

**ABSTRACTS OF THE TWENTY-EIGHTH ANNUAL  
MIDWINTER RESEARCH MEETING**

# **ASSOCIATION FOR RESEARCH IN OTOLARYNGOLOGY**



**February 19-24, 2005**

**The Fairmont New Orleans  
New Orleans, Louisiana**

**ABSTRACTS OF THE TWENTY-EIGHTH ANNUAL  
MID WINTER RESEARCH MEETING  
OF THE**

---

**A**ssociation for  
**R**esearch in  
**O**tolaryngology

---

**February 19 – 24, 2005**

**New Orleans, Louisiana, USA**

**Peter A. Santi, Ph.D.**  
*Editor*

Association for Research in Otolaryngology  
19 Mantua Road, Mt. Royal, NJ 08061 USA

## CONFERENCE OBJECTIVES

After attending the Scientific Meeting participants should be better able to:

1. Understand current concepts of the function of normal and diseased ears and other head and neck structures.
2. Understand current controversies in research methods and findings that bear on this understanding.
3. Understand what are considered to be the key research questions and promising areas of research in otolaryngology.

ISSN-0742-3152

The *Abstracts of the Association for Research in Otolaryngology* is published annually and consists of abstracts presented at the Annual MidWinter Research Meeting. A limited number of copies of this CD and previous books of abstracts (1978-2004) are available.

Please address your order or inquiry to:  
**Association for Research in Otolaryngology**  
19 Mantua Road  
Mt. Royal, NJ 08061 USA

**General Inquiry**  
Phone (856) 423-0041 Fax (856) 423-3420  
E-Mail: [headquarters@aro.org](mailto:headquarters@aro.org)

**Meetings**  
Phone: (856) 423-7222 Ext. 350  
E-Mail: [meetings@aro.org](mailto:meetings@aro.org)

This book was prepared from abstracts that were entered electronically by the authors. Authors submitted abstracts over the World Wide Web using Mira Digital Publishing's PaperCutter™ Online Abstract Management System. Any mistakes in spelling and grammar in the abstracts are the responsibility of the authors. The Program Committee performed the difficult task of reviewing and organizing the abstracts into sessions. The Program Committee Chair, Dr. Robert Shannon, the President, Dr. William Brownell, and Program Committee Member, Dr. John Middlebrooks constructed the final program. Mira electronically scheduled the abstracts and prepared Adobe Acrobat pdf files of the Program and Abstract Books. These abstracts and previous years' abstracts are available at: <http://www.aro.org>.

Citation of these abstracts in publications should be as follows:  
**Authors, year, title, Assoc. Res. Otolaryngol. Abs.: Abstract number.**

For Example:

Large, E., 2005, Nonlinear Time-Frequency Analysis: A Dynamical Systems Approach, Assoc. Res. Otolaryngol. Abs.: 1065.



## 2005 ARO MidWinter Meeting

*General Chair*

William E. Brownell, PhD (2004-2005)

*Program Organizing Committee*

Robert V. Shannon, PhD, *Chair* (2002-2005)

John P. Carey, M.D (2004-2007)

Robin L. Davis, PhD (2002-2005)

Michael P. Gorga, PhD (2002-2005)

Andrew K. Groves, PhD (2004-2007)

Leonard Kitzes, PhD (2004-2007)

Anna Lysakowski, PhD (2002-2005)

John Middlebrooks, PhD (2003-2006)

Kevin Ohlemiller, PhD (2003-2006)

Alan Palmer, PhD (2003-2006)

Joseph R. Santos-Sacchi, PhD (2004-2007)

Karen Steel, PhD (2004-2007)

Peter Santi, PhD, *ARO Editor, Council, ex officio*

William E. Brownell, PhD, *President, Council Liaison*

*Program Publications*

Peter Santi, PhD, *Editor*

*Diversity & Minority Affairs Committee*

Ann M. Thompson, PhD, *Chair* (2002-2005)

Henry J. Adler, PhD (2003-2006)

Ricardo Cristobal, MD PhD (2002-2005)

Xiaohong Deng, MS (2003-2006)

Jagmeet Kanwal, PhD (2003-2006)

Vishakha W. Rawool, PhD (2003-2006)

Duane Simmons, PhD (2003-2006)

Steven Rauch, MD, *Council Liaison* (2004-2005)

*Graduate Student/Postdoctoral Travel Awards*

Douglas Cotanche, PhD, *Chair* (2002-2005)

Laura Hurley, PhD (2003-2006)

Matthew Kelley, PhD (2002-2005)

Nathaniel T. McMullen, PhD (2002-2005)

Jennifer Stone, PhD (2002-2005)

*Physician Research Training*

Hilary A. Brodie, MD, PhD, *Chair* (2002-2005)

Carol A. Bauer, MD (2001-2005)

Holly H. Birdsall, MD, PhD (2001-2005)

Marc Coltrera, MD (2003-2006)

Diane Durham, PhD (2003-2006)

Bruce J. Gantz, MD (2002-2005)

Larry Lustig, MD (2003-2006)

Michael J. McKenna, MD (2001-2005)

Alan G. Micco, (2001-2005)

J. Gail Neely, MD (2002-2005)

Debara Tucci, MD (2003-2006)

James F. Battey, MD, PhD, NIDCD Dir., *ex-officio*

Maureen Hannley, PhD, Exec VP Rsch., *ex officio*

Ashley Wackym, MD, *Council Liaison* (2004-2005)

*Award of Merit Committee*

Peter Dallos, PhD, *Chair* (2003-2006)

Ellen Covey, PhD (2002-2005)

Ruth Anne Eatock, PhD (2004-2007)

Broyna J. B. Keats, PhD (2004-2007)

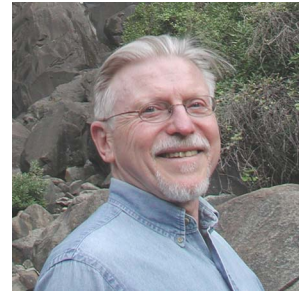
Lloyd Minor, MD (2003-2006)

Alan R. Palmer, PhD (2004-2007)

David Lim, MD, *Council Liaison* (2004-2005)

## President's Message

Welcome to New Orleans and our 28<sup>th</sup> Annual Midwinter Research Meeting. It is the first meeting of ARO in a major convention city and it promises, as in the past, to be scientifically important and stimulating. New Orleans and the Fairmont Hotel offer opportunities that should enhance the meeting experience.



The Program Committee and its Chair, Bob Shannon (who rotates off the committee this year), have once again done an efficient and thoughtful job of organizing the 1065 contributed and invited abstracts into poster and podium sessions. The scientific program begins Saturday evening with a workshop on Gene Microarray Technology. There are two other workshops on Sunday and Monday evening. The Presidential Symposium on Sunday morning is devoted to the structure and function of biological membranes. Five outstanding scientists address lipid-protein interactions that are at the heart of many sensory, developmental, neuronal and pharmacological events. Membrane-based cell signaling contributes to Planar Cell Polarity and Stereocilia Bundle Development which is the topic of one of the Sunday afternoon symposia. Other symposia at the meeting cover auditory pathways, cochlear implants, gap junctions, music and the brain, neuroethology, brain slices, hereditary hearing loss, and middle ear biomechanics.

The Award of Merit Committee and the ARO Council have selected Edwin W. Rubel for the 2005 Award of Merit. Ed will present the Presidential Lecture late Tuesday afternoon. His title "Gone Fishing; Can We Hook the Modulators of Hair Cell Survival in Zebrafish Lateral Line?" gives an indication as to why he is receiving the award. The Awards & Honors Ceremony that follows his lecture will elaborate on his career and contributions.

The association's journal JARO continues its ascent. The ARO research community together with JARO Editor-in-Chief Eric Young, associate editors and reviewers continues to improve our publication's citation index. Eric and his editorial office deserves a special thanks for initiating and maintaining the online prepublication of papers immediately on acceptance. The publication committee under the leadership of Drs. Popper and Popelka (co-chairs) continues to facilitate communication between the publisher, council and the editorial office helping to assure the fiscal viability of JARO and its important role in the ARO research enterprise.

Research trainees have benefited over the years from the generosity of the NIH/NIDCD, Deafness Research Foundation, American Academy of Otolaryngology - Head & Neck Surgery Foundation, Medtronic Xomed, and American Academy of Audiology/American Academy of Audiology Foundation (AAAF). These organizations sponsor the Travel Award Luncheon and Program which honors recipients of the Midwinter Meeting Travel Awards and their mentors. The Deafness Research Foundation deserves special thanks this year for significantly increasing its support. ARO Secretary/Treasurer, Betsy Keithley, as part of her role as in providing active oversight of ARO finances and documentation of council activities, made sure that applications for travel award and meeting funds were submitted. Betsy and Council Member Steve Rauch end their terms at this meeting. Please thank Betsy and Steve for their tireless efforts on behalf of ARO.

Their hard work has enhanced the organization and in many cases extended beyond the normal call of duty.

Returning and new exhibitors also contribute to the success of the Midwinter meeting with displays that keep us up to date on products, publications, grants and in some cases by sponsoring special receptions. Please be sure to thank them as their participation helps to keep our meeting costs down.

Our meeting in New Orleans would not have come about were it not for the support and hard work of many people. The wisdom and leadership of Council guided the decision to hold the 2005 Midwinter meeting at the Fairmont Hotel in New Orleans. We were able to move at practically the last possible moment because of the able assistance of our management firm (notably our Meetings Manager, Lisa Astorga, and our Executive Director, Darla Dobson). An *ad hoc* cite selection committee consisting of Bob Shannon, Charlie Liberman, myself and Lisa Astorga visited potential meeting venues and Council made the final decision. Bob Shannon, Lisa Astorga and the program committee had more than the usual stress of organizing the meeting at a new location. Please thank Bob, Darla, Lisa and all our Council members for their service during a stressful transition period.

The pressures that forced us to move to New Orleans also require we identify and commit to a meeting location for next year (2006) and beyond. A two year lead time is desirable in order to optimize meeting organization and membership attendance. Specifics about our exodus from the Adams Mark hotel and future meeting locations will be discussed during the business meeting on Monday evening. Please attend and make your wishes known. You will have a second opportunity to voice your opinions by completing the post-meeting questionnaire.

Now, let us celebrate science!

**Bill Brownell**



**Edwin W. Rubel, Ph.D.**  
**2005 Award of Merit Recipient**

Edwin W Rubel, Ph.D.  
2005 Award of Merit Recipient

Edwin W Rubel trained in Psychology at Michigan State University and received a doctorate in 1969 for the first comprehensive study of sensory coding in the developing central nervous system. His independent research program of the past three decades has retained a focus on behavior, particularly during auditory development. At the same time, Dr. Rubel's work has provided important insights into biological questions that tend to be viewed in purely cellular and molecular terms: hair cell regeneration, neuron cell death, and dendrite formation. In fact, each of these research areas is a successful offshoot from a laboratory that studies how the chicken auditory system develops and how that development is influenced by the environment.

After a postdoctoral fellowship at UC Irvine studying the physiology of polysensory association cortex, Dr. Rubel began his independent research career in 1971 as an Assistant Professor of Psychology at Yale University. There he began a series of experiments to determine how frequency is represented in the developing chick central auditory pathway. Behavioral experiments in normal and acoustically-deprived hatchling chicks used generalization of distress-call habituation to tones to show that there is perceptual sharpening during the first few days after hatching and that this maturation depends on normal acoustic experience. In parallel with these behavioral studies, Dr. Rubel began a series of experiments that have produced compelling examples of structure-function relationships in the auditory central nervous system. These cellular studies explored the organization and development of the second- and third-order neurons in the chick's auditory pathway, nucleus magnocellularis (NM) and nucleus laminaris (NL). Mapping studies revealed that there is a precise gradient of dendritic structure along the tonotopic axis of NL, which is thought to optimize interaural time difference detection at each frequency. Dr. Rubel (with Steven Young) then discovered that the projection from NM to NL serves as an anatomical delay line, consistent with the Jeffress coincidence-detector model of sound localization. Dr. Rubel then answered one of his initial research questions by showing (with Zaid Smith and Jeffrey Deitch) that the distinctive dorsal and ventral dendritic tufts of these NL neurons are independently maintained by afferent synaptic input from NM. Together, these studies formed one of the most successful fusions of behavioral and cellular neuroscience, and recommended the chick as an exceptional model for hearing research.

Although anatomical findings were consistent with a place code of frequency in the developing chick brainstem auditory nuclei, there was a paradox that had yet to be resolved. Whereas the cochlea itself begins to mature morphologically in the basal region (which responds to higher frequencies in adults), developing animals first respond behaviorally to relatively low frequencies. Dr. Rubel hypothesized that the basal cochlea was at first responsive to lower frequencies and only gradually shifted its responsiveness to higher frequencies. In one line of research begun after his move to the University of Virginia School of Medicine in 1977, Dr. Rubel (with Brenda Ryals) showed that the cochlear damage resulting from high intensity pure tones was found at successively more basal locations during development. In a second line of research,

taking advantage of his meticulous work on the normal development of NM topography, Dr. Rubel (with William Lippe) showed that the frequency map in NM did indeed shift during development. Similar observations have been made in many species over the past two decades, and the development of a shifting place code is now a broadly accepted principle.

One of Dr. Rubel's motivations for launching a systematic investigation of development in the bird auditory system was the mounting evidence that avian auditory neurons and hearing-related behaviors were quite sensitive to manipulation of sound-evoked activity. Experiments in his lab, in which the ear of chick embryos or hatchlings was surgically destroyed, revealed that there is a discrete period of life during which one-third of the neurons in NM die in the absence of cochlear nerve input. After moving to the University of Washington School of Medicine in 1985, Dr. Rubel devoted increasing efforts to understand the mechanisms of the rapid death of some auditory neurons and the survival of others after damage to the ear. The earliest studies (with Oswald Steward, Dianne Durham and Gwen Garden) showed that various cytological markers associated with oxidative metabolism and protein synthesis identified, within hours of deafening, those NM neurons destined to die. Dr. Rubel (with Richard Hyson) then demonstrated that afferent synaptic stimulation is necessary for survival of the NM neurons that otherwise die after deafferentation. Later work (with Lance Zirpel) showed that afferent stimulation acts via metabotropic glutamate receptors to maintain the normal intracellular calcium levels required for neuronal survival in NM. More recent experiments (with Sam Moustafapour) have shown that the normally brief postnatal critical period for susceptibility to deafening-induced cell death in the mouse cochlear nucleus can be extended by blocking expression of the *bcl2* gene or prevented by its over-expression. The chick NM is well-established as the leading model system for understanding the role of synaptic activity on neuron survival.

Dr. Rubel's work on hair cell regeneration in the bird cochlea is an interesting illustration of how basic research often begets clinically-relevant findings. His experiments on cochlear damage with ototoxic agents were initially designed to study the effects of auditory deprivation. Acoustic deprivation with earplugs had not produced significant changes in central auditory anatomy, and Dr. Rubel (with William Lippe) subsequently discovered that spontaneous activity was quite high prior to the onset of hearing. Thus, as he set about to identify a better way to deprive the brain of sound, one of the first studies (with Paul Lambert and Raul Cruz) looked at when cochlear damage first became apparent after exposure to noise or ototoxic drugs. The surprising finding was that damage decreased with survival time, suggesting a repair mechanism. Later, Dr. Rubel (with Brenda Ryals) used tritiated thymidine autoradiography to demonstrate that new cells were indeed generated within the damaged chick cochlea. We should emphasize that the experimental psychologist is never far from the lab bench. Most recently, Dr. Rubel (with Sarah Woolley) has shown that adult songbirds that are deprived of auditory input by hair-cell destruction recall their song when the hair cells regenerate, indicating that a stable template does not require persistent activation.



Dr. Rubel has clearly made key discoveries in diverse areas of developmental neurobiology, and his impact extends well beyond the hearing sciences. However, we in the auditory community have benefited the most from his imagination, energy, and intellect. About 100 students, scientists, and clinicians have been mentored in his laboratory, which has produced over 200 publications. Dr. Rubel founded the Virginia Merrill Bloedel Hearing Research Center, a thriving multidisciplinary enterprise that now embraces 12 departments and over 60 faculty at the University of Washington. He has also served our community as president of ARO and has been a forceful advocate for NIDCD from its inception. It is a welcome tribute that the 2005 Award of Merit should be presented to Edwin W Rubel for his scientific achievements, his scholarship, and his enduring commitment to understand the entire system, from hair cell to behavior.

Thomas N. Parks  
Dan H. Sanes

# Association for Research in Otolaryngology

Executive Offices

19 Mantua Road, Mt. Royal, NJ 08061 USA

Phone: (856) 423-0041 Fax: (856) 423-3420 E-Mail: [headquarters@aro.org](mailto:headquarters@aro.org)

Meetings Phone: (856) 423-7222 x 350 Meetings E-mail: [meetings@aro.org](mailto:meetings@aro.org)

## *ARO Council Members 2004-2005*

President: William E. Brownell, PhD  
Baylor College of Medicine  
Dept. of Otolaryngology & Comm. Sci.  
Houston, TX 77030

Secretary/Treasurer: Elizabeth Keithley, PhD  
University of California San Diego  
9500 Gilman Drive, 0666  
LaJolla, CA 92093

President-Elect: Lloyd B. Minor, M.D.  
Johns Hopkins University School of Medicine  
Department of Otolaryngology  
601 North Caroline Street, Room 6253  
Baltimore, MD 21287-0910

Editor: Peter A. Santi, PhD  
University of Minnesota  
Department of Otolaryngology  
Lions Research Bldg., Room 121  
2001 Sixth St. SE  
Minneapolis, MN 55455

Past President: Edwin M. Monsell, MD, PhD  
Wayne State University  
Department of Otolaryngology & HNS  
4201 St. Antoine 5E-UHC  
Detroit, MI 48201

Historian: David J. Lim, MD  
House Ear Institute  
2100 W. Third St., Fifth Floor  
Los Angeles, CA 90057

## *Council Members at Large*

Ashley Wackym, MD  
Medical College of Wisconsin  
Dept. of Otolaryngology  
& Comm. Sciences  
9200 West Wisconsin Avenue  
Milwaukee, WI 53226

Douglas A. Cotanche, PhD  
Children's Hospital  
Dept. of Otolaryngology FE 9  
300 Longwood Avenue  
Boston, MA 02115

Steven Rauch, MD  
Massachusetts Eye & Ear Infirmary  
Eaton Peabody Laboratory  
243 Charles Street  
Boston, MA 02114

## **Past Presidents**

1973-74 David L. Hilding, MD  
1974-75 Jack Vernon, PhD  
1975-76 Robert A. Butler, PhD  
1976-77 David J. Lim, MD  
1977-78 Vicente Honrubia, MD  
1978-80 F. Owen Black, MD  
1980-81 Barbara Bohne, PhD  
1981-82 Robert H. Mathog, MD  
1982-83 Josef M. Miller, PhD  
1983-84 Maxwell Abramson, MD  
1984-85 William C. Stebbins, PhD  
1985-86 Robert J. Ruben, MD  
1986-87 Donald W. Nielsen, PhD  
1987-88 George A. Gates, MD  
1988-89 William A. Yost, PhD  
1989-90 Joseph B. Nadol, Jr., MD  
1990-91 Ilsa R. Schwartz, PhD  
1991-92 Jeffrey P. Harris, MD, PhD  
1992-93 Peter Dallos, PhD  
1993-94 Robert A. Dobie, MD  
1994-95 Allen F. Ryan, PhD  
1995-96 Bruce J. Gantz, MD  
1996-97 M. Charles Liberman, PhD  
1997-98 Leonard P. Rybak, MD, PhD  
1998-99 Edwin W. Rubel, PhD  
2000-01 Richard A. Chole, MD, PhD  
2001-02 Judy R. Dubno, PhD  
2002-03 Richard T. Miyamoto, MD  
2003-04 Donata Oertel, PhD  
2004-05 Edwin M. Monsell, MD, PhD

## **Award of Merit Recipients**

1978 Harold Schuknecht, MD  
1979 Merle Lawrence, PhD  
1980 Juergen Tonndorf, MD  
1981 Catherine Smith, PhD  
1982 Hallowell Davis, MD  
1983 Ernest Glen Wever, PhD  
1984 Teruzo Konishi, MD  
1985 Joseph Hawkins, PhD  
1986 Raphael Lorente de Nó, MD  
1987 Jerzy E. Rose, MD  
1988 Josef Zwislocki, PhD  
1989 Åke Flóck, PhD  
1990 Robert Kimura, PhD  
1991 William D. Neff, PhD  
1992 Jan Wersäll, PhD  
1993 David Lim, MD  
1994 Peter Dallos, PhD  
1995 Kirsten Osen, MD  
1996 Ruediger Thalmann, MD & Isolde Thalmann, PhD  
1997 Jay Goldberg, PhD  
1998 Robert Galambos, MD, PhD  
1999 Murray B. Sachs, PhD  
2000 David M. Green, PhD  
2001 William S. Rhode, PhD  
2002 A. James Hudspeth, MD, PhD  
2003 David T. Kemp, PhD  
2004 Donata Oertel, PhD  
2005 Edwin W. Rubel, PhD

# Table of Contents

Abstract Number

Short Course	Gene Microarray Technology: An Introduction to Methods and Applications in Hearing Research	
Presidential Symposium		
A:	Membranes 101: Membrane Structure and Function .....	1-6
Symposia		
B:	Planar Cell Polarity and Stereocilia Bundle Development .....	7-12
C:	Corticofugal Auditory Pathways - Structure and Function .....	13-19
Poster		
D1:	Genetics: Gene Expression and CNS.....	20-28
D2:	Vestibular: Molecular.....	29-36
D3:	Cochlear Implants: Molecular Issues .....	37-44
D4:	Drug/Gene Delivery to the Inner Ear .....	45-54
D5:	Inner Ear Inflammation and Mitochondrial Hearing Loss .....	55-60
D6:	Inner Ear: Protection from Inflammation/Ischemia.....	61-64
D7:	Auditory Nerve.....	65-80
D8:	Aging: Human Studies.....	81-88
D9:	Auditory Brainstem: Molecular Aspects.....	89-102
D10:	Sound Localization: Physiology .....	103-120
D11:	Auditory Midbrain: Pharmacology, Plasticity and Tinnitus.....	121-134
D12:	Otoacoustic Emissions: Hearing Loss, Development .....	135-143
D13:	External or Middle Ear: Otitis Media .....	144-159
D14:	Clinical Audiology: Potpourri.....	160-171
D15:	Vestibular: Central .....	172-183
D16:	Vestibular: Clinical.....	184-205
D17:	Clinical Otolaryngology.....	206-219
D18:	Cochlear Implants: Channel Selectivity .....	220-228
D19:	Cochlear Implants: Clinical Issues .....	229-242
Workshop		
E1:	NIDCD Workshop: Part I-What's New at the NIH; Part II-New Investigators.....	243
Patient Advocacy Group Workshop		
E2:	Congenital Cytomegalovirus-Induced Hearing Loss: Who Needs To Know? .....	244-249
Symposia		
F:	The Brain's View of the Cochlear Implant .....	250-255
G:	Recent Advances in Understanding the Function of Gap Junctions.....	256-262
H:	Music and Auditory Neuroscience.....	263-267
Podium		
I:	Development/Regeneration .....	268-282
Poster		
J1:	Genetics: Human.....	283-294
J2:	Animal Models of Genetic Hearing Loss.....	295-309
J3:	Otoacoustic Emissions: Mostly DPOAEs .....	310-322
J4:	Basilar Membrane Mechanics .....	323-340
J5:	Tectorial Membrane and Others .....	341-349
J6:	Inner Ear Intrinsic Protective/Repair Mechanisms .....	350-360
J7:	Inner Ear Noise Injury: Prevention/Treatment .....	361-373
J8:	Hair Cells: Metabolic, Ototoxicity and Regeneration .....	374-387
J9:	Hair Cell Synapses.....	388-398
J10:	Inner Ear Anatomy and Physiology 1 .....	399-411
J11:	Aging: Animal Studies .....	412-433
J12:	Auditory Brainstem Physiology A .....	434-451
J13:	Auditory Cortex: Imaging, MEG and ERPs.....	452-471
J14:	Bilateral Cochlear Implants .....	472-478
J15:	Psychophysics: Hearing Impaired .....	479-485
J16:	External or Middle Ear: Cholesteotoma Plus a Potpourri.....	486-498

J17:	Clinical Audiology: Evoked Potentials.....	499-506
<b>Symposia</b>		
K:	Auditory Neuroethology: Getting Closer to the Real Acoustic World?.....	507-512
L:	Brain Slice Preparations for Studies of Signal Processing In the Auditory and Vestibular Systems: Reconciliation with in vivo Studies .....	513-517
<b>Podium</b>		
M:	Cochlear Implants.....	518-526
N:	Novel Techniques for Studying Lanyrinthine Structure and Function .....	527-536
<b>Poster</b>		
O1:	Development 1 .....	537-548
O2:	Regeneration 1.....	549-564
O3:	Inner Ear Noise Injury: Mechanisms.....	565-585
O4:	Inner Ear Ototoxic Injury: Mechanisms.....	586-601
O5:	Inner Ear Ototoxic Injury: Prevention/Treatment .....	602-609
O6:	Prestin and Hair Cell Mechanics .....	610-624
O7:	Hair Cell Molecular Biology and Development.....	625-641
O8:	Inner Ear Anatomy and Physiology 2 .....	642-656
O9:	Otoacoustic Emissions: SFOAEs, Efferent Effects.....	657-667
O10:	Auditory Brainstem: Physiology B.....	668-686
O11:	Auditory Midbrain: Pathways, Binaural and Frequency Selectivity.....	687-699
O12:	Auditory Cortex: Plasticity and Development.....	700-717
O13:	Animal Psychophysics.....	718-726
O14:	Psychophysics: Binaural and Learning.....	727-733
O15:	Cochlear Implants: Miscellaneous.....	734-748
O16:	Speech Perception .....	749-765
<b>Presidential Lecture</b>		
P:	Presidential Lecture and Award Ceremony .....	766
<b>Symposia</b>		
Q:	Hereditary Hearing Loss: From Humans to Mice and Back.....	767-772
R:	Integrating Middle-Ear Imaging, Physiology, Biomechanics.....	773-779
<b>Podium</b>		
S:	Inner Ear Mechanics .....	780-792
<b>Poster</b>		
T1:	Genetics: Mouse Models and Gene Characterization .....	793-804
T2:	Development 2 .....	805-829
T3:	Regeneration 2.....	830-840
T4:	Vestibular: Peripheral .....	841-860
T5:	Inner Ear Fluids and Membranes .....	861-874
T6:	Hair Cell Ion Channels .....	875-885
T7:	Hair Cell Transduction and Stereocilia.....	886-896
T8:	Inner Ear Anatomy and Physiology 3 .....	897-915
T9:	Middle Ear Function in Different Species.....	916-932
T10:	Auditory Brainstem: Effects of Trauma .....	933-951
T11:	Sound Localization Psychophysics .....	952-967
T12:	Auditory Midbrain: Temporal Features.....	968-979
T13:	Auditory Cortex: Temporal Features.....	980-993
T14:	Auditory Cortex: Structure and Function .....	994-1010
T15:	Cochlear Implant Physiology .....	1011-1025
T16:	Psychophysics: Miscellaneous.....	1026-1040
<b>Podium</b>		
U:	Inner Ear: Hair Cells.....	1041-1055
V:	Psychophysics: Complex Signals.....	1056-1065

## **1 Introduction - Membranes and the Association for Research in Otolaryngology**

**William Brownell<sup>1</sup>**

<sup>1</sup>*Baylor College of Medicine*

Membranes define the boundaries of cells and their organelles and help to maintain the electrochemical gradients that power biological processes. Biological membranes are composed largely of lipids and membrane proteins and they are a major role in a large portion of ARO related research. Outer hair cell electromotility is a direct conversion of the energy contained in the transmembrane electric field into mechanical force. Membrane interactions are important for synaptic vesicle exo- and endo-cytosis. Cell signaling events that underlie cellular development and the maintenance of neuronal polarization represent another area where membrane-based events are central. On the clinical side, many drugs exert their action by directly modulating the membrane. The purpose of the 2005 presidential symposium is to familiarize the membership with the composition, natural history and physical properties of cellular membranes and because of time constraints can convey only a portion of the excitement associated with the membrane revolution.

The first two talks provide an introduction to membranes at the molecular level. George Patterson discusses the movement of membrane lipids and proteins from the endoplasmic reticulum to the plasma membrane and back again. David Daleke focuses on the differences in lipid composition between the two leaflets of the membrane bilayer. Robert Cantor introduces membrane mechanics. He discusses lipid-protein interactions and how a broad range of drugs might alter those interactions. Sergey Sukarov provides a direct example of how membrane mechanics alter the structure and function of a bacterial stretch-activated channel. Eduardo Perozo concludes the symposium by describing lipid-protein interactions associated with the opening and closing of a voltage gated ion channel. Membrane biophysics is a vast subject and there are several topics that may be touched on but are not covered in a full seminar. These include membrane fusion, membrane rafts and cell signaling.

## **2 Membrane Trafficking in the Secretory Pathway**

**George Patterson<sup>1</sup>**, Jennifer Lippincott-Schwartz<sup>2</sup>

<sup>1</sup>*Cell Biology and Metabolism Branch, NICHD, NIH,*

<sup>2</sup>*National Institute of Cell Biology and Metabolism Branch, NICHD, NIH*

Organelles which comprise the secretory pathway, the endoplasmic reticulum, the Golgi apparatus, and the plasma membrane, maintain markedly different compositions of lipids and proteins while constantly exchanging material throughout the life of cell. Transmembrane proteins use two mechanisms to sort within the membranes of this pathway. In one, sorting sequences found in the cytoplasmic domain of many proteins are used for facilitating movement from one compartment to another or for retention within one compartment versus another. In a different mechanism,

the transmembrane domain itself determines the protein's localization and movement within the secretory pathway. Under this mechanism, proteins preferentially partition into or are excluded from specific lipid domains while moving within the secretory pathway. We have utilized confocal microscopy and a fluorescent protein tagged version of a temperature-sensitive vesicular stomatitis virus G protein (VSVG) as a model cargo molecule in the study of secretory pathway trafficking. At the non-permissive temperature, the VSVG is retained within the endoplasmic reticulum. Upon shift to the permissive temperature, it moves to the Golgi apparatus en route to the plasma membrane. Quantification of the fluorescence of the VSVG as it moves through these compartments indicates that it moves with first order kinetics from one compartment to the next. Movement of VSVG through the Golgi apparatus is of particular interest as this organelle is at the crossroads between the ER and the PM. Closer examination of VSVG cargo movement into and out of the Golgi apparatus suggests that this organelle behaves as a single interconnected compartment rather than as a series of separate cisterna, as generally thought. Our studies also suggest that the VSVG dynamically partitions into domains depleted of Golgi enzymes and it is from these domains that VSVG buds into transport carriers that traffick to the plasma membrane. These properties of VSVG movement through the secretory pathway provide a general framework for understanding the principles underlying secretory membrane sorting and transport within eukaryotic cells.

## **3 Generation and Maintenance of Transbilayer Phospholipid Asymmetry: Role of Flippases, Floppases and Scramblases**

**David Daleke<sup>1</sup>**

<sup>1</sup>*Indiana University*

Phospholipids in biological membranes are organized non-randomly across the bilayer. Glycolipids and the choline-containing phospholipids, phosphatidylcholine and sphingomyelin are enriched on the outer surface of the plasma membrane or the inner surface of internal organelles. In contrast, the amine-containing phospholipids, phosphatidylserine (PS) and phosphatidylethanolamine (PE), are found primarily in the cytofacial monolayer. This distribution is essential for the normal functioning of the membrane and the regulation of lipid asymmetry plays an important role in cell signalling. The appearance of PS on the surface of apoptotic cells signals the recognition and destruction by macrophages. The externalization of PS in stimulated platelets induces the activation of plasma clotting enzymes. Transbilayer asymmetry is maintained, and in some cases generated, by the action of a number of transporters that vary in their direction of transport, lipid specificity and requirement for energy. The most well-characterized of these transporters is the aminophospholipid "flippase" which catalyzes the ATP-dependent transport of PS and PE to the cytoplasmic surface of the plasma membrane. "Floppase" proteins transport lipids such as PC and cholesterol in the opposite direction and have been found to be members of the ABC class of transporters. "Scramblases" facilitate the

dissipation of transbilayer lipid gradients and are thought to play a role in equilibrating the distribution of newly-synthesized lipids across the membrane of the endoplasmic reticulum, as well as responding to cell signals, such as an increase in Ca<sup>2+</sup>, to induce the exposure of PS on the cell surface. The specificity of the transporters for their substrates and the presence or absence of the transporters in membranes may result in progressively greater transbilayer asymmetry as a membrane trafficks from the endoplasmic reticulum to the plasma membrane. The current challenges in this field are the purification, identification and functional reconstitution of these proteins.

#### References

- Daleke, D. L. (2003) Regulation of transbilayer plasma membrane phospholipid asymmetry. *J Lipid Res* 44, 233-242.
- Kol, M. A., de Kroon, A. I., Killian, J. A., and de Kruijff, B. (2004) Transbilayer movement of phospholipids in biogenic membranes. *Biochemistry* 43, 2673-2681.
- Sprong, H., van der Sluijs, P., and van Meer, G. (2001) How proteins move lipids and lipids move proteins. *Nat Rev Mol Cell Biol* 2, 504-513.

### **4 Bilayer Composition and the Activity of Membrane Proteins: Lateral Pressures and the Mechanism of Anesthesia**

**Robert Cantor<sup>1</sup>**

<sup>1</sup>*Dartmouth College*

The function of many integral membrane proteins involves conformational equilibria that are modulated by changes in bilayer composition. Such effects are likely to be of considerable physiological and pharmacological importance, but the underlying mechanisms are not well understood. We explore an indirect, nonspecific mechanism in which changes in bilayer composition alter the distribution of lateral pressures in the bilayer, which in turn causes a shift in the protein conformational equilibrium by altering the amount of mechanical work accompanying the transition. The physical origins of these lateral stresses in membranes, and the thermodynamic and mechanical basis for their coupling to protein conformational equilibria are outlined. Calculations predict significant redistributions of lateral pressure to accompany changes in lipid characteristics and admixture of amphiphilic solutes.

It is argued that this mechanism may well underlie general anesthesia. Although exceptions to the Meyer-Overton correlation, such as the cutoffs in potency of alkanes and alkanols with increasing chain length, are commonly cited as evidence against any membrane-mediated mechanism, many are actually predicted by this mechanism. The recent measurement of significant anesthetic potency of very long-chain polyhydric alkanols with regularly spaced hydroxyl groups is in agreement with predictions of the lateral pressure mechanism, but is inconsistent with a binding mechanism in which cutoff arises when a molecule exceeds the volume of a putative binding site.

In the continued presence of neurotransmitter agonists, ion currents of postsynaptic receptors undergo complex

modulation over long times. It is speculated that the underlying shifts in receptor conformational equilibria may arise indirectly, via the influence of neurotransmitters on the postsynaptic membrane. Such effects (concentration-dependent desensitization, inactivation, etc.) are predicted to be qualitatively consistent with electrophysiological results, both for excitatory and inhibitory receptors. If so, there are profound implications for general anesthesia, particularly with regard to the remarkably narrow range of sensitivity to anesthetics both within the human population and over a broad range of animal phyla.

#### References:

- Chem. Phys. Lipids* 101:45 (1999). "The influence of membrane lateral pressures on simple geometric models of protein conformational equilibria"
- Biophys. J.* 80:2284 (2001). "Breaking the Meyer-Overton rule: predicted effects of varying stiffness and interfacial activity on the intrinsic potency of anesthetics"
- Biochemistry* 42:11891 (2003). "Receptor desensitization by neurotransmitters in membranes: are neurotransmitters the endogenous anesthetics?"
- Biophys. J.* 76:2625 (1999). "Lipid composition and the lateral pressure profile in bilayers"

### **5 The MscL Stretch-Activated Channel: Where are We in Understanding the Conformational Transition and Protein-Lipid Interactions When Protein Structure is Known?**

**Sergei Sukharev<sup>1</sup>**

<sup>1</sup>*University of Maryland*

The bacterial mechanosensitive channel, MscL came in the spotlight not only as a prokaryotic osmoregulator, but also as a convenient model system for basic studies of primary events in mechanosensation [1]. The channel opens by tension transmitted directly through the surrounding lipid bilayer. The small size of the mscL gene allows for exhaustive mutagenesis, whereas its extremely large unitary conductance permits high-resolution electrophysiological recordings which capture not only closed and open but also intermediate states. The solved crystal structure of MscL homolog from *M. tuberculosis* [2] opened an opportunity for precise atomic-scale predictions of its gating process. A computational model of the MscL gating transition developed in collaboration with H.R. Guy (NIH) was supported by a variety of experiments [3-5]. It predicted that the homopentameric MscL complex undergoes a large iris-like expansion associated with tilting of transmembrane helices. The opening transition appears to involve two gates, the hydrophobic constriction in the middle of the pore (main gate) and the cytoplasmic gate formed by short N-terminal domains. The opening of the main gate produces large expansion of the protein complex, whereas the subsequent separation of the N-terminal gate results in a major gain in conductance. Analysis of easily opened gain-of-function mutants suggests that the tension at which the channel opens is critically dependent on the hydration properties of the pore interior [6]. On the other hand, many of the loss-of-function

mutations which reduce tension sensitivity and make the channel 'stiffer', are located at the protein-lipid boundaries adjacent to the lipid headgroups [7,8]. The gating was shown to be lipid context-dependent [9]. Obtaining a detailed and self-consistent physical picture of MscL gating, which includes the protein itself, surrounding lipid and water, will put us closer to understanding the principles of function in eukaryotic sensory channels.

1. Sukharev, S. and A. Anishkin. 2004. Mechanosensitive channels: what can we learn from 'simple' model systems? *Trends Neurosci.* 27:345-351.

2. Chang, G., R.H. Spencer, A.T. Lee, M.T. Barclay, and D.C. Rees. 1998. Structure of the MscL homolog from *Mycobacterium tuberculosis*: a gated mechanosensitive ion channel. *Science* 282:2220-2226.

3. Sukharev, S., M. Betanzos, C.S. Chiang, and H.R. Guy. 2001. The gating mechanism of the large mechanosensitive channel MscL. *Nature* 409:720-724.

4. Betanzos, M., C.S. Chiang, H.R. Guy, and S. Sukharev. 2002. A large iris-like expansion of a mechanosensitive channel protein induced by membrane tension. *Nat. Struct. Biol.* 9:704-710.

5. Perozo, E., D.M. Cortes, P. Somporpisut, A. Kloda, and B. Martinac. 2002. Open channel structure of MscL and the gating mechanism of mechanosensitive channels. *Nature* 418:942-948.

6. Yoshimura, K., A. Batiza, M. Schroeder, P. Blount, and C. Kung. 1999. Hydrophilicity of a single residue within MscL correlates with increased channel mechanosensitivity. *Biophys. J.* 77:1960-1972.

7. Maurer, J.A. and D.A. Dougherty. 2003. Generation and evaluation of a large mutational library from the *Escherichia coli* mechanosensitive channel of large conductance, MscL: implications for channel gating and evolutionary design. *J. Biol. Chem.* 278:21076-21082.

8. Yoshimura, K., T. Nomura, and M. Sokabe. 2004. Loss-of-function mutations at the rim of the funnel of mechanosensitive channel MscL. *Biophys. J.* 86:2113-2120.

9. Perozo, E., A. Kloda, D.M. Cortes, and B. Martinac. 2002. Physical principles underlying the transduction of bilayer deformation forces during mechanosensitive channel gating. *Nat. Struct. Biol.* 9:696-703.

## **[6] Structure and Dynamics of Voltage-Dependent K<sup>+</sup> Channels in the Lipid Bilayer**

**Eduardo Perozo<sup>1</sup>, S. Chakrapani<sup>1</sup>, L.G. Cuello<sup>1</sup>, D.M. Cortes<sup>1</sup>**

<sup>1</sup>*University of Virginia*

The fundamental processes that underlie ion channel function are permeation/selectivity and gating. In an effort to understand ion channel gating, we have used an approach that combines reporter-group spectroscopic techniques (spin labeling/EPR) and electrophysiological methods with classical biochemical and molecular biological procedures. We have focused our attention on a series of prokaryotic K<sup>+</sup> and mechanosensitive channels with different energy transduction mechanisms (proton binding, KcsA; membrane stretch, MscL; transmembrane

voltage, KvAP). Through site-directed spin labeling, cysteine chemistry was used to introduce nitroxide radicals into specific sites within these channels with high reactivity and specificity. EPR spectroscopy analysis of the spin labeled mutants yields two types of structural information: 1) mobility and solvent accessibility of the attached nitroxide through collisional relaxation methods and 2) distances between pairs of nitroxides through dipole-dipole interactions. In this presentation we will focus on the structure and dynamics of the voltage-dependent K channel KvAP in the context of the lipid bilayer. We show in reconstituted full-length KvAP and in the isolated voltage-sensing domain, that the S4 segment is highly flexible, consists of two helices separated by a short linker and lies at the protein-lipid interface, with most of the gating charges protected from the lipid environment. Accessibility and dynamics data position the S1 segment at the contact interface between the voltage sensing and pore domains. These results establish the general principles of voltage-dependent channel structure under physiological conditions and thus limit the types of structural models underlying voltage-dependent gating.

### References

1. Mchaourab, H., and Perozo, E. (2000) Determination of Protein Folds and Conformational Dynamics Using Spin-Labeling EPR Spectroscopy. in *Biological Magnetic Resonance* (S. Eaton, G. E., L. Berliner, Ed.) pp 155-218, Kluwer-Plenum, New York.

2. Cuello, L. G., Cortes, D. M., and Perozo, E. (2004) Molecular architecture of the KvAP voltage-dependent K<sup>+</sup> channel in a lipid bilayer *Science* 306, 491-5.

## **[7] Structural Features During Establishment of Hair Bundle Polarity and Orientation.**

**Andrew Forge<sup>1</sup>**

<sup>1</sup>*UCL Centre for Auditory Research, University College London*

The hair-bundle of a hair cell is asymmetric. Its morphological "polarity" is defined by the eccentrically positioned kinocilium behind the longest row of stereocilia. The "orientation" of a polarised hair bundle is not random but is closely related to that of its immediate neighbours. When hair bundles are first apparent the kinocilium is located at the centre of the cell and becomes surrounded by elongated microvilli of approximately equal height, but very rapidly it becomes eccentrically positioned and stereocilia begin to show differential lengths. The initial orientation of polarised bundles is approximately correct but the angles of orientation of adjacent bundles may vary quite widely. Orientation becomes "sharpened" subsequent to the initial hair cell differentiation. For example, in vestibular maculae of mice, in which in mature tissues hair bundle orientation reverses either side of the striola and the orientations in saccules is the opposite of those in utricles, initial orientation varies systematically across the maculae and the general orientation in utricles is the opposite of that in saccules. This implies the presence of orientation cues when hair cells first differentiate. However, the striola is not defined. Opposing orientations of hair bundles either side of a line of polarity

reversal is sharply delineated later. The establishment of polarity and orientation do not correlate with the production of the overlying extracellular matrices, nor asymmetric growth of the maculae. Prominent microtubules in differentiating hair cells, are initially generally aligned at right angles to the apical surface and are therefore unlikely to provide a substrate for establishing asymmetry across the cell surface. Microfilament assemblies aligned parallel to the apical surface and connecting to the adherens junctions in supporting cells from the earliest stages could be involved in providing a "framework" associated with hair bundle orientation.

## **8** Role of PDZ Proteins in Trafficking

Robert Wenthold<sup>1</sup>, Nathalie Sans<sup>1</sup>

<sup>1</sup>NIH

All cellular functions depend on protein-protein interactions that group individual proteins into complexes to optimize both the efficiency and the regulation of molecular processes. While all cells utilize such mechanisms, it is especially important for complex cells that contain discrete functional domains, such as polarized epithelial cells and neurons. Many types of protein-protein interactions have been identified, but one of the most significant for the organization of membrane-associated proteins, including ion channels and receptors, is the PDZ interaction. The term PDZ originates from the first three members of the family identified (postsynaptic density 95, PSD-95; discs large, DLG; zonula occludens-1, ZO-1). The PDZ domains in these proteins contain about 90 amino acids. More than 400 PDZ proteins are present in the human genome. Although a limited number of interactions involve internal sequences, most PDZ interactions involve the distal carboxyl-terminal sequence of proteins; for example, S and V of the last 3 amino acids of NMDA receptor NR2B subunit (-SDV) are critical for its interaction with PSD-95. Most PDZ proteins contain multiple protein-protein interacting domains, which can include several PDZ domains, thereby facilitating the organizing and clustering of groups of proteins. Thus, one of the major known functions of PDZ proteins is to cluster and organize multiple related signaling molecules at specialized points of function, of which the synapse is an excellent model. A less recognized function of PDZ proteins is their role in the trafficking of membrane proteins. Our research has focused on the trafficking of glutamate receptors, of which most subunits of both NMDA and AMPA subtypes have PDZ binding domains at their C-termini. Our results suggest that both AMPA and NMDA receptors interact with PDZ proteins early in the secretory pathway. These interactions may indicate pre-forming of the receptor complex found at the postsynaptic density and raise interesting questions concerning the role of the PDZ protein in the trafficking of membrane proteins, as well as the role of the membrane protein in the trafficking of the PDZ protein.

## **9** The USH1 Gene Network: Molecular Information Underlying the Cohesion of the Growing Hair Bundle

Christine Petit<sup>1</sup>, Vincent Michel<sup>2</sup>, Gaele Lefevre<sup>2</sup>, Aziz El-Amraoui<sup>2</sup>, Dominique Weil<sup>2</sup>, Kumar Alagramam<sup>3</sup>, Richard Goodyear<sup>4</sup>, Guy Richardson<sup>4</sup>, Avital Adato<sup>2</sup>

<sup>1</sup>Institut Pasteur & Collège de France, <sup>2</sup>Institut Pasteur,

<sup>3</sup>Case Western Reserve University, <sup>4</sup>University of Sussex

Today, five genes underlying the USH1 syndrome (sensorineural deafness associated to retinitis pigmentosa) have been identified. The USH1B gene, MYO7A, encodes myosin VIIa, the USH1C gene, USH1C, encodes harmonin, the USH1D gene, CDH23, encodes cadherin-23, the USH1F gene, PCDH15, encodes protocadherin15, and the USH1G gene, SANS, encodes Sans. Mouse models for each of these genes show an early disorganization of the hair bundle. By using yeast two-hybrid screens and biochemical approaches, we investigated the putative interactions between USH1 proteins. We found that they are all able to interact with the PDZ1 or PDZ2 domain of harmonin. Our results show that all these molecules but Sans are located in the hair bundle. In shaker-1 mouse mutants defective in myosin VIIa, harmonin b disappears from the tip of the hair bundle. Altogether, our results led us to propose that a network of USH1 proteins underlies the cohesion of the hair bundle.

We propose that 1) Sans is involved in the trafficking of some USH1 proteins, 2) myosin VIIa controls the targeting (or the maintenance) of harmonin b to the tip of the hair bundle, 3) the two cadherins form interstereociliar links that are anchored to the actin filaments of the stereocilia, thereby ensuring the cohesion of the hair bundle, and 4) harmonin b is implicated in this anchoring.

## **10** Regulation of Frizzled-Planar Cell Polarity Signaling

Marek Mlodzik<sup>1</sup>, Alex Djiane<sup>1</sup>, Gishnu Das<sup>1</sup>, Thomas Klein<sup>1</sup>, Jun Wu<sup>1</sup>, Jessica Reynolds-Kenneally<sup>1</sup>, Ursula Weber<sup>1</sup>, Andreas Jenny<sup>1</sup>

<sup>1</sup>Mt Sinai School of Medicine

Planar cell polarity (PCP) is evident in developmental processes and in the cellular organization of many organs in vertebrates and invertebrates. In *Drosophila*, PCP is manifest in all adult tissues, including ommatidial arrangement in the compound eye, or hair orientation in wing cells. In vertebrates, PCP-signaling governs convergent extension during gastrulation and organization of a wide variety of structures, including the orientation of body hair and sensory hair cells of the inner ear. PCP establishment requires the conserved Frizzled (Fz)-PCP pathway and the associated PCP genes regulating it. Mutations in PCP genes cause aberrant orientation of body hair or inner ear sensory cells in mice, or misorientation of ommatidia and wing hair in *Drosophila*. Fz-signaling is mediated by Dishevelled (Dsh). Here we provide mechanistic insight into Fz-Dsh signaling regulation. We show that diego (dgo) is, like fz, required in the R3 photoreceptor, it regulates Fz-signaling positively, and it binds directly to Dsh. The same region of Dsh can also be bound by Prickle (Pk) which inhibits Fz-PCP



signaling. Strikingly, the interactions of Dgo and Pk with Dsh are mutually exclusive. Our data indicate that Dgo and Pk compete for Dsh binding and upon binding modulate Fz-Dsh signaling positively or negatively. Thus the inhibitory effect of Pk on Dsh is antagonized by a direct interaction between Dgo and Dsh.

## **11 Planar Cell Polarity Regulates the Orientation of Asymmetric Cell Division in *Drosophila***

**Francois Schweisguth<sup>1</sup>**

<sup>1</sup>*Ecole Normale Supérieure*

During metazoan development, cell fate diversity is generated in part by asymmetric cell divisions, in which mother cells divide to produce two daughter cells with distinct developmental potentials. Adoption of different cell fates often relies on the polarised distribution and unequal segregation of cell-fate determinants, and thus requires polarization of the mother cell. In *Drosophila*, the sensory organ precursor (pl) cell divides asymmetrically within the plane of the dorsal thorax epithelium and along a stereotyped anterior-posterior (a-p) planar polarity axis. Two cell-fate determinants, Numb and Neuralized, localize at the anterior cortex and the mitotic spindle lines up along the a-p axis. Planar polarity of the pl cell is controlled by planar cell polarity (PCP). PCP proteins define two opposite cortical domains prior to mitosis. The Frizzled (Fz) receptor localizes at the posterior apical cortex whereas the transmembrane protein Strabismus (Stbm) and the cytoplasmic protein Prickle (Pk) co-localize at the anterior apical cortex. PCP genes provide a-p positional information to regulate the cortical localization of two protein complexes, the posterior Par3-Par6-aPKC complex and the anterior Dlg-Pins-Gai complex. Both complexes are required for the anterior localization of Numb and Neuralized. The Dlg-Pins-Gai complex may also regulate interactions between astral microtubules and the anterior cortex, thereby orienting the mitotic spindle along the a-p axis. In PCP mutants, these two complexes localize asymmetrically, opposite to each other, but at a random position relative to the a-p axis. Phenotypic analysis indicates that Stbm promotes the cortical localization of Pins at prophase and that Dsh acts antagonistically to Stbm by excluding Pins from the posterior cortex. Stbm may recruit Pins at the cortex via its interaction with Dlg. We propose that PCP signaling provides a spatial bias to promote the anterior localization of Pins at the cortex. We will discuss the possible implication of these findings for the orientation of mitotic spindle and other microtubule-based structures by PCP in vertebrates.

## **12 Vangl2 and Planar Cell Polarity in the Mammalian Inner Ear**

**Matthew Kelley<sup>1</sup>**

<sup>1</sup>*Porter Neuroscience Research Center*

The uniform orientation of stereociliary bundles within the sensory epithelia of the inner ear represents one of the most striking examples of planar cell polarity (PCP) in a vertebrate system. Recently, results from a number of laboratories have demonstrated that orthologs of

invertebrate PCP genes play similar roles in the generation of uniform stereociliary bundle orientation. However, other studies have identified molecules that appear to be uniquely involved in PCP in mammals. These results suggest that while the roles of the core molecules have been conserved, important differences in the regulation of PCP may exist between invertebrates and vertebrates.

One of the key molecules in regulation of PCP in the inner ear is Vangl2, a novel membrane protein that is expressed by *in situ* hybridization in both hair cells and support cells. To begin to understand the intracellular role of Vangl2 in the polarization of stereociliary bundles, we determined the subcellular localization of Vangl2 in developing hair cells and characterized its molecular interactions with other known and candidate, PCP molecules.

Results indicate that Vangl2 becomes asymmetrically localized to the proximal side (opposite side from the kinocilium) of developing hair cells. This localization is consistent with previous reports for the localization of Vang in *Drosophila* and suggests that Vangl2 is involved in restricting the final site of localization of the hair bundle, through modulation of cytoskeleton components. Vangl2 could function either in the formation of a complex that inhibits the activation of Dishevelled, a cytoplasmic effector of PCP, or alternatively, that Vangl2 could mediate the formation of molecular complexes that direct the movement of the developing kinocilium towards the opposite side of the cell.

## **13 Corticofugal Modulation and Plasticity in the Auditory System: An Overview**

**Nobuo Suga<sup>1</sup>**

<sup>1</sup>*Department of Biology, Washington University in St. Louis, MO 63130*

Compared with thalamocortical fibers, corticofugal fibers are much larger in number. This large number of corticofugal fibers is apparently necessary for adjustment and improvement of auditory signal processing in the frequency, amplitude, time and spatial domains. Focal electric stimulation of the auditory cortex (AC), used for the exploration of corticofugal function, evokes excitation (facilitation) and inhibition that spread into the subcortical auditory nuclei as well as into the AC surrounding the stimulation site. In terms of reorganization, the excitation and inhibition carry the message "join me" or "stay away," respectively. "Join me" evokes centripetal shifts of neural tuning curves (or receptive fields) for "expanded" reorganization, whereas "stay away" evokes centrifugal shifts in the tuning curves for "compressed" reorganization. Which of these contradictory messages is stronger than the other makes a big difference in reorganization. One type of reorganization can be changed into the other type by an application of an antagonist or agonist of GABA-A receptors to the AC. In the visual, auditory, and somatosensory cortices, corticofugal neurons facilitate subcortical neurons matched to the stimulated cortical neurons in tuning or receptive field and inhibit unmatched subcortical neurons. Such a positive feedback associated with lateral inhibition carries the message "send me better signals" to subcortical neurons. This message evokes the reorganization of cortical input for "egocentric selection."

Corticofugal modulation occurs even for the cochlear hair cells in a systematic way as the AC is electrically stimulated at a high rate. Corticofugal modulation (plastic changes) is augmented by the cholinergic basal forebrain when auditory fear conditioning is given to an animal, i.e., when a sound becomes behaviorally relevant to the animal. Therefore, the corticofugal system has a role in learning and memory (NIDCD DC 00175).

#### **14 Parallel Corticofugal Auditory Pathways: Multiple Streams for Auditory, Limbic, and Premotor Control.**

**Jeffery Winer<sup>1</sup>**

<sup>1</sup>*University of California at Berkeley*

One view of the auditory system postulates a hierarchy from cochlea to cortex with increases in integrative capacity and decreases in sensory map precision. Corticofugal projections might convey feedback for executive control of ascending streams of sensory information, but the nature of this control, and the neuroanatomical substrates for it, have not received the attention they merit. Some principles governing the corticofugal system are the subject of this report.

Auditory corticofugal connections (CC) descend as parallel systems to the medial geniculate body (MGB), inferior colliculus (IC), periolivary regions, cochlear nucleus, and the amygdala, striatum, and pontine nuclei. All 12 areas of cat auditory cortex (and corresponding regions in rodents) have corticofugal projections. The CC origins involve different cortical layers, independent neuronal populations, and unique target-specific axonal morphology. Each such difference is circumstantial evidence that the information carried by the several CC pathways is specific to the origins and targets within the particular subsystem.

Several principles emerge from the experimental data. First, in size, the CC projections often equal or exceed those of ascending pathways. Second, the CC laminar origin is projection—and target-specific, and few corticofugal neurons project to multiple targets. Third, CC axons are unique in certain targets: thus, the IC receives only thin axons while the MGB receives both slender and thick fibers. Fourth, many CC projections—even from non-tonotopic areas—have a topographic organization. Fifth, most areas project to the MGB, IC, striatum and pons; this implies that an area participates in different levels of integration by virtue of its central targets, including sensory and premotor roles.

This implies a role other than feedback for the corticofugal system, which appears integral to thalamic and midbrain reorganization and plasticity.

Supported by: USPHS grant RO1 DC02319-25.

#### **15 Projection Patterns and Targets of the Corticofugal Pathway to the Brainstem**

**Brett R. Schofield<sup>1</sup>**

<sup>1</sup>*U. of Louisville*

Early studies of descending pathways described a chain of projections from cortex to cochlea. Such chains were not demonstrated directly, but relied on assumptions about the

targets of cortical axons. It was assumed that cortical axons contact cells in the inferior colliculus (IC) whose axons descend to contact olivocochlear cells. Recent studies support some of the assumed contacts, but have also shown that direct cortical projections are more extensive than previously believed. The resulting view is one of a network of parallel descending pathways.

An issue that has been largely ignored is whether cortical axons contact ascending pathways. We demonstrated, first, that ascending projections from the IC and the superior olivary complex (SOC) arise from different cells than the descending projections. We then showed that corticofugal axons contact cells in each of these areas and in the cochlear nucleus that project to higher auditory centers.

Our results demonstrate that cortical axons contact cells of both ascending and descending auditory pathways at multiple levels of the brainstem, including the IC, SOC and cochlear nucleus.

In order to gain further insight into the functions of cortical projections, we examined projection patterns of individual cortical cells. Our results suggest two major patterns of projection. In the first, individual cells project to a single target. This pattern applies to the majority of projections to the brainstem, and is exemplified by cortical projections to the ipsilateral IC. In the second pattern, individual cells send axon collaterals to two or more targets. Many cells that project to the contralateral IC also project to the ipsilateral IC, and some of these cells also project to the CN. Fewer cells have such divergent projections (as opposed to a projection to a single target), but these projections could serve a unique function.

We conclude that corticofugal projections are in a position to modify activity at many points in the brainstem. Corticofugal targets include ascending and descending pathways as well as local circuits. Understanding the corticofugal system will require identifying how, and under what conditions, the cortex affects each of these brainstem targets.

Supported by NIH DC04391.

#### **16 Organization of Projections from Auditory Cortex to Cochlear Nucleus**

**David Ryugo<sup>1</sup>, Diana Molavi<sup>1</sup>, John Doucet<sup>1</sup>, Noah Meltzer<sup>1</sup>**

<sup>1</sup>*Johns Hopkins University*

It is well established that a descending auditory system parallels the more prominent ascending system. The ascending pathways convey information about the physical nature of the sound such as spectral composition, amplitude, shape of stimulus envelope, timing characteristics (phase, onset, duration), and binaural properties (time and intensity differences). In contrast, we propose that the descending system modulates the ascending system to facilitate recognition of stimulus motion, identity, and significance. These kinds of predictive attributes require involvement of other sensory and motor modalities as well as circuits for learning, memory, and emotion.

A first step in understanding the role of corticofugal systems is to determine which sets of neurons are functionally interconnected. We have been studying auditory cortex in rodents and examining the organization of its descending projections. Primary auditory cortex was identified by cyto- and myeloarchitecture, cytochrome oxidase staining, distribution of labeled layer Vc pyramidal cells following injections of the cochlear nucleus with a retrograde dye, and electrophysiologic recording and mapping criteria. Injections of neuronal tracers into primary auditory cortex of rats or mice retrogradely labeled thalamic neurons of the ventral division of the medial geniculate nucleus and anterogradely labeled terminal fields in the brain stem including the inferior colliculus, superior olivary complex, and cochlear nucleus. The terminal field in the cochlear nucleus was primarily ipsilateral and confined to the granule cell domain. Bouton endings from auditory cortex synapsed on the terminal dendrites of granule cells. The distribution of these bouton synapses implies that the auditory cortex exerts direct modulatory influence over the earliest stages of acoustic signal processing in the central nervous system.

Supported by NIH grants DC00232, DC04395, and DC00027.

### **17** Function of the Descending Auditory Pathways – Effects of Lesions and Electrical Stimulation

Josef Syka<sup>1</sup>

<sup>1</sup>*Institute of Experimental Medicine, Academy of Sciences of the Czech Republic*

Cortical neurons are able to exert control over the information processing in the inferior colliculus (IC), predominantly ipsilaterally. With the aim of understanding the function of the feedback pathway from the auditory cortex (AC) to the IC, we electrically stimulated the AC in the rat and recorded the responses of neurons in the IC. In addition, the IC's responses to sound were recorded before and after unilateral functional ablation of the AC by tetrodotoxin. AC stimulation produced a short latency excitation in the IC combined with a prolonged inhibition. Functional ablation of the AC resulted in a prolongation of the latency of some waves of the auditory evoked response in the IC, in changes in the responsiveness of IC neurons to acoustical stimuli and in changes in the synchronization of the firing of neuronal pairs recorded in the IC. The late part of the response of IC neurons to a tone burst was more influenced than the onset part. However, the discharge pattern of multiple unit responses, response thresholds and tuning were not altered during AC inactivation. Complete suppression of the corticofugal control of IC neuronal activity apparently produces in the IC a disorganization in the processing of acoustical signals. A further subject of our study was the feedback loop represented by pathways descending from the IC to the superior olive and the cochlear nucleus. Electrical stimulation of the IC in the rat resulted in a small depression of distortion product otoacoustic emissions (DPOAE); the maximal effect was observed when the stimulating electrodes were located in the rostro-medial or

ventral parts of the IC. The results indicate that electrical stimulation of the IC can activate the efferent system and produce changes in DPOAE by similar mechanisms as does acoustical stimulation of the contralateral ear. In general, the results suggest that a complex feedback system exists in the auditory system, involved in the control of auditory processing starting from the inner ear.

### **18** Corticofugal Modulation of Inferior Collicular Neurons in the Frequency and Amplitude Domains

Jun Yan<sup>1</sup>, Guenter Ehret<sup>2</sup>

<sup>1</sup>*University of Calgary*, <sup>2</sup>*University of Ulm*

A large number of neurons in the deep layers of the auditory cortex project to the subcortical auditory nuclei. Studies on bats unveiled that these corticofugal descending fibers implement a positive feedback to the subcortical nuclei as well as widespread lateral inhibition and improve auditory information processing in the frequency and time domains. To extend the research on the function of corticofugal systems, we have studied corticofugal modulation of collicular neurons of the house mouse in both frequency and amplitude domains. We have found that focal electrical stimulation of the primary auditory cortex facilitates the auditory responses of collicular neurons tuned to the same frequency as the best frequency (BF) of the stimulated cortical neurons, whereas it inhibits neurons tuned to different frequencies and shifts their frequency tuning towards the BF of the stimulated cortical neurons. In addition, we have found that focal electrical stimulation of the primary auditory cortex systematically changes the response properties of collicular neurons in the amplitude domain. That is, the minimum thresholds (MT) and dynamic ranges (DR) of collicular neurons are increased or decreased depending on the BF difference between stimulated cortical and recorded collicular neurons. When the cortical and collicular BFs are different from each other, cortical stimulation increases collicular MTs and decreases collicular DRs; the larger the difference in BF, the larger are the changes in collicular MTs and DRs. When the cortical and collicular BFs are similar to each other, cortical stimulation either increases or decreases the collicular MTs; it shifts collicular MTs toward the cortical MTs. Such shift in collicular MTs is linearly related to the MT difference between the cortical and collicular neurons. Our studies suggest that corticofugal control of lower auditory centers concerns the whole configuration of responsiveness to sounds not only to single parameters.

### **19** Corticofugal Modulation of Multi-Parametric Domain Processing in the Midbrain of the Big Brown Bat, *Eptesicus Fuscus*

Philip Jen<sup>1</sup>, Xiaoming Zhou<sup>1</sup>

<sup>1</sup>*University of Missouri*

Recent studies have shown that the massive auditory corticofugal system, which is topographically as well-organized as the ascending auditory system, improves on-

going subcortical auditory processing, and plays a role in experience-induced auditory plasticity. Studies in our laboratory show that corticofugal modulation of signal processing in the inferior colliculus (IC) of the big brown bat, *Eptesicus fuscus*, is specific and systematic in multi-parametric domains. Corticofugal modulation of collicular auditory sensitivity is observed when BF differences between IC and auditory cortical (AC) neurons are within 20 kHz. The smaller the BF differences are, the greater the degree of corticofugal modulation is. Corticofugal modulation also shifts collicular sensitivity in multi-parametric domains toward that of AC neurons when BF differences are within 7 kHz. The degree of multi-parametric shift is primarily dependent upon the relative sensitivity difference between IC and AC neurons but not upon the absolute sensitivity of IC and AC neurons. In directional domain, cortical electrical stimulation sharpens the directional sensitivity curves of IC neurons and shifts the best azimuthal angle (BAZ) toward that of AC neurons. In frequency domain, cortical electrical stimulation sharpens the frequency tuning curves of IC neurons and shifts collicular BF toward that of AC neurons. In amplitude domain, corticofugal modulation sharpens the rate-amplitude function and shifts the best amplitude (BA) toward that of AC neurons. The BF shift increases with BF differences; the BA shift increases with BA differences and the BAZ shift increased with BAZ differences. These multi-parametric shifts are minimal when IC and AC neurons have similar (matched) multi-parametric sensitivity. The adjustment of multi-parametric sensitivity of IC neurons toward that of AC neurons results in reorganization of collicular

sensitivity toward cortical sensitivity.

## **[20] The Jerker Mutation Slows Synaptic Responses and Increases Synaptic Depression at Synapses in the PVCN of Mice**

Xiaojie Cao<sup>1</sup>, Donata Oertel<sup>1</sup>

<sup>1</sup>Department of Physiology, UW-Madison

The jerker mutant mouse provides a model of deafness. These mice harbor a recessive mutation in *espin*, an actin bundling protein, that causes homozygote mice to be deaf (Steel and Bock, *Behav. Neurosci* 97:381, 1983; Zheng et al., *Cell* 102:377, 2000). We investigated the properties of synaptic transmission in the posteroventral cochlear nucleus (PVCN) of deaf jerker mice (*je/je*) with those in heterozygotes (*je/+*) and normal mice of the ICR strain (*+/+*). Stimulation of inputs, presumably auditory nerve fibers, evoked excitatory postsynaptic current (EPSCs) that were measured with whole-cell patch recordings from octopus cells and T stellate cells in slices from animals between 17 and 19 days old. Evoked EPSCs were broader and slower in mutant than in wild type mice. In T-stellate cells, decay time constants of EPSC were 0.47±0.03 msec in *je/je*, 0.31±0.04 msec in *je/+*, and 0.23±0.02 msec in *+/+* mice; in octopus cells they were 0.47 ±0.16 msec in *je/je*, and 0.34±0.09 msec in *+/+* mice. In T-stellate cells the widths of EPSCs at half amplitude were 0.61 ± 0.1 msec in *je/je*, 0.45 ± 0.04 msec in *je/+*, and 0.40 ± 0.05 msec in *+/+* mice. In octopus cells those

widths were 0.79 ± 0.16 msec in *je/je* and 0.74 ± 0.07 msec in *+/+* mice. Trains of shocks at 100 Hz evoked EPSCs that were more strongly depressed in deaf jerker mice than in normal animals. The second of a pair of pulses with a 10 msec interval evoked a synaptic current that was smaller than the first. The ratios of the second to the first evoked synaptic current in T-stellate cells were: 0.72±0.12 (n=5 *je/je*), 1±0.04 (n=5 *+/+*). In octopus cells ratios were 0.69±0.04 (n=6 *je/je*) and 0.94±0.07 (n=5 *+/+*). To test whether depression is affected differentially by desensitization of AMPA receptors, we tested how cyclothiazide affects responses to trains of shocks. We found that although cyclothiazide (100 iM) affects the amplitude and decay rate of individual evoked EPSCs, it does not alter the time course of depression.

This work was supported by NIH by the grant DC00176.

## **[21] Auditory Brainstem Response Waveform Analysis in the Math5 Mutant Mice Shows Interpeak Differences Suggestive of Defects in the Auditory Brainstem**

DF Dolan<sup>1</sup>, K Schacht<sup>1</sup>, L Grant<sup>1</sup>, L Kabara<sup>1</sup>, K Halsey<sup>1</sup>, G Dootz<sup>1</sup>, W Quirk<sup>2</sup>, S Schulz<sup>3</sup>, T Glaser<sup>3</sup>

<sup>1</sup>KHRI, University of Michigan, <sup>2</sup>Central Washington University, <sup>3</sup>Dept. Human Genetics, University of Michigan

Auditory Brainstem Responses (ABRs) were obtained in Math5 mutant mice on BALB/cJ background. Math5 is a basic helix-loop-helix (bHLH) transcription factor expressed during eye development that is essential for retinal ganglion cell formation. Math5 is also expressed in the auditory brainstem (VNLL/DNLL, MNTB, LSO and CN) (see Schulz et al. companion poster). Cells in the CN of Math5 (-/-) mice appear smaller when compared to corresponding cells in Math5 (+/-) mice. Since the ABR is the result of synchronous neural activity beginning with the auditory nerve and successively higher auditory nuclei, we compared the ABR waveforms from Math5 (+/+), Math5 (+/-) and Math5 (-/-). ABR thresholds at 4, 12 and 20kHz and DPOAEs were not significantly different for the three groups. We compared the latency of waves I through V and the interpeak intervals of waves I through V to tonal stimuli from 80-30dB SPL. The latency of waves I, II, IV and V were similar in each group across the stimulus intensity range. There were statistically significant differences (ANOVA) in Math5 (-/-) wave III latency compared to Math5 (+/+) and Math5 (+/-) groups. Interpeak latency differences were decreased for wave III-I and II-I and increased for waves IV-III and V-III in the Math5 (-/-) mice compared to the other groups. The waveform effects may result from anatomical changes in Math5 (-/-) mutants or an ongoing requirement for Math5 in central auditory function. These results suggest that the ABR may be used to indicate potential disruption of central auditory processing as well as auditory sensitivity.

Supported by NIH Grant P30 DC05188 (DFD), RO1 EY14259 (TG), 5 T32 GM 07544 (SMS), and 5 T32 DC00011 (SMS)

## **22 Math5 Gene Expression and Function in the Central Auditory System**

Sara M Schulz<sup>1</sup>, Richard Altschuler<sup>1</sup>, Susan Shore<sup>1</sup>, Joseph Brzezinski<sup>1</sup>, Keturah Schacht<sup>1</sup>, David F Dolan<sup>1</sup>, Thomas Glaser<sup>1</sup>

<sup>1</sup>University of Michigan

The basic helix-loop-helix (bHLH) transcription factor Atonal is required in *Drosophila melanogaster* for development of the eye and chordotonal organs. In mammals, these broad functions are partitioned between semi-orthologs *Math5* and *Math1*. *Math5* is transiently expressed in the eye, where it is needed for retinal ganglion cell (RGC) and optic nerve development. Conversely, *Math1* is required to form the cerebellum and mechanosensory structures, including sensory hair cells in the organ of Corti.

Using *Math5-lacZ* knockout mice, we have identified a novel expression domain for *Math5* in the adult brainstem that is remarkably co-extensive with central auditory pathways. In these mice, the *lacZ* histochemical marker is expressed in several major structures of the auditory brainstem, including the cochlear nucleus (CN), medial nucleus of the trapezoid body (MNTB), lateral superior olive (LSO), and lateral lemniscus (LL). Staining is particularly intense in the CN bilaterally, where *Math5* is expressed in roughly half of cells. *Math5-lacZ* was also detected in a small subset of fibers within the auditory nerve.

We have evaluated *Math5* <sup>-/-</sup> mutants for changes in brainstem anatomy, histopathology and auditory function. The size of *lacZ*-positive neurons in the CN is reduced in *Math5* <sup>-/-</sup> mice compared to *Math5* <sup>+/-</sup> littermates. Changes were also identified in the Auditory Brainstem Response (ABR) of *Math5* mutants, compared to wild-type and heterozygous mice in a BALB/cJ congenic background, consisting of alterations in the interpeak latencies (see companion poster by Dolan *et al*). Our results suggest a role for *Math5* in processing of binaural information by the auditory brainstem. While numerous mouse genetic models for sensorineural deafness exist, few are known that specifically affect central auditory processing. We are currently investigating the role of *Math5* during embryonic development of the auditory hindbrain.

Supported by NIH grants T32 DC00011 and T32 GM07544 (SMS), R01 EY14259 (TG), and P30 DC05188 (DFD).

## **23 Reliability of High-Throughput Gene Expression Analyses in the Central Auditory System**

David Friedland<sup>1</sup>, Rebecca Eernisse<sup>1</sup>, Paul Popper<sup>1</sup>, Joseph Cioffi<sup>1</sup>

<sup>1</sup>Medical College of Wisconsin

Changes in central auditory mechanisms in response to hearing loss may play a role in the development of tinnitus as well as the ability of an individual to respond to auditory stimuli after cochlear implantation. Indeed, the relationship between duration of deafness and efficacy of cochlear

implants appears to be more dependent on central processes rather than ear specific phenomena. Furthermore, abnormal cellular activity in the auditory brainstem is associated with the generation and percept of tinnitus. As such, many investigations have probed individual candidate genes and their role in the central auditory system. Fewer studies have assessed global gene expression by utilizing methods with the capacity to screen thousands of genes and transcripts. Such methods include gene chips and serial analysis of gene expression (SAGE).

In order to assess the reliability of these methods in central auditory investigations we used SAGE and Gene Chips to probe the transcriptomes of the subdivisions of the rat cochlear nucleus. SAGE has been previously described by our laboratory and we generated libraries of approximately 34,000 tags for each subdivision. The Gene Chip experiments were performed commercially and screened approximately 35,000 transcripts. Data from each experiment was assessed for internal reliability as well as for correlation between platforms.

The gene chip experiments were run in duplicate and there was excellent agreement in levels of expression between each chip. SAGE tags were assessed for reliability by RT-PCR and each transcript investigated was present in the original tissue. Correlation between the Gene Chips and SAGE was performed for high, moderate and low expression levels and showed good, but decreasing, correlation from the more common to the more rare transcripts.

This study has demonstrated the feasibility and reliability of high-throughput analyses of gene expression in the central auditory system. Both of the most frequently used methods provide valid information with good correlation between them. Combining data from these experiments has allowed a more precise assessment of cochlear nucleus gene expression and identified candidate genes subserving the unique physiologic properties seen in these regions and potentially altered in hearing loss and tinnitus.

Supported by the Triological Career Development Award and NIDCD K08 DC006227-01.

## **24 Microarray Analysis of Ion Transport-Related Genes in Semicircular Canal Duct Epithelium**

Nithyanandhini Raveendran<sup>1</sup>, Satyanarayana R. Pondugula<sup>1</sup>, Youping Deng<sup>1</sup>, Jun Chen<sup>1</sup>, Daniel C. Marcus<sup>1</sup>

<sup>1</sup>Kansas State University

Glucocorticoids are used in the treatment of Meniere's Disease, which is thought to be the manifestation of a disturbance of inner ear ion transport. We have shown that the semicircular canal duct (SCCD) epithelium is the site of cAMP-regulated Cl secretion and glucocorticoid-regulated Na absorption, and sought to determine whether glucocorticoids regulated the transcript expression of ion transport-related genes in SCCD cells. Primary cultures of SCCD cells from neonatal rats were grown on permeable supports. RNA was extracted from dexamethasone (DEX, 100 nM; 24 hr)-treated and untreated cultures. The quality

and quantity of RNA was assessed with an Agilent 2100 BioAnalyzer and processed for gene expression analysis with Affymetrix rat230A GeneChip microarrays. Signal expression of transcripts was analyzed using GeneChip Operating Software GCOS 1.1 and transcripts were considered to be present if at least two present calls and one marginal call in either the four untreated or the four treated sample groups were detected. For each transcript, expression comparison analysis was made between each untreated & DEX-treated sample to generate a signal log ratio (SLR) value; the t-test was performed on SLR to identify regulated gene expression. Fold change of the transcript level was derived from the median SLR. Genes were found to be present and regulated in groups thought to participate in: 1) transepithelial Na absorption [Pondugula et al. (2004) *Am J Physiol*], 2) transepithelial calcium absorption [Yamauchi et al. (2005) *ARO*], 3) water transport and 4) regulation of several signal pathways, including PI3-kinase (Na absorption) and cAMP/PKA (Cl secretion). We conclude that the presence and regulation of ion transport-related genes in SCCD cells can account for the observed transport phenomena and for the clinical observation that glucocorticoid administration leads to reduced episodes of vertigo in Meniere's patients. Supported by NIH-NIDCD grants R01-DC00212, NCRR P20 RR17686 & P20 RR16475.

## **[25] Global View of Expression Patterns of Mouse Utricle Development**

**MingQian Huang**<sup>1</sup>, Cyrille Sage<sup>1</sup>, S Zhong<sup>2</sup>, Yu GUO<sup>2</sup>, W Wong<sup>2</sup>, David Corey<sup>3</sup>, Cheng Li<sup>2</sup>, Zheng-Yi Chen<sup>1</sup>

<sup>1</sup>Massachusetts General Hospital and Harvard Medical School, <sup>2</sup>Department of Biostatistics, Harvard School of Public Health, <sup>3</sup>Howard Hughes Medical Institute and Harvard Medical School

To comprehensively understand the genes and pathways involved in the development and function of the inner ear, oligonucleotide microarray (GeneChip) technology was employed to profile global gene expression of the developing mouse utricle, from E10.5 through P12, at daily intervals. The study surveyed over 45,200 mouse genes and ESTs, and 26,000 genes/ESTs were detected in at least one of the utricle samples. 10.5% (4755) of the expressed transcripts were identified to be developmentally regulated.

Comparisons of expression patterns identified 1587 genes whose expression levels changed between two adjacent stages throughout development (a total of 21 comparisons). Surprisingly 1116 of these genes (70%) showed expression level changes at only five stages, indicating that they are the major transitional events in utricle development. Comparison between E12.5 and E13.5 revealed the largest number of genes within which the expression levels changed between two adjacent stages, coinciding with the beginning of terminal differentiation of the sensory epithelium. In situ hybridization studies of many genes showed that the patterns are indicative of their roles in progenitor cell production, hair cell and supporting cell specification, and demarcation for the inner ear sensory epithelium.

Clustering analysis identified co-regulated genes. We identified transcription factors and growth control genes which showed co-expression with the retinoblastoma gene (Rb), a gene that is critical in the cell cycle exit of sensory epithelium. Members of the Notch signaling pathway showed co-expression with Math1, raising the possibility of interactions between the two pathways.

Our studies identified many novel genes that are temporally regulated and potentially play significant roles during utricle development. This analysis provided a basis for similar studies of other inner ear organs such as the cochlea, and also aid in identifying deafness genes.

## **[26] Gene Expression Analysis of Specific Cell Types Isolated from Mouse Inner Ear Following Laser Capture Microdissection**

**Kumar Alagramam**<sup>1</sup>, Wen Wang<sup>1</sup>, Rick Davis<sup>2</sup>, Charles Wright<sup>3</sup>

<sup>1</sup>Otolaryngology-HNS, Case Western Reserve University, OH, <sup>2</sup>Division of Applied Research and Technology, NIOSH, Cincinnati, OH, <sup>3</sup>Otolaryngology-HNS, University of Texas Southwestern Medical Center, Dallas, TX

Laser Capture Microdissection (LCM) allows procurement of specific cell types from microscopic regions of tissue sections, which can then be used for gene expression analysis. Cryosections, rather than formalin-fixed paraffin embedded (FFPE) sections, are preferred because the recovery of quality RNA from FFPE sections can be quite challenging. However, the morphology of the various cell types within the inner ear is well preserved in FFPE sections (compared to cryosections) making it easier to identify the cell types and their boundaries. We explored the possibility of using FFPE for gene expression following LCM. Relatively pure populations of cells from the organ of Corti, spiral ganglion, and the maculae were isolated from eight-micron FFPE sections by LCM (Pixcell II, Arcturus, CA). RNA was extracted from captured cells, amplified and assessed for quality by gel electrophoresis. Expression of a select number of genes were tested by reverse transcription PCR and real-time PCR. We were able to detect the expression of several genes reproducibly. This included housekeeping gene Hprt, deafness genes (ex. Protocadherin 15) and other uncharacterized genes. While the house keeping genes were detected in all cell types, some of the other genes showed a restricted expression pattern. The method described here has potential use in many areas of hearing research. The sensitivity and accuracy of molecular profiling can be increased substantially by focusing the analysis on specific cell types within target tissues. For example, following noise exposure in mice, it would be highly desirable to perform gene expression analysis using RNA isolated from hair cells or spiral ganglion cells, instead of whole inner ear tissue or mixed populations of cells from surface preparations. Further, the method we describe here for mouse FFPE sections could be used for retrospective analysis of human archival ear tissue for investigation in search of disease mechanisms.

## **27 Investigation of MicroRNA Expression in Mouse Ear Development**

**Garrett Soukup<sup>1</sup>, Michael Weston<sup>1</sup>, Ken Morris<sup>1</sup>, Kirk Beisel<sup>1</sup>**

<sup>1</sup>*Creighton University*

RNA interference (RNAi) utilizes double-stranded RNA (dsRNA) to effect homology-dependent gene silencing in eukaryotic cells. The RNAi pathway is comprised of the action of Dicer and Argonaute proteins. Dicer is a ribonuclease III family member that specifically processes dsRNA to produce ~21 nucleotide species. Argonaute proteins subsequently utilize Dicer products as guide sequences to mediate post-transcriptional gene silencing of complementary mRNAs through either translational inhibition or mRNA cleavage. Disruption of Dicer-1 or Argonaute-2 function in transgenic mice leads to severe developmental defects and embryonic lethality, demonstrating that the RNAi pathway is requisite for organismal development. MicroRNAs (miRNAs) are Dicer products derived from highly conserved endogenous genes that function through the RNAi pathway to regulate target gene expression and guide developmental processes in eukaryotes. To date, 214 miRNA genes have been identified in mouse, where certain miRNA genes are differentially expressed among various tissue types. We therefore hypothesize that miRNAs play a critical role in development of the ear by prompting changes in gene expression that underlie cellular differentiation and maintenance. To begin to understand the role of miRNAs in ear development, we are presently working to identify known or novel miRNAs expressed in mouse ear at various developmental stages. Moreover, we have already identified one known miRNA precursor transcript represented in an inner ear expression library from adult mouse (~P35). Interestingly, the miRNA precursor resides within the untranslated region of a putative mRNA encoding a short polypeptide that is conserved among mouse, rat, and human. The identification of expressed miRNAs and potential target genes in mouse ear is expected to contribute to our understanding of the genetic mechanisms that underlie ear development and function.

## **28 Heterologous and Homologous Expression Systems for Functional Analysis of *Xenopus* Inner Ear Genes**

**David R. Sultemeier<sup>1</sup>, V. Bleu Knight<sup>1</sup>, Shannon J. Manuelito<sup>1</sup>, Michelle Hopkins<sup>1</sup>, Elba E. Serrano<sup>1</sup>**

<sup>1</sup>*New Mexico State University*

The size and inaccessibility of the inner ear pose challenges for investigations of gene regulation by conventional cell and molecular approaches. To address this problem, we are developing *Xenopus* homologous (inner ear) and heterologous (neural, muscle, kidney) in vitro systems for gene expression and promoter analysis. Here we present results of efforts to establish transfection protocols for three culture systems: primary cultures of larval *Xenopus* inner ear, primary dissociated neuron and muscle cultures prepared from embryonic *Xenopus* larvae, and the *Xenopus* kidney A6 line (ATCC CRL-8192). Culture viability was determined using vital dyes for

membrane integrity (trypan blue, propidium iodide) and metabolic activity (calcein-AM). Alexa-488 phalloidin was used to label F-actin in the mechanosensory bundles that typify hair cells of the vestibular and auditory organs. Immunofluorescent detection of acetylated-tubulin and myosin heavy chain verified the identity of neurons and muscle in culture. With our protocols, the *Xenopus* inner ear can be cultured for a week with some morphological changes and minimal cell death, while the *Xenopus* mixed nerve and muscle cultures can be sustained for over two weeks. A6 cells were used to optimize protocols for transient lipid-mediated (Lipofectamine) transfection with Clontech plasmids (pEGFP-actin, pEGFP-tubulin, pDsRed-Mito). Procedures were then applied to inner ear organ cultures, where transfection of bundles with GFP-actin could be detected. Presently, we are constructing plasmids that can be used to transfect the *Xenopus* cultures with fluorescent-tagged inner ear proteins. In future, we will use the culture systems to analyze promoter function, characterize genes screened from inner ear cDNA libraries (Serrano et al., Cell Mol Biol, 2001), and to identify tissue-specific features of inner ear gene expression. Funded by NIDCD DC03292 and NIGMS-SCORE GM08136 to EES and an NIGMS-RISE award to SM.

## **29 Mouse Vestibular Ganglion Cells Express Mitochondrial Uncoupling Protein 1 (Thermogenin)**

**Carey Balaban<sup>1</sup>, Ha-sheng Li-Korotky<sup>1</sup>, Tadashi Kitahara<sup>2</sup>**

<sup>1</sup>*University of Pittsburgh*, <sup>2</sup>*Osaka University*

Uncoupling proteins (UCPs) are a proton transporter family located in the mitochondrial inner membrane. Mitochondrial UCP activation is one factor that can influence the magnitude of the proton leak across the mitochondrial inner membrane. When activated, UCPs uncouple cellular respiration from ATP production, resulting in an increase in the basal proton leak and increased local heat dissipation. The classical UCP, UCP1 or thermogenin, is expressed predominantly in brown adipose tissue and is known to be thermogenic. This study provides the first documentation of UCP1 expression by vestibular ganglion cells. Four-week-old C57/BL6, CBA/J and BALB/c mice were divided into four groups (n=10 in each) as follows: a saline and NaHCO<sub>3</sub> vehicle injected control (CONT) group, a KM and NaHCO<sub>3</sub> vehicle injected (KM) group, a KM and DHB-injected (KM/DHB) group and a saline and DHB-injected (DHB) group. The KM and KM/DHB groups received daily injections of dose of 700 mg of KM base/kg body weight. The DHB and KM/DHB groups received 300 mg/kg body weight DHB. Mice received daily injections for two weeks. Tissues from three mice of each group were used for quantitative PCR, Western immunoblot analysis and immunohistochemistry (primary antibody: Santa Cruz Biotechnology goat polyclonal anti-UCP1). Quantitative PCR demonstrated 3.61 ± 0.74 fold UCP1 mRNA expression in the vestibular ganglion relative to the spiral ganglion across strains and protein expression was low but identifiable in Western immunoblots. Immunohistochemically-stained decalcified frozen sections

of the head showed granular UCP1-like immunoreactivity in vestibular ganglion cells. The DHB group showed a significant ( $p < 0.05$ ), 6-fold increase in UCP1 mRNA expression in both the vestibular ganglion and spiral ganglion. However, no commensurate changes were detected in either immunoblots or immunostaining. This lack of protein change mirrors findings in brown adipose tissue, which reflect a long (at least 5 day) time constant for translational changes to reflect changes in transcription. No changes in UCP1 mRNA expression were observed in other treatment groups. These findings suggest that UCP1 may play significant roles in both local thermogenic and fatty acid metabolic responses of vestibular ganglion cells during periods of low exposure to reactive oxygen species.

### **30 Identification of Low Abundance Otoconial Proteins**

Kang Tang<sup>1</sup>, Hua Yang<sup>1</sup>, Ronald Cerny<sup>2</sup>, Yunxia (Yesha) Lundberg

<sup>1</sup>Boys Town National Research Hospital, <sup>2</sup>University of Nebraska-Lincoln

Otoconia are dense biomineral crystals that overlay the sensory epithelium of the utricle and saccule in the vestibule and are required for gravity sensing and bodily balance. These crystals are composed of CaCO<sub>3</sub> and glycoproteins (otoconins). OC90, the predominant otoconin, has been identified, but the less abundant species remain elusive due to insufficient quantity. Here we report the purification and identification of the minor otoconins using a microbore HPLC separation system combined with the powerful Q-TOF mass spectrometry analysis.

### **31 Adenovirus-Mediated Gene Transfer in the Vestibular Epithelia of Mice and Guinea Pigs**

Chih-Hung Wang<sup>1</sup>, Masahiko Izumikawa<sup>1</sup>, Lisa Beyer<sup>1</sup>, Donald Swiderski<sup>1</sup>, Yehoash Raphael<sup>1</sup>

<sup>1</sup>Kresge Hearing Research Institute, Univ. of MI

Gene therapy has been shown to be applicable for protection and regeneration in the cochlea. This technology should also be useful for therapy in the vestibular epithelium. We set out to develop a method for efficient gene transfer in the vestibular epithelium of mice and guinea pigs. Using a canalostomy approach for adenovirus inoculation into the vestibular system, we observed reporter genes (*lacZ* and GFP) expressed in mature mouse and guinea pig vestibular sensory organs. In normal vestibular epithelia, transgene expression was restricted to the supporting cells of utricle, saccule and ampullae, whereas hair cells were negative. Following an ototoxic lesion by streptomycin treatment in the vestibular sensory epithelium, transgene expression was enhanced. To further characterize the conditions for transgene expression, different concentrations of streptomycin and different inoculation time courses following vestibulotoxicity were tested in guinea pigs. Transgene expression was more efficient when administered 2 weeks rather than 1 week after vestibulotoxicity. Higher concentrations of

streptomycin also enhanced gene expression, probably because of the increase in size and/or number of supporting cells. Transduction efficiency in the superior and lateral ampullae was higher than in other vestibular organs. The ability to express transgenes in mature mammalian vestibular supporting cells should allow for the development of gene-based therapies for vestibular disorders.

Supported by GenVec and by NIDCD grants R01-DC05401, R01-DC01634, R01 DC05053, P30-DC05188, NSC 93-2314-B-016-022, and TSGH-C94-23.

### **32 Sequencing of the Turtle Alpha-9 Nicotinic Acetylcholine Receptor Subunit Gene**

Peter Cameron<sup>1</sup>, Robert Gould<sup>1</sup>, Marcin Klapczynski<sup>1</sup>, Joseph C. Holt<sup>2</sup>, Jay M. Goldberg<sup>2</sup>, Anna Lysakowski<sup>1</sup>

<sup>1</sup>Univ. of Illinois at Chicago, <sup>2</sup>Univ. of Chicago

The red-eared slider turtle has been used as an in vitro model organism for inner ear research due to its robust ability to withstand anoxia. We and others have been using this turtle to investigate vestibular and auditory efferent innervation. One well established receptor for the inner ear efferent neurotransmitter, acetylcholine, contains the  $\alpha 9$  nicotinic acetylcholine receptor subunit ( $\alpha 9$ nAChR). To further investigate efferent function, we wanted to know the sequence of the homologous turtle gene in order to generate antibodies or probes for morphological localization. Thus we have sequenced the gene as a first step in this process.

RNA was extracted from turtle whole labyrinth and purified using a Qiagen RNeasy Mini kit. 97 ng of turtle RNA were converted to first strand cDNAs using an Invitrogen superscript kit. An initial PCR reaction was performed with degenerate primers based on nucleic acid sequences conserved among chick, fugu, and trout  $\alpha 9$ nAChR subunits. Multiple PCR products were generated and TA-cloned for subsequent analysis. One (~880bp) was amplified, sequenced and found to have significant (~80%) similarity to chick  $\alpha 9$ nAChR. 5' and 3' RACE reactions were performed on turtle cDNAs with primers specific to turtle  $\alpha 9$ nAChR. Two relevant 3' RACE products, one ~620bp and the other ~900bp (apparently the full 3' end), were generated and TA-cloned for subsequent analysis. To obtain the 5' end, several RACE reactions were performed with more turtle  $\alpha 9$ nAChR-specific reverse primers. Single products of the predicted size were obtained, TA-cloned, sequenced, and appeared to contain the full 5' end of the gene, which aligned well with chick  $\alpha 9$ nAChR (92% homology). Finally the full sequence was confirmed by amplification from turtle labyrinth cDNAs using a proofreading DNA polymerase combined with forward and reverse primers from the 5' and 3' untranslated regions (UTRs). The gene consists of 1860 bps, of which 69bps comprise the leading signal sequence, 1473bps the coding sequence, 151bps the 5' UTR and 176bps the 3' UTR. A splice variant (144bp deletion) was also detected. ProtParam and ProSite analyses of consensus sequences, such as transmembrane regions, glycosylation and



phosphorylation sites, and a Cys-loop ligand-gated ion channel signature characteristic of  $\alpha 9$  nAChRs. The sequence has been submitted to Genbank.

Supported by NIH R01-02058 (JMG) and NIH R01-02521 (AL).

### **33 Assessment of Differential Gene Expression in Vestibular Epithelial Cell Types using Microarray Analysis**

**Ricardo Cristobal**<sup>1</sup>, P. Ashley Wackym<sup>1</sup>, Joseph Cioffi<sup>1</sup>, Christy Erbe<sup>1</sup>, Joseph Roche<sup>1</sup>, Paul Popper<sup>1</sup>

<sup>1</sup>*Medical College of Wisconsin, Milwaukee, Wisconsin*

Current global gene expression techniques allow the evaluation and comparison of the expression of thousands of genes in a single experiment, providing a tremendous amount of information. However, the data generated by these techniques are context-dependent, and minor differences in the individual biological samples, methodologies for RNA acquisition, amplification, hybridization protocol and gene chip preparation, as well as hardware and analysis software, lead to poor correlation between the results. In the inner ear the acquisition of RNA from individual cell populations remains a challenge due to the high density of the different cell types and the paucity of tissue. Consequently laser capture microdissection was used to selectively collect individual cells and regions of cells from cristae ampullares followed by extraction of total RNA and amplification to amounts sufficient for high throughput analysis. To demonstrate hair cell specific gene expression, myosin VIIA, calmodulin, and alpha9 nicotinic acetylcholine receptor subunit mRNAs were amplified using RT-PCR. To demonstrate supporting cell specific gene expression, cyclin-dependent kinase inhibitor p27kip1 mRNA was amplified using RT-PCR. Subsequent experiments with alpha9 RT-PCR demonstrated phenotypic differences between type I and type II hair cells, with expression only in type II hair cells. Using the laser capture microdissection technique, microarray expression profiling demonstrated 408 genes with more than a five-fold difference in expression between the hair cells and supporting cells, of these 175 were well annotated. There were 97 annotated genes with greater than a five-fold expression difference in the hair cells relative to the supporting cells, and 78 annotated genes with greater than a five-fold expression difference in the supporting cells relative to the hair cells.

### **34 In Silico Analysis of the Rat Vestibular Periphery Transcriptome using a Normalized cDNA Library**

**Joseph Roche**<sup>1</sup>, P. Ashley Wackym<sup>1</sup>, Joseph Cioffi<sup>1</sup>, Christy Erbe<sup>1</sup>, Paul Popper<sup>1</sup>

<sup>1</sup>*Medical College of Wisconsin, Milwaukee, Wisconsin*

In order to begin understanding the transcriptome of the vestibular periphery, we characterized the inserts from 2400 cDNA clones isolated from a normalized *Rattus norvegicus* vestibular periphery cDNA library. The Wackym-Soares vestibular cDNA library was constructed from the saccular and utricular maculae, the ampullae of

all three semicircular canals, and Scarpa's ganglia containing the somata of the primary afferent neurons, microdissected from 104 male and female rats. The inserts from the 2400 randomly selected clones were sequenced from the 5' end. Each sequence was analyzed using the BLAST algorithm against the GenBank non-redundant, rat genome, mouse genome, and human genome databases to search for high homology alignments. Of the initial 2400 clones, 308 sequences (13%) were found to be of poor quality and were eliminated from the analysis. Of the remaining 2092 sequences, 919 (44%) were found to represent 756 unique genes having useful annotations that were identified in databases within the public domain or in the published literature; these sequences were designated as known characterized sequences. 1120 sequences (53%) aligned with 992 unique sequences had no useful annotations and were designated as known but uncharacterized sequences. The remaining 53 sequences (3%) did not align with significant homology to any previously identified sequences. The known, characterized sequences were analyzed with the FatiGO online data-mining tool to identify Level 5 biological process Gene Ontology (GO) terms for each alignment and to group alignments with similar or identical GO terms. Numerous genes were identified that have not been previously shown to be expressed in the vestibular system. Further characterization of the novel cDNA sequences identified may lead to the identification of genes with vestibular specific functions. Physiologic studies are necessary to further elucidate the roles of the identified genes and novel sequences in vestibular function.

### **35 Adenylate Cyclases in the Mammalian Vestibular Ganglia and Crista Ampullaris**

**Paul Popper**<sup>1</sup>, P. Ashley Wackym<sup>1</sup>, Wolfgang Siebeneich<sup>1</sup>, Christy Erbe<sup>1</sup>, Joseph Cioffi<sup>1</sup>

<sup>1</sup>*Medical College of Wisconsin, Milwaukee, Wisconsin*

Mechanical stimulation of vestibular hair cells results in vestibular afferent discharge, which is determined by interactions among neurotransmitters and neuromodulators identified within the vestibular epithelia. G protein and forskolin sensitive adenylate cyclase is a family of enzymes (AC1-AC9) that are key to integrating the signal transduction pathways activated in this process. Screening by PCR of a normalized cDNA library obtained from the Scarpa's ganglia and vestibular end organs of 104 Brown-Norway rats (*Rattus norvegicus*) showed that AC2, AC3, AC4, AC5, AC6, AC8 and AC9 transcripts are expressed in the vestibular periphery. RT-PCR of vestibular ganglia and end organ RNA extracts using primers for the above ACs yielded amplicons whose authenticity was confirmed by DNA sequencing. AC2 *in situ* hybridization signal was observed only in sections of Scarpa's ganglia and not in epithelia of cristae ampullares. Accordingly, in the crista ampullaris AC2-like immunoreactivity was observed only in nerve fibers throughout the epithelia but not in hair cells. Further investigation of the distribution of AC2 in the utricle and of the others ACs in the vestibular periphery is currently under way. Supported by NIDCD grants DC02971 and DC006571.

### **36** Characterization of Potentially Novel Transcripts Expressed in the Rat Vestibular Periphery

Joseph Cioffi<sup>1</sup>, Joseph Roche<sup>1</sup>, Christy Erbe<sup>1</sup>, Paul Popper<sup>1</sup>, P. Ashley Wackym<sup>1</sup>

<sup>1</sup>Medical College of Wisconsin

Changes in both the motion and position of the head are detected by specialized mechanoreceptors located in the vestibular apparatus. While some progress has been made in identifying the role of neurotransmitters, receptors, ion channels, signal transduction and other molecules in vestibular epithelia, significant gaps remain in our knowledge of the detailed molecular mechanisms and pathways subserving vestibular function. These mechanisms likely require the coordinated expression of large numbers of genes including those whose function may be poorly understood or are as yet unidentified. In an effort to better characterize the vestibular transcriptome, we have begun to systematically analyze cDNA clones obtained from a normalized cDNA library constructed from microdissected vestibular end organs and Scarpa's ganglia in the Brown Norway rat. Thus far, we have obtained DNA sequence information from 2,400 randomly selected clones. While the vast majority of sequences represent transcripts which have been previously characterized, 53 clones did not correspond with significant homology to any previously identified sequences in the public databases and therefore may represent novel genes. The 53 clones were prioritized using an algorithm that takes into consideration low degrees of homology to known genes with interesting functional annotations, the presence of a polyadenylation signal near the 3' terminus, and long open reading frames that may contain important functional domains or motifs. A subset of these clones was then chosen for gene expression analysis in major rat organs and tissues using RT/PCR. Several cDNAs were found to be differentially expressed in these tissues. The complete characterization of these novel transcripts and their encoded proteins may provide additional insights into vestibular function and the complex mechanisms controlling balance.

### **37** Cochlear Implant with Drug Delivery Function

Lisa Trejo<sup>1</sup>, Claude Jolly<sup>1</sup>, Guido Reetz<sup>1</sup>, Fabrice Beal<sup>1</sup>, Wolf-Dieter Baumgartner<sup>2</sup>, Joe Miller<sup>3</sup>

<sup>1</sup>MED-EL Corp, <sup>2</sup>University of Vienna Hospital, <sup>3</sup>Kresge Hearing Research Institute, University of Michigan Medical Center

#### Objective

Inner ear pharmacological treatment immediately after cochlear implantation through the electrode could preserve the neural substrate and increase the responsiveness to electrical stimulation. Neurotrophic factors, gene therapy, hair cell regeneration, or anti-oxidants could be combined with the electrical stimulation. Preservation of residual hearing could be enhanced. Strategies for inner ear treatment of sudden and progressive hearing loss, peripheral tinnitus could be derived from drug delivery with the cochlear implant.

#### Materials and methods

A hybrid device combining drug delivery with electrical stimulation is under development. The device consists of:

A MED-EL cochlear implant with a drug delivery channel incorporated within the electrode.

A permanently implanted micro-port with septum for the safe and reversible connection to a temporary implantable pump.

A fully implantable micro pump with a catheter terminated by a needle.

#### Results

The deep insertion electrode includes a channel of 200  $\mu\text{m}$  along the length of the electrode array. Two twin outlets 50  $\mu\text{m}$  in diameter permit fluid delivery to the basal turn of the scala tympani. The twin outlets are 180 degrees apart to ensure that fluid flow will face the perilymph. The electrode consists of a single line of 12 contacts and is based on the FLEX Technology.

The connection between the channel in the electrode and the removable pump is realized via a micro-port with septum that is permanently integrated at the cochlear implant housing. The pump may be connected to the port via a catheter and a 30 G non-coring needle. The needle-port connection ensures an immediate seal of the catheter within the electrode after pump removal, and provides optional re-connection. The fully implantable micro pump has a reservoir with the capacity to deliver a drug solution at a constant flow rate of 0.5  $\mu\text{l/hr}$  for 4 weeks. The reservoir is refillable through the scalp in order to permit long-term applications.

### **38** Substance Distribution in a Cochlea Model using Different Pump Rates

Gerrit Paasche<sup>1</sup>, Lars Bögel<sup>1</sup>, Martin Leinung<sup>1</sup>, Thomas Lenarz<sup>1</sup>, Timo Stöver<sup>1</sup>

<sup>1</sup>Medizinische Hochschule Hannover

Several recent reports on animal studies show the protective effects of neurotrophic factors (NF) on spiral ganglion cells (SGC). This is of particular importance since the number of SGCs is considered to be among the factors defining the effectiveness of cochlear implants. A device for local inner ear treatment is therefore of great interest. As described previously, we modified a Contour™ electrode, because this device already contains an inbuilt lumen (for carrying the stylet prior to insertion) and tested it for the purpose of drug delivery to the inner ear.

Three different electrode prototypes with openings at varying locations along the electrode array were used: a) release of the dye at the tip, b) release of the dye at the tip and the side of the electrode, c) release of the dye only at the side of the electrode (6mm from the tip). These prototypes were inserted into a plastic model of the scala tympani and the distribution of a coloured dye (methylene blue) was observed over time. A mechanical pump was used to drive the system at pump rates of 100  $\mu\text{l/h}$ , 10  $\mu\text{l/h}$ , and 1  $\mu\text{l/h}$ . The resulting series of pictures were transferred into gray-scale pictures and the dye concentration changes along the whole cochlea model were quantified using a small LabView program. Mean

values for all experimental conditions show that the distribution along the array is fastest having two outlets whereas only having an outlet at the side of the array can't be considered as sufficient. This setup is also suitable for evaluation of the amount of dye really being delivered from the different outlets and could easily be modified for a larger number of outlets.

Paasche.Gerrit@mh-hannover.de

### **39** The Effect of Corticosteroid on the Preservation of Hearing in Cochlear Implanted Guinea Pigs

**Qing Ye**<sup>1</sup>, Jan Kiefer<sup>2</sup>, Rainer Klinke<sup>3</sup>, Wolfgang Gstoettner<sup>1</sup>, **Jochen Tillein**<sup>3</sup>

<sup>1</sup>J.W.Goethe University, ENT Department, <sup>2</sup>Technical University Munich, ENT Department, <sup>3</sup>J.W.Goethe University, Department of Physiology II

Recently steroids have been applied locally during cochlear implant surgery, with the aim of reducing insertion trauma and improving the preservation of residual hearing. We previously showed that local application of a crystalline suspension of triamcinolone (40mg/ml), 'Volon A' improves recovery of hearing after cochleostomy. The present study tests the effect of locally applied Volon A on the hearing ability of guinea pigs after cochlear implantation.

Two groups of guinea pigs were implanted with a guinea pig electrode (MedEI) through a cochleostomy in the basal turn of the cochlea (insertion depth 3mm). In the first group (6 ears) 3µl of Volon A was carefully infused with a micro syringe before implantation while in the second group the same amount of saline was applied (control, 5 ears). A third group (7 ears) with a cochleostomy only served as an additional control. Hearing loss (HL) was tested before and after drug/saline application for 4 weeks postoperatively by measuring click evoked compound action potentials (CAPs) and frequency specific CAP audiograms via electrodes implanted near the round window.

Click evoked thresholds revealed a progressive HL in all groups, delayed by 1-2 weeks. From day 7, HL was most prominent for the saline group while HL of Volon treated animals was in the range of non implanted (cochleostomy only) animals or better. CAP audiograms showed similar trends with highest HL for the saline group and significant lower HL for the Volon group from day 14 onwards (t-test <0.05). Different frequency ranges were affected in the different groups. In the saline group HL was similar at all frequencies while in the Volon group highest HL was found above 10 kHz. In the non implanted group frequencies between 1-10 kHz were mostly affected..

The results indicate that Volon A may help to reduce the progressive hearing loss caused by electrode insertion trauma. The impact is likely to be based on long term effects such as reduction of inflammatory processes.

Supported by DFG & MedEI

### **40** Hypothermia Protects the Cochlea Against Electrode Insertion Trauma-Induced Hearing Loss

**Adrien Eshraghi**<sup>1,2</sup>, Thomas Balkany<sup>1</sup>, Jiao He<sup>1</sup>, Marek Polak<sup>1</sup>, Elliott Whitley<sup>1</sup>, Ophelia Alonso<sup>1</sup>, Dalton Dietrich<sup>1</sup>, Thomas Van De Water<sup>1</sup>

<sup>1</sup>University of Miami School of Medicine, <sup>2</sup>Miami VA Medical Center

Noise-induced threshold elevation of the cochlear microphonic is lessened if exposure occurs when the temperature of an exposed animal is below the normal body temperature. In contrast, multiple episodes of hyperthermia prior to noise exposure also reduces the magnitude of sensorineural damage and is associated with an increase level of heat shock protein within the cochlea. Mild hypothermia appears to have less associated risk than multiple exposures to hyperthermia.

Cochlear implantation involves the placement of a cochlear implant electrode array deep within the scala tympani. Because of an increasing trend to implant patients with residual hearing it is important to reduce damage during both preparatory surgery and placement of the electrode array within the cochlea. Recently we demonstrated in the laboratory rat that loss of hearing following electrode insertion occurs in two stages. There is an initial decrease in the auditory brainstem response (ABR) threshold of approximately 30 dB followed by a progressive loss of approximately 15 dB over the next 5 days.

The current study tests the hypothesis that mild hypothermia during surgery and cochlear implant electrode insertion has an otoprotective effect on hearing. Fisher 344 rats with normal ABR and DPOAE recordings were utilized. One ear was randomly selected for surgery and electrode insertion while the contralateral ear was the control. In group 1 (mild hypothermia), the rectal temperature was lowered to 34°C for 30 minutes prior to and through 30 minutes after electrode insertion. In group 2 (euthermia), the rectal temperature was maintained at 37° throughout the experiment. Testing was repeated immediately after surgery and over 7 days. Immediate post-insertion loss of auditory function of approximately 30dB occurred in both groups. However, in group 1 (37°C), there was an ongoing progressive loss in the range of 15 dB over the next 5 days while group 2 (34°C) had no progression over the initial hearing loss. Histopathology is presented using Eshraghi's classification of cochlear implantation trauma. The results support the hypothesis that hypothermia provides otoprotection against the progressive component of hearing loss caused by the trauma of preparatory surgery and electrode insertion.

#### **41 Assess Post-Treatment Efficacy of Glial Cell Line-Derived Neurotrophic Factor (GDNF) to Enhance Excitability and Survival of SGN**

Anette Fransson<sup>1</sup>, Göran Bredberg<sup>1</sup>, Josef Miller<sup>2</sup>, Mats Ulfendahl<sup>1</sup>

<sup>1</sup>Karolinska Institutet, <sup>2</sup>University of Michigan

The function of a cochlear prosthesis depends in part on survival and responsiveness of the spiral ganglion neurons (SGN). Neurotrophic factors enhance electrical sensitivity of the auditory nerve in deafened guinea pig (Fransson et al., ARO 2004); however recent evidence suggests the effect may be restricted to the period of treatment (Gillespie et al., Neuroreport 2004 May 19;15(7)).

The purpose of this study was to assess post-treatment efficacy of glial cell line-derived neurotrophic factor (GDNF) to enhance excitability and survival of SGN. 24 guinea pigs were deafened by transtympanic 15% neomycin. Three weeks after deafening the animals were implanted with a combined electrode and microcannal-pump (0.5µl/hour). The animals received a 4-week treatment of 1µg/ml GDNF or artificial perilymph (AP). The cannulae were disconnected from the osmotic pumps and sealed. Half the GDNF treated animals then received daily injections of antioxidants (Trolox 1mg/kg, ascorbic acid 20mg/kg, i.p.) while the other half received saline (i.p.). The group treated locally with AP was injected with saline (i.p.). All animals were injected with antioxidants or AP for 4 weeks and then sacrificed. Electrically-evoked ABRs (eABRs) were assessed weekly. Four-week GDNF treatment significantly lowered eABR thresholds compared to control animals. This difference was maintained throughout the 4-week period of no treatment. There was no significant difference between the GDNF groups subsequently treated with antioxidants and saline. This study clearly demonstrates that the positive electrophysiological effect of neurotrophic factor intervention is maintained for at least four weeks following treatment.

We gratefully acknowledge MEDEL GmbH (Austria) and Amgen (USA) for providing implant electrodes and GDNF, respectively, and the support of the European Commission (QLG3-CT-2002-01563) and NIH grant DC0382.

#### **42 CaMKII Mediates Prosurvival Signaling Pathways in Distinct Subcellular Compartments in Response to Depolarization in Neonatal Rat Spiral Ganglion Neurons (SGNs)**

Qiong Wang<sup>1</sup>, Jie Huang<sup>1</sup>, Shaheen Alam<sup>1</sup>, Steven Green<sup>1</sup>

<sup>1</sup>Department of Biological Sciences University of Iowa

We have previously shown that Ca<sup>2+</sup>/calmodulin-dependent protein kinases (CaMKs) are activated by nerve membrane depolarization, that mutant activated CaMKs support SGN survival, and that pharmacologic CaMK inhibition reduces the survival-promoting effect of depolarization. CaMKIV in SGNs is nuclear and promotes survival by activating the transcription factor CREB. Here,

we investigate CaMKII, another major CaMK isoform in SGNs. We find that *in vivo* CaMKII immunoreactivity (IR) is mainly cytoplasmic but nuclear CaMKII IR could be detected. We further investigated this in cultured SGNs using isoform-specific antibodies and found that CaMKIIβ IR is primarily cytoplasmic while CaMKIIα IR is both cytoplasmic and nuclear. This raises the possibility of distinct cytoplasmic and nuclear prosurvival signaling by CaMKII. To test this directly, we developed a specific and effective CaMKII inhibitor, GFP-AIP: a fusion of the CaMKII inhibitor peptide AIP to the C-terminal of GFP. We further restricted GFP-AIP to specific intracellular locations by addition of targeting signals, a Nuclear Export Signal (NES) or a Nuclear Localization Signal (NLS). We found that a lentiviral (FIV) vector could transduce cultured SGNs with high efficiency but only poorly transduces glia. GFP-AIP, NES-GFP-AIP and NLS-GFP-AIP constructs were expressed in cultured SGNs by conventional transfection or by FIV transduction. All three similarly reduced the ability of depolarization to promote SGNs survival, indicating that both cytoplasmic and nuclear CaMKII plays a role in depolarization-dependent prosurvival signaling. Because CREB is not required for CaMKII prosurvival signaling, these data suggest a novel prosurvival nuclear action.

#### **43 Blocking the MAPK/JNK Stress Activated Signal Cascade Prevents the Progressive Component of Electrode Trauma-Induced Hearing Loss**

Thomas Van De Water<sup>1</sup>, Adrien Eshraghi<sup>1</sup>, Jiao He<sup>1</sup>, Marek Polak<sup>1</sup>, Caihong Mou<sup>1</sup>, Christophe Bonny<sup>2</sup>, Azel Zine<sup>3</sup>, Thomas Balkany<sup>1</sup>

<sup>1</sup>University of Miami School of Medicine, <sup>2</sup>University of Lausanne, <sup>3</sup>University of Montpellier

The mitogen activated protein kinase (MAPK)/ c-Jun N Terminal Kinase (JNK) cell death signal cascade has been shown to play an important role in the apoptosis of oxidative-stress injured auditory hair cells. Blocking of this signal cascade has been shown to rescue injured hair cells and to prevent hearing loss. One such MAPK/JNK signal pathway inhibitor, D-JNKI-1 peptide, has been shown to prevent both hearing loss and loss of hair cells caused by exposure to either an aminoglycoside or sound trauma.

Insertion of an electrode into the scala tympani of a guinea pig causes a hearing loss that is both immediate and progressive. It is with this model of electrode trauma-induced hearing loss that we tested the efficacy of D-JNKI-1 peptide in preventing the progressive component of electrode trauma-induced hearing loss. Hearing of the guinea pigs was tested before and after electrode insertion trauma by pure tone evoked ABR and DPOAE recordings. D-JNKI-1 peptide in artificial perilymph was delivered into the scala tympani of the experimental animal immediately following electrode trauma and over 5 days. Controls consisted of the contralateral ears of untreated, electrode trauma animals and animals perfused with D-JNKI-1 peptide but not exposed to electrode trauma. There was no increase in the hearing thresholds of either the contralateral ears of the untreated, electrode insertion

trauma animals or in the ears of the animals perfused with D-JNKI-1 peptide without trauma. There was no change in the amplitudes of the DPOAEs of either of these two groups of control animals. There was a progressive increase in hearing thresholds following electrode insertion trauma in the untreated animals. This progressive increase in hearing thresholds following electrode insertion trauma was prevented in animals that were treated with scala tympani perfusion of D-JNKI-1. There was a progressive decrease in the amplitudes of the DPOAEs after electrode insertion trauma in the untreated animals. This trend did not occur in the electrode trauma animals treated with D-JNKI-1 perfusion. Initial results suggest that D-JNKI-1 peptide treatment is effective in preventing the progressive component of hearing loss initiated by electrode insertion trauma. Supported by a grant from MED-EL to TRV and TJB.

#### **44** Effects of Activity-Dependent Protein Kinases on Neonatal Rat Spiral Ganglion Neuron (SGN) Neurite Growth in Vitro

Marlan Hansen<sup>1</sup>, Damon Fairfield<sup>1,2</sup>, Papri Chatterjee<sup>1</sup>, Steven Green<sup>1,2</sup>

<sup>1</sup>*Depts. of Otolaryngology and,* <sup>2</sup>*Biological Sciences, University of Iowa, Iowa City, IA 52242, USA*

Hair cell loss leads to degeneration of SGN peripheral processes and eventual SGN death. Maintenance or regeneration of SGN peripheral processes is likely to improve cochlear implant performance, motivating us to investigate effects of electrical stimulation on SGN neurite growth. We have previously shown that chronic depolarization with 30 mM extracellular K<sup>+</sup> ("30K") promotes SGN survival in vitro, but neurite growth was reduced relative to that in neurotrophins (NTs). No significant difference was seen in neurite growth in BDNF or NT-3, and neither rescued the inhibition caused by 30K. Depolarization promotes survival by recruiting at least three distinct systems: cAMP-dependent protein kinase (protein kinase A, PKA), Ca<sup>2+</sup>/calmodulin-dependent protein kinase II (CaMKII) and CaMKIV. We had previously shown that transfecting SGNs with activated mutant CaMKII strongly inhibited neurite growth in the presence of NTs, suggesting that this could account for the effect of 30K. However, we now find that KN-62, a CaMK inhibitor, or transfection of SGNs with GFP-fused autacamtide-2-related inhibitory peptide, a highly specific CaMKII inhibitor, did not rescue 30K inhibition of neurite growth. Therefore, we have begun to investigate other depolarization-dependent intracellular signals and find that transfecting SGNs with GFP-tagged constitutively active PKA inhibits neurite growth in the presence of NTs. Current experiments are using subcellularly targeted PKA and PKI (a PKA inhibitor protein) to further investigate the effects of depolarization on neurite growth. We are also extending these studies to patterns of electrical stimulation more characteristic of those that occur physiologically or in implant users.

#### **45** Microfluidic System for Long Term Intracochlear Drug Delivery

Jason O. Firing<sup>1</sup>, Mark J. Mescher<sup>1</sup>, Sharon G. Kujawa<sup>2,3</sup>, William F. Sewell<sup>2,3</sup>, Michael J. McKenna<sup>2</sup>, Gerard J. Kujawa<sup>3</sup>, Jeffrey T. Borenstein<sup>1</sup>

<sup>1</sup>*Charles Stark Draper Laboratory,* <sup>2</sup>*Department of Otolaryngology and Laryngology, Harvard Medical School,* <sup>3</sup>*Eaton-Peabody Laboratory, Massachusetts Eye and Ear Infirmary*

Scientists and clinicians are making rapid progress in understanding the molecular mechanisms associated with cochlear and auditory nerve degenerative processes and in finding agents that can minimize degeneration and facilitate repair. Additional insight into the molecular signals involved in generating new hair cells is rapidly accumulating, and with this insight comes the promise of novel and precise drug treatments. Moreover, the extraordinary progress that has been made in defining the genes involved in a number of human genetic forms of deafness offers hope for gene-transfer and molecular approaches to treat these diseases. For therapies based on these discoveries to become clinically useful, it is necessary to develop a safe, precise, and programmable mechanism for the long term delivery of compounds to the inner ear.

In response to this need, we present a microfluidic system specifically designed for implantable intracochlear drug delivery and customized for clinical studies. The system employs a novel arrangement of pump, valves, and capillary tubing to achieve circulating flow of perilymph along with tunable periodic infusion and subsequent withdrawal of liquid volumes as small as 200 nL. The oscillating flow scheme enables long term perfusion of compounds of any desired concentration with optimized mixing, yet it results in negligible net volume addition to perilymph. All microfluidic components in the system are selected with a view towards miniaturization, and we also present progress and performance on microfabricated valves, pumps, and flow sensors. These microfluidic components will be incorporated into a self-contained implantable device sized to fit in the mastoid cavity of humans, providing a means for automated local drug delivery to the inner ear.

#### **46** Inner Ear Drug Delivery in Guinea Pig via a Recirculating Pump

Zhiqiang Chen<sup>1,2</sup>, Sharon G. Kujawa<sup>1,2</sup>, Michael J. McKenna<sup>1,2</sup>, Jason Firing<sup>3</sup>, Mark Mescher<sup>3</sup>, Jeffrey Borenstein<sup>3</sup>, William F. Sewell<sup>1,2</sup>

<sup>1</sup>*Harvard Medical School,* <sup>2</sup>*Massachusetts Eye and Ear Infirmary,* <sup>3</sup>*Draper Laboratory*

Therapies based on advances in cell and molecular biology will likely revolutionize the treatment of sensorineural hearing loss. Such treatments may require sequenced delivery of multiple and potentially unstable molecules for periods of months to years. Direct delivery of drugs to the inner ear will minimize side effects, enable access to tissues of interest, and profoundly increase target specificity. Our goal is to develop an implantable long-term drug delivery system for this purpose. Toward

this goal, we have developed a recirculating micropump that allows infusion of drugs into the cochlear perilymph through a single inlet hole in scala tympani of the basal turn (see Fiering et al., this meeting). Here we report the performance of a prototype, extracorporeal micropump in the guinea pig. We assayed base-to-apex distribution of two compounds with well characterized effects on cochlear physiology, salicylate (5 mM) and CNQX (100  $\mu$ M), using frequency specific effects on cochlear DPOAEs and auditory nerve CAPs (3 – 32 kHz). After insertion and sealing of the infusion line into the cochleostomy, the infusion line with drug delivery manifold and wire for recording the CAP were cemented to the bulla to prevent movement. We first established, with a direct infusion pump, safe parameters for net fluid delivery of artificial perilymph into the guinea pig cochlea (5  $\mu$ l/hr). We have determined that solutions infused in this manner reach cochlear regions far removed from the site of entry in scala tympani. Drug effects are largely reversible. With the prototype single-input recirculating micropump, we were able to rapidly and reversibly deliver drugs into the cochlea with no net fluid influx. As with the direct infusion pump, drugs reached cochlear regions significantly apical to the cochleostomy.

#### **47** A Method for Intracochlear Drug Delivery in Mouse

Zhiqiang Chen<sup>1,2</sup>, Anthony Mikulec<sup>1</sup>, Michael J. McKenna<sup>1,2</sup>, William F. Sewell<sup>1,2</sup>, Sharon G. Kujawa<sup>1,2</sup>

<sup>1</sup>Dept. of Otolaryngology and Laryngology, Harvard Medical School, <sup>2</sup>Eaton-Peabody Laboratory, Massachusetts Eye and Ear Infirmary

The confluence of two rapidly emerging research arenas - development of mouse models of human deafness and inner ear drug therapy for treatment and prevention of hearing loss - provides an opportunity for unprecedented approaches to study and treat deafness and other inner ear disorders. Toward such goals, we have begun to develop and test a method for intracochlear drug delivery in the mouse. Our technique provides for infusion of agents via a single inlet into basal turn scala tympani and for monitoring effects on cochlear physiology. In these studies, the bulla was exposed ventrally and the stapedial artery cauterized. An opening was made into the inferior-medial aspect of the bulla where the basal cochlear wall fuses with tympanic bulla, providing direct access to scala tympani of the basal turn. After demonstration of cochlear response stability with infusion of our control artificial perilymph solution (AP; 1  $\mu$ l/hr for 80 min), a drug with known effects on cochlear physiology (salicylate, 5 mM or CNQX, 100  $\mu$ M; 130 min) was introduced and its base to apex distribution assayed by frequency-specific effects on ABRs and DPOAEs (5.6 – 45.2 kHz).

For both drugs, effects were observed first and most significantly at our highest frequencies of test. Responses at progressively lower frequencies were compromised with continued drug infusion. As expected, the glutamate receptor blocker CNQX altered ABRs without significant effect on DPOAEs, while salicylate effects were observed in both metrics of function. Drug effects were reversible with AP wash (100-210 min), ruling out nonspecific or

traumatic effects of infusion. Results suggest that drugs delivered in this fashion to the cochlear base are distributed with time and continued infusion to more apical cochlear regions. This technique of local drug delivery with good preservation of cochlear physiology has immediate application in the study and treatment of forms of human hearing loss that can be modeled in the mouse.

Grant support: NIDCD R21 DC04983 (SGK); R01 DC00767 (WFS); RO1 DC03401-07 (MJM); P30 DC005209

#### **48** Feasibility of Superparamagnetic Nanoparticles for Drug Delivery to the Inner Ear

Natasha Mamedova<sup>1</sup>, Rick Kopke<sup>1,2</sup>, Jianzhong Liu<sup>1</sup>, Ronald Jackson<sup>3</sup>, Michael Costello<sup>3</sup>, Don Gibson<sup>4</sup>, Kenneth Dormer<sup>1,2</sup>

<sup>1</sup>Hough Ear Institute, <sup>2</sup>University of Oklahoma Health Sciences Center, <sup>3</sup>Naval Medical Center-San Diego, <sup>4</sup>NanoBioMagnetics Inc.

**OBJECTIVE:** An obstacle of inner ear medicine is effective, atraumatic, nontoxic delivery of therapeutic molecules, including genes, proteins, oligonucleotides to the fluid compartments of the inner ear. We sought to determine the feasibility of using superparamagnetic nanoparticles for targeted drug delivery.

**METHODS:** Silica-coated superparamagnetic nanoparticles (NP) were assayed for hermeticity and free radical generation using a hydroxyl radical spin trap agent and measuring ESR spectra. Similar particles were added to organotypic cultures of Corti's organ to assess in vitro toxicity. NP were placed on the round window membrane (RWM) of an anesthetized guinea pig. A 0.3 Tesla magnetic field was then applied on the opposite side of the RWM (20 min.) to draw the particles through the RWM into perilymphatic fluid, which was collected and assayed for the presence of NP. A similar experiment was performed on a fresh human cadaver temporal bone.

**RESULTS:** The NPs remained resistant to oxidation and no free radicals were formed. Exposure of mouse-pup organotypic Corti's organ culture to NP at a concentration of 100  $\mu$ g/ml for 24 hours demonstrated no hair cell loss after 3 days. NP were detected in guinea pig perilymphatic fluid and confirmed using transmission electron microscopy (TEM) with electron energy loss spectroscopy (EELS) and scanning electron microscopy with windowless, energy dispersive X-ray spectroscopy. NP were also detected in the perilymphatic fluid of human temporal bones as confirmed by TEM with EELS.

**CONCLUSIONS:** Silica-coated superparamagnetic NP were shown to be non toxic and susceptible to an external magnetic field. They could be rapidly and atraumatically pulled into inner ear perilymph. On-going experiments are aimed at payload attachment, polymer coatings, and in vivo studies of toxicity and therapeutic efficacy.

Sponsors: Office of Naval Research ; Shulsky Fund for Medicine & Research of the Jewish Communal Fund; and NanoBioMagnetics, Inc.

#### **49 Osmotic Mini-Pump Implantation Into the Mouse Vestibular System**

**Kaori Nakae<sup>1</sup>, Kohei Kawamoto<sup>1</sup>, Chiemi Himeno<sup>1</sup>, Narinobu Harada<sup>1</sup>, Hiromichi Kuriyama<sup>1</sup>, Toshio Yamashita<sup>1</sup>**

<sup>1</sup>*Kansai Medical University*

Osmotic mini-pump is one of the drug delivery systems into the inner ear and the method of placing it into the guinea pig cochlea had been established. However, there is no report to place the osmotic pump into the mouse inner ear because of the little size of it. Mice present an ideal model of inner ear research because their genome is being rapidly sequenced. Here we report the method of implanting the pump into the mouse vestibular system. Mice (25g) were implanted with an Alzet mini-pump and cannula for delivery of saline. Auditory brainstem responses (ABRs) were measured on day3 and day7 after the surgery and compared with baseline values. Also vestibular functions such as head tilt, circling behavior and swimming ability were scored everyday after the surgery. Saline control animals showed little or no change from baseline sensitivity for most frequencies in ABR. Vestibular functions had some damage immediately after the surgery, but it could be recovered within 7days. Utricles and cochleas were removed and processed for histological assessment. Our results showed that it is feasible to implant the osmotic mini-pump into the mouse inner ear and this method may be able to expand the drug induced research to the mouse inner ear.

#### **50 A Novel Neurotrophin Delivery Vehicle for the Inner Ear**

**Steven Feinberg<sup>1</sup>, John McGuire<sup>1</sup>, Terry Shibuya<sup>1</sup>, Leonard Kitzes<sup>1</sup>**

<sup>1</sup>*University of California - Irvine*

**Background:** Neurotrophins and neurocytokines have been shown to promote survival of spiral ganglion neurons following cochlear implant surgery in a guinea pig model. Chronic dosing strategies have previously been used, including mini-osmotic pumps, gene therapy, and stem cell transplantation. Although results have been favorable, there are various drawbacks to these techniques. Bolus dosing is a promising alternative to chronic dosing strategies, and has been shown to be equally effective in some models. Hyaluronic acid gel is an attractive candidate for bolus dosing of neurotrophins and neurocytokines.

**Objective:** To test hyaluronic acid gel as a potential delivery vehicle for neurotrophins and neurocytokines by measuring the release kinetics of brain-derived neurotrophic factor (BDNF) and ciliary neurotrophic factor (CNTF) from hyaluronic acid gel.

**Method:** Lyophilized BDNF and CNTF were dissolved in 20  $\mu$ L of 1% phosphate buffered saline and mixed in equal volumes with 1.4% hyaluronic acid gel. BDNF and CNTF were dissolved both alone and in combination to a concentration of 100 $\mu$ g/cc and 0.1  $\mu$ g/cc, respectively. The gel was pipetted in 40  $\mu$ L aliquots into 3 wells of a 96-well plate. The hyaluronic acid mixtures were then bathed in 100  $\mu$ L of phosphate buffered saline. The plate was

stored in a 37<sup>o</sup> C incubator and at time intervals ranging from 0 hours to 192 hours 1  $\mu$ L samples of supernatant were removed and stored at 2<sup>o</sup> C. Samples were analyzed using a commercially available enzyme linked immunosorbent assay specific for BDNF and CNTF. Plots of concentration versus time were obtained and analyzed.

**Results:** Data demonstrates a sustained release of both proteins, both alone and in combination. Both BDNF and CNTF achieved a sustained release over the time points evaluated. CNTF rapidly reached peak concentration within 4 hours and then steadily declined over 8 days, while BDNF achieved gradually increasing concentration over the course of the experiment.

**Conclusion:** BDNF and CNTF were readily dissolved in hyaluronic acid gel and achieved sustained release over 8 days. Our data demonstrates the release kinetics of BDNF and CNTF and may aid others in future work with neurotrophins. Hyaluronic acid may prove to be a viable option for the delivery of neurotrophins to the inner ear.

#### **51 Experiences with Delivery Approaches to the Rat Cochlea**

**Mark Praetorius<sup>1,2</sup>, Kim Baker<sup>2</sup>, Bernhard Schick<sup>3</sup>, Peter Plinkert<sup>1</sup>, Hinrich Staecker<sup>2</sup>**

<sup>1</sup>*University of Heidelberg*, <sup>2</sup>*University of Maryland*,

<sup>3</sup>*University of Erlangen-Nuremberg*

Sensorineuronal hearing loss refractory to conventional therapy may be a possible candidate for gene therapy in the future. Gene transfer to the cochlea has been approached mainly using various viral vectors (e.g. adenovirus, herpes simplex virus). Liposomes have been reported in comparison to various viral vectors to be least efficient in terms of gene transfer (Staecker et al, 2001). Another successful gene transfer was reported after placement of a liposome-soaked gelatine sponge at the round window membrane (Jero et al., 2001). We applied Cy3 labelled small silica particles and Cy3 alone. Also liposomes were tested carrying a plasmid with the green fluorescent protein and a CMV promotor. The agents were placed at the round window membrane or injected into the cochlea after utriculostomy (Praetorius et al., 2002). The results varied according to the application method. In cases of the utricular approach, a thorough transfection of the modiolar neuronal structures were observed. However, the extend of the detection of the GFP or Cy3 was variable. Until the viral vector systems can be substituted by a competitive transfective non viral agent, the search has to go on.

Jero J, Mhatre AN, Tseng CJ, Stern RE, Coling DE, Goldstein JA, Hong K, Zheng WW, Hoque AT, Lalwani AK. :Cochlear gene delivery through an intact round window membrane in mouse. *Hum Gene Ther.* 2001 Mar 20;12(5):539-48.

Praetorius M, Knipper M, Schick B, Tan J, Limberger A, Carnicero E, Alonso MT, Schimmang Th.: A novel vestibular approach for gene transfer into the inner ear. *Audiol Neurootol* (2002) 7: 324-334

Staecker H, Li D, O'Malley BW Jr, Van De Water TR.: Gene expression in the mammalian cochlea: a study of

## **52 Adenoviral Mediated Gene Delivery Occurs through Atypical Tropism in the Inner Ear**

Hinrich Staecker<sup>1</sup>, Mark Praetorius<sup>2</sup>, Chi Hsu<sup>3</sup>, Douglas Brough<sup>3</sup>

<sup>1</sup>University of Maryland, <sup>2</sup>University of Heidelberg, <sup>3</sup>Genvec Inc

Gene delivery to the inner ear has the potential to treat hearing loss and balance disorders. As more candidate therapeutic genes are being discovered, further understanding of the mechanisms involved in adenoviral vector transduction of the inner ear is needed. Multiply deficient and targeted adenovirus vectors have the potential to enhance safety and efficacy of a gene delivery candidate to treat hearing and balance disorders. The advantages that multiply deficient adenoviral vectors deleted of E1A, E1B, E3 and E4 for gene delivery to the inner ear have been shown. We have demonstrated that in the mouse the normal entry receptors for adenovirus are at a very low level in the inner ear which is inconsistent with the amount of gene delivery seen. Using capsid modified adenovirus vectors we have determined that efficiency of gene delivery in the inner ear is dependent on target volume and local vector concentration. Adenovirus capsids ablated of normal receptor interactions (CAR and integrin) are still capable of gene delivery suggesting that vector entry may occur through alternative pathways. While the ablated vector maintains efficient delivery within the inner ear, it has been shown to have a restricted tropism for gene delivery to tissue outside of the inner ear. These results have implications in designing safe adenovirus vectors for clinical applications to the inner ear.

## **53 Calcium Phosphate Nanoparticle-Mediated Gene Transfer in Rat Cochlear Organotypic Cultures and Cultured Spiral Ganglion Neurons**

Ping Wang<sup>1</sup>, Te-Chung Lee<sup>2</sup>, Dalian Ding<sup>1</sup>, Richard Salvi<sup>1</sup>

<sup>1</sup>Center for Hearing & Deafness, SUNY University at Buffalo, <sup>2</sup>Department of Biochemistry, SUNY University at Buffalo

The inner ear, which is surgically accessible and physically separated from the brain, is well-suited to targeted gene therapy. Viral vectors have typically been used to deliver therapeutically useful genes to the inner ear of animal models; however, health risks associated with viral-mediated gene transfer represent an obstacle for human clinical trials. Suitably constructed nanoparticles represent an alternative approach to gene delivery because of their low immunogenicity and the potential for tissue-specific targeting. To assess the efficacy of nanoparticle mediated gene expression, we constructed calcium phosphate nanoparticles carrying an EGFP reporter plasmid. Calcium phosphate-EGFP mediated gene transfer was first evaluated using small clusters of postnatal day 3 spiral

ganglion neurons (SGN). SGNs, grown in DMEM medium with 10% FBS, were treated for 5 h with calcium phosphate-EGFP nanoparticles and maintained in culture for several days. After 3 days in culture, samples were immunolabeled with fluorescently labeled neurofilament to identify neurons. Significantly, up to 80% of the SGN in the clusters were positive for EGFP. In addition, a large proportion of supporting cells around the SGN expressed EGFP. No evidence of toxicity was noted. In the second phase, organ cultures containing both hair cells and SGN were treated with calcium phosphate-EGFP nanoparticles to assess the efficiency and cell specific targeting. In organotypic cultures, EGFP positive cells were mainly seen in the periphery of the outer sulcus region and the SGN region; however, the number of labeled cells was less than isolated SGN clusters. Only a few EGFP positive cells were seen in the hair cell, interdental cell and inner sulcus cell region. These results suggest that calcium phosphate nanoparticles may be an effective delivery vehicle for transferring DNA to postnatal SGN as well as supporting cells in the outer sulcus. Other modified calcium phosphate nanoparticles are being evaluated for their efficiency and cell specific targeting.

(Supported by NIH grants P01 DC03600-01A1, R01 DC06630-01)

## **54 Effect of Adenoviral Vector Gene Delivery via the Round Window Membrane Treated with Phenol**

Mitsuya Suzuki<sup>1,2</sup>, Tatsuya Yamasoba<sup>2</sup>, Akinori Kashio<sup>1,2</sup>

<sup>1</sup>Tokyo Metropolitan Police Hospital, <sup>2</sup>University of Tokyo

Adenovirus could transfect a variety of inner ear cells through the round window membrane (RWM) treated with adenovirus vector and local anesthetic solution containing phenol (LA). Although this delivery system may be able to reliably transfect the organ of Corti, marked morphologic damage may occur at the basal turn of the organ of Corti. This study investigated the optimal exposure time of LA, which is needed to deliver adenovirus-mediated gene via the RWM without damage to the organ of Corti. We assessed morphologic and functional changes in the cochlea following application of both LA and adenovirus vector to the RWM. We characterized adenovirus-infected cells using a vector that carried the gene for green fluorescent protein (GFP) or beta-galactosidase (beta-gal). The vector was administered to the RWM treated with LA for 3, 7, 15 or 30 min.. Three days later, all animals were decapitated immediately after ABR tests. Hair cell damage was assessed morphologically in each animal using surface preparation technique or paraffin section. A statistically significant difference of the ABR threshold shifts at 4 KHz was found between the 3 or 7 min. treatment group and the 15 or 30 min. treatment group. There was a trend for greater threshold shifts at 12, 20 KHz in 15 or 30 min. treatment group as compared with the 3 or 7 min. treatment group, however, the difference was not significant. Surface preparation showed few scars in the organ of Corti of all cochlear turns in the 3 and 7 min. treatment groups. A large number of scars were observed in the cochlear basal turn in all animals in the 15



and 30 min treatment groups. Epi-fluorescence image showed GFP negative in all specimens in the 3 min. treatment group. No beta-gal expression was seen anywhere in the cochlea. These findings suggest the absent of adenovirus-infected hair cells and supporting cells in the 3 min. treatment group. We conclude that adenovirus vector administration via the RWM treated with LA for 7 min. may be suitable for safe and effective gene delivery to the guinea pig inner ear.

### **55 Induction of Hearing Loss in Mice with $\hat{\alpha}$ -Tubulin Immunization**

Mohammad Kermany<sup>1</sup>, Bin Zhou<sup>1</sup>, Jaechun Lee<sup>1</sup>, Xioping Du<sup>1</sup>, Jonathan Glickstein<sup>1</sup>, **Tai June Yoo<sup>1</sup>**

<sup>1</sup>*Univ. of Tennessee*

$\beta$ -Tubulin is an important molecule in the hair cells and supporting cells within the sensory epithelium and found to be an autoantigen in Ménière's disease. The objective of the study is to induce hearing loss in mice with varying doses of  $\beta$ -Tubulin antigen and evaluate the pathogenesis of autoimmune hearing loss induced by tubulin in mice.

5 weeks old Balb/C mice were subcutaneously injected with tubulin in dosage of 100, 200 and 300 ug and in CFA. Control mice underwent subcutaneous injection of PBS and CFA. Immunizations were boosted in IFA with 100, 200 and 300 ug tubulin per groups twice at one-week intervals, two weeks after the initial immunization. Control mice were given PBS in IFA at the contemporaneous boostertime as well.

The ABR and DPOAE were recorded three times as: a) before immunizations, b) 5 weeks after the first immunization and c) 9 weeks after the first immunization. The click and tone pips of 8, 16 and 32 kHz were generated using a Tucker Davis Technologies evoked generated equipment

Auditory thresholds were determined by increasing the sound intensity of the click and ton pips for each frequency stimulus from 15 dB to 90 dB first at 10 dB steps and then at 5 dB intervals and to the lowest level at which reproducible waves could be recognized. Every threshold was defined as the lowest stimulus level at which a distinguishable positive waveform (P2) in the evoked response tracing was evident.

In 100, 200 and 300 ug tubulin immunized groups, analysis of variance show significant difference in four weeks from 2 to 6 weeks of last boosting. ( $p < 0.05$ , mice# =28). Also t-test shows highly significant in comparison between controls and tubulin-immunized groups after 2 and 6 weeks from last boosting. Distortin product of 100, 200 and 300 ug tubulin immunization show abnormal result after 6 weeks from last booster immunization.

Morphological study of temporal bones shows that at 100 ug immunization group we did not observe abnormal changes. In both 200 and 300 ug tubulin immunized group we observe spiral ganglion damages as well as hair cells. Thus this study showed that  $\beta$ -tubulin is an autoantigen in animal model of hearing loss as well as in human autoimmune hearing loss patients.

Supported by NIH R0 1 DC005010-01

### **56 Pneumolysin, a Pneumococcal Protein, Induced Cochlear Hair Cell Death via a Calcium Dependent Apoptotic Pathway**

Maryline Beurg<sup>1</sup>, Aziz Hafidi<sup>1</sup>, Tim Mitchell<sup>2</sup>, Didier Dulon<sup>1</sup>  
<sup>1</sup>*EA-3665 University of Bordeaux 2, Hopital Pellegrin, Bordeaux, France,* <sup>2</sup>*Division of Infection and Immunity, University Glasgow, Glasgow, UK*

Pneumococcal meningitis can result in permanent sensorineural hearing loss. Deafness associated with meningitis is mainly due to cochlear damages, induced by the release of an exotoxin, pneumolysin (PLY). In cultures of rat organ of Corti, we showed that PLY induced, severe damages to cochlear hair cells, going from hair bundle disorganization to total cell loss. Apoptotic features in hairs cells (cell shrinkage, vacuoles) were observed in semithin sections of the explants. The toxic effect of PLY was dose-dependent. Surprisingly, PLY affected preferentially inner hair cells at low concentrations and both hair cell type at high concentrations. A Hill equation fit gave EC50 of 0.6 and 4 ng/ $\mu$ l for inner hair cell and outer hair cell respectively. Pneumolysin triggered in vitro cell death by an influx of calcium. Extracellular calcium appeared to enter the cell through a pore formed by the toxin. Buffering intracellular calcium with BAPTA prevented hair cell death. A mitochondrial apoptotic pathway was demonstrated by the use of an inhibitor of mitochondrial permeability transition pore. Blockers of caspases had not effect. Using a recombinant form of the toxin (eGFP-PLY), we studied the distribution of PLY binding in cochlear hair cells. The stain was distributed homogeneously in the plasma membrane, in the cuticular plate and in the stereocilia. The toxin distribution was comparable in IHCs and OHCs, and no significant difference in fluorescence intensity could be observed. The binding of PLY to the hair cell plasma membrane was required to induce cell death. Remarkably, increasing external calcium reduced cell toxicity by preventing the binding of PLY to hair cell membranes. Our results showed a main role of calcium - in triggering PLY-induced hair cell apoptosis - and in preventing the toxin from binding to its cellular target.

### **57 Bacterial Meningitic Deafness: Historical Development of Epidemiology and Cellular Pathology**

Robert Ruben<sup>1</sup>

<sup>1</sup>*Albert Einstien Colledge of Medicine*

Awareness that bacterial meningitis can cause disease of the labyrinth -- hearing and vestibular impairment -- occurred in the last third of the 19th century. Until the 1860's, the disease entity that we now recognize as bacterial meningitis was subsumed under the entity of hydrocephalus. Meningitis resulting in labyrinthitis and its associated hearing loss was first described by several authors during 1864 and 1865 but it was not integrated into the otological cannon until H. Knapp's 1871 publication. This report was incorporated by St. John Rossa in his textbook of 1873; Pollitzer, in 1882, included a fuller description of its clinical symptoms.

Analysis of records of the etiologies of students in 90 schools for the deaf in North America from 1817 – 1893 showed that prior to the mid 1870's meningitis was rarely identified as an etiology (<1%) but by the 1880's it accounted for 10% to 20% of all etiologies, with male preponderance. Rapid dissemination of the new medical information linking meningitis with deafness stimulated a more accurate epidemiology of childhood deafness.

Cellular pathology of meningitic labyrinthitis from the 1880's to the 1980's examined the ways bacteria invade the inner ear and their effects within the labyrinth. Human temporal bone studies were a major source of understanding of the pathological processes. Honda, in 1927, injected guinea pigs with live bacteria intracranially and serially observed the effects on the membranous labyrinth: acute bacterial labyrinthitis, secondary hemorrhagic, serous exudate, serous fibrinous exudate, suppuration and, at 36 hours, necrosis of the membranous labyrinth.

Lebel's 1988 observation of the effectiveness of Dexamethasone in preventing much deafness in children with meningitis stimulated examination of the role of immune response in relation to labyrinthitis. These studies have defined cellular processes that mediate the deleterious effects, and have indicated strategies for amelioration. Immunological mechanisms can account for some of the variable morbidity of unilateral, progressive, less-than-severe deafness.

### **[58] Human Trnu Related to Mitochondrial Trna Modification is a Modifier Factor for the Phenotypic Expression of the Deafness-Associated Mitochondrial 12S rRNA Mutation**

Qingfeng Yan<sup>1</sup>, Xiaoming Li<sup>1</sup>, Nathan Fischel-Ghodsian<sup>2</sup>, Min-Xin Guan<sup>1,3</sup>

<sup>1</sup>Cincinnati Children's Hospital Medical Center, <sup>2</sup>Cedars-Sinai Medical Center, <sup>3</sup>University of Cincinnati College of Medicine

Human mitochondrial 12S rRNA A1555G mutation has been associated with aminoglycoside and nonsyndromic deafness in many families of different ethnic backgrounds.

Our biochemical and genetic data showed that the A1555G mutation is the primary contributor to biochemical defect associated with deafness phenotype. Nuclear modifier genes have been proposed to modulate the phenotypic expression of this mutation. Here we identified the first nuclear modifier gene *TRMU* encoding a highly conserved mitochondrial protein related to tRNA modification. *TRMU* is ubiquitously expressed and more abundantly in tissues of high metabolic rates. We show that in families with the A1555G mutation there is highly suggestive linkage and linkage disequilibrium between microsatellite markers adjacent to *TRMU* and the presence of deafness. Sequencing of *TRMU* in deaf members of these families revealed a missense mutation (G28T) altering an invariant amino-acid residue (A10S) in the mitochondrial targeting sequence. Surprisingly, this mutation does not affect importing of Trnu precursors. Strikingly, the homozygous A10S mutation leads to the defect in mitochondrial tRNA metabolisms, specifically

reducing the steady-state levels of mitochondrial tRNAs. As a consequence, these defects contribute to the impairment of mitochondrial protein synthesis. The resultant biochemical defects aggravate the mitochondrial dysfunction associated with A1555G mutation, exceeding the threshold for expressing deafness phenotype. These findings indicate that the truncated *TRMU*, acting as a modifier factor, modulates the phenotypic manifestation of deafness-associated A1555G mutation.

This work was supported by Public Health Service grant DC04958 and DC05230 from the National Institute on Deafness and Other Communication Disorders, and NS44015 from the National Institute of Neurological Disorders and Stroke to M.-X.G. and United Mitochondrial Disease Foundation.

### **[59] Screening for the Common Mutations in the GJB2, GJB6 Genes and in Mitochondrial DNA in Patients with Non-Syndromic Hearing Loss of South Florida**

Xiao Mei Ouyang<sup>1</sup>, Li Lin Du<sup>1</sup>, Simon I Angeli<sup>1</sup>, Thomas J Balkany<sup>1</sup>, Denise Yan<sup>1</sup>, Xue Zhong Liu<sup>1</sup>

<sup>1</sup>University of Miami

Hearing loss (HL) is a common congenital disorder. In more than half of the cases, the cause is monogenic with the inheritance pattern being autosomal dominant (20%), autosomal recessive (80%), X-linked (1%) or mitochondrial (<1%). Nonsyndromic forms (NSHL) account for approximately 70% of genetic deafness. Mutations in the gene GJB2 (Cx26) underlie, depending on the population studied, up to 63% of autosomal recessive NSHL cases. The gene defect in GJB2 may cause NSHL through either a homozygous deletion of Cx26, or digenic inheritance of a Cx26 deletion and a Cx30 (GJB6) mutation in trans. Mutations in mitochondrial DNA (mtDNA) have also been implicated in NSHL. The objective of this study is to determine the frequency of mutations in GJB2, GJB6 (342-kb deletion) and in two common mitochondrial A1555G and A7445G mutations in NSHL patients of South Florida. Altogether, nine likely pathogenic GJB2 sequence changes were identified. Nineteen of 141 cases have mutations of one or both alleles of the GJB2 gene and seven of them are homozygous for the 35delG mutation. The most common mutation in the GJB2 gene, the 35delG mutation accounted for approximately 61% of the observed mutant alleles, followed by M34T and N206S, representing 11% and 7% respectively. We have identified the GJB6 (342-kb deletion) in two probands in the heterozygous state in a screening of 84 patients and found one case of digenic hearing loss due to 35delG (GJB2)/342 kb deletion (GJB6) in a total of 12 patients heterozygous for mutation in GJB2 investigated in our study. Finally, our screening of 186 patients revealed 3 subjects with the mtDNA A1555G and A7445G mutations in a homoplasmic state. This study shows that the common mutations in GJB2, GJB6 (342-kb deletion) as well as the mitochondrial A1555G and A7445G mutations are among the significant causes of non-syndromic deafness in patients of South Florida.

This work is supported by NIDCD 05575

## **60 Biochemical Characterization of the Mitochondrial 12S Rrna C1494T Mutation Associated with Maternally Inherited Aminoglycoside-Induced and Non-Syndromic Deafness**

Hui Zhao<sup>1,2</sup>, Wie-Yen Young<sup>2</sup>, Min-Xin Guan<sup>1,3</sup>

<sup>1</sup>Cincinnati Children's Hospital Medical Center, <sup>2</sup>Chinese PLA General Hospital, <sup>3</sup>University of Cincinnati College of Medicine

Biochemical characterization of mitochondrial 12S rRNA C1494T mutation associated with maternally inherited aminoglycoside-induced and non-syndromic deafness has been carried out by using cybrids constructed by transferring mitochondria from lymphoblastoid cell lines derived from the Chinese family into human mtDNA-less ( $\rho^0$ ) cells. 15 cybrids derived from five matrilineal relative of the Chinese family carrying the C1494T mutation, exhibited a significant decrease in the rate of mitochondrial protein synthesis, respiration and growth, compared with 9 control cybrids derived from three controls lacking the mutation. Furthermore, exposure to high concentration of paromomycin or neomycin caused a uniformed and significant average increase in doubling time in 15 cybrid cell lines derived from three symptomatic and two asymptomatic individuals in this family carrying the C1494T mutation, when compared to nine cybrids derived from three control cell lines. These results provide a direct biochemical evidence that the C1494T mutation is the novel mitochondrial DNA mutation associated with aminoglycoside-induced and nonsyndromic deafness. This data also suggest that the nuclear background plays a determining role in the aminoglycoside toxicity.

Grant support

This work was supported by Public Health Service grant DC04958 and DC05230 from the National Institute on Deafness and Other Communication Disorders, and NS44015 from the National Institute of Neurological Disorders and Stroke and United Mitochondrial Disease Foundation and Deafness Research Foundation to MXG

## **61 Glucocorticoids Restore Autoimmune Hearing Loss Through the Mineralocorticoid Receptor**

Dennis Trune<sup>1</sup>, Beth Kempton<sup>1</sup>, Sarah Parrish<sup>1</sup>, Steven Hefeneider<sup>1,2</sup>

<sup>1</sup>Oregon Health & Science University, <sup>2</sup>VAMC

Effective management of autoimmune hearing loss is achieved with glucocorticoids (prednisone, dexamethasone), although the underlying cochlear mechanisms are unknown. Studies of MRL/MpJ-Faslpr autoimmune mice have shown that inner ear pathology is limited to the stria vascularis and treatment with the mineralocorticoid aldosterone is as effective as prednisolone in reversing hearing loss (Trune & Kempton, *Hear. Res.* 155:9-20, 2001). The implication is that stria ion transport is compromised in systemic autoimmune diseases and the mineralocorticoid actions of glucocorticoids restore it. If this is the case, then prednisolone treatment while blocking the glucocorticoid receptor with its antagonist RU-

486 (mifepristone) should still restore hearing in autoimmune mice. MRL/MpJ-Faslpr mice (N=40) were tested for baseline ABR thresholds and then implanted with time release pellets providing 1.3 mg/kg of RU-486, 4 mg/kg of prednisolone, or their respective placebos. Animals were retested by ABR and serum analyses after one month of treatment. Serum immune complexes were measured to assess the immune suppressive effects of the prednisolone, which would be blocked by RU-486 because it is mediated through the glucocorticoid receptor. Autoimmune mice receiving either no drugs or RU-486 alone showed the normal progression of hearing loss coincident with systemic disease development. Thresholds at 32 kHz were higher in 65-80% of these mice. However, mice receiving prednisolone alone, or prednisolone + RU-486, had significantly better hearing after one month of treatment ( $p < 0.05$ ). Improved hearing was seen in 26% of prednisolone mice and 40% of prednisolone + RU-486 mice, while only 35-36% had higher thresholds. Thus, blockage of the glucocorticoid receptor with RU-486 did not prevent prednisolone from preserving, and even improving, hearing. Immune complexes were significantly elevated in all mice except those receiving prednisolone alone ( $p = 0.03$ ), demonstrating RU-486 did prevent glucocorticoid receptor-mediated immune suppression. These results offer strong evidence that the mineralocorticoid actions of glucocorticoids are relevant in the treatment of steroid responsive hearing disorders.

(Supported by R01 DC05593 & VA RR&D RCTR 597-0160).

## **62 Upregulation of HSP by Geranylgeranylacetone Protects the Cochlear Lateral Wall from Damage Induced by Acute Otitis Media**

Hiroshi Yamamoto<sup>1</sup>, Michihiko Sone<sup>1</sup>, Tsutomu Nakashima<sup>1</sup>, Takahiko Yoshino<sup>1</sup>

<sup>1</sup>Nagoya University School of Medicine

We investigated whether an acyclic polyisoprenoid antiulcer drug, geranylgeranylacetone (GGA), induces the expression of HSP70 in the rat cochlea. Immunoblotting revealed upregulation of HSP70 in the cochlea at 12 hours after transtympanic (local) or oral (general) administration of GGA, and this increased at 24 hours after administration. Positive immunohistochemical staining of HSP70 was observed in the organ of Corti, the spiral ganglion, the stria vascularis, the spiral ligament, and the perivascular portion of modiolar vessels. We therefore subsequently studied the effects of GGA as an HSP-inducer on inner trauma due to inflammation. Damage to the lateral wall due to otitis media induced by lipopolysaccharide inoculation was protected against by pretreatment with GGA, as assessed physiologically by measurement of cochlear blood flow and morphologically by electron microscopy. The results of the present study suggest that GGA can protect the cochlea against other injuries including those induced by noise, ototoxic drugs, and ischemia.

**63 The Neuroprotective and Therapeutic Effects of Intracochlear Administration of Basic Fibroblast Growth Factor on Streptococcal Meningitis Induced Sensorineural Hearing Loss in Mongolian Gerbils**

Moses D. Salgado<sup>1</sup>, Steven P. Tinling PhD<sup>2</sup>, Hilary A. Brodie MD, PhD<sup>2</sup>

<sup>1</sup>University Of California, Davis, <sup>2</sup>University Of California, Davis

Background: Basic fibroblast growth factor (bFGF) has been identified as an important neurotrophic factor involved in maintenance and repair of neurosensory epithelia. Studies have shown that bFGF may be involved in the regulation of inflammatory pathways and is involved in wound healing. Basic FGF is able to protect against trauma induced cochlear nerve degeneration, protect hair cells from acoustic over stimulation and ototoxic drugs. Given evidence that bFGF can confer protective effects within the cochlea it was important investigate the protective effects of bFGF against sensorineural hearing loss in a meningitis model.

Hypothesis: Intracochlear infusion of bFGF inhibits sensorineural hearing loss in post-meningitic gerbils.

Methods: Twenty Mongolian gerbils were infected by intrathecal injection of *Streptococcus pneumoniae* to induce meningitis. Simultaneously bFGF or artificial perilymph was directly infused into the cochlea through the round window membrane. An osmotic pump apparatus was implanted that continuously infused the treatments into the right cochlea of each animal for one week. Baseline ABR's were obtained prior to the infection and post-operative ABR's were obtained 8 weeks later at the time of sacrifice. The bullae were harvested, decalcified and embedded in plastic. Mid-modiolar sections of the cochlea were analyzed for histologic changes.

Results: Basic FGF was shown to decrease postmeningitic ABR dB threshold shifts when compared to the control group. Basic FGF was also shown to decrease the average dB threshold levels on the treatment side when compared to the non-treated side of a given animal within the treatment group. Histologic changes correlated well with the ABR findings.

Conclusion: Intracochlear infusion of bFGF was able to protect against sensorineural loss in this gerbil meningitis model. Basic FGF may function by down regulating the inflammatory cascade and protect inner ear function in pneumococcal meningitis.

**64 Human Recombinant Erythropoietin Protects Hair Cells in Rat Organ of Corti Explants Exposed to Ischemia**

Birgit Mazurek<sup>1</sup>, Nadejda Andreeva<sup>1</sup>, Nyamaa Amarjargal<sup>1</sup>, Heidemarie Haupt<sup>1</sup>, Hans Scherer<sup>1</sup>, Johann Gross<sup>1</sup>

<sup>1</sup>Charité-University Medicine Berlin

This study is designed to evaluate the effect of recombinant human erythropoietin (rhEPO) on ischemia-

induced hair cell loss in an organotypic cochlea culture. The results were compared with those obtained using insulin like growth factor-1 (rhIGF-1) and epidermal growth factor (rhEGF).

The apical, middle and basal parts of the organs of Corti (newborn rat, p.d. 3-5) were exposed to ischemia (3.5 h) in glucose-free artificial perilymph in a Billups chamber (pO<sub>2</sub> 10-20 mm Hg) without or with rhEPO (5.2 ng/ml, Roche), rhIGF-1 (50 ng/ml, R&D) or rhEGF (200 ng/ml, R&D). Controls were exposed to normoxia in artificial perilymph with glucose. 24 h after onset of ischemia, the cultures were stained using TRITC phalloidin (intact inner and outer hair cells), propidium iodide (necrotic nuclei) and in situ DNA End Labeling Assay (ISOL; apoptotic nuclei). The number of stained hair cells and nuclei/100 μm was counted.

Ischemia without growth factors induced a mean hair cell loss of 32% in the middle and basal cochlear parts. rhEPO and rhIGF-1 significantly reduced the hair cell loss by about 20 and 30%. rhEGF was not effective. Ischemia induced 1-7 necrotic and apoptotic nuclei/100 μm in the cochlear parts. rhEPO and rhIGF-1 significantly reduced the number of necrotic and apoptotic nuclei by about 50%.

rhEPO and rhIGF-1 attenuate the ischemia-induced hair cell loss by reducing apoptosis and necrosis. Binding of rhEPO to erythropoietin receptor activates several protein kinases and nuclear factor NF-kappa B. This results in activation of several proteins which support survival pathways. rhEpo has been in clinical use for more than a decade and found to be well tolerated. Clinical studies have to clarify whether rhEPO could be an effective therapy for the prevention of hearing loss via a hair cell protective mechanism.

**65 Selective Expression of Class III B-Tubulin in Type I Spiral Ganglion Cells**

Nigel Woolf<sup>1,2</sup>, Dawn Jaquish<sup>1,2</sup>, Anuradha Desai<sup>1,2</sup>, Fred Koehn<sup>1,2</sup>

<sup>1</sup>UCSD Medical School, <sup>2</sup>San Diego VAMC

Microtubules are cytoskeletal structures which are essential for numerous cellular functions. Tubulin, the primary component of microtubules, is an intracellular filamentous structure comprised of α and β monomers. At least seven different β-tubulin isotypes have been identified in vertebrates. Detailed descriptions of the distribution of the first four β-tubulin isotypes [βI, βII, βIII, βIV] in the cochlea of developing and adult gerbils have been reported previously (reviewed in H.C. Jensen-Smith et al., J. Neurocytol. 32:185, 2003). Notably, βI-, βII-, βIII- and βIV-tubulin were all expressed in gerbil spiral ganglion cells. To our knowledge, the distribution of β-tubulin isoforms in the adult mouse cochlea has not been reported. This study investigated βIII-tubulin expression in the cochlea of adult C.B-17 mice. βIII-tubulin was selected for our initial study because this isoform has been widely used for investigations of neurons and their precursors. Immunohistochemistry was conducted using a combination of well characterized anti-βIII-tubulin (monoclonal TUJ1 #MMS-435P or rabbit polyclonal #PRB-435P, Covance) and anti-peripherin (monoclonal

MAB1527 or rabbit polyclonal AB1530, Chemicon) antibodies. In the adult mouse cochlea  $\beta$ III-tubulin immunostaining was confined to spiral ganglion and Scarpa's ganglion cells. Earlier studies using neonatal mice reported  $\beta$ III-tubulin expression in both type I and type II spiral ganglion cells (Reid et al., *J Neurosci.* 24:733, 2004). In marked contrast, in adult mice type I spiral ganglion (peripherin negative) cells were intensely immunolabeled by anti- $\beta$ III-tubulin while type II spiral ganglion (peripherin positive) cells were not immunolabeled by anti- $\beta$ III-tubulin. The segregation of  $\beta$ III-tubulin isoforms in the two spiral ganglion cell subpopulations is consistent with growing evidence that the physiological functions of type I and type II spiral ganglion cells are different (Ibid; Jagger & Housley, *J. Physiol.* 552:525, 2003). [Supported by NIH DC02666, NIH DC00386, and the VA Research Service]

### **66** Glutamate Receptor Distribution in Murine Spiral Ganglion Neurons

Jacqueline Flores-Otero<sup>1</sup>, Robin L. Davis<sup>1</sup>

<sup>1</sup>Department of Cell Biology and Neuroscience, Rutgers University

Spiral ganglion neurons (SGNs), categorized by their innervation of the hair cell sensory receptors, are the first neural elements in the mammalian auditory system. Although little is known about the unmyelinated type II neurons that compose less than 10% of the ganglia, they innervate from 3 to 10 outer hair cells via multiple synaptic connections. Therefore, although few in number; these cells could play a significant role in auditory processing due to their multiple synaptic contacts. Differences in the type I / type II SGN innervation pattern, along with their distinctive electrophysiological properties (Reid, Flores-Otero, & Davis, *J. Neurosci.* 24, 2004) led us to hypothesize that there may also be differences in their neurotransmitter receptor composition. In order to address this issue we initiated a series of immunocytochemical studies to examine the distribution of glutamate receptors in SGNs.

We focused on the NMDA receptor distribution because of its modulatory role in synaptic transmission. An antibody to NR1, an obligatory subunit of the NMDA receptor, was utilized to determine the distribution of NMDA receptors, independent of their individual subunit composition. Using the Chemicon NR1 antibody (AB1516; lot# 23021043) we observed punctate anti-NR1 labeling that was highly enriched in type II SGNs relative to type I SGNs. This result is consistent with the idea that the type II SGNs are endowed with intrinsic and synaptic specializations required to carry out their function. Future experiments will determine whether additional NMDA receptor subunits are differentially distributed in type I and type II SGNs. Supported by NIH R01 DC01856 (RLD) and Gates Millennium Scholarship (JFO).

### **67** The Role of the Ih Current in Setting the Threshold Level of Spiral Ganglion Neurons

Qing Liu<sup>1</sup>, Robin Davis<sup>1</sup>

<sup>1</sup>Department of Cell Biology and Neuroscience, Rutgers University

Previous studies have shown that timing-related firing features of postnatal spiral ganglion neurons (SGNs), such as action potential latency, onset tau, and accommodation, vary according to cochlear location and presumably characteristic frequency (Adamson et al., *JCN*, 2002). In contrast to this, one might hypothesize that electrophysiological features related to other sub-modalities, such as intensity coding, would not co-vary with frequency, but, instead, would be uniform throughout the entire frequency range.

One channel type that could have a profound effect on neuronal threshold, and therefore, may contribute to intensity coding, is the hyperpolarization-activated cationic channel (Ih). In SGNs the steady-state activation of this channel type is characterized by a wide range of half-maximal voltages that varies from cell to cell, but does not correlate with cochlear location (Mo and Davis, *J. Neurophysiol.*, 1997). The present study is designed to determine whether the endogenous Ih current contributes to setting the wide range of thresholds observed in different SGNs.

Comparison of the amount of Ih inward rectification to the threshold voltage of each SGN for 16 whole-cell current clamp recordings from P5-P6 CBA/CaJ SGNs showed a clear relationship between inward rectification magnitude and threshold level ( $R^2=0.8$ ). Neurons with the greatest amount of inward rectification had the highest thresholds, whereas neurons with the least amount of inward rectification had the lowest thresholds.

In conclusion, our data support our hypothesis that Ih current magnitude sets the threshold voltage of SGNs. To date, we have observed that threshold does not vary systematically along the tonotopic axis, which is consistent with the idea that it is relevant to a frequency-independent coding parameter such as spontaneous rate.

Supported by NIH R01 DC01856.

### **68** Inhibition of JNK Signaling Inhibits Rat Spiral Ganglion Neurons (SGNs) Death in vitro

Shaheen Alam<sup>1</sup>, Steven Green<sup>1</sup>

<sup>1</sup>Dept. Biol. Sci. & Otolaryngol. Univ. Iowa, Iowa City, IA

Hair cells, the auditory sensory cells, are the sole presynaptic inputs to the SGNs. Destruction of the hair cells deafferents the SGNs, which then die gradually over a period of months to years, depending on the species. We have previously shown that the death of deafferented SGNs is apoptotic and that there is an increase in activity of a proapoptotic intracellular signaling pathway, the JNK-Jun pathway, in SGNs in vivo following hair cells loss. This is not marked in those SGNs that die within the first 2-3 weeks after deafening but is very marked in SGNs that die subsequently. These SGNs show significantly elevated phospho-Jun immunoreactivity (P-Jun IR) but not reduced

prosurvival signaling (assessed as phosphorylation of the prosurvival transcription factor CREB). Moreover, the appearance of increased P-Jun IR is highly correlated with appearance of TUNEL, a marker of apoptotic cells, indicating that the SGNs that have elevated P-Jun IR are those that are dying. SGNs cultured in the absence of neurotrophic stimuli show increased P-Jun IR, which is suppressed by depolarization, by addition of neurotrophins, or by addition of the JNK inhibitor SP600125 to the cultures. Jun phosphorylation via JNK signaling is causal to SGN death because addition of SP600125 to cultures prevents SGN death in vitro as effectively as does depolarization. While previous studies have shown that neurotrophins can suppress JNK activity via inhibition of its upstream activator MLK, suppression of JNK activity by depolarization has not been previously shown and the mechanism is not known. Current experiments are directed to determining this mechanism and to extending these results to SGNs in vivo. Supported by NIH grant DC02961

### **69** Determining the Refractory Period and Temporal Precision of Chick Primary Cochlear Afferents

Michael Avissar<sup>1</sup>, Adam C. Furman<sup>2</sup>, James C. Saunders<sup>2</sup>, Thomas D. Parsons<sup>3</sup>

<sup>1</sup>Department of Neuroscience, University of Pennsylvania,

<sup>2</sup>Department of Otorhinolaryngology - Head and Neck Surgery, University of Pennsylvania, <sup>3</sup>Department of Clinical Studies - New Bolton Center, University of Pennsylvania

The ability of a primary cochlear afferent to fire action potentials at a particular phase of a periodic stimulus (phase-locking) degrades with increasing stimulus frequency, in part due to its refractory period becoming greater than the stimulus period. We performed in vivo extracellular single unit recordings in 94 units from 17 chicks (*Gallus domesticus*). Each unit was stimulated repeatedly with a 40 ms tone burst 20 dB above rate-threshold at the characteristic frequency (CF) of that unit. Raster plots, post-stimulus time histograms, and interspike interval histograms (ISIH's) were generated for each unit as well as vector strength (VS) and temporal dispersion (TD) calculated. CF's ranged from 131 – 3984 Hz. VS's ranged from 0.084 – 0.92 as highest VS's were exhibited by the lower CF units. VS subsequently declined with a corner frequency of ~2 kHz as significant phase-locking was observed as high as 2832 Hz. TD's ranged from 0.059 – 0.88 ms and dropped as characteristic frequency increased. ISIH's showed characteristic peaks that tended to occur at integer multiples of the stimulus period. The first ISIH peak for cells between 100 – 300 Hz occurred either at an interval corresponding to one stimulus period or shorter intervals when multiple spikes occurred during a single stimulus cycle. The first ISIH peak of cells between 300 – 800 Hz all occurred at an interval corresponding to one stimulus period. Higher frequency cells showed a more scattered distribution of first ISIH peaks which usually occurred at an interval greater than one stimulus period. For these higher frequency cells, the first ISIH peak occurred at a mean interval of 1.58 ms (SD 0.46 ms),

which we will call the mean refractory period. Note that the TD's of these units can be orders of magnitude smaller than the refractory period. Thus, the refractory period only limits how often a unit can fire but it does not limit the precision of spike timing when the unit does fire.

### **70** What Can an Ancient Fish Tell Us About the Evolution of Directional Hearing and Frequency Selectivity?

Michaela Meyer<sup>1</sup>, Richard R. Fay<sup>2</sup>, Arthur N. Popper<sup>1</sup>

<sup>1</sup>University of Maryland, Department of Biology, <sup>2</sup>Parnly Hearing Institute and Department of Psychology, Loyola University, Chicago

We investigated frequency tuning and directional responses of single auditory nerve fibers in the lake sturgeon (*Acipenser fulvescens*), a primitive (or "ancient") fish. Sturgeon belong to the order Acipenseriformes, a group of fishes that separated from the "advanced" bony fishes, the teleosts, about 200 million years ago. Our analysis of sturgeon hearing focused on directional selectivity and frequency analysis by auditory neurons, and how responses from these neurons, as compared with other fishes, might contribute to our understanding of how early these basic tasks may have evolved in vertebrate history. Extracellular recordings were made from single afferent neurons during stimulation with a three-axis shaker system that generated linear translatory motion along various axes in the horizontal and mid-sagittal planes of the fish, thereby simulating acoustic particle motion. To test frequency responses, displacements were generated in the vertical plane and the frequency varied between 50 and 1000 Hz.

Spontaneous activity of different cells ranged from a high rate of firing to no activity. Thresholds in response to displacement stimuli differed between units. Most units had cosine-shaped directional response profiles in the horizontal and mid-sagittal planes. Preliminary data show that auditory nerve cells responded better to stimulus angles in the vertical plane at 90 ±20 degrees rather than in the horizontal plane. Such responses appeared to be correlated with the vertical orientation of the sensory epithelium and dorso-ventral orientation of hair cells on the epithelium that are innervated by these neurons. Preliminary data showed best frequencies between 100 and 300 Hz.

The results for sturgeon are consistent with general physiological features found in the periphery of other vertebrates with regard to different strength of spontaneous activity, varying thresholds, phase-coupling, and tuning of auditory nerve fibers. Directional response profiles are similar to those found in teleost fishes, indicating that the physiological mechanism encoding the direction of sound may have arisen very early in vertebrate history.

## **71 Predicting Lateralization Performance at High Frequencies from Auditory-Nerve Spike Timing**

**Anna Dreyer**<sup>1,2</sup>, Andrew Oxenham<sup>2,3</sup>, Bertrand Delgutte<sup>1,3</sup>

<sup>1</sup>*Eaton-Peabody Laboratory, Massachusetts Eye & Ear Infirmary*, <sup>2</sup>*Speech and Hearing Biosciences and Technology, Harvard-MIT Division of Health Sciences and Technology*, <sup>3</sup>*Research Laboratory of Electronics, Massachusetts Institute of Technology*

Psychophysical sensitivity to interaural time differences (ITD) in the envelope of high-frequency sinusoidally amplitude-modulated (SAM) tones is generally poorer than that to low-frequency pure tones (PT). ITD sensitivity at high frequencies might be improved using "transposed stimuli" (TS), which seek to produce the same temporal discharge patterns in high-frequency neurons as in low-frequency neurons for PT. Here, we study ITD sensitivity for PT, SAM tones and TS using neurophysiology, psychoacoustics and computational models.

Phase locking of auditory-nerve fibers in anesthetized cats was characterized using both the synchronization index and autocorrelograms. With both measures, phase locking is stronger for PT than for TS, and for TS than for SAM tones. Phase locking to SAM tones and TS degrades with increasing stimulus level, while remaining more stable for PT.

ITD discrimination was measured in humans for stimuli presented either in quiet or with band-reject noise intended to restrict listening to a narrow frequency band. Performance improves slightly with increasing stimulus level for all three stimuli both with and without noise. ITD sensitivity to TS is comparable to PT performance only in the absence of noise.

To relate psychophysical performance to auditory-nerve activity, we used an optimal binaural processor model with delay lines and coincidence detectors. In the no-noise condition, model performance is stable with stimulus level, consistent with psychophysics. However, in the band-reject noise condition, model performance for SAM tones and TS degrades with increasing level. The model also predicts worse-than-observed performance for TS relative to PT.

These results have implications for the relative roles of peripheral patterns of activity and the binaural processor in accounting for ITD sensitivity at low versus high frequencies.

Supported by NIH grants DC 02258, 05209 and 05216.

## **72 Spectral Coding Based on Cross-Frequency Coincidence Detection of Auditory-Nerve Responses**

**Michael Heinz**<sup>1</sup>

<sup>1</sup>*Johns Hopkins University*

Rate-based spectral coding in the auditory nerve (AN) degrades at high sound levels due to saturation. This degradation is partially overcome in the cochlear nucleus (CN), where an enhancement in spectral-shape coding occurs for several cell types. One possibility is that the

robust temporal representation of spectral shape in the AN is converted into a more robust rate code in the CN.

Nonlinear cochlear tuning associated with outer-hair-cell function produces level-dependent spatio-temporal patterns, which are characterized by increased correlation between nearby best frequencies (BFs) as level increases (Carney, 1994). This study evaluates the contribution of spatio-temporal patterns to enhanced spectral coding based on cross-frequency coincidence detection, a neural mechanism for decoding nonlinear phase cues. It is hypothesized that differences in the cross-frequency correlation near spectral peaks and troughs can be used to enhance spectral coding at high sound levels.

Responses of AN fibers were measured for vowel-like stimuli with spectral features (i.e., formants and troughs) shifted near the BF of each neuron to provide a measure of spectral coding. Shuffled cross correlograms (SCCs), which estimate the cross correlation between the responses of two AN fibers to the same stimulus as a function of delay, were used to predict the discharge rate of cross-frequency coincidence detectors. A method was developed to simulate the responses from several neurons with nearby BFs to the same stimulus using the responses of a single neuron to different stimuli with spectral features shifted around BF.

Vowels with F1 near BF demonstrated the same systematic level dependence in phase responses as for tones near BF. Constraints on using these nonlinear phase responses to overcome rate saturation, which are imposed by differences in traveling wave delays at different BFs, will be illustrated using SCCs.

Supported by an NOHR grant, and NIH/NIDCD grant P30 DC05211.

## **73 Coding of Pitch in the Auditory Nerve: Two Simultaneous Complex Tones**

**Erik Larsen**<sup>1,2</sup>, Leonardo Cedolin<sup>1,2</sup>, Bertrand Delgutte<sup>1,2</sup>

<sup>1</sup>*Massachusetts Institute of Technology*, <sup>2</sup>*Massachusetts Eye and Ear Infirmary*

Often, we listen to sounds consisting of harmonic complex tones in the presence of other harmonic complex tones, for example in symphonic music or in cocktail party situations. Perceptually, listeners can match the pitches of two instruments playing different notes, and a pitch difference aids in segregating sound sources. Physiologically, little is known about the neural basis for this ability. Thus, we investigated the representation of simultaneous pitches in the auditory nerve of anesthetized cats.

We measured the responses of single neurons to two simultaneous complex tones (missing fundamental, equal-amplitude harmonics) with a wide range of fundamental frequencies. The fundamental frequencies of the two tones differed by either 7% or 22%. Each harmonic was about 15 dB above the threshold at CF, corresponding to 20-50 dB SPL. Pitch estimates were obtained from both rate-place (average discharge rate against CF) and temporal (interspike interval distribution) representations of the stimulus.

Highly accurate (rms errors about 1%) estimates of both pitches of the two complex tones were obtained over

nearly the entire range of fundamental frequencies that was investigated using either of the two neural representations. For fundamental frequencies below about 1 kHz, best pitch estimates were obtained from the temporal representation. Also, the lower tone tended to be more prominently represented than the higher tone in interspike interval distributions, an effect reflecting the asymmetry of cochlear filtering. For fundamental frequencies above about 1.5 kHz, best pitch estimates were obtained with the rate-place representation. This limit may be lower in human, if cochlear tuning is sharper than in cat.

In conclusion, the auditory nerve faithfully transmits pitch information for simultaneous complex tones to higher auditory centers.

Supported by NIH Grants DC 02258 and 05209

## **74 Spatio-Temporal Representation of the Pitch of Complex Tones in the Auditory Nerve**

**Leonardo Cedolin<sup>1,2</sup>, Bertrand Delgutte<sup>1,3</sup>**

<sup>1</sup>*Eaton-Peabody Laboratory, Massachusetts Eye and Ear Infirmary,* <sup>2</sup>*Speech and Hearing Biosciences & Technology, Harvard-MIT Division of Health Sciences and Technology,* <sup>3</sup>*Research Laboratory of Electronics, Massachusetts Institute of Technology*

Previous studies of the coding of the pitch of complex tones in the auditory nerve suggest that neither a rate-place representation, nor a temporal representation based on interspike interval distributions fully account for psychophysical data. Here we explore an alternative spatio-temporal representation based on rapid changes in the phase of the cochlear traveling wave at the place of each resolved spectral component (Shamma, J. Acoust. Soc. Am. 78: 1622-1632).

We recorded from auditory-nerve (AN) fibers in anesthetized cats in response to equal-amplitude harmonic complex tones with a missing fundamental frequency (F0). For a given fiber, the F0 range was chosen so that the "harmonic number" CF/F0 varied from 1.5 to 4.5 in order to capture low-order harmonics likely to be resolved. We computed the derivative of the period histogram with respect to harmonic number in order to approximate a lateral inhibitory process operating on the spatio-temporal response pattern of the entire AN.

For F0s below about 1 kHz, the spatial derivative shows local maxima when the CF coincides with a harmonic of F0, thereby giving information about the frequencies of resolved harmonics. Resolved harmonics remain apparent in the spatial derivative even at stimulus levels where the average discharge rate is saturated. For F0s above 1 kHz, the spatio-temporal representation degrades due to poorer phase locking, while the rate-place representation improves as harmonics are better resolved. The spatio-temporal representation is thus consistent with the psychophysical upper F0 limit near 1 kHz to the pitch of missing-fundamental stimuli.

These results suggest that the spatio-temporal representation of pitch may be both more stable with

respect to stimulus level and more consistent with psychophysical data than the rate-place representation.

Supported by NIH grants DC 02258 and 05209.

## **75 Acoustic-Electric Interactions in the Auditory Nerve: Simultaneous and Forward Masking of the Electrically-Evoked Compound Action Potential**

**Kirill Nourski<sup>1</sup>, Paul Abbas<sup>1</sup>, Heil Noh<sup>1</sup>, Charles Miller<sup>1</sup>, Barbara Robinson<sup>1</sup>**

<sup>1</sup>*The University of Iowa*

Combined electric and acoustic stimulation (EAS) is a promising approach to improve the performance of cochlear implants in patients with residual hearing. In such patients, there may be auditory nerve fibers responsive to both acoustic and electric stimuli. Understanding of possible interactions between the two types of stimuli at the level of the auditory nerve is important for developing EAS stimulation paradigms. In this study, we investigated the time course of simultaneous and post-stimulatory effects of acoustic noise on the auditory nerve electrically evoked compound action potential (ECAP).

Adult guinea pigs were used in acute experiments. Broadband acoustic noise (400 ms duration) was used as a masker and biphasic electric pulses, delivered through an intracochlear wire electrode, were used as probe. The onset of the probe was varied relative to the onset of the masker. ECAPs were recorded from the auditory nerve trunk. Masking of ECAP by acoustic noise was measured as a decrease in ECAP amplitude relative to a control (unmasked) condition.

Simultaneous masking featured an onset effect followed by a recovery of ECAP to a steady state. The time course of the simultaneous effects was characterized by a two-component exponential function. Masking increased with both masker and probe level. Post-stimulatory ECAP recovery was non-monotonic: a rapid recovery was followed by a transient depression in ECAP amplitude. This effect was characterized a three-component exponential function with two decaying and a rising component.

Adaptation to acoustic stimulation clearly affects the auditory nerve responses to electric stimuli. Simultaneous masking follows a time course that is comparable to that of the adaptation to an acoustic stimulus. Forward masking functions suggest a multi-component process with refractoriness, adaptation, and subthreshold depolarization possibly contributing to the time course of the recovery.

Supported by NIH Contract N01-DC-2-1005



## **76 Treatment of Spiral Ganglion Explants with Corticosteroids Promotes Both Neuronal Migration and Neuritogenesis While Inhibiting Outgrowth of Fibroblasts**

Alexis D. Furze<sup>1</sup>, Deanna Kralick<sup>1</sup>, Ariel Grobman<sup>1</sup>, Craig Ettelman<sup>1</sup>, Adrien A. Eshraghi<sup>1</sup>, Thomas J. Balkany<sup>1</sup>, Thomas R. Van De Water<sup>1</sup>

<sup>1</sup>University of Miami

The auditory neurons of the spiral ganglion relay impulses from the peripheral auditory receptor to the central nervous system where the perception of sound is processed. In the case where the auditory hair cells have been lost, the auditory neurons become the primary receptor cells for hearing when stimulated by the electrode array of a cochlear implant. Neurotrophic factors (e.g. BDNF) have been assessed experimentally for their ability to stimulate neuritogenesis in spiral ganglion cell explants. In addition to enhancing neurite outgrowth, these neurotrophic factors have also been shown to contribute to the outgrowth of fibroblasts from the ganglion explants.

In an attempt to reduce fibroblastic outgrowth while maintaining the stimulation of neurite outgrowth, the current study investigated the action of several corticosteroid preparations on spiral ganglion explants. The corticosteroids tested included dexamethasone, methylprednisolone, and triamcinolone acetonide. Media preparations without neurotrophic or steroid supplementation and media supplemented with hrBDNF were used for comparison. Neurite and fibroblast outgrowth were quantified using computerized image analysis of images captured from an inverted microscope. Initial results of the current investigation show that spiral ganglion cell explants in media with either dexamethasone or triamcinolone acetonide treatment exhibited significant neurite outgrowth and suppression of fibroblastic outgrowth. The methylprednisolone group showed some neuritic outgrowth but little suppression of fibroblastic outgrowth.

These results suggest that the application of either dexamethasone or triamcinolone acetonide to an injured cochlea could promote neurite regeneration while minimizing fibrosis that leads to a decrease in the level of electrical stimulation required to evoke a response from the auditory neurons in Rosenthal's canal. The results of this study therefore may have a direct application to patients with residual hearing that undergo cochlear implantation and will be treated with bimodal stimulation. Supported by a grant from MED-EL Medical Electronics to TRV and TJB.

## **77 TEM Analysis of Innervation Patterns on Hair Cells in Normal Canary and a Canary with Progressive, Genetic, Inner Ear Abnormality (Belgian Waterslager Canary)**

Brenda Ryals<sup>1</sup>, Elena Sanovich<sup>2</sup>, Ron Petralia<sup>3</sup>, Robert Dooling<sup>2</sup>

<sup>1</sup>James Madison University, <sup>2</sup>University of Maryland, <sup>3</sup>NIDCD/NIH

Belgian Waterslager canaries (BWS) show a rapid, progressive, genetic inner ear abnormality, that results in minimal changes in the number of auditory nerve fibers (Gleich et al 2001) and cells in the first order cochlear nuclei (Kubke et al 2002) in adults. However, no studies have analyzed changes at the level of the adult hair cell synapse. Since many more hair cells are lost (~30%) than neural fibers (~12%) it has been suggested that the remaining adult BWS hair cells may have a greater afferent synaptic density than normal.

In the current study we use serial TEM sections from a position 80% of length from the basal tip of the basilar papilla (BP) to quantify synaptic density in non-BWS and BWS canary. At this position 14-16 hair cells are seen across the width of the non-BWS, BP. Preliminary results from serial reconstruction of 6 hair cells along the neural edge in non-BWS canary show at least two patterns of afferent innervation: 2 hair cells with 5-7 afferent synapses and an occasional single efferent synapse, and 4 hair cells with 1-2 large afferent synapses and no efferent synapses. These preliminary results suggest a synaptic density for neural hair cells in the apical region of the non-BWS, BP which may be similar to the synaptic density reported for neural hair cells in the apical region of barn owl BP (Fischer 1994).

Preliminary observations of TEM serial sections in BWS reveal only 6-8 hair cells across the width of the BP. Reconstruction of hair cells on the neural edge in BWS will be used to quantify synaptic density for comparison with patterns seen in non-BWS. These results offer the first direct measurements of synaptic density on apical hair cells in normal and genetically abnormal canary inner ear and provide a first step toward understanding the synaptic consequences of hair cell loss and regeneration in a bird with progressive, genetic inner ear abnormality.

(Supported by NIDCD R01DC001372 to RJD and BMR)

## **78 Influence of Hearing Loss on the Summed Post-Stimulus Time Histogram and Unit Response Obtained from an Analytic Treatment of the Compound Action Potential**

Jeffery Lichtenhan<sup>1</sup>, Mark Chertoff<sup>1</sup>, Katie Esau<sup>1</sup>

<sup>1</sup>University of Kansas Medical Center

Recently an analytic expression of the compound action potential (CAP) was obtained by convolving a gamma function representing a post-stimulus time histogram summed across auditory nerve fibers [P(t)] with a decaying sine wave representing a single-unit wave form (U(t); Chertoff, JASA 116(5), 2004). Fitting the analytic expression to tone-burst-evoked CAPs recorded from the round window of gerbils with normal auditory thresholds provided an in vivo estimate of P(t) and U(t). The goal of this work is to use the analytic expression to estimate neuronal survival in ears with peripheral hearing loss. The purpose of the present study is to determine the influence of hearing loss on P(t) and U(t).

CAP data were analyzed from our previous noise exposure study (Chertoff et al. JASA 114(6), 2003) where gerbils had been exposed to an 8 kHz band of noise at 117 dB SPL for durations ranging from 1 to 128 hours.

CAPs were recorded in response to 1-, 2-, 4-, 8-, and 16-kHz tone bursts presented at levels ranging from 100 to 15 dB SPL in 5-dB increments. For the current analysis, CAPs from 41 animals evoked by 100 dB SPL tone bursts were fit with the analytic expression using a nonlinear least squares fitting routine. Regression analysis was used to characterize changes in P(t) and U(t) as a function of average CAP threshold at 4, 8, and 16 kHz.

Results showed that P(t) and U(t) varied with hearing loss. For several frequencies, the delay and width of P(t) increased and the height decreased with hearing loss. This indicates that in addition to a decrease in the number of neurons, the location of neurons contributing to the CAP shift apically with high frequency hearing loss. U(t) showed less decay while the frequency of oscillation did not vary with hearing loss, which suggests that apical neurons may have a different discharge pattern than basal neurons, or perhaps the extracellular electrical medium changed as a result of noise exposure.

### **79** Effects of High Sound Pressure Levels in a Model of the Normal and Impaired Auditory Periphery

Muhammad Zilany<sup>1</sup>, Ian Bruce<sup>1</sup>

<sup>1</sup>*Electrical & Computer Engineering, McMaster University, 1280 Main St. W., Hamilton, Ontario, Canada*

A nonlinear phenomenological model for the responses of auditory nerve (AN) fibers in cat has been developed by Carney and colleagues (Carney, JASA 1993; Zhang et al., JASA 2001; Tan and Carney, JASA 2003). The most recent version adds a level-independent instantaneous frequency glide in the basilar membrane (BM) filter, as observed in BM and AN data. The Zhang et al. version of the model has been modified by Bruce and colleagues (JASA 2003) to study the effects of outer and inner hair cell impairment on the AN's representation of speech stimuli.

The goal of this work is to address the effects of high presentation levels on responses to vowels in cat AN fibers by incorporating a level-independent frequency glides in the BM filter of the Bruce et al. model and adding a filter path parallel to the main BM filter to explain multimodal excitation of AN fibers. This model now simulates the shifts in best-frequency (BF) observed in the impaired cochlea or in the normal cochlea at high intensities that can be explained by the interaction of the frequency glide with the nonlinear envelope of the impulse response of the BM. Thus, near 80-100 dB SPL the first formant (F1) AN response grows at the expense of the F2 response which is consistent with the physiological data (Wong et al., *Hear. Res.* 1998). The interactions of the parallel BM filter paths could explain the component 1 (C1)/component 2 (C2) transition usually observed near 100 dB SPL in the rate-level and phase-level functions of AN fibers, which presumably results from multimodal excitation. The implementation of frequency glides and C1/C2 transitions in the Bruce et al. model will be described, and the implications for the neural representation of speech in normal and impaired ears will be discussed.

[This work was supported by NSERC Discovery Grant 261736 and the Barber-Gennum Chair Endowment.]

### **80** Loss of Voltage-dependent Sodium Channels (Nav1.6) from the Spike Generators of the Cochlear Nerve in Mutant *qv<sup>3j</sup>* "Quivering" Mice

Waheeda A Hossain<sup>1</sup>, Matthew N Rasband<sup>1</sup>, D. Kent Morest<sup>1</sup>

<sup>1</sup>*University of Connecticut Health Center, Dept. of Neuroscience*

Previously we localized Nav1.6 channels to sites that may be axonal spike generators: ganglionic initial segments, recepto-neural segments beneath the hair cells, first hemi-nodes in the spiral lamina, and the nodes of myelinated fibers. "Quivering" mice have tremor and auditory dysfunctions attributed to mutations in the  $\beta$ IV-spectrin gene which, along with ankyrin G, stabilizes Nav1.6 channels. We hypothesized that this mutation may result in defective Nav1.6 localization in the cochlea. To test this, we used a highly specific antibody to localize Nav1.6 in the cochleas of quivering 3J mice and their age-matched wildtype littermates.

Compared to the wildtype, little or no staining for Nav1.6 appeared in the mutant organ of Corti, neither in the ganglionic or recepto-neural segments, although these fibers were stained for neurofilament-M. There was some labeling of the first hemi-nodes. Many of the nodes of Ranvier were labeled for Nav1.6, but they were often elongated and disrupted.

Since clustering of channels is critical for spike generation, it is significant that, in the mutant, Nav1.6 was disrupted in the axon initial segments of the cochlear ganglion neurons. The finding that Nav1.6 aggregation still occurs at the first hemi-node indicates that Nav1.6 can still cluster at nodes of Ranvier, even with mutant  $\beta$ IV-spectrin. These results suggest that auditory dysfunction in quivering 3J mice may result from impaired spike initiation in the recepto-neural segments of the afferent axons and flagging support of action potential propagation through the ganglion cell body.

Supported by NIH grants from NIDCD (DKM, WAH) & NINDS (MNR)

### **81** Progesterone Treatment Negatively Affects Hearing in Aged Women

Patricia Guimaraes<sup>1,2</sup>, Susan T. Frisina<sup>1,2</sup>, Frances Mapes<sup>2</sup>, SungHee Kim<sup>3</sup>, D. Robert Frisina<sup>1,2</sup>, Robert D. Frisina<sup>1,2</sup>

<sup>1</sup>*Otolaryngology Dept., Univ. Rochester Medical School,*

<sup>2</sup>*Int. Ctr. Hearing Speech Res., Nat. Tech. Inst. Deaf, Rochester Inst. Tech.,* <sup>3</sup>*ENT Dept., Daegu Fatima Hospital, Dong gu, Daegu, S. Korea*

The effects of female hormones on the development and aging of the human auditory system are not completely understood. We previously reported that hormone replacement therapy (HRT) can negatively impact on the hearing of aged women (Guimaraes et al., ARO Abstr. 2004). The purpose of the present study was to

retrospectively analyze and compare hearing abilities among post-menopausal human subjects (HRT vs. controls). Subjects were treated with Estrogen and Progesterone (E+P); Estrogen alone (E), and a third (control - NHRT) group did not receive any hormonal treatment. The data analyzed were obtained from a total of 54 subjects (N=17, E+P; N=9, E; N= 28, NHRT, matched for age). The criteria for subject selection were: age (60-86 years), relatively healthy medical history, absence of significant noise exposure, middle ear problems and current/heavy smoking. Subject groups were tested for pure tone audiometry, tympanometry, otoacoustic emissions, hearing-in-noise-test (HINT) and contralateral suppression of DPOAEs (distortion product otoacoustic emissions). Our results showed elevated pure tone thresholds in both ears with the "E+P" re the "E" and the control groups (ANOVA,  $p= 0.01$ ) for the right ear and a trend for the left ear. For DPOAE amplitudes, the "E+P" group presented with lower amplitude than "E" and the control groups with significant results for both ears: right ear (ANOVA,  $p=0.005$ ; interaction  $p=0.02$ ) and left ear (ANOVA,  $p=0.005$ ). As for the HINT results, the "E+P" group performed poorer than the "E" and the control groups (ANOVA,  $p=0.04$ ), across all background noise speaker locations. These findings suggest that the presence of progesterone as a component of HRT could be the cause of poorer hearing abilities in aged women taking HRT, affecting both the peripheral and central auditory systems.

Supported by NIH grants NIA P01 AG09524, NIDCD P30 DC05409 and the Int. Ctr. Hearing Speech Res.

### **82 Higher Aldosterone Levels Correlate with Lower Hearing Thresholds in Aged Humans**

**Sherif Tadros**<sup>1,2</sup>, Susan T. Frisina<sup>1,2</sup>, Frances Mapes<sup>1</sup>, D. Robert Frisina<sup>1,2</sup>, Robert D. Frisina<sup>1,3</sup>

<sup>1</sup>Int. Ctr. Hearing Speech Res., Nat. Tech. Inst. Deaf, Rochester Inst. Tech., <sup>2</sup>Otolaryngology Dept., Univ. Rochester Medical School, <sup>3</sup>Otolaryngology, Biomedical Engineering & Neurobiology Depts., Univ. Rochester Medical School

The biological bases of age-related hearing loss – presbycusis, are still being investigated. Hormonal levels may play a role in accelerating or slowing the course of presbycusis. Aldosterone hormone is a mineralocorticoid secreted by the adrenal cortex and controls serum sodium and potassium levels. Aldosterone has a stimulatory effect on expression of sodium-potassium ATPase (Na, K – ATPase) and sodium-potassium-chloride cotransporter (NKCC), both important cell membrane channel proteins. In the present investigation, the relations between serum aldosterone levels and presbycusis, and the correlation between these levels vs. the degree of presbycusis were examined in humans. Serum aldosterone concentrations were compared between normal hearing and presbycusis groups (ages 58 and above), for subjects without major medical problems, middle ear pathology or noise damage. Pure-tone audiometry (PTA), transient evoked otoacoustic emissions (TEOAE), the hearing in noise test (HINT) and gap detection thresholds were measured for each subject. A highly significant difference between subject groups in

serum aldosterone concentrations was found comparing normal vs. hearing loss groups (t-test,  $p=0.0002$ ,  $t=4.06$ ,  $df=45$ , and one-way ANOVA,  $p=0.0029$ ,  $F=5.44$ ,  $R$  squared= $0.275$ ). Highly significant correlations between PTAs in both right and left ears, and HINT scores, vs. serum aldosterone levels were also detected. On the contrary, no significant correlation was seen for TEOAE amplitudes, TEOAE suppression with contralateral noise, and gap detection. We conclude that aldosterone hormone may have a protective effect on hearing in old age, since higher levels were correlated with better hearing. This affects the peripheral and central auditory systems, and inner hair cells more than the outer hair cell system.

Supported by NIH: Grants P01 AG09524 from NIA, P30 DC05409 from NIDCD, and the International Center for Hearing and Speech Research, Rochester NY, USA

### **83 Quantitative Analysis of Age-Related Changes in the Stria Vascularis of Human Cochleae**

**Teruhisa Suzuki**<sup>1</sup>, Yukio Nomoto<sup>1</sup>, Takayuki Nakagawa<sup>2</sup>, Naofumi Kuwahata<sup>1</sup>, Hiroshi Ogawa<sup>1</sup>, Koichi Omori<sup>1</sup>

<sup>1</sup>Fukushima Medical University, <sup>2</sup>Kyoto University, Graduate School of Medicine

Human temporal bone and animal model studies have indicated that degeneration of the stria vascularis (SV) is included in the pathogenesis for age-related sensorineural hearing loss. However, there are few documents showing quantitative analysis of age-related changes of the SV in human cochleae. In this study, we quantitatively assessed age-associated atrophy of the SV using human temporal bones. We referred to medical records of 1278 human temporal bones and chose according to following criteria: 1) no histories of ear disease 2) no apparent hearing loss 3) no asymmetry in hearing levels. Then, 23 ears obtained from individuals under 50 years (younger group) and 31 ears obtained from individuals over 70 years (older group) were provided for morphological analysis. One mid-modiolus section of each temporal bone was used for quantitative analysis. We measured the areas of the cochlear duct and SV in each turn of cochleae, and calculated the SV ratio (area of SV/that of a cochlear duct x 1000). The difference in the hearing levels and SV ratio between two groups was statistically examined by unpaired t-test. The hearing levels for the younger group was 18.0 and 13.2 dB SPL (mean and SD) and for the older group 36.1 and 11.7 dB. The difference in the hearing level between the two groups was statistically significant. The SV ratios (mean and SD) in the basal turn of cochleae were 4.90 and 1.66 for the younger group and 3.63 and 1.18 for the older group, those in the middle turn were 4.92 and 1.06 for the younger group and 4.82 and 1.55 for the older group and those in the apical turn were 5.58 and 1.70 for the younger group and 4.97 and 1.77 for the older group. The difference in SV ratios in the basal turn between them was significant, but that in the middle or apical turn was not significant. These findings indicate that atrophy of the SV in the basal turn is included in common features in age-related degeneration of cochleae.

## **84** Aging and Auditory Temporal Order Recognition

Peter Fitzgibbons<sup>1</sup>, Sandra Gordon-Salant<sup>2</sup>, Sarah Friedman<sup>2</sup>

<sup>1</sup>Gallaudet University, <sup>2</sup>University of Maryland

This study investigated the effects of listener age and hearing loss on the recognition of temporal order within three-tone stimulus sequences. The stimulus sequences featured random permutations of the frequencies 500, 1000, and 2000Hz, with equal tonal inter-onset intervals (IOI) ranging from 150-500ms across conditions of different sequence presentation rates. For each sequence rate, the relative influences of tone duration and temporal spacing on order recognition were also examined by variation of the IOI duty cycle from 25-100%. The duty-cycle changes were implemented to determine whether variations in processing time would influence the recognition performance of older listeners. Based on earlier speech recognition data, we hypothesized that the performance of older listeners would benefit significantly by the extended tonal durations associated with larger sequence duty cycles. Listeners were younger (18-44yrs) and older (65-76 yrs) persons with either normal hearing or mild-to-moderate sensorineural hearing losses. The results showed temporal order recognition of all listeners was influenced primarily by sequence presentation rate, but was largely independent of tonal duty cycle. The performance of older listeners was generally poorer than younger listeners, with the largest age-related differences observed for the faster presentation rates. The effects of hearing loss on recognition performance were minimal.

## **85** Relationships Between Binaural Speech Intelligibility and Monaural Hearing Tests for Aged Listeners

SungHee Kim<sup>1</sup>, Susan T Frisina<sup>2,3</sup>, Fray M Mapes<sup>2</sup>, D. Robert Frisina<sup>2,3</sup>, Robert D Frisina<sup>2,3</sup>

<sup>1</sup>Daegu Fatima Hospital, Daegu, Republic of Korea,

<sup>2</sup>International Center for Hearing and Speech Research, NTID, RIT, Rochester, NY, USA, <sup>3</sup>Department of Otolaryngology, University of Rochester, Rochester, NY, USA

It is sometimes hard to classify the audiogram because of different audiometric configurations, particularly concerning bilateral hearing. It is well known that speech intelligibility predictors available today are to a large degree based on the articulation index (AI). The present study evaluates hearing parameters as predictors for speech intelligibility in different situations, using the hearing-noise-test (HINT) in subject groups with symmetrical and asymmetrical hearing loss. Retrospectively, the audiologic data was reviewed for 207 subjects who underwent pure tone audiometry and HINT. The symmetric hearing loss group (Gs) was defined as having less than 11 dB differences between the two ears. Their calculated AI differences ranged up to 0.15. The group with asymmetric hearing loss (Ga) had more than 0.15 of calculated AI interaural differences. To assess the effects of hearing loss, age was matched between the two groups. Group Gs (N=57, 72.7±6.2 SD yr) and group Ga

(N=30, 74.5±5.0 SD yr) were utilized to get the correlation coefficients between the hearing parameters (PTA averages, and AIs) and HINT results. In Gs, all HINT results were significantly correlated with PTA averages and AIs. HINT results in quiet (HINT Q) showed the best correlations, then HINT N0, HINT N270, and HINT N90, respectively. Interestingly, speech frequency PTA (0.5, 1 and 2 kHz) correlated better in the quiet condition, whereas the higher frequency PTA average (1, 2 and 4 kHz) correlated better with the background noise conditions. For Ga, the correlation with HINT Q was similar to that of Gs, however, the correlations for HINT N were worse than those of Gs. Higher frequency hearing is more important for the noisy listening conditions. In asymmetric hearing, the both ears in combination showed better correlates than one ear, in the HINT Q and N0.

Supported by NIH: Grants P01 AG09524, P30 DC05409, and the International Center for Hearing and Speech Research, Rochester NY, USA.

## **86** Measures of Auditory Perception as a Function of Age and Hearing Sensitivity

D Frisina<sup>1</sup>, David Eddins<sup>1,2</sup>, Chandler Marietta<sup>3</sup>

<sup>1</sup>International Center for Hearing & Speech Research, Rochester Institute of Technology, Rochester, NY,

<sup>2</sup>Psychoacoustics Laboratory, University at Buffalo, Buffalo, NY 14214, <sup>3</sup>Otolaryngology Department, University of Rochester School of Medicine, Rochester, NY 14642

It is well known that coincident with the aging process is a degradation in auditory function at multiple levels within the auditory pathway. A test-battery approach is frequently used to assess the auditory function at these different levels. One goal of the present study was to evaluate the degree to which the components of a test battery, composed of commonly used auditory tests, provide independent information about auditory function. The test battery was composed of speech, non-speech, and standard audiometric measures. Speech tests included monosyllabic word recognition (NU-6) in quiet, ipsilateral, contralateral, and diotic noise backgrounds; the HINT in quiet and noise presented from three locations (0, 90, 270 degrees); and the synthetic sentence index (SSI). Non-speech tests included the detection of 500 and 2000 Hz tones masked by spectrally notched noise and temporal gap detection in low-pass noise (500 and 4000 Hz). Standard audiometric measures included pure-tone threshold, the articulation index, spondee thresholds, and transient evoked otoacoustic emissions (TEOAE) in quiet or with contralateral suppression. To evaluate the primary factors of age and hearing abilities, four groups of twelve listeners (six male, six female) were tested: young normal hearing, elderly normal hearing, elderly mild hearing loss, and elderly moderate hearing loss. Preliminary analyses suggest a clear relationship between hearing sensitivity and performance on each of the speech in quiet and speech in noise tasks with poorer performance associated with degree of hearing loss. Likewise, performance indices on the notch-noise masking task also indicated an inverse relationship between hearing sensitivity and frequency selectivity. More detailed analysis will be used

to explore the relations among measures and their respective contributions to developing a profile of auditory function. (Work supported by National Institute on Aging, P01 AG09524).

### **87 Effects of Aging on the Perception and Neural Representation of Time-Varying Spectral Cues**

Ashley Harkrider<sup>1</sup>, Patrick Plyler<sup>1</sup>, Mark Hedrick<sup>1</sup>

<sup>1</sup>University of Tennessee

Differences in phonetic boundaries versus normal controls suggest that listeners with hearing impairment have difficulty categorizing stop consonant place of articulation based solely on the dynamic spectral information present in the second formant transition, even when stimuli are presented at increased levels. This may be due partly to a degraded ability of the central auditory nervous system (CANS) to process time-varying spectral cues. Because comparisons often are made between young listeners with normal hearing versus older adults with hearing impairment, the effects of aging, separate from hearing loss, on the CANS may not be considered. To determine if older versus younger listeners have more difficulty processing spectral cues, psychometric functions and slow cortical evoked responses were compared in 11 young (mean = 26 years) and 10 older (mean = 55 years) listeners with normal hearing. Stimuli were synthetic consonant-vowels along a /ba/ to /da/ to /ga/ place-of-articulation continuum in an unshaped and shaped condition. Shaped stimuli enhanced audibility of the spectral information present in the second formant transition. Behavioral and electrophysiological results indicate that aging significantly affected the processing of dynamic spectral information present in the second formant. For some measures, differences due to aging were minimized with spectrally-shaped stimuli.

### **88 Psychophysical Assessment of Hyperacusis in Tinnitus Patients**

Sylvie Hébert<sup>1</sup>

<sup>1</sup>Université de Montréal

It has often been suggested that tinnitus is associated with hyperacusis. However, empirical bases for this assumption are lacking. In a previous study (Hébert, & al, 2004), we had measured hyperacusis psychometrically in tinnitus patients and found that the group of patients with high tinnitus-related distress had a mean score that represents strong auditory sensitivity, and that was about 1.7 higher than the one obtained by the group of patients with low tinnitus-related distress and over three times higher than the one obtained by the matched control group. In this study, the psychoacoustical bases of sound intolerance were examined in tinnitus patients and controls without tinnitus. A categorical loudness scaling procedure was used. Three series of 1,000Hz tones of all possible sound levels (in 5dB steps) ranging between threshold level +5dB and discomfort level (up to 120dB HL) were presented. The extreme values (threshold and discomfort levels) were previously determined for each participant by a standard clinical procedure. Participants had to categorize each

sound as being Very weak, Weak, Comfortable, Loud, or Very loud. A psychophysical scale was built by subtracting the threshold value of each participant from his or her mean value found for each category (thus all participants had zero as threshold value). Results indicate that when comparing Tinnitus ears with Non-tinnitus ears in participants with unilateral tinnitus, there was no difference in sound levels in any category. However, when Tinnitus ears of tinnitus participants with either unilateral or bilateral tinnitus were compared with Non-tinnitus ears of Control participants with no tinnitus, lower levels were found in the Tinnitus group for all categories. For instance, a sound was judged comfortable at a lower intensity for Tinnitus participants than for Controls. This effect was maintained even when considering absolute values in the high intensity range (i.e., without subtracting the threshold value), where loudness recruitment should have kicked in, thus rendering unlikely an explanation of this effect as being attributable to hearing loss rather than to tinnitus. These findings therefore support the clinical observation and psychometrical assessment that Tinnitus patients have greater sensibility to sounds than Non-tinnitus patients, and that hyperacusis relies more likely on central, rather than peripheral, mechanisms.

### **89 Taurine Activates Glycine Receptors in Neurons of Rat Inferior Colliculus**

Han Xu<sup>1</sup>, Tian-Le Xu<sup>2</sup>, Lin Chen<sup>1</sup>

<sup>1</sup>Auditory Research Laboratory, School of Life Sciences, University of Science and Technology of China, <sup>2</sup>Institute of Neuroscience, Shanghai Institute for Biological Sciences, Chinese Academy of Sciences

Taurine (Tau) is one of the most abundant free amino acids in the mammalian nervous system including the auditory system. Tau has been known to play multiple roles in developmental and physiological functions. However, whether or not Tau regulates or modulates the neurotransmission of the central auditory system is not clear. In the present study, we investigated electrophysiological and pharmacological properties of Tau-activated currents in neurons of the inferior colliculus (IC) recorded with whole-cell patch clamp techniques. The neurons prepared for recordings were acutely and mechanically dissociated from the IC of Wistar rats aged P10-P14. Our data show that Tau activated an inward current and its half-maximal activation concentration was equal to 0.37 mM (n = 6) at a holding potential of -60 mV and under a condition of chloride equilibrium potential near 0 mV. The measured reversal potential of Tau-activated currents was close to theoretical chloride equilibrium potential. Strychnine, a glycine receptor antagonist, almost completely inhibited the currents evoked by Tau at both low (1 mM) and high (10 mM) concentrations. The Tau-activated current, however, was not affected by bicuculline, a GABA(A) receptor antagonist. An increase in Tau concentrations progressively reduced the current response to subsequent glycine application. Tau-activated current and glycine-activated current were mutually cross-desensitized by each other at saturated concentrations. Our study demonstrates that Tau activates glycine receptors rather than GABA(A) receptors under our

experimental conditions and is a full agonist on glycine receptors in this central auditory region. The study also indicates that the ionic mechanism of the action of Tau is an increase in chloride conductance across the neuronal membrane. Based on these results, we speculate that Tau may have a role in regulating or modulating the neurotransmission of the IC through influencing glycine receptors.

Supported by the National Natural Science Foundation of China (30270380) and the Knowledge Innovation Project from the Chinese Academy of Sciences (KSCX 2-SW-217).

## **90** Distribution of the Vesicular Glutamate Transporters VGLuT1 and VGLuT2 in Central Auditory Nuclei

Rafael Luján<sup>1</sup>, Joaquin Soriano<sup>1</sup>, Elena Caminos<sup>1</sup>, Carmen Diaz<sup>1</sup>, Juan Ramon Martinez Galán<sup>1</sup>, **Jose M. Juiz<sup>1</sup>**

<sup>1</sup>Medical School, Universidad de Castilla-La Mancha, 02006 Albacete, Spain

Glutamate is the major central excitatory neurotransmitter, including the auditory pathway. Identification of auditory neurons releasing glutamate is important to understand the functional organization of neuronal circuits involved in auditory processing. Such identification has been hampered by the lack of markers with sufficient specificity to label neurons and neuronal elements, particularly synaptic endings, involved in excitatory glutamatergic neurotransmission. Antibodies to glutamate, metabolic precursors, and synthetic or degradative enzymes are limited in that they label glutamatergic and non-glutamatergic neuronal populations. We analyzed the immunocytochemical distribution of the vesicular glutamate transporters VGLuT1 and VGLuT2 in central auditory nuclei. Wistar rats were perfused transcardially with 2 to 4% paraformaldehyde. Brain stem sections containing different auditory nuclei were incubated with anti-VGLuT1 or anti-VGLuT2 polyclonal antibodies and immunoreactivity was detected either with immunoperoxidase or immunofluorescence methods. VGLuT1 immunoreactivity was abundant and intense in the cochlear nucleus and superior olivary complex. Immunolabeling was present in structures resembling axonal endings, a finding confirmed using double labeling experiments with anti-synaptophysin antibodies. In the anteroventral cochlear nucleus and medial nucleus of the trapezoid body, many labeled endings had the usual morphology associated with endbulbs and chalyces of Held, embracing or decorating unlabeled cell bodies. Other VGLuT1 labelled structures had a more bouton-like appearance. With respect to VGLuT2, this transporter seemed to be less abundant than VGLuT1 and followed a different distribution pattern. Thus, VGLuT2 is present in bouton-like structures of the cochlear nucleus and superior olivary complex. Some regions and layers of the dorsal cochlear nucleus were particularly enriched in VGLuT2 immunolabeling. These findings strongly suggest that VGLuTs are specifically concentrated in excitatory synaptic endings. Differences in the distribution of VGLuT1 and VGLuT2 indicate that there may be molecular and

functional differences among populations of excitatory endings in auditory brain stem nuclei, which require further study.

Supported by grants PAI-03-015 (Consejería de Ciencia y Tecnología, JCCM) and BFI2003-09147-CO2-02 (Ministerio de Ciencia y Tecnología), Spain.

## **91** Central Auditory Pathways Mediating the Rat Acoustic Reflex

**Daniel Lee<sup>1,2</sup>**, Ronald DeVenecia<sup>1,2</sup>, John J. Guinan<sup>1,2</sup>, M. Christian Brown<sup>1,2</sup>

<sup>1</sup>Eaton-Peabody Laboratory, Massachusetts Eye and Ear Infirmary, <sup>2</sup>Department of Otolaryngology, Harvard Medical School

The neurons of the acoustic reflex pathway coordinate the activity of the middle ear muscles to protect the inner ear from intense acoustic stimuli and to reduce masking. The central auditory pathways mediating the reflex are poorly understood. Identifying the brainstem interneurons necessary for reflex function is essential to improving our understanding of these central pathways. Insight into these interneurons requires a sensitive assay of acoustic reflex function. An approach described by Relkin (ARO 2000-2001) is to monitor the change in levels of the primary tones and distortion product otoacoustic emissions (DPOAE) during a period of an acoustic reflex-evoking stimulus. We demonstrate such primary tone and DPOAE changes during the presentation of a contralateral broad band noise in the anesthetized rat. These changes could be explained by middle ear muscle contraction, which increases the impedance of the middle ear. Consistent with this view, administration of a neuromuscular blocker to paralyze the middle ear muscles results in elimination of the changes. Using this assay as our reflex metric, we investigated the regional distribution of acoustic reflex interneurons in the rat cochlear nucleus by focally injecting kainic acid. Kainic acid is a neurotoxin that destroys cell bodies while preserving axons of passage, such as the auditory nerve. Preliminary studies suggest that focal injections in the ventral cochlear nucleus result in elimination of noise-evoked primary tone and DPOAE changes. These findings imply that the central pathways of the acoustic reflex proceed through the ventral cochlear nucleus. Supported by the NIDCD.

## **92** Differential Expression of Potassium Channel Kv2.1 in the Adult Mouse Cochlear Nucleus

**Janet Fitzakerley<sup>1</sup>**, Mark Quale<sup>1</sup>

<sup>1</sup>University of Minnesota

In the cochlear nucleus (CN), as in other parts of the brain, neuronal excitability is modulated by the expression pattern of voltage-gated potassium channels. We determined previously that the delayed rectifier channel, Kv2.1, is expressed in the mouse CN, and that upregulation of Kv2.1 occurs during development (Fitzakerley et al., 2003). In this study, the pattern of distribution of Kv2.1 positive neurons and their identity was

more completely characterized using double-labeling immunohistochemical techniques and confocal imaging.

Kv2.1-immunohistochemical labeling was found in many cells, including most projection neurons, in all 3 CN subdivisions. As described previously, the octopus cell region of the posteroventral CN (PVCN) was notably devoid of Kv2.1-containing neurons. Kv2.1-labeled cells could be divided into two categories, depending upon the nature of the Kv2.1 clustering. A relatively small population of neurons had a punctate distribution of label surrounding the cell soma. These punctate cells were predominately found in granule cell domains, were less than 100  $\mu\text{m}^2$  in size, and many were glutaminergic in nature. Non-punctate cells predominated in the magnocellular regions of CN, and could be either glutaminergic or GABAergic. Cells of intermediate size were the most strongly labeled in these regions. Small immunoreactive puncta were scattered throughout all CN regions, including the octopus cell area.

Other researchers have suggested that restricted localization of Kv2.1 may play an important role in the contribution of this potassium channel to the regulation of dendritic  $\text{Ca}^{2+}$  transients (Antonucci et al., *Neuroscience*. 2001;108(1):69-81). If similar mechanisms are present in CN, it can be inferred from the data collected in this study that differential targeting of Kv2.1 may contribute to the unique patterns of dendritic excitability exhibited by CN neurons.

This research was supported by NIDCD grant #R29DC03737.

### **93 Intrinsic Mechanisms Regulating the Spike Timing of DCN Pyramidal Cells**

**Sarah E. Street<sup>1</sup>**, Paul B. Manis<sup>1</sup>

<sup>1</sup>*University of North Carolina Chapel Hill*

We previously reported that pyramidal cells of the dorsal cochlear nucleus (DCN) can fire reliable and precise trains of action potentials in response to time varying input, such as a frozen noise current. A number of different ion channels could play important roles in how these cells respond to time-varying inputs. Two particular channels that could influence behavior after a hyperpolarization are the hyperpolarization-activated cation current ( $I_h$ ), and a rapidly inactivating potassium current ( $I_{KIF}$ ). In the present experiments, we sought to determine how these channels influence spike timing in pyramidal cells in rat brainstem slices. In the first set of experiments, we tested whether blocking  $I_h$  with 10  $\mu\text{M}$  ZD7288 would decrease the reliability and precision of spike trains locked to the noise. There was no significant change in reliability and precision after blocking  $I_h$ . We next embedded a simulated IPSP (sIPSP) in the noise to test the contribution of  $I_h$  on reliability and precision after hyperpolarizations similar to those provided by inhibitory inputs. Blocking  $I_h$  also did not affect the reliability and precision of the spike trains after the sIPSP. The rapidly inactivating potassium current is thought to be generated by Kv4.2 channels. We found that r-Heteropodatoxin, a peptide toxin, was able to block at least part of  $I_{KIF}$  in outside-out somatic patches, consistent with the potential involvement of Kv4.2 in this

current. We then used dynamic clamp to subtract  $I_{KIF}$ -like currents from the cell. Subtracting small amounts of  $I_{KIF}$  with the dynamic clamp improved the precision of the first spike after the sIPSP. We conclude that  $I_{KIF}$  appears to play a role in regulating spike timing after an IPSP whereas  $I_h$  is less important. (Supported by DC00425 to PBM.)

### **94 Differential Regulation of Action Potential Signaling in Principal Neurons of the MSO and MNTB During Development.**

**Luisa Scott<sup>1</sup>**, Nace Golding<sup>1</sup>

<sup>1</sup>*University of Texas, Austin*

Principal neurons of the medial superior olive (MSO) exhibit biophysical specializations that allow them to detect microsecond interaural time differences. To address whether the intrinsic properties of MSO neurons mature after hearing onset, we made 103 whole-cell somatic current-clamp recordings (35°C) in brainstem slices from P14-38 gerbils. In the two weeks after hearing onset (~P12), a 3-fold reduction occurred in input resistance ( $20.3 \pm 2.3 \text{ m}\Omega$  to  $7.3 \pm 0.5 \text{ m}\Omega$ ) and membrane time constant ( $0.9 \pm 0.1 \text{ ms}$  to  $0.30 \pm 0.01 \text{ ms}$ ). Also, action potential (AP) amplitude at the soma decreased by nearly 6-fold ( $38.3 \pm 2.9 \text{ mV}$  to  $6.7 \pm 0.6 \text{ mV}$ ). These changes occurred largely in the first week of hearing. Further experiments suggest that the reduction in AP size does not reflect different initiation sites for small and large APs. During simultaneous somatic and dendritic current-clamp recordings, APs of all amplitudes were detected first at the soma and subsequently backpropagated into the dendrites with >60% attenuation at sites >80  $\mu\text{m}$  from the soma (P16-17; n=5). These experiments suggest that AP initiation occurs near the soma/axon with little backpropagation in the dendrites. Furthermore, in the presence of 40-80 nM dendrotoxin-K, the membrane time constant and input resistance increased ~3-fold and AP amplitude increased 4-fold (P20-21; n=5) showing that Kv1.1-containing K<sup>+</sup> channels contribute significantly to MSO neurons' electrophysiological features and are likely developmentally-regulated. In contrast with MSO neurons, input resistance, membrane time constant and AP amplitude remained comparatively stable in MNTB principal neurons (P14-37; n=18); thus, maturation of these parameters after hearing onset is not a general feature of all time-coding auditory neurons. Taken together, our findings display a dramatic, developmentally-regulated electrical segregation of the AP initiation zone and the somato-dendritic compartment in MSO neurons. Supported by DC 006877, 006341

### **95 Gene Transfection using Electroporation Visualizes Nociceptin Neurons in the Inferior Colliculus of the Rat**

**Motoi Kudo<sup>1</sup>**, Kousuke Taki<sup>1</sup>, Takaaki Nakamura<sup>1</sup>, Kiyoshi Kurokawa<sup>1</sup>

<sup>1</sup>*Shiga University of Medical Science*

Nociceptin (also called orphanin FQ) is an endogenous opioid-like peptide, of which function is known to be

distinct in many aspects from other opioids in the pain researches. In the auditory processing, nociceptin and its receptor system have been shown to play an important role at the midbrain levels, particularly associated with the regulation of neuropathological disorder such as tinnitus, audiogenic seizures and age-related hearing loss. In order to characterize nociceptin expressing neurons in the inferior colliculus (IC), we made a series of experiments as follows: cholera toxin B subunit (CTB) gene was connected with prepronociceptin promoter region 5kb long upstream to the exon I and designed to be expressed under the control of prepronociceptin promoter. This artificial DNA was injected into the IC, and an electric field was administered. 48h after the transfection, the rats were perfused. The brainstem was removed and detected for the reporter gene, CTB. Some of the IC neurons were successfully stained with anti-CTB antibody. These neurons were distributed not only in the external nucleus and the dorsal cortex but also in the central nucleus. In the double immunofluorescent paradigm, almost all the CTB immunoreactive neurons had GABA and nociceptin immunoreactivity. We thus successfully visualized nociceptin neurons throughout the IC. The present results substantiates crucial role of nociceptin in central auditory mechanisms, opening new opportunities in the treatment of the central hearing disorders.

Supported by Grants-in-Aid Scientific Research 15500234 and 15700273 from Japan Society for the Promotion of Science.

### **96 Upregulation of Sound-Induced c-Fos Expression in the nNOS Knockout Mouse**

**Meredith Garcia**<sup>1</sup>, **Jonathan Zoller**<sup>2</sup>, **Richard Harlan**<sup>1</sup>  
<sup>1</sup>Tulane University Health Sciences Center, <sup>2</sup>Tulane University

Upregulation of Sound-Induced c-Fos Expression in the nNOS Knockout Mouse.

Nitric oxide [NO] is a neuroactive molecule that is produced by the enzyme neuronal nitric oxide synthase [nNOS]. Our previous studies have demonstrated that inhibition of nNOS results in increased expression of the immediate-early gene c-Fos in the absence of sound, suggesting that NO may exert a tonic inhibitory effect in the central auditory system. To further characterize the role of nitric oxide neurotransmission in the central auditory system, we studied the effect of sound stimulation on c-Fos expression in the nNOS knockout mouse [nNOS KOM]. Our hypothesis was that basal and sound-induced levels of expression would be higher in nNOS KOM than in wild-type [WT] mice. nNOS KOM and appropriate WT controls were obtained from the Jackson Laboratory [Bar Harbor, ME] and were kept under sound attenuation on the night before the experiment. On the following morning, groups of mice [n=5] were either exposed to a 10 kHz tone pulse for 40 min, followed by 80 min of silence, or were kept in silence for 2 hr. Following this, they were deeply anesthetized with pentobarbital [100 mg/kg] and perfused transcardially with phosphate-buffered saline followed by 3% neutral buffered paraformaldehyde. Brains were removed and processed for c-Fos immunoreactivity [ir]

using procedures standard in our labs [e.g. Garcia et al 1995]. Levels of c-Fos-ir in the auditory systems of WT mice not exposed to sound were quite low. However, in the nNOS KOM, there was elevated expression of c-Fos-ir within the dorsal cochlear nucleus [DCN], inferior colliculus [IC] and primary auditory cortex [Au1] in the absence of sound. In sound-stimulated WT mice, there was increased c-Fos-ir in DCN, IC and Au1, but not in medial geniculate [MG]. In nNOS KOM, however, there was a much larger sound-induced increase of c-Fos-ir in DCN, IC, Au1 and also in MG. These data provide further support for an inhibitory role for NO in central auditory processing. Supported by a grant from the ATA to MMG.

### **97 No Regulation of c-Fos Expression by 7-Nitroindazole in the nNOS Knockout Mouse**

**Jonathan Zoller**<sup>1</sup>, **Richard Harlan**<sup>2</sup>, **Meredith Garcia**<sup>2</sup>

<sup>1</sup>Tulane University, <sup>2</sup>Tulane University Health Sciences Center

Our previous studies have shown that inhibition of neuronal nitric oxide synthase [nNOS] with the selective inhibitor 7-Nitroindazole [7-NI] results in increased expression of the immediate-early gene c-Fos in the absence of sound. To further characterize the role of the nNOS pathway in the central auditory system, we studied the effect of 7-NI on c-Fos expression in the nNOS knockout mouse [nNOS KOM]. Our hypothesis was that basal levels of c-Fos expression in the nNOS KOM would resemble that seen in the 7-NI treated rat, and that treatment of nNOS KOM with 7-NI would not have an effect on c-Fos levels with or without sound. nNOS KOM were obtained from the Jackson Laboratory [Bar Harbor, ME] and were kept under sound attenuation on the night before the experiment. On the following morning, groups of mice [n=5] received an injection of 7-NI [50 mg/kg, ip] or no injection, and 30 min later were exposed to a 10 kHz tone pulse for 40 min, followed by 80 min of silence, or were kept in silence for 2 hr. They were then deeply anesthetized [pentobarbital 100 mg/kg] and perfused transcardially with PBS followed by 3% buffered paraformaldehyde. Brains were removed and processed for c-Fos immunoreactivity [ir] using procedures standard in our labs [e.g. Garcia et al 1995]. In the nNOS KOM without sound, c-Fos-ir was elevated within the dorsal cochlear nucleus [DCN], inferior colliculus [IC] and primary auditory cortex [Au1], in a pattern that was similar to that seen in rats in response to 7-NI. In the nNOS KOM with sound, c-Fos levels were greatly increased over no sound, including increases in medial geniculate. In 7-NI treated nNOS KOM, in the presence or absence of sound, there was no difference in c-Fos-ir when compared to untreated nNOS KOM. These data show that inhibition of nNOS genetically or pharmacologically produces similar effects, and provide further support for an inhibitory role for NO in central auditory processing. Supported by a grant from the ATA to MMG.



## **98** Auditory Electrophysiology of the MdxCv3 and Dy Mice Show Abnormal Latencies Which May Provide Evidence for One Basis of Cognitive Defects Found in Duchenne Muscular Dystrophy

De-Ann Pillers<sup>1</sup>, J. Beth Kempton<sup>1</sup>, Dennis Trune<sup>1</sup>

<sup>1</sup>Oregon Health & Science University

**Introduction:** Neurosensory electrophysiology is characterized by two major markers: the amplitude of the response to a stimulus, and the time interval until the response peaks. In auditory physiology, this time interval is referred to as the latency, whereas in visual electrophysiology, it is known as the implicit time. We have shown abnormalities in the implicit time of the electroretinogram in the mdxCv3 mouse model versus the mdx which is normal, and sought to determine whether any parallels could be drawn in the auditory pathway.

**Methods:** Auditory brainstem response (ABR) audiometry to pure tones was used to evaluate cochlear function. 14 mdx, 4 mdxCv3, 9 dy, and 13 age-matched control (C57BL/6J and C57BL/10ScSn) male mice were tested. The ABR thresholds to tone-burst stimuli at 4, 8, 16, and 32 kHz were obtained for each ear and statistically compared (ANOVA) for potential group differences. Latencies were determined for wave IV and plotted against intensity.

**Results:** Both mdx and mdxCv3 mice demonstrated normal ABR thresholds when compared with controls. However, the latency response curves showed significant differences between the two mouse models. Although the mdx curve overlapped with that of the normal mice, that of the mdxCv3 showed significant shortening of the wave IV latency ( $p < 0.05$ ). On the other hand, dy mice had significantly higher thresholds and longer latencies than controls ( $p < 0.05$ ).

**Discussion:** Abnormalities in latency in auditory brainstem response testing can provide evidence for asynchrony in signal processing. Disorders with such asynchrony can be associated with cognitive defects. A subset of patients with Duchenne muscular dystrophy have cognitive defects ranging from dyslexia to mental retardation. Genotype-phenotype correlations in man have shown that 3' DMD mutations, such as that found in the mdxCv3 mouse, are predominantly associated with the cognitive defects. We speculate that the abnormal latency in the auditory response may provide evidence of a physiologic basis for these cognitive defects.

## **99** Changes in Arc and Homer Gene Expression in Rat Central Auditory System Following Sudden Hearing Loss-Preliminary Results

Bo Du<sup>1</sup>, Dalian Ding<sup>1</sup>, Ping Wang<sup>1</sup>, Wei Sun<sup>1</sup>, Haiyan Jiang<sup>1</sup>, Richard Salvi<sup>1</sup>

<sup>1</sup>Center for Hearing and Deafness, University at Buffalo

Sudden hearing loss from cochlear pathology is accompanied by roaring tinnitus and a significant decline in neural activity flowing from the cochlea into the central auditory system. Central auditory structures presumably

respond to this diminished neural input by rapidly altering the expression of genes and proteins related to synaptic function. Homer is a family of postsynaptic density (PSD) proteins that interacts with group I metabotropic glutamate receptors and other proteins that regulate synaptic activity. Arc (Arg3.1), an activity-regulated cytoskeleton-associated protein induced through NMDA-receptor dependent mechanisms, has been implicated memory formation and lesion-induced synaptic plasticity. Since Arc and Homer have been linked to changes in synaptic function, we hypothesized that Arc and Homer expression might be altered significantly during the early stages of sudden hearing loss. To test this hypothesis, we used quantitative RT-PCR to quantify the change in gene expression of Arc and Homer-1a in the rat cochlear nucleus (CN), inferior colliculus (IC) and auditory cortex (AC) 2-4 days following sudden hearing loss induced by co-administration of ethacrynic acid (EA, 100 mg/kg, iv) and gentamicin (150 mg/kg, im). Auditory function, measured with the ABR, was rapidly and permanently abolished following EA-GM treatment. Cochleas evaluated 2-4 d post-treatment showed a total loss of outer hair cells and ~40% loss of inner hair cells. Our preliminary results showed a large increase in Arc mRNA expression in AC and IC 2 days post-treatment followed by a rapid decline below control values by day 4. Arc expression in CN showed a large decline between 2 and 4 days post-treatment. Homer-1a expression in IC, AC and CN showed a significant decrease by day 2 and generally remained quite low except for the IC which showed some recovery on day 4. Our preliminary results suggest the changes of Arc and Homer-1a may play an important role regulating synaptic function in the central auditory pathway following sudden hearing loss.

Supported NIH R01 DC06630-01, American Tinnitus Association and Tinnitus Research Consortium

## **100** Developmental Differences in Death and Survival Gene Expression Could Define a Critical Period of Deprivation-Induced Neuron Loss in the Mouse AVCN

Julie Harris<sup>1,2</sup>, Edwin Rubel<sup>1,2</sup>

<sup>1</sup>University of Washington, Virginia Merrill Bloedel Hearing Research Center, Dept. Otolaryngology-HNS, <sup>2</sup>Graduate Program in Neurobiology and Behavior

Deprivation of peripheral input in young animals results in dramatic neuron death in the anteroventral cochlear nucleus while the same manipulation performed in older animals does not result in significant loss. The molecular basis underlying this critical period of differential susceptibility to loss of afferent input remains largely unknown. We used Affymetrix Mouse 430A Gene Chips to identify groups of genes differentially expressed in the cochlear nucleus during and after this critical period. Three ages were examined; during the critical period at postnatal day (P)7, when the critical period window closes at P14, and one week after the critical period ends at P21. Of the 22,690 genes surveyed, 380 genes were increased at P7 compared to both P14 and P21, and 381 genes were increased at both P14 and P21 compared to P7.

Interestingly, there were only 30 differentially expressed genes between the P14 and P21 CN. Of the 761 total genes that were differentially expressed during and after the critical period, 9 are directly involved in pro-apoptotic pathways and 7 have pro-survival roles. Importantly, 7 out of the 9 pro-apoptotic genes are expressed more highly during the critical period (e.g. caspase 3, BID, p75). In contrast, 5 out of the 7 pro-survival genes are expressed more highly after the critical period when AVCN neurons survive peripheral deprivation (e.g. ICAD, alphaB crystallin). We hypothesize that multiple neuroprotective mechanisms increase and pro-apoptotic factors decrease over development to protect mature neurons against stressful insults, making them less dependent on afferent input for survival. *Supported by NIDCD grants DC03829, DC07001, and DC04661*

### **101 Deafferentation-Induced Change in Glutathione S Transferase Expression in the Chick Cochlear Nucleus**

**Alexander Nicholas<sup>1</sup>**, Richard Hyson<sup>1</sup>

<sup>1</sup>Florida State University

Neurons in the chick cochlear nucleus, nucleus magonocellularis (NM), rely on activity from the auditory nerve for trophic support. If this activity is disrupted by cochlea removal, it results in atrophy, increased  $[Ca]^{2+}$ , altered oxidative enzyme capacity and ultimately the death of approximately 20-30% of the cells in NM. Previous studies in other systems have shown that the balance between prooxidant and antioxidant molecules is crucial in determining neuronal fate following stress induction. Moreover, those studies show an upregulation of detoxifying enzymes such as glutathione s transferase (GST) can initiate neuroprotective cascades. The purpose of this study was to determine whether GST, an antioxidant that has been known to protect cells following the induction of stress, is upregulated following deafferentation. Unilateral cochlea removal was performed on P7-P10 chicks. Subjects were then allowed to survive for periods ranging from 1 hour to 3 days. Immunocytochemistry was performed to visualize changes in GST expression. Opposite sides of the same tissue section were compared for analysis. GST expression dramatically increased as early as 6 hrs following cochlea removal. Interestingly, this elevation in GST coincides with an increased level of reactive oxygen species (ROS). This is also the time at which cells are dividing into living and dying populations based on analyses of protein synthesis. Taken together, these data support the hypothesis that ROS signaling may play a significant role in determining the fate of NM neurons following the loss of afferent input.

### **102 Early Postnatal K<sup>+</sup>-Cl<sup>-</sup> Cotransporter (KCC2) Expression does not Render Hyperpolarizing Effects of GABA in Spherical Bushy Cells of Gerbil**

**Ivan Milenkovic<sup>1</sup>**, Rostislav Turecek<sup>2</sup>, Thomas Reinert<sup>1</sup>, Marco Heinrich<sup>1</sup>, Mirko Witte<sup>1</sup>, Rudolf Rübtsamen<sup>1</sup>

<sup>1</sup>Faculty of Biosciences, Pharmacology, and Psychology, University of Leipzig, Leipzig, Germany, <sup>2</sup>Institute of Experimental Medicine, Academy of Sciences, Prague, Czech Republic

Spherical bushy cells (SBC) of the mammalian cochlear nucleus transmit phase-locked activity of the auditory nerve in pathways that contribute to sound localization based on interaural time differences. However, the firing of SBC is determined not only by an excitation through glutamate but rather by an interaction between excitatory and inhibitory inputs (GABAergic and glycinergic). Depolarizing action of GABA and glycine, observed as a striking developmental feature of diverse CNS structures, shift to hyperpolarizing during the second postnatal week, due to the Cl<sup>-</sup> extrusion maintained by the K<sup>+</sup>-Cl<sup>-</sup> cotransporter KCC2. Therefore, we addressed the expression of KCC2 in SBC and investigated GABA-evoked responses in early postnatal development by means of gramicidine-perforated patch clamp and Ca<sup>2+</sup> imaging. Obtained data revealed depolarizing, GABA<sub>A</sub>-receptor mediated, responses in SBC as mature as P14 (onset of hearing is at P12). E<sub>GABA</sub> was depolarized with respect to V<sub>m</sub> and exogenous GABA elicited dose-dependent Ca<sup>2+</sup> signals. Immunohistochemical staining of the AVCN revealed rather early KCC2 expression in SBC. While the anti-KCC2 immunoreactivity at P1 and P5 was rather diffuse, the shift in the distribution of KCC2 towards the SBC plasma membrane and proximal dendrites was observed between P7 and P9. The membrane staining remained pronounced in P14 and P30 SBC. Taken together, these experiments indicate that GABA could retain a depolarizing effect on SBC even after the onset of hearing. Moreover, they revealed that the expression of KCC2 and its incorporation into the plasma membrane are not sufficient *per se* to reverse the GABA<sub>A</sub>-mediated responses from depolarizing to hyperpolarizing. However, considering the maturity of the SBC examined, we cannot rule out the possibility that inhibitory neurotransmission in AVCN develops delayed with respect to the onset of hearing.

### **103 The Effects of Sounds Reflected from the Ground on the Spatial Response Fields of Neurons in the Gerbil Inferior Colliculus**

**Katuhiko Maki<sup>1</sup>**, Shigeto Furukawa<sup>1</sup>

<sup>1</sup>NTT Comm. Sci. Labs., NTT Corp.

In an ecologically realistic environment, sounds arriving at ears include sounds reflected from the ground as well as direct sound. We examined the auditory spatial response fields (SRF) of neurons in the inferior colliculus (IC) of anesthetized gerbils in the presence of sound reflected from the ground, and compared them with results obtained under traditional free-field conditions. The stimuli we used

were virtual acoustic space (VAS) stimuli, and they were presented to the gerbils binaurally through earphones. The VAS stimuli were generated based on the quasi-individual external-ear transfer functions (Maki and Furukawa, 2004, *ARO. Abs.*, 27: 612.) of a standing animal measured in the presence / absence of sandy ground, which was intended to simulate the Mongolian desert to which the gerbil is native. Single-unit responses were recorded from the central and the external nuclei of the IC (ICc and ICx, respectively). The ICc units exhibited several types of SRF. The presence of reflected sound tended to alter the SRF patterns. The effects of the reflection could be explained in terms of the interaction between the reflection-induced changes in the signal spectrum and the unit's frequency response area. In the ICx, a higher-order processing stage for the auditory space information, most units exhibited spatial tuning to specific direction in the contralateral hemisphere regardless of the presence of the reflected sound. We evaluated the sharpness of the SRF tuning of the ICx units by using the centroid vector length (CVL), which we calculated as follows: For stimulus directions where the spike rate was  $\geq 50$  % of the maximum rate, the response for each direction was presented as a vector with a length proportional to the spike rate and with a direction corresponding to the stimulus direction. The length of the sum of the vectors was defined as CVL. A greater CVL indicates sharper tuning. The CVL of about 30 % of the recorded ICx units increased by  $> 20$  % (i.e., tuning sharpened) in the presence of the reflected sound, and no units exhibited a CVL decrease of  $> 20$  %. The effects could not be explained in terms of the interaction between the signal spectrum and the unit's frequency response area. The results suggest that, in gerbils, the neural spatial selectivity measured in a free-field would underestimate the effective selectivity in an ecologically realistic environment.

### **104 Interaural Level Difference Discrimination Thresholds and Virtual Acoustic Space Minimum Audible Angles for Single Neurons in the Lateral Superior Olive** **Daniel J. Tollin<sup>1</sup>**

<sup>1</sup>*Department of Physiology, University of Wisconsin, Madison, WI*

Sound azimuth is determined by two main acoustical cues, interaural time and level (ILD) differences. Psychophysically, cats can discriminate changes in the azimuth of noise sources, the minimum audible angle (MAA), of 3-6°. When stimuli are presented to cats over headphones, ILDs of ~1 dB can be discriminated. The lateral superior olive (LSO) is one of the most peripheral structures in the auditory pathway at which inputs from both ears first converge. While it has been hypothesized that ILDs are first extracted at the LSO, it is unknown whether LSO neurons can signal changes in ILD or azimuth with a resolution comparable to the psychophysical data. To test this hypothesis, we examined the ability of LSO neurons of the barbiturate-anesthetized cat to signal changes in 1) the 'azimuth' of noise sources and 2) the ILDs of pure tones via the

discharge rates of the neurons. The virtual acoustic space technique was used to manipulate the 'azimuth' of stimuli presented independently to the two ears over headphones by digitally filtering noise with the head-related transfer functions of a 'standard' cat. ILDs for pure tones were manipulated by holding the signal level to one ear constant and varying the signal level at the opposite ear. Detection theory was used to compute the smallest increment in 'azimuth' and ILD just necessary to discriminate that change based on the discharge rate and associated response variability of each neuron. For midline sources, neural MAAs were as low as 2.3° with a median of 4.5° (N = 32 neurons). For off-midline sources, MAAs were as low as 1.4°. With a base ILD of 0 dB, ILD increments of  $< 1$  dB could be discriminated, with a median of 3.75 dB (N = 38 neurons). For base ILDs away from 0 dB, thresholds were as low as 0.5 dB. Individual LSO neurons at the first site of binaural interaction can signal changes in sound azimuth and in ILD that match or exceeded the behavioral capabilities of cats and humans. NIDCD R01-DC006865

### **105 Neural Correlates of Behavioral Thresholds to Interaural Time Differences**

**Charles Ebert, Jr<sup>1</sup>, Mihir Patel<sup>1</sup>, Charles Coffey<sup>1</sup>, Allen Marshall<sup>1</sup>, Jonathan Skaggs<sup>1</sup>, Douglas Fitzpatrick<sup>1</sup>**  
<sup>1</sup>*University of North Carolina*

One of the most important binaural cues for sound localization and separation of signals is the interaural time difference (ITD). Humans can detect an ITD as small as 10-20  $\mu$ s. However, animals tend to localize sound more poorly than do humans. Rabbits, for example, have sound localization thresholds of ~20°, while humans can localize sound within about 2°. Thresholds for ITDs in animals are generally not known. The acuity with which single neurons can detect ITDs is comparable to ITD threshold in humans, and it has therefore been suggested that behavioral thresholds follow the thresholds of the most sensitive neurons (Shackleton et. al. *J Neurosci* 23:716-724, 2003). To make this comparison directly, however, it is necessary to compare neural and behavioral thresholds to ITD in the same animal. For these reasons, we measured behavioral and neural discrimination of ITDs in the rabbit. The behavioral task was conditioned avoidance and the stimulus was broadband noise (500-1500 Hz). A tracking procedure was used to determine thresholds. The neural thresholds were measured in neurons of the inferior colliculus to similar stimuli, using signal detection methods. The behavioral threshold for ITDs across three animals ranged from 40-80  $\mu$ s, i.e. worse than in humans but comparable to a rabbit's sound localization threshold. The neuronal acuity in the best neurons was on the order of 15  $\mu$ s, which is roughly equivalent to values reported for human performance, but much better the rabbit's behavior. Thus, the behavior in rabbits was better predicted by the precision of the average neuron, rather than the best neuron. This indicates that ITDs are extracted via a population code using neurons with a range of tuning precision.

**106 The Representation of Interaural Timing Differences in the Inferior Colliculus Examined using High-Frequency “Transposed” Noise**

Sarah Griffin<sup>1</sup>, David McAlpine<sup>1</sup>

<sup>1</sup>University College London

Interaural timing differences (ITDs) in low-frequency sounds provide a cue for sound localisation and for signal detection in noise. In the Jeffress model (Jeffress 1948), ITDs are detected by a matrix of neurons tuned to specific ITDs and encoding discrete spatial positions; neurons in each frequency channel encode the full range of possible ITDs. Recent evidence does not support the Jeffress model in mammals. In vivo recordings in the medial superior olive of the gerbil (Brandt *et al.* 2001) and in the inferior colliculus (IC) of the guinea pig (McAlpine *et al.* 2002) and cat (Hancock & Delgutte 2004), suggest that ITD-sensitivity is dependent on neuronal characteristic frequency; low-frequency neurons were tuned to the longest ITDs and high frequency neurons were tuned to the shortest ITDs. In addition, a theoretical consideration of ITD coding concluded that a Jeffress matrix of neurons does not optimally encode low-frequency ITDs in the mammal.

ITDs are also detectable in the envelope of complex, high-frequency sounds. To determine whether recent observations of frequency dependence in ITD tuning is observed in response to ITDs in the envelope of high-frequency sounds, we investigated the range of ITDs encoded by neurons using high-frequency “transposed” noise. Single unit, extracellular recordings were made from the IC of guinea pigs in response to transposed noise with a constant spectrum level and a variable bandwidth. The ITD at the peak or trough of the ITD tuning function was estimated and compared with the envelope frequencies represented. Using this approach we address the question of how ITDs in the envelope of high-frequency sounds are represented in the IC, including the dependence of ITD tuning on modulation frequency, rather than pure-tone frequency.

*S.Griffin is sponsored by the Wellcome Trust 4 year PhD programme in Neuroscience.*

**107 The Effect of Intensity on ITD Tuning to Pure Tones**

Douglas C. Fitzpatrick<sup>1</sup>, Mihir R. Patel<sup>1</sup>, Charles S. Ebert, Jr.<sup>1</sup>, Joshua C. Demke<sup>1</sup>

<sup>1</sup>Univ. of NC at Chapel Hill

The auditory system compares the time of arrival of signals at each ear to localize sound sources and improve signal detection. To achieve this, binaural neurons fire when inputs from the two sides arrive in coincidence; however, due to peripheral processes, the times of arrivals of the inputs vary with intensity. Most models of how the brain processes ITDs are based on the Jeffress model and assume that inputs from both sides are from the same characteristic frequency (CF) region in the cochlea. If so, changing the intensity in both ears should affect the timing from both sides equally, thus causing no change in the

interaural delay. Other models however, use mismatched frequency inputs as the source of interaural delays. In this case, changing the intensity at both ears should affect the ITD tuning to pure tones. To test this, we recorded the ITD tuning to pure tones as the intensity was varied in neurons in the inferior colliculus (IC) of the unanesthetized rabbit. We used two paradigms, one was to record the ITD tuning while an interaural intensity difference (IID) was introduced, while the other was to vary the intensity at both ears equally. Most neurons show changes in ITD tuning when the IID was varied. In most neurons, the direction of change in the ITD tuning shifted toward longer ipsilateral delays as the intensity at the contralateral ear increased. When the intensity was varied equally in both ears most neurons also showed a shift in ITD tuning but the shift could be to increased ipsilateral or contralateral delays. These results are consistent with mismatched frequency inputs from the two sides and suggest that the mismatches can be in either direction. However, another possibility is that changes in ITD tuning with intensity are due to central inhibitory effects rather than peripheral effects. We are currently using frequencies well away from CF where peripheral changes with intensity should be minimal to test this possibility.

**108 The Representation of Sound Location Information among Neural Populations in the Inferior Colliculus**

Steven Chase<sup>1</sup>, Eric Young<sup>1</sup>

<sup>1</sup>Johns Hopkins University

Auditory processing occurs in multiple parallel streams in the auditory brainstem. These streams converge in the central nucleus of the inferior colliculus (ICC) in a manner that is not well understood. Ramachandran *et al.* (1999) have shown the existence of three classes of units (types V, I, and O) in the ICC of decerebrate cats that are hypothesized to receive their dominant input from the MSO, LSO, and dorsal cochlear nucleus, respectively. We use information theoretic techniques to probe the representation of sound information among these neural populations.

We have designed three sets of virtual space stimuli that vary in ILD and one of: ITD, the first spectral notch (SN) of head related transfer functions, or average binaural intensity (ABI). By quantifying the mutual information (MI) between the rate responses and the stimulus parameters, we can investigate separately the dual coding of the parameters with very few assumptions about the method of coding itself.

With the exception of the ABI/ILD stimulus set, we do not find a segregation of spatial location cue information among the unit types, despite the fact that the form of the representation (as assessed by rate v. parameter curves) varies with unit type. Rather, it appears that redundant copies of the information exist in each processing stream. When probing with the ABI/ILD stimulus set, we find that type-V units devote the majority of their response to ABI coding while type-I and -O units devote their responses to ILD coding. We find no differences in the overall representation of ILD among type-I and type-O units,

however, suggesting a convergence of binaural inputs to both unit types. In fact, when using a measure of binaural sensitivity that compares the fraction of variance accounted for by contralateral level manipulations to the fraction of variance accounted for by ipsilateral level manipulations, we find that type-I and -O units tend to show more binaural sensitivity than type-V units.

(Supported by NIH grants DC00115, DC05742, and DC05211)

### **109 Estimation of Preferred Spatial Direction in Guinea Pig Auditory Cortex: Spike Rate Vs. First Spike Latency**

**Susanne Sterbing-D'Angelo<sup>1</sup>**

<sup>1</sup>*Vanderbilt University*

It has been proposed that the latency of the onset response of neurons in the auditory cortex carries more information about acoustic space than the spike count. In this study, single-neuron responses to spatial sounds were recorded in the primary auditory cortex of the ketamine-anesthetized guinea pig. The spatial receptive fields were measured along perpendicular tracks to the cortical surface using high-impedance glass microelectrodes. Spatial broadband noise bursts were delivered via insertional earphones in a virtual auditory environment based on each animal's individual head-related transfer functions for sound directions distributed over the upper hemisphere. The analysis examined whether mean first-spike latency (FSL) and spike rate lead to the same estimate of the preferred direction (PD). Only neurons without spontaneous activity were included. Both PD estimates matched for only about 25% of the neurons. The estimate based on the shortest FSL deviated on average by 55 degrees (SD: 54 degrees) from the PD based on spike rate. Unlike spike rate, FSL often did not vary systematically or did not vary at all with sound direction, i.e., FSL values for all or most directions were within  $\pm 1$  SD of the FSL at PD based on spike rate. In general, the SD of FSL for each unit was small (median: 2.46 ms, mean: 5.14 ms). The results indicate that FSL codes sound source direction ambiguously, if at all, and lead to the conclusion that spike rate might be the more robust code for acoustic space in the primary auditory cortex.

### **110 Binaural Inhibition and Interaural Time Difference Coding in the Frog Dorsal Medullary Nucleus.**

**Jakob Christensen-Dalsgaard<sup>1</sup>, Morten Kannev<sup>1</sup>**

<sup>1</sup>*Institute of Biology, University of Southern Denmark*

The dorsal medullary nucleus (DMN) is the first nucleus in the anuran auditory pathway that is binaurally innervated and therefore a likely candidate for processing of the binaural cues for directional hearing, i.e. interaural time differences (ITDs) and interaural level differences (ILDs). We have studied binaural and directional processing in cells in the frog dorsal medullary nucleus (DMN) stimulated with dichotic sound (couplers) and free field sound. In the closed-field setup the two ears were decoupled acoustically by opening the mouth of the frog

(crosstalk less than -15 dB). We found a group of binaural cells where an excitatory response could be inhibited by contralateral stimulation at ITDs within 1 ms (typically when CL stimulus was leading). In a number of cells a further increase of CL stimulus intensity caused the inhibitory effect to decrease. Therefore, the cells in this population probably had at least three inputs: one IL excitatory input and two CL inputs, one excitatory and one inhibitory. In all binaural cells, including the high frequency cells (BFs up to 1.4 kHz) the inhibitory response showed periodicity with the period of the stimulus frequency. Therefore, the cells probably encode phase rather than onset disparities, which presupposes a phase locked input. In primary (VIIIth nerve) fibers phase locking is weak at frequencies above 1 kHz, but may still be sufficient to explain the results.

In free-field measurements the strength and timing of the binaural inputs will depend on sound direction as processed by the auditory fibers. Thus, the directionality of DMN cells is caused by both monaural directional cues generated by acoustical coupling of the eardrums and non-tympanic pathways as well as binaural interaction. Most DMN cells show ovoidal directional characteristics and the directionality is sharpened compared to that of auditory nerve fibers. We suggest that the sharpening is due to the inhibitory interactions.

### **111 Sound Localization in Monaurally Deafened Ferrets: Comparing Behavioural and Cortical Responses**

**Rob Campbell<sup>1</sup>, Andreas Schulz<sup>1</sup>, Andrew King<sup>1</sup>**

<sup>1</sup>*University of Oxford, Laboratory of Physiology*

We measured the behavioural accuracy of azimuthal sound localization at a range of sound levels (56-84 dB SPL) in adult ferrets that had been deafened in one ear during infancy. In addition to the obvious reduction in localization accuracy on the ablated side, the performance of these ferrets became significantly worse as the sound level was increased. This effect is not seen over this range of sound levels in animals with normal hearing. Physiological studies have shown that whilst the spatial receptive fields of cortical neurons increase in size at higher levels, the transmitted information relating to sound-source direction does not change. Such results have been used to argue for a role for auditory cortex in sound localization, even though cortical neurons do not appear to be specialized for this task. With a view to exploring this issue further, we recorded the free-field directional responses of cortical neurons in anaesthetized, monaurally-deafened ferrets. Azimuthal response profiles were measured using broadband noise bursts presented at two sound levels (56 and 84 dB SPL) and at the same locations as those used during behavioural testing.

Neural responses were approximated with von Mises basis functions to obtain an analytical description of each neuron's azimuthal response profile. A maximum likelihood approach was used to estimate the error between true stimulus direction and that predicted by the population of neurons. We observed marked similarities between localization accuracy measured behaviourally and the

predicted neural population error. Furthermore, preliminary analysis suggested that, in keeping with the behavioural data, the neural population errors were greater at higher sound levels.

This work was funded by the Wellcome Trust

### **112 Acoustic Measurements in a Typical Experimental Setting Used for Primate Neurophysiology**

**William D'Angelo<sup>1</sup>**, Alan Musicant<sup>2</sup>, Troy Hackett<sup>1</sup>, Susanne Sterbing<sup>1</sup>

<sup>1</sup>*Vanderbilt University*, <sup>2</sup>*Middle Tennessee State University*  
Historically, neurophysiological experiments with behaving primates have used an animal secured in a primate chair and tested in a small room. To study the auditory system, most approaches make use of external loudspeakers to approximate a "free field" condition. This paradigm includes experiments studying auditory spatial localization. We hypothesized that the use of external loudspeakers in this situation provides a confounded sound field that alters the cues used for sound localization. While some investigators have attempted to attenuate reflections by fitting the walls with acoustic foam, primate chairs often have three reflective surfaces close to the animal's ears. To test how the primate chair and a typical laboratory setup influence the sound field at the ears, we have measured binaural impulse responses using a KEMAR acoustic mannequin fitted with Knowles microphones. Data will be presented demonstrating the effects of 4" open-cell acoustic foam (AlphaWedge, Acoustical Solutions) covering the walls. Additionally, the acoustic effects of a typical primate chair were assessed by positioning the KEMAR head in the neckplate of the chair.

### **113 Auditory Stream Segregation in the Barn Owl's Space Map: Modeling**

**Clifford Keller<sup>1</sup>**, Terry Takahashi<sup>1</sup>

<sup>1</sup>*University of Oregon*

In a nature, sounds from multiple objects sum at the eardrums, generating complex cues for sound localization and identification. In this clutter, the auditory system must determine "what is where". We examined this process of stream segregation in the auditory space map of the barn owl (*Tyto alba*) using two virtual sources simultaneously emitting sinusoidally amplitude modulated (SAM'd) uncorrelated noises. The sources were separated horizontally, vertically, or diagonally by 30 deg. Each source's SAM (55 & 75 Hz) was our operational definition of sound identity. Here, we model the neural responses (reported separately) to these stimuli. We computed the time-varying, frequency-specific, average binaural level [ABL(t,f)] and interaural differences in time and level [ITD(t,f), ILD(t,f)] generated at the eardrums for all spatial configurations, using individualized head transfer functions. To predict a neuron's response for each stimulus configuration, binaural cues were converted to "distances" from a neuron's preferred values, estimated per Spezio et al. (2003 J N'sci 23:4677). A neuron's responses, weighted by its frequency tuning, were

assumed to be proportional to these distances. The contribution of each frequency band was summed and the predicted responses charted as a function of the sources' average positions. Like the recorded neurons, this model generated two foci of activity at appropriate locations, locked predominantly to the SAM of each source. Examination of the acoustics revealed that in some frequency bands, ITD & ILD fluctuated noisily, often attaining values far beyond that of each source. In other bands, the fluctuations were bounded by the values of each source. ITD & ILD, however, reached the values of each individual source at both 55 and 75 Hz, suggesting that binaural differences cannot be used, unambiguously, to assign temporal features to sources. ABL, by contrast, fluctuated in synchrony with either 55 or 75 Hz over large swaths of space surrounding each source. Multiplying ABL(t,f) with ITD(t,f) & ILD(t,f) allowed the binaural differences to select within these large swaths, generating focal regions responding in synchrony with the SAMs of the sources at those loci. This model behavior was confirmed neurophysiologically.

### **114 Auditory Stream Segregation in the Barn Owl's Space Map: Neurophysiology.**

**Terry Takahashi<sup>1</sup>**, Clifford Keller<sup>1</sup>

<sup>1</sup>*University of Oregon*

In a natural acoustical environment, sounds from multiple sources sum at the eardrums, generating complex cues for sound localization and identification. In this clutter, the auditory system must determine "what is where". We examined this process of stream segregation in the auditory space map of the barn owl (*Tyto alba*) using two sources simultaneously emitting sinusoidally amplitude-modulated (SAM'd), uncorrelated noise bursts in virtual auditory space (VAS). The AM of each source (55 & 75 Hz; 50% depth) constituted our operational definition of the sounds' temporal features. The sources, separated horizontally, vertically, or diagonally by 30° in VAS, were passed through the spatial receptive field (SRF) of isolated neurons in the owl's inferior colliculus (82 cells, 10 birds). The spike rates evoked were plotted as a function of the center of the VAS sound-source pair, generating a spatial response profile (SRP). The neurons responded to each source separately in all spatial configurations, generating SRPs with clearly segregated foci of activity at appropriate loci. The overall spike rate at each focus in the SRP, however, was lower than that evoked by a single source. The successful resolution of the two vertically-arranged sources cannot be explained by binaural cross-correlation because the two sources' interaural time differences were identical. The spike trains were also locked strongly to the AM of the source in the SRF (target), and the sound from the other source (masker), 30° away, had minimal influence. Two sources SAM'd at the same rate were successfully resolved, suggesting that the mechanism is based on differences of fine structure. The spike rate and synchrony to the target were stronger if the masker was farther than the target from the binaural acoustical axis, i.e., the direction giving rise to the highest average binaural level (ABL). Accordingly, the balance of the responses could be biased by changing the relative ABLs

of the two sources to compensate for the acoustical axis. The acoustical cues and the neuronal responses to these cues were modeled and are presented separately. (Supported by grants from the NIDCD (DC03925), McKnight Foundation)

### **115** Relative Contribution of Gna and Gklt Conductances in Dendrites of Mso Neurons

Gytis Svirskis<sup>1</sup>, Vibhakar Kotak<sup>1</sup>, Dan Sanes<sup>1</sup>, John Rinzel<sup>1,2</sup>

<sup>1</sup>Center for Neural Science, New York University, <sup>2</sup>Courant Institute of Mathematical Sciences, New York University

Sodium and  $I_{KLT}$  currents have been shown to be important for coincidence detection in MSO neurons. We investigated the properties of these currents in the dendrites with in vitro somatic recordings by using stimulation of synaptic terminals located on the dendrite and by altering dendritic membrane potential  $V_{den}$  with application of a DC field. Excitatory synaptic currents were evoked by passing negative current pulses through a pipette near the dendrite visualized with Lucifer Yellow. When soma membrane potential  $V_{soma}$  was hyperpolarized to -70mV, the evoked synaptic currents were biphasic in 55% of MSO cells, and the second component lasted <2ms. With  $V_{soma} = -40mV$ , the second component was absent. These properties suggest the presence of  $V_{den}$ -dependent, inactivating, inward currents, presumably sodium, in the dendrites of MSO neurons. In a second set of experiments, we used DC field stimulation to check for the presence of  $I_{KLT}$  in the dendrites after blockade of  $I_h$  current. Due to the nearly symmetric bipolar shape of MSO neurons a DC field changes  $V_{soma}$  relatively little compared to changes of  $V_{den}$ . Modeling results predict that if  $I_{KLT}$  is primarily dendritic its distal shunting biases  $V_{soma}$  responses toward hyperpolarization for both positive and negative DC fields. However, in experiments the small  $V_{soma}$  responses changed almost linearly as the field strength was varied from negative to positive suggesting the absence of dendritic  $I_{KLT}$ . The addition of DTX 1 (blocker of  $I_{KLT}$ ) enhanced the responses to DC field by eliminating shunting at the proximal membrane. Together, the results suggest that a dendritic  $G_{Na}$  enhances dendritic synaptic excitation and the role of  $G_{KLT}$  is restricted to the somatic region.

Supported by: NIH/NIMH MH62595-01, NIH DC00540

### **116** Intracellular Study of Auditory Coincidence Detector Neurons in Owls

Kazuo Funabiki<sup>1,2</sup>, Masakazu Konishi<sup>2</sup>

<sup>1</sup>Kyoto University Graduate School of Medicine, <sup>2</sup>Division of Biology, California Institute of Technology

The classical Jeffress model of sound localization uses axonal delay lines and coincidence detector neurons to encode interaural time differences (ITD). In the avian auditory system, the second order station, nucleus magnocellularis (NM), provides axonal delay lines and the third order station, nucleus laminaris (NL), coincidence detectors. However, little is known about the cellular mechanisms of coincidence detection, which have long been the subjects of discussion and modeling. Here, we

report the results of in vivo intracellular recordings from the barn owl's NL. We used coaxial glass electrodes in which one (microelectrode) was inserted into a patch-electrode type capillary. The inner sharp electrode was protected by the outer one during penetration into NL located 7-10 mm from the brain surface.

We isolated 140 NL cells from 16 owls and achieved intracellular recordings in 38 of them, as judged by a sudden DC potential drop and the resting membrane potential (mean resting potential = -58 ± 17 mV). NL neurons produced small spikes and oscillatory potentials whose waveform closely resembles the superposition of the tones delivered to the two ears (Sound Analogue PSPs:SAP). The amplitude of SAPs varied as a function of ITD from maximum for coincidence to minimum for out of phase signals. Spike rates changed in linear proportion to the amplitude of SAP. We assume that SAPs result from binaural convergence of phase-locked inputs from NM. Because the initial segment of the owl's laminaris neuron is covered with myelin, the spike initiating site is thought to be the 1st node of Ranvier, which is 60 micron away from the soma (Carr et al. 1993). This remote site accounts for the small spikes recorded in the soma.

### **117** Sensitivity of the Auditory Middle Latency Response of the Guinea Pig to Interaural Level and Time Differences

Shigeto Furukawa<sup>1</sup>, Katuhiro Maki<sup>1</sup>

<sup>1</sup>NTT Communication Science Labs, NTT Corp.

The auditory middle latency response (MLR) recorded from the temporal cortex of the guinea pig consists of robust positive and negative peaks for post-stimulus times of ~15 to ~40 ms. The present study examined the extent to which the MLR was sensitive to cues for sound localization such as the interaural level and time differences (ILD and ITD, respectively). The guinea pig was anesthetized with a mixture of ketamine-hydrochloride and xylazine, and a silver-ball electrode was placed on the dura over the auditory cortex as the active electrode. A needle electrode on the neck muscle served as the reference electrode. The stimulus was a biphasic click with a duration of 100  $\mu$ s, presented monaurally or binaurally with various ILD and ITD. We found a robust MLR to a contralateral click, whereas no appreciable response was observed for an ipsilateral click. As previously reported, the MLR exhibited a binaural interaction: the MLR amplitudes for diotic stimulation were intermediate between those for the contralateral and the ipsilateral stimulations alone. The MLR amplitudes decreased with ILD when the ipsilateral level was increased from -20 to +20 dB relative to the contralateral level. As regards the ITD, the MLR amplitudes decreased monotonically as the relative timing of the bilateral clicks was progressively varied from contralateral-leading to ipsilateral-leading. The steep slope of the amplitude-versus-ITD function fell within an ITD range of  $\pm 500 \mu$ s, which includes the guinea pig's physiological ITD range. The response reduction due to the ILD increase could be eliminated by decreasing the ITD by a certain amount, which was parallel to the psychophysical "time-intensity trading" in sound

localization exhibited by human listeners. The results imply that the binaural interaction in the guinea pig MLR reflects the neural processes that are involved in sound localization.

### **118 Sound Localization Deficits During Unilateral Or Bilateral Reversible Deactivation of Cat Primary Auditory Cortex And/Or the Dorsal Zone**

Shveta Malhotra<sup>1</sup>, Ameer J. Hall<sup>1</sup>, G. Christopher Stecker<sup>2</sup>, Ian A. Harrington<sup>3</sup>, Ewan A. Macpherson<sup>3</sup>, John C. Middlebrooks<sup>3</sup>, Stephen G. Lomber<sup>1</sup>

<sup>1</sup>University of Texas at Dallas, <sup>2</sup>VA Research Service, VA-NCHCS, <sup>3</sup>University of Michigan

Our earlier work has shown that combined unilateral deactivation of primary auditory cortex (A1) and the dorsal zone (DZ) results in sound localization deficits restricted to the contralateral hemifield. Recent physiological and anatomical studies suggest that DZ is both functionally and structurally distinct from A1. In this study, we examined the behavioral contributions of A1 and DZ to sound localization during both unilateral and bilateral reversible deactivation of each area. Cats were trained to attend to a central visual stimulus and then approach a 100-ms broadband, white-noise burst emitted from one of 13 loudspeakers arranged in an arc at 15-deg intervals. Each cat was implanted bilaterally with separate cryoloops over A1 and DZ. Prior to deactivation, normal performance at all positions was 90-95% correct. *Unilateral Deactivation:* Combined or single deactivations of A1 and DZ resulted in sound localization deficits in the contralateral, but not ipsilateral hemifield. On average, accuracy at all contralateral targets dropped by 86.3% during combined cooling of A1 & DZ, and by 49.7% and 35.4% during individual deactivation of A1 or DZ, respectively. During A1 cooling, the majority of errors were small in magnitude ( $\leq 30$  deg from the target), while during cooling of DZ the majority of errors were larger in magnitude ( $> 30$  deg from the target). *Bilateral Deactivation:* Deactivations of A1 & DZ resulted in accuracy dropping by an average of 87.0% (A1 & DZ), 55.2% (A1), and 25.9% (DZ). The median error magnitude was greatest during deactivation of DZ (45 deg - A1 & DZ, 30 deg - A1, 60 deg - DZ), as was the percentage of errors made to the incorrect hemifield (16.8% - A1 & DZ, 3.7% - A1, 26.2% - DZ). In summary, deactivation of A1 resulted in a large number of sound localization errors concentrated near the target, whereas deactivation of DZ resulted in errors that were less frequent, but more widespread across the entire field.

Supported by: NIDCD and NSF

### **119 Submillisecond Coincidence Detection Facilitated by Passive Soma Structure in the Owl's Auditory Neuron**

Go Ashida<sup>1</sup>, Kousuke Abe<sup>1</sup>, Kazuo Funabiki<sup>2</sup>, Masakazu Konishi<sup>3</sup>

<sup>1</sup>Graduate School of Informatics, Kyoto University,

<sup>2</sup>Graduate School of Medicine, Kyoto University, <sup>3</sup>Division of Biology, California Institute of Technology

Barn owls can locate prey in total darkness only by hearing. One of the acoustic cues for localization is the interaural time difference (ITD). Coincidence detector neurons in the nucleus laminaris (NL) of the barn owl's auditory system are known to detect time disparities of less than a few tens of microseconds for ITD computation, and this acuity has aroused much interest in both theoretical and experimental studies. Histological and physiological evidence suggest that spikes in the NL neuron are generated not at the initial segment but at the first node of Ranvier and that the soma passively receives back-propagating spikes.

We constructed a two-compartment NL neuron model consisting of a cell body and a first node, and systematically changed the excitability of each compartment to explore the relationship between somatic/nodal excitability and coincidence detection performance. When somatic excitability is set small and nodal excitability is large (passive soma conditions), spike shape is quite similar to the spikes observed in intracellular recordings in vivo. In our simulation, a neuron with more passive soma consistently achieves better performance in discriminating ITD for all the frequencies tested (2kHz, 4kHz, 6kHz). We also calculated the amount of the ionic flux in the model neuron during repetitive firing; this amount is a rough estimate for the energy cost of maintaining homeostasis of the cell. In a leaky cell like NL neuron, an active soma greatly increase the ionic flux, whereas somatic excitability does not affect much the ionic flux in a normal leak cell. These results indicate that a neuron with a less active soma achieves higher ITD sensitivity with lower energy costs. We conclude that the owl's NL neuron uses an unusual 'passive soma' design for computational and metabolic reasons.

### **120 Effects of Peripheral Processing are Evident in Neural Correlates of Precedence Effect**

Miles Paterson<sup>1</sup>, David McAlpine<sup>1</sup>

<sup>1</sup>UCL

The precedence effect describes the dominance of the first-arriving wave front on the perception of sound in a reverberant environment. Neurophysiological correlates of the precedence effect are observed as reduced responses to the second click of a binaural click pair. Evidence from high-frequency species such as bat and rat suggests a role for inhibitory neurotransmitters in the precedence effect. Recent modelling of psychophysical data, however, suggests that transient stimuli interact in the auditory periphery to alter the internal representation of the stimulus waveform, and this can account for the



precedence effect (Hartung and Trahiotis, 2001). The model predicts that peripheral interactions are greatest for neurons with narrow filter widths; in the mammalian auditory system, typically neurons with low best-frequency (BF). We examined the contribution of peripheral processing to the neural representation of binaural click pairs in the inferior colliculus (IC) of the guinea pig, comparing the neural representation of the waveform in the IC with the external stimulus waveform. Responses of IC neurons to the first click of a dual click stimulus are affected by the introduction of a second click within the localization dominance time frame. These effects are consistent with stimulus interactions due to peripheral processing. Thus, neural responses suggest the internal representation of click stimuli is well described by a peripheral processing model in which consecutive clicks interact monaurally to produce altered representation of binaural cues (Hartung and Trahiotis, 2001). The importance of low-frequency information to sound localization suggests that peripheral processing may well describe the phenomenon of localization dominance in precedence effect. Studies focusing on high frequency hearing may not translate well to species with low frequency hearing such as humans or, in the case of our experimental recordings, guinea pigs.

### **121 Does Tinnitus Increase Spontaneous Activity in the Inferior Colliculus?**

**Wei-Li Ma<sup>1</sup>**, Hiroshi Hidaka<sup>1</sup>, Bradford J. May<sup>1,2</sup>

<sup>1</sup>Center for Hearing and Balance, <sup>2</sup>Dept. of Otolaryngology-HNS, Johns Hopkins University

Previous studies have linked experimentally-induced tinnitus to increased spontaneous rates (SRs) in the central auditory system. Whether such changes are observed in the primary lemniscal pathways remains controversial. Our studies addressed this issue by recording single-unit activity in the central nucleus of the inferior colliculus. Groups of CBA/J mice were subjected to one of the three most common methods of tinnitus induction: bilateral sound exposure, salicylate treatment, and unilateral sound exposure. Our minimally invasive recording procedure required only light anesthesia to preserve normal SRs in an untreated control group.

No differences were observed in overall SRs between control subjects and either group of sound-exposed mice. Salicylate-treated mice exhibited a significant decrease in spontaneous activity. When single-unit activity was subdivided into transient versus onset responses, the salicylate-treated group also showed a high proportion of onset responses. Because this classification was associated with low SRs in treated and untreated subjects, the decrease in activity of salicylate-treated mice may reflect a sampling bias or a drug effect that increases the prevalence of onset responses.

Units also were classified according to the sharpness and symmetry of excitatory tuning curves using criteria proposed by Ehret and colleagues (Exp Brain Res 140:145-161, 2001). Relative to control data, the three treatment groups showed an increase in SRs that was confined to units with broad response areas (type III units).

Although this finding demonstrates tinnitus hyperactivity, an alternative explanation is that sound exposure and salicylate transformed sharply tuned type I and II units into type III responses by broadening cochlear frequency tuning. This misclassification is expected to inflate SRs in the type III response class because type I and II units tend to have higher spontaneous rates in control subjects. Supported by a Grant in Aid from the Tinnitus Research Consortium and NIH Grant P30DC05211.

### **122 Presynaptic GABAB Receptors Differentially Modulate AMPA and NMDA Receptor Mediated Synaptic Responses in the Rat's Central Nucleus of the Inferior Colliculus**

**Hongyu Sun<sup>1</sup>**, Jack B. Kelly<sup>1</sup>, Shu Hui Wu<sup>1</sup>

<sup>1</sup>Institute of Neuroscience, Carleton University, Ottawa, Ontario, Canada

Our previous study using *in vitro* brain slice techniques showed that synaptic inhibition mediated by GABA<sub>A</sub> receptors can be modulated by presynaptic GABA<sub>B</sub> receptors. The purpose of this study was to investigate the role of GABA<sub>B</sub> receptors in modulating synaptic excitation mediated by AMPA and NMDA receptors in the ICC.

Whole-cell patch clamp recordings were made from ICC neurons in brain slices of 9-16 day old rats. Postsynaptic currents in ICC neurons were evoked by electrical stimulation of the lemniscal inputs. Excitatory postsynaptic currents (EPSCs) were isolated pharmacologically by blocking GABA<sub>A</sub> and glycine receptors. EPSCs were further dissected into AMPA and NMDA receptor-mediated responses by adding the antagonists, CNQX and APV, respectively. The internal solution in the recording electrodes contained CsF, TEA and 4-AP which blocked K<sup>+</sup> channels that may be activated by postsynaptic GABA<sub>B</sub> receptors. The modulatory effects of GABA<sub>B</sub> receptors on EPSCs in ICC neurons were examined by bath application of the receptor agonist, baclofen, and the antagonist, CGP 35348.

The amplitudes of EPSCs in ICC neurons were reduced to 34.4±3.2% of the control (n=17) by baclofen (5-10 μM). The suppressive effect by baclofen was dose-dependent. The greatest sensitivity to baclofen was found with concentrations of 2 to 5 μM. The reduction of the EPSC amplitude was reversed by application of CGP35348 (100 μM). The ratio of the 2<sup>nd</sup> to 1<sup>st</sup> EPSCs (n=7) to paired pulse stimulation was increased from 0.61±0.01 to 0.99±0.02 after application of baclofen. All these results suggest that glutamatergic excitation in the ICC is modulated by presynaptic GABA<sub>B</sub> receptors. In addition, baclofen had differential effects on AMPA and NMDA receptor-mediated responses. Baclofen (5-10 μM) reduced NMDA EPSCs (n=7) by 75.9±8.1%, but AMPA EPSCs (n=9) by 51.4±3.3%. The difference in the reduction of two kinds of responses was statistically significant (p<0.01).

Supported by NSERC of Canada

## **123 Roles of AMPA and NMDA Mediated Excitation on Temporal Response Properties of Inferior Colliculus Neurons**

Jason Sanchez<sup>1,2</sup>, Donald Gans<sup>1,2</sup>, Jeffrey Wenstrup<sup>1</sup>

<sup>1</sup>Northeastern Ohio Universities College of Medicine, <sup>2</sup>Kent State University

This study investigated the effect of glutamate neurotransmission on basic auditory responses in the inferior colliculus (IC) of the mustached bat. Temporal response properties were examined to differentiate the roles of glutamatergic receptors  $\alpha$ -amino-3-hydroxy-5-methyl-4-isoxazolepropionic acid (AMPA) and *N*-methyl-D-aspartate (NMDA). Single unit responses were recorded in the IC before, during, and after local iontophoretic applications of selective glutamate receptor antagonists 1,2,3,4-tetrahydro-6-nitro-2,3-dioxo-benzo[f]quinoxaline-7-sulfonamide (NBQX) and ( $\pm$ )-3-(2-carboxypiperazin-4-yl)-propyl-1-phosphonic acid (CPP). Rate-level functions were obtained using long duration (61ms) acoustic stimuli presented at each unit's best frequency. The simultaneous application of the AMPA receptor antagonist NBQX and the NMDA receptor antagonists CPP completely eliminated all responses. For units with short first-spike latencies (<10ms) and phasic patterns, responses were significantly reduced or completely eliminated by NBQX. For most units with long first-spike latencies (>10ms) and tonic patterns, CPP eliminated the response while NBQX had minimal effect. This suggests that NMDA receptors can mediate excitation independent of AMPA-mediated responses. In some phasic units, a tonic response was revealed by application of antagonists to either the  $\gamma$ -aminobutyric acid (GABA<sub>A</sub>) receptor (bicuculine) or the glycine receptor (strychnine). For these units, CPP selectively reduced later excitation, while simultaneous application of NBQX and CPP completely eliminated the response. On occasion, however, the application of CPP reduced short latency phasic responses, suggesting that early excitation can be mediated by NMDA receptors. Additionally, for some long-latency tonic responses, NBQX eliminated later excitation indicating that AMPA receptors contribute to some later excitation. Supported by grants R01 DC00937 (J.J.W) and F31 DC007298-01 (J.T.S) from NIDCD.

## **124 Behavioral and Electrophysiological Assessment of Tinnitus in a Mouse Model**

Cynthia Prosen<sup>1</sup>, Brad May<sup>2</sup>

<sup>1</sup>Northern Michigan University, <sup>2</sup>Johns Hopkins University

Behavioral and electrophysiological assessment of tinnitus in a mouse model

Animal models of tinnitus are useful in determining the physiological basis of, and assessing treatment plans for, this debilitating condition. We used CBA/CaJ mice in a variety of control and experimental studies to develop an animal model of tinnitus.

Young female mice were trained to detect silent gaps in various levels of continuous broadband noise. After determining the lowest noise level that produced a detection threshold, a continuous 16-kHz tone was added

to the testing environment at tone levels from 30 to 75 dB SPL. This simulated 'tinnitus' resulted in a family of psychometric functions, which varied in threshold as a function of tone level. To induce tinnitus, the mice were unilaterally exposed to a 105 dB 16-kHz octave band of noise for one hour. Several days after noise exposure, the noise detection threshold was re-assessed, and tinnitus magnitude was estimated by matching the psychometric function to results obtained with tones prior to tinnitus induction. Subjects were then treated with gabapentin, an anti-seizure medication that has shown promising results in tinnitus patients. Changes in noise gap detection after sound exposure suggest that most mice experienced tinnitus, and that gabapentin reduced the tinnitus percept. Gabapentin had no effect on thresholds in normal-hearing or deafened animals.

*Supported by the Tinnitus Research Consortium*

## **125 Modelling the Effects of Spiral Ganglion Lesions on Tonotopicity and Receptive Fields in the Inferior Colliculus**

Christian Sumner<sup>1</sup>

<sup>1</sup>MRC Institute of Hearing Research

Damage to the cochlea produces changes in the tonotopicity and receptive fields of neurons in the auditory brain. Neurons apparently adapt to respond to a different range of frequencies corresponding to undamaged regions of the cochlea, and thresholds remain low. The effects are most noticeable in the high in the pathway (thalamus and cortex; e.g. Kamke et al., 2003) and several weeks after the cochlea damage (Robertson and Irvine, 1989). The mechanisms underlying this 'retuning' are unknown. Understanding the central effects of peripheral lesions is likely to lead to a better understanding of how the brain adapts to hearing impairment.

In the inferior colliculus (IC) changes in tuning occur immediately after lesions to a small number of spiral ganglion cells (Snyder and Sinex, 2002). The lesion effectively removes the input to the brain corresponding to a narrow range of best frequencies (BFs), whilst leaving mechanical filtering intact. The rapidity of the observed changes rules out slow plastic processes such as growth of axons or new synapses.

Here a computational model is presented which is intended primarily to account for the immediate changes observed in the IC. The model tests the hypothesis that the removal of peripheral input also removes inhibitory influences. This is often called 'unmasking'. When the cochlea is healthy, inhibition suppresses excitatory inputs from a wide range of BFs. The lesion removes the inhibition as well as some of the excitatory inputs, allowing the remaining excitatory inputs produce a response. The model reproduces the changes in tonotopicity and the range of changes in receptive fields observed in the inferior colliculus. The model therefore offers a 'proof-of-principle' for the unmasking hypothesis.

Kamke MR, Brown M, Irvine DRF (2003). *J Comp Neurol* 459:355-367.

Robertson D, Irvine DR (1989). *J Comp Neurol* 282:456-471.

### **126 Expressions of GABAA Receptors but not Glutamic Acid Decarboxylases Were Reduced in the Inferior Colliculus Following Long-Term Salicylate Overdose**

Jiunn-Liang Wu<sup>1</sup>, Tzai-Wen Chiu<sup>2</sup>, Paul Wai-Fung Poon<sup>3</sup>

<sup>1</sup>Department of Otolaryngology, <sup>2</sup>Basic Medical Institute,

<sup>3</sup>Department of Physiology, Medical College, NCKU

Tinnitus is a phantom perception of sound in the absence of acoustic stimulation with unclear pathophysiology. Acoustic trauma and ototoxic drugs (e.g. salicylate, SA) are known to cause this common hearing disorder in human and reproduced in animal models. In the animal models, SA-induced tinnitus is known to associate with over-activities at the central auditory system in particular the inferior colliculus (IC). Such over-activity could be the result of increased excitation and/or reduced inhibition to the neurons. IC is also known to have abundant GABAergic innervations, one of brain's commonest inhibitory systems. In this study, we explored the possible involvement of GABA in the SA-induced over-activity in the rat IC. After a 5-days SA treatment (250 mg/kg, i.p.), the expression level of GABAA receptor, and the GABA synthesizing enzyme glutamic acid decarboxylases (GAD) were measured with Western blotting. We found a decreased expression of beta 2 and beta 3 subunits of the GABAA receptor. On the contrary, there was an increased expression of both GAD65 and GAD67. This increase was paralleled with a concomitant increase in the number of GABA-positive cells in the IC revealed by immunohistochemistry. Results suggested that the increased neural activities in the IC following SA overdose could be related to a reduced GABAergic inhibition secondary to a decrease in GABAA receptor. The increased GAD expression, likely a compensatory action, was apparently ineffective to offset the loss of inhibition due to decreased GABAA receptors, resulting in over-activity in the IC.

(Supported in part by National Science Council, Taiwan.)

### **127 Role of Glycinergic and GABAergic Inhibition in Inhibitory Combinatorial Interactions in the Nuclei of the Lateral Lemniscus**

Kiran Nataraj<sup>1</sup>, Jeffrey Wenstrup<sup>1</sup>

<sup>1</sup>Dept. of Neurobiology, Northeastern Ohio Universities College of Medicine, Rootstown, OH 44272.

Some neurons in the nuclei of the lateral lemniscus (NLL) of mustached bats show inhibitory combinatorial interactions, in which the excitatory responses to best frequency (BF) tones are inhibited by a low frequency tone, tuned to frequencies one or more octaves below the BF. In 35 single NLL units, we examined the temporal and spectral features of inhibitory combinatorial interactions and the roles of glycine and  $\gamma$ -aminobutyric acid (GABA) in creating these interactions by local application of bicuculline (BIC: GABAA receptor antagonist) and/or strychnine (STRY: glycine receptor antagonist). Inhibitory combinatorial units formed two major groups based on the

response to the lower frequency signal. In the first group (n = 23, 66%), the low frequency tone evoked only inhibition, suppressing responses to the BF tone. In a majority of these units, the low frequency inhibition was tuned to frequencies within the fundamental harmonic of the sonar call (23-30 kHz), with the inhibition being mostly phasic. The low frequency inhibition was never eliminated by application of BIC. Application of STRY by itself or in combination with BIC eliminated this inhibition in 71% and 67%, respectively, of the units tested. In the second group (n = 12, 34%), the low frequency tone evoked an excitation followed by an inhibition. The inhibition following the excitation suppressed the responses to the BF tones. In all of these units, the low frequency inhibition was tuned to frequencies below the fundamental sonar harmonic (<23 kHz). These results suggest that: 1) some of the inhibitory combinatorial interactions are created in the NLL and require a glycine mediated mechanism and 2) inhibitory interactions in the NLL show distinct spectral and temporal features. In addition, we propose that inhibitory combinatorial interactions in the NLL could contribute to spectral integrative responses observed in the inferior colliculus. Supported by RO1 DC 00937 from NIDCD.

### **128 Response Properties of Inferior Colliculus Neurons with in vivo Whole-Cell Patch-Clamp Recording**

Ruili Xie<sup>1</sup>, George Pollak<sup>1</sup>

<sup>1</sup>University of Texas at Austin

Here we report on studies of whole-cell patch recordings from the inferior colliculus of awake Mexican free-tailed bats. The recordings were achieved at depths ranging from 300-600  $\mu$ m and cells were held for periods ranging from about 5-20 minutes. Upon encountering a neuron, we first made a gigaohm seal followed by break-in. We then evoked responses with a series of depolarizing and hyperpolarizing current steps to obtain membrane resistance and to determine whether the neuron displayed responses indicative of known intrinsic properties. We next recorded responses evoked by tonal frequencies that encompassed the receptive fields of the IC neurons and responses evoked by more complex stimuli, such as brief downward FM sweeps and to some of the communication calls emitted by this species.

A variety of different tuning curves were obtained but two types were of particular interest. One type displayed prominent EPSPs and prominent discharges with little or no inhibition evoked by any frequency. A range of frequencies evoked discharges that would comprise the excitatory receptive field with extracellular recordings. However, frequencies that flanked both the high and low frequency sides of the suprathreshold frequency range evoked prominent but subthreshold EPSPs. One noteworthy feature of these cells is that no IPSPs were evoked, including frequencies that were outside of those that evoked subthreshold EPSPs. In marked contrast were other cells in which tone bursts evoked only IPSPs and no EPSPs. The entire receptive fields of these cells were comprised only of tone evoked IPSPs. There were two additional features of these cells that are of interest.

The first is that a depolarizing current step of 200 pA evoked discharges that were sustained for the duration of the current step. The second is that some of these cells fired a burst of discharges to a downward FM sweep, whereas others responded to downward FM sweeps and to communication calls only with IPSPs. We suggest that these results show that there are numerous subthreshold events occurring in IC cells that would not be obvious with extracellular recordings.

Supported by NIH grant DC00268.

### **129 Inhibitory Fields of STRFs in the Inferior Colliculus are Lost when Inhibition is Blocked by Bicuculline**

Na Li<sup>1</sup>, Sari Andoni<sup>1</sup>, George Pollak<sup>1</sup>

<sup>1</sup>*University of Texas at Austin*

We derived spectral-temporal receptive fields (STRFs) from neurons in the inferior colliculus (IC) of awake Mexican free-tailed bats. The STRFs were generated by a set of dynamic moving ripple stimuli using methods of reverse correlation. The STRF characterizes the excitatory and inhibitory fields of each neuron but cannot distinguish between inhibition that is generated in the IC and inhibition that was generated in a lower nucleus. To distinguish between these two possible sites of inhibition, we compared the STRFs before and while GABAergic receptors were blocked with bicuculline. The idea is that if the inhibitory fields are generated in the IC, then blocking inhibition should partially or completely abolish the inhibitory fields, whereas if those fields are generated in a lower nucleus, then the application of bicuculline should cause no change in the inhibitory fields. In some neurons, we generated another STRF following recovery from bicuculline. We found that for most of IC neurons, the inhibitory fields, especially the lateral inhibitory fields, were partially or largely lost under the effect of bicuculline and were reacquired after recovery from the drug. This shows that most, if not all, of the inhibitory fields in those IC neurons are indeed generated by inhibition in the IC. Supported by NIH grant DC00268.

### **130 Pharmacology and Serotonergic Modulation of Synaptic Responses in the Rat's External Cortex of the Inferior Colliculus Studied using in Vitro Brain Slice Techniques**

Tarun K. Ahuja<sup>1</sup>, Shu Hui Wu<sup>1</sup>

<sup>1</sup>*Institute of Neuroscience, Carleton University, Ottawa, Ontario, Canada*

In mammals the IC can be divided into three anatomical subdivisions: the central nucleus (ICc), the dorsal cortex (ICd) and the external cortex (ICx). The ICx receives its primary inputs from the contralateral and ipsilateral ICc, auditory cerebral cortical areas and from regions of motor and other sensory systems. This wide array of primary projections from both auditory and non-auditory sources makes the ICx a unique structure within the auditory brainstem. To better understand the physiological function of the ICx, this study examined synaptic responses of ICx

neurons and identified neurotransmitters and types of receptors that mediated the evoked synaptic responses. We also investigated modulatory effects of serotonin (5-HT) on these responses.

Visual whole-cell patch clamp recordings were taken from ICx neurons (N=25) in coronal slices from rats between the ages of 8 to 11 days postnatal. To study the synaptic responses, a stimulating electrode was placed in the ICc to examine the direct inputs to the ipsilateral ICx. The resultant graded responses displayed a combination of excitatory/inhibitory potentials. The data showed that the majority of cells (60%) displayed an excitatory synaptic response, fewer were inhibitory (16%) and the remainder exhibited mixed responses (24%). Pharmacological analyses showed that the evoked responses were mediated by GABA, glycine and glutamate. The inhibitory responses were mediated predominantly through GABA<sub>A</sub> receptors and the excitatory responses through AMPA receptors. Application of 5-HT demonstrated a modulation of the elicited synaptic responses. The modulatory effects of 5-HT varied (i.e. suppression or enhancement), however, were quite prominent in the neurons tested. The effects of 5-HT on synaptic responses mediated by specific synaptic receptors were also examined. The results showed that 5-HT primarily influenced synaptic responses mediated by glutamate receptors.

Supported by NSERC of Canada

### **131 Activity Dependent Modulation of Tyrosine Hydroxylase in the Rat Midbrain**

Ling Tong<sup>1</sup>, Richard Altschuler<sup>1</sup>, Avril Genee Holt<sup>1</sup>

<sup>1</sup>*University of Michigan*

Auditory signals are relayed through major auditory brainstem centers and integrated in the inferior colliculus before processing in the auditory cortex. Using a gene microarray screen we previously identified tyrosine hydroxylase (TH), a key enzyme in the catecholaminergic pathway, as one of the genes that shows decreased expression in the inferior colliculus (IC) 3 and 21 days following deafness (Holt et al 2004). In the present study we followed up on this result by using immunocytochemistry to characterize the distribution of the catecholamine synthesizing enzymes TH, dopamine beta hydroxylase (DBH), and phenylethanolamine-N-methyltransferase (PNMT), in the IC and lateral lemniscus. Sprague Dawley rats were placed into one of three groups, normal hearing (n = 8), 21 (n = 5), or 90 (n = 5) days post-deafening (cochlear ablation). Hearing was assessed using auditory brainstem responses (ABRs). Only those animals showing a threshold shift of 75 dB or greater were included in the study. In normal hearing animals labeling for TH, and DBH, but not PNMT was observed in the IC and lateral lemniscus. There were many TH and DBH-immunoreactive puncta and small caliber axons in the IC. The fibers and puncta were found in all subdivisions of the IC with the heaviest labeling found in the external cortex. The TH labeled somata in the IC could be identified in the dorsal cortex and the central nucleus. The darkly labeled cells identified in the dorsal cortex were immunoreactive for TH, but not DBH or PNMT. The somata in the central

nucleus were immunopositive for both TH and DBH. In the nuclei of the lateral lemniscus both cells and fibers were identified in all three subdivisions. Deafness related changes were observed both at the 21 and 90 day time points. Deafness related changes were found in both the number of labeled fibers and cells as well as the intensity of the labeling. In the IC the number of cells decreased in both the dorsal cortex and the central nucleus and in the lateral lemniscus the number of TH positive neurons decreased in the intermediate nucleus. These results suggest that both dopaminergic and noradrenergic systems may be involved in mechanisms underlying deafness-related plasticity.

### **132** Maturation of Response Selectivity in the Inferior Colliculus

Zoltan Fuzessery<sup>1</sup>, Dustin Richardson<sup>1</sup>, Michael Coburn<sup>1</sup>

<sup>1</sup>University of Wyoming

In the adult pallid bat inferior colliculus, neuronal selectivity for the direction of the downward FM sweep of the biosonar pulse is created by an asymmetry in both the bandwidths and arrival times of low and high frequency inhibition, with the low frequency inhibition being broader, and arriving earlier. This inhibits responses to upward FM sweeps. Selectivity for the velocity (kHz/msec) of the sweep is created by either of two different mechanisms. The first is a delayed high frequency inhibition that suppresses the response as the FM sweep velocity slows. The second is a shortpass sound duration selectivity which inhibits responses to slower sweeps that remain within the excitatory tuning curve too long. The development of the circuitry underlying these forms of selectivity was assessed in young bats 2.5-7 weeks of age. Adult-like velocity tuning developed at 3 weeks of age, before sweep direction selectivity, and was created first by delayed high frequency inhibition. Duration selectivity did not become common until 5 weeks of age, when it too contributed to velocity tuning. Selectivity for sweep direction matured more slowly, and even at 7 weeks of age, pups possessed only half the percentage of selective neurons (34%) present in adults. The development of direction selectivity was associated with an increase in the bandwidth of low frequency inhibitory domains, and a decrease in the arrival time of this inhibition. Results suggest that some adult features of the inferior colliculus come online very early, while others require more time to develop.

### **133** Differential Expression of Shal, Kv4.2 and 4.3, Ion Channels in Auditory Brainstem and Midbrain Structures of the Big Brown Bat, *Eptesicus fuscus*.

Dennis Dever<sup>1</sup>, Ellen Covey<sup>1</sup>, J. H. Casseday<sup>1</sup>

<sup>1</sup>University of Washington

The specialized response properties of midbrain auditory neurons are not only shaped by extrinsic factors, such as patterns of connections and neurotransmitter distribution, but they are also strongly influenced by intrinsic properties. One such intrinsic property is ion channel distribution. Voltage-gated potassium channels regulate the membrane

potential of excitable cells and thus determine action potential rate and firing patterns. Shal-type potassium channels produce an outward current that activates and inactivates rapidly at low thresholds. This current, called the A-current, is thought to be responsible for creating transient firing patterns seen in neurons and cardiac cells. Interested in the possibility that this A-current shapes transient responses in the auditory system, we used antibodies directed toward the C-terminus of the Kv4.2 and Kv4.3 subunits to investigate the distribution of Shal channels in the central auditory system of *Eptesicus*. Both antibodies showed similar patterns of positive staining in the cochlear nucleus, medial nucleus of the trapezoid body, and medial superior olive. In the lateral lemniscus, staining was heaviest in the dorsal nucleus and in the columnar region of the ventral nucleus. The pattern of staining in the inferior colliculus differed for the two antibodies. Staining for Kv4.2 was found only in the ventral part of the inferior colliculus, while staining for Kv4.3 was evenly distributed throughout this structure. This positive staining for Kv4 channels in the central auditory system leads us to believe that these channels are important for shaping the specialized responses of cells found there. Differential patterns of distribution in the lateral lemniscus and inferior colliculus suggests that there may be functional differences that depend on neurons' intrinsic properties. Research supported by NIH DC-00607 and DC-00287.

### **134** Neonatal Plastic Changes at the Auditory Midbrain Depend Critically on the Times of Prolonged Sound Exposure

Tzai-Wen Chiu<sup>1</sup>, Paul Poon<sup>2</sup>

<sup>1</sup>Institute of Basic Medical Sciences, <sup>2</sup>Department of Physiology, National Cheng Kung University, Taiwan

The nature of plastic changes at the auditory midbrain following artificially enhanced sensory inputs was studied electrophysiologically in young rats during their first 5 weeks of life. Two prolonged sound exposure protocols were used: (a) weekly stimulation, or (b) monthly stimulation. The sound exposure (4 kHz pure tone, 65 dB SPL, 10 hrs/day) was given to litters of animals starting at different ages, viz., in week-1, -2, -3 or -4 for the weekly protocol, or week- 1 (to 4) or week- 2 (to 5) for the monthly protocol. Following weekly exposures, single units at the inferior colliculus (IC) showed the greatest increment in best frequency (BF) near the exposing frequency of 4 kHz when stimulation started in week-2 but not in week-3 or -4. Week-1 exposed group showed increased unit yield to sound compared to a non-responsive control group. After monthly exposures, week- 2 to 5 group showed a change in BF histogram very similar to the week-2 exposed group. But the same sound exposure starting a week earlier (i.e., the week- 1 to 4 exposed group) produced the most prominent and greatest relative increase in BF at 4 kHz. In this latter group, frequency tuning of units around 4 kHz was also significantly sharper than control. In marked contrast, other exposed groups which showed a broadened but not sharpened frequency tuning compared with their controls. Similar changes in BF at 4 kHz after week-2 sound exposure were not found at the cochlear

nucleus (CN). Results suggested that week-1 and week-2 are likely the critical period for BF changes at the midbrain. The present results on the neonatal plasticity do not however rule out the possible involvement of other structures lower than the IC (e.g., CN) particularly in the week- 1 to 4 exposed group.

### **135 Basilar-Membrane Motion Inferred from Otoacoustic Emissions and Psychoacoustic Measurements**

**Michael Epstein**<sup>1,2</sup>, Mary Florentine<sup>1,2</sup>

<sup>1</sup>*Department of Speech-Language Pathology & Audiology, Northeastern University,* <sup>2</sup>*Institute for Hearing, Speech & Language, Northeastern University*

The amplitude of tone-burst otoacoustic emissions, which arise on the basilar membrane, is believed to be proportional to basilar-membrane motion. If this is true, it should then be possible to assess basilar-membrane motion on the basis of otoacoustic emissions. The present study provides support for this possibility by comparing how relative basilar-membrane motion depends on signal level as inferred from emissions and from several psychoacoustic measures. Three psychoacoustic measurements believed to be associated with basilar-membrane motion were investigated: 1) pulsation threshold, 2) loudness functions derived from temporal integration, and 3) loudness functions derived from loudness matches between pure tones and multi-tone complexes. Six normal-hearing subjects took part in each of the experiments. Results of the psychoacoustic measurements and of the tone-burst otoacoustic emissions led to very similar estimations of basilar-membrane motion, especially in the pulsation-threshold data, which are more directly obtained measures. Accordingly, emissions could serve as an excellent tool—one that is objective, non-invasive, and rapid—for estimating relative basilar-membrane motion in normal-hearing subjects.

This research was supported by NIH/NIDCD Grants Nos. R01DC02241 and R01DC00187.

### **136 Ear Asymmetries in Middle-Ear, Cochlear and Brainstem Responses in Infants**

**Douglas Keefe**<sup>1</sup>, Michael Gorga<sup>1</sup>, Walt Jesteadt<sup>1</sup>

<sup>1</sup>*Boys Town National Research Hospital*

In a recent study of infants, Sininger and Cone-Wesson (Science, 305, 1581, 2004) examined ear asymmetries in overall otoacoustic emission (OAE) signal-to-noise ratios (SNR), and observed that the SNR for distortion product OAE (DPOAE) was larger on average in the left ear while the SNR for transient evoked OAE (TEOAE) was larger on average in the right ear. They concluded that the presence of such stimulus-guided asymmetry in the cochlear suggests that cochlear and brainstem asymmetries may serve to facilitate development of brain-hemispheric specialization for sound processing. The present study further explores the factors underlying these ear asymmetries using data obtained from a population of

1361 infants. Although the samples were entirely independent, the present data were collected as part of the same multi-center study (Norton et. al., Ear Hear. 21, 348-356, 2000) from which the data used by Sininger and Cone-Wesson were derived, using identical experimental paradigms and equipment. This should facilitate comparisons to their data and allow us to expand on their findings related to stimulus-guided asymmetry in the cochlea. In addition to examining ear differences in SNR collapsed across frequency, ear differences in signal and noise level will be evaluated separately, averaged across frequency and at individual ½ octave frequencies ranging from 1.5 to 4 kHz. ABR data also were collected and will be used to determine the extent to which ear asymmetries in brainstem responses relate to peripheral response asymmetries. In addition to the OAE and ABR data, ear-canal reflectance and admittance data were collected, allowing us to evaluate the influence of middle-ear function on ear asymmetries in cochlear (OAE) and brainstem (ABR) responses. [Work supported by the NIH – DC01958, DC003784, and DC002251].

### **137 Can Salicylate-Induced OHC Dysfunction Model Neonatal Cochlear Immaturity as Measured by DPOAE Suppression?**

**Carolina Abdala**<sup>1</sup>, Leslie Visser-Dumont<sup>1</sup>

<sup>1</sup>*House Ear Institute*

One of the DPOAE paradigms used to study cochlear function and, in recent years, cochlear immaturity, is DPOAE (2f1-f2) ipsilateral suppression. During ipsilateral suppression, f1 and f2 are presented simultaneously with suppressor tones centered around the primary tone frequencies. The suppressor is increased in level producing a systematic drop in the distortion product amplitude. Iso-suppression tuning curves (STC) can be measured using this technique, as can patterns of suppression growth across frequency. Several studies have consistently shown excessively narrow DPOAE suppression tuning curves in neonates, particularly at f2 = 6000 Hz, and to a lesser extent, at 1500 Hz. Additionally, suppression growth in infants is excessively shallow for low-frequency suppressor tones. Thus, DPOAE suppression appears to reflect a peripheral immaturity, although the cochlear source of this immaturity is not known. The outer hair cell (OHC) is a possible locus of functional immaturity in the newborn cochlea. One way to investigate this possibility is to produce a temporary OHC dysfunction in the adult cochlea and scrutinize the effect of this manipulation on DPOAE suppression. In the present study, DPOAE ipsilateral suppression and DPOAE Input/Output functions were measured at f2 = 1500 and 6000 Hz from two groups with impaired OHC function: normal-hearing subjects with temporary and reversible, salicylate-induced OHC dysfunction and mildly hearing-impaired subjects. Their results were compared to those obtained from a group of term neonates to address whether individuals with OHC dysfunction produce DPOAE results similar to individuals with immature cochlear function (i.e. neonates). If so, it is possible that one

source of the non-adultlike DPOAE suppression in neonates is immature OHC function. Preliminary results show that salicylates systematically alter DPOAE suppression results in normal-hearing adults at  $f_2 = 6000$  Hz and not at  $f_2 = 1500$  Hz. However, OHC dysfunction due to reversible salicylate ototoxicity or naturally occurring sensorineural hearing loss does not produce "neonatal-like" DPOAE suppression at either test frequency. The implications of this finding are considered and discussed.

### **138** Developmental Changes of Cochlear Active Mechanisms in the Time-Frequency Domain in Preterm Infants

**Gabriella Tognola**<sup>1</sup>, Marta Parazzini<sup>1</sup>, Paolo Ravazzani<sup>1</sup>, Ferdinando Grandori<sup>1</sup>

<sup>1</sup>*Istituto di Ingegneria Biomedica CNR, Piazza Leonardo da Vinci 32, 20133 Milan, Italy*

The analysis of click-evoked otoacoustic emission (CEOAE) changes in preterm infants during the first weeks after birth is a non-invasive and simple way to characterize the development of cochlear active mechanisms. Due to their strong time-varying properties, CEOAEs were studied with an ad hoc time-frequency approach - the wavelet transform (WT). By means of the WT, CEOAEs were decomposed into 12 frequency bands, spanning the 0.25-6.25 kHz range. For each band, the root-mean-square level and latency were studied as functions of both frequency and age.

Thirty four preterms were considered in this study (mean gestational age at birth 30.3 wks, s.d.=1.4 wks) for a total number of 58 tested ears. Each ear had a minimum of three and a maximum of 11 subsequent CEOAE measurements in a period ranging from 1 to 8 wks after birth. A total of 307 CEOAEs were thus obtained. Also, CEOAEs were measured from a control group of full-term babies (n=333) at the third day after birth.

Properties of CEOAE components were found to be related to the post-conception age (PCA) in that the levels and latency of CEOAE frequency components changed until the age of about 38 wk post-conception, whereas after 38 wk, CEOAE features were very similar to those of term newborns (see preliminary results in: G. Tognola, M. Parazzini, P. de Jager, P. Briennesse, P. Ravazzani, F. Grandori, "Cochlear maturation and otoacoustic emissions in preterm infants: a time-frequency approach", *Hear. Res.* 2004 [in press]). In particular, the CEOAE levels increased and latency decreased with age. The observed changes in CEOAE properties seem to reveal a development of cochlear active mechanisms, although contributions from outer and middle ear development cannot be excluded. Also, in agreement with previous physiological and behavioral findings, our results revealed that the development of CEOAE properties was not the same for all the frequencies, being greater for frequencies  $\leq 4$  kHz, and resembled the development of the cochlear partition, which proceeds from base to apex.

### **139** Does DPOAE Fine-Structure Contribute to Results in Automated Hearing Screening?

**Anne Mueller**<sup>1</sup>, Rudolf Leuwer<sup>1</sup>, Hannes Maier<sup>1</sup>

<sup>1</sup>*Universitaetsklinik Hamburg-Eppendorf*

The recording of DPOAE provides a quick and easy to handle tool for inner ear diagnostics in newborn hearing screening. DPOAE output levels at  $2f_1$ - $f_2$  depend on primary input levels, but also on the interference of different sources along the basilar membrane (Heitmann et al. 1998). In screening application with a priori chosen test frequencies measured output levels may be arbitrarily increased or decreased by the fine-structure and may not reflect the real state of the inner ear.

DPOAE responses were recorded using an AmDis device (GN Otometrics) in adults (n=1183, average age =26 y) with normal hearing threshold at 6 frequencies from 1 to 6kHz. To determine the influence of fine-structure on measured response levels DPOAEs were measured ( $L_1$ ,  $L_2=65$ , 55 dB SPL) with and without a third suppressor tone ( $L_{sp} = 55$  dB SPL). Both protocols were also used for measurements in newborns (n=230) with normal ABR screening result (Algo portable™). DPOAE responses with a SNR < 6dB were excluded from further analysis. Analysis of individual response level differences with and without suppressor in the adult group had a mean value (MV) of -0.1 to 0.3 (SD < 2.8 dB). Due to the distribution 5.6% of all measured responses were altered more than 5dB by the suppressor tone. Unlike in adults, response differences in newborn were normally distributed (MV = -0.3 to 0.8; SD = 2.1 to 6.2dB). As a result of the broader distribution 38% of DPOAE response levels were altered by more than 6dB by the suppressor tone and even 6% of the levels were altered by more than 9dB.

Our data suggest that interference and fine-structure has a significant impact on DPOAE results. Namely for newborn hearing screening those effects have to be taken into account. Existing methods need to be improved by countermeasures one of which is the use of a suppressor tone.

### **140** L1,L2 Response Areas for Lower- and Upper-Sideband DPOAEs Measured at Three F2/F1 Ratios in Normal and Noise-Exposed Rabbits

**Bart Stagner**<sup>1</sup>, Lyubov Nemanov<sup>2</sup>, Glen Martin<sup>1</sup>, Brenda Lonsbury-Martin<sup>3</sup>

<sup>1</sup>*Jerry Pettis Memorial Veterans Medical Center,*

<sup>2</sup>*University of Colorado,* <sup>3</sup>*University of Colorado Health Sciences Center*

It is well known that because of the nonlinear aspects of cochlear transduction presenting two tones simultaneously to the ear produces families of distortion-product otoacoustic emissions (DPOAEs) referred to as lower (LSB) and upper sideband (USB) DPOAEs. Most DPOAE literature focuses on the most prominent LSB DPOAE at the  $2f_1$ - $f_2$  frequency. However, by ignoring other DPOAEs, a considerable amount of information regarding cochlear nonlinearity is discarded. Thus, as more energy is applied to the nonlinearity, or as  $f_2/f_1$  ratios are

decreased, more sideband DPOAEs are produced. By studying multiple emissions, insight into changes in the cochlear nonlinearity, such as a shift in its operating point or changes in the response/growth map, can be appreciated that cannot be easily revealed by examining a single DPOAE. The purpose of the present study was to investigate LSB (2f1-f2, 3f1-2f2, 4f1-3f2, 5f1-4f2, f2-f1) and USB (2f2-f1, 3f2-2f1, 4f2-3f1, 5f1-4f2) DPOAE L1,L2 response areas in normal and noise-damaged rabbit ears as a function of f2/f1 ratio (1.05, 1.25, 1.4.) at different f2 frequencies (2, 4, 8, 11.3 kHz) over a range (45-75 dB SPL) of equal and unequal primary-tone levels. The right ears of eight rabbits were exposed monaurally for 2 h to a 2-kHz, 110-dB SPL octave-band of noise with the contralateral unexposed ear serving as a control. Experimental findings showed that in ears with moderate amounts of noise damage, USBs and LSBs behaved differently. That is, LSBs reflected cochlear damage in the exposed ear at both wide (1.4) and "standard" (1.25) f2/f1 ratios, while at narrow ratios (1.05), the 2f1-f2 DPOAE did not reflect the damage pattern. Unexpectedly, higher-order LSBs (4f1-3f2, 5f1-4f2) appeared to map the DPOAE losses at this narrow ratio. In contrast, USB DPOAEs either demonstrated no change or enhancement. As expected, in severely damaged ears, all DPOAEs were either reduced or eliminated. (Supported by NIDCD DC000613, DC003114).

#### **141 Detailed DPOAE Level/Phase Maps in Normal and Noise-Damaged Rabbit Ears: Insights Into Generation Processes**

Glen Martin<sup>1</sup>, Amy De La Garza<sup>2</sup>, Bart Stagner<sup>1</sup>, Brenda Lonsbury-Martin<sup>2</sup>

<sup>1</sup>Jerry Pettis Memorial Veterans Medical Center,

<sup>2</sup>University of Colorado Health Sciences Center

Knight and Kemp (2000) described a method in which they derived detailed plots of DPOAE level and phase as a function of f2/f1 ratio and DPOAE frequency. They identified two predominate DPOAE phase patterns consisting of horizontal phase banding, which was viewed as evidence for "wave-fixed" DPOAE generation, and vertical phase banding, which was ascribed to "place-fixed" DPOAEs. Shera and Guinan (1999) attributed these two modes to "distortion" and "reflection" generation mechanisms. We examined detailed DPOAE level/phase plots in normal and noise-damaged rabbit ears. It was hypothesized that noise damage would disrupt outer hair cell organization and thus alter the normal distribution of phase patterns. Primary tones were generated by a DSP on-board a personal computer and presented over ER-2 speakers. Ear-canal sound pressure, measured with an ER-10A microphone assembly, was sampled and synchronously averaged (n= 4) by the DSP. DPOAEs were measured in DPOAE frequency steps of approximately 44 Hz from 1.4-4.4 kHz in response to primary-tone sweeps at three levels (55/45, 60/55, 65/65 dB SPL), using constant f2/f1 ratios incremented in 0.025 steps from 0.025-1.5. DPOAE level was directly plotted while the phase was corrected for primary-tone phase variation and unwrapped before plotting. One ear of eight rabbits was exposed for 2 h to a 110-dB SPL, 10-kHz

octave-band of noise with the contralateral unexposed ear serving as a control. In unexposed ears the 2f1-f2 DPOAE showed phase patterns characteristic of "wave-fixed" DPOAEs with little evidence for "place-fixed" generation. In contrast, the 2f2-f1 DPOAE behaved like a "place-fixed" emission. Following noise exposure, the 2f1-f2 DPOAE exhibited a substantial number of vertical phase bands consistent with an increase in the amount of DPOAE generated by a reflection mechanism. Implications concerning DPOAE generation in normal rabbit ears will be discussed. (Supported by NIDCD DC000613, DC003114).

#### **142 Distortion Product Otoacoustic Emission Thresholds and Growth Functions in Normal-Hearing Individuals with Tinnitus And/Or Hyperacusis**

Grazyna Bartnik<sup>1</sup>, Monica Hawley<sup>2</sup>, Marek Rogowski<sup>1,3</sup>, Danuta Raj-Kozia<sup>1</sup>, Anna Fabijanska<sup>1</sup>, Craig Formby<sup>2</sup>

<sup>1</sup>The Tinnitus Clinic at the Institute of Physiology and Pathology of Hearing, Warsaw, Poland, <sup>2</sup>Department of Otolaryngology-HNS, University of Maryland School of Medicine, Baltimore, MD, <sup>3</sup>Medical University of Bialystok, Bialystok, Poland

The purpose of this study was to determine whether Distortion Product Otoacoustic Emission (DPOAE) responses, measured at the level of the cochlea, can be used to distinguish among patients reporting tinnitus and/or hyperacusis and, in turn, their responses from those of normal controls. Four groups with audiometrically normal-hearing sensitivity, including: (1) a control group, and three patient groups reporting (2) tinnitus alone, (3) hyperacusis alone, or (4) both tinnitus and hyperacusis, were tested using two types of DPOAE measures. The first measure was the DP-threshold response evaluated for fixed primary levels as a function of frequency (DP-gram). The second measure was DPOAE response growth (growth functions) for a range of primary levels evaluated between 45 and 70 dB SPL at 1000, 2000, and 4000 Hz. DP-grams were variable and did not clearly distinguish among the control and patient groups. The DP-threshold response successfully categorized 51-74% of the individuals included among the three patient groups as abnormal (outside of the 95% confidence range for the control group for at least one frequency). The average slopes of the DP-growth functions were consistently steeper for each of the patient groups than for the control group, but these slope values were indistinguishable among the patient groups. Slope values successfully categorized an individual as abnormal (outside of the 95% confidence range for the control group) in about 60% of the patients in each group. Thus, DPOAE measures can be used to distinguish controls from patients with tinnitus, hyperacusis, or both tinnitus and hyperacusis, but not to discriminate among the respective patient groups. These findings suggest that the pathology represented among these abnormal conditions is consistent at the level of the cochlea. Consequently, clinicians will likely need to use diagnostic tests targeted at higher centers of processing if



the individuals in these groups are somehow to be distinguished among themselves.

### **143 A Comparison of Stimulus-Frequency and Distortion-Product Otoacoustic Emissions for Monitoring Ototoxicity-Induced Hearing Loss**

**Dawn Konrad-Martin**<sup>1,2</sup>, David S. Phillips<sup>1,2</sup>, Kelly M. Reavis<sup>1</sup>, Jane S. Gordon<sup>1</sup>, Gene W. Bratt<sup>3</sup>, Stephen A. Fausti<sup>1,2</sup>

<sup>1</sup>Portland VA Medical Center, <sup>2</sup>Oregon Health and Science University, <sup>3</sup>Nashville VA Medical Center

In normal ears, otoacoustic emission (OAE) input-output (I/O) functions show a rapid, linear growth region at low input levels and a gradual, compressive growth region at moderate levels. The compressive-region slope of the I/O function (in dB/dB) may represent basilar membrane compression and can be used to extrapolate an OAE "threshold" that is correlated with pure-tone threshold [Boege and Janssen, *J. Acoust. Soc. Am.* 111, 2002]. Both OAE compression rate and threshold are likely associated with outer hair cell function and may be altered by ototoxic drugs. Stimulus-frequency (SF) and distortion-product (DP) OAE were measured in 20 normal-hearing and 19 hearing-impaired control subjects and in 9 experimental subjects receiving ototoxic drugs. SFOAEs extracted using a suppression paradigm (probe=f<sub>2</sub>, suppressor=f<sub>1</sub>, where f<sub>2</sub>/f<sub>1</sub>=1.03) and DPOAEs (f<sub>2</sub>/f<sub>1</sub>=1.2) were recorded at 11 f<sub>2</sub>'s (1 to 10 kHz) for L<sub>2</sub> held constant at a moderate level. I/O functions were obtained for L<sub>2</sub> varied in 5-dB steps (from 20 to 60 dB SPL for SFOAE and 20 to 65 dB SPL for DPOAE) and L<sub>1</sub> chosen to optimize the OAE level. I/O functions were obtained for each f<sub>2</sub> in normal-hearing controls, and for a limited (one-octave) range of f<sub>2</sub>'s near the highest frequency able to elicit a reliable OAE in hearing-impaired controls and experimental subjects. In each subject, OAE measurements were repeated on at least three occasions. SFOAE and DPOAE I/O function growth in normal ears often was compressive with mean slopes similar to those reported previously [Schairer et al., *J. Acoust. Soc. Am.* 114, 2003]. Compared to normal ears, SFOAE and DPOAE I/O functions in impaired ears had poorer thresholds, reduced maximum amplitudes and were less compressive with slightly steeper slopes. A comparison of SFOAE and DPOAE I/O functions was used to refine estimates of OAE threshold. Preliminary findings regarding the capability of DPOAE and SFOAE for predicting hearing change in patients receiving ototoxic drugs will be discussed. Supported by the Department of Veterans Affairs Rehabilitation Research and Development Service (C3213R and E3239V).

### **144 Association between Pathogenicity and Genic Diversity in *Haemophilus influenzae* and *Streptococcus pneumoniae***

**Michael L. Forbes**<sup>1</sup>, Jay Hayes<sup>2</sup>, Farrel J. Buchinsky<sup>2</sup>, Fen Ze Hu<sup>2</sup>, J. Christopher Post<sup>2</sup>, Garth D. Ehrlich<sup>2</sup>

<sup>1</sup>Department of Pediatrics, Allegheny General Hospital, Pittsburgh, PA, <sup>2</sup>Center for Genomic Sciences - ASRI/WPAHS

We hypothesize that bacterial genic diversity is positively correlated with virulence. To test this hypothesis, we injected 10 separate clinical isolates of *H. influenzae* into the bullae of chinchillas. Each animal was scored using a multiparameter scoring system that quantifies virulence on a 4 point scale. We found a wide range of pathogenicity among the strains. DNA sequence analysis of a subset of clones derived from a pooled genomic library prepared from the 10 clinical isolates was performed. From this analysis, we identified a set of unique genes not present in the reference strain, Rd. Distribution studies were performed to determine the percentage of each unique gene present in each isolate. No two isolates were the same, indeed there was a high degree of variability of genic distribution. When genic diversity was compared to pathogenicity, we found a 300% difference in genic diversity between the most and least pathogenic strains.. We then compared the degree of genetic diversity of the various strains with the pathogenicity index, and noted a linear relationship between pathogenicity and genetic diversity. A similar study was performed using clinical isolates of SP. Otitic changes occurred first in animals infected with Sp23, while Sp23 and Sp11 caused the most severe changes. Signs of sepsis as well as lethality was most demonstrable in those infected with Sp3 and Sp11. No association existed between severity of otoscopic changes and lethality. These data suggest that the degree of genic diversity appears linearly correlated to pathogenicity. This observation provides further support to the hypothesis that genetic diversity among prokaryotes may confer survival advantage. Additionally, we are using these findings to develop a bioassay to aid in the early, rapid diagnosis of sepsis.

### **145 Distribution of Novel (nonRd) Genes in 10 Clinical Isolates of *Haemophilus influenzae* and Novel (nonPA01) Genes in 12 Isolates of *Pseudomonas aeruginosa* from Pediatric Chronic Otitis Media Specimens**

**Kai Shen**<sup>1</sup>, Patricia Antalis<sup>1</sup>, Azad I. Ahmed<sup>1</sup>, John Gladitz<sup>1</sup>, Shujun Yu<sup>1</sup>, Sameera Sayeed<sup>1</sup>, Jay Hayes<sup>1</sup>, Bethany Dice<sup>1</sup>, Richard Dopico<sup>1</sup>, Benjamin Janto<sup>1</sup>, Sandra Johnson<sup>1</sup>, Randy Keefe<sup>1</sup>, Geza Erdos<sup>1</sup>, Robert A. Preston<sup>1</sup>, Robert W. Wadowsky<sup>2</sup>, J. Christopher Post<sup>1</sup>, Garth D. Ehrlich<sup>1</sup>, Fen Ze Hu<sup>1</sup>

<sup>1</sup>Center for Genomic Sciences - ASRI/WPAHS, <sup>2</sup>Children's Hospital of Pittsburgh, Pittsburgh, PA

We hypothesized that a bacterial species possesses a collection of genes far larger than the genome of any single bacterial strain and that the distribution of these component contingency genes among individual strains

within natural populations provide the bacterial species with an accessible reservoir for genetic exchange which confers a survival advantage to the population during polyclonal chronic infections. To test this notion of genomic plasticity, we studied 10 low-passage clinical isolates of *H. influenzae* (HI) and 11 low-passage clinical isolates of *P. aeruginosa* (PA), originally obtained from middle-ear effusions of patients with chronic otitis media and otorrhea. An ATCC strain of PA (Strain 27853) was also included in the study of *P. aeruginosa*. DNA sequencing was performed on 771 clones randomly chosen from a pooled genomic library of HI and 2,000 clones from a pooled genomic library of PA. Sequence analysis demonstrated that 72 (9.3%) of the HI clones were novel when compared to the Rd KW20 genome, and 125 (6.3%) of the PA clones were novel when compared to the PA01 genome. The distribution and expression of most of the novel HI and PA sequences among the component isolates was determined by PCR and RT-PCR-based analyses, respectively, using primers designed corresponding to the open reading frames (ORFs). All novel sequences which were transcribed in one or more of the clinical strains indicating that they corresponded to functional genes. These unique genes were non-uniformly distributed among the ten isolates of HI and the twelve isolates of PA. The studies on both species revealed an extensive genomic plasticity among the individual clinical isolates, supporting our hypothesis.

#### **146 Investigating the Role of the Com Operon in Competence and Transformation in Hemophilus Influenzae**

**Azad I. Ahmed<sup>1</sup>**, Kai Shen<sup>1</sup>, Garth D. Ehrlich<sup>1</sup>, Mandal Singh<sup>1</sup>, Richard Dopico<sup>1</sup>, Erica Schleifman<sup>1</sup>, Robert A. Preston<sup>1</sup>, Sandeep Kathju<sup>1</sup>, Rosemary J. Redfield<sup>2</sup>, J. Christopher Post<sup>1</sup>, Fen Ze Hu<sup>1</sup>

<sup>1</sup>*Center for Genomic Sciences - ASRI/WPAHS,*

<sup>2</sup>*Department of Zoology, University of British Columbia, Vancouver, BC, Canada*

The study of otitis media is changing our perception of the pathogenesis of chronic bacterial infections. We have established that the bacteria employ mucosal biofilms as a pathogenic mechanism that provides for persistent disease. We have also observed extensive genomic plasticity in *P. aeruginosa* and *H. influenzae* and have promulgated the Distributed Genome Hypothesis (DGH) to explain this diversity. The DGH states that genomic plasticity is a supra-virulence factor acting at the population level that provides for improved population survival through horizontal gene transfer mechanisms that provides for rapid adaptation to change in the environment. Successful chronic bacterial pathogens have evolved highly complex auto-transformation mechanisms for the uptake of species-specific DNA from the environment. However, transformation of clinical strains in vitro has not been described. We began by developing methods for transformation of clinical strains and then designed a study to investigate the evolutionary role of having a natural competence and transformation system present during infection. The com operon contains genes required for

competence and transformation. ComA is required for DNA uptake and therefore its deletion would render the cells both unable to take up and integrate DNA. ComE is required for transformation following uptake, therefore deletion would not affect uptake, but would abrogate transformation. In a test to see if transformability in *H. influenzae* is required for survival during chronic infection we constructed both comA and comE knockouts and are comparing the affect of these two knockouts (in syngeneic strains) to compete with wild type strains in an in vivo animal model of infection.

#### **147 Pseudomonas Aeruginosa Fluorescent Protein Reporter Vectors and the Investigation of Biofilm Formation**

**Luanne Hall-Stoodley<sup>1</sup>**, Joshua Levenson<sup>1</sup>, Bethany Dice<sup>1</sup>, Paul Stoodley<sup>1</sup>, Fen Ze Hu<sup>1</sup>, Laura Nistico<sup>1</sup>, Patricia Antalis<sup>1</sup>, Nathan Ehrlich<sup>1</sup>, Jay Hayes<sup>1</sup>, J. Christopher Post<sup>1</sup>, Garth Ehrlich<sup>1</sup>, Geza Erdos<sup>1</sup>

<sup>1</sup>*Center for Genomic Sciences - ASRI/WPAHS*

Otitis Media (OM) is the most common cause of acquired hearing loss in children. *Pseudomonas aeruginosa* (PA) is the most frequent pathogen that causes otorrhea. We have developed fluorescent protein (FP) vectors for use in 11 low passage clinical strains of PA from patients with otorrhea/OM obtained from Children's Hospital of Pittsburgh and Allegheny General Hospital to test biofilm-related gene activities. To identify genes of interest, in previous work a pooled genomic library was prepared using a fully robotic laboratory approach. The genomic library was then spotted onto nylon filter arrays and probed with labeled RNA from individual clinical PA strains grown as biofilms or in planktonic cultures. This approach demonstrated several novel genes that are absent in the reference PAO1 strain. The goal of the present work was to develop a reporter system that would allow imaging and detection of expression of these novel genes over time when PA clinical strains are grown 1) planktonically; 2) as a biofilm; and 3) as a mucosal biofilm growing on middle ear epithelium in vivo using the Chinchilla model of OM. Since commercial FP technologies use antibiotic selection with antibiotics to which the clinical PA strains are resistant, we successfully designed and constructed FP vectors using a gentamicin selection marker with and without a constitutive promoter. Novel gene promoters can then be spliced into the reporter vector and imaged using Confocal Laser Scanning Microscopy (CLSM). This technology enables us to investigate changes that occur when PA grows as a biofilm in vitro or in vivo during the infectious process. Using the clinical strains PittD and PittF with a cyan FP reporter vector, we have successfully demonstrated biofilm formation on glass, and on chinchilla middle ear mucosa early in infection with CSLM.

**148 Age-Dependent Changes in Expression Patterns of Pattern Recognition Receptors in Middle Ear Mucosal Epithelium in Lipopolysaccharide Induced Acute Otitis Media in Rats After Weaning**

Ha-Sheng Li-Korotky<sup>1,2</sup>, Juliane Banks<sup>2</sup>, Chia-Yee Lo<sup>2</sup>, William Doyle<sup>1,2</sup>

<sup>1</sup>University of Pittsburgh School of Medicine, <sup>2</sup>Children's Hospital of Pittsburgh

Background: Otitis media (OM) is the most common disease in infants and children at the age between 6 month and 2 year old. Lipopolysaccharide (LPS), endotoxin of Gram-negative bacteria, is present in a high percentage of the middle ear (ME) effusions. Related bacteria contain similar structural motifs that can be readily detected by host innate immunity as molecular patterns of infectious non-self, termed pathogen-associated molecular patterns (PAMPs). Host innate recognition molecules, known as pattern recognition receptors (PRRs), recognize PAMPs and activate both innate and adaptive immunity. ME mucosa (MEM) is the first line of defense. It remains, however, largely unknown how MEM responds to pathogen attack via PRRs' activation during early development. Aim: To define age-dependent expression patterns and molecular activities of the PRRs including CD14, LPS binding protein (LBP), and toll-like receptors (TLRs) in MEM during acute phase response to LPS in rats after weaning. Methods: MEs were inoculated with 15 µl of either PBS or LPS (*Pseudomonas aeruginosa*) in rats at 1 month (shortly after weaning) and 2 months of age. MEMs were collected and PRR transcript levels were assessed at 12 h and 48 h after ME challenge using real-time PCR. Results: No difference at the basal expression levels of PRRs was observed between the two age groups. Nevertheless, MEM of one-month-old rats was more responsive to LPS-induced inflammation than that of the 2-month-old rats, even though both age groups demonstrated similar expression patterns after LPS challenge. Profiles showed three expression patterns of PRRs in LPS challenged MEM: 1) acute induction of Cd14, Tlr2, Tlr5, and Tlr7 at 12 h; 2) increased molecular activity of Tlr8 from 12 h to 48 h; and 3) later elevation of Tlr9 at 48 h. Conclusion: MEM innate immunity undergoes changes in response to pathogen ligands after weaning. PRR hyper-reactivity and associated modulation of local innate and adaptive immune responses in the MEM of the young rats may play a role in predisposition to OM.

**149 Pneumococcal Biofilms and the Bacterial Plurality**

Fen Ze Hu<sup>1</sup>, Garth Ehrlich<sup>1</sup>, Kai Shen<sup>1</sup>, Bethany Dice<sup>1</sup>, Benjamin Janto<sup>1</sup>, Randy Keefe<sup>1</sup>, Azad Ahmed<sup>1</sup>, John Gladitz<sup>1</sup>, Jennifer Jocz<sup>1</sup>, Laura Kropp<sup>1</sup>, Nathan Ehrlich<sup>1</sup>, Richard Dopico<sup>1</sup>, Jay Hayes<sup>1</sup>, Robert A. Preston<sup>1</sup>, Joshua Levenson<sup>1</sup>, Prathapan Thiruvilangam<sup>1</sup>, Paul Stoodley<sup>1</sup>, Laura Nistico<sup>1</sup>, Joseph E. Kerschner<sup>2</sup>, Justin Hogg<sup>1</sup>, Susan Yu<sup>1</sup>, David P. Greenberg<sup>3</sup>, Karen Barbadora<sup>3</sup>, J. Christopher Post<sup>1</sup>, Luanne Hall-Stoodley<sup>1</sup>

<sup>1</sup>Center for Genomic Sciences - ASRI/WPAHS, <sup>2</sup>Medical College of Wisconsin, <sup>3</sup>Children's Hospital of Pittsburgh

*Streptococcus pneumoniae* (SP) is a major pathogen associated with otitis media (OM), the most common cause of hearing loss in children. Analyses of middle-ear biopsies using molecular diagnostics and confocal laser scanning microscopy (CLSM) suggested the presence of SP biofilms on middle-ear mucosa in children with OM. The current study used 8 of the most prevalent SP serotypes to determine if SP uses the pathogenic strategy of Bacterial Plurality that we have previously demonstrated for the OM pathogens, *Haemophilus influenzae* and *Pseudomonas aeruginosa*. Phenotypic plurality was evaluated by testing all strains for biofilm development in vitro, and genotypic plurality was studied by DNA sequencing. CLSM of adherent bacteria on glass and plastic demonstrated SP biofilms in vitro. Significantly, biofilm growth was shown over 9 days for strains that undergo autolysis within hours in planktonic culture, indicating that the metabolic state of the biofilm environment differs from planktonic forms. Strains also exhibited distinct biofilm structure: some formed large towers while others grew more uniform biofilms. Genomic libraries for each strain were prepared and DNA sequencing of ~ 800 random clones was performed. Homology searches revealed that ~ 5-15% of all clones were unique with respect to the TIGR 4 and R6 reference strains. PCR and RT-PCR-based assays were developed to examine the distribution patterns for 105 unique genes. Analyses revealed that no two clinical strains were alike; i.e. each strain contains a unique complement of distributed contingency genes. These findings support the distributed genome hypothesis of Bacterial Plurality where contingency genes among a bacterial population serve as a supra-virulence factor that enhances survival via horizontal gene transfer and rapid adaptation to environmental conditions through the reassortment of genes among strains within a population.

**150 A New Treatment Strategy for Otitis Media with Effusion**

Steven Hefeneider<sup>1,2</sup>, Stephen Kurtz<sup>2</sup>, Sharon McCoy<sup>1,2</sup>, Carol MacArthur<sup>3</sup>, Dennis Trune<sup>3</sup>

<sup>1</sup>Veterans Affairs Medical Center, Portland, OR, <sup>2</sup>Targeted Gene Delivery, Inc., Portland, OR, <sup>3</sup>Department of Otolaryngology, Oregon Health and Science University, Portland, OR

Otitis media with effusion (OME) is an inflammatory disease of the middle ear, primarily initiated by bacteria. OME is characterized by production of pro-inflammatory

cytokines by host immune cells within the middle ear, followed by fluid accumulation and mucosal thickening. The inflammatory immune response is initiated by intracellular signaling pathways that are activated by the interaction of pathogen-associated molecular patterns (PAMPs), found on bacteria, viruses, and fungi, with toll-like receptors (TLRs) on immune cells. This ligand/receptor interaction results in production of pro-inflammatory cytokines and upregulation of chemokines, leading to inflammation designed to contain and eliminate the pathogen. Vaccinia virus encodes immunoregulatory proteins, such as A52R, that can effectively inhibit intracellular signaling initiated by PAMP/TLR interaction, resulting in a diminished host immune response and enhancing viral survival. Here we report the identification and characterization of an 11 amino acid peptide derived from the A52R protein that, when linked to a 9-arginine cell transduction sequence, effectively inhibits cytokine secretion in response to TLR activation. The peptide had no effect on cytokine secretion resulting from cell activation that was initiated independent of TLR stimulation. Employing a mouse model of OME, administration of heat-inactivated *Streptococcus pneumoniae* into the middle ears of BALB/c mice resulted in a significant inflammatory response that was dramatically reduced with peptide treatment. Treatment with peptide resulted in marked reductions in fluid accumulation, number of inflammatory cells, and mucosal thickening in the middle ear. The identification of this peptide that selectively targets TLR-dependent signaling may have application in the treatment of chronic inflammation initiated by bacterial or viral infections.

### 151 Otitis Media in TNF-Deficient Mice

Joerg Ebmeyer<sup>1,2</sup>, Masayuki Furukawa<sup>1,3</sup>, Kwang Pak<sup>1</sup>, Eduardo Chavez<sup>1</sup>, Umay Ebmeyer<sup>1</sup>, David Broide<sup>4</sup>, Stephen Wasserman<sup>4</sup>, Allen Ryan<sup>1</sup>

<sup>1</sup>Department of Surgery/Otolaryngology UCSD School of Medicine, <sup>2</sup>Department of Otorhinolaryngology, Head and Neck Surgery University of Wuerzburg/Germany, <sup>3</sup>Department of Otorhinolaryngology-Head & Neck Surgery, Tohoku University, Sendai, Japan, <sup>4</sup>Department of Medicine UCSD School of Medicine

Tumor necrosis factor (TNF) has been reported to participate in the pathogenesis of bacterial otitis media (OM). It seems to mediate mucosal hyperplasia and can be found regularly in middle ear (ME) effusions. However, the impact of TNF on the course of bacterial OM has received relatively little attention.

The MEs of TNF-knockout mice (B6;129S6-Tnftm1Gkl/J, Jackson) were inoculated with nontypeable *Haemophilus influenzae* (NTHi) in accordance with a mouse model of experimental OM. The thickness of the ME mucosa as well as the number of inflammatory cells in the ME lumen were measured in microscopic sections on days one, two, three and five after challenge and compared to the findings in wild-type control mice (B6129SF2/J, Jackson).

In wild-type mice, mucosal hyperplasia was observed starting on day one and peaking on day two. By day five, the mucosa was back to normal. The number of inflammatory cells peaked on day one and was still

significant on day two. Five days after challenge, cells had cleared out of the ME cavity.

In TNF-knockout mice, the mucosal reaction to NTHi on the first three days was not significantly different to wild-type mice. However, on day five after challenge, the ME mucosa was not back to normal, but still unalteredly hyperplastic. Also, significant numbers of inflammatory cells in the ME lumen could be found throughout the observation period.

Our results indicate that TNF is essential in controlling bacterial OM. In the absence of TNF, bacterial infection can not be repelled in five days.

Supported by grant DC00129 from the NIH/NIDCD and by the German DFG (EB 260/1-1)

### 152 Intranasal Vaccination Against Pneumococcal Otitis Media in Neonatal Mice.

Albert Sabirov<sup>1</sup>, Dennis Metzger<sup>1</sup>

<sup>1</sup>Albany Medical College

*Streptococcus pneumoniae* is the leading bacterial cause of acute otitis media (OM) in infants and young children. The recently introduced pneumococcal conjugate vaccine, which is administered via the intramuscular route, is poorly protective against development of OM. In the present study, we tested the efficacy of intranasal (i.n.) vaccination with conjugate vaccine and interleukin-12 (IL-12) as a mucosal adjuvant against development of OM in neonatal mice. We employed two models of streptococcal OM: after direct middle ear (ME) challenge, and after intranasal challenge, which leads to nasopharyngeal colonization (NC). Neonatal wild-type (WT), IFN- $\gamma$  knockout (IFN- $\gamma^{-/-}$ ), and IgA knockout (IgA $^{-/-}$ ) mice were immunized i.n. with type 14 pneumococcal conjugate vaccine on days 7 and 14 after birth and treated with IL-12 (vaccine+IL-12 group) or PBS vehicle (vaccine only group) on days 7-10 and 14. I.n. vaccination of WT mice in the presence of IL-12 was found to significantly enhance the levels of specific antibodies (IgA, IgG1, IgG2a and total) in ME washes, nasal washes, and serum, and the levels of IFN- $\gamma^{-/-}$  in the ME. However, IL-12-mediated enhancement of mucosal and serum antibody responses did not occur in IFN- $\gamma^{-/-}$  mice. Increased numbers of specific IgA antibody-producing cells as well as IgA- and IgG-positive cells were detected in the ME and nasal mucosa after i.n. vaccination of WT mice in the presence of IL-12. Vaccine+IL-12 treated WT mice showed enhanced bacterial clearance from the ME, decreased NC and reduced incidence of OM. In addition, direct ME challenge of vaccine+IL-12 treated WT mice with a lethal dose of bacteria resulted in 89% survival. However, examination of nasal washes showed that IgA $^{-/-}$  mice failed to clear bacteria as efficiently as WT mice. There was no difference in the incidence of OM and NC between immunized and unimmunized IgA $^{-/-}$  mice. This suggests the importance of pneumococcus-specific IgA in protection against OM and NC. These results indicate that i.n. vaccination of neonatal mice in the presence of IL-12 is able to enhance ME mucosal and systemic immune responses to pneumococci, responses that were IgA and IFN- $\gamma$  dependent, and efficiently protect against both OM and invasive infection.

Supported by NIH grant AI41715 and a grant from Philip Morris, Inc.

### **153 Regulation of Mucosal Hyperplasia by Apoptosis During Bacterial Otitis Media**

**Masayuki Furukawa**<sup>1,2</sup>, Joerg Ebmeyer<sup>1</sup>, Won-Ho Chung<sup>1</sup>, Kwang Pak<sup>1</sup>, Nicholas Webster<sup>1</sup>, Allen Ryan<sup>1</sup>

<sup>1</sup>UCSD School of Medicine, <sup>2</sup>Tohoku University School of Medicine

Hyperplasia of the middle ear (ME) mucosa is an important component of otitis media (OM), involving substantial cell proliferation and differentiation. Hyperplasia contributes to the deleterious sequelae of OM, including the production of mucous secretions of ME effusions. Hyperplasia is also involved in fibrosis and other permanent damage that can occur in repeated and/or chronic OM. Return of the ME mucosa to normal during OM recovery involves the loss of large number of excess cells

The present study investigated the participation of programmed cell death, or apoptosis, in an animal model of bacterial OM. OM was induced by the inoculation of nontypeable Haemophilus influenzae into the rat middle ear cavity. The ME mucosa was dissected bilaterally from 5 rats at 7 time points spanning OM and recovery. Western blotting data clearly indicated that caspase 3 was present in the normal ME mucosa and at all 7 time points during OM, and that activation of caspase 3 occurred during OM. Cleaved caspase 3 (mol wt, 17kD) in the middle ear mucosa was first observed 24h after bacterial inoculation, was maximal at 72h and returned to undetectable levels by 5 d. Immunohistochemical analysis at 24 and 72h after bacterial inoculation revealed the presence of cleaved caspase 3 in a variety of cell types within the ME mucosa. The distribution of TUNEL labeled cells was similar to those showing cleaved caspase 3, further supporting the presence of apoptosis. The involvement of apoptosis relatively early in OM indicates that programmed cell death participates in the growth phase of hyperplasia, perhaps reflecting removal of cells with a resting phenotype, or pruning of excess proliferating cells. The high levels of caspase cleavage and TUNEL labeling later in OM further indicate that apoptosis plays a major role in recovery. Our data suggest that pharmacological intervention in programmed cell death may provide a novel method for pharmacological intervention in OM.

Supported by NIH/NIDCD grant DC00129.

### **154 Mucin Gene Cdna Sequence Characterization in Chinchilla Middle Ear Epithelium**

**Joseph Kerschner**<sup>1,2</sup>, Tanya Meyers<sup>1</sup>, Amy Burrows<sup>1</sup>

<sup>1</sup>Medical College of Wisconsin, <sup>2</sup>Children's Hospital of Wisconsin

Objectives: To identify mucin genes in chinchilla middle ear epithelium and characterize complimentary deoxyribonucleic acid (cDNA) sequences to facilitate further investigations into mucin pathophysiology.

Methods: Chinchilla mucin gene exploration and cDNA characterization was accomplished using reverse transcriptase-polymerase chain reactions (RT-PCR). Primer pairs were designed using consensus sequences available for human and rodent species. Chinchilla middle ear epithelium cell cultures (CMEEC) were established and explored for the expression of chinchilla mucin genes 1, 2, 4 and 5AC (cMuc1, cMuc2, cMuc4 and cMuc5AC). Identified cDNA amplicons for each of these genes were sequenced and homology compared to published sequences.

Results: CMEEC express the mucin genes cMuc1, cMuc2, cMuc4 and cMuc5AC. cDNA amplicons for these genes were able to be sequenced with lengths ranging from 66 to 362 base pairs. The chinchilla cDNA sequences expressed significant homology with published human and rodent cDNA for these mucin genes.

Conclusions: Chinchilla middle ear epithelium grown in culture expresses the mucin genes 1, 2, 4 and 5AC, which have been identified as important in mucin regulation in the middle ear. cDNA sequences corresponding to these mucin genes were identified and may serve as important molecular tools in future studies of otitis media using the chinchilla model.

### **155 The Bioelectric Response of Middle Ear Mucosa to Negative Ambient Pressure**

**David Mandell**<sup>1,2</sup>, Ryan Soose<sup>1</sup>, Corinne VanBeek<sup>2</sup>, Juliane Banks<sup>1</sup>, Patricia Hebda<sup>1,2</sup>

<sup>1</sup>Children's Hospital of Pittsburgh, <sup>2</sup>University of Pittsburgh School of Medicine

Background: The hydrops ex vacuo theory of otitis media with effusion (OME) states that middle ear underpressure from eustachian tube obstruction causes passive transudation of mucosal and interstitial fluid into the middle ear airspace. However, it is unknown if mucosal bioelectric changes may also contribute to the development and persistence of OME. In children prone to OME, middle ear pressure is often < -200 daPa. The effect of negative middle ear pressure on mucosal ion transport, and thus on mucosal absorptive or secretory properties, is unknown.

Objectives: To compare the effect of negative pressure versus atmospheric pressure on transepithelial sodium (Na<sup>+</sup>) absorption and chloride (Cl<sup>-</sup>) secretion.

Methods: Mongolian gerbil middle ear epithelial cell monolayers transformed with SV40 were exposed to 24 hours of either negative pressure (-250 daPa) or atmospheric pressure (control, 0 daPa) in airtight incubation chambers. Cells were then mounted into an Ussing chamber and transepithelial short circuit current (I<sub>sc</sub>) was measured.

Results: Middle ear cells exposed to negative pressure had similar baseline I<sub>sc</sub> and amiloride-sensitive transepithelial Na<sup>+</sup> absorption as controls. UTP-induced stimulation of transepithelial Cl<sup>-</sup> secretion was decreased with negative pressure exposure (I<sub>sc</sub> = 26.0 +/- 1.7 μA/cm<sup>2</sup>) when compared to controls (I<sub>sc</sub> = 35.7 +/- 3.3 μA/cm<sup>2</sup>), p=0.01. Pre-application of DIDS, a Ca<sup>2+</sup>-activated Cl<sup>-</sup> channel blocker, resulted in decreased response to UTP in controls, but not in cells exposed to negative pressure,

indicating that the change induced by negative pressure affects Ca<sup>2+</sup>-activated Cl<sup>-</sup> ion channels.

Conclusions: In cultured middle ear epithelial cells, exposure to negative pressure resulted in a decrease in UTP-induced Cl<sup>-</sup> secretion via Ca<sup>2+</sup>-activated Cl<sup>-</sup> channels. Decreased Cl<sup>-</sup> secretion may lead to decreased middle ear humidification and periciliary fluid depth, factors which might contribute to development and persistence of OME.

### **156 Middle Ear Epithelial Mucin Secretion in Response to Interleukin-1 $\beta$**

Erica A. Samuel<sup>1</sup>, Amy C. Burrows<sup>1</sup>, Joseph E. Kerschner<sup>1</sup>

<sup>1</sup>Medical College of Wisconsin

Otitis media is the most common diagnosis in pediatric patients who visit physicians for illness in the United States. Mucin production in response to otitis media causes significant sequelae including hearing loss and the need for surgical intervention. Variation in the quantity and character of middle ear secretions, specifically mucin secretion, are known to be important in the pathophysiologic mechanisms of otitis media. In addition, cytokines play an integral role in the mechanisms of otitis media, thus, investigating the effect of specific cytokines on the regulation of mucin secretion is vital to furthering our knowledge of the pathophysiology of otitis media.

We investigated the changes in mucin secretion from human middle ear epithelium (MEE) in response to interleukin-1 $\beta$ , an essential inflammatory mediator in otitis media. Human MEE cultures were established from a transformed cell line and exposed to 0, 2.5, 5, 10, 50, 100, and 200ng/mL concentrations of IL-1 $\beta$  in growth media for 16 hours after exposure to 5 $\mu$ Ci/mL tritiated glucosamine. The culture supernatant was then drawn off and loaded on sepharose columns after enzymatic degradation. The radioactivity of 2mL fractions was measured by liquid scintillation. The radioactivity was compared to the appropriate control to determine the amount of mucin produced.

Mucin production from human MEE increased in a dose-dependent manner in regard to IL-1 $\beta$  exposure. These findings add to our knowledge of the inflammatory processes involved in the development of otitis media and may provide new avenues for intervention and treatment in patients with otitis media.

### **157 Effect of Rimexolone Vs. Dexamethasone on Middle Ear Inflammation in Experimental Otitis Media in Chinchillas.**

Andrew Florea<sup>1</sup>, Aron Depew<sup>1</sup>, Seong Kook Park<sup>1</sup>, Jared Inman<sup>1</sup>, Rachele Wareham<sup>1</sup>, Kaalan Johnson<sup>1</sup>, Choong Won Lee<sup>1</sup>, G. Michael Wall<sup>2</sup>, Earnest John<sup>3</sup>, Timothy Jung<sup>3</sup>

<sup>1</sup>Loma Linda University Medical Center, <sup>2</sup>Alcon Laboratories, <sup>3</sup>Jerry L. Pettis Veteran's Administration Medical Center

Objective: Otitis media (OM) is one of the most common diseases in the pediatric population. Our previous studies showed treatment with systemic antibiotics and corticosteroids were more efficacious than antibiotics

alone. The purpose of this study was to determine effectiveness of topical application of corticosteroids on the outcome of OM. The long-term goal of this study is to find a better method of treatment of OM especially using topical treatment thereby avoiding systemic side effects.

Study Design and Methods: Three experimental groups were studied. Otitis media with effusion was induced in all groups of chinchillas by injecting lipopolysaccharide (LPS). Group 1 consisted of controls in three subgroups: Control-LPS alone; vehicle of dexamethasone (Control-dexa); vehicle of rimexolone (Control-rimex). Group 2 was treated with dexamethasone and included subgroups of separate concentrations of dexamethasone: 0.1% and 1% suspensions. Group 3 was treated with rimexolone and included subgroups of separate concentrations of rimexolone: 0.1% and 1% suspensions. A total of 60 animals were used – 36 for controls and 24 for experimental groups. All test substances (saline, rimex-vehicle, Dexa-vehicle, dexamethasone and rimexolone, 200 $\mu$ L) were injected at -2, 48 and 60 hours; LPS was injected at 0 hrs. Animals were monitored with daily otomicroscopy. At the end of 4 days, samples of MEE were collected for analysis and temporal bones harvested for histopathological studies.

Results: At the end of 4 days, only in five ears (3/20 1% dexamethasone, 1/20 1% rimexolone, and 1/20 0.1% rimexolone) the fluid had diminished to the point of being unobservable. The volume of MEE, thickness of mucoperiosteum, and the degree of inflammation of middle ear mucosa in 1% dexamethasone and 1% rimexolone was significantly less compared to other groups.

Conclusion: Topical corticosteroid treatment was effective in resolving inflammation of the middle ear mucosa in the experimental otitis media. Dexamethasone was more effective than rimexolone.

### **158 Role of Biofilm Formation on Adenoid Tissue in Recurrent Acute Otitis Media**

Abhishek Prasad<sup>1</sup>, Romy Yun<sup>2</sup>, Michael Haupt<sup>3</sup>, Richard Berk<sup>4</sup>, James Coticchia<sup>1</sup>

<sup>1</sup>Detroit Medical Center/Wayne State University, <sup>2</sup>Case Western Reserve University, <sup>3</sup>Wayne State University/Children's Hospital of Michigan, <sup>4</sup>Wayne State University School of Medicine

Biofilms account for 98% of bacterial growth in the natural environment. Previous investigators have demonstrated the importance of biofilm formation in otitis media with effusion and recurrent acute otitis media. It has been well established that adenoidectomy has utility in the management of recurrent acute otitis media (RAOM) as well as sinusitis refractory to medical management, regardless of the adenoid size. It has also been demonstrated by numerous investigators that otitis prone children have an increased nasopharyngeal carriage rate of middle ear pathogens. A possible mechanism for the benefit of adenoidectomy in these cases lies in the eradication of these middle ear pathogens. Certain species that are known middle ear pathogens such as *Hemophilus influenzae* are capable of forming biofilms, which are protective polysaccharide matrices generated by

bacteria under specific environmental stimuli. The ensuing mechanical barrier and decreased metabolic activity of bacteria in biofilms render these microorganisms resistant to antibiotic therapy. Other biofilm infections such as those that occur on artificial heart valves and intravenous catheters are extremely resistant to antimicrobial treatment and require removal of the device for eradication of the infection. As of yet to our knowledge, biofilms have not been demonstrated to exist in adenoidal tissue. In the present investigation, we recovered adenoid tissue from patients with recurrent acute otitis media. Utilizing scanning electron microscopy, adenoid images demonstrating colonies with high density microfibrillar networks consistent with extant images of biofilms on closely related tissue in the literature have been identified. This data suggests that some of the benefit derived from adenoidectomy in patients with RAOM may result from a mechanical debridement of biofilm microenvironments within adenoids, thereby eliminating a nasopharyngeal reservoir of these middle ear pathogens in resistant biofilms.

### **159** Expression of EGFR and MUC5AC in the Middle Ear Mucosa of Rat with Otitis Media Induced by Endotoxin

**Jae-Jun Song**<sup>1</sup>, Sung-Won Chae<sup>1</sup>, Jae-Gu Cho<sup>1</sup>, Kak-Hyun Jung<sup>1</sup>, Soon-Jae Hwang<sup>1</sup>

<sup>1</sup>*Korea University College of Medicine*

Expression of EGFR and MUC5AC in the middle ear mucosa of rat with otitis media induced by endotoxin

**Background and Objectives** :Otitis media with effusion(OME) is major cause of conductive hearing impairment in 2-4 years old. Mucin is a major component of middle ear effusion and controlled by several growth factor, especially epidermal growth factor(EGF) and its receptor(EGFR). This study aimed to analyze the relationship between EGFR and mucin gene(MUC5AC). **Materials and Methods** : Tissue samples from lipopolysaccharides induced inflammatory middle ear mucosa was achieved from rat. The protein of EGFR and MUC5AC was identified by Western blotting and mRNA expression was determined by reverse transcriptase-polymerase chain reaction (RT-PCR) at 0, 1, 3, 6, 12, 24hours, 3days and 7days. **Results** : By Western blotting, EGFR was detected at 1,3 days and MUC5AC at 3, 7days. By RT-PCR, EGFR mRNA was detected strongly at 6hours and MUC5AC mRNA at 3days. **Conclusions** : The expression of EGFR and MUC5AC within the middle ear mucosa were defined and mucin was expressed after the expression of EGFR. We thought that MUC5AC is up-regulated by EGF family and its receptor.

**KEY WORDS** : EGFR, MUC5AC, OME

### **160** Binaural Loudness Compensation with two Hearing Aid Fitting Strategies

**Uwe Baumann**<sup>1</sup>, Ingeborg Stemplinger<sup>1</sup>, Andrea Nobbe<sup>1</sup>, Josef Chalupper<sup>2</sup>, Kristin Rohrseitz<sup>2</sup>

<sup>1</sup>*Universität München/Großhadern*, <sup>2</sup>*Siemens Audiologische Technik/Erlangen*

Two different binaural loudness compensation strategies were tested in 20 subjects with a symmetric sloping high frequency sensorineural hearing loss. After an examination of the eardrum by microscopy and execution of pure tone audiometry including bone conduction and determination of uncomfortable loudness levels the subjects received the test hearing aid (Siemens Triano S BTE) and were fitted monaurally according to NAL-NL1. Binaural loudness compensation was realized by either simple -3 dB gain reduction or a level dependent compensation according to the suggestions for binaural fitting of NAL-NL1. Loudness rating was performed in an audiometric test room and the rating of the subject was recorded by means of a touch sensitive display. The task of the subject was to indicate the perceived loudness by assigning an appropriate position on a displayed bar with 270 millimeters length. The test signals were amplitude modulated narrow band noises (1/3 octave) with 4 different center frequencies (CF) and levels in between 30 and 90 dB SPL. In addition, CCITT noise was presented with 40, 65 and 90 dB. For a subjective rating of the pleasantness of the fitting a short piece of orchestral music and a traffic noise signal was presented with 2 different compression schemes (syllable/dual compression). In total, 5 conditions were tested (monaural left/right – contralateral earpiece in situ, ventilation plugged with plasticine, binaural without compensation, binaural -3 dB compensation, binaural compensation according to NAL-NL1). Binaural loudness summation was absent at 500 Hz CF, increased with higher CF and was most prominent at 4 kHz CF. The effect of binaural loudness reduction was highest with the adaptive NAL-NL1 based fitting and the results obtained with the -3 dB compensation method were close to monaural loudness judgments. A significant effect of compression scheme was observed for both music and street noise example with higher loudness ratings for the dual compression method.

### **161** Audiometric Threshold Shift Definitions: Simulations and Suggestions

**Robert Dobie**<sup>1,2</sup>

<sup>1</sup>*UC-Davis*, <sup>2</sup>*Dobie Associates*

Monitoring audiometry programs for noise-exposed workers and for patients receiving ototoxic drugs require definitions of significant threshold shift (STS) that maximize true positives (TPs) while minimizing false positives (FPs). For example, the Occupational Safety and Health Administration (OSHA) defines an STS as a 10 dB or greater shift for the worse, averaged across 2, 3, and 4 kHz, in either ear. Unfortunately, there is no obvious independent "gold standard" by which apparent threshold shifts can be categorized as TPs or FPs. Three surrogate validation methods have been available for real world studies, but each of them has serious drawbacks. Using

computer simulation of large groups of audiograms with plausible test-retest variability, with and without threshold shifts at different frequencies, it was found that the most accurate method of comparing one decision variable to another requires two patient groups similar in every respect except that one has been exposed to the potentially hazardous agent (noise or drug) and the other has not. When a non-exposed control group is unavailable, a second method, in which the number of negative shifts (apparent changes for the better) is used to estimate the number of FPs, was reasonably accurate for criterion values that yielded relatively small numbers of STSs, but was progressively inaccurate for criterion values that yielded larger numbers of STSs. The least accurate validation method characterized STSs that persisted on a third test as TPs and those that did not persist as FPs. This method systematically makes definitions that yield large numbers of STSs falsely appear to perform better (higher ratio of TPs to FPs) than definitions that yield fewer STSs, and makes definitions applied twice falsely appear to perform much better than definitions applied once. Previous studies of STS definitions for occupational hearing conservation programs have either failed to show the superiority of one STS definition over others, or have failed to consider the shortcomings of these surrogate validation methods. Thus, recommendations by several professional groups that OSHA should change its STS definition are not yet justified. Additional research with either new or old databases might show that a change in the OSHA STS definition would be desirable.

## **162** Hearing Loss in Workers Exposed to Different Types of Noise and Organic Solvents and Hand-Arm Vibration

Mariola Sliwinska-Kowalska<sup>1</sup>, Ewa Zamyslowska-Szmytko<sup>1</sup>, Malgorzata Pawlaczyk-Luszczynska<sup>1</sup>, Grazyna Tarnawska<sup>1</sup>

<sup>1</sup>NIOM

The severity of occupational noise-induced hearing loss could be significantly influenced by co-exposure to noise and chemicals, e.g. organic solvents. The consequences of noise exposure depend not only on the equivalent sound pressure level, but also on its impulsiveness.

The aim of the study was to evaluate hearing impairment in four groups of subjects: 427 dockyard workers co-exposed to steady-state noise (at the equivalent level  $95.5 \pm 1.8$  dBA) and organic solvent mixture; 161 dockyard workers exposed to impulse noise (at the equivalent level  $92.5 \pm 3.3$  dBA); 86 glass factory workers exposed to continuous steady-state noise only (at the equivalent level  $90.8 \pm 4.4$  dBA); and 204 control subjects exposed neither to noise nor to solvents or vibration. Gender and age were accounted for as confounding factors in all statistical analyses.

Audiometric results revealed the poorest hearing thresholds in the group exposed to impulse noise, lesser degree of hearing loss was seen in the groups exposed to continuous noise only, and continuous noise and organic solvent mixture.

There was no difference in the ABR results between study groups. The P-300 latency was prolonged in impulse-noise-exposed workers as compared with those exposed to steady-state noise, suggesting a central hearing effect of the impulse noise exposure, apart from the cochlear lesion. The results indicate that noise characteristics and co-exposure to noise and chemicals should be taken into account in evaluation of risk of occupational hearing loss.

## **163** Effects of GSM Cellular Phones on Human Hearing: the European Project GUARD

Paolo Ravazzani<sup>1</sup>, Lionel Collet<sup>2</sup>, Mark E. Lutman<sup>3</sup>, George Tavartkiladze<sup>4</sup>, Gyorgy Thuroczy<sup>5</sup>, Miltos Tsalighopoulos<sup>6</sup>, Virgilijus Uloza<sup>7</sup>, Ingrida Uloziene<sup>7</sup>, Steven Bell<sup>3</sup>, Annie Moulin<sup>2</sup>, Marta Parazzini<sup>1</sup>, Nathan A. Thomas<sup>3</sup>, Gabriella Tognola<sup>1</sup>

<sup>1</sup>Istituto di Ingegneria Biomedica CNR, <sup>2</sup>Université Claude Bernard Lyon1 and CNRS-UMR5020, Lyon, <sup>3</sup>Institute of Sound and Vibration Research, University of Southampton, <sup>4</sup>Research Centre for Audiology and Hearing Rehabilitation, Moscow, <sup>5</sup>"Frederic Joliot-Curie" National Research Inst Radiobiology and Radiohygiene, Dept of NIRR, Budapest, <sup>6</sup>AHEPA District General Hospital of Thessaloniki, <sup>7</sup>Kaunas University of Medicine, Biomedical Research Institute

The European multicenter project named GUARD involves nine centers and aims to assess potential changes in auditory function as a consequence of exposure to low-intensity electromagnetic fields (EMF) produced by GSM cellular phones.

Two experimental paradigms are used. The within-subject paradigm entails measurements before and after genuine or sham exposure to EMF in a repeated double-blind design. The between-subject paradigm uses two groups: heavy users and light users of cellular phones, where high users are defined as typically speaking for at least 30 minutes per day and low users are defined as typically speaking for less than 5 minutes per day. Participants are healthy young adults without any evidence of hearing or ear disorder. Tests for assessment of auditory function are: transient otoacoustic emissions (TEOAE), distortion product otoacoustic emissions (DPOAE), effects of contralateral acoustic stimulation (CAS) on OAE and auditory brainstem response (ABR). For the within-subject study only, the exposure consists of speech at a typical conversational level delivered via an earphone to one ear, plus genuine or sham EMF exposure, where EMF exposure utilizes the output of a consumer cellular phone at full power for 10 minutes. A system of phone positioning that allows participants to freely move their head without affecting exposure has been designed.

The final statistical analysis of the GUARD pooled data will be presented and discussed.

This work was financed by the Project GUARD "Potential adverse effects of GSM cellular phones on hearing" (European Commission, 5th Framework Programme, QLK4-CT-2001-00150, 2002-2004).



## **164 An Innovative Method for Developing a New Tinnitus Outcome Questionnaire: Use of a Web-Based Intranet to Solicit Expert Decisions Concerning Content Validity**

Mary B Meikle<sup>1</sup>, Thomas A. Creedon<sup>2</sup>, Harvey B. Abrams<sup>3</sup>, James A. Henry<sup>1</sup>, Craig W. Newman<sup>4</sup>, Sharon A. Sandridge<sup>4</sup>

<sup>1</sup>Oregon Health & Science University, Portland, OR,

<sup>2</sup>edit.Here.com, <sup>3</sup>VA Medical Center, St. Petersburg, FL,

<sup>4</sup>Cleveland Clinic Foundation, Cleveland, OH

Previous work at a number of clinics has resulted in at least 9 different English-language questionnaires for evaluating the severity and negative impact of tinnitus, and has yielded key concepts describing the negative effects of tinnitus (sleep disturbance, depression and anxiety, disruption of work and social activities, etc). However, it also highlights the need for a standardized instrument for clinical research into tinnitus treatments. Standardizing tinnitus measures would improve comparability of treatment effects between different clinics, and provide a more systematic basis for recruiting comparable subjects in different clinical trials. We addressed those needs by setting up a working group of 19 investigators with extensive experience in measurement, diagnosis, and/or treatment of tinnitus to derive a new tinnitus outcome questionnaire. To facilitate and record interactions between group members, a dedicated website will be described which presents discussion materials to the group and solicits members' input regarding content identification, item selection and response scaling for the new questionnaire. Customized web-based forms present the item content of each of the 9 questionnaires (totaling 195 separate items) interactively, requiring group members to rate each item in regard to two aspects of content validity: (1) representativeness with regard to one or more specific tinnitus effects such as sleep disturbance, depression, etc., and (2) the relevance of the item for measuring treatment-related change. Data will be presented illustrating the use of these techniques for optimizing the content validity of a proposed new tinnitus outcomes questionnaire. The data also indicate that the web-based approach to questionnaire development provides an effective method for developing consensus among members of this expert working group.

Supported by the Tinnitus Research Consortium.

## **165 Immunohistochemical and Ultrastructural Abnormalities in Muscle from A Patient with Sensorineural Hearing Loss Related to a 1555 A-to-G Mitochondrial Mutation**

Hideaki Kouzaki<sup>1</sup>, Mikio Suzuki<sup>1</sup>, Takeshi Shimizu<sup>1</sup>

<sup>1</sup>Shiga University of Medical Science

Abstract

Genetic studies indicate that hereditary of the inner ear to toxicity from aminoglycoside antibiotics is caused by a nucleotide 1555 A-to-G mutation in the mitochondrial 12S rRNA gene. Although the phenotype of patients with this mutation is one of nonsyndromic hearing loss, a possibility

of effects on other tissues containing numerous mitochondria like the inner ear, especially muscle, remains. We obtained atemporalis muscle specimen from a deaf patient with the A1555G mutation and found informative pathologic features including mosaic activity of cytochrome oxidase immunoreactivity and mitochondrial ultrastructure. These findings suggest that mitochondrial dysfunction from A1555G mutation extends beyond the inner ear.

## **166 Correlation of the Clinical Audiological Findings in Salicylate Intoxication with the Molecular Inhibition of the Electromotility of OHC by Salicylates**

Hermann Wecker<sup>1</sup>, Claudius Fauser<sup>2</sup>

<sup>1</sup>Evangelisches Waldkrankenhaus, Bonn, <sup>2</sup>Klinikum Rechts der Isar, TU Munich

We report about a young man with an acute moderate aspirin intoxication resulting in a bilateral symmetric hearing loss of 50 dB HL over all frequencies and tinnitus for five days. Otoacoustic emissions were absent on the first day of intoxication but could be measured again on the fifth day after the intoxication. There were no vestibular symptoms in this patient.

Since this is an observation in a single patient only we reviewed the literature for the audiological characteristics of salicylate induced hearing loss and possible molecular mechanisms.

Myers et Bernstein 1967 and others reported about salicylate induced elevations of the pure tone thresholds which correlated with serum salicylate levels. The sensorineural hearing loss was bilateral and symmetrical not exceeding 60 dB even in preexisting hearing losses. The hearing loss was completely reversible after cessation of salicylate intake.

These audiological findings correspond well with an inhibition of the cochlear amplifier. Outer hair cells of the mammalian cochlea actively change their cell length in response to changes of the membrane potential. This electromotility is generally considered the basis of cochlear amplification. Recently the gene for the integral membrane protein prestin was identified. In response to changes in the transmembrane voltage this protein in the OHC undergoes conformational changes which result in changes of the length of the outer hair cells. Coupling of motility and membrane voltage is mediated by intracellular anions, mainly Cl<sup>-</sup> anions. Oliver et al. recently showed that salicylates act as a competitive inhibitor of Cl<sup>-</sup> anions at the anion-binding site of prestin, the motor protein of the outer hair cell.

This molecular mechanism correlates well with the clinical audiological mainstays of aspirin-induced hearing loss, dose dependency, cochlear site of hearing loss and reversibility.

### **167 Auditory Processing Disorder (APD) in children: Not the problem?**

**Stuart Rosen<sup>1</sup>**, Mazal Cohen<sup>2</sup>, Iyngaran Vanniasegaram<sup>3</sup>  
<sup>1</sup>UCL, <sup>2</sup>Institute of Child Health, <sup>3</sup>St George's Hospital

There is currently much interest in the possible role of auditory processing disorders (APD) in the cognitive development of children, particularly regarding language and literacy. To investigate these links, we applied a battery of auditory tests to 32 school-age children who were referred for an auditory evaluation because of listening/hearing problems but who were all within normal limits for standard audiometric assessments (*suspected* APD - sAPD). Their performance was compared to a group of 33 age-matched controls. Neither backward nor simultaneous masking distinguished the two groups, but two simple discrimination tasks did: 1) a verbal task using consonant cluster minimal pairs of real words; 2) a non-verbal task using two short tone pairs differing in fundamental frequency at varying interstimulus intervals. Together, these two tasks detected impaired listening skills in 56% of the sAPD children but only 6% of the controls. Thus, a significant proportion of sAPD children appear to have genuinely auditory problems, although almost ½ appear to have no detectable deficit. A subgroup of the children was then tested on a variety of measures of cognitive skills. The sAPD group scored consistently lower than the controls on both verbal (vocabulary and grammar) and nonverbal skills. Strikingly, sAPD children with relatively good auditory performance did not differ on these measures of cognitive ability from sAPD children with poor auditory performance (unfortunately, no measure of reading ability was available). Therefore, although APD in children can be diagnosed to at least some extent, the presence or absence of APD appears to have little impact on the development of the verbal and nonverbal skills tested here.

### **168 Indicators of Peripheral Auditory Dysfunction in Auditory Processing Disorders**

**Prudence Allen<sup>1</sup>**, Chris Allan<sup>1</sup>  
<sup>1</sup>University of Western Ontario

Auditory Processing Disorders are frequently suspected in children who have normal hearing thresholds, but appear unable to learn efficiently and effectively through the auditory modality. These disorders are most commonly defined based upon their symptoms including for example, difficulty processing rapidly changing stimuli or difficulty understanding speech in degraded conditions. The underlying causes of these problems and their locus of origin within the auditory system have been the topic of much debate.

This paper will report initial results in a comprehensive study of children with suspected auditory processing disorders. The study includes clinical and experimental measures of auditory function, both behavioral and electrophysiologic, as well as standardized measures of phonology, language, memory, attention, academic achievement, and intelligence. In a substantial number of the over 40 children, aged 7 to 17 years, who have been

tested to date, significant abnormalities in peripheral measures of auditory physiology have been noted. Abnormalities include significantly elevated or absent acoustic reflex thresholds and/or missing or delayed waves of the auditory brainstem responses. These results are noted in spite of normal audiometric thresholds and middle ear function. Findings suggest that some central auditory processing disorders may have a relatively peripheral component. Results will be discussed in terms of a possible link with auditory neuropathy.

[This work is supported by the Canadian Language and Literacy Research Network.]

### **169 Development and Standardisation of a Test Battery for Research in Auditory Processing Disorder (APD): The Children's Auditory Processing Evaluation (CAPE).**

**Justin Cowan<sup>1</sup>**, Sally Hind<sup>1</sup>, Pauline Smith<sup>1</sup>, Melanie Ferguson<sup>1</sup>, Alison Riley<sup>1</sup>, Tim Folkard<sup>1</sup>, David Moore<sup>1</sup>  
<sup>1</sup>MRC Institute of Hearing Research

There are presently no standardised and scientifically validated tests to diagnose APD. Previously (Cowan et al., ARO, 2003), we presented a draft screening questionnaire, the APIC. Here, building on definitions of APD devised by the American Speech Hearing and Language Association and the British Society of Audiology, we present a research test battery consisting of audiological, psychoacoustic and cognitive components. The psychoacoustic component contains nine core auditory processing tests: masking level difference, gap detection, backward and simultaneous masking, frequency and amplitude modulation, temporal integration, and frequency and intensity discrimination. These tests are embedded within a series of computer games employing common procedures: a three-interval, three alternative forced choice adaptive response paradigm. Cognitive measures are general cognitive ability, attention, memory, phonological processing, language functioning, and literacy. Audiological tests are audiometry, tympanometry and distortion product OAE.

Normative data from children aged six to eleven years of age, quasi-randomly selected from local primary schools, will be presented. Analyses of test-retest reliability and the associations of specific auditory processing abilities with other cognitive abilities are currently being performed.

### **170 Long-Term and Short-Term Effects of Informational Counseling on Acceptance of Hearing Loss**

**Vishakha Rawool<sup>1</sup>**, Jessica Kiehl<sup>2</sup>  
<sup>1</sup>Southwest Missouri State University, <sup>2</sup>Audiologic consultants

Above the age of 65 years, every 1 individual out of three may have a hearing loss. However, only 20.7% of individuals with any hearing loss use hearing aids (Popelka et al., 1998). In theory, socially active individuals are more likely to use hearing aids. Social communications may lead to both awareness of loss through demands on communication and awareness of treatment of hearing

loss through better awareness of health related issues due to similar health-related concerns among peers. Also, research suggests that perception of stigma associated with hearing loss and hearing aid use decreases with increasing age. It is also likely that those socially active individuals who are simply unaware of their hearing loss due to slow progression of hearing loss may be more willing to accept the hearing loss following an audiological evaluation and informational counseling. In this study, 30 socially active older non-hearing aid users were administered the Survey for Client Acceptance of Hearing Loss and Aids (SCAHLA, Rawool, Hearing Review 2000). Audiograms were also obtained from the same individuals. Based on the criterion of 15 dB or worse pure tone average (0.5, 1 and 2 kHz) in the better ear, 24 participants had a hearing loss. Ten of these 24 individuals did not think that they had a hearing loss. A student clinician with limited training provided informational counseling to these individuals to see if such counseling will be effective in improving the acceptance of hearing loss among such individuals. Immediately following counseling five of the ten participants acknowledged the presence of hearing loss. However, one month following the counseling session, two of these five individuals reverted back to believing that they did not have a hearing loss. Thus, in the end, only 33% (3 out of 10) of the participants accepted the presence of a hearing loss following counseling by an inexperienced clinician. These results and results from SCALHA will be discussed.

### **171 At-Home Computer-Based Adaptive Training Improves Phoneme Processing in The Hearing Impaired**

**Glen A Bowman**<sup>1</sup>, G Christopher Stecker<sup>1</sup>, E William Yund<sup>1</sup>, Timothy J Herron<sup>1</sup>, Christina M Roup<sup>1,2</sup>, David L Woods<sup>1,3</sup>

<sup>1</sup>Human Cognitive Neurophysiology Lab, UC Davis and VANCHCS, <sup>2</sup>Speech and Hearing Science, Ohio State University, <sup>3</sup>Dept of Neurology, UC Davis

We evaluated the effects of PC-based at-home training on the phoneme identification ability of hearing-impaired patients. Patients were randomly assigned to training or control groups and given phoneme identification tests before and after hearing aid fitting. After preliminary testing, a personal computer was installed in the home of patients in the training group, along with software for presenting sounds, recording responses, and automatically reporting performance data via modem. Subjects trained for 40-60 minutes per day (5 days/wk) in a single-interval, nine-alternative forced-choice phoneme classification task. Training involved 27 consonant-vowel and 27 vowel-consonant phoneme pairs spoken by a male and female talker, and presented in continuous speech-spectrum noise. During training, the signal-to-noise ratio was adjusted on a trial to trial basis, using a 1-up, 1-down adaptive procedure. Phoneme-classification performance, assessed after one, two, four, and eight weeks, showed greater improvement in the trained groups at all test intervals, with little overlap between groups. Training-related improvements were similar in magnitude to the improvements associated with initial hearing aid fitting.

Improved phoneme detection performance was also seen for phonemes spoken by novel male and female voices not used during training. Supported by DC005814 and the VA Research Service.

### **172 The Interaction Between Respiration and Postural Control in a Virtual Environment**

**Michael Hoffer**<sup>1</sup>, Kim Gottshall<sup>1</sup>, Joseph Cohn<sup>2</sup>, Roy Strippling<sup>2</sup>, Carey Balaban<sup>3</sup>

<sup>1</sup>Department of Defense Spatial Orientation Center, <sup>2</sup>Naval Research Lab, <sup>3</sup>University of Pittsburgh

Traditional teaching asserts that balance and postural control are governed largely by inputs from the inner ears, the eyes, and somatosensory receptors in the ankles and hips. Recently a number of pieces of empirical evidence collected in our lab and in the labs of our collaborators have suggested that balance function may be influenced by several non-traditional inputs namely blood flow and respiration. In order to test the impact of respiration on postural control we placed individuals in a virtual environment composed of a tunnel with a projected image. The individuals stood on a force plate which was time synced with the virtual reality to record postural sway. In addition, the individuals were fitted with a cardio-respiratory apparatus to assess blood pressure and respiratory rate. This device was also time synced to the virtual display. Individuals were tested in pairs and underwent three trials in which they observed the scene with their partner controlling the figure that they represented and three trials in which they controlled the figure they represented in the scene. After each trial, the subjects filled out motion sickness questionnaires. In this paper we present the respiratory patterns of subjects as a function of role in the scenario, degree of motion intolerance reported by the subject, and in relation to their postural stability. In addition, we use other parameters studied in an attempt to argue that the respiratory pattern changes were utilized to allow the individuals to better control balance function and have a reduced level of "simulator sickness."

### **173 A Dual Track Treadmill in a Virtual Reality Environment as a Countermeasure for Neurovestibular Adaptations in Microgravity**

**Susan D'Andrea**<sup>1</sup>, Jay Horowitz<sup>2</sup>, Philip O'Connor<sup>2</sup>, John Oas<sup>1</sup>, Michael Kahelin<sup>1</sup>

<sup>1</sup>The Cleveland Clinic Foundation, <sup>2</sup>NASA Glenn Research Center

While the neurovestibular system is capable of adapting to altered environments such as microgravity, the adaptive state achieved in space is inadequate for 1G. This leads to gait and postural instabilities when returning to a gravity environment. New methods are needed to improve the understanding of the adaptive capabilities of the human neurovestibular system and to develop more effective countermeasures to eliminate deconditioning in space. The overall purpose of this research is to design, develop and test a dual track treadmill, which utilizes virtual reality in order to challenge the postural control system. The concept behind the current study is that by challenging the

neurovestibular system while walking or running, a treadmill can help to readjust the relationship between the visual, vestibular and proprioceptive signals that are altered in a microgravity environment. The treadmill has been designed to function with two belts and four actuators to both elevate and incline the tracks independently. Along with dual speed control, this arrangement will enable the system to replicate motion found during ascending and descending hills, going over rough terrain, turning corners and climbing stairs. Working in conjunction with the VR display, the treadmill system will provide an immersive environment for testing effects on the neurovestibular system.

Pilot studies were performed to evaluate the potential of the system to stimulate the neurovestibular system. Twenty subjects were tested running on a dual-track treadmill in simulated curve walking scenes. Subjects also participated in an extended trial consisting of walking 30 minutes in one randomly assigned condition. Before and immediately following testing, subjects ran a timed obstacle course. Results revealed that the combination of visual and proprioceptive stimuli provided by the VR system and the movement of the treadmill respectively, will significantly increase the stimulus to the neurovestibular system.

#### **174 Avian Gaze Stabilization: Why Move the Eyes When You Can Move the Head?**

**Asim Haque<sup>1</sup>**, Dora Angelaki<sup>1</sup>, J. David Dickman<sup>1</sup>

<sup>1</sup>*Washington University School of Medicine*

In birds, it is thought that head movements play a major role in the reflexive stabilization of gaze and vision. In this study, we investigated the contributions of the eye and head to gaze stabilization during rotations under both head-fixed (VOR) and head-free conditions in two avian species, pigeons (*Columba livia*) and quails (*Coturnix coturnix japonica*). These two species differ both in ocular anatomy (the pigeon has two distinct foveal regions in each eye as opposed to only one fovea in the quail) as well as in behavioral repertoires. Pigeons are arboreal, fly extended distances, and can navigate. Quails are primarily adapted for terrestrial niches and fly only short distances. Adult pigeons were chronically implanted with dual eye and head search coils, while dual eye coils were attached with cyanoacrylate on the corneas of Japanese quails. Each animal was placed beak-forward in a three-field AC magnetic coil system atop a motion delivery device. Frequency dynamic responses to rotational stimuli ranging from 0.01 – 2Hz yaw (20°/s), 0.02 – 4Hz pitch and roll (20°/s) were obtained under both head-free and head-fixed conditions in complete darkness. Unlike the head-fixed VOR gains which were under-compensatory for both species, gaze gains under head-free conditions were completely compensatory at high frequencies. This compensation was achieved primarily with head movements in the pigeon, but with combined head and eye-in-head contributions in the quail. In contrast, eye-in-head motion, which was significantly reduced for head-free compared to head-fixed conditions, contributed very little to overall gaze stability in pigeons. These results suggest that disparity between the stabilization strategies

employed by these two birds may be attributed to differences in species, including specific behaviors and ocular anatomy.

#### **175 The Axis of Eye Rotation During the Vestibuloocular Reflex Can Obey a Half Angle Rule.**

**Americo Migliaccio<sup>1</sup>**, Michael Schubert<sup>1</sup>, John Carey<sup>1</sup>, Charles Della Santina<sup>1</sup>, Lloyd Minor<sup>1</sup>, Richard Clendaniel<sup>1</sup>

<sup>1</sup>*Johns Hopkins University School of Medicine*

The aim of this study was to determine whether, under certain circumstances, a VOR/Listing's Law compromise strategy during vestibular head movements could generate a larger tilt in the axis of eye rotation than that predicted by the one-quarter angle rule. We measured 3D eye and head rotation axes using the scleral search coil technique during horizontal head-on-trunk and head-and-trunk (whole body) transient rotations with the head flexed and extended (0 deg, 15 deg, 30 deg) in eight subjects. The fixation target (124 cm) was placed such that the initial eye position always aligned with the naso-occipital axis. The head-on-trunk impulses consisted of low amplitude (~20 deg), high velocity (~150 deg/s), high acceleration (~3000 deg/s/s) rapid head rotations administered manually by the investigator. The head-and-trunk impulses consisted of passive, unpredictable, manual whole body rotations (about Earth-vertical and the body axis) with peak amplitude ~20 deg, velocity ~80 deg/s and acceleration ~1000 deg/s/s. Our results are consistent with a VOR/Listing's Law compromise strategy that produces an axis of eye rotation during the horizontal VOR that obeys a half angle rule when the eye and head have the same initial vertical position (re: space). This VOR/Listing's Law compromise strategy can account for the observed variable tilt in the axis of eye rotation depending on the initial eye and head positions and axis of head rotation. In addition, our results show that when the head is pitched down, the head-on-trunk horizontal rotation axis tilts forward (from Earth-vertical) by an amount equal to the head pitch angle, whereas when the head is pitched up, the head-on-trunk horizontal rotation axis is closer to Earth-vertical.

Supported by K08DC006216, R03DC005700, K23DC00196, R01DC02390, T32DC00027 and P30DC05211.

#### **176 Axes of Corrective Eye Movements Associated with Ipsilesional Head Thrusts in Persons with Vestibular Hypofunction**

**Michael Schubert<sup>1</sup>**, Americo Migliaccio<sup>1</sup>, John Carey<sup>1</sup>, C Matthew Stewart<sup>1</sup>, Lloyd Minor<sup>1</sup>, Richard Clendaniel<sup>2</sup>

<sup>1</sup>*Johns Hopkins University*, <sup>2</sup>*Duke University*

Various studies have identified unique characteristics of eye movements that correct gaze position and velocity errors that occur with rapid head rotations towards the lesioned ear for persons with unilateral vestibular hypofunction. Corrective eye movements are typically categorized as occurring at latencies that are early (50 – 100 ms) or late (> 170 ms) as measured from the onset of

the head rotation. The purpose of this study was to determine whether the axis of eye rotations for these corrective eye movements are similar to those generated by the VOR during contralesional head rotations. In addition we wanted to determine whether the magnitude of the corrective eye movements altered depending on the initial head position. Ipsilesional and contralesional horizontal head thrusts (~3000 deg/s/s, ~150 deg/s, ~10 deg amplitude) were delivered with the head positioned in neutral (0 deg) as well as  $\pm 30$  deg in pitch. We studied 5 subjects with unilateral vestibular hypofunction. The fixation target (124 cm) was placed such that the initial eye position always aligned with the naso-occipital axis. The axis of eye rotation during contralesional VOR head impulses was dependent on the pitch head position. In contrast, the magnitudes and axes of eye rotations for corrective eye movements (early and late) were similar and not dependent on pitch head position. However, the latencies of the early corrective eye movements appeared to be dependent on pitch head position (head pitched up 30 deg:  $72 \pm 14.5$  ms; head pitched down 30 deg:  $94 \pm 24$  ms,  $p < .001$ ). The corrective eye movements (early and late) associated with head rotations toward the lesioned side do not exhibit characteristics of a vestibular eye movement but are more similar to saccades.

Supported by K23 DC00196, R03 DC05700, T32 DC00023, R01 DC05040, K23 DC00196, P30 DC05211

### **177 Semicircular Canal Inactivation Abolishes Tilt-Translation Discrimination Property of Fastigial and Vestibular Nuclei Neurons**

Aasef Shaikh<sup>1</sup>, Shawn Newlands<sup>2</sup>, J. David Dickman<sup>1</sup>, Dora Angelaki<sup>1</sup>

<sup>1</sup>Washington University, <sup>2</sup>University of Texas Medical Branch

A sensory ambiguity exists in the encoding of translational motion by the vestibular system, because primary otolith afferents respond identically to inertial accelerations during self-motion and gravitational signals experienced as we change orientation in space. To study the neural basis for the resolution of this ambiguity, we recorded from neurons in the fastigial and vestibular nuclei of two fascicularis monkeys during combinations of tilt and translation that allow dissociation between translational and net linear accelerations. All stimuli were at 0.5 Hz, a frequency that activates both otolith and semicircular canals. When the semicircular canals were intact, only a small minority of central neurons modulated in proportion to the net gravito-inertial acceleration. The firing rates for the majority of the cells was satisfactorily fitted with a model that included two terms, a net linear acceleration arising from the otolith organs and an integrated angular velocity component that presumably arises from the semicircular canals. The relative phase of these two terms was appropriately matched on a cell by cell basis to cancel the gravitational acceleration component in the population activities. To further investigate the origin of this second signal, we recorded neural activities in the same animals after inactivation of all six semicircular canals. We found

that all cerebellar and brainstem vestibular neurons in the canal-inactivated animals responded like primary otolith afferents and encoded the net gravito-inertial acceleration. These results confirm that otolith-semicircular canal signal convergence is critical for detecting self-motion and solving the tilt-translation ambiguity.

This study was supported by NIH DC006540, EY12814, and DC04260; and NASA NNA04CC77G.

### **178 Parabrachial Nucleus Neuronal Responses to Off-Vertical-Axis Rotations in the Macaque 2: Comparison with Position-Trapezoid Responses**

Cyrus McCandless<sup>1</sup>, Carey Balaban<sup>1</sup>

<sup>1</sup>University of Pittsburgh

A novel population of brainstem neurons responsive to natural vestibular stimulation, located in the parabrachial (PBN) and Kölliker-Fuse nuclei of the alert macaque monkey has been described by Balaban and coworkers (Balaban et al., *J Comp Neurol*, 2002). Prior work examined responses of these units to periodic rotational stimuli in horizontal and vertical planes. Additional data has been presented demonstrating unique PBN unit responses to off-vertical-axis rotation (OVAR) stimuli (McCandless, et. al, *ARO* 2004). Here we report that unique spatial tuning properties expressed during OVAR stimulation are confirmed by position trapezoid stimulation. Two major types of OVAR responses are evident: 1) cosinusoidal spatial tuning with mean response phase differences (CW/CCW) of  $\sim 90^\circ$ , and 2) a long-lasting bias-type response in which the direction of rotation corresponds with a persistent increase or decrease in firing rate. These two response types frequently co-occur in the same units. Cosinusoidally-tuned OVAR responses were used to estimate static tilt sensitivity, with the surprising conclusion that the majority of units showed responses lags of approximately  $135^\circ$  during OVAR stimulation. Testing with position trapezoid stimulation in several directions of tilt in vertical planes confirmed these predictions in the majority of cases (mean difference =  $0.38\text{rad}$ ). These results demonstrate that vestibular responses in the PBN reflect highly processed self-motion information, with response lags much larger than might be accounted for by transmission and synaptic delays. Units of the PBN represent a novel and important new class of neurons with unique responses to natural vestibular stimulation. We believe that these neurons may relay integrative self-motion information to higher brain areas, particularly portions of the extended amygdala.

Supported by: **1 F31 DC006321-01**

### **179 Postural Prioritization Defines the Interaction Between Cognitive and Postural Task**

Mark Redfern<sup>1</sup>, Martijn Müller<sup>1</sup>, Joseph Furman<sup>1</sup>, J. Richard Jennings<sup>1</sup>

<sup>1</sup>University of Pittsburgh

Background: Dual-task effects between cognitive and postural control processes have been well established.

However, this interaction might not be entirely the result of a reciprocal interference effect, but rather may reflect a centrally modulated preparation biased toward a particular postural stimulus ('postural prioritization'). The purpose of this study was to determine if postural prioritization could be detected and to determine whether the amount of postural challenge influences the effect of a support surface movement on concurrent information processing. Methods: Twelve subjects (6 female;  $24.1 \pm 4.1$ ) participated in this study. Subjects performed a discrete Choice Reaction Time (CRT) task while standing on a platform that each subject knew would deliver either a block of non-destabilizing 'vibrations' (vibration only), or a block of destabilizing translations randomly mixed with vibrations (mixed perturbations). The CRT stimulus and postural stimulus were separated in time by 25, 125, or 325 ms. Results: For the mixed perturbation condition, RTs were significantly slower during the vibrations compared to the translations ( $p = 0.031$ ). These RTs for the vibrations during the mixed trials were also significantly longer than RTs during the vibration only condition ( $p = 0.019$ ). There was no significant difference between the RTs during the vibration only trials and the RTs during the translations of the mixed perturbations. Conclusion: These results suggest that when subjects were uncertain whether the upcoming postural stimulus would be destabilizing or not, i.e., a translation or a vibration, preparation was biased toward the destabilizing stimulus. The longer RTs for vibrations during the mixed trials suggest that subjects inhibited the postural response to the translation that did not occur. Thus, we propose that the postural control system prioritizes responses to potentially threatening perturbations and that inhibition of these prepared responses requires cognitive resources.

This study was supported by NIH grant R01 AG14116

### **180 Vestibular Otolith and Optokinetic Interactions using Counter-Rotation (pseudo-OVAR) in the Gerbil**

Galen Kaufman<sup>1</sup>, Scott Wood<sup>2</sup>, Michael Shinder<sup>1</sup>

<sup>1</sup>UTMB, <sup>2</sup>USRA

Eccentric counter-rotation, i.e. pseudo-off vertical axis rotation (pOVAR), provides a rotating gravito-inertial force vector to elicit otolith-mediated ocular reflexes without dynamic canal inputs. Gerbil pOVAR responses in the dark include complementary modulation of left and right slow phase eye velocity, with changes in both phase and bias velocity as a function of stimulus frequency. Six-canal plugging preserves the core pOVAR response and bias nystagmus, although the modulation amplitude is slightly reduced. Therefore, pOVAR with concomitant optokinetic stimulation can be used to examine otolith-visual interaction in the gerbil. Although the nature of their interaction is poorly understood, both the vestibulo-ocular and optokinetic reflexes (VOR, OKR) control non-foveate oculomotor function in the rodent. Together, head movements in the light generate gains near unity, with optokinetic and vestibular sensitivity preferring low and high frequencies, respectively. In the gerbil, several observations suggest that the VOR and OKR network

share substrate or are intimately connected. Both can be shown to have (functionally complementary) asymmetric temporo-nasal horizontal responses at low frequencies, and an optokinetic bias velocity interacts linearly with the VOR. Yet other results imply an attentional and/or gating function between the systems. For example, a pulse of sinusoidal rotation restarts the OKR after it has suddenly failed at high velocities. And the presence of an optokinetic field moving faster than that which causes eye movements alone nonetheless can suppress pOVAR bias velocity. We explored several paradigms where a rotating gravity vector was present during concurrent and natural or conflicting optokinetic field stimulation. With an optokinetic sinusoid superimposed on pOVAR, eye behavior switches neatly between an otolith bias nystagmus and optokinetic tracking in the dark and light, respectively. Periods of adaptation to this and constant velocity optokinetic stimulation during pOVAR drive VOR gains in specific ways that correlate with unique transcription factor expression patterns in vestibular and optokinetic circuitry.

### **181 Vestibulo-Collic Reflex (VCR) in Mice**

Michael King<sup>1</sup>, Keiji Takemura<sup>1</sup>

<sup>1</sup>University of Michigan

Vestibular function in small rodents such as mice is often assessed indirectly using behavior tests such as balance beam escape, rota-rod running or swim tests. Since these tests depend on complex behavior, it would be desirable to develop alternative tests more reflexively related to vestibular function. The vestibulo-collic reflex (VCR) is a reflex that attempts to stabilize head position in space during motion of the body. Similar to the better-studied vestibulo-ocular reflex, the VCR is subserved by relatively direct, short latency pathways linking vestibular nerve activity to cervical motoneurons. We measured the VCR using an electromagnetic technique often employed to measure eye movements; we attached a loop of wire (head coil) to an animal's head and placed the animal in an electromagnetic field. This method yielded accurate measurements of horizontal and vertical head position. To measure the VCR, the animal was gently restrained with its head free to move and subjected to sinusoidal or abrupt angular acceleration. Compensatory head movements in response to body rotation were assumed to be the VCR. To confirm that the compensatory head movements were in fact driven by the vestibular system, we plugged a horizontal canal unilaterally and then retested the animals 1, 2, 5, 8 and 15 days after the canal plug. Shortly after the surgery, (days 1 and 2) the putative VCR was completely blocked in response to abrupt rotations toward the lesioned side. Recovery commenced by day 5 and the responses were partially to fully recovered by day 15. Sinusoidal steady state responses were also blocked immediately after canal plugging, with partial recovery by day 15. We conclude that the compensatory head movements were vestibular in origin and likely to be the VCR.

Supported by a Pepper Center Development grant to W. M. King.

## **182 Vestibular Evoked Myogenic Potential (VEMP) Changes in Unaffected Ears of Unilateral Meniere's Syndrome**

**Steven D. Rauch**<sup>1,2</sup>, Brad S. Oriol<sup>1</sup>, Guangwei Zhou<sup>1</sup>, Sharon G. Kujawa<sup>1,2</sup>, John J. Guinan<sup>1,2</sup>, Barbara S. Herrmann<sup>1,2</sup>

<sup>1</sup>Mass. Eye and Ear Infirmary, <sup>2</sup>Harvard Medical School

We have shown previously that toneburst-evoked VEMP in ears affected by Meniere's disease (MD) exhibit a threshold elevation and loss of frequency tuning at 500 Hz compared to normal ears [Rauch et al 2004a]. We have also shown that, as a group, the unaffected ears of subjects with unilateral MD also show loss of 500 Hz frequency tuning and threshold elevation, though to a lesser degree than the affected ears. VEMP is as sensitive to side-of-disease as the most sensitive conventional vestibular test, bithermal calorics, in Meniere's syndrome [Rauch et al. 2004b]. Since a significant subset of unilateral MD patients eventually develop bilateral disease, these findings could indicate that VEMP is responsive to pre-symptomatic inner ear pathology. The present study was undertaken to confirm our previous findings in a larger dataset and to further characterize the VEMP changes seen in unaffected ears of unilateral MD.

Retrospective review identified 67 consecutive patients who had undergone both VEMP and routine vestibular function testing, of whom 49 had unilateral MD by AAO-HNS criteria. Findings previously observed in small datasets (loss of frequency tuning, threshold elevations and sensitivity to side of disease) were confirmed for the affected ears in this larger subject pool. The 49 subjects were divided into two groups based upon whether the VEMP thresholds of the unaffected ear were above or below the mean for all 49 unaffected ears. On average, the subset of unaffected ears with below-average thresholds demonstrated response tuning typical of normal ears, while the group with above-average thresholds showed loss of tuning, typical of MD. Ongoing monitoring of these "normal-like" and "Meniere-like" ears may eventually confirm whether VEMP is useful for presymptomatic diagnosis of bilateral MD.

(Supported by NIH-NIDCD Grant RO1-DC04425)

## **183 The Responses of the Vestibular Nucleus Otolith-related Neurons to Active and Passive Head Translation Movements.**

**Hongge Luan**<sup>1</sup>, Robert McCrea<sup>1</sup>

<sup>1</sup>University of Chicago

An accurate view of the external world depends on the ability to distinguish between sensory experiences produced by external forces and sensory events that are produced by self-generated movements. The distinction is presumably made by comparing sensory signals with an internal estimate of the sensory consequences of self-generated movements. In previous studies we reported that many secondary vestibular neurons in the vestibular nuclei that receive semicircular canal sensory inputs respond differentially to passive head movements. In the

present study we examined the firing behavior of 70 non-eye-movement related secondary vestibular neurons that receive inputs from the otolith organs during passive and active head translation. The majority (55/70) of these neurons were more sensitive to passive whole body translation than to active head translation. In many of the cells the differential sensitivity to passive translation could be attributed to convergent inputs from proprioceptive afferents that were dynamically matched to vestibular inputs. In other cells the cancellation of vestibular otolith inputs during active head translation appeared to be attributable to the addition of a central efference copy signal that was dynamically matched to the otolith input. We conclude that the distinction between self-generated head movements and externally produced head movements is made by the first neurons in the brain that receive input from the vestibular nerve.

## **184 Comparison of Body Translation Exercise and Head Motion Exercise on Vestibular Balance in Normal Individuals Who Have Been Artificially Spatially Disoriented**

**Kim Gottshall**<sup>1,2</sup>, Robert Moore<sup>2,3</sup>, Michael Hoffer<sup>1,2</sup>, Helen Cohen<sup>4</sup>

<sup>1</sup>Department of Defense Spatial Orientation Center, <sup>2</sup>Naval Medical Center San Diego, <sup>3</sup>San Diego State University,

<sup>4</sup>Baylor College of Medicine

The purpose of this study was to investigate the effects of vestibular physical therapy on adaptation of normal subjects who had been artificially visually spatially disoriented. Eighty male and female subjects who were identified as balance normal based on the results of computerized dynamic posturography (CDP) and the dynamic gait index (DGI) were randomly assigned to four experimental groups. Subjects were fitted with right diagonally shift lenses and retested by CDP and DGI. The control group was required to sit still for twenty minutes and view a video. Three active physical therapy groups were required to perform vestibular physical therapy tasks. Active group one performed body translation exercises and exercises with active head motion. Active group two performed body translation exercises without active head motion. Active group three performed all exercises with active head motion. Diagonal lenses were then shifted to the left. Subjects from all groups were again reassessed by CDP and DGI after control or active intervention. Lenses were then removed and subjects were retested to assure return to normal baseline status. There were no significant differences in the CDP scores within or between groups while wearing the distortion lenses. There was a significant difference in the DGI of all groups upon donning the lenses. However, the groups with right diagonal shifted lenses performing exercises with active head motion for twenty minutes displayed less spatial disorientation on DGI testing. The control group and the exercise group performing body translation exercises with no active head motion for twenty minutes did not significantly improve DGI scores. Subsequent shifting lenses diagonally to the left reduced the DGI score to initial

lens donning levels in all groups. All subjects returned to pre-test normal DGI scores within twenty minutes after removal of the distortion lenses. The results of this study indicate that vestibular exercises with head motion enhance adaptation to a specific visually artificially induced state of visual spatial disorientation. This primary adaptation to a specific artificial visual state does not transfer to a second novel artificial visual state.

### **185 Does Rizatriptan Reduce Motion Sickness in Patients with Migraine?**

**Joseph Furman<sup>1</sup>, Dawn Marcus<sup>1</sup>**

*University of Pittsburgh, Department of Otolaryngology, Department of Anesthesiology*

Motion sickness occurs in about half of persons with a history of migraine. Triptans, which are serotonin agonists, have been used successfully to treat migraine headaches. The current study tested the hypothesis that pre-treatment with rizatriptan would prevent both objective signs and subjective sensations associated with motion sickness in migraineurs. Subjects were ten persons between the ages of 23 and 41 years with a history of motion sickness who met the International Headache Society (IHS) criteria for migraine. Five subjects had no symptoms of a vestibular system abnormality; five subjects met criteria for migraine-related dizziness based on an adaptation of criteria established by Neuhauser. Exclusion criteria included a history of a recognized neurologic syndrome, e.g. Meniere's disease. Testing consisted of three sessions: a baseline vestibular battery and motion sickness provocation using both earth-vertical and off-vertical axis rotation two hours following pre-treatment with either oral rizatriptan 10mg or a placebo. Eye movements were measured with electro-oculography. Motion sickness was assessed using a questionnaire developed by Graybiel et al. Results indicated that motion sickness severity was lower following pre-treatment with rizatriptan in subjects with migraine-related dizziness but not in subjects with migraine without vestibular symptoms. There was no effect of rizatriptan on eye movement parameters in either group.

These findings suggest that pre-treatment with rizatriptan can reduce severe motion sickness symptoms in subjects with migraine-related dizziness in the absence of any changes in evoked eye movements. These pilot data suggest an important role for serotonin in the development of motion sickness symptoms in patients with migraine-related dizziness.

Supported by the National Headache Foundation, the Raymond & Elizabeth Bloch Educational and Charitable Foundation, and the Eye and Ear Foundation.

### **186 Symptom Expression During Virtual Reality Exposure**

**Susan Whitney<sup>1</sup>, Patrick Sparto<sup>1</sup>, Larry Hodges<sup>2</sup>, Joseph Furman<sup>1</sup>, Mark Redfern<sup>1</sup>**

*<sup>1</sup>University of Pittsburgh, <sup>2</sup>The University of North Carolina at Charlotte*

Background: The purpose of the study was to determine if full field virtual reality (VR) exposure results in different

symptom profiles in persons with vestibular disorders and controls. Methods: Subjects consisted of 3 symptomatic persons with a vestibular disorder and 10 healthy controls. The vestibular disorder group consisted of 2 women (59, 77 years) and 1 man (59 years). The control group consisted of 6 women and 4 men (mean age 41, range 22-75 years) Subjects performed 8 different head and eye coordination tasks, including: 20 deg eye saccades with head fixed, 100 deg gaze saccades, and gaze smooth pursuit. All eight tasks were performed on 6 different days, with each day denoting either a stationary (2 days) or moving background (4 days). The moving scenes were generated using a back-projected CAVE VR system that provided full-field antero-posterior motion. All subjects were asked to express their subjective units of discomfort (SUDS, 0 to 10 scale) and to complete the Simulator Sickness Questionnaire (SSQ, 16 items, 0 to 3 scale) after each 90-second trial. Responses were dichotomized into either a "no" (score of 0) or "yes" (score greater than 0, i.e. they experienced some symptom) immediately following each VR exposure for the SUDS, total SSQ, and each of the 3 SSQ subscales (nausea, disorientation, and oculomotor). Results: There was a significant association between subject group and the proportion of "yes" responses (chi-square,  $p < 0.001$ ) for all measures. The percentage of trials in which some symptoms occurred in the control and vestibular groups (CON:VEST) were as follows: SUDS: (23%:55%); SSQ total: (29%:60%); SSQ nausea: (11%:26%); SSQ disorientation: (5%:36%); and the SSQ oculomotor: (27%:60%). Conclusion: Patients with vestibular disorders appear to experience more discomfort than controls during virtual reality immersion.

Supported by NIH grants DC005384, DC05205 and DC05372

### **187 Visual Dependence in Postural Control and Spatial Orientation**

**Massimo Cenciari<sup>1</sup>, Patrick J. Loughlin<sup>1,2</sup>, Mark S. Redfern<sup>1,3</sup>, Patrick J. Sparto<sup>3,4</sup>**

*<sup>1</sup>Department of Bioengineering, University of Pittsburgh,*

*<sup>2</sup>Department of Electrical Engineering, University of Pittsburgh, <sup>3</sup>Department of Otolaryngology, University of Pittsburgh, <sup>4</sup>Department of Physical Therapy, University of Pittsburgh*

The purpose of this study was to determine if visual dependence for postural control is related to visual dependence for spatial orientation. Correlations between postural sway responses to sinusoidal moving scenes and reliance on visual cues for spatial orientation were studied. Results from 8 healthy adult subjects are reported here (mean age 27 years, range 22-35 yrs). Sway measurements via center of pressure (COP) were recorded during standing while subjects viewed an antero-posterior optic flow produced by a back-projected virtual reality system that encompassed 180 degrees of the visual field. Subjects stood on either a fixed or sway-referenced support surface during the trials containing visual motion at an amplitude of 16 cm peak-to-peak and constant frequencies of 0.1, 0.25, 0.4, 0.7, and 1 Hz for 60 seconds. Each test condition was repeated three times, for a total of 30 trials over two sessions. The first session consisted of



fixed platform trials, randomized by frequency of the moving scene, and the second session consisted of sway-referenced trials. Subjective visual vertical (SVV) was measured by having subjects seated in the dark align an initially tilted ( $\pm 40^\circ$ ) fluorescent rod to vertical. Visual orientation cues were altered by changing the background condition: black (no background), tilted frame ( $\pm 28^\circ$ ), or a rotating dotted pattern ( $\pm 30^\circ/s$ ). Two repetitions of each condition were conducted. Root-mean-square of the COP was used to quantify the amount of postural sway in response to the moving scene visual stimulus. The final angular deviation of the rod from vertical was used as a measure of reliance on visual information. A positive correlation was found between the amount of sway induced by the optic flow and the deviation of the rod from vertical ( $r=0.57$  to  $0.88$  for the various conditions studied). This result supports the concept of a common mechanism of visual dependence for balance and visual dependence for spatial orientation.

### **188** Ocular Reflex Phase During Off-Vertical Axis Rotation in Humans is Modified by Head-On-Trunk Position

Scott Wood<sup>1</sup>, Gilles Clément<sup>2</sup>, Pierre Denise<sup>3</sup>, Millard Reschke<sup>4</sup>

<sup>1</sup>USRA, <sup>2</sup>CNRS, <sup>3</sup>CHU de CAEN, <sup>4</sup>NASA

Constant velocity Off-Vertical Axis Rotation (OVAR) imposes a continuously varying orientation of the head and body relative to gravity. The ensuing ocular reflexes include modulation of both horizontal and torsional eye velocity as a function of the varying linear acceleration along the lateral plane. The purpose of this study was to examine whether the modulation of these ocular reflexes would be modified by different head-on-trunk positions. Ten human subjects were rotated in darkness about their longitudinal axis 20 deg off-vertical at constant rates of 45 and 180 deg/s, corresponding to 0.125 and 0.5 Hz. Binocular responses were obtained with video-oculography with the head and trunk aligned, and then with the head turned relative to the trunk 40 deg to the right or left of center. Sinusoidal curve fits were used to derive amplitude, phase and bias velocity of the eye movements across multiple cycles for each head-on-trunk position. Consistent with previous studies, the modulation of torsional eye movements was greater at 0.125 Hz while the modulation of horizontal eye movements was greater at 0.5 Hz. Neither amplitude nor bias velocities were significantly altered by head-on-trunk position. The phases of both torsional and horizontal ocular reflexes, on the other hand, shifted towards alignment with the head. These results are consistent with the modulation of torsional and horizontal ocular reflexes during OVAR being primarily mediated by the otoliths in response to the sinusoidally varying linear acceleration along the interaural head axis.

### **189** Reliance on Dynamic Visual Cues for Postural Control: Effect of Age is More Important Than History of Unilateral Vestibular Hypofunction

Patrick Sparto<sup>1</sup>, Joseph Furman<sup>1</sup>, Mark Redfern<sup>1</sup>

<sup>1</sup>University of Pittsburgh

**Background:** Young adult subjects with unilateral vestibular hypofunction (UVH) and healthy older adults demonstrate greater visually-induced sway than healthy young adult control subjects. The purpose of this study was to determine if the combination of advanced age and UVH synergistically result in even greater reliance on dynamic visual cues. **Methods:** Four groups of subjects were tested: four young adults (22-39 years) and eight older adults (58-80 years) with a history of UVH, and 4 young and 8 older age- and gender-matched controls. Eleven of the twelve subjects with UVH had a unilaterally absent caloric response; 1 had 67% loss. Subjects viewed sinusoidal anterior-posterior optic flow in a full field of view environment while standing on both a fixed and a sway-referenced platform. The optic flow consisted of nine trials each using a single frequency (0.1, 0.25, or 0.4 Hz) and a single amplitude (4, 8 or 12 cm). Anterior-posterior head sway was digitized at 20 Hz. Data were processed using a phaseless digital bandpass filter centered at the stimulus frequency of the optic flow. The root-mean-square (RMS) of the head sway was used to measure postural response. **Results:** Analysis of Variance revealed a significant effect of age on the magnitude of sway in response to optic flow ( $p = 0.005$ ); older subjects swayed 64% more than young adult subjects. There was no effect of UVH nor were there interaction effects with age. Additional significant effects were found for type of support surface, frequency, and amplitude ( $p < 0.001$ ) **Conclusion:** Age was a greater determinant of visually-induced sway than the presence of UVH. Moreover, the combination of advanced age and UVH did not result in a significantly greater reliance on dynamic visual cues than that associated with advanced age alone.

This study was supported by NIH grant K25-AG001049.

### **190** Response Characteristics of Nystagmus Elicited by the Dix-Hallpike Maneuver in Canalithiasis and Cupulolithiasis Subtypes of Benign Paroxysmal Positional Vertigo

Helen Cohen<sup>1</sup>, Kay T Kimball<sup>2</sup>

<sup>1</sup>Baylor College of Medicine, <sup>2</sup>Statistical Design and Analysis

The two subtypes of benign paroxysmal positional vertigo (BPPV) are canalithiasis and cupulolithiasis, putatively caused by otoconial matter adhered to the semicircular canal wall and the cupula of the crista ampullaris, respectively. The two subtypes are thought to be differentiated based on the temporal characteristics of the responses. Canalithiasis should have a longer latency to onset but shorter duration and cupulolithiasis should have a shorter latency and longer duration. We examined the records of patients who had been diagnosed with unilateral BPPV based on history and positive findings on the Dix-

Hallpike maneuver. Eye movements were recorded with either electrooculography or videooculography. Dependent measures were latency to onset of response, duration of response and maximum slow phase velocity of response. The data, modeled using ROC techniques, showed a wide range of responses. Shorter latencies were sometimes but not always associated with longer durations and longer latencies were usually but not always shorter durations. These data suggest that the distinctions between cupulolithiasis and canalithiasis can be blurred since responses occur in a range of temporal characteristics. Supported by NIH grant DC03602.

### **191 Value of Lying-Down Nystagmus in the Lateralization of Lateral Canal Benign Paroxysmal Positional Vertigo**

**Ja-Won Koo<sup>1</sup>**, So Young Moon<sup>1</sup>, Il Joon Moon<sup>1</sup>, Woo Sub Shim<sup>1</sup>, Ji-Yeon Yoo<sup>1</sup>, Ji Soo Kim<sup>1</sup>

<sup>1</sup>*Seoul National University Bundang Hospital*

Lateral canal benign paroxysmal positional vertigo (LC-BPPV) is characterized by horizontal direction-changing nystagmus induced by lateral head turning in supine position. According to the Ewald's second law, the direction of head turning that creates stronger response represents the affected side in geotropic nystagmus and the healthy side in apogeotropic nystagmus. However, it may not always be possible to lateralize the involved ear only by comparing the intensity of the nystagmus. We studied the values of lying-down nystagmus (LDN) in the lateralization of LC-BPPV. Retrospective study of 54 patients who had been diagnosed as having LC-BPPV in Dizziness Clinic of Seoul National University Bundang Hospital from May 2003 to February 2004 was performed. The directions of the nystagmus induced by lying down were compared with those determined by the Ewald's second law. Of the 54 patients, 32 (20 apogeotropic and 12 geotropic) patients showed horizontal nystagmus induced by lying down. The nystagmus was ipsilesional in 16 (80%) apogeotropic and contralateral in 9(75%) geotropic patients. In LC-BPPV, the LDN mostly beats toward the involved ear in the apogeotropic type, and directs to the healthy ear in the geotropic type. The direction of LDN may help lateralizing the involved ear in LC-BPPV.

### **192 Efficacy of a New Treatment Maneuver for Posterior Canal Benign Paroxysmal Positional Vertigo**

**Richard Roberts<sup>1</sup>**, Richard Gans<sup>1</sup>, Renee Montaudo<sup>1</sup>

<sup>1</sup>*The American Institute of Balance*

Posterior canal benign paroxysmal positional vertigo (PC-BPPV) is the most common cause of vertigo. The Semont Liberatory Maneuver (SLM) and Canalith Repositioning Maneuver (CRM) have been demonstrated to be successful in clearing PC-BPPV following 1-2 treatments by numerous independent investigators. Although these maneuvers are generally well-tolerated by most patients, certain populations may present with complications that contraindicate their use. For example, the SLM is not

indicated for patients with hip problems that might be aggravated during the required brisk lateral motion. While the CRM may be better tolerated by these patients, this maneuver requires the patient's neck to be hyper-extended. Hyper-extension of the neck is contraindicated for patients with osteoarthritis, spondylosis, or verteobasilar insufficiency. The SLM is preferable for these patients because there is no hyper-extension of the neck. We have developed a new treatment maneuver that is a hybrid of the SLM and CRM, the Gans Repositioning Maneuver (GRM). For 207 patients, the average number of treatments to resolve symptoms was 1.15. 80.5% of patients were cleared with one GRM treatment and 95.5% were cleared after two treatments. Recurrence rate within three months to two years post-treatment was 5%. There is no apparent clinician effect on treatment outcome. These findings are in agreement with efficacy data for other treatments, but with the advantage of use for a wider range of patients.

### **193 Postural Control in the Elderly with Benign Paroxysmal Position Vertigo - A Pilot Study**

**Judith White<sup>1</sup>**, Kathleen Coale<sup>2</sup>, Kelly Beaudoin<sup>3</sup>, Peter Catalano<sup>4</sup>, Nancy Cohen<sup>4</sup>, John Oas<sup>1</sup>

<sup>1</sup>*The Cleveland Clinic*, <sup>2</sup>*Rehabilitation Services, Lahey Clinic*, <sup>3</sup>*Balance Solutions*, <sup>4</sup>*Lahey Clinic*

In the elderly population, vestibular disorders and dizziness are associated with disability and risk of falls. Benign paroxysmal positional vertigo (BPPV) is responsible for a large percentage of dizziness in this population. Of older adult males in a VA setting complaining of dizziness, 34% had BPPV (Davis, 2004). Even in community dwelling elderly not complaining of dizziness, 9% had undiagnosed BPPV (Oghalai, 2000). Elderly patients with BPPV experience considerable functional impairment. When BPPV is present, postural instability has been documented using computerized dynamic posturography (CDP) (Blatt, 2000; Black, 1984; DiGirolamo, 1998). BPPV is treated with an office-based repositioning therapy which moves the patient's head into a series of positions to allow the debris to leave the affected canal. One study including 33 patients aged 38-91 suggested that younger patients were more likely to show recovery in postural stability after successful BPPV treatment (Blatt, 2000). The present study is a pilot to examine postural control recovery in 11 patients aged 65 and older who were diagnosed and treated for posterior canal BPPV in a tertiary care center. Postural control was assessed with the Dynamic Gait Index (DGI), Timed Up and Go test, and CDP performed at diagnosis (before canalith repositioning) and after successful treatment. Additional data included Vestibular Disorders of Daily Living Scale, Dizziness Handicap Inventory, vestibular testing (including oculomotor, caloric and sinusoidal vertical axis rotation) and full medical history. Results show a trend towards increased postural control scores, as measured by CDP and DGI, following successful canalith repositioning in this elderly sample. Total CDP score (t= -1.345 two tailed df=8 p<.215) and more significantly vestibular subscale CDP score (t= -1.737 two tailed df=8

p<.121) showed this trend. (Statistical significance may be limited by small sample size since this pilot study was not powered sufficiently to demonstrate significance). In addition, a notable 30% of the sample required repeated visits for bilateral BPPV, recurrent BPPV or persistent BPPV, suggesting that elderly patients may be at increased risk for these conditions. Additional research on postural control in the elderly with BPPV seems warranted.

### **194 False Positive Rate and Specificity for Yaw Axis Rotation Chair Testing in a Normal Active Duty Population**

**Derin Wester<sup>1</sup>, Todd Wagner<sup>1</sup>, Michael Hoffer<sup>1</sup>, Kim Gottshall<sup>1</sup>, Dennis Faix<sup>1</sup>**

<sup>1</sup>*Naval Medical Center San Diego*

Mefloquine (Larium) a commonly prescribed prophylaxis medication for malaria, has been recently proposed as a possible ototoxic exposure in deployed active duty and reserve military personnel. The Navy Environmental and Preventive Medicine Unit-5 in conjunction with the Centers for Disease Control and The Defense Spatial Orientation Center (DSOC) are investigating the proposed ototoxicity. In order to more effectively utilize objective rotation chair testing data it was necessary to determine the false positive rate and specificity in an asymptomatic and otherwise health active duty population and compare those measures against previously established DSOC clinical norms (Project Spin, 1996). 150 young to middle aged (ages 18-48) active duty volunteers who met stringent inclusion/exclusion criteria were tested with the standardized DSOC rotation chair clinical protocol. The assessment included tests of sinusoidal harmonic acceleration, oculomotor tests of gaze, smooth pursuit and saccadic eye movements, vestibular visual interaction, visual fixation suppression and velocity-step testing. Also, clinical testing with Frenzel goggles for spontaneous nystagmus, post-head-shaking nystagmus and positional nystagmus were completed as well as yaw-axis Halmagyi head thrust testing. Descriptive statistical analysis including mean, median, confidence interval on the mean and frequency distribution properties including normality were completed. New DSOC rotation chair norms were then established as well as the false positive rate and specificity for the Micromedical System 2000 Variable Yaw-Axis Rotation Chair.

### **195 Motorized Head Impulse Rotator for Horizontal Vestibulo-Ocular Reflex: Normal Responses**

**Timo Hirvonen<sup>1</sup>, Heikki Aalto<sup>1</sup>**

<sup>1</sup>*Helsinki University Central Hospital*

The angular vestibulo-ocular reflex (VOR) warrants gaze stability by providing compensatory eye movements during head movements. The head thrust sign provides a clinical tool to evaluate vestibular function with manual head impulses. The more precise quantification of the vestibular function is based on gain and latency calculation from the eye and head movement signals. We constructed

motorized head impulse rotator to attain more uniform and controlled stimulus.

Seventeen healthy controls (12 women and 5 men) with a mean age of 41(range 25-59) years were measured. The subject wore a boxer's helmet reinforced with plastic restraints, which could be fitted tightly. A DC-motor and gear combination moved two push-rods connected to joints on both sides of the helmet. The top of the helmet was fixed with a rotating joint to a bar that eliminated the lateral movement of the head. The desired short constant torque impulse was obtained by driving the motor with a pulse of increasing voltage to produce linear velocity increase. Fifty-six impulses randomized in direction and with an inter impulse interval of 1.17-2.20 s were delivered during 80 s.

The subject fixated on a LED target 140 cm ahead. The head position was measured with a rotation angle sensor and the eye position with an electro-oculography (EOG). Saccade calibration was performed before each test. The velocity gain was calculated at two points: during the period of 30 ms before the peak head velocity, and also when the head velocity was 100 - 120 °/s. The latency was calculated as the time difference (in ms) between the head and eyes reaching threshold velocity of 10°/s. The asymmetry (%) between sides was calculated as  $((\text{gainR} - \text{gainL}) / (\text{gainR} + \text{gainL})) * 100$ .

The mean velocity gain ( $\pm$  SD) at 30 ms interval before the peak head velocity was  $1.09 \pm 0.10$  with mean asymmetry of  $3.5 \pm 2.9\%$ . The mean gain at head velocities of 100-120 °/s was  $1.08 \pm 0.11$  and the mean latency was  $5.2 \pm 5.9$  ms.

Motorized head impulse rotator allowed reliable and fast quantification of the VOR. The gain and latency results of healthy controls were close to ideal for the target distance of 140 cm. The normative range for asymmetry remained within 10% making it a promising parameter for detection of unilateral weakness.

### **196 Contributions of Contralateral Sound to Vestibular-Evoked Myogenic Potentials**

**Shaum Bhagat<sup>1</sup>**

<sup>1</sup>*Louisiana State University*

Many ipsilaterally-measured sonomotor reflexes are influenced by the presence of contralateral sounds. Vestibular-evoked myogenic potentials (VEMPs), thought to reflect the vestibulo-collic reflex, can be elicited by monaural or binaural sound. The purpose of this investigation was to examine the effects of varying contralateral sound frequency on unilateral VEMP amplitude and latency characteristics. The participants were eighteen adults (4 male) with no history of vestibular or neurological disease. All participants were evaluated during monaural and binaural conditions. Monaural VEMPs were acquired with either air-conducted or bone-conducted 500-Hz tone bursts presented at 95 dB nHL and 70 dB nHL, respectively. These stimuli were simultaneously paired with 95 dB nHL contralateral tone bursts at 250, 500, 750 or 1000-Hz during the acquisition of binaural VEMPs. The results of the study indicated that air-conducted VEMP relative amplitudes in each of the four

binaural conditions were significantly decreased compared to the monaural condition. Larger differences between monaural and binaural conditions were seen when contralateral sounds were < 500 Hz. However, no significant changes in relative amplitude were seen amongst the conditions for bone-conducted VEMPs. Comparisons between monaural and binaural conditions revealed no significant differences in p13 or n23 latency across the conditions for either air-conducted or bone-conducted VEMPs. An explanation for the findings of the study is that activation of the contralateral acoustic reflex during the air-conducted VEMP binaural conditions causes an attenuation of sound transmission through the middle ear and lowers effective levels of sound from reaching the vestibule. The lack of change in bone-conducted VEMP amplitudes during the binaural conditions supports the conjecture that stimulation of the vestibule through bone conduction is largely accomplished without involvement of middle-ear sound transmission.

### **197 Comparison of Dynamic Subjective Visual Vertical Test (DSVV) and Computerized Dynamic Posturography (CDP) for Evaluation of Patients with Postural Instability**

Joel Goebel<sup>1</sup>, Nilubon Sangasilp<sup>1</sup>, Belinda Lindberg<sup>1</sup>

<sup>1</sup>*Dizziness and Balance Center, Washington University School of Medicine, St. Louis, MO*

#### Background

Computerized dynamic posturography (CDP) is the standard approach used to evaluate otolith inputs to postural control during the Sensory Organization Test (SOT). Recently, unilateral centrifugation test was developed to assess utricular function. This technique uses a vertical axis rotation that passes through one utricle which exposes the contralateral utricle to centrifugal acceleration at constant velocity while the ipsilateral vestibule is minimally stimulated. Unilateral otolith-ocular response and dynamic subjective visual vertical (DSVV) can be measured and hopefully demonstrate significantly different responses in unilateral vestibular patients versus normal subjects.

#### Hypothesis

We hypothesize that patients with abnormal SOT 5 or 6 scores will also demonstrate significant DSVV asymmetries.

#### Materials & Methods

We used DSVV and CDP to test 110 patients (ages 17-92, mean age 58 years) with vestibular disorders from October 2002–July 2004. The independent t-test was used to find the difference between the mean interaural SVV difference in patients who have normal versus abnormal SOT 5 (eye closed, support surface sway reference) and SOT 6 (eye open, visual and support surface sway reference) scores.

#### Results

SVV responses and mean DSVV differences in subjects with normal versus abnormal SOT 5 or 6 scores differed significantly ( $p < 0.05$ ). Mean DSVV differences of patients with normal versus abnormal SOT 5 scores were 2.81

degrees (SD=2.57) and 4.63 degrees (SD=3.6) respectively; and SOT 6 scores were 3.02 degrees (SD=2.84) and 4.82 degrees (SD=3.6) respectively.

#### Conclusion

Interaural DSVV differences and SOT 5 and 6 scores in these two groups were significantly correlated. We conclude that clinical DSVV may be useful for detecting utricular dysfunction in addition to the results of CDP.

### **198 Changes in the Axis of Rotation for Horizontal Head Movements Associated with Changes in Pitch Position**

Richard Clendaniel<sup>1</sup>, Americo Migliaccio<sup>2</sup>, Michael Schubert<sup>2</sup>, Amy Bastian<sup>3</sup>

<sup>1</sup>*Duke University Medical Center*, <sup>2</sup>*Johns Hopkins School of Medicine*, <sup>3</sup>*Kennedy Krieger Institute*

During tests of vestibular function it is thought that pitching the head forward 30° will bring the horizontal canals perpendicular to the axis of rotation. While this will work in situations where the axis of rotation remains in an earth vertical orientation (e.g. rotary chair test), it is not clear that the positioning will have the same effect during clinical tests such as the head thrust test. The purpose of this study was to assess the relationship between the axis of rotation for horizontal head movements and the position of the head in space.

Eight normal subjects (age 21 – 45) participated in this study. Head movements were recorded in 3D using an OPTOTRAK recording system. Infrared emitting diodes were securely attached to the lateral aspect of the subject's head. 15 – 20 high-acceleration, high velocity horizontal head impulses were passively applied. This paradigm was repeated with the head in neutral (Frankfort line horizontal), 15° and 30° anterior pitch, and 15° and 30° posterior pitch. The axis of rotation for each head position was determined relative to an earth fixed reference frame.

The results demonstrated that the axis of rotation shifted with the changes in head pitch position. When anterior and posterior pitch position data were grouped together, linear regression of the axis of rotation orientation on head position in pitch revealed a significant relationship ( $r^2 = 0.97$ ,  $p < 0.01$ ) between the two measures (slope of the regression line = 0.84). When the posterior pitch and anterior pitch data were analyzed separately, there were differences between the two data sets. For both positions, there were significant relationships between head position and the axis of rotation ( $r^2$  posterior pitch: 0.95; anterior pitch: 0.90; in both cases  $p < 0.01$ ). However, there were marked differences between the slopes of the regression lines (posterior pitch regression line slope: 0.93; anterior pitch regression line slope: 0.60). Tests for differences between these slopes were significant ( $p < 0.01$ ).

These results demonstrate that the axis of rotation for horizontal head movements shifts with the position of the head. Thus, tilting the head forward 30° during clinical tests will not place the horizontal canals perpendicular to the axis of rotation. The results can be explained by examining the biomechanics of the cervical spine.

## **199 Vestibular Evoked Myogenic Potential Assessment of Deaf and Hard of Hearing Subjects**

**Robert Ackley**<sup>1</sup>, Chizuko Tamaki<sup>1</sup>, Christopher Zalewski<sup>2</sup>, Carmen Brewer<sup>2</sup>

<sup>1</sup>Gallaudet University, <sup>2</sup>National Institutes of Health, NIDCD

Vestibular myogenic potentials (VEMPs) are a useful tool to measure saccular function. The test employs loud acoustic stimuli to elicit a myogenic response recorded from surface electrodes placed over the ipsilateral sternocleidomastoid muscle. The physiologic basis of the VEMP derives from anatomical connections between the saccule and the vestibulospinal tract to the motor neurons of the sternocleidomastoid. Preliminary findings conducted at the Gallaudet University Hearing Clinic corroborate published reports that subjects with vertigo, imbalance, or a history of these disorders frequently have VEMPs that are abnormal with respect to amplitude, latency and/or augmented calculations. Given that the evoking stimulus is acoustic, the effect of significant hearing loss on the VEMP is of clinical and research interest. However, there is a dearth of literature regarding clinical application of this procedure to Deaf and Hard of Hearing (HH) subjects. Although pilot data collected at Gallaudet indicates that this test is useful in assessing balance function in Deaf/HH patients, important baseline data is yet to be reported on these subjects. This study examines the feasibility and usefulness of VEMP on Deaf/HH subjects. Thirty (30) experimental subjects and 30 subjects with normal hearing are statistically compared. Preliminary indications suggest a small decrease in VEMP amplitude in Deaf/HH subjects when compared to control subjects with normal hearing. Categories of Deaf/HH subjects, including those with Connexin deafness and syndromic deafness, are reported in addition to Deaf/HH subjects with no known etiology.. Finally, case studies of subjects found to have vestibular symptoms, including Tullio Phenomenon and Meniere's symptoms, are reported anecdotally.

## **200 Age-Related Effects of Vestibular-Evoked Myogenic Potentials**

**Micah Bradshaw Klumpp**<sup>1</sup>, Shaum Bhagat<sup>1</sup>

<sup>1</sup>Louisiana State University

The vestibular-evoked myogenic potential (VEMP) is a sound-evoked reflex recorded by placing surface electrodes on the sternocleidomastoid (SCM) muscles. Recently, VEMPs have been introduced as a clinical test of saccule function. Previous research has established that degradation of the sensorineural structures of the cochlea and semicircular canals occurs with age in humans. However, little research exists on the frequency characteristics of the VEMP response across different age groups. Therefore, the purpose of this experiment was to examine the effects of tone burst frequency on p13 and n23 latencies in young (< 40 years) and middle-aged (40 years +) adults. Tone burst stimuli at 250 Hz, 500 Hz and 1000 Hz were used to record VEMPs in each subject. The results of the study indicated that p13 and n23 latencies

were unaffected by the frequency of the stimulus in both age groups. However, slight differences in VEMP latency were seen between age groups, with middle-aged subjects exhibiting prolonged p13 latencies compared to the young subjects. The preliminary results of this study suggest that age-related changes in tone burst VEMP latency occur beginning as early as the fourth decade. Further investigation of the effects of age on tone burst VEMPs is warranted.

## **201 Transfer of Optokinetic Activity to Perrotatoric and Galvanic Nystagmus**

**Lars-Uwe Scholtz**<sup>1</sup>, Dieter Schneider<sup>1</sup>, Hans Meyer-Rienecker<sup>2</sup>

<sup>1</sup>University of Wuerzburg, <sup>2</sup>University of Rostock

The influence of vestibular and optokinetic stimuli on the nystagmus slow phase velocity (SPV) in man was studied using different combinations of passive body rotation and optokinetic stimuli (1), of unilateral galvanic stimulation and optokinetic stimuli (2), and bilateral galvanic stimulation and optokinetic stimuli (3). The transfer of optokinetic activity was studied in 20 healthy subjects. The equation by Barratt and Hood (1988) were used as a function of transfer of activity. The following features were found: (1) an optokinetic stimulation following by passive body rotation in dark in the same direction induced an increasing of SPV (2) an optokinetic stimulation following by passive body rotation in dark in different direction induced a reduction of SPV (3) an optokinetic stimulation following unilateral galvanic stimulation in the same direction induced an increasing of SPV (4) an optokinetic stimulation following unilateral galvanic stimulation in different direction induced a reduction of SPV (5) an optokinetic stimulation following bilateral galvanic stimulation in the same direction induced an increasing of SPV (6) an optokinetic stimulation following bilateral galvanic stimulation in different induced a reduction of SPV. In summary, our results have shown that activity resulting from prior optokinetic stimulation can be stored and transferred to a subsequent vestibular response by non simultaneous stimulation.

## **202 Electrotactile Sensory Supplementation of Gravito-inertial References to Optimize Sensori-Motor Recovery of Postural Stability in Bilateral Vestibular Loss Subjects**

**F. Owen Black**<sup>1</sup>, Scott Wood<sup>2</sup>, Paul Bach-y-rita<sup>3</sup>, Yuri Danilov<sup>4</sup>, Mitchell Tyler<sup>5</sup>, Valerie Stallings<sup>1</sup>

<sup>1</sup>Neurotology Research, Legacy Clinical Research and Technology Center, Portland, OR, <sup>2</sup>University Space Research Association, Houston, Texas, <sup>3</sup>Departments of Orthopedics and Rehabilitation, and Biomedical Engineering, University of Wisconsin, <sup>4</sup>Department of Animal Health and Biomedical Science, University of Wisconsin, <sup>5</sup>Department of Biomedical Engineering, University of Wisconsin

Objective: To explore the effects of introducing gravito-inertial forces acting on the head via electrotactile inputs to the tongue for control of posture and movement.

Methods: Head acceleration (linear x,y) cues were "double" integrated, scaled to position inputs and presented via an electrotactile array to the subject's anterior tongue. Postural control performance in standing subjects was assessed using Computerized Dynamic Posturography (CDP) Sensory Organization Tests (SOTs) presented randomly to bilateral vestibular loss subjects (BVLs) before and after training sessions.

Results: All subjects fell on CDP SOTs 5 & 6 before training. Acquisition of normal or near-normal postural sway (three trial median SOT 5 & 6 scores normal or near normal) occurred within 4-5 days of training for most severe to profound BVL subjects. Retention of improved postural stability persisted for varying lengths of time among subjects (usually several days). Transfer to a more stable gait occurred in all subjects and also persisted for varying lengths of time after training. Some, but not all subjects reported resolution or improvement in oscillopsia.

Conclusions: To our knowledge, the acquisition, retention and transfer of postural stability using inertial electrotactile inputs to the tongue are accomplishments that no other vestibular rehabilitation, sensory substitution or biofeedback method has achieved in patients with profound bilateral vestibular loss. We hypothesize that time constants of adaptation (and retention after training) will be correlated with baseline levels of vestibular function and/or total training time. This hypothesis will be tested by studies including subjects with varying magnitudes of vestibular function loss.

### **203 Electrical Stimulation of the Human Inferior Vestibular Nerve can Induce the Vestibulocollic Reflex**

**Dietmar Basta<sup>1</sup>, Ingo Todt<sup>1</sup>, Arne Ernst<sup>1</sup>**

<sup>1</sup>*Dept. of ENT at ukb, Free University of Berlin, Germany*

Vestibular evoked myogenic potentials (VEMPs) are short-latency EMGs which are evoked by high-level acoustic stimuli in clinical practice. They can be recorded from the tonically contracted sternocleidomastoid muscle (SCM) as reported extensively before. The aims of the present study, however, were to study VEMPs upon direct electrical stimulation of the human inferior vestibular nerve. The responses were compared to acoustically evoked VEMPs to evidence the vestibulocollic reflex arch and their saccular origin, respectively.

Seven subjects were stimulated at the inferior branch of the vestibular nerve within the cerebello-pontine angle during otoneurosurgery. Subdermal needle electrodes were placed in the middle of the SCM of both sides. The EMG signals of the SCM were recorded upon bipolar electrical stimulation (0.4 – 1.0 mA; 0.2 ms duration; 4.7 Hz). These recordings were compared to air- and bone-conduction evoked VEMPs with respect to latency (P13/N23) and shape.

All subjects showed normal VEMPs upon acoustic stimulation with a latency of  $12.8 \pm 1.4$  ms for P13, and  $22.7 \pm 2.0$  ms for the N23 preoperatively. Upon direct electrical stimulation of the inferior vestibular nerve (IVN), a linear correlation of the response amplitudes of VEMPs and the stimulus was found with a threshold stimulus at

about 0.4 mA. The mean latency of the positive peak was  $9.1 \pm 2.2$  ms and  $13.2 \pm 2.3$  ms for the negative one. No contralateral SCM response was found. Electrical stimulation of the superior vestibular nerve did not result in any ipsi- or contralateral EMG response of the SCM.

The present results show experimental evidence of the vestibulocollic reflex by direct electrical stimulation of the human IVN for the first time. The method can be utilized to map VIIIth nerve subdivisions and to intraoperatively monitor IVN integrity in a real-time mode.

### **204 Eye Movements in Response to Electric Stimulation of the Human Ampullary Nerve**

**Conrad Wall<sup>1</sup>, Jean-Philippe Guyot<sup>2</sup>, Izabel Kos<sup>2</sup>**

<sup>1</sup>*Mass. Eye & Ear Infirmary, <sup>2</sup>Univ. Hospital of Geneva*

Two subjects having normal caloric responses in the stimulated ear were given multiphasic pulse trains of electric stimulation of their posterior ampullary nerve which was surgically exposed at the University Hospital of Geneva under local anesthesia using the procedure of Gacek. The procedure was approved by human studies committees of the participating institutions. Video oculography was used to record subjects' eye movements in the operating room. The stimulating pulse consisted of a 200 microsecond negative phase, followed by neutral and positive phases of the same duration. The duration of the fourth and final phase of each multiphasic pulse was systematically varied to give pulse repetition rates that ranged from 25 to 400 pulses per second. Stimulation was attempted at three stages of the operation in which thickness of the bone and other material between the 128 micron platinum stimulating electrode and the nerve was varied. The first stimulation was made before any drilling was attempted and produced no measurable response at the highest stimulus current level of 1 mA. A second attempt was made when the nerve canal became visible by the surgeon, with an estimated bone thickness of approximately 100 microns. In both patients, a pulse repetition rate of 200 pulses per second produced a robust vertical nystagmus without any apparent change in the slow component velocity of the horizontal slow component. Thus we replicate in humans the finding of Suzuki and Cohen in non-human primates for electric stimulation of the posterior semicircular canal that the plane of movement of the eye corresponds to the plane of the canal. This is a first step towards the demonstration in humans of the feasibility of a vestibular prosthesis using electric stimulation.

### **205 The Significance of Audiometric Testing in the Vestibular Patient: A New Perspective**

**Neil Cherian<sup>1</sup>, John G. Oas<sup>1</sup>, Craig Newman<sup>1</sup>, Sharon Sandridge<sup>1</sup>**

<sup>1</sup>*Cleveland Clinic Foundation*

Many vestibular syndromes do not manifest any audiologic symptoms. Vestibular diagnosis is often quite elusive with symptoms that have no physical marker. "Non-specific peripheral vestibular syndrome" is a common diagnosis. Audiometric studies in certain contexts may serve as surrogate markers of vestibular dysfunction.

Electrocochleography (EcochG) entails the monitoring of cochlear electrical potentials relative to the action potential of the auditory nerve. The test was commonly used to study endolymphatic pressures. This test, however, may be positive in patient's either without Meniere's syndrome or outside of a Meniere's attack. Vestibular testing may often provide information that is meaningful in the management of the vestibular patient, however, lateralizing features are not always present.

Vestibular test battery (VTB), comprehensive audiometry (pure tone and speech thresholds, and immittance studies) and EcochG results were reviewed of fifty patients presenting to the Cleveland Clinic Foundation's Vestibular Disorders clinic. Patient's meeting clinical criteria of Meniere's syndrome were excluded from the retrospective study to focus on abnormalities that may exist outside of endolymphatic hydrops. Patients were required to have normal hearing and no tinnitus by self-description to be included. Vestibular testing that indicated a partial peripheral vestibular loss and those with "non-specific peripheral vestibular disturbance" patterns were included.

Patterns of EcochG and audiometry, when analyzed along with vestibular testing, often suggest a lateralization that was not appreciable by vestibular testing alone.

The pathogenesis of vestibular dysfunction is polyfactorial and may affect audiologic pathways without providing audiologic symptoms. Audiometric studies in patients solely with vestibular symptoms may reveal audiologic deficits. This appreciation may help to elucidate the apparent variability of results that EcochG provides and why disorders such as tinnitus may often not manifest objective audiometric deficits. Newer testing modalities such as stacked ABR (auditory brainstem responses) and VEMP (vestibular evoked myogenic potentials) may help to further understand vestibular disorders.

## **206 Electro - Stimulation Therapy Versus Behavioural Therapy for Patients with Unilateral Vocal Fold Paresis: A Randomised Prospective Trial**

**Martin Ptok<sup>1</sup>, Daniela Strack<sup>1</sup>, Adrian Fourcin<sup>2</sup>**

<sup>1</sup>Medizinische Hochschule Hannover, <sup>2</sup>University College London

Different therapeutic methods have been proposed to reduce the adverse effects of unilateral vocal fold paresis (UVFP), including behavioural and surgical procedures.

In a clinical trial we compared a voice exercise treatment combined with electrolaryngeal – stimulation (ES) with conventional, nonsurgical voice therapy (CT). 25 patients with UVFP were randomly assigned to either procedure. All patients had recently diagnosed UVFP and no prior therapy.

CT was carried out by speech pathologists. For ES, stimulation parameters were adjusted by the laryngologist according to the degree of paresis. Then the patient was made familiar with the voice exercises. Stimulation supported voice exercises were subsequently carried on at home at least 3 times / day.

At the beginning of therapeutic interventions and at 3 months we measured several dependent variables. However, only maximum phonation time and an irregularity index were considered in evaluating effectiveness.

Data show that there is a slight though not significant effect in favour of ES.

Further research will be directed towards additional measures of effectiveness as well as efficacy parameters. At this point, however, ES for UVFP does not seem to be inferior to CT and thus may be considered for patients when adverse circumstances hinder the services of speech pathologists.

## **207 Effects of Botulinum Toxin Injection on Adductive Spasmodic Dysphonia "Baker" Shi<sup>1</sup>**

<sup>1</sup>Oregon Health & Science University

Spasmodic dysphonia (SD) is a form of focal dystonia of laryngeal muscles that disrupts voice and speech by causing a tight or strained voice with breaks and hoarseness. SD happens in about 0.001% of the population. Patients with SD experience tremendous difficulties with verbal communication. Surgical laryngeal muscle denervation and re-innervation have been used to treat SD with unpredictable results and significant side effects (i.e., vocal cord paralysis). Botulinum toxin, produced by clostridium botulinum, paralyzes skeletal muscles by blocking cholinergic synapses. Botox, a commercial preparation of botulinum toxin type A, has been used in treating SD since the 1980s.

This study attempted to quantify the perceived benefits of Botox treatment in SD patients. Sixteen patients consecutively seen at the Northwest Center for Voice and Swallowing at Oregon Health & Science University completed questionnaires regarding voice changes, side effects and effective duration related to Botox injection. On a visual numerical scale of 0 to 5, the patients rated perceived voice improvement (0 = no improvement, 5 = normal voice) and pre-/post-treatment symptoms severities (0 = no symptoms, 5 = very severe symptoms). Symptoms evaluated included tightness, breaks and hoarseness in voice. The mean age of this patient population was 63.5 years, with a female to male ratio of 3 to 1. Average dose delivered in this group of patients was 2.6 units/muscle with a range of 0.75 to 6.5 units/muscle based upon previous patient responsiveness.

All patients reported voice improvement following treatment. Average voice improvement rating was 4.4. Improvement was maintained for an average of 4.3 months (range, 2 to 11 months). Average ratings of tightness, breaks and hoarseness in voice and speech were reduced to less than 1 (0.7 to 0.9) after treatment, compared to 2.4 to 3.6 before injection. For all three symptoms, the changes were statistically significant ( $P_s = < 0.001$ ) as shown by paired T-test. Although perceived voice improvement tended to be associated with decreased symptoms, they were not always firmly correlated. Main side effects included breathiness in voice and dysphagia in the early period following Botox injection. Breathiness was generally mild to moderate (averaged at

2.4 on a 0 to 5 severity scale) and lasted on average 12.4 days. Dysphagia lasted for 4.5 days on average. These data indicate that Botox injection is effective in treating SD with satisfying voice improvement and tolerable side effects. However, there is significant inter-subject variability in response to Botox injection, in benefits, side effects, and dosage requirements. Possible meanings of the findings are discussed.

### **208 Percutaneous Endoscopic Gastrostomy (PEG) – A Long-Term Follow-Up Study in Head and Neck Carcinoma Patients**

Ylva Tiblom-Ehrsson<sup>1</sup>, Ann Langius-Eklöf<sup>2</sup>, Göran Laurell<sup>1</sup>  
<sup>1</sup>Department of Otolaryngology, Karolinska University Hospital, Stockholm, Sweden, <sup>2</sup>Department of Nursing, Karolinska Institute, Stockholm, Sweden

**Background:** Nutritional support is frequently provided for patients with head and neck carcinoma in an attempt to reduce morbidity and enhance quality of life. Most authors report a low incidence of complications related to use of percutaneous endoscopic gastrostomy (PEG). The background to the present investigation was a considerable difference between reported data and the clinical experience at a Swedish teaching hospital. We want to share our experience from a much higher incidence of adverse events that can be related to PEG.

**Methods:** A total of 156 consecutive head and neck carcinoma patients receiving PEG at Karolinska Hospital during the period 1992 to 1999 were retrospectively evaluated. Data were collected from medical and nursing records during the period January 1992 to June 2001. The patients were followed from diagnosis to death, or until June 2001.

**Results:** A surprisingly high incidence of fatal as well as less severe complications was found. Altogether 42 % had complications. Fatal complications were seen in connection to PEG tube placement, but severe and minor complications could occur much later.

**Conclusions:** It is important to select suitable candidates for a PEG. For a head and neck carcinoma patient with swallowing disorder a theoretically easy surgical procedure could turn into a potentially dangerous operation.

### **209 Optical Coherence Tomography and Image Analysis of the Aerodigestive Tract.**

James Ridgway<sup>1,2</sup>, R. Jackson<sup>2</sup>, U. Mahmood<sup>2</sup>, S Guo<sup>2</sup>, J Su<sup>2</sup>, W Armstrong<sup>1</sup>, t Shibuya<sup>1</sup>, r crumley<sup>1</sup>

<sup>1</sup>UCI Medical Center, <sup>2</sup>Beckman Laser Institute

**Background:** Early detection of head and neck cancer presents a difficult clinical problem. Tissue biopsy and histologic evaluation is common practice for early disease diagnosis. Unfortunately, this technique is invasive and may require multiple tissues samples from sensitive structures such as the vocal cords. Other non-invasive diagnostics including CT, MRI, and Ultrasonography lack the spatial resolution required for microstructure analysis and early detection. One promising technology that allows for in vivo microstructure characterization is Optical Coherence Tomography (OCT). Using light in analogous

fashion to B-mode ultrasound, OCT research have revealed the unique application of this technology in the analysis of the adult human upper aero-digestive tract. **Methods:** A high-speed, high resolution, real-time OCT imaging system was developed and applied with the in vivo imaging of oropharyngeal tissue in adult patients. This non-contact, non-invasive diagnostic tool combines a broadband light source and interferometry to produce high-resolution cross-sectional images (8-20µm) in biologic tissues and a depth of 1.5 -2.0 mm. **Results:** High-resolution images characterizing epithelium, basement membrane, and tissue microstructure were produced from studies in sixty adult patients. Correlation of OCT images with endoscopic and histologic observations was made in normal, benign, and pathologic conditions. **Conclusion:** Preliminary information of in vivo adult human upper aero-digestive tract will be presented. Highlights of instrument development and potential applications will be reviewed as our study broadens its analysis of the variable and complex disorders in head and neck surgery.

**Keywords:** Optical Coherence Tomography, oropharynx, in vivo, non-invasive, aero-digestive

### **210 Temporal Bone Findings on Computed Tomography Imaging in Branchio-Oto-Renal Syndrome**

Evan Propst<sup>1</sup>, Blake Papsin<sup>1</sup>, Karen Gordon<sup>1</sup>, Susan Blaser<sup>1</sup>

<sup>1</sup>The Hospital for Sick Children

**Objective:** To describe temporal bone findings using Computerized Tomography (CT) in individuals with Branchio-Oto-Renal Syndrome.

**Study Design:** Retrospective evaluation of CT findings in individuals with a clinical diagnosis of Branchio-Oto-Renal Syndrome.

**Patients:** Twenty patients with a clinical diagnosis of Branchio-Oto-Renal Syndrome from 13 families.

**Results:** Computerized Tomography findings included a funnel-shaped internal acoustic meatus, hypoplastic cochlea, hypoplastic or absent modiolus, absent lamina cribrosa, enlarged and medially-deviated facial nerve canal, hypoplastic horizontal semicircular canal, dilated vestibular aqueduct, fused ossicles, dilated Eustachian tube and medially-deviated carotid artery.

**Conclusion:** The association of findings on CT imaging can also strongly support the diagnosis of Branchio-Oto-Renal Syndrome. The distribution of these findings across affected individuals will be discussed.

### **211 3-D Virtual Model of the Human Temporal Bone: A Stand-Alone Downloadable Teaching Tool**

Haobing Wang<sup>1</sup>, Clarinda Northrop<sup>1</sup>, M. Charles Liberman<sup>1,2</sup>, Saumil Merchant<sup>1,2</sup>

<sup>1</sup>Massachusetts Eye & Ear Infirmary, <sup>2</sup>Harvard Medical School

We have developed a 3-dimensional (3-D) virtual model of a human temporal bone based on serial histological sections. The model is a powerful teaching tool for learning



the complex anatomy of the human temporal bone and for relating the 2-D morphology from a histological section to the 3-D anatomy.

The model was created from archival histologic sections from a 14-year old male. The specimen was formalin fixed, decalcified, embedded in celloidin, serially sectioned in the axial plane at 20 microns, stained with hematoxylin and eosin, and mounted on slides. Low-power views of every fifth section through the temporal bone were digitized and imported into Amira v3.1 (Mercury Computer Systems/TGS, San Diego, CA). The sections were aligned and segmented into anatomical "structures of interest".

The 3-D model is a surface rendering of these structures of interest, which currently includes (among others) the bone and air spaces of the temporal bone; the perilymph and endolymph spaces including cochlear aqueduct and endolymphatic duct and sac; the sensory epithelia of the cochlear and vestibular labyrinths; the ossicles and tympanic membrane; the middle-ear muscles; the carotid artery; and the auditory, vestibular and facial nerves. For each of these structures, the surface transparency can be individually controlled, thereby revealing the 3-D relations between surface landmarks and underlying structure. New structures of interest can be added within the Amira software.

The 3-D surface model can also be "sliced open" at any section, and the appropriate raw histologic image superimposed on the cleavage plane. Leafing through the section stack in this way provides a powerful view of the relation between microscopic images and 3-D anatomy. The image stack can also be re-sectioned in any arbitrary plane.

The model can be downloaded from the Eaton-Peabody Laboratory website (<http://epl.meei.harvard.edu/~hwang/3Dviewer/3Dviewer.html>) packaged within a freeware 3-D viewer, which allows full rotation and transparency control on any platform including Windows, Linux and Mac OSX. The native Amira files are also available upon request.

Model development supported by a core grant from the NIDCD (P30 DC05209).

## **[212] Hearing and Superior Semicircular Canal Dehiscence: Response to Air Conduction**

**Jocelyn Songer**<sup>1</sup>, Melissa Wood<sup>2</sup>, John Rosowski<sup>2</sup>

<sup>1</sup>*Speech and Hearing Bioscience and Technology, MIT,*

<sup>2</sup>*Massachusetts Eye and Ear Infirmary*

Superior semicircular canal dehiscence (SCD) syndrome affords a unique opportunity to study a novel pathology in otolaryngology, which was

first defined in 1998, and the mechanisms by which it affects hearing. An SCD is a break in the bone separating the superior canal from the cranial cavity. Patients with SCD syndrome present with a wide variety of symptoms: some present with vestibular symptoms, others present with auditory symptoms (including low-frequency conductive hearing loss) and still others present with both

auditory and vestibular symptoms. A mechanism for the vestibular and auditory symptoms has been suggested by Minor and Rosowski et al., which proposes that the SCD acts as a 'third window' in the inner ear, altering sound pathways and giving rise to both the auditory and vestibular symptoms. In this study we are focusing on the effect of dehiscence on audition and specifically how it affect both the cochlear potential and gross cochlear mechanics in response to air conducted sound. The effect of a surgically induced dehiscence on auditory responses to air conducted stimuli was evaluated in 5 chinchilla ears. We monitored the cochlear potential and stapes velocity (using laser Doppler vibrometry) in response to air conducted sound before and after the introduction of a dehiscence. Sound induced fluid motion within the dehiscent canal was also observed. A low frequency decrease in cochlear potential that was reversible upon plugging was observed in these five cases. Additionally, a reversible increase in stapes velocity in response to the introduction of a SCD was demonstrated. These findings are consistent with the hypothesis proposed by Minor et al. that the SCD acts as a 'third window' in the cochlea shunting volume velocity away from the cochlea, and leading to a low-frequency hearing loss. A preliminary model of the effect of the dehiscence on air-conducted hearing has also been developed. These findings, in conjunction with previous work demonstrating a low-frequency increase in bone-conduction sensitivity with SCD are consistent with clinical findings of conductive hearing loss in some SCD patients. [Supported by NICDC and NSF]

## **[213] Alleviating Effect of Intratympanic Injection of Latanoprost in Ménière's Disease. A Placebo-Controlled, Double-Blind, Pilot Study**

**Helge Rask-Andersen**<sup>1</sup>, Ulla Friberg<sup>2</sup>, Marianne Johansson<sup>3</sup>, Johan Stjernschantz<sup>4</sup>

<sup>1</sup>*Dept of Surgical Sciences, Unit of Otorhinolaryngology, Uppsala University,* <sup>2</sup>*Dept of Surgical Sciences, Unit of Otolaryngology, Uppsala University,* <sup>3</sup>*Synphora AB, Uppsala,* <sup>4</sup>*Dept of Neuroscience, Unit of Pharmacology, Uppsala University*

Objective: Latanoprost, a PGF<sub>2</sub>α analogue, is a selective FP prostanoïd receptor agonist that is widely used for treatment of glaucoma. The drug reduces the intraocular pressure by enhancing uveoscleral outflow of aqueous humor. The purpose of the present study was to investigate whether latanoprost alleviates the symptoms of Ménière's disease, the rationale being that the drug may reduce the endolymphatic pressure.

Methods: 10 patients with unilateral Ménière's disease were enrolled in the study. Preservative-free latanoprost solution (50 µg/ml) was administered once daily during three consecutive days by intratympanic injection. On days 4 and 14 after the first injection the patients underwent a thorough audiological examination. Vertigo/instability was assessed by the patients using a VAS-scale. The study was carried out according to a double-blind, crossover

protocol, each patient receiving both active treatment and placebo, with a washout period of 1-2 months.

Results: Latanoprost statistically significantly increased speech discrimination, and enhanced slightly, but statistically significant, hearing ability, determined as pure tone average. No clear-cut effect on tinnitus was seen, but a statistically significant 30% reduction in subjective vertigo/instability was recorded. Latanoprost was well tolerated in the ear. One patient was withdrawn from the study for a reason unrelated to the study drug.

Conclusion: Latanoprost statistically significantly alleviated symptoms of Ménière's disease in this first double-blind, placebo-controlled study. The results indicate that FP prostanoid receptor stimulation in the inner ear may be beneficial for the treatment of Ménière's disease. A dose-titration follow-up study is in progress.

## **214 Genotyping of Measles Viruses in Otosclerosis**

**Hans Peter Nierdermeyer<sup>1</sup>**, Tsana Gantumur<sup>2</sup>, Wolfgang Neubert<sup>2</sup>, Wolfgang Arnold<sup>1</sup>

<sup>1</sup>*Klinikum recht der Isar, Technical University Munich,*

<sup>2</sup>*Max-Planck-Institute of Biochemistry, Molecular Virology, Munich*

The nature of the triggering event in otosclerosis remains unknown, it appears to act on a complex genetic background. Detection of measles virus (MeV) by morphology and biochemistry within otosclerotic foci and epidemiologic data have suggested measles virus as an environmental stimulus on the development of otosclerotic foci. Immunohistochemical investigations have shown the expression of various MeV proteins within the otosclerotic focus. By the use of RT-PCR MeV related sequences have been detected in pulverized otosclerotic bone chips and in archived temporal bone section confirming the immunohistochemical data. Searching for an immune response of the inner ear immune system against MeV proteins increased anti MeV IgG amounts were detected in the perilymph of patients with otosclerosis. In situ RT-PCR allowed finally the localization of MeV sequences in osteoblasts, chondrocytes, macrophages and epithelial cells of the middle ear mucosa of the otosclerotic tissue. Determination of the virus strain needed large amounts of MeV RNA. Despite the use of nested primer amplification techniques MeV amounts for analysing large MeV RNA sequences were not sufficient. Recently more efficient cell culture technique protocols were employed which allowed detection of MeV RNA in osteoblasts cultured from otosclerotic bone chips. Using conventional guanidinium thiocyanate-phenol-chloroform method the sensitivity could be increased up to 5 positive cases out of 6 patients. Sequence analysis of the 456 nucleotides located on the Nc region revealed that all measles virus genome of our patients were grouped into the genotype A. Measles virus genotype A was present in central Europe during the prevaccination era. To this group are belonging only measles viruses isolated worldwide during 1950s and 1960s, different from the strains used for vaccination or employed as controls in our laboratories. Our results

support the view of a measles virus persistence in otosclerosis.

Supported by DFG NI 524/2-1 und KKF H-15/96

## **215 Randomized Placebo Controlled Trial of a Selective Serotonin Reuptake Inhibitor in the Treatment of Tinnitus**

Shannon Robinson<sup>1</sup>, Erik Viirre<sup>1</sup>, Jeffrey Harris<sup>1</sup>, Melissa Gerke<sup>1</sup>, Kelly Bailey<sup>1</sup>, Murray Stein<sup>1</sup>

<sup>1</sup>*UC San Diego*

Objective: To assess the efficacy of a selective serotonin reuptake inhibitor for tinnitus.

Design: 120 tinnitus patients participated in a randomized double blind placebo controlled trial. Paroxetine or placebo was increased to a maximally tolerated dose (up to 50 mg) and patients were treated for a total of 31 days at that dose.

Patients: Patients with chronic tinnitus were recruited through the UCSD Division of Otolaryngology, the local Otolaryngological and Audiology communities and advertisements. Exclusionary criteria included bipolar disorder, schizophrenia, alcoholism or drug dependence, use of psychoactive medications or medications that interact with paroxetine, suicidal ideation, and inability to hear at one's tinnitus sensation level. 58% of patients were male, 92% were Caucasian and the average age was 57. 26% of participants dropped out due to side effects.

Outcomes Measures: tinnitus matching, the Tinnitus Handicap Questionnaire (THQ), the question: how severe (bothersome, aggravating) is your tinnitus, Quality of Well-Being and psychological questionnaires.

Results: Paroxetine was statistically superior to placebo on the question "how aggravated are you by your tinnitus?",  $F(1,66)=6.54$ ,  $p=.013$ . Paroxetine was not statistically superior to placebo on any of the other tinnitus. Post-hoc analysis revealed individuals who achieved a dose of 50 mg/d did show improvement relative to placebo on a number of measures: 10db decrease in tinnitus in either ear [ $X^2(1, n=73) = 5.28$ ,  $p=.027$ ], THQ subscale 2 [ $F(1,76) = 8.36$ ,  $p=.005$ ], how severe is your tinnitus [ $F(1,39) = 5.46$ ,  $p=.025$ ], how bothered are you by your tinnitus [ $F(1, 40) = 4.82$ ,  $p=.034$ ], and how aggravated are you by your tinnitus [ $F(1, 55) = 8.01$ ,  $p=.006$ ].

Conclusions: These results suggest that the majority of individuals in this study did not benefit from paroxetine in a consistent fashion. The subgroup analysis is suggestive of benefit in patients who can tolerate higher doses.

## **216 Spontaneous Brief Unilateral Tinnitus: Prevalence and Properties**

**Robert Levine<sup>1</sup>**

<sup>1</sup>*Massachusetts Eye and Ear Infirmary*

Some forms of tinnitus, such as tinnitus following a loud sound, are experienced by most people and can be considered normal. Another type is spontaneous brief unilateral tinnitus (SBUT). To understand the relationship between SBUT and other types of problematic tinnitus we have undertaken a survey of some of its properties.

We interviewed 62 non-clinical subjects [from personal contacts] with normal or near normal hearing. 76% had experienced SBUTs at some time in their lifetime and 24% had never experienced a SBUT. There was no association between experiencing SBUTs and age, handedness, whether or not they had chronic tinnitus, or whether or not they could somatically modulate their tinnitus. Subjects who had experienced tinnitus after loud sound had a higher incidence of SBUTs than the general population.

4 subjects with normal hearing and SBUTs kept a log of their SBUTs for 4 months. Subjects had 0, 1, 11, and 36 SBUTs respectively. About 70% of SBUTs were in the right ear. Average duration was about 20 seconds. A pressure feeling was associated with about 60% of the SBUTs and could be longer or shorter than the SBUT. A subject who was a musician estimated the pitch as ranging between 100 to 1000 Hz.

Listening up to the ear of a subject at the time a SBUT was occurring never detected a corresponding sound.

Supported by ATA, & TRC.

### **[217] Development of the C3H/HeJ Mouse Model for the Study of Spontaneous Chronic Otitis Media and its Impact on the Inner Ear**

**Carol MacArthur<sup>1</sup>, Steven Hefeneider<sup>1,2</sup>, Sarah Parrish<sup>1</sup>, J. Beth Kempton<sup>1</sup>, Dennis Trune<sup>1</sup>**

<sup>1</sup>OHSU, <sup>2</sup>Portland VAMC

In spite of decades of study, it is still not clear how otitis media impacts the inner ear to cause sensorineural hearing loss. Temporal bone studies show inner ear pathology occurs in up to 67% of specimens with chronic otitis media. Inflammatory cells often are seen in the inner ear perilymphatic spaces, probably entering via the round window membrane. Our lab has recently described chronic otitis media in the C3H/HeJ mouse that has a defect in its toll like receptor 4 (TLR4). The C3H/HeJ mouse has a single amino acid substitution in its TLR4, making it insensitive to LPS. As a result, these mice cannot clear gram negative bacteria, such as *H. influenzae*, one of the major bacteria responsible for otitis media. This animal provides us the opportunity to study spontaneous chronic otitis media without experimental manipulation.

ABR thresholds in 7-8 month old C3H/HeJ mice showed that about half developed middle and inner ear disease. The significant elevation of thresholds suggested a sensorineural component in addition to the conductive loss. Middle and inner ear histology in 11 month old C3H/HeJ mice showed some degree of middle and inner ear inflammation in half the mice, paralleling the ABR data. Extensive inflammatory cell infiltration was seen in the middle ears along with fibrosis, mucosal hypertrophy and degeneration, fluid, breakdown of the round window membrane, and inner ear inflammation. The tissue of the round window appeared to be degenerated and replaced by fibrotic material. Furthermore, the inner ear had extensive inflammatory cell infiltration into the perilymphatic spaces. The organ of Corti was degenerated and occupied by inflammatory cells. All

these histopathologic changes have been reported in human inner ears during chronic otitis media. This spontaneous model of chronic otitis media will allow us to characterize the inner ear inflammatory processes that are induced by middle ear disease. (Supported by NIH R01 DC05593 and VA RR&D C2870R)

### **[218] Inhibition of Endogenously Produced Neuregulin Reduces Vestibular Schwannoma Cell Proliferation in Vitro**

**Papri Chatterjee<sup>1</sup>, Steven Green<sup>1</sup>, Marlan Hansen<sup>1</sup>**

<sup>1</sup>University of Iowa

Vestibular schwannomas (VSs) result from a benign proliferation of Schwann cells (SC) lining the vestibular nerves. Insight into the cellular mechanisms that contribute to VS growth may guide the development of non-operative treatment strategies for VSs. Previous studies suggest a role for the glial growth factor, neuregulin, in promoting SC neoplasia. We show here that VSs removed from human patients express neuregulin and its cognate ErbB2 and ErbB3 receptor protein-tyrosine kinases, as determined by immunoblot, confirming previous immunohistochemical findings. This suggests an autocrine mitogenic stimulation, further supported by our observation of ErbB2 tyrosine phosphorylation in these VSs, which indicates activation by neuregulin within the VS. VS cells proliferate in culture, as determined by BrdU uptake. The proliferation is enhanced by addition of exogenous neuregulin but is inhibited, even in the absence of exogenous mitogens, by addition of a neuregulin-blocking antibody or by the ErbB2 inhibitors, PD158780 (100 nM) or trastuzumab (Herceptin), an inhibitory humanized anti-erbB2 antibody. Conditioned media from cultured VS cells contains secreted neuregulin as demonstrated by immunoblot and promotes facial nerve SC proliferation, an effect that is reduced by co-treatment with a neuregulin-blocking antibody or trastuzumab. Together these data suggest that endogenously produced neuregulin contributes to VS proliferation in vitro and that blockade of this mitogen is a potential target for VS treatment.

### **[219] Kalman Filtering in Recording Auditory Evoked Potentials**

**Isaac Kurtz<sup>1</sup>, Aaron Steinman<sup>1</sup>**

<sup>1</sup>Vivosonic Inc.

Otoacoustic Emissions (OAE) and Auditory Evoked Potentials (AEP) are conventionally recorded using time averaging and the Fast Fourier Transform (FFT) method: Signals are first divided into data blocks, and these blocks are then averaged over time. Some methods employ weighted averaging to improve the signal-to-noise ratio. However, transient artifacts, like instant acoustic noises in OAE recording, or muscular artifacts in AEP recording, when averaged into the calculation, degrade the accuracy of the results, even if artifacts exceeding certain artifact-rejection threshold (ART) are rejected from averaging.

It was shown that Kalman filtering can be effectively employed for analyzing physiological signals, particularly in DPOAE recording, and that is faster and more accurate

than the FFT method (US Patents 6,463,411 and 6,778,955; Li et al, 2000). This paper will focus on the application of Kalman filtering to Auditory Brainstem Response (ABR) and Auditory Steady State Response (ASSR). We will show that it has major advantage over the FFT method in superior handling of artifacts. We will particularly focus on handling transient AEP artifacts: Kalman filtering does not "reject" time segments contaminated with transient artifacts, but rather extracts any useful information on the signal from such segments which results in better signal-to-noise ratio.

As a result, Kalman filtering can accurately record ABR and ASSR responses even in the presence of strong transient artifacts that would affect time-averaging recording. This unique ability assures the clinician of accurate, fast, and reliable OAE and AEP measurements in real-world environments. Results of ABR recording using Kalman filtering, as compared with averaging techniques, will be discussed.

## **220 Spectral Profile Discrimination Ability in Cochlear Implant Users**

**Ward R. Drennan<sup>1</sup>, Bryan E. Pfingst<sup>1</sup>**

<sup>1</sup>*University of Michigan*

The ability of cochlear implant users to discriminate a change in an electric profile (represented as current vs. electrode position) was investigated in listeners with Nucleus CI24R(CS) cochlear implants. This approach used static electric profiles as they would be presented through a speech processor given a static acoustic stimulus. In the first experiment, the independent variable was the number of active electrodes. Listeners were asked to detect a current increment in one of 1, 3, 7, 11 and 21 active electrodes. Sensitivity to differences in the electric profiles decreased with increasing number of electrodes. Current interaction and masking probably caused these effects. It is proposed that electric profile discrimination provides a measure suprathreshold channel interaction. This can be done by comparing current-level discrimination ability for one electrode to electric profile discrimination ability using an increment on one electrode in a multiple electrode profile. In a second experiment, the effects pulse rate and electrode spacing on electric profile discrimination were evaluated using clinically common parameters and a 7-active-electrode profile. Results were highly variable among listeners. Sensitivity was often best at the pulse rate used clinically. High pulse rates decreased electrical profile sensitivity substantially for some listeners. In a third experiment, listeners' abilities to hear a change in a 7-active-electrode profile were studied with the overall level randomly roved within an individual trial covering a range of 0, 10 or 20% of the dynamic range. One of five listeners was able to discriminate electric profile changes smaller than the amount of the rove. Listeners reported hearing variation in pitch that were not consistent with changes in the electric profile shape. These changes were possibly related to the size and shape of the electric fields which vary with level. Work supported by NIH/NIDCD F32 DC005893 and R01 DC03808.

## **221 Loudness Growth with Focused Electrical Stimulation: Model and Cochlear Implant Data**

**Leonid Litvak<sup>1</sup>, Gulam Emadi<sup>1</sup>, Anthony J. Spahr<sup>2</sup>**

<sup>1</sup>*Advanced Bionics Corporation*, <sup>2</sup>*Arizona State University*

Many cochlear implant strategies use monopolar stimulation, likely resulting in broad electrode activation patterns. Focusing stimulation by delivering opposite polarity current to adjacent electrodes may reduce this unwanted spread. We investigated activation patterns of focused stimulation in a biophysical model. Electrodes and neurons were arranged along parallel lines separated by distance  $d$ . For a given electrode, an effective spatial activation pattern was computed by assuming a homogeneous medium; activation from multiple electrodes was summed linearly. A neuron "fired" when the local net activation exceeded its threshold. Degree of focusing (based on current to the adjacent electrodes) ranged from  $s=0$  (monopolar) to  $s=1$  (tripolar). Regardless of distance  $d$ , the current needed for near-threshold activation was well-approximated by a monotonic relationship:  $I=I_0(d)/(1+s*K(d))$ , with fitted constants  $I_0(d)$  and  $K(d)$ . To achieve greater neural activation, the required current in some cases first increased and then decreased as a function of focusing. This non-monotonicity, likely related to side-lobes, occurred primarily for small electrode-to-tissue distances. We also measured the currents required for threshold and most-comfortable loudness as a function of focusing in 7 Clarion CII or HiRes90K cochlear implant users. The threshold data were accurately fit by the equation above (avg. correl. coef. = 0.99). The comfortable loudness data were non-monotonic in 3/13 cases, with the strongest case corresponding to the smallest electrode-to-tissue distance (predicted from the threshold data). The experimental confirmation of our model in terms of current levels suggests that it may also be useful with regards to predicting the spatial spread of neural activation. Namely, it predicts that optimal focusing constrains the same net neural activation to a smaller region as compared to monopolar stimulation. Such spatial constraint may have useful perceptual consequences.

## **222 Effects of High-Rate Pulse Trains on Electrode Discrimination in Cochlear Implant Users**

**Christina Runge-Samuelson<sup>1</sup>, Jill Firszt<sup>1</sup>, Marie Birnbaum<sup>2</sup>, Ashley Wackym<sup>1</sup>**

<sup>1</sup>*Medical College of Wisconsin*, <sup>2</sup>*University of Wisconsin*

STUDY AIM: High-rate pulse trains have been found to increase electric dynamic range in cochlear implant users [Hong et al.,2003]. The study aim was to investigate the potential for high-rate electrical pulse trains to improve electrode discrimination in a multi-electrode cochlear implant device. Electrode discrimination has been found to improve with increases in stimulation level [McKay et al.,1999; Pfingst et al.,1999], and Pfingst et al. (1999) found that electrodes with the poorest discrimination also had the smallest dynamic ranges. This effect has also been noted with electrode pitch-ranking abilities [Donaldson & Nelson, 2000]. Although the mechanisms

behind these results are unclear, the effects of level and dynamic range on electrode discrimination indicate that changes in dynamic range with high-rate pulse trains may affect electrode discrimination. **HYPOTHESIS:** High-rate pulse trains will increase dynamic range and improve electrode discrimination. **METHODS:** Subjects were users of the Clarion CII or HiRes 90K cochlear implant. Electrode discrimination was measured by presenting 1000 Hz sinusoids on two nearby electrodes with and without 5000 Hz pulses on adjacent electrodes. The 1000 Hz sinusoids were presented at several intensity levels, and were balanced for loudness at each intensity level prior to testing. The subjects reported whether the sounds were the same or different, and *d'* values were calculated. **RESULTS:** The presence of high-rate pulses increased the dynamic range for all subjects. Although there was variability within and among subjects, in general the *d'* values increased for most sinusoidal levels in the presence of high-rate pulses, consistent with an improvement in electrode discrimination. The possible mechanisms and implications of these results will be discussed.

*Supported by the NIH/NIDCD R03 DC006361-01A1 and intramural funds from the Department of Otolaryngology and Communication Sciences, Medical College of Wisconsin*

### **223 The Effects of Pulse Rate on Channel Interactions in Cochlear Implants as Revealed by Spectral Discrimination Tasks**

**Tim Green**<sup>1</sup>, Andrew Faulkner<sup>1</sup>, Stuart Rosen<sup>1</sup>

<sup>1</sup>*University College London*

Advances in cochlear implant design have resulted in large increases in the rate at which pulses can be delivered to the auditory nerve. Higher stimulation rates are advocated on the grounds that they allow an enhanced representation of temporal envelope information, and lead to patterns of neural responses that more closely resemble those found in normal hearing. However, the small number of studies that have assessed speech perception as a function of pulse rate have not provided a clear picture, with only limited evidence of benefits from high rates, and substantial differences across listeners. Potential benefits of high pulse rates may be counteracted by increased interaction between channels at higher rates. This possibility was assessed by measuring Clarion CII implant users' ability to discriminate spectral shape in moderately complex stimuli. This ability is both directly related to important auditory contrasts in speech, and depends upon the degree of channel interaction, since increased channel interaction will necessarily lead to smearing of spectral detail. Stimuli were complex periodic tones which had fundamental frequency in the human voice pitch range and featured two spectral peaks (formants). An eight-channel CIS processing strategy was implemented with several pulse rates within the range 250 – 5000 Hz. Just-noticeable differences (*jnds*) in formant frequency obtained for each formant, with the other formant static in frequency, will be reported.

### **224 Channel Interaction in Cochlear Implants as a Function of Pulse Rate, Phase Duration, and Stimulation Mode**

**Deniz Baskent**<sup>1</sup>, Robert Shannon<sup>1,2</sup>

<sup>1</sup>*House Ear Institute*, <sup>2</sup>*University of Southern California*

Cochlear implants with multiple electrodes stimulate auditory nerves at different locations along the cochlea. It is commonly assumed that good speech recognition requires independent activation of distinct tonotopic regions with minimal interactions between electrodes; such interactions can produce a result similar to spectral smearing. The electrical pulses produced by multiple electrodes can interact both spatially and temporally. However, little is known about the effect of basic electrical stimulation parameters on the degree of channel interaction. It is possible that high stimulation pulse rates could improve the temporal representation of the signal but reduce the spatial (tonotopic) resolution. Differences in pulse phase duration or amplitude could change the level of electrode interaction. Electrode stimulation configuration (monopolar or bipolar) is also assumed to affect channel interactions; bipolar stimulation is shown to result in smaller channel interaction at same stimulation levels. The present study used forward masking to measure electrode interaction patterns as a function of the stimulating pulse phase duration and the stimulation rate. Release of masking patterns were observed with masker and probe placed on the same electrode. To observe the spatial interactions the masker was placed on one electrode and the threshold elevation of the following probe signal on a different electrode was measured, as a function of cochlear location. Forward-masked electrode interaction patterns were compared for different stimulation configurations and parameters at several masker levels. Once the elevated thresholds were normalized with respect to subject's dynamic range, all patterns were similar, suggesting that the parameters used in the study have no significant effect on channel interactions.

[Supported by NIDCD Grant R01-DC-01526.]

### **225 The Tripolar Electrode Configuration and Measures of Channel Interactions in Cochlear Implant Subjects**

**Julie Arenberg Bierer**<sup>1</sup>

<sup>1</sup>*University of California, Epstein Laboratory*

Spatial and temporal interactions among cochlear implant channels reduce the effectiveness of multi-channel stimulation. One technique for potentially reducing channel interaction is to use stimulus channels that produce spatially restricted current fields. In this study, the effects of channel interaction were examined in 7 cochlear implant listeners by varying spatial current spread of one- and two-channel stimuli using three electrode configurations: monopolar (MP), bipolar (BP) and tripolar (TP). One- and two-channel stimuli were biphasic pulse trains. Channel interaction was quantified by the difference between one- and two-channel levels at threshold and maximum comfortable levels (MCL). Thresholds, MCLs, and dynamic ranges for one-channel

stimuli increased from MP to BP and further to TP. TP thresholds showed the most variability from channel-to-channel. The distribution of dynamic range was also more variable for TP. Two-channel trains were presented simultaneously or interleaved. Thresholds and MCLs were usually lower for two-channel compared to one-channel stimuli; the largest shifts occurred for the MP and simultaneous conditions. Shifts were nearly eliminated using TP. The TP channel interaction results were significantly correlated to speech perception performance. Also, in two of the subjects, speech perception testing was performed with 14-channel experimental speech processing strategies that employed each of the three configurations. Both subjects performed best on medial vowel identification with BP or TP strategies. On sentence and medial consonant identification, however, performance was best with MP, the experimental strategy most similar to the subject's clinical strategy. One- and two-channel data suggest TP is the most sensitive configuration to local, cochlear irregularities and has the lowest channel interactions.

### **226 Effects of Stimulation Rate, Mode, and Level on Modulation Detection by Cochlear Implant Users**

**John Galvin<sup>1</sup>, Qian-Jie Fu<sup>1</sup>**

<sup>1</sup>*House Ear Institute*

In cochlear implant (CI) patients, temporal processing is often poorest at low listening levels, making perception difficult for low-amplitude temporal cues that are important for consonant recognition. Presently, much CI research has been directed at enhancing temporal cues (e.g., high stimulation rates, prosthetic noise, etc.), with mixed results. It remains unclear how temporal processing may be affected by speech processor parameters such as stimulation rate and mode, especially at low listening levels. In Experiment 1, modulations detection thresholds (MDTs) were measured in Nucleus-22 users for both high and low stimulation rates, narrow and wide stimulation modes, as a function of loudness level and/or percent dynamic range (DR). Preliminary results show that for both rates, modulation detection was poorest at quiet listening levels, consistent with previous studies' results. However, MDTs were better across the entire DR for the lower stimulation rate, remaining relatively flat between 20 and 100 % DR; MDTs at the higher rate gradually worsened below 50 % DR. Similarly, better MDTs were observed in wide stimulation mode at low stimulation level. In Experiment 2, single-channel consonant recognition was measured for different stimulation rates and modes. The amplitude mapping function was systematically varied so that low-amplitude speech components were mapped to different regions of the electric DR. Preliminary results show that as the speech signal was mapped to progressively lower portions of the DR, recognition was significantly better at the lower stimulation rate; performance also deteriorated more steeply at the higher rate as the speech was mapped to lower portions of the DR. Overall, these results suggest that stimulation rate, mode, and level may significantly affect modulation detection and that interactions between these parameters

and amplitude mapping may strongly influence CI users' consonant perception.

### **227 Across-Channel Modulation Detection Interference in Cochlear Implants at Low modulation rates.**

**Anastasios Sarampalis<sup>1</sup>, Monita Chatterjee<sup>1</sup>**

<sup>1</sup>*House Ear Institute*

The ability of normal-hearing (NH) listeners to detect modulation is impaired in the presence of simultaneous modulated carriers at remote frequencies. This phenomenon has been termed modulation detection interference (MDI). The amount of interference generally shows broad tuning to modulation rate, being greatest when the target and interferer are modulated at the same rate. In cochlear implants (CIs), acoustic information is processed and delivered electrically in the form of amplitude modulations (AM) imposed on carriers stimulating tonotopically appropriate electrodes positioned inside the cochlea. MDI has been observed in electrical hearing at high modulation rates. The aim of the present study was to investigate across-channel MDI in electrical hearing at low modulation rates, which are important for carrying prosodic and segmental speech information. Modulation detection data were collected from 4 CI listeners (N-22 and N-24). The signal was 5-Hz pulse-width modulation presented on electrodes [10-13]. The interferer, when present, was delivered on electrodes [4-7]. It was either amplitude-modulated at rates of 2-15 Hz or unmodulated (amplitude at the peak of the modulated interferers). In a second experiment the interferer was modulated at the target rate (5 Hz), but the modulator phase was varied. The results indicated that performance was largely unaffected by the presence of an unmodulated interferer. Modulated interference, however, impaired the detectability of modulation. This effect showed tuning to modulation rate (peak interference at 5-7 Hz). The effect of relative modulator phase was small. It is concluded that across-channel MDI can be observed in electrical hearing at low modulation rates and that the effect is dependent on the modulation rate of the interferer. The tuning was much sharper than observed with NH listeners, indicating a possible difference in the processing of AM between electrical and acoustic hearing. [Supported by NIDCD R01DC04786].

### **228 Envelope Interactions in Cochlear Implant Listeners: Speech-Like Stimuli**

**Monita Chatterjee<sup>1</sup>, Sandra Oba<sup>1</sup>**

<sup>1</sup>*House Ear Institute*

Recent research has shown that cochlear implant (CI) listeners have particular difficulty with listening in the valleys of fluctuating maskers (Nelson and Jin (2004), J.A.S.A. 115, 2286-2294; Fu and Nogaki, J.A.R.O. In Press). It is likely that with speech maskers, modulation detection interference (MDI) plays an additional role. Kwon and Turner (2001, J.A.S.A. 110, 1130-1140) showed off-channel MDI in normal hearing listeners of spectrally reduced speech, as well as release from masking on-channel (presumably due to listening in the valleys). In

recent work, we have found significant amounts of MDI in CI listeners. Here, we present results from ongoing experiments conducted with stimuli that are more complex and speech-like, spatially (Exp. 1, using a two-channel masker) and temporally (Exp. 2, using two modulators in a single-channel masker). In Exp. 1, we measure spatial patterns of MDI produced by a two-channel (comodulated at 50 Hz) masker: the signal (also modulated at 50 Hz) is presented to the third channel, which is varied in location. Masker electrode locations were selected to correspond to F1 and F2 frequencies for specific vowels. Preliminary results indicate that energetic masking dominates when the signal is near the masker electrode locations (ie on-channel), while MDI dominates in off-channel locations. This pattern is broadly consistent with that observed in experiments with single-channel maskers. In Exp. 2, we introduce greater complexity in the temporal domain: the masker and the signal are both single channel stimuli, but each has two modulators, a fast (100 Hz) and a slow (10 Hz) modulator. The task is to detect the fast modulation in the signal channel. Preliminary results show evidence for both MDI and listening in the valleys in this task. The amounts of MDI and masking release vary with masker-signal distance and also show considerable intersubject variation. [Work supported by NIDCD R01 DC04786].

### **229 Effects of Stimulation Order and Rate on Speech Recognition for Two Cochlear Implant Signal Processing Strategies**

**Satoshi Iwasaki<sup>1</sup>, Yasuyuki Hashimoto<sup>1</sup>, Mitsuyoshi Nagura<sup>1</sup>, Kunihiro Mizuta<sup>1</sup>**

<sup>1</sup>*Hamamatsu University School of Medicine*

The cochlear implant (CI) provides a hearing sensation to profoundly deaf people. The mechanism underlying the variability is a hot discussion in CI speech processing. A number of studies have also been performed to address issues related to place-pitch, rate-pitch and electrode ranking. All of the above studies have used changes to stimulation patterns provided by speech processing strategies to achieve better speech recognition performance. In contrast to the studies mentioned above, we present an evaluation of a new cochlear implant signal processing strategy named Channel Selection by Pulse Estimation (CSPE), which generates stimulation patterns such that the electrode stimulation order and the electrode stimulation rate are directed by the location of the frequency bands of maximum instantaneous amplitude. Open-set speech recognition tests were performed to evaluate speech recognition using the CSPE strategy. Two signal processing strategies for multi-channel cochlear implant speech processors, the Nucleus ACE strategy and a strategy using channel selection by pulse estimation, were compared in a study of five subjects with cochlear implants, using Nucleus Implant Communicator stream tools. Subject-centered speech recognition tests were conducted on vowels, as consonant-vowel-consonant tokens, on consonants, as vowel-consonant-vowel tokens, and on multisyllabic words. Despite the very short learning experience with the CSPE strategy, four of the five subjects showed better consonant and vowel recognition, and three of the five subjects showed better multisyllabic

word recognition. The mean scores for consonant and vowel recognition were significantly better for the CSPE strategy, compared to the ACE strategy.

### **230 Combined Electric-Acoustic Stimulation: Pilot Study Outcomes and Preliminary Multi-Center Study Data**

**Patrick D'Haese<sup>1</sup>, Marcus Schmidt<sup>1</sup>, Lisa Trejo<sup>2</sup>, Amy Barco<sup>2</sup>, Ilona Anderson<sup>1</sup>, Jennifer Kingfield<sup>2</sup>**

<sup>1</sup>*MED-EL Worldwide Headquarters*, <sup>2</sup>*MED-EL Corporation*

Combined electric-acoustic stimulation (EAS) of the auditory system is based on a cochlear implant (CI) surgery that preserves residual low frequency hearing. The EAS system consists of a CI and hearing aid (HA) in the same ear.

Pilot studies have been conducted in Frankfurt and Vienna since 1999 (n=21) using an electrode insertion depth of approximately 20 mm with the aim to preserve low frequency residual hearing. Additionally, the European multi-center study and the United States multi-center clinical trial are currently underway to assess safety and efficacy of the EAS system.

In the pilot studies, the MED-EL C40+ was implanted in all cases. Various electrode variations were utilized as follows: standard electrode with partial insertion (~8 electrodes inserted to 20-22 mm); compressed electrode (12 electrodes inserted ~13 mm); and M-electrode (~10 electrodes inserted 20-22 mm). An overview of these results will be presented. Post-operatively, residual hearing was preserved in 18 of the 21 patients within 0-20 dB compared to pre-operative audiograms (13 within 0-10 dB; 5 within 11-20 dB). Audiograms are stable over time, except in one patient, who suffered from progressive hearing loss which continued to progress after the surgery. Progressive hearing loss is now an exclusionary criterion for EAS. Monosyllables and sentence testing in noise show a significant improvement over time for EAS patients in these pilot studies.

The United States EAS clinical trial utilizes a variation of the M-electrode array (not commercially available in the United States), which was developed in hope of reducing trauma during electrode insertion. The COMBI 40+ cochlear implant system is used for electrical stimulation combined with an Oticon Adapto hearing aid for acoustic amplification. Preliminary results from the clinical trial will be presented and discussed in terms of hearing preservation and speech perception outcomes.

### **231 Using Neural Response Telemetry (NRT) to Predict Programming Levels in the Nucleus 24 Cochlear Implant**

**John King<sup>1</sup>, Marek Polak<sup>2</sup>, Stacy Payne<sup>2</sup>, Ted Meyer<sup>1</sup>, Abby Turick<sup>1</sup>, Annelle Hodges<sup>2</sup>**

<sup>1</sup>*Medical University of South Carolina*, <sup>2</sup>*University of Miami Ear Institute*

Optimal performance with the Nucleus 24 cochlear implant requires accurate setting of the programming levels, including both threshold (T) and comfort (C) levels. In most cases, these levels can be appropriately set utilizing

behavioral and objective clinical techniques; however, alternative methods are sometimes required (i.e. when programming infants that do not have electrically-evoked stapedial reflexes or behaviorally-conditioned responses). Neural Response Telemetry (NRT) is gaining popularity as a potential means of objectively estimating programming levels; however, the proposed methods reported to date require the behavioral measurement of at least one electrode thus reducing the objectivity of such NRT-based methods. The use of NRT has been demonstrated to be an effective means of objectively predicting C levels in the Nucleus 24 (King et al., 2004 ARO abstract #882).

The purpose of this study was to determine whether NRT could be used to objectively predict T levels. Data from 22 adult Nucleus 24 recipients have been examined. Programming levels (T and C levels), NRT threshold ( $NRT_T$ ), and slope of the NRT growth function ( $NRT_{SLOPE}$ ) were obtained for all 22 electrodes. Subject age, length of deafness, and duration of cochlear implant use were also obtained as potential predictive factors. Multiple regression analysis was performed for individual electrodes to identify significant predictors of T levels, as well as to develop equations to estimate T levels.

$NRT_T$  was the only consistently significant predictor of T levels. For prediction of T levels,  $R^2$  ranged from .377 to .637 (mean  $R^2 = .523$ ). The mean difference between the predicted and clinically measured dynamic ranges (C levels - T levels) was only 9 programming units (sd = 6).

Overall, results indicate that NRT can be used objectively to closely predict programming levels. The use of NRT measures should be reserved for difficult cases rather than used as a default programming method.

### **232 ECAP Growth Functions and HiResolution Programming Levels in Pediatric CII Implant Subjects**

**Marc Eisen**<sup>1,2</sup>, Kevin Franck<sup>1,2</sup>

<sup>1</sup>Department of Otorhinolaryngology, University of Pennsylvania Medical Center, <sup>2</sup>Center for Childhood Communication, Children's Hospital of Philadelphia

In this study we sought to characterize the amplitude growth functions of the electrically evoked compound action potential (ECAP) in pediatric subjects implanted with the Clarion HiFocus electrode array with respect to electrode position and the presence or absence of a Silastic positioner. ECAP growth functions were measured for all electrodes along the implant's array in sixteen pediatric subjects. Nine of the patients were implanted with a Silastic positioner, while seven had no positioner. ECAP thresholds and growth function slopes were calculated. Fifteen of the 16 patients had psychophysical threshold and maximum comfort levels measured. Electrophysiologic growth function data was then compared to HiResolution psychophysical programming levels.

ECAP thresholds showed variability among patients, ranging from 178 to 920 nA at 32  $\mu$ s pulsewidth. ECAP thresholds did not depend on electrode position, but were lower in the presence of the Silastic positioner ( $p < 0.001$ ). Growth function slopes also showed considerable variation

among patients. Unlike thresholds, slopes decreased from apical to basal cochlear locations ( $p < 0.001$ ), but showed no difference between the absence and presence of the positioner. When ECAP thresholds were adjusted for each patient by the difference between M level and ECAP threshold at electrode 9, overall correlation between the two measurements was excellent ( $r = 0.98$ ,  $N = 224$ ).

In pediatric subjects with the Clarion HiFocus electrode, ECAP growth function thresholds decrease with the presence of the Silastic positioner, but are unaffected by electrode position along the array. Growth function slope, however, depends on electrode position along the array. ECAP thresholds can reliably predict stimulus intensities within the subjects' dynamic ranges, but considerable variability is seen between ECAP thresholds and HiRes programming levels.

### **233 Preliminary Results with the Advanced Telemetry Capabilities of the PULSARCI100 Cochlear Implant, Operating the EAP recording mode.**

Hansoerg Schoesser<sup>1</sup>, Kim Veekmans<sup>1</sup>, Phillipp Spitzer<sup>2</sup>, Jason Edwards<sup>3</sup>

<sup>1</sup>MED-EL Worldwide Headquarters, <sup>2</sup>University of Innsbruck, <sup>3</sup>MED-EL Corporation

The use of objective measures is very common in the field of cochlear implantation. These measures, especially the electrically evoked compound action potentials (EAP), might be helpful to simplify fitting procedures in difficult to test patients. Furthermore they are also advantageous for medical diagnosis as well as for research of technical features of the device.

The PULSARCI100, the latest cochlear implant developed by MED-EL Medical Electronics GmbH, offers additionally to the known impedance telemetry function from the COMBI 40+ implant, also extended back telemetry features, which give us the possibility of a direct measurement of the stimulation artifact, as well as the possibility to record EAP's directly in the cochlea.

To gather baseline data with standard EAP recordings, a research platform was set up, with software to evoke and record EAP's directly in the cochlea, through the electrode of the PULSARCI100 cochlear implant. Except for baseline data, EAP responses will also be recorded and compared for different sites along the cochlea and the possible change of the EAP response over time will be investigated, as well in adult as in pediatric patients. First clinical experience with the system, as well intra-operative as post-operative recordings, will be shown and discussed.



### **234 The Effect of Noise on Speech Recognition in Cochlear Implant Recipients with Prelingual and Postlingual Profound Hearing Loss Onset**

Jill Firszt<sup>1</sup>, Wolfgang Gaggl<sup>1</sup>, Christina Runge-Samuels<sup>1</sup>, P. Ashley Wackym<sup>1</sup>, Laura Holden<sup>2</sup>, Margaret Skinner<sup>2</sup>

<sup>1</sup>Medical College of Wisconsin, <sup>2</sup>Washington University School of Medicine

Recent published studies indicate improvements in open-set speech recognition scores for adults and older children with prelinguistic onset of profound hearing loss (Waltzman et al., 2002; Schramm et al., 2002). The purpose of the present study was to 1) determine speech recognition abilities for prelingually deafened adult recipients who achieve open-set speech recognition and use more current implant technology, and 2) compare measures of speech perception presented in noise for cochlear implant recipients who have either prelingual or postlingual deafness and equivalent scores in quiet. Subjects were adult implant recipients who had either prelinguistic onset of profound hearing loss (prior to age 3 years, Group 1), or postlinguistic onset of profound hearing loss with less than 10 years of auditory deprivation (Group 2) or 20+ years of auditory deprivation (Group 3). The mean length of auditory deprivation for Groups 1 and 3 was similar (33 and 28 years, respectively), however, the period of life during which the deafness occurred differed. Scores for the subjects in each of the three groups were matched on the Hearing in Noise Test (HINT) of sentence recognition when assessed in quiet at 60 dB SPL. All subjects were evaluated in the presence of noise at +8 dB signal-to-noise ratio. For each subject, the difference in performance in quiet and noise was calculated. A comparison of the score differences showed a larger decrease for those in Group 1 compared to either Groups 2 or 3. In other words, compared to postlingually deafened subjects of either short or long periods of deafness when matched for scores in quiet, there is a greater decrease in scores in the noise condition for prelingually deafened subjects. The implications of long periods of sensory deprivation and limited access to sound, particularly in childhood, are discussed.

Supported by Deafness Research Foundation, NIH/NIDCD K23DC05410

### **235 Speech Recognition Skills in the Elderly Cochlear Implant Population: A Preliminary Examination**

Marcia Hay-McCutcheon<sup>1</sup>, David B. Pisoni<sup>1,2</sup>, Karen I. Kirk<sup>1</sup>

<sup>1</sup>Indiana University Medical Center, <sup>2</sup>Indiana University Department of Psychology

It is generally accepted that as a group, elderly severe to profoundly deafened individuals receive significant speech recognition benefit following cochlear implantation (Chatelin et al., 2004; Francis, Chee, Yeagle, Cheng, & Niparko, 2002; Waltzman, Cohen, & Shapiro, 1993). The purpose of this retrospective study was to explore

individual speech recognition skills in the elderly cochlear implant population (i.e., 65 years of age and older) and to compare those skills with those of younger individuals (i.e., 40 to 59 years of age). A wide range of speech recognition performance, as determined from the CNC word list and the HINT sentences in quiet and in noise was observed. However, the mean percentage scores obtained for each group using these two speech recognition measures indicated no significant differences between the two different age groups. A subset of individuals was tested using the CUNY sentences presented in three different test conditions, auditory-alone, vision-alone and auditory-plus-vision. Although, the pre-implant auditory-alone and auditory-plus-vision scores did not predict post-implant performance, there was some evidence suggesting that vision-alone scores correlated with post-implant performance for the two different groups of participants. Additionally, examination of the auditory gain, the vision gain and the auditory-plus-vision gain derived from the cochlear implant suggested that the younger aged individuals received more auditory-alone and auditory-plus-vision benefit post-implantation than did the older aged individuals. Further prospective studies are required in order to assess the impact that age-related changes in the auditory pathway and/or cognition have upon the individual benefit that elderly cochlear implant recipients can receive from their devices.

### **236 Current Steering and Perceptual Channels in HiResolution Bionic Ear Users: Multi-Center Study of Cochlear-Implant Place/Pitch Relationships**

Mark Downing<sup>1</sup>, Jill B. Firszt<sup>2</sup>, Christina L. Runge-Samuels<sup>2</sup>, Dawn Burton Koch<sup>1</sup>, Leonid Litvak<sup>1</sup>

<sup>1</sup>Advanced Bionics Corporation, Valencia, CA, <sup>2</sup>Medical College of Wisconsin, Milwaukee, WI

This ongoing clinical investigation (seven study sites) is determining the number of perceptual channels (or different pitches) that can be resolved by postlinguistically deafened adults who use the HiResolution Bionic Ear. The number of perceptual channels is defined as the number of distinct pitches that can be heard as current is delivered to distinct locations along the cochlea. In the CII and 90K implants, the number of sites of stimulation can be increased beyond the number of electrode contacts. Through simultaneous delivery of current to pairs of adjacent electrodes, stimulation can be "steered" to sites between the contacts by varying the proportion of current delivered to each electrode of the pair.

Subjects were CII or 90K cochlear-implant users. After loudness balancing and pitch ranking electrode pairs (2-3, 8-9, 13-14), subjects identified the electrode with the highest pitch while current was varied proportionally between electrodes in each pair. Data from 38 implanted ears indicate that the number of perceptual channels that can be distinguished averages 5.7 for the basal electrode pair, 8.7 for the mid-array electrode pair, and 7.0 for the apical electrode pair. Assuming that the number of perceptual channels for these three electrode pairs are representative of the entire array, the potential number of

spectral channels can be calculated. For the subjects in the study to date, the number of possible channels ranges from 8 to 466. These results indicate that additional spectral resolution can be created using current steering. The eventual goal is to incorporate current steering into future sound-processing algorithms that will provide higher fidelity frequency resolution to Bionic Ear users.

### **237** Improvements in Speech-Perception Abilities Parallel Systematic Expansion of the Dynamic Range for Electrical Stimulation of Adult Med-EI Patients Over the First Year Post-Implantation

**Craig Formby**<sup>1</sup>, Kaulani Morgan<sup>1</sup>, Lisa Trejo<sup>2</sup>, Stephanie Moody-Antonio<sup>1</sup>

<sup>1</sup>University of Maryland School of Medicine, <sup>2</sup>MED-EL Corporation

The purpose of this study was to assess longitudinal patterns of change in electrical stimulation and speech-perception abilities for 25 Med-EI implant recipients. The de-identified data reported in this analysis were collected during an investigational study of the efficacy of the Med-EI implant (standard array) at 11 clinical sites from 19 post-lingually deafened adults and from six adults deafened before age 6. Their threshold (T) and maximum comfortable loudness (MCL) data (stimulation levels in  $\mu$ amps) and corresponding dynamic range (DR) values were measured for each of 12 electrode pairs in the implant array at activation, and at 1, 3, 6, and 12 months post-implantation. Also analyzed were corresponding patterns of change in their speech-perception scores for the HINT measured in quiet (HINT-Q) and noise (HINT-N) and for CNC monosyllabic words measured in quiet at 1, 3, 6 and 12 months post-implantation. Response patterns were grouped and analyzed in terms of cochlear-segment activation by apical (1-4), medial (5-8), and basal (9-12) electrode pairs and by the full array. Longitudinal trends of interest, based upon percent change in stimulation level between the 1-month post-activation and the 12-month tests, include:

(1) Improved 12-month T sensitivity (lower threshold responses) for the apical (9%), medial (14%), and basal (25%) segments, and for the full array (16%);

(2) Increased 12-month MCL values for the apical (30%), medial (30%), and basal (9%) segments, and for the full array (23%);

(3) Expanded 12-month DR values for the apical (40%), medial (42%), and basal (23%) segments, and for the full array (35%);

Improvements in speech-perception scores (HINT-Q: 71%; Hint-N: 113%; CNC: 79%) between the 1- and 12-month tests mirror systematic expansion of the DR over this period. Thus, DR expansion, resulting from the combined effects of reduced T and increased MCL values, parallels improvements in speech-perception abilities with the Med-EI implant over the 12-month evaluation period.

### **238** Attention to Infant-Directed Speech versus Adult-Directed Speech in Infants with Cochlear Implants: A Preliminary Report

**Tonya Bergeson**<sup>1</sup>, Kristen Spisak<sup>1</sup>

<sup>1</sup>Indiana University School of Medicine

Recent research has shown that hearing-impaired infants with cochlear implants (CIs) do not prefer speech sounds over silence, as measured by looking time at a checkerboard pattern (Houston, Pisoni, Kirk, Ying, & Miyamoto, 2003). The same infants are capable of discriminating these novel speech sounds even though they do not prefer them to silence. Are infants with CIs simply uninterested in speech sounds? It is well known that normal-hearing (NH) infants prefer the highly exaggerated characteristics of infant-directed (ID) speech to adult-directed (AD) speech. It might also be the case that implanted infants would attend more to speech over silence if the speech were presented in an ID manner. The present study investigated the effects of auditory deprivation and cochlear implantation on infants' attention to ID speech, AD speech, and silence. We tested NH 6- and 12-month-old infants (N = 14) and hearing-impaired infants with CIs (N = 3). Using an infant-controlled visual preference procedure, attention was measured by infants' looking time to a checkerboard pattern during auditory presentation of ID speech, AD speech, and silence. As expected, the results revealed that NH infants preferred to look at ID speech more than AD speech and silence. Surprisingly, all three hearing-impaired infants with CIs preferred silence to both ID speech and AD speech. These important new findings serve to broaden understanding of implanted infants' abilities to perceive and understand speech. [Supported by NIH/NIDCD Training Grant T32DC00012.]

### **239** Discrimination of Audio-Visually Presented Nonsense Words by Normal Hearing Infants and Hearing-Impaired Infants Who Use Cochlear Implants

**David Horn**<sup>1</sup>, Derek Houston<sup>1</sup>, Richard Miyamoto<sup>1</sup>

<sup>1</sup>Indiana University School of Medicine

A visual habituation procedure was used to investigate the ability of normal hearing (NH) infants and hearing-impaired (HI) infants with cochlear implants (CIs) to discriminate audio-visually presented nonsense words. During the habituation phase, infants were presented with an audiovisual display of a woman articulating one of two bi-syllabic nonsense words (see-pug, boo-dup) in the center of a large flat-screen TV monitor. Attention was measured by on-line recording of the infant's looking time during each trial. When looking time decreased to a pre-set habituation criterion, infants were presented with 14 test trials. Half of the test trials were videos of the same woman repeating the habituated nonsense word ("old" trials), while the other half were videos of the woman repeating both the old nonsense word and a novel nonsense word in alternating order ("novel" trials). Looking times during the novel trials were compared with looking times during the old trials. If infants could

discriminate between the old and novel nonsense words, they would look longer during novel trials than during old trials (visual recovery). We tested a group of HI infants ranging in ages from 18 months to 34 months who had used their CIs for an average of 12 months (6-22 months). We also tested a group of NH 9-month-old infants for comparison.

The results showed that the NH infants on average looked significantly longer during the novel trials than the old trials. Similarly, the HI infants on average looked significantly longer during the novel than during the old trials. When old and novel trials were compared for individual infants, we found that several NH infants showed significant visual recovery to the novel trials. So far, none of the individual HI infants have shown a statistically reliable visual recovery, although most trended in the hypothesized direction. These results suggest that HI infants with CIs are able to discriminate bi-syllabic nonsense words presented audio-visually. Further testing will be conducted to determine if this methodology is sensitive enough to detect significant discrimination in individual HI infants.

## **240** Communication Outcomes as a Function of Age at Cochlear Implantation in Congenitally Deaf Infants and Children: Is Younger Always Better?

Rachael Holt<sup>1</sup>, Mario Svirsky<sup>1,2</sup>

<sup>1</sup>Indiana University School of Medicine, <sup>2</sup>Purdue University

Accumulating evidence suggests that better outcomes are achieved by congenitally deaf children who receive cochlear implants (CIs) earlier rather than later in life. Fryauf-Bertschy et al. (1997) reported that children who receive CIs between 2 and 5 years of age tend to have better speech perception than children who receive one after 5 years of age. In examining speech and language development of children implanted in the second, third, or fourth year of life, Svirsky et al. (2004) found that children implanted before age 2 had significant advantages over children implanted later. Although these data support an "earlier is better" approach, they also beg the question of how early it is appropriate to perform cochlear implantation. Recently, infants as young as 6 months of age have received CIs in the United States. At least two concerns are raised when considering cochlear implantation in infants: anesthetic risk and the level of confidence in audiologic test results. As with any surgery requiring anesthesia, cochlear implantation in the first years of life carries potentially greater risks than in older populations. Also, although we have reliable objective measures of auditory function that can be used with infants, each has limitations that influence confidence in the results. These reasons make it especially important to evaluate potential benefits of cochlear implantation in infants. We compared speech perception and language development in children who received CIs in the first (n = 8), second (n = 38), third (n = 44), or fourth (n = 29) year of life. Participants were tested at approximately regular 6-month intervals for up to 4 years after implantation. Although, in general, results supported the "earlier is

better" hypothesis, infants implanted in the first year of life did not show an advantage over children implanted in the second year of life, at least though 2 to 2½ years of age.

## **241** The Effect of Cochlea Implant on Cognitive Functions in Deaf Children

Min-Sup Shin<sup>1</sup>, Soo-Kyoung Kim<sup>2</sup>, Seung-Ha Oh<sup>1</sup>

<sup>1</sup>Seoul National University College of Medicine, <sup>2</sup>Seoul National University Hospital

Objectives:

This study was conducted to examine improvements of cognitive and learning abilities after cochlear implant in deaf children. We also examined the relationships among cognitive improvements after cochlear implant, early educational experiences of deaf children and their mothers' depression.

Methods:

Subjects

Seventeen deaf children (mean age: 7 years 2 months) participated in this study. They were administered a neuropsychological test battery and reassessed by the same tests at 6 months follow up.

Instruments

- Leiter International Performance Scale-Revised
- Pictorial Test of Intelligence
- Attention Test
- Rey-Ostereith Complex Figure Test
- Grooved Pegboard Test

Results:

Deaf children showed age appropriate performances on simple visual-motor integration test before the cochlear implant. However, they showed poor performance on Rey-Ostereith Complex Figure Test and Grooved Pegboard Test, suggesting that even though deaf children have no problem in doing simple visual-motor task, they have difficulties performing tasks requiring more complex and delicate motor coordination and visual organization. At 6 months follow up after cochlear implant, they showed marked improvement on those tests up to normal range. Before the cochlear implant, deaf children's performances on vocabulary and information, and mathematics tests were at mild to moderate mental retardation levels. However, their performances on non-verbal tests were at average levels. At 6 months follow up, their cognitive functions such as verbal comprehension, concentration, and sequential processing were found to be much improved. Mothers' depression was negatively correlated with scores on information and mathematic subtests of Pictorial Intelligence Tests.

## **242 Audio-visual Integration in Speech Recognition by Children with Cochlear Implants**

**Frederic Wightman**<sup>1,2</sup>, Doris Kistler<sup>1,2</sup>, Kathryn Shaughnessy<sup>1</sup>, Douglas Brungart<sup>3</sup>

<sup>1</sup>University of Louisville, <sup>2</sup>Heuser Hearing Institute, <sup>3</sup>Wright-Patterson Air Force Base

When normally-hearing adults are shown the face of a talker who is speaking in a noisy environment, their speech reception thresholds improve as much as 15 dB over conditions in which the face is not visible. To assess the developmental aspects of audio-visual integration, adults and children were asked to respond to messages spoken by a target talker while ignoring messages that were spoken by a second distracting talker. Identification performance was measured at several target/distracter ratios (T/D) to estimate the threshold level for 80% correct responses (chance was 3%.) Two conditions were tested, an audio-only condition in which only the target talker's voice was presented and an audio-visual condition in which a synchronized video of the target talker's face was also presented. As expected, adult listeners obtained advantages as large as 15 dB from the visible face. Young normally-hearing children required a 10-15 dB higher T/D for threshold performance than normally-hearing adults but demonstrated no advantage from the visible face. This is consistent with previous studies of A/V integration in children. Children who had received a cochlear implant before age 2 produced T/D thresholds nearly the same as children with normal hearing and also showed no A/V integration.

## **243 NIDCD Workshop: Part I-What's New at the NIH; Part II-New Investigators**

**Jim Battey**<sup>1</sup>, **Amy Donahue**<sup>1</sup>, **Craig Jordan**<sup>1</sup>, and **NIDCD Staff**<sup>1</sup>

<sup>1</sup>NIDCD/NIH

This year's NIDCD workshop will have two mini-sessions. The first 30 minutes will provide an overview of "What's New at the NIH". Jim Battey, Craig Jordan and Amy Donahue will present updates on the NIH Roadmap, the NIH Neuroscience Blueprint, new and ongoing NIDCD and NIH initiatives and funding opportunities, as well as NIH policy and grants management changes that impact researchers.

The following hour will be the "NIDCD Workshop for New Investigators". This portion of the Workshop focuses exclusively on individuals at the training stages and on new investigators. The aim is to demystify the granting process and provide information on research and training funding mechanisms for the trainee/new investigator, leading to the status of independent investigator (R01). Following a brief overview, new investigators will choose one of three breakout sessions:

1. NIH 101: How does the NIH system work?
2. Training and Career Development (Fs and Ks): What do I need to know?
3. Transitioning to Independence: Should I apply for an R03 or an R01?

NIH 101 will provide practical information on how the NIH/NIDCD works (e.g., institute and study section assignments, application timelines, reviewer assignments, funding paylines, council activities, and the role of program and review staff).

Training and Career Development will include a profile of research training and career development mechanisms appropriate for new investigators, including mechanisms for predoctoral and postdoctoral fellows (F30, F31 and 32) and for clinically trained investigators (K08 and K23).

Transitioning to Independence will provide guidance on the appropriate grant mechanisms for early career stages, and will focus on the NIDCD Small Grant Award (R03). This session will also include a discussion of how to avoid mistakes commonly observed in the review process.

The breakout sessions are intended to allow ample time for questions and answers. Handouts from all three breakout sessions will be available.

## **244 Overview of CMV**

**Bracie Watson**<sup>1</sup>

<sup>1</sup>NIDCD/NIH

Congenital CMV infection is the most common congenital infection. The

incidence of CMV is estimated to range between 0.2% and 2.2%. In the U. S., the newborn incidence is estimated to range from 0.5% to 1.0% which would translate to approximately 40,000 new cases per year. While 10-15 percent of infants with congenital CMV are identified at birth, most cases are subclinical or asymptomatic and go undetected (85-90%). The public health impact of congenital CMV is mainly attributable to its effect on the central nervous system, including the auditory system. Our panelists will discuss the genetic, epidemiologic, and clinical impact of this disease as it relates to hearing.

## **245 Parent Concerns in CMV**

**Gayla Hutsell**<sup>1</sup>

<sup>1</sup>The Alexander Graham Bell Association from the Deaf and Hard of Hearing

The diagnosis of CMV is of immediate concern to the parent of a newborn infant. This much unknown and misunderstood infection leaves many questions and concerns that must be adequately addressed by professionals, including physicians, audiologists and counselors. The impact of CMV to the family is substantial, with one primary concern being the possibility of "spreading the infection" to other family members and friends. While infectious disease specialists can provide facts about

congenital CMV, support related to the emotional and social impact of CMV needs considerable attention. Encouragement and direction is particularly needed for treatment options and appropriate clinical and educational interventions.

## **246** Epidemiology of CMV Infection

**Karen Fowler<sup>1</sup>**

<sup>1</sup>*University of Alabama, Epidemiological Aspects of CMV*

The association between congenital cytomegalovirus (CMV) infection and sensorineural hearing loss (SNHL) was first described in 1964. However, despite these early reports of CMV and SNHL most congenital CMV infections today go unnoticed since ~90% of infected newborns have no clinically apparent disease at birth. The fact that congenital CMV infection can only be confirmed in the newborn period has made it difficult to estimate the proportion of SNHL that is attributable to congenital CMV infection in childhood populations. Approximately 30-50% children with clinically apparent disease (symptomatic) and 8-12% of children without clinically apparent (asymptomatic) congenital CMV infection will develop SNHL. Hearing loss due to congenital CMV infection varies in severity and the loss may be progressive or fluctuating. Complicating the diagnosis of SNHL in children due to congenital CMV infection is the fact that less than half of the hearing loss due to CMV infection is present at birth. Other CMV infected children may go on to develop delayed onset loss during the preschool and early school years. Although, most children with congenital CMV infection do not develop hearing loss, it remains unclear which children with congenital CMV infection will develop hearing loss and, among those who do develop loss, whether or not the loss will continue to deteriorate.

## **247** Medical Aspects of Congenital CMV Infection

**Margaret Kenna<sup>1</sup>**

<sup>1</sup>*Harvard University, Children's Memorial Hospital*

CMV is the most common cause of intrauterine infection, and the fetus may become infected during pregnancy. Primary infection with CMV is much more likely to be transmitted to the fetus, and 15% of infants with primary infection will have clinical symptoms of disease ranging from mild to severe. In contrast, intrauterine transmission of reactivated CMV infection occurs less commonly, and only rarely results in symptomatic disease after birth.

Congenital cytomegalovirus (CMV) occurs in approximately 1/100 newborns. Ten percent of this number (1/1000) will present with symptomatic disease in the neonatal period, including prematurity, intrauterine growth retardation, jaundice, microcephaly, petechiae, thrombocytopenia, hepatosplenomegaly, other signs of hepatitis, and sensorineural hearing loss (SNHL). Symptoms developing after the neonatal period include microcephaly, seizures, developmental delay and cognitive impairments, and up to 60% will also develop SNHL. Another 10-15% of initially asymptomatic infants will develop hearing loss or other cognitive impairments without the other signs and symptoms.

Recent studies at the University of Alabama have shown encouraging results with the use of ganciclovir to stabilize or prevent the hearing loss in infants with congenital CMV detected in the newborn period. However, since the results of the University of Alabama studies have only recently

become available, and ganciclovir administration is not without concern, routine neonatal screening for congenital CMV is not performed. Since the SNHL secondary to congenital CMV is not always present at birth, using the UNHS programs to guide a search for CMV will miss up to half the potentially treatable hearing losses. It may therefore be time to consider the development and implementation of neonatal screening for congenital CMV infection.

## **248** Audiological Aspects of Congenital CMV

**Diane Sabo<sup>1</sup>**

<sup>1</sup>*University of Pittsburgh*

Cytomegalovirus is a major cause of non-hereditary sensorineural hearing loss in children. The majority of infants affected are asymptomatic with only about 10% of infants with congenial CMV showing symptoms. Hearing loss can be present in both children who are symptomatic as well as those who are asymptomatic, although the prevalence of hearing loss is higher in children who are symptomatic. The hearing losses in both those who are symptomatic and asymptomatic can be of delayed onset and/or progressive. This presentation will review the audiologic findings of children with symptomatic and asymptomatic congenital CMV.

The hearing loss in congenital CMV may be present at birth or occur after the neonatal period and is the most common cause of acquired non-genetic SNHL. Delayed onset occurs in about 18%, with a mean age of onset of 27 months. The hearing loss is progressive in 50%, fluctuates 22-35% of the time, and is often asymmetric. At birth, the hearing loss may be profound and bilateral or the hearing may be normal. Because of the delayed onset of the SNHL in many of these infants, one third to one half of the eventual hearing losses will be missed by universal newborn hearing screening (UNHS) programs.

## **249** Animal Models of Inner Ear CMV Infection

**Elizabeth Keithley<sup>1</sup>**

<sup>1</sup>*University of California, San Diego*

Abstract Unavailable

## **250** Patterns of Excitation in the Inferior Colliculus Produced by Intracochlear Electrical Stimulation in Cats and Guinea Pigs: Models of Cochlear Implant Stimulation.

**Russell Snyder<sup>1</sup>**, Boh Bonham<sup>1</sup>, Steve Rebscher<sup>1</sup>, Patricia Leake<sup>1</sup>

<sup>1</sup>*University of California*

Contemporary human cochlear implants (CIs) use intracochlear electrodes with several electrical contacts to activate the auditory nerve array. The contacts of these devices are distributed along the cochlear spiral, and activation of each pair of contacts (consisting of an active and one or more return contacts) is thought to excite a restricted, unique and tonotopically appropriate population

of auditory nerve fibers. Psychophysical and clinical studies indicate that these devices allow open-set speech reception in many users. Our studies seek to understand mechanisms that underlie this performance by focusing on the many factors that influence the spatial (spectral) and temporal distribution of neural activity evoked across the tonotopic organization of the central nucleus of the inferior colliculus. Among these factors are: the orientation and separation of the active and return contacts in a pair, the mode of stimulation (monopolar, bipolar and tripolar), the rate and amplitude of the electrical pulses, the recent activation history of the neuronal populations (forward masking), and the number of populations activated at any one time (simultaneous masking with two-channel stimulation). We will review the results of our multichannel intracochlear electrical stimulation experiments in deaf animal models. These models are designed to accurately reflect CI stimulation in humans. We will compare the patterns of activation produced by electrical stimulation with those evoked by acoustic stimuli in these animal models.

NIDCD NO1-DC-02-1006, NO-1-DC-03-1006

### **251 Binaural Interactions in the Auditory Midbrain with Bilateral Cochlear Implants**

**Zachary M. Smith**<sup>1,2</sup>, Bertrand Delgutte<sup>1,3</sup>

<sup>1</sup>*Eaton-Peabody Laboratory, Massachusetts Eye & Ear Infirmary, Boston, MA,* <sup>2</sup>*Harvard-MIT Division of Health Sciences and Technology, Cambridge, MA,* <sup>3</sup>*Research Laboratory of Electronics, Massachusetts Institute of Technology, Cambridge, MA*

The neural processing of binaural cues in normal-hearing listeners is essential for accurate sound localization and speech reception in noise. Bilateral implantation seeks to restore the advantages of binaural hearing to cochlear implant users. While psychophysical tests show good sensitivity to interaural level differences with bilateral implants, sensitivity to interaural timing differences (ITD) is generally poor. To better understand the neural processing of ITD with electric stimulation, we recorded from single-units in the inferior colliculus (IC) of acutely deafened, anesthetized cats implanted bilaterally with intracochlear electrode arrays. Stimuli were electric pulse trains with and without sinusoidal amplitude modulation (SAM).

The discharge rates of the majority of cells in the central nucleus of the IC were sensitive to ITD for low-rate (40 pulses per sec - pps) pulse trains. Best ITDs and tuning widths were similar to those seen for acoustic stimulation with clicks. For many neurons, however, well defined ITD sensitivity existed only over a small range (2-3 dB) of stimulus levels near threshold. As pulse rate was increased, responses became largely limited to the onset and ITD tuning degraded. When high-rate (1000 pps) pulse trains were amplitude modulated (40 Hz), sustained responses were again observed and good ITD sensitivity sometimes reappeared. When ITD was independently controlled in the modulation and carrier of SAM stimuli, about twice as many cells showed sensitivity to ITD in the modulation than in the carrier. However, modulation ITD functions were broad with little or no change in discharge

rate within the physiological range of ITD, at least for this low modulation frequency.

These results suggest that precise control of the interaural timing of carrier pulses and/or temporal sharpening of modulation waveforms may be important for effectively delivering ITD cues with bilateral cochlear stimulation using a continuous interleaved sampling (CIS) strategy.

*Supported by NIH grants DC05775 and DC05209.*

### **252 Auditory Cortex Activity in Congenitally Deaf Cats Evoked by Electrical Cochlear Stimulation**

**Rainer Hartmann**<sup>1</sup>, Jochen Tillein<sup>1</sup>, Silvia Heid<sup>1</sup>, Rainer Klinke<sup>1</sup>, Andrej Kral<sup>2</sup>

<sup>1</sup>*J.W. Goethe-Universität, Physiologie II, Theodor Stern Kai 7, 60590 Frankfurt, Germany,* <sup>2</sup>*Universitätsklinikum Hamburg-Eppendorf, Martinistr. 52, 20246 Hamburg, Germany*

The plasticity of the central auditory system of congenitally deaf cats (CDC) was investigated by chronic electrical stimulation with a cat cochlear implant (CI).

Young CDCs were implanted with an electrode array and stimulated using a 1-channel analogue signal processor 24 hrs/d, 7 days/w. To register the development of synchronized cortical activity in these cats by the use of the CI, 4 electrodes (spacing 2 x 2 mm) were chronically implanted epidurally above the auditory cortex A1. With a telemetric setup evoked potentials (EPs) in awake animals were recorded during noise- and tone-burst stimulation. Frequency difference limen, determined with the Mis-Match-Negativity method, was 1/2 octave (500 Hz range).

In acute experiments, the responses of the ipsi- and contralateral primary auditory cortices (A1) and the surrounding auditory fields to pulsatile electrical cochlear stimulation were examined in acutely deafened normal cats (controls) and CDCs under anaesthesia.

The synaptic activity of layers I – VI in cortical columns was investigated by recording field potentials (middle and long latency potentials MLP, LLP) and cell activity by multi- and single-unit activity in penetration tracks every 300 µm with pairs of micro-electrodes. The synaptic currents of distinct cortical layers were evaluated with the current source density (CSD) method. The synchronization of MLP and LLP activity was calculated by correlation of the amplitudes and latencies, that of spike activity was determined by cross-correlograms.

Chronic electrical stimulation in CDCs through the CI induced enlargement of evoked MLP activity at the surface as well as in deeper cortical layers. The shape of the MLP changed in the first 6 months and came closer to normal controls. The CSDs showed stronger synaptic sinks/sources especially in the infragranular layers. The correlation of amplitudes and latencies of MLPs was layer specific and significant for electrode distances < 1mm.

*Supported by DFG SFB 269*

## **253** Transmission of Temporal Information from a Cochlear Implant to the Auditory Cortex

### **Cortex**

**John Middlebrooks<sup>1</sup>**

<sup>1</sup>*University of Michigan*

The majority of cochlear-implant speech processors signal temporal features of sounds by extracting the amplitude envelopes of sounds and using those envelopes to modulate electrical pulse trains that are presented to intracochlear electrodes. Presumably, if temporal information is to contribute to recognition of speech and other sounds, the modulation waveforms must be represented in some form in the auditory cortex. We are evaluating the ability of auditory cortical neurons in anesthetized guinea pigs to synchronize to sinusoidally amplitude-modulated electrical pulse trains and to detect temporal gaps in ongoing pulse trains. We tested modulation frequencies and depths comparable to those provided by speech processors. A signal detection procedure indicated the threshold for modulation detection based on cortical phase locking. Modulation sensitivity was greater for monopolar cochlear stimulation than for a narrow bipolar configuration and was greater for 254-pulse-per-second (pps) carrier rates than for 4069-pps rates. Modulation sensitivity varied among cortical layers. Supragranular and granular cortical layers showed threshold modulation depths of 10-30% for 30-to-60-Hz modulation, whereas with few exceptions, phase locking was largely absent in infragranular layers was at those frequencies. At lower modulation frequencies, e.g., 20 Hz, modulation thresholds averaged ~10% throughout most cortical layers. Maximum cut-off frequencies for modulation detection generally were much lower than 100 Hz, suggesting that the temporal resolution of the auditory cortex is on the order of ~10 ms. Contrary to that suggestion, thresholds for gap detection in the cortex could be as low as 2 ms. Overall, the temporal sensitivity of cortical neurons corresponds well to perceptual capabilities of human cochlear-implant users.

Supported by NIH grants RO1 DC04312 and P30 DC05188. Recording probes furnished by U-M CNCT (supported by P41-RR09754).

## **254** PET and fMRI Studies of Speech Perception and Their Application to Cochlear Implantation.

**Sophie Scott<sup>1</sup>**

<sup>1</sup>*University College London*

Functional imaging techniques have permitted us to establish the relationship between human auditory anatomy and function. This has also allowed us to draw parallels with the wealth of data now emerging about primate and mammalian auditory cortical anatomy and function. We have been using PET and fMRI to establish the neural basis of human speech perception: this has revealed a left lateralised system, in which distinct fields associated with the processing of intelligible speech, sensory-motor integration in speech perception, and short term transient representations of the speech signal can be distinguished. In contrast, right temporal lobe regions are

more selectively interested in regions with pitch variation, in speech or music. Of particular interest for applications to clinical groups are connections between early acoustic areas and prefrontal and premotor cortex. Our studies suggest these regions are recruited to aid perceptual processing when speech is degraded or novel, or presented in noise. We are currently extending our PET studies to study individuals who have been fitted with cochlear implants, and in my presentation I will illustrate how the location and extent of activation to speech stimuli differs from a hearing control group.

## **255** Pharmacologic Activation of Dormant Cortex in the Restoration of Speech and Language Following Cochlear Implantation

**Michael Devous<sup>1,2</sup>**, Emily Tobey<sup>1,2</sup>, Peter Roland<sup>1</sup>, Wendy Ringe<sup>1</sup>, Kristi Buckley<sup>2</sup>, Thomas Harris<sup>1</sup>, Gary Overson<sup>2</sup>

<sup>1</sup>*UT Southwestern Medical Center*, <sup>2</sup>*University of Texas at Dallas*

A major consequences of long-term deafness is a change in the neural architecture of the central nervous system (CNS). Cochlear implantation has been observed to enhance or preserve CNS structure and function under such situations. However, a great deal of variation exists in the post-implantation performance of adults with cochlear implantation. Previous work by our laboratory indicates that regional cerebral blood flow (rCBF) responses in primary and association auditory cortices measured by Single Photon Emission Computed Tomography (SPECT) are blunted in cochlear implant users relative to normal hearing control subjects, and the severity of blunting is greatest in cochlear implant patients with poor speech perception. This study used SPECT imaging to determine if pharmacologic stimulation paired with auditory habilitation enhances speech perception performance of individuals with cochlear implants. Such an intervention has proven successful in restoring speech in post-stroke aphasics and in restoring motor function in stroke victims. All subjects have pre-treatment rCBF SPECT imaging during a control (no auditory stimulation) and auditory speech stimulation while watching and listening to a video-taped story. Subjects received 10 mg d-amphetamine or placebo 60 min prior to a one hour intensive aural habilitation therapy session occurring twice a week for two months. Treatment consists of a multi-step rehabilitation program developing listening skills for speech. At the conclusion of the therapy sessions, rCBF imaging (control and monaural speech stimulation) is repeated along with the audiologic speech perception assessments. Comparison of pre- to post-treatment rCBF images (voxel-wise analyses employing SPM) demonstrated significant increases in activation of primary and association auditory cortices in both good and poor cochlear implant users. Further, comparison of pre- to post-treatment speech perception measures (e.g., auditory word comprehension) have demonstrated 40% increases in speech perception. These finding demonstrate substantial efficacy for pharmacologically assisted therapy.

## **256 Regulation of Connexin-Mediated Cell-Cell Signaling: Development of Peptidomimetic Inhibitors.**

**W. Howard Evans<sup>1</sup>**

<sup>1</sup>*Dept. Med. Biochemistry and Wales Heart Research Institute, Cardiff University Medical School*

Cells are invariably in partnership with others and communicate directly and extensively. Connexins (Cx) are nonglycosylated proteins in vertebrates that function as oligomeric membrane channels facilitating cell-cell signaling. In gap junctions, docked Cx hexameric channels organised as linear arrays at cell contact points allow direct intercellular signaling exemplified by propagation of calcium waves and unidentified small ions and molecules across groups of cells. Calcium wave spread also occurs in a paracrine mode by release of ATP across nonjunctional plasma membrane Cx hemichannels. Specific pharmacological inhibition of Cx mediated signaling can be a powerful tool for its analysis. Short peptides corresponding in sequence to selected extracellular loop domains are 'clean' reversible reagents allowing manipulation of signaling in cells expressing various Cxs owing to the conserved sequences on the two exposed loop domains of these proteins. Patch clamp studies show that binding of Cx peptidomimetics blocks electrical conductance of Cx hemichannels. In metabolic stress, Cx peptidomimetics block the release of ATP and calcium signaling by cells occurring via the hemichannels. The mechanism of action on cell signaling via Cx channels by this new class of inhibitors is now being elucidated.

## **257 Connexin Disorders of the Skin – Clinic, Genetics, and Pathogenesis**

**Gabriele Richard<sup>1</sup>**

<sup>1</sup>*Jefferson Institute of Molecular Medicine*

The list of human connexin disorders is growing and includes numerous diverse phenotypes affecting the skin and its appendages. Dominant mutations in the connexin gene GJB2 (Cx26) manifest with an array of different allelic disorders, including sensorineural hearing loss (SNHL) alone or in association with palmoplantar keratoderma, erythrokeratoderma, adnexal or mucosal involvement. The most severe disorder is Keratitis-Ichthyosis-Deafness (KID) syndrome, which also predisposes to mucocutaneous infections and squamous cell carcinoma. Our molecular studies of more than 15 patients revealed that nearly 80% of KID patients carry the de novo mutation D50N, located in the first extracellular loop of Cx26, which might interfere with both connexon assembly and channel function. However, we recently discovered that KID syndrome is genetically heterogeneous and may be caused by missense mutations in GJB6 encoding the closely related Cx30, whose mutations may also manifest with SNHL, hidrotic ectodermal dysplasia or nail dystrophy. The epidermal disorder erythrokeratoderma variabilis is also genetically heterogeneous and due to defects in two co-expressed connexin genes, GJB3 (Cx31) and GJB4 (Cx30.3). Nature and location of pathogenic mutations in both connexin genes are strikingly similar, including the amino terminus

and membrane spanning domains, thus emphasizing their structural/functional importance. Recent in vitro studies demonstrated that the majority of mutant connexin isoforms with a cutaneous phenotype fails to form visible gap junction plaques at plasma membranes and induces cell death. Furthermore, co-expression with different wildtype connexins revealed a dominant negative effect, suggesting direct molecular interactions between numerous connexin isoforms, which are critical for normal development, differentiation and function of stratifying epithelia of ectodermal origin. Tissue-specific, spatial or temporal interferences of mutant connexins with other partner connexins might help to explain the broad phenotypic spectrum of epidermal connexin disorders.

## **258 Gap Junction Distribution and Connexin Expression in the Inner Ear**

**Andrew Forge<sup>1</sup>, Daniel Jagger<sup>1</sup>, Regina Nickel<sup>1</sup>**

<sup>1</sup>*UCL Centre for Auditory Research, University College London*

Gap junctions are present between supporting cells of inner ear sensory epithelia in all vertebrate classes. Some of them contain over 100,000 channels. Dye transfer reveals extensive 2-dimensional intercellular communication between supporting cells, which in the organ of Corti resolves into two coupled compartments separated by the pillar cells. In the mammalian cochlear lateral wall, gap junctions are associated with strial intermediate and basal cells, where they may occupy up to 30% of the plasma membrane area, and with fibrocytes in the spiral ligament. The onset and rise in EP during cochlear development coincides temporally with the formation and increase in number of basal cell gap junctions. Connexin (cx)26 and cx30 co-localise in the supporting cells of the organ of Corti and in the cochlear lateral wall. Studies of transfected HeLa cells show cx26 and cx30 can form heteromeric channels. Immunogold labelling and immunoprecipitation suggest heteromeric cx26/cx30 channels are present in cochlear tissues, and selective dye transfer indicates gap junctions in the organ of Corti are not cx26 homomeric. Heteromeric cx26/cx30 channels have not been reported in any other mammalian tissue. In chickens, a particular connexin –chicken-(c-)cx31- is expressed uniquely in the inner ear. Its molecular structure is "chimeric-like" for mammalian cx26 and cx30 and its distribution mirrors that of cx26/cx30 in the mammalian inner ear. The restricted expression of c-cx31 may indicate it has particular properties necessary for support of inner ear function. If this were true for heteromeric cx26/cx30 channels in mammals, it could be one factor underlying the non-syndromic effects of some deafness-causing cx26 mutations. Chick basilar papillae (bp) also contain cx43 which is absent from chick utricles. Cx43 maybe associated with asymmetric dye transfer, preferentially in the neural direction, observed in bp. It may also have a role in maintaining mitotic quiescence in the bp.



## **259** Characterization of Connexins Expressed in the Inner Ear and Other Organs, using Targeted Mouse Mutants.

Klaus Willecke<sup>1</sup>

<sup>1</sup>University of Bonn

Characterization of connexins expressed in the inner ear and other organs, using targeted mouse mutants.

Willecke, K., Ott, T., Zheng-Fischhöfer, Q., Schnichels, M., Eiberger, J., and Söhl, G.

Institut für Genetik, Abt. Molekulargenetik, Universität Bonn, Römerstr. 164, 53117 Bonn, Germany

According to a recent survey, there are 20 connexin genes present in the mouse genome and 21 in the human genome (cf. Söhl and Willecke, 2003, *Cell Communication and Adhesion* 10: 173-180). Connexins (Cx) are expressed cell type specifically but most of them show overlapping expression in several cell types. Cx26 and Cx30 are expressed in cochlear supporting cells, fibrocytes, in the stria vascularis, and in other tissues. Previously we have shown together with external coworkers that transgenic mouse mutants with defects in Cx26 or Cx30 coding DNA exhibit hearing defects as do patients with mutations in these genes. Here we report on the morphological reorganization of the stria vascularis in Cx30 deficient mice (collaboration with D. Koch, M. Kibschull, J. Lautermann, K. Jahnke and E. Winterhager, University of Duisburg-Essen, Germany). These transgenic mouse mutants are valuable models to clarify the mechanism of this hearing loss in mouse and man.

Recently we have characterized several new transgenic mouse mutants with defects in connexin genes that are expressed in the inner ear and other organs of mouse and man. In these mutants we had replaced the coding region of the connexin by a reporter gene that allows to identify the cell type by a cell autonomous assay. In contrast, the identification of connexin expressing cell types with connexin antibodies can usually not discriminate between two contacting cells, since gap junction channels are located in the plasma membrane of contacting cells. Connexins appear to fulfill unique functions in certain cell types but can replace each other functionally in other cell types. This is probably the main reason for the large diversity of connexin genes in the mouse and human genome.

## **260** Characterization of Mutant Connexins Linked to Human Disease: Molecules to Mice

Dale Laird<sup>1</sup>, Tamsin Thomas<sup>1</sup>, Xiangun Gong<sup>1</sup>, Greg Veitch<sup>1</sup>, Elizabeth McLachlan<sup>1</sup>, Donglin Bai<sup>1</sup>, Gerald Kidder<sup>1</sup>, Joanne Gittens<sup>1</sup>, Dan Tong<sup>1</sup>, Qing Shao<sup>1</sup>

<sup>1</sup>University of Western Ontario

Connexin mutations are linked to human diseases that include inherited non-syndromic deafness, various skin diseases and oculodentodigital dysplasia (ODDD). ODDD is an autosomal-dominant human disorder where patients display symptoms of congenital craniofacial and limb deformities suggestive of defective osteoblast function. The consequences of connexin mutations on transport, assembly, stability and function can potentially result in

either gain- or loss-of-function changes in channel activity. In our studies we have expressed diseased-linked Cx43 and Cx26 mutants and examined their transport, assembly and function in mammalian cells that include organotypic keratinocyte cultures. While the Cx43 G21R, G138R, and G60S mutants readily traffic to the cell surface, these mutants showed complete loss of function, not unlike the Cx26 G59A mutant. However, the loss-of-function Cx26 D66H mutant was not stabilized at the cell surface but was localized to the trans Golgi network. Importantly, when any of these mutants were co-expressed with their wild-type connexin counterpart, they dominantly inhibited gap junction function and trans-dominantly inhibited the function of other connexin family members. We propose that only some Cx26 mutants interact with other connexins co-expressed in keratinocytes, resulting in reduced overall gap junctional intercellular communication and skin disease. As an animal model of connexin-linked disease, we have obtained a Cx43G60S mutant mouse line from Dr. Janet Rossant (University of Toronto) that has classical ODDD abnormalities. Interestingly, granulosa cells obtained from these mice, where both mutant and wild-type Cx43 are thought to be equally expressed, have only residual gap junction coupling, further suggesting that mutant Cx43 has a dominant effect on wild-type Cx43. These mutant mice will serve as models for understanding the pathophysiology of ODDD mutations. Supported by the CIHR to DWL, DB and GMK.

## **261** Approaching the Functions of Connexins in the Inner Ear

Martine Cohen-Salmon<sup>1</sup>, Christine Petit<sup>2</sup>, Klaus Willecke<sup>3</sup>, Francisco Del Castillo<sup>1</sup>

<sup>1</sup>Institut Pasteur, <sup>2</sup>Institut Pasteur & College de France, <sup>3</sup>Bonn University

Intercellular communication through gap junctions is crucial for the proper functioning of the inner ear. Mutations in three gap junctions genes CX26, CX30, and CX31 are responsible for deafness. In particular, mutations in CX26 account for as many as 50% of all cases of prelingual hearing impairment, making the molecular analysis of CX26 a standard of care for diagnosis and counseling of patients. In the cochlea, gap junctions assemble in two distinct cellular networks, i.e. the epithelial network connecting all supporting cells of the sensory epithelium, and the connective tissue network, which is composed of fibrocytes, and also includes basal, and intermediate cells of the stria vascularis. Aside from Cx26 and Cx30, which are the major connexins in the cochlea, many other connexin genes are expressed in the inner ear, the precise expression pattern of which needs to be determined. We have recently demonstrated that Cx43 is expressed in the bone of the otic capsule, while Cx45 is present only in the inner ear vascular system. In order to get insight into the role of gap junctions in the inner ear physiology, we developed two complementary approaches: (1) The search for molecular partners of connexins in the inner ear, by means of the yeast two-hybrid technique. (2) Gene inactivation in mice, either ubiquitous or targeted to various inner ear cell types. We have shown that both the ubiquitous absence of Cx30 and

the absence of Cx26 in the epithelial gap junction network, lead to degeneration of the organ of Corti soon after hearing onset. Cx26- and Cx30- containing gap junctions would therefore be crucial for cell survival in the organ of Corti. They could provide a route to transport K<sup>+</sup> secreted by sensory hair cells after their depolarization, away from the sensory epithelium. We have also established that the endocochlear potential needs Cx30 to develop, and that Cx26 participates to the EP maintenance. With various animal models in hands, we attempt to address the molecular mechanisms underlying the observed physiological defects and try to determine the role of each connexin in the different inner ear cell types.

## **262 Permeability and Gating Mechanisms of Gap Junctions, and Their Implications for Disease.**

**Bruce Nicholson<sup>1</sup>**

<sup>1</sup>*The University of Texas Health Science Center at San Antonio*

Gap junctions represent perhaps the most complex family of channels so far described in terms of the diversity of permeants that they allow to be exchanged between cells, and the variety of gating mechanisms that are known to regulate them. Given their ubiquitous presence in most organ systems, it is also not surprising that mutations in their constituent proteins (connexins, or Cx) been linked to a remarkable diversity of human diseases, including the most common heritable form of asymptomatic sensorineural deafness. Our laboratory has been using a variety of biophysical, biochemical and mutational strategies to investigate the molecular basis of channel gating and pore permeability for metabolites, and how they contribute to normal and aberrant behavior of the channels. We have mapped the pore lining of Cx32 gap junctions and demonstrated that channels composed of different connexins have very different permeabilities in terms of both physical cut-off sizes, and specialized affinities for permeants that are likely to have evolved for specific functions in each tissue. In addition, evidence for structural similarities and differences between the permeability and pore structures of intercellular and hemichannel conformations of connexins will be presented. We have also made significant progress in defining the molecular basis of voltage gating in connexins, including mapping the location of the gate and interhelical interactions that appear important in the transduction of this response. This mapping has proven particularly instructive in an analysis of disease, as some mutations linked to deafness appear to affect gating in a way that can explain apparently contradictory reports of their recessive and dominant nature in the literature.

## **263 Processing of Music by the Human Auditory Cortex: Neuroimaging Evidence**

**Robert Zatorre<sup>1</sup>**

<sup>1</sup>*Montreal Neurological Institute*

The human auditory cortex has evolved specialized mechanisms for processing the information contained in our acoustic environment. Among the more complex and

interesting of these signals are speech sounds and musical patterns; it is perhaps not surprising that these aspects of auditory processing are unique to humans. Data will be presented bearing on the organization of the human auditory cortices as they pertain to the processing of these types of sounds using functional neuroimaging techniques. In particular, it is argued that studying musical processes offers useful insights into the functional organization of this system. We will discuss studies examining functional differences between auditory cortical regions within and between the cerebral hemispheres, and how these differences may relate to higher-order processing of music. Together, the data contribute towards a better model of how auditory cortical organization underlies auditory cognitive processes.

## **264 Investigating Human Auditory Cortical Dynamics using Musical Sequences and Magnetoencephalography (MEG).**

**Aniruddh Patel<sup>1</sup>**

<sup>1</sup>*The Neurosciences Institute*

Human communication relies heavily on complex and rapidly changing acoustic sequences. Thus there is a growing need in human auditory neuroscience for techniques which monitor stimulus-related cortical activity over time. We have been developing one such technique based on the auditory steady-state response (aSSR), an ongoing neural oscillation with sources in the primary auditory cortex. The aSSR is produced in response to amplitude modulation of an acoustic stimulus, and is present as long as the stimulus is on. In this talk I will discuss aSSR dynamics in relation to tone sequence structure, pitch perception, and attention. Specifically, I will present evidence that 1) the phase of the aSSR reflects the pattern of carrier frequency variation in long acoustic sequences, 2) in a subpopulation of cells involved in aSSR generation, aSSR phase reflects the perceived pitch of a stimulus, and 3) that attention modulates the degree of temporal coordination of aSSR activity between the hemispheres.

## **265 Local and Global Analysis of Pitch Sequences**

**Tim Griffiths<sup>1,2</sup>, Jessica M. Foxt<sup>1</sup>, Lauren Stewart<sup>3</sup>, Jason D. Warren<sup>3</sup>**

<sup>1</sup>*Auditory Group, Newcastle University Medical School, Newcastle-Upon-Tyne*, <sup>2</sup>*Wellcome Department of Imaging Neuroscience, University College, London*, <sup>3</sup>*Wellcome Department of Imaging Neuroscience, University College, London*

The concept of local and global analysis of pitch sequences is well established in musicology, where local corresponds to the actual pitches within a sequence and global the patterns of 'ups' and 'downs' irrespective of the actual pitches present. We have been studying local and global analysis using 'generic' sequences, distinct from conventional western melodies, where the octave is split into equal divisions other than 12. The idea is to probe mechanism relevant to analysis of a broad range of stimuli including speech, using the local and global concepts

derived originally from work on music. Behavioral work will be presented that addresses the significance of pitch sequence analysis as a mechanism relevant to reading ability. A further study addresses the mechanism of learning of pitch sequences in musically unsophisticated adults and demonstrates that i) improvement in contour analysis can occur after training ii) this improvement can occur whether the training uses a 'local' or a 'global' paradigm. The work supports models based on serial mechanisms for pitch-sequence analysis where global processing precedes local processing. Functional imaging work is in progress that addresses the neural bases for local and global analysis using similar stimuli.

## **266 The Neural Basis of Harmony.**

**Gerald Langner<sup>1</sup>**

<sup>1</sup>*Darmstadt University of Technology*

Harmonicity is a fundamental property of signals in a world of resonances. This is particularly true for acoustic communication in animals, speech, and music. Many communication sounds are periodic vibrations, which elicit the perception of a pitch and are composed of a fundamental frequency and multiples of this fundamental (harmonics). Moreover, because of physical constraints many sound sources tend to favor sequences of sounds with harmonically related fundamentals. Therefore, for all communicating animals, including man, it would be of advantage if their auditory systems were able to detect and discriminate harmonicity of acoustic signals. In contrast to cochlear frequency analysis, temporal processing of periodicity information includes harmonic analysis as a by-product. This is because with temporal correlation of any kind as an underlying mechanism, neurons tuned to a fundamental have a tendency to also respond to higher harmonics, thereby indicating the harmonic relationships of particular sounds.

Tuning to harmonic and harmonically related sounds was studied both electrophysiologically and also with the 2-deoxyglucose technique (2-DG) in the auditory midbrain of gerbils. Stimuli were sinusoidal amplitude modulations or harmonic complexes with various fundamental frequencies.

Many neurons in the ICC are tuned to modulation frequencies and arranged in periodicity maps orthogonal to the tonotopic map. More than half of the periodicity tuned neurons in the ICC were found to react like comb-filters during the first 30 to 60 ms of their responses to periodic signals. Similarly, with the 2-DG technique we found that single harmonic sounds evoke regular response patterns in the ICC. This indicates that in addition to neurons which are tuned to that particular periodicity, neurons which are tuned to corresponding subharmonics are also activated to a certain extent. Results from iontophoretic experiments indicate that these harmonic responses are suppressed by inhibition. It is likely that the source of the underlying inhibition which is precisely synchronized to the signal periodicity is the ventral nucleus of the lateral lemniscus (VNLL). Since results from tracer studies have demonstrated that the VNLL receives feedback from the ICC, the VNLL was also investigated for a spatial

representation of periodicity information with the 2-DG technique.

The results indicate that low pitch is represented dorsally and high pitch ventrally in the VNLL. A 3-D-analysis of the VNLL gave evidence for a helical periodicity map with 7 to 8 turns, reminiscent of the well-known pitch helix of music psychology.

## **267 Music Processing in Children and Adults: The Effects of Experience and Brain Maturation**

**Gottfried Schlaug<sup>1</sup>**

<sup>1</sup>*Beth Israel Deaconess Medical Center and Harvard Medical School*

It has been proposed that melody and rhythm processing may be lateralized to the right and left hemispheres, respectively. However, the picture of hemispheric dominance for these functions may be dependent on factors such as brain maturity and music training, with data supporting right hemisphere dominance for music tasks in non-musicians and left hemisphere dominance in musicians. The effects of brain maturity on the development of the neural basis of music processing are still uncertain. I will present data from our longitudinal study in children learning to play a musical instrument and several cross-sectional studies in adults (musicians and non-musicians) that have examined the effects of brain maturity and music training on the neural basis of rhythm and melody discrimination.

## **268 FGF Signaling and its Regulation During the Development of the Mouse Ear**

**Suzanne Mansour<sup>1</sup>, Chaoying Li<sup>1</sup>**

<sup>1</sup>*Department of Human Genetics, University of Utah*

Our lab studies the roles of FGF signaling in the development of the mouse peripheral auditory system. We showed previously that a two-step FGF signaling cascade, involving Fgf8, Fgf3 and Fgf10 initiate mouse inner ear development. FGF signals activate intracellular signaling pathways, including the ERK/MAPK cascade. Signaling through MAPKs is subject to negative feedback regulation at a variety of levels. For example, *Drosophila puc*, which encodes a dual-specificity phosphatase (DSP), is a transcriptional target of signaling through the DJNK MAPK pathway and feeds back to dampen signaling by inactivating DJNK. We are investigating the roles of ERK-specific mammalian DSPs. *Dusp6* is expressed at sites of FGF signaling and in periotic mesenchyme, which gives rise to the ossicles and otic capsule and participates in reciprocal signaling with the otic epithelium. To determine the role of *Dusp6* in ear development and to address the hypothesis that *Dusp6* functions in the ERK pathway similarly to *puc* in the DJNK pathway, we investigated *Dusp6* transcription in embryos with reduced FGF signaling and analyzed mice lacking *Dusp6*. *Dusp6* mRNA was reduced in embryos with reduced signaling through either Fgfr1 or Fgfr2. Loss of *Dusp6* caused dominant perinatal lethality with reduced penetrance. Both *Dusp6*<sup>+/-</sup> and *Dusp6*<sup>-/-</sup> embryos had increased levels of pERK and

Erm, suggesting activation of the ERK pathway. Affected pups were small and had craniosynostosis, reflecting activation of FGF signaling similarly to that seen in humans and mice with activating mutations in FGF receptors. In addition, the otic capsule and ossicles of small *Dusp6*<sup>-/-</sup> pups were abnormal. Consistent with these observations, small *Dusp6*<sup>+/-</sup> or *Dusp6*<sup>-/-</sup> pups that survived until P21 had increased ABR thresholds. Further characterization of the development of these phenotypes, progress in identifying genes redundant with *Dusp6* and in determining which FGF/ERK pathways *Dusp6* regulates will be presented.

### **269 Sprouty2, a Mouse Deafness Gene, Regulates Cell Fate Decisions in the Auditory Sensory Epithelium by Antagonizing FGF Signaling**

**Katherine Shim**<sup>1</sup>, George Minowada<sup>2</sup>, Donald Coling<sup>3</sup>, Gail Martin<sup>1</sup>

<sup>1</sup>University of California, San Francisco, <sup>2</sup>Case Western Reserve University, <sup>3</sup>University at Buffalo, The State University of New York

The auditory sensory epithelium (organ of Corti), where sound waves are converted to electrical signals, comprises a highly ordered array of specific types of sensory receptor cells and non-sensory supporting cells. Perturbations in this pattern can result in hearing deficits. We find that *Sprouty2*, which encodes a negative regulator of signaling via FGF receptors and other receptor tyrosine kinases, is required for normal hearing, and that *Spry2* null mutants display a significant abnormality in the cellular architecture of the organ of Corti: instead of two pillar cells, there are three, and this causes structural abnormalities in the tunnel of Corti. We provide evidence that the third pillar cell results from an early postnatal fate change, whereby a Deiters' (supporting) cell differentiates into an extra pillar cell. Both this fate change and hearing loss can be partially rescued by reducing *Fgf8* dosage in *Spry2* mutants. Our results provide evidence that precise modulation of FGF signaling by *SPRY2* is essential for establishing the cellular architecture of the organ of Corti and for hearing.

### **270 Integration of the Auditory Apparatus in the Chicken: Induction of the Middle and Outer Ear**

YiHui Zou<sup>1,2</sup>, HongXing Zhuang<sup>2,3</sup>, Raj Ladher<sup>1</sup>

<sup>1</sup>Sensory Development, RIKEN CDB, Kobe, Japan, <sup>2</sup>Plastic Surgery Department, Tsinghua University, Beijing, China, <sup>3</sup>Dept of Otolaryngology - Head and Neck, General Hospital of PLA, Beijing, China

The auditory apparatus of higher vertebrates consists not only of the inner ear to process mechanical stimuli into neural impulses, but also requires the tight integration of the middle ear to transduce and amplify sound waves and the external ear through which the sound is channeled. We wish to understand the embryological nature of this integration, and understand how the inner ear and middle ear can be so intimately linked. Previously we have found that a signal emitted by the cephalic paraxial mesoderm,

FGF19, can induce overlying adjacent non-neural ectoderm to adopt an otic fate, by acting through the neural ectoderm. We hypothesized that this patch of mesoderm could organize middle ear development through its action on the endoderm; this specific endoderm would then induce the middle and external ear (external auditory meatus - EAM) of the chick.

By making use of the quail – chick chimera system, we can successfully duplicate both middle ear (colomnella) and EAM of the chick when we implant an ectopic piece of pharyngeal endoderm taken from the 1st and 2nd pharyngeal arches. We have also shown that the same cephalic paraxial mesoderm that induces the inner ear can indeed respecify other cephalic endoderm to adopt a 1st to 2nd pouch fate. We show that FGF19 protein is a substitute for the cephalic paraxial mesoderm, leading to the tempting conclusion that FGF19 may play a role in the integration of the auditory apparatus.

### **271 Differential Guidance Cues in Auditory versus Vestibular Sensory Primordia in the Chicken Cochlear Duct**

**Andrea Campero**<sup>1</sup>, Donna M. Fekete<sup>1</sup>

<sup>1</sup>Purdue University, West Lafayette, IN

During otocyst development, a postmitotic neuron of the statoacoustic ganglion navigates a process through the periphery to contact only one of several incipient sensory organs. In the cochlear duct of the chicken, neuronal processes are confronted with a choice between two functionally distinct sensory primordia—the auditory basilar papilla and the vestibular lagena macula. One hypothesis is that the two types of sensory tissues express guidance factors that differentially affect auditory vs. vestibular afferents. This can be tested by asking whether afferents of one type are repelled by sensory primordia of the other. Alternatively, afferents may be attracted towards ectopic sensory patches of the right type if confronted with them on the way to their normal target. We can artificially create such choices by forced Wnt/ $\beta$ -catenin signaling, which generates ectopic vestibular patches in auditory territory. This situation affords the opportunity to ask whether ectopic vestibular patches will be innervated, and if so by which neuronal population.

We use RCAS virus to deliver an activated form of  $\beta$ -catenin to the right otocyst on E3. On E11 embryos are frozen, sectioned and immunostained to detect axons, hair cells, vestibular supporting cells, and ectopic  $\beta$ -catenin. Uninjected left ears serve as controls and show normal innervation. Two distinct results are seen depending upon the size of the ectopic patch. Small ectopic patches within the basilar papilla have little or no innervation. These data suggest that guidance cues expressed by converted vestibular patches may repel nearby auditory axons. In contrast, larger ectopic patches are innervated, although the identity of the innervating neurons is unknown. We predict they are vestibular afferents, and suggest that the afferents reach these patches without traversing auditory territory, or that vestibular-specific attractants are strong enough to overcome auditory repulsion. Tract tracing is being conducted to test this idea.

## **272 Expression of $\beta$ -catenin and Effects of $\beta$ -catenin Gain and Loss of Function in the Developing Mouse Organ of Corti**

Jose Gurrola II<sup>1</sup>, Chad Woods<sup>1</sup>, Montcouquiol Mireille<sup>1</sup>, Kelley Matthew W.<sup>1</sup>

<sup>1</sup>NIDCD/NIH

While the development of the mammalian auditory sensory epithelia (Organ of Corti) remains an area of much research, little is known about the factors regulating the determination of cell fate and patterning.  $\beta$ -catenin ( $\beta$ -cat) is a cytoplasmic protein known to link transmembrane cadherins to the cytoskeleton. Moreover, it can act as a transcriptional activator in the canonical Wnt/ $\beta$ -cat pathway.  $\beta$ -cat's role in the development of the auditory sensory epithelia has yet to be fully determined. Studies in which  $\beta$ -cat was over-expressed in chicken embryo otocysts suggest  $\beta$ -cat induces a change in sensory hair cell morphology from acoustic to vestibular. Based on these results, it seems likely that  $\beta$ -cat could be involved in the determination of sensory hair cell fate in the organ of Corti. To begin to examine the roles of  $\beta$ -cat in the organ of Corti, we determined the sub-cellular pattern of expression for  $\beta$ -cat in the mouse cochlear duct at different developmental time points. Membranous expression was found throughout the organ of Corti at different stages, while nuclear staining was not observed in any cells. Based on these results, we generated both gain and loss-of-function models for  $\beta$ -cat. Since complete deletion of  $\beta$ -cat results in lethality by E7, we utilized a Cre-lox recombination system in order to study the effects of deletion of  $\beta$ -cat in the otocyst. Results indicated that loss of  $\beta$ -cat leads to a complete absence of all inner ear structures. To examine effects of increased  $\beta$ -cat signaling, wild type and the non-ubiquitinatable S37A mutant forms of  $\beta$ -cat were transfected into E13-E14 mouse explants. Transfected cells did not express Myosin VI, a marker for both auditory and vestibular hair cells. Based on these results it seems likely that while  $\beta$ -cat plays an integral role in the development of the sensory epithelia, the introduction of  $\beta$ -cat alone is not sufficient to induce hair cell fate in the mammalian cochlea.

## **273 The Role of Atoh1 in the Development and Evolution of the Peripheral and Central Mammalian Auditory System**

Feng Feng<sup>1</sup>, Bernd Fritsch<sup>1</sup>

<sup>1</sup>Creighton University

The mechanosensory cells of the vertebrate ear have become a prime example for a 'deep, molecular based homology'. This is so because a critical developmental factor, the bHLH gene *atoh1*, is highly conserved across phyla and can be interchanged between vertebrates and invertebrates to govern species specific mechanosensory development. Based on these findings it appears likely that mechanosensory cells that use this or closely related bHLH genes for their development are homologous no matter how different they appear at a morphological level. Recent experimental work suggests that *Atoh1* may also be associated with the formation of the cochlear nuclei. Like the cerebellar granule cells, the

granule cells of the dorsal cochlear nuclei of mice require the bHLH gene *Atoh1* for their development. Descriptive analysis of gene expression domains suggest that the vestibular and possibly parts of the auditory nuclei may derive from a neurogenin 1 expressing domain, an expression domain of the very same gene that also regulate sensory neuron formation in the ear. We have recently investigated the formation of cochlear nuclei in *Atoh1* and *Neurog1* null mutant mice histologically as well as by tracing their connections to the inferior colliculus. *Atoh1* null mutant mice are known to lose embryologically a number of dorsal nuclei of the hindbrain such as the external cuneate nucleus and the cerebellum. Our data now suggest that auditory nuclei are almost completely absent in *Atoh1* null mice at E18.5. We verified this using a second marker, *Neurod1*, a gene that is also expressed in the cerebellum and the cochlear nuclei. Our results either through investigation of the area that contains *Atoh1* positive neurons in *Atoh1* null mice or through analysis of *Neurod1* expressing cells in *Atoh1* null mice or through analysis of central projections through retrograde filling with lipophilic dyes all suggest that most, if not all, cochlear nuclei neurons are absent at E18.5 *Atoh1* null mutant mice. We are currently investigating the central projection of spiral neurons and the connection of cochlear neurons in earlier stages to verify that the absence of cochlear nuclei is not due to a secondary loss due to a reduction of spiral ganglion consequential to the absence of differentiated hair cells. If this is a true lack of formation of cochlear nuclei, the highly conserved gene governing mechanosensory cell development across phyla has assumed an evolutionary novel function in the CNS.

## **274 Immortalized Mouse Inner Ear Cell Lines Reveal a Role for Chemokines in Promoting Outgrowth of SAG Neurons**

Lynne Bianchi<sup>1,2</sup>, Zeeba Daruwalla<sup>1</sup>, Ayo-Lynn Richards<sup>1,2</sup>, Ian White<sup>1</sup>, Susan Allen<sup>2</sup>, Kate Barald<sup>2</sup>

<sup>1</sup>Oberlin College, <sup>2</sup>University of Michigan, Ann Arbor

The target-derived factors necessary to promote initial outgrowth from the statoacoustic ganglion (SAG) have not yet been fully characterized. In the present study, immortalized mouse inner ear cell lines that maintain characteristics of developing inner ear sensory epithelia were screened for survival and neurite-promoting activity. A positive conditioned medium was tested for the presence of chemokines, molecules not previously investigated for SAG-promoting activity. One candidate molecule, MCP-1, was detected in the conditioned medium, and subsequently localized in inner ear tissues by immunohistochemistry. A receptor for MCP-1 was also detected on SAG neurons. In vitro studies demonstrated that function-blocking MCP-1 antibodies decreased the amount of SAG neurite outgrowth induced by the conditioned medium and that MCP-1 protein was able to promote outgrowth when added to antibody-treated cultures. The use of the immortalized cell lines proved valuable in identifying a candidate co-factor that promotes outgrowth of early stage SAG nerve fibers.

Grant Sponsors: NIH/NIDCD R15DC05587 and NSF0114831 to LMB; NIH/NIDCD R01DC04184, and R01DC05939 to KFB; and an Oberlin–University of Michigan Collaboration Award to LMB, KFB

### **275 Otopetrin 1 is Required for Otolith Formation in the Zebrafish *Danio Rerio***

Inna Hughes<sup>1</sup>, Brian Blasiolo<sup>2</sup>, David Huss<sup>1</sup>, Mark E. Warchol<sup>1</sup>, Nigam P. Rath<sup>3</sup>, Belen Hurler<sup>4</sup>, Elena Ignatova<sup>1</sup>, J. David Dickman<sup>1</sup>, Ruediger Thalmann<sup>1</sup>, Robert Levenson<sup>2</sup>, David M. Ornitz<sup>1</sup>

<sup>1</sup>Washington University School of Medicine, <sup>2</sup>Pennsylvania State University College of Medicine, <sup>3</sup>University of Missouri, St. Louis, <sup>4</sup>National Genome Research Institute, NIH

The receptors responsible for detecting linear acceleration make up one of the phylogenetically oldest sensory systems. Three large extracellular biomineral particles, otoliths, have evolved in the fish inner ear to transduce the force of linear motion into neuronal signals. Mammalian ears contain thousands of small particles called otoconia that serve a similar function. Loss or displacement of these structures can be lethal for fish and is responsible for age related balance disorders and Benign Paroxysmal Positional Vertigo in humans. Mutations in a novel gene, *Otopetrin 1* (*Otop1*), encoding a multi-transmembrane domain protein, causes non-syndromic otoconial agenesis and a severe balance disorder in mice. Here we show that morpholino mediated knock-down of zebrafish otopetrin 1 leads to otolith agenesis without affecting the sensory epithelium or other structures within the inner ear. Despite lack of otoliths in early development, otolith formation partially recovers in some fish after 2 days. However, the otoliths are malformed, lack an organic matrix and often form inorganic calcite crystals. These studies demonstrate that *Otop1* has an essential and conserved role in the timing of formation and the regulation of the calcium carbonate crystal polymorph of developing otoliths.

### **276 Topographic Organization of Macular Sensory Epithelia is Independent of Natural Stimulation**

Larry Hoffman<sup>1</sup>, Sherri Jones<sup>2</sup>, Timothy Jones<sup>2</sup>

<sup>1</sup>UCLA, <sup>2</sup>East Carolina University

The present study was undertaken as a component of a larger investigation of the role that natural stimulation plays in the development of structural and physiologic features of vestibular sensory epithelia. The principal strategy is to compare two strains of otoconia-deficient mutant mice (head-tilt (*het* [*Nox3<sup>het</sup>*]) and tilted (*ttt* [*Otop1<sup>ttt</sup>*]) homozygotes) to normal heterozygous littermates. The only known common phenotype of the homozygous mutants is the absence of otoconia within the otolithic membranes of the utricle and saccule, rendering these epithelia incapable of transducing linear head movements and orientation within the Earth's gravitational field. In the present study, we focused upon the topographic organization of hair cell morphologic polarization vectors (MPVs). This fundamental feature of hair cell morphology appears at approximately the same developmental stage

as the otolithic membrane. It is not known whether natural stimulation plays a role in the maintenance of the topographic organization of hair cell MPVs through adulthood. Adult utricular and saccular epithelia from *het*, *ttt*, and normal mice were obtained from temporal bones infused with 4% paraformaldehyde. Epithelia were dissected in cold phosphate buffered saline. Specimens were processed with phalloidin conjugated to Alexa-488 (Molecular Probes, Inc.) to label the stereocilia bundles and tight junctions at the epithelia surface then mounted on flat slides and analyzed via confocal microscopy. We measured various parameters at regular spatial loci across the entire epithelial surface, including MPVs and hair cell density. There were no differences in any of these parameters among epithelia from *het*, *ttt*, and normal animals. These findings indicate that natural stimulation is not required to maintain the exquisite organization of hair cell MPVs. The results also demonstrate the absence of secondary phenotypic sequelae associated with the otoconial deficiency. Supported by NIDCD R01 DC05776.

### **277 p27KIP1 Regulates the Timing of Cell Cycle Exit in the Developing Organ of Corti**

Feng Liu<sup>1,2</sup>, Yun-shain Lee<sup>1</sup>, Neil Segil<sup>1,3</sup>

<sup>1</sup>Gonda Department of Cell and Molecular Biology, House Ear Institute, USA, <sup>2</sup>Neuroscience Program, University of Southern California, USA, <sup>3</sup>Department of Cell and Neurobiology, University of Southern California School of Medicine, USA

The cell cycle is strictly regulated during development to produce the correct number of sensory hair cells and supporting cells required for the formation of a functional organ of Corti. In the developing cochlea, p27KIP1, a cyclin-dependent kinase inhibitor, has been shown to be expressed at the time when the sensory progenitor cells exit the cell cycle, and its absence leads to prolonged cell division within the prosensory domain. To further define the roles of p27KIP1, we studied the pattern of p27KIP1 expression in comparison with the pattern of the cell cycle exit. We found that the p27KIP1 expression is initiated in the apex of the E12 cochlea, and spreads to the whole cochlea by E15. This gradient of p27 upregulation is immediately followed by the apical-to-basal gradient of the cell cycle exit of sensory progenitor cells. In the absence of p27KIP1, the apical-to-basal gradient of the cell cycle exit within the prosensory domain is gone, indicating that p27KIP1 functions by driving the sensory progenitor cells out of the cell cycle. Furthermore, even though the sensory progenitor cells do not stop dividing at the normal time in p27KIP1<sup>-/-</sup> mice, hair cell precursors exit the cell cycle in a basal-to-apical gradient between E14.5 and E17.5, in parallel with the normal timing of hair cell differentiation. Together, our results indicate that p27KIP1 is required for regulating the normal timing of cell cycle exit in the organ of Corti, and in its absence, there appears to be a more direct link between the stimulus for differentiation and cell cycle withdrawal.

## **278** Hair-Cell-Specific Deletion of Retinoblastoma Gene (Rb1) Led to Production of Functional Hair Cells Postnatally

Cyrille Sage<sup>1</sup>, MingQian Huang<sup>1</sup>, Melissa Vollrath<sup>2</sup>, Doug Vetter<sup>3</sup>, David Corey<sup>2</sup>, Zheng-Yi Chen<sup>1</sup>

<sup>1</sup>Massachusetts General Hospital and Harvard Medical School, <sup>2</sup>Howard Hughes Medical Institute and Harvard Medical School, <sup>3</sup>Department of Neuroscience, Tufts University School of Medicine

Mammalian hair cells lack self-renewal capacity, thereby making it particularly challenging to restore hearing and balance via hair cell replacement.

Previously we have shown in a conditional knockout mouse model in which the retinoblastoma gene (Rb1) is deleted in the inner ear, hair cells were able to proliferate. Functional hair cells were generated through cell division in the embryos.

In order to further study the specific effect of pRb in hair cells postnatally, we have generated new pRb conditional knockout mice, with cre under the control of Pou4f3 (Brn-3.1) promoter. Rb1 is specifically deleted in the hair cells and the mice were able to survive postnatally.

The hair cells without pRb undergo cell division. Continuous hair cell proliferation was observed in the pRb<sup>-/-</sup> vestibular system in 6-week old mice. Therefore lack of pRb in the vestibular system does not lead to hair cell death. The supernumerary hair cells in the knockout mice were the result of hair cell division, rather than from the conversion by supporting cells. Using various cellular markers it was illustrated that the proliferating hair cells were highly differentiated. FM1-43 uptake and patch clamp studies on the P4 and P6 pRb<sup>-/-</sup> utricular hair cells showed functional characteristics similar to control hair cells.

Finally to investigate the role of pRb in maintaining postmitotic status of the hair cells, both embryonic and postnatal floxP-Rb utricles were infected with adenovirus carrying cre-recombinase. BrdU, PCNA and hair cell marker labeling showed that the postmitotic hair cells re-entered cell cycle, after acute elimination of pRb function.

We have therefore demonstrated that pRb is involved in both cell cycle exit and maintenance of quiescence of hair cells. Functional hair cells can be continuously generated in postnatal pRb<sup>-/-</sup> inner ear, strongly indicating the possibility that a transient and reversible block of pRb function may be sufficient to produce functional hair cells in adult inner ear.

## **279** Possible Involvement of ADP-Ribosylation Factors in Repair of Hair Cells

Glen Watson<sup>1</sup>, Patricia Mire<sup>1</sup>, Hanho Park<sup>1</sup>

<sup>1</sup>University of Louisiana Lafayette

Previously, we have investigated 'repair proteins' secreted by sea anemones in response to trauma to their hair bundle mechanoreceptors. A specific chromatographic fraction named 'fraction beta' has biological activity comparable to the complete repair protein mixture. Fraction beta apparently includes replacement linkages including tip links that are installed into the damaged

mechanoreceptors. In addition, fraction beta likely includes accessory proteins involved in installing the replacement linkages. Fraction beta restores function to hair cells in superficial neuromasts of blind cave fish. Thus, repair mechanisms may be largely evolutionarily conserved. We here report our initial results in screening a cDNA library prepared in traumatized anemones. Anti-beta detection of a fusion protein has revealed a lambda clone with a DNA insert having considerable sequence homology to human ADP-ribosylation factors 5 and ADP-ribosylation factor like 8. These are small G-proteins that activate ADP-ribosyltransferases, enzymes that add ADP-ribose groups to proteins to modify their behavior. Both ADP-ribosylation factors and ADP-ribosyltransferases are known to occur (in other systems) on the apical cell surface. The possibility that such factors may be involved in hair cell repair is supported by experiments in which exogenously added GTP with beta enhances the rate of recovery of vibration sensitivity by approximately 4 fold as compared to that for beta alone. Supported by NIDCD DC05514.

## **280** Identification of Signaling Pathways Involved in Sensory Regeneration in the Avian Ear using Gene Expression Profiles and RNAi

R. David Hawkins<sup>1</sup>, Stavros Bashiardes<sup>1</sup>, Veena Bhonagiri<sup>1</sup>, David Alvarado<sup>1</sup>, Steven Woolley<sup>1</sup>, Rose Veile<sup>1</sup>, Judy Speck<sup>1,2</sup>, Mark E. Warchol<sup>1,2</sup>, Michael Lovett<sup>1</sup>

<sup>1</sup>Washington University School of Medicine, <sup>2</sup>Central Institute for the Deaf

We have recently conducted the first large-scale gene expression profile during sensory regeneration in the avian inner ear. Sensory epithelia (SE) from both the cochlea and utricle were separately profiled following damage by either laser ablation or neomycin treatment. Epithelial cells were then profiled for transcription factor (TF) expression at various points during the regenerative process. A detailed analysis of changes in gene expression, involving more than a hundred microarray comparisons, identified over 100 TFs that were differentially expressed in both the cochlea and utricle after injury. However, only a subset of these genes were common to both treatments in both organs. Many of these shared TFs are members of key signaling cascades such as the TGF- $\beta$  and Pax-Eya-Six-Dach pathways. In order to determine the role of these factors in regeneration, we then treated cultures of dissociated progenitor cells with siRNAs for selected TFs. Immunofluorescence and microarray-based gene expression measurements determined that RNAi was effective in knocking-down both protein and gene expression levels of these TFs. Knockdown of most of the targeted genes had no effect on cell proliferation. However, reduction of PAX2, JUNB, and CEBPG gene expression levels resulted in significant inhibition of proliferation. In addition, we identified common downstream effects on gene expression amongst different RNAi experiments. This allowed us to identify intersections between pathways (e.g., between JUNB and CEBPG). Genes that showed co-variation across time courses, or after RNAi, were searched for common DNA

motifs by bioinformatics approaches. In this way we identified motifs that are conserved across multiple species and between co-varying genes. These represent putative regulatory elements that may control the co-expression of these genes.

### **281 Mitotic Hair Cell Generation by Postnatal Cochlear Supporting Cells**

Angelika Doetzlhofer<sup>1</sup>, Patricia White<sup>1</sup>, Yuan Shain Lee<sup>1</sup>, Andy Groves<sup>1</sup>, Neil Segil<sup>1</sup>

<sup>1</sup>House Ear Institute

Loss of sensory hair cells in the inner ear is a major cause of deafness in humans. The highly specialized mechanosensory hair cells of the mammalian cochlear are only formed during embryogenesis and no regeneration occurs after hair cell loss. In contrast, birds and other non-mammalian vertebrates are able to regenerate hair cells by stimulation of neighboring supporting cells. Whether the lack of cochlear hair cell regeneration in mammals is caused by inability of postnatal supporting cells to generate hair cells or by a lack of appropriate stimuli is unknown.

To test if mammalian supporting cells have the capacity to generate hair cells, we purified postnatal cochlear supporting cells and cultured them in the presence of epidermal growth factor and periotic mesenchyme. Such conditions have been previously shown to allow embryonic hair cell progenitors to divide and differentiate into hair cells (Doetzlhofer et al., 2004). To isolate postnatal cochlear supporting cells, a transgenic mouse line in which GFP is expressed under the control of p27/Kip1 was used. The exclusive expression of the GFP reporter gene in supporting cells allows the isolation of supporting cells with 96% purity.

Our data indicates that purified postnatal cochlear supporting cells retain the ability to re-enter the cell cycle and divide. Importantly some of these newly mitotic supporting cells act like hair cell progenitors, which over time, differentiate to express many characteristics of mature hair cells.

### **282 Neuronal Growth Toward Regenerated Hair Cells Following Math1 Gene Therapy in Deafened Guinea Pigs**

Shelley Batts<sup>1</sup>, Mark Crumling<sup>1</sup>, Masahiko Izumikawa<sup>1</sup>, Yehoash Raphael<sup>1</sup>

<sup>1</sup>Kresge Hearing Research Institute, Univ. of MI

Hair cell (HC) loss in the organ of Corti causes permanent and irreversible hearing impairment, as mammals are unable to replace lost HCs. *Math1*, the mouse homolog of atonal, generates new HCs when expressed in the cochlea (Kawamoto et al., Gao et al). This study sought to characterize the innervation of regenerated HCs at two weeks, one month, and two months following systemic deafening and *Math1* over-expression. Young adult guinea pigs were deafened with kanamycin and ethacrynic acid, and four days later were inoculated into the scala media of the left cochlea with a recombinant adenovirus vector with the *Math1* gene insert (Ad. *Math1*). Control

deafened animals were inoculated with adenovirus vectors with no gene insert (Ad.empty), or deafened without an inoculation. Auditory brainstem responses (ABRs) were measured before deafening, before inoculation, and either two weeks, one month, or two months post-inoculation. After the last ABR measurement, animals were sacrificed and cochleae prepared for histological assessment using whole-mounts stained for synapsin and neurofilament. New HCs were observed in cochleae of *Math1*-inoculated ears, but not in control ears. Control ears exhibited little neurofilament or synapsin staining at two weeks after deafening and progressively less at one and two months, confirming regression of neurons in deafened ears. *Math1*-inoculated ears also exhibited minimal staining for neurofilament or synapsin at 2 weeks, but more neurofilament staining was evident at 1 and 2 months. More important, inoculated cochleae exhibited synapsin staining indicating numerous mature nerve terminals in the organ of Corti. These results demonstrate neurite growth in the *Math1*-treated organ of Corti and suggest that new HCs produce the neurotrophic factor(s) required to attract auditory nerve fibers.

Supported by GenVec and NIH/NIDCD Grants R01-DC01634, R01-DC05401, R01-DC05053 and P30-DC05188.

### **283 Presence of Human Papillomavirus in Nasal Inverted Papilloma**

Shawn McKay<sup>1</sup>, Lucie Grégoire<sup>2</sup>, Fulvio Lonardo<sup>3</sup>, Patrick Reidy<sup>1</sup>, Wayne Lancaster<sup>4</sup>

<sup>1</sup>Otolaryngology, Wayne State University, Detroit, MI,

<sup>2</sup>Immunology/Microbiology, Wayne State University,

Detroit, MI, <sup>3</sup>Pathology, Wayne State University, Detroit,

MI, <sup>4</sup>Center for Molecular Medicine and Genetics, Wayne State University, Detroit, MI

The objectives of the study were to detect human papillomavirus (HPV) sequences in nasal inverted papillomas (NIP) lesions, and to demonstrate HPV is involved in the progression of NIP to sinonasal squamous cell carcinoma (SSCC).

A retrospective study was performed on 14 patients diagnosed with NIP within the last 12 years. Of these 14 patients, 3 developed SSCC.

Eighteen formalin fixed paraffin-embedded tissues were obtained for these 14 patients. After DNA extraction, PCR was performed, followed by hybridization using HPV 6, 11, 16, 18 specific DNA probes, in an attempt to identify HPV type in each specimen. After RNA extraction, the integration status of the HPV genome was evaluated based on the level of E7 and E5 viral transcripts, assessed by quantitative real-time PCR.

HPV sequences were detected in samples from 4 of the 14 patients with NIP. All 3 patients with SSCC harbored HPV sequences; 2 patients carried HPV 18, while 1 patient was positive for HPV 6. Of the 11 patients diagnosed with NIP, only 1 patient was positive for HPV DNA (HPV type 11). This difference in HPV positivity between NIP and SASCC is statistically significant (p= 0.01, Fisher's exact test, two tailed).



Viral transcripts were detected in all 3 SSCC. Since HPV early transcripts are polycistronic, loss of 3' transcript sequences (E5) and retention of 5' sequences (E7) indicates integration. One of 3 SSCC containing HPV 18 sequences showed a E7/E5 ratio of 120:1.

HPV sequences were detected in NIP using a limited number of types of HPV (6, 11, 16, 18), 4 of 14 patients being positive. Additional probes should be used to determine the frequency of HPV in NIP.

HPV transcripts were present in SSCC, and in one sample, there was integration of the viral genome.

Additional studies are needed to determine the exact role of HPV in NIP and progression to SSCC.

## **284 Two Mutations in Epidermodysplasia Verruciformis 1 (EVER1) Gene are not Contributors to the Susceptibility to RRP**

Farrel J. Buchinsky<sup>1</sup>, Joseph Donfack<sup>1</sup>, J. Christopher Post<sup>1</sup>, Craig S. Derkay<sup>2,3</sup>, Suzanne M. Leal<sup>4</sup>, Stephen F. Conley<sup>5</sup>, Sukgui Choi<sup>6</sup>, Garth D. Ehrlich<sup>1</sup>

<sup>1</sup>Center for Genomic Sciences - ASRI/WPAHS, <sup>2</sup>Children's Hospital of the Kings's Daughters, Norfolk, VA, <sup>3</sup>Eastern Virginia Medical School, <sup>4</sup>The Department of Molecular and Human Genetics, Baylor College of Medicine, Houston, TX, <sup>5</sup>Children's Hospital of Wisconsin, <sup>6</sup>Children's National Medical Center, Washington, DC

Infections with human papilloma virus (HPV) HPV 6 and 11 may result in recurrent respiratory papillomatosis (RRP). While millions of children are exposed, relatively few develop clinical evidence of the disease and the aggressiveness of the course is highly variable. We have postulated that genetically encoded host susceptibility is the basis for this wide variability and are currently collecting specimens in collaboration with the RRP Task Force (Buchinsky et al., 2004). As part of this effort, we investigated the potential role of a gene that has been implicated in another HPV-related disease known as epidermodysplasia verruciformis (EV). EV is a rare autosomal recessive genodermatosis characterized by abnormal susceptibility to HPVs. RRP and EV are phenotypically similar as they both can cause recurrent epithelial warts, that could ultimately become malignant. Ramoz et al. (2002) mapped a susceptibility locus for EV1 to chromosome 17q25. Subsequently the same group identified two mutations EVER1-280C/T and EVER1-1726G/T in the EVER1 gene that are associated with EV. Tate et al. (2004) recently described two novel mutations (EVER1-744C/A and EVER1-892-2A/T) in the same gene also associated with EV. Based on the phenotypical similarity between RRP and EV, we wanted to test whether these four mutations could account for the susceptibility to RRP. We genotyped EVER1-744C/A and EVER1-892-2A/T by allele-specific PCR in 25 RRP patients recruited as part of the collaborative study. None of the 25 patients showed the mutant alleles (EVER1-744A and EVER1-892-2T). These results suggest that EVER1-744A and EVER1-892-2T do not contribute to RRP disease. EV patients are more susceptible to HPV 5 or 8 as opposed to RRP patients to HPV 6 and 11; the absence of these two mutations might reflect genetic susceptibility to different

species of HPV. However, studies are underway to determine whether EVER1-280C/T and EVER1-1726G/T might account for the susceptibility to RRP.

## **285 Assessment of Genetic Counseling Services for Hearing Loss**

Heidi Rehm<sup>1,2</sup>, Anna Frangulov<sup>3</sup>, Janet Horgan<sup>4</sup>, Margaret Kenna<sup>3,5</sup>

<sup>1</sup>Pathology, Harvard Medical School, <sup>2</sup>Harvard-Partners Center for Genetics and Genomics, <sup>3</sup>Otolaryngology and Communication Disorders, Children's Hospital Boston, <sup>4</sup>ALM Program, Harvard University, <sup>5</sup>Otology and Laryngology, Harvard Medical School, Boston, MA, USA

**Objective:** We performed 2 survey studies to determine the effectiveness of genetic counseling (GC) in 2 groups of patients who underwent genetic testing (GT) for hearing loss (HL).

**Methods:** In the 1st study, a survey was sent to parents of 80 children with HL, the majority of whom had negative GT results. Some of the questions addressed what the parents remembered about the GT results, whether they had counseling, and who provided it. The survey also asked 5 "quiz" questions to assess respondent knowledge of GT. In the 2nd study a similar survey was sent to 80 families who were positive for biallelic Connexin 26 (Cx26) mutations.

**Results:** 47 parents responded to the 1st survey. Only 34% had a passing score on the quiz. Those who saw a genetic professional (GP) scored much better (70% correct) than those who did not (38% correct). 38% who had Cx26 testing did not know if any mutations were found. Yet 76% of respondents reported being satisfied with their understanding of GT (ARO 2004). To date 27 responses to the 2nd survey have been received. The performance on the 2nd study quiz is much better (89% passing). Whether or not a GP was seen did not have a significant impact on score (82% passed with GP vs. 93% without GP). Despite improved quiz performance, satisfaction with their understanding of GT did not change from the 1st study (78% vs. 76%).

**Conclusions:** The 1st study suggested parents were uneducated about GT implications and were not likely to pursue resources to improve their understanding. In contrast, the 2nd study showed that families with Cx26 HL were more educated, despite inconsistent GP involvement. The results suggest that it is important for families who are negative for Cx26 receive genetic counseling, given that many will have an unidentified genetic cause for the HL, and be unsuspectingly more likely to have a 2nd child with HL. These families also need to be aware that new genetic tests may be available in the future that could help diagnose the HL.

## **286 High Density SNP Mapping of Auriculo-Condylar Syndrome**

Jason Johnson<sup>1</sup>, Chris Cunniff<sup>1</sup>, Patricia Roberts<sup>2</sup>, David Duggan<sup>2</sup>, **Glenn Green**<sup>3</sup>

<sup>1</sup>University of Arizona, <sup>2</sup>Translational Genomics Research Institute, <sup>3</sup>University of Michigan

Auricular-Condylar Syndrome is characterized by maldevelopment of the ear and mandible and has been identified in several different ethnic populations. We recently identified a large family with several affected members where this disease is inherited in an autosomal dominant fashion with variable expressivity. To exclude previously hypothesized candidate genes and identify the disease causing gene whole genome linkage analysis was performed.

Genomic DNA was isolated from study participants from whole blood samples using standard techniques. A genomewide search was undertaken using the GeneChip Mapping 10K Xba 142 2.0 Array containing 10,204 SNP markers (Affymetrix, USA). The mean intermarker distance was 258 kb, and the mean heterozygosity of markers was 0.38. Compared to the standard microsatellite genome scan (~1 microsatellite every 10 cM), this represents a greater than 50-fold increase in mapping resolution. SNP genotypes were obtained by following the Affymetrix protocol for the GeneChip Mapping 10K 142 2.0 Xba Array. Two-point and haplotype based LOD scores were determined using Varia (Silicon Genetics, USA).

SNP mapping was able to exclude several phenotypically similar genes including the predominant gene for Treacher Collins syndrome. A high linkage area was identified. Fine mapping of this area will enable us to delineate the region to examine for candidate genes.

## **287 A Genetic and Functional Study of the V27I/E114G Genotype: Is It a Cause of GJB2-Related Deafness?**

**John Greinwald**<sup>1</sup>, Lynne Lim<sup>1</sup>, Wenxue Tang<sup>2</sup>, Hongwei Dou<sup>3</sup>, Muhammed Ali<sup>4</sup>, Valentina Pilipenko<sup>3</sup>, John Bradshaw<sup>5</sup>, Xi Lin<sup>2</sup>, John Greinwald<sup>3,5</sup>

<sup>1</sup>Cincinnati Children's Hospital Medical Center, <sup>1</sup>Department of Otolaryngology Head and Neck Surgery, National University Singapore, National University Hospital, Singapore <sup>2</sup>Departments of Otolaryngology and Cell Biology, Emory University School of Medicine, Atlanta, GA <sup>3</sup>Center for Hearing and Deafness Research, Cincinnati Children's Hospital Medical Center, Cincinnati, OH, <sup>4</sup>Dhaka Health Care, Dhaka, Bangladesh, <sup>5</sup>Department of Otolaryngology, University of Cincinnati College of Medicine, Cincinnati, OH

Mutations in the *GJB2* gene are a major cause of congenital non-syndromic sensorineural hearing loss (SNHL). The V27I and E114G alleles in *GJB2* are thought to be sequence variants that are not associated with hearing loss. We previously reported a higher prevalence of the V27I/E114G compound heterozygote genotype among subjects with SNHL compared to hearing controls in 2 Asian SNHL populations. We hypothesize that V27I

and E114G in the compound heterozygote state may result in SNHL.

After appropriate institutional review board approvals, a total of 87 unrelated subjects with idiopathic SNHL (40 from Singapore/47 from Bangladesh) and 92 subjects with no SNHL (50 from Singapore/42 from Bangladesh) were enrolled. Most subjects from Singapore were of Chinese ancestry (85.0%). The prevalence of known biallelic hearing loss related *GJB2* mutations among the Singaporean and Bangladeshi subjects with SNHL was 17.5% (7/40) and 2.1% (1/47), respectively. There was a high prevalence of V27I and E114G alleles at 15.0% and 8.8%, respectively, among the SNHL group compared to 8.0% and 3.0%, respectively, among hearing controls. At total of 10 SNHL subjects from both groups (11.5%) were identified with V27I/E114G and had severe-profound SNHL, while 1 other subject had a borderline-mild mixed loss. One subject with the V27I/E114G genotype was found among the hearing controls. Genetic analysis confirmed the V27I and E114G alleles were on unique chromosomes.

In-vitro testing of the functional significance of the V27I/E114G genotype was performed using dye transfer and intercellular Ca<sup>++</sup> signaling transfer experiments in a HEK293 cell culture model. Dye transfer was nil in the V27I/E114G injected cells, while all wild type injected cells showed normal dye transfer. E114G heterozygote injected cells all showed dye transfer, but 7/14 (50%) showed weak transfer. Our data suggest that V27I/E114G may play a role in *GJB2* related deafness.

## **288 Audiologic and Clinical Phenotype-Genotype Relationships in Children with Connexin 26 Mutations**

**Margaret Kenna**<sup>1,2</sup>, Anna Frangulov<sup>1</sup>, Heidi Rehm<sup>2,3</sup>

<sup>1</sup>Children's Hospital Boston, <sup>2</sup>Harvard Medical School, <sup>3</sup>Harvard-Partners Center for Genetics and Genomics, Boston, MA, USA

Objective: To compare the audiologic and clinical phenotype to the genotype in patients with biallelic Connexin 26 (Cx26) mutations

Methods: Children birth-18 years of both sexes and all races/ethnicities with sensorineural HL (SNHL) were studied. Cx26 testing was offered as part of the HL evaluation. Otoacoustic emission (OAE) and auditory brainstem evoked response (ABR) testing were used in infants to establish hearing thresholds and to confirm behavioral results in older children. Hearing was reported as the pure tone average (PTA) in dBHL of 500, 1000 and 2000 Hz for the worst ear; normal (0-20), mild (21-40), moderate (41-55), moderately severe (56-70), severe (71-90), or profound (>90). Progressive HL was defined as change at 1 frequency of 15dB or 10dB at 2 frequencies.

Additional collected information included computed tomography (CT) of the temporal bones (TB), developmental status, and other clinical, laboratory or radiographic findings.

Results: 100 patients (88 probands) were identified between 1999 and 2004; 63 were female. 78 were White, 12 Asian, 3 biracial, and 7 unknown. Initial PTA was

normal 5, mild 22, moderate 9, moderately severe 6, severe 13 and profound 40. All "normal PTA" had HL at > 2000 Hz, so not calculated into the PTA. 30% of the total had progression in at least 1 frequency. Of the 24 identified Cx26 mutations the most common were 35delG, M34T, 167delT and V37I. 15 patients had either homozygous or compound heterozygous M34T mutations; the HL in all cases was mild to moderate.

6 patients had cochlear anomalies on CT. 6 children had pervasive developmental delay or autism. 2 had congenital urinary tract anomalies and 1 had a cardiac arrhythmia.

Conclusions: Children with biallelic Cx26 mutations had wide variability of HL with a 30% progression rate. 15 children had TB CT anomalies or other important clinical findings; the relationship to Cx26 status is uncertain. Arguments supporting the pathogenicity of the M34T mutation are presented.

### **289 Novel Deletions in the DFNB1 Locus in Subjects with Autosomal Recessive Non-Syndromic Hearing Impairment**

Montserrat Rodriguez-Ballesteros<sup>1</sup>, Luis A. Aguirre<sup>1</sup>, Francisco J. del Castillo<sup>1</sup>, Araceli Alvarez<sup>1</sup>, Manuela Villamar<sup>1</sup>, Margarita Olarte<sup>1</sup>, Miguel A. Moreno-Pelayo<sup>1</sup>, Felipe Moreno<sup>1</sup>, **Ignacio del Castillo<sup>1</sup>**

<sup>1</sup>Unidad de Genética Molecular, Hospital Ramon y Cajal, Madrid, Spain

DFNB1-deafness, caused by mutations in the gene encoding connexin-26 (GJB2) on 13q12, is the most frequent subtype of autosomal recessive non-syndromic hearing impairment. Molecular testing for GJB2 mutations has become a standard diagnostic approach for subjects presenting with this disorder. However, genetic diagnosis is complicated by the fact that 10%-50% of affected subjects with GJB2 mutations carry only one mutant allele. A 309-kb deletion truncating the GJB6 gene (encoding connexin-30) was shown to be the accompanying mutation in up to 50% of these deaf GJB2 heterozygotes in different populations. We have investigated the existence of other DNA rearrangements at the DFNB1 locus. Here we report the molecular characterization of two novel deletions at DFNB1, found in trans with GJB2 mutant alleles in affected subjects. One of these deletions, named del(GJB6-D13S1854), spans 232 kb and removes the first two exons of GJB6. It took place by Alu/Alu unequal homologous recombination, involving an AluY repeat inside GJB6 intron 2, a mechanism which might generate other deletions at DFNB1. This mutation accounts for 25% of the affected GJB2 heterozygotes which remained unresolved after screening for the 309-kb deletion in our cohort of Spanish patients. The other deletion spans about 200 kb, and it does not alter the GJB6 gene. Diagnostic tests for the novel deletions were developed.

### **290 Differences in Transdominant Effects of Cx30 Mutations**

James Sipp<sup>1</sup>, Yanping Zheng<sup>1</sup>, Shoab Ahmad<sup>1</sup>, Xi Lin<sup>1</sup>

<sup>1</sup>Emory University

Introduction

Human Cx30 mutations are found to cause either congenital sensorineural hearing loss (e.g., mutation T5M) or autosomal dominant skin disorder (Clouston syndrome, e.g., mutations G11R, A88V, V37E). It is unknown why Cx30 point mutations at different locations cause distinctive diseases.

Methods

We reconstituted GJs in a GJ-deficient cell line (HEK293) containing disease-causing Cx30 mutations (T5M, V37E, G11R and A88V). Plasmid DNA containing Cx30 mutation only, or mixed (1:1) with wild type Cx30 or Cx26 were used in transfections. Co-transfections of the mutant and wild type Cxs were verified by tagging Cxs with fluorescent protein reporters with different colors (eGFP or DsRed). The ionic and biochemical permeabilities of reconstituted GJs were evaluated by intercellular Ca<sup>++</sup> transfer and fluorescent dye diffusion assays, respectively. Our results showed that the Cx30 mutation T5M selectively affected biochemical, but not ionic, permeability of GJs. Not only T5M mutation is dominant for homomeric Cx30 GJs, it is also transdominant for heteromeric GJs consisting of Cx26 and Cx30. In contrast, the Cx30 mutations that cause skin disorders (G11R, A88V, and V37E) did not form GJs in vitro after transfections.

Conclusions

We are currently investigate whether these Cx30 mutation exert any transdominant on heteromeric GJs consisting of Cx26 and Cx30. Cochlear gap junctions (GJs) consist of diverse types of connexins (Cxs). Hexameric co-assembly of Cx26 and Cx30 into GJs is the dominant form of GJs found in the cochlea of mice. Differences in Cx30 mutants' ability to transdominantly affect the function of heteromericly assembled GJs in the cochlea is an attractive hypothesis we are currently pursuing. We are currently testing whether Cx26 GJs are functional when co-expressed with Cx30 mutations (G11R, A88V, and V37E) that cause skin disorders.

### **291 SLC26A4 Gene is One of the Major Gene of Non Syndromic Hearing Loss**

Françoise Denoyelle<sup>1,2</sup>, Sebastien Albert<sup>1</sup>, Helene Blons<sup>2,3</sup>, Delphine Feldmann<sup>2,3</sup>, Alain Joannard<sup>4</sup>, Sebastien Schmerber<sup>5</sup>, Bruno Delobel<sup>6</sup>, Jacques Leman<sup>7</sup>, Hubert Journel<sup>8</sup>, Helene Catros<sup>9</sup>, Helene Dollfus<sup>10</sup>, Marie-Madeleine Eliot<sup>11</sup>, Albert David<sup>12</sup>, Catherine Calais<sup>13</sup>, Valerie Drouin-Garraud<sup>14</sup>, Marie-Françoise Obstoy<sup>15</sup>, Patrice Tran Ba Huy<sup>16</sup>, Didier Lacombe<sup>17</sup>, Françoise Duriez<sup>18</sup>, Christine Francannet<sup>19</sup>, Pierre Bitoun<sup>20</sup>, Christine Petit<sup>2,21</sup>, Erea-Noel Garabedian<sup>1,2</sup>, Remy Couderc<sup>2,3</sup>, Sandrine Marlin<sup>2,22</sup>

<sup>1</sup>Service d'ORL, Hopital d'enfants Armand-Trousseau, Paris, France, <sup>2</sup>INSERM U587, <sup>3</sup>Service de Biochimie et de Biologie Moléculaire, Hôpital d'Enfants Armand-Trousseau, AP-HP, Paris, <sup>4</sup>Service de Pédiatrie, CHU, Grenoble, France, <sup>5</sup>Service d'ORL, CHU, Grenoble, France, <sup>6</sup>Centre de Génétique, Hôpital St Antoine, Lille, France, <sup>7</sup>Centre Rochin, Lille, France, <sup>8</sup>Unité de Génétique Médicale, CHR, Vannes, France, <sup>9</sup>Centre G Deshayes, Auray, France, <sup>10</sup>Service de Génétique médicale, Hôpital de Haute-pierre, Strasbourg, France, <sup>11</sup>Service d'ORL,

Hôpital de Hautepierre, Strasbourg, France, <sup>12</sup>Service de Génétique, Hôtel Dieu, Nantes, France, <sup>13</sup>Service d'ORL, Hôtel Dieu, Nantes, France, <sup>14</sup>Service de Génétique, Hôpital Charles Nicolle, Rouen, France, <sup>15</sup>Service d'ORL, Hôpital Charles Nicolle, Rouen, France, <sup>16</sup>Service d'ORL, Hôpital Lariboisière, AP-HP, Paris, France, <sup>17</sup>Unité de Génétique Médicale, Hôpital Pellegrin, Bordeaux, France, <sup>18</sup>Service d'ORL, Hôpital Pellegrin, Bordeaux, France, <sup>19</sup>Unité de Génétique Médicale, Hôtel Dieu, Clermont Ferrand, France, <sup>20</sup>Service de Pédiatrie, Hôpital Jean Vedier, AP-HP, Bondy, France, <sup>21</sup>Unité de Génétique des Déficients Sensoriels, Institut Pasteur, Paris, France, <sup>22</sup>Unité de Génétique Médicale, Hôpital d'Enfants Armand-Trousseau, AP-HP, Paris, France.

Mutations of the SLC26A4 (PDS) gene underlies either a syndromic deafness characterized by congenital sensorineural hearing loss and goitre (Pendred syndrome), or a congenital isolated deafness (DFNB4). In this report 112 patients from 103 unrelated families, with documented non syndromic childhood deafness and inner ear malformation (enlarged vestibular aqueduct, cochlear dysplasia), were genotyped for SLC26A4 using DHPLC molecular screening and sequencing. Seventy seven allelic mutations were observed in 103 unrelated families, and eighteen had never been reported. Most mutations were found in exons 6, 10, 16, 19 and 14, and many of them had already been described in Pendred syndrome. Prevalence of SLC26A4 mutations was 36.9% (38/103) and prevalence of compound heterozygous 19.4% (20/103). Among patients with SLC26A4 mutations, deafness was more severe and more fluctuant than in patients with no mutation ( $p < 0.05$ ). According to the prevalence of inner ear anomalies, SLC26A4 mutations could underlie up to 6% of non syndromic hearing impairments.

## **292 A Large Chinese Family with Autosomal Dominant Late-Onset Progressive Non-Syndromic Hearing Loss Also Maps to DFNA4 Locus**

**Qiu-ju Wang**<sup>1,2</sup>, Chun-ye Lu<sup>2</sup>, Wei-yan Yang<sup>1</sup>, Dong-yi Han<sup>1</sup>, Yan Shen<sup>2</sup>

<sup>1</sup>Institute of Otolaryngology, Chinese PLA General Hospital, <sup>2</sup>Chinese National Human Genome Center, Beijing,

A large Chinese family with autosomal dominant late-onset progressive, high frequency hearing loss with the average onset of 25 years old was also mapped in DFNA4 locus. Genomic DNA was isolated from whole blood of 42 of 66 family members, who received clinical auditory evaluations. 384 markers covered the 22 autosomes were obtained from Perkin-Elmer Applied Biosystems (ABI Prism Linkage Mapping sets, version 2). DNA was PCR amplified and genotyped on an ABI Prism 3700 DNA sequencer according to standard protocol. Alleles were analyzed with Gene-mapper software (version 3.0). The resulted in significant evidence for linkage to the markers D19S420 and D19S918 (two-point lod-score of 4.97 and 5.74 at  $\theta = 0.0$ ) and a candidate critical region of 19.92cM between markers D19S223 and D19S571. One deafness locus DFNA4 (American pedigree) had been

mapped to 19q13 at 24.07cM interval between D19S414 and D19S246 in 1995 and the second pedigree (German) had been mapped to 19q13.3-q13.4 at 14cM interval between D19S412 and D19S571 in 2002. The region we mapped in Chinese pedigree located on the center of the two intervals and showed partial overlap with the previously reported DFNA4 and the German pedigree critical regions. The maximal LOD score at the marker D19S918 we mapped was 5.74 at  $\theta = 0.00$  showed close linkage at marker D9S918. We are not able to find the mutations in the candidate genes of KCNA7, KPTN, KCNN4 and KCNJ14 and turn to perform the MYH14 gene mutations in the Chinese family.

This work was supported by a grant from the National High Tech Development Project (2004AA221080), a grant from National Nature Science Foundation (A30370782) and Beijing Science and Technology Major Project (No. H020220020610) grant.

## **293 Polymorphisms and Mutation of CTL2 Gene**

**Thankam Nair**<sup>1</sup>, Pavan Kommareddi<sup>1</sup>, Steven Telian<sup>1</sup>, Alexander Arts<sup>1</sup>, Thomas Carey<sup>1</sup>

<sup>1</sup>University of Michigan

CTL2 is a recently identified and sequenced protein that is abundantly expressed in inner ear supporting cells. Disruption of CTL2 function by antibody binding leads to hair cell death and hearing loss. CTL2 is encoded from a 2.1 kb open reading frame that uses either of two promoters, (CTL2 P1 and CTL2 P2) and alternate first exons resulting in a protein of 704 or 706 amino acids respectively. CTL2 P1 is the predominant inner ear isoform. It differs in the first 10 amino acids from the CTL2 P2 sequence that predominates in most other tissues. Mutations and polymorphisms play an important role in human disease. We examined cDNAs from 4 human vestibular tissues (VTs) and 4 squamous cell carcinoma (SCC) cell lines for CTL2 single nucleotide polymorphisms (SNPs). Of the five known polymorphic sites in CTL2, two are silent and three at codons 98, 154, 470 (based on the CTL2 P2 sequence) result in an amino acid change. CTL2 P1 sequences were found in all VT samples and only one SCC. All 4 SCCs had a codon 68 GAT-GAC polymorphism, whereas all of the VTs had GAT. Since both GAT and GAC code for asparagine this does not alter the protein. VT from a Meniere's patient expressed both the CGA (arginine) and the CAA (glycine) alleles at codon 152. Interestingly, all of the other VTs expressed arginine and all of the SCCs had the glycine allele at this locus. We also found a previously unreported TTC>CTC base change at codon 602 phenylalanine to leucine that was present only in UM-SCC-74B and could represent a mutation in this SCC cell line. SNPs that alter the amino acid may affect the functional properties of proteins. The full significance of the SNPs we observed in this small sample are not yet known, but an expressed polymorphism in a patient with Meniere's disease and a novel change in a cancer cell line are suggestive that these changes may have functional consequences.

## **294 Genetic and Functional Characterization of PFET1, an Abundantly Expressed Fetal Cochlear Transcript with High GC-Content**

Sharon Kuo<sup>1</sup>, Weining Lu<sup>2</sup>, Arti Pandya<sup>3</sup>, Chinweike Ukomadu<sup>4</sup>, Joe Adams<sup>5</sup>, Cynthia Morton<sup>6</sup>

<sup>1</sup>*Speech and Hearing Bioscience and Technology, Harvard-MIT Division of Health Sciences and Technology,* <sup>2</sup>*Department of Pathology, Brigham and Women's Hospital,* <sup>3</sup>*Medical College of Virginia,* <sup>4</sup>*Department of Medicine, Brigham and Women's Hospital,* <sup>5</sup>*Department of Otolaryngology, Harvard Medical School,* <sup>6</sup>*Departments of Pathology and Ob/Gyn, Brigham and Women's Hospital*

PFET1/Pfet1 (Predominantly Fetal Expressed T1 domain) is an evolutionarily conserved intronless gene with a 70% GC-rich ORF encoding a 6 kb transcript in human and three transcripts of approximately 4, 4.5, and 6 kb in mouse. The protein, pfetin, is predicted to contain a voltage-gated potassium channel tetramerization (T1) domain. Initial findings revealed a striking preferential expression of the human 6 kb transcript in fetal organs with highest levels of transcript present in cochlea and brain. Immunohistochemistry analysis with pfetin antibody, a polyclonal antibody raised against a synthetic peptide to PFET1 sequence, detects a variety of positively stained cells in cochlea and vestibule of human, monkey, mouse, and guinea pig, including type I vestibular hair cells. Developmental Northern blot analysis shows a differential level of PFET1 transcripts between mouse embryonic developmental days 6.5 and 16.5; immunohistochemistry is in progress to determine cellular expression of pfetin during this developmental time frame. Immunoprecipitation studies are also underway to determine pfetin's binding partners, of particular interest given the presence of the T1 domain. Presently, there are no known deafness loci mapped in close proximity to PFET1/Pfet1 on human (at 13q12) or mouse (on 14) chromosomes. To detect potential pathogenetic sequence variants within the PFET1 ORF (given the GC-richness of the PFET1 ORF and the associated bias towards deamination of CpG dinucleotides as a common molecular cause of mutations in humans), a panel of DNAs is being sequenced from individuals likely to have a genetic etiology for their hearing loss. To pursue further the function of pfetin, we are studying its homolog in zebra fish; PFET1 has two zebra fish homologs, leftover and righton, that have largely been studied to date for their asymmetric expression patterns in the habenula. Developmental whole mount zebra fish in situ experiments are planned corresponding to the mouse developmental expression time points in addition to double knockdown studies with morpholinos.

## **295 Strial Pathology in Lupus Mouse Strains**

Michael Ruckenstein<sup>1</sup>, Michael Patterson<sup>2</sup>, Micah Cohen<sup>1</sup>, Michael Anne Gratton<sup>1</sup>

<sup>1</sup>*University of Pennsylvania,* <sup>2</sup>*University of Miami*

Strial pathology has been described in the MRL-Fas<sup>lpr</sup> Lupus mouse strain. The etiology of this pathology is not inflammatory and remains unclear. We hypothesized that if this pathology was secondary to the underlying systemic autoimmune syndrome, then similar cochlear pathology should be observed in all Lupus strains. Cochlear function and ultrastructure was evaluated in the MRL/lpr and the NZB(BxW)F1 Lupus strains, 2 strains that do not share genetic backgrounds. Elevations in ABR thresholds and strial degeneration were observed in the MRL/lpr strain, but not in the NZB mouse. These results suggest that the observed strial degeneration does not result from the autoimmune Lupus-like syndrome observed in these mice.

## **296 Hypoxia: A Mechanism for the Susceptibility of Alport Mice to Noise?**

William Snyder<sup>1</sup>, Kate Barrett<sup>1</sup>, Kristen Bateman<sup>1</sup>, Michael Anne Gratton<sup>1</sup>

<sup>1</sup>*University of Pennsylvania*

Alport syndrome is a group of genetic disorders resulting from mutations in  $\alpha 3(\text{IV})$ ,  $\alpha 4(\text{IV})$  or  $\alpha 5(\text{IV})$  collagen. This disease is characterized by a progressive glomerulonephritis, a high frequency sensorineural hearing loss, and ocular abnormalities. The mouse model of Alport syndrome, which lacks  $\alpha 3(\text{IV})$  collagen, has all the hallmarks of human disease. Defects in the collagen IV gene in the Alport mouse result in thickened strial capillary basement membranes. The Alport mouse is susceptible to noise in comparison to the resistance to excessive noise displayed by its wild-type littermate.

Hypoxia-inducible factor-1 (HIF-1) is an important transcription factor that regulates genes involved in tissue oxygen homeostasis. In the presence of normal oxygen levels HIF-1 is degraded, but in the presence of hypoxia, HIF-1 expression is stabilized. We hypothesized that the thickened strial capillary basement membranes in the Alport mouse might cause hypoxia by impeding transfer of energy substrate from the blood to strial tissue, especially when physiologically stressed by exposure to moderate levels of noise. Functionally, increased latency of Wave V of the ABR response has been noted in following induction of hypoxia.

Expression of HIF-1 was evaluated using immunohistochemistry with antibodies specific for the HIF-1 $\alpha$ , HIF-2 $\alpha$  and HIF-1 $\beta$  subunits. Immunopositivity was noted in the stria vascularis of the Alport mice with greater reactivity noted in Alport mice exposed to 8 hours of 106 dB SPL, 8-17kHz noise. Immunoreactivity was noted in cochlear tissues of wild-type littermates only after exposure to 6 hours of 8% oxygen/92% nitrogen gas. Analysis of Wave V latency revealed a significant increase in the ABR response of Alport mice when compared to their wild-type littermates. The activation of HIF-1 and increased ABR latency in the Alport mice suggest that hypoxia may be a contributing factor to the hearing loss associated with Alport syndrome.

## **297** VLGR1 Mutant Mice Exhibit Severe Peripheral Auditory Pathology

Edward J. Walsh<sup>1</sup>, JoAnn McGee<sup>1</sup>, Noelle Feldbauer<sup>1</sup>, Jo Ellen Boche<sup>1</sup>, D. Randy McMillan<sup>2</sup>, Perrin C. White<sup>2</sup>

<sup>1</sup>Boys Town National Research Hospital, <sup>2</sup>UT Southwestern Medical Center

The VLGR1 (MASS1) gene encodes the “very large G protein-coupled receptor 1”, composed of ~6300 amino acids including a very large extracellular domain, 7 transmembrane domains and a highly conserved cytoplasmic carboxyl terminus. Mutations of the VLGR1 gene are associated both with Usher syndrome type 2C in humans, characterized by moderate to severe hearing loss and retinitis pigmentosa, and with audiogenic seizures in mice.

In this study, auditory brainstem responses (ABRs), distortion product otoacoustic emissions (DPOAEs), and microscopy were used to assess the integrity of the auditory periphery of VLGR1 mutant mice produced through targeted mutagenesis of the transmembrane and cytoplasmic domains (VLGR/del7TM). Although waveform morphology of ABRs recorded from affected animals appeared normal at stimulus levels exceeding 110 dB SPL, homozygous mutant animals were profoundly impaired, with thresholds in the range of 100 dB SPL across the audible frequency range. DPOAEs were not detected in mutant animals.

Consistent with functional studies, light microscopy demonstrated extensive cochlear pathology in two-month-old mutant mice. Significant outer hair cell loss in the basal half of the cochlea became progressively worse in more basal regions. Additionally, both inner hair cells and pillar cells were lost in the extreme base, leading to complete collapse of the end organ in affected areas. Examination of 20-day-old mutant mice suggests the inaugural pathology involves the integrity of stereociliary bundles associated with both inner and outer hair cells.

These findings confirm that VLGR1 mutations cause deafness in mice as well as humans and support the view that VLGR1 plays a crucial role in the maintenance of cochlear function.

Supported by NIH DC04566.

## **298** Development of Summating Potentials in Normal and Hypothyroid (Tshrhyl Mutant) Mice

JoAnn McGee<sup>1</sup>, Noelle Feldbauer<sup>1</sup>, Edward J. Walsh<sup>1</sup>

<sup>1</sup>Boys Town National Research Hospital

Like cochlear microphonic (CM) potentials, summating potentials (SP) can be elicited from normal animals by intense airborne sounds at least one day before auditory brainstem responses (ABR) can be reliably elicited in neonatal, altricial mammals, like the mouse. During the earliest responsive period, SPs dominate evoked potential records containing both SP and the ABR. In addition, the interval between the onset of the SP and ABR Wave I decreases in early maturational stages as neural elements underlying the response acquire adultlike properties. These findings collectively suggest that cochlear systems

develop earlier than do retrocochlear, neural systems underlying peripheral responsiveness. As with ABR, SP develops later in hypothyroid mice than in normal animals and findings reported here suggest that both neural and sensory abnormalities contribute to observed otological deficits.

The animal model used to evaluate the development of SP and ABR in hypothyroid animals was the *Tshr<sup>hyt</sup>* mutant mouse. A single locus autosomal recessive mutation in a membrane spanning segment of the thyrotropin receptor results in profound, congenital thyroid gland hypoplasia in affected individuals and that condition leads to profound congenital hypothyroidism when the trait is expressed in the homozygous state.

SPs and ABRs were acquired simultaneously from anesthetized mice using standard evoked potential methods. As in normal animals, SP dominated the record in young hypothyroid mice, but it is notable that SP thresholds were typically lower than ABR thresholds in a subset of relatively young animals. These findings suggest that hypothyroidism associated acoustic insensitivity is complex, with both sensory and neural contributions.

Research was supported by NIDCD grant DC04566.

## **299** Usherin Binding to Integrins Mediates Both Cell Adhesion and Cell Signaling: Usherin Interaction with A1B1 Integrin is Central to Usherin Function.

Gautam Bhattacharya<sup>1</sup>, Michael Anne Gratton<sup>2</sup>, Daniel Meehan<sup>1</sup>, Delimont Duane<sup>1</sup>, Edward Walsh<sup>1</sup>, JoAnn McGee<sup>1</sup>, **Dominic Cosgrove<sup>1</sup>**

<sup>1</sup>Boystown National Research Hospital, <sup>2</sup>University of Pennsylvania

Usher syndrome type IIa is the most common of the Usher syndromes, and thus the leading single genetic cause of combined deafness and blindness in the world. The gene responsible encodes a novel basement membrane protein we named usherin. In recently published work, we used biochemical characterization to show that usherin specifically interacts with type IV collagen, and that the interaction stabilizes usherin in the basement membrane superstructure. Usherin also specifically interacts with integrins a1b1, a3b1, and a5b1 on retinal pigment epithelial cells, and integrin a3b1 and a5b1 on stria marginal cells. We have created usherin knockout mice, and through parallel analysis found that usherin knockout mice and integrin a1-null mice both display a similar progressive retinal pathogenesis. This data suggests that retinal pathogenesis for both of these animal models is rooted in a progressive alteration of retinal pigment epithelial (RPE) cell function. We have established and qualified RPE cell culture systems from normal mice, usherin knockout mice, and integrin a1 knockout mice. Using these systems, we show that absence of the usherin protein from matrix results in dysregulation of specific matrix metalloproteinases, which appears linked to integrin a1b1 signaling. This may contribute to the observed retinal pathogenesis in the two knockout mice. While we observe a structural abnormality in the stria vascularis of

usherin knockout mice, there is no change in ABR thresholds out to nine months of age. RPE cells from normal mice adhere significantly better to testicular basal lamina from normal mice compared to that from usherin knockout mice, demonstrating a role for usherin in cell adhesion. The microvilliary processes of RPE cells from usherin knockout mice show focal detachment from the underlying basal lamina, consistent with the cell adhesion studies. These data support a central role for usherin/integrin interactions in both cell adhesion and cell signaling.

(Supported by R01 DC04844 and R01 DC006442)

### **300 Anti-Clarin-1 AAV-CBA-Delivered Ribozymes Induce Apoptosis in the Cochlea of Mouse**

**AA Aarnisalo**<sup>1</sup>, L Pietola<sup>1</sup>, J Joensuu<sup>1</sup>, J Isosomppi<sup>2</sup>, A Dinculescu<sup>3</sup>, AS Lewin<sup>3</sup>, WW Hauswirth<sup>3</sup>, E-M Sankila<sup>2,4</sup>, J Jero<sup>1</sup>

<sup>1</sup>Dept. ORL, Univ. Helsinki, Finland, <sup>2</sup>Biomedicum Helsinki Folkhalsan Institute of Genetics, Helsinki, Finland, <sup>3</sup>Dept. Ophthalmology and Molecular Genetics, Univ. Florida Gainesville, Florida, USA, <sup>4</sup>Dept Ophthalmology, Univ. Helsinki, Finland

Usher's syndrome type III (USH3A) is caused by mutations in the gene encoding Clarin-1. In USH3A the hearing loss and retinitis pigmentosa are progressive, with variable vestibular function. Clarin-1 is a member of the transmembrane 4 superfamily (TM4SF) and it is expressed in the organ of Corti and spiral ganglion cells of the mouse. We have used an AAV-2 vector containing ribozymes to knock-down the level of clarin-1 mRNA in the cochlea.

Three hammerhead ribozymes were designed to specifically recognize and cleave wild type mouse clarin-1 mRNA. Rz 166, which cuts right before the start codon following the GUC triplet, was used for inner ear micro-injections. By using a micromanipulator and a microinjector we injected 1 µl of the AAV-2-Rz or a control AAV-2 vector containing GFP marker gene to cochlea of CD-1 mice. The survival times were 1 week and 1 month. The animals were perfusionfixed transcardially and cochleas were removed. Perilymphatic fixation was also used. The cochleas were mounted in paraffin and sectioned.

AAV-GFP showed expression in the organ of Corti, stria vascularis and in the endothelial cells lining the scala vestibuli and tympani. Also few vestibular epithelial cells showed fluorescence for GFP. The apoptotic effect of anti-clarin-1 AAV-CBA-delivered ribozymes was evaluated with TUNEL-staining. After one month apoptotic hair cells and apoptotic cells in the stria vascularis were seen. Significantly less apoptotic cells were found in the cochleas of the control animals. Also apoptotic cells in the vestibular epithelium were observed. However, no apoptotic ganglion cells were seen.

As a TM4SF protein, clarin most probably acts on the postsynaptic surface. The cleavage of clarin-1 mRNA by the vector-delivered ribozymes seems to induce apoptosis. The ganglion cells showed no apoptosis, which can be due either to the injection technique or viral vector used. The

role of apoptosis in the progression of USH3A needs further evaluation.

### **301 A Histological Study of the German Waltzing Guinea Pig**

**Paula Mannström**<sup>1</sup>, Zhe Jin<sup>1</sup>, Leif Järlebark<sup>1</sup>, Mats Ulfendahl<sup>1</sup>

<sup>1</sup>Center for Hearing and Communication Research, Karolinska Institutet

The German waltzing guinea pig is a new strain of animal exhibiting balance problems and profound deafness. The homozygous animals are deaf from birth except at the lowest frequencies in the newborn animals. The inheritance is autosomal recessive and the heterozygotes (carriers) appear to have normal vestibular and auditory functions. However, the carriers are less susceptible to noise as compared to normal animals [Skjönsberg et al., in prep].

In this study the structural changes in the cochlea were characterized using both light and electron microscopy in adult waltzers and at different embryonic stages. In the adult cochlea, Reissner's membrane had collapsed over the organ of Corti. The sensory cells had degenerated and the stria vascularis was thinner as compared to normal animals. Flatmount preparations of the stria vascularis showed that the pigment granules appeared in clusters rather than in a network pattern as in normal animals. The embryonic development of these animals appeared normal until around embryonic day 40 when changes in stria vascularis were observed. The cell layer was thinner and narrower, and the intercellular spaces appeared wider. In addition, Reissner's membrane was starting to fall down onto the organ of Corti. At this stage, the sensory cells showed no signs of degeneration suggesting that the hair cell changes occur secondary to strial damage. The heterozygotes showed no histological alterations.

It is suggested that a genetic defect manifested during the development of stria vascularis disturbs the ionic composition of the endolymph, which causes the Reissner's membrane to collapse.

### **302 Progression of Inner Ear Pathology in Ames Waltzer Mice**

**Karen Pawlowski**<sup>1,2</sup>, Charles G. Wright<sup>1</sup>, Kumar N. Alagramam<sup>3</sup>

<sup>1</sup>University of Texas Southwestern Medical Center,

<sup>2</sup>University of Texas at Dallas, <sup>3</sup>Case Western Reserve University

We examined several lines of Ames waltzer mice, which vary in the nature of their mutation, to determine if the variation in extent of pathology correlated with the extent of genetic mutation. The severity of changes in the inner ear correlated positively with the extent of mutation in the Pcdh15 gene from postnatal day 2 (P2) up to 12 months. By evaluating cellular and subcellular changes that correlate with the severity of the mutation in several Pcdh15 alleles, we can better determine the role of Pcdh15 in the development of the organ of Corti. Mice harboring in-frame deletion mutations (Pcdh15av-J and

Pcdh15av-2J) had less disorganization of stereocilia and cuticular plates in the organ of Corti than the presumptive functional null alleles (Pcdh15av-3J and Pcdh15av-Tg) at P2-P10. The difference in severity of changes was also seen by light microscopy in immature (P15-P20), adult (P25-P50) and older adult (6.5 – 12 months) animals, where mice harboring mutations Pcdh15av-J and Pcdh15av-2J had slightly less severe organ of Corti damage, less spiral ganglion cell loss, less saccular damage, and fewer changes in the spiral ligament, spiral limbus and stria vascularis than those harboring mutations Pcdh15av-3J and Pcdh15av-Tg. Electron microscopic analysis suggests the location of the earliest pathology in the auditory system due to mutation of Pcdh15 in Ames waltzer mice is in inner and outer hair cell cuticular plates. The abnormalities include disorganization of the stereocilia, the actin mesh within the cuticular plate and, in severe cases, displacement of the kinocilium and alteration of the shape of the cuticular plate. Observed changes in the cuticular plate could reflect changes in hair cell structure that affect the organization of the stereocilia. Observed changes in tissues other than the organ of Corti could reflect the effect of the Pcdh15 mutation on these structures since they also express Pcdh15. Research supported by a grant from NIDCD to KA.

### **303 Morphological Analysis of Ames Waltzer (av) Mice and Developmental and Spatial Expression of Protocadherin 15**

Yayoi S. Kikkawa<sup>1</sup>, Karen S. Pawlowski<sup>1,2</sup>, Charles G. Wright<sup>1</sup>, Kumar N. Alagramam<sup>3</sup>

<sup>1</sup>Dept. Otolaryngology-HNS, University of Texas Southwestern Medical Center, Dallas, TX., <sup>2</sup>Behavior and Brain Science, University of Texas at Dallas, TX., <sup>3</sup>Dept. Otolaryngology-HNS, Case Western Reserve University, Cleveland, OH.

The Ames waltzer (*av*) mouse is a model for Usher syndrome 1F (USH1F) that develops deafness and vestibular dysfunction associated with disorganized inner ear stereocilia. Observations with light and scanning electron microscopy show disruption of the cuticular plate during development, followed by degeneration of the organ of Corti and subsequent spiral ganglion cell loss.<BR>

To detect the onset of cuticular plate disorganization in *av* mice, we studied morphology of hair cells during early development (E17.5-P10) by electron microscopy and cytoskeletal arrangement in the hair cell was studied by phalloidin staining of whole-mount mouse cochlea. The *av* mice showed delayed development and improperly oriented stereocilia bundles as early as P0.<BR>

The gene that harbors the *av* mutation is protocadherin 15 (*Pcdh15*). *Pcdh15* is predicted to be a transmembrane protein and it is suspected to be involved in cell-cell interaction and signal transduction. To localize the expression of *Pcdh15* and relate the timing of the expression of *Pcdh15* to the timing of the first appearance of the phenotype, we applied immunohistochemical methods to the wild type mice to determine its expression pattern. The most consistent labeling was seen on the lateral side of the inner hair cell, either in a supporting cell

or in the nerve endings, and in the spiral ligament and the spiral ganglion. The surface of the cuticular plate was also labeled in the tissues from younger animals. These results suggest *Pcdh15* is one of the critical components in a pathway required for normal development and organization of the cuticular plate structures. *Research supported by a grant from NIDCD to KA.*

### **304 Progressive Hearing Loss is Linked to Genetic Ablation of BK Channel A-Subunit**

Marcus Mueller<sup>1</sup>, Matthias Sausbier<sup>2</sup>, Marlies Knipper<sup>1</sup>, Peter Ruth<sup>2</sup>, Markus Pfister<sup>1</sup>

<sup>1</sup>Otolaryngology, University of Tübingen, Elfriede Aulhornstr. 5, Tübingen, Germany, <sup>2</sup>Institute of Pharmacology, University of Tübingen, Auf der Morgenstelle 8, Tübingen, Germany

The large-conductance voltage- and calcium-activated potassium (BK) channel is expressed in inner (IHC) and outer hair cells (OHC). An important role of BK channels in mammalian cochlear neurotransmission at the presynaptic level was established: BK channels are a major player in repolarizing IHCs (Rüttiger et al., PNAS 2004). Mice deficient in BK channel  $\alpha$ -subunit (BK  $\alpha$ -/-) developed a progressive high-frequency hearing loss starting at an age of 2 months, concomitant with a progressive OHC degeneration. In this study, we extended hearing analysis in wild-type (wt) and BK  $\alpha$ -/- mice by measuring audiograms over a period of 15 months. In addition to the high-frequency hearing loss, BK  $\alpha$ -/- mice older than 6 month revealed also a low-frequency hearing loss. The hearing loss was progressive at all measured frequencies, resulting in a complete deafness of BK  $\alpha$ -/- mice older than 12 months. The present data clearly show that lack of BK channel  $\alpha$ -subunit in the inner ear leads to a progressive hearing loss starting in adult mice. In conclusion, BK channel  $\alpha$ -subunit is not necessary for normal development of hearing in mice, but for maintaining normal hearing function in adult mice. Thus, mutations in the BK channel  $\alpha$ -subunit encoding gene *slo 1* may be a susceptibility factor for progressive deafness in humans. Supported by Fortune-Foundation

### **305 Functional and Morphological Examinations of a Mouse Model Created by a Conditional Knockout of GJB2 Gene**

Takashi Iizuka<sup>1</sup>, Katsuhisa Ikeda<sup>1</sup>

<sup>1</sup>Juntendo university

Hereditary deafness affects about 1 in 2,000 children and mutations in the GJB2 gene are the major cause in various ethnic groups. GJB2 encodes connexin26, a putative channel component in cochlear gap junction. However, the pathogenesis of hearing loss caused by the GJB2 mutations remains obscure. The generation of a mouse model to study the function of connexin26 during hearing has been hampered by the fact that *gjb2* knockout mice are embryonic lethal. We generated targeted disruption of *gjb2* using Cre recombinase controlled by P0. Targeted disruption of *gjb2* caused profound deafness. Auditory brainstem response (ABR) derived from tone bursts in



knockout mice resulted in elevation of threshold by 60 to 80dB in all frequencies (8,12,16,20kHz). Histological analysis showed collapse of the organ of Corti in the mutant mice, and this collapse may be due to disruption of gap junction of Cx26, but not tight or adherens junctions. Eventually, apoptotic changes are suggested to result in the cell death of the organ of Corti.

### **306 Connexin Permeability Defects and Hereditary Deafness**

Valeria Piazza<sup>1</sup>, Martina Beltramello<sup>1</sup>, Feliksas Bukauskas<sup>2</sup>, Fabio Mammano<sup>1,3</sup>

<sup>1</sup>Venetian Institute of Molecular Medicine, Padova, Italy,

<sup>2</sup>Department of Neuroscience, Kennedy Center, Albert Einstein College of Medicine, <sup>3</sup>Department of Physics, Padova, Italy.

The most common forms of genetic deafness have been prevalently associated with mutations in connexin 26 (Cx26). We have compared the V84L and the related V95M mutants of human (h)Cx26, as both consist in the substitution of a highly conserved valine. In dual patch-clamp recordings, the mean intercellular conductance of V84L was higher ( $g_j=45\pm 15nS$ , mean $\pm$ S.D.,  $n=13$ ) than in the wt hCx26 controls ( $g_j=27\pm 15nS$ ,  $n=9$ ). However the rate of  $[Ca^{2+}]_i$  elevation in cell n.2, due to injection of  $IP_3$  (100-500  $\mu M$ , MW 420) in cell n.1 of a coupled pair was reduced by 66% in V84L compared to controls. The V95M mutant showed lack of  $IP_3$  transfer, paralleled by null electrical conductance. Our data revealed a highly significant,  $91\pm 4\%$  reduction of the apparent permeability coefficient to  $IP_3$  [ $p_j=P/g_j$ ], i.e. total permeability,  $P_j$  ( $cm^3/sec$ ), normalized to the indirect index of channel number,  $g_j$ ] in V84L compared to wt hCx26. Surprisingly, we found no difference in the diffusion of Lucifer Yellow (LY, MW 443), between HeLa cells expressing wt hCx26 or V84L. To probe the relevance of our findings for the patho-physiology of the inner ear, we exploited organotypic cultures of the rat cochlea. Delivery of  $IP_3$  via the patch pipette (100-500  $\mu M$ ) to a single Hensen's cell in the organ of Corti bathed in suramine (200  $\mu M$ ), resulted in the rapid elevation of the  $[Ca^{2+}]_i$  in the patched cell, and  $Ca^{2+}$  signals propagated to the nearest neighbours. Delivering  $IP_3$  to a single Hensen's cell (100  $\mu M$ ) in a naïve organ culture elicited a  $[Ca^{2+}]_i$  elevation in the patched cell followed by a complex pattern of oscillations in the surrounding cells. Our experiments with HeLa cells and cultures of inner ear sensory epithelium show that point mutations in Cx26 that leave electrical communication intact yet reduce metabolic coupling mediated by  $IP_3$ . By blocking the propagation of calcium waves through support cells of the organ of Corti, these mutations hinder the formation of a functional syncytium.

### **307 Development of a COCH "Knock-In" Mouse Model for DFNA9**

Nahid Robertson<sup>1</sup>, Theru Sivakumaran<sup>1,2</sup>, Sara Hamaker<sup>1</sup>, Cynthia Morton<sup>1,2</sup>

<sup>1</sup>Brigham and Women's Hospital, <sup>2</sup>Harvard Medical School  
Four missense mutations in the FCH/LCCL domain of COCH have been found in the dominantly-inherited

deafness and vestibular dysfunction at the DFNA9 locus. Two other missense mutations have been reported in the same domain in two simplex cases. Because of the late-onset and progressive nature of DFNA9, and accumulation of abnormal acidophilic deposits in DFNA9-affected inner ears, we speculated that COCH mutations act in a dominant negative fashion. Therefore, to create a mouse model that would most closely replicate DFNA9, we decided to generate a mouse "knock-in" by introducing one of the COCH missense mutations (G88E).

The targeting construct consists of ~5.6kb of 129/SvJae (agouti color) mouse *Coch* genomic sequence spanning introns 3 to 8. A neomycin positive selection cassette, flanked by loxP sites, was introduced into intron 5, and a thymidine kinase was placed upstream for negative selection. A short homologous recombinant arm of ~1.7kb and a long arm of ~3.9kb are at either side of *neo*. Transfection of J1 embryonic stem (ES) cells with the *Coch* mutant construct was performed. Screening of 240 ES cell clones revealed four homologous recombinants. The integrity of the recombination, the loxP sites, the mutation, and exons were confirmed by PCR, Southern blot analysis, and sequencing.

Two ES cell clones (#68 and #160) that had homologous recombination and no detectable sequence alterations were micro-injected into C57BL/6 (black coat color) blastocysts for implantation into pseudopregnant females. Clone # 160 yielded only two pups, despite implantation of a total of ~100 blastocysts into eight recipients. The male pup (50% chimeric) was bred to six C57BL/6 females resulting in a total of 36 offspring, all with black color, indicating that germline transmission of the targeting construct is not likely to have occurred. Micro-injection of clone #68 has resulted in 18 chimeric pups (11 male, 7 female) which have not yet been assessed for germline transmission.

### **308 Cochlear Defects in Deaf Gata3 Mice, a Model for HDR Syndrome.**

J.Hikke van Doorninck<sup>1</sup>, Marjolein van Looij<sup>1,2</sup>, Ruben van der Giessen<sup>1</sup>, Jacqueline van der Wees<sup>3</sup>, Frank Grosveld<sup>3</sup>, Chris I de Zeeuw<sup>1</sup>

<sup>1</sup>Dpt Neuroscience, Erasmus MC, <sup>2</sup>ENT Erasmus MC, <sup>3</sup>Dpt Cell Biology, Erasmus MC

The transcription factor GATA3 is essential for multiple organs: mutation of a single allele causes hypoparathyroidism, deafness and renal dysplasia in patients, called HDR syndrome. A similar phenotype is observed in genetically modified mice that carry a mutated *Gata3* allele. While deletion of both *Gata3* alleles leads to a complete absence of otic vesicle development and early death of the embryo, heterozygous *Gata3* mice show hearing loss from postnatal day 16 onwards. These mice can therefore serve both as a model to study deafness in the HDR syndrome and to study the function of GATA3 in general. Analysis of adult *Gata3* heterozygous mice shows a progressive degeneration of the organ of Corti. We did not see any morphological or physiological abnormalities in the brains of mutant mice and therefore conclude that the hearing loss is of cochlear origin. A direct assay of

outer hair cell function by measuring otoacoustic emissions showed a clear deficit in *Gata3* heterozygous mice to respond to sound. To investigate the hair cell phenotype further we did light and EM microscopy that revealed specific vacuoles in *Gata3* mutant outer hair cells associated with degeneration. Scanning EM showed aberrant morphology of the stereocilia on the cochlear hair cells in young mutant mice but a functional test of the transduction channel by FMI-43 loading did not show differences between mutant and wild type mice.

### **309** Bilirubin Ototoxicity in Jaundiced Gunn Rats Evaluated by ABR and DPOAE

Hee-Yeon Shim<sup>1</sup>, Jihwan Woo<sup>1</sup>, Young Ju Sung<sup>2</sup>, Sang Min Lee<sup>1</sup>, In-Young Kim<sup>1</sup>, Yang-Sun Cho<sup>2</sup>, Won-Ho Chung<sup>2</sup>, Sung Hwa Hong<sup>2</sup>

<sup>1</sup>Department of Biomedical Engineering, College of Medicine, Hanyang University, Seoul, Korea, <sup>2</sup>Department of Otorhinolaryngology-Head & Neck Surgery, Sungkyunkwan University School of Medicine

Accumulation of unconjugated bilirubin, especially in newborns, in the central auditory pathway and basal ganglia may cause neurological damage and deafness. Effect of unconjugated bilirubin on the brain is known well through auditory brainstem responses (ABRs). However, effect of unconjugated bilirubin on the cochlea is not defined completely. This study was performed to evaluate the bilirubin ototoxicity using ABR and DPOAE in jaundiced Gunn rats before and after sulfadimethoxine injection.

Experiments were conducted on littermate P19(postnatal 19 days) homozygous(jj) and one heterozygous(nj) Gunn rats, five littermate P21 jj and one littermate nj Gunn rats. P21 jj and nj Gunn rats were re-tested in three weeks in the same condition. DPOAE in Sprague Dawley rats was measured for comparing with the results from Gunn rat experiments. ABRs were measured with auditory stimuli of 100-microsecond pulse width click and DPOAEs were measured at 8kHz, 16kHz and 22kHz before and after sulfadimethoxine.

Thresholds of ABR were increased in P19 and P21 groups starting within the first day after injection and became normalized at 10 days after injection. The interwave intervals I ?III and I ?V were increased and normalized. Even though sulfadimethoxine injection induced significant ABR abnormalities in P19 and P21 groups, no DPOAE abnormalities were found in these groups. Unconjugated bilirubin induced pathologic changes at or higher than the brainstem level with intact cochlear function. ABR abnormalities were only observed in P19 and P21 groups because the level of bilirubin in blood is higher and the central auditory pathway is more immature than P42 group. We also found the possibility of spontaneous reversibility of the hyperbilirubinemia-related ototoxicity.

This work was supported by grant No. (R01-2002-000-00392-0 ) from the Basic Research Program of the Korea Science & Engineering Foundation.

### **310** Otoacoustic Emissions Measured in Rhesus Monkeys (*Macaca Mulatta*) and Spotted Hyenas (*Crocuta Crocuta*)

Dennis McFadden<sup>1</sup>, Edward G. Pasanen<sup>1</sup>, Jessica Raper<sup>2</sup>, Kim Wallen<sup>2</sup>, Mary L. Weldele<sup>3</sup>, Stephen E. Glickman<sup>3</sup>, Ned J. Place<sup>3</sup>

<sup>1</sup>Dept of Psychology, Center for Perceptual Systems, University of Texas, Austin, TX 78712, <sup>2</sup>Yerkes National Primate Research Center, Dept of Psychology, Emory University, Atlanta, GA, <sup>3</sup>Dept of Psychology, University of California, Berkeley, CA 94720

In humans, otoacoustic emissions (OAEs) are generally stronger in females than in males and stronger in right ears than in left. These differences exist in newborns as well as in adults, strongly implying that the sex differences are attributable, at least in part, to prenatal hormonal mechanisms. Specifically, it appears that prenatal exposure to high levels of androgens weakens the cochlear amplifiers and thus the OAEs. Little is known about sex and ear differences in the OAEs of other species. Both CEOAEs and DPOAEs were measured in 33 female and 27 male rhesus monkeys (located at Yerkes NPRC in Atlanta) and in 13 female and 14 male spotted hyenas (located at UC Berkeley). Most of the rhesus monkeys were tested on multiple occasions at different points in the annual breeding cycle.

In rhesus, CEOAEs were significantly stronger in females than in males; DPOAEs were also stronger in females, but not significantly. Similar effects are seen in humans. This has implications for the Shera and Guinan argument about the specific cochlear mechanisms contributing to the different types of OAE. The magnitude of the sex difference fluctuated seasonally because the OAEs for the male rhesus became weaker during the breeding season when androgen levels would be the highest. Thus, we have evidence for both organizational and activational effects of hormones on OAEs.

Spotted hyenas are highly unusual among mammals in that the females are larger than the males, are dominant over the males, and have genitalia that are highly masculinized. This masculinization begins during prenatal development, and is known to involve exposure to high levels of androgens prenatally. If prenatal androgen exposure does weaken the cochlear amplifiers, then the OAEs in female spotted hyenas should not follow the human (and rhesus) pattern of being stronger than in males. In fact, both the CEOAEs and DPOAEs in spotted hyenas showed no sex (or ear) differences.

Supported by NIDCD grant.

### **311** In Search of a Harmonic Distortion Mechanism

Jill Lodde<sup>1</sup>, Robert Withnell<sup>1</sup>

<sup>1</sup>Indiana University

The 2f1-f2 distortion product otoacoustic emission (DPOAE) is thought to arise primarily from the complex interaction of components that come from two different cochlear locations. Such distortion has its origin in the nonlinear interaction on the basilar membrane of the

excitation patterns resulting from the two stimulus tones, f1 and f2. Fahey et. al. (2000) suggest that this view for the origin of the 2f1-f2 DPOAE is incomplete and that this distortion product may also be produced as a quadratic difference tone, the cochlear harmonic of f1 interacting nonlinearly with the f2 excitation pattern. We measured the 2f1-f2 DPOAE in guinea pig before and after acoustically traumatizing the basal region of the cochlea (the origin of the harmonic of f1). Pure tone stimuli, f1 and f2, were presented with an onset phase difference of 90 degrees, the 2f1-f2 DPOAE obtained being an amplitude-modulated waveform;  $f_2/f_1 = 1.2$  and  $f_2 = 8000$  to  $8940$  Hz. Data will be analyzed by determining the equation of best fit for each amplitude-modulated 2f1-f2 DPOAE time domain waveform using a least-squares-fit technique and equations of best fit compared pre and post acoustic trauma for each 2f1-f2 DPOAE. The results of the analysis will be discussed in terms of a harmonic mechanism contributing to the guinea pig DPOAE.

### **312** Level Dependent Changes in the Generator and Reflection Components of DPOAE

Glenis Long<sup>1</sup>, Carrick Talmadge<sup>2</sup>, Jungmee Lee<sup>1</sup>

<sup>1</sup>Graduate Center CUNY, <sup>2</sup>University of Mississippi

The effects of changes in primary level on DPOAE are evaluated using frequency-modulated primaries (log frequency sweeps) which maintain a constant frequency ratio (Long et al., 2004, ARO Midwinter Meeting Abstr. 102). We use 8s/octave sweeps to evaluate the DPOAE fine structure, and 2s/octave sweeps to evaluate the generator component alone. The reflection component is examined using vector subtraction and IFFT analysis of the 8s/octave data. Using this procedure we have obtained data over a wide range of levels ( $L_2=20-80$  DB SPL.  $L_1=39\text{dB}+0.4*L_2$ ) and frequencies ( $f_2$  sweeping from 1000-4000,  $f_2/f_1=1.22$ ) in one session, permitting evaluation of changes in the relative level of components with level. We also test the hypothesized changes in the fine structure and phase of DPOAE at higher primary levels (Talmadge et al., 2000:JASA,108:2911-2932)

### **313** OpenDP: A DPOAE System with Specifiable Stimulus Parameters

Edward Smith<sup>1</sup>, Sandra Gordon-Salant<sup>1</sup>, Erin McAlister<sup>1</sup>, Robert Dooling<sup>1</sup>

<sup>1</sup>University of Maryland at College Park

This presentation describes development of a DPOAE research system called OpenDP.

The impetus for designing this platform was to permit operator control of virtually all stimulus parameters. The software is implemented using Matlab. End users customize stimulus generation and analysis to meet specific research needs using clear interface windows. System hardware consists of a TDT RP2.1 real-time processor and an Etymotics Research ER10c microphone/dual sound source.

Features of the system and design techniques to achieve valid DP results will be detailed. These features include

parameters of the primaries, data collection procedure, and analysis techniques. Noise rejection is accomplished after data collection, allowing the user to select the basis for noise rejection – time domain or frequency domain. Sample data will show the effects of these options.

Pilot data will be presented that compare results obtained with OpenDP and two clinical systems using a common clinical protocol. Analyses of results suggest that data obtained from individuals with normal hearing using OpenDP are comparable to those obtained with clinical DPOAE systems, when stimuli, data collection, and analyses are defined similarly. Advantages and new directions of the OpenDP system will be summarized.

OpenDP system development is supported by NIH grant DC 04664.

### **314** Temperature Dependence of Distortion Product Otoacoustic Emission in the Frog: Differences Between the Amphibian and the Basilar Papilla

Sebastiaan W. F. Meenderink<sup>1</sup>, Pim Van Dijk<sup>2</sup>

<sup>1</sup>University Maastricht, Dept. of ORL, Maastricht, The Netherlands, <sup>2</sup>University Hospital Groningen, Dept. of ORL, Groningen, The Netherlands

The frog inner ear includes two papillae with high sensitivity to airborne sound: the amphibian papilla and the basilar papilla. The amphibian papilla is sensitive to low frequencies ( $100 < CF < 1200$  Hz in *R. pipiens*) and the basilar papilla is tuned to a higher frequency ( $1500 < CF < 2000$  Hz in *R. pipiens*). Both papillae generate distortion product otoacoustic emissions (DPOAEs), but only the amphibian papilla is presumably involved in the generation of spontaneous otoacoustic emissions. Furthermore, DPOAEs from the amphibian papilla are more sensitive to physiological insults than those from the basilar papilla. These differences have led to the hypothesis that DPOAEs from the basilar papilla result from a passive nonlinearity. If so, these emissions would not rely on biochemical energy sources and their generation may be independent on temperature.

We measured DPOAEs from the amphibian and basilar papilla in the frog, *Rana pipiens pipiens*. Extensive measurements of DPOAE level for a range of  $L_1$  and  $L_2$  levels were performed. In the amphibian papilla, the amplitude of DPOAEs evoked with low stimulus levels showed a clear dependence on the temperature of the animal. In contrast, DPOAEs from the basilar papilla did not exhibit such dependence on temperature.

We infer that DPOAEs from the basilar papilla apparently do not depend on biochemical energy sources, and thus cannot result from an active mechanism. These results place the frog's basilar papilla in a possibly unique position within vertebrate hearing: no other hearing organ, including the frog's amphibian papilla, is thought to rely on passive hearing mechanisms alone. Given the poikilothermic nature of frogs, the passive basilar papilla provides the frog with consistent spectral information, regardless of ambient and body temperature.

### **315 Optimal Stimulus Parameters for Recording Distortion Product Otoacoustic Emissions (Dpoaes)**

Tiffany Johnson<sup>1</sup>, Stephen Neely<sup>1</sup>, Cassie Garner<sup>1</sup>, Michael Gorga<sup>1</sup>

<sup>1</sup>Boys Town National Research Hospital

Using a new method for recording DPOAE responses with continuously varying stimulus levels (Neely et al., 2004), we investigated the combined influence of primary-level differences ( $L_1$ - $L_2$ ) and primary-frequency ratio ( $f_2/f_1$ ) on DPOAE level. DPOAE responses were recorded in 20 subjects with normal hearing for the following stimulus conditions:  $f_2 = 1, 2, 4,$  and  $8$  kHz;  $f_2/f_1 = 1.05$  to  $1.4$  in steps of  $0.05$ ; 4 different relationships between  $L_1$  and  $L_2$ , including a path individually optimized to produce the largest DPOAE. The results suggest that the  $L_1$ - $L_2$  producing the largest DPOAE level varies with other stimulus parameters. For broadly spaced primaries at low  $L_2$ 's, the largest DPOAE level was obtained when  $L_1$  was much higher than  $L_2$ , with  $L_1$  remaining relatively constant as  $L_2$  increased. As  $f_2/f_1$  decreased, optimal DPOAE levels were observed when  $L_1$  was closer to  $L_2$ , and increased as  $L_2$  increased. A mean-optimal  $L_1$ - $L_2$  was derived from the average of the individually optimized  $L_1$ - $L_2$  for each stimulus condition. For every stimulus condition, average DPOAE levels for the mean-optimal  $L_1$ - $L_2$  were equivalent to or larger than those observed for other primary-level combinations, including those defined by the scissor paradigm (Kummer et al., 1998) and those in which  $L_1$ - $L_2 = 10$  dB for all  $L_2$ 's. The largest DPOAE levels at all  $f_2$ 's were observed for  $f_2/f_1$  between  $1.15$  and  $1.3$ , with a tendency for the ratio to decrease as  $f_2$  increased. Taken together, these results indicate that the  $L_1$ - $L_2$  and  $f_2/f_1$  values that typically have been recommended for recording DPOAE responses do not result in the largest average DPOAE levels in subjects with normal hearing. [Work supported by the NIH – NIDCD R01-DC02251, T32-DC00013, P30-DC04662].

### **316 Measurement of Distortion Product Otoacoustic Emissions (Dpoaes) by using an External Acoustic Canal Model of Mice**

Yuya Narui<sup>1</sup>, Katsuhisa Ikeda<sup>1</sup>

<sup>1</sup>Juntendo university

In recent years many studies regarding the measurement distortion product otoacoustic emissions (DPOAEs) in mice were performed for researching inner ear functions (outer hair cell functions), although most reports have utilized the same instrumentation as that used in human. There are some problems due to the differences of external auditory canal (EAC) and audible frequencies. In order to resolve such problems, we designed an EAC model.

First, EAC of a mouse is smaller and more complex than that of human. An external diameter is about 2mm and the narrowing portion exist at about 2mm distant from tympanic membrane in EAC of a mouse, therefore the shape and size of ear probe must be appropriate for the

vibration of the air that transmitted from the tympanic membrane.

The second is the decline of sound pressure due to the reduced size of probe. By using an EAC model high frequency sound ( $>7$  kHz) has been difficult to detect from reduced probe. In order to resolve those problems we improved the probe and the EAC model, and we measured sound pressure at side of tympanic membrane in the EAC model output from probe and opposite position. The detailed results will be presented.

### **317 Spectral Features of Low-Frequency Modulation of DPOAEs**

Lin Bian<sup>1</sup>, Mark Chertoff<sup>1</sup>

<sup>1</sup>University of Kansas Medical Center

A low-frequency bias tone can modulate distortion product otoacoustic emissions (DPOAEs). As a result of biasing cochlear transducer, the temporal feature of DPOAEs is an amplitude modulation (AM) of the distortion products (DPs). Within a half cycle of the bias tone, the typical modulation patterns of the DPs show shapes of the appropriate derivatives of the sigmoid-shaped transducer function (Bian et al., 2004, JASA 115:2159). This leads to possibilities of non-invasively obtaining the cochlear transducer function from DPOAEs. Since previous methods that measure the modulated DPOAEs are primarily focused on single DP frequency, little is known about the whole spectrum of the low-frequency modulation of DPOAEs. In gerbils, ear-canal acoustics were measured while presenting a two-tone signal and a 25-Hz bias tone with 20-Pa peak-amplitude. The spectral characteristics were examined with fast Fourier transformation and the DPOAEs were identified with an algorithm based on the formulation of DPs from a nonlinear system (Bian et al., 2002, JASA 112:198). The most prominent feature was the presence of sidebands around DPOAE frequencies. For a particular DP, there were 4-6 equally spaced frequency components within either the upper or lower sideband. For DPs up to the fifth order, the averaged total bandwidth was about 300 Hz. The largest amplitude of the sideband component in the sidebands was more than one half of the magnitude of the DP. The effects of primary level on the sideband components were examined. As carriers, the DPOAEs envelopes follow the variation in nonlinear characteristics of the cochlear transducer during low-frequency biasing. Therefore, demodulation of AM emissions would reveal the hair-cell transducer function inside the cochlea. Moreover, spectral analysis of AM emissions provides alternative means of deriving cochlear transducer functions with a variety of substitutes if one particular DP does not show a typical modulation pattern.

Supported by NIH-NIDCD grants: R03 DC006165 and R01 DC02117

### **318 Similarity of Group Delays of Basilar-Membrane Vibrations and Distortion-Product Otoacoustic Emissions in Chinchilla**

**Qin Gong**<sup>1</sup>, Andrei Temchin<sup>1</sup>, Jonathan Siegel<sup>1</sup>, Mario Ruggero<sup>1</sup>

<sup>1</sup>Northwestern University

Comparisons of distortion-product otoacoustic emissions (DPOAEs) and basilar-membrane (BM) vibrations simultaneously recorded in the same ears of chinchillas and gerbils indicate that the group delay of  $2f_1$ - $f_2$  DPOAEs ( $\tau_{\text{DPOAE}}$ ) measured with fixed  $f_2$  and swept  $f_1$  ( $\tau_{\text{swept-}f_1}$ ) is nearly identical to BM group delay at the characteristic frequency (CF),  $\tau_{\text{BMCF}}$ , at basal sites with CF =  $f_2$  [Narayan et al., ARO MWM Abstr. 21: 181, 1998; Ren, Nature Neurosci. 7: 333-334, 2004]. Recently, Ruggero (ARLO 5: 143-147, 2004) showed that  $\tau_{\text{swept-}f_1}$  and  $\tau_{\text{BMCF}}$  are also similar at other basal sites of the gerbil cochlea and at basal and apical sites of the guinea pig cochlea. Here we extend those findings by comparing  $\tau_{\text{DPOAEs}}$  and  $\tau_{\text{BMCFs}}$  for responses to moderate-level stimuli throughout the chinchilla cochlea.  $\tau_{\text{BMCFs}}$  were taken from the BM literature and also derived from Wiener-kernel analyses of responses to noise of auditory-nerve fibers (Temchin et al., ARO MWM Abstr. 18: 174, 1995). DPOAEs were stimulated by tones  $f_1$  and  $f_2$  ( $f_2 > f_1$ ) with  $f_2$  set at 25, 35 or 45 dB SPL and  $f_1$  level = 15 dB +  $f_2$  level.  $\tau_{\text{DPOAEs}}$  were measured from the slopes of  $2f_1$ - $f_2$  phase-vs.-frequency functions for fixed  $f_2$  & swept  $f_1$  ( $\tau_{\text{swept-}f_1}$ ) and fixed  $f_1$  & swept  $f_2$  ( $\tau_{\text{swept-}f_2}$ ). The dependencies of  $\tau_{\text{DPOAEs}}$  on frequency ( $\tau_{\text{swept-}f_1} = 2.135f_2^{-0.55}$  and  $\tau_{\text{swept-}f_2} = 2.587f_2^{-0.413}$ , with  $\tau$  expressed in ms and  $f_2$  in kHz) closely bracketed the  $\tau_{\text{BMCFs}}$  in the entire frequency range of comparison, 300 Hz-18 kHz. The arithmetic means of  $\tau_{\text{swept-}f_1}$  and  $\tau_{\text{swept-}f_2}$  were statistically indistinguishable from  $\tau_{\text{BMCF}}$  (see abstract by Siegel, Cerka, Recio-Spinoso, Temchin, van Dijk, and Ruggero, this ARO MW Meeting). This similarity between  $\tau_{\text{BMCF}}$  and  $\tau_{\text{DPOAE}}$ , consistent with the findings of Narayan et al. (op. cit.), Ren (op. cit.) and Ruggero (op. cit.), is not predicted by any established theory of DPOAE generation and raises the possibility that  $\tau_{\text{BMCFs}}$  in other species, including humans, can also be derived from DPOAE delays.

### **319 Mechanism Responsible for DPOAE Tuning**

**Paul Fahey**<sup>1</sup>, Barden Stagner<sup>2</sup>, Glen Martin<sup>2</sup>

<sup>1</sup>University of Scranton, <sup>2</sup>Jerry Pettis Memorial Veterans Medical Center

It is commonly observed that the levels of the  $2f_1$ - $f_2$  and the  $3f_1$ - $2f_2$  distortion product otoacoustic emissions (DPOAEs) show a bandpass shaped level versus frequency generation curve. For constant value of  $f_2$ , as  $f_1 \rightarrow f_2$  levels increase and then decrease. It has been hypothesized that this effect is due to: (1) a second filter, (2) suppression of distortion generation by the primary tones, (3) re-emission of distortion products from the distortion product place (on the basilar membrane), (4) the presence of an even order nonlinearity and (5) cancellation of the DPOAE due to the vector addition of multiple sources of distortion product. In this study distortion products are produced

under conditions where there will be minimal vector cancellation of multiple DPOAE sources. It is observed that under this condition, there is no or minimal bandpass shape of the DPOAE generation curve. Therefore, this data supports the hypothesis that the bandpass shape is due to vector cancellation from multiple sources.

### **320 The Allen-Fahey Experiment Extended**

**Egbert de Boer**<sup>1</sup>, Alfred Nuttall<sup>2,3</sup>, Ning Hu<sup>4</sup>, Yuan Zou<sup>2</sup>, Jiefu Zheng<sup>2</sup>

<sup>1</sup>Academic Medical Center, <sup>2</sup>Oregon Hearing Research Center, Oregon Health & Science University, <sup>3</sup>Kresge Hearing Research Institute, University of Michigan, <sup>4</sup>Department of Otolaryngology, Chinese Navy General Hospital, Beijing P.R. China

An ingenious experiment has been performed by Allen and Fahey (J. Acoustic. Soc. Am. 92, 178-188, 1992), in which they attempted to estimate the gain of the cochlear amplifier by comparing responses to the  $2f_1 - f_2$  distortion products (DP) in the outer ear canal (otoacoustic emissions) and from an auditory nerve fiber. Results were essentially negative. A variation of that experiment is reported here. Where DP responses in the outer ear canal (*otoacoustic emissions*) are compared with *mechanical responses of the basilar membrane*. Results confirm and extend those of Allen and Fahey entirely. Apparently, the gain of the cochlear amplifier cannot be measured in this way. It is argued that the retrograde DP wave going to the stapes is most likely reduced in magnitude—at its source—by wave interferences when the two primary frequencies approach each other (Shera, *in Biophysics of the cochlea: from molecule to model*, World Scientific, Singapore). Such an amplitude reduction does not take place in the forward-going DP wave to the location tuned to the DP frequency. This explanation is illustrated on the basis of results of our earlier experiments on the movements of the basilar membrane. This study has been supported by NIH NIDCD DC 00141, NIH NIDCD R01 004084.

### **321 Dependence of Distortion on Cochlear Transducer Characteristics**

**Alec Salt**<sup>1</sup>, Ruth Gill<sup>1</sup>

<sup>1</sup>Department of Otolaryngology, Washington University Medical School, St. Louis, MO

The cochlea generates distortion primarily due to the known nonlinear transduction characteristics of the hair cells. An understanding of how distortion varies with stimulation conditions requires detailed knowledge of the transducer characteristics under different stimulation conditions. In the present study, cochlear microphonics (CM) recorded from the round window were analyzed by fitting Boltzmann functions using methods established by Kirk et al. (Hear Res 112, 69, 1997). Derived parameters include transducer slope ( $z$ ), saturation voltage ( $P_{\text{sat}}$ ) and operating point ( $P_o$ ; representing the position on the transducer curve at zero-crossings of the stimulus). Derived transducer parameters were compared as stimulus frequency and level were varied systematically. For a 500 Hz stimulus,  $z$  was little changed as level was

varied from 75 to 95 dB SPL, while  $P_{\text{sat}}$  increased by more than a factor of two.  $P_o$  was typically negative for low stimulus levels but became positive for levels of 100 dB SPL and higher. With higher frequency stimulation at 90 dB SPL,  $z$  decreased progressively,  $P_{\text{sat}}$  remained unchanged and  $P_o$  became more positive. At frequencies where  $P_o$  became close to zero, very low levels of second harmonic distortion were observed. These changes account for the decreases in second and third harmonic distortions as frequency increases. Analysis of CM responses to two tones presented simultaneously showed similar slope and operating point characteristics, but differences in  $P_{\text{sat}}$  were observed at both high and low frequencies. We conclude that for a given stimulus condition, the amount of distortion generated depends on the both the transducer curve properties and on the region of the transducer curve over which the stimulus operates. As cochlear transducer properties are dynamic and vary with the applied stimulus frequency and level, an understanding of these relationships is necessary to interpret distortion data.

Study supported by NIH/NIDCD DC01368

### **322 Influence of Low Frequency Biasing on Distortion Generation by the Cochlea.**

**Alec Salt**<sup>1</sup>, Hillary Henson<sup>1</sup>

<sup>1</sup>*Department of Otolaryngology, Washington University Medical School, St. Louis, MO*

Previous work has shown that even-order distortions,  $2f$  ( $2^{\text{nd}}$  harmonic),  $f_2-f_1$  and  $f_2+f_1$  acoustic emissions, are more sensitive to treatments that displace the cochlear partition than are odd-order distortions,  $3f$  ( $3^{\text{rd}}$  harmonic) and  $2f_1-f_2$  emissions. Even-order distortions may thus provide a tool for the study and diagnosis of endolymphatic hydrops. In the present study, changes in distortion were evaluated during displacement of the cochlear transducer by low-frequency (5 Hz) bias tones applied at levels from 80 to 120 dB SPL. Probe stimuli for harmonic distortions ( $2f$ ,  $3f$ ) were 500 Hz tone bursts at 90 dB SPL and for  $2f_1-f_2$ ,  $f_2-f_1$  and  $f_2+f_1$  acoustic emissions were 4 kHz ( $f_1$ ) and 4.8 kHz ( $f_2$ ) delivered at 55 to 95 dB SPL. Distortion levels were determined in cochlear microphonics (CM) recorded from the round window and in acoustic emissions in the external ear canal. Distortions were quantified in 8 independent collection windows, equally spaced within 1 cycle of the bias tone. In addition, the cochlear transducer operating point was quantified by analysis of the cochlear microphonic waveforms. Low frequency biasing caused predictable, sinusoidal changes in operating point. Bias-induced changes of  $2f$  in the CM were consistent with a V-shaped dependence on operating point (distortion increasing as operating point moves in either direction away from zero), as predicted by simulation of the cochlear transducer. Based on this known dependence, it is possible to derive operating point status of the transducer from bias-induced distortion changes. Furthermore, an analysis of bias induced changes of  $2f$ ,  $f_2-f_1$  or  $f_2+f_1$  recorded from the ear canal permits transducer operating point status to be derived from acoustic emissions measurements. Our findings demonstrate that distortions are present at the level of the external ear canal

that can be interpreted in terms of the resting position of the cochlear transducer.

Study supported by NIH/NIDCD DC01368

### **323 Effects of Coiling on Cochlear Micromechanics**

**Hongxue Cai**<sup>1</sup>, Daphne Manoussaki<sup>2</sup>, Richard Chadwick<sup>1</sup>

<sup>1</sup>*Section on Auditory Mechanics, NIDCD, Bethesda, MD 20892*, <sup>2</sup>*Center for Cell Dynamics, Friday Harbor Laboratories, University of Washington, WA 98250*

The mammalian cochlea is a complex spiral-shaped organ, which is often uncoiled for cochlear mechanics modeling. In those few studies where coiling has been considered, the cochlear partition was reduced to the basilar membrane only. Here we extend our recently developed hybrid WKB/finite-element micromechanics model to include curvature effects, which were previously ignored. In this study, we take into consideration coiling and use a realistic cross-section geometry including the tilt of the basilar membrane with respect to the modiolar axis. We also include the microstructure of the organ of Corti and tectorial membrane, to model the apical region of a guinea-pig cochlea, where the curvature is the greatest. For simplicity, we neglect the pitch of the helix in the helicoidal coordinates and formulate the governing equations of the fluid and solid domains in a modified cylindrical coordinate system which involves  $r$ , the radial distance from the modiolar axis,  $s$ , the arc length along the coiled cochlear duct, and  $z$ , the modiolar axis. The WKB perturbation analysis is used to treat the propagation of the traveling wave along the arc length  $s$ , and the  $O(1)$  system of the governing equations is solved in the  $r$ - $z$  plane using the finite-element method. We then investigate the effects of coiling on the wave number of the traveling wave, the shear gain, and the vibrational modes of the basilar membrane, the organ of Corti and the tectorial membrane, by comparing our simulation results to those of our straightened cochlear model.

### **324 A New Cochlear Fluid Inertia Mechanism of Bone Conduction Hearing**

**Tianying Ren**<sup>1,2</sup>

<sup>1</sup>*Oregon Health & Science University*, <sup>2</sup>*Xi'an Jiaotong University*

Although the bone-conduction hearing test has been routinely performed in all otological clinics to diagnose and differentiate hearing losses, its mechanism remains unknown. Two generally accepted mechanisms of bone-conduction hearing are compressional and inertial bone conduction. In the compression model, the cochlear shell is alternately compressed by an applied vibratory force. Due to volume differences between the two perilymphatic scalae and stiffness differences between the two cochlear windows, a pressure differential must develop across the cochlear partition, resulting in its displacement. In the inertial model, a relative motion is set up between the ossicular chain and the temporal bone, which leads to cochlear stimulation in much the same way as air-conducted sound. The above theories were tested in this study by conducting the following experiments: (1) direct

measurement and comparison of bone-conducted sound-induced basilar membrane vibrations and those evoked by air-conducted sounds, (2) observation of the effects of opening the round and oval windows on bone-conduction hearing. (3) investigation of the relationship of the round window membrane, stapes footplate, and cochlear bony shell vibrations evoked by bone-conducted sound. It was found that transfer functions and longitudinal patterns of bone-conducted sound-induced basilar membrane vibration were very similar to those induced by air-conducted sound. Opening the round and oval windows did not change bone-conducted sound-induced compound cochlear action potentials or basilar membrane vibration significantly. Bone-conducted sound caused a translatory motion of the cochlear bone and stapes, with no significant relative motion between the stapes and surrounding bone. These data conflict with current theories, and demonstrate that it is cochlear-fluid inertia rather than bone compression, middle-ear ossicular chain inertia, or middle ear-dependent secondary mechanisms that causes bone-conduction hearing.

Supported by NIH-NIDCD and VA RR&D Center Grant, Portland, VAMC.

### **325 Modulation of Cochlear Tuning by Electric Current**

**Egbert de Boer**<sup>1</sup>, Alfred Nuttall<sup>2,3</sup>, Yuan Zou<sup>2</sup>, Jiefu Zheng<sup>2</sup>

<sup>1</sup>Academic Medical Center, University of Amsterdam,

<sup>2</sup>Oregon Health & Sciences University, <sup>3</sup>Kresge Hearing Research Institute, University of Michigan

Local electrical stimulation of the cochlea can give rise to otoacoustic emissions, proving that mechanically sensitive elements are excited. There is ample evidence that the sound waves, which produce the emissions, are generated by Outer Hair Cells (OHCs). These are also the cells that play a crucial part in the amplification that the cochlear waves undergo, and these cells are believed to be the (major) site of cochlear nonlinearity. One of the manifestations of nonlinearity is the compression of basilar-membrane response amplitudes for stronger acoustical stimuli, which can be explained by saturation of OHCs. If that theory is correct, it should be possible to influence cochlear amplification by direct current. Such an effect has been reported by Parthasarathi et al. (J. Acoust. Soc. Am. 113, 442-452, 2003). A constant current (50 or 100 microamperes) from a positive voltage applied to an electrode in scala vestibuli relative to one in scala tympani was found to induce an increase in cochlear gain, whereas a negative voltage had the opposite effect. In the present study the same problem is approached from a different side. The maximum length of a current pulse is 5  $\mu$  s, one fourth of the period of the acoustical stimulus. Hence we generated four stimulus signals in which the current pulses occurred in four different segments of the period. By special processing of the four corresponding responses we obtained basilar-membrane responses with the same frequency resolution (20 Hz) as in our earlier work. In addition, the response functions were made into "composite-spectrum files" and subjected to "inverse

solution analysis". In that way the set of parameters of the best-fitting model, in particular, the impedance function of the organ of Corti (generally known as the basilar-membrane impedance) is determined from the measured response. From the results we conclude that the variations in the impedance differ from what we anticipated. In particular, we found *in the region of the peak* no discernible variations of the imaginary part (i.e., the stiffness part) of the impedance associated with current stimulation. *Closer to the stapes* we found the stiffness to be smaller with positive current. Variations of the real part agreed with the variations in response amplitude. This study has been supported by NIH NIDCD DC 00141

### **326 Two Tone Distortion in Intracochlear Pressure in the Basal Turn of Gerbil Cochlea** **Wei Dong**<sup>1</sup>, Elizabeth Olson<sup>1</sup>

<sup>1</sup>Columbia University

Two-tone distortion has been studied at different levels of the auditory system: perceptual (eg Zurek and Sachs, 1979), neural (eg Kim et al., 1980), in auditory emissions (see review article by Probst et al.) and in basilar membrane (BM) motion (eg, Robles et al., 1997, Cooper and Rhode, 1997). This report provides the first detailed study on two-tone distortion in the intracochlear pressure close to the BM. It also extends the previous mechanical measurements of two-tone distortion components by studying more distortion family members and doing relatively detailed frequency sweeps.

Pressure responses to double tones were recorded from the scala tympani (ST, close to the BM) at a region that is tuned to ~20 kHz, in turn one of the gerbil cochlea and scala vestibuli (SV, close to the stapes) using intracochlear sensors.

Consistent with the previous mechanical measurements of two-tone distortion in BM, distortion products (DPs) in the pressure close to BM were frequency and level dependent. The greatest and most numerous DPs were observed at the lowest primary frequency ratio (1.05) and when the sensor was close to the BM. The decay of DPs with distance from BM differed from that of the primaries, and the difference is easily explained by the fast-wave pressure that essentially fills the cochlea at primary frequencies. At a ratio of 1.05 the individual members of the distortion family were tuned quite similarly to the primaries – ie, they were all tuned to ~ the best frequency. However, the high-side DPs (eg. 2f2 – f1) showed a slightly less steep cutoff than the primaries. The phase-vs-frequency of the distortion components paralleled that of the primaries for frequencies in the vicinity of the BF, consistent with their being locally generated in the region of the sensor. For stimulus frequencies that were somewhat lower than the BF, the phase of the DPs often diverged from that of the primaries, suggesting that the measured DPs had been generated at different (presumably more apical) locations.

### **327 Alterations of in Vivo Cochlear Electromotile Responses by Chlorpromazine**

Jiefu Zheng<sup>1</sup>, Yuan Zou<sup>1</sup>, Alfred Nuttall<sup>1,2</sup>

<sup>1</sup>Oregon Hearing Research Center, Oregon Health & Science University, Portland, Oregon 97239, U.S.A.,

<sup>2</sup>Kresge Hearing Research Institute, The University of Michigan, Ann Arbor, Michigan 48109, U.S.A.

We have reported that chlorpromazine (CPZ), an antipsychotic drug that alters plasma membrane biomechanics and outer hair cell (OHC) electromotile responses, affects acoustically evoked basilar membrane (BM) motion and that an OHC-mediated reduction of cochlear amplification is likely involved (Zheng and Nuttall, ARO Abstract 1215, 2004). Here we further investigate the effects of CPZ on the electromotile responses in living guinea pig cochleas. The BM velocity in response to locally applied current (100 micro-A rms, 5-70 kHz, through scala vestibuli vs. scala tympani electrodes) was measured at the site corresponding to the best frequency (BF) of around 17 kHz using a laser interferometer. CPZ in artificial perilymph was infused locally into the scala tympani of the basal cochlear turn. The locally applied current evoked BM responses in the OHC region are featured by large, narrow-frequency tuned peaks near the BF and a relatively smaller, broadly tuned response at higher frequencies up to 70 kHz with a prominent dip near 50 kHz. The BM velocity magnitude both around the BF and at higher frequencies was substantially reduced by CPZ, and the degree of reduction was comparable with that caused by salicylate (SAL). Interestingly, the frequency of the dip in BM response around 50 kHz significantly shifted upwards in a CPZ concentration-dependent manner accompanied with corresponding phase change. In contrast, SAL did not induce an unambiguous shift in the dip frequency. These results implicate that CPZ modulates cochlear amplification via its effects on the OHC plasma membrane biomechanics in addition to or rather than a direct effect on the OHC motor, the prestin.

Supported by NIDCD R01 DC00141

### **328 Influence of Electrically-Induced Somatic Mobility of Outer Hair Cells on the Basilar Membrane Motion**

Manuela Nowotny<sup>1</sup>, Anthony W. Gummer<sup>1</sup>

<sup>1</sup>Department Otolaryngology, University Tubingen, Tubingen, Germany

For a better understanding of the amplification process in the mammalian inner ear the electrically-induced transverse vibration patterns of the organ of Corti (OC) were investigated at different radial and longitudinal locations: i) on the reticular lamina (RL) and ii) on the basilar membrane (BM). Velocity was measured using a laser-interferometer (Polytec OFV 302) with a depth resolution of  $\pm 1.8 \mu\text{m}$  from the focus plane (at -10 dB).

The results derive from an in vitro preparation of the first (N=16), second (N=26) and third (N=22) turn of the guinea-pig cochlea with a characteristic frequency (CF) of 0.8–24 kHz. The turn of interest was isolated by removal of

the lateral part of all other turns. Reissner's membrane was left intact, allowing better preservation of the tectorial membrane (TM). For electrical stimulation, two platinum electrodes and one gold electrode were used; the latter also served as a mirror for illumination from the tympanic side of the organ. The stimulus frequency was between 480 Hz and 70 kHz.

The amplitudes of the BM motion exhibited a CF-independent resonance between 11–21 kHz at all measured radial and longitudinal positions (except below the HeCs). There was a local minimum in the amplitudes at frequencies below this resonance. At CF, displacement amplitudes were about five times lower on the BM than on the respective positions on the RL. On the BM, the region near the modiolus (extending from the inner sulcus cells to the inner pillar cells) exhibited a phase delay with respect to the HeC region. This was about 160° in the basal turn and 90° in the medial turn. No phase difference was detected in the apical turn between these two regions. At CF, at every measured radial position, the BM vibrated counterphasic to the RL in the basal turn. In the medial and apical turns the modiolus region and the HeCs region vibrated in-phase on the BM and RL and out-of-phase in the OHC region. The phase response showed distinct phase shifts corresponding to the characteristic amplitude response.

The measured electrically-induced vibration pattern of the BM and RL, together with the data from the TM (Nowotny et al. 2004 ARO, Abstract 1002) provides a clearer picture about the influence of somatic mobility of OHCs on the motion of the organ of Corti.

*This work was supported by the Deutsche Forschungsgemeinschaft, Gu 194/5-1,2.*

### **329 Tributyl-Tin Rescues Salicylate Ototoxicity in Outer Hair Cells by Promoting Chloride Influx.**

Lei Song<sup>1</sup>, Joseph Santos-Sacchi<sup>1</sup>

<sup>1</sup>Otolaryngology and Neurobiology, Yale University School of Medicine

The Cl ionophore tributyl-tin (TBT) enhances Cl exchange across the outer hair cell (OHC) plasma membrane (Song and Santos-Sacchi, ARO, 2003). This additional Cl pathway provided by TBT supplements the cell's natural lateral membrane Cl conductance,  $G_{\text{metL}}$ , enhancing the influence of extracellular Cl on prestin activity. Intracellular salicylate is known to depress prestin activity and shift its voltage dependence, as gauged by nonlinear capacitance measures (NLC; Kakehata and Santos-Sacchi, J. Neuroscience, 1996), and this action is likely dependent on competition between Cl and salicylate for an anion binding site on prestin (Oliver et al, 2001). Thus, we reasoned that TBT, which has no direct effect on prestin, could overcome salicylate effects on prestin by permitting an enhanced Cl influx. We evaluated this hypothesis using whole cell voltage clamp on isolated OHCs. Pipette solutions contained 5 mM Cl, and extracellular solutions contained 140 mM Cl to mimic an in vivo Cl gradient across the OHC lateral membrane. Extracellular perfusion with graded salicylate concentrations reduces NLC in a



graded fashion, and washout recovers NLC. The subsequent re-perfusion of the same graded salicylate concentrations with the addition of TBT (1  $\mu$ M) reduced salicylate ototoxicity by up to an order of magnitude. Dose response curves show that the susceptibility to salicylate ototoxicity depends on the intracellular Cl concentration; with 5 mM Cl intracellular, OHCs are about one order of magnitude more susceptible to salicylate ( $K_{1/2}$ : 146  $\mu$ M) than with 140 mM intracellular ( $K_{1/2}$ : 1.6 mM; Kakehata and Santos-Sacchi, 1996). The presence of TBT shifts the salicylate dose response curve toward that of the 140 mM Cl intracellular condition. This is a result of enhanced Cl influx since in the absence of a Cl gradient across the membrane (e.g., 140 mM inside and 140 mM outside) TBT cannot rescue the effects of salicylate. We hypothesize that TBT offers a way to modulate the cochlear amplifier in vivo by regulating Cl homeostasis in the OHC.

Supported by NIDCD grant DC 00273.

### **330 Modulation of Cochlea Amplification by Tributyltin and Salicylate**

Alfred Nuttall<sup>1,2</sup>, Jiefu Zheng<sup>1</sup>, Joseph Santos-Sacchi<sup>3</sup>

<sup>1</sup>Oregon Hearing Research Center, Oregon Health & Science University, <sup>2</sup>Kresge Hearing Research Institute, University of Michigan, <sup>3</sup>Section of Otolaryngology, Dept. of Surgery, Yale University

Modulation of cochlea amplification by tributyltin and salicylate.

Nuttall, Zheng, Santos-Sacchi

Cochlear amplification depends on the proper function of prestin, the outer hair cell motor protein. Intracellular chloride ions have been shown to 'activate' prestin causing a shift in the OHC nonlinear capacitance that is accompanied by a change in cell length and stiffness. Further, there is evidence that chloride acts in ways other than simply carrying capacitive charge. Chloride can induce a shift of prestin's operating voltage range. An increase of OHC intracellular chloride concentration will shift the operating range in the hyperpolarizing direction increasing the 'gain' of the OHC voltage-to-length relationship as the cell's operating point shifts. The purpose of current study is to explore for cochlear amplification changes (as an indirect measure of changes in prestin activity) with manipulations OHC intracellular chloride. Tributyltin (TBT) is used as a chloride ionophore to raise intracellular chloride concentration (Song and Santos-Sacchi, ARO, 2004). Salicylate is used to chemically compete with chloride's action on prestin, reducing chloride's effectiveness and shifting the OHC operating point in the depolarizing direction. We measure the basilar membrane (BM) velocity tuning curves to indicate the status of cochlear amplification. Guinea pigs were surgically prepared for laser Doppler velocimeter measurements of BM motion in the basal turn while prestin-affecting agents were topically applied to the organ of Corti at the measurement location. A perilymphatic perfusion system allowed applications of artificial perilymph to be delivered into the basal turn (2  $\mu$ l/min) containing TBT (50  $\mu$ M), salicylate (1 to 10 mM) or combinations of the two agents. We observed that TBT

improved the magnitude of the BM velocity response by 3-6 dB near the best frequency (approximately 17 kHz) for low sound level stimuli. The **improvement** of cochlear sensitivity is a highly unusual result. The combination of salicylate and TBT resulted in a salicylate concentration-dependent reduction of cochlear sensitivity from the TBT elevated level. Washout of the salicylate restored the enhanced level of cochlear amplification provided by TBT. These results indicate that TBT (via chloride flux) and salicylate compete with each other to modulate cochlear sensitivity (amplification). Further, intracellular chloride concentration is able to modulate the gain of OHC electromotility. This increased OHC gain is translated into enhanced traveling wave motion, by the process of cochlear amplification.

Supported by NIH NIDCD DC 00141 and DC 00273.

### **331 An Analytic Model for the Mechanical Point Impedance of the Organ of Corti**

Charles R. Steele<sup>1</sup>, Marc P. Scherer<sup>2</sup>, Chandramouli Chandrasekaran<sup>2</sup>, **Anthony W. Gummer<sup>2</sup>**

<sup>1</sup>Stanford University, Dept. Mechanical Engineering, USA,

<sup>2</sup>University Tubingen, Dept. Otolaryngology, Germany

An analytical model has been developed which is able to reproduce the previously measured point-impedance spectrum of the guinea-pig organ of Corti (Scherer and Gummer, 2004, Biophys. J. 87:1378). The model consists of an infinite, isotropic or orthotropic plate which is attached to ground by a spring at the load point, and is immersed in a viscous fluid. Despite its simplicity (compared to the structure of the organ), the isotropic model can be fitted to the data surprisingly well. Introducing material damping for the spring improves the fit, while introducing plate orthotropy provides no further refinement. Most importantly, all parameters of the new model have a physical interpretation, so that material properties can be extracted from the fit. Initial results show that the thickness of the plate is of the order of 1  $\mu$ m for a Young's modulus of  $10^9$  Pa (a typical value for collagen, microtubules, spectrin, etc.). We conclude that the point impedance of the reticular lamina is dominated by the bending of the surface together with the associated fluid forces, while the rest of the organ mainly acts as a spring with material damping.

This work was supported by a grant from the Deutsche Forschungsgemeinschaft DFG Gu 194/5-1.

### **332 A Sandwich Model of the Gerbil Cochlea That Includes the Electroanatomy of Hair Cells and Scalae**

Shan Lu<sup>1</sup>, David Mountain<sup>1</sup>, **Allyn Hubbard<sup>1</sup>**

<sup>1</sup>Boston University

A hydromechanical sandwich model of the cochlea employing outer hair cell (OHC) force generation creates a slow-traveling pressure wave inside the organ of Corti, which is principally responsible for enhanced (amplified) response of the basilar membrane (BM). This model has been shown generally to mimic physiological data using

physiologically-realistic parameters, including actual dimensions of the gerbil cochlea and measured BM stiffness values.

The present model differs from our previous versions of sandwich models, because the electrical characteristics of OHC and cochlear scalae have been included. Previously, hair cell force generation was made directly proportional to reticular lamina (RL) displacement. In this new model, the OHC consists of apical and basal membrane portions, which have membrane conductance and capacitance in parallel. The apical conductance varies nonlinearly as a function of the stereocilia displacement. Scala media (SM) fluid resistance creates a longitudinal coupling, as does the scala vestibule (SV) and scala tympani (ST). SM also has membrane conductances and capacitances to ST and SV. Intracellular and stria vascularis batteries were also included in this model. All the parameters were gleaned from previously published experimental data, albeit, some were "adapted" to the gerbil cochlea, in the case that gerbil data did not exist.

The model produces both mechanical and electrical data that to some extent mimic data collected in animal experiments. Cochlear microphonic at low frequencies compared well with our own data and those from the literature. The mechanical data were compared with those of Ren [Ren, T., Nuttall, A., Basilar membrane vibration in the basal turn of the sensitive gerbil cochlea, Hearing Research 151 2001, 48-60] whose characteristic frequencies are in the vicinity of 13 kHz. In this frequency range, the baso-lateral membrane voltage produced by RL displacement is substantially reduced due to low pass filtering; hence an artificially increased gain between baso-lateral membrane voltage and hair cell force production is required to approximate physiological data.

This work was supported by NIH.

### **333 Predicting Cochlear Response using a Global Cochlear Model with Mechanical-Electrical-Acoustic Coupling**

**Karl Grosh<sup>1</sup>, Sripriya Ramamoorthy<sup>2</sup>, Niranjan Deo<sup>1</sup>**

<sup>1</sup>University of Michigan, <sup>2</sup>Bose Corporation

Predictions of response of the mammalian cochlea to acoustic and electrical input are obtained using a linear three-dimensional physiologically based finite element model. The model includes a micro-mechanical model for the cochlear structures, a two-duct acoustic model with structural-acoustic coupling at the basilar membrane (BM) and a global electrical circuit to model conductances in the different scalae. Incorporation of the electrical domain in the model enables computation of the cochlear microphonic and other cochlear potentials. Model response to pure acoustic input, round window electrical stimulation, and bipolar electrical stimulation will be presented. Effects of random perturbations of certain parameters (e.g. BM stiffness) on electrically evoked emissions will be shown. Model simulations indicate that RC cut off of the hair cells is overcome by tectorial membrane resonance. Model predictions agree well with recent experimental findings by Grosh et. al. (2004, J. Acous.

Soc. Am., 115(5): 2178-2184). This project is funded by NIH NIDCD R01 - 04084.

### **334 Laser Irradiation of the Basilar Membrane**

**Gentiana I. Wenzel<sup>1</sup>, Bahman Anvari<sup>2</sup>, Amaan Mazhar<sup>2</sup>, Brian Pikkula<sup>2</sup>, Chul-Hee Choi<sup>1</sup>, John S. Oghalai<sup>1</sup>**

<sup>1</sup>Dept. of Otolaryngology- Head and Neck Surgery, Baylor College of Medicine, Houston, TX 77030, USA, <sup>2</sup>Dept. of Bioengineering, Rice University, Houston, TX 77005-1892, USA

The basilar membrane is tonotopically tuned based on the spatial variation of its mass, stiffness and damping. These biophysical properties are mainly defined by its constituent collagen fibers. We sought to assess the effect of laser irradiation on collagen within the basilar membrane using histological analysis. Excised guinea pig cochleae were perfused with trypan-blue as an exogenous chromophore ( $\lambda_{max}$ :607nm). A 600nm pulsed dye laser (3ms pulse duration) with radiant exposure of 30 J/cm<sup>2</sup> was used to irradiate the cochleae. The cochleae were fixed in paraformaldehyde, stained with picosirius-red, and analyzed using polarized light microscopy to visualize collagen organization. Laser irradiation reduced the birefringence within the basilar membrane as well as within other stained collagen-containing structures. Larger reductions in birefringence were measured when more laser pulses were given. The effects were similar across all turns of each cochlea. In vivo experiments on mice with the same technique are currently being performed. Our preliminary results suggest that by 2 weeks after laser irradiation, new collagen deposition has occurred in the basilar membrane, causing it to thicken. Additionally, there is a strong inflammatory response throughout *scala tympani* and *scala vestibuli*. Laser irradiation causes immediate and long-term alterations in collagen organization within the cochlea that can be visualized with polarization microscopy. These alterations may affect cochlear tuning. Ongoing research is aimed at analyzing the effect of laser irradiation on cochlear function.

Supported by NIH grants DC05131 and DC006671 (J.S. Oghalai)

### **335 Stiffness Properties of the Gerbil Organ of Corti as Measured in the Hemicochlea**

**Alicia Quesnel<sup>1</sup>, Claus-Peter Richter<sup>1</sup>**

<sup>1</sup>Northwestern University, Department of Otolaryngology-Head and Neck Surgery, Chicago, IL, U.S.A.

The past decade has brought remarkable advances in understanding how the ear works. Accurate descriptions of basilar membrane motion patterns are now available for the base and the apex of the mammalian cochlea. Although these advances are remarkable, fundamental questions remain unanswered, for example the mechanism by which the patterns of vibration contribute to the cochlear amplifier. Thus, by investigating the physical and dynamic properties of the basilar membrane, the organ of Corti, and the tectorial membrane, we will better understand the mechanism by which each structure may

contribute to the cochlear amplifier. These measurements are possible in vitro in the gerbil hemicochlea.

Driving point stiffnesses of the reticular lamina with its supporting structures and the tectorial membrane were determined with a piezoelectric sensor. Measurements were made at several radial positions and at five locations along the cochlea from base to apex. Furthermore, using a stiff probe, static images of the stepwise indentation of the reticular lamina were captured to monitor relative displacements of structures within the organ of Corti. Images were captured at three locations, over the first, second, and third outer hair cells and displacement was measured using NIH-Image.

Stiffness values at the reticular lamina approximately matched the stiffness values of the TM for each of the five locations along the length of the cochlea. Reticular lamina displacement along the radial direction was like a beam. Moreover, the displacement of the reticular lamina was greater than the OHC displacement at the base of the outer hair cells, which was larger than the Deiter's cell displacement, which was greater than the displacement of the BM.

In summary, the stiffness of the reticular lamina and tectorial membrane are approximately matched. A stiffness gradient exists between the basilar membrane and reticular lamina.

Supported by the NSF (IBN-0077476 and IBN-0415901)

### **336** Optical Coherence Tomography of the Organ of Corti

Steven L. Jacques<sup>1</sup>, Scott Matthews<sup>2</sup>, Guiju Song<sup>3</sup>, Alfred L. Nuttall<sup>2,4</sup>

<sup>1</sup>Biomedical Engineering/Dermatology, Oregon Health & Science University, <sup>2</sup>Oregon Hearing Research Center, Oregon Health & Science University, <sup>3</sup>Biomedical Engineering, Oregon Health & Science University, <sup>4</sup>Kresge Hearing Research Institute, University of Michigan

An optical coherence tomography system (OCT) is an interferometric measurement that is scanned axially versus depth (z) and laterally versus position (x) to yield an x-z image of a tissue structure with 10 μm x 10 μm spatial resolution, based on the backscatter of coherent light. OCT allows such 10 μm axial resolution despite viewing the organ of Corti through a small hole in the bone of the cochlea, using a low numerical aperture lens. In this report, an OCT operating at 1310 nm imaged, *in vitro*, a formalin-fixed organ of Corti within the dissected cochlea of a guinea pig, demonstrating the ability to localize an interferometric signal at the front (basilar membrane) versus rear (reticular lamina) surfaces of the organ of Corti. These surfaces presented optical reflectivities of about 10<sup>-5</sup> to 10<sup>-4</sup>, with a signal-to-noise exceeding 100:1. This result suggests that the scanner of the OCT system can be positioned at either the front or rear surface to detect 10-nm movement with a 10:1 signal-to-noise. To illustrate an interferometric measurement, a glass coverslip was held by one edge in free space, and the OCT scanner was immobilized and positioned to align with the front air-glass surface. An audio sound system generated a free field that induced vibrations in the

coverslip. The OCT system recorded a time trace and its Fourier transform yielded the frequency spectrum. The system could monitor acoustic frequencies in the 100 Hz to 25 kHz range. This report describes initial steps toward developing a dual-channel OCT system that can simultaneously and independently detect the phase and amplitude of both the front and rear surfaces of the organ of Corti. Supported by NIH R01-DC00141, R55 DC06273-01 and R24-ER000224.

### **337** Predicting DPOAEs using a Model of The Cochlea Incorporating Voltage Controlled Stiffness Coupled to a Forward/Reverse Model of the Ear Canal/Middle Ear

D Sen<sup>1</sup>, Raymond Louie<sup>1</sup>, J B Allen<sup>2</sup>

<sup>1</sup>University of New South Wales, <sup>2</sup>University of Illinois (Urbana Champaign)

In this paper, we report on the ability of a 'passive', non-linear model of the cochlea to produce distortion-product otoacoustic emissions (DPOAE). The model is passive in that it does not incorporate negative damping to explain the non-linearities observed in the cochlea. The model [1] is non-linear due to a model of the outer hair cell (OHC) motility that causes a stiffness change in the Basilar Membrane (BM).

To evaluate the model's ability to predict DPOAE levels, we implemented forward models of the ear canal (EC) and middle ear (ME) with two-ports which incorporate characteristics of the EC [2], ME [3] and cochlear impedance  $Z_c(\omega)$  [4]. Since reciprocity holds for the EC and ME [3], the same two-ports were used to implement a reverse model of the EC/ME.

The two sinusoidal pressure stimuli  $P_{ec_k} \sin(\omega_k t + \phi_k)$ , introduced in the EC was modified by the forward admittance  $A_f(\omega)$  to calculate the stapes particle velocity,

$u_s(t) = P_{ec_k} |A_f(\omega_k)| \sin(\omega_k t + \angle A_f(\omega_k) + \phi_k)$ . The  $u_s(t)$  is the input to the cochlear model which calculates the BM velocity  $\xi(x,t)$  as a function of time  $t$  and position  $x$ , along the cochlea. The reverse stapes particle velocity was approximated by  $\xi(x=0, t \gg T_l)$ , where  $T_l$  is the time at which transient effects end. This is then converted to an EC pressure using  $P_{ec_r}(\omega) = Z_c(\omega) \xi(0, \omega) H_{me_r}(\omega)$  where  $H_{me_r}(\omega)$  is the reverse transfer function.

The results indicate that a voltage controlled stiffness model of OHC is able predict DPOAEs with similar accuracy to those using active models of the OHCs[5].

#### References

- [1] Sen, D. & Allen, J.B., "Benchmarking a two dimensional cochlear model against experimental auditory data", ARO, 2001
- [2] Fletcher, N., "Acoustic Systems in Biology", Oxford University Press, 1992.

[3] Puria, S., "Measurements of human middle ear forward and reverse acoustics: Implications for otoacoustic emissions", *JASA*, 113(5), 2003.

[4] Puria, S. & Allen, J.B., "A parametric study of cochlear input impedance", *JASA*, 89(1), 1991.

[5] Neely, S.T., Gorga, M.P. & Dorn, P.A., "Distortion product and loudness growth in an active nonlinear model of cochlear mechanics", *Mechanics of Hearing*, 1999.

### **338 Low-Frequency Biasing of Quadratic**

#### **DPOAE**

**Lin Bian<sup>1</sup>**

*<sup>1</sup>University of Kansas Medical Center*

Cochlear transduction demonstrates a compressive nonlinearity, from which distortion product otoacoustic emissions (DPOAEs) are generated. Quadratic difference tone (QDT,  $f_2-f_1$ ) is related to the asymmetric saturation of the transduction. It is formulated that at low signal levels QDT magnitude is proportional to the absolute value of the second derivative of a sigmoid-shaped transducer function evaluated at an operating point (Bian et al., 2002, *JASA* 112:198). With a low-frequency bias tone, the operating point is systematically shifted along the transducer curve, and subsequently a cochlear transducer function can be derived from measuring the QDT magnitude. In gerbils, DPOAEs were biased by 25-Hz tones with various peak amplitudes. The primary levels ranged from 50-75 dB SPL. QDT magnitudes measured at the peaks and troughs of the bias tone showed a "V-shaped" pattern similar to the absolute second derivative of the transducer function. Center-notch of the modulation pattern with 20 dB in average depth pinpointed to inflection-point of the transducer function. In time-domain, QDT magnitude was enhanced at the peaks and troughs of the bias tone, and suppressed around zero-crossings. Within one bias tone period, the QDT magnitudes showed two "V-shaped" patterns each associated with the rise or fall of bias pressure. The double modulation pattern indicated that the transduction contained hysteresis. Physiologic indices that characterized the modulation pattern varied with primary levels. The results are consistent with the findings of cubic difference tone (CDT,  $2f_1-f_2$ ) (Bian et al., 2004, *JASA* 115:2159), but differ in their prominence at high signal levels and suppressions at zero-crossings. In addition to CDT, low-frequency modulated QDT can be used in estimating cochlear transducer function and its hysteresis. Moreover, the center-notch obtained with multiple-level bias tones may serve as an indicator for the position of cochlear partition.

*Supported by NIH-NIDCD grant: R03 DC006165*

### **339 Further Evidence of a Cochlear Fluid Compression Wave in Otoacoustic Emission Generation**

**Tianying Ren<sup>1,2</sup>, Wenxuan He<sup>1,2</sup>, Alfred L. Nuttall<sup>1,3</sup>**

*<sup>1</sup>Oregon Health & Science University, <sup>2</sup>Xi'an Jiaotong University, <sup>3</sup>The University of Michigan*

It is commonly believed that the cochlea emits sounds through backward-traveling waves. This prevailing theory

was challenged by a recent study (Ren, *Nature Neuroscience* 7:333-334, 2004), which demonstrated that there is no detectable backward traveling wave and that the stapes vibrates earlier than the basilar membrane at the emission frequency. Based on these experimental facts, a cochlear fluid compression wave was proposed to be responsible for backward propagation of the emissions in the cochlea. This study was criticized for the use of high primary stimulus levels and a high noise floor for scanning interferometry of the basilar membrane vibration. In response to this critique, the basilar membrane vibration at cubic DPOAE frequencies was measured at several longitudinal locations on the basilar membrane. The noise floor of the measurement was significantly decreased by the use of reflective beads on the basilar membrane. It was found that the phase of the emission decreases with the emission frequency. The slope of the phase-frequency curve measured from an apical location is always steeper than that measured from its basal locations. This phase-location relationship is not stimulus intensity- or other stimulus parameter-dependent, although the magnitude-frequency function can change with such variables. Derived from the distance between two measured locations and their phase difference, the propagation velocity demonstrates that the basilar membrane vibration at the emission frequency propagates from base to apex through the observed region. The wave speed decreases with the emission frequency increase. The data describe a typical forward traveling wave, and provide further evidence for the cochlear-fluid compression wave as the main mechanism for the cochlea to emit sounds.

*Supported by NIH-NIDCD and VA RR&D Center Grant, Portland, VAMC.*

### **340 Medial Olivocochlear Efferent Inhibition of Basilar-Membrane Click Responses**

**John Guinan<sup>1</sup>, Nigel Cooper<sup>2</sup>**

*<sup>1</sup>Eaton-Peabody Lab, Mass. Eye & Ear Infirmary, Harvard Medical School, 243 Charles St. Boston MA02114,*

*<sup>2</sup>MacKay Institute of Communication & Neuroscience, Keele University, Staffordshire, ST5 5BG, UK*

Despite the insights that click responses provide, the effects of medial olivocochlear (MOC) efferents on basilar-membrane (BM) responses to clicks have not been studied previously. In the basal turn of the cochlea in anesthetized guinea pigs, we measured BM motion in response to clicks with and without brainstem electrical stimulation of MOC efferents. We report here preliminary results on MOC fast effects on BM click responses using paradigms that separate MOC fast and slow effects (MOC inhibition = BM response just before each shock train minus BM response during the shock train).

Stimulation of MOC efferents inhibited BM click responses with a pattern that depended on time after the click and appeared qualitatively similar in good and poor preparations (efferent effects >10 dB or <2 dB). In the first half-cycle of the click response, there was little or no inhibition. In later cycles, MOC inhibition built up, reached a maximum near the peak amplitude of the click response, and then declined in absolute magnitude. However,

expressed as a fraction of the normal response at that time, the inhibition was largest during the declining part of the click response. MOC inhibition produced a small phase advance that was greatest near the maximum of the response.

The pattern of MOC inhibition of BM click responses appears to fit the hypothesis that MOC efferents decrease the gain of the cochlear amplifier. These BM results are in strong contrast to results from cat auditory-nerve (AN) fibers which show MOC inhibition of the first peak (or earliest part) of click responses for CFs up to at least 8 kHz, as well as inhibition in the decaying part of the response. Assuming no species differences, the BM and AN results together imply that MOC efferents, in addition to reducing the gain of the cochlear amplifier, must also reduce some other motion or process that produces the first peak of the AN click response.

Supported by NIDCD RO1DC00235, P30DC005209, and the Royal Society.

### **341 Electrical Properties of the Isolated Tectorial Membrane Measured with a Microfabricated Planar Clamp Technique**

**Roozbeh Ghaffari<sup>1,2</sup>, Dennis Freeman<sup>1,2</sup>**

*<sup>1</sup>Massachusetts Institute of Technology, <sup>2</sup>Harvard-MIT Speech and Hearing Biosciences and Technology Program, 77 Massachusetts Ave. 36-805*

The tectorial membrane (TM) clearly plays a mechanical role in the cochlea. However, the presence of charged macromolecules (Thalman et al, 1993) in the TM suggests that electrical properties may also be important. Traditional micropipet techniques to quantify fixed charge (Steel, 1983) have proven to be difficult. The main difficulty has been in creating an electrical seal to the TM. We overcame this problem with a novel microfabricated planar clamp designed with dimensions comparable to those of the TM. The planar clamp placed the TM as an electrochemical barrier separating two baths of different ionic strength. Fixed charges in the TM created a Donnan potential difference between the baths. This potential depends on the fixed charge concentration (cf) and ionic strength of the baths. Thus by measuring the potential difference at several ionic strengths, we can determine the cf of the TM. We tested the validity of this technique on artificial gels with known fixed charge. We then applied the planar clamp technique to measure the cf of TMs from mice. In both artificial gels and TM, the electrical recordings were stable and repeatable. Furthermore, in both systems, the dependence of potential on bath ionic strength was well fit by a gel model (Freeman and Weiss, 1997). From the gel model fit, the TM was found to contain -26 mmol/L of fixed charge. This cf value is larger than previous estimates based on microelectrode measurements, which is consistent with the notion that there was a poor seal. This cf value is also slightly larger than TM fixed charge estimates based on composition, which may be because only 75% of the TM composition is known. The value of cf measured with the planar clamp suggests that electrostatic repulsion can have a significant mechanical effect. Although fixed charge is shielded by

surrounding mobile ions, we estimate that -26 mmol/L of fixed charge will contribute 1.8 kPa to the TM bulk modulus in vivo.

### **342 Measuring the Equilibrium Bulk Modulus for the Tectorial Membrane with Osmotic Stress: Caveats of using Polyethylene Glycol**

**Kinuko Masaki<sup>1,2</sup>, Thomas Weiss<sup>1,2</sup>, Dennis Freeman<sup>1,3</sup>**

*<sup>1</sup>MIT, <sup>2</sup>Harvard/MIT Speech and Hearing Bioscience and Technology, <sup>3</sup>Harvard/MIT Speech and Hearing Bioscience and Technology*

The equilibrium bulk modulus of the isolated mouse tectorial membrane (TM) was measured by applying osmotic pressure with polyethylene glycol (PEG). This method has been introduced previously (Masaki et al, 2002) but two issues remained to be resolved. First, the relation between PEG concentration and osmotic pressure does not obey van't Hoff's law but is a nonlinear function of both molecular weight (MW) and concentration. A theory to quantify this nonlinear relation had been developed for PEG with MW below 40 kDa (Hasse et al., 1995). To test this theory for higher MW PEGs, we measured the stress-strain relation of polymethacrylic acid (PMAA) gels using 511 kDa PEG. The result was comparable to that previously measured using hydraulic pressure (Quinn and Grodzinsky, 1993) indicating that the theory can be applied even at these large MWs. Second, we investigated whether PEG entered the TM by measuring the strain using solutions that exerted the same osmotic pressure prepared with PEGs of different MW (20 - 511 kDa). The TM strain was found to be independent of MW for MW  $\geq$  100 kDa. From this result, we inferred that PEG does not enter the TM if the MW is greater than 100 kDa. Once these two issues were resolved, the equilibrium stress-strain relation was measured using several concentrations of 511 kDa PEG. The stress-strain relation of the TM was nonlinear, exhibiting larger equilibrium bulk modulus at higher osmotic pressures. At low osmotic pressures, the equilibrium bulk modulus was estimated to be 1.1 kPa. Therefore, properly accounting for the nonlinearity of PEG-induced osmotic pressure leads to lower estimates of equilibrium bulk modulus than previously reported. Moreover, from the known relation of PEG MW and radius (Bhat and Timasheff, 1992), the maximum pore size was estimated to be 16 nm. This implies that ions and small solutes can freely diffuse into the TM but larger organic molecules such as proteins are excluded.

### **343 Hearing Loss Measured by DPOAEs Correlates with an Increase in Equilibrium Bulk Modulus of Tectorial Membranes from Col11a2 -/- Mouse Mutants**

**Kinuko Masaki<sup>1,2</sup>, Gary Chan<sup>1</sup>, Richard Smith<sup>3</sup>, Dennis Freeman<sup>1,2</sup>**

*<sup>1</sup>MIT, <sup>2</sup>Harvard/MIT Speech and Hearing Bioscience and Technology, <sup>3</sup>U. of Iowa Hospitals & Clinics*

Type XI collagen is quantitatively a minor fibrillar component of the tectorial membrane (TM). Mutations in COL11A2, one of the genes that encodes type XI collagen,

are known to cause non-syndromic hearing loss (DFNA13) in humans. The DFNA13 audio profile is characterized by hearing loss that preferentially affects the middle frequencies. Hearing thresholds as measured by ABR click-responses in a mouse mutant homozygous for a targeted deletion of this gene are increased by 40-50 dB (McGuirt et al., 1999). To determine the frequency specificity of the hearing loss in both heterozygote and homozygote Col11a2 mouse mutants, we recorded distortion product otoacoustic emissions (DPOAEs). In particular, we measured the 2f1-f2 component of the DPOAEs, with f2 chosen to be 1.2\*f1. The DPOAEs of heterozygotes and homozygotes were similar for f < 10 kHz and f > 25 kHz, however at frequencies between 10 and 25 kHz, Col11a2 -/- mouse mutants had about a 50 dB increase in thresholds as compared to Col11a2 +/- mouse mutants. This pattern of mid-frequency hearing loss is similar to the DFNA13 audio profile. To determine if the differences in hearing thresholds between Col11a2 -/- and Col11a2 +/- mouse mutants reflected changes in material properties of the TM, the equilibrium stress-strain relation was measured using 511 kDa polyethylene glycol (PEG) to exert an osmotic pressure. For a given PEG concentration, TMs from Col11a2 -/- mouse mutants were found to shrink less compared to TMs from wild-type Col11a2 +/+ mouse. These results suggest that targeted deletion of Col11a2 causes an increase in the equilibrium bulk modulus of the TM. Increase in equilibrium bulk modulus may be responsible for the elevated threshold at mid-frequencies found both in COL11A2 -/- mouse mutants and humans with DFNA13. (Supported in part by grant R01 DC03544 to RJHS and DF)

#### **344 TectaY1870C Missense Mutation Increases the Equilibrium Bulk Modulus of the Tectorial Membrane**

**Kinuko Masaki**<sup>1,2</sup>, Guy Richardson<sup>3</sup>, Dennis Freeman<sup>1,2</sup>  
<sup>1</sup>MIT, <sup>2</sup>Harvard/MIT Speech and Hearing Bioscience and Technology, <sup>3</sup>Univ. of Sussex, UK

Alpha-tectorin is one of the major glycoproteins of the non-collagenous, striated-sheet matrix of the mammalian tectorial membrane (TM). Mutations in TECTA, the gene encoding alpha-tectorin, cause both dominant and recessive forms of hereditary deafness in humans. A transgenic mouse with a missense mutation in TECTA, the TectaY1870C mouse, was created to provide a model for a severe, prelingual, dominant form of deafness resulting from this mutation in the Austrian DFN8/12 family. The TMs of these mice have a number of morphological abnormalities. The mice have a 70-80 dB hearing loss (Legan et al., in preparation). To determine if the observed ultrastructural changes affect the material properties of the TM, we measured the stress/strain relation of TMs isolated from normal and mutant mice. TMs were isolated and placed on a microscope stage, and volume changes were measured by tracking the positions of fluorescent beads attached to the TM surface. Osmotic stress was applied by bathing the TM in artificial endolymph solutions (AE) containing various concentrations of polyethylene glycol (PEG) with a molecular weight of 511 kDa. In AE, the TMs

from TectaY1870C/+ mice were approximately 20-33% thinner than those of normal TMs from wild type Tecta+/+ mice. For a given PEG concentration, the TMs of TectaY1870C/+ mouse mutants shrank less than half as much as the TMs of control mice, suggesting that the TM of the TectaY1870C/+ mouse has a higher bulk modulus than that of the wild type Tecta+/+ mouse. Since mutations in TECTA are only known to affect the TM (Legan et al., 2000), these findings suggest that hearing loss found in these mutants may be due to a decrease in TM thickness or an increase in the TM equilibrium bulk modulus.

#### **345 Measuring Mechanical Properties of the Isolated Tectorial Membrane at Audio Frequencies with a Microfabricated Probe**

**Jianwen Gu**<sup>1</sup>, Alexander Aranyosi<sup>1</sup>, Werner Hemmert<sup>2</sup>, Dennis Freeman<sup>1</sup>

<sup>1</sup>MIT, <sup>2</sup>Infineon

Although shearing forces exerted by the tectorial membrane (TM) clearly play a role in driving hair bundle deflection, relatively little is known about the TM's relevant mechanical properties. Few direct measurements of TM shear impedance exist, and those have been limited to frequencies below 100 Hz. To extend the frequency range, we developed novel microfabricated probes for measuring shear impedance of the TM. The probes consisted of systems of cantilevers designed to apply forces in two dimensions. Several designs were specified using CAD layout tools, and multiple copies of each design were manufactured from silicon using a commercial MEMS foundry (MEMSCAP). We tested various designs and selected the one with impedance best matched to that of the TM. The chosen probe was calibrated and could exert forces with amplitudes in the range 30-300 nN at frequencies in the range 10-9000 Hz. The resulting magnitudes of TM displacements were between 10 and 150 nm and depended nearly linearly on force amplitude. The impedance of the TM consisted of elastic and viscous components, which remained proportional through the entire frequency range studied. Radial impedance was about three times larger than longitudinal impedance. The magnitude of the displacement of surrounding tissue decreased as distance from the probe increased, and space constants were approximately 30 um in both radial and longitudinal directions. These results suggest (1) the elasticity of the TM is linear and probably does not contribute to compressive nonlinearity in the cochlea; (2) the TM is viscoelastic even at frequencies as high as 9000 Hz; (3) the TM cannot be modeled as a low-order mechanical system consisting of masses, springs, and dashpots; and (4) the TM can couple motions of adjacent longitudinal sections within the cochlea.

#### **346 cAMP-Dependent Protein Kinase Phosphorylation of Myosin-1C**

**Emilie Miller**<sup>1</sup>, Peter Gillespie<sup>1</sup>

<sup>1</sup>Vollum Institute and Oregon Hearing Research Center, Oregon Health and Sciences University

Adaptation of mechanical transduction in hair cells of the inner ear is mediated by an unconventional myosin,

myosin-1c (Myo1c). When cAMP is increased in hair bundles, the mechanically sensitive organelles of hair cells, the resting open probability ( $P_o$ ) of the transduction channel decreases. Because reduced force production by the adaptation motor would decrease  $P_o$ , these results suggested the possibility that phosphorylation of Myo1c by cAMP-dependent protein kinase (PKA) underlies the effect of cAMP on transduction. Between the ATP-binding head domain and first calmodulin-binding IQ domain of Myo1c there is a consensus PKA phosphorylation site present at Ser-701. A synthetic peptide incorporating the putative PKA site and the first IQ domain was phosphorylated by PKA in a calmodulin-independent manner; moreover, calmodulin bound equally well to both phosphorylated or unphosphorylated peptides. Using baculovirus infection of SF9 cells, we co-expressed with calmodulin both a truncated Myo1c (HIQ) that included the head and IQ domains and a Myo1c fragment (IQT) that incorporated the IQ domains and the lipid-binding tail. Both Myo1c recombinant proteins were phosphorylated in vitro by PKA; surprisingly,  $Ca^{2+}$  substantially increased phosphorylation of each. These results implied that  $Ca^{2+}$  altered the conformation of Myo1c near Ser-701, independent of its effects on calmodulin binding. The PKA phosphorylation site is located at a region between the head and neck domains of the protein, which may form a pliant hinge. We hypothesize that phosphorylation of this critical position alters the force exerted by Myo1c, affecting adaptation in vivo.

### **347 Noise Exposure Induced Increase of NO Derivatives in the Guinea Pig Cochlea**

**Weiju Han**<sup>1,2</sup>, **Xiao-Rui Shi**<sup>1</sup>, **Alfred L. Nuttall**<sup>1,3</sup>

<sup>1</sup>Oregon Hearing Research Center, Oregon Health & Science University, <sup>2</sup>Dept of Otolaryngology, The General Hospital of Chinese PLA, Beijing, <sup>3</sup>Kresge Hearing Research Institute, University of Michigan

Early after the discovery of the signal transducing physiological functions of the free radical nitric oxide (NO) in the vasculature and nervous system, it became evident that NO could also participate as a cytotoxic effector molecule and/or a pathogenic mediator. Nitric oxide mediated pathology depends on the formation of reactive intermediates, such as the peroxynitrite ( $ONOO^-$ ).  $ONOO^-$  can nitrate free tyrosine and tyrosine residues of proteins. Therefore increases in tyrosine nitration reflect the amount of  $ONOO^-$  produced by oxidative stress. The 3-nitrotyrosine has been revealed as a relevant biomarker of NO-dependent oxidative stress. Here we have investigated the distribution of NO derivatives, nitrotyrosine (NT) and 3-nitrotyrosine (3-NT), in the cochlear lateral wall tissue and the organ of Corti from the guinea pig using the whole mount surface preparation and/or frozen sections methods. Guinea pigs were exposed to 120 dB broadband noise, 4 h/day, for 2 consecutive days. The immunoactivity of NT and 3-NT in the noise exposure animal was compared with the control animals using fluorescence immunohistochemistry method. The NT and 3-NT staining were found in the inner hair cells (IHCs), outer hair cells (OHCs), and the stria vascularis of the lateral wall. An increased NT and 3-NT signal was

observed in IHCs, OHCs, and stria vascularis of the lateral wall following exposure to the broadband noise. Relatively high levels of 3-NT immunoactivity were detected in the OHCs after broadband noise exposure. In addition to immunoactivity labeling of NO derivatives, the specimens were double labeled either with phalloidin, a probe for F-actin, to observe the whole cell shape or with propidium iodide (PI), a DNA intercalator, to detect apoptotic cells. Following noise exposure, quite a few OHCs loss and a few OHCs apoptosis were observed in organ of Corti. The data indicate that noise exposure leads to production of NO derivatives in the cochlea stria vascularis and organ of Corti. This is consistent with the known increase of NO production by loud sound stress and suggests that NO derived free radicals participate in the cochlear pathophysiology of noise-induced hearing loss. Tissue distribution and quantitation of 3-nitrotyrosine open new avenues for the understanding of NO cytotoxic effect. Supported by NIH NIDCD R01 DC 00105.

### **348 Cochlear Slow Adaptation with Pressure Applied to the Otic Capsule**

**Yuan Zou**<sup>1</sup>, **Jiefu Zheng**<sup>1</sup>, **Tianying Ren**<sup>1</sup>, **Alfred Nuttall**<sup>1,2</sup>

<sup>1</sup>Oregon Hearing Research Center, Oregon Health & Science University, Portland, OR, 97239, USA, <sup>2</sup>Kresge Hearing Research Institute, The University of Michigan, Ann Arbor, MI, 48109, USA

When a constant force is applied to the surface of the otic capsule, a slow adaptation of the cochlear microphonic (CM) occurs. This CM change is associated with a shift of the outer hair cell (OHC) stereocilia operating point (Zou Y., *et al*, 2004 ARO). In the current work, the operating point shifts were analyzed based on the 2<sup>nd</sup> and 3<sup>rd</sup> harmonics of CM, and the calcium and nitric oxide (NO) dependence of this CM adaptation are studied. CM was evoked by a low level 400 Hz pure tone and recorded using a differential electrode in the first turn. CM adaptation was induced by applying a constant force to the cochlear bony shell over scala tympani using a blunt probe at the 18 kHz best frequency location in guinea pigs. This force caused a sudden reduction of CM amplitude, which then underwent a slow partial recovery toward the initial level with a time constant of about 10~30 s. Removing the force caused an overshoot of CM, which returned to the control level with a time constant 30-60 s. Quadratic distortion of the round window signal and the cubic distortion product otoacoustic emissions showed very similar pattern of alteration as the CM. The recovery may be due to a dynamic shift in the OHC transduction operating point. The overshoot recovery pattern is cochlear sensitivity-related. For poor cochlear sensitivity, the overshoot is nearly absent. In high sound pressure level (>90 dB SPL) evoked CM, the overshoot did not occur. Perilymph perfusion of BAPTA-AM (300  $\mu$ M) abolished the overshoot, while NO inhibitor L-NAME (1 mM) and NOS substrate L-arginine (1 mM) did not effect the overshoot in sensitive animal. The data indicate that in the normal cochlea this slow recovery and overshoot are not NO related but are calcium dependent.

Supported by: NIDCD DC00141 & DC04554

### **349** Group Delays in the Auditory Nerve of the Cat

Marcel van der Heijden<sup>1</sup>, Philip Joris<sup>1</sup>

<sup>1</sup>Laboratory of Auditory Neurophysiology K.U.Leuven, Belgium

Group delays derived from auditory nerve (AN) responses provide important information on cochlear travel times. A particular advantage of neural data is their complete coverage characteristic frequencies (CFs), including CFs from the mid-frequency region for which very few cochlear-mechanical data are available. In a previous study [J. Neurosci. 2003 23:9194-9198] we showed that group delays can be determined with good (~20-microsecond) accuracy from neural responses to irregularly spaced tone complexes. The method is based on an analysis of the coding of envelope of the tone complex. It yields estimates of group delays for fibers of arbitrary characteristic frequency and a wide range of stimulus frequencies.

Here we present a large collection of data on group delays obtained from AN recordings from 10 cats. The dependence of group delay on CF, stimulus frequency and stimulus level is analyzed. The data are discussed in terms of cochlear traveling waves. Evidence is presented for a qualitative difference in patterning of group delays between the apical and basal portions of the cochlea.

Supported by the Fund for Scientific Research - Flanders (G.0083.02) and Research Fund K.U.Leuven (OT/10/42). MvdH was supported by a K.U.Leuven fellowship (F/00/92).

### **350** Expression and Induction of the Kidney Injury Molecule-1 (KIM-1) in the Rat Cochlea by Cisplatin

Debashree Mukherjee<sup>1</sup>, Craig Whitworth<sup>1</sup>, Leonard Rybak<sup>1</sup>, Vickram Ramkumar<sup>1</sup>

<sup>1</sup>SIU School of Medicine

Cisplatin is a widely used chemotherapeutic agent used in the treatment of various solid tumors such as testicular, ovarian, and bladder cancers. Dose-limiting side effects include ototoxicity and nephrotoxicity. Recently, a novel protein, termed kidney injury molecule-1 (KIM-1), was identified in renal proximal tubular epithelial cells whose expression was induced by cisplatin. It has been proposed that this molecule aids in the regenerative process of the kidney following toxic injuries. Since the cochlea bears a number of similarities to the kidney and is sensitive to drugs known to produce nephrotoxicity, we investigated whether this tissue also expresses KIM-1. Using reverse transcriptase (RT) PCR, we have identified KIM-1 in the rat cochlea and in an Organ of Corti transformed cell line (Ock-3). Administration of cisplatin (13 mg/kg, i.p.) resulted in ~3-fold induction in KIM-1 expression by 3 days. This increase in expression was time-dependent, with the highest increase observed by 3 days. This pattern of expression was similar to that observed in the kidneys obtained from these animals. In addition, exposure of Ock-3 cells to cisplatin (2.5  $\mu$ M) produced a similar increase in KIM-1 expression. We conclude that the induction of KIM-1 in the cochlea could constitute a

compensatory response to cochlear damage and mediate some form of regeneration to aid in healing process.

### **351** Heme Oxygenase-1 Attenuates the Cisplatin-Induced Apoptosis of Auditory Cells via Modulating Oxidative Stress

HyungJin Kim<sup>1</sup>, YunHa kim<sup>1</sup>, Eunsook Kim<sup>1</sup>, Channy Park<sup>1</sup>, Hongseob So<sup>1</sup>, Raekil Park<sup>1</sup>

<sup>1</sup>Vestibulocochlear Research Center, Wonkwang University School of Medicine

Heme oxygenase-1 (HO-1) is the rate-limiting enzyme in heme catabolism, which leads to the generation of carbon monoxide (CO), biliverdin and free iron. One of three mammalian HO isoforms, HO-1, is a stress-responsive protein and known to modulate cellular functions such as cytokine production, cell proliferation and apoptosis. However, its protective effect against cisplatin-cytotoxicity on auditory cells remains to be elusive. In this study, we investigated whether induction of HO-1 provided the protective effect against cisplatin-cytotoxicity. Treatment with hemin and cobalt protoporphyrin IX (CoPPIX), well known HO-1 inducers, apparently induced HO-1 mRNA and protein expression in a time- and dose-dependent manner, and significantly suppressed the apoptosis of HEI-OC1 auditory cells. Cytoprotective effect of CoPPIX was significantly abrogated by the inhibition of HO-1 enzymatic activity with zinc protoporphyrin  $\text{L}$  (ZnPPIX). In addition, treatments with hemin and CoPPIX prior to cisplatin-exposure significantly decreased the generation of ROS to control levels. Additional experiments also showed that bilirubin and carbon monoxide (CO) generated by HO-1 was directly involved in the cytoprotective effect by HO-1. Therefore, these results suggest that HO-1 serves as a safeguard against cisplatin-cytotoxicity through the modulation of cellular redox balance.

This work was supported by the Korea Science & Engineering Foundation (KOSEF) through the Vestibulocochlear Research Center (VCRC) at Wonkwang University in 2004

### **352** CB1 Cannabinoid Receptor is Expressed in the Mammalian Cochlea

Claudius Fauser<sup>1</sup>, Thorsten Briede<sup>1</sup>, Hans Niedermeyer<sup>1</sup>, Elmar Oestreicher<sup>1</sup>

<sup>1</sup>Klinikum recht der Isar, Technical University Munich

Cannabinoids have been shown to exert neuroprotective effects in several models of neurotoxicity in the CNS. The cannabinoid system is a neuromodulatory system which comprises the cannabinoid receptor type 1 (CB1).

In the inner ear excitotoxicity is a common pathomechanism in different cochlear traumas like noise or ischemia. As there is limited information on CB1 receptors in the auditory system, we investigated the distribution of CB1 receptors in the mammalian cochlea of adult gerbils.

Following local application of saline, salicylate or glutamate via the round window niche, animals were sacrificed and cochleas were removed. After fixation with



paraformaldehyde and decalcification 3-5 $\mu$  slices of the cochlea were stained with CB1 antibody (Acris, Germany) and a fluorescent secondary antibody.

All Animals showed specific staining of type I and type II spiral ganglion cells. This staining was slightly stronger after treatment with salicylate and glutamate. No specific stain was found in the organ of Corti or stria vascularis. Interestingly, in adjacent slices we were able to co-localize the NMDA receptor subunit NR1.

The results demonstrate the existence of CB1 cannabinoid receptors in the mammalian cochlea. As previous studies also showed colocalisation of CB1 with gabaergic and glutamatergic neurons in the CNS, our results suggest a similar neuroprotective and neuromodulatory function of the cannabinoid system in the cochlea.

### **353 Calcipressin1: A Stress Inducible Gene Expressed in the Cochlea**

**Kevin Leahy**<sup>1</sup>, Lawrence Lustig<sup>2</sup>, Paul Fuchs<sup>1</sup>

<sup>1</sup>Department of Otolaryngology, Head and Neck Surgery, Johns Hopkins, <sup>2</sup>Department of Otolaryngology-Head & Neck Surgery, UC San Francisco

Free radicals are emerging as major components of cochlear damage following exposure to ototoxic insults such as the aminoglycosides, chemotherapeutic drugs, and acoustic trauma. Calcium also plays a role in the cellular response to oxidative stress, rising to activate a host of calcium-dependent processes. In turn, cellular pathways exist to compensate for these stress-induced changes. For example, Csp1, a member of the calcipressin family (Csp1, Csp2, and Csp3), can be induced both by free radical stress (H<sub>2</sub>O<sub>2</sub>) and by elevation of intracellular calcium. The calcipressins obtain their name from the ability to inhibit calcineurin, a serine/threonine phosphatase implicated in a variety of calcium-mediated processes, including excitotoxicity and apoptosis. These characteristics make Csp1 an interesting molecule to study with respect to stress tolerance by the cochlea. We report here the expression of Csp family members (Csp1 and Csp2) in the cochlea at the level of mRNA. The expression of Csp1 was demonstrated in cochlear tissue derived from mice and rats. A potential chicken Csp1 homologue was detected by RT-PCR with mRNA derived from basilar papilla (including hair cells and supporting cells). Using RT-PCR we demonstrated that the two major splice variants of calcipressin (Csp1.1 and Csp1.4) are expressed in the rat cochlea. However, when outer hair cell/Deiters' cells were selectively isolated for RT-PCR, only Csp1.1 was detected. Additionally, in the mouse cochlea other members of the Csp1 signal transduction cascade were detected by RT-PCR, namely calcineurin and NFAT. These findings not only show the presence of a stress-regulated mRNA in the cochlea, but suggest that whatever role this molecule plays in the inner ear may be conserved across vertebrates. Supported by NIDCD DC00276 and P30 DC05211.

### **354 Hair Cell and Synaptic Responses to High-Level Noise Exposures in the Amphibian Papilla of the Bullfrog.**

**Dwayne Simmons**<sup>1</sup>, Helena Wotring<sup>1</sup>, Craig Johnson<sup>1</sup>, Angela Schrader<sup>1</sup>, Rebecca Hooper<sup>1</sup>

<sup>1</sup>Washington University

The bullfrog amphibian papilla (AP), although lacking a basilar membrane, is a sensitive frequency analyzer that is tonotopically organized and generates distortion-products (DPs). Our goal was to investigate the temporal course of hair cell and synaptic recovery following short (4 hour) and long (20 hour) noise exposures at 155 dB SPL.

The MAGUK family members are abundant at submembranous sites of cell-cell contacts including the postsynaptic density. We find that PSD-95 immunoreactivity is especially robust in rostral AP regions and among mature hair cells. This immunoreactivity is punctate in appearance, forming bead-like plaques that encircle the basolateral portion of the hair cell nucleus. Consistent with the presence of afferent terminals on hair cells PSD-95 immunoreactivity is contained mostly within the subnuclear region of the hair cell and is concentrated at synaptic terminal regions. At excitatory synapses, PSD-95 binds NMDA and kainate receptors as well as potassium channels

After high-level noise exposures either for short or long periods, there was a 20-30 dB drop in DP levels between 500 and 1000 Hz over a 24-hour period. DPs recovered to normal levels within 3 - 4 days. Following long periods of sound overexposure, hair cells displayed significantly more damage, including extruding hair cells, fragmenting hair cells, and hair cells with missing hair bundles. However some hair cells within the sound-damaged region retained some of their synaptic endings that were closely associated with PSD-95 immunoreactivity. Following shorter periods of sound overexposure, hair cells displayed mostly missing hair bundles within the sound damage region and unexpectedly, an increase in the number and amount of PSD-95 immunoreactivity. At 9 days following long noise overexposures, there was a significant decrease in the number of isolated PSD-95 and co-localized myosin and PSD-95 fragments, and small PSD-95 clusters were seen on hair cells. Recovering hair cells in the damaged region were labeled with PSD-95 suggesting they were contacted by synaptic endings.

### **355 Regulation of Gene Expression of GDNF-, NGF- and Tgfb- Family Members in Rat Modiolus Following Neomycin-Induced Deafness**

**Kirsten Wissel**<sup>1</sup>, Patrick Wefstaedt<sup>1</sup>, Heike Rieger<sup>1</sup>, Joseph M. Miller<sup>2</sup>, Thomas Lenarz<sup>1</sup>, Timo Stöver<sup>1</sup>

<sup>1</sup>ENT Department, Medical University of Hannover,

<sup>2</sup>Kresge Hearing Research Institute, University of Michigan

Hair cell loss following drug- and noise-induced trauma induces apoptosis in spiral ganglion cells (SGC). It has been shown that nerve growth factors, especially members of the transforming growth factor b (TGF-b) superfamily, play key roles for the protection of SGC and enhance the

functional excitability of the auditory nerve in response to stress. The aim of the present study was to determine gene expression patterns of the glial cell line-derived neurotrophic factor (GDNF), nerve growth factor (NGF) and transforming growth factor beta (TGF $\beta$ ) family members and their corresponding receptors in the modiolus and inferior colliculus of deafened rats. Adult rats were deafened by local inner ear injection of 10% neomycin and sacrificed after 26 days. The gene expression of GDNF, persephin, artemin and neurturin, their receptors GFRa1, GFRa2, GFRa3 and c-ret, BDNF, the tyrosine kinase receptors trk A, B and C as well as TGF $\beta$ 1, TGF $\beta$ 2, the receptors TGF $\beta$ R1 and TGF $\beta$ R2 was determined by semiquantitative RT-PCR using GAPDH expression as an internal standard. Furthermore, the expression of the selected neurotrophic factors were localized in the cochlear tissues by FITC-immunohistochemistry. Gene expression levels of persephin as well as of artemin, GDNF and c-ret were slightly downregulated in IC following deafening. In contrast artemin, GDNF, GFRa1, GFRa2, GFRa3 and c-ret RNA expression were strongly upregulated in modiolus of deafened rats. These data suggest endogenous survival effects of artemin and GDNF as well as their receptors GFRa1, GFRa3 and c-ret on SGC over a certain period following deafening. In congruence to the RT-PCR results expression of artemin, GDNF, GFRa1 and c-ret were localized mainly in the spiral ganglion cells.

### **356 The PI 3-Kinase/Akt Pathway in Chronic Aminoglycoside Ototoxicity**

**Andra Talaska<sup>1</sup>**, Hongyan Jiang<sup>1</sup>, Su-Hua Sha<sup>1</sup>, Jochen Schacht<sup>1</sup>

<sup>1</sup>*Kresge Hearing Research Institute, University of Michigan, Ann Arbor, MI 48109*

The PI 3-kinase/Akt pathway plays a crucial role in response to extracellular signals. Its activity is regulated by tyrosine receptor kinases that can respond to hormonal signals, e.g. growth factors. A key downstream effector of PI 3-kinase is the serine-threonine kinase Akt which is activated by phosphatidylinositol-3,4,5-trisphosphate (PIP3), the product of the PI 3-kinase reaction. We investigated this pathway in response to the chronic administration of kanamycin. Adult CBA/J mice subcutaneously received kanamycin base at 700 mg/kg, twice per day for 7 days. Under this condition, there was no permanent threshold shift, but a temporary hearing loss was seen at 14 days (i.e. 7 days after cessation of treatment). Phosphatidylinositol-4,5-bisphosphate (PIP2) increased and PIP3 decreased in outer hair cells at 7 days. Phosphorylated Akt (p-Akt) also decreased. Co-treatment with salicylate, a protective agent against aminoglycoside ototoxicity, restored PIP3 in outer hair cells and also increased p-Akt. Details of the downstream pathways of PI 3-Kinase and Akt were followed in the HEI-OC1 cell line. The sum of our results indicates that the PI 3-kinase/Akt pathway may rescue outer hair cells from aminoglycoside ototoxicity.

Supported by the research grant DC-03685 from the National Institute on Deafness and Other Communication Disorders, NIH.

### **357 Hair Cell Specific Proteins are Found in Cochlear Supporting Cells After Hair Cells Degenerate**

Karen Abrashkin<sup>1</sup>, Masahiko Izumikawa<sup>1</sup>, Donald Swiderski<sup>1</sup>, **Yehoash Raphael<sup>1</sup>**

<sup>1</sup>*Kresge Hearing Research Institute, Univ. of MI*

Hair cell death leads to permanent hearing loss in mammals. One possible approach to preserve hearing is to salvage and rehabilitate injured hair cells, but this requires a better understanding of the mechanism of scarring, whereby supporting cells replace degenerating hair cells in the organ of Corti. Specifically, it is necessary to determine whether degenerating hair cells are (a) extruded from the organ of Corti or (b) remain within the epithelium and are removed via phagocytosis by supporting cells or by macrophages. Here we tested the hypothesis that supporting cells can phagocytose dying outer hair cells. We lesioned the organ of Corti with ototoxic drugs or noise exposure, and stained the tissue with an antibody to prestin, a protein specific to outer hair cells. We examined whole mounts and plastic sections of the auditory epithelium, comparing normal and lesioned organ of Corti tissues. We determined that supporting cells in areas of hair cell loss contained clumps of prestin. These data suggest that supporting cells phagocytose dying hair cells, and that prestin is a stable protein. With this knowledge in hand, we may now pursue the signal that initiates phagocytic activity of supporting cells, and determine if increasing the threshold for this activity may spare hair cells in the face of trauma. Our data suggest that among other roles, supporting cells act as glial-like cells and remove dead hair cells from the auditory epithelium.

Supported by NIH/NIDCD Grants R01-DC01634, R01-DC05401, R01-DC05053, and P30-DC05188.

### **358 Induction of Heat Shock Proteins by Heat and Noise Stress in the Normal and Aging Mouse Cochlea**

**Margaret Lomax<sup>1</sup>**, Tzy-Wen Gong<sup>1</sup>, Gary Dootz<sup>1</sup>, Lynne Fullarton<sup>1</sup>, Kristina Mitchem<sup>1</sup>, Catherine Lomax<sup>1</sup>, David Dolan<sup>1</sup>, David Kohrman<sup>1</sup>, Richard Altschuler<sup>1</sup>

<sup>1</sup>*University of Michigan Kresge Hearing Research Institute, Ann Arbor, MI USA*

Hearing loss is a major health problem for both the young and old. Excessive noise can cause either transient or permanent hearing loss. Approaches for protecting the cochlea from noise damage throughout life would be highly desirable. Our research has focused on the role of a major protective mechanism controlled by the heat shock transcription factor 1 (HSF1) in the cochlea. Many different stresses can activate HSF1, leading to DNA binding and induction of genes for heat shock proteins (Hsps). To understand how HSF1 protects the cochlea from noise stress, we have used mouse genetic models that lack HSF1. We previously identified genes activated by noise stress in the rat cochlea (Cho et al., in press) and showed maximum induction 2 hr following noise overstimulation. We examined induction of Hsp genes in

wild-type, Hsf1<sup>+/-</sup>-heterozygotes, and Hsf1<sup>-/-</sup>-mice, using both heat shock and noise stress. Levels of cochlear mRNA for eight Hsps were measured by quantitative RT-PCR with TaqMan probes. Genes encoding heat shock proteins Hsp25, Hsp47, Hsp70 (Hsp70.1, Hsp70.3), Hsp84, Hsp86, and Hsp110 were induced following heat stress in heterozygotes, but not in Hsf1<sup>-/-</sup> null mice. In wild-type CBA mice, induction of Hsp25, Hsp70.1, and Hsp70.3 by heat stress decreased with age (between 12 – 22 months), suggesting that this decrease might contribute to presbycusis. The induction of Hsps by noise over stimulation was examined following exposure to BBN (2-20 kHz) presented for 2 hr at increasing intensities (98 dB, 106 dB, and 120 dB SPL). Induction was greatest at 106 dB. Maximum induction for most Hsp genes occurred 4 hr following the noise exposure. The notable exception was Hsp32, which showed maximum induction at 6 hr. These studies suggest that Hsf1-controlled induction of Hsp genes following noise over stimulation may play a protective role in the cochlea. To examine the effect of noise stress in the Hsf1<sup>-/-</sup> mouse cochlea with age, we have created a new mouse model in which we replaced sensitive allele of the Ah1 locus on Chr 10 with the resistant allele from CBA. We are examining the hearing sensitivity of these Hsf1<sup>-/-</sup>-Ah1R mice and their sensitivity to noise-induced hearing loss with age.

(Supported by NIH grants P01 DC02982 (MIL; RA) and P30 DC005880)

### **359 The Role of Metallothioneins in Protection from Noise Damage.**

Ana Vazquez<sup>1</sup>, Jerel Garcia<sup>1</sup>, Helena Yip<sup>1</sup>, Tejas Patel<sup>2</sup>, Michael Anne Gratton<sup>2</sup>

<sup>1</sup>University of California Davis, <sup>2</sup>University of Pennsylvania  
Inbred mice strains exhibit widely different susceptibilities to noise damage. The 129Sv/Ev and 129X1/SvJ are highly resistant to noise-induced hearing loss (NIHL) (Yoshida, 2000; Gratton et al. 2002 ARO abs: 251). In contrast, the C57BL/6J and B6.CAST (B6) are susceptible to noise damage. Taking advantage of these strain differences, we investigated what molecules may be relevant to the development of NIHL by comparing the levels of gene expression before and after noise exposure (Vázquez and Gratton, 2004, ARO abst 382). Total RNA was isolated from the membranous labyrinth of 129 and B6 mice.

Gene expression profiling revealed upregulation of a subset of stress-related genes in both mice strains. Genes in the metallothionein family showed higher levels of expression in the 129 mice relative to those in the B6 mice. Upregulation of metallothionein I and II was noted in each strain after noise exposure; however the upregulation in the 129 mice was more dramatic.

Metallothioneins are small proteins that have protective roles against various types of cellular insults in the liver, heart and brain. These proteins, which are very rich in cysteine and methionine, bind metals. In this study, we report the expression of metallothionein isoforms I, II and III in the mouse membranous labyrinth, as well as the noise-induced alterations in their expression for the 129

and B6 mice. Western blot and immunohistochemical analyses were used to confirm and localize the cochlear expression of metallothionein at the protein level. Metallothionein knockout mice had comparable baseline ABR thresholds however; they exhibited higher susceptibility to NIHL than their parental strain (129 SvImJ). Our preliminary data indicates that higher basal levels and a upregulation of metallothionein contribute to the resistance to NIHL exhibited by 129 mice.

Supported by R01-DC006442-01 to MAG and R21-DC04990 and R01-DC006421-01 to AEV.

### **360 Gap Junction Involvement in Damage-Induced ERK1/2 Activation in Neonatal Mammalian Cochlear Cultures**

Manuela Lahne<sup>1,2</sup>, Jonathan Gale<sup>1,2</sup>

<sup>1</sup>Department of Physiology, UCL, London, UK, WC1E 6BT,

<sup>2</sup>Centre for Auditory Research, The UCL Ear Institute, London, UK, WC1X 8EE

After hair cell damage or death surrounding non-sensory support cells close the wound in order to maintain the physiological environment and function of surviving hair cells. The mechanisms that signal damage and induce such wound closure in the inner ear are poorly understood. Candidate signalling molecules include the extracellularly regulated kinases 1 and 2 (ERK1/2), members of the MAP kinase family.

We investigated ERK1/2 activation in response to both laser-induced and mechanical damage in neonatal rat cochlear cultures. Cultures were stained with a phospho-specific antibody to the activated form of ERK1/2. Damage induced transient activation of ERK1/2 in support cells. ERK1/2 was not activated in hair cells. The activation spread non-uniformly from the damage site predominantly along the rows of Deiters' and inner phalangeal cells. The spread was maximal 5 to 10 min post-damage. Carbenoxolone (CBX, 75 µM) reduced the spread at 5 min suggesting that gap junctions carry a signal necessary for ERK1/2 activation.

We recently showed that damage triggers a rise in cytoplasmic calcium (Ca<sup>2+</sup>) that travels from the damage site as an intercellular wave requiring extracellular ATP release (Gale et al. 2004). We tested the role of gap junctions in the spread of the intercellular Ca<sup>2+</sup> wave. CBX significantly reduced the rise in cytoplasmic Ca<sup>2+</sup> associated with the damage-induced Ca<sup>2+</sup> wave by 46 % at 50 µm and 62 % at 150 µm longitudinally from the damage site. Lateral spread of the Ca<sup>2+</sup> wave into outgrowing Claudius-like cells was also affected, with the wave failing to pass through all cells. Applying CBX together with apyrase (40 U/ml), which degrades ATP, resulted in a greater reduction in Ca<sup>2+</sup> wave spread than either treatment alone and near complete prevention of ERK1/2 activation. We are currently testing whether the Ca<sup>2+</sup> wave is necessary for damage-induced ERK1/2 activation in this system.

Supported by the Royal Society, the Wellcome Trust and an MRC studentship.

### **361 Amitriptyline Attenuates Noise-Induced Trauma in Guinea Pig**

Yasunori Osumi<sup>1</sup>, Masao Yagi<sup>1</sup>, Kohei Kawamoto<sup>1</sup>, Hiromichi Kuriyama<sup>1</sup>, Mototane Komeda<sup>2</sup>, Mikiya Asako<sup>1</sup>, Toshihiko Kaneko<sup>1</sup>, Toshio Yamashita<sup>1</sup>

<sup>1</sup>Kansai Medical University, <sup>2</sup>Saiseikai Izuo Hospital

Cochlear epithelium damage attributable to noise is a major cause of permanent hearing loss. This study evaluates the protective effect of amitriptyline, antidepressant drug, against noise-induced hearing loss. Hartley guinea pigs with normal hearing as initially assessed by auditory brainstem response (ABR) measurement, were used in this study. Animals injected with amitriptyline (30mg/kg) intraperitoneally were designated as the experimental group and animals injected saline intraperitoneally were designated as the control group. After administration, each animal was exposed to 120 dB SPL octave band noise, centered at 4kHz, for 24 hours. One day before noise exposure, and three days and seven days after noise exposure we measured ABR threshold shift at 4kHz, 8kHz, and 16kHz. After the measurement of the ABR, we decapitated the animals and the ears were removed for histological evaluation. In experimental group, average ABR threshold shift between pre-noise and post-noise were approximately 15dB three days after exposure and approximately 10dB seven days after exposure. In control group, average ABR threshold shift between pre-noise and post-noise were approximately 25dB three days after exposure and approximately 20dB seven days after exposure. There was a tendency that outer hair cell loss of the experimental group was less than that of control group. This result indicates that amitriptyline attenuates noise-induced trauma in guinea pig.

### **362 Carbamathione in the Prevention of Glutamate Excitotoxicity in Chinchilla**

Xianxi Ge<sup>1</sup>, John Coleman<sup>1</sup>, Jianzhong Liu<sup>1</sup>, Elizabeth Harper<sup>1</sup>, Gavin Jones<sup>1</sup>, Richard Kopke<sup>1</sup>, Ronald Jackson<sup>1</sup>

<sup>1</sup>Naval Medical Center San Diego

**Objectives:** It has been well documented that acoustic overexposure produces excessive glutamate, which in turn causes excitotoxicity to the synapses. Our laboratory has extensively investigated the pharmacological intervention of noise-induced cochlear damage. Based on our previous success, we hypothesized that glutamate excitatory-induced injury might be prevented by pharmacotherapy. The aim of this study was to observe the effects of carbamathione (CARB), a glutamate antagonist, in the prevention of glutamate excitotoxicity in chinchilla cochlea. **Methods:** 16 chinchillas were equally divided in two groups. Each group received noise exposure (NE =octave band, 105 dB SPL, centered at 4kHz for six hours) with either saline or CARB (5.2mg/kg) treatment. Treatments were given one hour before and after noise and Bid for two days prior to and after NE. Animals were humanely euthanized at two hours and three weeks. Cochleae were processed using transmission electron microscopy. Auditory brainstem response was performed to determine hearing threshold. In another set of experiments

perilymphatic glutamate concentration was measured using microdialysis method in no noise controls (n = 5) and in NE animals with (n = 6) or without (n = 6) CARB treatment.

**Results:** Synapses below the inner hair cells exhibited edema in NE-animals two hours post-NE, and edema was diminished at three weeks. No synaptic edema was demonstrated with CARB treatment both at two hours or three weeks after noise. Perilymphatic glutamate concentration was 0.65±0.63  $\mu$ M in no noise controls, 1.35±0.70  $\mu$ M in noise exposure animals, and 0.56±0.23  $\mu$ M in noise exposure with CARB treatment after two hours NE (P<0.05). Hearing thresholds were increased in both noise-exposed groups with either saline or with CARB treatment (P>0.5).

**Conclusion:** The findings of this study indicate that CARB, a glutamate antagonist, reduces the production of glutamate and prevents inner hair cell synaptic edema.

Funded by the Office of Naval Research

### **363 The Effect of Carbamathione, Acetyl-L-Carnitine, Or N-Acetylcysteine on Perilymphatic Microdialysates of Glutamate, Aspartate and Cysteine After Noise Exposure**

Gavin Jones<sup>1</sup>, Erland Arning<sup>2</sup>, Jianzhong Liu<sup>1</sup>, Elizabeth Harper<sup>1</sup>, Xianxi Ge<sup>1</sup>, Teodoro Bottiglieri<sup>2</sup>, Richard Kopke<sup>1</sup>, Ronald Jackson<sup>1</sup>

<sup>1</sup>Naval Medical Center San Diego, <sup>2</sup>Baylor University Medical Center

The aim of the study was to measure perilymphatic levels of glutamate (Glu), aspartate (Asp), cysteine (Cys) and total glutathione (reduced and oxidized GSH) in animals after noise exposure (NE) and in NE-animals that were pre-treated systemically with either: (1) the NMDA receptor antagonist, carbamathione (CARB), (2) the antioxidants, N-acetylcysteine (NAC) or (3) acetyl-L-carnitine (ALCAR). No-noise animals served as controls for comparisons. Cochlear amino acids (Glu, Asp, Cys) and GSH were sampled using inner ear microdialysis. Dialysate samples were taken every 30 minutes for two and a half hours before NE and for two and a half hours during NE. Amino acid and GSH concentrations were normalized with respect to their averaged pre-NE readings. When control values (no NE) were compared to the NE-only group, Cys, Asp and Glu levels were elevated, but total GSH levels did not increase. CARB treatment resulted in a significant reduction in Glu and Asp and an increase in Cys levels. ALCAR treatment was followed by a reduction in Glu and Asp levels, while the Cys levels were actually increased compared to NE-control values. NAC-treated animals showed decreases in Glu and Asp levels that were in between control and NE values but with no change in Cys levels. Total GSH levels in controls were similar to the NE group. For all three pre-treated compounds there was no difference in GSH across all conditions. These results suggest that the NMDA receptor-antagonist may facilitate the reduction of the transmitters Glu and Asp, which may confer protection against excitotoxicity injury. The antioxidants, NAC and ALCAR, may also provide protection against excitotoxicity. Perilymphatic GSH

(reduced and oxidized) as measured by this methodology in either the NE or the pre-treated drugs conditions may not be a reliable measure of inner ear oxidative state.

### **364 Role of p53 in Noise-Induced Hearing**

#### **Loss: Protection with Pifithrin and CH65**

**Anna Rita Fetoni**<sup>1</sup>, Donald Henderson<sup>2</sup>, Bo-Hua Hu<sup>2</sup>, Gaetano Paludetti<sup>1</sup>, Thomas Nicotera<sup>3</sup>

<sup>1</sup>Dept. Otolaryngology - Università Cattolica S. Cuore Roma, Italy, <sup>2</sup>Center for Hearing and Deafness - University at Buffalo, <sup>3</sup>Molecular & Cellular Biophysics, Roswell Park Cancer Institute - Buffalo, NY

Recent studies suggest that p53 may play an important role in initiating apoptosis in cochlear hair cells. Zheng et al. (2003) observed that Pifithrin-alpha (PTF), a p53 inhibitor, protects against cisplatin-induced hair cell loss in organotypic cochlear and vestibular cultures. Carney et al. (2004), has demonstrated protection against noise-induced hearing loss (NIHL) using CH65, a putative inhibitor of pp60c-src protein tyrosine kinase. The goal of the present study was to determine the role of p53 in apoptotic signaling following exposure to noise and whether p53 expression could be blocked using CH65 or PTF. Chinchillas were used. One ear received a 30 µl drop of CH65 or PFT, the other control ear is treated with vehicle. Fifteen minutes after the chinchillas were exposed to 75-pairs of impulse noise at 155 dB pSPL. Auditory thresholds were measured with ABR responses, then the animal was anesthetized and the unfixed cochleas were stained with propidium iodide (PI) and p53 immunolabeling. Additional animals were assessed at 4 and 24 hours after noise. Both apoptosis and necrosis coexist in the cochlear lesion after noise exposure. Impulse noise caused an upregulation of phospho-p53 serine 30 minutes after the expression of p53 increased in hair cells survival 24 hours after noise exposure. Treatment of the round window before exposure with either CH65 or PFT decreased the apoptotic and necrotic cells and suppressed the p53 immunolabeling. These data suggest that p53 activation occurs in response to noise via changes in cellular attachment and/or increases in oxidative stress and confirm the pivotal role of p53 in the cell death pathway. Suppression of p53 expression with CH65 and PFT constitute a potential protective strategy against NIHL.

[Research supported by NIDCD P01-DC03600-1A1 grant; Dr. Donald Henderson, P.I.]

### **365 A Comparison of the Protective Function of an Antioxidant (L-NAC) and a Src Inhibitor (CH65)**

**Donald Henderson**<sup>1</sup>, Bo Hua Hu<sup>1</sup>, Eric Bielefeld<sup>1</sup>, Sarah Hynes<sup>1</sup>, David Przynosch<sup>1</sup>

<sup>1</sup>Center for Hearing and Deafness, SUNY Buffalo

Both the antioxidant n-acetyl cysteine (L-NAC) and the Src inhibitor CH 65 have been used to protect the cochlea from hazardous noise. To date, CH65 has only been used locally on the round window (Harris et al., 2004). In the current study, the two drugs were administered

systemically. L-NAC was delivered intraperitoneally at a dose of 325 mg/kg (Kopke et al., 2000). CH65 was delivered sub-cutaneously at a dose of 50 mg/kg. The noise exposure was a 4kHz octave band of noise at 100 dB SPL for 6 hours/day for 4 days. The drugs were administered once each day, 30 minutes prior to the onset of the noise exposure. The animals' hearing was estimated using surgically-implanted chronic recording electrodes in the inferior colliculi. Thresholds were recorded at .5, 1, 2, 4, and 8 kHz prior to the noise exposure, and then on Days 1, 4, 8 and 21 after the noise exposure. The chinchillas were then sacrificed and the hair cells were counted for cochleograms. The control animals showed a maximum temporary threshold shift of 65 dB at 8 kHz on Day 1 that recovered to 20-25 dB by Day 21. By contrast, the treated animals had 10 to 20 dB less TTS at Day 1, and an average 10 dB less permanent threshold shift. There were no significant side effects (ie: appetite loss, weight loss, lethargy, etc) related to either of the drug treatments. CH65 produced at least as much protection as L-NAC, but at a significantly lower concentration.

Research supported by NIDCD grant P01-DC03600-1A1.

### **366 Role of Retinoic Acid in Hearing Preservation of Mice During Noise Exposure**

**Joong Ho Ahn**<sup>1</sup>, Hun Hee Kang<sup>2</sup>, Young-Jin Kim<sup>1</sup>, Nam-Kyung Yeo<sup>1</sup>, Jong Woo Chung<sup>1</sup>

<sup>1</sup>dpt of Otolaryngology, Asan Medical Center, <sup>2</sup>Asan Institute of Life Science

Objective:

To evaluate the role of retinoic acid in hearing preservation of mice during noise exposure

Methods:

We used 100 gm mice with normal Preyer's reflex. Mice in retinoic acid group were fed with all-trans retinoic acid 1 mg/kg for 2 days before and during 3-day noise exposure. Mice in control group and sesame oil group were fed with same volume of water and sesame oil respectively. Audiologic tests with auditory brainstem response (ABR) were done in all mice before 3-day noise exposure and 1 week after. Samplings of temporal bone of mice in all groups were carried out and we checked the photographs of FITC-phalloidin and TUNEL stain to detect apoptosis.

Results:

Average hearing threshold of mice was 12.5 ± 2.6 dBnHL before noise exposure. Hearing thresholds measured 7 days after noise exposure were 38.57 ± 6.27 dBnHL in retinoic acid group (n=7), 78.8 ± 4.8 dBnHL in control group (n=4), and 75 ± 7.1 dBnHL in sesame oil group (n=7). In FITC-phalloidin stain, there was 10 % degeneration of outer hair cells in retinoic acid group, while 25.75 % and 16.75 % degenerations were found in control and sesame oil group individually. TUNEL-labeled nuclei were observed significantly in large numbers in control and sesame oil groups than in retinoic acid group.

Conclusion:

Retinoic acid plays a role in hearing preservation of mice during noise exposure.

### **367 Preservation of Hearing by Cobalt Chloride in Noise-exposed Mice**

Hun Hee Kang<sup>1,2</sup>, Jeong Eun Shin<sup>1</sup>, Joong Ho Ahn<sup>3</sup>, Jong Woo Chung<sup>3</sup>

<sup>1</sup>University of Ulsan, <sup>2</sup>Asan Institute for Life Science, <sup>3</sup>Asan Medical Center, University of Ulsan, College of Medicine

Hypoxia-inducible factor-1 (HIF-1) was expressed in the inner ears of mice exposed to noise, suggesting hypoxic damage in noise-exposed inner ears. Because HIF-1 may protect against cerebral infarction in hypoxic rat, the precise role of HIF-1 must be elucidated in the inner ear.

In this study, we induced HIF-1 expression in inner ear by the injection of cobalt chloride and observed the protective role against noise-induced hearing loss.

BALB/c mice, which have normal Preyeri's reflex and a normal hearing threshold, were used. The hearing level of each mouse was analyzed by measuring the auditory brainstem response (ABR). Broad band click sound (300 - 10,000 Hz) was generated by a personal computer and amplifier and delivered through a speaker equipped in noise booth. Mice were exposed continuously for 3 hours per day to 120 dB SPL broad band click sound for 3 consecutive days. In experimental group, cobalt chloride (60 mg / kg) was daily injected into intra-peritoneum 2 hours before the noise exposure for 3 days.

Subsequent to ABR measurements, both cochleae were removed and immunofluorescent staining was performed with FITC-phalloidin.

Mice exposed to noise for 3 consecutive days (n=20) experienced an increase in hearing threshold from 15.0 dB hearing level (HL) to 55.0 dB, 80.0 dB, and 76.6 dB HL in 3 days, 5 days, and 10 days later, respectively. In the mice injected with cobalt chloride (n=7), hearing level was increased from 12.5 dB to 54.1 dB in 3 days later. Hearing level, however, was partly recovered after 5 days. (45.0 dB and 37.5 dB in 5 days and 10 days later)

Through the surface preparation with FITC-phalloidin, more hair cells were preserved in cobalt chloride injection group.

Through this study, cobalt chloride may have a protective effect on noise-induced hearing loss. Though this protective effect may be due to the induction of HIF-1, further study on precise mechanism is needed.

### **368 Extended Oral Dosing of Ebselen in Rats Shows Continued Improvement in Auditory Protection from Noise.**

Eric Lynch<sup>1</sup>, Rende Gu<sup>1</sup>, Carol Pierce<sup>1</sup>, James LaGasse<sup>1</sup>, Huy Tran<sup>1</sup>, Jerry Glattfelder<sup>1</sup>, Jonathan Kil<sup>1</sup>

<sup>1</sup>Sound Pharmaceuticals, Inc.

Glutathione Peroxidase (GPx) is a key enzyme for hair cell protection in animal models of noise induced hearing loss (NIHL). We and others have shown that the GPx mimic, ebselen (SPI-1005), provides significant protection from NIHL in rats (Lynch et al., 2004) and Guinea pigs (Pourbahkt and Yamasoba, 2003) when dosed orally at 4-10 mg/kg.

In our current studies, we extended the dosing schedule from 3 days to 14 days (4 mg/kg, bid, po) starting one day

before noise exposure (113 dB SPL, 4-16 kHz OBN, 4 hours) and continuing for 12 days post noise exposure. Controls were dosed with vehicle only using the same schedule. Physiology was evaluated by ABR testing. Thresholds were determined using click and pure tone (4, 8, 12, 16 kHz) stimuli at multiple time points up to 15 weeks following noise exposure. Morphologic evaluations were performed on whole cochleae stained with DAPI to detect cell nuclei and TRITC-phalloidin to detect F-actin. Hair cells were also labeled with the mechanotransduction dye, AM1-43, prior to fixation. ABR data indicated that ebselen provided significant long lasting protection from NIHL at all tested frequencies for both the 3 and 14-day dosing schedules. Interestingly, the 14 day dosing schedule resulted in continued improvements in ABR thresholds at 6 and 9 weeks versus 3 weeks post noise exposure, up to 7 weeks after the last dose of ebselen. DAPI, phalloidin, and AM1-43 labeling indicated the presence of mechanotransducing hair cells throughout the cochlea of treated and control rats.

Damaging levels of reactive oxygen species (ROS) and reactive nitrogen species (RNS) continue to be produced in the cochlea for up to two weeks following noise exposure (Yamashita et al., 2004), suggesting that a therapeutic window exists for the prevention and treatment of NIHL. Our data show that by extending ebselen treatment for 2 weeks post noise, a greater reduction in ABR threshold shift and OHC loss is achieved.

### **369 D-JNKI-1, a Potent C-Jun N-Terminal Kinase (JNK) Inhibitor Protects Against Acoustic Trauma-Induced Auditory Hair Cell Death and Hearing Loss.**

Jing Wang<sup>1,2</sup>, Christophe Bonny<sup>3</sup>, Jérôme Ruel<sup>1,2</sup>, Ladrech Sabine<sup>1</sup>, Thomas Meyer<sup>2</sup>, Jean-Luc Puel<sup>1</sup>

<sup>1</sup>INSERM U583 and Université de Montpellier 1, <sup>2</sup>Auris Medical, <sup>3</sup>Division de Génétique Médicale, CHUV

Acoustic trauma is the major cause of hearing loss in industrialised nations. Intense sound exposure principally affects the viability of sensory hair cells via the mitogen activated protein kinase (MAPK) cell death signaling pathway that incorporates c-Jun N-terminal kinase (JNK).

We evaluated the otoprotective efficacy of D-JNKI-1, a cell permeable peptide that blocks the MAPK/JNK signal pathway. Our results indicate that acoustic overstimulation (6 kHz, 120 dB SPL during 30 minutes) causes a release of cytochrome c from mitochondria into the cytoplasm of the damaged hair cells prior to the activation of downstream cell death effector molecules, e.g. caspase 3. In addition, DNA fragmentation in cochlear hair cells and ganglion cells was observed suggesting an apoptosis mechanism of hair cell death. The MAPK/JNK signaling pathway is associated with injury, and blocking of this signaling pathway prevented apoptosis in damaged areas. Direct application of D-JNKI-1 into the scala tympani of the guinea pig cochlea via an osmotic minipump prevents DNA fragmentation, and hair cell degeneration. This was confirmed by functional tests demonstrating a clear dose-dependent reduction (ED50 = 2,31 µM) of permanent hearing loss and complete protection at 100 µM D-JNKI-1.

Although less efficient than intracochlear perfusion, the local application of D-JNKI-1 onto the intact round window membrane rescues the cochlea even when applied after acoustic trauma within a therapeutic window of 24 hours.

These results indicate that the MAPK/JNK signal pathway is involved in acoustic trauma-induced hair cell loss and permanent hearing loss. Blocking this signal pathway with D-JNKI-1 is of potential therapeutic value for protection of both the morphological integrity and physiological function of the organ of Corti after acoustic trauma.

### **370 Creatine Attenuates Noise-Induced Hearing Loss**

**Shujiro Minami**<sup>1,2</sup>, Tatsuo Matsunaga<sup>3</sup>, Daisuke Yamashita<sup>1</sup>, Kaoru Ogawa<sup>1</sup>, Jochen Schacht<sup>2</sup>, Josef Miller<sup>2,4</sup>

<sup>1</sup>*Department of Otolaryngology, Keio University,* <sup>2</sup>*Kresge Hearing Research Institute, University of Michigan,*

<sup>3</sup>*National Institute of Sensory Organs, National Tokyo Medical Center,* <sup>4</sup>*Center for Hearing and Communication, Karolinska Institutet*

Energy depletion and free radical formation have been implicated in noise induced hearing loss (NIHL). To better define the role of these factors in NIHL, we measured the effectiveness of creatine (enhances ATP energy storage) and tempol (free radical scavenger) to attenuate NIHL. Guinea pigs were exposed to 120 dB SPL 1 OBN centered at 4 kHz for 5 h. Experimental groups (n = 6 each) included: untreated controls, 3 % creatine diet (2 wk prior to noise exposure), tempol (3 mM in drinking water 2 wk prior to exposure), and creatine + tempol treated. The noise-only group showed auditory brainstem response (ABR) threshold shifts on day 1 of 47dB (4 kHz), 67dB (8 kHz), and 73dB (16 kHz), and on day 10 of 30 dB (4 kHz), 50dB (8 kHz), and 47 dB (16 kHz). Creatine-treated subjects showed smaller ABR threshold shifts on day 1 of 29 dB, 51 dB and 49 dB, and on day 10 of 22 dB, 43 dB and 33 dB at 4, 8, and 16 kHz, respectively. Tempol alone also achieved significant protection on day 10 (24 dB, 42 dB, 34 dB threshold shifts) but not on day 1. ABR shifts in the combination treatment group were not significantly different from the creatine group, except at 16 kHz on day 10 (24 dB). Hair cell loss on day 10 was significantly attenuated in all treatment groups (creatine, tempol, or combination) compared to animals exposed to noise only but there were no significant differences between the treated groups. Our results indicate that the restoration of ATP levels is important in attenuating both temporary and permanent NIHL while the scavenging of free radicals contributes mostly to protection from permanent NIHL.

This work was supported by NIH grant DC04058, General Motors Corporation and the Lynn and Ruth Townsend Professorship

### **371 Post-Exposure Administration of Edaravone, a Free Radical Scavenger, Attenuates Acoustic Trauma.**

**Kuniyoshi Tanaka**<sup>1</sup>, Tsuyoshi Takemoto<sup>1</sup>, Hiroaki Shimogori<sup>1</sup>, Takefumi Mikuriya<sup>1</sup>, Kenji Takeno<sup>1</sup>, Hiroshi Yamashita<sup>1</sup>

<sup>1</sup>*Yamaguchi University School of Medicine*

It is known that increased reactive oxygen species in the cochlear perilymph following noise stress have toxicity to the cochlea. This study investigated the effects of edaravone against the noise-induced hearing loss in the guinea pigs. Edaravone is a free radical scavenger that is clinically used in Japan. A tiny hole was made adjacent to the round window in each guinea pig's right ear, and edaravone (1.722 x 10<sup>-2</sup> M) was infused through this hole by osmotic pump. The left ear was kept intact as a control. The animals were divided into four groups. Group I (n=7) received edaravone during exposure to noise (130 dB SPL, 3 h). Group II (n=8), III (n=7) and IV (n=4) received edaravone 9 h, 21 h and 33 h after the noise exposure, respectively. Seven days after the exposure, we assessed the shift in auditory brainstem response (ABR) thresholds to evaluate cochlear function and observed histopathological characteristics of the sensory epithelia. In Group I, II and III, the shift in ABR thresholds and the proportion of defective outer hair cells were decreased in edaravone-treated ears in comparison to those in untreated ears. In Group IV, however, there was no difference with those in treated ears and untreated ears. The smallest shift and proportion were observed in Group II. These data suggest that edaravone administration may be clinically effective for acoustic trauma, especially within 21 h after the noise exposure.

### **372 Single Oral Dose of Geranylgeranylacetone Induces Heat Shock Proteins in Cochlear.**

**Takefumi Mikuriya**<sup>1</sup>, Tsuyoshi Takemoto<sup>1</sup>, Kuniyoshi Tanaka<sup>1</sup>, Kenji Takeno<sup>1</sup>, Kazuma Sugahara<sup>1</sup>, Hiroaki Shimogori<sup>1</sup>, Hiroshi Yamashita<sup>1</sup>

<sup>1</sup>*Yamaguchi university school of medicine*

Geranylgeranylacetone (GGA) is accepted as an inducer of the heat shock proteins (Hsps) at gastric mucosa, hepatocytes, heart, and brain, and that its response may function to protect those tissues. At last MidWinter Meeting, we showed that GGA administered locally protected cochlea hair cells from acoustic trauma histologically. But we thought that it is difficult that GGA was administered continuously for further trial because of the property of GGA which was settled easily. As same as other tissues, if oral dose of GGA could induce Hsps at cochlea, the way might be effective. So the purpose of this study is to investigate whether single oral dose of GGA can induce Hsps at cochlea and oral administration have protective effect of cochlea hair cells. We used Hartley guinea pigs, and to evaluate cochlear function, we assessed thresholds of the auditory brain stem response (ABR). For histological assessment, we observed the sensory epithelium using surface preparation technique. GGA (600mg/kg) was administered orally and we

investigated the expression of HSP 70, 40 in cochlea by western blot analysis. Next, to clarify the role of heat shock response, after animals were exposed to intense (130 dB SPL) noise for three hours, GGA was given orally once a day for a week. Seven days after the sound exposure, ABR threshold were recorded and we observed the second turn of the organ of Corti. Western blot analysis showed that the expression of Hsp 70, 40 was increased. After the noise exposure, there were fewer defects on outer hair cells of organ of Corti in GGA treated ears than those of the control's, but not significantly. Otherwise, the threshold shifts up in the treated animals to the same level as those in the untreated animals. This result shows that oral dose of GGA have potential to protect cochlea hair cells from acoustic trauma histologically.

### **373** Hearing Rescue After Noise Trauma Guang-Di Chen<sup>1</sup>

<sup>1</sup>University of Oklahoma

Hearing loss due to hair cell death is irreversible, because auditory hair cells in the mammalian cochlea cannot regenerate. However, many noise-damaged hair cells survive in the cochlea for a long time without hearing-related function, leading to a permanent threshold shift (PTS). We believe that noise-induced hearing loss (NIHL) due to hair cell non-lethal injury is treatable. It has been reported that fibroblast growth factor receptor (FGFR) and epidermal growth factor receptor (EGFR) increased in the cochlea after noise exposure. FGF1 is thought to be released from the traumatized nerve endings following damaging auditory stimuli and to initiate recovery and repair processes. Cochlear perfusion with FGF1, FGF2, or EGF was found to promote hearing recovery following noise exposure. In this study, rats (about 250g) were exposed to an octave band noise (10-20 kHz) at 110 dB SPL for 4 hours. Immediately after the noise exposure, the rats (n=5) received cisterna magna injection with 0.2 $\mu$ g FGF1 and 2 $\mu$ g EGF. Control animals were injected with saline only. The growth factor treatment significantly promoted recovery of the cochlear functions.

### **374** Expressions of ATP-Gated Purinergic (P2) Receptors in the Cochlear Outer Hair Cells

Ni Ji<sup>1</sup>, Hong-Bo Zhao<sup>2</sup>

<sup>1</sup>Dept. of Biology, Berea College, Berea, KY 40404, <sup>2</sup>Dept. of Surgery-Otolaryngology, University of Kentucky Medical Center, Lexington, KY 40536

It has been known for a long time that extracellular ATP can influence cochlear active hearing function. Although both ATP-gated ionotropic purinergic (P2X) and metabotropic purinergic (P2Y) receptors have been identified in the mammalian cochlea, the expressions of P2 receptors in outer hair cells (OHCs) remain largely unclear. Both of P2X and P2Y receptors have seven subtypes, each of which plays different roles in cellular functions. In this experiment, the expressions of subtypes of P2X and P2Y receptors in outer hair cells were screened by using immunofluorescent staining and confocal microscopy. OHCs were freshly isolated from the organ of Corti of

guinea pigs and were stained with specific antibody to each subtype of P2X and P2Y receptors. Immunofluorescent staining showed OHCs with strong labeling for subtypes of P2X2, P2X7, and P2Y4. The labeling for P2X4 and P2Y2 receptors was very weak, and no labeling was detected in staining for P2X1, P2X3, P2Y1, and P2Y12 subtypes. The labeling for P2X7 and P2Y4 was distributed through the whole cell membrane, including the OHC lateral wall, while the labeling for P2X2 was mainly restricted at the cell apical and basal parts, consistent with previous reports. The data indicated that there are multiple subtypes of P2 purinergic receptors expressed in OHCs, which may play different roles in OHC electromotility and cochlear functions.

Supported by NIHDCD DC04618 and DC05989 to HBZ

### **375** Extracellular ATP Mediates Outer Hair Cell Electromotility

Ning Yu<sup>1,2</sup>, Hong-Bo Zhao<sup>1</sup>

<sup>1</sup>Dept. of Surgery – Otolaryngology, University of Kentucky Medical Center, Lexington, KY 40536, <sup>2</sup>Dept. of Oto., CPLA General Hospital, Beijing, China, 100853

Adenosine triphosphate (ATP) is an important intracochlear mediator that can influence otoacoustic emission, indicating involvement in mediation of the active cochlear mechanics. Although expressions of ATP-mediated purinergic receptors (P2 receptors) have been reported in outer hair cells (OHCs), it is still unclear whether ATP can influence OHC electromotility. In this experiment, freshly isolated OHCs from the guinea pig cochlea were voltage-clamped under a whole cell configuration to study the influence of ATP on the voltage dependent nonlinear capacitance, which is an electronic signal associated with OHC electromotility. Extracellular application of ATP caused a reversible, dose-dependent depolarizing shift in the voltage at the peak of nonlinear capacitance ( $V_{pkCm}$ ). The shift was detectable in response to application of ATP as low as 3.6 nM. At the 36  $\mu$ M concentration, the mean shift was 11.22 $\pm$ 5.43 mV (n=11). Pre-application of 50  $\mu$ M pyridoxal-phosphate-6-azophenyl-2', 4'-disulfonic acid tetrasodium (PPADS), a P2X receptor antagonist, could block  $V_{pkCm}$  depolarizing shift. Removal of extracellular  $Ca^{2+}$  also inhibited this ATP-induced depolarizing shift in nonlinear capacitance, while using 10 mM BAPTA to chelate intracellular  $Ca^{2+}$  did not block this shift, indicating that this shift is relative to extracellular  $Ca^{2+}$  but irrelative to intracellular  $Ca^{2+}$  release. Neither removal of extracellular and/or intracellular  $K^+$  nor blockage of potassium channels could eliminate the ATP effect. The results indicated that ATP can influence OHC electromotility through P2 receptors on cell surface at normal physiological concentration.

Supported by NIHDCD DC04618 and DC05989 to HBZ



### **376 Vesicular ATP Release from Cells of the Guinea Pig Organ of Corti**

Xiao-Rui Shi<sup>1</sup>, Peter Gillespie<sup>1</sup>, Alfred Nuttall<sup>1,2</sup>

<sup>1</sup>Oregon Hearing Research Center, Oregon Health & Science University, <sup>2</sup>Kresge Hearing Research Institute, University of Michigan

P2X2 purinergic receptors are found at the apical surfaces of sensory hair cells, suggesting that extracellular ATP is important as an autocrine or paracrine mediator of hair cell function. In this study, we investigate the mechanism of Na<sup>+</sup> entry into hair cells of the *in vitro* preparation of the organ of Corti and the possible ATP release from organ of Corti cells. To detect intracellular Na<sup>+</sup>, the fluorescent dye Sodium Green was used. The organ of Corti from adult guinea pigs was isolated and maintained in an organ bath with constant perfusion of artificial perilymph solution. Amiloride was continuously present in the medium to prevent ion influx through mechano-electric transduction channels. Under these conditions, there is a gradual increase in the Na<sup>+</sup> fluorescent intracellular signal both for inner and outer hair cells over the one hour observation time period. The rate of increase of Na<sup>+</sup> signal was significantly reduced when the P2X2 inhibitor pyridoxyl 5-phosphate 6-azophenyl-2',4'-disulfonic acid (PPADS; 100 μM) was also present in the medium. Washout of PPADS caused a sharp increase in the fluorescent signal rate of increase. Depletion of extracellular ATP with ATP phosphohydrolase (0.125 to 0.5 units/ml, Sigma Units) also significantly reduced the rate of Na<sup>+</sup> signal increase. To determine if the apparent extracellular ATP was caused by vesicular release from the cells of the organ of Corti, we used different inhibitors of cellular vesicular traffic. Treatment of the tissue with BAPTA-AM (30 μM) significantly reduced the Na<sup>+</sup> signal. Blocking cAMP synthesis (SQ 22536; 250 μM) or vesicular transport with LY 294002 (10 μM) also reduced the Na<sup>+</sup> signal. Taken together, these results show an activation of P2X2 receptors on hair cells occurs via vesicular ATP release. Although the specific cells responsible for the ATP release are not known, the data suggest the possibility of autocrine control by hair cells of their apical membrane ionic conductances. Supported by NIH NIDCD DC 00105, 00141, 004571 and 002368

### **377 Alteration of Activator Protein 1 DNA Binding Activity in Gentamicin Induced Hair Cell Degeneration.**

Andrea Albinger<sup>1</sup>, Ivan Hegyi<sup>1,2</sup>, Ivana Nagy<sup>1</sup>, Morana Bodmer<sup>3</sup>, Stephan Schmid<sup>1</sup>, Daniel Bodmer<sup>1</sup>

<sup>1</sup>Department of Oto-Rhino-Laryngology, Head and Neck Surgery, University Hospital Zürich, Frauenklinik,

<sup>2</sup>Department of Pathology, Institute of Clinical Pathology, University Hospital Zurich, Schmelzbergstr, <sup>3</sup>Swiss Federal Institute of Technology (ETHZ), Raemistr. 101, 8092 Zurich, Switzerland

Sensorineural hearing loss (SNHL) is associated with damage of cochlear hair cells (HCs) and/or of the neurons of the auditory pathway. This damage can result from a variety of causes, e.g. genetic disorders, aging, exposure

to certain drugs such as aminoglycosides, infectious disease and intense sound overexposure. Intracellular events that mediate aspects of aminoglycoside mediated damage to HCs have been partially unraveled. Several independent research groups have demonstrated a crucial role of mitogen activated protein kinase (MAPK) signaling in aminoglycoside induced ototoxicity.

MAPKs are important mediators of signal transduction from the cell surface to the nucleus. Jun N-terminal kinases (JNK), members of the MAPK family, are strongly activated in cell culture conditions by stress-inducing stimuli, including ultraviolet light (UV), heat shock and tumor necrosis factor; therefore they are also referred to as stress-activated protein kinases (SAPKs). In HCs, the JNK signaling pathway was shown to be activated by aminoglycoside treatment. Activation of JNK leads to phosphorylation and thereby activation of transcription factors and consequently to altered gene expression. There are many nuclear JNK substrates including c-Jun, ATF2, Elk-1.

One of the downstream targets of JNK is the transcription factor activating protein -1 (AP-1). AP-1 is a dimeric complex composed of members of the Fos and Jun proteins. A variety of different stimuli are known to induce AP-1 activity. Induction of AP-1 is thought to play a central role in reprogramming gene expression in response to external stimuli. In this study we have analyzed the effect of gentamicin treatment on the downstream targets of JNK. Our results demonstrate that gentamicin treatment of explants of Organ of Corti (OC) results in increased AP-1 binding activity. The main component of these AP-1 complexes is the c-Fos protein. Moreover, we show that the AP-1 induction is transient and occurs exclusively in HCs of OC explants.

### **378 Mechanisms of Rapid Hair Cell Death Induced by Co-Administration of Cisplatin and Ethacrynic Acid in Chinchilla**

Dalian Ding<sup>1</sup>, Haiyan Jiang<sup>1</sup>, Richard Salvi<sup>1</sup>

<sup>1</sup>Center for Hearing & Deafness, SUNY at Buffalo

Hair cell damage is difficult to induce in chinchillas using cisplatin (CIS) alone; however, if CIS is co-administered with ethacrynic acid (EA) there is rapid and widespread destruction of inner hair cells (IHC) and outer hair cells (OHC). The cell death pathways involved in CIS/EA induced ototoxicity are poorly understood; however, the initial stages of ototoxicity are likely to involve reactive oxygen species generated by these ototoxic agents, secondary ischemic effects caused by EA-induced impairment of blood flow in stria vascularis, and/or enhanced entry of cisplatin into the cochlea due to EA-induced disruption of the blood-cochlear barrier. To elucidate the apoptotic pathways involved in rapid CIA/EA induced hair cell death, we simultaneously administered CIS (80 mg/kg, i.m.) and EA (40 mg/kg, i.v.) to chinchillas and evaluated cell death signaling pathways 6, 12, 18, 24, or 48 h after treatment. Apoptosis mediated by the receptor-mediated, initiator caspase 8 signaling was first seen in some hair cells in the base of the cochlea at 6 h post-treatment, but by 12 h, caspase 8 activation had

increased and extended well into the second cochlear turn. Activation of executioner caspase 3 first was first seen in basal turn hair cells around 12 post-treatment. At 18 h post-treatment, severe damage was evident in the cuticular plate and staining with propidium iodide, which intercalate with DNA, revealed extensive nuclear condensation and fragmentation, an anatomical hallmark of apoptosis. By 24-48 h post-treatment, most OHC and IHC in the basal turn and many in the middle turn were completely destroyed. Importantly, no activation of initiator caspase 9 affecting mitochondria was seen within this assessment time window. These results suggest that the rapid loss of hair cells following CIS/EA treatment primarily involves apoptotic cell death pathways initiated by caspase 8 and followed by activation of executioner caspase 3. These results suggest that CIS/EA damage may start from the cell surface receptors such as Fas or tumor necrosis factor receptor 1 (TNFR1).

Supported by NIH grants P01 DC03600-01A1 & R01 DC06630-01

### **379 Cochlear Hair Cell Damage Caused by Application of Kanamycin Through the Round Window Membrane**

**Yasuyuki Hashimoto<sup>1</sup>, Satoshi Iwasaki<sup>1</sup>, Mitsuyoshi Nagura<sup>1</sup>, Kunihiro Mizuta<sup>1</sup>**

<sup>1</sup>*Hamamatsu University School of Medicine*

We investigated cochlear outer hair cell damage caused by kanamycin under a drug delivery system. IntraEAR Animal Round Window micro Catheter® (Durect, Cupertino, CA) was placed at the round window niche of guinea pigs and kanamycin was administered by an electronic micropump. Two doses of Kanamycin (345 mg/ml, 172.5 mg/ml) and saline were delivered at a rate of 0.1 ml/hr for 1 or 2 hours. Catheter was then removed and the middle ear was flushed with saline. Four days after the treatment, the animals were decapitated and their cochleae were microdissected. The specimens were examined using a scanning electron microscope.

No significant damage was observed in control group that was treated with saline alone. At the dose of 172.5mg/ml, one hour treatment by kanamycin resulted in 42.8% outer hair cell loss in the basal turn and 1.1% loss in the second turn. Two hour treatment resulted in outer hair cell loss of 79% in the basal turn and 34.2% in the second turn. At 345 mg/ml, one hour treatment gave rise to 89.6% outer hair cell loss in the basal turn and 28.3% in the second turn. 2-hour treatment led to total destruction of outer hair cells without any significant difference among basal and second turns.

The hair cell loss that we observed was both dose-dependent and treatment duration-dependent. Our results thus indicate that we controlled damage area in the cochlea by drug doses and treatment duration with the drug delivery system through round window membrane.

### **380 Phosphatidylserine Exposure on the Outer Leaflet of Cochlear Hair Cell Plasma Membranes is Induced by in Vitro Sodium Loading**

**Xiao-Rui Shi<sup>1</sup>, Peter Gillespie<sup>1</sup>, Alfred L. Nuttall<sup>1,2</sup>**

<sup>1</sup>*Oregon Hearing Research Center, Oregon Health & Science University, <sup>2</sup>Kresge Hearing Research Institute, University of Michigan*

Apoptotic or necrotic cell death is characterized by the early exposure of phosphatidylserine (PS) at the outer leaflet of the plasma membrane. Using annexin V fluorescent labeling, we previously reported that incubation of adult organ of Corti tissues in artificial perilymph solution caused rapid exposure of phosphatidylserine (PS) on the external leaflet of inner hair cell (IHC) apical plasma membranes. To test if PS externalization is caused by early apoptosis or necrosis, we treated the isolated organ of Corti with z-VAD-fmk (50  $\mu$ M), a broad-spectrum inhibitor of caspases. PS externalization was unchanged with this treatment. Moreover, mitochondrial membrane potential (measured using 100 nM TMRM) remained normal, swollen nuclei were not observed, and DNA condensation or fragmentation (assayed with 1 mg/ml propidium iodide) were also not detected. By contrast, we have found that PS externalization is highly correlated with high intracellular Na<sup>+</sup> fluorescent signals as measured with Sodium Green dye. Blocking Na<sup>+</sup> influx by inhibiting the mechano-electronic transduction channels with 500  $\mu$ M amiloride hydrochloride and P2X ATP channels with 100  $\mu$ M PPADS greatly reduced external PS exposure. Similar results were seen when Na<sup>+</sup> in the bath was replaced with N-methyl-D-glucamine. These results indicate that PS exposure on the external leaflet, presumably via phospholipid scrambling, results from Na<sup>+</sup> influx. Limited regional externalization at the apical pole may arise because the apical pole of the HC is a unique 'compartment', which regulates plasma membrane permeability and composition differently than the basolateral region of the cell. Supported by NIH DC00105, DC00141, DC004571 and DC002368.

### **381 Effect of Ouabain Treatment on Inner Hair Cell Ultrastructure**

**Spicer, S.S.<sup>1</sup>, Lang, H.<sup>1</sup>, Schmiedt, R.<sup>1,2</sup>, Schulte, B.A.<sup>1</sup>,**

<sup>1</sup>*Department of Pathology and Laboratory Medicine, Medical University of South Carolina, 165 Ashley Avenue, Charleston, South Carolina, 29425, <sup>2</sup>Department of Otolaryngology-Head and Neck Surgery, Medical University of South Carolina, 165 Ashley Avenue, Charleston, South Carolina, 29425*

Administering the Na,K-ATPase antagonist ouabain via the round window has been shown to ablate type I spiral ganglion neurons in the gerbil cochlea and produce an animal model of nerve deafness (Schmiedt et al, JARO 3:223, 2002). Neurosensory inner hair cells (IHCs) differ from neurons in possessing a unique population of crowded synaptic vesicles that fill the basal half of the cell (Spicer et al, J. Comp. Neurol. 409:424-37, 1999). The present inquiry addressed the question raised by the model concerning the fate of inactive synaptic vesicles in

IHCs that lack synaptic connections to radial nerves. Cochleas of 12 young adult gerbils were examined by electron microscopy at intervals up to 2 months following induction of nerve deafness by 0.5 hr, application of 50  $\mu$ l of 1mM ouabain to the round window niche. The IHCs of these animals consistently showed degradation of the synaptic vesicle population to an equally large population of solid grain-like structures. This change provided evidence that the cell deactivated the synaptic vesicles in lieu of a mechanism for exocytosing or catabolizing them. The basal region of three of the cochleas exhibited another pathologic change that involved formation of one or more large, compacted islands apparently composed of coalesced vesicles. These islands differed from autophagic lysosomes in lacking a delimiting membrane and disclosed again an inability to lyse or destroy vesicles catabolically. In addition, one cochlea revealed an involution of stereocilia associated with conversion of the upper half of the cell under the utricular plate to a crystalline-like array of parallel aligned laminae.

### **382 High Concentrations of Chlorpromazine are Lethal to HEK and Cochlear Outer Hair Cells.**

**Daniel Chelius<sup>1</sup>**, Rosen Ugrinov<sup>1</sup>, Cynthia Shope<sup>1</sup>, William Brownell<sup>1</sup>

<sup>1</sup>*Baylor College of Medicine*

The antipsychotic, cationic, amphipath chlorpromazine (CPZ) intercalates into lipid bilayers, often changing membrane architecture and function. CPZ reversibly shifts the voltage-displacement function for outer hair cell (OHC) electromotility and increases both the cochlear compound action potential threshold and the distortion product otoacoustic emission threshold, likely via its effect on the membrane-based OHC motor mechanism. CPZ may indirectly influence cochlear function in the current treatment of psychiatric disorders and the investigational treatment of certain malignancies. We designed this study to examine the effects of CPZ on OHC viability. Because wild-type human embryonic kidney (HEK) cells are frequently used as a cell model in OHC research (e.g. transfection with the OHC membrane-protein prestin), we initially applied CPZ to HEK cells. Using trypan blue as a marker of cell death and the *annexin-V* fluorescent probe as a marker of apoptosis, we noted a concentration dependent increase in HEK cell proliferation up to 10  $\mu$ M CPZ. Above 10  $\mu$ M, apoptosis occurred and increased with concentration. After exposure to 100  $\mu$ M CPZ, all HEK cells began apoptosis within 25-45 minutes and were dead within one hour. When OHCs were exposed to 100  $\mu$ M CPZ for one hour, we observed an increased rate of basolateral cell membrane annexin labeling (11%) versus control (5%). Additionally, 19% of CPZ exposed OHCs demonstrated cytoplasmic clumping of annexin, indicating the induction of membrane pores. Cytoplasmic labeling was not observed in control OHCs, which demonstrated apical membrane labeling with annexin similar to that in IHCs as reported by Shi et al in a 2004 ARO abstract. Our results suggest that CPZ may not be ototoxic at its antipsychotic therapeutic concentrations; but, at levels that

have been proposed for its use as an antineoplastic agent it may lead to hearing loss.

Supported by NIDCD research grant NIH RO1 DC00354.

### **383 Meniere's Disease, an Explanation for the Cochlear Symptoms of Hydrops**

*Withdrawn*

### **384 Transfection of Math1 into Neural Stem Cells**

**Wen-Hann Tan<sup>1</sup>**, Mark A. Parker<sup>1,2</sup>, Douglas A. Cotanche<sup>1,2</sup>

<sup>1</sup>*Department of Otolaryngology, Children's Hospital Boston*, <sup>2</sup>*Department of Otology and Laryngology, Harvard Medical School*

Transfection of Math1 into Neural Stem Cells

Mouse atonal homolog 1 (Math1), the murine homolog of the *Drosophila* atonal gene, is required for the production of inner ear hair cells. Math1 encodes a member of the basic helix-loop-helix transcription factor family, and is thought to be involved in the differentiation of various subsets of neural precursors. Previous studies have shown that Math1-null knock-out mice do not develop any hair cells, while over-expression of Math1 in cochlear explants leads to excess production of hair cells. This supports the essential role of Math1 in the formation of cochlear hair cells. The overall aim of our research is to regenerate inner ear hair cells that have been damaged or lost. We hypothesize that by over-expressing the Math1 gene in a population of relatively undifferentiated cells placed in an appropriate environment, hair cells can be produced. Neural stem cells provide an attractive vehicle for the delivery and expression of the Math1 gene into the damaged cochlea because they retain the capacity to differentiate into all types of neuronal cells appropriate to the local environment and demonstrate the capacity to migrate to the site of neuronal injury. As the first step towards this goal, we have transfected c17.2 neural stem cells with a plasmid containing the Math1 gene using a calcium phosphate mixture. We will present data that demonstrate the effects of overexpression of Math1 in neural stem cells *in vitro*.

### **385 Co-Culture of Mouse Cochlea with Cells Derived from Embryoid Bodies**

**Tsuyoshi Takemoto<sup>1</sup>**, Kazuma Sugahara<sup>1</sup>, Kuniyoshi Tanaka<sup>1</sup>, Hiroshi Yamashita<sup>1</sup>, Akira Nakai<sup>2</sup>

<sup>1</sup>*Department of Otolaryngology Yamaguchi University School of Medicine*, <sup>2</sup>*Department of Biochemistry and Molecular Biology Yamaguchi University School of Medicine*

It was thought that hair cells of the inner ear of mammals do not regenerate after injury, although in birds and lower vertebrates hair cells regenerate spontaneously. Recently some studies about hair cell regeneration in mammals were reported using viruses, cell transplantation. We report the co-culture of mouse cochlea with cells derived from embryoid bodies (EBs). EBs were obtained from

mouse embryonic stem (ES) cells expressed green fluorescent protein (GFP). ES cells were differentiated to EBs in vitro using hanging drop technique. EBs were dissociated with trypsin-EDTA. Temporal bones were removed from 6d-old mice and picked up organ of cortis in PBS with 6 % glucose. They were incubated in DMEM F12 / 3g/l glucose/ N2supprement medium at 37 °C with 5 % CO<sub>2</sub> for 2 days. Then cells derived from EBs were added to cultured tissues and co-cultured for 3 days. For histological examination, cultured tissues were fixed with 4 % paraformaldehyde in PBS for 12 hours and stained sensory epithelium with phalloidin TexasRed. Then we observed cultured tissues under a fluorescent micro scope. Cultured organ of cortis for 7days were observed. They had same appearances compared with tissues observed immediately after removed so we thought that in this model organ cultures of corti were kept good condition for 7 days. The tissues co-cultured for 3 days were observed. Cells expressed GFP were attached to out side of sensory epithelium layer and no cells were identified in sensory epithelium layer.

### **386** Alteration of the Expression Patterns of Musashi-1 in the Guinea Pig Cochlea Following Hair Cell Injury Induced by Ototoxic Agents

Chie Miyajima<sup>1</sup>, Tatsuya Yamasoba<sup>1</sup>, Kenji Kondo<sup>1</sup>, Hideyuki Okano<sup>2</sup>

<sup>1</sup>University of Tokyo, <sup>2</sup>Keio University School of Medicine

Musashi-1 (Msi1), a neural RNA-binding protein, is highly enriched in neural precursor cells that are capable of generating both neurons and glia during embryonic central nervous system and therefore is regarded as a neural stem cell marker. The wide expression of Msi1 in the supporting cells suggests that those cells might have the potential to become hair cell progenitors once the hair cells are injured. In the current study, we investigated if Msi1 expression was altered in the mature guinea pig cochlea following significant hair cell loss induced by ototoxic agents.

Young albino guinea pigs were deafened by the systemic application of kanamycin sulfate (400 mg/kg, s.c.) followed 2 hours later by ethacrynic acid (50 mg/kg, i.v.). The animals were euthanized 1, 3, 7, and 28 days following it, and the cochlea was fixed with 4 % PFA, decalcified in 10 % EDTA, and embedded in paraffin. Sections parallel to the modiolus were immunostained using a monoclonal antibody for Msi1 (14H1).

In the normal cochlea, Msi1 immunoreactivity was confined to the nuclei of a variety of supporting cells, such as Deiters cells and outer and inner pillar cells, whereas there was no immunoreactivity in the inner or outer hair cells. The hair cells showed significant degeneration already 1 day following deafening, and the pattern of the subcellular localization of Msi1 immunoreactivity in the supporting cells changed over time. Msi1 immunoreactivity became obscure in the nuclei and discernible relatively predominantly in the cytoplasm 1 through 7 days following deafening. The Msi1

immunoreactivity returned to be nuclear predominant pattern 4 weeks after deafening.

It is worth mentioning that Msi1 is localized predominantly in the cytoplasm of CNS progenitor cells and that the subcellular localization of Msi1 in the supporting cells in the inner ear changes from the cytoplasmic predominance to the nuclear predominance during the first 2 weeks after birth. Considering these findings, diffuse spread of Msi1 immunoreactivity into the cytoplasm of the supporting cells soon after the completion of hair cell loss seems to imply that Msi1 plays some role during scar formation, such as introduction of hair cell regeneration, although some other mechanisms, such as expression of p27Kip1, strictly inhibit this potential.

### **387** New Hair Cells Induced in vivo in Adult Chinchilla Vestibular Epithelium by ad-Hath1

Dalian Ding<sup>1</sup>, Jianyong Shou<sup>2</sup>, Wei-Qiang Gao<sup>2</sup>, Richard Salvi<sup>1</sup>

<sup>1</sup>University at Buffalo, <sup>2</sup>Genentech Inc

Hair cells in the mammalian auditory and vestibular systems can be destroyed by traumatic insults (e.g., ototoxic drugs, aging, noise, infections); however, damaged cells do not regenerate leading to permanent auditory or vestibular deficits. Math1 and its human homolog, Hath1, are members of the basic helix-loop-helix transcription factor genes that, in certain cell types, are sufficient to promote the production of new hair cells. In the past few years, several groups have exploited this finding and have used plasmid- (Zheng and Gao, 2000) or viral-mediated Math1/Hath1 gene therapy to promote the differentiation of supporting cells into hair cells in postnatal rat cochlear or adult rat vestibular cultures (Shou et al., 2003) or mature guinea pig (Kawamoto et al, 2003) inner ears. To extend these results to an in vivo model, we infused an adenovirus carrying Hath1 plus EGFP genes (ad-Hath1-EGFP) or EGFP alone (ad-EGFP) into the adult (1-2 years) chinchilla vestibular cavity. After 2-4 weeks, the animals were sacrificed and evaluated by confocal and scanning electron microscopy for evidence of new hair cells. After treatment with ad-Hath1-EGFP, new, presumptive hair cells (pHC) with stereocilia bundles and expressing EGFP were seen in several regions of vestibular epithelium. In some cases, ectopic pHC were found in small, circumscribed islands well outside the normal sensory cell region while in other cases ectopic pHC were located in loose clusters. Ectopic pHC were also seen in the non-sensory, dark cell region of the macula of the utricle. Importantly, ectopic pHC were never seen in chinchillas treated with ad-EGFP. EGFP expressing pHC were also seen along the border of the sensory cell region as well as within the cristae and maculae itself. These results suggest virally mediated gene transfer of Hath1 can be used to drive the differentiation of supporting cells into hair cells in adult animals. (Support by NIH grants P01 DC03600-01A1 & R01 DC06630-01)

### **388 Synaptic Potentials at the Inner Hair Cell Afferent Synapse**

Eunyoung Yi<sup>1</sup>, Elisabeth Glowatzki<sup>1</sup>

<sup>1</sup>Johns Hopkins School of Medicine

Inner hair cell (IHC) ribbon synapses in the mammalian cochlea are the first site of chemical transmission in the auditory pathway. Postsynaptically, fast transmission is mediated by rapidly-gating AMPA receptors at the afferent dendrites of auditory nerve fibers. To achieve rapid and reliable signaling, however, the receptor currents must be reliably converted into suprathreshold postsynaptic potentials with short latency. Here, we compare excitatory postsynaptic currents (EPSCs,  $n=1066-1464$ ) and potentials (EPSPs,  $n=162-1593$ ) both recorded from the same IHC afferent dendrite ( $n=3$ ), to identify postsynaptic mechanisms enabling rapid and reliable transmission. In apical turns of 7-12 day-old rat cochleae we recorded spontaneous or 'evoked' (by 15 mM extracellular  $K^+$ ) postsynaptic events from afferent dendrites using whole-cell patch clamp (Glowatzki and Fuchs, 2002). In general, the EPSP waveform was 2-4 times prolonged relative to that of the EPSC (time constant of decay 2-4 ms vs. 1 ms). As we have shown before, EPSC amplitude distributions were highly skewed with a peak at about 30-40 pA and values up to 800 pA (at -90 mV at room temperature). In comparison, while EPSP amplitudes varied from 1 to 40 mV overall their distributions were normalized relative to the highly skewed distribution of the postsynaptic currents. EPSP amplitudes were not affected by 1  $\mu$ M TTX. These results suggest that passive properties and possibly the postsynaptic voltage-dependent potassium conductances play an important role in shaping the EPSPs. During depolarizing voltage steps, we observed rapidly activating inward and outward currents, presumably through voltage-gated sodium and potassium channels ( $n=10$ ). Supported by the NICDC DC006476 to EG and DC05211.

### **389 Channel Noise and Quantal-Size Variability in Bouton Afferents of the Turtle Posterior Crista**

Jay M. Goldberg<sup>1</sup>, Joseph C. Holt<sup>1</sup>, Anna Lysakowski<sup>2</sup>

<sup>1</sup>University of Chicago, <sup>2</sup>University of Illinois, Chicago

Shot-noise theory, particularly Rice's extension of Campbell's theorem, can be used to estimate quantal size ( $q_{size}$ ) and quantal rate ( $q_{rate}$ ) from the variance ( $\lambda_2$ ) and skew ( $\lambda_3$ ), the second and third cumulants of high-pass filtered records. In applying the theory, the contributions of instrumental and channel noise to  $\lambda_2$  must be eliminated. Instrumental noise can be estimated from the  $\lambda_3$  vs  $\lambda_2$  relation. Channel noise was estimated from the response to bath-applied AMPA during periods when quantal activity was momentarily abolished by inhibitory mechanical stimulation. From the AMPA response, the relation between the mean ( $\lambda_1$ ) of the dc-coupled record and  $\lambda_2$  provided an estimate for the size of individual channel openings,  $\lambda_1/v = 1.24 \pm 0.36 \mu$ V (mean  $\pm$  SE,  $n = 5$ ). Resting quantal activity typically leads to a depolarization,  $\lambda_1 = 1$  mV. The variance contributed by channel noise at rest is obtained from the

product,  $\lambda_1 \cdot v = 1.25 \times 10^{-3} \text{ mV}^2$ , approximately 3% of the typical resting  $\lambda_2 = 4.5 \times 10^{-2} \text{ mV}^2$ .  $q_{size}$  is typically 0.4 mV. From the ratio,  $\lambda_1/v/q_{size}$ , an individual mEPSP involves the opening of 300 channels. This is about 10 times larger than the corresponding estimates for central synapses. Part of the difference can be explained by the larger postsynaptic densities of hair-cell, as compared to central, synapses.

The findings have implications for the distribution of  $q_{size}$ s. Deconvolution of quantal records indicates that  $q_{size}$ s are approximately gamma distributed with a  $cv = 0.4$ . Theoretically, a second estimate of  $cv$  can be obtained from shot-noise estimates involving the fourth cumulant ( $\lambda_4$ ), as well as  $\lambda_2$  and  $\lambda_3$ . Unfortunately,  $\lambda_4$  has a large statistical variability and is perturbed by inadvertent, but unavoidable variations in  $q_{rate}$ . Instead, we can infer  $\lambda_4$  from the above estimate of channel noise. The inferred  $\lambda_4$  leads to the same  $q_{size} cv$  as does deconvolution.

### **390 Quantal (QT) and Non-Quantal Transmission (NQT) in Bouton Afferents of the Turtle Posterior Crista**

Joseph C. Holt<sup>1</sup>, Jay M. Goldberg<sup>1</sup>

<sup>1</sup>University of Chicago

We had previously emphasized NQT involving type I hair cells. NQT also takes place between type II hair cells and bouton endings. During sinusoidal mechanical stimulation, afferents show a periodic modulation of membrane potential ( $v_{mod}$ ). On average, two-thirds of  $v_{mod}$  is a consequence of QT, while the remaining one-third is NQT. To investigate the etiology of NQT, we blocked glutamate QT presynaptically by lowering external  $Ca^{2+}$  or postsynaptically with CNQX. Even after complete QT block,  $v_{mod}$  persists, but is reduced in amplitude, typically by >50%, from control estimates of NQT. The persistence provides independent evidence for NQT. The amplitude reduction implies that some, but not all, of NQT is due to glutamate spillover. To confirm the latter suggestion, we used TBOA, a blocker of glutamate transporters. Consistent with the suggestion, TBOA enhances NQT even as it reduces QT. In addition, TBOA can result in a progressive phase lag of  $v_{mod}$  and a long lasting depolarization, implying the persistence of transmitter beyond the stimulus cycle in which it is released. Because it persists after glutamate block, NQT must involve some mechanism besides glutamate accumulation. A candidate is  $K^+$  accumulation. Receptor currents are carried out of hair cells by  $K^+$ , which may accumulate extracellularly during excitatory stimulation. To explore this possibility, we studied the effects of bath application of 10 mM  $K^+$  and of 30 – 300  $\mu$ M DIDS, a blocker of K-Cl co-transporters among other things. Both agents led to similar results, greatly reducing QT, while having a much smaller effect on NQT; the action on QT appears to be postsynaptic as quantal size is much more affected than quantal rate. It remains to be seen whether the agents enhance NQT after glutamate block. Regardless of mechanism, NQT is of

potential functional importance since the depolarization it produces can result in large changes in spike rate.

### **391 Membrane Potential Changes Influence Membrane Transcytosis of Outer Hair Cells**

Csaba Harasztosi<sup>1</sup>, Toshihiko Kaneko<sup>1,2</sup>, Anthony W. Gummer<sup>1</sup>

<sup>1</sup>University Tubingen, Dept. Otolaryngology, Germany,

<sup>2</sup>Kansai Medical University, Dept. Otolaryngology, Japan

Hair cells are known to exhibit rapid endocytic activity around the cuticular plate. Using the fluorescence dye FM1-43 we have previously shown evidence that trapped vesicles at the apical pole are transported to the basal pole in guinea-pig cochlear outer hair cells (OHCs) (P448, ARO 2004). This dye dissolves reversibly into the outer leaflet of surface membranes and is trapped by endocytosis. The purpose of this study was to clarify the effect of depolarization on membrane transcytosis of OHCs.

OHCs were mechanically isolated from the adult guinea-pig cochlea. FM1-43 dye (10  $\mu$ M) was applied locally to OHCs by pressure injection. Fluorescence changes of FM1-43 were monitored using confocal laser scanning microscopy (Zeiss LSM510). The patch-clamp technique in whole-cell configuration was used to depolarize OHCs.

Holding the membrane potential at -60 mV, continuous application of FM1-43 dye evoked a monotonic increase of the fluorescence signal with time, in both the apical and the basal regions of the OHC. The slope of this time dependence was reduced as a result of depolarizing the cell to 0 mV. Normalized to control, depolarization to 0 mV reduced the slope of the time dependence to  $0.29 \pm 0.14$  (mean  $\pm$  SD) and  $0.26 \pm 0.17$ , respectively, in the apical and basal regions. This effect was reversible. While application of CdCl<sub>2</sub> (200  $\mu$ M), a potent voltage-gated Ca<sup>2+</sup> channel blocker, did not block the effect of depolarization in the apical region ( $0.50 \pm 0.26$ ), it did in the basal region ( $0.99 \pm 0.18$ ).

These results indicate that depolarization influences membrane transcytosis in OHCs and facilitates exocytotic activity of OHCs by opening voltage-gated Ca<sup>2+</sup> channels.

### **392 Analysis of Non-stationary Fluctuations of Exocytotic Capacitance Changes in Mouse Inner Hair Cells**

Darina Khimich<sup>1</sup>, Primoz Pirih<sup>1,2</sup>, Fred Wolf<sup>3</sup>, Tobias Moser<sup>1</sup>

<sup>1</sup>University of Goettingen, <sup>2</sup>University of Groningen, <sup>3</sup>MPI for Nonlinear Dynamics

Ribbon synapses are specialized structures, found in neurons driven by graded potentials. It has been proposed that ribbons act as attractors or reservoirs for the synaptic vesicles, thus enabling multivesicular release and rendering these synapses able of transmitting information over a broad dynamic range of stimuli with short latency. We have applied non-stationary fluctuation analysis to repetitively evoked exocytotic capacitance steps in perforated patch clamp recordings from inner hair cells (IHC). To reveal the apparent quantal vesicle size and thus give insight into the statistical properties of the fusion

mechanism we have developed some enhancements of the non-stationary fluctuation analysis (e.g. demixing of crosstalk between the lock-in channels, trend-correction procedures, bootstrapping randomization for the estimation of the quantal size confidence interval). Preliminary results have shown that the apparent quantal vesicle sizes, estimated with this method, are similar to the real size of a single vesicle, suggesting statistical independence of individual vesicles in the mature mouse inner hair cells.

### **393 Effects of ATP- $\gamma$ -S on Endocytosis and Exocytosis in Frog Sacculus Hair Cells**

Mark Rutherford<sup>1</sup>, William Roberts<sup>1</sup>

<sup>1</sup>Institute of Neuroscience, University of Oregon

Whole-cell recordings of membrane capacitance have revealed differences in depolarization-evoked synaptic vesicle fusion and subsequent compensatory endocytosis when ATP in the internal solution is replaced with the poorly hydrolyzable substrate, ATP- $\gamma$ -S. Compared to the standard ATP condition, we observed decreased exocytosis in response to continuous depolarization as well as deficits in the degree of membrane retrieval after stimulation under conditions of competitive inhibition of ATP. Preliminary results also suggest an effect on steady-state membrane cycling. An apparent decrease in endocytosis at rest results in a steady upward drift in membrane capacitance when ATP is replaced with ATP- $\gamma$ -S. Contrary to previous findings in retinal bipolar cells, paired pulse depression does not differ between the two conditions. The presence of functional refilling of the releasable vesicle pool in the seconds between pulses suggests that the reduced exocytotic burst during brief depolarization results from an inhibition of fast resupply of vesicles to release sites when ATP- $\gamma$ -S replaces ATP in frog sacculus hair cells.

### **394 Role of the Calcium-Activated Potassium Channel SK2 in Olivocochlear System Development and Function.**

Douglas E. Vetter<sup>1</sup>, Stephane F. Maison<sup>2</sup>, Julian Taranda<sup>3</sup>, Chris T. Bond<sup>4</sup>, A. Belen Elgoyhen<sup>5</sup>, M. Charles Liberman<sup>2</sup>, John P. Adelman<sup>4</sup>

<sup>1</sup>Tufts Univ. School of Medicine, <sup>2</sup>Eaton Peabody Lab, Mass. Eye and Ear Infirmary, <sup>3</sup>INGEBI, Univ. Buenos Aires, <sup>4</sup>Vollum Inst., Oregon Health Sciences Univ., <sup>5</sup>INGEBI, UBA-CONICET Buenos Aires

Efferent transmission at outer hair cells involves ligand-gated calcium entry via nicotinic acetylcholine receptors (nAChR) composed of  $\alpha 9$  and  $\alpha 10$  subunits. This then activates calcium sensitive, small conductance K channels, resulting in hyperpolarization of the cell and suppression of cochlear responses. The K channel is thought to be the apamin sensitive SK2 channel. The present study tests this hypothesis, and further investigates the role of SK2 in the inner ear, using SK2 gene null mice (Bond et al., 2004).

Cochlear function in SK2 null mice was assessed by comparing amplitude vs. level functions for ABRs and

DPOAEs to those from wildtype littermates. Efferent transmission was assessed by electrically activating the olivocochlear (OC) bundle and measuring DPOAE amplitude suppression. Morphology of efferent terminals was assessed by examination of cochlear whole mounts and cryostat sections immunostained for vesicular acetylcholine transporter or synaptophysin.

Baseline cochlear function was unaffected by SK2 deletion: ABRs and DPOAEs were similar in knockouts and wildtypes. In contrast, effects on efferent transmission were profound: OC stimulation in wildtypes always elicited large and rapid suppression of DPOAEs; similar stimulation in the SK2 null mice never suppressed DPOAEs, and sometimes produced a small, slow enhancement of DPOAE amplitude. Morphological investigation revealed profound alterations of OC terminal morphology: OC boutons on outer hair cells were less numerous and significantly smaller than in wildtype controls.

These results definitively illustrate that the SK2 channel is functionally coupled with the hair cell nAChR and participates in the production of classic suppressive OC effects. However, SK2 channel activity also appears necessary for the normal development and/or maintenance of the efferent synaptic contacts themselves.

Support- DC006258 (DEV), DC0188 (MCL), Fundación Antorchas (ABE and DEV)

### **395** Role of the $\alpha 10$ nAChR Subunit Gene in the Development and Function of the Olivocochlear System

**Douglas E. Vetter**<sup>1</sup>, Eleonora Katz<sup>2</sup>, Stephane F. Maison<sup>3</sup>, Julian Taranda<sup>4</sup>, Chenghang Huang<sup>1</sup>, M. Charles Liberman<sup>3</sup>, A.Belen Elgoyhen<sup>5</sup>, Jim Boulter<sup>6</sup>

<sup>1</sup>*Dept. of Neuroscience, Tufts Univ. School of Medicine,*

<sup>2</sup>*INGEBI-CONICET, Univ. Buenos Aires,* <sup>3</sup>*Eaton Peabody Lab, Mass. Eye and Ear Infirmary,* <sup>4</sup>*INGEBI, Univ. Buenos Aires,* <sup>5</sup>*INGEBI, UBA-CONICET Buenos Aires,* <sup>6</sup>*Dept. of Psychiatry and Biobehavioral Sci., UCLA*

It is well known that acetylcholine (ACh) is a major neurotransmitter of the olivocochlear (OC) system, and that hair cell nicotinic acetylcholine receptors (nAChR) are encoded by the  $\alpha 9$  and  $\alpha 10$  nAChR subunit genes. While  $\alpha 9$  functions as a homomeric receptor in heterologous expression assays, generation of the native hair cell-like physiology requires  $\alpha 10$  co-expression. Also, normal endogenous changes in the expression level of  $\alpha 10$  mRNA during postnatal development correlates with sensitivity of IHCs to ACh. However, the precise function played by the  $\alpha 10$  gene in auditory processing is unknown. We have therefore generated  $\alpha 10$  gene null mutant mice to assess the role of the  $\alpha 10$  gene in auditory processing.

nAChR  $\alpha 10$  mutant mice were genetically engineered using standard gene targeting techniques. Homozygous  $\alpha 10$  mutant mice breed normally and show no overt behavioral phenotype. We have analyzed the hearing of these mice using ABR and DPOAE assays and examined whether ACh can induce electrophysiological responses in IHCs of the knockout mice. We have also examined the

nature of the OC innervation in the  $\alpha 10$  knockouts. No changes in threshold (relative to wildtype littermates) were observed in the  $\alpha 10$  null mice as assessed by ABR across a frequency spectrum spanning 8-32kHz. DPOAE amplitudes were likewise unchanged compared to wildtype controls. Whole cell electrophysiological recordings of IHCs obtained from acutely excised P8-9 organs of Corti revealed no ACh-inducible responses or K-induced synaptic activity in IHCs. By contrast, wildtype and heterozygous littermates showed robust ACh-evoked responses and K-induced synaptic activity. Immunostaining using antibodies staining nerve terminals revealed hypertrophied OC synaptic terminals on OHCs similar to those we described for the  $\alpha 9$  knockout mice.

Support- DC 006258 (DEV), DC0188 (MCL), Fundación Antorchas (ABE and DEV), Tobacco Related Disease Res. Prog. (10RT-0136) and UCLA Stein-Oppenheimer Endowment Award (JB)

### **396** Calcium Release Channels of the Efferent Synaptic Cistern in Cochlear Hair Cells

**Hakim Hiel**<sup>1</sup>, Paul A. Fuchs<sup>1</sup>

<sup>1</sup>*Johns Hopkins University School of Medicine*

Physiological studies support the involvement of intracellular calcium release channels, (ryanodine-sensitive channels – RyRs - and inositol 1,4,5 triphosphate-activated receptors - IP3Rs), in efferent modulation of cochlear hair cells. Such channels may mediate release from the 'synaptoplasmic cistern' closely associated with efferent synaptic contacts on hair cells. In the present work we sought to identify calcium release channel subtypes that are expressed in cochlear hair cells of both rat and chicken, experimental models used in physiological studies of hair cell inhibition. Using RT-PCR methodology we established that only RyR1 mRNA was expressed in apical outer hair cells (OHCs) of the rat, while both RyR1 and IP3R1 mRNAs were present in chicken hair cells. *In situ* hybridization was conducted with radioactive riboprobes for IP3R1 and RyR1 mRNA. In the chicken basilar papilla, IP3R1 mRNA was present in the hyaline cell area, and in short ('outer') hair cells in the high frequency region of the basilar papilla, paralleling the densest distribution of efferent endings. However, RyR1 riboprobes gave no signal in the chicken cochlea (but did label Purkinje cells in cerebellar tissue in the same sections). In the rat cochlea (both adult and neonatal - P10), IP3R1 mRNA was detected in the spiral ligament, inner sulcus cells and especially Hensen's cells, but not in sensory hair cells. However, RyR1 mRNA was detected in the synaptic pole of OHCs in the apical and middle turns of the cochlea, but not in IHCs and supporting cells. RyR1 mRNA was absent from the high frequency region (basal turn) of the adult rat cochlea. In the P10 rat, RyR1 mRNA was present in OHCs throughout the cochlea, with no apparent gradient along the tonotopic axis. These observations suggest that calcium release from the synaptoplasmic cistern found at efferent synapses on cochlear hair cells may be controlled by various and potentially novel molecular mechanisms.

### **397 Evoked Efferent Inhibition of Cochlear Hair Cells.**

Juan Goutman<sup>1</sup>, Jee-Hyun Kong<sup>2</sup>, Elisabeth Glowatzki<sup>1</sup>, Paul Fuchs<sup>1</sup>

<sup>1</sup>Department of Otolaryngology, Head and Neck Surgery, Johns Hopkins, <sup>2</sup>Department of Neuroscience, Johns Hopkins

Central cholinergic neurons project to the cochlea where they form synapses on outer hair cells (OHCs) in the adult, and on neonatal inner hair cells (IHCs). The effects of spontaneous efferent transmitter release have been described in both IHCs and OHCs. Here we describe a method of electrically stimulating efferent action potentials to characterize evoked release of ACh onto cochlear hair cells. A bipolar electrode was placed on the organ of Corti, directly beneath the row of IHCs in an excised apical turn of the rat cochlea (P7-P13). When neonatal IHCs were voltage-clamped to -90 mV at room temperature, single efferent shocks (1 Hz) evoked transient inward currents of variable amplitude (inhibitory postsynaptic currents - IPSCs). The average amplitude (for 621 events in 6 cells) was  $-35.1 \pm 10.8$  pA with a decay time constant of  $21.6 \pm 0.5$  ms. The IPSC waveform varied as a function of membrane potential, becoming biphasic at -60 mV and entirely outward positive to -30 mV. The later outward component reversed polarity near  $E_K$ . Efferent IPSCs could be blocked reversibly by 100 nM strychnine and were eliminated completely when 1  $\mu$ M tetrodotoxin was added to the bath. The evoked IPSCs had equivalent waveforms to, and slightly larger amplitudes than ongoing spontaneous IPSCs observed in the same IHCs. When two electrical shocks were presented with a 5-25 ms interval, the second shock produced IPSCs that were 37% larger than those evoked by single shocks, with an increased probability of occurrence. This result suggests that efferent release of neurotransmitter can be facilitated by repetitive activity, as observed previously in the turtle inner ear. Electrical stimulation provides an important tool to examine the full range of efferent effects on cochlear hair cells. Preliminary efforts show that these same methods can be used to study evoked efferent inhibition of OHCs. Supported by NIDCD DC006476, HFSP RGY-19/2004 (EG), DC01508 (PF) and P30-DC05211.

### **398 Association of SK2 and Alpha 9-Containing Acetylcholine Receptors in the Mouse Cochlea, an Affinity Purification Approach.**

Payam Mohassel<sup>1</sup>, Jerel Garcia<sup>1</sup>, Chan-De Zhan<sup>1</sup>, Liping Nie<sup>1</sup>, Weighong Fen<sup>1</sup>, Ebenezer Yamoah<sup>1</sup>, Ana Vazquez<sup>1</sup>

<sup>1</sup>University of California Davis

To ensure the sensitivity of the auditory system, the outer hair cells of the mammalian cochlea (OHCs) receive feedback from the brainstem through cholinergic fibers that form synapses at their base. The ensuing response of the OHCs, modulates the cochlear amplifier in the presence of background noise, and sharpens frequency selectivity.

Previous studies of other investigators have demonstrated that efferent inputs activate acetylcholine receptors (ACh  $\alpha 9/\alpha 10$ ) in OHCs. These receptors are permeable to  $Ca^{2+}$ ; and  $Ca^{2+}$  influx activates a small conductance  $Ca^{2+}$ -activated  $K^+$  current that results in membrane hyperpolarization. We hypothesized that the SK channels and the ACh  $\alpha 9/\alpha 10$  receptors are co-localized at the base of OHC and that their association involves other protein(s).

When immunoprecipitation using alpha 9 specific antibodies was performed from cochlear extracts, the immunoprecipitate was shown to contain SK2 by western blot analysis. However, no SK2 band could be detected when the immunoprecipitation was performed from extracts of cultured cells expressing SK2 and the ACh  $\alpha 9/\alpha 10$  receptors. Thus, cochlear protein(s) not expressed in the cultures cells seem to be required for the close association of SK2 and the ACh  $\alpha 9/\alpha 10$  receptors.

The proteins immunoprecipitated from mouse cochlea extracts using either antibodies specific for  $\alpha 9$  and in a second set of experiments antibodies to SK2 were analyzed by two-dimensional gel electrophoresis. A set of 17 proteins was detected in both, the  $\alpha 9$ -precipitation study and the SK2 study. None of these proteins could be detected using similar analysis with other antibody. Our data indicate that the SK2 channel and the ACh  $\alpha 9/\alpha 10$  receptors coassemble as part of protein complexes that require the presence of other protein(s) expressed in the cochlea but not in cultured cells. Mass spectrometry may help confirm the identity of some of these proteins.

Supported by R01-DC003826 to ENY and R01-DC006421 to AEV

### **399 Reactive Blue-2, an Inhibitor of P2Y4 Receptor, Increases $K^+$ Secretion in Strial Marginal Cells of the Rat Cochlea.**

Jeong Hwa Heo<sup>1</sup>, Seung-Ha Oh<sup>1</sup>, Sun O Chang<sup>1</sup>, Chong-Sun Kim<sup>1</sup>, Young Ho Kim<sup>2</sup>, Jun Ho Lee<sup>2</sup>

<sup>1</sup>Department of Otolaryngology, Seoul National University, College of medicine, <sup>2</sup>Department of Otolaryngology, Seoul National University College of Medicine, Boramae Hospital

Purinergic signaling has been implicated in the ionic homeostasis of cochlear endolymph (Housley and Thorne, 2000). One of sites regulated by purinergic receptors is the marginal cell in the stria vascularis. P2Y4 receptor is present at the apical membrane of which function is the decrease of  $K^+$  secretion and P2Y2 receptor at the basolateral membrane of which function remains unclear. Recently, reactive blue-2 (RB-2) was reported to be an inhibitor of rP2Y4 receptor expressed in *Xenopus* oocytes. The reported order of potency was RB-2 > BzATP >> suramin. The purpose of this study is to investigate the effects of rP2Y4 receptor inhibitors on the apical membrane of marginal cells where rP2Y4 receptor is expressed. Currents outflowing from the strial marginal cells were monitored at 37°C by voltage-sensitive vibrating probe technique which has been used near the small area of native membrane (Lee and Marcus, 2003). Surprisingly, the application of RB-2 increased the short circuit current



(*Isc,probe*) in a dose-dependent manner. There was a rapid peak response and then decreased, but stayed above or below baseline current level. RB-2 inhibited the response of UTP.. Suramin showed little response, but at high concentration there was a small increase of *Isc,probe*. Surprisingly, BzATP showed decrease of *Isc,probe* like an agonist for rP2Y4 receptor. The contrary action of BzATP would be possible if we consider that it is also an agonist for rP2Y4 receptor, which is not yet determined precisely. This result suggests that the increase of K<sup>+</sup> secretion by rP2Y4 receptor antagonists is caused by receptor desensitization. In other words, in the context of normal ionic homeostasis, there is a basal tonic secretion of ATP into the endolymph from the apical membrane of the marginal cells (Munoz et al, 2001), and it is likely that the secreted ATP is inhibiting K<sup>+</sup> secretion in some degree, which would be released by the application of antagonists.

#### **400 Blood Labyrinth Barrier Permeability Assessment by Evans Blue Extravasation**

**Steven K. Juhn<sup>1</sup>, Bo-Hyung Kim<sup>1</sup>, Patricia A. Schachern<sup>1</sup>, George L. Adams<sup>1</sup>**

<sup>1</sup>*Department of Otolaryngology, University of Minnesota Medical School, Minneapolis, Minnesota*

An existence of blood labyrinth barrier (BLB) similar to blood brain barrier has been demonstrated in the cochlea and this barrier appears to be an important factor to maintain the biochemical homeostasis of the inner ear (Juhn et al, 2001). The effects of inflammatory mediators produced in the process of middle ear inflammation on the inner ear have not been thoroughly studied. It is assumed that the inflammatory mediators that pass through the round window membrane (RWM) result in structural and biochemical changes in the inner ear tissues leading to auditory dysfunction.

The aim of this study was to compare the effect of inflammatory mediators (Interleukin 1 beta and tumor necrosis factor alpha) on the BLB permeability by measuring the Evans Blue (EB) concentration in the lateral wall tissues and auditory function.

Chinchillas weighing 400 to 500g were used in this study. Interleukin 1 beta (5ng/ml) and TNF alpha (10ng/ml) soaked in gelfoam were applied to the RWM. Five hours after the application, EB (2%) solution was injected via femoral vein and 1 hour after the EB injection, temporal bones were removed and lateral walls from the cochlea were dissected. Explants were homogenized and centrifuged. The optical density of EB in the supernatant after extraction was measured at 620 nm wavelength with the spectrophotometer. The concentration of EB (ng/ug wet weight of explant) was obtained by standard curve (50-500 ng/ml EB solution). Results were expressed as nanogram per milliliter of EB in 1 microgram of explant (ng/ug).

Our preliminary studies with EB dye extravasation after lipopolysaccharide (LPS) application on the RWM demonstrated the leakage of EB through BLB in the lateral wall tissues (stria vascularis and spiral ligament). The amount of EB in the lateral wall tissues increased with time after the application of LPS on the RWM and correlated

with the inner ear function evaluated by ABR. It was interesting to observe the differences of EB concentration in the lateral wall tissues after the application of IL 1 beta and TNF alpha on the RWM. Functional assessment of the inner ear with ABR after the application of the inflammatory mediators was also performed.

This is the first attempt to quantify the degree of BLB permeability after inflammatory mediator application on the RWM.

Supported by NIDCD grant : P30 DC4660-0341

#### **401 Ultrastructural Localization of Megalin in the Rat Vestibular Dark Cells and Endolymphatic Sac Epithelial Cells**

**Kunihiro Mizuta<sup>1</sup>, Yasuyuki Hashimoto<sup>1</sup>, Maki Arai<sup>1</sup>, Satoshi Iwasaki<sup>1</sup>**

<sup>1</sup>*Hamamatsu University School of Medicine*

Megalin is expressed by a wide variety of absorptive epithelial cells including kidney proximal tubule cells, type II pneumocytes, parathyroid cells, epididymal epithelial cells, and cells of yolk sac, among others (Christensen and Birn, *Nat Rev Mol Cell Biol.* 3: 256-66, 2002). It is an endocytic receptor for multiple ligands including plasminogen, plasminogen activator-inhibitor complexes, lactoferrin, lipoprotein lipase, aprotinin and Ca<sup>2+</sup>.

We have previously found the distribution of megalin in the cochlear duct using the immunogold technique with the antibody raised against megalin of the rat kidney proximal tubules (Mizuta et al., *Hear. Res.* 129, 83-91, 1999). Megalin may also be involved in endocytosis in the vestibular organ and endolymphatic sac. To examine this possibility, we extended our immunocytochemical investigation to the rat inner ear cells with special attention to vestibular dark cells and endolymphatic sac epithelial cells.

Dark cells of the utricle and semicircular canal were labeled on the apical surface, but not on the basolateral surface. This localization pattern resembles kidney proximal tubule cells. Immunoreactivity was also detected in endolymphatic sac epithelial cells. In contrast, virtually no gold particles were seen on sensory cells and supporting cells in vestibular apparatus.

It is well known that the maintenance of endolymphatic fluid depends on cells lining the endolymphatic space. Ligands are still unclear, but our data indicates that megalin is likely to play an important role in regulating fluid homeostasis of the inner ear.

#### **402 Alpha-MSH as an Emergency Hormone of the Inner Ear?**

**Angela Meyer-zum-Gottesberge<sup>1</sup>**

<sup>1</sup>*University Düsseldorf*

The homeostatic control of body fluids and electrolytes involves a complex interaction of hormonal and neural mechanisms. At present, we focused on a hormone system that may play a role in early stage of fluid disturbances in the inner ear - melanocytes stimulating hormone (a-MSH). Alpha-MSH and related melanocortins have a wide range of physiological effects, including nerve

regeneration, functional recovery, and others. Based on in vitro and in situ ultrastructural and immunohistochemical investigation we identified several cells types that may locally produce  $\alpha$ -MSH and cells containing

MC1-R receptors. Furthermore, our results indicate that melanocytes of the inner ear are under MSH control and their activation and their intercellular interaction may be dynamically controlled by extracellular (endolymphatic)  $\text{Ca}^{2+}$ . Therefore we proposed that melanocytes provide a regulatory network for the maintenance of the inner ear homeostasis. They may play a crucial role as an initial modulatory factor during the development, when function (electric and ionic gradients) is maintained and during pathological conditions, when the ionic and electric gradients fail and corrections are required. Alpha-MSH may participate as an emergency system in the regulation of the inner ear homeostasis.

### **403 Localization of Prostanoid Receptors and Cyclo-oxygenase Enzymes in the Cochlea of Guinea Pig and Man**

Johan Stjernschantz<sup>1</sup>, Parri Wentzel<sup>1</sup>, Helge Rask-Andersen<sup>2</sup>

<sup>1</sup>Dept of Neuroscience, Unit of Pharmacology, Uppsala University, <sup>2</sup>Dept of Surgical Sciences, Unit of Otorrhinology, Uppsala University

**Objective:** Prostanoid receptors are widely distributed in the eye, and selective FP prostanoid receptor agonists, e.g. latanoprost, are used for the treatment of glaucoma. The purpose of the present study was to investigate the localization of the FP prostanoid receptor in the cochlea to understand which tissues exogenous FP receptor agonists are likely to exert effect on in the cochlea. As control we have studied the distribution of the EP1 and EP3 prostanoid receptors and in addition we have investigated the localization of the cyclo-oxygenase (COX) enzymes involved in the production of endogenous prostaglandins.

**Methods:** Cochleas were obtained fresh from guinea pigs and two patients who underwent intracranial surgery for meningioma tumors. The tissues were fixed, decalcified and processed for immunohistochemistry according to routine techniques. Appropriate controls comprised incubation without primary antibodies, or incubation in the presence of specific blocking peptides of the primary antibodies.

**Results:** The FP prostanoid receptor was found abundantly distributed in the organ of Corti, stria vascularis, spiral limbus, and the spiral ganglion, both in guinea pig and man. The immunohistochemical staining of the EP1 and EP3 prostanoid receptors in the corresponding structures was significantly weaker, and sometimes completely lacking. Weak staining of the COX-1 enzyme was found in the cochlear structures whereas the COX-2 enzyme appeared to be lacking.

**Conclusion:** The abundant distribution/expression of the FP prostanoid receptor in the cochlear structures suggests a physiological role for PGF<sub>2a</sub> in the cochlea. Based on the findings it is reasonable to anticipate FP prostanoid receptor agonists to exert pharmacologic effect in the inner

ear. The COX-1 enzyme appears to be constitutively expressed in the cochlea in contrast to COX-2.

### **404 Immunolocalization of Orphanin FQ in rat cochlea**

Soochuen Kho<sup>1</sup>, Ivan Lopez<sup>1</sup>, Chris Evans<sup>1</sup>, Ishiyama Gail<sup>1</sup>

<sup>1</sup>University of California at Los Angeles

Orphanin FQ, an endogenous opioid like neuropeptide and its receptor ORL-1 play a role in the regulation of hearing. A previous study has shown increased auditory brainstem response (ABR) thresholds after loud noise exposure in ORL-1 knockout mice as compared to wildtype. ORL-1 is expressed in the auditory brainstem. The nucleus of the brachium of the inferior colliculus as well as the dorsal nucleus of the lateral lemniscus express ORL-1. The ORL-1 ligand, orphanin FQ is also expressed in the auditory brainstem, specifically in the medioventral and lateroventral periolivary nuclei. In this study, we demonstrate the expression of orphanin FQ in the cochlea endorgan using immunohistochemistry. Temporal bones were harvested from six Sprague Dawley male rats. Sections were embedded in OCT compound and cryostat midmodiolar sections were made. Immunohistochemistry was performed on these sections using rabbit polyclonal antibody raised against orphanin FQ and visualized under light microscopy. There was differential staining amongst the spiral ganglion cells. Intense staining was seen in the cytoplasm of type I spiral ganglion cells. In addition, the area under the outer hair cells stained strongly. This area is usually occupied by olivocochlear efferents and Deiter cells.

### **405 Identification of CIC-2 and CIC-K2 Chloride Channels in Cultured Rat Type IV Spiral Ligament Fibrocytes**

Chunyan Qu<sup>1</sup>, Fenghe Liang<sup>1</sup>, Zhijun Shen<sup>1</sup>, Samuel Spicer<sup>1</sup>, Bradley Schulte<sup>2</sup>

<sup>1</sup>Department of Pathology and Laboratory Medicine, Medical University of South Carolina, Charleston, South Carolina, <sup>2</sup>Department of Otolaryngology-Head and Neck Surgery, Medical University of South Carolina, Charleston, South Carolina

Voltage-gated chloride channels (CICs) function as important mediators of cellular ion homeostasis and cell volume regulation. Previously, we have used immunohistochemical and RT-PCR approaches to demonstrate the expression of the CIC-K isoforms in type II, IV and V fibrocytes of the rodent spiral ligament. All three of these fibrocyte subtypes are involved in  $\text{K}^+$  recycling in the mammalian cochlea, thus it is important to understand the precise mechanisms regulating their membrane conductance and the role played by CICs in this process. Here, we provide evidence that  $\text{Cl}^-$  conductance in type IV fibrocytes is mediated predominantly by CIC-2 and CIC-K2. A secondary cell line, derived from explants of the rat spiral ligament underlying and inferior to the spiral prominence, was characterized immunohistochemically with protein markers specific to various spiral ligament cell types. The cultures were

immunopositive for vimentin, Na,K-ATPase, the Na,K,Cl-cotransporter and creatine kinase isozyme BB, but not for cytokeratins and Ca-ATPase. This immunostaining profile differed from that of cultured type I or type II fibrocytes and is indicative of the type IV subtype. Evaluation of the cultures by RT-PCR and Western blot analysis confirmed the presence of both CIC-2 and CIC-K2. Whole-cell patch clamp recordings identified two biophysically distinct Cl<sup>-</sup> currents in the cultured cells. One, an inwardly rectifying Cl<sup>-</sup> current activated by hyperpolarization or decreasing pH, corresponded with the properties of CIC-2. The other, a weak outwardly rectifying Cl<sup>-</sup> current regulated by extracellular Cl<sup>-</sup> and Ca<sup>2+</sup>, resembled the channel characteristics of CIC-K2 when expressed in *Xenopus* oocytes. These findings suggest that at least two functionally different chloride channels are involved in regulating membrane anion conductance in cultured type IV spiral ligament fibrocytes.

#### **406 Immunohistochemical Localization of Alport, Type IV Collagen Antigens in Bovine and Primate Cochleas**

Peter Santi<sup>1</sup>, Clifford Kashtan<sup>1</sup>

<sup>1</sup>University of Minnesota

Alport syndrome is characterized by a hereditary nephritis and sensorineural hearing loss and appears to be caused by mutations in genes that code for the novel alpha 3, 4, and 5 chains of type IV collagen. We have previously immunolocalized Alport type IV collagen antigens in the human cochlea to the basement membrane associated with the basilar membrane/organ of Corti, and the inner and outer sulcus cells (Kleppel et al., *Am. J. Path.* 134:813, 1989; Kleppel et al., *Lab. Invest.* 61:278, 1989). The purpose of this investigation was to extend those findings using the same Alport antibodies against antigens in bovine and primate kidney and cochlear tissues. Bovine tissues were obtained from a local abattoir and primate tissues were obtained from a Rhesus monkey through a University of Minnesota tissue-sharing program. Tissues were fixed with Carnoy's fixative, decalcified with EDTA, and cryosectioned. Indirect immunohistochemistry was used to demonstrate the alpha 1, 3, 4, and 5 type IV collagen antigens using mouse monoclonal antibodies that were generated against human Alport antigens. Alpha 1 reacted with all of the basement membranes in the cochlea and kidney. Alpha 3, 4, and 5 showed some differences in their reactivity but primarily reacted with the glomerular basement membrane of the kidney. In the cochlea, these antibodies reacted with basement membranes primarily associated with the basilar membrane/organ of Corti, and the inner and outer sulcus cells. Less reactivity by the antibodies was observed in basement membranes of some vessels, including those of the spiral limbus, ligament, and stria vascularis, and in the tension fibroblasts of the spiral ligament. We will discuss the possible functional significance of the distribution of these novel type IV collagen chains in the cochlea in regard to the recent report by Merchant et al. (*Laryngoscope* 114:1609, 2004) of a mechanical separation between the basilar membrane and the organ of Corti in cochleas from humans with Alport syndrome.

Supported by NIDCD.

#### **407 Ryanodine-Induced Vasodilation Inhibits Ca<sup>2+</sup> Sparks in Gerbil Spiral Modiolar Artery.**

Keil J. Regehr<sup>1</sup>, Casey L. Devore<sup>1</sup>, Philine Wangemann<sup>1</sup>

<sup>1</sup>Kansas State University

Ryanodine receptors have been implicated in the dilation of vascular smooth muscle cells and cardiac muscle cells. Ryanodine receptors are located in the membrane of the sarcoplasmic reticulum and have been shown to mediate vasodilation via sudden Ca<sup>2+</sup>- and ryanodine-sensitive Ca<sup>2+</sup> release (sparks) from the sarcoplasmic reticulum. Ryanodine has a concentration-dependent effect on ryanodine receptors, stimulating the receptor at 10<sup>-6</sup> M and inhibiting at 10<sup>-5</sup> M. Inhibition of the ryanodine receptors induces vasoconstriction. The goal of this study was to determine whether 10<sup>-6</sup> M ryanodine causes a vasodilation and whether this vasodilation would coincide with an increase in spark frequency and/or amplitude. Vessel diameter was monitored by video microscopy, and Ca<sup>2+</sup> sparks were recorded by confocal fluo-4 microfluorometry. 10<sup>-6</sup> M ryanodine caused a vasodilation and reduced the amplitude and frequency of Ca<sup>2+</sup> sparks and waves. Time control experiments demonstrated that Ca<sup>2+</sup> sparks maintained their amplitude and frequency over the duration of the experiment. These findings suggest that Ca<sup>2+</sup> sparks may not be the sole causal link between the ryanodine receptor and vascular diameter.

Supported by NIH-R01-DC04280

#### **408 Sphingosine-1-Phosphate Induced Vasoconstriction of the Spiral Modiolar Artery is Mediated by RhoA/Rho kinase-Dependent Ca<sup>2+</sup> Sensitization of the Contractile Apparatus**

Elias Q. Scherer<sup>1</sup>, Elmar Oestreicher<sup>1</sup>, Wolfgang Arnold<sup>1</sup>, Ulrich Pohl<sup>2</sup>, Steffen-Sebastian Bolz<sup>2</sup>

<sup>1</sup>ENT-Department, Technical University of Munich, Germany, <sup>2</sup>Institute of Physiology, Ludwig-Maximilians University, Munich, Germany

Increased tone of the spiral modiolar artery (SMA) may cause ischemia of the inner ear, resulting in sudden hearing loss. We have previously shown that the sphingolipid mediator sphingosine-1-phosphate (S1P) induces constriction of the SMA via activation of Rho kinase. S1P is synthesized by sphingosine kinase (Sphk1); degraded by S1P phosphohydrolase 1 (SPP1); and acts as a specific ligand for a group of G-protein-coupled receptors (S1PR<sub>1-5</sub>). To date, this signalling pathway has not been fully characterized in the SMA.

SMA were isolated from gerbil cochleas and cannulated on glass micropipettes; transmural pressure was set to 25 mmHg. Vascular diameter and vascular smooth muscle cell (VSMC) intracellular Ca<sup>2+</sup> ([Ca<sup>2+</sup>]<sub>i</sub>) were measured simultaneously. Ca<sup>2+</sup> sensitivity of the contractile apparatus was evaluated by correlating [Ca<sup>2+</sup>]<sub>i</sub> and vascular diameter after increasing extracellular Ca<sup>2+</sup> under depolarizing conditions. RT-PCR was used to characterize the mRNA expression of S1PR<sub>1-3</sub>, Sphk1 and SPP1.

Translocation of RhoA to the VSMC plasma membrane, a measure of its activation, was assessed using immunofluorescence and confocal microscopy.

The SMA expressed mRNA for S1PR<sub>1-3</sub>, Sphk1 and SPP1. S1P induced dose-dependent, long-lasting vasoconstriction with an EC<sub>50</sub> of 200nM (i.e., within the physiological range of plasma S1P concentrations; n=13). In the presence of 100nM S1P, the relationship between [Ca<sup>2+</sup>]<sub>i</sub> and diameter was shifted to the left. The Rho kinase inhibitor Y27632 (1μM) completely abolished this effect. S1P-induced translocation of RhoA to the VSMC plasma membrane confirmed the activation of this GTPase.

We conclude that the critical components of S1P signaling are expressed in the SMA; S1P-induced vasoconstriction is partially mediated through enhanced RhoA/Rho kinase activity, which augments Ca<sup>2+</sup> sensitivity. We therefore propose that S1P signalling is a physiologically relevant regulator of SMA tone.

#### **409 Multiple Membrane Actions of Dopamine in Guinea Pig Spiral Modiolar Artery**

**Yu-Qin Yang<sup>1</sup>, Alfred Nuttall<sup>1</sup>, Zhi-Gen Jiang<sup>1</sup>**

<sup>1</sup>Oregon Health & Science University

Dopamine (DA) has been identified as an important central and peripheral neurotransmitter implicated in cochlear function, circulation regulation as well as in Parkinsonism, schizophrenia and drug abuse ((d'Aldin et al., 1995; Eybalin et al., 1993) (Reitsamer et al., 2004). The enzyme for synthesis of DA, tyrosine hydroxylase, has been immunocytochemically localized to fibers innervating blood vessels including the spiral modiolar artery (SMA, (Jiang et al., 1999; Qiu et al., 2000; Usami et al., 1988). We also reported previously that pretreatment with dopamine antagonists, especially D<sub>1</sub> antagonist, attenuates dopamine induced cochlear blood flow increases. Using intracellular recording method on the *in vitro* SMA preparation, we found: 1) Dopamine, in presence of 100 nM prazosin, induced a concentration-dependent hyperpolarization in the majority of smooth muscle cells that had a low resting potential (~-40mV), not in cells with high RP near -75 mV. The EC<sub>50</sub> is about 20 μM. 2) Dopamine caused a depolarization in the majority of high RP cells, which was largely blocked by a α<sub>1</sub>-receptor antagonist 100 nM prazosin and, in some cases, unmasked a hyperpolarization. The DA-depolarization was suppressed by 1 mM 4-aminopyridine. 3) The DA-hyperpolarization was blocked by 10 μM haloperidol and a D<sub>1</sub> antagonist R(±)-SCH23390 (1 μM), but not by 1 μM sulpiride, a D<sub>2</sub> antagonist. 3) The D<sub>1</sub> agonist, (±)SKF81297, but not D<sub>2</sub> agonist quinpirole, mimicked DA in causing a hyperpolarization sensitive to R(±)-SCH23390. We conclude that, in guinea pig *in vitro* SMA, dopamine elicits dual membrane actions: first, a hyperpolarization via activation of D<sub>1</sub> receptors and, second, a depolarization by stimulation of a α-adrenoceptor. *Supported by DRF, NIH NIDCD DC 004716 (ZGJ) and DC00105 (ALN).*

#### **410 Cholinergic Involvement of Neuromuscular Transmission in Guinea-Pig Spiral Modiolar Artery**

**Bing-Cai Guan<sup>1</sup>, Yu-qin Yang<sup>1</sup>, Zhi-Gen Jiang<sup>1</sup>**

<sup>1</sup>Oregon Health & Science University

It has been suggested in arteries of several organs that acetylcholine (ACh) mediates part of neuromuscular transmission but remains unclear in cochlear vessels (Guan et al., 2004; Hashitani et al., 1998). We reported previously that transmural stimulus-evoked excitatory junction potential (EJP) was not completely blocked by combined antagonists for α-adrenergic and P2X receptors (Jiang et al., 2000; Jiang et al., 1999), and sparse nerve fibers and terminals reactive to choline-acetyltransferase-antibody were identified in guinea-pig spiral modiolar artery (SMA) as well as its upstream artery (Guan et al., 2004). We also found that ACh caused a depolarization and contraction in smooth muscle cells, in addition to an endothelium-dependent hyperpolarization and relaxation (Jiang et al., 2003). ACh-induced hyperpolarization and depolarization were both blocked by 4-DAMP, an M<sub>3</sub> receptor-selective antagonist. In this study, using intracellular recording on *in vitro* SMA, we found: 1) 50 nM 4-DAMP or atropine reduced the amplitude of evoked EJP by 42.9±3.8 % (n=20, p<0.001) and 43.8 ± 4.1% (n=14, p<0.01) respectively in the cells that had a high resting potential (RP, ~-70 mV), whereas had little effect on the EJP of low RP (~-40 mV) cells (p>0.05, n=23), though a few of such cells manifested repeatable 4-DAMP and atropine inhibition of EJP (n=3). 2) In the presence of 4-DAMP, the remaining component of the EJP was 38.1±10.3% suppressed by 0.1 μM prazosin plus 0.1μM idazoxan (n=8, p<0.05) and 17.5±6.2% by 10 μM PPADS, a P2X receptor antagonist (n=8, p<0.05). 3) 4-DAMP had no effect on depolarizations induced by norepinephrine or by ATP (n≥6). We conclude that cochlear artery receives a cholinergic innervation, and an excitation of these cholinergic nerve fibers may cause ACh release at the terminals, which mediates an excitatory neuromuscular transmission to the SMA smooth cells via activation of M<sub>3</sub> receptors. *Supported by DRF, NIH NIDCD DC 004716 (ZGJ).*

#### **411 Acetylcholine-Induced Depolarization is Mediated by Opening of a Non-Selective Cation Channel and Closing a Potassium Channel in Guinea Pig Spiral Modiolar Artery**

**Zhi-Gen Jiang<sup>1</sup>, Bing-Cai Guan<sup>1</sup>, Yu-Qin Yang<sup>1</sup>**

<sup>1</sup>Oregon Health & Science University

We reported that, in addition to an endothelial-dependent hyperpolarization, acetylcholine (ACh) causes a depolarization in smooth muscle and endothelial cells of the spiral modiolar artery (SMA, Jiang et al., 2001). The ACh-depolarization is often robust in cells that have a high resting potential (HRP, ~-70 mV) but small or being masked by a robust ACh-hyperpolarization in low RP (~-40 mV) cells. The ACh-hyperpolarization is generated by an activation of Ca-activated potassium channels (K<sub>Ca</sub>), whereas the ionic mechanism of ACh-depolarization in

vascular cells remains unclear (Jiang et al., 2004). The latter issue became important as we found that the evoked EJP in the SMA was partially sensitive to muscarinic receptor antagonists, indicating a possible involvement of cholinergic neuromuscular transmission (Guan et al., 2004). Using isolated SMA preparations and intracellular recording method, we found in current study that: 1) When  $K_{Ca}$  was blocked by charybdotoxin or nimodipine, ACh-depolarization was associated with a small decrease or no significant change in input resistance, 2) The amplitude of ACh-depolarization was reduced by membrane depolarization (up to  $-10$  mV) in some cells but slightly enhanced or no change in others; 3) ACh-depolarization was 62% attenuated by 1 mM La and 27% reduced by 10  $\mu$ M flufenamic acid, and 47% suppressed by 1 mM 4AP, but not sensitive to 50 nM charybdotoxin, 10  $\mu$ M nifedipine, 1  $\mu$ M nimodipine or 10  $\mu$ M quinidine; 4) ACh-depolarization, as well as  $-$ hyperpolarization, was inhibited by 10 mM caffeine, whereas nominal Ca-free solution often temporarily enhanced ACh-depolarization. We conclude that ACh-induced depolarization is probably generated by dual mechanisms: one is activation of a non-specific cation channel and the other inactivation of a voltage-dependent potassium channel ( $K_v$ ). ACh membrane effects all involve an intracellular calcium mobilization. Supported by a grant of NIH NIDCD DC004716 to ZGJ.

#### **412 Stem Cell Therapy for Age-related Hearing Loss**

Yafei Du<sup>1</sup>, Debin Lei<sup>1</sup>, Mingbo Han<sup>1</sup>, Jianxin Bao<sup>1</sup>

<sup>1</sup>Washington University in St Louis

Abstract

Functional decline of the nervous system is a cardinal feature of normal aging. Currently, there is no effective way to reverse age-related neuronal loss. UB/OC-1 and adult omental stem cells were found to be able to "transdifferentiate" into various cell types such as neurons both *in vitro*. The hypothesis to be tested in this proposal is whether there is a population of adult omental stem cells capable of differentiation into hair cells.

UB/OC-1 cells. We first examined possible expression of Math1 in this cell line under various conditions. We next established a co-culture model to examine the interactions between UB/OC-1 cells and primary spiral ganglion neurons from E16 mice.

In summary, our preliminary data suggested: (1) contrary to a previous report, Math1 was induced in UB/OC-1 cells under differentiation conditions; (2) although UB/OC-1 cells express most of molecular markers specific for hair cells, molecular cascades for hair cell differentiation may be de-regulated; (3) with Math1 over-expression, molecular pathways for normal hair cell differentiation were partially restored although these cells were not able to make synaptic contacts with spiral ganglion neurons.

Adult omental stem cells after Math1 over-expression. To evaluate whether adult human omental stem cell marrow cells can be induced to express molecular markers specific for hair cells after overexpression of Math1, we infected human adult omental stem cells with an adenovirus

expressing HATH1 (human Math1) and enhanced green fluorescent protein (EGFP). Three days after the infection, hair cell specific markers such as myosin VI and VII could be readily detected in the infected cells by immunocytochemistry, while uninfected cells did not show any immunoreactivities against the same hair cell specific markers. Even more interestingly, a rearrangement of actin network was observed in these cells over-expressing Math1 by using phalloidin staining, a dye specific for hair bundles. The infected cells (green) showed more intensive and unique phalloidin staining pattern while a straight actin network (red) was observed in the rest of uninfected cells at the same visual field. Thus, human adult omental stem cells were induced to express molecular markers for hair cells and also change their actin network *in vitro*.

#### **413 Progressive Hearing Loss and Loss of Central Neurons in DBA/2J Mice are Ameliorated by Very Early Initiation of Treatment with an Augmented Acoustic Environment**

James Willott<sup>1,2</sup>, Sandra McFadden<sup>3</sup>, Dalien Ding<sup>3</sup>, Haiyan Jiang<sup>3</sup>

<sup>1</sup>University of South Florida, <sup>2</sup>The Jackson Laboratory,

<sup>3</sup>University at Buffalo

DBA/2J (D2) mice exhibit early genetic progressive sensorineural hearing loss that is severe by 2 months of age. This is ameliorated by nightly exposure to an augmented acoustic environment (AAE) consisting of 70 dB SPL broad-band noise bursts. Thresholds of auditory brainstem responses (ABRs) indicated significant lessening of progressive hearing loss when AAE treatment was initiated around weaning (age 25 days). However, treatment begun very early (prior to the onset of hearing at about 2 weeks postpartum) resulted in even greater amelioration of ABR threshold elevations.

In D2 mice, hearing loss is accompanied by a significant loss of neurons in the anteroventral cochlear nucleus (AVCN) by age 55 days. Similar loss of neurons also occurred in mice for which AAE treatment had begun at 25 days of age. In contrast, the early AAE treatment resulted in no loss of AVCN neurons by 55 days of age. No sex differences were observed in peripheral or central AAE effects.

Supported by NIH grant R01 AG07554

#### **414 Delay Age-Related Hearing Loss by Trimethadione**

Yafei Du<sup>1</sup>, Kevin Ohlemiller<sup>1</sup>, Debin Lei<sup>1</sup>, Mingbo Han<sup>1</sup>, Jianxin Bao<sup>1</sup>

<sup>1</sup>Washington University in St Louis

Delay age-related hearing loss by trimethadione

Abstract Age-related hearing loss is a common condition affecting elderly persons. Currently, there is no effective way to delay this process. Consistent with a recent finding from a drug screen of *Caenorhabditis elegans*, we have identified trimethadione as the first drug able to delay presbycusis in mice. Trimethadione is effective in slowing down age-related increase of hearing

thresholds in both male and female mice, although the effect is more dramatic on female C57BL/6J mice. Trimethadione does not significantly change insulin/IGF signaling pathways, which suggests other independent signaling pathways may be involved in this aging process.

In the inbred C57BL/6J mouse, which has been used extensively as an animal model for presbycusis, age-related hearing loss can be detected by auditory brainstem recording (ABR).

We examined the hearing threshold in both male (n=10, 9 month-old) and female (n=10, 10 month-old) mice by ABR testing, and then started to feed half the animals with trimethadione. Two months later, ABR testing was performed again on these mice. Compared to control female mice, hearing thresholds were significantly lower at all seven frequencies tested (from 5K to 56.6K) in female mice fed with trimethadione. By calculating the hearing threshold shift for each animal, we also found a significant delay of age-related threshold up-shift in mice fed trimethadione across all frequencies tested. For male mice, the same trend was observed across all frequencies tested although the effect of trimethadione was slightly less dramatic than that observed in female groups. Considering that these "middle-age" mice only received trimethadione for two months, the effect of this drug was surprisingly strong. Thus, we identified the first drug able to delay age-related hearing loss, which has no significant effects on the insulin/IGF signaling pathway.

Trimethadione, already approved by FDA for clinical treatment of convulsion activity, is not similar to the structure of these compounds. Thus, this drug has a different mechanism of action to delay age-related hearing loss. It is exciting to consider the possibility of testing this drug on its therapeutic effects on age-related degenerative diseases.

#### **415 The Heterozygous Deafwaddler Mouse is a Model for Age-Related Hearing Loss (AHL)**

**Brendan McCullough<sup>1</sup>**, Bruce L Tempel<sup>1</sup>

<sup>1</sup>*University of Washington*

Hearing loss is a sensory disorder that affects over 20 million people in this country alone. Recent experiments in our lab indicate that the heterozygous deafwaddler mouse is a model for hearing loss. This phenotype is the result of loss or dysfunction in the plasma membrane calcium ATPase isoform 2 (PMCA2), which is critical for calcium extrusion in the stereocilia of hair cells in the organ of Corti. Mice homozygous for a mutation in the gene encoding this protein are profoundly deaf and ataxic; heterozygotes display partial hearing loss in a haplo-insufficient manner. In young animals, this hearing loss is as great as ~50 dB at high frequencies, while leaving low frequencies largely unaffected. To better characterize the hearing loss seen in these animals, we have genetically manipulated the amount of PMCA2 activity available and examined the progression of hearing loss over time. Preliminary results demonstrate that hearing loss progresses to include lower frequencies with age. Furthermore, the rate of this progression depends on the

amount of PMCA2 activity present. This pattern of hearing loss resembles the age-related hearing loss (AHL), or presbycusis, seen in humans and suggests a mechanism involving the cochlear amplifier.

#### **416 Hormone Replacement Therapy Diminishes Outer Hair Cell Function in Perimenopausal CBA Mice**

**Katharine Price<sup>1</sup>**, Patricia Guimaraes<sup>1</sup>, Xiaoxia Zhu<sup>1</sup>, Olga N. Vasilyeva<sup>1</sup>, Robert D. Frisina<sup>2,3</sup>

<sup>1</sup>*Otolaryngology Dept., Univ. Rochester Medical School,*

<sup>2</sup>*Otolaryngology, Biomedical Engineering & Neurobiology Depts., Univ. Rochester Medical School,* <sup>3</sup>*Int. Ctr. Hearing Speech Res., Biosciences Dept., Rochester Inst. Technology*

Recent research has indicated that the use of hormone replacement therapy (HRT) has many negative side effects on women's health. Its effect on presbycusis and auditory measures, specifically distortion product otoacoustic emissions (DPOAE), contralateral suppression of DPOAEs (CS), and brainstem-evoked responses (BSER) have not been tested rigorously using animals. This study examines these physiological processes using the CBA mouse. Middle aged, perimenopausal CBA mice (15 mon, n=19) were randomized to treatment or placebo groups. Baseline measures of CS, DPOAE and BSER were obtained, followed by subcutaneous placement of a time released pellet of either 17 $\beta$  estradiol (n=7, 0.006 mg/day), progesterone + 17 $\beta$  estradiol (n=6, 0.4 mg/day + 0.006mg/day, respectively) or placebo (n=6). Longitudinal data (3 mon) were obtained across three conditions: CS, BSER and DPOAE. Data obtained for CS indicated no statistically significant changes longitudinally, in treatment compared to placebo, or between treatment groups. BSER values also showed no statistically significant changes across the same testing conditions. DPOAE measures obtained in the estrogen and progesterone + estrogen treatment groups showed statistically significant decreases within the midlevel frequencies (13-30 kHz) when compared longitudinally and to placebo (p<.05). These findings suggest that both estrogen and progesterone + estrogen therapy may not provide the protective effect to the auditory system as once thought. Consequently, data obtained in this study suggest that hormone replacement therapy may actually impair outer hair cell functioning before a measurable effect in hearing sensitivity is obtained using BSER. Ongoing experiments examine longitudinal cochlear physiological changes at later time points.

Supported by NIH grants NIA P01 AG09524, NIDCD P30 DC05409 and the Int. Ctr. Hearing Speech Res.

#### **417 Prolonged Estrogen Suppression and Decreased Otoacoustic Emissions in CBA Mice**

**Daniel R. Olney<sup>1</sup>**, Xiaoxia Zhu<sup>1,2</sup>, Scott K. Thompson<sup>1</sup>, Robert D. Frisina<sup>2,3</sup>

<sup>1</sup>*Otolaryngology Dept., Univ. Rochester Med. Sch.,* <sup>2</sup>*Int.*

*Ctr. Hear. Speech Res., Nat. Tech. Inst. Deaf, Rochester*

*Inst. Tech., <sup>3</sup>Otolaryngology, Biomedical Eng., Neurobiology Depts., Univ. Rochester Med. Sch.*

Evidence has recently emerged describing hormonal effects on presbycusis – age-related hearing loss, in particular, circulating estrogen levels have effects on otoacoustic emissions (OAEs) and contralateral suppression of OAEs (CS). Estrogen levels may play a protective role on the hearing apparatus and lack of estrogen may accelerate age-related hearing declines. Distortion product OAEs (DPOAEs) and CS of DPOAEs are non-invasive, physiological techniques, where DPOAEs assess outer hair cell integrity, and CS of DPOAEs measures medial olivocochlear efferent system function. We have shown that female mice implanted with the estrogen blocker tamoxifen have an early decrease of CS, but DPOAEs and auditory brainstem responses (ABRs) remain intact compared to controls. The focus of the present study is: What effects will prolongation of estrogen blockade have on the auditory system as CBA mice age? CBA mice previously implanted with tamoxifen (N=12) or placebo (N=12) and studied from 6-15 weeks of age were further investigated. At 15 weeks, the tamoxifen treated mice were re-implanted with tamoxifen and the placebo group were re-implanted with placebo pellets. ABRs, DPOAEs, and CS were measured at three week intervals thereafter. We found that CS in the tamoxifen treated mice at 15 weeks of age were decreased compared to untreated mice, however, CS of tamoxifen treated mice equilibrated with the control group as they aged to 21 weeks. While the tamoxifen treated group maintained DPOAEs up to 15 weeks, our analysis showed a decline of DPOAEs from 15 to 21 weeks compared to the untreated mice. Likewise, ABRs of the estrogen-suppressed mice showed an increase in thresholds compared to the untreated mice. We therefore conclude that in addition to negatively affecting the CS of DPOAEs, continued estrogen suppression does, indeed, affect DPOAE magnitudes and ABR thresholds.

Supported by NIH grants NIA P01 AG09524, NIDCD P30 DC05409 and the Int. Ctr. Hearing Speech Res.

#### **418 Estrogen Blockade Reduces Auditory Feedback in CBA Mice**

**Scott K. Thompson<sup>1</sup>**, Xiaoxia Zhu<sup>1</sup>, Daniel R. Olney<sup>1</sup>, Robert D. Frisina<sup>2,3</sup>

<sup>1</sup>*Otolaryngology Dept., University of Rochester Medical School, <sup>2</sup>Otolaryngology, Biomedical Engineering & Neurobiology Depts., Univ. of Rochester Medical School, <sup>3</sup>Biosciences Dept., Rochester Inst. Technology*

Although age-related hearing loss is a virtually universal problem among the elderly, it is well known that differences exist in auditory anatomy and physiology as well as the progression of presbycusis between males and females. Evidence also suggests that these observations may be accounted for at least in part, by different circulating estrogen levels. We hypothesized that if estrogen does indeed play a role in presbycusis, suppression of circulating estrogen levels, while controlling for other factors, should influence the development and progression of hearing loss. Distortion product otoacoustic

emissions (DPOAEs) and contralateral suppression (CS) of DPOAEs are non-invasive, effective techniques of measuring the integrity of the auditory system. While DPOAEs provide an accurate assessment of outer hair cell integrity, CS of DPOAEs is thought to serve a protective role for cochlear function. One fact that supports this hypothesis is that declines in CS of DPOAEs generally precede DPOAE declines. This study's objective was to examine the effects of estrogen suppression on age-related changes in DPOAEs and CS of DPOAEs in CBA mice. CBA mice were obtained at 6 weeks of age and baseline ABRs, DPOAEs, and CS of DPOAEs were obtained. While still anesthetized, half of the female animals (N=12) received a shoulder implantation of the estrogen antagonist, tamoxifen, while the other half (N=12) received a placebo injection. Serial DPOAEs and CS of DPOAEs were then obtained at three-week intervals over a period of nine weeks. Analysis showed that while DPOAEs were maintained over the study interval, CS of DPOAEs decreased significantly with age in the study group. By contrast, no such declines were observed in either the female control animals or the group of untreated male mice. We conclude therefore, that estrogen suppression negatively affects CS of DPOAEs. We also hypothesize that if, as suggested, CS of DPOAEs does serve a protective purpose, further administration of tamoxifen should result in continued declines of CS of DPOAEs and eventual DPOAE declines.

Supported by NIH grants NIA P01 AG09524, NIDCD P30 DC05409 and the Int. Ctr. Hearing Speech Res.

#### **419 Medial Olivocochlear Function Declines Very Rapidly in the C57Bl/6 Mouse: A Longitudinal Study**

**Xiaoxia Zhu<sup>1,2</sup>**, Marjorie S. Waterman<sup>1</sup>, David Tuttle<sup>1</sup>, Robert D. Frisina<sup>2,3</sup>

<sup>1</sup>*Otolaryngology Dept., Univ. Rochester Med. Sch., <sup>2</sup>Int. Ctr. Hear. Speech Res., Nat. Tech. Inst. Deaf, Rochester Inst. Tech., <sup>3</sup>Otolaryngology, Biomedical Eng. & Neurobiology Depts., Univ. Rochester Med. Sch.*

The C57Bl/6 mouse is a useful model of presbycusis, as it displays an accelerated age-related peripheral hearing loss in the high frequencies in young adulthood. The medial olivocochlear (MOC) efferent system plays a role in suppressing cochlear outer hair cell (OHC) responses for contralateral stimulation. Our previous studies have shown that the function of the MOC system declines with age prior to OHC degeneration, as measured by suppression of distortion product otoacoustic emissions (DPOAEs) in humans and CBA mice. The aim of this study was to determine the time course of early hearing loss in C57s in more detail. Auditory brainstem response (ABR), DPOAEs and contralateral suppression (CS) of DPOAEs were collected for C57s (8 male, 8 female) from 6 weeks (wk) of age bi-weekly. ABR thresholds were recorded (3-48 kHz) using tone bursts. DP-grams were obtained with L1/L2 =65/50 dB SPL, f1/f2=1.25, (5.6-44.8 kHz). DPs were recorded in quiet and with a contralateral noise (3-30 kHz) or pure tone (12 kHz) at 55 dB SPL. For the contralateral noise, CS was observed at all frequencies at 6wk, but was

lost at middle (15-30 kHz) and high (30-45 kHz) frequencies by 8wk.CS at all frequencies with the contralateral pure tone was minimal at 6 wk. For high frequencies, the DP-gram declines began at 8 wk and were statistically significantly declined by 12wk. For the middle frequencies, declines occurred at 16wk and for the low frequencies (5-15 kHz) declines were significant at 40wk. ABRs at 48 kHz changed by 14wk, at 32 kHz declines occurred at 16w, and at 24 kHz decreases took place at 24wk. In conclusion, the C57Bl/6 mouse has good MOC function at 6wk, but it declines quickly, preceding the rapid progression of peripheral age-related hearing loss in this mouse strain: elevations of ABR and behavioral thresholds, reductions in DPOAE amplitudes.

Support: NIH Grants P01 AG09524 from NIA, P30 DC05409 from NIDCD, and the Int. Ctr. Hear. Speech Res., Rochester NY, USA.

#### **420 Aging and Progression of Hearing Loss in Mice Lacking Muscarinic Acetylcholine Receptor Subtype 3**

**Ken Ito**<sup>1</sup>, Shinichi Iwasaki<sup>1</sup>, Minoru Matsui<sup>1</sup>

<sup>1</sup>University of Tokyo

Acetylcholine plays various important roles in cochlear physiology. However, in the inner ear, the function of muscarinic metabotropic acetylcholine receptors was less elucidated than that of nicotinic ionotropic acetylcholine receptors. It has been shown that acetylcholine mobilized, via muscarinic metabotropic receptors, intracellular calcium stores (Rome et al. 1999) and activated a non-selective cation conductance in spiral ganglion neurons (Ito and Dulon, 2002). It was suggested that main muscarinic subtype involved in spiral ganglion neurons was M3. Khan et al. (2002) showed that muscarinic receptor subtypes (M1 to M5) were differently distributed in the mammalian cochlea. Immunoreactivity for M3 was found in outer hair cells, inner hair cells, Deiter's cells, spiral ganglion neurons, and capillaries. In the present study, we investigated progression of age-related hearing loss between M3 knock-out mice and their wild type counterparts (C57BL/6J). Auditory brain stem response thresholds were measured using tone bursts ranging from 4 to 20 kHz at the age of 3, 6, and 12 months. No significant difference was found between M3 knock-out mice and wild type mice at 3 months. At 6 months, auditory brain stem thresholds were significantly elevated in M3 knock-out mice compared to those in wild type mice. At 12 months, the threshold difference was more manifest, especially in lower frequencies. These results indicated that age-related hearing impairment was more prominent in mice lacking M3 receptors. A preliminary histopathological study on M3 knock-out mice showed loss of outer hair cells and relatively preserved inner hair cells and spiral ganglion neurons.

#### **421 Age-related Changes in Kv 3.1b Expression in the MNTB of CBA/CaJ Mice.**

**Martha L Zettel**<sup>1</sup>, Robert D Frisina<sup>1</sup>

<sup>1</sup>Dept of Otolaryngology, University of Rochester Medical Center, Rochester, NY

Neurons of the medial nucleus of the trapezoid body (MNTB) transmit phase locked information very precisely, and voltage-gated potassium channels are implicated in regulating their temporal properties. In our ongoing study of age-related declines in temporal processing, we reported a 76% decrease in the mean optical density (MOD) of Kv3.1b staining in the MNTB of 15 month-old CBA/CaJ mice vs. 3 month-old mice. To examine this change further we determined overall MOD, cellular MOD, somatic area, and density of KV3.1b + cells in high, mid, and low frequency regions of the MNTB in 3, 15, 24, and 31 month-old CBA/CaJ mice. Auditory brainstem response curves for these mice showed good thresholds until 31-mon., when a flat 40dB elevation occurred. The MOD of KV3.1b + cells showed only very small declines in all frequency regions between 3 and 15 months of age and after 15 months remained stable through very old age. Unlike other studies we did not find a strong medial to lateral somatic MOD gradation but the number of KV 3.1b + cells/mm<sup>2</sup> was significantly higher in the high frequency region. The number of KV 3.1b + cells/mm<sup>2</sup> changed little with age. Cells in the lateral region showed a significant age-related decline in mean cell area that was not found in other regions. In contrast to the somatic MOD data, significant declines in KV3.1b expression were found in the neuropil of all regions, with the lateral low frequency region declining by 15 mon. and the mid and high frequency regions by 24 mon. In conclusion, the decline in KV3.1b expression in old CBA/CaJ mice was due almost entirely to loss of neuropil expression rather than cellular expression, and large increases in ABR thresholds in the oldest animals were not mirrored by large KV3.1b declines.

Support: NIH-NIA Grant P01 AG09524, NIDCD P30 DC05409, and the Int. Center Hearing & Speech Research, Rochester NY.

#### **422 Gja1 Gene Expression in the CBA Mouse Cochlea Decreases with Age**

**Amir Taslimi**<sup>1,2</sup>, Mary D'Souza<sup>1</sup>, Xiaoxia Zhu<sup>1</sup>, Martha Lynch-Erhardt<sup>1</sup>, Andrew Brooks<sup>3</sup>, Robert D. Frisina<sup>1,2</sup>, Dina Newman<sup>2</sup>

<sup>1</sup>Otolaryngology Dept., Univ. Rochester Med. Sch.,

<sup>2</sup>Biosciences Dept., Rochester Inst. Technology,

<sup>3</sup>Functional Genomics Center, Univ. Rochester Med. Sch.

Age-related hearing loss (presbycusis) is a neurodegenerative condition that affects the majority of our elderly population. The molecular mechanisms of this disease are unclear, and no human genes that cause susceptibility to or protection from presbycusis have yet been identified. However, many mutations are known to cause congenital deafness in humans, with the connexin (CX) family being the major gene family involved. Connexins are gap junction proteins (multimers of connexins) that are responsible for intercellular adhesion,



communication and ion flow, particularly for K<sup>+</sup> ions. Mutations in CX26 (*Gjb2*), CX30 (*Gjb6*), CX31 (*Gjb3*) and CX43 (*Gja1*) have been linked to autosomal dominant or recessive forms of deafness in humans. This study investigates age-related variations in the gene expression of connexins in cochlear tissue of CBA mice. The sample set was segregated into 4 groups based on age, distortion-product otoacoustic emissions and auditory brainstem response measurements: young adult with good hearing (N=8), middle-aged with good hearing (N=17), old with mild presbycusis (N=9) and old with severe presbycusis (N=6). RNA isolated from the cochleae (left and right) of each mouse was reverse transcribed into cDNA and hybridized to an Affymetrix™ GeneChipR M430A containing probes for >20,000 murine genes. Gene chip analysis revealed that *Gja1* expression in cochlear tissue decreased significantly, as age increased and hearing deteriorated. Ongoing confirmations with quantitative real-time PCR on the cDNA from the cochlear samples are being conducted. We hypothesize that failure to replace damaged or degraded connexins due to lowered gene expression of *Gja1* during aging may be an important underlying cause of presbycusis.

Supported by NIH grants NIA P01 AG09524, NIDCD P30 DC05409 and the Int. Ctr. Hearing Speech Res.

#### **423 Pathogenic Mechanism for PHFHL: Genetic Load and Dynamic Gene Expression in the Aging Cochlea.**

Kirk Beisel<sup>1</sup>, Sonia Rocha-Sanchez<sup>1</sup>, Ken Morris<sup>1</sup>, Bechara Kachar<sup>2</sup>, Bernd Fritsch<sup>1</sup>

<sup>1</sup>Creighton University, <sup>2</sup>NIDCD/NIH

Mutations in KCNQ4 are associated with progressive high frequency hearing loss (PHFHL) in DFNA2 patients. We propose that quantitative production of aberrant Kcnq4 proteins during aging influences the progression and severity of PHFHL. In order to test this hypothesis we examined the spatiotemporal expression of Kcnq4  $\alpha$  subunits and the associated alternatively spliced transcript variants in developing and aging mouse cochleae. Whole mount immunohistochemistry was done to examine the cellular expression pattern of KCNQ4  $\alpha$  subunits. These data confirmed our early whole mount in situ hybridization results (Beisel et al., 2000) showing KCNQ4 expression in P21 cochleae with a basal > apical longitudinal gradient in both SGN and IHCs, and a reciprocal gradient in OHCs. Kcnq4 exhibits a regional staining pattern in all vestibular end-organs with both Type I and Type II HCs showing expression. An increasing KCNQ4 expression in both auditory and vestibular hair cells was observed with age. Analysis of older mice (P120) showed higher levels of IHC KCNQ4 immunostaining in the middle turn. The relative qualitative and quantitative utilization of the various splice variants was analyzed using spatial distinct cochlear apical and basal fragments and Kcnq4 variant-specific RT-PCR primers and real time quantitative PCR (QPCR) primers and probes. Both RT-PCR and QPCR demonstrated that the four Kcnq4 splice variants also exhibit a differential spatiotemporal pattern. All these data combined indicate that KCNQ4 is topologically expressed in hair cells and is

not HC-type specific. Overall, KCNQ4 upregulation in four month old mice challenges the idea of inner ear maturity being synonymous with static expression levels, thereby suggesting that the inner ear is a very dynamic system and changes in gene expression pattern occur over time. Thus, these data are consistent with quantitative production of aberrant Kcnq4 proteins during aging influences the progression and severity of PHFHL. Thus, variation in the onset, progression and severity of PHFHL phenotypic profile may be due to the impact of an increasing genetic load upon the aging cochlea.

#### **424 Gene Microarray Analysis of the CBA Mouse Cochlea Reveals Age-Related Changes in Glutamate Expression**

Ryan Susa<sup>1,2</sup>, Mary D'Souza<sup>1</sup>, Xiaoxia Zhu<sup>1</sup>, Martha Lynch-Erhardt<sup>1</sup>, Andrew Brooks<sup>3</sup>, Robert D. Frisina<sup>1,2</sup>

<sup>1</sup>Otolaryngology Dept., Univ. Rochester Med. Sch.,

<sup>2</sup>Biosciences Dept., Rochester Inst. Technology,

<sup>3</sup>Functional Genomics Ctr., Univ. Rochester Med. Sch.

Glutamate (Glu) is the main excitatory neurotransmitter at the hair cell/auditory nerve synapse. Its role in age-related hearing loss – presbycusis – is unknown. In the current study, 40 CBA mice were evaluated using auditory brainstem responses (ABRs) and distortion product otoacoustic emissions (DPOAEs). The mice were divided into 4 groups with respect to age and auditory profile: young adult (N=8), middle-aged (N=17), old-aged mild presbycusis (N=9), and old-aged severe presbycusis (N=6). The young and middle-age groups had similar ABR thresholds and DPOAE magnitudes while the two old-aged groups showed significant differences in both auditory tests, consistent with the increased variability of hearing, characteristic of presbycusis. Cochlear cDNA samples from each mouse's RNA were assessed with the Affymetrix™ *mus musculus* M430A GeneChipR, using 1 array per mouse. GeneTraffic RMA analysis and non-parametric one-way ANOVA analysis indicated 6 Glu-associated genes that showed significant age effects: *Glud* [glutamate dehydrogenase]; *Pgcp* [plasma glutamate carboxypeptidase]; *Mglap* [matrix gamma-carboxyglutamate protein]; *Grid2* [glutamate receptor, ionotropic, delta 2]; *Slc1a4* [solute carrier family 1 (glutamate/neutral amino acid transporter), member 4]; and *Grin2C* [glutamate receptor, ionotropic NMDA2C (epsilon 3)]. The *Grid2* and *Grin2C* receptor genes are up-regulated with respect to age, while *Slc1a4* is down-regulated, implying a possible buildup of glutamate presynaptically. *Glud* and *Pgcp*, genes that code for Glu metabolic enzymes, are down-regulated with respect to age, suggesting less cochlear Glu synthesis, a possible response to the presynaptic Glu buildup. Currently, the 6 Glu-associated genes expressions are being validated by real-time PCR and further studied with PathwayAssist™ to correlate Glu gene expression with associated cochlear neurotransmission pathways.

Supported by NIH grants NIA P01 AG09524, NIDCD P30 DC05409 and the Int. Ctr. Hearing Speech Res.

#### **425 Differential GABA Microarray Gene Expression Data for Aging CBA Mice**

Mary D'Souza<sup>1</sup>, Martha Zettel<sup>1</sup>, Xiaoxia Zhu<sup>1</sup>, Martha Lynch-Erhardt<sup>1</sup>, Andrew Brooks<sup>2</sup>, Robert D. Frisina<sup>1,3</sup>

<sup>1</sup>Otolaryngology Dept., Univ. Rochester Med. Sch.,

<sup>2</sup>Functional Genomics Ctr., Univ. Rochester Med. Sch.,

<sup>3</sup>Int. Ctr. Hear. Speech Res., Biosciences Dept., Rochester Inst. Tech.

Differential expression of GABA may effect cochlear functioning with age, particularly in regard to the auditory efferent system. We applied a Robust Multi-Chip Analysis (RMA) approach to microarray data to identify changes in GABA gene expression in CBA mice cochleae. When analyzing the entire cochlear partition, the baseline expression of GABA is relatively low, but GABA is of high biological importance for neurotransmission in the auditory efferent system. Four age groups of mice were used: young adult (N=8) and middle aged (N=17) with good hearing, and old mild (N=9) and severe presbycusis (little or no hearing, N=6), classified with DPOAE and ABR data. cDNA extracted from RNA of each mouse (left and right) cochlea was hybridized for use in one Affymetrix M430A chip/mouse. Thirty one differentially expressed GABA genes were observed by Robust Multi-Chip analysis by placing each hybridization in a group of its own. Functional groups of GABA genes included GABA-A, GABA-A transporters, GABA-B, and GABA-C, and some genes in each group displayed fold changes of 1-2 with age. One- and two-way ANOVAs were utilized to make further investigations of age effects. In addition, real-time PCR analysis of 8 representative genes showing significant age effects were performed on microarray-tested samples. Eight Real time primer/probes of GABA genes representing 26% (8/31) of the total number of GABA genes, and 12% (1/8) of the selected (significant p-values) genes were validated by real time PCR analysis. Real-time PCR experiments are ongoing to complete validations of the microarray data for the 31 GABA genes of interest.

Supported by NIH grants NIA P01 AG09524, NIDCD P30 DC05409 and the Int. Ctr. Hearing Speech Res.

#### **426 PTEN-Linked Apoptotic Signaling Pathways in Age-Related Hearing Loss**

Su-Hua Sha<sup>1</sup>, Andra Talaska<sup>1</sup>, Maria Angeles Vicente-Torres<sup>1</sup>, Jochen Schacht<sup>1</sup>

<sup>1</sup>Kresge Hearing Research Institute, University of Michigan, Ann Arbor, MI 48109

With an increasing life span of our population, age-related hearing loss will have an ever greater impact on health care and quality of life. However, the mechanisms responsible for age-related hearing loss are multifactorial and largely unclear. Resistance to oxidative stress has been identified as a factor of longevity in a variety of organisms. Conversely, reactive oxygen species (ROS) have been implicated in age-related pathologies, including age-related hearing loss in animals. We have demonstrated (ARO 2004) in CBA/J mice that oxidative stress increased and the intrinsic antioxidant defenses such as SOD2 decreased in the aged cochlea. In this

study, we investigate PTEN (a tumor suppressor and PIP3 phosphatase) -linked apoptotic signaling pathways and their relation to hair cell death. PTEN increased and p-Akt, a downstream target of PIP3, decreased in the aged cochlea. Pro-apoptotic Bcl-2 family members such as Bid, Bim, Bad increased, cytochrome C was released from mitochondria to cytosol, a complex of cytochrome C with caspase 9 was formed, and cleavage of caspase 9 increased. Finally, endonuclease G (Endo G) translocated into nuclei of outer hair cells and both apoptotic and necrotic cell death occurred in outer hair cells at an age of 18 month. The sum of these data indicates that the intrinsic antioxidant status is compromised in the aged cochlea and that PTEN regulated signaling pathways may contribute to hair cell death in presbycusis.

Supported by pilot grants to Dr. Sha from the National Institute of Aging (for aged animals) and from the Claude Pepper Older Americans Independence Center at the University of Michigan.

#### **427 Effects of Dietary Antioxidants on Auditory Neurons and the Stria Vascularis in Aged Beagle Dogs**

Tima Le<sup>1</sup>, Elizabeth M Keithley<sup>1,2</sup>

<sup>1</sup>University of California, San Diego, <sup>2</sup>Veterans Affairs Medical Center, San Diego, CA

Presbycusis is a significant problem for the aging population. Among the cochlear structural changes are the deterioration of spiral ganglion neurons (SGN) and stria vascularis (SV). One theory accounting for the degenerative changes is the inability to reduce free radicals that result from respiration and cause damage to molecular structures. In fact, dietary antioxidants can reduce cognitive dysfunction and neuronal degradation with age. The objective of this study was to determine the ability of dietary antioxidants (D, L-alpha-tocopherol acetate, L-carnitine, D, L-alpha-lipoic acid, and ascorbic acid) given during the last quarter of a beagle's life span to reduce SGN and SV degeneration. 2 groups of aged dogs (10-15 years) were created: an antioxidant group (n=11) and a control group (n=9). These were compared to young dogs (<4 years; n=5). The temporal bones were generously given to us by Dr. Carl Cotman. H&E stained paraffin sections were used for histological analysis. All aged groups had less SGN density than the young group. The antioxidant group, however, had greater SGN density than the control group. The basal turn showed the largest loss of cells, however, the antioxidant group had more cells (38% loss) than the control group (54% loss) (p<0.0001). In the apical turn, the antioxidant group had 12% more cells than the control group. The SV in the aged dogs was about 20-27% thinner relative to the young dogs in all turns. The antioxidant group had less SV degeneration in both the basal and apical turns relative to the control group. It was concluded that a high antioxidant diet, even during the last 25% of the life span, can slow some of the progression of cochlear degeneration. The greatest effects were seen in the basal and apical turns, where the largest losses occur.

Support: Cotman Laboratory, UCI, Irvine, CA; NIDCD DC RO-1 003395; Medical Research Service of the Department of Veterans Affairs.

#### **428 Anatomical Changes are Correlated with Early Functional Declines in the C57 Mouse Auditory System**

**Olga Vasilyeva**<sup>1,2</sup>, Xiaoxia Zhu<sup>1,2</sup>, Martha Lynch-Erhardt<sup>1,2</sup>, Robert D. Frisina<sup>2,3</sup>

<sup>1</sup>Otolaryngology Dept., Univ. Rochester Med. Sch., <sup>2</sup>Int. Ctr. Hear. Speech Res., Nat. Tech. Inst. Deaf, Rochester Inst. Tech., <sup>3</sup>Otolaryngology, Biomedical Eng. & Neurobiology Depts., Univ. Rochester Med. Sch.

Two useful animal models for studying age-related hearing loss – presbycusis - are the CBA and C57 mouse strains. CBAs have a slow hearing loss that progresses on a time frame similar to human presbycusis, when one corrects for different absolute lifespans. Contrarily, C57s have a very rapid, high-frequency hearing impairment. Both strains show high amplitude DPOAEs as young adults (6 weeks), and CBAs show significant contralateral suppression of DPOAEs (CS) – indicating a normally functioning medial olivocochlear efferent system (MOC). Measurements at young adult ages of CS in C57s reveal a fast time course for an age-related decline in the MOC. Significant CS was found in 6-week old C57s, but this significantly declined by 8 weeks, and was absent thereafter. The dorsomedial periolivary (DMPO) region contains many of the cell bodies of origin for the efferent system. The present investigation aimed to uncover neuroanatomical underpinnings of the rapid age-related decline of the MOC in young adult C57s, as contrasted with CBAs that have a robust MOC response as young adults. To accomplish this, a neuroimaging system was used to make cell density and perikaryal size measurements in DMPO region where cell bodies of the efferent system reside in CBA/J, (14 weeks, n=7), and C57BL/6J (6 weeks, n=4; 10 weeks, n=6) mice. It was found that using a variety of cell size measurements, in Nissl stained sections that cells declined in size and number, comparing 6 and 10-week old C57s, and in both cases these declines were relative to 14-week old CBAs. These findings suggest that rapid decreases in neuron size and number may underlie part of the noteworthy decline in the functioning of the young adult C57 efferent system.

Supported by NIH Grant P01 AG09524 from NIA, NIH Grant P30 DC05409 from NIDCD, and the Int. Ctr. Hearing Speech Res., Rochester NY, USA.

#### **429 Noise-Induced and Age-Related Hearing Loss Interactions: Evidence of a Misspent Youth?**

**Sharon G. Kujawa**<sup>1,2</sup>, M. Charles Liberman<sup>1,2</sup>

<sup>1</sup>Dept. of Otology and Laryngology, Harvard Medical School, <sup>2</sup>Eaton-Peabody Laboratory, Massachusetts Eye and Ear Infirmary

Unraveling the relative contributions of noise exposure and aging to the aggregate hearing loss in older adults is

challenging, as it is impossible to know all of the factors contributing to a hearing loss seen at an advanced age. In mouse models, however, lifetime noise exposures can be carefully controlled, manipulated and delivered to animals of identical genetic backgrounds at any age. Such work has not only revealed inter-strain differences in age-related and noise-induced hearing loss (AHL, NIHL) susceptibilities; it has also revealed important intra-strain differences in hearing loss magnitude related to age-at-exposure and post-exposure time. A key, unresolved issue in the mouse as well as in the human is whether the noise-damaged ear ages differently from the unexposed ear.

In the present series, effect of age-at-exposure vs. age-at-test on threshold shifts recorded in CBA/CaJ mice was assessed by exposing groups of mice at different ages (8-16 kHz OBN, 2 hr, 100 or 103 dB SPL at 4-6, 16, 32, 64 or 96 wk) and holding them without further exposure with unexposed, age-matched cohorts for different post-exposure times (1 day, 2, 16, 32, 64 or 96 wk) before final physiologic testing (ABR, DPOAE; 5.6-45.2 kHz) and retrieval of cochlear tissues. Two major findings emerged: First, young ears (exposed at 4-6 wk) are substantially more vulnerable than those exposed at any of the other ages sampled here. Threshold shifts are larger at short post-exposure times, extend across a broader range of frequencies, and show less recovery from acute insult by 2 weeks post exposure. Second, when such animals are maintained without additional exposure for months to years, there can be further changes in cochlear physiology and histopathology. Depending on exposure level, threshold elevations can progress beyond those expected by simple addition of noise + age effects, and evidence of diffuse neuronal loss can be observed even in regions with good preservation of hair cells.

NIDCD R21 DC04983 (SGK), P30 DC005209 (MCL)

#### **430 Exaggerated Startle Reflex to Low Frequency Tone Bursts in C57BL/6J Mice with Progressive Hearing Loss: A Longitudinal Aging Study.**

**James Ison**<sup>1</sup>, Peter Rivoli<sup>1</sup>, Jason Moore<sup>1</sup>, Paul Allen<sup>1</sup>

<sup>1</sup>University of Rochester

The cochlea of the C57BL/6J mouse degenerates with age beginning at about 1 to 2 months, with a high- to low-frequency pattern of regional loss. This peripheral pathology is accompanied by central tonotopic reorganization from the IC to cortex, with former high frequency areas now sensitive to low frequencies (e.g., Willott, J. Neurophys. 1986). A cross-sectional study has shown that hearing loss in this mouse leads to an exaggerated acoustic startle for low frequency tone bursts (Ison & Allen, JARO, 2003). Here we present the results of a longitudinal study, in which a group of 12 mice (8F, 4M) were tested to 52 weeks of age, every other week with threshold and superthreshold ABR tests (3 to 48 kHz) and DPOAE tests beginning at 6 weeks of age (the DPOAE not reported here), with ASR tests (3, 6, 12, and 24 kHz at 60 to 110 dB SPL) on alternate weeks, beginning at 9 weeks of age. Both threshold and suprathreshold ABR measures showed progressive hearing loss with increased age

beyond 10 weeks of age, more rapidly for high compared to low frequencies. The ASR showed an immediate gradual decline for all frequencies, less rapid for 3 and 6 kHz compared to 12 and 24 kHz tones. But starting at about 26 weeks of age the declining ASR trajectory reversed for 3 kHz and 6 kHz tone bursts at 110 dB, with a similar enhanced ASR at lower levels appearing later with advancing age. The final level of ASR responding to 110 dB was 3 to 4 times that of the 9-10 week old mice, and some one-year old mice responded even at 60dB, this never seen in hearing mice of any strain. All mice showed ASR exaggeration, though the age at onset varied: this accounts for the inter-subject variability of the earlier study. These data are consistent with the physiological data showing over-representation of these frequencies in the IC, but given the known pathways of the ASR through the VCN but not the IC, the functional change in the ASR is most likely due to changes in downstream modulation of the ASR, not changes within the reflex pathway. The strength and reproducibility of this effect in this mouse suggests its potential utility as a target model for testing interventions intended to ameliorate other consequences of auditory hyperexcitability, e.g., tinnitus and hyperacusis. Supported by USPHS grant PO1 AG09524.

### **431 Behavioral Gap Detection Deficits in the Fischer Brown Norway (FBN) Rat Model of Presbycusis**

**Jeremy Turner<sup>1</sup>**, Jennifer Parrish<sup>1</sup>, Larry Hughes<sup>1</sup>, Hong-Ning Wang<sup>1</sup>, Thomas Brozoski<sup>1</sup>, Carol Bauer<sup>1</sup>, Donald Caspary<sup>1</sup>

<sup>1</sup>*Southern Illinois University School of Medicine*

Presbycusis is one of the most common ailments of the elderly, affecting 1/3 of the over- 65 population. Presbycusis is characterized, in part, by difficulty in processing complex, rapidly changing signals such as speech, especially in a noisy environment. Humans, mice and gerbils show age-related temporal processing deficits with a loss in the ability to detect short duration gaps embedded in a background noise. The present study examined whether gap detection deficits are also present in the FBN rat model of presbycusis. Behavioral gap detection functions were measured in young (4-6 mo) and aged rats (28-30 mo) using acoustic startle reflex methods. Gaps of variable duration were embedded in background noise and subjects responded to the presence of a gap. Detectable changes in the acoustic background (including gaps) that precede (optimally by 60-100 ms) an acoustic startle stimulus serve as a "warning" stimulus reducing the amplitude of the startle reflex. Longer, more easily detectable gaps in the background produce a greater reduction of the startle reflex. In the present study, gaps (removal of the 75dB broadband noise for durations of 0, 1, 2, 3, 4, 5, 10, 15 and 50 ms) were pseudorandomly presented 100 ms before a 115 dB noise startle stimulus. Ten trials of each gap-startle combination were run and the reduction of the startle reflex relative to the 0 ms (startle only) condition was recorded. Consistent with previous studies in humans and other animals, aged rats exhibited significantly longer gap thresholds than young animals. Aged rats also exhibited a flatter gap function

than young animals; even long gaps of 50 ms in a 75 dB noise were less salient to aged rats. Preliminary data suggest that gap detection in aged FBN rats can be improved by operant training to discriminate a variety of stimuli, including silence, from low-level background noise. In contrast, this training procedure had no effect on the gap detection performance of young adult FBN rats.

### **432 Cross-Spectral Channel Gap Detection in the Aging CBA Mouse**

**Jason Moore<sup>1</sup>**, Paul Allen<sup>1</sup>, James Ison<sup>1</sup>

<sup>1</sup>*University of Rochester*

The purpose of the current study is to investigate the effect of aging on both within- and between-channel gap processing and to determine if the effect of aging varies with marker frequency. Previous aging studies (e.g. Barsz et al., *Neurobiol Aging*, 2002) have used within-channel gaps in broadband noise and typically have found a significant but modest effect of age on temporal acuity. However, "cross-spectral channel" gaps may be more common in realistic listening situations, so here we describe cross-spectral channel gap detection using prepulse inhibition of the acoustic startle response in the CBA mouse model of presbycusis. Gap detection was examined in 12 young (2 months), middle-aged (12 months), and old (24 months) CBA/CaJ mice by presenting gaps between two 1/2-octave band pink noise markers (70 dB SPL) in the presence of a 50 dB pink noise background. The markers ranged in center frequency from 6 to 38 kHz, yielding both within-channel and between-channel conditions. In the young and middle-aged mice, within-channel gaps were more effective than between-channel gaps, and high frequency within-channel gaps were more effective than low-frequency within-channel gaps. For between-channel gaps, the better conditions had a low frequency marker preceding the gap and a high frequency following, compared to the reverse. While all conditions produced appreciable inhibition in the young and middle-aged mice, PPI was only observed in old mice for high frequency within-channel conditions. These data indicate that aging significantly reduces auditory temporal acuity, and that the magnitude of this effect is dependent on the spectral contents of the stimuli both preceding and following the gap.

### **433 Colony-Wide Analysis of Mouse Auditory Brainstem Responses (II): Maturation, Gender and Aging Effects in C57BL/6J and CBA/CaJ Mice**

**Peter Rivoli<sup>1</sup>**, James Ison<sup>1</sup>, Jason Moore<sup>1</sup>, William O'Neill<sup>1</sup>, Paul Allen<sup>1</sup>

<sup>1</sup>*Univ. Rochester*

The CBA/CaJ and the C57BL/6J mouse strains have been useful in providing models of two kinds of aging in the auditory system, a genetically programmed rapid loss in the C57, a gradual loss of threshold sensitivity apparent only as the mouse approaches near-senescence in the CBA. We have been gathering ABR absolute thresholds in these two strains for some years, and at present we have

965 CBA and 829 C57 ABR records collected at different ages. Because our other experiments use stimuli that approximate "comfortable hearing levels" in humans, we have been recently examining these records to determine the suprathreshold levels as well as the threshold ABR. The initial results presented here extend the classic results of Li and Borg (*Acta. Otol.*, 1991) by providing ABR measures across stimulus levels, and also, given the recent reports by Willott and his colleagues (e.g., Willott and Bross, *J. Comp. Neurol.*, 2004) and by Henry (*Hear. Res.*, 2002) showing that the rate of hearing loss in the C57 mouse accelerates in the middle aged female, we provide data on the appearance of sex differences with age in these two strains. The details of our techniques are given in the companion poster (Allen et al., ARO, 2005). The C57 mice lost about 50 dB at their most sensitive region between 2 and 12-18 months, while the CBA lost but 10 to 20 dB between 2 months and 28 months of age. Hearing loss in the C57 mouse progressed from high to low frequencies as is commonly observed, but with a small initial loss across the spectrum that has been noted in some prior reports. Sex differences in threshold in the mid frequencies (particularly at 16 kHz) appeared at 8 months of age. These favored the male, and were still present in the oldest group of 12 to 18 month old mice. This effect was significant, but relatively small (i.e. averaging ~10 dB). No systematic sex differences appeared in CBA thresholds at any age, and RMS analyses at the highest stimulus level (90 dB SPL) indicated that there were no consistent sex differences in the suprathreshold ABR across either strain. It is interesting that the maximum suprathreshold ABR declined in the CBA between the ages of 3 and 12-18 months of age, though there was little apparent change in the ABR threshold over this period.

#### **434 Development of GABAergic Inputs and Inhibition in Chicken Nucleus Magnocellularis**

**MacKenzie Howard<sup>1</sup>**, R. Michael Burger<sup>1</sup>, Edwin Rubel<sup>1</sup>  
<sup>1</sup>*University of Washington*

Neurons of nucleus magnocellularis (NM), a division of the avian cochlear nucleus involved in temporal processing, receive GABAergic inputs arising primarily from the superior olivary nucleus. These inputs elicit an unusual depolarizing response that potently inhibits action potentials (APs) by activating low voltage activated K<sup>+</sup> conductances (I<sub>KL</sub>) that shunt excitatory inputs. We investigated the development of synaptic responses mediated by GABA<sub>A</sub> receptors (GABA<sub>A</sub>Rs), responses mediated by agonist application, and I<sub>KL</sub>. We used whole-cell current and voltage clamp recordings at embryonic (E) days E12, 14, 18 and 21. While glutamatergic responses were prevalent as early as E12, E14 was the earliest age at which bicuculline- (Bic) sensitive GABA<sub>A</sub>ergic postsynaptic currents (IPSCs) were reliably evoked. In all E12 neurons tested, puff pipette application of the GABA<sub>A</sub>R agonist muscimol elicited Bic-sensitive currents, suggesting the presence of GABA<sub>A</sub>Rs in the absence of synaptic input. The I<sub>KL</sub> contribution to the inhibitory response was measured using current step protocols. Current injection generally resulted in a single AP at the

stimulus onset, followed by a steady state depolarization. Some E12 neurons fired multiple spikes before the steady state was reached. E12 cells also showed a depolarized AP threshold relative to more mature neurons. Membrane rectification during the steady state became progressively stronger over development. Our data suggest that GABA<sub>A</sub>Rs are expressed prior to inhibitory synaptogenesis, which occurs between E12 and E14. Additionally, GABAergic AP generation is controlled by AP threshold at younger ages but by other intrinsic properties, such as strengthening I<sub>KL</sub>, at older ages. Supported by DC00466, DC04661, DC00395, T32-DC05361.

#### **435 Inhibition Shapes Monaural Response Properties in Avian Nucleus Magnocellularis Neurons**

**R. Michael Burger<sup>1,2</sup>**, Rudolf Rübsamen<sup>3</sup>, Edwin Rubel<sup>1,2</sup>  
<sup>1</sup>*University of Washington*, <sup>2</sup>*Virginia Merrill Bloedel Hearing Research Center*, <sup>3</sup>*University of Leipzig*

In the avian brainstem, nucleus magnocellularis (NM) contains second order neurons that receive excitatory input from 2-4 auditory nerve fibers and GABAergic inhibition from the ipsilateral Superior Olivary Nucleus (SON). Phase-locked output of NM neurons provides excitatory binaural input to n. laminaris where coincident input is encoded for the analysis of interaural time differences. Previous studies have established the cellular specializations and response properties of NM neurons that allow them to phase-lock to an acoustic stimulus and have extensively described the cellular physiology of the GABAergic input. Yet, previous *in vivo* studies have not investigated the functional role of this inhibitory input in the coding of acoustic information in NM. We have recorded from NM neurons *in vivo* with multibarrel pipettes which allowed us to iontophoretically apply antagonists of GABAergic signaling. Several response properties are modified by GABAergic inhibition: 1) Inhibition shapes the input/output functions of NM neurons such that the range of intensities over which NM neurons vary their firing rate is increased by inhibitory feedback; it extends the dynamic range; 2) Long-lasting (100-300ms) suppression of discharges following the offset of the signal appears to be partially generated by GABAergic input; 3) GABAergic inhibition is involved in the broadband suppression of NM responses to CF tones by stimuli outside of the excitatory tuning curve. Interestingly, in most neurons the quality of phase-locking, as measured by vector strength, was not influenced by blocking inhibition. These results suggest that inhibition shapes the NM responses to frequency and intensity parameters but phase-locked responses to the fine structure of the stimulus are independent of inhibitory input. Clearly, despite the small number of inputs to NM, its output reflects substantially more processing than a simple relay of its auditory nerve inputs. Supported by NIDCD grants: DC04661, DC0046, DC00395

### **436 Total Serum Bilirubin Level and Auditory Brainstem Function in the Developing Neonate**

**Gerald Popelka<sup>1</sup>**

<sup>1</sup>*Stanford University*

Bilirubin molecules resulting from catabolized red blood cells are produced in substantial levels in the majority of neonates during the 14 day period after birth. It is well known that high-level exposures to bilirubin cause permanent neural damage to the auditory neural pathways. However, little is known about the effects of lower-level exposures, including whether they are acute or chronic. Our overall research focus is to understand the relation between bilirubin exposure and auditory neural effects. This determination requires auditory measures that are reliable and accurate enough to separate toxic effects from normal maturational changes, and noninvasive to allow multiple measures during the developmental period. Previously we showed that our non-invasive auditory brainstem responses are accurate enough to isolate maturational changes. The experiments reported here investigated the relation between these sensitive auditory measures and bilirubin level (total serum bilirubin in mg/dl) in a cross-sectional research design. Measures were made in the period after birth when bilirubin levels rise, but were restricted to neonates with bilirubin levels less than those requiring a total blood transfusion. After accounting for maturational changes, the auditory neural measures were significantly lower than normal in all cases where serum bilirubin levels were elevated. Future research will involve similar experiments in a longitudinal research design to better quantify the magnitude of the bilirubin exposure and determine any temporal relation between blood levels and auditory effects.

NIH Grant 5 R42 DC003614-03

### **437 Colony-Wide Analysis of Mouse Auditory Brainstem Responses (I): Maturational Effects in Several Strains of Young Mice**

**Paul Allen<sup>1</sup>, Jason Moore<sup>1</sup>, William O'Neill<sup>1</sup>, Peter Rivoli<sup>1</sup>, James Ison<sup>1</sup>**

<sup>1</sup>*University of Rochester*

The mouse is a critical model for investigating the molecular and genetic bases of hearing and its disorders (see Willott's Handbook, 2001), and this has encouraged the increasing study of the mouse ABR (e.g., Erway et al. 2001) because of its apparent simplicity and objectivity. ABRs are typically reported only as thresholds, however, since our other experiments use stimuli that approximate "comfortable hearing levels" in humans, we are interested in analyzing super-threshold ABR. Here we provide initial findings from our ongoing effort to characterize this response. Measurements were made from Avertin anaesthetized mice using needle electrodes at the vertex and mastoid, and hind limb. Tone-pip stimuli (5ms; 3, 6, 12, 16, 24, 32, 48 kHz; 10-90 dB SPL) were generated and ABR waveforms measured (11/s, duplicates of 100 reps) using TDT System II and 3 DSP workstations in

conjunction with BioSig. Three ABR metrics were used to compare young adult mice (3-6, 6-12, 12-18 weeks) CBA/CAJ (N=37;218;163), C57BL6 (N=44;181;103), and C3H/FeJ (N=36;39;4) and F1 hybrids CBAxC57 and CBAxC3H. These metrics are 1) S/N ratio calculated from the RMS of high-pass filtered waveforms at each level and frequency; and 2) Objective thresholds obtained from S/N measures; compared to 3) "by eye" subjective thresholds. S/N ratios increase with stimulus level in all strains and are largest near the best frequency (~12kHz). Save for C57 mice, which show an interaction between maturation and progressive hearing-loss, S/N ratios increase with increased age, however the youngest C3H mice start with a relatively mature S/N pattern and do not increase appreciably with age. The pattern of S/N vs frequency and level of the C57xCBA is like that of the CBA parent, while the C3HxCBA hybrids appear to have stronger ABR responses than either parent strain. The two methods of threshold determination provide similar mean values. An initial analysis including only the CBA mice indicates that frequency differences in the super-threshold RMS can be eliminated by equating for sensation level, but this holds only for 12 kHz and above: the growth of S/N with increasing level seems abnormally low at lower frequencies, 3 and 6 kHz in these analyses. These initial findings attest to the promise of the super-threshold ABR. Supported by USPHS grant PO1 AG09524.

### **438 Representation of Pitch in the Human Brainstem May Be Influenced by Language Experience**

**Anathanarayan Krishnan<sup>1</sup>, Jack Gandour<sup>1</sup>, Yisheng Xu<sup>1</sup>**

<sup>1</sup>*Purdue University*

Evidence from the behavioral, neuropsychological, and functional neuroimaging literature has consistently implicated left cortical regions in the processing of pitch patterns associated with lexical tone by native speakers, but not non-native speakers, of tone languages. These cross-language differences suggest that pitch processing varies depending on language experience at the level of the cerebrum. Cross-language data from evoked electric and magnetic responses elicited during pre-attentive stages of speech processing further show that activation of left auditory cortex varies depending on language experience. The question then arises whether early, pre-attentive stages of pitch processing at the human brainstem level may also be influenced by language experience. The scalp-recorded human frequency-following response (FFR) reflects sustained phase-locked activity in a population of neural elements within the rostral brainstem. It has been shown to encode both the spectral features and voice pitch of steady-state and time-variant speech sounds. FFRs were elicited from native speakers of Mandarin Chinese and English in response to the four Mandarin tones. Autocorrelation measures of pitch strength and pitch tracking revealed that the Chinese group exhibits stronger pitch representation and smoother pitch tracking than the English group. A between-group comparison on individual harmonics indicated stronger intensity of h2 in the Chinese group, whereas intensity was stronger in the English group for higher harmonics (h3-h5).

These FFR findings support the possibility of neural plasticity at the brainstem level that is induced by language experience that may be enhancing or priming linguistically-relevant features of the speech input.

#### **439 EarLab: Large-scale Simulation of Auditory Pathways**

**David Mountain**<sup>1</sup>, David Anderson<sup>1</sup>, Glenn Bresnahan<sup>1</sup>, Socrates Deligeorges<sup>1</sup>, Allyn Hubbard<sup>1</sup>, Viktor Vajda<sup>1</sup>  
<sup>1</sup>*Boston University*

The rapid increase in the available experimental data has not always led to a comparable increase in our understanding of how physiological systems function. One approach to bridging this gap is to develop biologically realistic simulation systems. These systems can be used to integrate available information and to develop new hypotheses. They can also be used to predict the outcomes of experimental and therapeutic manipulations.

The EarLab simulation environment is an example of such a system that can be used for studies of the auditory system. The underlying EarLab software architecture is designed to be able to represent any physiological system or group of systems and uses interchangeable modules, each of which represents a different component of the physiological system. The modules are designed to be configured at run time and to use species-dependent parameters that are loaded at run time. Simulation outputs can either represent continuous variables such as sound pressure or instantaneous neural firing rate, or point processes such as the times of occurrence for individual action potentials. The simulation environment also includes software tools for data visualization and analysis.

Several example applications will be presented ranging from neural processing of sound source location to examples of neural activity evoked by a cochlear implant.

Supported by NIH award DC04731.

#### **440 A Modeling Study of Notch Noise Responses of Type III Units in the Gerbil Dorsal Cochlear Nucleus**

**Xiaohan Zheng**<sup>1,2</sup>, Herbert Voigt<sup>1,2</sup>

<sup>1</sup>*Boston University*, <sup>2</sup>*Hearing Research Center*

A computational model of the neural circuitry of the gerbil dorsal cochlear nucleus (DCN), based on the MacGregor neuromine, was used to investigate type III unit (P-cell) responses to notch noise stimuli. The DCN patch model is based on a previous computational model of the cat DCN (Hancock and Voigt, 1999). According to the experimental study of Parsons et al. 2001, the responses of gerbil DCN type III units to notch noise stimuli are similar to those of cat DCN type IV units. This suggests that type III units in gerbil DCN may serve as spectral notch detectors. In this modeling study a simplified notch noise response plot - rate vs. notch cutoff frequency plot - was used to compare model responses to the experimental results. Parameter estimation and sensitivity analysis of three connection parameters within the DCN patch have been studied and shows the model is robust, providing reasonable fits to the experimental data from all 14 type III units examined.

[Work supported by a grant from NIDCD and Boston University's Biomedical Engineering department]

#### **441 A Network Model of Avian Brainstem: Effects of Superior Olivary Nucleus Inhibition**

**Vasant K. Dasika**<sup>1</sup>, John A. White<sup>1</sup>, Laurel H. Carney<sup>2</sup>, H. Steven Colburn<sup>1</sup>

<sup>1</sup>*Boston University*, <sup>2</sup>*Syracuse University*

Empirical data from avian brainstem neurons suggest that inhibition can increase interaural-time-difference (ITD) coding sensitivity across sound-level. Using a computational model, we assess the impact of feedback inhibition from the superior olivary nucleus (SON) on the ITD sensitivity observed in nucleus laminaris (NL). A bilateral network model is constructed consisting of SON and NL, as well as nucleus magnocellularis (NM) and nucleus angularis (NA). Individual cells are specified as modified leaky-integrate-and-fire cells whose time constants decrease and thresholds increase with SON inhibitory input. Acoustic sound-level is reflected in the discharge rate of the auditory-nerve fibers which innervate the brainstem circuit. Simulations indicate that with SON inhibitory feedback, ITD sensitivity is maintained in NL over a threefold range in auditory-nerve discharge rate. In contrast, without SON feedback inhibition, ITD sensitivity in NL is significantly reduced as input rates are increased. Feedback inhibition is most beneficial in maintaining ITD sensitivity at the highest input rates, which correspond to high-sound-level conditions in the functioning organism. With SON inhibition, ITD sensitivity in NL is maintained for both interaurally balanced inputs (simulating an on-center sound source) and interaurally imbalanced inputs (simulating a lateralized source). In addition to SON's negative feedback control on the network, two factors further expand the dynamic range of the ITD coding system. The first is the empirically observed temporal buildup of SON inhibition, and the second is the presence of reciprocal inhibitory connections between the ipsilateral and contralateral SON. Our model indicates that SON inhibitory feedback in the avian auditory brainstem can substantially improve the dynamic range of ITD coding, which in turn would improve spatial hearing. [Supported by NIH: NIDCD R01 DC00100 (VKD,HSC); R01 DC01641 (LHC); and NINDS R01 NS24425 (JAW).]

#### **442 in Search of an Optimal Stimulus.**

**Michael Anderson**<sup>1</sup>, Kechen Zhang<sup>1</sup>, Eric Young<sup>1</sup>

<sup>1</sup>*Biomedical Engineering, Johns Hopkins Univ, Baltimore, MD, USA*

A stimulus that can most effectively drive a neuron is often called the optimal stimulus and is expected to correspond to a maximum in the stimulus-response relationship such that any small deviation of the stimulus from the optimum always reduces the response. In search of an optimal stimulus, we played random sounds generated by adding pure tones with random amplitudes and recorded the responses of single neurons in the cochlear nucleus of cat. Neurons in the auditory system have responses to such random stimuli that are described using second order or quadratic models better than linear models (Yu and Young

2000, 2004). The existence of an optimal sound as described above has strong implications that can be tested experimentally. One implication is that any quadratic model close to the optimum should never have a positive eigenvalue. However, we found that all cochlear nucleus neurons have quadratic model eigenvalues with both positive and negative signs. This result implies a saddle shape property in that the same stimulus can cause both a maximal and a minimal response, depending on how the stimulus is changed. The saddle shape property predicts that among all stimuli allowable in an environment or producible by the experimental setup, the stimulus that elicits the largest response must always lie on the boundary of the allowable stimuli. We directly tested this theoretical prediction by combining two sounds corresponding to two eigenvalues of opposite signs and confirmed the existence of a saddle in the response, and hence the nonexistence of an optimal stimulus. The origin of the saddle property can be demonstrated explicitly by analyzing realistic neural network models. Our results indicate that nonlinear auditory responses depend on sound parameters in such a complex manner that they cannot be adequately described in terms of optimal stimuli. Supported by NIH grants DC000115 and DC005211.

#### **443 A Model Study of the Effect of the Afterhyperpolarization on the Sound-Level Sensitivity of the LSO Chopper Units**

Yi Zhou<sup>1</sup>, H. Steven Colburn<sup>1</sup>

<sup>1</sup>Hearing Research Center, Boston University, MA 02215

The discharge rates of neurons in the lateral superior olive (LSO) are sensitive to overall level and to interaural level difference (ILD). The temporal patterns in responses to tone bursts of LSO neurons exhibit various chopper frequencies and inter-spike interval (ISI) statistics. This study explores the correlation between characteristics of afterhyperpolarization (AHP) of the membrane and statistics of discharge intervals. This study further addresses the question of whether variations in the intrinsic membrane properties can yield the differences in rate-ILD functions observed among LSO neurons. We use a simple leaky integrate-and-fire model with an adapting AHP channel to simulate LSO neurons. The dynamics of the AHP conductance is characterized by the increment of the conductance (gAHP) after a spike and its decay time constant (tauAHP). The model is stimulated by stochastic inputs of either current or synaptic conductance. The simulations test the model with a large/small gAHP and a long/short tauAHP (2x2 conditions).

In simulations with fixed current strength, Poisson-like ISI histograms are generated by the model when gAHP is small and Gaussian-like ISI histograms when gAHP is large. The discharge irregularity, however, is more prominent when tauAHP is long, which leads to broader ISI histograms. When gAHP is large and tauAHP is long, the slope of the rate vs. current-strength function is shallower than that when gAHP is small and tauAHP is short. This is due to the amount of accumulation of the AHP conductance shunting the membrane. In simulations with excitatory synaptic inputs, the above values of gAHP

and tauAHP yield slow-chopper, fast-chopper, and bimodal types of responses to tonal stimuli as observed in the cat LSO (Tsuchitani 1985, J Acoust. Soc Am 77(4):1484-1496). Adding inhibitory inputs to the model decreases the discharge rate. The slope of the rate-ILD function (generated by varying the input strength of inhibition) depends on gAHP and tauAHP. The model will also be used to test the influence of the dynamics of AHP on the model responses to stimuli with rich temporal information such as envelop-modulated tones. [Supported by NIH DC 00100]

#### **444 Measurement and Modeling of Cable Properties and Optimal Input Delay Profiles in Octopus Cells of the Ventral Cochlear Nucleus**

Matthew J. McGinley<sup>1,2</sup>, Yaniv Lazimy<sup>1</sup>, Ramazan Bal<sup>1,3</sup>, Donata Oertel<sup>1</sup>

<sup>1</sup>University of Wisconsin, Madison, <sup>2</sup>Oregon Health and Sciences University, Portland, <sup>3</sup>Mustafa Kamal University, Turkey

Octopus cells have unique morphological and electrical properties that may compensate for the traveling wave delay in the activation of auditory nerve fibers. To test this hypothesis, we have measured the current and voltage response to hyperpolarizing steps in voltage and current clamp respectively, in the whole-cell configuration. Recordings were made with Sylgard-coated pipettes, with and without compensation for whole cell capacitance and series resistance ( $8.4 \pm 0.4 \text{ M}\Omega$ ).

Pipettes contained biocytin so that recordings could be associated with their particular morphology. A digital representation of each cell's morphology was created with NeuroLucida and analyzed with Neuroexplorer (MicroBrightField, Vermont). For five octopus cells, the average somatic and dendritic surface areas were  $1260 \pm 350$  and  $6800 \pm 1900 \mu\text{m}^2$ , respectively. The average length from the cell body to the tip of terminal dendrites was  $153 \pm 12 \mu\text{m}$ .

For four representative octopus cells, the input resistance was  $6.6 \pm 0.6 \text{ M}\Omega$  and the resting potential was  $-62 \pm 3 \text{ mV}$ . Time constants were extracted from the responses of cells after correction for the kinetics of the hyperpolarization-activated conductance,  $g_h$ . Two time constants were resolved in voltage responses to current pulses:  $0.46 \pm 0.13$  and  $1.3 \pm 0.2 \text{ ms}$ . Three time constants were resolved in current responses to voltage pulses:  $0.17 \pm 0.03$ ,  $0.39 \pm .08$ , and  $1.9 \pm 0.7 \text{ ms}$ .

Digital morphologies were imported into Neuron (Yale University) to create a model of each cell, and the model was adjusted so its response matched the recordings. From this model we extract the cytoplasmic resistivity, the membrane resistance and capacitance of the cell body and dendrites, and the electrical length of the dendrites. We determine the temporal profile of input arrival, as a function of position in the dendritic tree, which is optimal to elicit firing.

This work was supported by a grant from the NIH DC 00176.



#### **445 Comparison of Several Models for Monaural Tone-in-noise Detection to Gerbil AVCN Responses**

Yan Gai<sup>1,2</sup>, Laurel H. Carney<sup>1,3</sup>

<sup>1</sup>*Institute for Sensory Research, Syracuse University,*  
<sup>2</sup>*Dept. of Biomedical & Chemical Engineering,* <sup>3</sup>*Depts. of Biomedical & Chemical Engr., and Electrical Engr. & Computer Science*

Several cellular models with auditory-nerve (AN) inputs give similar predictions of human monaural detection of tones in reproducible noise, in terms of detection thresholds, and hit and false-alarm rates for individual maskers. These models include the phase-opponency model (Carney et al, *Acustica*, 88:334-346, 2002), the same-frequency inhibition and excitation model (Nelson & Carney, *JASA*, in press, 2004), the lateral-inhibition model, the autocorrelation model, and the cancellation model (de Cheveigne, *JASA* 103:1261-1271, 1998). These physiologically based models can be directly compared to responses of antero-ventral cochlear nucleus (AVCN) neurons. Because of their different structures, these models predict very different response properties, more so for relatively simple stimuli such as amplitude-modulated (AM) tones than for tone-in-noise stimuli. Here extracellular responses of anesthetized gerbil AVCN cells to AM tones across a range of modulation frequencies are compared to model predictions for the synchrony to the envelope and to the fine structure, the PST histogram, the average rate, and the cumulative phase relative to the stimulus envelope. A specific property that is not emphasized in previous AVCN studies is the characteristic phase, which indicates whether a neuron phase locks to the peak, the valley, or elsewhere in the stimulus envelope. Characteristic phase provides fundamental information about the responses of these cells with general implications for model structures, such as the characteristic frequencies of converging AN inputs and the nature of their interaction. Supported by NIH NIDCD-01641.

#### **446 Auditory Sensitivity in the Eastern Screech Owl**

Elizabeth Brittan-Powell<sup>1</sup>, Bernard Lohr<sup>1</sup>, Caldwell Hahn<sup>2</sup>, Robert Dooling<sup>1</sup>

<sup>1</sup>*University of Maryland College Park,* <sup>2</sup>*USGS - Patuxent Wildlife Research Center*

Auditory sensitivity in the eastern screech owl (*Megascops asio*) was measured using the auditory brainstem response (ABR). The typical screech owl ABR waveform showed two to three prominent peaks occurring within 5 ms of the stimulus onset. As sound pressure levels increased, ABR peak latency decreased and peak amplitude increased for all test stimuli. With increasing stimulus rate, the latency of ABR peaks increased and amplitude decreased. The shape of the screech owl audiogram derived from the ABR is similar to the audiogram of the barn owl except at highest frequencies. Based on the ABR, screech owls hear best between 1.5 and 6.4 kHz with the most acute sensitivity between 4-5.7 kHz. Preliminary data suggest that there may be a

difference in overall auditory sensitivity between the color morphs of this species. Generally, changes in the ABR waveform to stimulus intensity and repetition rate are comparable to what has been found in other birds.

#### **447 Efferent Effects on Cochlear Whole-Nerve Responses and its Antimasking Effects Through Electrical Stimulation of the Inferior Colliculus**

Wei Zhang<sup>1</sup>, DF Dolan<sup>1</sup>

<sup>1</sup>*Kresge Hearing Research Institute, University of Michigan, Ann Arbor, MI*

The mammalian cochlea is innervated by the lateral (LOC) and medial (MOC) olivocochlear efferent systems. These two systems have different peripheral terminations in the cochlea and different origins in the brainstem. Studies of the MOC have a rich history leading to potential roles in peripheral processing. Recent studies now suggest that LOC activation also influences the neural output of the cochlea. Both systems regulate different components of cochlear function. The detection of signals in noise while activating each efferent system is the focus of this study. Electrical stimulation (ES) within the inferior colliculus (IC) can evoke either MOC or LOC efferent effects within the cochlea. The effect of IC ES on the cochlear whole-nerve action potential (CAP) and the distortion product otoacoustic emission (DPOAE) defines which system is activated. The effects of IC ES on the masked CAP are measured.

Anesthetized, paralyzed and respiration pigmented guinea pigs (300-400g) were used. TDT hardware and software were used to generate acoustic, ES and data collection. ES (biphasic rectangular pulses (phase 0.4 ms) at 100Hz) was achieved with bipolar insulated platinum electrodes (0.2mm), set 0.5-1 mm apart and placed in and around lateral cortex (LC) of IC. Tone and noise were presented either simultaneously or in a forward masking paradigm.

ES of the LC region can produce "typical" MOC effects or alter the CAP independent of frequency or stimulus level. In some animals both MOC and LOC effects were observed in both ears. With ES, CAP enhancement can be seen in the masking paradigms. Usually the enhancement occurred at high signal levels. At low signal level, the masked CAP amplitude with IC ES is reduced compared to the tone alone condition. Different antimasking effects could occur between ears, either bigger in one ear or absent in the other ear. The effect of eliminating the efferent pathways by transaction will be presented.

Supported by NIH Grant RO1 DC004194 and P30 DC05188 (DFD).

#### **448 Hebbian and anti-Hebbian Learning Rules in the Dorsal Cochlear Nucleus**

Thanos Tzounopoulos<sup>1</sup>, Larry Trussell<sup>1</sup>

<sup>1</sup>*Oregon Health & Science University*

The dorsal cochlear nucleus (DCN) may detect spectral cues for sound localization and integrate this information with multimodal sensory inputs from diverse areas of the brain. Excitatory parallel fibers carry sensory inputs to the

apical, spiny dendrites of fusiform and cartwheel cells, while auditory nerve fibers carry acoustic inputs to the basal dendrites of fusiform cells. Cartwheel cells form a network of interneurons that inhibit fusiform cells, a primary output neuron of the DCN. We have previously shown (Tzounopoulos et al., 2004) that the DCN exhibits cell-specific spike-timing dependent plasticity (STDP). For example, in fusiform cells, spikes evoked 5 ms after parallel-fiber EPSPs leads to potentiation (LTP), while spikes peaking 5 ms before EPSPs leads to depression (LTD). By contrast, this EPSP-then-spike protocol leads to depression in cartwheel cells, while no plasticity results from the reverse sequence. Such Hebbian and anti-Hebbian plasticity may operate in concert to alter the output of this nucleus. We have now investigated the cellular mechanisms underlying the anti-Hebbian LTD found in cartwheel cells. The NMDA receptor antagonist, APV (100 mM), blocked the induction of LTD. Also, intracellular application of the Ca<sup>2+</sup> chelator BAPTA (20 mM) blocked LTD, arguing for an induction mechanism requiring postsynaptic Ca<sup>2+</sup>. However, coefficient of variation (CV) and paired-pulse ratio analysis revealed a presynaptic expression mechanism. In the pursuit of a retrograde message that could confer postsynaptic induction but presynaptic expression, we discovered that AM-251 (5 mM), an antagonist of endocannabinoid receptors, blocked LTD in cartwheel cells. AM-251 also blocked depolarization-induced suppression of inhibition (DSI) and excitation (DSE), a short-term retrograde plasticity. Finally, mGluR1 receptor antagonists LY 367385 (50 mM) and MPEP (4 mM) did not block either LTD or DSE/I. We propose that anti-Hebbian LTD in cartwheel cells is mediated by endocannabinoid signaling. Supported by the NIH (R37-NS028901).

#### **449 Lateral Asymmetry in Auditory Physiology of the Neonate**

**Yvonne Sininger**<sup>1</sup>, Barbara Cone-Wesson<sup>2</sup>  
<sup>1</sup>UCLA, <sup>2</sup>University of Arizona

Asymmetry in cortical processing of auditory stimuli has been well documented. Recently, asymmetric function at sub-cortical levels of the human auditory system has been demonstrated. We showed that DPOAEs are larger in the left ear of neonates and TEOAEs are greater from the right (Science, 2004 305:1581). This study looks for asymmetry in the ABR of neonates and evaluates two possible mechanisms. **Study one**, designed to investigate asymmetry in infant ABRs, analyzed data of 2205 neonates (full-term and high-risk infants) from a previous study (Ear Hear, 2000, 21:383). ABRs were obtained to 30 and 69 dB nHL click stimuli in both ears. Amplitude asymmetry was found in the ABR. Wave V was larger from the right ear. Peak latency was significantly shorter from the right at 30 dB and for peaks III and V at 69 dB. Right ear wave I-wave V interpeak intervals were generally shorter but some interaction was found with risk group. **Study two** investigated possible mechanisms of asymmetry: asymmetric activation of the medial olivocochlear (MOC) system and asymmetric synaptic or neural transmission efficiency. ABRs were evoked by 70 dB clicks in both ears of 44 neonates. To evaluate the MOC

contribution, responses were elicited with and without contralateral noise. To evaluate synaptic/neural transmission, two stimulus rates (7 and 55 cps) were used. Significantly greater amplitude reduction was found in left ear ABR from contralateral masking but no comparable asymmetry in latency was revealed. The rate study found no significant asymmetry in peak amplitude or latency as a function of rate, suggesting that there is no asymmetry of synaptic transmission. The overall findings confirm asymmetry in brainstem level auditory function in neonates. The ABRs evoked by the right ear stimulation were found to have larger amplitudes and generally shorter latencies. The amplitude of the ABR from the left ear is suppressed by contralateral noise to a greater extent than the ABR from the right. This indicates that asymmetrical activation of the MOC is a plausible explanation for ABR amplitude asymmetry.

#### **450 Auditory Brainstem Responses to Airborne Sounds in the Aquatic Frog *Xenopus laevis*: Correlation with Middle Ear Characteristics**

**Bharti Katbamna**<sup>1</sup>, John Brown<sup>1</sup>, Charles Ide<sup>2</sup>

<sup>1</sup>Speech Pathology & Audiology, Western Michigan University, Kalamazoo, MI, <sup>2</sup>Environmental Institute, Western Michigan University, Kalamazoo, MI

Previous measurements of tympanic disk mobility and middle ear characteristics in the South African clawed frog *Xenopus laevis* indicate that the vibrational profile of the disk depends on the air enclosed in the middle ear cavity. In adults the frequency response of the disk to airborne sounds has been shown to be nearly flat with a maximum velocity of 0.3 mm/s at 1 kHz. Best levels of distortion product otoacoustic emissions are also measured in the 1.0-1.2 kHz range. In this study we recorded auditory brainstem responses (ABR) in response to airborne sounds and showed that best hearing sensitivity ranges were determined by the volume of the middle ear cavity. In newly metamorphosed frogs (body mass 0.7-0.9 g, snout-vent length 1.8-2.2 cm) best hearing sensitivities were measured in the 2.2-3.0 kHz range, whereas the optimal hearing sensitivity in older adults (body mass 83-90 g, snout-vent length 10-11 cm) ranged from 1.0-1.4 kHz. Measurements of middle ear volume reconstructed from serial sections of the head showed approximate volume in the 0.005-0.0075 cc range in newly metamorphosed frogs, which translated to resonant frequencies of 2.6-3.0 kHz. In older adults middle ear volumes ranged from 0.03-0.08 cc, so that resonant frequencies shifted to 1.0-1.6 kHz region. Thus, differences in best hearing sensitivity appear to be correlated to variation in the middle ear volume at least for airborne sounds. Moreover, these results are comparable to peak frequency vibration profiles of the tympanic disk and explain the occurrence of peak amplitudes of distortion product otoacoustic emissions in the 1.0-1.2 kHz region reported in literature.

Supported in part by the Western Michigan University Faculty Research and Creative Activities Support Fund and the EPA grant #R83023501-0.

### **451 Survival and Integration of Monkey Neuronal Progenitor cells differentiated from Embryonic Stem Cell in Auditory Brain Stem Slice Cultures**

Charoensri Thonabulsombat<sup>1,2</sup>, Shoukhrat M. Mitalipov<sup>3</sup>, Don P. Wolf<sup>3</sup>, Petri Olivius<sup>2,4</sup>

<sup>1</sup>Department of Anatomy & Institute of Science & Technology, Mahidol University, Thailand, <sup>2</sup>Center for Hearing and Communication Research, Karolinska University Hospital, Stockholm, Sweden, <sup>3</sup>Oregon National Primate Research Center, Oregon Health & Science University Beaverton, OR 97006, <sup>4</sup>Department of Clinical Neuroscience, Section of Otorhinolaryngology, Karolinska Institute, Sweden

The poor regeneration capability of the mammalian inner ear has initiated different approaches to enhance the functionality after injury. Development of animal transplantation models will be necessary to study the safety and efficacy monkey neuronal progenitor cells (NPCs) of cell transplants. An interesting approach alternative is to use implant with the potential to establish synaptic contacts with the cochlear neurons and with the perspective to develop into a functional auditory unit. ES cell-induced neural progenitor cells (NPCs) have been shown to develop into morphologically mature neurons and glia cells in serum-free medium containing fibroblast growth factor (FGF)-2 before neural differentiation was induced. We developed a co-culture system as a rat brainstem slice preparation to study the integration of the monkey NPCs implant within the cochlear nucleus. Following in vivo retrograde labeling with Dil, neuronal components of the auditory system, including that of the cochlear nucleus, were dissected out and transferred to a petri dish. Thus monkey NPCs were implanted into brainstem slices from postnatal rats. The slices contained neurons of the cochlear nucleus. The slices were 300 µm thick and the monkey NPCs were grown together as an organotypic co-culture on membrane. However, we evaluate the integration of monkey NPCs engineered to express green fluorescent protein (GFP) into the rat brain slices. After integration into the brain slice, GFP+ donor NPCs were able to differentiate into neuron and glia cells as evaluated by their relevant antibodies.

The results demonstrate that organotypic slice cocultures present a useful model to study the regeneration of the respective neurons for up to five weeks in vitro and the cocultured monkey NPCs generate neurons and glia cells capable of integrating into the brain circuitry.

### **452 Cortical and Cognitive Consequences of Brainstem Timing Deficits**

Karen Banai<sup>1</sup>, Trent G Nicole<sup>1</sup>, Steven Zecker<sup>1</sup>, Nina Kraus<sup>1</sup>

<sup>1</sup>Auditory Neuroscience Laboratory, Northwestern University, 2240 Campus Drive, Evanston, IL, USA

The search for a unique biological marker of language-based learning disabilities (LD) has so far yielded inconclusive findings. In this study we investigated whether

brainstem timing deficits had specific consequences with respect to higher order processing of stimulus differences.

We have tested a large group of children with LD and normal learning children ages 8-16 years. The LD group was divided into two subgroups with normal and abnormal transient brainstem response to the speech syllable /da/. The cortical mismatch responses (MMNs) elicited by a just-perceptibly different /da-ga/ pair and the behavioral and cognitive profiles of the two LD subgroups and the controls were compared.

At the group level, the magnitude of the cortical MMN response was smaller in both LD groups compared to controls. Analyzed on an individual subject basis, MMNs were present among the majority of controls, but only in a minority of LDs. LDs with abnormal transient brainstem response had on average more severe speech discrimination, reading, spelling and cognitive difficulties and they were more likely to exhibit abnormal cortical processing of fine stimulus differences compared to LDs with intact brainstem function. Consequently, abnormal brainstem timing appears to negatively impact cortical processing of sound.

We suggest that abnormal brainstem function may serve as a marker of a distinctive subgroup of LDs, with poorer speech perception, reading and spelling and abnormal processing of stimulus change. This marker is reliable at the individual level. On the other hand, the MMN is a less sensitive marker, since abnormal MMNs characterizes the majority of LDs and sub-grouping LDs by their MMN does not yield distinguishable groups in terms of reading, speech perception or cognitive ability.

Supported by NIH NIDCD RO1-01510

### **453 Contralateral Noise Changes Activation in Left Human Auditory Cortex During the Distinction Between Words and Pseudowords**

Nicole Behne<sup>1</sup>, Henning Scheich<sup>1</sup>, Andre Brechmann<sup>1</sup>

<sup>1</sup>Leibniz-Institute for Neurobiology Magdeburg

Recently we suggested that presenting information-bearing stimuli to one ear and noise to the other ear may be a general tool to determine hemispheric specialization in auditory cortex (AC). Using this approach we confirmed that directional categorization of frequency modulation is mainly processed in right AC by showing an influence of contralateral noise exclusively on right AC activation. In the present fMRI study we tested if there is an exclusive influence of contralateral noise on left AC activation in a semantic decision task that is known to be processed mainly in left AC.

Pseudowords and semantically neutral words with neutral prosody were presented monaurally or binaurally and had to be distinguished by 16 subjects. The monaural presentation took place either with or without contralateral white noise.

The activation in both AC on contralateral word stimulation was stronger than on ipsilateral stimulation as expected from electrophysiological studies showing that the contralateral auditory pathway is stronger than the

ipsilateral. During additional presentation of contralateral noise the activation in right AC was similar to the condition without noise. Whereas in left AC we found a stronger activation on left ear word stimulation with contralateral noise than without noise. This can be explained assuming a left hemispheric specialization for semantic decision tasks.

These results together with that of the directional categorization study suggest that the activation on ipsilateral information-bearing stimuli can be up-regulated by presenting noise to the contralateral ear exclusively in the hemisphere specialized for a given task. Therefore this paradigm may be useful to determine yet unknown hemispheric specialization of the auditory cortex.

#### **454 Time Imaging of Human Auditory System Activity in Cochlear Implant Users**

**Curtis W. Ponton<sup>1</sup>, Jos J. Eggermont<sup>2</sup>, Manfred Fuchs<sup>1</sup>**

<sup>1</sup>*Compumedics Neuroscan*, <sup>2</sup>*University of Calgary*

The ability to image central auditory system activation provided by cochlear implant (CI) stimulation remains limited, particularly for children. The use of neuroimaging techniques such as positron emission tomography (PET) is normally restricted to adult CI users because of the exposure to radioactive binding agents. Functional magnetic resonance imaging (fMRI) also has limited application because of the incompatibility of strong scanner magnetic fields with CI hardware. Electrophysiological measures of brain activity such as evoked potentials have lower spatial resolution than PET and fMRI, but can be applied to both children and adult cochlear implant users. Moreover, evoked potentials provide exquisite measures of time-based processing in the auditory system, far superior to PET and fMRI. Unfortunately, most evoked potentials studies of cochlear implant users have limited analyses to a very small number of electrode recording sites on the head. With high density multi-channel evoked potential recordings, advanced data processing techniques such as independent components analysis and current density reconstruction provide the capacity to spatially and temporally localize cortical activity with a combined precision absent from other imaging techniques. This presentation will demonstrate a dissection of auditory system responses, illustrating the timing and cortical location of auditory-evoked activity in the normal-hearing population and in individuals who use cochlear implants. Results will show that early on, areas of cortical activation are similar for both normal-hearing and CI users. However, subsequent stages of processing may differ greatly between these groups. These findings provide further evidence of differences in cortical processing of auditory input for cochlear implant users, specifically for children with longer periods of deafness prior to receiving a cochlear implant.

#### **455 Human Auditory Cortical Sensitivity to Changes in Interaural Correlation**

**Maria Chait<sup>1</sup>, Jonathan Z. Simon<sup>1</sup>**

<sup>1</sup>*University of Maryland, College Park*

Sensitivity to interaural correlation (IAC), the similarity of the sound waveforms at the two ears, plays a key role in auditory scene analysis and the process of extracting objects from background. Psychophysically, listeners' sensitivity to changes in IAC is asymmetrical such that discrimination is very fine for deflections from IAC=1 (completely correlated signals) but decreases significantly for deflections from IAC=0 (uncorrelated signals). The present study explores the neural mechanisms that underlie this behavior. We use the high temporal resolution of MEG recording to investigate the timing of IAC processing in cortex and the degree of correspondence between behavioral and electrophysiological measures.

Signals are 1100 ms long, consisting of 800 ms of interaurally correlated (IAC=1) or uncorrelated (IAC=0) wide-band noise, followed by 300ms of the same wide band noise with different degrees of IAC (1, 0.8, 0.6, 0.4, 0.2, 0). Auditory cortical responses were recorded using a 160 channel whole head MEG system (KIT, Kanazawa, Japan). The response to the change in correlation was characterized by sequential increases in activity in 3 temporal windows ~70ms, ~130ms and ~200ms post change in correlation. These physiological responses tracked behavioral responses by peaking earlier for correlated references and for bigger changes in correlation. Additionally, we note differential hemispheric contribution to the responses such that the right hemisphere dominated in the early time-window, and the left hemisphere in the later responses. The response at ~130ms correlated most with behavior, and most interestingly, exhibits different (opposite) dipolar patterns for changes from reference IAC of 1 and 0. The comparison between electrophysiology and behavior indicates that these cortical brain responses are more acute to changes in correlation than what is reflected in behavioral detection.

This work was supported by R01 DC05660 to David Poeppel

#### **456 Auditory Cortex Function in Subjects with Steep High-Frequency Hearing Loss; a fMRI Study**

**Dave R. M. Langers<sup>1</sup>, Walter H. Backes<sup>1</sup>, Pim Van Dijk<sup>2</sup>**

<sup>1</sup>*University Hospital Maastricht, Dept. Radiology,*

*Maastricht, The Netherlands,*

<sup>2</sup>*University Hospital Groningen, Dept. ORL, Groningen, The Netherlands*

Numerous animal studies have shown functional reorganization of the auditory cortex following peripheral hearing loss. In induced high-frequency hearing loss, frequencies just below the imposed lesion become over-represented in the auditory cortex (e.g. Rajan and Irvine, *Audiol. Neurotol.* 3, 123-144, 1998). The present study utilizes functional MRI to investigate whether similar effects can be observed in humans with steep high-frequency hearing loss.

Eight hearing impaired subjects and 10 normal hearing controls were tested. In the hearing-impaired subjects (5 unilateral, 3 bilateral), thresholds in the affected ears were 20 dB nHL or better at 250, 500, and 1000 Hz, and 70 dB or worse at 4000 and 8000 Hz. Subjects performed a 2AFC-task, and detected tones (500 ms) in 1/3-octave noise bands (1500 ms). Tone frequencies were 125, 500, 2000, and 8000 Hz, respectively. Tone and noise levels were aimed at 60 dB SL each, but were never above 85 dB SPL. Stimuli were presented in a new double-scan sparse imaging blood-level-oxygen-dependent MRI protocol (TR=13.5 s and 2.5 s alternatingly).

A SPM-analysis showed a low-to-high frequency gradient on Heschl's gyrus in the anterolateral to posteromedial direction. In addition a complicated pattern of tonotopic organization on the planum temporale was observed. Hearing-impaired subjects displayed a similar, but more erratic, tonotopic organization. In unilaterally affected patients (n=5) activation extent and level was significantly increased for stimulation of the affected ear at 2000 and 8000 Hz, in comparison to stimulation of the unaffected side.

Several explanations may account for the observed responses. Frequencies at the edge of the hearing loss may have increased representation in the auditory cortex, similar to the effects shown in other mammals (e.g. Rajan and Irvine, 1998). This may be due to increased recruitment at cochlear level, but may also be the result of plastic changes in the central auditory pathways.

(Supported by the Maastricht University Research Fund and the Heinsius Houbolt Foundation)

#### **457 Analysis of Cerebral Glucose Metabolism Between Normal and Deaf Cats using microPET**

**Min-Hyun Park<sup>1</sup>**, Seung-Ha Oh<sup>1</sup>, Hyo-Jeong Lee<sup>1</sup>, Byung Yoon Choi<sup>1</sup>, Jin Su Kim<sup>2</sup>, Jae Sung Lee<sup>2</sup>, Dong Soo Lee<sup>2</sup>, Sun O Chang<sup>1</sup>, Chong-Sun Kim<sup>1</sup>

<sup>1</sup>Department of Otolaryngology, Seoul National University, College of medicine, <sup>2</sup>Department of Nuclear medicine, Seoul National University, College of medicine

**Objects:** The glucose metabolism of primary auditory cortex was decreased in deaf patients. (Naito et al, 1997) The purpose of this study is to evaluate the changes of glucose metabolism in the brain auditory cortex using a cat model with FDG-PET.

**Methods:** We obtained positron emission tomography (PET) images of cat brain using a microPET R4 scanner (Concorde Microsystems Inc., Knoxville, TN) in 3 normal cats and 2 deafened cats. Before getting PET images, cats were kept fasting state since last midnight. They were anesthetized with ketamine (Veterinary Ketalar) 100mg/kg and xylazine (Rompun) 10mg/kg intramuscular injection and ketamine was injected intravenously every 30 minutes for keeping the anesthesia. After anesthesia, transmission image was acquired by singles mode using <sup>68</sup>Ge line source for 30 minutes. Then <sup>68</sup>Ge line source was removed, F-18-FDG was injected intravenously and emission image was acquired by coincidence mode for 30 minutes. 3D data was sorted into a set of 2D data by using

Fourier rebinning and the image was reconstructed by using 2D Ordered Subset Expectation Maximization (subset:16, iteration:4). For evaluation of decreased glucose metabolism in auditory cortex, we drew region of interest in auditory cortex, and measured the mean counts of the area in brain PET image. Cerebellum was regarded as reference region in PET image so got the mean counts of cerebellum. Count ratio (= mean counts of auditory cortex / mean counts of cerebellum) was compared between normal and deafened cats.

**Results:** The count ratio of glucose metabolism in three normal cats was 2.49±0.13(standard deviation), and in the deafened cats, the count ratio were 2.23 (deaf duration was 5 months), and 2.52 (deaf duration was 2 months).

**Conclusion:** We identified decreased glucose metabolism in auditory cortex in deafened cat (Deaf duration was 5 months) (Statistical significance could not be achieved due to small number of cases).

#### **458 Central Auditory Development in Children with Bilateral Cochlear Implants.**

**Anu Sharma<sup>1</sup>**, Michael Dorman<sup>2</sup>, Kathryn Martin<sup>3</sup>, Phillip Gilley<sup>3</sup>

<sup>1</sup>University of Texas at Dallas, <sup>2</sup>ASU, <sup>3</sup>UTD

We examined the longitudinal development of the Cortical Auditory Evoked Potential (CAEP) in several children who were fitted with bilateral cochlear implants before age 3.5 years or after age 7 years. The age cut offs (<3.5 years for early implanted and >7 years for late implanted) were based on the sensitive period for central auditory development described by Sharma et al. 2002 [Ear and Hearing, 23; 532-539]. Children who received bilateral implants by age 3.5 years showed rapid development in CAEP waveform morphology and P1 latency. In the case of a child who received his first implant by age 3.5 years and his second implant after age 7 years, CAEP responses elicited by the second implant were similar to late implanted children. Data from other children who received their second implant after the sensitive period will be presented. Our preliminary evidence and data from animal models suggests that long-term stimulation of auditory pathways ipsilateral to an implant may not be sufficient to preserve the plasticity of those pathways. This outcome is in contrast to the preservation of plasticity (after early implantation) of the pathways contralateral to the implant.

Supported by: NIH R01DC004552-05 and NIHR01 DC006257

#### **459 The Effects of Selective Auditory Attention Recorded from Human Electrooculograms**

**Michael Neelon<sup>1</sup>**, Prakash Khanikar<sup>1</sup>, Justin Williams<sup>1</sup>, Lisa Ruehlow<sup>1</sup>, P. Charles Garell<sup>1</sup>

<sup>1</sup>University of Wisconsin - Madison

A central question in electrophysiological research is whether selective attention modulates exogenous components of the averaged auditory event-related potential (ERP), or instead arises outside of modality-

specific cortex to create a possibly overlapping processing negativity. The greater signal gain and anatomical precision of intracranial electrocorticograms (ECoG) were used in the current work to investigate these issues in more detail.

Data were recorded from subdural electrodes placed on temporal cortex in six patient-volunteers undergoing diagnostic procedures for medically intractable epilepsy. Patients performed a dichotic listening task in which they alternately attended to or ignored a series of tone pips presented contralateral to electrode location and with varying mean interstimulus intervals (ISI). To control attention, patients had to respond to rare frequency deviants embedded among common standard frequency tones.

ERP components were isolated based on electrode location, latency and polarity of peak negative and positive deflections between 70-120ms and 121-220ms post-stimulus, respectively. In general, largest ERP components and changes in components due to attention were both recorded from the posterior superior temporal gyrus (pSTG). Differences between attend and ignore conditions were assessed for each patient individually using non-parametric tests. For the two time windows studied, respectively, three and five patients showed consistently enhanced intracranial ERPs in the attend relative to ignore conditions. The results suggest that selective attention can enhance early auditory cortical responses, with the largest effects seen in pSTG. These findings are consistent with the theory that attention can modulate exogenous auditory components in a gain-like manner.

#### **460 The Handshaking Model of Brain Function and the AXS Test Battery: A New Strategy for Assessing the Physiology of Rostro-Caudal Relations in the Human Auditory Nervous System**

Judith Lauter<sup>1</sup>

<sup>1</sup>Stephen F. Austin State University

Top-down modulation in sensory systems is a physiological prerequisite for selective attention, whether the goal is attending to one sensory modality vs. others, or focusing on specific aspects of a stimulus array within the same modality. While substantial research has been directed to describing corticofugal and other anatomical bases of this type of neural control, less is known about the physiology of top-down modulation, particularly in humans, in spite of obvious applications for clinical conditions such as attention deficit and hyperactivity. The Auditory Cross-Section (AXS) Test Battery provides a relatively inexpensive, noninvasive, and coordinated approach to assessing top-down modulation in the auditory system, by quantifying physiological features at three levels -- the peripheral ear (e.g., otoacoustic emissions, OAEs), the brainstem (Repeated Evoked Potentials version of the Auditory Brainstem Response, REPs/ABR), and auditory cortex (quantitative electroencephalography, qEEG). The Handshaking Model of Brain Function offers an approach to interpreting AXS-

Battery data, on the analogy of Hughlings Jackson's conclusions regarding top-down modulation in the motor system. That is, lower levels of a sensory system are considered as having an inherent degree of activity which is subject to modulation by higher levels, ranging from more suppressed (associated with increased activity at more rostral levels) to more released (associated with decreased activity at more rostral levels). In addition, such modulation can be readily quantified in terms of: amplitude of background activity, latency and amplitude of evoked responses, and the repeatability of evoked responses. Sample data will be presented illustrating correlated changes in cortex, brainstem and ear during manipulations such as methylphenidate, antihistamines, nicotine, and biofeedback.

#### **461 The Processing of Vocal Expressions of Emotion in Human Auditory Cortex Studied with fMRI**

Disa Sauter<sup>1</sup>, Jane Warren<sup>2</sup>, Jade Wiland<sup>1</sup>, Frank Eisner<sup>3</sup>, Sophie Scott<sup>4</sup>

<sup>1</sup>UCL, <sup>2</sup>MRC Clinical Science Centre, <sup>3</sup>MPI Psycholinguistics, Nijmegen, <sup>4</sup>Institute of Cognitive Neuroscience, UCL

Recent functional imaging studies have indicated that, as in the non-human primates, there is a left lateralised 'what' stream of processing important in the neural representation of speech (Scott et al, 2000). In this study, we investigated the neural systems important in the perception of non-linguistic information – specifically paralinguistic expressions of emotion. We used two negative and two positive emotional expressions - disgust, anger, amusement and triumph - based on our previous work (Sauter, Calder and Scott, under review). Neural responses were measured using 3T fMRI. Relative to a signal correlated noise baseline, the paralinguistic expressions of emotion activated bilateral superior temporal gyri and sulci, lateral and anterior to primary auditory cortex, consistent with the processing of non linguistic vocal cues in the auditory 'what' pathway. The activation extended posteriorly into the superior temporal sulcus on the right. There were some emotion specific responses seen – most notably amusement, characterized by laughter, was associated with greater activation extending into both temporal poles, amygdale and insula cortex. Further work will attempt to determine the extent to which this is a consequence of contagion, or the role of laughter as a salient social cue. This study has confirmed an important role for the auditory 'what' pathway in the processing of non-verbal expressions, indicating that in the human this may not be specific to the processing of spoken language.

## **462** Monitoring Brain Response After Cochlear Implantation in Prelingually Deaf Children

Yasuhiro Osaki<sup>1,2</sup>, Takako Iwaki<sup>1,3</sup>, Satoru Kohno<sup>4</sup>, Jun Hatazawa<sup>1</sup>, Masashi Takasawa<sup>1</sup>, Hiroshi Nishimura<sup>1</sup>, Naohiko Oku<sup>1</sup>, Katsumi Doi<sup>1</sup>, Takeshi Kubo<sup>1</sup>

<sup>1</sup>*Osaka University School of Medicine*, <sup>2</sup>*Mount Sinai School of Medicine*, <sup>3</sup>*Aichishukutoku University*, <sup>4</sup>*Shimadzu Corporation*

Activation of the temporal cortex was investigated in adult deaf patients after cochlear implantation by means of positron emission tomography (PET). However, cortical response to auditory stimuli in deaf children with cochlear implants (CIs) has not yet been understood. Objective evaluation of the function of central auditory system is important because it is difficult to obtain reliable behavioral response from very young children when their CIs are adjusted. In this study, we measured activation of the temporal cortex in nine prelingually deaf children with CIs by means of near-infrared spectroscopy (NIRS). Near-infrared (NIR) light emitted from a transmitter optode penetrates the tissue to a certain depth and undergoes partial absorption by blood hemoglobin (Hb) along the banana-shaped light path. By measuring the reflected light detected at a receiver optode placed 3 cm from the transmitter one, concentration change of oxyhemoglobin (oxyHb), deoxyhemoglobin (deoxyHb), and total hemoglobin (totalHb) in the cerebral cortex between two optodes can be calculated. Since the amounts of oxyHb, deoxyHb, and totalHb in cerebral circulating blood are altered depending on the activation of local brain, NIRS can be used to monitor local brain response noninvasively. We used three transmitter and three receiver optodes. Hb concentration was monitored in seven sites of the temporal cranium region contralateral to the CI. Written informed consent was obtained from the parents before the experiments. The protocol was in compliance with the ethical committee of the institute. Concentration of oxyHb and/or totalHb increased in seven of nine subjects during the auditory stimuli. DeoxyHb increased in three subjects and decreased in other three subjects. These results, similar to those reported in normal neonates, demonstrate activation of the temporal cortex in prelingually deaf and early-implanted children when cochlear implantation was successful.

## **463** Variations of N100m Responses in Auditory Evoked Magnetic Fields

Kanako Yamada<sup>1</sup>, Yuko Suzuka<sup>1</sup>, Masanori Higuchi<sup>2</sup>, Natsuko Hatsusaka<sup>2</sup>, Koichi Tomoda<sup>1</sup>

<sup>1</sup>*Kanazawa medical university*, <sup>2</sup>*Kanazawa Institute of Technology*

Purpose: In recent, magnetoencephalography (MEG) is well suited for studies of human auditory cortex. The waves of P50m, N100m, and P200m were observed in auditory evoked magnetic fields. It revealed that there were some differences and patterns of responses especially in N100m. The purpose of this study was to investigate interaction of auditory pathway at the level of primary auditory cortex by changing stimulus side of the ear.

Methods: We examined auditory responses in healthy 17 subjects, 8 males and 9 females, including 3 left handed. The corresponding auditory evoked magnetic fields with stimuli to the right ear, left ear and both ears were recorded using a 320-channel whole-head MEG system developed by Kanazawa Institute of Technology. The stimuli were 1kHz short tone burst of 50ms duration with the interstimulus interval of about 1s. The responses were averaged by 100 stimulus presentations of each measurement.

Results: We could find clear response peaks such as N100m and P200m in 16 subjects. It revealed that there were some patterns of responses especially in N100m and it was not simple to determine contra lateral dominance or hyperactivity of right auditory cortex than left, and there were some differences with previous studies. In this measurement, we could classify them into three major groups using the isofield contour map and peak latency of N100m. The 1st group was the general type which is contra lateral dominance and slightly hyperactivity of right hemisphere in both ears of stimulus. The 2nd group showed right hemisphere dominance even in right ear of stimulus. The 3rd group showed left hemisphere dominance even in left ear of stimulus. Left handed 3 subjects were all involved in this group. As a special case in the 2nd group, one subject showed almost no response in the left hemisphere. This subject has normal hearing ability by audiometry and no anatomical abnormality by MRI and PET.

Conclusions: It was revealed that there were individual variations of N100m responses in auditory evoked magnetic fields. The explanation of individual variation is required further investigations of binaural integration and interaural differentiation.

## **464** A Characterization of Potentials Evoked by Intracortical Microstimulation in Gerbil Primary Auditory Cortex (AI)

Achim Engelhorn<sup>1</sup>, Daniel Ensberg<sup>1</sup>, Matthias Deliano<sup>1</sup>, Henning Scheich<sup>1</sup>, Holger Schulze<sup>1</sup>, Frank W. Ohl<sup>1</sup>

<sup>1</sup>*Leibniz-Institut für Neurobiologie, Magdeburg*

For a better understanding of the processes underlying the information exchange between sensory cortex and cortical neuroprostheses basic knowledge is needed about how the cortex responds to electrical stimulation as a putative carrier of information and behaviourally relevant meaning. Therefore, a parametric study has been conducted in the auditory cortex of the Mongolian gerbil (*Meriones unguiculatus*).

Biphasic charge-balanced pulses were applied with variations in pulse amplitude, pulse phase duration and the combination of both. Typical components of the electrically evoked potentials were characterized and compared with auditory evoked potentials. Finally, collision-like experiments were performed by means of combined electrical and acoustic stimulation to draw inferences about the nature of the electrically, and respectively, acoustically evoked neuronal populations.

## **465 Asymmetric Hemodynamic Responses of the Auditory Cortex in Normal Hearing and Unilateral Hearing Loss Subjects**

Jill B. Firszt<sup>1</sup>, Wolfgang Gagli<sup>1</sup>, Christina L. Runge-Samuelson<sup>1</sup>, P. Ashley Wackym<sup>1</sup>, John L. Ulmer<sup>1</sup>, Robert W. Prost<sup>1</sup>, Edgar A. DeYoe<sup>1</sup>

<sup>1</sup>Medical College of Wisconsin

When evoked by monaural stimulation, the central auditory system shows stronger activation in the contralateral compared to the ipsilateral hemisphere (Zatorre et al., 1992). This amount of asymmetry between hemispheres has been shown to differ between normal hearing (NH) and unilateral hearing loss (UHL) subjects for both click stimuli and auditory evoked potential measures (Ponton et al., 2001) as well as pulsed tonal stimuli and functional magnetic resonance imaging (fMRI) findings (Scheffler et al., 1998). The purpose of this study was to investigate the hypothesis that, using speech stimuli, UHL subjects show an increase in symmetric activation patterns between hemispheres compared to NH subjects. Normative data were collected in NH listeners for presentation of monaural and binaural speech stimuli using hemodynamic responses measured during fMRI experiments. UHL subjects were tested with the same stimuli in the hearing ear. Preliminary results indicate that in NH subjects, 1) responses are stronger in the contralateral compared to ipsilateral hemisphere, and 2) binaural stimulation results in stronger responses than monaural stimulation. Although there was variability within and across subjects in the UHL group, some subjects have more symmetric hemodynamic responses compared to NH subjects. The comparison between UHL and NH subjects will be presented with respect to activation of the contralateral and ipsilateral hemispheres and the spatial distribution of activity (e.g., transverse temporal gyrus and planum temporale).

Supported by NIH/NIDCD K23DC05410

## **466 Auditory Streaming in Humans: Possible fMRI Correlates in Auditory Cortex**

E. Courtenay Wilson<sup>1,2</sup>, Jennifer Melcher<sup>2</sup>, Christophe Micheyl<sup>3</sup>, Alexander Gutschalk<sup>2</sup>, Andrew Oxenham<sup>3</sup>

<sup>1</sup>Speech and Hearing Bioscience and Technology Program, MIT, <sup>2</sup>Eaton-Peabody Laboratory, Massachusetts Eye and Ear Infirmary, Boston, MA, <sup>3</sup>Research Laboratory of Electronics, MIT, Cambridge, MA

The aim of this study was to identify neural correlates of auditory stream segregation in humans using blood oxygenation level dependent (BOLD) functional magnetic resonance imaging (fMRI). The stimuli consisted of alternating-frequency 100-ms tone bursts (ABAB) presented over 32 s. The frequency difference between the A and B tones was 0, 1/8, 1, or 20 semitones (ST). These values were chosen to elicit either integration (one-stream percept; 0 ST), segregation (two-stream percept; 20 ST), or an intermediate percept (fluctuation between one and two streams). Subjects' psychophysical responses were recorded simultaneously with their fMRI measurements. We examined both the temporal shape and the overall levels of activation across conditions of

repeating tone pairs. While some differences in temporal response were observed, they were subtle compared to differences in the overall amount of activation. In particular, fMRI activation in auditory cortex increased in amplitude and extent with increasing frequency separation between tones. Correspondingly, the psychophysical results showed an increasingly segregated (i.e., two-stream) percept with increasing frequency difference. At one level, the fMRI results may reflect increased segregation of neural activity along the tonotopic axis with increasing tone separation. At another, they may indicate that population neural activity in auditory cortex increases with increasing number of perceived streams. [Supported by Hertz Foundation Fellowship and by NIH grant R01DC05216 and P30DC005209.]

## **467 Effects of Continuous Broadband Noise on Tone-Evoked Activations in Human Auditory Cortex**

G Christopher Stecker<sup>1</sup>, Teemu Rinne<sup>1</sup>, Isaac H Liao<sup>1</sup>, Xiaojian Kang<sup>1</sup>, E William Yund<sup>1</sup>, Timothy J Herron<sup>1</sup>, David L Woods<sup>1,2</sup>

<sup>1</sup>Human Cognitive Neurophysiology Lab, UC Davis and VANCHCS, <sup>2</sup>Dept of Neurology, UC Davis

A significant challenge for auditory functional magnetic resonance imaging (fMRI) is the control of acoustic noise present in the scanning environment. Although ambient noise can be minimized through sparse imaging procedures and passive attenuation, some residual environmental noise---e.g., "pump noise" generated by coolant-handling machinery---remains audible. Pump noise varies acoustically from scanner to scanner, complicating between-study comparisons, and its spectrotemporal complexity may interfere with activations caused by complex acoustic stimuli. One potential means for controlling the effects of pump noise is to present sounds mixed with a low-level continuous broadband masking noise. Here we examine the effects of such maskers on tone-evoked BOLD fMRI activations in human auditory cortex.

Runs consisted of 21.6-s blocks of auditory stimulation (sequences of 120-ms pure tones) or silence. The blocks were presented either with or without a continuous broadband noise masker, the level of which was adjusted psychophysically to provide equal detectability across frequency, of tone sequences embedded in pump noise. Tone sequences were presented 15 dB above masked thresholds at a mean frequency of 225, 900, or 3600 Hz (varying between blocks), with individual tones varying by  $\pm 5$  semitones. During the recordings, the subjects performed auditory or visual one-back matching tasks.

Full-brain images were acquired using sparse echo-planar imaging (TR=10.8 s) at 1.5 Tesla. Functional data were projected to high-resolution flat maps of each subject's cortical surface for analysis. In all subjects, sound presented in silence produced widespread activation of auditory cortex (Heschl's gyrus and adjacent regions of middle superior temporal gyrus). In general, a subset of lateral activations was maintained when sounds were presented with the continuous masker, while medial



activations were more markedly attenuated. Despite similar detectability of tones across subjects, some showed more widespread reductions. These results suggest differential sensitivity of auditory cortical fields to continuous noise and corresponding differential specialization for auditory stimulus processing. They also have important implications for the use of masking noise to control the effects of environmental noise in fMRI experiments.

Supported by DC005814, VA Research Service, and the Academy of Finland

#### **468 Auditory Steady State Responses to Broadband Noise in Human Auditory Cortex**

**Yadong Wang<sup>1</sup>**, Nayef Ahmar<sup>1</sup>, Juanjuan Xiang<sup>1</sup>, David Poeppel<sup>1</sup>, Jonathan Simon<sup>1</sup>

<sup>1</sup>*University of Maryland*

Natural sounds, including speech, have an instantaneous modulation rate and bandwidth that change from one segment to the next. Neural responses to natural sounds, however, are computationally challenging to analyze. Neural responses to intermediate stimuli, sinusoidally amplitude modulated noise of systematically varied bandwidth, allow computationally simple analysis while still preserving features crucial to natural sounds. A whole-head 160-channel MEG system was used to acquire auditory evoked responses from 5 human subjects. The auditory Steady State Response (aSSR) was analyzed as a function of changing bandwidth and modulation frequency, with particular attention paid to the complex phase of the response. Complex field patterns were fit to complex single equivalent current dipoles. We find that response magnitude is not significantly affected by increasing bandwidth.

#### **469 The P1N1 Response to Intensity Changes at a Rapid Rate in 9-11 Year-Olds and Adults**

**Elizabeth Dinces<sup>1</sup>**, Elyse Sussman<sup>1</sup>

<sup>1</sup>*Albert Einstein College of Medicine*

The sound environment consists of rapidly changing spectrotemporal acoustic cues. An inability to normally process intensity changes within an acoustic signal may affect sound perception. This study assesses encoding of intensity in the auditory N1 at a rapid stimulus presentation rate in children. We presented tones with a stimulus onset asynchrony of 100 ms to investigate the auditory N1 response to four intensity levels (66dB, 74dB, 78dB and 86dB) in a group of 9-11 year olds and compared their responses to that of adults. The N1 latency and amplitude responses to the different intensities were similar in both groups. The N1 amplitude increased as intensity increased. ERPs can be used to study rapid (e.g., 100 ms) encoding of acoustic features in 9-11 year olds

#### **470 Phase Tracking of Slow and Rapid Tone Sequences in Human Auditory Cortex**

**Huan Luo<sup>1,2</sup>**, Yadong Wang<sup>3</sup>, David Poeppel<sup>1,2</sup>, Jonathan Simon<sup>1,3</sup>

<sup>1</sup>*Neuroscience and Cognitive Science Program, University of Maryland College Park*, <sup>2</sup>*Department of Biology, University of Maryland College Park*, <sup>3</sup>*Electrical and Computer Engineering Department, University of Maryland College Park*

The phase of the auditory steady-state response (aSSR) to sinusoidally amplitude modulated tone sequences depends on the frequency of the carrier tone. It has been shown that the response phase can track changes in the carrier frequency for long tone durations (400 ms) for analysis windows as short as below 50 ms (Patel & Balaban, 2004). Since phase tracking performance, especially for a short analysis time window, should decrease for rapidly changing tone sequences, we investigated the phase tracking performance of rapid tone sequences as well as slow tone sequences. The carrier frequency shifting speed was changed by varying the duration of the tones in the sequence from 400ms to 20ms, and the phase of the aSSR was extracted with analysis window lengths ranging from 20ms to 200ms. We find that the overall performance of phase tracking (measured by the correlation between tone carrier frequency track and the phase of the aSSR) decreases as the tone sequence becomes more rapid and such decrease is mainly due to shorter analysis temporal windows. The implication is that the ability of the brain to track carrier frequency change is determined by both duration of analysis window and stimuli carrier changing rate.

The work was supported by NIH R01 DC05660 to David Poeppel.

1, Patel, A. D. & Balaban, E., 2004, Human auditory cortical dynamics during perception of long acoustic sequences: phase tracking of carrier frequency by the auditory steady-state response. *Cerebral Cortex*, 14: 35-46

#### **471 Optical Imaging of Intrinsic Signals in Rat Olfactory Bulb for Enantiomer Pair Stimulation**

**Hikaru Uchida<sup>1</sup>**, Toru Miyazawa<sup>2</sup>, Tokio Sugai<sup>1</sup>, Koichi Tomoda<sup>1</sup>, Norihiko Onoda<sup>1</sup>

<sup>1</sup>*Kanazawa medical university*, <sup>2</sup>*University of Michigan Medical school*

The odor signals received by sensory neurons are transmitted to glomeruli of the olfactory bulb (OB). Recently, the technique of intrinsic signal imaging in rat or mouse OB was applied to map the glomerular activities of various odorants. In this study, we adapted this technique to determine whether the spatial pattern of glomerular activity in the rat provided a basis for enantiomer discrimination.

After anesthesia, a skull overlying the dorsal surface of the OB was thinned. Intrinsic signal images of reflected light (646 nm) were collected using a CCD camera. Each trial consisted of a pair of records with and without odor

stimulation at 2 min intervals. This trial was repeated 6-8 times. Then, averaged differential images with and without stimulation were calculated and significant ( $p < 0.05$ ) regions were statistically defined as active regions. Five enantiomer pairs (camphor, carvone, fenchone, limonene, and menthol) were used as odor stimuli.

Each member, (-) or (+), of enantiomer pairs activated one or more glomeruli and (-) and (+), of an enantiomer pair activated them in fairly similar regions. Some glomeruli however, showed differences in concentration-threshold between (-) and (+). Further, concentration-response curves to an enantiomer pair were near parallel with each other. On the other hand, other glomeruli have similar concentration-response curves and concentration thresholds. A common effect of increasing concentration was a large increase in the glomerular signal intensity. Results indicated that the glomerular activity patterns of an enantiomer pair were similar, but some glomeruli were differentially activated. Thus, it is suggested that subtle differences in sensory neuron responses to enantiomer pairs might make functional differences in glomerular representation, such as differences in combinations of the number of responsive glomeruli and their locations.

#### **472 Final Results of a US Multi-Center Bilateral Study Investigating Speech Perception and Localization Ability**

**Amy Barco**<sup>1</sup>, Emily Buss<sup>2</sup>, Patrick D'haese<sup>3</sup>, Robert Wolford<sup>2</sup>, Marian Zerbi<sup>1</sup>

<sup>1</sup>MED-EL Corporation, <sup>2</sup>University of North Carolina, <sup>3</sup>MED-EL Worldwide Headquarters

A multi-center study within the United States to investigate bilateral cochlear implantation in post-linguistically deafened adults implanted with the MED-EL COMBI 40+ recently concluded with 12-month data on 30 subjects. Final results for all subjects (group and individual subject data) will be reported.

Speech perception testing in noise was completed using direct audio input (DAI) (6- and 12-month intervals). Speech and noise materials were recorded onto CDs using HRTFs. A decision tree was utilized to determine the appropriate signal-to-noise ratio for bilateral speech testing using CUNY sentences in noise.

Localization testing was conducted in the horizontal-plane using a source identification task (4- and 13-month intervals). Testing was conducted in an anechoic chamber. The participant's task was to identify which of 20 loudspeakers emitted the sound. Data analyses include assessments of random error and response bias as well as overall error. Localization was evaluated separately for two signals, a Gaussian noise burst and a speech sample.

Analysis of the initial 12 patients' grouped data indicated significant head shadow, binaural summation and squelch effects. The majority of individual subjects showed all three effects at 12-months, while far fewer showed all three at 6-months. These results suggest that bilateral benefits of speech in noise may be acquired over time.

Additionally, 5 subjects were tested in both the sound field and using DAI on the same day to verify the test

procedure. Results indicated that both procedures measure binaural benefit, thus verifying the methodology.

As a group, subjects performed significantly better in the bilateral condition on all localization tasks. Data showed that individuals performed between normal and near chance in the bilateral condition.

#### **473 Bilateral Cochlear Implants and Binaural Beat Perception**

**Christopher Long**<sup>1</sup>, Robert Carlyon<sup>1</sup>, Claire Fielden<sup>2</sup>, Huw Cooper<sup>2</sup>, Daniel Downs<sup>1</sup>

<sup>1</sup>MRC Cognition and Brain Sciences Unit, <sup>2</sup>Hearing Assessment and Rehabilitation Centre, Selly Oak Hospital

Normal-hearing listeners exploit binaural information both to improve speech understanding in noise and to localize sounds. Our overall goal is to understand how such information, and the consequent real-life benefits, can be made available to bilateral cochlear implant users.

We are studying binaural beat perception by bilateral implant users. An important clinical goal is to identify, for a given patient, which pairs of interaural electrodes provide binaural cues. Assuming that beats can only be heard when stimuli are presented to appropriately matched electrodes, beat detection may be used to identify appropriate electrode pairs. It could form the basis of a simple fitting technique usable with existing clinical software and equipment, without the need to synchronize stimulation between the two implants.

Interaural time difference (ITD) and binaural beat detection were measured with four subjects, using 100pps pulse trains. The ITDs were presented in a 2IFC task in which the ITD led on the left ear in one interval and on the right in the other. Subjects indicated whether the sound moved from left to right or vice versa. All performed significantly above chance with ITDs of 234 $\mu$ sec on a given electrode pair.

Using the same electrode pairs as above, two of four subjects have shown significant binaural beat sensitivity in a cue plus 2IFC task. Subjects were told to pick the interval which contained the different sound. In two intervals, a 100pps pulse train was presented to both ears with zero ITD. In the signal interval the pulse rate was 100pps in the left and 101pps in the right ear and the ITD initially led by 3750 $\mu$ sec at the left ear, and lagged by the same amount by the end of the 750msec stimulus.

These preliminary results show that binaural beats are usable by cochlear implant users. A modified version of our method may form the basis of an interaural fitting technique.

Supported by the RNID.

#### **474 Effects of Interaural Time Differences in Fine Structure and Envelope on Lateral Discrimination in Bilateral Electrical Hearing**

**Piotr Majdak**<sup>1</sup>, Bernhard Laback<sup>1</sup>, Wolf-Dieter Baumgartner<sup>2</sup>

<sup>1</sup>*Acoustic Research Institute, Austrian Academy of Sciences,* <sup>2</sup>*ENT Department, Vienna University Hospital*

Localization of sound sources is partly based on interaural time differences (ITDs). For lower frequencies, the neural stimulation pattern is synchronized to the phase of the carrier signal. Interaural difference of the phase, so called fine structure ITD, is important for determining the lateral position of the sound source. Bilateral cochlear implant (CI) listeners currently use stimulation strategies which encode ITD in the temporal envelope but which do not transmit ITD in the fine structure due to the constant phase in the electrical pulse train. The arbitrary interaural phase difference between the pulse trains causes uncontrolled fine structure ITD.

To determine the necessity for encoding ITD in the fine structure, ITD-based lateralization was investigated systematically with CI listeners and normal hearing (NH) subjects. Lateralization discrimination was tested at different pulse rates for various combinations of independently controlled envelope ITD and fine structure ITD. Special stimuli were used whose basic parameters are based on speech signals.

Fine structure ITD had the strongest impact on lateralization at lower pulse rates, with significant effects for pulse rates up to 800 pulses per second. At higher pulse rates, lateralization discrimination depended on the envelope ITD only. It is concluded that bilateral CI listeners benefit from transmitting fine structure ITD at lower pulse rates.

A comparison of the performance between CI and NH listeners reveals sufficient comparability, suggesting that tests with NH subjects could predict performance of CI listeners.

#### **475 Experience Improves Minimum Audible Angle in Children with Bilateral Cochlear Implants 15 Months Post-Activation of the Second CI**

**Patti Johnstone**<sup>1</sup>, Ruth Litovsky<sup>1</sup>, Smita Agrawal<sup>1</sup>, Shelly Godar<sup>1</sup>, Aaron Parkinson<sup>2</sup>, B. Robert Peters<sup>3</sup>, Jennifer Lake<sup>3</sup>

<sup>1</sup>*University of Wisconsin--Madison,* <sup>2</sup>*Cochlear Americas,* <sup>3</sup>*Dallas Cochlear*

Children with bilateral cochlear implants (CIs) perform poorly on localization tasks when tested at 3-9 months after receiving their second CI (Litovsky et al., 2004, *Bilateral Cochlear Implants in Adults and Children, Archives of Otolaryngology Head and Neck Surgery*, 648-655). This result contrasted with our findings that adults show improved localization with bilateral CIs, and that in both adults and children, speech intelligibility in noise is significantly better with bilateral than with unilateral listening modes. We thus continued with follow-up testing at 15-18 months. Data from 10 children with bilateral CIs

tested between 3-, 9-, and 18- months post-2nd-surgery will be presented. Testing was conducted under bilateral and unilateral conditions. Right/Left discrimination was measured at positions ranging from +/- 2.5 to +/- 90 degrees, using noise and/or speech stimuli with overall level either fixed (60 dB SPL) or roved (+/- 4 dB). Performance was better when tested bilaterally than unilaterally for 5/10 children. Training during the test, as well as post-surgery experience resulted in significant improvement in performance in some children. Results will also be compared to measures from children with CI+HA where better performance with bilateral devices was seen for 1/6 children.

#### **476 Effects of Experience on Sound Localization with Bilateral Cochlear Implants**

**Becky B. Poon**<sup>1,2</sup>, Donald K. Eddington<sup>1,2</sup>, H. Steven Colburn<sup>1,3</sup>

<sup>1</sup>*Speech and Hearing Bioscience and Technology, Massachusetts Institute of Technology,* <sup>2</sup>*Cochlear Implant Research Laboratory, Massachusetts Eye and Ear Infirmary,* <sup>3</sup>*Hearing Research Center, Boston University*

Five bilateral cochlear implant (CI) listeners are being studied as part of a research program to improve performance with bilateral CIs. All subjects received their second CI after a year of monolateral experience. The implant systems (Clarion II with HiFocus electrodes and positioners) are identical except for two of the subjects, who have a positioner in only one ear. The mapping of analysis channel to electrode for the two independent sound processors (CIS strategy) was based on three characteristics of sensations elicited by stimulating interaural electrode pairs: fusion, relative pitch, and sensitivity to interaural time differences (ITD).

Sound-localization performance was measured both prior to receiving their second CI processor and periodically thereafter. The experiment is conducted in a reverberant, single-wall, IAC room with an array of seven or thirteen loudspeakers each positioned 5 feet from the subject and placed at equal intervals on a 180-degree arc extending from opposite the subject's left ear to opposite the subject's right ear. Broadband noise bursts were presented in a 1-interval, 7-alternative, forced-choice task, without feedback. Constant- and roved-level conditions were measured.

Data collected so far show an improvement in bilateral sound-localization performance with bilateral experience. Preliminary analysis indicates that bilateral benefit, as defined by the difference between monolateral and bilateral localization performance, increases with increasing bilateral stimulation in daily life. Also, there appear to be changes in sound-localization strategies used by the subjects.

It is known that ITD is a primary cue for sound localization for normal-hearing listeners. Measurements of ITD sensitivity of our bilateral CI subjects are underway. As the data become available, analysis of the correlation between each subject's sensitivity to ITD and sound localization performance will be made. [Support provided by the NIH-

#### **477 Effect of Interaural Electrode Pairing on Binaural Sensitivity in Bilateral Cochlear Implant Users**

Ruth Litovsky<sup>1</sup>, Smita Agrawal<sup>1</sup>, Gary Jones<sup>1</sup>, Belinda Henry<sup>1</sup>, Richard Van Hoesel<sup>2</sup>

<sup>1</sup>Univ. Wisconsin Madison, <sup>2</sup>Bionic Ear Institute, Melbourne  
Binaural sensitivity was studied in 8 adults with bilateral cochlear implants (BICI-N24). Effect of electrode pairing across the two cochleas was investigated by selecting pairs based on pitch magnitude estimation. Single electrodes positioned in the basal, medial or apical portions of each cochlea were each systematically paired with the complimentary electrodes in the opposite ear (up to 9 possible combinations). Stimuli were electrically pulsed signals, 100 pps, 300 ms duration. Sensitivity to interaural time and level (ITD and ILD) differences was measured using a 2-interval discrimination paradigm; lateralization of the same stimuli was measured using an identification task. Results suggest that (1) both sensitivity and identification are highly variable across subjects; (2) ITD thresholds range from 50-2,000  $\mu$ s; (3) ILD thresholds range from and 1-10 current levels, but the majority of subjects show sensitivity to differences of  $\pm 1$ ; (4) several subjects are unable to use ITD cues, but are good at using ILDs; (5) when ITD sensitivity is present, electrode pairs that are closely matched by pitch/place produce the best performance. (6) Effects of pitch/place on ILD sensitivity are also at times present but are less pronounced. In some cases, numerous hours of training were required before ITD and/or ILD measurements were possible, due to difficulties with perceived fusion and/or lateralization of the sound images. In summary, these findings suggest that electrode pairing with approximate pitch/place matching may be necessary for enhanced performance in BICIs, and that when a relatively large group of bilateral patients is surveyed, sensitivity is quite variable. In addition, patients with the best ITD sensitivity had adult-onset deafness, while those with poorer performance had congenital or childhood-onset deafness. It may, therefore, be possible in some cases to predict performance from the patient's clinical history.

#### **478 Interaural Time Differences in Temporal Fine Structure, Onset, and Offset in Bilateral Electrical Hearing**

Bernhard Laback<sup>1</sup>, Piotr Majdak<sup>1</sup>, Wolf-Dieter Baumgartner<sup>2</sup>

<sup>1</sup>Acoustics Research Institute, Austrian Academy of Sciences, <sup>2</sup>ENT Department, Vienna University Hospital  
Interaural time differences (ITDs) are important for speech reception in noise and localization of sound sources. The normal auditory system encodes ITD information both in the phase and in the amplitude envelope. Bilateral cochlear implant (CI) listeners currently use stimulation strategies which transmit ITD via the envelope, but not through the carrier (so-called fine structure) due to the

constant phase in the electrical pulse train. To determine the benefit to be expected from transmitting fine structure ITD in CI systems, the effects of different ITD types have to be separated.

The relative contributions of fine structure, onset, and offset ITD to lateralization discrimination were studied for unmodulated pulse trains. Bilateral CI listeners and normal hearing (NH) subjects listening to acoustic simulations of CI stimulation were tested. Experiment I presented ITD in the fine structure, the onset and/or offset, or the entire signal. The CI listeners showed high sensitivity to ITD in the fine structure at low pulse rates and decreasing relative weight of fine structure ITD with increasing pulse rate, as opposed to increasing relative weight of onset ITD. Experiment II verified that lateralization performance in experiment I was indeed mediated via binaural processing and not influenced by monaural cues. Experiment III measured the effect of pulse number on the relative weighting of fine structure and onset/offset ITD at a rate of 100 pulses per second. For longer stimuli (containing more than 8 to 16 pulses, depending on the subject) the just noticeable differences were determined almost entirely by fine structure ITD. Overall, the results indicate that bilateral CI listeners are most sensitive to ITD in the fine structure at lower pulse rates. The results of the NH subjects showed close agreement with those of the CI listeners, suggesting that CI performance can be predicted from experiments with NH listeners.

#### **479 Binaural Loudness Summation for 5- and 200-Ms Tones in Normal and Impaired Hearing**

Shani Whilby<sup>1</sup>, Mary Florentine<sup>1,2</sup>, Eva Wagner<sup>1,2</sup>

<sup>1</sup>Department of Speech-Language Pathology & Audiology, Northeastern University, <sup>2</sup>Institute for Hearing, Speech & Language, Northeastern University

Because most people with hearing losses listen with both ears, understanding the influence of hearing losses on binaural loudness is important for rehabilitation with hearing aids. This study measured binaural loudness summation for 5- and 200-ms tones as a function of level in listeners with normal and impaired hearing. The stimuli were 1-kHz tones presented at levels ranging from 10 to 90 dB sensation level. Sixteen listeners (eight normal and eight with losses primarily cochlear in origin) made loudness matches between equal-duration monaural and binaural (diotic) tones using an adaptive 2AFC procedure. Binaural loudness summation was taken as the difference in the levels of the monaural and binaural tones at which they were judged equal in loudness. The present results corroborate existing data for 200-ms tones and provide new data for 5-ms tones. Our results show that, on average, the amount of binaural loudness summation is about the same for 5- and 200-ms tones. The group data for normal and impaired listeners are in reasonable agreement with data in the literature. For both normal and impaired listeners, the data indicate that the loudness of a tone—whether 5 or 200 ms—is greater if it is heard binaurally than if it is heard monaurally. The magnitude of this increase changes as a function of level. For normal

listeners, summation is about 4 dB at 20 dB SPL, increases to about 10 dB at 60 dB SPL, and decreases to about 5-6 dB at 100 dB SPL. For impaired listeners with moderate losses, the average summation is about 3 dB at 65 dB SPL, which increases to about 6 dB at 90 dB SPL, and decreases to about 5 dB at 100 dB SPL. However, group data do not accurately represent the behavior of all impaired listeners. Implications for fitting binaural hearing aids are discussed. [Work supported by NIH/NIDCD Grants No. R01DC02241 and R01DC02241-07S1.]

#### **480 Effects of Modulation Waveform and Age on Detection of Frequency Modulation**

**Ning-ji He<sup>1</sup>, Judy R. Dubno<sup>1</sup>, John H. Mills<sup>1</sup>**

<sup>1</sup>*Medical University of South Carolina*

Detection of frequency modulation (FM) with low modulation rates has been used as an index of frequency discrimination. Using a 1000-Hz carrier frequency, Sek and Moore (2000) observed that FM detection improved for quasi-trapezoidal frequency modulation with increases in steady-state time (Tss) from 0 ms (sinusoidal frequency modulation) to 160 ms. However, using a 6000-Hz carrier frequency, the effect of Tss was minimum, suggesting that FM detection is partly mediated by a temporal mechanism, such as phase-locking of the auditory nerve. A similar frequency-dependent trend was observed in frequency discrimination (He, Dubno, and Mills, 1998), where age-related declines were larger at low frequencies and decreased as frequency increased. Here, detection of frequency modulation was measured for younger and older adults as a function of Tss (0 and 80 ms). The carrier frequencies were 500 and 4000 Hz and the modulation frequency was 5 Hz. Each stimulus was 600 ms in duration and was presented at 75 dB SPL. FM detection was measured using two psychophysical methods: constant stimuli and three-interval-forced choice. In general, the constant stimuli method resulted in higher FM thresholds than the forced choice method. The effect of Tss varied with age, carrier frequency, and psychophysical method. For all conditions, age-related declines in FM detection were larger at 500 Hz than at 4000 Hz. Thus, these results, showing age-related declines in FM detection, are consistent with previously observed age-related declines in frequency discrimination. [Supported by NIH/NIDCD]

#### **481 Temporal and Spectral Resolution of Hearing in Patients with Precipitous Hearing Loss: Gap Release of Masking (GRM) and the Role of Cognitive Function**

**Martin Vestergaard<sup>1</sup>**

<sup>1</sup>*Research Centre Eriksholm*

Non-speech auditory abilities can be used to measure auditory performance in hearing-impaired listeners. The use of non-speech measures is motivated by the notion that hearing-aid performance can be narrowed down to psychoacoustic abilities such as frequency selectivity and temporal acuity. The idea is to explain the relationships between psychoacoustic properties of hearing and

audiological measures like speech recognition scores. Since speech recognition involves discriminating between subtleties in the spectral and temporal domains, temporal and spectral resolution of hearing may explain some of the variance in the ability of listeners to recognize speech.

The purpose of the experiment was to measure temporal and spectral resolution of hearing in new hearing-aid users over a period of time post-fitting and to demonstrate the extent to which performance changes over time. For one-octave wide maskers with and without spectral and temporal gaps, masking was measured repeatedly over 3 months post-fitting. GRM was characterized as the release from masking under the gap conditions. The cognitive skills of the participants were assessed with two tests for measuring working memory capacity and lexical vigilance.

The results showed an increase in temporal resolution of hearing over time. While masking by one-octave wide maskers without gaps was constant over time, GRM increased over time for maskers involving a temporal gap. Moreover, at low frequency where the subjects had normal hearing-threshold levels, they performed as hearing-impaired for the spectral-gap condition. For the temporal-gap condition, they performed as normally hearing at both low and high frequency. The results suggest that patients with precipitous hearing loss do not maintain normal spectral resolution through the low-frequency region, in which the hearing threshold is otherwise normal. Surprisingly, the results also showed moderate though highly significant correlation between lexical vigilance and GRM.

#### **482 Induced Loudness Reduction in Hearing-Impaired Listeners**

**Eva Wagner<sup>1,2</sup>, Bertram Scharf<sup>1,3</sup>, Mary Florentine<sup>1,2</sup>**

<sup>1</sup>*Institute of Hearing, Speech and Language,*

<sup>2</sup>*Communication Res. Lab., SPLA Dept. (106A FR),*

*Northeastern University, Boston, <sup>3</sup>Dept. of Psychology (125 NI), Northeastern University, Boston*

The present study extends the measurement of induced loudness reduction (ILR) to listeners with losses of primarily cochlear origin. Under ILR, the loudness of a weaker tone declines when preceded by a stronger tone, a phenomenon also known as loudness recalibration. Many papers have shown that in normal hearing, the average amount of ILR under optimal stimulus conditions is approximately 10 dB. While varying noticeably among listeners, with standard deviations of the order of 5 to 7 dB, ILR is stable within listeners, as evident in high correlations between the individual amounts of ILR measured under various stimulus conditions. The present experiment tested seven listeners with unilateral or asymmetric hearing losses, which varied at the tested frequencies from 36 to 58 dB HL (thresholds: 44 to 66 dB SPL) in the poorer ear and from -1 to 38 dB HL (thresholds: 7 to 46 dB SPL) in the better ear. A 2AFC adaptive procedure was used to obtain loudness matches between test tones at 70 dB SPL — with and without a preceding inducer at 80 dB SPL — and a comparison tone at a distant frequency. The inducer and test tones were always at the same frequency, chosen on the basis of

each listener's audiogram. The results show that the loudness of the test tone was reduced by the stronger inducer an average of 11 dB (ranging from 5 to 24 dB) in the less impaired (including three normal) ears and an average of 9 dB in the more impaired ear (ranging from 4 to 14 dB); the average difference of 2 dB between the better and poorer ears is not statistically significant. There was no difference, even though measurements in the poorer ears were made at low sensation levels, where ILR has been shown to be very small in normal ears. This finding suggests that ILR depends more on SPL (or loudness level) than on sensation level. Altogether, it appears that ILR is within normal range in listeners with hearing losses of primarily cochlear origin.

(Supported by NIH/NIDCD Grant No. R01 DC 02241).

### **483** Discrimination of Temporal Fine Structure by Listeners with Sensorineural Hearing Loss

Amanda Lauer<sup>1</sup>, Michelle Molis<sup>2</sup>, Marjorie Leek<sup>2</sup>

<sup>1</sup>University of Maryland, <sup>2</sup>Walter Reed Army Medical Center

The effects of cochlear damage on perception of temporal fine structure are largely unknown. In this study, the ability of normal-hearing (NH) listeners and listeners with mild to moderate sensorineural hearing loss (HI) to discriminate harmonic complexes with similar envelope shapes but different temporal fine structure was measured. Complexes were constructed of equal-amplitude harmonic components with fundamental frequencies (F0s) ranging from 50 to 800 Hz. Component starting phases were selected according to either the positive or negative versions of the Schroeder phase algorithm (Schroeder, 1970), resulting in either increasing or decreasing phases as harmonic frequency increases within a complex. Listeners were asked to discriminate between the positive and negative Schroeder-phase complexes for each F0. Within these pairs of complexes, the temporal fine structure of one is the reverse of the other, but the long-term amplitude spectra and the temporal envelopes are the same. Stimulus amplitudes were either fixed at 80 dB SPL or were randomly roved on each presentation over a 10-dB range centered on 80 dB. In addition, NH listeners listened at about 20 dB sensation level (SL). At presentation levels of 80 dB, NH listeners could discriminate the two waveforms nearly perfectly when the F0s were less than 200-400 Hz, but fell to chance performance for higher F0s. Performance of HI listeners at 80 dB SPL was variable across subjects and almost always started to decline for lower F0s than was observed for NH listeners; however, chance performance was reached at similar F0s. In contrast, when NH subjects listened at about 20 dB SL, their discrimination was poorer than HI listeners at all F0s. This suggests that, even though these stimuli were above thresholds for all listeners, the lower sensation levels of the HI listeners accounted for at least part of their poorer performance. Roving presentation levels had little effect on performance by NH listeners, but reduced performance by HI listeners by about 10 to 20 percentage points. The differential

impact of roving level for NH and HI listeners suggests a greater ambiguity in the perception of HI listeners, as well as a weaker perception of timbre differences. [Supported by R01 DC00626 to MRL]

### **484** Temporal Integration: A New Model for the Effects of Hearing Loss

Peter Heil<sup>1</sup>, Heinrich Neubauer<sup>1</sup>

<sup>1</sup>Leibniz Institute for Neurobiology Magdeburg

For every species examined, the SPL needed to detect a sound decreases as sound duration increases, a trading relationship referred to as a temporal integration function. It is often assumed that the parameter ultimately integrated over time is sound intensity, and that the integrator is located centrally. We have shown that thresholds are much better specified as the temporal integral of the sound's amplitude envelope than of its intensity, and we have provided strong evidence that the integrator resides in the auditory pathway's first synapse (Heil & Neubauer, *J Neurosci* 21:7404-7415, 2001 and *Proc Natl Acad Sci USA* 100:6151-6156, 2003). We proposed a statistical integrator that reaches threshold by summation of chance (possibly exocytotic) events. This physiologically plausible mechanism agrees well with the observed slope of the temporal integration function.

In listeners with sensori-neural hearing losses, that slope seems reduced, but it is not fully understood why. Here we propose that in such listeners there may be an elevation in the baseline above which the sound's amplitude can be effective in driving the system, in addition to a reduction in sensitivity. We test this simple model on thresholds to tones of different temporal envelopes and durations obtained from cats before and after hearing loss (Solecki & Gerken, *JASA* 88:779-785, 1990).

We document that our model constitutes a successful alternative to the model currently favoured to account for altered temporal integration in listeners with sensori-neural hearing losses, viz. reduced peripheral compression (Moore & Oxenham, *Psychol Review* 105:108-124, 1998). Our model does not seem to be at variance with physiological observations and also accounts for a number of phenomena observed in such listeners with suprathreshold stimuli (Neubauer & Heil, *JARO* 5:in press).

Supported by grants of the Deutsche Forschungsgemeinschaft to P. Heil

### **485** Factors Affecting Sample Discrimination for Frequency in Hearing-Impaired and Normal-Hearing Listeners

Joshua Alexander<sup>1</sup>, Robert Lutfi<sup>1</sup>

<sup>1</sup>University of Wisconsin- Madison

Less-than-ideal performance when discriminating complex tone patterns is often attributed either to inefficient weighting strategies or to internal noise. Sensitivity to frequency differences can be several times worse for hearing-impaired (HI) listeners than for normal-hearing (NH) listeners, which has implications for how internal noise and ideal weights are conceptualized. We introduce

a modified version of Berg's efficiency analysis [Berg, J. Acoust. Soc. Am. 88, 149-158 (1990)] that attributes less-than-ideal performance to three factors: sensory noise (limits in sensitivity), central noise (inconsistency in the decision-making process), and nonoptimal decision weights. NH and HI listeners (13 in each group) identified on 2IFC trials which of two multitone complexes were sampled from a distribution higher in mean frequency. Each multitone complex consisted of six simultaneous tones presented at 82dB SPL with center frequencies spaced five ERBs apart between 257 and 6930Hz. For each center frequency, sensory noise was estimated from obtained difference limens and decision weights were estimated from multiple regression of the listeners' trial-by-trial responses and the frequency difference of each tone across the two intervals. Generally, listeners' decision weights were not appropriate for their sensitivities. Results indicate that, while each group was equally influenced by central noise, HI listeners weighted information less efficiently than NH listeners even after accounting for differences in sensitivity. [Supported by NOHR and NIDCD.]

#### **486 Epidermal Hyperplasia on the Tympanic Membrane and Deep External Canal: I. Histopathologic Changes**

**Leslie Michaels<sup>1</sup>, Ricardo Persaud<sup>1</sup>, Jianning Liang<sup>1</sup>, Sava Soucek<sup>2</sup>, Anthony Wright<sup>1</sup>**

<sup>1</sup>University College London, Royal National Throat Nose and Ear Hospital, <sup>2</sup>St. Mary's Hospital, London

A study of stained step sections of temporal bones was carried out to determine the histological features of epidermal hyperplasia on the tympanic membrane and deep external canal. From the fetal period through the early years of childhood the epidermis in these regions is composed of at least 10 layers of pale-staining, mainly spherical, cells. The normal mature epidermis is thin and composed of five or fewer layers of dark-staining cells with spindle shaped nuclei.

In some mature ears a marked change in the appearance of the epidermis to one resembling that of the developing fetus and young child is seen. This fetal type epidermis (FTE) replaces varying lengths of epidermis on tympanic membrane and/or deep canal and displays offshoots growing down into subepidermal tissue, which sometimes penetrate collagen layer of tympanic membrane to enter middle ear. Keratosis is frequent on the surface and may also be seen in the invading FTE where it produces small keratin cysts. Severe chronic otitis media (inflammatory exudate, glandular metaplasia and/or tympanosclerosis) is present in all mature middle ears with FTE. This type of hyperplasia may be seen in several structurally distinct conditions such as retraction pocket, cholesteatoma of the deep external canal and keratosis obturans. FTE invading into the middle ear, in some cases is indistinguishable from acquired cholesteatoma.

Severe local inflammation can thus alter the mature epidermis to become the more vigorous FTE. This enhances the concept that auditory epithelial migration is

the persistence of fetal growth, previously based only on the finding that it follows the pathways of the latter.

#### **487 Epidermal Hyperplasia on the Tympanic Membrane and Deep External Canal: II. Clinical Types and Pathologic Correlates**

**Ricardo Persaud<sup>1</sup>, Leslie Michaels<sup>1</sup>, Jianning Liang<sup>1</sup>, Sava Soucek<sup>2</sup>, Anthony Wright<sup>1</sup>**

<sup>1</sup>University College London, Royal National Throat Nose and Ear Hospital, <sup>2</sup>St. Mary's Hospital, London

We describe the clinical forms manifested by epidermal hyperplasia on the tympanic membrane and deep external canal and suggest pathologic correlates for each entity on the basis of our temporal bone study (see I).

**Retraction pocket:** This is an invagination of part of the tympanic membrane into the middle ear as a result of chronic otitis media. Middle ear cholesteatoma is a known complication. Replacement of mature epidermis by fetal type epidermis (FTE) is likely to be present and ingrowths of FTE into the middle ear may lead to cholesteatoma.

**Keratosis and keratosis obturans of tympanic membrane and deep external canal:** In these conditions migration has been shown to be defective or absent and this leads to the accumulation of keratinous material. It is conceivable that a latent chronic otitis media is associated with FTE replacement of the affected mature epidermis with subsequent production of the excessive keratin.

**Cholesteatoma of deep external canal:** Clinically, this condition is characterised by ulceration and the build-up of epidermis in a localised area of the bony canal with underlying osteonecrosis. Downgrowth of replacement FTE, probably triggered by inflammation and/or trauma, is likely to be the early pathologic change associated with this disease.

In each of these clinical conditions, it is our conjecture that FTE hyperplasia is the cause of the lesion or its complication. Therefore, prompt and adequate treatment of otitis media could reduce the incidence of these entities by preventing the development of FTE hyperplasia.

#### **488 Invasion of Human Keratinocytes by Otopathogenic *Pseudomonas Aeruginosa***

**Robert Nason<sup>1</sup>, Jae Jung<sup>1</sup>, Eric Wang<sup>1</sup>, Richard Chole<sup>1</sup>**

<sup>1</sup>Washington University School of Medicine

Aural cholesteatomas are epithelial inclusions which commonly occur medial to the tympanic membrane as a result of otitis media. They consist primarily of a matrix of hyperproliferative keratinocytes and are chronic in nature. Furthermore, most aural cholesteatomas become superinfected by pathogenic bacteria, the most prevalent being *Pseudomonas aeruginosa*. Infection of cholesteatoma exacerbates its clinical aggressiveness and like the disease itself, the infection seen in cholesteatoma is characterized by chronicity. Bacterial adhesion and invasion of keratinocytes are important in the initiation and progression of infection and may provide a mechanism for the chronicity of this infection.

In our study, we used 12 clinical isolates of otopathogenic *Pseudomonas aeruginosa* obtained from patients with

cholesteatoma. *Pseudomonas aeruginosa* invasion was determined by its propensity to invade human keratinocytes *in vitro*.

PAO1, a well defined laboratory strain, was used as a control for all experiments. Adhesion assays show that the majority of our clinical isolates (10 of 12) have enhanced adherence to keratinocytes while only one strain was less adherent ( $p < 0.05$ ). For our invasion studies, 9 strains were appropriate for study. Results showed that all of our clinical isolates were more invasive than PA001, a non-invasive, non-cytotoxic strain, and 3 clinical isolates were more invasive than PAO1. These results demonstrate the first report of *Pseudomonas aeruginosa* invasion of keratinocytes. We hypothesize that these mechanisms may be involved in the persistence of infection seen in cholesteatoma and chronic otitis externa. Future studies will further examine the role of *Pseudomonas aeruginosa* in the pathogenesis of keratinocyte infections and cholesteatoma.

#### **489** Expression of Placenta Growth Factor(PLGF) in Cholesteatoma

Jae-Jun Song<sup>1</sup>, Sung-Won Chae<sup>1</sup>, Jae-Gu Cho<sup>1</sup>, Soon-Jae Hwang<sup>1</sup>

<sup>1</sup>Korea University College of Medicine

**Background and Objectives :** Middle ear cholesteatoma is characterized by the presence of a keratinizing squamous epithelium with hyperproliferative features. Such growth can only be supported by abundant blood vessels. Angiogenesis is particularly important in many normal and pathologic processes, including wound healing and inflammation. Because proliferating tissues require an enhanced blood supply, angiogenesis appears to be a prerequisite for the expansion of cholesteatoma. This study aimed to analyze the presence of the angiogenic growth factor in the human cholesteatoma, especially placenta growth factor (PLGF). **Materials and Methods :** Tissue samples from the human cholesteatoma and normal auditory meatal skin were recovered from patients during operation. PLGF was localized by immunohistochemical staining and mRNA expression was determined by reverse transcriptase-polymerase chain reaction (RT-PCR). **Results :** By immunohistochemical study, PLGF was detected in basal and parabasal layer of cholesteatoma, but not found in normal auditory meatal skin. By RT-PCR, PLGF mRNA was detected in the epithelium of cholesteatoma. **Conclusions :** The expression and localization of PLGF within the cholesteatoma were defined. We thought that PLGF is one of the angiogenic growth factor found in the cholesteatoma, and participates in the neoangiogenesis of cholesteatoma .

**KEY WORDS :** PLGF, Cholesteatoma, Angiogenesis, VEGF

#### **490** Role of *Pseudomonas Aeruginosa* Lipopolysaccharide on Osteoclastogenesis and Toll Like Receptor Activation

Lei Zhuang<sup>1</sup>, Jae Jung<sup>1</sup>, Richard A. Chole<sup>1</sup>

<sup>1</sup>Washington University School of Medicine

In aural cholesteatoma, the accumulation of keratin debris and persistent infection causes an inflammatory response in the middle ear. The expanding mass of keratin and inflammatory cells progressively erode surrounding bone leading to hearing loss and vestibular dysfunction. It is now clear that bone loss accompanying these chronic infections is the result of enhanced osteoclast development and activity. While many bacterial products may be involved, lipopolysaccharide (LPS) is believed to be a major mediator of inflammation and osteolysis. However, the exact mechanisms by which LPS activates this resorptive process is unknown. Specifically, there is little information as to whether LPS enhances osteoclastogenesis by directly targeting osteoclast precursors, or indirectly, via intermediary cells such as osteoblasts.

In this study, we investigated the role of *Pseudomonas aeruginosa* (PA) LPS in osteoclastogenesis *in vivo* and *in vitro*. *In vivo* model was established by implanting PA LPS directly onto the calvaria of mice. Osteoclasts were generated *in vitro* using two different methods: isolated bone marrow monocyte (BMM) and BMM with osteoblast co-cultures. Using RT-PCR on both *in vivo* and *in vitro* samples, we examined the expression of cytokines, markers of osteoclastogenesis and toll like receptor (TLR) activation by PA LPS.

Our results show that although PA LPS induces osteoclast formation *in vivo*, a suppressive effect of LPS was observed *in vitro* with isolated BMM cultures. However, PA LPS induced osteoclastogenesis in the co-culture system suggesting that PA LPS acts indirectly via interaction with osteoblasts or stromal cells rather than directly on the osteoclast precursors themselves. This hypothesis is further supported by RT-PCR results which show that PA LPS does not induce RANKL expression in isolated BMM, but it does in co-cultures. Additionally, RT-PCR results indicate that multiple TLRs, including TLR2, TLR4 and TLR9, are expressed in response to PA LPS. Future studies will investigate the role of each of these putative LPS receptors in osteoclastogenesis.

#### **491** Characterization of the Fiber Structures of the Tympanic Membrane Pars Tensa

Magnus von Unge<sup>1</sup>, Johan Knutsson<sup>1</sup>, Dan Bagger-Sjöbäck<sup>1</sup>

<sup>1</sup>Karolinska Institute

**Background:** The genesis of the most severe chronic disease of the middle ear – cholesteatoma – is still under debate. There is no doubt that retraction of the tympanic membrane is one important feature in this process. It is still unclear how and why these retractions develop. In our previous studies we have shown that inflammation of the middle ear may cause a loss of stiffness in the tympanic membrane. The morphological investigations did not show



reduced numbers of fibers in these acute or semi-acute situations, and no structural deterioration of fibers – yet stiffness was lost. Edema was present in the lamina propria, but it is not clear whether the spatial separation of the fibers, caused by edema, is the full explanation of the stiffness loss.

In a long-term, negative middle ear pressures situation it is likely that such a weakening of the tympanic membrane may lead to retractions, that later may expand into cholesteatoma formations. Our aim is to study the fibers of the tympanic membrane, normal and in pathological situations. In a first step the fiber types in the lamina propria will be identified. It is presumed that these fibers are collagens. We used immuno-histochemical methods to detect the presence of the most common collagens in the pars tensa in Sprague-Dawley rats. The presentation reveals fresh, preliminary data.

Results: Collagen I was expressed in the basilar membranes of the pars tensa as well as within the lamina propria, but was not expressed in the annulus fibrosus (annular ring). Collagen II was also expressed in the basilar membranes of the pars tensa and within the lamina propria. Furthermore it was significantly expressed within the annulus fibrosus. Collagen III and IV results are under way.

Discussion: The first results in our effort to investigate the character of the important stiffness bearing structures of the lamina propria pars tensa are presented. This is the one basic step in a stairway of investigations aiming to enlighten the mechanisms behind the patophysiology of cholesteatoma – perhaps the most important riddle of middle ear pathology.

#### **492 Region-Of-Interest Micro-CT of the Middle Ear: A Practical Approach**

**Stefan L.R. Gea<sup>1</sup>**, Willem F. Decraemer<sup>1</sup>, Joris J.J. Dirckx<sup>1</sup>  
<sup>1</sup>*University Of Antwerp*

Computed micro-tomography ( $\mu$ CT) is a powerful non-destructive imaging technique. The CT scanner records first a large number of x-ray projection images while the object is rotated over 180° with small steps (e.g. 0.9°). These images serve then as input for a back-projection algorithm that calculates a stack of virtual slices through the object. To obtain a correct slice reconstruction the object must remain entirely within the x-ray beam while it is rotated. When this requirement is not fulfilled the sectional images will be corrupted due to incompleteness of the input data.

Region-of-Interest (ROI) scanning is a method where the scanning is restricted to a small object region -deliberately or forced by the shape or size of the object- so that parts of the object run out of the x-ray beam during the rotary scan. The input data for the back-projection algorithm is therefore incomplete and errors will be generated in the grey level values (which are measures for the local x-ray absorption coefficient) in the section images. In this study we will show that, if we are not interested in the grey level, but only in the shape of imaged structures we can still use the normal back-projection algorithm and exploit the ROI

to our favour to increase the magnification and hence the resolution of the images.

Several phantom objects with varying material parameters were scanned at different magnifications so that smaller and smaller ROI's were obtained. We found that while the resolution improves drastically with ROI scanning compared to global scanning, no shape artefacts are observed. As a cost the noise in the section images increased, but signal to noise ratio remained sufficiently high. Next we scanned rat temporal bones. Small details such as the lenticular process or the joint between malleus and incus became clearly visible in an ROI scan -even when large parts of the temporal bone exceeded the FOV-, while they could not be discerned on a global scan of the temporal bone.

#### **493 Nitinol Shape-Memory Malleus-To-Footplate Prosthesis**

**Glenn Knox<sup>1</sup>**

<sup>1</sup>*University of Florida*

The aim of this study is to determine the efficacy of a shape-memory alloy, Nitinol, as a component of an improved malleus-to-footplate prosthesis. After development of the Nitinol stapedectomy prosthesis (“Smart Prosthesis”) as described by our group previously, the plan for developing an analogous malleus-to-footplate prosthesis was initiated. Various diameters of Nitinol wire and temperature transition variants were analyzed with regard to ease of deformation, response to heating, and strength. The size and geometry of the closed hook was determined by measurement of 50 malleus cadaver bones. Several heat sources for activating the shape memory were evaluated, including electrocautery, lasers, and warm water. Trial surgeries were then performed on human temporal bones in the laboratory. The closure characteristics of the Nitinol loop were studied. Preliminary human subject trials were then instituted. In all cases, a low heat condition was ample to activate the shape memory characteristics of the hook and return it to a closed position after it had been opened. Laser power was generally set well below the power needed for removing bone. The Nitinol loop closed snugly around the malleus with application to the top of the hook with a low temperature laser setting. Almost any heat source was effective. Preliminary results in human subjects showed excellent air-bone closure. The Nitinol loop holds uniform contact around the malleus. The Nitinol malleus-to-footplate prosthesis greatly simplifies ossicular reconstruction. Because of the nature of the Nitinol wire, it can never over-crimp. As shown previously by our group, the Nitinol stapes prosthesis has been successfully implemented for otosclerosis surgery. The analogous nitinol malleus-to-footplate prosthesis is the next logical step. All these characteristics make the prosthesis advantageous for ossicular reconstruction.

#### **494 Transfer Function of an Implantable Middle Ear Hearing Device Calculated from Psychoacoustic Measurements**

Bernd Waldmann<sup>1</sup>

<sup>1</sup>Otologics LLC

The middle ear transfer function for the Otologics MET Ossicular Stimulator is a measure of transducer coupling efficiency and variability. It was calculated as acoustic threshold (in dB HL) minus implant threshold (in units of electrical drive level into the transducer). It can be used to convert audiological requirements, e.g. minimum required unaided hearing loss or desired functional gain, to electrical specifications and vice versa. In a clinical trial the transfer function was ca. 10 dB higher for frequencies around 1 kHz than for lower and higher frequencies. In this trial, 50% of patients had a transfer function in a  $\pm 5$  dB range around the median; in a separate study with a larger number of participating surgeons, the range was initially higher. Intraoperative measurements that provide guidance to the surgeon regarding optimal positioning of the transducer can improve results and reduce variability of coupling.

The transfer function calculated from psychoacoustic measurements in patients correlates with a corresponding transfer function in cadaver studies, derived from stapes velocity measurements under implant and acoustical stimulation.

#### **495 Force Loading and Changes in Transfer Function of an Implantable Hearing Aid Transducer (METTM, Otologics ) Due to Pressure Differences Across the Tympanic Membrane.**

Hannes Maier<sup>1</sup>, Bernd Waldmann<sup>2</sup>, Rudolf Leuwer<sup>1</sup>

<sup>1</sup>HNO Universitaetsklinik Hamburg-Eppendorf, Germany,

<sup>2</sup>Otologics LLC, USA

In implantable hearing aids sound is directly coupled into the middle ear ossicles. In the Otologics Middle Ear Transducer™ (MET), the transducer body is anchored in the temporal bone with a sound transmitting tip fitting into a drilled hole in the incus body. Force loading of this connection is critical for proper sound transmission. After implantation this loading is also subject to external forces e.g. movements of the ossicular chain due to pressure differences across the tympanic membrane. Theoretically, this additional loading could affect sound transmission characteristics or even damage the transducer.

To investigate the effect on sound transmission, 6 fresh (<36h) human temporal bones were implanted with transducers. Proper coupling of the transducer was achieved by driving the transducer with a multitone signal (0.25Vs, 0.25 – 6 kHz, 4/oct) and measuring the vibration response near the coupling point with a Laser Doppler Velocimeter. Measurements were performed while applying pressure (0,  $\pm 5$ ,  $\pm 10$ ,  $\pm 20$ ,  $\pm 40$ ,  $\pm 80$  hPa) to the outer ear canal. The same signal as before was used to measure the forward transfer function from the transducer to the ear drum and the reverse transfer function from the

transducer to the ear canal using an ER-10c probe in the outer ear canal.

Velocity responses to sound stimulation, i.e. passive hearing, was most affected by pressure at low frequencies (< 0.6 kHz). Responses were maximal at 0 hPa while at the highest and lowest pressures velocity amplitudes were decreased by approx. 20dB.

Velocity and microphone responses to transducer stimulation had a less pronounced dependency (<10dB) on ear canal pressure again with a maximum response at 0 hPa.

Most importantly, the application and release of the pressure over the entire range did not lead to permanent changes (before/after) in response behaviour at 0 hPa. This indicates that moderate pressures, as they may occur when the Eustachian tube is blocked, do not permanently affect the implant.

#### **496 Evaluation of Obliterating Materials in the Guinea Pig Dorsal Bullae of Temporal Bone**

Myung-Koo Kang<sup>1</sup>, Byung-Gun Park<sup>1</sup>, Chan Ho Hwang<sup>1</sup>, Woo-Yong Bae<sup>1</sup>

<sup>1</sup>Dept. of Otolaryngology, Dong-A University, Busan, 602-715, Republic of Korea

When using implant materials for obliteration of the dorsal bullae of the temporal bone, several aspects, such as inflammation, absorption and regeneration as well as osteoconduction of these materials, have to be considered. The present study was undertaken to determine and to compare by morphological observations the characteristics of bone wax, fibrofatty tissues or bone graft materials (Lubboc) as obliterating materials in the guinea pig.

The guinea pigs were used to perform obliteration of the dorsal bullae of the temporal bone by the bone wax, fibrofatty tissues or bone graft materials (Lubboc). Twelve weeks after implantation, the animals were sacrificed, and histological sections were prepared. Histological evaluations were performed to determine changes of the dorsal bullae mucosa of the temporal bone and the implanted materials.

Where bone wax was used for obliteration, histological evidences indicated inflammatory reactions within the dorsal bullae mucosa of the temporal bone. Large amount of absorption was observed in case of using the fibrofatty tissue. On the other hand, in case of using bone graft materials (Lubboc), real bonds between new bone and native bone were observed, also mature trabecular bone were observed traversing throughout the entire implant materials. Bone formation as induced by bone graft material (Lubboc) implantation appeared to be a physiological reaction, which was further supported by observation of extensive neovascularization within the graft material.

Based on our current observations, we consider the bone graft material (Lubboc) as a superior implant material to bone wax and fibrofatty tissues.

#### **497 Management of the Patulous Eustachian tube**

**Sören Wenzel**<sup>1</sup>, Hartwig Seedorf<sup>1</sup>, Thomas Kucinski<sup>1</sup>, Hannes Maier<sup>1</sup>, Rudolf Leuwer<sup>1</sup>

<sup>1</sup>Hamburg University Medical School

**Objectives:** Treatment outcomes of patients with patulous eustachian tube (pET) disorder are often poor. The mechanism of the pET includes the atrophy of the medial pterygoid muscle acting as a modulator for the tensor veli palatini muscle as a new decisive aspect. The aim of this study was to develop a conservative therapy being based on this muscular synergy and to examine its long-term outcome. Besides, a safe and definitive surgical method was to be evolved for refractory cases.

**Methods:** In a study of thirty-four concurrent patients with pET symptoms individual pathomorphism and the therapeutical approaches were investigated. Eighteen patients attended a special physical therapy to train and strengthen the medial pterygoid and the tensor veli palatini muscle. Three patients got a surgical obstruction of the tubal environment by an implantation of autologue cartilage chips.

**Results:** Eleven patients showed a complete and long-lasting resolution of their complaints six months after the physical therapy. The distressing symptoms were significantly improved in eleven patients who required no further treatment. The three patients with the surgical obstruction showed a complete reversal of the symptoms.

**Conclusion:** If we look at the rate of success and the negligible invasiveness of the physical therapy, irrespective of the pathogenesis, the training of the medial pterygoid and the tensor veli palatini muscle should be the first therapeutic step. In cases of persistent or recurrent complaints of the pET, obstructing surgical augmentation of the tubal environment with autologue cartilage chips could follow.

#### **498 Effect of Dexamethasone on Nitric Oxide induced Ototoxicity**

**Choong Won Lee**<sup>1</sup>, Andrew Florea<sup>2</sup>, Timothy Jung<sup>1</sup>, Earnest John<sup>1</sup>, Aron Depew<sup>2</sup>, Jared Inman<sup>2</sup>, Rachele Wareham<sup>2</sup>, Kaalan Johnson<sup>2</sup>

<sup>1</sup>Jerry L. Pettis Veteran's Administration Medical Center,

<sup>2</sup>Loma Linda University Medical Center

**Background:** Intratympanic dexamethasone has been shown previously to be effective in the treatment of hearing loss caused by many different factors. In our previous study, it was found that nitric oxide (NO) releasing compound, S-nitroso-N-acetylpenicillamine (SNAP) and peroxy-nitrite releasing compound, 3-morpholiniosydnonimine (SIN-1), caused significant hearing loss when applied to the round window membrane (RWM) in a chinchilla animal model. Additionally, based on our in vitro studies of the effects of NO on isolated outer hair cells (OHCs), we demonstrated that NO is cytotoxic to OHCs.

**Objective:** The purpose of this study was to determine whether dexamethasone can prevent the hearing loss caused by exogenous NO (SNAP and SIN-1).

**Method:** After obtaining initial hearing thresholds using ABR, the NO-donor-compound, SNAP, or the peroxy-nitrite-donor-compound, SIN-1 were placed on the RWM, and baseline ABR hearing thresholds as well as post-application ABR hearing thresholds were obtained at one, two, four and eight hour intervals. In the dexamethasone + SNAP group, dexamethasone was applied one hour prior to SNAP application on the RWM.

**Results:** Three groups were studied: SNAP, SIN-1, and dexamethasone + SNAP treated groups.

SNAP treated animals (n=9) developed a mean hearing loss of  $53.9 \pm 5.8$  dB at 8 hours post-application. SIN-1 treated animals (n=9) developed a mean hearing loss of  $44.6 \pm 4.9$  dB at 8 hours post-application. Dexamethasone + SNAP treated animals developed a mean hearing loss of  $18.3 \pm 1.7$  dB at 8 hours post-application. The difference between the dexamethasone + SNAP treated animals and the SNAP and SIN-1 treated animals began to be significant at 4

hours post-application and continued to remain significant through 8 hours post-application.

**Conclusion:** These findings suggest that pretreatment with dexamethasone can reduce hearing loss induced by exogenous nitric oxide.

#### **499 Frequency Domain Deconvolution of Overlapping Auditory Evoked Responses**

**Ozcan Ozdamar**<sup>1,2</sup>, Jorge Bohorquez<sup>1</sup>, Rafael Delgado<sup>1,3</sup>

<sup>1</sup>University of Miami Department of Biomedical Engineering, <sup>2</sup>University of Miami Department of Otolaryngology, <sup>3</sup>Intelligent Hearing Systems

Recently we introduced the Continuous Loop Algorithm Deconvolution (CLAD) method (Delgado and Ozdamar, J.A.S.A., 2004) to deconvolve overlapping evoked responses obtained at arbitrarily selected non-isosynchronous stimulus sequences. CLAD method is a generalized version of the Maximum Length Sequence (MLS) based deconvolution algorithms that works for most sequence patterns and operates in the time domain. In this study, frequency domain formulation of CLAD is developed and applied for the extraction of transient responses from convolved recording obtained at high stimulation rates. The formulation allows for a faster execution of CLAD by using standard Fourier Transform algorithms and avoiding the inversion of large matrices in the time domain approach. The frequency domain CLAD displays the frequency characteristics of the response extraction and shows the attenuation and amplification of noise in different frequencies, thus, allowing for custom designing of the stimulus sequences for a desired noise elimination effect. This also clarifies the previously unexplained susceptibility of some stimulus sequences to noise. The newly developed methodology is used with the previously developed and new stimulus sequences for the extraction of all types of transient auditory evoked responses (brainstem, middle latency and late latency) acquired at high stimulus rates. The results of this study show the MLS or Legendre methods as special cases of the deconvolution theory and describe the limitation of the deconvolution process.

## **500 A Novel Method for Simultaneous Acquisition of Auditory Steady State and Transient Responses**

**Erdem Yavuz**<sup>1</sup>, Ozcan Ozdamar<sup>1,2</sup>, Rafael Delgado<sup>1,3</sup>, Jorge Bohorquez<sup>1</sup>

<sup>1</sup>University of Miami Department of Biomedical Engineering, <sup>2</sup>University of Miami Department of Otolaryngology, <sup>3</sup>Intelligent Hearing Systems

A novel method is designed for the simultaneous acquisition of Auditory Steady State Response (ASSR) and Auditory Transient Response (ATR) counterparts. The method is based on the recently introduced Continuous Loop Algorithm Deconvolution (CLAD) algorithm (Delgado and Ozdamar, J.A.S.A., 2004). Specially tailored CLAD sequences are generated while ensuring equal spacing between all stimuli except one slightly jittered stimulus. A single non-equally spaced stimulus causes two non-equal Inter Stimulus Intervals (ISI) in CLAD's circular continuum. The non-isochronous stimulus is used to eliminate the singularity problem associated with steady-state stimuli and allow the recovery of the ATR. The selected sequence is used to evoke Quasi Steady-State Response (QSSR) which is similar to ASSR with the difference of two deviant ISIs. Acquired raw recording is used to extract the ATR. The effect of the non-isochronous stimulus is calculated using the ATR and subtracted from the raw recording. Then the jittered ATR component is estimated and corrected in the CLAD response sequence to provide a derived steady state response. The proposed method is evaluated with simulations and real recordings from subjects using click stimuli. The method is capable of reconstructing steady state responses and transient responses from single recording.

## **501 Electrocochleography to High-Frequency Toneburst with Ear Canal Electrode**

Brianne Davis<sup>1</sup>, Dwayne Paschall<sup>1</sup>, Candace Hicks<sup>1</sup>, Steven Zupancic<sup>1</sup>, **Ming Zhang**<sup>2</sup>

<sup>1</sup>Texas Tech Univ Health Sciences Ctr, Dept Speech-Language & Hearing Sciences, <sup>2</sup>\*Texas Tech Univ Health Sciences Ctr, Dept Speech-Language & Hearing Sciences, [ming.zhang@ttuhsc.edu](mailto:ming.zhang@ttuhsc.edu)

The use of ear canal electrodes in electrocochleography (ECochG) has not been fully studied in response to tonebursts, especially to high-frequencies. Recording high frequency cochlear microphonic (CM) is challenging. Using tonebursts of different frequencies may lead to a potential approach to assess the conditions of the cochlea in specific regions. ECochG can assess conditions of both cochlea and auditory nerve, but neither otoacoustic emission (OAE) nor ABR alone can assess both. In addition, the OAE is attenuated by the middle ear during backward transmission (Zhang & Abbas, 1997), while ECochG is not. Moreover, the threshold of compound action potential (CAP) in ECochG is lower than that in ABR. Electrode placement in ECochG varies in configuration. Tympanic Membrane electrodes (TM-trode) can be better in many aspects than invasive TransTympanic electrodes (TT-trode) (Ferraro & Durrant,

2002), while ear canal electrodes (EC-trode) can record usable responses. The advantages of using ear canal electrodes and toneburst stimulation has been described (Zhang and Paschall et al, 2003). These advantages include no risk to and no load on TM (perhaps benefiting higher frequency transmission), low and stable electrode impedance, easy application, no stress on patient, applicable to young ages, applicable to minor TM conditions, simultaneous OAE recordings, etc. Recording with mid-high frequency toneburst has also been discussed. In this study the use of high frequency tonebursts and ear canal electrode was examined. The CM waveform was recordable but not as prominent as that of lower frequencies. The CM amplitude was small. The latency of CAP was short. The presence of CM waveform and absence of CAP to high frequency toneburst may indicate a functioning cochlear basal region but nonfunctioning high frequency auditory nerve fibers. The issues related to ECochG to high-frequency toneburst with ear canal electrode are also discussed.

## **502 Auditory Brainstem Responses (ABRs) in Neonates Exposed to Repeated Courses of Antenatal Corticosteroids**

**Michael Church**<sup>1,2</sup>

<sup>1</sup>Wayne State University SOM, <sup>2</sup>NICHHD MFMU Network

The neonatal ABR, a sensitive measure of brain maturation, can help determine if repeated courses of antenatal corticosteroids (AC) had a beneficial or harmful effect on infant brain and auditory function. Our objective was to determine if repeated AC had any effects on the neonatal ABR. We performed an ancillary study at 6 of the 19 centers that conducted a double-blind, placebo-controlled clinical trial of repeated AC. Consenting women <32 wks gestation, who were at high risk for preterm birth and had received one course of AC, were randomized to receive additional weekly courses of AC (Betamethasone) or placebo. ABR testing was performed on infants prior to discharge. The ABRs were evoked by 45 and 70dB clicks delivered to the right and left ears separately, utilizing standard procedures and recording equipment. The ABR's Wave V latencies were analyzed by the Wei-Lachin procedure which adjusts for the correlation due to twins ( $p < 0.05$  considered significant, 2-tailed test). We enrolled 49 mothers, 11 of whom carried twins, giving 60 infants who were ABR tested. Fifty-one infants had complete sets of ABR data. The repeated AC ( $n=24$ ) and placebo ( $n=27$ ) groups respectively had right ear Wave V latencies (mean $\pm$ SD) of  $7.93 \pm 0.60$  vs  $7.63 \pm 0.65$  msec ( $p=0.08$ ) and left ear Wave V latencies of  $7.73 \pm 0.60$  vs  $7.62 \pm 0.52$  msec ( $p=0.41$ ) – where longer latencies suggest less maturity. A power analysis (80% power), using an infant's highest Wave V latency value from either ear, indicated that a total 260 infants (130/group) would be needed to achieve statistical significance. Results from the 45 dB condition were very similar. The number of additional weekly treatment courses (range = 1-8), gestational ages at birth and at ABR testing did not differ between groups; whereas birth weight, head circumference and length were smaller in the repeated AC group ( $p < 0.05$ ). In conclusion, repeated AC treatments did not significantly affect

neonatal brain development as assessed by the ABR's Wave V latencies, despite significant effects on birth size. (Supported by grant U10 HD27917)

**503 Estimation of Hearing Thresholds in Rats : Comparison of Flat-Noise Carrier Auditory Steady State Response(FNC-ASSR) and Click Auditory Brainstem Response(C-ABR)**

See Youn Kwon<sup>1</sup>, Myung Soon Kim<sup>2</sup>, Sam-Mi Yu<sup>2</sup>, Yang Sun Cho<sup>2</sup>, Sung Hwa Hong<sup>2</sup>, Sang Min Lee<sup>1</sup>, In Young Kim<sup>1</sup>

<sup>1</sup>Department of biomedical engineering, Hanyang University, <sup>2</sup>Department of Otolaryngology-Head and Neck Surgery, Sungkyunkwan University School of Medicine

Auditory brainstem response (ABR) has been used for measuring hearing thresholds in animal research. However, click ABR has some physical restrictions to measure hearing thresholds, such as not-flatness of sound energy in high frequency region and limits of stimulus level. Clinically, with ASSR, it is assumed that hearing thresholds could be estimated in severe to profound hearing loss even if ABR has no responses. We hypothesized, if flat noise(white noise) is used as a carrier frequency, it would stimulate the whole cochlea like click in ABR and flat-noise carrier auditory steady-state response (FNC-ASSR) would represent the whole range of hearing without distortion. In addition, using ASSR, we could measure rather accurate hearing thresholds in animal models with profound hearing loss, which show no response to C-ABR. The objective of this study is to determine usefulness of FNC-ASSR technique for estimating hearing ability in comparison with wide-band click ABR in normal hearing animals. Left ears of 6 SD rats, ranging from post-natal day (PND) 31 to 39, with normal hearing were tested for the hearing thresholds with C-ABR and FNC-ASSR using TDT neurophysiology workstation. C-ABR was evoked by rarefaction click with 100 us pulse width. Stimulus for FNC-ASSR was made using 100% amplitude modulation with flat noise carrier frequency ranging from 0 to 50kHz. To find the best modulation frequency of FNC-ASSR, we varied modulation frequency from 45Hz to 500Hz at 70dB SPL. In comparison of hearing thresholds, there are no significant differences between using C-ABR and FNC-ASSR. We confirmed that FNC-ASSRs showed reliable responses at of the modulation frequency over 75Hz. In rat experiments, FNC-ASSR thresholds were well correlated with C-ABR thresholds and FNC-ASSR might provide an useful tool for hearing threshold estimation in animal research.

Supported by grant of the Korea Health 21 R&D Project, Ministry of Health & Welfare, Republic of Korea. (02-PJ3-PG6-Ev10-0001)

**504 A Computational Approach to Hearing Aid Design: Minimization of Distortion in Impaired Auditory Nerve Fiber Responses in Adverse Acoustic Environments**

Courtney C. Lane<sup>1</sup>, Don H. Johnson<sup>1</sup>

<sup>1</sup>Rice Univ.

To improve hearing aid performance in adverse listening environments, we approach the design of hearing aids in a new way. We compute the distortion induced by hearing impairment by comparing normal and impaired model auditory-nerve-fiber responses. We then simulate various hearing-aid algorithms to determine how effective they are in reducing distortion. In this way, we can determine when and how impairment affects the fiber responses, and within the same framework, we can objectively optimize hearing aid performance under a variety of realistic conditions.

We measure the distortion in the impaired fiber responses using the Chernoff distance, which quantifies how well normal and impaired responses can be discriminated. Our stimuli are sentences in quiet, speech babble, and broadband noise. We use an auditory nerve fiber model (Heinz et al., ARLO, 2001) that simulates responses for both a normal human auditory periphery and a periphery with impaired outer hair cells.

For speech in quiet, impaired fibers with characteristic frequencies (CFs) between formants tend to respond to frequency components far from CF, as reported in other studies (e.g. Miller et al., JASA, 1997). As a consequence, the optimal hearing aid gain for each individual fiber varies dramatically as a function of CF. Compared to the results in quiet, results were qualitatively, but not quantitatively similar for sentences in speech babble and broadband noise, indicating that hearing aid parameters need adjustment as the acoustic background changes.

Overall, we are able to use this computational approach to probe the effects of hearing impairment and listening conditions on auditory nerve fiber responses to speech. This approach allows us to make testable hypotheses about which hearing aid algorithms to use for different listening conditions so that the impairment-induced distortion is reduced to nearly zero.

**505 Wireless Communications in Otoacoustic Emissions and Auditory Evoked Potentials**

Yuri Sokolov<sup>1</sup>, Roger Zhang<sup>1</sup>, George Long<sup>1</sup>

<sup>1</sup>Vivosonic Inc.

Auditory Evoked Potentials (AEP) and Otoacoustic Emissions (OAEs) are conventionally recorded using systems that include AEP electrodes and OAE probe(s), and an electronic interface device connected to a computer via cable. Noises, which are introduced largely by electrical and magnetic fields produced by surrounding equipment, wireless-communication devices such as computers, LANs, PDAs, mobile phones, contaminate physiological responses, and make the tests more difficult and long. Yet, in conventional AEP or OAE systems, long cables, typically 6' (2 m) are necessary to reach the patient, while many places are difficult to reach, such as

an infant incubator, operating room, or a rotating chair or centrifuge. In such cases, cables become not only a source of noise, but make the tests difficult or impossible.

We employed wireless Bluetooth® communication between the computer and the data-collecting interface module. Bluetooth® is a wireless communications protocol that enables computers and other digital devices communicate via broad radio-frequency band. Our experiments show that Bluetooth® does not introduce noise to OAE and AEP itself because it has very low energy, below the background level of electromagnetic field, but is strong enough to communicate within about 30 ft (10 m) even through walls.

This wireless interface module for auditory electrophysiology is a universal platform: It performs ABR, ASSR, DPOAE, and TEOAE tests, and has the potential to add other testing modalities on the same platform. It is operated by a microprocessor, controlled from a remote computer through Bluetooth®, and powered by batteries.

In clinical environment, the module can be placed on the adult's chest, or placed next to a baby, or be held by the baby's mother. Testing can be performed anywhere within the reach of Bluetooth®, including situations where cabled instruments cannot be used at all. Importantly, removing the cable from the system reduces electromagnetic noise pick-up and test time, depending on background noise in the testing area where a shielded room is unavailable. Results of OAE and ABR recording using wireless interface will be discussed.

### **506 Novel Method of Reducing the Effect of Electric and Magnetic Fields on Auditory Evoked Potentials**

**Isaac Kurtz<sup>1</sup>, Yuri Sokolov<sup>1</sup>**

<sup>1</sup>*Vivosonic Inc.*

Electric and magnetic fields in clinical Audiology environment significantly affect the quality of evoked potential measurements. Because of their small magnitude, ASSR and ABR signals are particularly susceptible to interference. The presence of electric and magnetic interference in clinical environments is a growing problem. Due to non-linearities in electronic amplifiers, broadband radio-frequency equipment such as cellular telephones that operate well above the frequency range of evoked potentials can cause significant interference in the bandwidth of clinical interest.

This paper will quantify the relationship between measured field levels in the test environment and noise in evoked potential measurements. Average electric fields in offices in the United States (5 Hz – 2 kHz band) have a typical range of 1-200 V/m and average magnetic fields are typically in the range of 0.1-200 mG. Our experiments have shown that in the presence of moderate levels of mixed electric and magnetic fields of 12 V/m and 5.5 mG, ABR morphology and the reliability of latency measurements is degraded when conventional ABR equipment and clinical protocols are used.

The relationship between the electric field level and measured noise depends on the length of electrode cables and impedance mismatch between the signal electrodes,

while the noise due to magnetic fields depends on the area encompassed by the cable leads. Both electric and magnetic field noise are affected by preamplifier specifications and field-patient geometry. The effect of radio-frequency interference on evoked potential measurements depends on preamplifier linearity. Novel techniques for reducing the effects of electric and magnetic fields on evoked potential measurements will be discussed. These techniques include amplification of signals at the electrode site, in-situ, and passive filtering of high-frequency signals prior to preamplification.

### **507 Complex Pitch Analysis in Non-human Primates and its Implication for Object Processing in Auditory Cortex**

**Xiaoqin Wang<sup>1</sup>**

<sup>1</sup>*Laboratory of Auditory Neurophysiology, Dept. of Biomedical Engineering, Johns Hopkins University*

The pitch of complex sounds is an important component in forming an auditory object. Its perception is one of the most fundamental auditory behaviors, but its underlying neural mechanism in the brain remains elusive. While psychophysics on pitch perception has predominantly been conducted in humans, evidence has shown that many animal species are also capable of perceiving pitch and pitch-related acoustic patterns. Our laboratory has investigated neural correlates of pitch in auditory cortex of marmosets, a non-human primate species with a hearing range similar to that of humans. It has been shown that there is a similarity in the organization of auditory core and belt areas among primate species. Our recent experiments revealed neurons in a restricted area of the low-frequency region of auditory cortex that encoded the pitch embedded in harmonic complex sounds, even when the fundamental frequency component was removed or masked by noise. In contrast, the repetition rate of complex sounds is analyzed at both low- and high-frequency regions of marmoset auditory cortex. Together these results demonstrate that temporal modulation analysis is a general function carried out by the primary auditory cortex (A1) across the tonotopic axis, whereas pitch analysis is a specialized function performed by neurons located in a distinct region of auditory cortex. The significance of the pitch-encoding neurons is that their function represents a transformation from acoustic to perceptual dimension, a crucial step in auditory object recognition. Because A1 receives well-tuned inputs from lemniscal MGB and contains neurons highly selective for acoustic features of sounds, these findings suggest that the synthesis of complex auditory objects take place outside of A1 in auditory belt or parabelt areas where inputs from both A1 and non-lemniscal MGB are combined. Finally, our findings mirror recent human imaging studies that identified pitch-processing areas in human auditory cortex.

## **508 Scene Analysis in the Ascending Auditory System**

Israel Nelken<sup>1</sup>

<sup>1</sup>Hebrew University

When presented with mixtures of sounds, neurons in primary auditory cortex often respond to one member of the mixture, even when another member is much more intense. Furthermore, neurons in auditory cortex show memory to previous stimulation history at multiple time scales. Therefore, I will argue that neurons in auditory cortex respond to specific auditory objects rather than to the physical characteristics of the mixture. These properties arise in several stages along the ascending auditory system, and will be illustrated with data from the inferior colliculus, the auditory thalamus and primary auditory cortex of halothane-anesthetized cats.

## **509 Pitch-Sequence Analysis in Auditory Cortex**

Michael Brosch<sup>1</sup>

<sup>1</sup>Leibniz-Institut fuer Neurobiologie

Behaviorally significant information is contained in the spectro-temporal patterning of the adjacent tones in a sequence. To elucidate neuronal mechanisms in auditory cortex underlying the representation of such patterns we tested how neurons respond to two or more consecutive tones. We observed that depending on the frequency and time separation of the tones the response of neurons to an individual tone can be suppressed or enhanced both by preceding and succeeding tones. These suppressive and enhancing effects generate neuronal sensitivities for various spectro-temporal patterns that match the properties of many environmental sounds.

## **510 Auditory Stream Segregation in Primary Auditory Cortex (A1) of Awake Monkeys**

Yonatan Fishman<sup>1</sup>, Mitchell Steinschneider<sup>1</sup>

<sup>1</sup>Albert Einstein College of Medicine, Bronx, NY 10461

Sounds originating from multiple sound sources often impinge upon the ear simultaneously or in rapid succession (e.g., speakers' voices at a cocktail party or musical instrument sounds of an orchestra). A cardinal task of the auditory system is to organize the complex sound input into perceptual "objects" representing individual sound sources in the environment (auditory scene analysis). Auditory stream segregation is a fundamental feature of auditory scene analysis and denotes how interleaved sequences of sounds are perceptually decomposed into distinct "streams" corresponding to individual sound sources. The neural bases of stream segregation are only beginning to be understood. In the present study, sequences of alternating high and low tones, similar to those used in psychoacoustic experiments on stream segregation ('...ABAB...'), were presented to awake macaques while neural activity was recorded in primary auditory cortex (A1). Tone frequency separation ([Delta]F), tone presentation rate (PR), and tone duration (TD) were systematically varied to examine whether neural

responses correlate with effects of these variables on perceptual stream segregation. 'A' tones were fixed at the best frequency of the recording site, while 'B' tones were displaced in frequency from 'A' tones by an amount = [Delta]F. As PR increased, 'B' tone responses decreased in amplitude to a greater extent than 'A' tone responses, yielding neural response patterns dominated by 'A' tone responses occurring at half the alternation rate. Increasing TD, while keeping PR constant, facilitated the differential attenuation of 'B' tone responses. These findings parallel psychoacoustic data and suggest a physiological model of stream segregation, whereby increasing [Delta]F, PR, or TD enhances spatial differentiation of 'A' tone and 'B' tone responses along the tonotopic map in A1.

## **511 Looking for Neural Correlates of Stream Segregation in Humans and Monkeys**

Christophe Michey<sup>1</sup>, Biao Tian<sup>2</sup>, Alexander Gutschalk<sup>3</sup>, E. Courtenay Wilson<sup>1,3</sup>, Jennifer R. Melcher<sup>3</sup>, Andrew J. Oxenham<sup>1</sup>, Robert P. Carlyon<sup>4</sup>, Josef P. Rauschecker<sup>2</sup>

<sup>1</sup>MIT Research Laboratory of Electronics, Cambridge, MA,

<sup>2</sup>Georgetown Institute for Cognitive & Computational Sciences, Georgetown University, Washington, DC,

<sup>3</sup>Eaton-Peabody Laboratory, Massachusetts Eye and Ear Infirmary, Boston MA, <sup>4</sup>MRC Cognition & Brain Sciences Unit, Cambridge, UK

An essential aspect of auditory scene analysis is the organization of temporal sound sequences into "streams" corresponding to physical sound sources in the environment. The neural basis of auditory stream formation remains unclear. We will summarize recent findings obtained using single-unit recordings in the auditory cortex of macaque monkeys, together with magneto-encephalographic (MEG) and functional magnetic resonance imaging (fMRI) recordings in humans. Stimuli were sequences of tones at two frequencies (A and B), arranged into repeating temporal patterns (ABAB... or ABA\_ABA...). Depending on factors such as frequency separation (dF), inter-stimulus interval (ISI), time since sequence onset (T), and listener's attention, these sequences are perceived as either one or two streams. Single-unit recordings during 10-second ABA sequences showed a complex dependence on both dF and T which paralleled that measured psychophysically in humans. This suggests that the build-up of auditory streaming is reflected in long-term neural adaptation to repeating tone sequences in auditory cortex. Long-latency MEG responses to ABA sequences showed a dependence on dF and ISI consistent with psychophysical data. The MEG responses to perceptually ambiguous but physically identical sequences were found to differ depending on the listener's percept. Preliminary fMRI results with AB sequences also indicate differences in bold-signal wave-shapes depending on dF. These findings reinforce the idea that auditory stream formation is reflected in auditory cortex activity. Perspectives for future research include the development of new tasks that permit tighter coupling between behavioral and neurophysiological measures of streaming. [Support by NIH R01 DC003489 to J. Rauschecker, NIH R01 DC05216 to A. Oxenham, EPSRC Life Sciences Network GR/M90146 to C. Darwin, Hertz

## **512 Cortical Neural Mechanisms in Auditory Scene Analysis**

Shihab Shamma<sup>1</sup>

<sup>1</sup>*University of Maryland*

Humans and animals can parse complex acoustic information arising from multiple sound sources into meaningful auditory "streams". While seemingly effortless, the neural mechanisms underlying auditory streaming are varied and complex. They likely include processes that: (1) extract clean views of simultaneous multiple source spectra based on harmonicity and onset cues; (2) construct more elaborate representations that highlight timbre attributes consistent across sequences of such views; (3) rapidly adapt neural receptive fields in order to segregate responses to different sources. In this talk, we shall review physiological findings in the cortex pertinent to these issues and discuss their functional significance within a computational model of auditory scene analysis.

## **513 Emergence of Action Potential Firing in Vestibular Nucleus Neurons from Chick Brain Slice Preparations.**

Kenna Peusner<sup>1</sup>, Mei Shao<sup>1</sup>, June C Hirsch<sup>1</sup>

<sup>1</sup>*George Washington Univ. Med. Center*

Patch-clamp recordings and pharmacological testing were performed on brain slices of the chick tangential nucleus, a vestibular nucleus whose principal cells (PCs) control posture and balance. Many properties recorded in slices are similar to those obtained from intact animals. A good measure of a neuron's functional integrity is its output signals encoded as firing rate. Firing rate results from integrating vestibular and non-vestibular synaptic inputs with intrinsic membrane properties. In 5 day hatchling (H5) slices, PCs fire spikes spontaneously at  $30 \pm 8$  Hz, in keeping with rates recorded extracellularly from intact hatchlings (du Lac and Lisberger, 1992). However, at resting membrane potential, spontaneous spike activity is not observed in young embryos from E10-E16. By H1, spontaneous spiking appears in about half of the PCs, where it depends on synaptic transmission. Finally, by H5, spontaneous spiking is recorded in most PCs, where it depends on intrinsic membrane properties. At E10 and E13, some PCs generate single spikes on depolarization, while at E16, PCs begin to show repetitive firing on depolarization. Repetitive firing is recorded in all PCs by H5, concurrent with a down-regulation of a dendrotoxin-sensitive potassium current. Interestingly, even at E10, vestibular-nerve stimulation produces glutamatergic postsynaptic responses in some PCs. Thus, PC development includes: (1) Spontaneous spike activity appears after birth, first depending on synaptic transmission and later on intrinsic membrane properties. (2) Repetitive firing on depolarization appears during the perinatal period, coinciding with changes in potassium channels. (3) On vestibular-nerve stimulation, some PCs generate glutamatergic postsynaptic responses as early as E10. In summary, slices are important preparations for

developmental studies, and may also be advantageous to investigate vestibular compensation at the cellular level. Supported by NIH grants R01 DC05004 and R01 DC00970.

## **514 Synaptic Inhibition and Plasticity at Auditory Relays**

Larry Trussell<sup>1</sup>

<sup>1</sup>*Oregon Health & Science University*

Recent studies of auditory brainstem nuclei have documented cell physiological behavior which suggest that plasticity in circuit function may be a common feature of the early levels of sound processing. Many of these analyses employ brain slices preparations made from young rodents, and patch clamp recordings. In the calyx of Held nerve terminal, for example, repetitive presynaptic stimuli results in depression of synaptic function. Moreover, multiple transmitter systems exert powerful modulation of glutamate release from the calyx. Inhibitory transmitter systems working on postsynaptic neurons are now being revealed in greater detail, systems whose functions in vivo have not been well appreciated. Similar properties are seen at end-bulbs synapses. In addition, in both cochlear nucleus and olivary nuclei, long-term changes in synaptic function are being resolved. Are these diverse observations really telling us something about auditory function in vivo? As discussed in this presentation, while computations of acoustic information may indeed be dictated by ongoing refinements in synaptic function, the slice preparation, and patch clamping, have attendant technical limits that must be considered in evaluating recent literature.

## **515 In Vitro Studies of Plasticity in Vestibular Nucleus Neurons During Vestibular Compensation**

Mayank Dutia<sup>1</sup>

<sup>1</sup>*University of Edinburgh*

"Vestibular compensation", the behavioral recovery that follows damage to one vestibular labyrinth or nerve, is an attractive model of de-afferentation induced plasticity in the adult brain. Recent studies of medial vestibular nucleus (MVN) neurons in vitro have revealed potential mechanisms of cellular plasticity that may be involved in the early stages of compensation after unilateral labyrinthectomy. These include rapid changes in the functional efficacy of GABA-A and GABA-B receptors, and changes in the intrinsic neuronal excitability of MVN cells, and the re-modelling of the remaining excitatory and inhibitory synaptic inputs to the deafferented MVN neurons. The extent to which these proposed cellular mechanisms of plasticity may be reconciled with in vivo experimental findings, will be reviewed.



## **516 Intrinsic Electrical Excitability: How Do We Bridge the Gap from In Vitro to In Vivo?**

**Paul B. Manis<sup>1</sup>**

<sup>1</sup>*University of North Carolina Chapel Hill*

In the auditory system, the cochlear nucleus has provided a unique model system in which it has been possible to relate the expression patterns of ion channels to the sensory responses of the neurons, in part because of our knowledge about the detailed behavior of the auditory nerve. This has been largely accomplished through the use of brain slice and isolated cell preparations that allow detailed biophysical analysis of channels and synapses. However, to more fully explain the in vivo responses of cells to sound, the consequences of afferent convergence and other ongoing network activity must also be considered against the context of the cell's intrinsic integrative mechanisms. Recent advances in the application of computational methods have allowed us to begin to integrate our knowledge of individual neurons into more realistic scenarios of neural networks and synaptic drive. Another way to test specific hypotheses about the biological mechanisms of neural integration involves the use of "dynamic clamp" systems that allow the simulation (or substitution) of arbitrary ionic conductances in neurons using computations in real time. It thus becomes possible to simulate synaptic activity to a cell in a controlled manner, while simultaneously manipulating the integrative mechanisms (ion channels, receptor kinetics, synaptic dynamics) in otherwise intact cells. It is also feasible to isolate parts of the cellular system that may be otherwise inaccessible, to determine their contributions to information processing by the rest of the cell. There are both advantages and some significant limitations to this method. This presentation will discuss both the analysis of intrinsic conductances and their contribution to auditory processing, as well as approaches that can be used to incorporate and evaluate the local neuronal circuits and afferent inputs, in order to study the relationship between cellular events and in vivo responses to sensory stimuli

## **517 Regulation of Spike Timing by GABAergic Interneurons in Auditory Cortex**

**Matthew I. Banks<sup>1</sup>, Yakov I. Verbny<sup>1</sup>, Elliott B. Merriam<sup>1</sup>**

<sup>1</sup>*University of Wisconsin*

*In vivo* studies of auditory cortex (ACx) have focused on the responses of single cells to simple acoustic stimuli. This approach has provided insight into encoding of stimuli at the cellular level, but how intracortical circuitry affects population-based coding is unclear. We are interested in how GABAergic cells shape firing patterns in cortical networks. *In vivo*, intracortical inhibition sharpens frequency tuning and onset timing of pyramidal cell responses to auditory stimuli. Networks of mutually connected GABAergic interneurons are capable of generating stable firing patterns that may underlie integration of stimulus features. Brain slices offer an opportunity to explore how interneurons regulate the spatial and temporal spread of excitation, and how connections between cells influence the types of stable firing patterns that emerge upon activation of the network.

In auditory thalamocortical slices, we identified GABAergic cells underlying feedforward vs. feedback inhibition in ACx, and thus the structural basis for inhibitory connections that regulate responses to thalamic and cortical input. Feedforward interneurons predominate in layer IV (LIV), are weakly excited by thalamic input, and have diverse morphology. Feedback interneurons predominate in LI and typically had horizontally-oriented dendritic trees and axonal projections. In paired recordings from LI interneurons the incidence of gap junctions was 24% and inhibitory coupling was 13%. Synaptic strength and kinetics influenced the types of activity that emerged in two-cell networks upon tonic activation. LI networks exhibited bistable behavior, frequently transitioning between 0 and 180° phase lags. Prolonging inhibition or increasing gap junction coupling strength promoted synchrony. Networks of LI cells may underlie oscillations observed upon stimulation of paralamina thalamic nuclei, and enhanced synchrony with prolonged inhibition may underlie cortical synchronization under general anesthesia.

## **518 Reproducing Auditory Outcomes with Simulated Neural Activation Patterns**

**J. Brandon Lafen<sup>1</sup>, Thomas Talavage<sup>2</sup>, Mario Svirsky<sup>3</sup>,**

**N. Ellen Taylor<sup>1</sup>, Thomas Ng<sup>1</sup>, Heidi Neuburger<sup>3</sup>**

<sup>1</sup>*Rose-Hulman Institute of Technology*, <sup>2</sup>*Purdue University*, <sup>3</sup>*Indiana University School of Medicine*

This presentation demonstrates the use of a perceptual difference framework in reproducing clinical outcomes and results from human auditory experiments. The framework uses models of auditory systems (*e.g.*, the Auditory Nerve Model of Heinz, *et al.*, and the Auditory Image Model of Patterson, *et al.*) to simulate neural activation patterns (NAPs) within the auditory nerve. Differences between NAPs correspond to perceptual distinctions in the original acoustic signals. The framework can compare perceptual effects among all hearing scenarios that produce auditory nerve activity (*e.g.*, normal hearing, impaired hearing, and hearing with a cochlear implant). Results from two experiments are presented: (1) perceptual difference correlates to closed-set confusion scores from normal-hearing (NH) and cochlear implant (CI) subjects and (2) measured pure-tone thresholds of NH subjects to tones altered to reflect cochlear hearing loss.

The first experiment compares perceptual difference scores between utterances to actual confusion scores from NH and CI subjects. Models of both the NH and CI auditory systems are used to produce NAPs for comparison with respective human-subject data. Perceptual difference scores increase with dissimilarities between NAPs and this increase corresponds to a lower probability of confusion. Thus, there is an inverse correlation between perceptual difference scores and human confusion data. This provides for *a priori* prediction of closed-set confusion results.

The second experiment demonstrates the reproduction of elevated thresholds from simulated cochlear hearing loss within NH subjects. NAPs of pure tones are altered to reflect various types of cochlear hearing loss. The altered NAPs are transformed by an inverse process to a sound

that simulates the tone, now reflecting the hearing-loss. When presented to a NH subject, the resulting neural activation should reflect the modeled hearing loss.

### **519 Effect of Filtering Spacing and Correct Tonotopic Representation on Melody Recognition: Implications for Cochlear Implants**

**Kalyan Kasturi<sup>1</sup>**, Philip Loizou<sup>1</sup>

<sup>1</sup>*University of Texas-Dallas*

Several studies reported that cochlear implant listeners perform poorly on melody identification tasks. The ability of cochlear implant subjects to perceive melodic information seems to be limited by many factors, including poor complex pitch perception. This is partly due to the fact that current implant processors convey primarily envelope information and no fine-structure cues.

In the proposed study, we investigate whether filter spacing is a potential factor that might influence melody recognition. Most devices use a logarithmic or mel-type filter spacing, which is appropriate for speech signals, but not for music, which is based on a highly-structured semitone scale. We therefore hypothesize that a filter spacing scheme that corresponds to a musical semitone structure might better capture pitch information for music perception.

To test the above hypothesis, we synthesized melodies using noise-vocoder simulations based on two different filter spacings: logarithmic and semitone-based. The number of channels was varied from 2 to 40. The synthesized melodies were presented to normal-hearing listeners for identification. Results indicated that the semitone filter spacing consistently yielded better performance than the conventional logarithmic spacing. Nearly perfect melody recognition was achieved with only four channels of stimulation based on the semitone filter spacing. In a second experiment we frequency transposed the synthesized melodies to 1 and 3 kHz and examined performance using twelve channels of stimulation. Performance degraded significantly for the frequency-transposed melodies. The experiments demonstrate that the envelope cues can be effective cues to complex pitch perception (e.g., melody recognition) provided that the right envelope information is extracted from the signal and sent to the right place of stimulation in the cochlea.

### **520 Sound Processing for Improved Pitch Perception in Cochlear Implantees**

**Johan Laneau<sup>1</sup>**, Jan Wouters<sup>1</sup>, Marc Moonen<sup>2</sup>

<sup>1</sup>*Lab. Exp. ORL - Katholieke Universiteit Leuven*, <sup>2</sup>*ESAT SCD - Katholieke Universiteit Leuven*

Music perception and appraisal is very poor in CI subjects partly because (musical) pitch is inadequately transmitted by the current clinically used sound processors which limit CI recipients' performance. A new sound processing scheme (F0mod) is designed to optimize pitch perception, and its performance for music and pitch perception is compared in four different experiments to that of the current clinically used sound processing scheme (ACE) in

six Nucleus CI24 subjects. In the F0mod scheme, slowly varying channel envelopes are explicitly modulated sinusoidally at the fundamental frequency (F0) of the input signal with 100% modulation depth and in phase across channels to maximize temporal envelope pitch cues. The results of the four experiments show that: 1) F0-discrimination of single formant stimuli was not significantly different for the two schemes, 2) However, F0-discrimination of musical notes of five instruments was three times better with the F0mod scheme for F0 up to 250 Hz, 3) Melody recognition of familiar Flemish songs (with the rhythm cues removed) was higher with the F0mod scheme, 4) Estimates of musical pitch interval, obtained in a musically trained CI subject, matched more closely the presented intervals with the F0mod scheme. These results indicate that explicit F0-modulation of the channel envelopes improves music perception in CI subjects.

### **521 Encoding Fine Structure for Improved Speech Understanding in Cochlear Implant Subjects**

**Selin Kucukoglu<sup>1</sup>**, Danielle Davidian<sup>1</sup>, Leslie Collins<sup>1</sup>

<sup>1</sup>*Duke University*

Current signal processing techniques used in cochlear implants only encode amplitude and envelope information. Even though this strategy usually provides good speech recognition in quiet, speech recognition in noisy environments where most social interactions and communications occur is often poor. It has been suggested that incorporating frequency information other than that which is provided solely through place stimulation via the extracted envelope of the signal would improve temporal resolution, thus improving speech recognition in noise. One approach that has been proposed is varying the stimulation rate on individual electrodes depending on the frequency of the signal. Zeng, Nie, Stickney and Kong (10th Joint Symposium on Neural Computation Proceedings, 2003) acoustically modeled this approach by encoding the slowly-varying frequency-modulated signal along with the envelope and demonstrated promising results. We have evaluated an alternative approach which uses multiple carrier frequencies, instead of a single carrier frequency, to modulate the envelope. This simpler model might result in an easier implementation for the actual cochlear implant; there would be fewer number of predefined pulse rates that would encode fine structure. We have studied speech recognition performance with 2, 4 and 8 carrier frequencies per analysis band as a function of noise level. The frequencies presented in each band are determined via short time Fourier transform and mapped to the desired carrier frequencies. Our results are comparable to Zeng et al's. and suggest that there is an improvement in speech recognition scores as the number of carrier frequencies increase, but that performance plateaus fairly quickly.

## **522 Using Both Place and Rate Pitch Cues to Improve Cochlear Implant Music Perception**

Hongbin Chen<sup>1</sup>, Fan-gang Zeng<sup>1</sup>

<sup>1</sup>University of California, Irvine

Hearing and Speech Research Laboratory, Department of Biomedical Engineering, University of California, Irvine, California 92697-1275, USA

Pitch perception depends on both the site of stimulation (place pitch) and the periodicity of stimulation (rate pitch). The majority of current cochlear implant processors extract the temporal envelope from a number of spectral bands and use it to amplitude modulate a pulse train of constant rate on each individual electrode. Such a processing strategy has provided a high level of speech intelligibility but minimal melody recognition. The present study systematically manipulated the site of stimulation and the rate of stimulation to improve cochlear implant music perception. In the place only condition, up to 6 electrodes were stimulated individually with a frequency resolution of ¼ to 1 octave per electrode and a constant stimulation rate (100 or 1000 Hz). In the rate only condition, a single electrode (near apex, middle, or base) was stimulated with the stimulation rate varying linearly as a function of the note frequency. In the combined place and rate condition, melodies were encoded by varying both the electrode and the stimulation rate. As a baseline measure, three subjects used their clinical processors to achieve an average score of 24% correct in a closed-set melody recognition test. The results showed improved performance with all three experimental conditions with the best average score of 38% for the rate only condition, 64% for the place only condition, and 84% for the combined condition. This result suggests that both place and rate cues contribute independently to pitch perception and cochlear implant listeners can use both to improve their music perception. Novel processing strategies can be developed to incorporate these cues with the traditional temporal envelope cue for improved performance in music perception, tonal language understanding, and speech recognition in noise.

## **523 Evidence from Auditory Brainstem Implants of a Modulation-Specific Auditory Pathway That is Critical for Speech Recognition**

Robert Shannon<sup>1</sup>, Vittorio Colletti<sup>2</sup>

<sup>1</sup>House Ear Institute, <sup>2</sup>University of Verona

Excellent speech understanding has been observed in patients with prosthetic electrical stimulation of the cochlear nucleus. Psychophysical tests reveal that the difference between listeners with high and low speech understanding is not due to overall neuronal survival in the cochlear nucleus, the quality of electrode placement or the specificity of stimulation by individual electrodes, but is related to the ability to detect amplitude modulation. The difference in speech understanding was dramatic between patients whose deafness was caused by vestibular schwannomas on the VIII nerve or from other causes of VIII nerve loss. The relation between etiology, modulation

detection and speech recognition suggests that tumor growth and resection has selectively damaged a physiological processing pathway specialized for modulation. This suggests that modulation specialized cells represent a critical pathway for speech recognition and their loss impairs speech recognition even when other cell types survive. [Partially funded by NIH and Cochlear Corp.]

## **524 Electrophysiological Assessment and Validation of the Auditory Midbrain Implant (AMI).**

Minoo Lenarz<sup>1,2</sup>, Hubert H Lim<sup>1</sup>, David J Anderson<sup>1</sup>, Jim Patrick<sup>3</sup>, Thomas Lenarz<sup>2</sup>

<sup>1</sup>Kresge Hearing Research Institute, <sup>2</sup>Medical University of Hannover, <sup>3</sup>Cochlear Ltd. Australia

Based on several clinical and neurophysiological findings, the inferior colliculus central nucleus (ICC) is an appropriate target for prosthetic stimulation of the central auditory pathway (Lenarz et al., ARO MWM 2004, Lim and Anderson, Proc. IEEE EMBS Conf. Neural Eng., 2003, 193-196). The AMI (Cochlear Ltd.) is a central auditory prosthesis designed for penetrating microstimulation of the human ICC. In order to investigate the electrophysiological properties of the AMI and validate its ability to provide low-threshold, frequency-specific stimulation, a set of acute experiments based on electrical stimulation of the ICC and multi-unit cortical recordings was performed in guinea pigs.

In these experiments, a multichannel Michigan electrode was positioned along the tonotopic gradient of the primary auditory cortex (A1) and the AMI electrode was inserted along the tonotopic gradient of the ICC. The best frequency (BF) for each site in A1 and ICC was determined in response to pure tone acoustic stimuli to ensure both electrodes were aligned along similar frequency ranges. Each ICC site was stimulated with single, biphasic, charge-balanced, monopolar pulses (200 µs/phase) and the corresponding neural activity was recorded in A1. Based on the results, frequency-specific stimulation is achievable using the AMI. Stimulation threshold levels to evoke A1 activity ranged between 10 to 40 µA, which is well within the safe limits suggested for stimulation of the central nervous system (Agnew and McCreery 1990). These findings suggest that the AMI may provide an alternative approach for hearing restoration in the patients with bilateral retro-cochlear deafness.

This work was supported by Cochlear Ltd. Australia, NIH/NIDCD T32 DC00011 and NIH/NIBIB P41 EB2030.

## **525 Psychophysical Detection Thresholds for Electrical Stimulation of the Inferior Colliculus: Comparison to Cochlear Implant Thresholds**

**Bryan E. Pfingst**<sup>1</sup>, Hubert H. Lim<sup>1</sup>, Deborah J. Colesa<sup>1</sup>, Gina L. Su<sup>1</sup>, Jennifer M. Benson<sup>1</sup>, James A. Wiler<sup>1</sup>, Sanford C. Bledsoe<sup>1</sup>

<sup>1</sup>*University of Michigan*

Central auditory prostheses are required in cases of deafness where the auditory nerve is absent or inaccessible by cochlear implants. The inferior colliculus central nucleus (ICC) offers a potentially attractive site for prosthetic stimulation due to its orderly tonotopic organization and relatively good surgical accessibility in humans (Lenarz et al., ARO MWM 2004). Neurophysiological studies (Lim and Anderson, Proc. IEEE EMBS Conf. Neural. Eng., 2003, 193-196) support the hypothesis that this site should have low current requirements and provide good channel independence. In this study, we compare psychophysical thresholds obtained with electrical stimulation in the ICC of the guinea pig to thresholds obtained with cochlear implant stimulation in the same species. In contrast to the case with cochlear stimulation, electrode configuration (TP, BP, MP) for ICC stimulation had little effect on threshold, consistent with the hypothesized effect of placing electrodes in close proximity to the target neurons. However, contrary to our hypothesis, psychophysical detection thresholds for stimulation in central and caudal ICC were high, often falling within or above the upper third of the range of thresholds obtained with monopolar cochlear stimulation. At these locations, psychophysical detection thresholds for ICC stimulation were also generally higher than thresholds for eliciting multiunit responses in auditory cortex, in contrast to the relationship seen with cochlear stimulation. For the most rostral penetrations, thresholds below the typical cochlear implant thresholds have been observed. Possible explanations for the relatively high psychophysical thresholds in some ICC regions are being explored. These include issues related to location, spatial extent, and timing of stimulation as well as anesthesia and plasticity. This work was supported by NIDCD R01 DC03389 and NIBIB P41 EB2030.

## **526 Rostrocaudal Location of Electrical Stimulation Within an ICC Lamina Affects A1 Responses – Implications for a Midbrain Auditory Prosthesis**

**Hubert H. Lim**<sup>1</sup>, David J. Anderson<sup>1</sup>

<sup>1</sup>*University of Michigan*

We have previously shown that electrical stimulation of the inferior colliculus central nucleus (ICC) can produce low threshold, localized, frequency-specific responses in primary auditory cortex (A1) suggesting that a frequency-place coding scheme could be utilized for a midbrain auditory prosthesis (MAP) [Lim & Anderson, ARO, 2004]. However, the complex organization within an isofrequency lamina of the ICC makes it difficult to predict the place and manner of stimulation in the ICC that will elicit the most

useful auditory percepts. Therefore, we investigated the effects of electrical stimulation of different regions within an isofrequency lamina of the ICC on cortical activity. Multichannel Michigan electrodes were used to stimulate different regions within an ICC lamina and simultaneously record unit activity along the tonotopic gradient of A1 in guinea pigs. Our results indicate that electrical stimulation of more rostral regions within an ICC lamina produce spatially (across the tonotopic gradient) and temporally diffuse onset responses as well as strong evoked potentials in A1. As the site of stimulation moved more caudally within an ICC lamina, the cortical response patterns became more spatially and temporally localized and evoked potentials were weaker. In caudal and central ICC, we have observed cases where weak or no activity was elicited in A1 in response to stimulation levels up to 56  $\mu$ A (monopolar, 200  $\mu$ sec/phase). These findings suggest that inhibition may play a more dominant role in more caudal ICC regions. In light of a MAP, stimulation of more rostral regions may provide lower behavioral thresholds due to stronger evoked potentials but at the cost of greater overlap across frequency channels. In more caudal ICC regions, enhanced frequency specificity may be achieved; however, more complex stimulation patterns may be necessary to overcome the inhibitory interactions that prevent activation of higher auditory centers when simple monopolar pulses are used. Future studies will assess both the behavioral and electrophysiological significance of more complex stimulation strategies of different regions within and across ICC laminae to better understand how to optimally implement a MAP.

Supported by NIH/NIDCD T32 DC00011 and NIH/NIBIB P41 EB2030

## **527 The Zebrafish (*Danio rerio*) as an Animal Model for the Identification of Otolith Proteins**

**Richard Kollmar**<sup>1</sup>, Amy Stevenson<sup>1</sup>, Young-Jin Kang<sup>1</sup>, Peter Yau<sup>1</sup>

<sup>1</sup>*University of Illinois at Urbana-Champaign*

The constituent proteins of otoliths are likely key regulators of otolith growth; however, only three proteins out of one or two dozen have been sequenced so far. In this study, we evaluated the zebrafish (*Danio rerio*) as an animal model for the identification of otolith proteins because of its extensive genomics infrastructure. First, we determined that the electrophoretic pattern of otolith proteins from the zebrafish in a polyacrylamide gel was very similar to those from other ray-finned fishes. Next, we obtained a full-length sequence for zebrafish Otolith-matrix protein (Otomp) by molecular cloning; it was between 73% and 81% identical to its orthologs from rainbow trout, medaka, torafugu, and spotted green pufferfish. Together, these results suggested that the protein complement of zebrafish otoliths is representative of those from actinopterygians in general. We then identified a carp otolith protein by *de novo* sequencing with a tandem mass spectrometer and querying databases of zebrafish sequences. We found that this cross-species approach required minimal amounts of material, time, and labor, and that it could be

widely applicable to proteins from other species. We concluded that the zebrafish promises to be instrumental in the identification and characterization of actinopterygian otolith proteins.

**528 Synapsin-like Immunoreactivity is Present in Hair Cells and Efferent Terminals of the Toadfish Crista Ampullaris**

**Gay R. Holstein<sup>1</sup>**, Giorgio P. Martinelli<sup>1</sup>, Robert Nicolae<sup>1</sup>, Todd M. Rosenthal<sup>1</sup>, Victor L. Friedrich, Jr.<sup>1</sup>

<sup>1</sup>*Mount Sinai School of Medicine*

The synapsins are presynaptic membrane-associated proteins involved in neurotransmitter release. They are differentially expressed in tissues and cells of the central and peripheral nervous system. In vestibular end organs of mammals, synapsin I-like immunoreactivity has been reported in efferent and afferent terminals and in afferent nerve calyces surrounding type I hair cells. It has recently been demonstrated that synapsin I, canonically viewed as "neuron-specific", interacts with cytoskeletal components of non-neuronal cells including osteoblasts, epithelial cells, HeLa and NIH/3T3 cells. These findings reinforce the importance of examining the presence and role of this protein in different cells and tissues. Toward that end, the present study was conducted to examine the localization of synapsin-like immunolabeling in the vestibular sensory epithelium of the toadfish, *Opsanus tau*. Synapsin immunostaining was visualized by immunofluorescence detection in wholemounts of the toadfish crista ampullaris using multiphoton laser scanning microscopy and by electron microscopic visualization of postembedding immunogold labeling. Western blots confirmed that the synapsin antibody detects synapsins I and II in this fish. The immunolabeling results demonstrated that synapsin-like immunoreactivity is present in vestibular hair cells, as well as in efferent boutons of the toadfish crista ampullaris. Afferent endings were not labeled. Staining in hair cells was not associated with the synaptic ribbons, suggesting that there is an additional, non-synaptic role for the synapsins in some non-neuronal cells of vertebrates. The observed association between synapsin-like immunoreactivity and non-vesicular membrane profiles in toadfish vestibular hair cells suggests that synapsin may regulate the movement of synaptic vesicle precursor membrane, or even membranes not directly related to synaptic transmission. Moreover, while the cristae of amniote and anamniote species share many functional attributes, differences in their synaptic vesicle-associated protein profiles appear to reflect their disparate hair cell populations.

Supported by DC 01837.

**529 Title: Adding Channel Gating to Finite Element Models of Vestibular Hair Cell Bundles: A New Tool to Study Mechanoelectric Transduction**

Jung-Hoon Nam<sup>1</sup>, John Cotton<sup>1</sup>, John Grant<sup>1</sup>

<sup>1</sup>*VA Tech*

A dynamic finite element (FE) model of the vestibular hair cell is combined with prevalent theories of mechanoelectric transduction (MET), represented by channel gating and adaptation. The FE model explicitly describes the full three-dimensional bundle morphology and individual gating channel for each tip link. Also considered are the mechanical effects of the fluid-drag on the bundle, and a material description of lateral links that allows for kinking when the tension is low. Mechanical deformation of the kinocilium, stereocilia, and links (tip, lateral, and kinocilia) are computed from the FE analysis. Further, Ca<sup>2+</sup> dynamics, which play a key role in hair cell adaptation, are modeled to describe the change of Ca<sup>2+</sup> concentrations at the adaptation sites. The proposed single channel-gating scenario considers (1) tip link tension, and (2) Ca<sup>2+</sup> concentration inside the stereocilia tip, as deterministically governing MET channel gating. Simulated results were found to reproduce the prominent characteristics of in vitro hair cells: bundle compliance matching with activation curve and twitch response (fast movement followed by transient rebound) in accordance with the fast adaptation. Finally, the striola and extrastriola vestibular hair cells are simulated to present detailed information on the dynamics of individual tip links, Ca<sup>2+</sup> concentrations and MET channels.

**530 Intracellular Responses of Hair Cells of the Horizontal Semicircular Canal**

**Stephen Highstein<sup>1</sup>**, Jon Art<sup>2</sup>, Katherine Breneman<sup>3</sup>, Richard Rabbitt<sup>4</sup>, Richard Boyle<sup>5</sup>, Gay Holstein<sup>6</sup>, **Stephen Highstein<sup>7</sup>**

<sup>1</sup>*Washington University School of Medicine*, <sup>2</sup>*Univ. Illinois, Chicago*, <sup>3</sup>*Univ. Utah*, <sup>4</sup>*Univ. Utah*, <sup>5</sup>*NASA-Ames*, <sup>6</sup>*Mt. Sinai School of Medicine*, <sup>7</sup>*Washington University School of Medicine*

Sharp microelectrodes were employed in-vivo to record from hair cells of the horizontal semicircular canal of the oyster toadfish, *Opsanus tau*, in order to examine their responses in-vivo. Records were taken in current and voltage clamp using a single microelectrode switch clamp (NPI) switching at 30 kHz. Microphonic recording was also performed employing an endolymphatic electrode. Indentation of the long and slender limb of the canal (Rabbitt et al., 1995) was utilized for step and sinusoidal stimuli. In a subset of experiments, the endolymphatic voltage was also polarized (Highstein et al., 1996) to investigate the voltage dependence of hair cell receptor currents and the microphonic potential. For frequency sweeps from 2-600 Hz, a fenestra was made in the canal side of the ampulla to permit a ball (~100 micron diameter) on a slender stalk to be inserted into the endolymph. For low-frequency sinusoidal and step stimuli, hair cell receptor current and voltage modulation, and microphonic gain and phase were relatively flat across the frequency

range tested, closely mimicking hair bundle displacements. There were no appreciable frequency-dependent gain increases or phase advances observed, in contrast with those typically present in records taken from primary afferents under similar circumstances (Highstein et al., 1996, Rabbitt et al., 2004). Additionally, during sinusoidal stimulation, first-harmonic hair cell receptor potentials and currents and the microphonic increased nearly linearly with increasing stimulus intensity (Rabbitt et al., 2004). Receptor currents and microphonic potentials appear linearly related to translabyrinthine endolymphatic voltage, reversing at about -10 to -15 mV, relative to perilymphatic ground. Hair cells were subsequently visualized and localized in the crista following intracellular injection of neurobiotin.

(Supported in part by NIDCD R55 DC05585 and PO-1 DC01837)

### **531** Early Development of Spontaneous Synaptic Activity in Vestibular Nucleus Neurons from Chick Embryo Brain Slices.

Mei Shao<sup>1</sup>, June C Hirsch<sup>1</sup>, Kenna D Peusner<sup>1</sup>

<sup>1</sup>George Washington Univ. Med. Center

Principal cells (PCs) of the chick tangential nucleus are vestibular nucleus neurons participating in the vestibular reflexes, which control posture and balance. Previous patch-clamp recordings on brain slices have shown that excitatory (sEPSC) and inhibitory (sIPSC) spontaneous synaptic currents undergo major changes during the perinatal period. Using Cs-gluconate pipet solution, the frequency of sEPSCs increased from E16 (0.6 Hz) to hatching (1.5 Hz), while sIPSCs changed from mainly GABAergic to glycinergic events. In the present study, spontaneous synaptic activity was characterized at E10 and E13, when PCs begin to generate action potentials on depolarization. At -60 mV, the frequency of inward currents recorded at E10 (0.3 Hz  $\pm$  0.1, n=8) and at E13 (0.6 Hz  $\pm$  0.2, n=9) was not significantly different ( $p > 0.05$ ). Inward currents were blocked by CNQX, indicating they were AMPA receptor-mediated events. At +10 mV, the frequency of outward currents recorded at E10 (0.8 Hz  $\pm$  0.3, n=7) and at E13 (1.0 Hz  $\pm$  0.3, n=11) was not significantly different ( $p > 0.05$ ). The outward currents were GABAergic in all the PCs tested at E10 (n=7). At E13, most PCs (7/10) exhibited both GABAergic (75%) and glycinergic currents (25%), while the remaining cells (3/10) showed GABAergic currents only. Decay time and halfwidth of sIPSCs were significantly faster at E13 ( $p < 0.05$ ) than at E10, but sEPSC kinetics did not change significantly between E10 and E13 ( $p > 0.05$ ). In comparison to data obtained at E16 and H1, the spontaneous events recorded at E10/E13 exhibited lower frequency and slower kinetics. In summary, at times before vestibular nucleus neurons can generate repetitive spike firing essential for vestibular reflex function, GABAergic events predominate, with little AMPA or glycinergic activity. Supported by NIH grant R01 DC05004.

### **532** Vestibulo-Cerebellar Zones Controlling Principal and Accessory Eye Muscles in a Canal Plane using Pseudorabies Virus Recombinants

Isabelle Billig<sup>1</sup>, Carey Balaban<sup>1</sup>

<sup>1</sup>University of Pittsburgh School of Medicine

Distinct populations of Purkinje cells in the flocculus/ventral paraflocculus were suggested in mammals to modulate vestibulo-ocular reflex (VOR) eye movements in the plane of semicircular canal pairs. For example, stimulation of a central longitudinal zone of the flocculus/ventral paraflocculus evokes ipsilateral eye movements in the horizontal plane. Recently, the use of the retrograde transsynaptic transport of two isogenic pseudorabies virus (PRV) recombinants provided direct evidence in rats that most Purkinje cells in the ventral paraflocculus project to vestibular nuclear neurons controlling both the ipsilateral medial rectus and contralateral lateral rectus. Hence, the ventral paraflocculus and flocculus may exert influence upon distinct VOR pathways. Growing evidence suggests that the anatomical organization of the flocculus-vestibular nucleus pathways may be a representation to simultaneously modulate reflex pathways for both principal and accessory muscles for eye movement in the plane of a semicircular canal. To test this, the two PRV recombinants were injected into the medial rectus and superior rectus muscles of the same eye, respectively, and transsynaptically-infected cells were detected using dual-labeling immunofluorescence. Three populations of labeled Purkinje cells were detected bilaterally in both flocculi/ventral paraflocculi. Two populations replicated only one reporter while a third contained both viruses (i.e., dual-labeled). Most dual-labeled cells were located in the flocculi, particularly in the rostral half of the ventral surface of flocculi, in areas shown previously to project to the superior and rostral medial vestibular nuclei. This result further supports the hypothesis that the ventral paraflocculus may influence conjugate horizontal VOR pathways through collateralization, whereas the flocculus may instead provide a monocular control of multiple eye muscles. These monocular connections may be an effective way of maintaining VOR adaptive performance when the eyes are in different eccentricities or for controlling the disconjugate linear VORs.

This work was supported by NIH grant: RO3-DC005911 (I.B.).

### **533** Significance of Vestibular and Visual Inputs During Allothetic and Idiothetic Maze Learning to Fos Expression in the Rodent Brain

Michael Shinder<sup>1</sup>, Galen Kaufman<sup>1</sup>

<sup>1</sup>UTMB

Locomotion and navigation rely upon visual and vestibular input to create and use internal representations of the world to get from one place to another. Visual and vestibular information impart distinct information. Allothetic representations, exocentric references about the external

world, are dominantly visual. Idiothetic representations, internal references about one's orientation to that external world, are dominated by vestibular input. Allothetic and idiothetic references can be used together or independently to navigate. We trained rodents to learn a maze using each reference independently, and evaluated regional Fos activation patterns in the brain. Allothetic place learning utilized local visual landmarks, while idiothetic response learning did not. The training produced equivalent locomotor activity, but learning to properly navigate the maze required different behavioral strategies dependent upon different cues. We demonstrate that the non-visual response learning required vestibular sensory input, as bilateral vestibular lesions abolished the ability to perform this type of maze learning. Idiothetic vestibular dependent maze learning resulted in Fos activation patterns that differed from allothetic based learning in the striatum and hippocampus, as well as the cingulate cortex, temporal and parietal association cortices, and retrosplenial cortex. Idiothetic patterns were characterized by stronger temporal, parietal, and cingulate cortex labeling than that seen after allothetic reference learning. Maze learning following vestibular lesions was impaired or failed, and resulted in reduced Fos labeling that nonetheless covered the same regional patterns as seen in normal animals learning the maze with a similar strategy. There were two exceptions: First, the Fos labeling became more lateralized in bilaterally lesioned animals using either allothetic or idiothetic strategies, reflecting the laterality of the behavior. Second, the vestibular brainstem labeling was strongly increased in the nucleus prepositus hypoglossi in animals using idiothetic strategies above that seen in unlesioned animals and in lesioned allothetic learners. The labeling increase may reflect descending inputs to the prepositus attempting to increase sensitivity to inputs that are not available.

### **534 FAR and NEAR Target Dynamic Visual Acuity: Bilateral Vestibular Deficit Patients**

**Eric Landsness<sup>1</sup>, Jacob Bloomberg<sup>2</sup>, Brian Peters<sup>2</sup>, F. Owen Black<sup>3</sup>**

<sup>1</sup>University of Wisconsin School of Medicine, <sup>2</sup>NASA Johnson Space Center Neuroscience Laboratory,

<sup>3</sup>Neurotology Research, Legacy Clinical Research and Technology Center

**Background:** Semi-circular canals and otoliths differentially contribute to gaze stability and visual acuity at different visual target distances. Subjects with impaired vestibular function often report oscillopsia and decreased visual acuity during active and passive movements. A locomotion paradigm that functionally characterizes loss of gaze control could provide insight regarding relative otolith and canal contributions to ocular globe stability and dynamic visual acuity.

**Objective:** Quantify changes in visual acuity in a population of bilateral vestibular deficient subjects during quiet stance and gait.

**Methods:** Six bilateral vestibular loss (BVL) subjects (25-79 years), and 4 sex and age-matched normals participated. Subjects were tested twice, five months apart.

After obtaining visual acuity while standing quietly, subjects walked on a treadmill at 1.12 m/s while viewing visual targets at either 4 meters (FAR) or 0.5 meters (NEAR).

**Results:** When compared to the FAR condition, the NEAR condition showed significantly larger decrements ( $F=11.5$ , 68 degrees of freedom,  $p=0.00000034$ ) in dynamic visual acuity for both controls and BVL patients. Comparison between the subject groups indicated that BVL patients have statistically significant larger decrements in visual acuity for both FAR and NEAR conditions ( $F=44$ , with 4,68 degrees of freedom  $p<0.000001$ ).

**Conclusions:** 1) Significant changes were observed in NEAR versus FAR target dynamic visual acuity in both controls and BVL patients. 2) Significant changes were observed when comparing controls to BVL patients in the NEAR and FAR condition. The observed changes in controls versus BVL patients may be explained by the affect of altered vestibular contributions to ocular globe stability (absent or reduced linear VOR). Future studies will include independent measures of the LVOR in controls and BVL subjects.

### **535 Comparative Study of the Gaze Stabilization Test (GST) and Dynamic Visual Acuity Test (DVAT) for detecting patients with unilateral vestibular dysfunction**

**Joel Goebel<sup>1</sup>, Nilubon Sangasilp<sup>1</sup>, Belinda Lindberg<sup>1</sup>**

<sup>1</sup>Dizziness and Balance Center, Washington University School of Medicine, St. Louis, MO

**Background**

The Gaze Stabilization Test (GST) is a new quantitative clinical test which assesses the VOR by measuring visual acuity at different velocities of head movement. The GST measures maximum head velocity (in degree/second) where the subject can still maintain visual acuity. In contrast, the Dynamic Visual Acuity (DVAT) measures changes in optotype size recognition during head movement.

**Objectives**

This study evaluated the sensitivity, specificity and reliability of the Gaze Stabilization Test and the Dynamic Visual Acuity test for detecting patients with unilateral vestibular dysfunction.

**Methods**

Fourteen unilateral vestibular dysfunction patients (43-81 years, mean age 66 years) and ten normal subjects (23-78 years, mean age 39 years) were enrolled in this study. The subjects are scheduled blindly into two hour test sessions. After baseline static visual acuity is obtained, 3 subsequent trials of the DVAT (120 deg/s head velocity as threshold for displaying the baseline optotype) and 3 trials of the GST (three optotypes above baseline) were performed in random order. The main outcome measure for the GST was maximum head velocity and for the DVAT was change in optotype from baseline.

**Results**

Both the GST and DVAT were reliable in detecting patients with unilateral vestibular loss. (Intraclass correlation

coefficient [ICC] =0.85 and 0.75 respectively) Using the criterion for abnormal test at normal mean DVA logMAR + 2SD (0.1737+0.14), the sensitivity of DVAT was 61.5% and the specificity of DVAT was 100%. The sensitivity of the GST was 56% and the specificity was 100% at the normal mean head velocity – 2SD cut point (152.8 -62.96 deg/sec)

#### Conclusion

In this pilot study, the Gaze Stabilization Test was comparable to the Dynamic Visual Acuity Test in sensitivity and specificity for detecting unilateral vestibular dysfunction. The optimal optotype size for GST is yet to be determined although three optotypes above baseline yielded acceptable results for this study.

### **536** Imaging the Membranous and Bony Labyrinths with CT and MR Microscopy

Scott Eggers<sup>1</sup>, Robert H. Brey<sup>2</sup>, **John (Jack) Lane**<sup>3</sup>, Robert Witte<sup>3</sup>, O'Dell Henson<sup>4</sup>, Colin Driscoll<sup>2</sup>, Jon Camp<sup>5</sup>, Richard Robb<sup>5</sup>

<sup>1</sup>Mayo Clinic, Rochester MN, <sup>2</sup>Mayo Clinic, Otorhinolaryngology, <sup>3</sup>Mayo Clinic, Radiology, <sup>4</sup>UNC at Chapel Hill, <sup>5</sup>Mayo Clinic, Biomedical Imaging Resource

#### Background:

Anatomic definition of the bony and membranous labyrinth in the clinical setting remains limited. Ultra-high resolution CT and MR imaging for use in the research laboratory on small animals and pathologic specimens has given rise to the field of imaging microscopy.

#### Objectives:

Demonstrate new imaging techniques to display the separation between the membranous and bony labyrinthine structures and apply this to a new interactive teaching tool.

#### Methods:

We used these techniques to image human temporal bone cadaveric specimens using 9 Tesla MicroMR and MicroCT in order to delineate labyrinthine structures that have previously only been seen using standard light microscopy.

#### Results:

Volume data acquisition resulted in 20um voxel size for MicroCT and 78 um voxel size for T2-weighted microMR imaging at 9T. Segmentation of the 9T dataset allowed separation of the endolymphatic structures from the perilymphatic space within the cochlea and semicircular canals. These structures were then reconstructed into 3 dimensional images that could be viewed interactively as a 3D sectional data exploration tool. We juxtaposed high-resolution MicroCT images of the bony labyrinth with 9 Tesla MicroMR images of the membranous labyrinth to highlight the utility of these techniques.

#### Conclusions:

By utilizing recent advances in imaging technology, we have resolved finer detail views of temporal bone structures than ever possible before in undissected specimens. This approach to the study of the inner ear avoids tissue destruction inherent in histopathologic preparations. We highlight the utility of MR and CT

microscopy in teaching normal anatomy of the inner ear. This will further the understanding of the inner ear's complex anatomy in an effort to aid practicing physicians in the clinical setting.

### **537** Initiating Inner Ear Induction: a Role for FGF8 in Otic Development.

**Raj Ladher**<sup>1</sup>, Tracy Wright<sup>2</sup>, Suzi Mansour<sup>2</sup>, Gary Schoenwolf<sup>2</sup>

<sup>1</sup>RIKEN Center for Developmental Biology, <sup>2</sup>University of Utah School of Medicine

The precursor of the inner ear, the otic placode, arises from a disc of thickened ectoderm adjacent to the caudal hindbrain. Substantial progress has been made in characterizing the molecular and cellular interactions that lead to the induction of the otic placode and have provided insights on the development of the inner ear.

In the chick, the otic placode is induced by the synergistic action of two signals, one from the cephalic paraxial mesoderm located subjacent to the neural plate of the caudal hindbrain and the other from the overlying neural ectoderm. In the chick, the mesodermal signal, Fgf19, initiates overlying ectoderm to express Wnt8c and Fgf3. It is apparent that the position of the otic placode is due to the localized action of the mesodermal inducers. We wished to determine the events that cause the localization of the mesodermal inducers of the otic placode. We have uncovered a role for Fgf8 in the induction of the localized mesodermal otic inducers. Fgf8 is expressed in the endoderm subjacent to Fgf19, and is both sufficient and necessary for the expression of Fgf19 in the mesoderm. Abrogation of the expression of Fgf8 in the endoderm can block the development of the otic placode. Additional evidence from the mouse using null and hypomorphic alleles will be consistent with this scheme. The data presented supports a role for the localized action of Fgf8 initiating the localized expression of the mesodermal inducer of the otic placode.

### **538** In Vitro Differentiation and Apoptosis of Auditory Myofibroblasts: A Smooth Muscle Actin EGFP Transgenic Mouse Model

**Cristina Bertolotto**<sup>1,2</sup>, Dynio Honrubia<sup>1,2</sup>, Dora Acuna<sup>1</sup>, Sebastian Wachsmann-Hogiu<sup>1,2</sup>, Valeria Ubal<sup>1</sup>, Ali Pirooz<sup>1,2</sup>, Arash Moghimi<sup>1,2</sup>, Daniel Farkas<sup>1,2</sup>, Charles Simmons<sup>1,2</sup>

<sup>1</sup>Cedars-Sinai Medical Center, <sup>2</sup>David Geffen School of Medicine at UCLA

**Background:** Myofibroblasts are specialized mesenchymal cells that contribute to developmental fibrotic disorders, tissue development and repair. Myofibroblasts must ultimately differentiate but then disappear from areas of injury by programmed cell death. The role myofibroblasts play during normal auditory development and their response to trauma are unknown.

**Hypothesis:** Myofibroblasts can be cultured from the auditory system of mice and stimulated to differentiate and undergo apoptosis *in vitro*.



**Design/Methods:** We developed an  $\alpha$  smooth muscle actin (SMA) enhancer/promoter driven transgenic mouse line expressing EGFP in myofibroblasts and smooth muscle cells. Cochleae and ossicles from EGFP positive mice were dissected and primary cell cultures established. A clonally expanded, SV40T immortalized cell line was established. Cultured cells were subjected to photodynamic laser exposure and/or proteasome inhibition with lactacystin (200ug/ml) to induce apoptosis. Cells were analyzed by real time confocal, immunofluorescence microscopy with image analysis.

**Results:** Primary and immortalized cochlear cell cultures expressed EGFP positive myofibroblasts. Immunofluorescence revealed expression of  $\alpha$  SMA, desmin, and vimentin. Photodynamic laser exposure or proteasome inhibition induced fluorescent aggregates formation, nuclear propidium iodide uptake, and apoptosis. Myofibroblasts exhibited increased EGFP fluorescence, followed by abrupt extinction of fluorescence during apoptosis.

**Conclusions:** Primary and immortalized fibroblasts can be cultured from cochlea and ossicles of an  $\alpha$  SMA EGFP transgenic mouse line and stimulated to differentiate into fluorescent myofibroblasts *in vitro*. These auditory myofibroblasts can be specifically stimulated to undergo apoptosis. Further investigation will address the role of myofibroblasts in auditory and vestibular system pathology and their molecular mechanisms of differentiation and apoptosis.

### **539 Cochlear Alterations in Transgenic Mice Lacking the Neurotogenic Region of Saposin C: Progressive Deafness and Altered Innervation Patterns**

Omar Akil<sup>1</sup>, Hakim Hiel<sup>2</sup>, Jee-Hyun Kong<sup>2</sup>, Suchitra Parameshwaran<sup>2</sup>, Elisabeth Glowatzki<sup>2</sup>, Lawrence Lustig<sup>1</sup>  
<sup>1</sup>University of California San Francisco, <sup>2</sup>Johns Hopkins University

Prosaposin is the precursor of four glycoprotein activators (saposins) for lysosomal hydrolases, and has lipid transfer properties and neurotogenic effects. Auditory structure and function was studied in a previously created transgenic mouse (Sun et al, 2002) in which a chimeric saposin C had its neurotogenic region replaced by the non-neurotogenic sequence of saposin B. Compared to wild type (+/+) mice, transgenic mice lacking the neurotogenic region of saposin C (-/-) showed normal hearing at 16 days, but deafness by 22 days, as measured by ABR. While at 11 days there was very little histologic difference between (+/+) mice and (-/-) mice, by 3 weeks transgenic mice demonstrated hypertrophy in the region of the inner hair cell and supporting tissues, with a severe loss of outer hair cells. These effects were more pronounced in the apex compared to the base of the cochlea. Immunofluorescent staining showed exuberant overgrowth of afferent (anti-Neurofilament-200 Ab) and efferent (anti-synaptophysin Ab) neurites in the region of the inner hair cell. Recordings from inner hair cells of the homozygote mice display normal I-V curves and responses to applied acetylcholine. Together, these data suggest that the neurotogenic region

of saposin C is required for normal cochlear innervation and the development of hearing.

### **540 The Nuclear Receptor COUP-TFI Plays a Role in Cytokinesis**

Patricia Pardo<sup>1</sup>, Patricia Yotnda<sup>1,2</sup>, Feng Lin<sup>1,3</sup>, John Kwon<sup>1,3</sup>, Haiying Liu<sup>1,3</sup>, Fred A. Pereira<sup>1,4</sup>

<sup>1</sup>Baylor College of Medicine, <sup>2</sup>Shell Center for Gene Therapy, <sup>3</sup>Huffington Center on Aging, <sup>4</sup>Otorhinolaryngology

COUP-TFI is an orphan member of the superfamily of nuclear receptors. It usually acts as a transcriptional repressor impeding the induction of genes by other nuclear receptors such as RXR, RAR, and TR, which are required for development of normal hearing. COUP-TFI<sup>-/-</sup> mice are completely deaf due to morphogenetic alterations in the organ of Corti with loss of high frequency hair cells before maturation of hearing. COUP-TFI<sup>-/-</sup> mice also have an increased loss of neural crest cells as they divide, migrate and mature during development of the glossopharyngeal ganglion. In *Drosophila*, the homologue of COUP-TFI Seven-up (Svp) is required for the development of the fly kidney, the Malpighian tubules, where Svp loss-of-function provokes a reduced number of cells by affecting the number of cell divisions without affecting cell fate or cell death. Thus, we explored the possibility that COUP-TFI function could influence the cell cycle in mammalian cells by studying the effects of its loss-of-function and over-expression in mouse embryonic fibroblasts (MEFs) and in HeLa cells. Consistent with a role in the cell cycle, COUP-TFI<sup>-/-</sup> MEFs have a reduced proliferative capacity and they accumulate at the G2/M stage of the cell cycle with increasing passages. Close inspection of MEFs in culture revealed an increase number of cells at mitosis, as detected by the increased number of phosphohistone H3 (mitotic marker) positive cells. Intriguingly, most of these cells were found at cytokinesis, with late passage cells having longer cytokinetic bridges, a characteristic seen in gene mutations that have difficulties to complete cytokinesis. Over-expression of COUP-TFI has a more dramatic effect, with a higher proportion of cells found at cytokinesis and they have abnormal cytokinetic bridges, even at early passages. These results indicate that COUP-TFI function is cell-autonomously required in MEFs and is necessary for normal progression through mitosis and cytokinesis. This work is supported by DC04585.

### **541 Roles of Dishevelled Genes in Growth and Polarity of the Organ of Corti**

Sharayne Mark<sup>1</sup>, Xiaohui Zhang<sup>1</sup>, Jianbo Wang<sup>2</sup>, Xi Lin<sup>1</sup>, Andres Collazo<sup>3</sup>, Neil Segil<sup>3</sup>, Anthony Wynshaw-Boris<sup>2</sup>, Ping Chen<sup>1</sup>

<sup>1</sup>Emory University School of Medicine, <sup>2</sup>UCSD School of Medicine, <sup>3</sup>House Ear Institute

During development, the precursors of the organ of Corti differentiate within the postmitotic primordium to form a mosaic consisting of alternating rows of sensory and supporting cells. This process is accompanied by extension of the sensory epithelium and acquisition of a

characteristic planar cell polarity (PCP), manifested with the formation of precisely organized and uniformly oriented actin-rich stereociliary bundles on the apical surface of all hair cells. Recent studies identified the association of stereocilia defects with genes in a conserved PCP pathway and genes involved in actin filament polymerization/organization. However, it is not clear how these morphogenetic events are coordinated. Here we show that dishevelled (Dvl) genes may mediate divergent downstream pathways to regulate the patterning of stereocilia and the extension of the organ of Corti. Dishevelled proteins consist of multi-functional domains, essential for transducing PCP and canonical Wnt pathways, and capable of interacting with cytoskeleton network for actin reorganization. In the null mice of two homologous Dvl genes, Dvl1 and Dvl2, the organ of Corti is shorter and wider, the stereocilia are less developed, and toward the middle and apical region of the cochlea the stereocilia of hair cells are misaligned. The cellular localization of Dvl2 further supports the role of dishevelled in the orientation and growth of the stereocilia. Dvl2 is localized to the lateral edge on the apical cortexes of the hair cells in wild-type animals, exhibiting a polarized sub-cellular localization across the organ of Corti. This polarized localization of Dvl2 is disrupted in animals that exhibit stereocilia mis-orientation. Dvl2 is also physically associated with stereociliary bundles. These data together implicated the involvement of dishevelled genes in both the growth and orientation of the stereocilia, and in coupling the extension of the organ of Corti with establishment of PCP in the organ of Corti.

#### **542 Effects of Ethanol on the Development of Sensory Hair Cells in Embryonic Zebrafish**

**Jonathan Matsui**<sup>1,2</sup>, Ana Egana<sup>1</sup>, Kevin Koo<sup>1</sup>, John Dowling<sup>1</sup>, Douglas Cotanche<sup>2,3</sup>

<sup>1</sup>Department of Molecular and Cellular Biology, Harvard University, <sup>2</sup>Department of Otolaryngology, Children's Hospital, Boston, <sup>3</sup>Departments of Otolaryngology and Laryngology, Harvard Medical School

Some children who are born to mothers who have consumed alcohol during pregnancy present a number of morphological, cognitive, and sensory abnormalities, including hearing deficits, collectively known as fetal alcohol syndrome (FAS). The goal of this study is to determine if the zebrafish is a good model system to study auditory abnormalities caused by exposure to ethanol during embryogenesis. Stereocilia bundles are observable at 2 days post-fertilization (dpf) and by 5 dpf sensory hair cells are clearly distinguishable by light microscopy. Zebrafish embryos were raised in fish water supplemented with varying concentrations of ethanol (1%-2% by volume) from 2 dpf through 5 dpf. Both untreated controls and embryos receiving 1% ethanol appeared morphologically normal. Embryos treated with 1.25% and 1.5% ethanol began to show different morphological characteristics including a slightly flatter forebrain, swollen heart, and swollen gut. Embryos treated with 1.75% and 2% ethanol had numerous morphological problems including a curved body (dorsal curve), extremely swollen heart with blood sometimes pooling in the chamber, rounded forebrain,

irregular jaw, and smaller eyes. Hair cell morphology was examined using light and fluorescent microscopy. Ethanol treatment resulted in a drastic reduction in the number of sensory hair cells in the utricle. We also examined the effects of ethanol on the development of sensory hair cells in neuromasts found in the lateral line. Neuromasts were labeled with the fluorescent vital dye, DASPEI, which is preferentially taken up by hair cells. Fish were scored for the presence or absence of hair cells in each of the lateral line neuromasts. There was a dose dependent decrease in the number of lateral line neuromasts that were stained with DASPEI. At the higher ethanol concentrations (1.5%-2%), embryos had irregular DASPEI staining patterns indicating that the ethanol interfered in the development of the lateral line. Embryos treated with 2.00% ethanol had very few neuromasts indicating the absence of hair cells.

Funded by the National Institutes for Health EY 14790 and the NOHR Foundation (JM); Knights Templar Eye Foundation (AE); Howard Hughes Medical Institute (KK), NIH EY 00811 (JD); NIH DC01689, Deafness Research Foundation, Samuel P. Rosenthal and Dossberg Foundation, and the Sarah Fuller Fund (DC).

#### **543 Transforming Growth Factor-Beta Participates in Both the Physiological and Pathological Regulation of Inner Ear Development by Retinoic Acid**

Wei Liu<sup>1</sup>, Sydney Butts<sup>1</sup>, Geming Li<sup>1</sup>, **Dorothy Frenz**<sup>1</sup>

<sup>1</sup>Albert Einstein College of Medicine

Retinoic acid (RA) is a vitamin A derivative that participates in patterning and regulation of inner ear development. Either excess RA or RA deficiency during a critical stage of otic morphogenesis can produce teratogenic effects. Previous studies have shown that in utero exposure to a high dose of RA results in severe inner ear malformations that are associated with reduced levels of endogenous transforming growth factor-beta (TGF-B). In this study, the effects of a teratogenic dose of RA on levels and patterns of expression of TGF-B receptor (TGFBRII) and downstream Smad2 are investigated in the developing mouse inner ear. The expression pattern of endogenous RA receptor-alpha (RAR-alpha) and the ability of an RAR-alpha specific antisense oligonucleotide (AS) to modulate otic capsule chondrogenesis are demonstrated in the inner ear and in culture respectively. We show that TGFBRII and Smad2 are downregulated in the malformed RA-exposed inner ear. In addition, a marked suppression of chondrogenesis occurs in RAR-alpha AS-treated cultures. Analysis by quantitative real-time RT-PCR indicates that this suppression of chondrogenesis is associated with a reduction in endogenous levels of TGF-B in comparison to levels in control cultures. Supplementation of cultures with exogenous TGF-B can partially overcome the chondrogenic suppression produced by RAR-alpha AS treatment. Our findings show that both excess RA and deficiency in RA by blocking of RAR-alpha produce changes in TGF-B signaling, supporting TGF-B in the physiological and pathological regulation of inner ear development by RA.

### **544 The Effects of Prenatal Cytomeglovirus Infection on Cochlear Development in the Rhesus Macaque (*Macaca mulatto*).**

Steven Tinning<sup>1</sup>, Alice Tarantal<sup>2</sup>, Shan-Shan Zhou<sup>3</sup>, Peter Barry<sup>3</sup>

<sup>1</sup>University of California, Davis, <sup>2</sup>California National Primate Research Center, <sup>3</sup>Center for Comparative Medicine, UC Davis

Control (N = 22) and experimental (N = 37) rhesus monkeys (*Macaca mulatto*) from 70 days gestation through 3-month old infants were compared immunohistochemically and by light and electron microscopy (EM) to determine viral distribution and the histopathologic effects of prenatal cytomegalovirus (CMV) infection during cochlear development. Fetal monkeys were infected intracranially (within the cerebrospinal fluid) or intraperitoneally under ultrasound guidance at the end of the first trimester. They were fixed either by immersion or transcardial perfusion with mixed aldehydes. Left ears were processed for plastic thin section histomorphometry and EM. Right ears were processed for wax immunohistochemistry. Cells with "owl eye" viral inclusion morphology were seen in wax and plastic sections. Intracellular EM viral morphology included virions, capsids and dense bodies characteristic of those previously reported for human and guinea pig CMV. Immunohistochemical detection of viral antigens was seen from 70 through 90 days gestation. Labeled cells were localized in the developing spiral ganglion and the inflammatory infiltrate of the modiolus and connective tissue of the exterior cochlear surface. They were absent from the developing organ of Corti, spiral ligament and stria vascularis although some positive cells were present in the inflammatory infiltrate of the connective tissue matrix filling the nascent scala tympani and vestibuli. Pre-natal pathology was largely confined to the developing spiral ganglion and eighth nerve. Post-partum animals demonstrated overall retention of cochlear structure including the scala media. However, there was a distinct loss of cellularity within the spiral ganglion, spiral ligament, stria vascularis and organ of Corti. Pre-natal infection with CMV in rhesus monkeys appears to primarily affect the spiral ganglion and processes of the eighth nerve with possible inflammatory bystander damage to the substructures of the scala media.

### **545 Transcriptional Control of the Potassium Channel KCNQ4**

Harald Winter<sup>1</sup>, Claudia Braig<sup>1</sup>, Ulrike Zimmermann<sup>1</sup>, Jiang Zuo<sup>2</sup>, Hyun-Soon Geisler<sup>1</sup>, Karl Bauer<sup>3</sup>, Thomas Weber<sup>2</sup>, Marlies Knipper<sup>1</sup>

<sup>1</sup>Tuebingen Hearing Research Center, Molecular Neurobiology, <sup>2</sup>St. Jude Children's Research Hospital, <sup>3</sup>Max-Planck-Institute for Experimental Endocrinology

Cochlear outer hair cells are responsible for the frequency-resolving capacity of the mammalian inner ear. Electrical stimulation during the hearing process induces rapid length changes of these cells, transduced by the novel

motor protein prestin (Zheng et al., 2000, Nature 405). Recently Karkovets et al., 2000, PNAS 97 reported the expression pattern of a novel potassium channel, KCNQ4, in hair cells and neurons of the auditory and vestibular systems, the expression of which is linked to nonsyndromic dominant deafness, DFNA2. In outer hair cells this channel is presumed to be similar to the unusual potassium selective "leak" current, termed IK,N, which is responsible for the repolarisation of the outer hair cells. We noted an alteration of the subcellular distribution of the outer hair cell motor protein prestin coincident to an alteration of the subcellular distribution of KCNQ4 prior to the onset of hearing. As the prestin expression itself as well as its subcellular distribution revealed as being under control of thyroid hormone (TH) (Weber et al., 2002, PNAS 99), we analysed the effect of TH on KCNQ4 expression. By analysing various rat and mouse-models of hypothyroidism, we can show that the expression of KCNQ4 is also dependent on TH. Sequence analysis identified putative thyroid response elements in the upstream region of KCNQ4 gene which were tested for functionality using reporter gene assays and electromobility shift assays. The data suggest a TH-dependent mechanism of regulation of the KCNQ4 expression which is different of that observed for the motor protein prestin. While prestin expression is enhanced by TH (Weber et al. 2002, PNAS 99) expression of KCNQ4 is under repression of TR $\alpha$  aporeceptors and TH is needed to overcome this repression during development (Winter et al, submitted). New data concerning the repressive effect of TR $\alpha$  aporeceptors during final differentiation processes of the hair cells will be presented by analysing mutant mouse and cre/lox mouse models.

Supported by a grant from the Deutsche Forschungsgemeinschaft DFG KN316/4-1 and the Interdisciplinary Center of Clinical Research (Tübingen, Germany).

### **546 Number of Spiral Ganglion Neurons in Newborn Mouse Cochlea and Their Survival and Growth Characteristics in Dissociated Culture**

Donna S. Whitlon<sup>1</sup>, May Tso<sup>1</sup>, Webster Edpao<sup>1</sup>, Kathleen Ketels<sup>1</sup>, Claus Peter Richter<sup>1</sup>

<sup>1</sup>Department of Otolaryngology, Feinberg School of Medicine, Northwestern University

Published estimates of the number of spiral ganglion neurons in newborn or early postnatal mouse cochleas are variable, ranging from 4400 to 16,000. This uncertainty in the actual size of the intact neuronal population interferes with determining the percentage of spiral ganglion neurons that survive in dissociated culture. In vitro experiments aiming to examine a consistently representative sample of spiral ganglion neurons depend on accurate population counts. Using unbiased stereology techniques, we have counted every neuron in serial 5 micron sections of complete cochleas from newborn CD-1 mice, and find approximately 8000 neurons. This is in agreement with a few of the published reports (Postigo et al., 2002; Agerman et al., 2003; Luikart et al., 2003; Farinas et al, 2001). We

have developed a new procedure for preparing dissociated cultures of the spiral ganglion from newborn mice. In the presence of serum and growth factors, survival is improved by inclusion of the adjacent non-neural tissue (Limbus+spiral lamina) in the dissociated culture. The method routinely permits 15-25% survival of the total number of neurons in the starting material. Consistent with the results of Marzella et al (1997), two day survival in the presence of the neurotrophic factors NT3 + BDNF is increased by the inclusion of the cytokine, LIF. The survival effect of LIF on these neurons is mainly on those from the apical, rather than the basal turn. In addition, we report that inclusion of LIF increases the lengths of the longest neurites by approximately 47%, but has little or no effect on the length of the shorter process. LIF causes an increase in the percentage of bipolar neurons in the culture from 44% to 76% and a decrease in the percentage of monopolar neurons from 52% to 13%. In longer term cultures (7-10 days) neurons arrange themselves in stereotypic patterns that are similar in appearance to those formed by endogenous laminin and entactin but not to those formed by endogenous fibronectin or tenascin. These results demonstrate the regulation of growth and morphology of spiral ganglion neurons by composition of the medium, and suggest that growing neurites in vitro may follow patterns of molecules generated by the underlying non-neural cells. (Supported by grant #R01DC00653 from the NIDCD).

#### **547 Developmental Changes in Spiral Ganglion Cell Counts: Revisited**

**Webster Edpao<sup>1</sup>, Gagan Kumar<sup>1</sup>, Claus-Peter Richter<sup>1</sup>**

<sup>1</sup>*Northwestern University Feinberg School of Medicine*

Gerbils provide an ideal animal model to study the development of the auditory system. Final cochlear maturation occurs after birth. It has been reported that the number of spiral cells changes drastically between postnatal three and seven. Cell counts decrease by 27% (Echteler and Nofsinger; JCN 425:436; 2000). A similar finding has been reported for rats (Rueda et al., Acta Otolaryngol. 104: 417; 1987). Furthermore, Rueda and coworkers (Neurosci Res. 45:401; 2003) argued that hypothyroidism prevents developmental neuronal loss during auditory organ development.

This poster revisits developmental changes in spiral ganglion cell counts in the gerbil. Gerbil cochleae were harvested at postnatal day 0 (N=3) and at postnatal day 7 (N=2). They were then embedded in Epon-Resin and serial sectioned into 5 µm thick slices. The slices were mounted on glass slides. A stereologic method was used to count the spiral ganglion cells on every slice. The values for each of the slices were summed to obtain the total number of spiral ganglion cells for each cochlea. Interestingly, no significant change in spiral ganglion cell counts could be observed between the two age groups. This contrasts the previously reported results. Our average spiral ganglion cell counts were 23895±2058 for zero day old animals and 24521±360 for seven day old animals.

Methodology differences may account for the discrepancy between our results and the published data. Previous

estimations of total cell counts were achieved by using profile counts of every tenth section of a serial sectioned cochlea. Raw counts were then multiplied by ten and corrected for overcounting. In contrast, we used a stereologic method and counted every slice. It is possible that the rapid growth, which occurs between postnatal day three and seven may account for the underestimation of the total number of cells in the adult animals using the profile counting method.

Supported by the American Hearing Research Foundation

#### **548 The Role of Gli3 in Mouse Inner Ear Patterning**

**Jinwoong Bok<sup>1</sup>, Doris Wu<sup>1</sup>**

<sup>1</sup>*National Institute on Deafness and other Communication Disorders*

Previously, we have shown that Sonic hedgehog (SHH) is required for patterning the ventral inner ear structures in mouse and chicken, and the source of SHH is the ventral midline structures, the floor plate and notochord. GLI3 is a zinc finger transcriptional regulator and it can act as either an activator or repressor depending on the level of SHH signaling. It has been shown that the limb and neural tube defects observed in *Shh*<sup>-/-</sup> single mutant are partially rescued in *Shh*<sup>-/-</sup> and *Gli3*<sup>-/-</sup> double mutants. To understand the role of *Gli3* in mouse inner ear development and its interaction with SHH function, we examined normal expression patterns of *Gli* genes in the developing inner ear. In addition, we analyzed inner ears of mutant mice with various genetic combinations of *Shh* and *Gli3* mutant alleles.

*Gli3* expression in the otocyst is relatively uniform. In contrast, expression of another member of the *Gli* gene family, *Gli1*, is graded, stronger in the ventral and weaker in the dorsal region of the otocyst, consistent with their relative distances from the source of SHH in the ventral midline. These results suggest that the expression of *Gli1* but not *Gli3* in the inner ear is dependent on SHH, similar to what has been reported in other systems.

Inner ears from *Gli3* mutants lack the lateral semicircular canal, and the anterior semicircular canal is often missing or truncated. Yet, all sensory organs are present including the lateral crista. The dorsal malformations observed in *Shh*<sup>-/-</sup> mutants are rescued in the *Shh*<sup>-/-</sup>;*Gli3*<sup>+/-</sup> mice, probably due to an improved neural tube structure. In *Shh*<sup>-/-</sup>;*Gli3*<sup>-/-</sup> double mutants, the ventral inner ear structures that are absent in *Shh*<sup>-/-</sup> mutants are partially rescued. Dorsally, the inner ears display a phenotype similar to the *Gli3*<sup>-/-</sup> single mutants. These results suggest that GLI3 normally acts as a repressor of SHH functions in the ventral inner ear but its activity is independently required for canal development.

**549 Voltage-Sensitive and Ligand-Gated Channels in Differentiating Fetal Neural Stem Cells Isolated from the Non-Hematopoietic Fraction of Human Umbilical Cord Blood**

Wei Sun<sup>1</sup>, Leonora Buzanska<sup>2,3</sup>, Krystyna Domanska-Janik<sup>2</sup>, Michal K. Stachowiak<sup>3</sup>, Richard J. Salvi<sup>1</sup>

<sup>1</sup>Center for Hearing & Deafness, SUNY at Buffalo,

<sup>2</sup>Institute of Experimental and Clinical Medicine, Warsaw, Poland, <sup>3</sup>Molecular and Structural Neurobiology and Gene Therapy Lab, SUNY at Buffalo

Neural stem cells (NSC) hold potential for treating neurodegeneration in the peripheral or central auditory system; however, limited supply of embryonic and adult NSCs and the problem of immunological rejection make this impractical for humans. An alternative is to use bone marrow stromal cells that reportedly can integrate into damaged rat brain and differentiate into astrocytes and neurons. Human umbilical cord blood (HUCB) cells represent another source of multipotent stem cells with low antigenicity and high expansion potential. Recent studies have shown that NSC can be isolated from the non-hematopoietic fraction of HUCB. Nondifferentiated HUCB-NSC can be induced to differentiate into neuron-like cells expressing neuron-specific cytoskeletal markers; however, the functional properties of these cells are unknown. To address this issue, we used whole cell patch clamp recordings and immunocytochemistry to identify voltage-gated channels and ligand gated receptors on HUCB-NSC. NSC-D, which acquired neural phenotypes following attachment to polylysine/laminin surface and treatment with dBcAMP/ascorbic acid, displayed 2 types of voltage-sensitive currents, an inward rectifying potassium current (Kir) and an outward rectifying potassium current (IK+). Kir currents, reversibly blocked by external Cs+ or Ba2+, were present on most nondifferentiated and differentiation-induce NSC (NSC-D). In contrast, IK+ were absent from nondifferentiated NSC, but were present on 40% of NSC-D. IK+ was blocked completely by externally applied TEA and 4-AP and partially by Cd2+, but was not affected by Cs+. NSC-D expressing IK+ generated narrow depolarizing voltage spikes in response to current steps. Many NSC-D were immunopositive for glutamate, glycine, ACh-nicotinic, DA, 5-HT, and GABA receptors. Kainic acid (KA) induced an inward current in a small proportion of NSC-D. KA, glycine, DA, ACh, GABA, and 5-HT partially blocked the Kir current through their respective receptors. These results suggest that HUCB-NSC can differentiate toward neuron-like cells with functional voltage and ligand gated channels and appear to have the potential to differentiate into neurons if transplanted into the human auditory brain or spiral ganglion.

Supported by NIH P01 DC03600-01A1

**550 Hematopoietic Origin of Mesenchymal Cells and Fibrocytes in the Adult Inner Ear**

Hainan Lang<sup>1</sup>, Yasuhiro Ebihara<sup>2,3</sup>, Bradley A Schulte<sup>1,4</sup>, Richard A Schmiedt<sup>1</sup>, Samuel S Spicer<sup>4</sup>, Nancy Smythe<sup>1</sup>, Makio Ogawa<sup>2,3</sup>

<sup>1</sup>Department of Otolaryngology - Head & Neck Surgery, Medical University of South Carolina, <sup>2</sup>Department of

Medicine, Medical University of South Carolina, <sup>3</sup>Department of Veterans Affairs Medical Center, Charleston, SC, <sup>4</sup>Department of Pathology and Lab Medicine, Medical University of South Carolina

Bone marrow derived progenitor and stem cells have shown surprising plasticity with a capacity to differentiate into a variety of specialized cells. Bone marrow contains hematopoietic stem cells (HSCs) and progenitors and various types of stromal cells. To test the hypothesis that some cell types in cochlea are derived from HSCs, we transplanted a clonal population of HSCs derived from a single HSC into tail veins of lethally irradiated C57BL/6-Ly-5.1 mice. HSCs were prepared from bone marrow cells of transgenic enhanced green fluorescent protein (EGFP) mice (C57BL/6-Ly-5.2) by fluorescence-activated cell sorting. The clonally engrafted mice showed high-level and multilineage hematopoietic engraftment. Direct observation of EGFP epifluorescence or EGFP immunofluorescence was performed on inner ear tissues 2-5 months after transplantation. Many EGFP+ cells were found in the inner ears of transplanted mice in several areas including 1) types I, III, IV and V fibrocytes in the spiral ligament, 2) limbal fibrocytes, 3) fibrocytes in the saccule, utricle and ampulla, 4) bone-associated fibrocytes, 5) mesenchymal or tympanic covering cells under the basilar membrane, 6) unidentified cells in Rosenthal's canal and the cochlear and vestibular nerves and 7) unidentified cells in Reissner's and the round window membranes. These results suggest that many types of mesenchymal cells including fibrocytes in the adult inner ear are derived continuously from HSCs.

Supported by NIH NIA R01AG14748, NIDCD R01DC00713, NHLBI R01HL69123 and NHLBI R01HL57375.

**551 Sonic Hedgehog and Retinoic Acid Synergistically Promote Sensory Lineage Specification from Adult Pluripotent Stem Cells**

Eri Hashino<sup>1</sup>, Takako Kondo<sup>1</sup>, Scott Johnson<sup>1</sup>, Mervin Yoder<sup>1</sup>

<sup>1</sup>Indiana University School of Medicine

Recent studies demonstrated that stromal cells isolated from adult bone marrow have the competence of differentiating into neuronal cells *in vitro* and *in vivo*. However, the capacity of marrow stromal cells (MSCs) to differentiate into lineage-specific neurons and the identity of molecular factors that confer MSCs with the competence of a neuronal subtype have yet to be elucidated. Based on our flow cytometric analysis showing that the majority of purified MSCs constitutively express patched1 and RAR $\alpha$ , high-affinity receptors for Sonic hedgehog (Shh) and retinoic acid (RA), respectively, we hypothesized that MSCs are sensitive to Shh and/or RA signaling. To test this hypothesis, we incubated MSCs that had been exposed to neural induction reagents in the presence of Shh and/or RA. Shh and RA in combination, but not alone, induced more than 200-fold increases in *GATA3*, *Irxd2*, *Sox10*, *calretinin* and *GluR4* mRNAs, all of which are expressed during development in inner ear

sensory neurons. In addition, the differentiated MSCs displayed a range of mature neuron-specific antigens, including MAP2, TUJ1, NeuN and NF160. However, *Brn3a* was not detectable in MSCs that were treated with Shh and RA. To test the possibility that hitherto unknown proteins in the microenvironment surrounding the otocyst have effects on *Brn3a* expression, we incubated MSCs with E10 mouse hindbrain/somite/otocyst conditioned medium. Incubation with the conditioned medium for 3 days induced a 150-fold increase in *Brn3a*. Expression of *neuroD* and *neurogenin1* was also increased albeit at a lesser extent than that of *Brn3a*. These results demonstrate that Shh and RA exert synergistic effects on neural-competent MSCs to promote sensory neuron differentiation. The results also imply the existence of an unidentified protein(s) in the embryonic microenvironment that acts as a sensory differentiation factor.

### **552 Embryonic Organ of Corti Promotes Neuronal Differentiation and Axon Outgrowth from Adult Pluripotent Stem Cells in Vitro**

**Takako Kondo<sup>1</sup>, Eri Hashino<sup>1</sup>**

<sup>1</sup>*Indiana University School of Medicine*

Establishment of a successful cell-based therapy to replace damaged auditory neurons depends on the optimization of a host microenvironment in which donor stem cells can differentiate, extend their axonal processes and establish synaptic connections with hair cells in the organ of Corti. To investigate the interactions between adult pluripotent stem cells and host cochlear tissues in vitro, we established a three-dimensional co-culture system. Marrow stromal cells (MSCs) were isolated from TgN(ACTbEGFP) mice, in which enhanced GFP is expressed in most tissues including the bone marrow. Our flow cytometry analysis showed that approximately 93% of MSCs isolated from TgN(ACTbEGFP) mice were GFP-positive. Organ of Corti tissues were removed from E18 C57BL/6 mice and placed in 8-chamber slide wells. For each culture, one organ of Corti was embedded into rat type I collagen. Four to five hours after the start of incubation, GFP-positive MSCs at  $1 \times 10^3$  cells/5  $\mu$ L were placed onto collagen using a micropipette. On the following day, the medium was replaced with neural induction medium and incubation continued for an additional 3 days. In the presence of an organ of Corti explant, MSCs survived and propagated vigorously, but upon exposure to the neural induction medium, withdrew from the cell cycle and differentiated into neurons. In addition, the MSCs began expressing several sensory neuron-specific antigens, *Brn3a*, *GluR4* and *calretinin*, along with pan-neuronal markers, including *NF160*, *MAP2*, *tau* and *TUJ1*. Furthermore, MSC-derived neurons extended their processes towards outer hair cells in the organ of Corti explant. These results strongly suggest that protein(s) secreted from the embryonic cochlea have the ability (1) to regulate the expression of sensory neuron markers, and (2) to act as chemoattractant (s) for MSC-derived neurons.

### **553 Transplantation of Stem Cells Into the Embryonic Inner Ear**

**Kwang Pak<sup>1,2</sup>, Elisabeth Sauvaget<sup>1,2</sup>, Yan Li<sup>1</sup>, Allen F. Ryan<sup>1,2</sup>**

<sup>1</sup>*Department of Surgery/Otolaryngology, University of California, San Diego*, <sup>2</sup>*Veterans Affairs Medical Center, La Jolla, California, USA*

Sensorineural hearing loss and vestibular disorders are commonly caused by the loss of hair cells and/or primary sensory neurons. Stem cells have been successfully transplanted into the brain, suggesting the possibility of inner ear transplantation for replacement strategies. Furthermore, in utero transplantation is a promising approach to potential treatments of such disorders. In order to explore the potential of stem cell transplants into the inner ear, we performed exo utero and in utero injections of rat neural stem cells and mouse embryonic stem cells, stably transformed with GFP, into the region of the inner ear in embryonic day 14.5 (e14.5) mouse embryos. External landmarks were used to guide the injections. For exo utero transplants, dams were sacrificed at e18.5. After in utero injections, mice were sacrificed on postnatal day 0, 7 and 14. Controls included injection of killed GFP+ cells and free GFP.

Embryonic stem cells survived the transplant well, with most mice showing GFP+ cells in the region of the inner ear. When GFP+ cells were localized within the inner ear, they were found preferentially in the modiolus and spiral ganglion. In contrast, few cells were present in inner ear epithelia. With increased survival time, mortality increased, perhaps reflecting continued growth of the stem cells that were commonly observed in brain. Neural stem cells were observed in the inner ear after exo utero injection, typically in fluid spaces. However, neural stem cells were not observed in the inner ear after in utero transplantation. Typically, only a few cells were observed in brain adjacent to the ear.

The results indicate that embryonic stem cells have the potential to integrate into the inner ear, at least within the modiolar structures. Future studies will determine whether the cells adopt inner ear phenotypes, and how stem cell transplantation compares to that of embryonic inner ear cells.

Supported by the Research Service of the VA and by NIH/NIDCD grant DC00139.

## **554 The Potential of Embryonic Stem Cell-Derived Neurons for Innervation Into the Organ of Corti**

**Masahiro Matsumoto**<sup>1</sup>, Takayuki Nakagawa<sup>1</sup>, Tae-Soo Kim<sup>1</sup>, Toru Higashi<sup>1</sup>, Tomoko Kita<sup>1,2</sup>, Tatsunori Sakamoto<sup>3</sup>, Ken Kojima<sup>1</sup>, Tetsuji Sekiya<sup>1</sup>, Juichi Ito<sup>1</sup>

<sup>1</sup>*Department of Otolaryngology-Head and Neck Surgery, Graduate School of Medicine, Kyoto University,* <sup>2</sup>*Horizontal Medical Research Organization, Kyoto University Graduate School of Medicine, Kyoto, Japan,* <sup>3</sup>*Organogenesis and Neurogenesis Group, Center for Developmental Biology, RIKEN, Kobe, Japan*

Embryonic stem (ES) cells have been expected as a source for cell therapy for replacement of neural systems including spiral ganglion neurons. In this study, we investigated the potential of ES cell-derived neurons for innervation into the organ of Corti using explant culture systems. We used the co-culture of ES cells with PA6 cells, mouse skull bone marrow cells, as a method for neural induction of ES cells. ES cells genetically labeled with EGFP gene were used. Colonies that formed on the PA6 layer during the 6 days of culture were collected, and prepared as cell suspensions. Cochlear sensory epithelia obtained from P3 mice were co-cultured with ES cell suspensions for 7 days. Cochlear specimens cultured without supplement of ES cells were used as controls. At the end of the culture period, specimens were fixed with 4% PFA and provided for histological analysis in whole mounts or cross sections. Histological analyses demonstrated massive elongation of neurites from ES cells and attachment of the neurites to hair cells. Expression of synaptophysin was observed in the neurites of ES cell-derived neurons adjacent to the basal or basolateral portion of hair cells. These findings indicate a high potential of ES cell derived neurons as transplants for replacement of spiral ganglion neurons.

## **555 Functionality of Cochleae Received ES Cell Transplantation Into the Modiolus**

**Takayuki Nakagawa**<sup>1</sup>, Tuyoshi Endo<sup>1</sup>, Tomoko Kita<sup>1</sup>, Masahiro Matsumoto<sup>1</sup>, Tae-Soo Kim<sup>1</sup>, Koji Iwai<sup>1</sup>, Tetsuya Tamura<sup>1</sup>, Takayuki Okano<sup>1</sup>, Tatsunori Sakamoto<sup>2</sup>, Toru Higashi<sup>1</sup>, Ken Kojima<sup>1</sup>, Tetsuji Sekiya<sup>1</sup>, Fukuichiro Iguchi<sup>1</sup>, Juichi Ito<sup>1</sup>

<sup>1</sup>*Kyoto University,* <sup>2</sup>*RIKEN*

We have reported that ES cells treated with the stromal cell inducing activity (SDIA) can survive and differentiate into neurons following transplantation into the modiolus of deafened cochleae. ES cell-derived neurons exhibited massive elongation of their neurites and expression several neurotransmitters in the modiolus of cochleae. However, the functionality of cochleae received transplantation of ES cells was not insufficient. Sham-operated cochleae demonstrated no electrically evoked auditory brainstem responses (eABRs), while transplanted cochleae showed eABRs. However, thresholds of eABRs for transplanted cochleae were apparently higher than non-operated ones. These findings strongly suggest necessity of refinement of methods for transplantation. Here we report the functionality of cochleae received ES

cell transplantation by the refined method. We used mouse ES cells genetically labeled with GFP after treatment with the SDIA for 6 days as transplants. Hartley guinea pigs deafened by kanamycin and ethacrynic acid were used as recipient animals. We made a small perforation (approximately 180 micro meter in diameter) at the bony wall of Rosenthal's canal in the basal turn of cochleae. ES cells were introduced into the cochlear modiolus from this perforation via a polyimide tube. We specially paid attention to avoid injury to cochlear nerve fibers. Three weeks later, we measured eABRs of transplanted cochleae and contra-lateral, non-operated ones. Transplanted cochleae exhibited significantly lower eABR thresholds in comparison with those of non-operated ones. We will discuss the relationship between functionality and morphology of transplanted cochleae.

## **556 Transplantation of Embryonic Stem Cell-Derived Neurons Into Vestibular Sensory Epithelia In Vitro**

**Tae Soo Kim**<sup>1</sup>, Takayuki Nakagawa<sup>1</sup>, Masahiro Matsumoto<sup>1</sup>, Toru Higashi<sup>1</sup>, Tomoko Kita<sup>1,2</sup>, Tatsunori Sakamoto<sup>3</sup>, Ken Kojima<sup>1</sup>, Juichi Ito<sup>1</sup>

<sup>1</sup>*Department of Otolaryngology-Head and Neck Surgery, Graduate School of Medicine, Kyoto University,* <sup>2</sup>*Horizontal Medical Research Organization,* <sup>3</sup>*Organogenesis and Neurogenesis Group, Center for Developmental Biology, RIKEN*

We have reported the possibility of hair cell replacement in vestibular epithelia by transplantation of neural stem cells. Recent studies have suggested the potential of transplantation of embryonic stem (ES) cells for the treatment of inner ears. In the current study, we investigated the potential of ES cell transplantation for treatment of vestibular sensory epithelia. ES cells pre-treated with stromal cell-derived inducing activity, which induces efficient neural differentiation of ES cells, were used as transplants. Utricles dissected from P3 mice were used as recipients. Vestibular sensory epithelia were isolated by the thermolysin treatment, and cultured in serum-free medium for 24 h. Vestibular epithelia were then co-cultured with ES cell-derived cells for 7 days. Organotypic cultures of vestibular epithelia without ES cells were used as controls. Immunohistochemistry for class III beta tubulin were revealed massive elongation of neurites from ES cell-derived cells into vestibular epithelia. Some neurites from ES cell-derived cells attached to the basal or basolateral portion of sensory hair cells. Immunohistochemistry for synaptophysin indicated the formation of synaptic connections between neurites from ES cell-derived cells and sensory hair cells. These findings indicate the potential of ES cell-derived cells for replacement of neural tissues in vestibular systems.

## **557 Expression of Myosin VIIa in Embryonic Stem Cells Treated with the Stromal Cell-Derived Inducing Activity**

**Toru Higashi**<sup>1,2</sup>, Takayuki Nakagawa<sup>2</sup>, Tomoko Kita<sup>2,3</sup>, Shinji Takebayashi<sup>2</sup>, Tae-Soo Kim<sup>2</sup>, Masahiro Matsumoto<sup>2</sup>, Kouji Iwai<sup>2</sup>, Tatsunori Sakamoto<sup>4</sup>, Juichi Ito<sup>2</sup>

<sup>1</sup>*School of Medicine, Kyoto University*, <sup>2</sup>*Department of Otolaryngology, Head & Neck Surgery, Graduate School of Medicine, Kyoto University*, <sup>3</sup>*Horizontal Medical Research Organization, Graduate School of Medicine, Kyoto University*, <sup>4</sup>*Organogenesis and Neurogenesis Group, Center for Developmental Biology, RIKEN*

Embryonic stem (ES) cells are capable of self-renewal and pluripotency. They have therefore been considered as a basis for cell therapy in a range of organs. Co-culture of ES cells with PA6 stromal cells can induce differentiation into different types of neural cells including sensory progenitors. In the current study, we examined expression patterns of myosin VIIa and other hair cell-markers in ES cells co-cultured on PA6 stromal cells supplemented with BMP4 at different time points. ES cells were co-cultured on the layer of PA6 cells and BMP4 was supplemented in the culture medium 3, 4 or 5 days after the beginning of co-culture. After 6 day-culture, SDIA-treated ES cells were collected and cultured on the mesh in GMEM medium supplemented with 10% knockout serum replacement/1 mM pyruvate/0.1 mM nonessential amino acids/0.1 mM 2-mercaptoethanol for 7 days, and fixed with 4% PFA and provided for immunohistochemistry. A part of ES cells supplemented BMP4 from day 3 or 4 exhibited expression of myosin VIIa. Myosin VIIa-positive cells were surrounded by class III beta-tubulin-positive cells. No myosin VIIa-positive cells were found in ES cells supplemented BMP4 from day5. On the other hand, no expression of Pax2, calbindin, Math1 or Brn3c was identified in myosin VIIa-positive cells. These findings suggest that early exposure to BMP4 induces differentiation of ES cells into Myo7a-positive cells, but not an actual immunophenotype of hair cells.

## **558 Induction of Differentiation of Otic Progenitor Cell Lines Into the Hair Cell Immunophenotypes by DMSO**

**Koji Iwai**<sup>1</sup>, Ken Kojima<sup>1</sup>, Sunaho Tamura<sup>2</sup>, Shinji Takebayashi<sup>1</sup>, Tomoko Kita<sup>1</sup>, Takayuki Nakagawa<sup>1</sup>, Juichi Ito<sup>1</sup>

<sup>1</sup>*Kyoto university hospital*, <sup>2</sup>*Keihanna sinkori hospital*

Induction of differentiation of otic progenitor cell lines into the hair cell immunophenotypes by DMSO

We have previously shown that multipotent otic progenitor cells were established from embryonic day 12.5 (E 12.5) rat otocysts by use of serum free culture medium containing epidermal growth factor (EGF). The progenitor cells possess potentials to differentiate into not only sensory epithelial cell lineages but also neural cell lineages. However, the precise differentiation mechanism has not yet been determined. Here, we have attempted to induce differentiation in the cell cultures by using dimethyl sulfoxide (DMSO). The several reports have shown DMSO

has abilities to induce immature cell cultures to differentiate into mature cell phenotypes.

Before the induction of differentiation, 90% of the progenitor cells were immunoreactive for nestin (one of immature cell markers), while 3% of progenitor cells only positive for myosin7a (one of hair cell markers). After treatment of DMSO, the number of nestin positive cells decreased (4% of the progenitor cells), suggesting that the addition of DMSO led to the decrease in the number of undifferentiated cells. On the other hand, DMSO treatment resulted in the appearance of myosin7a positive cells (85% of the progenitor cells), while it showed no effect on neurofilament (NF200) and neuron specific enolase (NSE) levels which are known as markers of neural cell lineages.

Our results suggest that DMSO has a potential to induce the differentiation of the otic progenitor cell line to hair cells, but not to neural cells, from the otic progenitor cells in vitro. The results of this study should help to further understand the mechanism of differentiation multipotent otic progenitor cells.

## **559 Stem Cell-Derived Neural Progenitor Grafts Re-Innervate the De-Afferented Organ of Corti in Vivo**

C. Eduardo Corrales<sup>1,2</sup>, Luying Pan<sup>1,2</sup>, Stefan Heller<sup>1,2</sup>, M. Charles Liberman<sup>1,2</sup>, **Albert Edge**<sup>1,2</sup>

<sup>1</sup>*Department of Otolaryngology, Harvard Medical School*, <sup>2</sup>*Eaton-Peabody Laboratory, Massachusetts Eye and Ear Infirmary 243 Charles Street, Boston, MA 02114*

We are attempting to regenerate spiral ganglion neurons in animal models of primary neuronal degeneration using fetal cells and stem cells as a source for neurons. Mouse embryonic stem (ES) cells that had been selectively guided to become neural progenitors were assessed for their ability to generate new neurons that could re-innervate the organ of Corti after chemical de-afferentation.

Application of ouabain to the round window niche (day 0) in gerbils results, within one week, in the loss of >90% of spiral ganglion neurons without significant hair cell damage (Schmiedt et al, JARO 3:223-233, 2002). Neural progenitor cells derived from R1-EYFP mouse ES cells were suspended in medium and microinjected into the modiolus via the round window niche (day 7-21) into the treated ear. Animals were immunosuppressed from the day of transplantation until tissue harvest, from 2 to 90 days later. CAPs and DPOAEs were measured bilaterally at the time of surgery and at the time of tissue harvest. The transplanted cells identified by endogenous EYFP expression survived and could be found in clearly identifiable clusters in the modiolus of the basal and middle turns of the cochlea. The grafts derived from the neural progenitors express neuronal markers and send out processes. Tracking of the immunohistochemically stained processes through semi-serial sections indicates that, after 2-3 months, the neurons have grown preferentially toward the organ of Corti. The neurites cross the spiral ganglion, where few original neurons remain, and continue in large numbers through the osseous spiral lamina into the



sensory epithelium that lacks host spiral ganglion cell innervation.

The growth of neuronal processes from grafted neuronal progenitor cells into the organ of Corti suggests that the stem cell-derived neurons can follow the passage left by the degenerated neurons in response to cues for regeneration from the host cochlear sensory epithelium. These data are currently allowing us to examine the connections that these replacement neurons are establishing with hair cells and raise the possibility that functional recovery in cases of primary neuronal degeneration may be achievable.

Supported by NIDCD grants DC006789 (AE), DC00188 (MCL), P30 005209 (MCL) and DC006167 (SH).

### **560** Formation of Synapses between Hair Cells and Engrafted Neurons in the in Vitro Organ of Corti

Rodrigo Martinez-Monedero<sup>1,2</sup>, C. Eduardo Corrales<sup>1,2</sup>, Math Cuajungco<sup>1,2</sup>, Stefan Heller<sup>1,2</sup>, Albert Edge<sup>1,2</sup>

<sup>1</sup>Department of Otolaryngology, Harvard Medical School, <sup>2</sup>Eaton-Peabody Laboratory, Massachusetts Eye and Ear Infirmary, 243 Charles Street, Boston, MA 02114

We are attempting to regenerate spiral ganglion neurons and hair cells using stem cell-derived neural and inner ear progenitors. To determine the optimal conditions for cell engraftment, we developed an in vitro model system in which we specifically eliminate either spiral ganglion neurons or hair cells by means of drug treatment as well as genetic manipulation and then test the ability of stem cell-derived progenitor cells to engraft and regenerate neurons and hair cells. Organ of Corti culture was established from P0-P3 mice and was performed for up to 14 days. The specific ablation of spiral ganglion neurons was achieved by treatment with  $\beta$ -bungarotoxin for 48 h leaving the hair cells intact. Hair cells could be removed from the organ of Corti by treatment with gentamicin for 48 h. Organ of Corti culture from neurogenin 1-/- mice was established at P0 (the homozygous mice do not survive beyond P0) and yielded cultures lacking spiral ganglion neurons. The organ of Corti after  $\beta$ -bungarotoxin treatment had a similar appearance to that from a neurogenin1-/- mouse as detected by immunostaining with antibodies for  $\beta$ -III tubulin and parvalbumin 3.

Primary neurons derived from P1 spiral ganglion were tested first in the denervated organ of Corti and were shown to grow processes toward the sensory epithelium where they formed synapses with hair cells (shown by  $\beta$ -III tubulin and synapsin staining). Neurons formed connections with outer hair cells and inner hair cells, and in some cases branched to form synapses with multiple outer hair cells. To compare the capacity of other cell types to the P1 spiral ganglion neurons, the same conditions were used with embryonic spiral ganglion cells and neurons derived from embryonic and adult inner ear stem cells isolated from vestibular and cochlear tissues. Adult inner ear stem cells gave rise to neurons in co-culture with the denervated organ of Corti, and these neurons grew processes that made contact with hair cells.

The in vitro assay system is useful for testing conditions for engraftment of transplanted cells and for investigation of mechanisms of regeneration of the organ of Corti. The progenitor cell types that perform best in this in vitro system are candidates for in vivo regeneration experiments.

Supported by National Institutes of Health grants DC006789 (to AE) and DC006167 (to SH).

### **561** Expression of p27Kip1 and Hair Cell Differentiation in Adult Mouse Cochlear Progenitor Cell Culture

Patricia Wilson<sup>1</sup>, Hong-Bo Zhao<sup>1</sup>

<sup>1</sup>Dept. of Surgery-Otolaryngology, University of Kentucky Medical Center, Lexington, KY 40536

During organic development rapid down-regulation of a cell cycle inhibitor, p27<sup>Kip1</sup>, is associated with Math1 gene expression in hair cell differentiation. p27<sup>Kip1</sup> persists at high expressive levels in mammalian supporting cells after birth, but has no expression in hair cells. Previously we have shown that some cells derived from the cochlea of adult mice and guinea pigs possess stem progenitor cell properties, as these cells are capable of proliferation and differentiation in cell culture. In this study, the cochlear sensory epithelia of adult mice were micro-dissected and dissociated cells were cultivated using the cell culture technique that we developed for guinea pig cells. Three mouse cell lines (C, D and F) that have been passaged multiple times with retention of stable morphological phenotypes were characterized by immunofluorescent staining. All three mouse cell lines were positive for Nestin and Brn3.1c, revealing progenitor cell characteristics. Cell line C and D showed negative staining for p27<sup>Kip1</sup>, but Math1 was detectable in double staining. In cell line F, staining for p27<sup>Kip1</sup> was positive but Math1 staining was undetectable. In addition, positive staining for hair cell markers Myosin VIIa and prestin could be found in cell line C and D, but not in cell line F. These data supported our hypothesis that p27<sup>Kip1</sup> may negatively control hair cell generation.

Supported by National Organization for Hearing Research Foundation and UKMC Research Fund

### **562** Overexpression of Bcl-2 Promotes Embryonic Stem Cell Survival in the Gerbil Inner Ear

Hainan Lang<sup>1</sup>, Richard A Schmiedt<sup>1</sup>, Michelle Hedrick<sup>2</sup>, Ling Wei<sup>2</sup>, Bradley A Schulte<sup>1,2</sup>

<sup>1</sup>Department of Otolaryngology - Head & Neck Surgery, Medical University of South Carolina, <sup>2</sup>Department of Pathology and Lab Medicine, Medical University of South Carolina

Mouse embryonic stem (ES) cells can survive and differentiate into neural phenotypes after direct transplantation into Rosenthal's canal of the gerbil (Lang et al., ARO Abs. 27: 93, 2004). However, apoptotic cell death was found in some implanted ES cells at one to four weeks after transplantation. Here we investigated the effects of overexpressing the anti-apoptotic gene bcl-2 on

mouse ES cell survival after transplantation. Gerbil cochleas were deafened by applying ouabain to the round window membrane which resulted in the complete loss of type I ganglion neurons. Wild type (wt, D3 cell line) and human bcl-2 overexpressing ES cells (bcl-2 ES cells) were differentiated in vitro using the 4-/4+ method (Wei et al., Stroke 34: 29, 2003). A volume of 1  $\mu$ l with an ES cell density of 2-4 x 10<sup>7</sup> cells/ml was injected into Rosenthal's canal and the perilymph of ears one to seven days after ouabain exposure. Physiologic and histologic examination of the cochleas was performed one to six weeks after implantation. Surviving bcl-2 ES cells were found in about 93 % of the implanted cochleas (n = 27), whereas wt ES cells survived only in about 63 % of the cochleas (n = 11). Thus, overexpression of bcl-2 significantly enhanced the survivability of the implanted ES cells. In addition, angiogenesis was seen within bcl-2 ES cell colonies in three implanted cochleas four weeks after transplantation, whereas, angiogenesis was never seen in cochleas implanted with wt ES cells. The rescue of type I neurons was seen in the apical turn of one cochlea that received bcl-2 cells 18 hours after ouabain exposure. In this cochlea, compound action potential thresholds to low frequency stimuli were almost normal.

Supported by NIH/NIA R01AG14748, NIDCD R01DC00713, NINDS R01NS37372, NINDS R01NS45155 and AHA-Burgher Award 10063N.

### **563 Neural Stem Cells Differentiate into Cochlear Cell Types after Transplantation**

**Mark Parker**<sup>1,2</sup>, Brianna Gray<sup>1</sup>, Deborah Corliss<sup>1</sup>, M Charles Liberman<sup>2,3</sup>, Evan Y Snyder<sup>4</sup>, Richard P Bobbin<sup>5</sup>, Douglas Cotanche<sup>1,2</sup>

<sup>1</sup>Childrens Hospital-Boston, <sup>2</sup>Harvard Medical School, <sup>3</sup>Eaton Peabody Laboratory-MEEI, <sup>4</sup>Burnham Institute, <sup>5</sup>LSU Health Sciences Center

We transplanted c17.2 Neural Stem Cells (NSCs) into the of cochleas of sound damaged mice and guinea pigs then determined the cell fates of transplanted cells using immunohistochemistry and fluorescent in situ hybridization (FISH). We found that the transplanted NSCs migrated throughout the cochlea and differentiated into both neural and non neural cochlear tissue depending upon their location within the cochlear microenvironment. For instance, transplanted NSCs that had migrated to the spiral ganglion adopted both the morphology and expression patterns of Type 1 spiral ganglion neurons, satellite cells, and Schwann cells. Additionally, transplanted stem cells that had migrated to the organ of Corti had adopted both the morphologies and expression patterns of inner phalangeal cells, pillar cells, dieter's cells and hair cells. These results indicate that the cochlear microenvironment plays a key role in regulating NSC differentiation into specific cell types of the organ of Corti and auditory nerve. Moreover, it suggests that the mature cochlea retains signals necessary to direct NSC differentiation into cochlear cells, even though it cannot regenerate these cells on its own. Our results provide promise that NSCs may eventually be used therapeutically to replace damaged cochlear tissue.

### **564 NT-3 Enhances the Neuronal Differentiation of Grafted Neural Stem Cells in an Ototoxin-Damaged Mouse Cochlear Explant**

**Sophie Martin**<sup>1</sup>, Christopher Cederroth<sup>2</sup>, Cecile Dromard<sup>1</sup>, Philippe Hugnot<sup>1</sup>, Thomas Van de Water<sup>3</sup>, Jean Luc Puel<sup>1</sup>, Azel Zine<sup>1</sup>

<sup>1</sup>INSERM U583, <sup>2</sup>Department of Zoology, University of Genava, Switzerland, <sup>3</sup>Cochlear Implant Research Program, University of Miami Ear Institute, Department of Otolaryngology

Most types of acquired hearing loss arise from damage to, or loss of, cochlear hair cells and associated spiral ganglion neurons. Numerous studies have indicated that neural stem cells (NSC) are immature, multipotent cells that have retained the capacity to differentiate into a variety of cell types depending on their response to local environmental cues. The initial objective of our research is to assess the ability of NSC to integrate into injured cochlear sensory epithelium and to replace damaged hair cells and/or associated auditory neurons. To this end, we isolate NSC from the spinal cords of embryonic GFP transgenic mice and grafted them into organotypic cultures of ototoxin-damaged postnatal day-3 mouse cochleae. The expression of GFP, hair cell, and neuronal differentiation markers were evaluated at 3 to 7 days post-grafting. Our data indicate that a supplementation of the culture medium with neurotrophin-3 (NT3) enhanced NSC expression of neuronal markers (MAP2, neurofilament) at the expense of astrocytic differentiation marker (GFAP). In contrast, NT-3 supplementation did not enhance the expression of any of the hair cell differentiation markers (Math-1 and Myosin 7a). There was a significant difference in the neuronal differentiation in the NT-3 supplemented, ototoxin-damaged cochlear explants as compared to the level obtained in the NT-3 non-supplemented, damaged, control explants. In the NT-3 supplemented ototoxin-damaged explants, a large number of the grafted NSC were found to differentiate into neurons that also generated peripheral processes.

These findings suggest that combining NSC grafting with an adequate level of neurotrophin support can create a useful strategy to repair and/or replace lost or damaged auditory neurons in a traumatized cochlea.

### **565 Interaction of Tamoxifen with Noise Induced Hearing Loss**

**Jagan Pillai**<sup>1</sup>, Jonathan Siegel<sup>1</sup>

<sup>1</sup>Northwestern University

The ototoxicity of the commonly used anticancer drug Tamoxifen and its interaction with noise exposure was evaluated in mongolian gerbils. A randomized double blind study was conducted whereby the animals were injected i.p with either Tamoxifen (~10mg/kg) or placebo. Five hours after injection of Tamoxifen or a placebo, the gerbils were exposed to a 108 dB SPL one-third octave narrow band noise centered at 8 kHz for 30 minutes. Compound Action Potential (CAP) thresholds, Distortion Product Otoacoustic Emissions (DPOAE), and Stimulus Frequency

Otoacoustic Emissions (SFOAE), were measured 30-35 days after noise exposure. To test the effect of Tamoxifen on hearing in the absence of noise exposure, CAP, DPOAE, SFOAE, were measured 30-35 days after administering a Tamoxifen or placebo injection in a second group of gerbils.

In gerbils exposed to both noise and Tamoxifen, the mean CAP thresholds were significantly increased in the frequency range of maximum expected noise damage (8-15Khz). A smaller increase in average thresholds in the 1-7Khz range of frequencies not expected to be affected by the noise was also noted. In contrast, there was no significant difference in the CAP thresholds between the Tamoxifen and control groups not exposed to noise.

It was concluded that Tamoxifen potentiates the effects of noise exposure on hearing loss. The higher thresholds consistently seen across most frequencies in the Tamoxifen group following noise exposure could be due to the additive ototoxic effect of Tamoxifen and other factors that may have been influenced by noise. For example, decreased blood flow and decreased oxygenation to the organ of Corti, that affects the entire cochlea, may have potentiated the ototoxic effect of Tamoxifen, even in regions not expected to be damaged by noise exposure.

Supported by NIH grant R01 DC03416

### **566 Towards Intracochlear Monitoring of Reactive Oxygen Species During Noise Exposure**

**Alexander Scheeline**<sup>1</sup>, Jonathan H. Siegel<sup>2</sup>, Theodore E. Lapainis<sup>1</sup>, Roger W. Smith<sup>1</sup>, Christopher T. Sorce<sup>1</sup>

<sup>1</sup>University of Illinois at Urbana-Champaign, <sup>2</sup>Northwestern University

Oxidative stress is correlated with noise-induced hearing loss. Whether radical generation in the *Stria* or reactive oxygen species (ROS) diffusion from cells injured or killed by intense sound are the source of such stress remains unclear. Pharmacological data are ambiguous. To clarify the mechanisms by which ROS damage cochlear cell membranes, we are developing implantable sensors. These are three-electrode amperometric sensors with enzyme-modified working electrodes to monitor hydrogen peroxide, superoxide, and (potentially) other oxidizable or reducible species simultaneously. The pseudoreference junction is tungsten/tungsten oxide embedded in polypyrrole, and the counter electrode is polypyrrole on gold. Mongolian gerbils will be used as test subjects. Methods for fabricating biocompatible amperometric sensors are described, calibration and interference issues are addressed, and we demonstrate the effect of noise-induced convection on sensor response. By characterizing the sensors in synthetic perilymph, matrix mismatch between calibration and *in situ* measurement is minimized.

### **567 Oxidative Stress Pathways in the Potentiation of Noise-Induced Hearing Loss by Acrylonitrile**

**Benoit Pouyatos**<sup>1</sup>, Caroline Gearhart<sup>1</sup>, Laurence Fechter<sup>1</sup>

<sup>1</sup>Loma Linda VA Medical Center

We hypothesize that disruption of intrinsic antioxidant defenses is a key mechanism whereby chemical contaminants potentiate noise-induced hearing loss (NIHL). This hypothesis was tested using acrylonitrile (ACN), a widely used industrial chemical whose metabolism is associated with significant potential for oxidative stress. ACN conjugates glutathione (GSH), depleting this important antioxidant rapidly. A second pathway involves oxidation by cytochrome P450 2E1 (CYP2E1) that leads to the formation of cyanide as a by-product, which can in turn inhibit superoxide dismutase (SOD). We have shown recently that ACN can potentiate NIHL and cochlear hair cell loss, even when noise levels approach permissible human exposure levels. However, the relative involvement of GSH depletion and/or cyanide production in this mechanism of potentiation is still unknown. Determining the relative contribution of these two pathways by compromising the alternate branch pharmacologically will further delineate the role of specific antioxidants in the protection of the cochlea, thus enhancing the therapeutic possibilities. In the present study, we focused on the oxidative metabolism of ACN that leads to cyanide production. Long-Evans rats were exposed to an octave band noise (97 dB), or to noise in combination with ACN. In an additional group of noise-exposed animals, ACN was injected in conjunction with 4-methylpyrazole (4MP), a drug that prevents ACN from being oxidized by CYP2E1, in order to prevent cyanide formation. 4MP injection preceding ACN reduced cyanide formation to undetectable levels. While rats treated with both ACN and noise showed a profound loss of DPOAE amplitude relative to rats receiving noise alone, 4-MP treatment offered protection against the disruptive effect of ACN+noise. However, the protection was not complete suggesting that GSH depletion might also be involved in that potentiation. Supported in part by grants OH03481 and DC05503.

### **568 Genetic Impairment of Ceruloplasmin, an Iron Regulatory Protein, Promotes Noise-Induced Hearing Loss (NIHL) and Age-Related Hearing Loss (ARHL)**

**Kevin K. Ohlemiller**<sup>1</sup>, Patricia M. Gagnon<sup>1</sup>

<sup>1</sup>Washington University Medical School, Department of Otolaryngology

Mutations that impair cellular regulation of reactive oxygen species (ROS) can promote NIHL and ARHL (Ohlemiller et al., JARO, 2000; ANO 1999; McFadden et al., JCN, 1999). Since iron can participate in reactions that generate ROS, disruption of iron metabolism may have a similar effect on hearing. We evaluated the impact of a null mutation for ceruloplasmin (Cp), a protein that helps clear iron from many tissues, on both NIHL and ARHL in mice.

Cp knockout (KO) and wild type (WT) mice kindly provided by Dr. Z. Leah Harris (Harris et al., PNAS, 1999) on an inbred C57BL/6 background were bred at our facility. Cp KOs are outwardly healthy and have normal fecundity and lifespan. Male and female KO (n=8) and WT (n=12) mice underwent ABR testing (5, 10, 20, 28.3, and 40 kHz) at 2.5 mos of age, followed by broadband noise exposure (4-45 kHz, 110 dB SPL, 15 min), and retest 2 wks post-exposure. Cp KO mice showed significantly higher thresholds than WT, both before and after exposure (2-way ANOVA,  $p < 0.001$ ). KO thresholds ranged 2-10 dB and 0-15 dB higher than WT thresholds before and after exposure, respectively. In a separate experiment, thresholds in 6 mo old Cp KO (n=8) and WT (n=12) mice were compared, then compared again at 9 mos. Cp KO mice showed significantly higher thresholds at both ages (2-way ANOVA,  $p < 0.001$ ). KO thresholds ranged 2-18 dB and 5-14 dB higher than WT thresholds at 6 and 9 mos, respectively.

Our data show that genetic disruption of iron metabolism can promote both NIHL and ARHL, and support a mechanistic link between cochlear injury and apparent aging processes. Oxidative stress may be fundamental to this relation. While hearing loss promoted by Cp dysfunction appears sensorineural, it remains to be confirmed that it is principally due to iron storage within cochlear sensory cells, and not secondary to systemic effects of iron storage.

(Supported by NIH DC03454 to KKO)

### **569 Noise-Damage vs. Exposure-Level Functions in 'Resistant' Strains of Mice: Divergent Behavior Suggests Different Underlying Mechanisms**

Lija M. Enas<sup>1</sup>, M. Charles Liberman<sup>2,3</sup>, Bruce L. Tempel<sup>4,5</sup>, Sharon G. Kujawa<sup>2,3</sup>

<sup>1</sup>Dept. of Audiology, Massachusetts Eye and Ear Infirmary,

<sup>2</sup>Dept. of Otolaryngology, Harvard Medical

School, <sup>3</sup>Eaton-Peabody Laboratory, Massachusetts Eye

and Ear Infirmary, <sup>4</sup>Dept. of Otolaryngology-HNS,

University of Washington, <sup>5</sup>V.M. Bloedel Hearing Research Center

Study of noise-induced hearing loss in mice has revealed several particularly noise-resistant strains. 129S6/SvEvTac (129S6) and MOLF/Ei (MOLF), for example, show much smaller noise-induced permanent threshold shifts (NIPTS) than CBA/CaJ (CB) after identical exposure (8-16 kHz OBN, 103 dB SPL, 2 hr) when evaluated by ABR and DPOAE (5.6-45.2 kHz) 2 weeks post-exposure. The resistant strains also show smaller threshold shifts 1 day post-exposure, especially at frequencies below the exposure band. Moreover, when CB exposure level is reduced so that 1-day shifts match those of 129S6 or MOLF at a higher SPL, the subsequent recovery in CB is less complete than for the resistant strains. These results suggest that noise resistance in 129S6 and MOLF arises both in the mechanisms governing the initial response to the exposure, as well as from enhanced recovery from acute damage.

Present studies of the two resistant strains, however, suggest that mechanisms underlying their resistance differ. First, noise damage vs. exposure level functions are qualitatively different for 129S6 and MOLF. As exposure levels increase from 94 to 106 dB SPL, NIPTS in 129S6 grows very slowly. In contrast, MOLF reaches a critical exposure level above which NIPTS increases rapidly with exposure level. MOLF is resistant in that this critical SPL is higher than that in CB (103 vs. 97 dB SPL), shifting its noise damage vs. level function rightward relative to CB. 129S6 is resistant in that, within the exposure range tested, there is no critical level above which the NIPTS growth accelerates. Second, for CB and MOLF, the lowest frequency at which a criterion NIPTS occurs decreases dramatically (place moves apically) as exposure level increases. For 129S6, the frequency of this criterion NIPTS moves little – and then increases slightly (place moves basally) – as exposure level is increased. Comparisons of the underlying cochlear histopathology are underway.

NIDCD R21 DC04983 (SGK), RO1 DC00188 (MCL), P30 DC005209 (MCL), RO1 DC006305 (BLT)

### **570 Hearing Loss in Mice Lacking TRPV4 Channels**

Keiji Tabuchi<sup>1</sup>, Akiko Nakamori<sup>1</sup>, Akira Hara<sup>1</sup>

<sup>1</sup>Institute of Clinical Medicine, University of Tsukuba

The sense of hearing relies on the sensory hair cells and their transduction channels localized at the tips of stereocilia of hair cells. The transduction channels are mechanosensitive nonselective cation channels opened by deflections of the stereocilia. Transient receptor potential channel vanilloid subfamily 4 (TRPV4), a member of TRP family, is a mechanosensitive nonselective cation channel, which has been implicated as a transducer of acoustic stimuli. On the other hand, Greene et al. (2001) have reported that DFNA25, an autosomal dominant nonsyndromic hearing loss, maps to 12q21-24 and that TRPV4 is one of candidate genes in this region. We therefore examined the effects of disruption of TRPV4 in mice on cochlear functions by analyzing auditory brainstem response (ABR) and distortion-product otoacoustic emission (DPOAE). TRPV4-knockout mice (TRPV4<sup>-/-</sup>) were produced and maintained on a C57BL/6 background (4th generation). Sex and age-matched wild type mice (TRPV4<sup>+/+</sup>) were used as controls. ABR and DPOAE testings were performed on the mice of 8 and 24 weeks of age. There was no statistically significant difference in the ABR threshold or DPOAE amplitude between the TRPV4<sup>-/-</sup> and the TRPV4<sup>+/+</sup> mice at 8 weeks of age. However, the ABR threshold was significantly elevated in the TRPV4<sup>-/-</sup> mice as compared with the TRPV4<sup>+/+</sup> mice at 24 weeks of age although disruption of the TRPV4 did not affect the DPOAE amplitude. In addition, the auditory threshold shift was significantly larger in the TRPV4 knockout than in the TRPV4<sup>+/+</sup> mice one week after the acoustic overexposure of 128 dB SPL for 4 hours. The present findings suggest that TRPV4 does not encode an essential component of a transduction channel of hair cells of mice and that disruption of TRPV4

causes delayed-onset hearing loss and makes the cochlea vulnerable to acoustic injury.

### **571 Bcl-2 Genes Regulate Noise-Induced Hearing Loss**

Daisuke Yamashita<sup>1,2</sup>, Shujiro Minami<sup>1,2</sup>, Kaoru Ogawa<sup>1</sup>, Josef Miller<sup>2,3</sup>

<sup>1</sup>Department of Otolaryngology, Keio University Hospital, Tokyo, Japan, <sup>2</sup>University of Michigan, Kresge Hearing Research Institute, Ann Arbor, Michigan, <sup>3</sup>Center for Hearing and Communication, Karolinska Institutet, Stockholm, Sweden

Proteins of the Bcl-2 family have been implicated in control of mitochondrial apoptotic pathways modulating neuronal cell death, including noise-induced hearing loss (NIHL). This protein family includes anti-apoptotic and pro-apoptotic members. In this study, we assessed the expressions of anti- and pro-apoptotic Bcl-2 genes, represented by Bcl-xL and Bak, respectively, following noise exposures yielding permanent threshold shift (PTS) or temporary threshold shift (TTS).

Auditory brainstem responses (ABRs) were assessed at 4, 8 and 16KHz before and 1, 3, 7 and 10 days following exposure to 120 dB SPL, 4 kHz OBN, 5h (PTS) or 100 dB SPL, 4 kHz OBN, 1h (TTS), n=5 each at each exposure level. This was followed on day 10 by sacrifice and quantitative hair cell assessment. ABR thresholds increased following both exposures, fully recovering following the TTS exposure, and showing a 24dB (4kHz), 44dB (8kHz) and 45.5dB (16kHz) mean shift on day 10 following the PTS exposure, which was also accompanied by extensive outer hair cell loss in the 4 kHz region. Twenty-five additional animals were sacrificed on day 1 following both exposures, plus 5 unexposed controls, for immunohistochemical assessment (n=15) and hair cell counts (n=10). Following the PTS exposure Bak was clearly expressed in outer hair cells, while Bcl-xL was expressed (outer hair cells) only following the TTS exposure. These results indicate the important role of Bcl-2 family proteins in regulating cell death or survival in NIHL and specifically suggest that Bcl-xL protects dying cells in TTS, while Bak promotes apoptosis in PTS.

This work was supported by NIH grant DC 04058, General Motors, and the Ruth and Lynn Townsend Professorship.

### **572 Noise Exposure Activates Proapoptotic Bcl-2 Family Members in the Mouse Cochlea**

Maria Angeles Vicente-Torres<sup>1</sup>, Yajun Guan<sup>1</sup>, Su-Hua Sha<sup>1</sup>, Jochen Schacht<sup>1</sup>

<sup>1</sup>Kresge Hearing Research Institute, University of Michigan, Ann Arbor, MI-48109-0506

Acoustic trauma induces several molecular events, such as the formation of free radicals or the activation of different proteases, kinases and phosphatases, which lead to the death of cochlear sensory hair cells. The aim of the present study was to evaluate the state of some pro-apoptotic Bcl-2 family members in a mouse model of noise exposure. CBA mice were exposed to a broadband noise (2-20 kHz) for 2 hours or kept in silence. The intensity of

the stimulus was: 96 dBA or 106 dBA. Exposure to 96 dBA provoked a temporary threshold shift of about 40 dB at two hours after the cessation of the stimulus, which was gradually recovered and disappeared 3 days after the stimulus. However, exposure to 106 dBA provoked a permanent threshold shift of 40 dB from one week after the noise exposure on. Pro-apoptotic Bcl-2 family members were analyzed by Western blot from 10 min to 5 h after exposure. The bands corresponding to Bid and Bad decreased in cytosolic fractions of cochleae exposed to a permanent threshold shift inducing noise. The results could indicate the cleavage of Bid and the dephosphorylation of Bad, events which could inhibit the antiapoptotic Bcl-2 system. The activation of these proteins could be an early stage of the initiation of a cell death cascade after noise exposure.

This work was supported by the research grant DC-06457 from the National Institute on Deafness and other Communication Disorders, NIH.

### **573 Small Gtpase Pathways in Noise-Induced Hearing Loss**

Hongyan Jiang<sup>1</sup>, Su-Hua Sha<sup>1</sup>, Jochen Schacht<sup>1</sup>

<sup>1</sup>Kresge Hearing Research Institute, University of Michigan, Ann Arbor, MI 48109

Overstimulation of energy metabolism such as in noise trauma may cause intracellular ATP depletion and permeability changes of mitochondria. This imbalance in the energy status can activate cell death pathways. In this study, we investigated Rho GTPase-linked signaling pathways in CBA/J mice exposed to a broad band noise (2-20 kHz, 106 dB, 2 hours). This exposure results in a permanent threshold shift of about 40 dB at 12 and 24 kHz. F-actin in stereocilia decreased and was partially missing 3 hours after noise exposure. Active Rac1 (Rac1-GTP) in the cochlea increased up to 1 hour and then maintained stable until 5 hours. Conversely, active Rho A (Rho-GTP) decreased immediately and continued to decrease until 5 hours. AIF decreased and endonuclease G was translocated into the nuclei of outer hair cells one hour and 5 hours after noise exposure. PI staining showed apoptotic nuclei of outer hair cells at the 3 hour time point and later. We next investigated the relationship between Rac1/Rho A and ATP depletion in a HEI-OC1 cell line. Following ATP depletion, Rac1-GTP increased and endonuclease G translocated into the nuclei. The sum of these results indicates that activation of small GTPase signaling pathways through ATP depletion may contribute to noise-induced hearing loss.

Supported by the research grant DC-06457 from the National Institute on Deafness and Other Communication Disorders, NIH.

## **574 Correlation of Cochlear Pathology with ABR Threshold Shift and DPOAE Level Shift Following Exposure to Low-Frequency Noise**

Devon Snow<sup>1</sup>, Gary W Harding<sup>1</sup>, Barbara A Bohne<sup>1</sup>

<sup>1</sup>Washington University School of Medicine

ABR thresholds & DPOAE levels were determined before & 1-3 times after a 24-h exposure to a 0.5-kHz OBN at 95 dB SPL. At termination, the EP was recorded in the 1st turn & carbon tracer injected into the endolymphatic space (ES). After 45 min, the cochlea was fixed with OsO<sub>4</sub>, plastic-embedded & dissected as a flat preparation. Quantitative data on hair-cell losses were collected. Cytocochleograms were prepared with ABR threshold shifts (TS) & DPOAE level shifts (LS) overlaid. Based on the functional results, organ-of-Corti (OC) segments in the 2nd & 1st turns were sectioned at a radial angle for light & TEM study. Four chinchillas were terminated by 3 h post-exposure (0-d); two were terminated at 1 wk. At 0 d, the animals had a TTS of 20-60 dB over 0.5-10 kHz & a TLS of 10-50 dB over 2-10 kHz. EP averaged 84 mV, similar to controls. OHC loss ranged from 2.2-10.5% & 0.8-2.8% in the apical & basal halves of the OC, respectively. IHC loss was negligible throughout the OC. Viewed by phase contrast microscopy, most missing OHCs were found to have been replaced by immature phalangeal scars & cellular debris was seen in the ES & Nuel spaces. Most remaining hair cells had normal shapes & stereocilia arrays. Hair-cell loss & damage were insufficient to account for the TTS & TLS. Over the extent of the TTS & TLS, the nerve fibers & endings below the IHCs were not damaged, while the outer pillar bodies were either non-parallel or buckled. By 1 wk, the TS & LS had improved considerably; EP averaged 77 mV. The pillars were buckled over a smaller linear distance in the OC that was aligned with the frequency range of the residual TS & LS. Immature scars were still visible in the reticular lamina but the amount of cellular debris was decreased. We conclude that in the chinchilla, the most consistent pathological correlates of noise-induced TTS & TLS are an accumulation of cellular debris in cochlear fluids & injury to supporting cells that uncouples the stereocilia from the tectorial membrane.

## **575 Noise-induced Loss of Spiral Ligament Fibrocytes in Mice**

Joe Adams<sup>1</sup>

<sup>1</sup>Mass. Eye & Ear Infirmary

The locations and specializations of type I and type II fibrocytes have strongly implicated them in K<sup>+</sup> ion recycling from perilymph to the stria vascularis. In contrast, the localizations and specializations of type III and type IV fibrocytes have thus far provided few clues regarding their functional roles. Based upon their finding that type IV fibrocyte loss precedes sensory cell loss in C57BL/6 mice Hequembourg and Liberman suggested that loss of these fibrocytes may result in other cochlear cells being more vulnerable. Noise exposure of CBA/CaJ mice induces degeneration of type IV fibrocytes in ways that are very different from hair cell degeneration patterns. For example, following 92 dB 8-16 kHz noise exposures type IV

fibrocytes in the upper basal turn degenerate. This exposure level is 18 dB less intense than that required to produce loss of hair cells at the place of maximal basilar membrane motion. Furthermore, the site of type IV cell loss following 4-8 kHz noise exposures is the same as that produced by higher frequency noise exposures. Noise-induced loss of fibrocytes at this location may be associated with damage to sensory cells located in the lower basal turn. Degeneration of type IV cells can occur rapidly and the region of cell loss expands to include type III fibrocytes when high level noise exposures are utilized. If loss of type III and type IV fibrocytes creates vulnerabilities in sensory cells as Hequembourg and Liberman suggested, and if noise-induced losses of type III and type IV cells are associated with damage to basal turn sensory cells, then vulnerabilities associated with type III and type IV losses should be detectable by assaying the status of sensory cells in the extreme basal turn.

Supported by grants DC03929 and P30 DC 005209.

## **576 The Spiral Ligament Participates in Cochlear Inflammation Following Acoustic Trauma**

Kunihiro Sato<sup>1</sup>, Peter Billings<sup>1</sup>, Elizabeth M. Keithley<sup>1,2</sup>

<sup>1</sup>University of California, San Diego, <sup>2</sup>VA Medical Center, San Diego

Hearing loss following acoustic trauma results from cochlear damage. This damage is associated with an inflammatory-like response. We investigated the morphology and location of cells expressing CD45 (leukocyte common antigen) and F4/80 (a marker of activated macrophages), as well as ICAM-1 (intercellular adhesion molecule) expression following acoustic trauma. Swiss-mice were exposed to an octave-band noise (8-16 kHz) at 118 dB for 2 hours and sacrificed 0.5, 1, 2, 4, 7, and 14 days later. All animals had severe hearing loss, 90 dB or more, at every survival time. Non-exposed cochleae showed only a few immunopositive cells with anti-CD45 or anti-F4/80 antibody and constitutive expression of ICAM-1 by venules and fibrocytes in the lower part of the spiral ligament. Following acoustic trauma, the number of CD45(+) cells was increased dramatically, reaching its maximum at 2 days, decreasing slightly at 4 and 7 days. By 14 days most CD45(+) cell were gone. CD45(+) cells were most predominant within the spiral ligament, but detected also in the stria vascularis, scala tympani, and scala vestibuli in lower numbers. Most CD45(+) cells also expressed F4/80, but some F4/80(+) cells did not express CD45. Morphologically, CD45 and/or F4/80 immunopositive cells comprised two types of cells: round/oval cells throughout the cochlea, which are likely to be recruited macrophages, and irregularly-shaped cells with a few processes in the spiral ligament, which are likely to be activated microglia. Following acoustic trauma ICAM-1 expression was detected in an increased number of spiral ligament fibrocytes. These results imply that both leukocyte recruitment and activation of resident cells within the spiral ligament are important in cochlear responses to acoustic trauma.

### **577 Pro-Inflammatory Cytokine Expression in Noise Induced Damaged Cochleae**

Masato Fujioka<sup>1</sup>, Sho Kanzaki<sup>1,2</sup>, Hirotaka James Okano<sup>3</sup>, Kaoru Ogawa<sup>1</sup>, Hideyuki Okano<sup>3</sup>

<sup>1</sup>Department of Otolaryngology, Keio University School of Medicine, <sup>2</sup>Department of Otolaryngology, Tokyo Electricity Hospital, <sup>3</sup>Department of Physiology, Keio University School of Medicine

Among various organs, pro-inflammatory cytokines are highly expressed after tissue damages such as traumatic, mechanical damage and ischemia. We evaluated the expression of pro-inflammatory cytokines in noise-induced damaged cochleae.

**Materials and Methods:** 4-6-week old SD rats with normal Preyer's reflex were exposed to the noise (4kHz OBN 124dB SPL) for 2 hrs. 0,3,6,12,24hr, 3,5,7,14,28 day after the noise exposure, we dissected whole cochleae and examined for 10 cytokines with RT-PCR analysis.

Among these, 3 cytokines (TNF-alpha, IL-1beta, IL-6) were highly expressed in the early phase of noise induced hearing loss (NIHL). To test the time course of the expression levels of the three cytokines in detail, we used RT-PCR method with a TaqMan probe. Furthermore, we examined the localization of TNF-alpha and IL-6 by immunohistochemistry.

**Results:** TNF-alpha was highly elevated immediately after the noise exposure. IL-6 was elevated afterward, but the expression was diminished earlier than 12 hours. Both cytokines were highly expressed in the lateral wall fibrocytes, especially in the spiral ligament, but not in the stria vascularis. In the basement membrane fibrocyte, only IL-6 expression was detected.

**Discussion:** After the traumatic damage, excessively elevated pro-inflammatory cytokines are sometimes toxic in various organs. Our data suggest that the similar inflammatory pathway might be also involved in NIHL, and this observation might have pathophysiological meanings.

### **578 Inducible NOS Does not Participate in the Early Stage of Noise-Induced Hearing Loss Development.**

Irina Omelchenko<sup>1</sup>, Alfred Nuttall<sup>1,2</sup>

<sup>1</sup>OHSU, OHRC, <sup>2</sup>University of Michigan, KHRI

One of the multiple ways for development of noise-induced hearing loss is damage of Organ of Corti due to oxidative stress. Nitric oxide (NO) plays a double role in this process. It can enhance the oxidative damage caused by hydrogen peroxide or to react with superoxide and form the peroxynitrite as well as can intercept the reactive species such as the hydroxyl radical and convert them to less damaging and easier utilized compounds (1). All three variants of nitric oxide synthase (NOS) participate in NO production. However, their activation is suggested to be time-dependent in inner ear in animals treated with LPS (2).

In our in vivo experiments the cochleae of male guinea pigs were implanted with an osmotic pump to perfuse the non-selective NOS inhibitor L-NAME or selective inhibitor of inducible NOS L-NIL for 3 weeks. During this period of time, animals were exposed to 122 dB SPL wide band loud sound for three hours and ABR tested at several post sound exposure time points.

We did not observe an effect of inducible NOS inhibitor L-NIL on temporary ABR threshold shift. ABR data at 7 and 14 days after sound exposure showed slightly better recovery at frequencies 24-32 kHz. However, data from ears perfused with the non-selective NOS inhibitor L-NAME showed both a smaller temporary ABR curve shift and a better recovery compare to the non-treated ears at all frequencies checked (4-32 kHz). This result suggests that NOS activation and NO production are involved in development of loud sound-induced hearing loss. Also, that neuronal NOS and endothelial NOS but not inducible NOS participate in forming of temporary threshold shift.

References:

1. Murphy M.P., (1999), *Biochimica et Biophysica Acta*, 1411, 401-14.
2. Takumida M. et al., (2001), *Acta Otolaryngol.*, 121(1), 16-20.

Supported by NIH NIDCD R01 DC 00105

### **579 Overexpression of NMDA Receptor Subunit NR1 After Local Glutamate and Salicylate Application**

Thorsten Briede<sup>1</sup>, Claudius Fauser<sup>1</sup>, Wolfgang Arnold<sup>1</sup>, Hans Niedermeyer<sup>1</sup>, Elmar Oestreicher<sup>1</sup>

<sup>1</sup>Klinikum recht der Isar, Technical University Munich

In the cochlea NMDA receptors play a key role in reconnection of dendritic processes from surviving neurons to inner hair cells after excitotoxicity or noise trauma. Furthermore, NMDA receptors are required for the formation of functional synapses during development. Salicylate seem to activate NMDA receptors as demonstrated in electrophysiological and behavioural studies.

In this study we performed an immunohistochemical study to localize and characterize the expression behaviour of NR1, a subunit of NMDA receptors, in the adult gerbil cochlea after glutamate and salicylate intoxication.

Salicylate and glutamate were applied locally to the round window niche. After 24 hours animals were sacrificed and cochleas were removed. After fixation with paraformaldehyde and decalcification 3-5µ slices were stained with NR1 antibody (Chemicon, GERMANY) and detected by fluorescent antibody.

Saline treated animals showed specific staining in spiral ganglion cells as shown in previous studies. We could not detect any specific reaction in the organ of Corti or stria vascularis. Glutamate treated animals demonstrated strongly enhanced staining in spiral ganglion cells while no reaction could be demonstrated in the organ of Corti. Salicylate treated animals showed moderate enhancement of specific staining in spiral ganglion cells and, additionally, in outer hair cells.

The results demonstrate an overexpression of NMDA-NR1 subunit in spiral ganglion cells after excitotoxicity induced by glutamate as well as salicylate intoxication. Salicylate treatments lead to additional expression of NR1 in outer hair cells. The mechanism of NMDA receptor activation seems to be independent of the trauma. Further studies are needed to investigate the molecular basis of NMDA receptor activation.

### **580** Reduced Outer Hair Cell Membrane Fluidity by Intense Noise Leading to a Permanent Hearing Loss

Guang-Di Chen<sup>1</sup>, Hong-Bo Zhao<sup>2</sup>, Ben Fowler<sup>3</sup>, Julie Maier<sup>3</sup>

<sup>1</sup>University of Oklahoma, <sup>2</sup>University of Kentucky, <sup>3</sup>OMRF

Noise-induced hearing loss results from hair cell damage in most cases, but details of the mechanism are still unclear. Damage to outer hair cell (OHC) stereocilia may affect OHC receptor potential and then the cochlear amplification by affecting the OHC electromotility. However, loss of the cochlear amplification was often observed without damage to OHC receptor potential (Chen and Liu, 2004). In this study, guinea pigs were exposed to an 8-kHz octave band noise at 110 dB SPL for 3 hours. The noise exposure induced a permanent threshold shift (PTS) at frequencies around 8 kHz due to the loss of the cochlear amplification. However, there was no hair cell loss, no obvious injury of the hair cell stereocilia, and no permanent loss of the OHC receptor potential (by CM measurement). Effect of the noise exposure on OHC plasma membrane fluidity was determined *in vitro* in this study by laser bleaching technique. In the control OHCs, the membrane fluidity increased with the cell length. The relationship between the OHC plasma membrane fluidity ( $D$ ) and the cell length ( $L$  in  $\mu\text{m}$ ) can be expressed as:  $D = 0.02L + 0.64$ . Interestingly, in the noise-exposed animals, membrane fluidities of those OHCs with length in 40-70 $\mu\text{m}$  were significantly reduced compared to the control levels ( $p < 0.05$ ), while the longer and shorter OHCs had similar membrane fluidities as the control OHCs. It is known that the long hair cells respond to low frequency and the short hair cells respond to high frequency. The noise exposure caused membrane fluidity reduction only in those OHCs with lengths of 40-70 $\mu\text{m}$ , which distribute in the 2<sup>nd</sup> and 3<sup>rd</sup> turns. The noise-induced PTS was observed only at frequencies around 8 kHz (2-12 kHz), which correspond to the cochlear region of about 33-66% from the apex in the 2<sup>nd</sup> and 3<sup>rd</sup> turns (15-75% from the apex). Therefore, the cochlear functional loss appeared to result from the OHC membrane fluidity alteration. The OHC plasma membrane seemed more vulnerable to noise exposure than the stereocilia. The membrane fluidity alteration may affect the cochlear micromechanics and the OHC electromotility, leading to a loss of the cochlear amplification.

### **581** Temporary Suppression of SDH Activity in the Chinchilla Cochlea Following Exposure to Impulse Noise

Bo Hua Hu<sup>1</sup>, Donald Henderson<sup>1</sup>

<sup>1</sup>Center for Hearing and Deafness, State University of NY at Buffalo

Decreases in cochlear metabolism have been considered to be a major factor leading to hair cell (HC) damage following a noise exposure. The current study was designed to delineate the relationship between the metabolic status of individual HCs and their viability. The activity of succinate dehydrogenase (SDH), an important mitochondrial enzyme involved in ATP synthesis in the electron transport chain of mitochondria, was examined in chinchilla cochleas following an exposure to impulse noise at 155 dB SPL, an exposure that led to extensive HC loss in the first and second cochlear turns. The viability of HCs was assessed with propidium iodide (PI) staining, and cell death pathways were determined with TUNEL staining. The results showed that, at 5 min after the noise exposure, SDH staining was significantly decreased in most HCs in the upper first and the entire second cochlear turns. Only a small portion of HCs in this region maintained relative normal SDH staining. Interestingly, PI staining revealed that the HCs with stronger SDH staining were dying cells, whereas the HCs having decreased SDH activity were viable cells. SDH activity in the damaged region started to recover 4 hours to 1 day after the noise exposure, although the cochlear pathology continued to develop during this period of time. The extent of SDH recovery was associated with the severity of noise damage. Reappearance of SDH staining was seen in both viable and dying cells. For the dying cells with apoptotic phenotype, the SDH staining was consistently strong. In contrast, the SDH activity in the dying cells with necrotic manifestation was various. Some necrotic cells had strong SDH staining, where others had very weak staining. The results of the study suggest that there is a temporary suppression of SDH activity in the noise-damaged, but still viable, HCs. Whether the SDH suppression is protective or detrimental needs to be addressed in future studies. (Supported by NIDCD 1R03DC006181-01 to Bo Hua Hu, Ph.D.)

### **582** Superior Cervical Ganglion Ablation Influences Recovery of Cochlear Function After Noise Exposure

Eric Bielefeld<sup>1</sup>, Bo Hua Hu<sup>1</sup>, Donald Henderson<sup>1</sup>

<sup>1</sup>Center for Hearing and Deafness, SUNY Buffalo

The current study was undertaken in a continuing effort to better understand the involvement of cochlear sympathetic efferent fibers in noise-induced damage. The fibers from the superior cervical ganglion (SCG) have been implicated in modulating noise-induced hearing loss (Borg, 1982, Hildesheimer et al., 1991, 2002; Horner et al., 2002). In the current study, we explore the effects of unilateral and bilateral SCG ablation on threshold shift from noise exposure, as measured with inferior colliculus (IC) evoked potentials, distortion product otoacoustic emissions (DPOAE), and outer hair cell (OHC) loss. SCG's were



isolated at the level of the bifurcation of the carotid artery and removed unilaterally in 15 chinchillas. Another 8 chinchillas underwent bilateral ablation. 20 animals were employed as sham controls. Each animal was implanted with IC electrodes and exposed to a 4 kHz octave band noise for one hour at 108 dB SPL. Hearing thresholds and DPOAE input/output functions were measured at one day, three days, one week, and three weeks after the noise. After the three-week test, animals were sacrificed and OHCs were counted for cochleograms. Results showed improved recovery of DPOAE amplitudes after noise exposure in animals that underwent SCGectomy, as well as lower evoked potential threshold shifts relative to sham controls. Effects of SCGectomy on OHC loss were small. Results of the study suggest that sympathetic fibers do exert some influence on susceptibility to noise, but the influence is not a major one.

Research supported by NIDCD grant P01-DC03600-1A1.

### **583** Effects of Low Frequency Sonar on Fishes

Arthur N. Popper<sup>1</sup>, Michele B. Halvorsen<sup>1</sup>, Andrew S. Kane<sup>2</sup>, Diane L. Miller<sup>1</sup>, **Michael E. Smith<sup>1</sup>**, Jiakun Song<sup>1</sup>

<sup>1</sup>Department of Biology, University of Maryland, College Park, MD 20742, <sup>2</sup>Department of Veterinary Sciences, University of Maryland, College Park, MD 20742

There has been considerable concern raised as to whether new high intensity sonar, and particularly SURTASS Low Frequency Active (LFA) sonar, may have adverse effects on marine animals. This study is the first to examine the behavior, hearing, and sensory and gross pathology of fish exposed to an LFA source. Experiments were conducted at the U.S. Navy Sonar Facility at Seneca Lake, NY. Groups of rainbow trout (*Onchorynchus mykiss*) were exposed to three 108-second bursts of LFA sounds with nine minutes between each burst (193 dB re 1  $\mu$ Pa, frequency modulated from 150 to 300 Hz). The sound levels were equivalent to those encountered approximately 10 m from the LFA sonar. Following exposure, animals had hearing measured using auditory brainstem response (ABR) and were then prepared for examination of ear tissue using scanning electron microscopy. Additional fish were retained for necropsy or ABR testing on the second day.

Fish behavior in the test tank was normal during and after testing, except that the fish exhibited startle responses at the onset of sound presentation. Fish survived for up to three days post testing (until used for various tests). There was no apparent gross damage to the swim bladder or any organ system, and the sensory hair cells of the ears were fully intact.

Compared to controls, fish exposed to sound showed a statistically significant hearing loss at 400 Hz, although a similar trend occurred at 200 Hz. Thresholds for control fish were no different than for baseline fish (fish which were not placed in the test cage or lowered in the water). Hearing recovery will be examined in future tests.

This experiment is the first to test the effects of actual sonar signals on any fish species. There was no apparent gross effect on the fish even several days post exposure,

but hearing loss was considerable at the frequency of best hearing for this species. Previous studies have suggested that only sounds that are at least 60 dB above threshold cause hearing loss in fishes, which could explain why hearing loss was greatest at 400 Hz. The sounds to which fish were exposed in these tests probably represent a "worst case scenario" for fish exposed to sonar from a moving boat, since highest sound levels would only be present at the closest pass of the sonar to the fish.

### **584** Loci Contributing to Noise Resistance in 129S6 Mice

**Bruce Tempel<sup>1</sup>**, Valerie Street<sup>1</sup>, Jeremy Kallman<sup>1</sup>, Robert Silverstein<sup>1</sup>, Linda Robinson<sup>1</sup>, Charles Liberman<sup>2</sup>, Sharon Kujawa<sup>2</sup>

<sup>1</sup>VMBHRC, University of Washington, <sup>2</sup>MEEI, Harvard University

Some strains of mice (e.g., C57BL/6J) are highly vulnerable to noise-induced hearing loss (NIHL), while others (129S6, MOLF) are highly resistant, and one commonly studied strain (CBA) is intermediate. Toward identifying the genetic basis of noise resistance, we have undertaken an unbiased genetic approach that screens the entire genome of 129S6 and identifies loci contributing endogenously to the phenotype of noise resistance. In this quantitative trait locus (QTL) mapping study, offspring from a cross between 129S6 and CBA were backcrossed to the recessive parent (129S6) and the N2 individuals noise exposed (8-16 kHz, 103 dB SPL, 2 hr) then evaluated by ABR and DPOAE (5.6-45.2 kHz) at two weeks post-exposure. We found that approximately 1 in 10 of the N2 animals showed post-exposure thresholds similar to the 129S6 parental strain. Assuming roughly equal contributions from each locus, 10% penetrance suggests that 3 to 5 different loci contribute to the trait of noise resistance. Whole genome scans at 5 to 10 cM resolution were performed on 25 resistant N2 mice. Four chromosomal regions where 129S6 homozygosity occurred at a frequency of 0.75 ( $p < 0.01$ ) or higher were identified in the resistant N2 mice.

These results suggest that resistance to NIHL is a complex trait with 3-5 genes contributing to the phenotype in 129S6 mice. Ongoing studies are underway to narrow the genetic intervals at each locus and to identify candidate genes using expression profiling techniques. Ultimately, identification of the genes that contribute to noise resistance in mice will clarify mechanisms underlying noise-induced cochlear damage and will have ramifications for preventing or minimizing NIHL in humans.

(Supported by NIDCD RO1 DC006305)

## **585 Elevation of Superoxide Dismutase Increases Acoustic Trauma from Noise Exposure**

### **Exposure**

**Tomoko Kita**<sup>1,2</sup>, Takayuki Nakagawa<sup>1</sup>, Fukuichiro Iguchi<sup>1</sup>, Tsuyoshi Endo<sup>1</sup>, Takayuki Okano<sup>1</sup>, SuHua Sha<sup>3</sup>, Jochen Schacht<sup>3</sup>, Atsushi Shiga<sup>4</sup>, TaeSoo Kim<sup>1</sup>, Juichi Ito<sup>1</sup>

<sup>1</sup>*Department of Otolaryngology, Head and Neck Surgery, Graduate School of Medicine, Kyoto University,* <sup>2</sup>*Horizontal Medical Research Organization, Graduate School of Medicine, Kyoto University,* <sup>3</sup>*University of Michigan, Kresge Hearing Research Institute,* <sup>4</sup>*Department of Otolaryngology, Aichi Medical University*

The generation of superoxide has been implicated as a cause of cochlear damage from excessive noise. Cu/Zn superoxide dismutase (SOD1) will generally protect against superoxide-mediated tissue injury, but protection by this enzyme against noise trauma is controversial. The aim of the present study was to elucidate effects of increasing SOD1 on noise-induced hearing loss. We compared ABR threshold shifts between C57BL/6 mice administered lecithinized SOD1 (PC-SOD) and those applied physiological saline, and between C57BL/6 mice overexpressing SOD1 and littermates. The activity of SOD and catalase was assessed in cochlear specimens obtained from animals treated with PC-SOD and those with saline. Noise exposure caused significantly higher threshold shifts in PC-SOD-treated animals than physiological saline-treated ones. Cochlear tissues of PC-SOD-treated animals exhibited significant elevation of the levels in the SOD activity, but not in the catalase activity, in comparison with saline-treated ones. Transgenic mice overexpressing SOD1 suffered a significantly higher ABR threshold shift than non-transgenic littermates from noise exposure. These findings indicate that increasing SOD1 enhances auditory dysfunction following noise exposure. Our data point to the complexity of ROS homeostasis in the cochlea and measures of protection for auditory function.

## **586 Limiting Iron Status Confers Neuroprotection from Chronic Mild Carbon Monoxide Exposure in the Developing Auditory System of the Rat**

**Douglas Webber**<sup>1</sup>, Lopez Ivan<sup>1</sup>, Rose Korsak<sup>1</sup>, Sean Hirota<sup>1</sup>, Dora Acuna<sup>2</sup>, John Edmond<sup>1</sup>

<sup>1</sup>*UCLA,* <sup>2</sup>*Cedars Sinia Medical Center*

Iron deficiency and chronic mild carbon monoxide (CO) exposure are nutritional and environmental problems that can be experienced in common. Ambient concentrations of CO increase from the incomplete combustion of fossil fuels and from cigarette smoke; CO is ubiquitous to air in some communities. Carbon monoxide can bind to heme in proteins such as in hemoglobin and in cytochrome c oxidase, causing decreased function. We propose that mild chronic CO exposure creates an oxidative stress condition that impairs the neurons of the spiral ganglion. We have examined the effect of chronic mild CO exposure and iron status on auditory development in the rat. The CO exposed rats have decreased amounts of neurofilament

proteins and increased copper, zinc-superoxide dismutase (SOD1) in the neurons of the spiral ganglion. The increase in SOD1 produces hydrogen peroxide favoring the Fenton reaction that promotes oxidative stress. Rat pups exposed to CO have decreased basal c-Fos expression in the central nucleus of the inferior colliculus. However, the CO exposed group with decreased iron status exhibited in their cochlea an up-regulation of transferrin, whereas their expression of neurofilament proteins and of SOD1 were similar to controls. The normal expression of SOD1 and a reduced iron status does not promote oxidative stress in the cochlea. As a result, basal c-Fos expression in the CIC is the same as in controls. We conclude that the developing cochlea is selectively affected by mild CO exposure causing an increase in oxidative stress, while a limiting iron status ameliorates the effect caused by mild CO exposure by averting conditions that facilitate oxidative stress.

## **587 Cisplatin Induced the Death of Auditory Cells Through Proinflammatory**

**HyungJin Kim**<sup>1</sup>, JaeHyung Lee<sup>1</sup>, SeJin Kim<sup>1</sup>, David J Lim<sup>2</sup>, Channy Park<sup>1</sup>, **Raekil Park**<sup>1</sup>

<sup>1</sup>*Vestibulocochlear Research Center, Wonkwang University School of Medicine,* <sup>2</sup>*House Ear Institute, CA, USA*

Cisplatin is a widely used chemotherapeutic agent that is also highly ototoxic. A number of evidences in cytotoxic mechanism of cisplatin, including perturbation of redox status, increase in lipid peroxydation, formation of DNA adduct, have been suggested. However, the role of proinflammatory cytokines in cisplatin cytotoxicity of auditory cells has not yet been demonstrated. For the first time, we clearly demonstrated that cisplatin induced secretion and expression of proinflammatory cytokines including TNF-(, IL-1( and IL-6, in HEI-OC1 auditory cells as well as chemokines such as and IFN-inducible protein 10/CXCL10, thymus-expressed chemokine (TECK) /CCL25. Neutralization of proinflammatory cytokines by antibodies also attenuated the cisplatin-induced cell death. Additionally, exogenous treatment with proinflammatory cytokines increased expression of chemokines as well as death of HEI-OC1 auditory cells. Our findings may provide a pivotal understanding of the pathophysiology of hair cell damage caused by ototoxic drugs including cisplatin.

This work was supported by the Korea Science & Engineering Foundation (KOSEF) through the Vestibulocochlear Research Center (VCRC) at Wonkwang University in 2004.

## **588 Further Evidence for Aminoglycoside-Permissive Cation Channels in Inner Ear Explants**

**Peter Steyger**<sup>1</sup>, **Payal Razdan**<sup>1</sup>, Andrew Hordichok<sup>1</sup>, Nathan Spencer<sup>1</sup>, Katherine Johnson<sup>1</sup>

<sup>1</sup>*Oregon Hearing Research Center, Oregon Health & Science University, Portland, Oregon, 97239, USA*

Deafness and nephrotoxicity are serious consequences of aminoglycoside (AG) therapy. In cultured kidney cells, we

demonstrated that the non-endocytotic component of fluorescently-labeled gentamicin (GTTR) uptake was regulated by TRPV1 channel agonists and antagonists (pH, Ca<sup>++</sup>, RTX). Here we report the influence of these modulators on GTTR uptake in explants of bullfrog and murine inner ears.

After live incubation with GTTR; washed, fixed and delipidated inner ear explants displayed extensive cytoplasmic and intra-nuclear GTTR labeling. GTTR uptake was little reduced at 4°C, demonstrating that GTTR uptake was not dependent on endocytosis. Potassium depolarization of explants decreased GTTR uptake. Reduced pH (pH 5) increased GTTR uptake. The specific, competitive, TRPV1 agonist RTX, enhanced GTTR uptake at 0.16 mM Ca<sup>++</sup>, but reduced GTTR uptake at physiological Ca<sup>++</sup> levels. Low (0.16 mM) Ca<sup>++</sup> media had greater GTTR uptake compared to zero Ca<sup>++</sup> media.

In TRPV1 +/- cochlear explants, GTTR uptake was clearly altered, being observably higher or lower than wildtype explants, further suggesting that TRPV1 channels are involved in regulating GTTR uptake mechanisms.

Regulation of GTTR uptake by specific agonists and antagonists of TRPV1, in combination with competitive inhibitors (Ca<sup>++</sup>), provides further insight for developing new therapeutic mechanisms to prevent aminoglycoside toxicity.

*Funded by NIDCD R01 04555 and R21 06084*

### **589** Quantitative and Microscopical Evidence for Non-Endocytotic Uptake of GTTR Into the Cytoplasm and Nucleoli

Katherine Johnson<sup>1</sup>, Peter Steyger<sup>1</sup>

<sup>1</sup>Oregon Hearing Research Center, Oregon Health & Science University, Portland, Oregon, 97239, USA

Our previous studies have shown that cytoplasmic and nuclear uptake of fluorescently labeled gentamicin (GTTR) occurs by an endocytosis-independent mechanism, is competitively inhibited by cold (unlabeled) gentamicin, and is modulated by known agonists/antagonists of the TRPV1 channel (pH, Ca<sup>2+</sup>, RTX, and iodo-RTX).

We developed a fluorescent microplate assay using the MDCK kidney cell line to quantify the modulation of GTTR uptake by these agonists/antagonists. Our results confirm our confocal microscopy observations that cold gentamicin reduced GTTR uptake, following incubation at either 37°C for two hours or at room temperature for ten minutes (precluding endocytosis).

In addition, to verify the observed cytoplasmic and nuclear distributions of GTTR, we performed gentamicin immunocytochemistry on GTTR-treated and cold gentamicin-treated cells. Gentamicin immunolabeling was localized throughout the cytoplasm but was absent from the nucleolar-like structures within the nucleus for both treatments. However, GTTR co-localizes with a RNA-specific fluorophore that label nucleolar-like structures in the nucleus. This suggests that the interaction between the gentamicin molecule and its binding site in the nucleolus is also interfering with the antigenic site, preventing nuclear-specific immunoreactivity.

These studies demonstrate that microscopical observations of fluorescent gentamicin uptake by a rapid, bio-regulatory, non endocytotic pathway into the cytoplasm and nucleus can be independently corroborated by quantitative fluorescence assays, histochemistry and immunocytochemical methods.

*Funded by NIDCD R01 04555 and R21 06084.*

### **590** Platinum-DNA-Adducts in the Inner Ear of the Guinea Pig

Jan Peter Thomas<sup>1</sup>, Jürgen Thomale<sup>2</sup>, Bernd Liedert<sup>2</sup>, Jürgen Lautermann<sup>3</sup>

<sup>1</sup>Department of Otorhinolaryngology, University of Essen, Germany, <sup>2</sup>Institute of cellular biology, University of Essen, Germany, <sup>3</sup>Department of Otorhinolaryngology, University of Bochum, Germany

Sensorineural hearing loss is a typical side-effect of cisplatin. Previous studies mainly refer to free-radical-induced damage of the inner ear after administration of cisplatin. Until now platinum-DNA-adducts in the inner ear have not been examined.

10 guinea pigs were injected with a single dose of cisplatin (12.5 mg/kg body weight). 4, 8 and 48 h after injection the cochleae were removed and fixed in Carnoy solution. After staining with DAPI for visualization of DNA and antibodies against platinum-DNA-adducts the specimen were examined by fluorescence microscopy.

There was marked fluorescence in the marginal cells of the stria vascularis but not in the spiral ligament or the neurosensory epithelium. The platinum-DNA-adduct-concentration in the marginal cells of the stria vascularis was three times higher than in the basal and intermediate cells. In outer hair cells platinum-DNA-adduct concentrations were not increased.

These findings support ultrastructural studies showing early morphological damage to the marginal cells after cisplatin application. Therefore in cisplatin ototoxicity damage to the stria vascularis is an early event which may lead to a decreased endolymphatic potential and consecutive loss of hair cells.

### **591** Changes in the Transcription Factor AP-1 Within Inner Ear After Treatment with Ototoxic Drugs

Sho Kanzaki<sup>1,2</sup>, Yoshiaki Fujinami<sup>3</sup>, Reiko Nagashima<sup>3</sup>, Shujiro Minami<sup>2</sup>, Kiyokazu Ogita<sup>3</sup>, Kaoru Ogawa<sup>2</sup>

<sup>1</sup>Tokyo Electricity Power Hospital, <sup>2</sup>Keio University Medical School, <sup>3</sup>Setunan University

Aminoglycoside antibiotic (kanamycin) and diuretic agent (ethacrinic acid) were used in clinical use. The combination of these drugs induced hearing loss due to hair cell damage and apoptosis. The activity of the early response transcription factor activator protein-1 (AP-1) is enhanced by acoustic trauma including those that alter the cellular oxidation/reduction status (Ogita 2001, Shizuki, 2002, Matsunobu 2003). In this study, we investigated AP-1 DNA binding in the guinea-pig cochlea and vestibule following treatment with ototoxic drugs, ethacrinic acid and

kanamycin, which have been known to produce reactive oxygen species.

Guinea pigs were administered kanamycin (400mg/kg, i.m.) and then ethacrynic acid (50mg/kg, i.v.) 2 h later, following by preparation of nuclear extracts in discrete inner ear structures to test AP-1 DNA binding. AP-1 DNA binding was enhanced in the organ of Corti, lateral wall, spiral ganglion, by 14 days after the treatment. This enhancement induced by ototoxic drugs was more potent and longer in the organ of Corti compared in spiral ganglion neuron. Enhancement of AP-1 DNA binding was also seen in the vestibular organs. Immunohistochemical study showed that the organ of Corti, lateral wall, spiral ganglion, and vestibules had positive cells to AP-1 proteins.

Our data suggested that AP-1 could modulate several apoptotic and protective genes in inner ear damaged by ototoxic drugs. Ototoxic drug-induced enhancement of AP-1 binding has different responses and tissue specificity from those induced by acoustic trauma. This model was also very suitable for testing the effect of neurotrophic factor in survival of spiral ganglion neurons.

### **592 Proteomic Analysis of Cisplatin-Induced Cochlear Damage**

**Donald Coling<sup>1</sup>**, Dalian Ding<sup>1</sup>, Maciej Lis<sup>2</sup>, Rebecca Young<sup>3</sup>, Kenneth Blumenthal<sup>2</sup>, Richard Salvi<sup>1</sup>

<sup>1</sup>*Center for Hearing and Deafness, University at Buffalo,*

<sup>2</sup>*Department of Biochemistry, University at Buffalo,*

<sup>3</sup>*Department of Medicine, University at Buffalo*

Cisplatin is a widely used chemotherapeutic agent whose use is limited by severe side effects which include nephrotoxicity, neurotoxicity, ototoxicity and vestibulotoxicity. Recent studies suggest that the transcription factor, p53, plays an important role initiating cisplatin-induced apoptosis. Suppression of p53 with pifithrin- $\alpha$  (PFT) results in a reduction in caspase-1 and -3 activities and significant protection against cisplatin-induced hair cell loss. To identify changes in protein expression induced by cisplatin, we have used 2 dimensional differential gel electrophoresis (2D-DIGE) and matrix-assisted, laser desorption-ionization/time of flight (MALDI-TOF) analysis of cochlear sensory epithelium from a P2 rat organ culture model. In initial experiments, sensory epithelium was cultured for 3 h in serum free BME medium in the presence or absence of 1 mM cisplatin. Proteins were labeled with either of two Cy-dye DIGE fluors, Cy3 or Cy5. Proteins from cisplatin-treated cultures labeled with Cy3 were mixed with proteins from untreated cultures labeled with Cy5 and separated on the same gel by 2D electrophoresis. In control dye swapping experiments, dyes used to label proteins were switched. As an added control, equal amounts of protein from each treatment were mixed and labeled with Cy2. An equal amount of the Cy2-labeled proteins was used as an internal standard to control for gel to gel variability. Gels were scanned for Cy2, Cy 3 and Cy5 by fluorescence imaging. Replicate analysis of results from 6 gels (twelve pairs of conditions) revealed 1.5 – 1.8 fold cisplatin-induced increases in the expression of 5 proteins and 1.5

– 6.4 fold decreases in the expression of 16 proteins ( $p < 0.01$ , ANOVA). Experiments are underway to identify the proteins by MALDI-TOF, to confirm their change in expression by Western blot analysis and immunofluorescent microscopy and to verify their role in cisplatin-induced apoptosis.

### **593 Ethacrynic Acid Exacerbates Cisplatin-Induced Hair Cell Loss in Chinchillas and Reduces DPOAEs**

**Andrew Baschnagel<sup>1</sup>**, Dalian Ding<sup>1</sup>, Haiyan Jiang<sup>1</sup>, Richard Salvi<sup>1</sup>

<sup>1</sup>*University at Buffalo*

Chinchillas show a dramatic difference in ototoxicity from two closely related platinum-based anticancer drugs, carboplatin versus cisplatin (CIS). High doses of carboplatin reliably induce massive inner hair cell (IHC) damage and substantially less outer hair cell (OHC) loss in chinchillas. In contrast, cisplatin typically leads to death of the chinchilla, but little hair cell loss. Since cisplatin-induced hair cell damage is extremely difficult to induce in chinchillas, we co-administered with CIS (0.2, 0.4 or 0.8 mg/kg, i.p.) and ethacrynic acid (EA, 40 mg/kg, i.v.) and determined the amount and pattern of CIS+EA induced hair cell destruction and the change in DPOAE amplitude. CIS alone resulted in little or no hair cell loss at these concentrations. However, when if EA was administered at the same time as CIS, there was rapid and widespread destruction of IHC and OHC and large reduction in DPOAE. The 0.8 mg/kg dose of CIS plus EA resulted in nearly total loss of IHC and OHC over the basal 80% of the cochlea and abolished DPOAEs at f2 frequencies 1200-12000 Hz. EA plus a CIS dose of 0.4 mg/kg resulted in a relatively flat IHC loss ranging from 50-80% throughout the cochlea; the OHC lesion showed the typical base-to-apex gradient with roughly 95% OHC loss in the basal half of the cochlea decreasing to 40% in the apex. EA plus 0.2 mg/kg of CIS resulted in a flat IHC lesion ranging from 30-60% throughout the cochlea and a gradient of OHC loss that decreased from 95% in the base to 10% in the apex. With the 0.2 mg/kg dose of CIS, DPOAEs were absent at the high frequencies and greatly reduced at the lowest frequencies where there was partial retention of OHC. Thus, CIS can induce massive hair cell lesions in chinchillas, but only when it is co-administered with EA. Combined treatment with CIS and EA results in a peculiar, flat IHC lesion reminiscent of that seen with carboplatin and the typical OHC loss gradient that decreases from base to apex. (Supported by NIH grants P01 DC03600-01A1 & R01 DC06630-01)

### **594 Environmental Effects on Stress Granule Formation in Hair Cells of the Cultured Avian Basilar Papilla Following Gentamicin Treatment**

**Julia K. Anderson<sup>1</sup>**, Dominic A. Mangiardi<sup>2</sup>, Nicole J. Falk<sup>1</sup>, Jonathan I. Matsui<sup>1,3</sup>, Douglas A. Cotanche<sup>1,4</sup>

<sup>1</sup>*Children's Hospital Boston, Department of Otolaryngology,* <sup>2</sup>*Boston University, Department of*

Biomedical Engineering,<sup>3</sup>Harvard University, Department of Cellular and Molecular Biology,<sup>4</sup>Harvard Medical School, Department of Otology and Laryngology

Aminoglycoside antibiotics have known ototoxic side effects and can lead to permanent hearing and balance disorders through loss of inner ear sensory hair cells. Aminoglycosides induce hair cells to activate programmed cell death pathways and undergo apoptotic death. Recent studies have implicated kinase activation in aminoglycoside-induced hair cell death, as evidenced by the formation of stress granules in hair cells following gentamicin injection and through studies showing inhibition of the c-Jun-N-terminal kinase pathway can protect hair cells from aminoglycoside exposure. The aim of this study was to determine the factors that affect the formation of stress granules in organ culture with and without exposure to gentamicin. Additionally, we examined the effect of kinase inhibitors on the formation of stress granules and the correlation between stress granule formation and later stages of apoptosis such as caspase-3 activation. Formation of stress granules was greatly enhanced under certain medium conditions even without gentamicin, and was not inhibited by staurosporine. In other conditions, stress granules were not induced to form either with or without the presence of gentamicin in the culture medium. In situations where stress granules were observed, activation of caspase-3 occurred with or without the presence of gentamicin. In situations where stress granules were not observed, caspase-3 activation was consistently more abundant in hair cells of gentamicin treated epithelia. These results link the formation of stress granules with activation of programmed cell death pathways. However, stress granule formation is not necessary for gentamicin-induced apoptosis in hair cells in vitro despite their formation in affected hair cells following an in vivo injection of gentamicin. Determining the signaling events that link stress granule formation to the downstream events of apoptosis may isolate differences in the apoptotic signaling in hair cells in response to gentamicin in vitro versus in vivo.

### **595 In-Vitro Models Do not Reflect In-Vivo Ototoxicity of Aminoglycosides**

**Yajun Guan<sup>1</sup>, Hong-Yan Jiang<sup>1</sup>, Andra Talaska<sup>1</sup>, Shu-Hua Sha<sup>1</sup>, Jochen Schacht<sup>1</sup>**

<sup>1</sup>Kresge Hearing Research Institute, University of Michigan, Ann Arbor, MI 48109

*Aminoglycosides cause permanent hearing loss via damage to the sensory hair cells. In-vitro studies have suggested the involvement of caspase-9 and caspase-3, mitochondrial permeability changes, and activation of JNK and its upstream signaling components in hair cell death. Information from such in-vitro studies is frequently extrapolated to in-vivo ototoxicity. However, there is little direct information on cellular and molecular mechanisms of aminoglycoside ototoxicity in vivo. Our current study investigates whether in-vitro studies indeed can reliably predict responses to aminoglycosides in vivo.*

*HEI-OC1, an immortalized mouse cell line derived from the organ of Corti, expresses several molecular hair cell*

*markers. It is sensitive to aminoglycosides, and can be considered a convenient way to screen for ototoxic chemicals and to investigate toxicity mechanisms. However, our results indicate that this in-vitro system responds to aminoglycoside stimuli (1 mM gentamicin treatment, up to five days) distinctly differently than the in-vivo system (CBA mice, 700 mg kanamycin/kg bodyweight, twice daily for 14 days). In the HEI-OC1 cell line, transcription factor AP-1 is activated by gentamicin treatment, while NF-kB does not respond. In contrast, in-vivo, NF-kB but not AP-1, is up-regulated upon kanamycin treatment. Consistent with other in-vitro studies, caspase-3 was found to be significantly activated by gentamicin in the HEI-OC1 cell line, while Endo G activation and translocation could not be detected. On the other hand, caspase-3 activation could not be detected after in-vivo treatment, while activation and translocation of Endo G was apparent. The distinct responses of AP-1 and NF-kB and the activation of different cell death pathways indicate that different signaling pathways and the expression of different sets of genes are involved in acute and chronic drug actions and that in-vitro results can not necessarily be extrapolated to in-vivo responses. This fact is especially important for the design of protective therapies against aminoglycosides ototoxicity.*

*Supported by the research grant DC-03685 from the National Institute on Deafness and other Communication Disorders, NIH*

### **596 Increased Outer Hair Cell Loss when Cisplatin therapy is combined with Oral Ethanol**

**Geming Li<sup>1</sup>, Dorothy Frenz<sup>1</sup>, Dilip Madnani<sup>2</sup>**

<sup>1</sup>Albert Einstein College of Medicine, <sup>2</sup>Montefiore Medical Center

Cisplatin is a chemotherapeutic agent effective in the treatment of a broad spectrum of tumors. However, its treatment side effects, particularly its ototoxicity and nephrotoxicity, limits its therapeutic window. Previous studies in our lab have shown that treatment with the antioxidant L-Methionine, either locally or systemically, can protect against the auditory receptor damage and loss of hearing acuity produced by cisplatin ototoxicity. However, local delivery is an invasive procedure while systemic delivery compromises the anti-tumor activity of Cisplatin. In our search for other otoprotective molecules against cisplatin, we studied the phytoalexin, Resveratrol (3,5,4-trihydroxy trans-stilbene), shown to have potent antioxidant and cancer chemopreventive properties. The Resveratrol was administered via orally using ethanol as a solvent. Our preliminary results indicated increased outer hair cell loss in those rats administered both cisplatin and Resveratrol in ethanol solution, versus cisplatin alone and no damage with Resveratrol used alone. Further investigation as to why the Resveratrol with Cisplatin increased outer hair cell loss led us to ethanol, the solvent for Resveratrol, as the potential etiology. Ethanol has been shown to increase membrane fluidity and could increase cisplatin concentrations inside hair cells, potentiating its ototoxicity. We will present our results, showing increased

outer hair cell damage with the concomitant use of intraperitoneal Cisplatin with oral ethanol in a rat model. This has potential clinical implications whereby those patients undergoing Cisplatin chemotherapy should be counseled in the use of alcohol during treatment.

### **597 A PI3K Pathway Mediates Hair Cell Survival and Opposes Gentamicin Toxicity in Neonatal Rat Organ of Corti**

Won-Ho Chung<sup>1</sup>, Kwang Pak<sup>2</sup>, Allen Ryan<sup>2</sup>

<sup>1</sup>Sungkyunkwan University School of Medicine Seoul Korea, <sup>2</sup>UCSD School of Medicine and VA medical center

Gentamicin is well known to promote hair cell (HC) death in the inner ear, but it also appears to activate opposing pathways that promote HC survival. In combination with the work of others, our previous study has indicated that a K-Ras-Rac-JNK signal transduction pathway is important for HC death and an H-Ras-Raf-MEK-Erk pathway is involved in promoting HC survival (Battaglia et al. *Neurosci.* 122: 1025, 2003). However, our data also suggested that a Ras-independent survival pathway for activation of MEK might be stimulated by gentamicin. To investigate alternatives to the Ras-Raf-MEK-Erk pathway in promoting HC survival, organ of Corti explants were exposed to gentamicin combined with inhibitors of signal transduction pathways also known to activate MEK in other cell types. When gentamicin was combined with a PI3K inhibitor (LY294002, 10, 50 $\mu$ M), a PKC inhibitor (calphostin C, 50, 100nM) or a PKB/Akt inhibitor (SH-6, 10 $\mu$ M), HC damage was significantly increased compared to gentamicin alone. In contrast, a PLC $\gamma$  inhibitor (U73122, 5 $\mu$ M) did not affect HC damage when combined with gentamicin. These results indicate that PI3K promotes HC survival via its downstream targets, PKC and PKB/Akt. This suggests that both MEK and MEK-independent survival pathways are activated during gentamicin exposure of HCs, acting in opposition to pathways that promote HC death. In contrast, PLC $\gamma$  activation of PKC does not appear to play a role in the HC response to gentamicin.

Acknowledgements: Research was supported by funds from NIH/NIDCD grant DC00139 and the research service of the Veteran Administration.

### **598 Dose-Dependent Protection and Toxicity of C-Jun N-Terminal Kinase Inhibition in Aminoglycoside Exposed Hair Cells**

Felipe Santos<sup>1</sup>, David Raible<sup>1</sup>, Edwin Rubel<sup>1</sup>

<sup>1</sup>University of Washington

The MAP-JNK signal transduction pathway has been shown to be involved in the apoptotic response of sensory hair cells following aminoglycoside-induced ototoxicity. Inhibitors of this pathway have resulted in protective effects on hair cell survival in some aminoglycoside exposure protocols. If protective compounds are to be used therapeutically, it is necessary to examine the biological activity of these compounds over a broad range of aminoglycoside and protective compound dosing strategies. In the present study we examine dose-dependent variations in the biological response of MAP-

JNK inhibitors, varying both aminoglycoside and inhibitor dose.

Five day post fertilization zebrafish (*Danio rerio*) were exposed to vital fluorescent dyes FM 1-43 and Yo-Pro-1 to identify hair cells of the lateral line *in vivo*. Larvae were exposed to 0, 25, 50, 100, 200 and 400  $\mu$ M neomycin for one hour and the number of remaining hair cells determined, establishing a neomycin dose-response curve. To determine whether hair cells were protected by MAP-JNK inhibitors, larvae were pretreated with MAP-JNK inhibitors at 1, 10, 50, 100 and 200  $\mu$ m for 1 hour, before exposure to all neomycin doses.

The results show both statistically significant protective and toxic effects of the MAP-JNK inhibitors on hair cell survival. The results emphasize the multiplicity of effects of biologically active compounds in dynamic systems. Modulators of hair cell toxicity provide important insight into the biology of hair cell death and survival yet not all modulators may be of therapeutic value.

### **599 Sentinel Modulates Hair Cell Toxicity in the Zebrafish Lateral Line**

K N Owens<sup>1,2</sup>, D W Raible<sup>1,2</sup>, E W Rubel<sup>2,3</sup>

<sup>1</sup>Biological Structure, <sup>2</sup>VM Bloedel Hearing Research Center, <sup>3</sup>Otolaryngology-HNS, University of Washington

Loss of mechanosensory hair cells in the inner ear is a leading cause of hearing impairment. One of the more experimentally tractable cause of hair cell loss is exposure to ototoxic drugs, which include aminoglycoside antibiotics, and the anti-neoplastics, cisplatin and carboplatin. In wildtype zebrafish, *Danio rerio*, lateral line hair cells are killed by aminoglycosides in a consistent, dose-dependent manner. The external location of the lateral line allows visualization and manipulation of hair cells *in vivo*. To identify factors that affect hair cell death or survival, we screened zebrafish for mutations that modulate aminoglycoside-induced lateral line hair cell death. Larvae are exposed to neomycin at 5 days post fertilization, stained with the vital dye DASPEI and evaluated for presence of hair cells. Animals are screened with high (200  $\mu$ M) or low (25  $\mu$ M) doses of neomycin to identify mutations conferring resistance or sensitivity, respectively. We have identified a recessive mutant, *sentinel*, which exhibits neomycin resistance. This mutant has a cosegregating sinusoidal body phenotype; animals appear otherwise normal as young larvae. Lateral line development in *sentinel* mutants is relatively normal at the ultrastructural level. Rapid uptake of the vital dye FM1-43, which is associated with mechanotransduction, occurs normally in *sentinel* mutants. Thus, initial components of the mechanotransduction pathway are likely to be intact. Aminoglycosides can enter the hair cells of *sentinel* mutants rapidly, suggesting that the mutation alters response downstream of drug entry. The *sentinel* mutant has a wildtype response to cisplatin, indicating that there is not a disruption of general cell death components used by both ototoxic agents. We have positionally mapped the mutant allele and are in the process of identifying the altered gene.

## **600 p53 Mediates Cisplatin-Induced Hair Cell Death in Vitro**

Alan Cheng<sup>1</sup>, Richard Morrison<sup>2</sup>, Edwin Rubel<sup>1,2</sup>

<sup>1</sup>Department of Otolaryngology-HNS, University of Washington, <sup>2</sup>Department of Neurological Surgery, University of Washington

Sensory hair cell loss is a well-documented side effect of cisplatin (CP) treatment. However, its mechanism of inducing hair cell death is still not completely understood. The caspase family of proteases has been found to mediate hair cell death, but the signaling pathways controlling their activation have not been clearly defined. One proposed regulator of this process is the p53 protein, which has been found to mediate cell death induced by a variety of genotoxic agents including CP (Dempke et al., 2000, *Anticancer Drugs* 11:225). In the inner ear, one recent study found that a p53 inhibitor, pifithrin- $\alpha$  (PFA), prevented caspase-3 activation and hair cell death in CP-treated rat cochleae in vitro (Zhang et al., 2003, *Neurosci* 120:191). The following experiments have been designed to test the hypothesis that p53 mediates CP-induced hair cell death. Whole organ cochleae harvested from wildtype postnatal 3- to 5-day-old mice were incubated with 0-100  $\mu$ g/ml CP for 24hr. A subset of these cultures was co-treated with PFA. At the end of the incubated period cochleae were fixed and labeled for hair cells. Cochleae were also harvested from p53-deficient mice and treated with 0-50  $\mu$ g/ml CP for 12-24hr. The 24-hr treatment group was analyzed for hair cell survival and the 12-hr group was labeled for activated caspase-3. Our data indicated that hair cell survival decreased in a dose-dependent manner with increasing doses of CP. Co-treatment with 100 $\mu$ M PFA significantly improved hair cell survival at both 10 and 25  $\mu$ g/ml CP. Hair cell survival was significantly elevated in the p53-deficient cochleae at each treatment dose (10-50 $\mu$ g/ml). When compared to wildtype cochleae, hair cell derived from p53-/- cochleae exhibited significantly less caspase-3 activation after 12hr CP treatment. Our data suggest that p53 mediates CP-induced hair cell death in a caspase-3 dependent manner. Supported by the Deafness Research Foundation.

## **601 TEA Amelirates Cisplatin-Induced Caspase-3 Activation in Spiral Ligament Fibrocytes**

Zhijun Shen<sup>1</sup>, Fenghe Liang<sup>1</sup>, Bradley Schulte<sup>1</sup>

<sup>1</sup>Medical University of South Carolina

We have previously shown that cisplatin-induced apoptosis in type I spiral ligament fibrocytes involves the activation of BK channels. Using annexin V-FITC/PI, we also have demonstrated that cisplatin-induced apoptosis in these cells is dose- and time-dependent. Inhibition of the endogenous BK channels significantly reduced the apoptosis in type I spiral ligament fibrocytes. In the current study, we investigated the effects of blockage of the BK channels on cisplatin-induced activation of caspases in these cells.

Type I spiral ligament fibrocytes cultures were incubated with 40  $\mu$ M cisplatin for up to 72 hours. Quantitative analysis of apoptosis was performed using annexin V-

FITC/PI and carboxyfluorescein labeled substrates for caspases -3, -8 and -9/PI with flow cytometry. Annexin V binding showed a significant increase at 24 hours that plateaued around 48 hours. Activity for caspases-8 and -9 was moderately elevated at 72 hours. In contrast, treatment with 40  $\mu$ M did not affect caspase-3 activity within 72 hours. However, caspase-3 showed a dose-dependent activation profile when incubated with 80, 160 and 320  $\mu$ M cisplatin for 48 hours, with a peak at 160  $\mu$ M. At 160  $\mu$ M dose level, cisplatin-induced activation of caspase-3 was significantly reduced by co-incubation with 10 mM TEA for 48 hours, a more than 50% reduction in apoptosis.

Based on these data, we concluded that (1) Cisplatin may activate both caspases-8 and -9 as up-stream signaling mediators in the pathways and (2) Blockage of the BK channels significantly ameliorates the cisplatin-induced activity of caspase-3 and apoptosis in type I spiral ligament fibrocytes in vitro.

[Supported by DC 5148 and DC 00713 from NIH/NIDCD]

## **602 The Effects of Insulin-Like Growth Factor I(IGF-1) on the Hair Cell Survival in the Explant Culture of Mouse Utricular Epithelium**

Ji Yeong Park<sup>1</sup>, Byung Yoon Choi<sup>1</sup>, Sun O Chang<sup>1</sup>, Chong-Sun Kim<sup>1</sup>, Seung Ha Oh<sup>1</sup>

<sup>1</sup>Seoul National University, College of Medicine, Seoul, South Korea

Background and Objectives

IGFs are known to regulate a proliferation during hair cell development and regeneration. In order to analyze the effect of IGF- I on hair cell survival, we used the explant culture of mouse utricular epithelium with ototoxic damage using neomycin.

Materials and Methods

Utricular epithelial sheets were separated from postnatal day 3-5(P3-P5) ICR mice with 0.5mg/ml thymoysin in DMEM for 20 min at 37 °C, based on the method reported previously(Zheng et al.1997). The poly -L- lysine coated coverslip was placed into an individual dish that was filled with the culture medium (DMEM, 4.5mg/ml glucose, antibiotics and antimycotics ) supplemented with 1% fetal bovine serum (GIBCO). After 1 day culture, the hair cells were incubated with neomycin with different concentrations (0 to 1mM) for 24 hrs. The effect of IGF-1(50ng /ml) on the hair cell survival was evaluated after phalloidin staining.

Results

Neomycin over 0.5mM induced hair cell damage by 29  $\pm$  10 % compared to control (P < 0.05). In a group with combined neomycin and IGF- I treatment, around 10% of hair cells were damaged.

Conclusions

This study suggests that IGF I promotes hair cells survival in neomycin-induced acute damage condition.

### **603 T-Type Calcium Channel Blocker**

#### **Flunarizine Activates the Nrf2/HO-1 Signaling**

HyungJin Kim<sup>1</sup>, Junghan Lee<sup>1</sup>, SungYeol Park<sup>1</sup>, MyungJa Yun<sup>1</sup>, Federico Kalinec<sup>2</sup>, **Hongseob So<sup>1</sup>**

<sup>1</sup>Vestibulocochlear Research Center, Wonkwang University School of Medicine, <sup>2</sup>House Ear Institute, CA, USA

NF-E2-related factor-2 (Nrf2) regulates the gene expression of phase II detoxification enzymes and antioxidant proteins through an enhancer sequence of the antioxidant-response element (ARE). Our previous study has shown that flunarizine significantly prevented the cisplatin-cytotoxicity on HEI-OC1 auditory cells. Here, we further investigated whether Nrf2/HO-1 signaling was directly involved in protective effect of flunarizine against cisplatin-cytotoxicity. Flunarizine induced nuclear translocation of Nrf2 within 2-4 h of exposure. Consistent with this observation, flunarizine significantly increased the ARE-driven luciferase gene activity. Overexpression of wild type Nrf2 significantly protected the cisplatin-cytotoxicity whereas dominant negative Nrf2, lacking the transcriptional activation domain, inhibited the protective effect of flunarizine. Furthermore, cobalt protoporphyrin IX (CoPPIX), a well known Nrf2 and HO-1 inducer, also enhanced the translational expression and nuclear translocation of Nrf2 accompanied with inhibitory effect against cisplatin-cytotoxicity. In addition, flunarizine increased the transcriptional expression of HO-1, whose inhibitor hemoglobin abrogate the cytoprotective effects against cisplatin-cytotoxicity. Taken together, these results suggest that T-type calcium channel blocker, flunarizine antagonized cisplatin-cytotoxicity in HEI-OC1 auditory cells via up-regulation of Nrf2/HO-1 signaling

This work was supported by the Korea Science & Engineering Foundation (KOSEF) through the Vestibulocochlear Research Center (VCRC) at Wonkwang University in 2004.

### **604 Caspase Inhibitors, but not c-Jun N-Terminal Kinase Inhibitor Treatment Prevent Cisplatin-Induced Hearing Loss**

**Jing Wang<sup>1,2</sup>**, Sabine Ladrech<sup>1</sup>, Philippe Brabet<sup>1</sup>, Jean-Louis Pujol<sup>3</sup>, Jean-Luc puel<sup>1</sup>

<sup>1</sup>INSERM U583 and Université de Montpellier 1, <sup>2</sup>Auris Medical, <sup>3</sup>Pneumologie Oncologique, CHU Montpellier and Université Montpellier 1

Cisplatin (CDDP) is a highly effective chemotherapeutic agent, but with significant ototoxic side effects. Apoptosis is an important mechanism of cochlear hair cell loss following exposure to an ototoxic level of CDDP. This study examines intracellular pathways involved in hair cell death induced by CDDP exposure in vivo to develop effective therapeutic strategies to protect auditory receptors from CDDP-initiated hearing loss.

Guinea pigs were treated with systemic administration of CDDP. Cochlear hair cells from CDDP-treated animals exhibited classic apoptotic alterations in their morphology. Several important signaling events that regulate the death of CDDP-injured cochlear hair cells were identified. CDDP

treatment induced the activation and redistribution of cytosolic Bax, and the release of cytochrome c from injured mitochondria. Activation of caspase-9 and caspase-3, but not caspase-8 was detected after treatment with CDDP, and the cleavage of fodrin by activated caspase-3 was observed within damaged hair cells. Intracochlear perfusions with caspase-3 inhibitor (z-DEVD-fmk) and caspase-9 inhibitor (z-LEHD-fmk), but not caspase-8 inhibitor (z-IETD-fmk) and cathepsin B inhibitor (z-FA-fmk), prevent both hearing loss and loss of sensory cells. Although the SAPK/JNK signaling pathway is activated in response to CDDP toxicity, intracochlear perfusion of D-JNKI-1, a JNK inhibitor, did not protect against CDDP ototoxicity, but instead potentiated the ototoxic effects of CDDP. The results of the present study demonstrate that blocking a critical step in apoptosis may be a useful strategy for preventing harmful side effects of CDDP ototoxicity in patients having to undergo chemotherapy.

### **605 Protection from Cisplatin Ototoxicity by Salicylate and Manganese Superoxide Dismutase In Vivo**

**Andrew K. Patel<sup>1</sup>**, Anand N. Mhatre<sup>2</sup>, Ting-Ting Huang<sup>3</sup>, Holly Van Remmen<sup>4</sup>, Anil K. Lalwani<sup>2</sup>

<sup>1</sup>University of California, San Francisco, <sup>2</sup>New York University School of Medicine, <sup>3</sup>Stanford University School of Medicine, <sup>4</sup>University of Texas Health Science Center at San Antonio

Cisplatin (cis-diamminedichloroplatinum(II) (CDDP)) is a widely used, highly effective, oncolytic agent with serious dose-limiting ototoxic side-effects. Cisplatin toxicity targets sensory hair cells in the cochlea with histopathology similar to that caused by aminoglycosides or reactive oxygen species (ROS), with the exception that the observed toxicity is preferential for outer versus inner hair cells. Protective antioxidants against aminoglycoside ototoxicity include acetylsalicylic acid (aspirin). Superoxide dismutases (SODs) form the first line of defense in vivo against damage mediated by the superoxide anion, the most common ROS. We tested the hypothesis that application of the antioxidant aspirin or in vivo overexpression of Mn SOD (SOD2) will provide protective effect against cisplatin-induced ototoxicity. Protective effects of aspirin (100 mM) and SOD2 against cisplatin (16 mg/kg intraperitoneally) were assessed in CD1 mice and SOD2 transgenics (mice overexpressing SOD2), respectively. Pre- and post-treatment status of inner and outer hair cell function was assessed using auditory brainstem threshold responses (ABRs) using free field click stimulus and distortion product otoacoustic emissions (DPOAEs), respectively. A 20 dB elevation of ABR thresholds and loss of otoacoustic emissions (in 30% of the subjects) was identified in control animals exposed to cisplatin. In contrast, preservation of ABR thresholds and distortion product otoacoustic emissions was identified in aspirin-supplemented CD1 mice and the SOD2 transgenics exposed to cisplatin, thus demonstrating protection against cisplatin ototoxicity. The demonstration of the protective effect of these reagents provides further evidence for a role of ROS in cisplatin ototoxicity and



provides a validation for their application for the preservation of hearing.

This work was supported by a Howard Hughes Medical Institute Research Fellowship.

### **606 Sodium Thiosulfate Versus Saline in the Ototoxic Protection Against Cisplatin in the Guinea Pig Model**

**Rose Mary Stocks, M.D., Pharm.D.**<sup>1</sup>, Herbert Gould, Ph.D.<sup>2</sup>, **Gabriel Phillips, B.S.**<sup>3</sup>, **Sreekrishna Donepudi, M.D.**<sup>3</sup>, Xiaoping Du, M.D.<sup>4</sup>, Kristin Hamre, Ph.D.<sup>4</sup>

<sup>1</sup>Department of Otolaryngology, University of Tennessee Health Science Center, <sup>2</sup>School of Audiology and Speech-Language Pathology, University of Memphis, <sup>3</sup>University of Tennessee Health Science Center, <sup>4</sup>Department of Anatomy and Neurobiology, University of Tennessee Health Science Center

**Objective:** To compare the effects of sodium thiosulfate (STS) and saline (control) administered continuously to the middle ear space (MES) of Hartley albino guinea pigs (HAGP) receiving a standard ototoxic regimen of cisplatin (CP).

**Design:** Prospective study.

**Setting:** Animal research facility.

**Methods:** Baseline hearing of the HAGP was assessed by auditory brain stem recordings (ABR) at 2, 8, 16, and 32 kHz. Then, STS was administered continuously via a surgically-placed mini-osmotic pump (Alzet 2002) to the MES of one ear for 20 days. Similarly, the other ear of the same animal received saline and served as a control. The treatment ears were randomized between the left and right side to eliminate surgical bias. CP doses (1 mg/kg) were given subcutaneously each day for a 15-day period. On day 20, the pumps were removed. Four weeks later, the post-treatment ABRs were performed at the same frequencies and the animals were subsequently sacrificed. The temporal bones were harvested and the cochleas were histologically prepared. The outer hair cells were counted and compared.

**Results:** Seventeen HAGP (initial weight 200-250gms) were studied. As expected, treatment with CP resulted in hearing loss bilaterally, and there was a frequency effect with greater hearing loss at higher frequencies. However, STS protection did not result in significantly less hearing loss post treatment compared to the control ear. Histological data was consistent with the hearing test results.

**Conclusion:** The data from this study does not indicate a significant role for STS or saline in protection against CP-induced ototoxicity. In a previous similar study which showed protection by STS, those animals received a progressively lower dose of CP based on body weight. Some of the animals in this study actually received up to 18% more CP. This demonstrates that there is a limit to the protection that STS provides. The otoprotection from STS is apparently not enough to withstand a larger dose of CP.

### **607 PD98059 Protects Cochlear Hair Cells from Cisplatin**

**Dalian Ding**<sup>1</sup>, Irene Lanzoni<sup>2</sup>, Elisa Corbacelli<sup>2</sup>, Maurizio Previati<sup>2</sup>, Haiyan Jiang<sup>1</sup>, Ping Wang<sup>1</sup>, Richard Salvi<sup>1</sup>

<sup>1</sup>Center for Hearing & Deafness, SUNY at Buffalo,

<sup>2</sup>University of Ferrara, Italy

The early stage of cisplatin-induced ototoxicity is thought to arise from the production of reactive oxygen species that damage hair cells. Cisplatin activates multiple signal transduction pathways including members of the mitogen-activated protein kinases (MAPK) such as extracellular signal-regulated kinases 1 and 2 (ERK1/2) which results in phosphorylation of P53 and activation of caspases. We have previously shown that cisplatin upregulates P53 expression in the inner ear during the early stages of cisplatin-induced apoptosis (Zhang et al., *Neurosci*, 2003). PD98059 is an inhibitor of ERK1/2 which can block the phosphorylation of p53. In the present study, we examined the potential protective effects of PD98059 against cisplatin ototoxicity using cochlear organotypic cultures. Cochlear explants were cultured with various concentrations of cisplatin (0.1, 0.2, 0.5, 1.0, 2.0, or 5.0mM), PD98059 (100, or 500µM) or the combination of both drugs. Stereocilia were labeled with fluorescently-conjugated phalloidin to quantify the degree of hair cell loss; fluorescently-labeled inhibitors of caspase-3, caspase-8 and caspase-9 were used to identify apoptotic signaling pathways and Western blots were used to identify phosphorylation of P53 and ERK. Cisplatin activated receptor-mediated caspase-8 and executioner caspase-3 during the first 24 h, but did not activate mitochondrial-mediated caspase-9 at this time point. Addition of PD98059 to cisplatin-treated cultures greatly reduced caspase-8 and caspase-3 activity during the first 24 h of cisplatin treatment and significantly enhanced hair cell survival during the first 24 h of cisplatin treatment; however, this protective effect disappeared after 48 h of cisplatin treatment. Western blots showed significant upregulation of P53 and ERK expression after 12 h of cisplatin treatment; the addition of PD98059 significantly reduced the expression of P53 and ERK expression. These results suggest the early stages of cisplatin ototoxicity may involve oxidative stress induced activation of the ERK1/2 signaling pathway leading to subsequent activation of P53 and apoptosis via caspase-8 and caspase-3 signaling. The mechanisms underlying delayed hair cell death with PD98059 treatment are currently being investigated.

Supported by NIH grants P01 DC03600-01A1 & R01 DC06630-01

### **608 Protection of Adult Vestibular Hair Cells Against Aminoglycoside Toxicity by Inhibition in the JNK Signaling Pathway**

**Kazuma Sugahara**<sup>1,2</sup>, Lisa L. Cunningham<sup>3</sup>, Edwin W Rubel<sup>1</sup>

<sup>1</sup>Virginia Merrill Bloedel Hearing Research Center, Dept. Otolaryngology-HNS, Univ. Washington, <sup>2</sup>Dept. Otolaryngology, Yamaguchi Univ., Sch Med., <sup>3</sup>Dept.

c-Jun N-terminal kinase (JNK) is a member of the mitogen-activated protein kinase family. In a variety of cell types, phosphorylation of JNK in response to stress facilitates apoptotic cell death. Several studies have now shown that inhibition of the JNK signaling pathway can provide some protection to cochlear hair cells. However, little is known about the role of JNK in vestibular sensory cells in mammals and the degree of protection at different aminoglycoside exposure levels has not been well described. The purpose of this study is to investigate the role of JNK in mammalian vestibular hair cell death induced by aminoglycoside exposure. Cultured utricles from mature CBA/CaJ mice were used. CEP-11004 was used as an indirect inhibitor of JNK signaling. Utricles were cultured with neomycin (0, 1, 4 mM) and CEP-11004 (0, 0.1, 0.2, 0.5, 1.0  $\mu$ M). Phospho-specific antibodies showed phosphorylation of JNK and c-Jun in the utricles of the utricles with neomycin, but not utricles cultured without neomycin. CEP-11004 inhibited the phosphorylation of both JNK and c-Jun 12 h after exposure to neomycin. We replicated previous results showing protection against moderated aminoglycoside exposure; 92.4% of extrastricular hair cells survived when cultured with 1 mM neomycin and 1.0  $\mu$ M CEP-11004, compared to 76.1% survival with only neomycin. The protective effect of the inhibitor showed the dose-response relationship (0.1-1.0  $\mu$ M), though high concentrations (2.0  $\mu$ M) of the inhibitor were toxic. In addition, the inhibitor did not provide any protection at the high dose of neomycin (4 mM). Where effective, inhibition of JNK was coupled with loss of caspase-9 activation in hair cells. These data indicate that inhibition of JNK provides some protection of mammalian vestibular hair cells, but the dosage range of both toxicant and protectant over which protection is seen is limited.

### **609 Heat Shock Inhibits Ototoxic Drug-Induced Hair Cell Death**

**Lisa Cunningham**<sup>1</sup>, Carlene Brandon<sup>1</sup>

<sup>1</sup>Medical University of South Carolina

Human hearing and balance impairments are often due to death of sensory hair cells. These cells are hypersensitive to death induced by noise exposure, aging, and some therapeutic drugs. Two major classes of ototoxic drugs are the aminoglycoside antibiotics and the antineoplastic agent cisplatin. Exposure to these drugs results in hair cell death that is mediated by the activation of specific apoptotic proteins. The induction of heat shock proteins (HSPs) in response to cellular stress is a ubiquitous and highly-conserved response that can significantly inhibit apoptosis in some systems by inhibiting apoptotic proteins. HSP induction occurs in hair cells in response to a variety of stimuli. Given the ubiquitous nature of HSP induction in response to cellular stress, we hypothesized that HSP induction is an important modulator of hair cell death and survival in response to ototoxic drug exposure. In order to begin to test this hypothesis, we have developed a method for inducing HSP expression in the adult mouse utricle *in vitro*. Utricles are cultured at 37°C overnight before being heat shocked at 43°C for 30 minutes and then returned to

37°C for 6 hours. This protocol reliably produces a robust upregulation of HSP-70 mRNA and HSP-70 protein, but does not result in death of hair cells. The heat shock protocol has a significant protective effect against both cisplatin-induced and neomycin-induced hair cell death in the utricle preparation. Six hours after heat shock, control and heat-shocked utricles were exposed to neomycin (1 mM) or cisplatin (15  $\mu$ g/ml) for 24 hours. Utricles were then fixed and hair cells were counted. Heat shock treatment significantly inhibited hair cell death caused by exposure to neomycin ( $p < 0.05$  for  $n = 7-13$  utricles per condition). The heat shock treatment also had a protective effect against cisplatin-induced hair cell death ( $p < 0.001$  for  $n = 9-12$  utricles per condition). These data indicate that heat shock can protect hair cells against ototoxic drug-induced death.

### **610 Modeling High-Frequency Electromotility of Cochlear Outer Hair Cell in Microchamber Experiment**

**Zhijie Liao**<sup>1</sup>, Aleksander Popel<sup>1</sup>, William Brownell<sup>2</sup>, Alexander Spector<sup>1</sup>

<sup>1</sup>Johns Hopkins University, <sup>2</sup>Baylor College of Medicine

Cochlear outer hair cell (OHCs) electromotility is critical for the amplification and sharp frequency selectivity of the mammalian ear. This property of OHCs is particularly pronounced for high-frequency conditions. Microchamber experiments permit experimental investigation of OHC high-frequency performance. In this study, we simulate the OHC electrical-mechanical behavior in the microchamber. Our model takes into account the inertial and viscous properties of the fluids inside and outside the cell as well as the viscoelastic and piezoelectric properties of the cell composite membrane (lateral wall). The closed ends of the cylindrical cell were considered as oscillatory rigid plates. The solution to the problem was obtained in terms of Fourier series, and model results are consistent with experimental results (Dallos and Evans, 1995; Frank et al., 1999). We analyzed the conditions of the interaction between the cell and pipette and found that the amount of slip along the contact surface could have a significant effect on the cell electromotile response. The viscosity of the external fluid was assumed to be equal to that of water, and the viscosity of the internal fluid was varied within a range with the upper bound of 10 times greater than the water viscosity. The viscosity of the OHC wall is not presently available. This parameter was chosen on the basis of information on other cell types. Finally, the cell's electrically evoked length changes were computed as a function of frequency, and their dependence on the viscosities of both fluids and of the cell wall was analyzed. We also estimated the distribution of the viscous losses inside the fluids. The proposed approach can help in a better understanding of the high-frequency OHC electromotility under experimental and physiological conditions.

Supported by NIDCD research grants R01 DC 02775 & DC00354.

## **611 High-Frequency Force Generation in Constrained Cochlear Outer Hair Cell: A Model Study**

Zhijie Liao<sup>1</sup>, Aleksander Popel<sup>1</sup>, William Brownell<sup>2</sup>, Alexander Spector<sup>1</sup>

<sup>1</sup>Johns Hopkins University, <sup>2</sup>Baylor College of Medicine

The outer hair cell (OHC) electromotility is critical for the amplification and frequency selectivity of the mammalian hearing process particularly at high-frequencies. The manner by which high-frequency forces might be generated by this membrane-based, piezoelectric-like mechanism requires analysis of the constraints to the OHC in situ. We examine the force generated by OHC as a feedback to vibration of the basilar membrane (BM). In this study, a model of constrained OHCs is developed in order to simulate the in vivo condition where the OHCs are located between the relatively stiff basilar and tectorial membranes. The OHC is modeled as a viscoelastic and piezoelectric cylindrical shell interacting with viscous intracellular and extracellular fluids. The constraint imposed on the cell is represented by a spring with adjustable stiffness. The solution to the problem is obtained in the form of Fourier series. The results of the model are consistent with several experiments under both low and high frequency conditions (Hallworth, 1995; Iwasa and Adachi, 1997; Frank et al., 1999). It was found that constrained OHCs can achieve a much higher corner frequency than unconstrained isolated OHCs. The frequency enhancement depended on the stiffness of the constraint. For the stiffness of the spring equal to that of the BM at the basal turn of cochlea, the computed force was constant up to 100 kHz. This is because a more constrained cell has smaller amplitude of vibration, resulting in a reduction of energy loss both in the viscous fluids and the viscoelastic cell wall. This model describing OHC as a local active element can be effectively incorporated into a global cochlear model considering cochlear hydrodynamics as well as the graded BM stiffness and OHC length.

Supported by NIDCD research grants R01 DC 02775 & DC00354.

## **612 Characterization of an Apparent Voltage-Dependent Resistance in the Outer Hair Cells**

Rosen Ugrinov<sup>1,2</sup>, Brenda Farrell<sup>1</sup>, Cynthia Shope<sup>1</sup>, William Brownell<sup>1</sup>

<sup>1</sup>Baylor College of Medicine, Houston, Texas 77030, USA,

<sup>2</sup>Institute of Solid State Physics, Bulgarian Academy of Sciences, Sofia 1784, Bulgaria

The bell-shaped voltage-dependent membrane capacitance,  $C_m$ , of the outer hair cells (OHC) is well characterized. It is frequently calculated from admittance with a dual sinusoidal stimulus. Current is measured with voltage-clamp in whole-cell configuration on cells whose ion channels are blocked. The calculations are based on a conventional equivalent circuit containing a capacitor (membrane capacitance,  $C_m$ ) with a resistor in parallel (membrane resistance,  $R_m$ ) and both in series with a resistor (the pipette resistance,  $R_s$ ). The OHC  $R_m$ , contained in this model shows a robust voltage-

dependence. A plot of the  $R_m$  versus DC voltage exhibits two peaks that are separated by a trough. The first peak ( $> 5x$  baseline) is at a voltage slightly negative to the voltage of the peak of the nonlinear  $C_m$ . The second peak is of much lower magnitude ( $\sim$  baseline) and at a voltage more positive than the peak of the  $C_m$ , but still within the range of the bell-shaped capacitance. The trough ( $<$  baseline) is centered between the two peaks at a voltage more positive than the voltage at peak capacitance. We observe qualitatively similar  $R_m$  vs. voltage plot with prestin transfected human embryonic kidney cells. In addition, we find that salicylate diminishes the voltage dependent  $R_m$ , just as it decreases the nonlinear  $C_m$ . This suggests that prestin is required to observe both the nonlinear  $R_m$  and  $C_m$ . When  $R_m$  is measured by a DC protocol, incrementing 10 mV steps from -150 to 150 mV (each step 100 ms), we do not observe the peaks and trough. In this case the current vs. voltage curve is similar to that of cell membranes with low conductance around zero voltage and reduced resistance at the extreme voltages. Because membrane resistance is not expected to be dependent on the recording procedure this observation suggests that the conventional equivalent circuit does not fully represent the electrical circuit of the OHC.

Supported by NIDCD research grants R01 DC 02775 & DC00354.

## **613 Optimization of Culture Conditions for Established Stable Prestin-expressing CHO Cell Lines**

Koji Iida<sup>1</sup>, Kouhei Tsumoto<sup>1</sup>, Katsuhisa Ikeda<sup>2</sup>, Izumi Kumagai<sup>1</sup>, Toshimitsu Kobayashi<sup>3</sup>, Hiroshi Wada<sup>1</sup>

<sup>1</sup>Tohoku University, <sup>2</sup>Juntendo University School of Medicine, <sup>3</sup>Tohoku University Graduate School of Medicine

Electromotility of outer hair cells (OHCs) is believed to be a major factor in cochlear amplification that enables high sensitivity, wide dynamic range and sharp frequency selectivity of hearing in mammals. This motility is thought to be based on voltage-dependent conformational change of the motor protein prestin embedded in the lateral wall of the OHC. Since identification of prestin, intensive research has been done using prestin-expressing cells to elucidate the function of prestin. However, the motor function of prestin at the molecular level is still unclear. To obtain knowledge about the function of prestin, it should be studied using not only prestin in cells, but also prestin in solution. For this purpose, a method of obtaining a large amount of prestin as material is required. To obtain prestin, we established prestin-expressing cell lines using transfected CHO cells by limiting dilution cloning. The stable expression and the activity of prestin expressed in the generated cell lines were confirmed. In the established cell lines, although the expression levels were lower than those in OHCs and transiently prestin-expressing TSA201 cells, the stable expression of prestin is advantageous for obtaining prestin molecules. In the present study, to efficiently obtain prestin from these cell lines, the type of culture medium, the time course of the quantity of the cells and the amount of prestin per unit number of cells were examined. As a result, it was clarified that cells should be

cultured in serum-free medium as suspension cells and should be harvested around 48 hours after passage.

### **614 Imaging of the Cytoplasmic Face of the Prestin-expressing CHO Cell Membrane by Atomic Force Microscopy**

Michio Murakoshi<sup>1</sup>, Takashi Gomi<sup>1</sup>, Hiroshi Wada<sup>1</sup>

<sup>1</sup>*Tohoku University*

High sensitivity of mammalian hearing is believed to be achieved by cochlear amplification. The basis of this amplification is thought to be the motility of outer hair cells (OHCs), i.e., the elongation and contraction of their longitudinal length in response to acoustical stimulation. The origin of this motility is concerned with a membrane protein distributed over the lateral membrane of the OHCs. This protein has recently been identified and termed prestin (Zheng et al., 2000). From the molecular weight of prestin, the size of prestin can be speculated to be approximately 7 nm in diameter if its shape is assumed to be a cube. However, prestin per se has not directly been observed yet. In this study, to visualize prestin, an attempt was made to observe the plasma membrane of the prestin-expressing CHO cells by atomic force microscopy (AFM). First, CHO cells on the substrate were sonicated to leave the sheets of the plasma membrane on the substrate. The cytoplasmic face of the prestin-expressing CHO cell membrane was then observed by AFM in liquid. At a low magnification scanning, i.e., imaging of large area (10  $\mu\text{m} \times 10 \mu\text{m}$ ), the large globular structures with a diameter of approximately 100 nm were recognized. Therefore, high-magnification AFM images, i.e., imaging of small area (0.5  $\mu\text{m} \times 1.0 \mu\text{m}$ ), were obtained at the membrane areas without such heterogeneous structures with over 100 nm in diameter, because the size of the membrane proteins is the order of 10 nm. As a result, particle-like structures were recognized in the plasma membranes of both untransfected CHO cells and prestin-expressing CHO cells. However, statistical analysis indicated that density of particle-like structures with an estimated diameter of 8-13 nm in the plasma membrane of the prestin-expressing CHO cells was significantly higher than those in untransfected CHO cells. Results show that not all but the majority of these particle-like structures are likely to be prestin.

### **615 Development and Expression of Helper-Dependent Adenovirus Containing Prestin in HEK 293 Cells**

Anping Xia<sup>1</sup>, Rosen Ugrinov<sup>1</sup>, Gentiana Wenzel<sup>1</sup>, Feng Lin<sup>1</sup>, Cynthia Shope<sup>1</sup>, Philip Ng<sup>1</sup>, Fred Pereira<sup>1</sup>, William Brownell<sup>1</sup>, John Oghalai<sup>1</sup>

<sup>1</sup>*Baylor College of Medicine*

Prestin is a membrane protein necessary for outer hair cell (OHC) electromotility. We sought to create an adenoviral (Ad) vector for gene transfer experiments containing the prestin gene. Rather than using a more routine Ad5 viral serotype that lacks the E1 and E3 regions of the native viral DNA, we created a helper-dependent adenovirus (HDAd) that contains no native viral DNA. Thus in theory,

toxic side effects from the viral vector should be reduced. Gerbil prestin cDNA was inserted into a shuttle pCMV-IRES-hrGFP plasmid. Then, a hemagglutinin (HA) tag was added in front of prestin as an aid for later immunofluorescence analysis. The pCMV-HA-Prestin-IRES-hrGFP DNA fragment was excised and inserted into a stuffer HDAd DNA plasmid. This plasmid contains no viral DNA except for the inverted terminal repeats necessary for DNA replication and the packaging signal necessary for encapsulation of the vector genome. The HDAd DNA was transfected into 293Cre cells and the titer increased by serial coinfections with a helper adenovirus bearing a packaging signal flanked by loxP sites. Cre-mediated excision rendered the helper virus genome unpackageable, but still able to replicate and provide all of the necessary trans-acting factors for propagation of the HDAd. Finally, the HDAd vector was purified by CsCl<sub>2</sub> ultracentrifugation to a concentration of 5x10<sup>12</sup> viral particles/ml. The HDAd containing prestin was applied to HEK 293 cells at multiplicity of infections (MOI) ranging from 10-800 and cultured overnight. The gene reporter protein GFP was visible under fluorescent microscopy in all dishes with an MOI > 330. At MOIs > 600, over half the cells were infected. We performed whole-cell voltage clamp experiments to measure the non-linear capacitance in infected cells and in uninfected controls. Infected cells demonstrated a bell-shaped voltage-dependent non-linear capacitance of about 2 pF that peaked at -40 mV that was absent in controls. This study demonstrates that HDAd with prestin can infect HEK 293 cells and cause them to develop a non-linear capacitance. Studies to assess the infection rate and viral toxicity in an in vivo preparation are underway.

Supported by NIDCD Grants R01 DC 02775 & DC00354 (WEB), DC04585 (FAP) & DC006671, The American Hearing Research Foundation, and The Caroline Weiss Law Fund for Research in Molecular Medicine (JSO)

### **616 Preliminary Study of Prestin's Oligomerization**

Jing Zheng<sup>1</sup>, Alex Orem<sup>1</sup>, Guo-Guang Du<sup>1</sup>, Charles T. Anderson<sup>1</sup>, Peter Dallos<sup>1</sup>

<sup>1</sup>*Northwestern University*

Prestin is the motor protein in the lateral membrane of outer hair cells (OHCs). Prestin is a member of the solute carrier family 26, it has 744 amino acids and provides the molecular basis for OHC's electromotility, which is crucial for frequency selectivity and sensitivity of mammalian hearing. It is thought that these abundantly expressed motor proteins constitute the 11-nm particles present in the plasma membrane of OHCs. Since the estimated size of a prestin-monomer is too small to form an 11-nm particle, the possibility of prestin's oligomerization is studied.

We have inserted Prestin cDNA into different expression systems. When prestin was studied in SDS-PAGE/Western blot experiments, two bands were consistently found in different host cells including prestin-expressing OHCs and prestin-expressing yeast. The size of the higher molecular-weight band is about twice that of the lower prestin band. These data imply that prestin may

exist as a dimer or multimer. In order to test this possibility, prestin was further studied in a yeast two-hybrid system. The interactions between prestin-bait/prestin-prey and prestin-bait/C-terminus-of-prestin-prey were tested. Our data suggest that prestin molecules can associate with themselves, and that their C-terminus fragments (499-744 a.a) are involved in this association. When the C-terminus fragment alone is expressed in yeast, multiple bands were found on a Western blot, including a dimer. These data indicate that the C-terminus can exist as multiple forms of oligomers. The oligomeric structure of the full-length prestin is under further study. [Supported by Grant DC00089 and The Hugh Knowles Center Leadership Fund]

### **617 The Outer Hair Cell Electro-Mechanical Wave**

**Sarah Clifford**<sup>1</sup>, William Brownell<sup>2</sup>, Richard Rabbitt<sup>1</sup>

<sup>1</sup>University of Utah, <sup>2</sup>Baylor College of Medicine

Distributed systems that efficiently store energy in both kinetic and potential forms give rise to propagating waves – acoustic waves and shear waves in elastic materials are two examples. Resonance in these systems results from reflections at the boundaries and constructive interference of multiple traveling waves moving in various directions. We have previously reported (ARO, 2004) the presence of resonance in isolated outer hair cells (OHCs). Here we examine the nature of the wave behavior that would be expected to underlie OHC resonance. It was modeled from first principles to account for the structure and properties of the OHC lateral wall including: 1) the fluid mass entrained by movement of the plasma membrane; 2) the electrical constraint imposed by the presence of the sub-surface cisterna (SSC); and 3) the electrical properties of the plasma membrane (PM). The model predicts the presence of electro-mechanical waves that propagate along the lateral wall. Energy storage is alternately electrical and mechanical and the waves are dispersive. They decay as they propagate due to both electrical and mechanical losses. The space constant decreases with increasing frequency, consistent with the cochlear map and the correlation between OHC length and best frequency. The functional importance of the SSC is to increase intracellular axial resistance and thereby direct current from the transduction channels to the piezoelectric-like lateral wall. This increases motile responses to injected current by reducing both the effective input capacitance and the current losses through the basal membrane in a frequency dependent manner. The SSC is also predicted to slow the wave propagation speed. Voltage-dependent capacitance observed in OHCs is predicted exclusively on the basis of a nonlinear piezoelectric coefficient without the need to invoke a voltage-dependent permittivity (supported by NIDCD R01 DC04928 & DC00354).

### **618 Expression and Purification of the Slc26a5 Transmembrane Protein: Prestin**

**Feng Lin**<sup>1,2</sup>, Haiying Liu<sup>1,2</sup>, Amir Gafur<sup>1,2</sup>, Heather Alger<sup>1,2</sup>, William E. Brownell<sup>1,3</sup>, Amy L. Davidson<sup>1,4</sup>, Fred A. Pereira<sup>2,5</sup>

<sup>1</sup>Baylor College of Medicine, <sup>2</sup>Huffington Center on Aging, <sup>3</sup>Otorhinolaryngology, <sup>4</sup>Molecular Virology and Microbiology, <sup>5</sup>Molecular and Cellular Biology

Prestin is a novel Slc26 (solute carrier 26 family) multi-pass transmembrane protein of the basolateral wall in outer hair cells (OHC) in the organ of Corti. It is functionally required for OHC electromotility and for the sensitivity and frequency-resolving capacity of the mammalian ear. A structural-functional understanding of prestin is required to determine how it enhances charge movement and force production in the membrane. To accomplish this goal we have utilized an inducible yeast expression system to over-express and purify full-length prestin to partial homogeneity. Gerbil prestin cDNA was cloned in-frame and downstream to the ubiquitin (Ub) and glutathione-S-transferase (GST) proteins to create a fusion protein Ub-GST-prestin in the yeast expression vector PCBGST-1. This construct was transformed into the protease deficient yeast BJ2168, which allows for stabilized high-level expression of exogenous protein. Growth of this strain in the presence of CuSO<sub>4</sub> induces stabilized expression of Ub-GST-prestin, which is endogenously processed to yield GST-prestin that was detected by immunofluorescence in transport vesicles and in the plasma membrane (PM). Purification of prestin was achieved by isolating the crude PM fraction and extraction with detergents prior to glutathione-Sepharose capture and elution. Testing of numerous detergent combinations yielded varying efficiencies of extraction from membranes with DDM (n-dodecyl-beta-D-maltoside) and NOG (n-octyl-beta-D-glucopyranoside) offering the best extractions as determined by Western blot, Coomassie and silver stained analyses to determine the extent of purity of extracted prestin. A plentiful source of biologically active and pure prestin will facilitate ongoing projects to determine the biophysical properties of prestin. Supported by NIDCD R01 grants: DC 02775 & DC 00354 (WEB), DC 04585 (FAP) and GM 49261 (ALD).

### **619 Prestin Transport: Temporal and Spatial Co-Localization with Intracellular Markers**

**Donald Yoo**<sup>1</sup>, Feng Lin<sup>1</sup>, Haiying Liu<sup>1</sup>, Julie-Anne Goddard<sup>1</sup>, William Brownell<sup>1</sup>, Fred Pereira<sup>1</sup>

<sup>1</sup>Baylor College of Medicine

Prestin, a member of the SLC26 family of anion transporters, has garnered intense interest as the membrane protein that is crucial for the membrane-based electromotility of mammalian outer hair cells (OHC). The electrical signature of the electromotile response is a charge movement called non-linear capacitance (NLC). The NLC has been demonstrated to be both gained by cells transfected with functional prestin, and is lost in OHCs lacking functional prestin. While prestin is thought to reside in or around the plasma membrane in order to confer NLC to the cell, the details of its synthesis and

transport, and its precise location in the cell, have yet to be determined. We show that prestin requires 12 hours to be fully expressed in the plasma membrane of transfected HEK-293 cells; interestingly, this expression is not uniform throughout the plasma membrane but shows a punctate distribution. Through colocalization studies with clathrin, LAMP2, caveolin, and endoplasmic reticulum (ER) markers by immunofluorescence staining, we present evidence that prestin does not colocalize with clathrin, while it does show colocalization with LAMP2, caveolin and the ER. Transport within these vesicles is consistent with prestin's identity as a membrane protein. Knowledge of the timing and details of prestin's transport to and position in the basolateral plasma membrane of the OHC is critical to further elucidating the significance of this novel membrane protein.

## **620 Unraveling the Outer Hair Cell RC Paradox**

**Richard Rabbitt<sup>1</sup>**, Sarah Clifford<sup>1</sup>

<sup>1</sup>*University of Utah*

The physiological role of voltage-driven outer hair cell (OHC) somatic electromotility has been called into question based on the mere presence of plasma membrane capacitance – a biophysical feature of virtually all cells that would be expected to sharply attenuate receptor potential modulations of OHCs at auditory frequencies. Relatively recent data on the rapidly adapting kinetics of OHC transduction currents (Kennedy et al., 2004 *Nat. Neurosci.*, 6(8):832), and evidence of electro-mechanical resonance and waves in the OHC lateral wall (Rabbitt et al., ARO 2004) led us to revisit this question from a theoretical perspective. For this, we applied first physical principles to derive a model of OHC electro-mechanics consisting of an electrical cable equation directly coupled to a mechanical wave equation. This model was further coupled to an empirical model of transduction current adaptation. Results indicate that there is no RC paradox. Two factors are responsible. For low-frequency stimuli, below the characteristic best frequency (CF), the model predicts that the kinetics of transduction current adaptation effectively cancels the adverse effect of hair cell capacitance. As the frequency is increased, above the adaptation corner and above CF, the effect of outer hair cell electro-dynamics is predicted to generate sustained responses via wave propagation along the lateral wall. The net result is a robust somatic motile response to hair bundle displacements that is predicted to extend into the ultrasonic frequency range (supported by the NIDCD R01 DC04928).

## **621 Perilymph Osmolarity Modulates Cochlear Function**

**Chul-Hee Choi<sup>1</sup>**, Alexander A Spector<sup>2</sup>, John S Oghalai<sup>1</sup>

<sup>1</sup>*Baylor College of Medicine*, <sup>2</sup>*The Johns Hopkins University*

Outer hair cells (OHCs) have an intracellular turgor pressure, but maintain a cylindrical shape because of their elastic lateral wall cytoskeleton. In vitro, changing the osmolarity of the extracellular fluid produces changes in

OHC morphology, compliance, and force production. We sought to determine the effects of changing perilymph osmolarity on cochlear function. First, we created a mathematical model of cochlear mechanics using several unique biophysical properties of the OHC such as its orthotropic cytoskeleton, its intracellular turgor pressure, and the longitudinal and radial vectors related to electromotility force generation. The simulation demonstrated that hypo-osmotic perilymph (260mOsm) increased and hyper-osmotic perilymph (340mOsm) decreased basilar membrane velocity at the characteristic frequency by approximately 20 dB. There was little change in basilar membrane velocity at frequencies away from the characteristic frequency and there was no change in the phase of basilar membrane velocity. Second, we tested the hypothesis experimentally by perfusing the guinea pig cochlea with hypo- or hyper-osmotic artificial perilymph made by changing the glucose concentration. After perfusing hypo-osmotic perilymph, compound action potential thresholds decreased 5-10 dB and distortion product otoacoustic emissions thresholds decreased 2-3 dB across the frequency range of 4-20 kHz (n=8). These effects reversed after washout with artificial perilymph of normal osmolarity (300mOsm). The opposite effects were seen when hyper-osmotic perilymph was perfused. Compound action potential thresholds increased 10-20 dB and distortion product otoacoustic emissions thresholds increased 3-5 dB. These findings suggest that changing perilymph osmolarity modulates cochlear function by affecting OHC electromotility via changes in cell turgor pressure. The magnitude of the measured effects is consistent with the predictions of our mathematical model. We are currently measuring basilar membrane velocity with a laser doppler vibrometer to lend additional support to this hypothesis.

Supported by NIH grants: NIDCD DC05131 and the National Organization for Hearing Research Foundation (J.S.Oghalai), and DC00354 (A.A.Spector)

## **622 Advanced Optical Techniques for Investigating Outer Hair Cell Plasma Membranes**

**Jennifer N Greeson<sup>1</sup>**, Louise E Organ<sup>1</sup>, Robert M Raphael<sup>1</sup>

<sup>1</sup>*Rice University*

The outer hair cells (OHCs) of the mammalian cochlea operate as mechano-electrical transducers, converting changes in membrane potential into mechanical forces manifested as axial length changes. This somatic deformation is termed electromotility and is responsible for the remarkable sensitivity and frequency selectivity of the mammalian auditory system. Although the complete mechanism of electromotility is not presently understood, the discovery and localization of prestin to the OHC plasma membrane promotes the importance of the membrane in both OHC and cochlear behavior. A complete understanding of the individual constituents of the plasma membrane, both lipids and proteins, as well as their interactions, is crucial to future analyses of OHC function. A major research goal in our laboratory is to

apply advanced fluorescent microscopy techniques to examine lateral mobility, protein-protein interactions, and molecular orientation within the OHC plasma membrane. We are currently implementing fluorescence recovery after photobleaching (FRAP) in a variety of cellular model systems to evaluate the membrane diffusion of lipids, lipid analogues, and proteins. We are also utilizing fluorescence resonance energy transfer (FRET) to assay the degree of prestin self-association in transfected human embryonic kidney (HEK) cells. Finally, we are employing fluorescence polarization microscopy (FPM) to model the orientation of membrane-embedded fluorescent molecules. This preliminary work will allow for sophisticated quantitative studies of the components and activity of OHC plasma membranes.

### **623 Effects of Tarantula Toxin and Amphipathic Ions on the Membrane Motor of Outer Hair Cells**

**Jie Fang**<sup>1</sup>, Kuni Iwasa<sup>1</sup>

<sup>1</sup>*National Institutes of Health*

The membrane motor of outer hair cells is sensitive to membrane tension[1] as well as mechano-sensitive ion channels are. Such sensitivity should allow chemical agents that modify lipid bilayers to affect these proteins' activity. Indeed, amphipathic ions trinitrophenol(TNP) and chlorpromazine (CPZ) open bacterial mechanosensitive channel MscL[2] and GsMTx4, a hydrophobic peptide from tarantula venom, closes a vertebrate stretch-activated cation channel (SAC)[3]. Here we report the effects of these amphipathic ions on the membrane motor of outer hair cells.

Unlike salicylate (anionic amphipath) and gadolinium ion (blocker of the stretch sensitive cation channel) these amphipathic ions do not significantly reduce the motility or motor charge, indicated by the peak height of the nonlinear capacitance. Instead, these ions, both cations and anions, induce positive shifts in the voltage dependence of the membrane motor. The shift was 10 mV for 0.5 mM TNP (anionic), 20 mV for 0.05 mM CPZ (cationic), 20 mV for 0.005 mM GsMTx4 (cationic). The value for CPZ is consistent with an earlier report[4]. The effective doses of these chemicals for the membrane motor are similar to those for mechanosensitive channels. These induced shifts change the operating point of the motor and have the effect of reducing the motile response of outer hair cells in physiological conditions.

We interpret that these shifts in the voltage dependence of the membrane motor is due to an increased tension felt by the motor. Insertion of these amphipathic ions to lipid bilayer adjacent to the motor deforms the membrane at the interface. Specifically in the case of the membrane motor, these ions have the effect same as increased membrane tension. That in turn favors the stretched conformation of the motor, leading to positive shifts in its voltage dependence. In contrast, salicylate seems to interact with the motor in a more specific manner.

[1] Iwasa, *Biophys J*, 65 (1993) 482-498

[2] Martinac and Kung, *Nature*, 348 (1990) 261-263

[3] Suchyna et al., *J Gen Physiol*, 115 (2000) 583-598

[4] Lue et al., *Otolaryngol Neck Head Surg*, 125 (2001) 71-76

### **624 Effects of Auditory Nerve Compression on Cochlear Microphonic Harmonics**

**Jorge Bohorquez**<sup>1</sup>, Ozcan Ozdamar<sup>1,2</sup>, Krzysztof Morawski<sup>3</sup>, Fred Telischi<sup>1,2</sup>, Rafael Delgado<sup>1,4</sup>, Erdem Yavuz<sup>1</sup>

<sup>1</sup>*University of Miami Department of Biomedical Engineering*, <sup>2</sup>*University of Miami Department of Otolaryngology*, <sup>3</sup>*Silesian Medical School Department of Otolaryngology*, <sup>4</sup>*Intelligent Hearing Systems*

Cochlear microphonics (CM), the first two harmonics (CM2 and CM3) and cochlear blood flow (CBF) were simultaneously recorded using a specially designed otic probe, placed into the round window (RW) niche, during experimentally induced compressions of the internal auditory artery (IAA) and cochleo-vestibular nerve (CVN) complex in rabbits. Electrocochleographic (ECoChG) recordings were made using tone burst (5 ms 4KHz of 70 and 80 dB SPL) stimuli during CVN/IAA compressions lasting 1, 3, 5 and 10 minutes. Using digital filters, CM, CM2 and CM3 were extracted from the ECoChG and their amplitudes and phases were tracked. A total of 62 compressions were analyzed. The amplitude of CM followed that of CBF during the induced ischemic episodes while CM phase remained relatively unaffected. CM2 amplitude, however, showed dramatic changes during compressions displaying an overshoot immediately after the onset of compression and then disappeared during the ischemic event, followed by a second overshoot at the compression offset. Unlike CM phase, CM2 phase was more active during the compression, going to zero following the compression onset and showing a 180° phase shift (i.e., polarity inversion) after the release of compression. The third harmonic (CM3) showed a similar behavior to the fundamental component (CM). A model of outer hair cell (OHC) mechano-electrical transduction transfer function was used to explain the behavior of CM harmonics. A Boltzman mechano-electrical transduction transfer function of OHC activity explains the existence and phase characteristics of CM and its harmonics. Cochlear ischemia appears to change the bias factor of the transfer function. In this study, CM harmonics are found to be very sensitive to CVN/IAA manipulation and compressions. In a clinical neuro-monitoring system, these signals may be useful in monitoring cochlear function during skull base surgery to prevent post-operative hearing loss.

### **625 Expression and Localization Studies of the TMC1 Protein**

**Tomoko Makishima**<sup>1</sup>, Rachel Macnamara<sup>1</sup>, Kiyoto Kurima<sup>1</sup>, Andrew Griffith<sup>1</sup>

<sup>1</sup>*NIDCD, NIH*

Mutations in *TMC1/Tmc1* can cause dominant (DFNA36, Beethoven) and recessive (DFNB7/11, deafness) hearing loss in humans and mice. *TMC1/Tmc1* is a novel gene predicted to encode a multi-pass transmembrane protein with no significant sequence similarity to genes of known

function. *Tmc1* mRNA is expressed in mouse cochlear and vestibular hair cells, but its function remains unknown. Antibodies were generated against mouse TMC1 in order to determine its location in the inner ear. We immunized rabbits with a synthetic 20-amino acid peptide corresponding to a portion of the C-terminal tail or a GST-fusion protein containing all 60 amino acids of the C-terminal tail. We validated the specificity of the antibodies by western blot, immunoprecipitation, and indirect immunofluorescence analyses of COS-7 cells expressing recombinant TMC1.

Western blot analysis demonstrated that TMC1 is an approximately 100-kDa glycosylated protein. Immunofluorescent staining of TMC1 expressed in COS-7 cells revealed a reticular pattern indicative of localization in the endoplasmic reticulum. When antisera were used to stain inner ears of C57BL/6J mice, the strongest signal was detected in the area surrounding the cuticular plate (i.e. the pericuticular necklace) of both cochlear and vestibular hair cells. This staining pattern was observed only for mice at postnatal day 10 or older, consistent with previous reports of *Tmc1* mRNA being detectable only after postnatal day 5.

The pericuticular necklace is thought to be a site of active endocytotic, and perhaps exocytotic, vesicular trafficking in hair cells. Although some proteins located in the pericuticular necklace are also detected in stereocilia, anti-TMC1 antibodies did not stain stereocilia. TMC1 may be required for endocytotic, exocytotic, or membrane trafficking processes at the apices of hair cells, or for signaling events related to these processes.

## **626 Hair-Cell Expression of Plasma Membrane Ca<sup>2+</sup>-ATPase Splicing Region a Isoforms**

Jennifer K. Hill<sup>1</sup>, Emanuel Strehler<sup>2</sup>, Peter G. Gillespie<sup>1</sup>

<sup>1</sup>Oregon Health & Science University, <sup>2</sup>Mayo Clinic College of Medicine

Hair cells maintain their mechano-electrical sensitivity by regulating Ca<sup>2+</sup> that enters through transduction channels. Most Ca<sup>2+</sup> that enters the bundle through these channels is extruded by the plasma membrane Ca<sup>2+</sup>-ATPase (PMCA). There are four PMCA genes (PMCA1-4), each of which has two splice regions (A and C); alternative splicing in these regions therefore generates a variety of isoforms. We previously showed that PMCA2 was the only PMCA isoform located in hair bundles; moreover, the predominant splicing region C version of PMCA2 in rat and frog hair bundles was the "a" variant and in frogs, the splicing region A form was the "v" variant (Dumont et al., *J. Neurosci.*, 21:5066; 2001). By contrast, we were unable to identify the specific splicing region A isoform in mammalian hair cells, although we found by RT-PCR only the "w", "x", and "z" splice forms in cochlea and vestibular organs. In PMCA2 expressed in MDCK cells, splicing region A, which determines the "v", "w", "x", "y", or "z" isoforms, apparently dictates apical versus basolateral targeting; "w" was the only region A variant to traffic to the apical membrane of this polarized-epithelial cell line (Chicka & Strehler, *J. Biol. Chem.* 278, 18464; 2003). To

determine conclusively the specific bundle isoform of PMCA2 in rat hair cells, we examined the splicing region A variant expression using immunohistochemistry. Because we found strong immunoreactivity for the "w" splice variant in hair bundles and did not detect expression of either the "x" or "z" variants, we conclude that PMCA2aw is the bundle isoform of PMCA in rat hair cells.

(Supported by DC04571).

## **627 A Comparison of Scala Media and Scala Tympani Helper-Dependent Adenovirus Injection in Mice**

Gentiana I. Wenzel<sup>1</sup>, Drew Sawyer<sup>1</sup>, Brad Evans<sup>1</sup>, Anping Xia<sup>1</sup>, Donna J. Palmer<sup>2</sup>, Philip Ng<sup>2</sup>, Fred A. Pereira<sup>3</sup>, John S. Oghalai<sup>1</sup>

<sup>1</sup>Dept. of Otolaryngology- Head and Neck Surgery, Baylor College of Medicine, Houston, TX 77030, USA,

<sup>2</sup>Department of Molecular and Human Genetics, Baylor College of Medicine, Houston, TX 77030, USA, <sup>3</sup>Huffington Center on Aging, Baylor College of Medicine, Houston, 77030 TX, USA

Adenoviral gene transfer experiments in mice have focused on delivering the virus via the perilymph. One downside of this approach is that the infection rate of cells within the organ of Corti is low. We sought to compare the rate of hearing preservation and the efficiency of gene transfer to the organ of Corti using *scala media* (SM) and *scala tympani* (ST) injection techniques. Anesthetized, wild type C57BL mice were infected with 1µl of a viral suspension (8x10<sup>9</sup> viral particle/µl) of a Helper-Dependent adenovirus (HDA) containing the LacZ gene. SM injections were performed by drilling a cochleostomy over the spiral ligament in the second cochlear turn and injecting the virus using a micropipette pulled to a tip diameter of about 10 µm. The ST injection was performed by opening the round window membrane and applying a virus-soaked gelfoam. Auditory brainstem response (ABR) measurements were performed over the frequency range of 4-34 kHz after opening the bulla and cochlea but before viral infection, and after four days of incubation. Whole mount preparations of the cochleae were then studied. The SM injection technique was performed on 6 mice, 5 of which demonstrated infection of the organ of Corti after 4 days. All of the mice had normal ABR thresholds after opening the bulla, 1 mouse lost all ABRs after opening the cochlea, and 2 mice lost all ABRs after 4 days of incubation. In the 3 mice that were infected and maintained some residual hearing, the mean threshold shift caused by opening the cochlea was 27±19 dB and the viral injection was 9±9 dB. The ST injection technique was performed on 11 mice, 5 of which demonstrated infection of the organ of Corti after 4 days. Again, all of the mice had normal ABR thresholds after opening the bulla, but no mice lost all ABRs after opening the cochlea or after 4 days of incubation. In the 5 mice that were infected, the mean threshold shift caused by opening the cochlea was 11±4 dB and the viral injection was 8±5 dB. Our results suggest that the SM injection technique is more traumatic than ST injection, but that the efficiency of organ of Corti infection is better. Further studies are underway to



decrease the trauma associated with this technique and to determine the rate of hair cell infection.

Supported by DC 006671, The American Hearing Research Foundation (JSO)

### **628 A Novel Bovine Virus Efficiently Transduces Inner Ear Neuroepithelial Cells**

**Mark Schneider**<sup>1</sup>, Agnieszka Rzadzinska<sup>2</sup>, Giovanni Di Pasquale<sup>1</sup>, Ioannis Bossis<sup>1</sup>, John Chiorini<sup>1</sup>, Bechara Kachar<sup>1</sup>

<sup>1</sup>NIH, <sup>2</sup>Sanger Institute

Hearing and balance depend on the function of the inner ear sensory epithelium and genetic disruption of the cellular composition or arrangement of the sensory epithelia due to receptor hair cells or specialized supporting cell damage leads to hearing loss and vestibular dysfunctions. These peripheral hearing disorders make good targets for gene therapy; however, development requires efficient gene transfer methods for the inner ear. Herein, we characterized the cellular tropism of a novel adeno-associated bovine virus vector (BAAV) in cultured inner ear epithelia and compared this vector with other serotypes of adeno-associated viruses, AAV2, -4, and -5. To help identify transduced cells, we used beta actin-GFP as a reporter gene because this fusion protein is progressively incorporated into stereocilia. We found BAAV had the highest transduction efficiency. BAAV transduced up to 48% of vestibular and 16% of auditory hair cells as well as a number of supporting cells with no apparent pathological effects. The number of transduced cells significantly increased in both a dose and time dependent manner. Transduction was independent of the maturation state of the cells and was observed in both PD 2 and PD 10 cultures. Interestingly, even after several days of incubation with BAAV, hair cells demonstrated varying progression of beta actin-GFP incorporation, which suggests that the onset of viral transduction can occur throughout the course of the experiment. Of the other tested AAVs, AAV2 and AAV5 transduced only a small percentage of inner and

### **629 Dynamic Expression of COUP-TFI and II in Development and Functional Maturation of the Organ of Corti**

**Louisa Tang**<sup>1</sup>, Heather Alger<sup>1</sup>, Feng Lin<sup>1</sup>, Fred Pereira<sup>1,2</sup>

<sup>1</sup>Huffington Center on Aging, Baylor College of Medicine, One Baylor Plaza, Houston, TX 77030, <sup>2</sup>Department of Otorhinolaryngology, Baylor College of Medicine, One Baylor Plaza, Houston, TX 77030

COUP-TFs (chicken ovalbumin upstream promoter transcription factors) are orphan members of the steroid/thyroid hormone receptor superfamily for which the ligands have not been identified. Two members, COUP-TFI and COUP-TFII, share a high degree of identity and regulate many aspects of mammalian development, differentiation, metabolism and homeostasis. Although the general expression patterns of COUP-TFI and II in the mouse embryo is reported, their precise expression profiles in the inner ear is unclear. Since the COUP-TFI

mutant is reported to be deaf, in this study, we systemically examined the temporal and spatial expression profiles of COUP-TFI and II transcripts and protein during the development of murine cochlea, and in the post-natal functional maturation of the organ of Corti. We found that both COUP-TFI and II were expressed during the onset of otocyst formation. Their expressions were dynamic in the developing sensory epithelium where COUP-TFI expression up-regulation correlated with the differentiation of hair cells and support cells whereas COUP-TFII expression was down-regulated with progression of hair cell differentiation. Moreover, no COUP-TFII was expressed in functionally maturing hair cells during post-natal development. Interestingly, the nuclear COUP-TFI receptor protein was not only found in the nucleus but was also detected in the cytoplasm of functionally maturing hair cells and in pillar cells. Collectively, although COUP-TFI and II are homologues within the COUP-TFs family, their expression patterns in the developing murine cochlea are different. Their restricted pattern of expression during cochlea development suggests that COUP-TFI and II each may play vital but different roles in regulating the differentiation and formation of a functional hearing system. (This work is supported by grant DC04585)

### **630 Mind the Gap: Selective Dye Transfer Supports the Existence of Heteromeric Connexons in the Organ of Corti**

**Daniel Jagger**<sup>1</sup>, Andrew Forge<sup>1</sup>

<sup>1</sup>University College London

Cochlear gap junctions may be constructed from unique heteromeric connexons, comprising connexin 26 (cx26) and cx30. The disruption of such channels may explain the non-syndromic nature of certain types of inherited deafness. Groups of HeLa cells co-expressing cx26 and cx30 are unable to pass Lucifer yellow (LY; mw 443, charge -2), but do pass neurobiotin (NB; mw 287, +1). HeLa cells expressing only cx26 pass LY and NB; cells expressing cx30 alone pass NB only. Here we have explored native gap junctions in the developing rat organ of Corti, by studying dye transfer in cochlear slices from birth to the onset of hearing (P0-P12).

Dyes were co-loaded into single supporting cells during whole-cell patch recordings. NB (visualised by CY3-conjugated streptavidin) and LY spread were observed by confocal microscopy. At P0 there was transfer of LY and NB between supporting cells around inner hair cells (IHC), but dye transfer was restricted between supporting cells of outer hair cells (OHC). By P8 there was extensive transfer of both dyes between supporting cells of IHC or OHC, and between heterotypic pillar cells. At P12 LY was retained in single supporting cells. However, NB passed freely between OHC supporting cells, or between IHC supporting cells. There was no transfer of NB between heterotypic pillar cells at P12. There was no dye transfer into hair cells at any age.

The results suggest a change in the connexin composition of organ of Corti gap junctions during development. By hearing onset, the lack of Lucifer yellow transfer argues against continued expression of homomeric cx26

connexons. The data supports the existence of cochlea-specific heteromeric cx26/cx30 connexons. Also, supporting cells of the functioning organ of Corti appear organized into distinct medial and lateral compartments. Supported by The Royal Society, Defeating Deafness, and The Wellcome Trust.

### **631 Identification of Genes Expressed in Zebrafish Hair Cells**

**Brian McDermott**<sup>1,2</sup>, Jessica Baucom<sup>1,2</sup>, A.J. Hudspeth<sup>1,2</sup>  
<sup>1</sup>*Rockefeller University*, <sup>2</sup>*Howard Hughes Medical Institute*

In its role as a sensory receptor that converts mechanical stimuli into electrical responses, a hair cell contains distinctive structures with specialized molecular components, including the hair bundle that mediates mechanotransduction and presynaptic active zones that permit tonic vesicular release. Because of the paucity of starting material in each vertebrate ear, on the order of tens of thousands of hair cells, and the unavailability of a pure population of hair cells, few of the hair cell's specialized molecular components have been identified and a comprehensive census of the cell's molecular constituents has yet to be accomplished.

We are using the zebrafish as a model system for the study of the acousticolateralis system. Hair cells in the inner ear of the zebrafish mediate the sense of hearing and equilibrium, whereas those in the lateral-line system participate in rheotaxis. The zebrafish offers many advantages for studying the acousticolateralis system, including rapid aural development, optical clarity, robust forward and reverse genetic methods, and transgenic methodologies.

As a starting point for an understanding of the molecular constituents of the hair cell, we have used DNA microarray technology to identify the transcripts present in adult zebrafish hair cells. Methods have been developed to rapidly isolate small, pure populations of hair cells from the lagena of the inner ear. RNA from these populations has been amplified, labeled, and hybridized to oligonucleotide microarrays. The amplification process that was used produced greater than a million-fold increase in labeled RNA from the transcripts contained in 200 hair cells. The hair-cell transcriptome of the zebrafish includes genes involved in cytoskeletal function, vesicular fusion, transcription, and ion flow across membranes. Among these are homologs of genes that, when mutated, produce deafness in humans and mice. The transcription profile also encompasses genes of undetermined function. Using the genetic techniques applicable to the zebrafish, we shall investigate the roles that some of these genes' products play in hair-cell development and function.

This research was supported by grant DC00241 from the National Institutes of Health.

### **632 A Secretory-Type Protein Interacts with the A-Type Channel in the Cochlea**

**Bernd Sokolowski**<sup>1</sup>, Dmytro Duzhyy<sup>1</sup>, Margaret Harvey<sup>1</sup>, Joerg Karolat<sup>1</sup>

<sup>1</sup>*University of South Florida*

Sensory and ganglion cells of the chick express an A-type channel (Kv4.2) that is blocked by the polyunsaturated fatty acid, arachidonic acid (Sokolowski et al., *J. Neurosci*, 24:6265-78, 2004). Previously, we examined potential interacting partners of Kv4.2, using the yeast two-hybrid system (Duzhyy et al., *ARO Abst* 461, 2004). These experiments showed that a protein with a pentraxin domain (PPTX) interacts with the N-terminal end of Kv4.2. Here, we report the characteristics of PPTX, which colocalizes with Kv4.2 in both cochlear hair cells and ganglion cells. PPTX contains 433 amino acids with a signal sequence containing a cleavage site at the N-terminus. Experiments using Na<sup>+</sup>-carbonate suggest that PPTX is a peripheral membrane protein as opposed to a protein containing two transmembrane regions, as predicted by hydrophobicity analysis. Additionally, our experiments show that PPTX is a secretory protein. When CHO cells are transfected with full-length recombinant PPTX, both wild type and truncated PPTX are expressed in cellular lysates and in secreted products. Mutations of the signal peptide cleavage site inhibit the expression of these variants. Experiments with brefeldin A, which blocks the classical ER-Golgi pathway to secretion, show that most truncated variants follow this path, except for one, which follows a non-classical route to secretion. Functional studies suggest that PPTX does not alter the inactivation kinetics of Kv4.2, as demonstrated by whole cell recordings of CHO cells, nor does it act as a shuttle protein, as demonstrated in COS cells. PPTX belongs to the family of "long" pentraxins that include neuronal pentraxins, apexin, and tumour necrosis factor-stimulated gene-14. Moreover, PPTX is a member of a superfamily of proteins that includes laminin-G and thrombospondins. Site-directed mutagenesis of the Kv4.2 N-terminus may provide insights into PPTX-Kv4 functional interactions.

Supported by NIDCD grant DC43095 to BHAS.

### **633 Regional Kcnq4 Expression in the Developing Vestibular End-organs**

**Sonia Rocha-Sanchez**<sup>1</sup>, Ken Morris<sup>1</sup>, Liliana Minichiello<sup>2</sup>, Carla Sciarretta<sup>2</sup>, Bechara Kachar<sup>3</sup>, Bernd Fritzsche<sup>1</sup>, Kirk Beisel<sup>1</sup>

<sup>1</sup>*Creighton University*, <sup>2</sup>*EMBL, Monterotondo*, <sup>3</sup>*NIDCD/NIH*

Mammalian otolith sensory epithelium is composed by two types of hair cells (HCs): Type I, enclosed in a large calyx afferent ending, and Type II, connected on its basolateral surface by bouton afferent endings. Kcnq4, a member of the KCNQ voltage-gate K<sup>+</sup> ion channel gene family, was thought to be expressed primarily in Type I HCs and possibly in the afferent calyxes (Kharkovets, et al. 2000). However, the precise cellular localization of Kcnq4 is not yet resolved. Whole mount immunohistochemistry was done using Kcnq4 antibodies to determine the spatiotemporal developmental pattern in the vestibular system. Our results clearly demonstrate a topographical

expression and upregulation of Kcnq4 during development. Kcnq4 expression was detected as early as E18.5 restricted to the striolar region HCs in both utricle and sacuole. During the postnatal maturation period Kcnq4 expression showed an increase, such that by P21, both utricle and sacuole striolar and extrastriolar HCs were stained. However striolar HCs still exhibited the highest levels of expression. By P35 striolar and extrastriolar HCs showed comparable staining. The same pattern of expression was observed to the HCs in the three cristae. In these end-organs the expression started in the central zone HCs, spreading over the entire sensory epithelia as the mice aged. Quantitative PCR analysis using microdissected utricle striolar and extrastriolar regions confirmed the ImHChem results, revealing significant Kcnq4 expression differences between tissues (at P21) and ages (P21 vs. P35). In order to test any HC specificity in the expression of Kcnq4, we have performed ImHChem in TrkB PLC- $\gamma$  mutant mice, which lack the calyx nerve ending formation. No differences were observed between mutant and wild type mice, showing HC staining even in the absence of a calyx. Our data demonstrate that Kcnq4 exhibits a regional staining pattern in all vestibular end-organs with both Type I and Type II HCs showing expression.

### **634 Developmental Regulation of BK-Type Potassium Channel Expression in the Chicken Basilar Papilla**

R. Keith Duncan<sup>1</sup>, Graham Atkin<sup>1</sup>, Yi Li<sup>1</sup>

<sup>1</sup>University of Michigan

Immature hair cells exhibit spontaneous, slowly-repetitive calcium spikes. However, as development approaches the onset of hearing, hair cells acquire fast, calcium-dependent potassium (BK) currents, turning the immature cells into functional sensory receptors. Interestingly, gene products encoding BK  $\alpha$  subunits are present in the chicken basilar papilla as early as embryonic day 12 (E12), up to 7 days before the appearance of BK currents on E19 (J.B. Yang and P.A. Fuchs, unpublished). Quantitative PCR results in our laboratory show that the relative abundance of BK  $\alpha$  and  $\beta_1$  subunits is unchanged between E17 and posthatch. Therefore, the delay between gene expression and function remains unclear. We have used immunohistochemistry to localize BK channel expression in chick hair cells, to test whether the sudden appearance of BK currents is correlated with an increase in protein expression. Cryosections of chick basilar papillae were obtained throughout late-stage development, between E10 and posthatch. In the mature animal, antibodies to the BK  $\alpha$  subunit produced extensive staining at the basal pole of tall hair cells, the soma of the cochlear ganglion, and nerve fibers extending to the tall hair cells. Label was present at the synaptic pole of the hair cells throughout development, but increased in intensity from E10 to E16. The intensity and extent of the staining was similar between E16 and posthatch. Since both hair cells and neurites were labeled, it was difficult to distinguish between pre- and post-synaptic staining. For this reason, we also performed immunofluorescence on isolated hair cells. These results

suggest that BK expression is initially confined to a cytoplasmic compartment (E10-E12), followed by diffuse expression (E14-E18), and then clustering at the hair cell synapse (E18-posthatch). Punctate clusters were more prevalent in apical hair cells, similar to the tonotopic distribution of presynaptic release sites.

### **635 Functional Significance of Developmental Changes in Calcium Dependence and Calcium Efficiency of Exocytosis in Mouse Inner Hair Cells**

Stuart Johnson<sup>1</sup>, Walter Marcotti<sup>1</sup>, Corne Kros<sup>1</sup>

<sup>1</sup>School of Life Sciences, University of Sussex, Falmer, Brighton BN1 9QG, UK

Synaptic vesicle exocytosis is generally considered to have a high-order dependence on presynaptic Ca<sup>2+</sup> entry, but recent studies at olfactory and visual sensory synapses have shown the relation to be almost linear (Murphy *et al.* 2004, *J Neurosci* 24: 3023-3030; Thoreson *et al.* 2004, *Neuron* 42: 595-605). We examined the Ca<sup>2+</sup> dependence of exocytosis from inner hair cells (IHCs) of the mammalian auditory system at different stages of development.

Developmental changes in the coupling between Ca<sup>2+</sup> entry and exocytosis were studied in apical-coil mouse IHCs. Ca<sup>2+</sup> currents ( $I_{Ca}$ ) and changes in membrane capacitance ( $\Delta C_m$ ) were recorded from cells maintained at body temperature, using physiological (1.3 mM) extracellular Ca<sup>2+</sup>. The magnitudes of both  $I_{Ca}$  and  $\Delta C_m$  increased with maturation from embryonic stages until postnatal day 6 (P6). Subsequently,  $I_{Ca}$  declined to a steady level of around -100 pA from P13 while the Ca<sup>2+</sup>-induced  $\Delta C_m$  remained constant. This increased the apparent Ca<sup>2+</sup>-efficiency of exocytosis with development, consistent with a previous study on mouse IHCs using 10 mM extracellular Ca<sup>2+</sup> (Beutner & Moser 2001, *J Neurosci* 21: 4593-4599). The Ca<sup>2+</sup> dependence of exocytosis was obtained by varying the size of  $I_{Ca}$  and recording  $\Delta C_m$ . Synaptic transfer functions, where  $\Delta C_m$  was plotted against  $I_{Ca}$ , indicated that the Ca<sup>2+</sup> dependence of vesicle release changed with maturation from a fourth power relation in immature cells to an approximately linear one in mature cells. This change applied to vesicles released from both an identified readily releasable pool (RRP) and a slower secondary pool of vesicles.

We conclude that the linear Ca<sup>2+</sup> dependence of mature IHC exocytosis would make mature cells ideally suited for fine intensity discrimination over a wide dynamic range. The high-order dependence in immature cells would promote reliable signalling of action potential activity.

*Supported by the MRC*

### **636 Uptake of FM1-43 and Methylene Blue by Developing Auditory Hair Cells**

David Furness<sup>1</sup>

<sup>1</sup>School of Life Sciences, Keele University, Keele, UK

The dyes FM1-43 and methylene blue (MB) enter hair cells through the mechano-electrical transducer channels (Gale *et al.* 2001; *J Neurosci* 21: 7013-7025; Farris *et al.* 2004; *J*

Physiol 558: 769-792), although FM1-43 is also endocytosed at the hair-cell apex (Griesinger et al. 2001; Eur J Neurosci 20: 41-50). The development of uptake of FM1-43 by hair cells appears to coincide with acquisition of tip links in equivalent-aged samples, which suggests that tip link formation is required for transduction (Geleoc and Holt 2003; Nat Neurosci 6: 1019-1020). In the present study the uptake of MB and FM1-43 has been examined along the apico-basal gradient of hair-cell maturation in 0 and 1 pnd mouse cochleae and compared directly with the extent of hair-bundle differentiation in the same samples using high resolution SEM. Cochleae were immersed in FM1-43 in HBSS for a maximum of 10 s to reduce endocytosis, followed by 3 - 5 min in 0.1% MB in HBSS, examined by confocal and transmitted light microscopy, then fixed and prepared using the OTOTO technique for SEM. Uptake of both FM1-43 and MB showed a cochleotopic gradient with greater proportions of hair cells taking up the dyes towards the base. However, whilst all basal hair cells took up both dyes, many apical hair cells preferentially took up either one or other dye but not both and apical IHCs were more likely to take up dye than apical OHCs. SEM revealed that hair bundles of both basal and apical hair cells which were MB or FM1-43 positive had a clearly defined staircase with multiple links around the stereociliary tips, whereas apical hair cells which were FM1-43 and MB negative had poorly developed staircase and links. These results suggest that although MB and 'rapid' FM1-43 uptake begins when hair bundles have developed a staircase and links, the two dyes enter by distinct routes that develop independently and it is therefore unlikely that both are taken up through transducer channels.

### **637 Transgenic Expression of Cre Recombinase from the Brn3.1 Locus**

**Robert Mlynski**<sup>1</sup>, Stefan Hansen<sup>1</sup>, Wilfried Rossoll<sup>2</sup>, Dominik Brors<sup>1</sup>, Christoph Aletsee<sup>1</sup>, Michael Sendtner<sup>2</sup>, Allen F. Ryan<sup>3</sup>, Stefan Dazert<sup>4</sup>

<sup>1</sup>ENT Department, University of Wuerzburg, Germany,

<sup>2</sup>Clinical Neurobiology, University of Wuerzburg, Germany,

<sup>3</sup>Dept. of Surgery/Otolaryngology, University of California San Diego, USA, <sup>4</sup>Dept. of Otolaryngology, University of Essen, Germany

Cre recombinase mediated tissue-specific gene targeting is a powerful tool for studying development and differentiation of inner ear cells. For this purpose we wanted to generate a transgenic mouse, that expresses the Cre recombinase in a spatial and temporal pattern like that observed for the hair cell specific transcription factor Brn3.1.

In order to ensure tissue-specific expression of the Cre recombinase without disabling the target gene, we used a cassette containing an internal ribosome entry site (IRES) followed by the Cre recombinase coding region. The IRES-Cre cassette was inserted into the 3'-untranslated region of the mouse Brn3.1 gene by homologous recombination.

To confirm tissue specific expression of Cre, these transgenic mice were mated to lacZ reporter strains (ROSA26). Here we report Brn3.1 specific Cre

recombinase activity in the inner ear visualized by lacZ staining at various developmental stages.

### **638 Characterization of Y61G-Myo1c Knock-In Mice**

**John D. Scarborough**<sup>1,2</sup>, Eric A. Stauffer<sup>3</sup>, Susan K.H. Gillespie<sup>1,2</sup>, Jeffrey R. Holt<sup>3</sup>, Peter G. Gillespie<sup>1,2</sup>

<sup>1</sup>Oregon Health & Science University, <sup>2</sup>Oregon Hearing Research Center & Vollum Institute, <sup>3</sup>University of Virginia

Myosin-1c was recently shown to participate in hair-cell adaptation by a chemical-genetic strategy in transgenic mice expressing a mutant version of Myo1c (Y61G) (Holt et al. *Cell* 108:371-381, 2002). Application of a specific ADP-analog inhibitor (NMB-ADP) for Y61G-Myo1c into transgenic hair cells blocked adaptation, but had no effect on adaptation in wild-type cells. Moreover, transgenic hair cells displayed robust adaptation in the absence of inhibitor. These results revealed a critical function for Myo1c in vestibular hair-cell adaptation, but did not rule out the possibility of another myosin motor playing a similar role in the hair bundle and left Myo1c's role in cochlea unanswered. To determine whether Myo1c mediates hair-cell adaptation in *all* hair cells, we replaced the wild-type *Myo1c* allele with the Y61G allele by a gene-targeting knock-in strategy in mice. We injected Y61G-Myo1c targeted clones into C57B6 blastocysts, which produced chimeras that transmitted to the germline. As expected, both heterozygous and homozygous progeny appear normal. Immunoblot analysis of multiple tissues with a Myo1c-specific antibody showed that homozygous knock-in mice produce full-length Y61G-Myo1c at wild-type levels. Using a Y61G-specific antibody, we also selectively detected Y61G-Myo1c in inner ear tissues from homozygous mice but not wild-type. Delivery of NMB-ADP through a whole-cell recording pipette into utricular hair cells revealed that the analog blocked adaptation to positive deflections in 80% of homozygous cells tested but not in wild-type cells. These mice will be used as an alternative test of Myo1c's role in the vestibular system and to investigate its role in the cochlea.

### **639 Myosin VI in Fish Ears**

**Allison B. Coffin**<sup>1</sup>, Matthew W. Kelley<sup>2</sup>, Arthur N. Popper<sup>1</sup>

<sup>1</sup>University of Maryland, <sup>2</sup>National Institutes of Health

Myosin VI is an important hair cell protein, with myosin VI mutations resulting in hereditary deafness. Recent work in other labs has identified zebrafish (*Danio rerio*) myosin VI mutants that show physiological defects in mechanotransduction. These studies also show that there are two myosin VI paralogs expressed in zebrafish, *myo6a* and *myo6b*. Here, we characterize myosin VI expression and distribution in the ears of zebrafish and other fishes such as American shad (*Alosa sapidissima*) and oscar (*Astronotus ocellatus*). We use immunocytochemistry to show that myo6 is found in at least some hair bundles of all species examined in this study. Myosin VI is distributed throughout the cytoplasm and hair bundles in all zebrafish inner ear hair cells, while it is not found in utricular hair bundles in other species. Western blotting shows that our antibody binds a single protein of 150 kDa,

suggesting that it is specific for myo6b. We further examined antibody specificity by expressing zebrafish myo6 antigens in mammalian cell lines and examining myo6 gene expression by RT-PCR. Both myo6 genes were successfully amplified from zebrafish inner ear tissue. Since work in other labs suggests that myo6a is not expressed in larval zebrafish ears, we used *in situ* hybridization to study gene expression patterns for myo6a in the adult ear. Our work adds depth to current studies of myo6-associated hereditary deafness and suggests that comparative studies between zebrafish and other fishes such as shad that differ in myo6 protein distribution will help elucidate the function of this critical hair cell protein. Comparisons between the two myo6 paralogs will further aid in functional studies and shed light on hair cell evolution.

#### **640 Quantitative Analysis of Basilar Papilla Epithelia Health and Hair Cell Protein Distribution using Confocal Microscopy**

**Dominic A. Mangiardi**<sup>1</sup>, David C. Mountain<sup>1</sup>, Douglas A. Cotanche<sup>2,3</sup>

<sup>1</sup>*Boston University, Department of Biomedical Engineering,*

<sup>2</sup>*Childrens Hospital Boston, Otolaryngology Department,*

<sup>3</sup>*Harvard Medical School, Department of Otolaryngology and Laryngology*

A semi-automated tool was created in Matlab to quantitatively describe the health of stereocilia on sensory hair cells in whole-mount confocal montages of the chick basilar papilla. The goal was to provide a tool to aid in assessing the efficacy of agents that may protect hair cells of the basilar papilla from aminoglycoside-induced death. The analysis aims to provide a qualitative assessment of the number of hair cells and their health within small segments of the epithelium through comparison to a library of images characterized by the user. The program provides quantification of the entire epithelium in this manner, providing better spatial resolution of damaged areas in less time than previously utilized methods, thus enabling higher throughput. The analysis was expanded to include analysis of caspase-3 labeling across the entire epithelium in combination of assessment of stereocilia health. The program was utilized to monitor epithelial degeneration in a culture setting with and without exposure to the aminoglycoside gentamicin and to screen whether various agents including the tetracycline derivative minocycline and kinase inhibitor staurosporine were able to alleviate gentamicin damage in the cultured chick basilar papilla.

An additional tool was developed to quantify changes in protein labeling on the single hair cell level. From high magnification confocal z-series images of the basilar papilla, single hair cells were segmented into three regions in 3D space: stereocilia, nucleus, and cytoplasm. Within these regions, the amount of fluorescence from a particular protein label was described. This analysis was developed to facilitate quantitative description of changes in protein distribution or location within hair cells undergoing death or regeneration.

#### **641 Endogenous Calcium Buffering of Chick Cochlear Hair Cells**

**Matthew M. Giampola**<sup>1</sup>, Thomas D. Parsons<sup>2</sup>

<sup>1</sup>*University Of Pennsylvania School of Medicine,*

<sup>2</sup>*University Of Pennsylvania School of Veterinary Medicine*

Cochlear hair cells transduce the mechanical energy of acoustic waves into a neural code that is ultimately perceived as sound. Mechanical deflections of stereocilia result in cell membrane depolarizations that modulate neurotransmitter release. The nature of acoustic stimuli requires the encoding of high frequency information, and thus, the hair cell provides a unique opportunity to study the presynaptic mechanisms that regulate the temporal control of transmitter release. Membrane capacitance recordings were made from isolated cochlear tall hair cells (THC) of White Leghorn chickens (8-20 days old), using tight-seal patch clamp techniques. Capacitance changes reflect increases in cell surface area due to the fusion of synaptic vesicles. Cells were depolarized with voltage clamp steps from a holding potential of -81 mV to -21mV for durations from 100 ms to 500 ms. Perforated-patch recordings provided a measure of vesicle-pool activation under endogenous buffering conditions, as electrical access to the cell was gained via inclusion of the pore-forming antibiotic nystatin (200µg/ml) in the pipette solution. Whole-cell patch clamp allowed us to vary buffer conditions by introducing different known concentrations of slow and fast buffers to identify the buffering capacity which best approximates endogenous buffering conditions. Preliminary studies indicate that endogenous calcium buffering capacity of synaptic vesicle exocytosis is better mimicked by millimolar concentrations of a fast buffer (1.6mM BAPTA) than by submillimolar concentrations of a slow buffer (0.2mM EGTA). This observation is consistent with previous reports in other lower vertebrates of hair cell calcium buffering of potassium channel activation and transduction channel adaptation. Such strong calcium buffering is thought to be important for the temporal precision of hair cell signaling.

#### **642 Usherin Interaction with Fibronectin is a Critical Element of Usherin Function**

**Gautam Bhattacharya**<sup>1</sup>, Dominic Cosgrove<sup>1</sup>

<sup>1</sup>*Boys Town National Research Hospital*

Usher syndrome type IIa is the most common of the Usher syndromes, and thus the leading single genetic cause of combined deafness and blindness in the world. The gene responsible encodes a novel basement membrane protein we named usherin. In recently published work, we used biochemical characterization to show that usherin specifically interacts with type IV collagen, and that the interaction stabilizes usherin in the basement membrane superstructure. Using information from the human mutation database for missense mutations in the usherin gene, we showed that type IV collagen interacts specifically with the b-loop of the LE domain of usherin. We now show that the LE domain of usherin interacts specifically with fibronectin as well. The two molecules co-localize in both the retina and the cochlea. Co-immunoprecipitation experiments were used to establish

the direct interaction in extracts from both the cochlea and the retina. Biacore interaction data using purified full-length recombinant usherin and purified fibronectin show that this interaction is of high affinity and 1:1 stoichiometry. The same panel of mutant fusion peptides employed for the type IV collagen studies were used in co-immunoprecipitation studies with fibronectin. Interestingly, only mutations in the d-loop abolish the ability of the LE domain to interact with fibronectin. These data show that binding sites in the LE domain for type IV collagen are distinct from binding sites for fibronectin. Further, these data establish a critical role for usherin/fibronectin interaction in usherin function. (Supported by R01 DC04844)

### **643 Expression of Pituitary Adenylate Cyclase-Activating Polypeptide Receptor (PAC1-R) Splice Variants in the Cochlea: New Splice Variants**

**Maher D. Abu-Hamdan**<sup>1</sup>, Marian J. Drescher<sup>1</sup>, Khalid M. Khan<sup>2</sup>, James S. Hatfield<sup>3</sup>, Dennis G. Drescher<sup>4</sup>

<sup>1</sup>Department of Otolaryngology, Wayne State University School of Medicine, Detroit, MI, <sup>2</sup>Department of Biological Sciences, Aga Khan University, Karachi, Pakistan, <sup>3</sup>Electron Microscopy Laboratory, Veterans Affairs Medical Center, Detroit, MI, <sup>4</sup>Departments of Otolaryngology & Biochemistry, Wayne State University School of Medicine, Detroit, MI

Pituitary adenylate cyclase-activating polypeptide (PACAP), through its receptor PAC1-R, upregulates catecholaminergic and cholinergic function. Previously, Toma et al. (Assoc. Res. Otolaryngol. Abstr. 26: 155, 2003) demonstrated mRNA expression of PACAP precursor protein and the short form of the PACAP receptor (PAC1-R) in the rat cochlea. We have now obtained evidence that additional splice variants of PAC1-R are expressed in the cochlea including two new variants. Specific primers, encompassing the splice variant region in the third intracellular loop of PAC1-R, directed amplification of hop1, hop2, and hip cDNA from lateral wall subfractions. Further, a new splice variant was detected in the lateral wall, which, otherwise like hop1 in sequence, has a deletion of 193 bp downstream from the splice region, predicted to alter second messenger transduction. These four additional splice variants were not detected in organ of Corti or spiral ganglion microdissected cochlear subfractions. Another new splice variant has been detected, specifically in the organ of Corti, with a deletion of the first 8 out of the 21 amino acids deleted in the PAC1-R-vs splice variant of the N-terminus. Overall, these findings indicate the expression of mRNA for a total of 5 PACAP splice variants in the lateral wall, 2 in the organ of Corti and 1 in the spiral ganglion. PAC1-R protein has been immunolocalized to neural elements (apparently efferent) associated with both inner and outer hair cells. Within the stria vascularis, immunoreactivity was associated with the basolateral extensions and tight junctions of marginal cells, as well as in conjunction with melanin particles. A role for PAC1-R in modulation of afferent neural activity in the inner ear via dopaminergic

efferents is hypothesized. The multiple expression of splice variants for PAC1-R in the lateral wall may facilitate differential signal transduction pathway regulation of K<sup>+</sup> extrusion to endolymph.

### **644 Glucocorticoid Regulation of Genes Involved in Sodium Transport by Semicircular Canal Duct (SCCD) Epithelium**

**Satyanarayana R. Pondugula**<sup>1</sup>, Nithyanandhini Raveendran<sup>1</sup>, Daniel C. Marcus<sup>1</sup>

<sup>1</sup>Kansas State University

We have shown that semicircular canal duct (SCCD) epithelium absorbs Na<sup>+</sup> under glucocorticoid (GC) control [Pondugula et al., *Am J Physiol*, 2004]. We sought to determine the presence of genes involved in control of Na<sup>+</sup> transport in SCCD epithelia and whether their level of expression was regulated by GC. RNA was extracted from dexamethasone ([DEX], 100 nM; 24 hr)-treated and untreated primary cultures of SCCD epithelia and used for quantitative real-time RT-PCR. We found that the transcripts for  $\alpha$ ,  $\beta$  &  $\gamma$  subunits of epithelial sodium channel (ENaC);  $\alpha_1$ ,  $\alpha_2$ ,  $\alpha_3$ ,  $\beta_1$ ,  $\beta_2$ , &  $\beta_3$  isoforms of Na,K-ATPase; 2.3, 3.1 & 7.1 isoforms of inwardly rectifying potassium channel (Kir, IC<sub>50</sub> for Ba<sup>2+</sup>: 210  $\mu$ M); glucocorticoid receptor (GR); mineralocorticoid receptor (MR); 11 $\beta$ -hydroxysteroid dehydrogenase type 1 (11 $\beta$ -HSD1) & 11 $\beta$ -HSD2 isoforms; serum-and glucocorticoid-regulated kinase (SGK) and neural precursor cell expressed developmentally downregulated 4-2 (Nedd4-2) are expressed in SCCD epithelia. On the other hand, transcripts for  $\alpha_4$  Na,K-ATPase; Kir3.4, 6.1 & 6.2 and sulfonyl urea receptor 2 (SUR2) were not expressed. DEX not only up-regulated the transcript expression of  $\alpha$ -ENaC (~ 4.1fold),  $\beta_2$ - (~ 2.3 fold) &  $\beta_3$ - (~ 8.4 fold) Na,K-ATPase, Kir3.1 (~ 2.7 fold) & Kir7.1 (~ 2.3 fold), SGK (~ 3.9 fold) and Nedd4-2 (~ 2.1 fold) but also down-regulated the transcript expression of GR (~ 3.2 fold) and 11 $\beta$ -HSD1 (~ 2.3 fold). Transcripts for GR and 11 $\beta$ -HSD1 were expressed higher, compared to MR and 11 $\beta$ -HSD2 respectively, in the absence of DEX. These findings are consistent with the genomic stimulation by GC of electrogenic Na<sup>+</sup> transport by SCCD epithelia. Water would passively follow the active Na<sup>+</sup> extrusion from endolymph. Increased Na<sup>+</sup> absorption and regulation of Na<sup>+</sup> transport-related genes by GC in SCCD epithelia can account for the therapeutic action of GC in the treatment of vertigo in Meniere's patients. Supported by NIH-NIDCD grant R01-DC00212, NCRR P20 RR17686 & P20 RR16475.

### **645 Regulation of Epithelial Calcium Channel Expression by Vitamin D in Inner Ear of Rat: Gene Microarray and qRT-PCR**

Daisuke Yamauchi<sup>1</sup>, Nithya Raveendran<sup>1</sup>, Satyanarayana Pondugula<sup>1</sup>, Suresh B. Kampalli<sup>1</sup>, Joel D. Sanneman<sup>1</sup>, Donald G. Harbidge<sup>1</sup>, Daniel C. Marcus<sup>1</sup>

<sup>1</sup>Kansas State University

The low luminal calcium concentration of mammalian endolymph in the inner ear is required for normal hearing and balance. However, the molecular basis of calcium absorption and its regulation is not yet understood. Recently, two epithelial calcium channels were detected in the apical membrane of calcium-absorbing epithelia, kidney (ECaC1, CaT2, TRPV5) and intestine (ECaC2, CaT1, TRPV6). We extracted RNA from nonsensory tissues from the cochlea, the semicircular canal ducts (SCCD) from the vestibule and primary cultures of SCCD for gene microarray and quantitative RT-PCR (qRT-PCR) analyses; the identity of PCR products was verified by sequencing. Gene microarrays revealed the presence of transcripts for ECaC1 and ECaC2 expressed in primary culture of SCCD epithelium of rats as well as other components of transepithelial calcium absorption: plasma membrane calcium-ATPase 1 (PMCA1) and Na<sup>+</sup>/Ca<sup>2+</sup> exchanger 2 and 3 (NCX2, NCX3), but not calbindin. The presence of ECaC1 and ECaC2 in the native and cultured SCCD and in the native nonsensory tissues of the cochlea was substantiated by qRT-PCR. Transcripts for NCX1, NCX3, PMCA1, PMCA4, calbindinD9k and calbindinD28k were also detected in SCCD cultures by qRT-PCR. The expression of ECaC1, but not ECaC2, was found to significantly increase in SCCD epithelia after exposure to 1,25-dihydroxyvitamin D<sub>3</sub> for 24 hours, and transcripts for the vitamin D receptor were found to be present. These observations suggest that ECaC1, ECaC2 and the other proteins that support absorption of calcium likely play an important role in regulation of calcium concentration in the endolymph of the inner ear, and that this transport is under the regulation of vitamin D. Supported by NIH-NIDCD grant R01-DC00212, NCRP P20 RR17686 & P20 RR16475.

### **646 Sequencing of Gerbil Pendrin mRNA and Analysis for Alternative Splicing**

Rajanikanth J. Maganti<sup>1</sup>, Sairam V. Jabba<sup>1</sup>, Kathryn Mohney<sup>1</sup>, Philine Wangemann<sup>1</sup>

<sup>1</sup>Kansas State University

Pendrin, an anion transporter, encoded by the SLC26A4 gene, is highly expressed in the inner ear and thyroid. Mutations of SLC26A4 is associated with Pendred syndrome characterized by sensorineural deafness and goiter. The human gene consists of 21 exons and the protein of 780 amino acids (~86 kDa) predicted to contain 12 transmembrane domains. The purpose of this study was to determine the mRNA sequence from gerbil pendrin since the gerbil is an established animal model for functional inner ear studies and to analyze whether tissue-specific alternative splice variants exist that would point to tissue-specific variations of pendrin function. We employed RT-PCR, RACE, TA-cloning and DNA

sequencing to obtain the gerbil pendrin mRNA sequence including the 3'UTR. Sequence homology of gerbil pendrin mRNA was 90, 90 and 84% to mouse, rat and human mRNA, respectively. Sequence analysis of transcripts obtained from gerbil inner ear, thyroid and kidney provided no evidence for the presence of tissue specific splice variants. Three potential glycosylation sites were conserved between mouse, rat, human and gerbil pendrin. One additional site was conserved between mouse, rat and gerbil. In conclusion, these data demonstrate that structural and functional properties of pendrin are preserved between species and that the gerbil can be used as an animal model to study the function of pendrin in the inner ear.

Supported by NIH-R01-DC01098

### **647 Free Radical Stress Mediated Nitration in Stria Vascularis May Underlie Loss of KCNJ10 K<sup>+</sup> Channel Function in Pendred Syndrome**

Sairam V. Jabba<sup>1</sup>, Erin M. Itza<sup>2</sup>, Philine Wangemann<sup>1</sup>

<sup>1</sup>Kansas State University, <sup>2</sup>Imperial Valley College

Pendred syndrome, a common autosomal-recessive disorder characterized by congenital deafness and goiter, is caused by mutations of SLC26A4, which codes for pendrin, an anionic exchanger, which is highly expressed in the inner ear and secretes HCO<sub>3</sub><sup>-</sup> into endolymph. We investigated the relationship between pendrin and deafness using mice that have (*Slc26a4*<sup>+/+</sup>) or lack a complete *Slc26a4* gene (*Slc26a4*<sup>-/-</sup>). Stria vascularis of *Slc26a4*<sup>-/-</sup> mice lacked the KCNJ10 K<sup>+</sup> channel, was hyperpigmented and did not generate an endocochlear potential (Wangemann et al., 2004). The hypothesis that the loss of the endocochlear potential is due to free radical stress was evaluated by confocal immunocytochemistry using an antibody against nitrotyrosine. Tissue preparations consisted of cryosections from the gerbil kidney and whole mounts of stria vascularis from *Slc26a4*<sup>-/-</sup> and *Slc26a4*<sup>+/+</sup> mice. Specificity of the anti-nitrotyrosine antibody was evaluated in kidney sections either untreated or treated with 100 μM peroxyntrite. Nitrotyrosine immunostaining was enhanced in kidney sections treated with peroxyntrite in presence of CO<sub>2</sub>/HCO<sub>3</sub><sup>-</sup>. Nitrotyrosine immunostaining was significantly enhanced in whole mounts of stria vascularis from *Slc26a4*<sup>-/-</sup> mice. Nitration was concentrated around the pigmentation. These observations suggest that free radical stress contributes to the loss of KCNJ10 K<sup>+</sup> channel that leads to the loss of the endocochlear potential and results in deafness.

Supported by NIH-R01-DC01098

## **648** Microarray and Q-PCR Based Gene Expression Analysis of Stria Vascularis of a Pendred Syndrome Mouse Model.

Philine Wangemann<sup>1</sup>, Alisha Oelke<sup>1</sup>, Anantha S. B. Gollapudi<sup>1</sup>, Ruchira K. Singh<sup>1</sup>, Sairam V. Jabba<sup>1</sup>, Rajanikanth J. Maganti<sup>1</sup>

<sup>1</sup>Kansas State University

Pendred syndrome, a common autosomal-recessive disorder characterized by congenital deafness and goiter, is caused by a mutation of SLC26A4, which codes for pendrin, an apically located Cl<sup>-</sup>/HCO<sub>3</sub><sup>-</sup> exchanger. We investigated the relationship between pendrin and deafness using mice that have (*Slc26a4*<sup>+/+</sup>) or lack a complete *Slc26a4* gene (*Slc26a4*<sup>-/-</sup>). Stria vascularis of *Slc26a4*<sup>-/-</sup> mice lacked the KCNJ10 K<sup>+</sup> channel, was hyperpigmented and did not generate an endocochlear potential (Wangemann et al., 2004). The present study was performed to further explore the causal relationship between the loss of pendrin and loss of KCNJ10 that ultimately leads to deafness. Total RNA was isolated from microdissected stria vascularis with a yield of ~10 ng per animal and prepared for gene array analysis using the Affymetrix Small Sample protocol. Gene array analysis was performed using Affymetrix 420 2.0 mouse chips. Transcripts of interest were quantified by quantitative RT-PCR in total RNA obtained from microdissected stria vascularis and spiral ligament. Quantification of 18S rRNA served as a standard. Changes by less than factor 2 were considered insignificant. Expression of the calcium-activated chloride channel, carbonic anhydrase 3 and lysozyme was significantly upregulated in stria vascularis of *Slc26a4*<sup>-/-</sup> mice compared to *Slc26a4*<sup>+/+</sup> mice; expression of carbonic anhydrase 2 and 13 and the anion exchanger AE2 were unchanged. Expression of the calcium-activated chloride channel, carbonic anhydrase 2, 3 and 13, the anion exchanger AE2 and lysozyme appeared significantly upregulated in spiral ligament. Upregulation in spiral ligament was considered apparent since losses in tissues masses of spiral ligament in *Slc26a4*<sup>-/-</sup> mice could have changed ratios of cell types comprising spiral ligament. Our data suggest that loss of the HCO<sub>3</sub><sup>-</sup> transporter pendrin induces compensatory upregulation of HCO<sub>3</sub><sup>-</sup> generating enzymes and transporters.

Supported by NIH-R01-DC01098

## **649** Characterization of the Head Bobber Locus and Inner Ear Phenotype

Giuseppina Somma<sup>1,2</sup>, Heather Alger<sup>1</sup>, Pawel Stankiewicz<sup>1</sup>, Svetlana A. Yatsenko<sup>1</sup>, Wilbur Harrison<sup>1</sup>, Paul A. Overbeek<sup>1</sup>, Fred A. Pereira<sup>1</sup>

<sup>1</sup>Baylor College of Medicine (Houston, Tx), <sup>2</sup>University of Tor Vergata (Rome, Italy)

Many genes involved in the proper formation of the inner ear have been identified in the past few years by analyzing mutant mice affected by deafness and balance disorders. Head Bobber is a transgenic mouse characterized by reduced size at puberty, deafness, circling behavior and repetitive head tilting. Histological analysis of the Hb inner

ear, that appear significantly smaller in the mutant compared to the wild type, has shown an absence of the semicircular canals and malformation of the cochlea duct. The semicircular canal region presents as a single chamber with the anterior, posterior and lateral semicircular canals and associated cristae poorly distinguishable in mutant mice homozygous for the Hb locus. Within the cochlear duct, the stria vascularis is poorly developed before birth. After birth, the Reissner's membrane collapses by P3 and the tectorial membrane is flattened onto the sensory hair cells. This phenotype is associated with alterations in extracellular matrix components in the tectorial membrane. Molecular cloning of the Hb locus reveals that the insertion of the transgene caused a deletion of about 650 Kb in the distal part of chromosome 7F3, approximately 300kb telomeric to the Nkx5.1 (Hmx3) locus. We are currently identifying the specific genes affected in Hb mice particularly in structures of the inner ear.

## **650** Osteoprotegerin (OPG) Knockout Mice Have Abnormal Otic Capsule Remodeling and Progressive Hearing Loss

Andreas Zehnder<sup>1,2</sup>, Sharon G. Kujawa<sup>1,3</sup>, Arthur G. Kristiansen<sup>2</sup>, Joe C. Adams<sup>1,2</sup>, Michael J. McKenna<sup>1,2</sup>

<sup>1</sup>Department of Otolaryngology, Harvard Medical School, <sup>2</sup>Department of Otolaryngology, Massachusetts Eye and Ear Infirmary, <sup>3</sup>Eaton-Peabody Laboratory, Massachusetts Eye and Ear Infirmary

Unlike all other bones in the body, the otic capsule has virtually no significant bone remodeling following development. We have previously demonstrated that osteoprotegerin (OPG), a potent inhibitor of osteoclast formation and function, is produced at high levels within the spiral ligament, secreted into the perilymph, and diffuses into the surrounding otic capsule bone. These findings have led to the speculation that OPG may play an important role inhibiting otic capsule remodeling and protecting the sensory function of the inner ear. To further investigate this hypothesis, we have studied the histology and physiology of OPG knockout mice. The homozygote knockouts demonstrate abnormal osteoclastic bone resorption within the otic capsule and the ossicles. They also develop progressive, apparently mixed (conductive and sensorineural) hearing loss. The conductive component of the hearing loss may be related to resorptive changes within the ossicles. The cause of the sensorineural hearing loss remains unclear. Elucidation of the factors responsible for the inhibition of otic capsule remodeling will be important for the understanding of pathologic processes affecting the otic capsule such as otosclerosis and the development of better forms of treatment in the future.

This work was supported by NIDCD grant 5 RO1 DC03401-07.



## **651** Characterizing a Second Prestin Knockout Mouse Derived from the 129S1 Strain

Kristin Huynh<sup>1</sup>, Mary Ann Cheatham<sup>1</sup>, Jing Zheng<sup>1</sup>, Peter Dallos<sup>1</sup>

<sup>1</sup>Northwestern University

Studies using the prestin knockout mouse indicate that removal of prestin is associated with losses of sensitivity, frequency selectivity and OHC motility (Liberian et al. 2002; Cheatham et al. 2004). Here we provide data obtained from a second prestin knockout mouse that was produced commercially. *In vivo* recordings from the round window indicate that the phenotype is very similar to that of the original knockout generated by Jian Zuo's group at St. Jude Children's Research Hospital. For example, CAP thresholds are shifted in a frequency dependent manner from ~45 dB at 5 kHz to ~55 dB at 25 kHz. CAP tuning curves at 12 kHz are flat for masker frequencies between 2 and 18 kHz. Although CAP and CM input-output functions at 6 kHz show a shift in sensitivity at low levels, both responses approach wildtype magnitudes at high levels where the amplifier has less influence. This behavior, however, is not observed at higher frequencies, where high-level CAP and CM responses are well below those in controls. These reductions are associated with hair cell loss, which afflicts both knockout models. In order to confirm that the loss of sensitivity and frequency selectivity are due to a loss of prestin, we performed immunohistochemistry using anti-prestin tagged with FITC. Results indicate that the loss of function phenotype is associated with a loss of prestin protein. Cochlear segments from knockout mice showed no fluorescence while wildtype mice displayed a fluorescent signal targeted to the OHC's lateral membrane. The linkage shown here between the loss of prestin protein and abnormal cochlear function, validates the original knockout model and attests to the importance of OHC motor function for signal coding in the auditory periphery. (Work supported by The Hugh Knowles Center and Grant #DC00089 from NIDCD).

## **652** Cochlear Phenotypes in Mice with Targeted Deletion of Putative Olivocochlear Receptors.

Stéphane F. Maison<sup>1,2</sup>, Thomas W. Rosahl<sup>3</sup>, Gregg E. Homanics<sup>4</sup>, William Wisden<sup>5</sup>, Neil M. Nathanson<sup>6</sup>, Jurgen Wess<sup>7</sup>, John E. Pintar<sup>8</sup>, M. Charles Liberman<sup>1,2</sup>

<sup>1</sup>Harvard Medical School, <sup>2</sup>Massachusetts Eye & Ear Infirmary, <sup>3</sup>Merck Sharp and Dohme, <sup>4</sup>University of Pittsburgh, <sup>5</sup>University of Heidelberg, <sup>6</sup>University of Washington, <sup>7</sup>NIH-NIDDK, <sup>8</sup>Rutgers University

Immunocytochemistry suggests that olivocochlear (OC) terminals contain several neurotransmitters including ACh, GABA and dopamine, as well as peptidergic modulators including CGRP, urocortin and enkephalins. The well-studied phenomenon of OC-mediated suppression arises from cholinergic interactions with  $\alpha 9/\alpha 10$  nicotinic receptors on outer hair cells. The function of other transmitter/receptor systems in both inner and outer hair cell areas is less well understood.

To explore the functional roles of non-nicotinic components of OC transmission, we characterized the cochlear phenotype of 7 GABA-A ( $\alpha 1$ ,  $\alpha 2$ ,  $\alpha 5$ ,  $\alpha 6$ ,  $\beta 2$ ,  $\beta 3$ ,  $\delta$ ), 3 muscarinic (M1, M3, M5) and 1 opioid ( $\mu$ OR) receptor type knockout line by measuring 1) ABRs and DPOAEs at frequencies from 5.6 to 45.2 kHz, 2) the magnitude of DPOAE suppression evoked by electric stimulation of the OC bundle, 3) their sensitivity to noise overexposure and 4) cochlear histopathology by light microscopy.

Cochlear abnormalities were seen only in GABA-A knockouts. With  $\alpha 5$ ,  $\beta 2$  or  $\beta 3$  GABA-A deletion, cochlear sensitivity was reduced: ABR thresholds were elevated by as much as 40 dB. DPOAE threshold shifts were comparable to ABR shifts in  $\beta 3$  mutants, but were significantly smaller than ABR shifts in  $\alpha 5$  and  $\beta 2$ , suggesting GABAergic effects on IHCs, spiral ganglion cells or synaptic transmission between them.  $\beta 3$  mutants showed gross cochlear dysfunction at 6 wks and dramatic abnormalities in both afferent and efferent innervation of hair cells. The  $\alpha 5$  and  $\beta 2$  lines showed progressive dysfunction, with near normal responses at 6-8 wks. In addition, effects of  $\beta 2$  deletion were more pronounced in males than females. Shock-evoked OC suppression of cochlear responses and sensitivity to noise overexposure were unaffected in the  $\beta 2$  line.

The present results suggest that the GABAergic component of the OC system contributes to the development and/or maintenance of normal function in both IHC and OHC areas.

Research supported by RO1 DC00188 and P30 DC 005029

## **653** Microarray Based Comparison of Amplification Methods for Nanogram Amounts of Total RNA

Ruchira K. Singh<sup>1</sup>, Rajanikanth J. Maganti<sup>1</sup>, Sairam V. Jabba<sup>1</sup>, Philine Wangemann<sup>1</sup>

<sup>1</sup>Kansas State University

Gene profiling of RNA samples from micro-dissected tissues or needle biopsies requires amplification prior to microarray analysis. A novel system, based on single primer isothermal linear amplification (SPIA) has recently been introduced (Ovation, Nugen). SPIA was run concurrently with a T7-based system employing two rounds of amplification (TwoRA, Small Sample Protocol, Version II, Affymetrix) or one round of amplification (OneRA, Standard Protocol, Affymetrix). Targets were prepared in triplicate by OneRA from 10  $\mu$ g, by TwoRA from 10 ng and by SPIA from 100, 30, 10 and 3 ng of mouse kidney (MK) or mouse universal reference (MUR) RNA and analyzed using high-density Affymetrix Mouse 430 2 GeneChips. More genes were called present in target populations prepared from 10 ng RNA by TwoRA than by SPIA. In MUR RNA, 13,895 targets were called present by both TwoRA and SPIA and an additional 5,929 or 3,093 targets were called present by TwoRA or SPIA, respectively. All 13 selected TwoRA- and all 13 SPIA-specific targets were verified by RT-PCR. Reproducibility, measured as call concordance between replicates, was slightly higher for targets prepared from 10 ng MK RNA by

TwoRA (91.4%) than by SPIA (88.4%). Sensitivity was computed as minimal fold-increase in signal intensity necessary for significance and was similar for TwoRA and OneRA. Sensitivity of SPIA was 13% less than OneRA. Similar results were obtained for MK and MUR RNA. Signal intensity ratios between MK and MUR RNA were computed. Correlation of ratios between TwoRA and OneRA ( $R=0.94$ ) was better than between SPIA and OneRA ( $R=0.84$ ). In conclusion, TwoRA and SPIA amplified overlapping sets of genes. Target preparation by SPIA can be performed from as little as 3 ng of RNA, was faster and resulted in cDNA, which is more stable than cRNA and can be used in a variety of gene expression platforms.

Supported by R01 DC 01098, P20 RR16475, NIH-P20-RR017686, Nugen Corporation, NSF MRI 0421427.

### **654** Lentiviral Vector Mediated Inner Ear Gene Expression using Different Promote

Maoli Duan<sup>1</sup>, Dongguang Wei<sup>1</sup>, Busheng Tong<sup>1</sup>, Mats Ulfendahl<sup>1</sup>, Cecilia Lundberg<sup>2</sup>

<sup>1</sup>Karolinska Institutet, <sup>2</sup>Lund University

Gene therapy constitutes a unique tool to modify the endogenous faulty mechanisms involved in hearing disorders. Adeno, adeno-associated viral vector gene therapy has provided certain information but due to their higher immune reaction by the host in vivo study, consequently limits their application in the inner ear. Lentiviral (LV) vector has more promising for inner ear gene therapy based on the following reasons:

a) Lower immune response from the host; b) can target both dividing and non-dividing cells; c) Cochlear hair cells and spiral ganglion cells are non-dividing cells. Thus, LV mediated gene expression in the inner ear may be longer and more effective, and consequently obtain better results using LV compared to other vectors.

The aim of the present study is to test different promote such as CMV, CAG, PKG and Ef1a using LV, and compare their effectiveness. Reporter genes are GFP and LacZ. Thus, we can find better promote for LV gene therapy in the inner ear.

### **655** Transplantation of Stem Cells Into the Lateral Wall of the Inner Ear

Elisabeth Sauvaget<sup>1,2</sup>, Kwang Pak<sup>1</sup>, Yan Li<sup>1</sup>, Patrice Tran Ba Huy<sup>2</sup>, Allen Ryan<sup>1</sup>

<sup>1</sup>Otolaryngology and neurosciences, UCSD and VAMC, La Jolla, CA, USA, <sup>2</sup>Otolaryngology department, Lariboisiere hospital, Paris, France

A number of inherited and acquired hearing disorders involve damage to the cells of the spiral ligament and stria vascularis. In order to explore potential replacement strategies for such cells, we transplanted a variety of types of stem cells into the lateral wall, and explored their potential to express molecules known to be important for the function of the lateral wall.

Neural stem cells, embryonic stem (ES) cells, bone-marrow-derived stem cells and cells harvested from the fetal lateral wall were used. We employed cells expressing

either green fluorescent protein or yellow fluorescent protein in order to trace the cells after transplantation. Some embryonic stem cells were differentiated in vitro into a mesodermal cell phenotype prior to transplantation. Cells were transplanted in vivo against the lateral surface of the lateral wall, after a deliberate damage of the ligament either mechanically, chemically or cryogenically. The cochleas were then evaluated for the survival and integration of transplanted cells and for expression of tissue-appropriate proteins by immunocytochemistry.

After 7 to 10 days, 60% of the cochleas showed survival of transplanted cells, that in the majority of cases formed clusters in the scala vestibuli close to the ligament. In 20 to 25% of cases, the cells were adjacent to or integrated into the spiral ligament, in some cases coming quite near the stria vascularis but never entering it. Regarding the different types of stem cell, the rate of integration in the spiral ligament was around 20% for neural stem cells and for undifferentiated ES cells, slightly higher for differentiated ES cells. Less integration was seen for bone marrow stem cells and for the cells harvested from the fetal lateral wall. Regarding the type of injury, integration in the ligament was more frequent after mechanical injury than after chemical or cryogenic injuries, which could be explained by severe cochlear inflammation that was common after chemical or cryogenic injury. Within one week after transplantation, some stem cells exhibited expression of molecular markers of spiral ligament cells, including connexin 26 and S100.

Supported by NIH/NIDCD grant DC00139, and by the Medical Research Service of the VA.

### **656** The Mouse Cochlea Database: 2D Atlas, Interactive Java Measuring Tools, Virtual Reality 3D Reconstructions, and the Digital Cytocochleogram

Peter Santi<sup>1</sup>, Anbon Cheng<sup>1</sup>, Thomas Forsythe<sup>1</sup>, Ian Rapson<sup>1</sup>, Arne Voie<sup>2</sup>

<sup>1</sup>University of Minnesota, <sup>2</sup>Spencer Technologies

The purpose of this presentation is to describe our progress in the development of several resources of the Mouse Cochlea Database (MCD). Using OPFOS image stacks, 2D atlases from two mouse cochleas (CBA and C57 strains) have been produced and are available on the MCD website. The image stacks are raw OPFOS images taken in a midmodiolar plane through the complete cochlea. We have developed a Java Applet, which allows for zooming, panning, and measuring of distance and area of structures on the images. Oblique sectioning of the 2D images to produce orthogonal sections of the cochlea using the Amira program is being developed so investigators can obtain accurate morphometric information from the 2D atlas. 3D reconstructions of the mouse cochlea have been completed using manual segmentation of the different cochlear structures. These reconstructions are presented as QuickTime movies in which the cochlea is rotated in horizontal/vertical planes. Amira and QuickTime VR Authoring Studio have been used to produce QuickTime virtual reality (VR) presentations of the 3D reconstructions in which a user

can interactively examine any desired plane of the cochlea. We have also developed an open source database (MySQL) indexing model, which allows all resources within the MCD to be searched by keyword. Lastly, the Digital Cytochoeogram resource of the MCD has been programmed as a Java Applet, which allows for more interactive morphometric measurements on the organ of Corti/basilar membrane surface preparations. This should make it easier for users to prepare Digital Cytochoeograms of their surface preparation specimens. Supported by a grant from the NIDCD.

### **657 Coherent-Reflection Models of Reflection-Source Oaes with and Without Slow Transverse Retrograde Waves**

**Christopher A. Shera**<sup>1,2</sup>, Arnold Tubis<sup>3</sup>, Carrick L. Talmadge<sup>4</sup>

<sup>1</sup>Eaton-Peabody Laboratory, <sup>2</sup>Harvard Medical School, <sup>3</sup>Institute for Nonlinear Science, UCSD, <sup>4</sup>National Center for Physical Acoustics, University of Mississippi

Current theories of reflection-source (or place-fixed) OAEs based on coherent cochlear wave reflection from distributed mechanical perturbations (e.g., Shera & Zweig 1993; Zweig & Shera 1995; Talmadge et al. 1998; 2000) incorporate a model of the cochlear amplifier in which active forces exerted within the cochlear partition couple into the transverse motion of the partition. As a result, OAE theories have assumed that backscattered energy couples primarily into the classical transpartition pressure wave that drives the motion of the partition. This modeling strategy was based on the considerable body of evidence that relates the production of low-level evoked and spontaneous OAEs to the mechanisms that serve to amplify the transverse motion of the basilar membrane. In principle, however, the generation and back-propagation of fast compressional (longitudinal) waves provides an additional mechanism for energy to escape from the inner ear. Indeed, mounting albeit not unequivocal evidence suggests that such a mechanism may be contributing to mammalian OAEs (e.g., Wilson 1980; Sivaramakrishnan 1991; Ren 2004; Ruggero 2004). To explore the production of compression-wave OAEs at the phenomenological level, we formulate a toy macromechanical cochlear model that incorporates a "squeezable" cochlear partition (e.g., Shera & Zweig 1992). Model parameters can be adjusted to yield OAEs produced by coherent-reflection mechanisms involving variable mixtures of both slow transverse waves (i.e., the "traditional" coherent-reflection mechanism) and fast compressional waves. Despite differences in the mechanisms of back-propagation, the principal physical mechanisms operating in the traditional coherent-reflection model (e.g., mechanical irregularity, phase-coherent summation, and dynamical spatial-frequency filtering) also play an important role in shaping the characteristics of possible compression-wave OAEs.

*Supported by the NIDCD, National Institutes of Health.*

### **658 Stimulus Frequency Otoacoustic Emissions Elicited by Transient Tones in Noise**

**Douglas H. Keefe**<sup>1</sup>, Kim S. Schairer<sup>1</sup>, John C. Ellison<sup>1</sup>, Denis F. Fitzpatrick<sup>1</sup>, Walt Jesteadt<sup>1</sup>

<sup>1</sup>Boys Town National Research Hospital

Stimulus frequency otoacoustic emissions (SFOAE) provide a frequency-specific test of cochlear function that may be useful in studying mechanisms underlying a listener's ability to detect tones in noise. An objective adaptive procedure to measure the detection threshold of SFOAE suppression by a noise or other elicitor has been developed that is similar to psychophysical adaptive procedures. This allows estimation of behavioral and SFOAE thresholds using an identical earphone probe insertion and stimuli. The SFOAE threshold at each noise suppressor level is the lowest probe level that produces a detectable SFOAE residual. Two studies were performed with normal-hearing subjects to evaluate the feasibility of measuring SFOAE thresholds using a 3-down, 1-up adaptive procedure. In experiment 1, SFOAE thresholds for a 4-kHz probe were obtained as a function of frozen noise type (broadband or notched noise), noise level, probe duration, and suppression condition. Experiment 2 studied a potential SFOAE correlate to the overshoot effect, in which the behavioral detection threshold of a tone pip in noise improves when the pip is delayed 200 ms after noise onset compared to a 1 ms delay. A supplementary measurement using a 250-Hz tone in noise tested whether each noise stimulus elicited the middle-ear muscle reflex. Results will address the extent to which cochlear nonlinearity may account for behavioral variations in the detection of tones in external noise. (Research supported by NIDCD grants DC03784, DC006648, DC006342, DC04662).

### **659 Measuring the Spatial Extent of Action of a Near-Probe Suppressor that Demonstrates SFOAEs**

Jonathan Siegel<sup>1,2</sup>, Amanda Cerka<sup>1,2</sup>

<sup>1</sup>Northwestern University, <sup>2</sup>Department of Communication Sciences and Disorders

Brass and Kemp (1993) reasoned that a moderate-level suppressor tone near the frequency of a low-level probe tone would reveal the presence of a stimulus frequency otoacoustic emission (SFOAE) even if the emission generators extended some distance basal to the place of the probe tone. We used a dual suppressor paradigm in chinchillas to examine the spatial extent of action of a near-probe suppressor. The SFOAE evoked by a 30 dB SPL probe tone was revealed by adding a 55-70 dB suppressor tone near the frequency of the probe. The SFOAE revealed by a second higher frequency suppressor, varied from 0-70 dB, was also measured. Then the emission was measured with both suppressors presented simultaneously. If each suppressor acts only near its characteristic place, then the emission revealed by both suppressors presented simultaneously should equal the vector sum of the emissions revealed by each of the two suppressors presented alone (additivity prediction).

But if the near-probe suppressor removes SFOAE generators that are also removed by the higher frequency suppressor, then the additivity prediction will fail to the extent to which both suppressors act on the same subset of emission generators.

The additivity prediction failed in most conditions for suppressor levels of 65 dB SPL or lower: the SFOAE demonstrated by the higher frequency suppressor was nearly always reduced by the lower-frequency suppressor, but was never enhanced. This result implies that, contrary to the suggestion of Shera et al. (2004 ARO MWM), suppressors an octave or more above the frequency of the probe tone do not generate a signal that is not present in the absence of the suppressor. Parallel results were obtained in simultaneous measurements of cochlear microphonic (CM) at the probe frequency. Both the SFOAE and CM data appear to be completely accounted for by a single mechanism of two-tone interaction in the hair cell transducer.

Supported by NIH grant DC-00419 and Northwestern University.

### **660** Origin of Stimulus Frequency Otoacoustic Emissions in the Hair Cell Transducer: Evidence from Near-threshold Two-Tone Acoustic and Microphonic Suppression

Jonathan Siegel<sup>1,2</sup>, Amanda Cerka<sup>1,2</sup>

<sup>1</sup>Northwestern University, <sup>2</sup>Department of Communication Sciences and Disorders

We tested two predictions of a two-state Boltzmann model of the hair-cell transducer (Kros et al., 1995) for the two-tone suppression measurements used to separate the stimulus tone from the stimulus frequency otoacoustic emission (SFOAE) it evokes. The model predicts that, for a probe tone with amplitude small enough not to drive the transducer appreciably into its nonlinear range, the threshold for suppressing the response to the probe tone by a second tone (the suppressor) is reached when the amplitude of the suppressor exceeds the transducer's quasilinear range. The suppression threshold is nearly independent of the amplitude of the probe tone under these conditions. The model also predicts that suppression of the probe by a suppressor with level well above suppression threshold should be evident at probe levels 20-30 dB below that at which the probe exceeds the transducer's quasilinear range.

Experiments in chinchillas confirmed both of these predictions, for suppressor tones with frequencies near that of the probe or as much as several octaves higher. These results were quantitatively similar for suppression measured as an SFOAE or in the cochlear microphonic (CM) signal at the probe frequency recorded from extracochlear electrodes, suggesting that SFOAEs are directly related to the population transducer currents giving rise to the CM. There was no evidence of low-pass filtering that should be evident if the SFOAE originated in the voltage-driven prestin motors. The harmonic content of the CM and the SFOAE was also similar, with the second harmonic larger than the third harmonic. The CM and

SFOAE suppression both disappeared following the death of the animal with a similar time course. The SFOAE thus appear to be generated by the transducers of hair cells in a large cochlear region, require the driving force that powers the CM and are susceptible to suppression by tones near neural threshold.

Supported by NIH DC-00419 and Northwestern University.

### **661** Map of Basilar-Membrane Delays Reveals Fast Exit of Stimulus-Frequency Otoacoustic Emissions from the Chinchilla Cochlea

Jonathan Siegel<sup>1</sup>, Amanda Cerka<sup>1</sup>, Alberto Recio-Spinoso<sup>2</sup>, Andrei Temchin<sup>1</sup>, Pim van Dijk<sup>3</sup>, Mario Ruggero<sup>1</sup>

<sup>1</sup>Northwestern University, <sup>2</sup>University of Wisconsin, Madison, <sup>3</sup>University Hospital Groningen, The Netherlands

When stimulated by tones, the ear emits tones of its own, stimulus-frequency otoacoustic emissions (SFOAEs). We compared their latencies in chinchilla with a unique map of basilar-membrane group delay, measured at the characteristic frequency (CF), as a function of CF:  $\tau_{\text{BMCF}} = 0.496 + 1.863\text{CF}^{-0.771}$  (with  $\tau$  expressed in ms and CF in kHz). The map was constructed using second-order Wiener-kernel analysis (van Dijk, Wit, Segenhout & Tubis, J.A.S.A. 95: 904-919, 1994) of responses to noise of auditory-nerve fibers innervating most of the length of the cochlea and corroborated by measurements, culled from the literature, of vibrations at several basal and apical basilar-membrane sites. SFOAE latencies were similar to, or shorter than, basilar-membrane delays for frequencies >4 kHz and <4 kHz, respectively. Such short latencies imply very fast propagation of SFOAEs in the cochlea, perhaps via acoustic waves, and indicate that SFOAEs with frequency <4 kHz arise from regions distributed basal to the sites where traveling waves reach their peaks. These results contradict a key prediction of the widely-accepted "theory of coherent reflection filtering" (Zweig and Shera, J.A.S.A., 98: 2018-2047, 1995; Shera and Guinan, J.A.S.A., 113: 2762-2772, 2003), namely that the latencies of SFOAEs evoked by low-level tones approximately equal twice the basilar-membrane group delays at the CF.

### **662** Measurement of Stimulus-Frequency Otoacoustic Emissions using Amplitude-Modulated Suppressor Tones

Stephen Neely<sup>1</sup>, Tiffany Johnson<sup>1</sup>, Cassie Garner<sup>1</sup>, Michael Gorga<sup>1</sup>

<sup>1</sup>Boys Town National Research Hospital

Although methods are available for measuring SFOAEs without the use of a suppressor tone, SFOAEs are typically obtained by taking the difference in sound pressure at the probe frequency between measurements made with and without a suppressor tone at a nearby frequency. Underlying this method is the fact that the suppressor tone reduces or eliminates the SFOAE, so that it is fully present only in measurements without the suppressor. We present a variation of this method in which

the amplitude of the suppressor tone is varied continuously. The effect of using an amplitude-modulated suppressor is to cause the SFOAE to also be modulated at the same rate. Modulation shifts the SFOAE to frequencies slightly above and below the probe frequency. These SFOAE sidebands are separated from the probe frequency by an amount equal to the modulation frequency of the suppressor. This feature allows the AM-SFOAE to be separated from the probe frequency using spectral methods instead of subtraction methods. To demonstrate this technique, we measured AM-SFOAEs in normal-hearing subjects. The suppressor used for these measurements was amplitude modulated at a rate of 6-Hz with a modulation depth of 99%. Besides the amplitude modulation, the levels of both the probe and the suppressor were varied continuously at a much slower rate of 1 cycle/minute. This level variation allowed the measurement of SFOAE I/O functions with a single stimulus. Heterodyne analysis was used to recover the AM-SFOAE from the recorded waveform. SFOAE level was computed from the power sum of the upper and lower sidebands. These SFOAE levels in normal-hearing subjects were similar to levels reported by others using the subtraction method. Cavity measurements and measurements in subjects with cochlear implants were used to verify that the responses in normal-hearing subjects were of cochlear origin. One possible advantage of the AM-SFOAE method is that it makes it possible to exclude the influence of heartbeat, which can be shown to also modulate the amplitude of the SFOAE. However, other possible artifacts in the measurement, such as subject swallowing and cable rub, remain problematic for the heterodyne-analysis method. [Work supported by grants from NIH-NIDCD.]

### **663 Efferent OAE suppression and binaural interactions**

**David Kemp**<sup>1</sup>, Ju-Yin Hsueh<sup>2</sup>, Jonathan Slightam-Wearne<sup>2</sup>  
<sup>1</sup>University College London England, <sup>2</sup>Institute of Laryngology and Otology

Efferent suppression of OAEs is known to take times of the order of 100-200ms to become fully established after the onset of contralateral or ipsilateral stimulation and a similar time to decay. Despite this sluggish response its origin in the MOC leaves open the possibility that the intensity of efferent suppression is to some extent dependant on the precise temporal relationship between the stimuli arriving at the two ears i.e. a dependence on the inter-aural time differences which facilitate localisation.

We report on experiments designed to explore the characteristics of TEOAE suppression in human subjects. In the first experiments the rise and fall time constants of the suppression following contralateral, ipsilateral and bilateral white noise stimuli were determined to be of the order of rise time 90ms and fall time 200ms. We found evidence of positive synergistic behaviour in binaural amplitude suppression.

We could obtain comparable levels of suppression by replacing the white noise with click stimuli

In the second series of experiments synchronised click stimuli were given to both the OAE measurement ear and the suppressor ear. We searched any dependence of TEOAE level on the inter-aural time difference between the clicks using ITDs of up to 10ms.

Long measurement runs were necessary but we succeeded in demonstrating small systematic and repeatable differences in TEOAE levels related to ITD in some subjects. We interpret this as ITD dependant efferent suppression. The form of the dependence differed between subjects making it unlikely that this aspect of efferent activity is functional at the cochlear level but the results suggest that OAE suppression is a byproduct of functional activity in the MOC.

### **664 Distortion Product Otoacoustic Emission (DPOAE) Fine Structure is Responsible for the Variability of DPOAE Contralateral Suppression Effect** **Xiao-Ming Sun**<sup>1</sup>

<sup>1</sup>Wichita State University

DPOAEs can be altered in amplitude by contralateral acoustic stimulation, known as DPOAE contralateral suppression effect since an amplitude reduction was caused in majority of cases. It is generally accepted that such effect is an auditory reflex mediated by the olivocochlear efferent system. A number of studies have demonstrated the potential of DPOAE contralateral suppression measurement to be a noninvasive tool in assessing functional status of the auditory efferent system. However, this procedure has not been widely utilized in clinical practice. Limited dynamic range of the effect and large variability may be the major reasons. Previous investigations in humans showed, in average, up to 2 dB of reduction in DPOAE amplitude by contralateral sounds and sizable inter-subject variability. No-change or even increase in DPOAE amplitude occurred in some cases under certain testing conditions. Are these relevant to DPOAE fine structure? DPOAEs measured over frequency with higher resolution exhibit fine structure, characterized by a series of peaks and troughs in the amplitude-frequency function, indicating the variation of DPOAE amplitude. In this study, the 2f1-f2 DPOAE was measured in human ears over the frequency range from 0.5 to 7 kHz in absence and contralateral presence of broadband noise. The frequency steps used were 17 per 0.1 octave and the frequency ratio of f2/f1 was kept at 1.22 with the primary levels of L1=65 dB and L2=50 dB SPL. The contralateral noise was present at a level 20 dB below the middle-ear reflex threshold of the test ear. The preliminary results displayed a fine structure-dependent variation of DPOAE contralateral suppression effect. In general, for frequencies at the peaks in the fine structure, contralateral noise resulted in the largest reduction in DPOAE amplitude. At the troughs, the reduction evidently decreased or vanished and in many cases, DPOAEs were enhanced in amplitude. DPOAE phase showed alteration in the reverse pattern.

## **665** Effects of Selective Attention on DPOAE Amplitude and Rapid Adaptation in Humans

Rony Aouad<sup>1</sup>, Tom Heil<sup>1</sup>, David W. Smith<sup>1</sup>

<sup>1</sup>Hearing Research Laboratories, Duke University Medical Center, Durham, North Carolina

It has been suggested that the medial efferent innervation of outer hair cells might play a role in mediating selective auditory attention at the auditory periphery. The present study investigated the effects of selective attention on the  $2f_1$ - $f_2$  DPOAE in humans. DPOAE ( $2f_1/f_2 = 1.21$ ,  $L_1 = 70$  dB SPL,  $L_2 = 65$  dB SPL) levels were measured simultaneously in both ears for a range of  $f_2$  frequencies (1.2 to 10.0 kHz). The  $f_2$  frequency producing the largest amplitude DPOAE was used for further testing. Two experiments are reported. In the first experiment, DPOAE recordings were compared under two conditions; while the subject was reading a book (ignoring the tones) and while counting the eliciting tones (attending). In the second experiment, DPOAEs recorded while the subject was watching a movie with subtitles (no sound; not attending) were compared with DPOAEs measured while counting tones (attending). Forty-eight human subjects participated in the first experiment and twenty-one in the second, with most being female (79% and 76% respectively). The magnitudes and time constants for the rapid DPOAE adaptation component was similar across all recording conditions. The DPOAE steady-state levels, however, were statistically different when compared while subjects read a book (non-attending; 17.8 dB) with levels measured while counting the tones (attending; 17.5 dB) ( $p < 0.003$ ). The steady-state levels of the slow adaptation components were also statistically different under the condition of reading DVD subtitles (non-attending; 17.8 dB) compared with the tone counting condition (attending; 16.8 dB) ( $p < 0.001$ ). Interestingly, attending to the movie (moving, dynamic visual objects) produced a much larger difference in DPOAE levels, compared with reading (static objects). These data provide evidence that selective auditory attention can modulate auditory activity, likely through the action of the medial olivocochlear efferent system, at the most peripheral aspects of the auditory system.

## **666** Anesthetic Effects on Middle Ear Muscles and the Medial Olivocochlear Reflex in Rats

Joseph Smith<sup>1</sup>, Anita Sterns<sup>2</sup>, Beth Prieve<sup>2,3</sup>, Charles Woods<sup>1,2</sup>

<sup>1</sup>Department of Otolaryngology and Communication Sciences, Upstate Medical University, Syracuse, NY,

<sup>2</sup>Institute for Sensory Research, Syracuse University,

<sup>3</sup>Communication Sciences and Disorders, Syracuse University

To study the medial olivocochlear (MOC) reflexes in animals, sedation is usually required. A major concern is that anesthetic agents reduce the MOC reflex. An investigation was done to explore the effects that two popular cocktails, acetylpromazine-ketamine (AK) and xylazine-ketamine (XK), and historically important, sodium pentobarbital (NaP), have on the middle ear muscle (MEM) reflex and the MOC reflex in rats. MOC reflexes

were studied by observing changes in DPOAE level and phase during ipsilateral stimulation (onset adaptation) and contralateral presentation of a broadband noise (suppression) while the rats were under sedation from one of the anesthetic agents. DPOAEs from each animal were measured once per week; each week the rats were anesthetized with a different one of the three agents. At the third week after the last recordings were made, the MEMs were sectioned and the set of measurements was repeated. Similar to previous research from our lab, onset adaptation and contralateral suppression were smaller after MEM section, consistent with interpretation that these effects are mediated mostly by the MEM reflexes in the rat. Contralateral suppression before MEM section for AK and XK were similar to each other and greater than that seen with NaP. DPOAE onset adaptation was significantly greater for AK than for XK and NaP, which were similar to each other. There were no significant differences in onset adaptation or contralateral suppression between the NaP and post MEM section groups, demonstrating that NaP affected the MEM reflex. Although the data from the NaP and post MEM section groups were not significantly different, DPOAE phase leads in 5 of 9 rats suggest that in individual animals, the MEM reflex may be reduced but not abolished by using NaP.

## **667** DPOAE Adaptation Reflex Strength: Is It a Predictor of Susceptibility to Noise?

Åsa Skjönsberg<sup>1,2</sup>, Karin Halsey<sup>3,4</sup>, Lisa Kabara<sup>3,4</sup>, Mats Ulfendahl<sup>1,2</sup>, David Dolan<sup>3,4</sup>

<sup>1</sup>Karolinska Institutet, Institution for Clinical Neuroscience,

<sup>2</sup>Center for Hearing and Communication Research, and Dept. of Otolaryngology, <sup>3</sup>University of Michigan, <sup>4</sup>Kresge Hearing Research Institute

The aim of this study was to explore any correlations between efferent-mediated DPOAE reflex strength and different guinea pig strains in order to determine if a genetic component affects the DPOAE reflex strength for different populations. It was also to investigate any correlations between susceptibility to noise-induced hearing loss and the DPOAE reflex strength for different populations.

In this study we used guinea pigs from three different strains. These strains were selected from earlier studies where the susceptibility to noise-induced hearing loss was determined. One of the strains had elevated resistance to noise trauma, another of the strains had diminished resistance to noise trauma. Third strain served as control.

The animals were anaesthetized with ketamine 58.8 mg/kg, xylazine 2.4 mg/kg, and acepromazine 1.2 mg/kg, and the  $2f_1$ - $f_2$  DPOAE ( $f_1 = 8$  kHz, and  $f_2/f_1 = 1.2$ ) DPOAE adaptation was measured with a minimum of 144 level combinations of the primary tones L1 and L2. Adaptation was measured with a resolution of one dB steps initially, and in the region of maximum reflex, the resolution was increased to 0.4 dB steps of L1 and L2. The DPOAE reflex strength for each animal was defined as the difference between maximum positive adaptation and the maximum negative adaptation.

There were no significant differences in the average adaptation magnitude among the strains included in this study. From this we conclude that the DPOAE adaptation reflex strength is not a predictor for a population's susceptibility to noise trauma, using the methods described.

### **668 Interaural Correlation Discrimination with Broadband and Narrowband Noise: Performance of Auditory Nerve and Cochlear Nucleus Fibers**

**Dries Louage<sup>1</sup>**, Marcel van der Heijden<sup>1</sup>, Philip Joris<sup>1</sup>

<sup>1</sup>*Laboratory of Auditory Neurophysiology, KULeuven*

Human listeners are able to detect tiny changes in interaural correlation, and their performance is better for narrowband than for broadband noise. Classic models of binaural interaction that are based on analytical descriptions of auditory nerve (AN) inputs overestimate performance and predict an opposite bandwidth dependence [Gabriel and Colburn, 1981, JASA 69:1394]. We used real spike trains from AN and cochlear nucleus (CN) fibers of cats to calculate the correlation jnds of an optimal binaural processor.

Eight Gaussian frozen broadband noises with the same SPL and duration were presented many times to each fiber. The normalized correlation between the tokens ranged from 0.996 to -1. For each fiber, all possible combinations of two spike trains obtained with different noises were used as the input to a simple coincidence detector with an integration window of 50  $\mu$ s. The coincidence counts at different delays were transformed into a decision variable (DV). For each correlation, the distribution of DV was approximately Gaussian. The separation of the DV distributions for different stimulus correlations was expressed in units of standard deviation ( $d'$ ). The same procedure was repeated for responses to narrowband noises (bandwidth=100 Hz) centered on the characteristic frequency (CF) of the fiber.

The binaural processor yielded lower correlation jnds ( $d' = 1$ ) when fed with CN fibers compared to AN fibers, at both high and low CFs. When large interaural delays were available to the binaural processor, bandwidth dependence of jnds agreed with psychophysical data. These results suggest that, in the context of correlation discrimination, coding by CN fibers is superior to that by AN fibers and that correlation discrimination is shaped by the presence of large internal delays.

Supported by the Fund for Scientific Research - Flanders (G.0083.02) and Research Fund K.U.Leuven (OT/10/42).

### **669 Encoding of Steep, Rising Spectral Edges by Neural Circuits in the Dorsal Cochlear Nucleus**

**Lina Reiss<sup>1</sup>**, Eric Young<sup>1</sup>

<sup>1</sup>*Johns Hopkins University*

One possible function of DCN is discrimination of behaviorally relevant stimuli like HRTFs, spectral cues used for vertical sound localization. Previously, we showed that a majority of 24/37 DCN Type IV neurons encodes the

locations of spectral notches and bands with an excitatory peak response to rising spectral edges aligned near BF (Reiss and Young, ARO 2004). Since Type II inhibition to Type IV units often occurs at frequencies below BF (Voigt and Young, 1990; Spirou and Young, 1991), we proposed that this spectral asymmetry of inhibition and excitation is the mechanism for edge sensitivity.

To confirm this proposed mechanism, in the current experiment we recorded from Type IV and Type II neurons in the DCN of the decerebrate cat. We presented notch noise (NN) center frequency sweeps, or a series of notch noise stimuli with the notch center frequency varied within a two-octave range around the unit's BF. We also presented band noise (BN) sweeps. Analysis of Type IV tone response maps showed that edge sensitivity in Type IV units is correlated with inhibition centered on average  $\sim 0.1$  octaves below BF. We also found that 7/7 Type II units respond strongly to NN centered off BF, and Type II responses to NN and BP sweeps align with the inhibition of Type IV responses to rising edge frequencies just below the peak and far above the peak, but shifted by  $\sim 0.1$  octave down, consistent with the above finding.

There is also additional inhibition of Type IV units to rising edge frequencies just above the peak for all notch widths tested (1/16-2 oct). Computational simulations based on current models of DCN processing (Nelken and Young, 1994; Hancock and Voigt, 1999) show that WBI inputs account for this inhibition to NN with narrow notch widths, but not wide notch widths. Therefore, a new component is needed in the DCN model to fully explain this additional inhibition. This shaping of edge sensitivity by inhibition to rising spectral edges both below and above BF suggests the specialization of DCN for edge sensitivity along the tonotopic gradient.

Supported by NIH grants DC00115, DC05211; NIH predoctoral fellowship DC00441.

### **670 Nonlinear Spectral Processing Models of Neurons in the Cochlear Nucleus**

**Sharba Bandyopadhyay<sup>1</sup>**, Eric Young<sup>1</sup>

<sup>1</sup>*Johns Hopkins University*

Neurons in the cochlear nucleus, especially the dorsal cochlear nucleus (DCN), are known to exhibit nonlinearities in spectral processing. Spectral processing models, where spectral level is transformed into rate through a linear gain function (an estimate of the neurons spectral receptive field, Yu and Young 2000), do well at predicting responses to novel stimuli in most CN neurons. Often a second order polynomial nonlinearity improves model predictions. However among the different types of cochlear nucleus neurons, Type IV neurons in DCN most often cannot be modeled this way. Here we present results of using nonlinear models based on sigmoidal gain control. Responses to random spectral shape (RSS) stimuli with varying degrees of fluctuations (spectral contrast) were fit with these gain functions, in which gain changes with spectral level. For most cochlear nucleus neuronal types, the nonlinearity obtained is very close to that obtained with second order models. The departure from second order models is manifest primarily in the responses to high

spectral contrast stimulus sets (12 dB standard deviation). In these cases, predictions are slightly improved when the gain-control model is used, relative to second order models. However for DCN Type IV units, there is larger improvement in predictions, as measured by fraction of the response variance predicted by the model. The nature of the sigmoidal nonlinearity for Type IV units is that the sensitivity at the best frequency decreases for increasing spectral deviations. Models, that include interactions between frequencies, are being investigated. Supported by NIH grants DC00115 and DC005211.

### **671 Wideband Suppression in Cochlear Nucleus: A Role in Grouping by Common Onset?**

**Stefan Bleeck**<sup>1</sup>, Neil Ingham<sup>1</sup>, Jesko Verhey<sup>2</sup>, Ian Winter<sup>1</sup>  
<sup>1</sup>University Cambridge, <sup>2</sup>Universität Oldenburg

Sounds that start at the same time are judged as originating from the same source. Darwin and Sutherland (Q. J. Exp. Psychol 1984. 36A, 193-208) demonstrated the effect of onset asynchrony: the perception of the vowel /l/ changes to /e/ by manipulating the harmonics around F1. Extending the augmented component before the vowel reduced this change. The change could be restored by using a 'captor' tone which was switched on with the asynchronous harmonic but off when the vowel started.

We hypothesise that (i) the reduced effect of the asynchronous component occurs because it has adapted before the other components begin (ii) a 'captor' tone that groups with the leading segment reduces the neural response to that segment by activating an across-frequency inhibition from a wideband inhibitor (iii) the reduction in neural response is effectively a release from adaptation; (iv) the offset of the captor terminates the inhibition and the response to the continuation of that component is now enhanced and (v) because the captor offset occurs at the same time as the other components begin, all partials effectively have a common onset time, and so group together.

As a preliminary test of the above hypothesis we measured the responses of single units in the cochlear nucleus of anesthetized guinea pigs to two-tone complexes. One tone was placed at the unit's best frequency (BF) while the second tone – the 'captor' – was positioned in the unit's inhibitory sidebands. The captor tone was always turned off before the termination of the BF tone. For 36 units (n = 65) an increase in response to the BF tone was observed at the termination of the captor tone. This effect was most prominent in units classified as chopper and primary-like with a notch. These results suggest that wideband inhibition/suppression may play a role in grouping by common onset.

Supported by the BBSRC

### **672 Binaural Properties of Ventral Cochlear Nucleus Neurons**

**Alberto Recio**<sup>1</sup>

<sup>1</sup>University of Wisconsin

Responses of ventral cochlear nucleus (VCN) neurons and auditory nerve fibers to ipsilateral short-duration tones in the anesthetized chinchilla were obtained in the presence of contralateral sounds (tones and broadband noise). Inhibitory effects by contralateral stimuli were observed only in the responses of chopper neurons and not in the auditory nerve or other types of VCN neurons. Such effects were most prominent for responses evoked by near-threshold, ipsilateral best frequency (BF) tones. The strength of inhibition also depended on the frequency and level of the contralateral tone, being the largest for near BF tones. Inhibitory effects by broadband noise were usually stronger than the effects obtained using tones.

Current thinking holds that contralateral inhibition is mediated by commissural fibers, whose axons travel along the intermediate acoustic stria (IAS). Disruption of the contralateral IAS, however, failed to affect the inhibition. Dislodging of the contralateral ossicles did remove the inhibitory effects.

### **673 Contralateral Single Neuron Receptive Fields in the Mammalian Cochlear Nucleus**

**Neil Ingham**<sup>1</sup>, Stefan Bleeck<sup>1</sup>, Ian Winter<sup>1</sup>

<sup>1</sup>University of Cambridge

Wideband inhibition can improve the detection of signals in amplitude-modulated noise [eg Neuert et al 2004 J Neurosci 24: 5789-97] when both signal and noise are presented ipsilaterally. Improvements in ipsilateral signal detection have been demonstrated psychophysically when noise is presented contralaterally. Here, we measure the effect of changing the frequency and level of a contralateral tone on single neurons in the guinea-pig cochlear nucleus. Pure tone receptive fields were recorded (n=58) using combinations of monaural and binaural stimuli. Many neurons showed no evidence of neural responses originating from the contralateral ear (n=25). However, 27 neurons responded with activity patterns that were suggestive of contralateral inhibitory input. In several cases (n=10), the inhibition was evident at relatively high contralateral stimulus levels and at frequencies below the ipsilateral best frequency (BF); "off-BF inhibition". For the remainder (n=17), the contralateral tone evoked an inhibitory pattern which produced a 'negative' of the ipsilateral excitatory receptive field. In many cases, this inhibition extended to low stimulus levels, close to the threshold stimulus level for an ipsilateral tone; "on-BF inhibition". A few neurons (n=6) exhibited responses consistent with excitatory input from the contralateral ear. Our results are in agreement with previously published studies of the cochlear nucleus [Mast 1970 J Neurophys 33: 108-15; Mast 1973 Br Res 62: 61-70; Joris & Smith 1998 J Neurosci 18: 10157-70; Shore et al 2003 Exp Brain Res 153: 427-35]. We have extended these studies into the domain of the pure tone receptive field, where the relative inhibitory/excitatory strength as a function of both frequency and level can be assessed. These preliminary



data suggest that the improvement of signal detection in noise at the level of the cochlear nucleus may be reduced if the noise is presented to the contralateral ear.

Supported by the Wellcome Trust.

### **674 Responses of Neurons in the Rat's Ventral Nucleus of the Lateral Lemniscus to Monaural and Binaural Stimulation**

Huiming Zhang<sup>1</sup>, Jack B. Kelly<sup>1</sup>

<sup>1</sup>*Psychology Department, Carleton University, Ottawa, Canada K1S 5B6*

We made recordings from the rat's ventral nucleus of the lateral lemniscus (VNLL) and examined the responses of single neurons to monaurally and binaurally presented sounds. We determined the characteristic frequency (CF), the threshold at CF, the shape of the frequency tuning curve, and the temporal firing pattern for responses to a 100 ms tone burst presented to the ear contralateral to the recording site. We also recorded responses to a long duration (10 sec) amplitude modulated tone presented to the contralateral ear. The shape of the modulation transfer functions for firing rate and vector strength, the maximum level of synchronization, the best modulation frequency and the upper cut-off frequency for synchronous discharges were determined. In addition, we studied single unit responses to 100 ms dichotic tone bursts. We found that many neurons in VNLL were sensitive to binaural level differences. To determine whether the responses were dependent on local synaptic excitation in VNLL, we recorded activity before and during the release of NBQX, a selective AMPA receptor antagonist. The drug was released at the recording site by iontophoresis from a pipette fixed to the recording electrode. In most cases the AMPA receptor antagonist rapidly and substantially reduced the number of spikes evoked by acoustic stimulation. The data suggest that the responses, including those sensitive to binaural level differences, were recorded from VNLL neurons rather than fibers of passage.

Research supported by NSERC of Canada.

### **675 Binaural Interactions Shape the Responses of Dorsal Cochlear Nucleus Units to Virtual Space Stimuli.**

Oleg Lomakin<sup>1</sup>, Kevin Davis<sup>1</sup>

<sup>1</sup>*Department of Biomedical Engineering, University of Rochester, Rochester, NY 14642*

Physiological and behavioral evidence suggests that the dorsal cochlear nucleus (DCN) plays an early role in the processing of monaural pinna-derived spectral cues to the location of broadband sounds in space. DCN principal cells (type IV units) do not require binaural stimulation to exhibit their directional sensitivity; yet, these neurons receive inputs from the contralateral cochlear nucleus as well as descending projections from multiple binaural nuclei. Single-unit studies suggest that the net effect of these commissural and efferent projections is usually inhibitory, particularly when activated by broadband noise. To investigate the effects of these contralateral inputs in the DCN, the responses of type IV units to binaural virtual

space (VS) stimuli were compared to those elicited by monaural stimulation. Head-related transfer functions (HRTFs) were used to filter broadband noise spectra to synthesize binaural VS stimuli in the frontal field. When VS stimuli were presented to the ipsilateral ear, type IV units showed a tuned inhibitory response that followed a diagonal contour from low ipsilateral elevations to high contralateral elevations. This trough in the elevation functions coincided with a spectral notch in the HRTF at the unit's best frequency. When tested with binaural VS stimuli, type IV units showed a tuned inhibitory response for elevation only in the ipsilateral hemifield; responses were largely inhibitory throughout contralateral space. In comparison to monaural responses, binaural responses to VS stimuli showed enhanced sensitivity to the elevation of a sound source in ipsilateral space (i.e. a deeper trough) but reduced sensitivity in contralateral space (i.e. the response was lateralized). These results demonstrate that the contralateral inputs to the DCN are functionally relevant in natural listening conditions, and that one role of these inputs is to enhance DCN processing of spectral sound localization cues produced by the pinna. Supported by NIDCD grant R01 DC 05161-04.

### **676 The Medial Nucleus of the Trapezoid Body: an in vivo Electrophysiological Study in Rat.**

Sandra Tolnai<sup>1</sup>, Olga Hernández<sup>2</sup>, Rudolf Rübsamen<sup>1</sup>, Manuel S. Malmierca<sup>2</sup>

<sup>1</sup>*Faculty of Biosciences, Pharmacology, and Psychology, University of Leipzig, Leipzig, Germany,* <sup>2</sup>*Auditory Neurophysiology Unit. Lab Neurobi Hear, Fac Med. University of Salamanca, Salamanca, Spain*

The medial nucleus of the trapezoid body (MNTB) transforms excitatory inputs from the globular bushy cells into inhibitory inputs and projects widely within the superior olivary complex. For many years, the MNTB neurons were thought to play a passive role in audition because of the unique morphology of their input, the calyx of Held that allows a fast and reliable synaptic transmission. However, the MNTB has recently become a main object of investigating synaptic processes and basic electrophysiological *in vivo* studies in rats – the most commonly used animal model for *in vitro* studies – are virtually pending. Therefore the main aim in the current study was a systematic characterization of MNTB neurons to acoustic stimulation. Pigmented rats (Long Evans) were anesthetized with urethane (1.5 mg/kg i.p.), and acoustic stimuli generated in a TDT system II were delivered through a closed field system. The present study is based on the responses of 59 single units. We determined the units' frequency response areas (FRAs), obtained rate intensity function and post-stimulus time histogram at the units' characteristic frequency (CF). In addition, we investigated the responses to sinusoidal amplitude modulated signals at the units' CF. Recording sites were histologically verified in each experiment. Consistent with previous studies, MNTB units solely responded to stimuli presented to the contralateral ear. The majority of units exhibited V-shaped FRAs. We complemented this subjective classification by applying quantitative measures,

e.g. inverse slope of upper and lower FRA borders. Rate intensity functions were mainly monotonic and post-stimulus time histograms mostly primary-like. Units phase-locked to sinusoidal amplitude modulated signals, typically with a low-pass transfer characteristic. Our data provide the basis for further investigations especially with respect to the interaction of excitation and inhibition at the calyx terminal itself.

**Acknowledgments:** This study was supported by grants from the Spanish DGES (BFI-2003-09147-02-01) and JCYL-UE (SA040/04) to MSM. OH held a fellowship from the Spanish MCYT (FP-2000-5811 and BFI 2000/1358).

### **677 Dynamic Clamp Analysis of Jitter Reduction and Latency upon Convergence of Many Synaptic Inputs**

**Matthew Xu-Friedman<sup>1,2</sup>, Wade Regehr<sup>2</sup>**

<sup>1</sup>University at Buffalo, SUNY, <sup>2</sup>Dept. Neurobiology, Harvard Medical School

Precise action potential timing is important in sensory acuity and motor control. We used dynamic clamp to mimic synaptic inputs to test the effectiveness of convergence of a large number of synaptic inputs on reducing spike timing variability ("jitter") and in controlling spike latency. We systematically varied the total conductance ( $G_{tot}$ ), number ( $N$ ), timing variability ( $SD_{in}$ ), and input distribution and examined the effect on firing in the postsynaptic cell. Changing  $G_{tot}$  caused large shifts in postsynaptic spike latency. These latency shifts were unaffected by changes in  $N$ , and thus appeared to be determined by the amplitude of individual inputs. The effect of  $G_{tot}$  on jitter reduction depended on the input distribution: optimal jitter reduction for the Gaussian distribution occurred with  $G_{tot}$  2-3 times threshold, whereas for the alpha distribution jitter in first spike latency showed continued reduction with higher  $G_{tot}$ . When  $G_{tot}$  became sufficiently high, the postsynaptic cell could spike multiple times, which interfered with jitter reduction. Secondary spikes were particularly prominent when  $SD_{in}$  was much longer than the refractory period of the cell. Under *in vivo* conditions, the effectiveness of convergence could be compromised by use-dependent changes in synaptic strength and by variability in the number of active inputs, which both affect  $G_{tot}$ . However, our results indicate that convergence is resistant to these factors because the events that cause the greatest skew in latency are rare.

### **678 Blocking Input from the Ventral Nuclei of the Lateral Lemniscus Alters Response Areas and Duration Sensitivity of Inferior Colliculus Neurons in Rats and Bats**

**David Perez-Gonzalez<sup>1,2</sup>, Manuel S. Malmierca<sup>2</sup>, Ellen Covey<sup>1</sup>**

<sup>1</sup>BATLAB, Department of Psychology, University of Washington, Box 351525, Seattle, Washington, USA, <sup>2</sup>Cell Biol and Pathol, Auditory Neurophysiol Unit, Lab Neurob Hearing, INCYL. Fac Med, Univ Salamanca

The ventral nuclei of the lateral lemniscus (VLL) is a major source of monaural excitatory and inhibitory input to the

inferior colliculus (IC). Responses from single neurons in the IC of big brown bats (*Eptesicus fuscus*) and Long-Evans rats (*Rattus norvegicus*) were recorded extracellularly before, during and after reversible blocking of the VLL by iontophoretic injections of kynurenic acid, a broad-spectrum antagonist of glutamate receptors. We analyzed the effect of blocking VLL on IC neurons' frequency response areas (FRA), rate-intensity functions (RIF), duration-intensity functions and responses to amplitude- and frequency modulated sounds. Most IC units (91% in bats, 81% in rats) showed some kind of change in their discharge rate after inactivation of the VLL. These changes typically affected both response areas and RIFs, but did not affect discharge patterns. In rats, the FRA of 65% of affected neurons was modified in a non-level-dependent way, mainly by a decrease in firing rate and uniform downward shift of the RIF. The other 35% showed level-dependent increases and/or decreases in firing rate. In bats, level-dependent changes occurred in 60% of the affected units, most of them showing a decrease in firing at high levels and an increase (or no change) at lower levels. VLL inactivation also affected duration sensitivity in both rats and bats. For some long pass duration sensitive neurons, blocking the VLL caused them to respond to short durations and changed their duration response functions from long-pass to all-pass. These results suggest that the VLL provides transient, short-latency inhibition that normally prevents some IC neurons from responding to short sounds. Blocking VLL had little or no effect on IC neurons' responses to modulated sounds.

Supported by the Spanish JCYL-FSE (SA040/40, MSM) and DGES (BFI-2003-09147-02-016, MSM, DPG) and by the NIH-NIDCD (DC00607, EC, DPG).

### **679 Stimulation Rate Dependent Broadening in the Dorsal Nucleus of the Lateral Lemniscus, Implications for Context Dependent Processing in the Central Auditory System**

**Jeremy Smalling<sup>1</sup>, Albert Feng<sup>1</sup>**

<sup>1</sup>University of Illinois

Echolocating bats such as the little brown bat (*Myotis lucifugus*) emit discrete sonar signals in a context dependent manner. The rate of sonar emissions is low (5 to 20 emissions per second) during the prey search phase, and the rate is increased progressively, when a bat pursues a flying insect, up to 100 to 200 emissions per second during the terminal buzz. Previously we have shown that the frequency tuning curves of inferior colliculus (IC) neurons are dynamic; a unit's tuning curve at low stimulation rates (SRs) can not accurately predict its frequency tuning at higher, more behaviorally relevant SRs. Typically, the frequency response range ( $W$ ) of midbrain auditory neurons becomes narrower with increasing SR, presumably conferring a greater perceptual frequency resolution. There is evidence (see also Jen et al., 2002) that this SR-dependent change involves local synaptic inhibition (i.e. GABAergic and glycinergic inhibition within the midbrain). The rate-dependent

mechanism underlying this context dependent change in local synaptic inhibition remains unclear.

In this study, we investigated whether or not SR similarly influences the frequency and amplitude response properties of single neurons in the auditory cortex and the dorsal nucleus of the lateral lemniscus (DNLL). We found that, as in the IC, cortical neurons also displayed SR-dependent narrowing of frequency tuning. However, at the DNLL an increase in SR primarily produced a broadening of W. Since the DNLL gives an inhibitory projection to the IC, SR-dependent broadening of W in the DNLL would likely create SR-dependent narrowing of W in the IC. Thus, SR-dependence may be found as early as the DNLL in the form of SR-dependent broadening of frequency tuning. This dependence is preserved at the levels of the midbrain and auditory cortex, but is found in the form of SR-dependent sharpening of frequency tuning. The implications for these findings in context-dependent sound processing will be presented.

### **680** Response Properties of Neurons in the Dorsal Cochlear Nucleus of the Unanesthetized Mouse

**Nathaniel Sawtell**<sup>1</sup>, Richard Felix<sup>2</sup>, Thanos Tzounopoulos<sup>3</sup>, Christine Portfors<sup>2</sup>

<sup>1</sup>Neurological Sciences Institute, Oregon Health & Science University, <sup>2</sup>Washington State University, <sup>3</sup>Oregon Hearing Research Center and Vollum Institute, Oregon Health & Science University

The dorsal cochlear nucleus (DCN) is a cerebellum-like structure that integrates ascending auditory nerve input with descending multimodal inputs conveyed by parallel fibers. Similar cerebellum-like sensory structures in fish are adaptive sensory processors in which plasticity at parallel fibers subtracts predictable features from the sensory inflow. Recent in vitro studies in mouse DCN have demonstrated cell-specific spike timing-dependent plasticity at parallel fiber synapses. As a first step towards understanding the roles of descending inputs and synaptic plasticity in auditory processing in the mouse DCN, we have characterized the auditory response properties of DCN neurons in the unanesthetized mouse. We focused primarily on putative cartwheel and fusiform cells, both of which receive plastic input from parallel fibers. We recorded responses of well-isolated single-units in the DCN to tones, combinations of tones and broad-band noise. After obtaining characteristic frequency (CF) and minimum thresholds (MT), we obtained measures of response magnitude to tone burst stimuli (50 ms, 0.5 ms rise/fall) across the hearing range of the mouse (6-100 kHz) at varying levels of intensity (at minimum 10, 30 and 50 dB above threshold). Rate-level functions were also obtained for broad-band noise stimuli (50 ms, 0.5 ms rise/fall time). To assess excitatory and inhibitory frequency response areas in neurons with little or no spontaneous activity, we used a two-tone paradigm in which one tone was set at CF and MT and the frequency of a second, simultaneously presented, tone varied in frequency. Based on these data most neurons could be categorized according to previously defined post-stimulus

time histogram and excitatory-inhibitory area schemes. Cartwheel cells were identified on the basis of complex-spikes, recording location, and characteristic responses to sound. Most cartwheel cells had broad excitatory frequency tuning curves and long-latency responses to sound. Tone-evoked responses in cartwheel cells typically consisted of a complex-spike burst followed by a pause and a variable number of simple spikes. Response properties and proportions of various unit types recorded in the unanesthetized mouse DCN are compared to those reported previously for the anesthetized mouse and for other species.

### **681** Duration Sensitive Neurons in the Medial Nucleus of the Trapezoid Body (MNTB) and Superior Paraolivary Nucleus (SPON) of the Rat

**Alexander Kadner**<sup>1,2</sup>, Albert Berrebi<sup>1,2</sup>

<sup>1</sup>West Virginia Univ. School of Medicine, <sup>2</sup>Sensory Neuroscience Research Center

Our previous work has shown that single unit responses from the SPON of the rat are tuned to stimulus duration (Kulesza & Berrebi, ARO abstracts, 2004). Neurons in this nucleus receive strong tonotopic inhibitory input from MNTB, show no spontaneous activity and respond transiently to the offset of BF tones. In contrast, MNTB neurons show spontaneous activity and primary-like, sustained responses that continue for about 5 ms after the stimulus offset. This sustained response is followed by a period of up to 50 ms during which spontaneous activity is suppressed.

We recorded responses from single neurons in both the SPON and the MNTB. The stimuli used were BF tones presented at 20 dB above threshold with durations from 2 to 1000 ms. We measured the mean spike rate and median first spike latency during a time window 5-80 ms after the stimulus offset. In most MNTB neurons, mean spike rate decreased and first spike latency increased, indicating that the period of suppressed spontaneous activity got longer as stimulus duration was increased. In some cases this increase was observed for durations up to 1000 ms, whereas in other cases saturation was reached at shorter durations. The offset response of the SPON neurons also fell in this time window. The mean spike rate of these responses tended to increase with stimulus duration, but saturation and a reduction of mean spike count for longer durations were also observed in some units.

These data support the notion that the SPON offset response is triggered by release from MNTB-derived inhibition during the period of suppressed spontaneous activity. The duration of this suppression largely determines the duration of the offset response in SPON neurons.

Supported by NIDCD RO1 DC-06626 to ASB.

## **682** Characterization and Function of Low Threshold Potassium Channels in Principal Neurons of the MSO

Nace L. Golding<sup>1</sup>, Paul J. Mathews<sup>1</sup>

<sup>1</sup>Section of Neurobiology and Institute for Neuroscience, University of Texas, Austin, TX 78712

Low threshold K<sup>+</sup> currents ( $I_{K(LT)}$ ) shape the time course and pattern of synaptic excitation and action potential firing in brainstem auditory neurons concerned with temporal coding. To understand the biophysical properties, subunit composition and role these channels play in the medial superior olive (MSO), we made whole-cell voltage clamp recordings from MSO principal cells in brainstem slices of P17-21 gerbils.  $I_{K(LT)}$  was isolated pharmacologically by inclusion of 1  $\mu$ M TTX, 10 mM TEA, and 50  $\mu$ M ZD7288 to block Na<sup>+</sup>, high threshold K<sup>+</sup> and h currents, respectively. Cells were held at -60 mV, and outward currents were activated from a -80 mV prepulse to voltages between -70 and 0 mV (750 ms step duration).  $I_{K(LT)}$  activated at -65 mV and ranged in amplitude from  $63 \pm 18$  pA to  $1734 \pm 265$  pA between -65 and -45 mV (n=8). These currents showed fast activation and slow inactivation kinetics between -60 and -45 mV ( $\tau_{act}$ :  $0.62 \pm 0.08$  ms to  $1.31 \pm 0.14$  ms,  $\tau_{inact}$ :  $329 \pm 26$  ms to  $234 \pm 17$  ms). Outward currents evoked by voltage steps between -65 mV and -45 mV were blocked by over 90% by bath applied dendrotoxin-K (80 nM, n=5), indicating that Kv1.1-containing channels mediate the majority of  $I_{K(LT)}$  in these neurons. A similar blockade of current was also apparent in responses to brief trains of simulated EPSP voltage commands delivered at 250 or 500 Hz (n=2).  $I_{K(LT)}$  activated with temporal fidelity in response to EPSP commands, and the timing of the current was correlated with the repolarizing phase of the EPSPs. Accordingly, whole-cell current clamp recordings confirmed that a dendrotoxin-sensitive current increased EPSP repolarization rate and decreased EPSP duration in responses to increasing simulated EPSC injections. Taken together, these experiments suggest that Kv1.1-containing channels mediate the majority of  $I_{K(LT)}$  in MSO principal neurons. This current sharpens subthreshold EPSPs and therefore increases the temporal resolution of binaural coincidence detection.

Supported by DC 006877, DC 006341

## **683** Optical Imaging Studies of the Dorsal Cochlear Nucleus in Response to Acoustic and Electric Stimulation

Jinsheng Zhang<sup>1</sup>, James Kaltenbach<sup>1</sup>

<sup>1</sup>Department of Otolaryngology-Head & Neck Surgery, Wayne State University, Detroit, MI 48201

We are investigating the use of optical imaging for observing the spatial patterns of neural activation in the dorsal cochlear nucleus (DCN) of hamsters during acoustic and electric stimulation. The patterns of response were studied in the DCN, in vivo, following application of a voltage sensitive dye, Di-2-ANEPEQ, to the DCN surface. Electrophysiological recordings 60-90 minutes following dye application revealed no significant toxicity of Di-2-ANEPEQ that affected the frequency tuning properties of

DCN neurons. We examined areas of activation in response to each of a series of test stimuli consisting of pure tones ranging in frequency from 2 to 20 kHz. For each stimulus condition, images were collected over a stimulus interval of 400 ms and averaged over 32 stimulus repetitions. The obtained images revealed areas of activation with definable epicenters. These epicenters shifted from lateral to medial locations on the DCN surface with increases in stimulus frequency. Comparison with electrophysiological data indicated a close parallel between the tonotopic gradient defined by optical imaging and that defined by the distribution of characteristic frequencies. In contrast to this medial-lateral gradient in frequency, no systematic shifts in optical response were observed along the rostrocaudal axis of the DCN with changes in stimulus frequency. In addition, a buildup pattern has been observed in the optical responses of the DCN to tones. This buildup pattern is comparable to the 'buildup' response pattern that many DCN fusiform cells exhibit in single unit recordings. The principal temporal and spatial features of these optical responses will be examined. We are currently comparing the optical responses the DCN to acoustic stimulation with those following electric stimulation of the parallel fibers. (This work was supported by NIDCD grant R21DC006041).

## **684** Integration Window for Detection of Inputs in Neurons of the Ventral Cochlear Nucleus

Matthew J. McGinley<sup>1,2</sup>, Aldo R. Rodrigues<sup>1</sup>, Donata Oertel<sup>1</sup>

<sup>1</sup>University of Wisconsin, Madison, <sup>2</sup>Oregon Health and Sciences University, Portland

Bushy and octopus cells of the ventral cochlear nucleus, but not T stellate cells, express a low-voltage-activated potassium current (IKL) that truncates firing after one or a few action potentials soon after the onset of a step depolarization. To understand how this current affects responses to synaptic activation, we have studied the voltage responses of these neurons to current ramps in whole-cell current-clamp. An electrical circuit model of the electrode and cell in the recording configuration was solved for the case of ramp waveforms, to allow accurate corrections to be made of series resistance and pipette capacitance throughout the ramp.

When depolarized from the resting potential with current ramps, bushy cells have a threshold in the rate of depolarization (dV/dt) that is significantly slower ( $p < .0001$ ) than octopus cells. Bushy cells must be depolarized faster than  $3.8 \pm 1.7$  mV/ms (n=12) to fire an action potential, contrasting with  $10 \pm 2.5$  mV/ms (n=12) for octopus cells (Ferragamo and Oertel, J. Neurophys. 87: 2262, 2002). When ramps are applied from a depolarizing or hyperpolarizing holding current, the dV/dt threshold does not change substantially. In bushy cells, as in octopus cells, the rate of depolarization threshold is alleviated in the presence of 66 nM  $\alpha$ -dendrotoxin, so that the cell fires in response to even slow depolarizing current ramps. Stellate cells were confirmed not to have a dV/dt

threshold and fire even in response to very slow depolarizations.

The time to threshold for the slowest suprathreshold current ramp, the time during which the cell must be depolarized to elicit a spike, was defined as the integration window. The integration window was 5 to 10 ms for bushy cells and about 1 ms for octopus cells. Stellate cells have an effectively unlimited integration window, so that their temporal integration will be limited entirely by the decay time of excitatory synaptic inputs.

This work was supported by a grant from the NIH DC 00176.

### **685 Analysis of Mossy Fiber Projections from Brainstem Nuclei to the Cochlear Nucleus in Rats**

Xiping Zhan<sup>1</sup>, Tan Pongstaporn<sup>1</sup>, David K Ryugo<sup>1,2</sup>

<sup>1</sup>Center for Hearing Sciences, Department of Otolaryngology, <sup>2</sup>Department of Neuroscience, School of Medicine, Johns Hopkins University

The dorsal cochlear nucleus (DCN) resembles a cerebellar folium in terms of structural organization, homologous cell types, and kinds of inputs. Afferents to these separate structures can appear as bouton endings or mossy fibers (MFs). We are studying inputs to the cochlear nucleus with light and electron microscopy in order to identify postsynaptic targets. We have injected biotinylated dextran amine into the cuneate nucleus, spinal trigeminal nucleus, pontine nuclei, or lateral reticular nucleus of rats. Animals were histologically processed for analysis after a 4-14 day post-injection survival period. We observed a projection to the granule cell domain (GCD) of the cochlear nucleus from each of these structures. Labeled terminals appeared as small boutons or large lobulated endings called MFs. The synaptic targets of the small bouton endings were cell bodies or dendrites of unidentified neurons. MFs from the cuneate and spinal trigeminal nuclei were closely associated with the terminal dendritic claws of granule cells, and formed many punctate synapses with these dendrites. In contrast, MFs from the pontine nuclei contacted thick dendritic shafts of mitral or unipolar brush cells and formed long undulating synapses. Granule cells project to the DCN but the targets of mitral and unipolar brush cells are unknown. All MFs contained round synaptic vesicles, and the synaptic complexes were loosely ensheathed by glial lamellae. We are working on identifying the other synaptic targets of boutons and MFs, especially from the lateral reticular nucleus. A 3-D analysis of different MFs will be presented. It is our working hypothesis that GCD neurons form distinct functional circuits and receive inputs from MFs of different origins.

Supported by NIH/NIDCD grant DC04593

### **686 Projections of the Spinal Trigeminal Nucleus to the Inferior Colliculus in the Guinea Pig**

Jianxun Zhou<sup>1</sup>, Susan Shore<sup>1</sup>

<sup>1</sup>Kresge Hearing Research Institute, University of Michigan, Ann Arbor, MI 48109

We have previously demonstrated projections from the spinal trigeminal nucleus (Sp5) to the ipsilateral cochlear nucleus (CN) that terminate primarily in the marginal area (Zhou and Shore, *J. Neurosci. Res.*, 2004). To further elucidate the trigeminal-auditory pathways in the guinea pig, we examined Sp5 projections to the inferior colliculus (IC) using retro- and anterograde tracers. We have begun to functionally characterize these pathways by identifying their neurotransmitters. Injections of retrograde tracers into the external nucleus of IC (ICx) resulted in labeled cells primarily in the contralateral Sp5. Anterograde injections into Sp5 resulted in terminal labeling predominately in the contralateral ICx. The terminal distribution exhibited a restricted laminar pattern extending from ventro-medial to dorso-lateral mainly in layer 3 of ICx. The labeled endings in ICx were en passant or small terminal boutons, but not large, irregular swellings which are often observed in the Sp5 projections to CN. Interestingly, the same region of ICx receiving Sp5 projections also received terminal endings from a different anterograde tracer placed in the CN. Preliminary data on localization of neurotransmitters for the Sp5 - ICx pathway revealed double labeling of anterogradely labeled terminal endings in IC with Vesicular Glutamate transporter 1 (VGluT1). VGluT1 accumulates glutamate in synaptic vesicles, and is a prime marker for glutamatergic neurons. These results provide anatomical evidence that the trigeminal projection to ICx may be important in the integration of cross-modal information. This integration could be involved in processing self-produced vocalizations (Tammer et al., *Behav. Brain Res.*, 2004).

Supported by NIH grant 5 R01 DC004825-03 and Tinnitus Research Consortium

### **687 Effect of Inhibitor on Binaural Sensitivity to Noise**

John Agapiou<sup>1</sup>, David McAlpine<sup>1</sup>

<sup>1</sup>University College London

Neurons in the medial superior olive (MSO) receive inputs from both the ipsilateral and contralateral cochlear nuclei and are thought to act as coincidence detectors, firing maximally when ipsilateral and contralateral inputs arrive synchronously. The response of these neurons to interaurally time delayed broadband noise is band-pass-like, with maximal discharge rate evoked at a particular interaural time difference (ITD). This "best ITD" is thought to reflect an internal interaural delay mechanism and has been suggested to arise from differences in the axonal propagation time of signals from the two ears (Jeffress, 1948) or from slight mismatches between the contralateral and ipsilateral cochlear filter delays ("stereausis", Shamma, 1989). Recently however, both of these theories have been challenged by the finding that the internal delay

appears to be determined largely by glycinergic input to the MSO (Brand et al., 2002).

Responses of delay sensitive cells in the inferior colliculus (IC) and dorsal nucleus of the lateral lemniscus (DNLL) were obtained from anaesthetised guinea pigs using a noise stimulus subjected to both interaural time and interaural phase delays (Yin et al., 1987). Analysis of the shape of the envelope of the responses revealed both ITD dependent and ITD independent deviations from a band-pass like response.

A simple model of binaural sensitivity was developed, incorporating the effects of stereausis, monaural nonlinearity, axonal delays and inhibition in MSO. Analytical determination of the response of the model to the noise stimulus revealed that while ITD independent distortions could be explained by monaural nonlinearities, ITD dependent distortions could not be a consequence of either axonal delays or stereausis. The distortion in DNLL was observed to be skew-like, consistent analytically with the reported effects of inhibition in MSO (Brand et al., 2002), while the more complex response patterns in IC were consistent with additional convergence of multiple delay sensitive inputs (McAlpine et al., 1998).

#### References

- Brand A, Behrend O, Marquardt T, McAlpine D, Grothe B (2002) *Nature* 417: 543-547.
- Jeffress LA (1948) *J Comp Physiol Psychol* 41: 35-39.
- McAlpine D, Jiang D, Shackleton TM, Palmer AR (1998) *J Neurosci* 18: 6026-39.
- Shamma SA, Shen NM, Gopalaswamy P (1989) *J Acoust Soc Am* 86: 989-1006.
- Yin TC, Chan JC, Carney LH (1987) *J Neurophysiol* 58: 562-83.

### **688** Olivary and Extra-olivary Sources of Cholinergic Input to the Cochlear Nucleus

Susan D. Motts<sup>1</sup>, Brett R. Schofield<sup>1</sup>

<sup>1</sup>*U. of Louisville*

The cochlear nucleus (CN) has a well-known cholinergic input that acts on a variety of cell types in the dorsal and ventral CN. The source of this cholinergic input has been examined in a single study done in rats (Sherriff and Henderson, 1994, *Neurosci.* 58:627-33). The source comprises two groups of cells in the superior olivary complex (SOC): olivocochlear cells, whose axons provide collaterals to the CN, and other SOC cells that project to the CN but not to the cochlea. The presence of olivocochlear collateral projections to the CN has now been shown in several species, but little is known about other possible cholinergic inputs. We combined retrograde tracing with immunohistochemistry for choline acetyltransferase (ChAT; a synthetic enzyme for acetylcholine and a specific marker of cholinergic cells) to identify the sources of cholinergic inputs to the CN in guinea pigs.

We injected Fast Blue or red fluorescent beads into the CN. After time for transport, the brain was fixed by perfusion (4% paraformaldehyde) and processed to mark cholinergic cells with green immunofluorescence (goat

anti-ChAT [Chemicon AB144P] followed by biotinylated rabbit anti-goat and AlexaFluor 488 streptavidin). Double-labeled cells (containing tracer and immunofluorescence) were observed bilaterally in the ventral nucleus of the trapezoid body in the SOC. Additional double-labeled cells were located outside the superior olivary complex in the pedunclopontine tegmental nucleus (PPT) and the laterodorsal tegmental nucleus (LDT). Cells in these nuclei were located predominantly on the ipsilateral side, and on both sides were more numerous in the PPT than in the LDT.

The PPT and LDT constitute the pontomesencephalic cholinergic nuclei and are well known for projections to thalamus and many brainstem nuclei. They are components of the ascending reticular activating system and play an important role in arousal and sleep/wake cycles. They have not previously been identified as sources of projection to the CN. It seems likely that projections from these nuclei could modulate responses of CN cells to acoustic stimuli, perhaps in accord with general levels of arousal. It will be important in future studies to consider the projections from these nuclei when discussing the possible roles of cholinergic inputs to the CN.

Supported by NIH DC04391.

### **689** The Central Gray and the Inferior Colliculus: An Auditory-Limbic Interface.

David T. Larue<sup>1</sup>, Jorge J. Prieto<sup>2</sup>, Jeffery A. Winer<sup>1</sup>

<sup>1</sup>*University of California at Berkeley, Berkeley, California,*

<sup>2</sup>*University Miguel Hernández, Alicante, Spain*

Studies of the corticotectal and tectothalamic projections have shown that the auditory midbrain has important relations with the limbic system. Anterograde tracer deposits in cat insular and temporal limbic-related auditory association cortex label the CG near the IC (Winer et al., *J. Comp. Neurol.* 400:147-174; 1998). In the rat, cortical areas Te2 and Te3 project to the same region (Arnault and Roger, *J. Comp. Neurol.* 302:110-123; 1990).

We now report that WGA-HRP or BDA deposits in the cat and rat inferior colliculus (IC) label both axons and neurons in the dorsolateral central gray (CG). Small HRP injections in the mustached bat (Wenstrup, Winer and Larue, unpublished observations) and the mouse (Frisina et al., *J. Acoust. Soc.* 101:2741-2753; 1996) produce a similar labeling pattern. A projection from the amygdala to the IC is further evidence of an auditory midbrain-limbic relationship (Marsh et al., *J. Neurosci.* 22:10449-10460; 2002).

The cat and rat have three similar types of CG neurons projecting to the IC: small neurons (~6 µm in diameter), medium-sized (~8 µm) spindle-shaped cells with bipolar dendrites, and large multipolar cells (~10 µm) with vertical dendritic fields. Labeled cells cluster in dorsolateral CG and are sparse elsewhere. Afferent axons range from 0.5–3 µm thick; some are beaded while others are smooth. Some travel in the commissure of the IC; others cross the IC directly. Axons ~0.8 µm thick can be followed almost to the aqueduct. The projection is reciprocal, with axons often labeled near filled neurons. The projection is

heaviest ipsilaterally, but axons ring the entire CG and occasional contralateral somata are labeled.

The dorsolateral CG may be a limbic target mediating autonomic reflexes from novel or biologically significant acoustic stimuli. The limbic-affiliated cortical input suggests a cortico-tectal-central gray circuit modulating autonomic responses triggered by sound.

Supported by USPHS grant R01DC02319-25.

### **690 Involvement of Ephrins and Eph Receptors in Establishing Early Pattern Formation in the Auditory Midbrain**

**Mark Gabriele<sup>1</sup>, Jaime Robenolt<sup>1</sup>, Amanda Laz<sup>1</sup>, C. David Jaynes<sup>1</sup>**

<sup>1</sup>*James Madison University*

Eph receptors constitute the largest known family of receptor tyrosine kinases. Together with their corresponding ligands, the ephrins, this family of molecules is thought to oversee several processes that are essential for establishing order in the developing nervous system (e.g. cell migration, axonal pathfinding, and axonal pattern formation within selected targets). The present study focused on the auditory midbrain, or inferior colliculus (IC). The inferior colliculus is an important site of convergence for numerous ascending and descending projections arising from the auditory brainstem and cortex. Most of the inputs to the central nucleus of the IC are highly ordered and organized into patterns of afferent bands or patches. Previous findings in our laboratory have shown that this precise pattern formation, while absent at birth, appears gradually over the first postnatal week and is well established by the onset of hearing (postnatal day 12 in rat). The present study began to explore the hypothesis that Eph/ephrin interactions are in part responsible for the described early pattern formation. Immunocytochemistry was utilized to determine whether certain members of the Eph/ephrin family (ephrin-B2, B3, A5, and EphA4) are expressed during this critical period. Preliminary findings suggest that ephrin-B3 may serve to demarcate compartmental boundaries of the central nucleus during early inferior collicular development.

### **691 Correlates of Binaural Masking Level Difference measured in High Frequency Neurons in Cats and Owls**

**Frank Endler<sup>1</sup>, Dina Farkas<sup>2</sup>, Ali Asadollahi<sup>1</sup>, Israel Nelken<sup>2</sup>, Hermann Wagner<sup>1</sup>**

<sup>1</sup>*Institute for Biology II, RWTH Aachen University,* <sup>2</sup>*The Alexander Silberman Institute of Life Sciences, Hebrew University*

In humans, threshold for detecting a tone within a masking noise decreases about 12-15dB when either the tone or the noise is inverted in one ear (binaural masking level difference, BMLD). We studied correlates of BMLD in two model systems of auditory processing, cats and barn owls. Whereas BMLD in mammals was thought to be restricted to low frequencies (presumably because of failure of phase locking), barn owls show phase locking and sensitivity to interaural time difference (ITD) in high

frequencies. We have therefore hypothesized that barn owls should show BMLD in high frequencies as well. With a special stimulus called the 'transposed stimulus', constructed by multiplying a high-frequency carrier by a low-frequency envelope simulating the firing of auditory nerve fibers, humans also show exquisite ITD sensitivity in high frequencies. The neuronal correlates of BMLD in high-frequency neurons, were studied in the primary auditory cortex (A1) of cats and in the inferior colliculus (IC) of barn owls. IC neurons sensitive to ITD showed influence of the tone phase on the detection threshold of a tone stimulus presented together with a masking noise of constant loudness at the best noise ITD (54 neurons, 37% had positive BMLDs, 45% negative and 18% no influence). These data demonstrate for the first time that BMLD is present in high-frequency neurons of the barn owl's IC. In cat A1, ITD sensitivity was present in high-frequency neurons (6-13 kHz) when using transposed stimuli. Best ITDs were in the physiological range, and tuning width could be less than 200  $\mu$ s, even when the modulator frequency was 64 or 128 Hz. BMLD was present as well, and was often expressed by changes in firing patterns.

### **692 Thalamic Origin of Descending Axons that Project to Olivocochlear Neurons in the Gerbil**

**Nobuyuki Kuwabara<sup>1</sup>**

<sup>1</sup>*Anatomical Sci. and Neurobiol., University of Louisville Sch. of Med., Louisville, KY*

Direct descending projections from neurons in the medial geniculate body (MGB) to the olivocochlear (OC) neurons were demonstrated previously (Kuwabara et al., '03, ARO Abstr., 27:87). Olivocochlear cells are also known to receive projections from inferior colliculus (IC), which in turn receives descending projections from the upstream MGB (Kuwabara and Zook, '00, Brain Res. 878:79-87; Winer et al., '02, Hear. Res. 168:181-195). In this study retrograde prelabeling technique was combined with anterograde axonal labeling in uniquely cut slices to examine whether IC-projecting MGB cells project further to OC cells.

Olivocochlear neurons of the gerbil were prelabeled using a retrograde tracer (Fluoro-Gold, Fluorescein-conjugated Cholera Toxin-B subunit or HRP) injected in the cochlea. Inferior colliculus was also given a large injection of Fluoro-Gold or fast blue to prelabel MGB cells that have descending axons. Angled parasagittal brain slices were subsequently made. These slices contained ipsilateral auditory cell groups at the level ranging from the thalamus to the lower brainstem that had prelabeled OC cells. The anterograde marker biocytin was focally injected with visual guidance into the area of the MGB that exhibited prelabeled cells in these slices.

Biocytin-labeled axons with terminals and *en passant* varicosities were found in close apposition to the cell body and proximal dendrites of prelabeled OC neurons. Some of the observed axons were the collaterals of those projecting to the IC. The area of MGB that contained both the prelabeled IC-bound cells and the cells that projected to OC cells included the medial and approximately half of

the dorsal divisions. The ventral third of the ventral division, which also exhibited prelabeled cells after IC injection, did not show descending axons projecting to OC cells. These results suggest that there are distinct populations of MGB cells that project to IC cells, OC cells or both.

(Supported by NSF-IBN9987660)

### **693 Interaural Level Differences Shift Interaural Time Difference Sensitivity in the Inferior Colliculus Consistent with Changes in Auditory Nerve Phase Locking**

Liangfa Liu<sup>1</sup>, Trevor Shackleton<sup>1</sup>, Alan Palmer<sup>1</sup>

<sup>1</sup>MRC Institute of Hearing Research, Nottingham, UK

In both the squirrel monkey and cat, the response phase of auditory nerve fibres (ANFs) at low frequencies, where the activity is phase-locked to the stimulus waveform, is level dependant: for frequencies above and below the characteristic frequency there are progressive phase leads and lags as the sound level is increased. These phase locked spikes are transmitted to the medial superior olive (MSO), where cells fire most vigorously when there are coincident spikes from both left and right ears. It has been shown that interaural level differences cause shifts in the interaural phase that produces maximum activity (best phase: BP) of the coincidence detectors, presumably as a result of the level dependence of the ANF responses. However, the relation of the signals to the neurones best frequency was not very clear. We measured interaural phase difference sensitivity of 72 cells in the inferior colliculus of the anaesthetised guinea pig as a function of frequency and interaural level difference. We fixed the level of a contralateral tone at 20 or 30 dB re threshold and varied the level of the ipsilateral tone in 10 or 15 dB steps above and below this level. For all units there was a "null" frequency (not necessarily the best frequency) where this made no difference to the ITD curves. For 28/41 units which showed some effect, for frequencies below the null frequency, BP moved more contralaterally with increase in the ILD (i.e. contra more intense). Above the null frequency BP moved ipsilaterally with increasing ILD. For the remaining 13/41 these changes in BP were reversed. The changes in BP were maximally about 0.2 cycles. Preliminary results suggest that changes in response phase with level in ANFs are in the same direction and magnitude as the binaural effects.

### **694 The Representation of Sound Frequency in the Primate Inferior Colliculus.**

Uri Werner-Reiss<sup>1</sup>, Nathaniel Greene<sup>1</sup>, Abigail Underhill<sup>1</sup>, Ryan Metzger<sup>1</sup>, Jennifer Groh<sup>1</sup>

<sup>1</sup>Dartmouth College

Previous studies in numerous species have demonstrated that the inferior colliculus (IC) contains a topographically-organized representation of sound frequency, but comparatively little is known about the representation of sound frequency in primates. Information regarding this representation is critical for understanding IC function, and will be useful for cross-species comparisons.

We assessed the sensitivity of IC neurons to tones of different frequencies in two awake rhesus monkeys. Our aim was to determine the population profile of IC activity as a function of sound frequency, for sounds at a fixed intensity (53 dB SPL). Electrodes entered the IC at an angle of 33 deg. lateral from vertical in the coronal plane, and multiunit activity was assessed every 500 microns. Experiments were conducted in a single-walled sound attenuation chamber, and sounds were delivered from a loudspeaker located in the contralateral hemifield.

We found that low frequency tones activated multiunit clusters throughout the IC and at all depths, whereas high frequency sounds activated primarily multiunit clusters at deeper (more ventral) depths. Bandwidth increased with recording depth as well. In short, high frequency sounds activated a smaller population of neurons than did low frequency sounds, and these high-frequency responsive neurons were located at more ventral locations. Although neural clusters at ventral locations were more likely to respond to high frequency sounds than were neural clusters at shallower depths, the ventral neurons also responded to low frequency sounds, and we did not find a correlation between recording depth and "best" frequency at this fixed sound intensity.

These findings are consistent with a previous study from the IC of rhesus monkeys (Ryan and Miller, J. Neurophysiol. 1978) which showed a preponderance of sensitivity to low frequencies. Our results are also consistent with a previous study in *Macaca fascicularis* monkeys (Webster et al., Exp. Brain Res. 1984), which showed that high frequency sounds activated the ventral region of the IC. Taken together, our results clearly support the view that sound frequency information is organized topographically in the IC, with higher frequency sounds preferentially activating neurons at more ventral locations (Zwiers et al., J. Neurosci., 2004).

### **695 Competitive Interaction Shapes Development of Afferent Segregation in Banded Projections from the Dorsal Nucleus of the Lateral Lemniscus to the Inferior Colliculus**

Samuel Franklin<sup>1</sup>, Judy K. Brunso-Bechtold<sup>1</sup>, Craig K. Henkel<sup>1</sup>

<sup>1</sup>Wake Forest University School of Medicine, Department of Neurobiology and Anatomy

In the central nucleus of the inferior colliculus (IC) inputs from multiple hindbrain auditory nuclei converge with other inputs to form interdigitating bands. The segregation of bands reflects specific combinations of afferent inputs or synaptic domains that determine complex response properties of IC neurons. We hypothesize that afferent bands from the dorsal nucleus of the lateral lemniscus (DNLL) develop in the IC through competitive interactions. Unilateral cochlear ablation (UCA) creates an imbalance of spontaneous activity generated by the cochlea. A previous study (Gabriele et al., 2000, J. Neurosci. 20:6939-6949) showed that the pattern of afferent DNLL bands in IC was disrupted after early UCA. To address the possibility that disruption of band development by UCA was related to



deafferentation resulting from cell loss in auditory hindbrain nuclei, experiments were undertaken in which UCA was performed after the sensitive period for cell death. After 3 days survival, brains were fixed and DNLL projections were labeled by placing glass pins coated with the carbocyanine dye, Dil in the DNLL commissure. In control cases, labeled DNLL inputs segregated into bands in both ICs. After late UCA, cochlear nucleus volume measurements indicated less than 30% atrophy which was significantly less shrinkage than after early UCA. Also, the density of labeled cells in the left and right DNLL was symmetric after late UCA in contrast to the asymmetric density observed after early UCA. In the IC contralateral to the UCA, the intensity of Dil label was markedly reduced but bands were clearly preserved. In the IC ipsilateral to UCA, the intensity of Dil label was as great as or greater than control cases but there was no regular pattern of alternating bands. The results confirm earlier findings that segregation of afferent inputs into bands in developing IC is disrupted by UCA and suggest that this plasticity is dependent on an imbalance of spontaneously active inputs to the IC and not simply on sprouting that fills deafferented synaptic space.

Supported by NIH grant DC04412

### **696** Population Coding of Sound Level Depends on Stimulus Statistics

Isabel Dean<sup>1</sup>, David McAlpine<sup>1</sup>, Nicol Harper<sup>1</sup>

<sup>1</sup>University College London

The auditory system accurately codes sound levels ranging from those that move the basilar membrane by only a fraction of the width of an atom, up to levels 10<sup>12</sup>-fold greater. How auditory neurons code this range of levels is unknown; neural discharge rates tend to vary with level over only a limited portion of the full range of hearing. We tested whether neurons alter their tuning to sound level according to the statistics of the stimulus, so as to improve the coding accuracy of the neural population for different stimulus distributions.

Extracellular recordings were made from 54 single neurons in the inferior colliculi of anaesthetised guinea pigs. Diotic white noise stimuli were presented continuously for 5s; every 50ms, the level was randomly selected from a defined distribution. 75 stimulus iterations were presented in rapid succession. The full range of levels presented was 21-96dB SPL. The level distribution consisted of one or more regions of more probable levels, from which levels were selected with 0.8 probability.

We found that neural rate-level functions adjust according to the statistics of the stimulus. Increasing the mean level caused rate-level functions to shift along the level axis. Using point estimation theory, we examined whether the neural population code for sound level improved with the changes in rate-level functions. The changes in tuning altered the range of levels most accurately coded by the neural population: the point of highest accuracy lay just above the mean level, and levels just above the mean level of a given stimulus were coded best by tuning curves adjusted to that stimulus. Extending the range of level fluctuations also caused rate-level functions to change,

such that the range of levels most accurately coded by the neural population was extended. Lastly, for bimodal level distributions, the population code adjusted so as to improve coding accuracy at levels just above the midpoint of both peaks in the stimulus distribution.

### **697** Neuronal Response Characteristics in the Inferior Colliculus of the Awake Ferret

Peter Marvit<sup>1</sup>, Heather Dobbins<sup>1</sup>, Yadong Ji<sup>1</sup>, Barak Shectter<sup>1</sup>, Didier Depireux<sup>1</sup>

<sup>1</sup>U. Maryland, Baltimore

Much of what is known about the neuronal response of inferior colliculus (IC) comes from anesthetized preparations; however, it is unclear to what extent the effects of anesthesia change the response properties. We report here on the first in a series of experiments characterizing IC neurons in the awake ferret--an auditory generalist. Classical stimuli (pure tones, clicks, and AM tones) and dynamic ripples were presented to the animal in order to compute response measures and derive spectro-temporal receptive fields (STRFs). With these measures, we assess the degrees of linearity in the neuronal response and identify possible sub-populations amongst the sample set. We compare and contrast our results with those obtained from anesthetized ferrets, and with relevant studies in other species.

### **698** Addition of Harmonic Complexity Increases Response Selectivity for Features of Periodic Frequency Modulated Stimuli in the Inferior Colliculus

Wm. Owen Brimijoin<sup>1</sup>, William O'Neill<sup>1</sup>

<sup>1</sup>University of Rochester

The filter properties of auditory neurons are typically described in terms of simple signals and this leads to the conclusion that selectivity for sounds is largely dependent on the amount of energy around a neuron's best frequency. We demonstrate that energy outside the standard response area is intimately involved in selectivity for complex sounds. We recorded complete data sets from 29 single units in the IC of the mustached bat. We generated mono- and multi-harmonic sets of 12 sinusoidally frequency modulated stimuli based on a prototype that decreased geometrically in modulation bandwidth from 60 ± 7.44 kHz to 60 ± 0.0036 kHz and included an unmodulated endpoint (60 ± 0 kHz). The endpoints of the multi-harmonic synthetic continuum were modeled after two mustached bat social vocalizations described by Kanwal et al (1994). Both sets of stimuli were tailored to the BEF of the unit and presented at MT+20 dB. We quantified total spikes and phase locked activity in response to the two stimulus sets. Responses to both sets were categorized as having low-, band-, high- and all-pass response profiles with respect to modulation bandwidth. With respect to total spikes, three systematic differences in the responses to the mono- versus multi-harmonic stimulus sets were observed. First; mono-harmonic stimuli tended to evoke a greater number of spikes than the multi-harmonic set in the majority of units (79%). Second; the

modulation bandwidth that evoked the maximal response was smaller for the multi-harmonic set than for the mono-harmonic set in all but one unit. Third; excluding units suppressed completely by the multi-harmonic stimulus, most (78%) units with band-pass response profiles responded to a narrower range of modulation bandwidths in the multi-harmonic set than in the mono-harmonic set. Correspondingly, units with low- or high-pass response profiles tended to have lower and higher modulation cutoff points respectively or became band-pass (78%). With respect to phase-locked activity, apart from those effects related to response suppression, we did not observe systematic differences in the responses to mono- versus multi-harmonic stimulus sets. We conclude that the addition of multiple harmonics in synthetic communication sounds serves to increase the selectivity of IC units to particular dimensions of those sounds.

### **699 Multiple Low-Frequency Inputs to Combination-Sensitive Neurons as Recorded by Single- and Multi-Channel Electrodes from the Mustached Bat Inferior Colliculus.**

**Kianoush Sheykhosslami<sup>1,2</sup>, Donald Gans<sup>2</sup>, Jeff Wenstrup<sup>2</sup>**

<sup>1</sup>Case Western Reserve University, <sup>2</sup>Northeastern Ohio Universities College of Medicine

Combination-sensitive neurons respond to the combination of temporally and spectrally distinct components of the mustached bat's sonar or social vocalizations. This study examines the presence of multiple low frequency bands with distinct combinatorial interactions. Well-isolated single units were recorded with micropipettes, while multi-unit responses were obtained using 16-channel linear electrode arrays (Michigan) with 50 or 100  $\mu\text{m}$  spacing between recording sites. Of 84 single units from 58-112 kHz representations of the inferior colliculus (IC), 40.3% display an excitatory response to low-frequency sounds tuned in the range of the fundamental biosonar (23-30 kHz, 15.8%) or sub-sonar (10-22 kHz, 24.5%) components. We reported previously that sub-sonar low frequency sounds inhibit a unit's best high frequency response for the duration of the low-frequency tone (tonic inhibition). Of 84 combination sensitive neurons, 30% show dual combination sensitivity patterns that include tonic inhibition at sub-sonar frequencies and either phasic inhibition (15.5%) or facilitation (14.5%) at fundamental biosonar frequencies. Multi-channel recordings from 50% of 26 penetrations show similar multiple low frequency sensitivities. For these penetrations, 57% of recording sites showed this multi-low frequency response. Frequency response curves, as well as combinatorial properties, indicate that tuned responses to both low frequency bands are functionally distinct. Other work suggests that the origin of these low frequency responses is different. Responses tuned to 23-30 kHz originate in nuclei of the lateral lemniscus and IC, while responses in the 10-22 kHz range are present in the cochlear nucleus. The data further suggest that multi-channel recordings can reproduce many of the complex responses observed in

single unit recordings, and further suggest that multi-low frequency responses may be clustered within the IC.

Supported by RO1 DC00937 from NIDCD.

### **700 Auditory Interhemispheric Transfer in Patients with Congenital Abnormalities of the Commissural Pathways Due to a PAX6 Mutation.**

**Doris-Eva Bamiou<sup>1</sup>, Frank E. Musiek<sup>2</sup>, Sanjay Sisodiya<sup>3</sup>, Samantha Free<sup>3</sup>, Anthony Moore<sup>4</sup>, Veronica van Heyningen<sup>5</sup>, Linda Luxon<sup>1</sup>**

<sup>1</sup>National Hospital for Neurology and Neurosurgery, London, <sup>2</sup>Communication Sciences, University of Connecticut, <sup>3</sup>Department of Clinical and Experimental Epilepsy, Institute of Neurology, UCL, <sup>4</sup>Institute of Ophthalmology, and Moorfields Eye Hospital, London, <sup>5</sup>MRC Human Genetics Unit, Edinburgh

PAX6 encodes a transcriptional regulator that is essential for brain morphogenesis. Patients with a heterozygous PAX6 mutation have absent or hypoplastic anterior commissure and may have a reduced size corpus callosum. Both these formations contain auditory interhemispheric fibers.

We assessed central auditory function in 8 patients with a PAX6 mutation and 8 age- and sex-matched controls. Brain MRI results were available for all PAX6 subjects. Subjects and controls had baseline audiometric tests, and central auditory tests, which included the dichotic digits, rhyme and CVs, frequency and duration pattern, and a Gap in Noise tests.

The anterior commissure was absent in 5 and hypoplastic in 1 subject. The callosal area was reduced in 3 subjects. All subjects and controls had normal peripheral hearing. The PAX6 group had a greater left ear deficit in the dichotic digit and the dichotic CVs tests and a greater right ear advantage in the dichotic rhyme test than controls ( $p < 0.05$ ). The PAX6 group gave worse scores than the control group in the frequency and duration pattern tests ( $p < 0.05$ ). The Gap in Noise test results were similar in patients and controls.

The PAX6 group had significantly worse results in tests that require interhemispheric transfer (dichotic speech and pattern tests) than the control group, but similar results in the Gap in Noise test, which does not require such transfer. Our results may reflect deficient auditory interhemispheric transfer in the PAX6 group. The profile in the PAX6 group was very similar, albeit less severe, than the profile of patients who have undergone surgical section of the corpus callosum. This profile could be attributed to the absence/aplasia of the anterior commissure and/or deficiency of the corpus callosum, although other subtler abnormalities of the central auditory pathway, undetected by MRI may also have contributed to our findings.

## **701** Tone Frequency Maps and Receptive Fields in Developing Chinchilla Auditory Cortex

Martin Pienkowski<sup>1</sup>, Robert Harrison<sup>1,2</sup>

<sup>1</sup>Auditory Science Laboratory, The Hospital for Sick Children, <sup>2</sup>Department of Physiology & IBBME, University of Toronto

Neurons in sensory/motor pathways typically respond preferentially to particular stimulus features (or motor commands); examples in hearing are sound frequency, amplitude and frequency modulation rate, location of the sound source, even complex fragments of species-specific vocalizations. The basis for such 'feature extraction' is often a precise spatial map, whose component units are selective for some (narrow) part of the stimulus feature range. How are precise (i.e., highly ordered) spatial maps established? To what extent does their development proceed under genetic control (via chemoaffinity, etc.), before being consolidated by patterned neural activity? Also, what can be consolidated by spontaneous activity (e.g., afferent bursting; loop oscillations), and what requires input from the external (acoustic) environment? There is growing evidence, for instance, that the representation of visual space in cortex (retinotopic map) requires waves of spontaneous bursts across retinal ganglion cells. In the auditory system, such bursts have also been observed during early development, but their role in tonotopic map refinement remains unclear.

In this study, single-unit responses to tone pip stimuli were isolated from numerous microelectrode penetrations of auditory cortex in the anesthetized, developing chinchilla (*Ianiger*), a precocious rodent. Hearing sensitivity and spike firing rates were high (mature) in the youngest age group tested (P2-P4). Significantly, tonotopic organization in the core primary areas was well-ordered (mature), and neurons were sharply tuned in these near-newborn animals. Thus, the refinement of diffuse tonotopic projections to chinchilla auditory cortex appears to occur in utero, where external (and maternal) sounds are considerably attenuated, and may not contribute significantly to the mechanisms involved. On the other hand, tonal receptive fields steadily increased in 'complexity' to adulthood (at least past P30); here complexity was defined as spectral-temporal integration across distinct tonotopic channels. This integration may take place subcortically (e.g. thalamocortically), or via lateral connections between cortical columns, or both. The increasing complexity may reflect the emergence of selectivity, for example, for the 'harmonic stacks' and 'frequency glides' which recur most frequently in the repertoire of chinchilla calls; this hypothesis requires further testing.

## **702** Perceptual Learning and Top-Down Influences in Auditory Cortex Plasticity

Daniel Polley<sup>1</sup>, Elizabeth Steinberg<sup>2</sup>, Michael Merzenich<sup>3</sup>

<sup>1</sup>Keck Center for Integrative Neuroscience, University of California San Francisco, <sup>2</sup>Columbia University, <sup>3</sup>University of California, San Francisco

Previous work has shown that the neural encoding of sound frequency, intensity, and modulation rate in the adult primary auditory cortex (AI) can be reorganized through perceptual learning processes. Although plasticity can occur independently in each of these representational domains, it is unclear whether functional reorganization in adult AI primarily reflects a bottom-up process in which the statistics of sensory inputs drive reorganization or top-down process in which cognitive factors such as attention and task demands influence the direction and domain of functional reorganization. In the present experiment, adult rats were trained in either a sound intensity or sound frequency recognition task. Importantly, the sensory stimuli for both tasks were an identical set of tone pips that varied independently in intensity and frequency. Thus, rats were trained with an identical sensory stimulus set but their attention was drawn to completely separable features of those stimuli.

High-density mapping of frequency and intensity tuning in AI and ventral auditory field performed at the conclusion of training revealed dissociable forms of plasticity that were specific to the demands of the perceptual learning task. In frequency-trained rats the area of the tonotopic map with CF values at or near the target frequency was 13.3% greater than naïve control rats ( $p < 0.05$ ). The representational area of the same frequencies in intensity-trained rats was not significantly different than naïve controls. Examination of the intensity tuning profiles from the same recording sites reveals the opposite relationship. In intensity-trained rats we observed a 20.7% increase in the percentage of recording sites that were most effectively driven by sound levels at or near the target intensity compared to naïve controls ( $p < 0.001$ ). The percentage of recording sites most responsive to the target intensity in frequency-trained rats was not different from naïve controls. Therefore, top-down factors such as attention and task demands can strongly influence the expression of plasticity in the adult auditory cortex.

## **703** Cortical Representation of Hearing Restoration in Patients with Sudden Deafness

Mikio Suzuki<sup>1</sup>, Hideaki Kouzaki<sup>1</sup>, Takeshi Shimizu<sup>1</sup>, Hiroya Kitano<sup>2</sup>

<sup>1</sup>Shiga University of Medical Science, <sup>2</sup>Tottori University

Normally, unilateral auditory stimulation produces activation predominantly in the contralateral auditory cortex (cross projection). The few reports characterizing auditory brain activation in patients with hearing loss suggest a degree of plasticity in the adult auditory cortex. In animals, such plasticity has been observed within 6 h after inner ear ablation. To characterize brain activity in response to auditory stimuli during recovery from acute hearing loss, functional magnetic resonance imaging was

performed at two time points in 11 patients with sudden deafness in the right ear, and 10 subjects with normal hearing. In the acute phase, right-ear auditory stimulation induced only a small response in the auditory cortex, limited to the left hemisphere. In the recovery phase, the auditory response was more extensive than in the acute phase. Stimulation of the left ear induced a more extensive response in the left than right hemisphere in both acute and recovery phases, which differed from the pattern in normal subjects. Alteration of cortical response in deafness occurs earlier than suggested by previous reports.

#### **704 Binaural Interaction in the Auditory Cortex of Patients with Adult-Onset Unilateral Sensorineural Hearing Loss**

**Ken-ichi Kaneko**<sup>1,2</sup>, Hanna Renvall<sup>2</sup>, Juha-Pekka Vasama<sup>3</sup>, Nobuya Fujiki<sup>4</sup>, Riitta Hari<sup>2</sup>

<sup>1</sup>Department of Otolaryngology, Fukui Red Cross Hospital, 2-4-1Tsukimi, Fukui, Japan, <sup>2</sup>Low Temperature Laboratory, Helsinki University of Technology, Otakaari3A, Espoo, Finland, <sup>3</sup>Department of Otorhinolaryngology, Tampere University Hospital, Tampere, Finland, <sup>4</sup>Department of Otolaryngology, Otsu Red Cross Hospital, 1-1-35Nagara, Otsu, Japan

Adult-onset unilateral hearing loss causes imbalance of inputs between the two ears and may change responses of the central auditory pathways. We examined unilateral sensorineural hearing-impaired patients to evaluate binaural interaction in the central auditory pathways. We applied frequency-tagging of magnetoencephalographic (MEG) signals, recently introduced as a new tool to study binaural interaction in the human auditory pathways (Fujiki et al., 2002). We measured 8 patients suffering from moderate adult-onset unilateral sensorineural hearing loss and 8 normal-hearing controls. Cortical steady-state fields (SSFs) to binaural and monaural amplitude-modulated sounds (carrier frequency 1 kHz) were measured with a 306-channel whole-scalp neuromagnetometer. The modulation frequencies were 39.1 Hz for the right ear and 41.1 Hz for the left. In control subjects, responses to binaural stimuli were suppressed more in the ipsilateral than the contralateral hemisphere when the stimulus loudness for both ears was equal, but no such hemispheric differences were observed when the stimulus loudness was different between ears. In patients, binaural suppression was stronger in the ipsilateral than the contralateral hemisphere for intact-ear input, even when the loudness between ears was different, while for impaired-ear input there was no significant difference between hemispheres when the stimulus loudness was equal. Binaural suppression differed in the hearing-impaired patients compared with normal-hearing control subjects, likely reflecting plastic changes in the auditory pathways of patients with moderate unilateral hearing loss.

#### **705 Changes in NMDA and Arc Gene Expression in Auditory Cortex During Auditory Learning**

**Richard Salvi**<sup>1</sup>, Wei Sun<sup>1</sup>, Eduardo Mercado III<sup>1</sup>, Ping Wang<sup>1</sup>, Xiaojun Shan<sup>1</sup>, Te-Chung Lee<sup>1</sup>

<sup>1</sup>University at Buffalo

During development, the auditory cortex goes through critical periods in which experience strongly influences cortical function and structure. For example, exposure to continuous noise impedes the segregation and functional development of rat auditory cortex; however, normal cortical segregation and function can be restored if older rats are returned to an acoustically rich environment. During development, changes in the response properties of neurons in auditory cortex are correlated with changes in the distribution of NMDA receptors NR2A and NR2B. NR2A mRNA expression is initially weak, but progressively increases during development whereas NR2B mRNA levels are high throughout development, but decline in adulthood. Since NR2A and NR2B receptors are thought to play important roles in learning and memory, we hypothesized that mRNA expression levels of NR2A and NR2B would change significantly when adult rats learned to discriminate novel auditory stimuli. To test this hypothesis, we evaluated 3 groups (6/group) of rats, Naïve (N), Short-Term Trained (STT) and Long-Term Trained (LTT). Food restricted rats were placed in operant chambers equipped with a nose-poke to initiate a trial, and 2 response levers to signal if they heard a low-frequency click train (right lever) or a high-frequency tone (left lever). LTT (14 sessions) rats discriminated clicks from tones at better than 90% accuracy whereas the accuracy of STT (3 sessions) rats was ~80%. N rats were simply placed in the chamber and given free access to food. Afterwards, the auditory cortex (AC) was removed and the tissue prepared for quantitative RTPCR to determine the relative change in gene expression of NR2A and NR2B, Arc and Homer 1-A genes compared to beta-actin. Western blotting was performed to determine protein expression. NMDA receptor 2A and 2B gene expression and protein levels decreased significantly as auditory discrimination improved whereas expression of Arc, an immediate early gene involved in memory stabilization, increased. Homer-1A, an immediate early gene that modulates glutamate receptor function, showed a slight increase in expression with increase in auditory learning; however, the change was not statistically significant. These results suggest that changes in NMDA receptors 2A and 2B and Arc enhance experience-dependent cortical remodeling and auditory learning. (Supported by NIH grants P01 DC03600-01A1, R01 DC06630-01 & NIH K01 MH067952-02)

#### **706 Effects of Maternal Experience on Auditory Cortical Responses to Pup Calls in Mice**

**Robert C. Liu**<sup>1,2</sup>, Christoph E. Schreiner<sup>3</sup>

<sup>1</sup>UCSF Depts. of Otolaryngology and Physiology, <sup>2</sup>Emory Dept. of Biology, <sup>3</sup>UCSF Dept. of Otolaryngology

A communicative stimulus carries varying levels of behavioral significance for different individuals, depending

on one's experience with that sound and its source. For example, a baby's cry can make a stronger impression on a mother worried about her infant, compared to a nulliparous female who does not have these concerns. How do such behavioral distinctions manifest in the underlying neural activity? One possibility is that early sensory processing is similar in these two individuals, but that subsequent neural stations diverge in their coding to support separate behavioral contingencies. We use the mouse communication system to investigate this at the level of the auditory cortex.

Isolated mouse pups emit ultrasonic whistles that elicit maternal searches and retrievals. The behavioral significance of the pup call differs for mothers and nulliparous, pup-naive females: the former prefer the calls to non-communicative sounds, while the latter do not (Ehret et al, 1987). Do auditory responses to calls differ for the two animal groups? We explored this in ketamine and medetomidine anesthetized CBA/CaJ female mice that had either recently weaned their pups (mothers) or had no pup-rearing experience (naive). We compared auditory cortical responses to various pup calls around the typical frequency and duration of 64 kHz and 50 ms. Significant differences in both spike count and timing among the population responses are evident, especially among neurons with characteristic frequencies in the ultrasound range. These coding changes may facilitate the processing of pup calls as behaviorally significant. Future work can explore whether pup experience alone or hormones are responsible for these differences.

Supported by NIDCD, and the Sloan and Swartz Foundations.

### **707 Long-Term Cortical Plasticity Evoked by Electric Stimulation and Acetylcholine Applied to the Auditory Cortex**

**Xiaofeng Ma<sup>1</sup>**, Nobuo Suga<sup>1</sup>

<sup>1</sup>*Department of Biology, Washington University in St. Louis, MO 63130*

Reorganization of the frequency map in the central auditory system is based on best frequency (BF) shifts of auditory neurons. In the big brown bat, conditioning with acoustic stimulation followed by electric leg-stimulation causes short-term collicular and long-term cortical BF shifts. These BF shifts can also be evoked by a 30-min-long focal electric stimulation of the auditory cortex (ESa). They are basically the same as those evoked by conditioning. However, the cortical BF shift is short-term. This short-term cortical BF shift becomes long-term as ESa is combined with electric stimulation of the cholinergic basal forebrain. These findings indicate that the BF shifts are evoked by the cortical neural net and corticofugal feedback, not by the association of auditory and somatosensory stimuli in the medial division of the medial geniculate body (MGBm), and that acetylcholine play an essential role in augmenting and maintaining the cortical BF shift. Therefore, we studied whether the long-term cortical BF shift (plastic change) can be evoked by electric stimulation and acetylcholine (ACh) applications to the auditory cortex (AC). In the big brown bat, we found that a

45-min-long ACh application to the AC during and after ESa increases the cortical BF shift and changes the short-term to long-term BF shift: nine of the 12 BF shifts studied showed no sign of recovery even 6 hours after the ESa. Since an increased cortical ACh level appears to last ~150 min after a 30 min-long conditioning (Ji and Suga 2003), the 45 min-long ACh application is not unnaturally long. Our current result is an additional demonstration that the long-term cortical BF shift is evoked by the neural net intrinsic to the auditory system, without the auditory and somatosensory association in the MGBm and that this BF shift is amplified and lengthened by the cholinergic system which is activated by the neural pathway excluding the MGBm-Amygdala pathway. (NIDCD 00175).

### **708 Environmental Influence in Cortical Map Reorganization Generated by Basal Forebrain Activation**

**Rafael Carrasco<sup>1</sup>**, Amanda Puckett<sup>1</sup>, Pritesh Pandya<sup>1</sup>, Roshini Jain<sup>1</sup>, Alyssa McMenamy<sup>1</sup>, Joanna Gibbons<sup>1</sup>, Raluca Moucha<sup>1</sup>, Christopher Heydrick<sup>1</sup>, Michael Kilgard<sup>1</sup>

<sup>1</sup>*University of Texas at Dallas*

One of the ongoing goals of our research effort has been to determine the rules that govern remodeling of tonotopic maps in primary auditory cortex (A1) of young adult rats. It has previously been documented that massive and progressive reorganization of A1 can occur with daily episodic activation of neuromodulatory inputs paired with tonal stimuli (Kilgard & Merzenich, 1998). In previous studies, the magnitude of representational reorganization in A1 was determined twenty-four to forty-eight hours after the last conditioning session. An open question is how long these experimental manipulations on cortical representation endure under different environmental conditions. Therefore, the major goal of this study has been to determine the duration and decay of cortical map reorganization after the cessation of one month of daily conditioning.

To determine the progressive decay of A1 map reorganization, a 19 kHz tone was repeatedly paired with electrical activation of the basal forebrain ~350 times a day for one month in over twenty-four animals. Cortical representation of tones was determined by conducting acute mapping experiments one to twenty days after the termination of the basal forebrain-tone pairing procedure. In addition to confirming robust map reorganization twenty-four hours after the last conditioning session, our preliminary results reveal long lasting changes in cortical representation for at least twenty days after the last conditioning session. Ongoing experiments are trying to determine the influence of environmental conditions in cortical map reorganization. We hypothesize that cortical representation after NB stimulation may be influenced by environmental settings.

Supported in part by R03-DC04534-02 (MPK), the McDonnell Foundation, and the Callier Excellence in Education Fund.

### **709 Scopolamine Attenuates Salicylate-Induced Plasticity and Tinnitus Activity in Auditory Cortex of the Gerbil**

Elisabeth Wallhäusser-Franke<sup>1</sup>, Claudia Mahlke<sup>1</sup>, Bessy Cuautle-Heck<sup>1,2</sup>, Gerald Langner<sup>1</sup>

<sup>1</sup>Institute of Zoology, Darmstadt University of Technology, Darmstadt, Germany, <sup>2</sup>Universidad Autonoma de Puebla, Puebla, Mexico

Salicylate is widely used for experimental tinnitus induction in animal models. A high dose of salicylate causes hearing impairment, reduces activity in the inferior colliculus, but increases activity in auditory cortex (Wallhäusser-Franke et al., 1996). In addition, it evokes upregulation of markers of neuronal plasticity in primary auditory cortex, and in the central nucleus of the amygdala (CeA) (Mahlke and Wallhäusser-Franke, 2004). CeA, the main output structure of the amygdala, is activated by different stressors and by different ways of experimental tinnitus induction (Wallhäusser-Franke et al., 2003). We hypothesized that irregularities in auditory input, coinciding with enhanced levels of attention or stress that activate CeA promote the induction of tinnitus as indicated by cortical activity. CeA influences cortical excitability and plasticity through various avenues, among others by activating neurons in the cholinergic basal forebrain, which in turn synapse on muscarinic cortical receptors. We suggested that blocking the cholinergic influence attenuates salicylate-induced plasticity in auditory cortex.

Young adult, male gerbils were injected i.p. with salicylate (350 mg/ kg bodyweight) or with a mixture of salicylate (350 mg/kg) and the muscarinic antagonist scopolamine (0.5; 1 or 3mg/kg). The gerbils stayed in their familiar environment at all times. Exactly 5 h after the injection they received an overdose of anesthetic which was followed by perfusion. Brains were sectioned horizontally on a vibratome at a thickness of 50 µm. Alternate sections were reacted with a c-fos or an arg3.1/arc antibody (both Santa Cruz) following published protocols.

In accordance with our former results, numbers of arg3.1-immunoreactive neurons (IRN) were particularly enhanced in the high frequency domain of AI after injecting salicylate, whereas a simultaneous injection of scopolamine reduced the number of arg3.1-IRN in this region substantially. Numbers of c-fos IRN were also reduced, but were still increased compared to saline controls after injecting 3 mg/kg scopolamine. As expected, scopolamine did not reduce numbers of arg3.1- or c-fos IRN in the amygdala.

The cholinergic input from the amygdala may provide a mechanism for long-term enhancement of neuronal transmission in auditory cortex. Since this may be the substrate of chronic tinnitus, our results open perspectives for a pharmacological treatment of tinnitus.

### **710 Complementary Neural Systems for the Experience-Dependent Integration of Mate-Choice Cues in European Starlings**

Keith W. Sockman<sup>1</sup>, Timothy Q. Gentner<sup>2</sup>, Gregory F. Ball<sup>3</sup>

<sup>1</sup>University of North Carolina, <sup>2</sup>University of California, San Diego, <sup>3</sup>Johns Hopkins University

The courtship song of a male songbird provides an honest signal of his quality, and females choose among prospective mates based on between-male variation in these auditory cues. When prior experience of the female European starling (*Sturnus vulgaris*) is not controlled, long songs induce stronger mate-preference behavior and greater forebrain expression of the immediate early gene (IEG) ZENK in females than short songs do. Thus, mean song length is a phenotypic parameter instrumental in mediating female mate-choice decisions and forebrain responses. But choice of a particular mate phenotype may arise out of experience with the very phenotypes under consideration. Here, we compared the experience-dependent modulation of ZENK with that of another IEG, FOS, and report that ZENK and FOS expression in the auditory forebrain regions of the caudomedial mesopallium and caudomedial nidopallium show different modulation properties that complement natural variation in song length. ZENK expression was greater in response to novel long than to novel short songs following a 1-wk experience with long but not short songs. In contrast, FOS expression was greater in response to novel long than to novel short songs following a 1-wk experience with short but not long songs. Thus, the ZENK and FOS signaling pathways of the female auditory forebrain are made sensitive to variation in song length by experiences with songs at opposite ends of the starling song-variation continuum, suggesting the presence of complementary neural systems tuned in register with the natural axis of stimulus variation fundamental to the species' natural history.

### **711 BDNF Affects Synaptogenesis in the Developing Rat Auditory Cortex**

Scott Schachtele<sup>1</sup>, Michael Dailey<sup>1</sup>, Steven Green<sup>1</sup>

<sup>1</sup>University of Iowa

The developmental elimination and reorganization of central nervous system (CNS) synapses occurs in several sensory systems, including the auditory system. In the CNS, acquisition of synaptic function in auditory neurons precedes both the establishment of mature auditory hair cell thresholds as well as hearing-evoked activity in central auditory neurons, suggesting that hearing onset may correlate with the reorganization of synaptic contacts in the auditory cortex. Indeed, developmental perturbations of the cochlea's tonotopic organization is reflected in the organization of the auditory cortex. The neurotrophin BDNF is known to be an important regulator of synapse formation and dendritic branching patterns during CNS development. We have therefore initiated an investigation of the effects of BDNF on synapse formation in the neonatal rat auditory cortex, using a cortical slice preparation in which synaptic interactions are maintained and which are highly accessible to gene transfer and other

experimental manipulations. Cortical slices were prepared from postnatal day (P5) rats and maintained for at least 7 days *in vitro* corresponding to the period surrounding onset of hearing and the rapid formation of central synaptic connections in the rat. We used biolistic transfection ("gene gun") to introduce into cortical neurons a PSD95-GFP fusion protein that fluorescently labels postsynaptic sites, allowing them to be observed directly in live and fixed slices. We have observed a reduction in synaptic density on basal dendrites in slices incubated with exogenous BDNF relative to control slices. We are now investigating intracellular signaling used by BDNF to mediate these changes in synapse density and the effects of BDNF on auditory cortical neuron dendritic branching patterns. Supported by NIH grant DC02961.

### **712** Cortical Activity Patterns Emerging with Discrimination Learning of Auditory Stimuli and of Intracortically Applied Electrical Stimuli Differ in Their Spatial Organization

Matthias Deliano<sup>1</sup>, Achim Engelhorn<sup>1</sup>, Daniel Ensberg<sup>1</sup>, Henning Scheich<sup>1</sup>, Frank Ohl<sup>1</sup>

<sup>1</sup>Leibniz Institute for Neurobiology

The generation of meaningful perception on the basis of patterned electrical stimulation will be a critical step in the development of a sensory cortical neuroprosthesis [1,6]. In the present work it is proposed that successful patterned multi-site electrical stimulation will rely on a better understanding of cortical processes already involved in the generation of meaningful perception induced by single-site stimulation.

We have recently shown that with discrimination learning of acoustic stimuli, spatially distributed activity patterns emerge in the  $\beta$ - and  $\gamma$ -band of the ongoing Electrocorticogram (ECoG) recorded from the primary auditory cortex (AI) of the Mongolian gerbil. These patterns are related to the meaningful interpretation of the stimuli by the animal [2,3,4].

Electrical stimulation of the cortex is likely to interfere with the endogenous cortical dynamics from which these activity patterns emerge. In the present study we therefore compared the patterns found with the discrimination learning of acoustic stimuli and with intracortical microstimulation (ICMS). Using a GO/NO-GO paradigm animals were trained to discriminate ICMS delivered to different sites within AI [5]. Learning induced cortical activity patterns emerging with electrical stimulation were spatially more focal than with acoustic stimulation. This indicates principle differences in the modes how cortical dynamics is recruited to form discernable percepts when using acoustic or electrical stimuli. To improve the perceptual interpretation of neuroprosthetic stimulation, we aim at the development of an interactive cortical neuroprosthesis permitting proper timing and shaping of ICMS conditional on the instantaneous cortical state.

[1] Brindley, G.S. & Lewin, W.S. (1968) *J. Physiol.*

[2] Ohl, F.W. et al. (2001) *Nature*.

[3] Ohl, F.W. et al. (2003a) *Biol. Cybern.*

[4] Ohl, F.W. et al. (2003b) *Rev. Neurosci.*

[5] Scheich, H. and Breindl, A. (2002) *Audiol. Neurootol.*

[6] Schmidt, E.M. et al. (1996) *Brain*.

### **713** Salicylate Induces Alteration of Behavior and Responses of Auditory Neurons in an Animal Model for Tinnitus

Lukas Rüttiger<sup>1</sup>, Susanne Kilian<sup>1</sup>, Elmar Oestreicher<sup>2</sup>, Justin Tan<sup>1</sup>, Saida Hadjab<sup>1</sup>, Marlies Knipper<sup>1</sup>

<sup>1</sup>THRC Hearing Research Center, University Clinic Tübingen, <sup>2</sup>Technical University of Munich

Behavioral conditioning studies on rats have been proven to be a valid animal model for the evaluation of acute and chronic phantom auditory experience (tinnitus). We recently developed an animal model for short-term acute induced phantom auditory sensations in rats on the basis of systemic application of salicylate (Rüttiger et al., 2003). The expression of activity dependent genes in cochlear spiral ganglion neurons and auditory cortical tissues after application of salicylate - systemically and also locally to the round window of the cochlea - has been shown to be highly specific for excitability changes in the auditory system (Tan et al. 2004, Hadjab et al. 2004). However, the changes of gene expression differed for local and systemic application in auditory cortical tissues. The question arises how the response of auditory neurons is correlated to the expression changes of activity dependent genes and to the performance of rats in the behavioral animal model after local application of salicylate to the cochlea or system injection. Single cell recordings are presented and discussed in the context of salicylate induced phantom auditory experiences, neuronal excitability, and auditory sensory deprivation as indicated by the expression of activity dependent genes.

Supported by the Deutsche Forschungsgemeinschaft DFG 316/3-1, DFG 316/4-1 and Fortune 816-0-0. SH was partially supported by the European Commission, Marie Curie Training Site, HEARING (QLG3-CT-2001-60009).

### **714** Altered Intrinsic Optical Responses in Auditory Cortex with Early Induction of Cortical Microgyri.

Heather L. Read<sup>1</sup>, Nathan C. Higgins<sup>1</sup>, Monty A. Escabi<sup>2</sup>

<sup>1</sup>Department of Psychology, University of Connecticut,

<sup>2</sup>Department of Engineering, University of Connecticut

Behavioral and cortical field responses to rapid sound sequences are altered in rats with cortical microgyri (MG) in somatosensory cortex. However, there is no direct evidence that auditory cortical function is altered in animals with MG. In the present study bilateral MG were induced in somatosensory cortex post-natal day 1 (P1) prior to ear opening and cortical maturation in rats. Auditory cortical function was examined in the mature MG animals and compared with sham treated animals. No differences in the early auditory brainstem responses were observed for the two groups. Auditory cortex response properties were mapped with a continuous intrinsic optical imaging technique (Kalatsky and Stryker, 2003). Sounds were delivered binaurally and consisted of transient pure tones of exponentially ascending or descending frequency.

Significant optical response amplitudes for four auditory cortical regions were observed in shams and microgyrics. However, the frequency gradient or cochleotopic map in auditory cortex was degraded in animals with MG. These data suggest that temporal processing deficits observed previously may be associated with altered acoustic response properties in auditory cortex. Sponsored by the National Institute of Child Health and Development (NICHD).

### **715 Do Salient Temporal Cues Play a Role in Dynamic Receptive Field Plasticity in A1?**

**Jonathan Fritz<sup>1</sup>**, Mounya Elhilali<sup>1</sup>, Nicol Harper<sup>1,2</sup>, Christine Haisfield<sup>1</sup>, Pingbo Yin<sup>1</sup>, Shihab Shamma<sup>1</sup>

<sup>1</sup>University of Maryland, <sup>2</sup>University College London

Do neurons in primary auditory cortex (A1) adapt to the presence of salient temporal cues in auditory tasks? By taking multiple “snapshot” measurements of spectrotemporal receptive fields (STRFs) of single neurons in A1, we can measure STRF shape changes which occur as the animal performs auditory tasks. We have previously demonstrated task-related dynamic spectral changes in STRF shape while the animal performed spectral tasks such as tone detection or discrimination (Nature Neuroscience, 6, 1216-23, 2003). To discover whether A1 neurons show task-related responses during performance of a temporal task we trained ferrets, using conditioned avoidance behavioral techniques, on temporal as well as spectral tasks. The temporal tasks were: (1) gap detection, (2) click rate detection, (3) click rate discrimination and (4) tone duration discrimination. All tasks were variations on a basic task paradigm, in which the animal learned to discriminate between a set of similar reference stimuli and distinct target stimuli in the presence of background rippled noise. Successful performance required attention to the presence of salient acoustic cues such as silent gaps (15-50 ms) in TORCs (temporally orthogonal ripple combinations), rapid (10-20 Hz) sets of clicks, changes in click rate in TORC-click combinations or changes in tone duration in TORC-tone combinations. Preliminary data (from recordings from >50 neurons) indicate a variety of STRF changes in the temporal dimension during temporal task performance including (a) changes in response latency, (b) changes in response duration, (c) “sharpness” of response onset and offset. We shall discuss these results in light of our adaptive hypothesis of task-related, attentional modulation of A1 receptive fields.

### **716 The Other Side of the Coin of Cortical Plasticity – Receptive Field Stability in Ferret A1**

**Mounya Elhilali<sup>1</sup>**, Serin Atiani<sup>1</sup>, Yao Li<sup>1</sup>, Mahdvi Jain<sup>1</sup>, Jonathan Fritz<sup>1</sup>, Shihab Shamma<sup>1</sup>

<sup>1</sup>University of Maryland

In order to form a consistent and stable representation of the acoustic scene, it might be useful for cortical neurons to maintain stable receptive fields. However, recent studies suggest that cortical neurons can be modified throughout adulthood and may change response properties quite rapidly. We have shown that task-related plasticity can

lead to changes in the shape of the spectrotemporal receptive field (STRF) of A1 neurons within minutes (Nature Neuroscience, 6, 1216-1223, 2003). The challenge is to understand how the brain forms stable images of objects in the evolving acoustic scene given the presence of dynamic cortical receptive field properties. Although cortical changes can be induced by attentional focus on acoustic cues during task performance, an important issue is the degree of intrinsic receptive field stability in the awake, non-behaving, quiescent animal. This is important to measure to provide a benchmark for comparison with task-related changes. The observed STRF task-related changes can be more confidently attributed to learning-induced plasticity when a comparison to “spontaneous” plasticity is made. To gauge spontaneous plasticity, we measured, compared and analyzed series of successive STRFs gathered over time from the same neuron in the “passive” awake ferret. We also describe the properties of A1 neurons with “stable” or “labile” STRFs (during acoustic task performance) which can be intermingled in the same recording site or penetration. These observations offer deeper insight into neuronal receptive field stability in A1.

### **717 Spectro-Temporal Processing in the Auditory Cortex of a Microgyric Rat Model.**

**Monty Escabi<sup>1</sup>**, Nate Higgins<sup>1</sup>, Heather Read<sup>1</sup>

<sup>1</sup>University of Connecticut

Cortical anatomical anomalies have been observed in children with developmental dyslexia, a disorder associated with impaired speech and language processing. We are investigating the cortical processing in a rat model with focal microgyria (MG) in somatosensory cortex (S1). Previous studies have established a correlation between the presence of microgyri and acoustic processing deficits in rats. We hypothesize that focal microgyria could lead to changes in the auditory cortex (A1) organization which directly affect spectral and temporal sensitivities in A1. To this end, we are recording single cell activity from A1 neurons in MG+ and MG-control animals and mapping sound sensitivities with dynamic ripple spectro-temporal receptive fields, noise-burst modulation transfer functions and pure tone tuning curves. Such methods are allowing us to quantitatively identify the mechanisms and principles underlying impaired processing in the MG+ rat auditory cortex. (supported by NICHD: HD20806).

### **718 Possible Model of Attention-Deficit Disorder in Lead-Exposed Chicks**

**Lincoln Gray<sup>1</sup>**

<sup>1</sup>University of Texas Medical School

Early lead exposure is associated with an increased risk of attention-deficit disorders in humans. In this experiment we suggest a possible parallel in an animal model. Masked thresholds were estimated in newborn chicks exposed to two levels of early lead poisoning (88 and 132 mg/kg) and in two control groups (un-injected and saline-injected). Two µl per gram of egg weight of the solutions (0.9% NaCl, 80.6 or 120.9 mg/ml lead acetate) were



injected into the large air space at 14 days of incubation (start of auditory function). Receiver operating characteristics were constructed from momentary delays in the subjects' peeping when they heard the signal. The signal was a 250-Hz pure tone. The masker was band-pass noise: 500-800 Hz presented at 30 dB above estimated threshold. We might predict little or no masking because all frequencies in the masker are at least an octave away from the signal, certainly more than the critical band. But normal neonates (both human and avian) show elevated thresholds under these conditions, termed "distraction masking" by L. Werner. Lead exposure had no effect on sensitivity to either the signal ( $p=.22$ ) or the masker ( $p=.69$ ) when these were presented alone. These control listening conditions suggest that the lead exposure does not affect absolute thresholds. Importantly, lead-exposed chicks had decreased responses to the signal in the presence of the masker ( $F_{1,21} = 8.7$   $p < .01$ ). The effect of the off-band masker suggests that early lead poisoning either delays the normal developmental trend of decreasing distraction masking, or makes off-frequency noise more distracting. Such results are conceptually similar to what might be expected from lead-exposed children who frequently present with attention deficits but normal audiograms. Children with attention deficits are more distracted by background sounds. Blood lead levels in the lead-exposed chicks were in the range of what is experienced by many children (about 20  $\mu\text{g/dl}$ ).

### **719** Discrimination of Echo Roughness in the Fruit-Eating Bat *Phyllostomus discolor*

Sven Schörnich<sup>1</sup>, Uwe Firzlaff<sup>1</sup>, Lutz Wiegrebe<sup>1</sup>

<sup>1</sup>Department Biologie II/LMU Munich

Through echolocation, bats are not only able to detect an object in the darkness, but also to gather information about its structure. It has been shown that the fruit-eating bat *Phyllostomus discolor* is able to use the roughness (i.e. the amount of the envelope fluctuation) of a virtual object's impulse response as a parameter for the classification of complex natural objects like trees or bushes [Grunwald et al. PNAS 101, 5670-5674]. The roughness of an object's impulse response is quantified as the base-ten logarithm of its 4th Moment ( $\log_{10}M_4$ ).

In the current psychoacoustical playback experiment we investigate the ability of *P. discolor* to discriminate echoes generated with a fixed reference roughness from echoes with several higher test roughnesses. In a two-channel playback setup, the ultrasonic emissions of the bat are recorded with two microphones and convoluted both with an impulse response possessing the reference roughness and with an impulse response with a test roughness. The resulting echoes are played back over the two speakers, and the bats are trained to crawl towards the speaker delivering the echo with the reference roughness.

Discrimination performance is assessed as a function of the test roughness.

When the reference roughness was 1.8, the test roughness had to be at least 2.5 for significant discrimination.

When the reference roughness was 2.5, the test roughness had to be at least 2.8.

Experiments with additional reference roughnesses are in progress.

These psychophysical results are compared with the performance of electrophysiologically recorded cells from the auditory cortex of *P. discolor*. These cells were stimulated with synthetic echoes consisting of the impulse responses from the psychophysical experiments convolved with a standard *P. discolor* echolocation call. In 21 % of the recorded cells, the rate responses obtained with these stimuli are monotonically related to the impulse-response roughness.

### **720** Robustness Found in Synthesized Coo-Like Sound Discrimination by Japanese Macaques

Hiroshi Riquimaroux<sup>1</sup>, Yasunari Sasaki<sup>1</sup>

<sup>1</sup>Doshisha University

The present study investigated how monkeys establish robustness in perception of communication-related sounds when frequency and time parameters were independently and systematically manipulated. Two adult Japanese monkeys participated in the experiment. They were trained to discriminate between harmonically structured synthesized sounds with (S+) and without the second harmonic components (S-) on Go-Nogo paradigm for water reward. They successfully learned to discriminate between S+ and S-. In testing sessions we systematically and independently varied the height/depth of frequency peak and shifted the peak location in time. No feedbacks were given in the test sessions. The animals clearly discriminated synthesized sounds with and without the second harmonic component regardless the peak height/depth or location in time. One animal showed consistent responses to test stimuli with variation of peak height/depth only depending upon the harmonic structure while some individual gradient was observed on the temporal peak variation. On the other hand, another animal presented stable responses to test stimuli with temporal peak variability while some preference was found for the peak frequency differences. The findings have shown robustness of coo-like sound discrimination based upon the harmonic structure and may imply existence of different individual strategies in establishing categories of communication sound perception.

Study supported by Special Coordination Funds from the Science and Technology Agency and a grant to RCAST at Doshisha University from the MEXT of Japan.

### **721** Comodulation Effects in a Songbird: Comodulation Detection Difference

Ulrike Langemann<sup>1</sup>, Mark Bee<sup>1</sup>, Georg Klump<sup>1</sup>

<sup>1</sup>Oldenburg University

The common modulation of signal envelopes as well as the common onset of signal components provide cues exploited by the auditory system for auditory grouping and signal segregation. In a comodulation detection difference (CDD) task, signal detection is enhanced if the temporal

envelope of the signal band is different from the correlated flanking noise bands. Here we present CDD data in a model species that shows perceptual effects of auditory grouping and comodulation very similar to those observed in humans.

Five European starlings (*Sturnus vulgaris*) were trained in a Go/NoGo paradigm to report the detection of a signal band (SB) centered at 2 kHz (bandwidth 100 Hz, 60 or 400 ms duration) surrounded by six flanking bands (FBs, bandwidth 100 Hz, 600 ms duration). The SB was either switched on together with the FBs or was delayed by 100 ms. There were three conditions (1) FBs and SB had the same envelope (correlated), (2) FBs had a common envelope that was different from the envelope of the SB (co-uncorrelated), (3) the envelopes of all band were uncorrelated (all-uncorrelated). The spectrum level of the noise bands was either 15 or 50 dB. Signal detection theory was applied to determine the level of the signal band at detection; threshold criterion was a  $d'$  of 1.8.

Masker level, signal duration and the different conditions each had a significant effect on signal detection. In comparison to humans (McFadden & Wright 1990, JASA 88: 711-724) starlings were not affected by the delayed onset of the signal band. The difference for signal detection in correlated maskers versus co-uncorrelated maskers (the CDD effect) was on average 3.7 dB at 15 dB and 4.6 dB at 50 dB masker level. Signal detection in all-uncorrelated maskers was about 1 and 6 dB worse compared to correlated maskers at 15 dB and 50 dB, respectively. For short duration SBs, signal detection was impaired by about 5 and 7 dB compared to long SBs at 15 dB and 50 dB, respectively.

Supported by the DFG, FOR 306, and NSF grant INT-0107304

## **722 Auditory Short-Term Memory for Tonal Signals in a Songbird**

**Melanie Zokoll<sup>1</sup>, Ulrike Langemann<sup>1</sup>, Georg Klump<sup>1</sup>**

<sup>1</sup>*Oldenburg University*

To evaluate a sequence of acoustic communication signals it is necessary to keep the previous elements in memory. This not only applies to the analysis of speech by a human observer, but also to the analysis of a long sequence of elements in the song of a bird. Female European starlings (*Sturnus vulgaris*), for example, base their mate choice on the diversity of elements that an individual male sings (Eens et al. 1991, Behaviour 116: 210-238). To assess the diversity of elements that a female hears in a song she needs to store information about the elements in short-term memory. Thus, starlings should be suitable models to investigate the role and mechanisms of auditory short-term memory. In this study we applied a delayed-matching-to-sample (DMTS) paradigm to estimate the extent of the short-term memory stores.

Starlings were trained in a Go/NoGo procedure. In each trial of a session comprised of a total of 90 trials, a series of up to 6 identical sample tones and a final test tone were presented with random inter stimulus intervals (range 1-10 s). The frequency of the test tone either was the same as that of the sample tones (NoGo-Stimulus) or it was

different (Go-Stimulus). The test tone frequency (range between 1 and 4 kHz) became the sample tone frequency of the next trial. The 400-ms tones were presented with a level that randomly varied between 58 and 64 dB SPL (average 61 dB SPL). Memory performance was expressed as the proportion of correct responses in relation to the total number of pairs of sample and test stimulus that were presented with a specific delay. The short-term memory duration was measured as a function of the delay between the last sample and the test. The results suggest a rather long persistence of auditory short-term memory in this bird species.

Supported by the DFG, International Graduate School "Neurosensory Science, Systems and Application" and FOR 306 "Hörobjekte".

## **723 Quinine Induced Tinnitus Like Behavior using Schedule Induced Polydipsia Avoidance Conditioning (SIP-AC)**

**Edward Lobarinas<sup>1</sup>, Guang Yang<sup>1</sup>, Wei Sun<sup>1</sup>, Richard Salvi<sup>1</sup>**

<sup>1</sup>*Center for Hearing and Deafness University at Buffalo*

Quinine, an anti-malarial drug that can induce tinnitus when administered at high doses, has been used to investigate the neural and biochemical mechanisms underlying tinnitus; however, meaningful interpretation of the biological results would be aided by behavioral measures of quinine-induced tinnitus. We are aware of only one behavioral study in which quinine-induced tinnitus was measured with a lick suppression technique (Jastreboff et al., 1991; Arch Otolaryngol Head Neck Surg). To confirm and extend the behavioral findings, we used our newly developed technique, Schedule Induced Polydipsia Avoidance Conditioning (SIP-AC) (Lobarinas et al, 2004, Hear Res) to assess quinine-induced tinnitus. Food-restricted rats auto-shaped to lick for water under scheduled delivery of food pellets at 1 minute intervals (Schedule Induced Polydipsia). The polydipsic behavior was then put under the control of a shock avoidance paradigm by training the rats to lick for water only when it was quiet and to refrain from licking when either noise (4 to 20 kHz) or a pure tone (16 kHz) were present to avoid foot shock, i.e., avoidance conditioning. Rats were trained to a criterion of >90% of licks in quiet and <10% licking in the presence of sound. Following training, rats were injected with quinine. Preliminary data show that quinine induced tinnitus-like behavior, by reducing the number of licks in quiet but did not affect licking behavior in the presence of sound. The data were consistent with a reduced ability to perceive the quiet intervals and with the presence of a phantom sound. After terminating quinine injections, licking in quiet increased to pre-drug levels suggesting that the phantom sound of tinnitus had disappeared. These results are consistent with previous published data in which quinine or salicylate was used to induce tinnitus. SIP-AC can be used as a technique that allows the time course of tinnitus onset and recovery to be measured in individual animals and allows for within and between animal comparisons.

## **724 Effect of Listening Strategy on the 'Pitch' Strength of Complex, Harmonic Sounds in Chinchillas: Stimulus Generalization with Split-Test Stimuli**

**William P. Shofner<sup>1</sup>, William M. Whitmer<sup>1</sup>**

<sup>1</sup>*Loyola University Chicago*

The perception of 'pitch' strength in chinchillas is dependent on the stimulus used for training. Behavioral data from animals trained to discriminate a cosine-phase harmonic tone complex (COS) from wideband noise (WBN) suggest animals rely more heavily on temporal information in the envelope, whereas data from animals trained to discriminate infinitely iterated rippled noise (IIRN) from WBN suggest animals rely more heavily on information in the fine structure. These results imply that chinchillas weigh high frequency information more when discriminating COS from WBN and weigh low frequency information more when discriminating IIRN from WBN. To test this hypothesis, stimulus generalization experiments were carried out using split-test stimuli. In experiment 1, chinchillas were trained to discriminate COS from WBN and tested with tone complexes in which phase was split between frequency regions. In this split-phase condition, responses to complexes made of random-phase low frequencies, cosine-phase high frequencies were similar to responses to the COS training stimulus. However, responses to complexes made of cosine-phase low frequencies, random-phase high frequencies were generally lower than their responses to the COS training stimulus. In experiment 2, chinchillas were trained to discriminate IIRN from WBN and tested with noises in which the spectral ripple was split between frequency regions. In this split-rippled condition, responses to noises made of rippled-spectrum low frequencies, flat-spectrum high frequencies were high, whereas responses to noises made of flat-spectrum low frequencies, rippled-spectrum high frequencies were generally lower than their responses to the IIRN training stimulus. The results suggest that chinchillas listen across all frequencies, but give more weight to high frequencies when discriminating COS from WBN and give more weight to low frequencies when discriminating IIRN from WBN.

Supported by NIDCD R01 DC005596

## **725 Equal Loudness Contours for the Domestic Cat**

**Nicole Little<sup>1</sup>, Brad May<sup>1</sup>**

<sup>1</sup>*Johns Hopkins University*

Previous electrophysiological studies from our laboratory suggest that speech encoding in hearing-impaired cats may be improved by enhancing the spectral contrast of steady-state vowels. Attempts to validate these amplification strategies in animal behavioral studies have met with limited success because contrast-enhanced vowels appear to evoke an unnaturally rapid growth of loudness in impaired cats. Our ongoing studies are

attempting to quantify and control these recruitment effects by characterizing loudness perception in normal and hearing-impaired cats. Our psychophysical scaling procedures are founded on the traditional assumption that equal response latency signifies equal loudness. These reaction time measures reproduce most of the well-known features of human loudness functions when applied to normal cats. The effects of sensorineural hearing loss on the perceived loudness of simple tones and spectrally complex vowels will be demonstrated with data from the same cats after they have been exposed to an intense noise with peak energy at vowel formant frequencies.

This work funded by NIH grants DC000109 and DC05211.

## **726 Duration Discrimination in the Mouse (*Mus musculus*)**

**Karin Klink<sup>1</sup>, Georg Klump<sup>1</sup>**

<sup>1</sup>*Oldenburg University, IBU, Fak. V*

Signal duration is an important parameter of sounds evaluated by the auditory system, and in the inferior colliculus neurons of the mouse and of other mammals duration-dependent response patterns have been found (e.g., Brand et al. 2000, *J. Neurophysiol.* 84: 1790-1799). It has been postulated that duration-specific responses in the auditory system result either from an adequately timed interaction of excitation and inhibition (e.g. Casseday et al. 2000, *J. Neurophysiol.* 84: 1475-1487) or from the integration of activity over time. Thus, a reduced inhibition (e.g., by applying the glycine antagonist strychnine) should lead to a change in the duration discrimination capability if the first mechanism dominates the analysis whereas the activity-integrating mechanisms do not rely on inhibition. Here we present psychoacoustical data on the accuracy of duration discrimination in the house mouse and evaluate the effect of strychnine on the perception of signal duration.

The increment-detection thresholds for 3 reference durations (50ms, 100ms, 200ms) and two signal-level conditions (fixed versus randomized level by  $\pm 3$  dB) were found to vary significantly with the reference duration ( $p=0.009$ , RM ANOVA), but did not differ between conditions with a fixed and a randomized tone level (see also Klink & Klump, *J. Comp. Physiol. A*, in press). Thus, a simple energy-integration mechanism does not explain the behavioral data. There was no significant difference between sessions with strychnine and control sessions ( $p>0.05$ , RM ANOVA). This suggests that the mechanism underlying duration discrimination does not necessarily involve inhibition. It could be based on responses observed in long-pass neurons in the mouse inferior colliculus that would require a summing up of neural activity over the duration of the stimulus as is suggested by clock-counter models of duration perception (Creelman 1962, *J. Acoust. Soc. Am.* 34: 582-593).

(Supported by the DFG, SFB 517)

## **727** Role of Masker Predictability in the Cocktail Party Effect

Gary Jones<sup>1</sup>, Ruth Litovsky<sup>1</sup>

<sup>1</sup>University of Wisconsin-Madison

A cocktail party is an unpredictable auditory environment. Masking consists of an energetic component due to target and maskers exciting the same auditory filters and an informational component which is believed to reflect uncertainty. With speech maskers there is a substantial informational component, with greater release from masking when there is actual or perceived spatial separation between target and maskers than is found with other broadband maskers such as Gaussian noise or modulated noise. In the current experiments subjects identified a target word spoken by a male talker presented in free field amidst 0, 1 or 2 maskers arrayed in the horizontal plane in a 40 AFC task. Ten masking conditions were used, and predictability of the masking condition was varied from 10% to 80%. We hypothesized that fixed SNR percent correct and spatial release from masking increase with increasing predictability. There was high individual variability in percent correct and in spatial release from masking and neither measure showed a significant effect of predictability. This suggests predictability of the spatial location of maskers is less important than predictability of other features such as content and that existing clinical measures adequately estimate spatial release from masking in normal hearing subjects.

## **728** The Effects of Distractor Frequency on Monaural Intensity Discrimination Under Monotic and Dichotic Conditions

Daniel Shub<sup>1,2</sup>, Tracy Pogal-Sussman<sup>2</sup>, H. Steven Colburn<sup>1,2</sup>

<sup>1</sup>Speech and Hearing Bioscience and Technology, Massachusetts Institute of Technology, <sup>2</sup>Hearing Research Center, Boston University

This study measured and modeled the effects of distractor frequency on intensity discrimination. Subjects were simultaneously presented both a tonal target and a tonal distractor and asked to discriminate target intensity. The 600-Hz target was presented at the left ear. The level of the distractor was roved over a 30 dB range on an interval-by-interval basis, and both the frequency of the distractor and the ear at which it was presented (either ipsilateral or contralateral to the target) were varied. The psychophysical discrimination thresholds varied with both the spectral proximity of the distractor to the target and the ear at which the distractor was presented. Distractors with frequencies close to the target frequency, within 100 Hz, decreased performance (thresholds above 5 dB and under some conditions as large as 10 dB) to a greater extent than spectrally remote distractors (thresholds approaching 2 dB). For a given distractor frequency, thresholds were higher when the distractor was presented ipsilateral to the target; contralateral distractors, however, still had a significant effect.

The detection theoretic modeling used the sum of the energies of the target and distractor after gamma-tone filtering (centered at 600 Hz), regardless of the ear at

which the distractor was presented, and when the distractor was presented at the ear contralateral to the target the "lateral position" was also included. In agreement with the psychophysical results, for frequencies within 100 Hz of the target the modeled thresholds show a strong dependence upon distractor frequency. Additionally, within this frequency range, the model thresholds for ipsilateral distractors were higher than for contralateral distractors, consistent with the "lateral position" carrying additional information. Inconsistent with the psychophysical results is that outside this frequency range the model thresholds showed little influence of the distractor. This is hypothesized to be a result of a mismatch between the tails of the gamma-tone filter and an actual auditory filter. [Supported by NIH grants R01 DC 00100 and 1 F31 DC006769-01]

## **729** Consequences of Across-Frequency Convergence Following Binaural Integration

Torsten Marquardt<sup>1</sup>, David McAlpine<sup>1</sup>

<sup>1</sup>University College London

Inspired by recent physiological findings, we present a new model of mammalian binaural hearing that explains a wide range of binaural unmasking data. This model is based on internal phase-, rather than time-, delays. Consequently, the range of interaural timing differences within one frequency channel is restricted to interaural phase delays within plus and minus half a cycle ("Pi-limit"). The activation pattern across frequency channels, however, reveals information about interaural time delays of any length. The necessary across-frequency convergence has the consequence of producing an apparently wider binaural critical band. The lack of knowledge about the specific convergence pattern lead us to a simple convergence strategy in order to model results of binaural unmasking experiments: from each off-frequency channel we choose the internal phase-delay that exhibits lowest masker activation. These activations are then summed using a frequency-weighting function, and combined with the activation in the signal-frequency channel at a phase delay that shows the highest signal-to-noise ratio for the dichotic stimulus condition. This simplified convergence strategy models surprisingly well psychophysical results of v.d. Heijden & Trahiotis (1999, Masking with Interaurally Delayed Stimuli: The use of "Internal" Delays in Binaural Detection. JASA 105(1), 1999, 388-399.), Sondhi & Guttman (Width of the Spectrum Effective in the Binaural Release of Masking. JASA 40(3), 1966, 600-606) and data from an experiment in which we applied flanking noise bands, similar to Sondhi & Guttman (1966), to the double-delayed masking stimulus paradigm of v.d. Heijden and Trahiotis (1999). The data from our experiment reveal that the binaural critical bandwidth appears to be smaller in the double-delayed, compared with the single-delayed, masking condition, consistent with our model. In addition, our data cannot be explained by a single-frequency channel model, such as that of v.d. Heijden and Trahiotis (1999). Across-frequency convergence is essential to explain a wide range of binaural phenomena, and obviates the need for long internal delays, i.e. beyond the Pi-limit.

Supported by Medical Research Council, U.K.

### **730 Vertical-Plane Localization of Sounds with Distorted Spectral Cues**

Andrew T. Sabin<sup>1,2</sup>, Ewan A. Macpherson<sup>1</sup>, John C. Middlebrooks<sup>1</sup>

<sup>1</sup>Kresge Hearing Research Institute, University of Michigan, <sup>2</sup>Department of Communication Sciences and Disorders, Northwestern University

For human listeners, the primary cues for localization in the vertical plane are provided by the direction-dependent filtering of the pinnae. Vertical-plane localization generally is accurate for broadband sounds, but when such sounds are presented at near-threshold levels or at high levels with short durations (< 20 ms), the apparent location lies closer to the horizontal plane than does the physical location (elevation gain < 1). In the present study, we tested the hypothesis that these effects result from distorted peripheral representations of sound spectra in addition to the effects of poor signal-to-noise ratio (near-threshold sounds) or lack of temporal integration (short, high-level sounds). Human listeners indicated the apparent position of 100-ms, 50-60 dB SPL, wideband noise-burst targets by orienting their heads. The targets were synthesized in virtual auditory space and presented over headphones. Faithfully synthesized targets were interleaved with targets for which the directional transfer functions (DTFs) were manipulated in one of three ways: DTF notches were filled in, DTF peaks were levelled off, or the DTF spectral profile was compressed or expanded in magnitude, decreasing or increasing the spectral contrast of DTF features. Manipulated stimuli retained natural interaural difference cues. As notches were filled in progressively or peaks clipped progressively, elevation gain decreased in a graded manner similar to that observed as level is reduced below 30 dB or, for brief sounds, increased above 50-60 dB SPL. As contrast was reduced, gain dropped only at the most extreme reduction (25% of normal), but increasing contrast (by up to 400%) had no effect. The results are consistent with the hypothesis that loss of representation of DTF spectral features contributes to reduced elevation gain at low and high sound levels. [Funded by NIDCD grants R01 DC00420 and P30 DC05188]

### **731 Generalisation of Learning with ITD Discrimination Across Frequency and Type of Cue**

Daniel Rowan<sup>1</sup>, Mark Lutman<sup>1</sup>

<sup>1</sup>University of Southampton

A previous study<sup>1</sup> compared the ability of normal-hearing 'naïve' listeners to learn to discriminate low-frequency ongoing interaural time difference (ITD) or high-frequency interaural level difference (ILD), two important cues to localisation. The authors concluded that learning for ILD had a longer time course and only partially transferred across frequency (~0.6 octaves), interpreted in the context of known differences in the processing of the two cues. *Are differences in learning apparent with the discrimination of low-frequency ITD and high-frequency envelope-based ITD cues?* We have addressed this using a 128-Hz tone and a 128-Hz tone 'transposed' to 4000 Hz; ITD

sensitivity with these stimuli is comparable in highly trained listeners<sup>2</sup>, thereby minimising a confounding effect of differential overall sensitivity when interpreting learning. Twenty naïve listeners were trained over 2160 trials with one or other stimulus or served as untrained controls. Performance was measured with both stimuli and sinusoidally amplitude modulated (SAM) tones during pre- and post-training sessions. ITD discrimination was measured using a 1-cue, 3-alternative forced-choice task and listeners were trained using a modified Levitt 2-down, 1-up adaptive procedure<sup>3</sup>. Overall, performance on pre-training was comparable for unmodulated and transposed stimuli but better than with SAM, although inter-individual variation was apparent. This reinforces the notion that ongoing ITD processing is functionally uniform across frequency. Both training groups learned more than untrained controls but the learning with either trained stimulus transferred entirely to the untrained stimuli. That is, learning generalised across both frequency (~5 octaves) and type of ITD cue. This generalisation may reflect commonality in the necessary listening strategies for optimal performance (e.g. detection of decorrelation) or the pooling across frequency in the underlying processing for ITD discrimination.

This research was supported by a grant from the Royal National Institute for Deaf People (RNID)

1 Wright BA, Fitzgerald MB. Proc Natl Acad Sci USA 2001;98:12307-12

2 Bernstein LR, Trahiotis C. J Acoust Soc Am 2002;112:1026-36

3 Trahiotis C, Bernstein LR, Buell TN, Spektor Z. J Acoust Soc Am 1990;87:1359-61

### **732 Virtual Sound Localization using PCA-modified, Non-individualized Head Related Transfer Functions**

Jinyu Qian<sup>1</sup>, David A. Eddins<sup>1</sup>

<sup>1</sup>Psychoacoustics Laboratory, University at Buffalo, Buffalo, NY 14214

Sound localization cues generally include both binaural and monaural information. Interaural time (ITD) and interaural intensity differences (IID) provide two important binaural cues for sound localization. For sounds coming from the median sagittal plane (MSP), where ITDs and IIDs alone cannot account for sound localization, spectral cues in the head related transfer functions (HRTFs) play a critical role, both monaurally and binaurally. Two types of experiments can be performed to study sound localization cues. One is free-field sound localization, in which the subject must judge the sound source location following a sound presented from a loudspeaker in a specific location. The other is virtual sound localization, in which the subject must specify an apparent sound source location based on a 3D auditory image for a synthesized sound delivered binaurally by headphones. Compared to free-field experiments, virtual sound localization allows more systematic manipulation of various acoustic cues. Several virtual sound localization studies have focused on the perceptual consequences of specific spectral modifications

of the HRTFs. An efficient way to represent the underlying structure in a highly variable data set such as HRTFs is principal component analysis (PCA). In a previous study involving PCA analysis of HRTFs, we illustrated a theoretical relationship between the resulting principal directions and sound source locations. The current project investigated a corresponding perceptual relationship by measuring the virtual sound localization abilities of six normal-hearing listeners using HRTFs reconstructed with various combinations of principal directions. The data demonstrate a relationship between some but not all principal directions and the ability to identify specific sound source locations. The use of non-individualized rather than subject-specific HRTFs, however, may have resulted in less accurate localization performance. (Supported by NIH NIDCD DC04403).

### **733 Training Requirements Necessary for Frequency-Discrimination Learning Over Multiple Sessions**

**Beverly A. Wright<sup>1</sup>**, Matthew B. Fitzgerald<sup>1</sup>, Christopher C. Stewart<sup>1</sup>, Jeanette A. Ortiz<sup>1</sup>

<sup>1</sup>*Northwestern University*

The ability to discriminate tones of different frequencies can improve with multiple-session practice, but little is known about the training requirements that are necessary to obtain such learning. Here, we compared learning on a frequency-discrimination task across listeners who were trained with one of three regimens that differed in the number of trials per session and in whether or not each session also included training on a task other than frequency discrimination. In all cases, the training consisted of repeated threshold measurements, over 6 to 10 sessions on separate days, using an adaptive (3-down/1-up), two-interval forced-choice procedure with a 1-kHz pure-tone standard. Seven listeners who practiced only frequency discrimination for 360 trials per session (~0.5 hour) did not improve significantly more than untrained controls ( $p=.526$ ), whereas five listeners who practiced for 900 trials per session (~1 hour) nearly did ( $p=.092$ ). Finally, unexpectedly, eight listeners whose training alternated between frequency and duration discrimination every 120 trials for a total of 720 trials per session (360 trials per discrimination task) showed marked improvements in frequency discrimination relative to untrained controls ( $p=.005$ ). Taken together, these results suggest that some critical amount of practice per session (>360 trials) is required to obtain improvements on frequency discrimination over multiple training sessions. However, not all of the practice need be on frequency discrimination: Practice on a different task (duration discrimination) actually appears to enhance improvements on frequency discrimination, at least when the standard stimulus is the same. [Work supported by NIH.]

### **734 Encoding Dilemma Between Fundamental Frequency and Speech Intelligibility in Cochlear Implants**

**Jeff Carroll<sup>1</sup>**, Fan Gang Zeng<sup>1</sup>

<sup>1</sup>*Department of Biomedical Engineering, University of California Irvine, California, 92697-1275, USA*

As speech intelligibility continues to improve in cochlear implant users, attention has been paid to other aspects of auditory perception such as the encoding of the fundamental frequency (F0). Based on the importance of resolved harmonics in complex pitch perception, Geurts and Wouters suggested that the density of low frequency channels be increased to improve F0 discrimination. The present study examined the relationship between F0 encoding and speech intelligibility as a function of channel density. A total of 8 channels were used to construct the following 4 processing strategies: the Greenwood map and three with 6 channels in low (0.1-0.5 kHz), middle (0.5-1.5 kHz) or high frequency (1.5-5 kHz). The remaining 2 channels covered the rest of the 0.1-5 kHz overall bandwidth. Finally, the contribution of temporal envelope cues was examined by setting the envelope low-pass cutoff to 50, 160 and 500 Hz. Eight normal-hearing subjects participated in this study via a cochlear-implant simulation. The F0 discrimination task used a 2IFC, three-down, one-up adaptive procedure in which the listener chose the sentence with higher pitch as processed by the STRAIGHT program. The intelligibility task was to listen to IEEE sentences from a single talker and to type as many recognizable keywords as possible. For the 50- and 160-Hz low-pass stimuli, the low-frequency condition showed a significant 3-semitone improvement in F0 discrimination over the Greenwood, middle- and high-frequency conditions but significantly lower intelligibility of only 20% as compared to the 60-85% intelligibility with the other three conditions. The cutoff frequency had a significant effect with the 160- and 500-Hz conditions performing 9-10 semitones better than the 50-Hz condition. The result suggests that F0 discrimination and speech intelligibility rely on different frequency regions and future cochlear implant design should consider this difference to improve performance for both tasks.

### **735 Relative Contribution of Temporal Cues and Spectral Profile to Voice Gender Discrimination**

**Sherol Chinchilla<sup>1,2</sup>**, Geraldine Nogaki<sup>1</sup>, Qian-Jie Fu, Ph.D.<sup>1</sup>

<sup>1</sup>*House Ear Institute*, <sup>2</sup>*California State University, Northridge*

Despite limited access to spectral and temporal cues, cochlear implant (CI) users are somewhat able to discriminate voice gender. The present study explored the relative contributions of spectral and temporal cues to normal hearing (NH) subjects' voice gender discrimination, while listening to multi-channel simulations of CI processing. The output spectrum was either matched (relative to normal) or upwardly-shifted to simulate the spectral shift associated with CIs; the envelope filter in each channel was varied to examine the contribution of

temporal cues. Voice gender discrimination was tested with two talker sets, in which the mean fundamental frequency (F0) between male and female talkers was either widely or narrowly separated. Results showed that for both talker sets, 16 spectral channels were needed before subjects could use the spectral profile to identify voice gender; when the speech spectrum was shifted, 32 channels were needed. Given enough temporal cues, the spectral profile had a relatively small effect on discrimination when the F0 was widely-separated between male and female talkers. When there was little F0 separation between male and female talkers, the spectral profile had a much stronger effect; however, 16 or more channels were needed before listeners could attend to the profile. These results will be taken and compared with those of CI users. A comparison of averages between both groups should indicate what cues CI users are relying on in discriminating voice gender.

Supported by NIDCD-RO1-DC004993

### **736 Auditory Training with Spectrally Shifted Speech: An Implication for Cochlear Implant Users' Auditory Rehabilitation**

**Geraldine Nogaki<sup>1</sup>**, Qian-Jie Fu<sup>1</sup>, John J. Galvin<sup>1</sup>

<sup>1</sup>*House Ear Institute*

After implantation, post-lingually deafened cochlear implant (CI) patients must adapt to both spectrally-reduced and -shifted speech patterns; the time course of this adaptation generally occurs during the first 3-6 months of implant use and may continue for many years. To see if intensive training can accelerate this learning process, 16 naive, normal-hearing listeners were trained with spectrally-shifted speech via an 8-channel acoustic simulation of CI speech processing. Baseline vowel and consonant recognition was measured for both spectrally-shifted and -matched speech. Short daily training sessions were conducted over 5 consecutive days, using 3 different training protocols and one test-only protocol. Because the spectral upshift and compression was so severe, subjects initially scored at chance level on the vowel test. For the test-only protocol, no improvement was seen over the 5-day period. Similarly, sentence training provided little benefit for vowel recognition. However, over 5 days of targeted phoneme training (either preview of the vowel tokens produced by a different talker set or training with novel stimuli that targeted vowel contrasts), subjects' recognition of spectrally-shifted vowels significantly improved. This improvement did not generalize to the spectrally-matched vowel and consonant tokens, suggesting that subjects adapted to the specific spectral shift, rather than to the 8-channel processing in general. Interestingly, significant improvement was observed in the recognition of spectrally-shifted consonants; the largest improvement was observed with targeted vowel contrast training, which did not include any explicit consonant training. These results show that targeted phoneme training can accelerate adaptation to spectrally-shifted and -compressed speech patterns. Auditory rehabilitation tools that provide targeted phoneme

training may be an effective approach toward improving the speech recognition of adult cochlear implant users.

### **737 Relative Effectiveness of Training Methods for Adaptation to Spectrally-Shifted Speech**

**Andrew Faulkner<sup>1</sup>**, Stuart Rosen<sup>1</sup>, Andrew Jackson<sup>1</sup>

<sup>1</sup>*Dept. Phonetics and Linguistics, UCL, UK*

Adaptation to spectrally-shifted speech is found in both normal listeners and users of cochlear implants. New implant users are likely to benefit from training designed to accelerate this adaptation. Here we consider two factors in such training. 1) What is the relative effectiveness of analytic training focussed on specific speech sounds compared to a global approach based on meaningful connected speech? 2) Is adaptation to a large spectral shift facilitated by exposure to a gradually increasing shift?

Three groups of normal-hearing listeners were trained with spectrally-shifted noise-vocoded speech. One group received analytic training requiring identification of /vowel-consonant-vowel/ bisyllables and /b-vowel-d/ words. Global training required identification of words in simple sentences. A fixed spectral shift equivalent to a 6 mm basalward basilar membrane shift was always used in analytic training. Global training used either this fixed shift or an adaptively varied spectral shift that tracked 50% intelligibility. Training ran for approximately 3 hours: each presentation included two response opportunities followed by text feedback. Pre- and post-training measures with unshifted and 6 mm-shifted vocoded speech were vowel and consonant identification, and simple (BKB) and more complex (IEEE) sentences. An untrained control group was also tested.

There were no significant differences in training effects between the fixed and adaptive shift. However outcomes were dependent on test and training materials. Post-training sentence scores with shifted speech did not differ between the analytic training group and controls, but both groups trained with sentences showed improved performance over controls. Outcomes were quite different for vowel identification. Here only the analytic training group showed higher performance than controls. If the goal is to improve speech understanding, then connected speech materials seem to be more effective than analytic materials.

### **738 "Vowel Spaces" of Subjects Listening to Frequency-Shifted Vocoded Speech**

**Mario Svirsky<sup>1,2</sup>**, Michael Rerko<sup>1</sup>, Heidi Neuburger<sup>1</sup>

<sup>1</sup>*Indiana University School of Medicine*, <sup>2</sup>*Purdue University*

Postlingually deaf cochlear implant (CI) users must learn to interpret an auditory signal that is spectrally degraded and may be shifted in frequency with respect to the percepts received when they had normal hearing. One way to investigate listeners' perception of such degraded auditory input is to examine their internal representation of vowel categories using the "vowel space" (VS) task. In this task, synthetic vowels varying in first and second formant frequency (F1 and F2) are arranged in a grid on a

computer screen. Listeners select the regions of the grid that sound like different pre-specified vowels. We predicted that the initial post-implant VS's of postlingually deaf CI users would be systematically shifted with respect to normative values, as listeners tried to compensate for the frequency shift. However, this prediction was wrong. The present study aimed to investigate the effect of a spectrally degraded, frequency shifted signal on the VS of listeners who (unlike CI users) have not suffered long term deafness or differing patterns of neural survival. This was done by studying the VS's of 12 normal hearing subjects listening to an 8-channel vocoder where the output of each channel modulated a band of noise, a common way of acoustically simulating CI output. The noise bands were systematically shifted with respect to the vocoder filters. Measured in mm along the basilar membrane, the frequency shift ranged from 0 to 6.5 mm. Results as a function of frequency shift were highly nonlinear. Average VS's under frequency shifts up to 2.5 mm were very close to normal, while shifts of 4.5 mm or more resulted in highly distorted VS's. These results suggest that listeners identify vowels by giving more weight to inter-formant differences than to absolute formant frequency values, because the former are less affected by frequency shifts. The complicated VS patterns for larger frequency shifts may be associated with listeners mistaking an upwards-shifted F1 for a low F2.

This work was supported by NIH-NIDCD grant R01-DC03937.

### **739 Effect of Low-Noise Noise Carriers on Speech Intelligibility in Simulations of Cochlear Implant Processors with Normal-Hearing Listeners**

**Nathaniel A. Whitmal<sup>1</sup>**, Sarah F. Poissant<sup>1</sup>, Richard L. Freyman<sup>1</sup>, Karen S. Helfer<sup>1</sup>

<sup>1</sup>*University of Massachusetts*

The speech perception capabilities of cochlear implant patients are often simulated in normal-hearing listeners with multi-channel vocoders that modulate a series of tone or narrow-band Gaussian noise carriers. Published data (Dorman, *et al.*, JASA 102:2403-2411, 1997) show that speech recognition for subjects trained with correct-answer feedback is relatively unaffected by carrier type. In contrast, results presented at last year's ARO MidWinter meeting (Whitmal, *et al.*, 2004) showed that subjects with limited training who listened to sentences in quiet and in noise processed by 6-channel tone and noise vocoders were better able to understand the tone-vocoded sentences. Intelligibility differences were attributed to both training and carrier-based perturbations in the speech envelope, an important source of intelligibility cues for vocoded speech (Kwon and Turner, JASA 110:1130-1140, 2001).

The goal of the current study was to determine the extent to which these intelligibility differences were caused by fluctuations in the speech envelope. The results of Whitmal, *et al.* were replicated and extended to include comparisons with vocoded speech using low-noise noise carriers (Kohlrausch, *et al.*, Acustica 83:659-669, 1997)

with flat envelopes and narrow-band spectra respectively resembling the envelopes and spectra of the original tone and noise carriers. A coherence analysis showed that the correlations between the envelopes of unprocessed and vocoded sentences were higher for tone and low-noise noise carriers than for Gaussian noise carriers. Despite the higher correlation, only minor differences were observed between intelligibility scores for the low-noise noise and Gaussian noise vocoders, thus discounting the influence of envelope fluctuations. Preliminary results attributing the original intelligibility differences to inter-carrier spectral differences will be discussed.

Work supported by NIDCD DC01625.

### **740 Loudness Adaptation in Acoustic and Electric Hearing**

**Qing Tang<sup>1</sup>**, Sheng Liu<sup>1</sup>, Fan-Gang Zeng<sup>1</sup>

<sup>1</sup>*Univ of California, Irvine*

Hearing and Speech Research Laboratory, Department of Biomedical Engineering, University of California, Irvine, California 92697-1275, USA

The present study aims to compare loudness adaptation between normal-hearing and cochlear-implant subjects. Loudness adaptation for 367-second pure tones was measured in normal-hearing subjects at three frequencies (125, 1000, and 5000 Hz) and three levels (30, 60, and 90 dB SPL). Similarly, loudness adaptation for 367-second pulse trains was measured in cochlear implant subjects at three stimulation rates (125, 1000, and 5000 Hz) and three levels (10%, 50%, and 90% of the electric dynamic range). In addition, electrodes were stimulated at apical, middle and basal cochlear position with both monopolar and bipolar modes. Five normal-hearing and five Clarion C-I cochlear-implant subjects participated in this experiment. Loudness adaptation was measured using the method of successive magnitude estimation. Similar to the previous results, we found that loudness adaptation increases with decreasing level and increasing frequency. In addition, we observed slight but significant loudness enhancement at 90 dB SPL. Despite the large individual variability, we found in cochlear-implant subjects that loudness adaptation depends on level, but not on stimulation rate, electrode and mode. The present results suggest that loudness adaptation is of most likely central origin, depending on the degree and distribution but not the phase locking of the neural firing.

### **741 The Effect of Poor Intensity Resolution in Individual Channels on Speech Recognition in Cochlear Implants**

**Chandra Throckmorton<sup>1</sup>**, Leslie Collins<sup>1</sup>

<sup>1</sup>*Duke University*

Although cochlear implant users often have good speech recognition in quiet, an implant still does not restore perception to the level of acoustic sensation. Acoustic models have recently been employed to explore the degree to which this can be attributed to limitations of the device or of physiology, e.g. the effects of insertion depth, number of channels, and dynamic range. Loizou *et al.*



(JASA, 2000) used acoustic models to investigate intensity resolution. The amplitude range of each channel was divided into the same number of quantization steps to model intensity resolution (fewer steps result in poorer resolution). Their results indicate that 4-8 steps provide asymptotic performance given a reasonable number of channels (8 or 6 out of 20). Fewer spectral channels increased the importance of intensity resolution in terms of speech recognition.

Nelson et al. (JASA, 1996) has demonstrated that intensity resolution may vary across the electrode array. This study focuses on the effect that poor resolution in individual channels may have on overall speech recognition. For this study, an eight-channel acoustic model was used in which one of the channels had only two quantization steps while the rest had sixteen. This allowed for determination of whether poor resolution in individual channels could affect speech recognition as well as whether the level of the effect was channel dependent. For the channels that contain a relatively small portion of speech energy (very low and very high frequency bands), poor resolution had little effect on speech recognition. The effects increased for channels containing a greater proportion of the speech energy. Also, consonant recognition tended to be more affected than vowel recognition indicating possible distortion of temporal information through the loss of intensity resolution.

#### **742 Identifying Poorly Performing Channels in Cochlear Implants through Confusion Matrix Analysis**

**Jeremiah Remus<sup>1</sup>, Leslie Collins<sup>1</sup>**

<sup>1</sup>*Duke University*

Impairments to the ideal speech presentation, which can result from various physiological or psychophysical conditions, are one factor affecting how much benefit severely deafened individuals receive from cochlear implants. Studies of the effects of impairments often use acoustic models to examine impairments on all channels; however isolated impairments affecting a small number of electrodes are more common and have been shown to negatively affect speech recognition performance. Assessing cochlear implant device performance on an electrode-by-electrode basis requires extensive, time-consuming tests.

In this study, methods for screening poorly performing electrodes are evaluated using vowel confusion data from normal-hearing subjects tested with acoustic models and cochlear implant patients. In normal-hearing subjects, confusion patterns for vowel tokens in noise with missing spectral information were measured using an eight channel acoustic model with individual channels removed. The missing channel model represents the most severe case of a poorly performing channel, with no speech information transmitted on the channel under investigation. Preliminary results indicate successful identification of the missing channels using the vowel confusion matrices for each acoustic model. Additionally, analysis of vowel confusion matrices from three cochlear implant patients, each previously identified as having indiscriminate

electrodes that significantly affect speech test performance, resulted in some success in identifying the indiscriminate electrodes, encouraging further investigation. A technique that quickly identifies potential poorly performing channels would allow researchers, and ultimately clinicians, to develop and implement alternate speech presentations that maximize transmission of critical speech information.

#### **743 The Impact of Limited Spectral Information and Pitch Anomalies on Melody Recognition in Cochlear Implants**

**Patrick Crosby<sup>1</sup>, Chandra Throckmorton<sup>1</sup>, Leslie Collins<sup>1</sup>**

<sup>1</sup>*Duke University*

As cochlear implant patients achieve greater success in understanding speech, examining areas in which implant performance is less than desired becomes important. Music perception requires relatively precise pitch information, thus presenting unique challenges to current speech-oriented implant designs that are limited in terms of spectral channels. In addition, anomalies associated with channel interactions that have been shown to affect speech perception may also impair music perception. Kong et al. (Ear & Hearing, 2004) investigated the effect of limited spectral information by measuring the ability of subjects to identify melodies with and without rhythm. They found that without rhythm, normal-hearing subjects may need as many as 32 spectral channels.

This study is an extension of the Kong et al. work. First, the effect of limited spectral information on melody recognition (with and without rhythm) was investigated in normal-hearing subjects using two acoustic models: all filters presented for each time sample (ranging from 2 to 32 filters), and 6 out of 20 filters (6/20F) presented for each time sample. Melody recognition improved as the number of spectral channels increased, including the case of the 6/20F model in which the number of presented filters is low but the number of spectral channels is high. Second, the effect of pitch anomalies on melody recognition was investigated. The pitch anomalies used were non-tonotopic pitch order and missing channels as described by Throckmorton and Collins (JASA, 2002) modeled in high, mid, and low frequency portions of the filter bank. With rhythm, these pitch anomalies had little effect on melody recognition. However, without rhythm, missing channels and, to some extent, pitch reversals resulted in a noticeable drop in performance. These results suggest that correction of pitch anomalies may be important for improving music perception, especially when accurate temporal information is not available.

#### **744 Sensitivity to Acoustic Speech Cues in Acoustic and Electric Hearing**

**Eric W. Healy<sup>1</sup>, Cheryl F. Rogers<sup>1</sup>, Allen A. Montgomery<sup>1</sup>**

<sup>1</sup>*Dept. Communication Sciences and Disorders, University of South Carolina, Columbia, 29208*

The majority of work measuring sensitivity to acoustic cues in cochlear implant (CI) users has employed simple stimuli presented directly to the electrode array. In the current

study, difference limens (DLs) were measured under conditions that more closely approximate natural listening conditions. Synthesized words were presented in soundfield to age-matched normal-hearing (NH) and CI listeners, who detected increases in either frequency, amplitude or duration in a middle stressed syllable using an adaptive 3I-2AFC procedure. In accord with previous work, frequency DLs were considerably larger than normal for the CI listeners. However, in contrast to previous work that has shown far finer than normal amplitude sensitivity, amplitude DLs for the CI listeners were equal to, or greater than, those of the NH listeners. Duration DLs also tended to be larger for the CI listeners. Greater sensitivity to isolated cues was only weakly associated with speech recognition scores of individual CI listeners, but the ability of individual CI listeners to combine simultaneously occurring frequency and amplitude cues was more strongly related to speech recognition. These results have the potential to clarify the abilities and limitations of both current device processors and their users. [Work supported by NIH/NIDCD]

### **745 Evaluation of a Noiseband-Based Cochlear Implant Simulator: Consonant Perception**

N. Ellen Taylor<sup>1</sup>, Karen Hardy-Bruce<sup>2</sup>, Thomas Talavage<sup>3,4</sup>, J. Brandon Laflen<sup>1</sup>, Mario Svirsky<sup>4</sup>, Heidi Neuburger<sup>4</sup>

<sup>1</sup>Rose-Hulman Institute of Technology, <sup>2</sup>Kettering University, <sup>3</sup>Purdue University, <sup>4</sup>Indiana University School of Medicine

Cochlear implants (CIs) are proven medical devices that can restore hearing to the profoundly hearing impaired, though with an efficacy that can vary significantly across individuals. Variability in perceptual performance, etiology of hearing loss, and the locations of electrode arrays in the cochlea have prompted the use of CI simulators with normal hearing (NH) listeners to evaluate optimal CI performance. However, it remains an open question whether noiseband-based simulators can produce auditory nerve activity that effectively models that produced by CI electrical stimulation.

Consonant identification (24 pre-recorded phonemes) was compared between 32 CI users at 1 year post-implantation, and NH listeners following 0 and 15 hours (21 and 10 listeners) of exposure to an 8-channel noiseband-based CI simulator configured to mimic a 6.5mm basalward shift. Confusion matrices were used to evaluate performance of the CI and NH groups for preservation of three phonemic features: voicing, place of articulation and manner of articulation. In addition to rates of correct identification, patterns of phoneme misidentification were evaluated using paired t-tests across the CI and NH groups. While preservation rates for each feature were similar over the set of phonemes, the performance on individual phonemes varied appreciably. Some phonemes (e.g., /aka/, /ara/) led to equivalent performance between the two groups, while others (e.g., /ada/, /ava/, /aza/) exhibited differences in patterns of confusion that were significant at the  $p < 0.05$  level.

Further, it was observed that the NH group performed significantly better (in terms of correct identification) after 15 hours of training than actual CI users after 1 year of implant use. These results suggest while noiseband-based CI simulators effectively model the acoustic signal degradation associated with real CIs, the encoding of speech in the auditory nerve produced by CI electrical stimulation is not yet well-modeled.

### **746 Speech Evoked Cortical Potentials as a Function of Cochlear Implant Channel Number**

Lendra Friesen<sup>1</sup>, Kelly Tremblay<sup>1</sup>, Neeru Rohila<sup>1</sup>, Richard Wright<sup>1</sup>, Robert Shannon<sup>2</sup>, Deniz Baskent<sup>2</sup>

<sup>1</sup>University of Washington, <sup>2</sup>House Ear Institute

Studies exploring the relationship between cortical auditory evoked potentials (CAEPs) and perception in cochlear implant (CI) listeners are generally based on CAEP waveform morphology, often without mention of implant parameters. This is potentially problematic because device factors could affect waveform morphology. For example, the number of active channels could be a confounding variable since the number of channels affects spectral and temporal information being delivered to the CANS. As the number of CI channels decrease, frequency resolution becomes poorer in the output signal from the device. If the number of active channels in the implant evokes different neural responses, erroneous conclusions could be made about auditory system development or the auditory systems ability to represent sound.

The purpose of this study was to determine if the number of active CI channels used affects the latencies and amplitudes of CAEPs and perception. For behavioral testing, 20 presentations of 12 CVC tokens from the Hillenbrand vowel test were presented to 7 normal hearing monolingual adults. Conditions consisted of unprocessed spoken words and processed versions simulating 2, 4, 8, 12, and 16 implant channels. Subjects were asked to select the token they heard. For the purpose of comparing perceptual and physiological responses, percent correct scores for the word /hid/ and /heed/ were extracted from the overall performance score. Then, those same stimuli were used to evoke the N1 and P2 responses. N1-P2 responses were evoked in six stimulus conditions (2, 4, 8, 12 and 16 channels, as well as the unprocessed version). For both speech tokens, CAEP waveform morphology differed as a function of channel number. Similar to our previously published findings, perception also changed as a function of channel number (Friesen et al. 2001). The relationship between perception and physiology, as a function of channel number, will be addressed. (Funded by NOHR)

## **747 Cochlear Implant-Mediated Listening of Rhythm, Melody, and Language: A H2-[15]O PET Study**

Charles Limb<sup>1,2</sup>, Anne Molloy<sup>1</sup>, Allen Braun<sup>1</sup>

<sup>1</sup>National Institutes of Health, <sup>2</sup>Johns Hopkins Hospital

Cochlear implant (CI) technology has revolutionized the treatment of profound sensorineural hearing loss. Rehabilitative efforts have thus far focused on language perception. Relatively little is known, however, about CI-mediated perception of non-linguistic auditory stimuli, such as music.

We used H2-[15]O PET to study brain activity in 4 adults who received right-sided CIs for postlingual deafness with at least one year of implant use. Four normal hearing adults were selected as controls. During scanning, subjects listened to rhythms, melodies, and sentences. Rhythms consisted of simple percussive patterns without pitch. Melodies consisted of popular children's songs played solely in quarter notes. Language stimuli consisted of CID sentences. After each scan, recall tasks were used to assess perception. Imaging data were smoothed, normalized, and realigned using SPM 99. Contrast analyses ( $p < 0.001$ ) were then performed to identify regions of activity in Talairach space.

For language, CI subjects had greater activity in bilateral middle temporal gyri compared to controls, whereas controls had greater activity in right inferior parietal lobule and left middle frontal gyrus. For melody, CI subjects had greater activity in left middle frontal gyrus and inferior parietal lobule, whereas controls had greater right superior frontal gyrus activity. Melody perception in CI patients was significantly worse than in controls. For rhythm, CI subjects had greater activity in right middle frontal gyrus, post- and pre-central gyrus, and left inferior parietal lobule activity, whereas controls had greater right inferior parietal lobule and left middle temporal gyrus activity.

These data allow the delineation of specific activation patterns in CI patients according to basic musical elements, and show differences between processing of musical and linguistic stimuli. These findings are germane to our understanding of CI-mediated listening of non-linguistic auditory stimuli.

## **748 Left Lateral Occipitotemporal Gyrus, not Primary Auditory Cortex, Predicts Outcome of Cochlea Implementation in Congenital Deaf Children**

YuneSang Lee<sup>1</sup>, Eunjoo Kang<sup>1</sup>, Hyejin Kang<sup>1</sup>, DongSoo Lee<sup>1</sup>, HyoJeong Lee<sup>2</sup>, Seung-Ha Oh<sup>2</sup>, Chong Sun Kim<sup>2</sup>

<sup>1</sup>Dept. of Nuclear Medicine, Seoul National University, College of Medicine, Seoul, Republic of Korea, <sup>2</sup>Dept. of Otolaryngology, Seoul National University, College of Medicine, Seoul, Republic of Korea

Brain plasticity is known to play a critical role in acquiring function of speech perception after cochlea implantation (CI) in congenital deaf. However, it is still controversial whether pre-surgical activity of primary auditory cortex (A1), or other cortical region is critical for CI outcome.

A group of congenital deaf children ( $n=36$ , age: 1.6 ~12.1 yr) were scanned with  $F^{18}$ -FDG PET before the CI surgery. 2 years later, auditory performance of CI-deaf children was measured with Korean version of CID (Central Institute of Deaf). Regions of interest of various regions (ROI) including A1 were delineated.

Left occipitotemporal gyrus was the only region showing a significant negative correlation between glucose metabolic activity of ROIs and CID score, not in A1 or superior temporal region. The extent of hypometabolic region within this area, compared to normal hearing adults was positively associated with the better auditory performance. No significant correlation with age or group difference was found in left occipito-temporal or A1.

These results suggest that congenital deaf children could well acquire auditory speech perception after CI, if their left occipitotemporal gyrus remains relatively less active until first influx of auditory signal. Further research will be required to understand how the brain plasticity of this region affects the level of speech hearing after CI.

## **749 Vocal Intensity Responses to Perturbations in Voice Loudness Feedback**

Charles Larson<sup>1</sup>, Jay Bauer<sup>2</sup>, Timothy Hain<sup>1</sup>

<sup>1</sup>Northwestern University, <sup>2</sup>University of Wisconsin Milwaukee

Recent studies have demonstrated compensatory voice fundamental frequency ( $F_0$ ) responses to perturbations in pitch feedback, suggesting close linkage between auditory feedback and voice control. These compensatory responses help to stabilize voice  $F_0$  around a target pitch. The present study tested the hypothesis that analogous compensatory mechanisms also help stabilize voice intensity. Twenty subjects produced sustained vowel phonations (/u/) at a normal (75 dB SPL) or soft (69 dB SPL) vocal intensity while receiving voice loudness-shifted stimuli (0 (control),  $\pm 1$ ,  $\pm 3$  or  $\pm 6$  dB SPL, 200 ms duration). Voice and auditory feedback waveforms were digitized on-line (10 kHz, 12 bit sampling, 5 kHz filtered), and subsequently transformed into an RMS wave in off-line analysis. Event-related averaging techniques were used to generate average changes of voice intensity following onset of the loudness-shifted feedback signal for each subject per block. A computer algorithm detected responses as a change in voice intensity beginning at least 50 ms following the stimulus and exceeding a magnitude of at least twice the SD of the pre-stimulus mean. Results showed that all subjects responded to the stimuli with compensatory changes in vocal intensity. There were greater numbers of responses to the 3 (76/80) and 6 (70/80) dB stimuli compared with the 1 (56/80) dB stimuli. Collapsed across stimulus magnitude, response magnitudes were significantly larger for the soft (0.99 dB) voice intensity condition compared to the normal (0.78 dB) voice intensity condition ( $F = 10.2$ ,  $df = 1,200$ ,  $p < 0.002$ ). Collapsed across voice intensity condition, response magnitudes were significantly greater for the 3 dB (0.99 dB) and 6 dB (0.98 dB) stimuli compared to the 1 dB (0.63 dB) stimuli ( $F = 10.7$ ,  $df = 2,199$ ,  $p < 0.0001$ ). Response latencies were significantly shorter for the 3 dB (377 ms)

stimuli compared with the 1 dB (430 ms) and 6 dB (437 ms) stimuli ( $F = 5.9$ ,  $df = 2,199$ ,  $p < 0.004$ ). There were no significant differences in latency as a function of sustained voice intensity condition. This study confirms the hypothesis that the audio-vocal mechanism responds to brief perturbations in auditory feedback loudness with compensatory vocal intensity responses. The likely function of this mechanism is to help stabilize voice intensity.

### **750** Speech Responses to Perturbations of Feedback Loudness

**Theda Heinks-Maldonado<sup>1</sup>**, John Houde<sup>1</sup>

<sup>1</sup>*University of California San Francisco*

One of the key questions about the neural control of speech production is the role that auditory feedback plays in the process. In this study we investigate if speakers show fast compensatory changes to brief perturbations of the loudness of their feedback. The subjects speech from the microphone was amplified and fed into an Eventide Ultraharmonizer (model 7000) that introduced brief (400ms) +/- 10dB perturbations to volume of the subject's speech. For both amplitude perturbation types we found compensatory responses in all subjects, which occurred at a similar latency to that previously observed in responses to pitch perturbations. We conclude that voice amplitude and pitch may be controlled by the same feedback system.

### **751** The Effect of Visible Speech on Perceptual Rating of Pathological Voices

**Huib Versnel<sup>1</sup>**, Jan Martens<sup>1</sup>, Philippe Dejonckere<sup>1</sup>

<sup>1</sup>*Dept of Otorhinolaryngology, University Medical Centre Utrecht*

Perceptual rating and acoustic measures are used in the speech voice clinic to evaluate voice disorders. A common rating tool is the GRBAS scale where G stands for grade, R for roughness, B for breathiness, A for asthenicity (hypofunction) and S for strain (hyperfunction). Common acoustic measures are among others jitter, shimmer and noise-to-harmonics-ratio. The rating is performed by experienced phoniatricians, laryngologists or speech therapists and it might vary considerably between raters. Ratings do not correlate well with acoustic measures, thus the former cannot simply be replaced by the latter.

We investigated whether visible speech shown to the rater influences the perceptual rating. The visible speech in our study consisted of spectrograms of a sustained vowel /a/. Specifically, the effect of visible speech on the interrater agreement and the correlation between acoustic and perceptual parameters was studied. Six experts evaluated seventy pathological voices in two sessions, first without and, after a few months, with visible speech. The GIBAS scale was used for voice assessment, where instability is an addition to the GRBAS scale. The multi-dimensional voice program (MDVP, Kay Elemetrics Corp.) was applied to obtain acoustic parameters of the sustained /a/.

We found a significant positive effect of the visible speech on the agreement among raters. The interrater agreement was larger with than without visible speech, especially for

roughness and breathiness. Thus, visible speech enhances the reliability of the GRBAS scale. Visible speech had no effect on the correlations between perceptual and acoustic parameters. This finding confirms the notion that pathological voices need to be multidimensionally assessed and that perception and acoustics are two distinct dimensions.

### **752** Release from Masking in Patients with Multiple Sclerosis

**David Lilly<sup>1</sup>**, Michele Hutter<sup>1</sup>, Richard Wilson<sup>2</sup>, Dennis Bourdette<sup>1,3</sup>, Stephen Fausti<sup>1</sup>, M. Samantha Lewis<sup>1</sup>

<sup>1</sup>*VA Medical Center, Portland, Oregon*, <sup>2</sup>*VA Medical Center, Mountain Home, Tennessee*, <sup>3</sup>*Oregon Health and Science University*

Multiple sclerosis (MS) is an immune-mediated disease of the central nervous system that, in its classic form, is characterized histologically by focal loss or destruction of myelin sheath (demyelination). We hypothesize that asymmetric demyelination of nervous tissue in segments of the auditory system can disrupt the normal timing and processing of binaural auditory information for some patients with MS. If, for a given patient, this situation reduces the masking-level differences (MLD) for 500 Hz and for speech, it also should reduce spatial release from masking and thus the patient's ability to understand speech in multi-talker babble.

The patient group for this study comprised 20 patients with a clinical diagnosis of "definite" MS and a control group of 20 subjects without MS. Each MS patient and each matched control was seen for three experimental sessions. During the first session we evaluated monaural auditory function. During the second session we evaluated: 1) masking-level differences for 500 Hz at comfortable levels that were judged to be equally loud; 2) masking-level differences for two-syllable words; and 3) performance on the Staggered-Spondaic-Word (SSW) test. During the third session we measured speech intelligibility binaurally in the sound field for short (IEEE) sentences in a babble surround of 16 speakers talking simultaneously. The target sentences always were presented at 65 dBA Leq. The babble was varied systematically over the range from +10 dB to -16 dB signal-to-noise ratio.

In this study, most of our patients with MS had significantly more difficulty understanding speech in a background of multi-talker babble than control subjects when both groups were matched with respect to age, to sex and to audiometric configuration. Moreover, for MS patients with this apparent reduction in spatial release from masking, masking-level differences for 500 Hz and for two-syllable words also were reduced. On average, these same MS patients also had a "left-ear deficit" on the SSW test.

### **753 Categorical Perception of Speech Stimuli in Children at Risk for Reading Disability**

Joshua Breier<sup>1</sup>, Jack Fletcher<sup>1</sup>, Lincoln Gray<sup>1</sup>

<sup>1</sup>University of Texas Medical School

Children determined to be at risk (n = 24) or not at risk (n=13) for reading difficulty listened to tokens from a voice onset time (VOT) (/ga/ - /ka/) or tone series played in a continuous unbroken rhythm. Changes between tokens occurred at random intervals, and children were asked to press a button as soon as they detected a change. For the VOT series, at-risk children were less sensitive than not-at-risk children to changes between tokens that crossed the phonetic boundary. Maps of the group stimulus space produced using multidimensional scaling of reaction times for the VOT series indicated that at-risk children may attend less to the phonological information available in the speech stimuli and more to subtle acoustic differences between phonetically similar stimuli than not-at-risk children. Better phonological processing was associated with greater sensitivity to changes between VOT tokens that crossed the phonetic boundary and greater relative weighting of the phonological compared to the acoustic dimension across both groups. Findings suggest a possible low-level mechanism for deficits in phoneme perception that have been observed in children with reading disability.

### **754 Speech Unmasking in Free Field in Preschool Children**

Soha Garadat<sup>1</sup>, Ruth Litovsky<sup>1</sup>

<sup>1</sup>University of Wisconsin-Madison

Previous work in our lab using spondees (CRISP) has shown that, similar to adults, children ages 4-7 show spatial release from masking (SRM) in free field on the order of 5-6 dB. Speech unmasking, however, has not been evaluated in very young children due to the lack of an age-appropriate test. This study validated a new test (CRISP-Jr) with age appropriate lexicon and interactive tools designed for preschoolers. The test was first validated through intra-subject SRTs comparisons in 4-5 year-olds using both tests. CRISP-Jr was then utilized to measure SRM in 3-year-old children. Targets were presented at 0° (front), in quiet, and in the presence of a speech interferer located either at 0° or 90°. Using a 4AFC paradigm, subjects pointed to a picture matching the heard target word and received feedback. Results show that the amount of masking and SRM in the 4-5 year-old group were comparable for the two tests, but SRTs were generally higher with the CRISP-Jr test. In the cross-age comparison, the 3-year-old children had higher SRTs than 4-5 year-olds; however, there was no difference between the two groups in the amount of masking or SRM. This suggests that auditory abilities involved in source segregation may be fairly well developed by early childhood.

### **755 Temporal Landmarks in the Ensemble Response of the Auditory Nerve Distinguish Stop Consonants for Naturally Produced and Shannon Synthesized Speech**

Jeremy Loebach<sup>1</sup>, Robert Wickesberg<sup>1</sup>

<sup>1</sup>University of Illinois

Although the perception of speech has been proposed to rely on features in the detailed frequency spectrum of the acoustic speech signal, studies have demonstrated that accurate perception occurs for speech signals that have been spectrally reduced (van Tasell et al, 1987; Shannon et al, 1995). Shannon and colleagues divided the acoustic spectrum of speech into 1 to 4 broad frequency bands, and used the amplitude envelopes for each band to modulate equivalent bands of noise. This produced a stimulus that lacked the spectral detail of the original stimulus, but preserved the overall temporal information. Shannon et al. (1995) found that as the number of bands in the stimulus increased from 1 to 4, subjects' accuracies in identifying the speech sounds increased from chance to near normal. Speech perception occurred with reduced spectral information, as long as the temporal information of the signal was maintained. The purpose of the present study was to examine the encoding of temporal information in the auditory nerve for naturally produced and Shannon speech.

Responses to naturally produced and 1, 2, 3 and 4 band Shannon versions of the tokens of /ba/, /pe/, /di/ and /to/ were recorded from individual auditory nerve fibers in ketamine anesthetized chinchillas. The ensemble response of the auditory nerve was computed for each token. Temporal patterns were observed in the ensemble responses to the natural tokens that could distinguish stop consonants across voicing and place of articulation. Similar patterns were observed for the Shannon tokens, with overall pattern similarity to the natural response increasing as the number of bands increased from 1 to 4. These physiological results parallel the findings of Shannon and colleagues. Sufficient temporal landmarks are contained in the ensemble auditory nerve response for the identification of stop consonants, and may be essential for their perceptual recognition.

### **756 Recognition of Temporally Smeared Time-Intensity Envelope of Speech as a Function of Signal-To-Noise Ratio**

Yang-soo Yoon<sup>1</sup>, David Gooler<sup>1</sup>

<sup>1</sup>University of Illinois

The goal of the study was to investigate the relationship between temporal processing ability and speech recognition as a function of signal-to-noise ratio (SNR). Stimuli were generated from 16 consonant-vowel (CV) sounds of the Linguistic Data Consortium. For each CV sound, the time-intensity envelope of speech was extracted from each of 26 critical bands by the Hilbert transformation. Temporal smearing of these processed signals was produced by applying low-pass filters with one of five cut-off frequencies (2, 4, 8, 16, and 32 Hz). Articulation matrices for 16 CV sounds in the forms of

unprocessed speech, processed speech without smearing, and processed speech with smearing were measured as a function of SNR (-5, 0, 5, 10, 25, and 100 dB). The results showed that the mean percent correct recognition across SNRs was dependent on the speech condition: 73.4% for the unprocessed speech, 37.96% for the processed without smearing speech, and 22.2% for the smeared speech. All measured values were well above chance (6.25%). Interestingly, SNR had a limited effect on CV recognition, especially for processed speech with and without smearing. Performance with unprocessed speech remained almost constant as SNR increased. Results for processed speech without smearing remained the same up to 10 dB SNR, and then gradually increase from 32% to 42% correct at 25 dB SNR. These results indicate that a similar amount of speech information was available to listeners even at the lowest SNR (-5 dB). Performance for processed speech with smearing remained about 22% independent of both SNR and amount of smearing. It suggests that there exists a SNR degrading temporal information maximally. It may also suggest that some temporal envelope cues such as manner, voicing, and segment duration are present in the lowest SNR and in narrowest band (2 Hz). The data suggest that listeners with hearing loss can have important prosodic information from envelope cues in between 2 and 32 Hz time-intensity variation.

### **757 A Time-Frequency Representation of Temporal Modulations in Critical Bands for Speech**

**Bryce Lobdell<sup>1</sup>, Sandeep Phatak<sup>1</sup>, Jont Allen<sup>1</sup>**

<sup>1</sup>*University of Illinois*

speech Plomp and Mimpen (1979) and Steeneken and Houtgast (1980), working with speech signals, were among the first to emphasize the importance of modulation processing to speech intelligibility. Houtgast (1989) [followed by Dau (1999)] argued that the auditory system detects modulation frequencies between 1/2 to 20 [Hz] via a modulation filter bank. These early conjectures were confirmed by Drullman (1994) who measured the intelligibility of speech signals having filtered modulation frequencies. Once these envelope modulation frequencies are reduced, recognition scores dropped. Shannon (1995) showed that decimating the spatial (place) resolution still allowed modest intelligibility of nonsense speech sounds. Finally Carlyon and Shamma (2003) showed, using physiological data, that the Ferret brain encoded these modulations. Given the importance of modulation processing to speech perception, there is a need for a visual representation of temporal envelope modulations in cochlear critical bands. A visual spectrographic tool called the CMSgram is described in which the intensity envelope is color coded by the modulation frequencies. Low (.5-4 Hz) frequencies are represented by red, mid (4-8 Hz) by green and high (8-20 Hz) by blue. We hypothesize that color-coded features in the CMSgram may be used to explain confusions in human perception of speech sounds. The CMSgram shows features which are not obvious in a spectrogram, but are known to be perceived. CMSgrams

of speech sounds will be compared across groups of confusable and non-confusable nonsense speech sounds.

### **758 Measuring Nonsense CV Confusions Under Speech-Weighted Noise**

**Sandeep Phatak<sup>1</sup>, Bryce Lobdell<sup>1</sup>, Jont Allen<sup>1</sup>**

<sup>1</sup>*University of Illinois*

Humans have a unique ability to accurately decode nonsense speech sounds in high levels of background masking noise. The focus of this research is to analyze the speech sound confusions via an under-utilized metric called the confusion matrix (CM)  $P_{\{s,h\}}(SNR)$ , defined as the probability of reporting sound 'h' after speaking sound 's'. A widely deployed alternative measure, the performance intensity (PI) function, is a certain average over the CM. Thus the CM contains key diagnostic information, like perceptual grouping of sounds, that is averaged away (i.e., removed) in the PI metric. Miller and Nicely (1955) (MN55) used the CM to analyze consonant confusions with "white" noise, and found that the consonants are perceptually grouped into three categories: Voice, Unvoiced and Nasals. As the SNR increases, the high frequency information, which is masked at lower SNR, becomes perceptible and the first two groups split into subgroups: Stop-Plosives and Fricatives. This has become a commonly used basis for classifying consonant sounds. However, a recent study (UIUC-summer04) for 4 vowels and 16 consonants, with speech-weighted noise, shows that these groupings depend on the background noise spectrum. A strong effect of the place of articulation on the perceptual groupings is observed in the UIUC-summer04 data. Unlike the flat-spectrum noise in MN55, the speech-weighted noise did not mask the high frequency information, resulting in less confusions and small groups for alveolar (/s/, /z/) and post-alveolar (/sh/, /zh/) fricatives. Since, the low frequency information was highly masked by speech-weighted noise, voicing errors were high. The nasals, which have the spectral energy concentrated at low frequencies, form a tight group (i.e., the two nasals are confused with each other, but not with other consonants). The dental (/f/, /v/) and labiodental fricatives (/th/ as in 'that', /th/ as in 'think') show a tight group, but with a very poor recognition rate, even at the best SNR. The CM is an excellent tool for analyzing the inner workings and diagnose the deficiencies of cochlear implants and hearing aids.

### **759 Speech Recognition with Amplitude and Frequency Modulations**

**Fan-Gang Zeng<sup>1</sup>, Kaibao Nie<sup>1</sup>, Ginger Stickney<sup>1</sup>, Ying-Yee Kong<sup>1</sup>, Michael Vongphoe<sup>1</sup>, Ashish Bhargave<sup>1</sup>, Chaogang Wei<sup>2</sup>, Keli Cao<sup>2</sup>**

<sup>1</sup>*University of California, Irvine*, <sup>2</sup>*Peking Union Medical College, Beijing*

Amplitude modulation (AM) and frequency modulation (FM) are commonly used in communication, but their relative contributions to speech recognition have not been fully explored. To bridge this gap, we derived slowly-varying AM and FM from speech sounds and conducted listening tests using stimuli with different modulations in

both normal-hearing and cochlear-implant subjects. We found that although AM from a limited number of spectral bands may be sufficient for speech recognition in quiet, FM significantly enhances speech recognition in noise as well as speaker and tone recognition. Additional speech reception threshold measures revealed that the FM advantage is particularly critical for speech recognition with competing voice and is independent of both spectral resolution and stimulus similarity. These results suggest that AM and FM provide independent yet complementary contributions to support robust speech recognition under realistic listening situations. Encoding FM may improve auditory scene analysis, cochlear-implant and audio-coding performance.

### **760 High Signal-To-Noise Ratio “Islands” and Their Role in the “Cocktail-Party Effect”**

**Pierre Divenyi<sup>1,2</sup>**

<sup>1</sup>VA Medical Center, Martinez, CA 94553, <sup>2</sup>East Bay Institute for Research and Education

Listening to the speech of a target talker in babble noise or reverberation distracters (=the “cocktail-party effect”, or CPE) affects intelligibility, especially for hearing-impaired and/or elderly individuals. However, normal-hearing young listeners can perform surprisingly well even in negative signal-to-noise ratio (S/N) situations. One likely reason for this is that, because the envelope fluctuations in both the target and the distracters produce relatively high S/N “islands”—kernels of mostly stressed syllables—that carry much needed information regarding speaker identity and spatial location, vowel identity, consonant manner and place of articulation, as well as sentence context. This information appears to facilitate access to target information in adjacent low-S/N segments in the signal that, without the “islands”, would be masked by the distracter. In the present experiments, we investigated the amount and type of information contained in the “islands” in various conditions influencing general and frequency-specific S/N, as well as their effect on overall intelligibility. The results suggest further explanation for poor CPE performance by elderly individuals with little or no hearing loss. [Supported by Grant AG-07998 by National Institute on Aging, and by the VA Medical Research.]

### **761 Speech Recognition in Sensorineural Hearing Loss as a Function of Spectral Channels and Implications for Cochlear Implants**

**Deniz Baskent<sup>1</sup>**

<sup>1</sup>House Ear Institute

Speech recognition by normal-hearing (NH) listeners improves as a function of spectral channels when tested with a noiseband vocoder simulating cochlear implant (CI) processing. Speech recognition by CI users, however, saturates around eight channels and does not improve as the number of electrodes activated increases (Friesen et al., J. Acoust. Soc. Am. 110, 2001). The main limiting factor is believed to be the current spread and the resulting channel interactions. In sensorineural hearing loss the

auditory filters are broadened, which might also result in reduced number of effective spectral channels (Turner et al., J. Speech Hearing Res. 42, 1999). The purpose of the present study is to investigate whether the limitation in the spectral information transmission in CIs comes from the reduced frequency-selectivity due to hearing loss or whether it is caused by the inefficiency of the implant processing in delivering the information. If the limitation comes from the auditory system rather than the device signal processing then simply increasing the number of channels of the device will not increase information transmission. HI subjects with moderate sensorineural hearing loss and NH subjects participated in the study. The speech stimuli were processed with noiseband vocoder with varying number of channels and in background noise of varying level. The stimuli were amplified linearly to comfortable listening levels for HI subjects, also maximizing the speech spectrum above the hearing threshold. To control for audibility effects, NH listeners were tested at different sound levels: same SPL and SL levels as HI group average and most comfortable listening level. To control for spread of activation NH group was tested with smeared filters. The preliminary results show a limitation in the performance of HI group in high background noise levels, similar to CI listeners, which can not be explained by limited audibility only.

[Supported by NOHR Grant.]

### **762 Incidental Complex Auditory Category Learning in a Computer Game Task**

**Travis Wade<sup>1</sup>, Lori Holt<sup>1</sup>**

<sup>1</sup>Carnegie Mellon University

This study examined the perceptual learning of spectrally complex non-speech auditory categories in a novel incidental, interactive multi-modal training paradigm. Participants played a computer game in which they were required to navigate through a three-dimensional space while responding appropriately to animated characters encountered along the way. Each character's appearance in the game correlated with a sound category distribution, a randomly selected member of which was repeated each time the character was encountered. As the game progressed, the speed and difficulty of required tasks increased and characters became gradually more difficult to identify by visual patterns alone. As a result, quick identification of approaching characters by means of sound patterns was, while never required or explicitly encouraged, of gradually increasing benefit. After a thirty-minute session, participants performed a categorization task, matching sounds to characters encountered during game play. Despite not being informed of audio-visual correlations beforehand, participants showed reliable learning of these patterns at post-test. Post-test performance was shown to be related to several measures of success at the game task, and learning was also sensitive to differences in category structure analogous to patterns seen in speech categories. Category knowledge resulting from the game was shown to be quantitatively different from that gained from an explicit grouping task involving the same categories. Results are discussed with respect to the mechanisms and information sources

involved in the acquisition of complex, context-dependent phonetic categories.

### **763 Hemispheric Lateralisation in Speech Perception Does not Arise from Simple Acoustic Properties of Speech Stimuli.**

**Sophie Scott<sup>1</sup>**, Stuart Rosen<sup>2</sup>, Richard Wise<sup>3</sup>

<sup>1</sup>University College London, <sup>2</sup>UCL, <sup>3</sup>MRC Clinical Sciences Centre

Many theories of the neural basis of speech perception posit that 'temporal' or 'rapid' features of the speech signal are both crucial to processing speech and are preferentially processed in the left temporal lobe. Typically, this is contrasted with 'spectral' or 'slow' processing preferences in the right temporal lobe. While there is considerable evidence from functional imaging studies for a right temporal preference for signals with pitch variation, this is not synonymous with 'spectral' processing. There is also no evidence for a left temporal lobe preference for the introduction of modulations in non-speech signals. We present a PET study, in which we separately manipulated the amplitude and spectral modulations in the speech signal, independently of speech intelligibility. Thirteen subjects listened passively to the acoustic stimuli. As with non-speech signals, amplitude and spectral modulations resulted in bilateral superior temporal responses. Additive effects of amplitude and spectral modulations, which sounded like unintelligible speech, were seen in the right superior temporal sulcus (STS), a result not predicted by theories of speech perception which link the left hemisphere to the acoustic properties of speech. In contrast, in the conditions where the additive effects were constructed to result in intelligible speech, the activation was strongly left lateralised in the anterior STS, suggesting that the left temporal lobe dominance in speech perception derives from domain specific linguistic processing, rather than non-linguistic acoustic processing.

### **764 Audio-Visual Integration in Speech Perception: An Fmri Study using the McGurk Effect**

**Sonja Tomaskovic<sup>1</sup>**, Lavinia Slabu<sup>1</sup>, Remco Renken<sup>1</sup>, Esther Wiersinga-Post<sup>1</sup>, Femke de Smit<sup>1</sup>, Hendrikus Duifhuis<sup>1</sup>

<sup>1</sup>Department of Biomedical Engineering, University of Groningen, BCN NeuroImaging Center

In speech perception both auditory and visual information is important. Especially in a noisy environment visual information can improve speech intelligibility. How auditory and visual information is combined is largely unknown. To investigate this process we used the McGurk effect. This effect is a useful tool for studying audio-visual (AV) integration, since, in the McGurk effect, the auditory perception is changed due to AV integration. E.g., when the speech sound /aba/ is presented while a moving mouth pronouncing the sound /aga/ is shown, hearing /ada/ indicates AV integration. In psychophysical experiments the strength of the McGurk effect was studied as a function of AV synchronicity. AV time shifts ranging from -520 ms to

+520 ms were used. Based on psychophysical data fMRI stimuli for minimum, intermediate or maximal strength of the McGurk effect were selected. The sparse sampling technique was used to record the fMRI data. Given the assumption that the strength of the McGurk effect reflects the strength of AV integration, we expected to find a correlation in brain activation and AV synchronicity of areas involved in AV integration. Preliminary results did not show such a correlation. In accordance with previous studies, we did find significant activation in auditory cortex for silent lip-reading.

### **765 Response of Auditory Cortex to Speech Feedback Perturbations**

**John Houde<sup>1</sup>**, Srikantan Nagarajan<sup>1</sup>, Theda Heinks-Maldonado<sup>1</sup>

<sup>1</sup>University of California San Francisco

Several studies have shown that speaking suppresses the normal response to speech sounds in auditory cortex and associated regions. Our own studies suggest that this suppression reflects a comparison between actual auditory input and a prediction of that auditory input. Based on these initial studies, we have developed a model, derived from modern control theory, for how auditory feedback is processed during speech production. Here, we test this model by using whole-head magnetic source imaging (MSI) to monitor activity in auditory cortex as speakers respond to brief perturbations of the pitch or amplitude of their speech. Prior studies and our own work have shown that such speech perturbations cause compensatory responses in speech motor output. MSI recordings were acquired at the onset of feedback perturbations as the subject continuously vocalized (speak) and also when the subject passively listened to recordings of the perturbed feedback (listen). For both conditions, the feedback perturbations caused M50, M100, and several subsequent response peaks, with most peaks delayed from their normal latency. No large differences were seen in M100 amplitude across conditions or perturbation types. However, for both M50 and the post-M100 response peaks, amplitudes were generally larger in the speak condition than in the listen condition for all perturbations.

### **766 Gone Fishing; Can We Hook the Modulators of Hair Cell Survival in Zebrafish Lateral Line?**

**Edwin W. Rubel**

**Abstract Unavailable**

### **767 Hearing Loss in Humans – Where are we in 2005?**

**Richard Smith<sup>1</sup>**

<sup>1</sup>University of Iowa

Nonsyndromic deafness is an extremely heterogeneous condition that most often segregates as a monogenic trait. As of September 2004, the Hereditary Hearing Loss Homepage reported 51 dominant, 39 recessive and 6 X-linked nonsyndromic deafness-causing loci, and 20, 21 and 1 genes, respectively, that encode a diverse spectrum



of proteins required for normal inner ear function. These proteins play biological roles as adhesion molecules (cadherin 23), in the cytoskeleton (diaphanous 1, espin), as enzymes (TMPRSS3) and extracellular matrix components (cochlin,  $\alpha 2(XI)$  collagen, otoancorin,  $\alpha$ -tectorin), in the gap junction system (connexin 26, connexin 30, connexin 31, connexin 43), as ion channels and transporters (KCNQ4, pendrin), integral membrane proteins (TMC1, TMIE), molecular motors (myosin IIA, myosin VI, myosin VIIA, myosin XVA), macromolecular organizers (harmonin), in synaptic function (otofelin), as tight junctions (claudin 14), in transcription as transcription regulators (EYA4, POU3F4, POU4F3, TFCP2L3) and in translation (12S rRNA tRNA-Ser(UNC)). Not unsurprisingly, the function of many other proteins is not yet known ( $\mu$ -crystalline, DFNA5, stereocilin, wolframin).

Exploring the interaction of these proteins is enabling us to define a more comprehensive model for the molecular basis of hearing and deafness, and to translate this knowledge back from the laboratory bench to the clinical arena. Already the evaluation of nonsyndromic deafness has been transformed from a diagnosis of exclusion to a definitive diagnosis based on molecular genetic analysis. The future promises a rich understanding of how mutations in specific proteins impact normal function to cause deafness. Based on this knowledge, gene- and mutation-specific habilitation options will be developed to provide therapeutic options for persons with defined types of deafness. Preventing progression or averting of some forms of deafness are goals that will be achieved in the not-so-distant future.

## **768 Histopathologic Phenotypes of Genetic Deafness in Humans**

Saumil Merchant<sup>1,2</sup>

<sup>1</sup>Massachusetts Eye and Ear Infirmary, <sup>2</sup>Harvard Medical School

There are over 350 different genetic conditions causing hearing loss but temporal bones from less than 50 of these syndromes have been examined to determine the histopathologic phenotypes. To date, over 60 genes responsible for hearing loss have been cloned, but the number of types of genetic deafness in which the molecular defect was known and the otopathology reported is less than 12 on a world-wide basis.

A knowledge of the pathologic basis of disease is central to the study of medicine, including disorders affecting the ear. Otology is unique in that the inner ear is inaccessible during life and so conventional techniques of pathologic studies such as biopsy and surgical excision are not feasible. Consequently, insight into the pathologic basis of ear disease can only be obtained by postmortem study of temporal bones. While animal models can provide valuable information regarding the molecular bases of inner ear disorders, it is important to verify the validity of these models by comparison with the human otopathology. Studying human specimens can also generate hypotheses regarding mechanisms of hearing loss which can then be tested experimentally in a suitable animal model. Thus,

human and animal otopathology become complementary to each other.

Some of the genetic deafness's where the histopathology has been reported and the molecular mutation ascertained include DFNA9, Waardenburg's syndrome, Mohr-Tranebjaerg syndrome, MELAS, Alport's syndrome and Usher's syndrome. These studies have shown that the histopathological phenotypes differ depending on the genetic defect. Some of these cases will be reviewed to highlight the implications of the phenotypes for understanding the pathophysiology of the hearing loss, for improving its diagnosis and for providing potential therapeutic targets for pharmacologic or gene therapy.

The application of molecular biologic assays involving genomics and proteomics to the study of temporal bones has the potential to transform our understanding of the pathophysiology of many genetic disorders. Before this promise can be realized, one has to overcome several serious technical obstacles that hinder the retrieval of genomic and proteomic information from the human inner ear. These technical challenges and potential solutions will be reviewed.

Supported by NIDCD.

## **769 A Molecular Geneticist's View of Mouse Models for Genetic Deafness**

Jian Zuo<sup>1</sup>

<sup>1</sup>St. Jude Children's Research Hospital

The use of transgenic and knockout mouse models is a powerful approach to the elucidation of gene function in the ear. Here I will present recent development on creating gene-targeted mice that include tissue specific knockout, knockin, transgenic overexpressing models. To create knockout mice, one can use the ready-to-use gene-trapped embryonic stem (ES) cells, targeting constructs, and ES cells with point mutations in specific genes. New targeting constructs can easily be created by modifying bacterial artificial chromosomes (BACs). For tissue specific gene targeting, the Cre-loxP technology has been proven efficient and nine independent mouse lines have been reported to date with Cre recombinase activity in the ear. Many of the mouse strains with loxP sites in specific genes of interest are already available. To achieve temporal control of gene expression in ear, one can use a new version of Cre (CreER). To overexpress genes of interest in specific tissues, one can create transgenic mice by modifying BACs with reporters such green fluorescent protein (GFP), or using the Cre-loxP technology. To reduce the expression of genes of interest, one can insert loxP sites and other selection markers in specific genes, and compare to heterozygous and homozygous knockout mice. To minimize variation in hearing phenotypes and avoid undesired hearing defects, mutant mice in the common gene-targeting background strains (129 and C57B6) should be transferred into congenic CBA/CaJ, a strain with "gold standard" normal hearing, by successive backcrosses. Valuable mutant strains can be maintained, distributed, and cryopreserved in one of four NIH-sponsored Mutant Mouse Regional Resource Centers.

Supported by the American Lebanese Syrian Associated Charities (ALSAC), NIH Cancer Center Support CORE grant (CA21765), and NIH grants to J.Z. (DC04761, DC05168, DC06471, EY12950, and MH61971).

### **770 Phenotype Assessment in Mouse Models of Genetic Deafness.**

**M. Charles Liberman**<sup>1,2</sup>, Stephane Maison<sup>1,2</sup>

<sup>1</sup>Massachusetts Eye and Ear Infirmary, <sup>2</sup>Harvard Medical School

The increasing ease with which the mouse genome can be manipulated in controlled and precise ways has made it an attractive model system in which to study the affects of genetic modifications on hearing. Transgenic mouse lines have been studied to better understand the normal function of particular gene products in the ear and to probe the mechanisms underlying a variety of hearing disorders. This talk will summarize 1) the current state-of-the-art with respect to techniques available to assess murine auditory function in vivo, and their relative strengths and weakness; and 2) some of the problems and pitfalls involved in phenotypic assessment which arise because of systematic differences among different inbred mouse strain, and because the creation of many transgenic lines involves hybridization of the genome of two different inbred strains. Research supported by RO1 DC0188 and P30 DC005209

### **771 Mouse Models for Usher Syndrome**

**Karen P Steel**<sup>1</sup>, Richard Libby<sup>2</sup>, Ralph Holme<sup>2</sup>, Walter Marcotti<sup>3</sup>, David Williams<sup>4</sup>, Corne Kros<sup>3</sup>

<sup>1</sup>Wellcome Trust Sanger Institute, <sup>2</sup>MRC Institute of Hearing Research, <sup>3</sup>University of Sussex, <sup>4</sup>University of California San Diego

People with the most severe form of Usher syndrome have deafness and balance problems from birth, and develop progressive retinitis pigmentosa during the first decade of life. At least eleven genes can be involved in Usher syndrome, and several of these have been identified following discovery of the mouse orthologue. We have examined mice with mutations in two of these genes, *Myo7a* and *Cdh23*. Both show primary defects of the stereocilia bundle projecting from the top of sensory hair cells in the inner ear. This bundle normally forms a neat V-shaped array on cochlear hair cells, but in the mutants, the array becomes progressively more disorganised during development. Electrophysiological recordings from single *Myo7a* mutant hair cells together with the known localisation of *Myo7a* protein just below the cell membrane covering the stereocilia suggest that *Myo7a* serves to anchor the cell membrane to the actin core, and loss of this anchoring function affects the mechanical opening of the transduction channel located in stereocilia membranes as well as cohesion of the bundle into its normal array. In the eye, electroretinography reveals reduced a- and b-wave amplitudes in some mutant alleles of *Myo7a* and *Cdh23*, and these mutants are also relatively resistant to light-induced retinal damage, suggesting that *Myo7a* and *Cdh23* molecules are involved in photoreceptor cell activation. These findings provide clues to the underlying

pathological processes in humans with *MYO7A* and *CDH23* mutations.

### **772 Mouse Models of Branchio-Oto-Renal (BOR) Syndrome**

**Rick A Friedman**<sup>1</sup>

<sup>1</sup>House Ear Institute

The development of the mammalian ear is directed by a series of tissue movements and inductive interactions that promote spatial patterning and cellular differentiation. The identification of genes intimately involved in these processes is facilitating our understanding of the complexity of ear development and the molecular pathogenesis of some forms of inherited hearing loss. Genetic hearing loss can be divided into two broad classes, nonsyndromic and syndromic. A number of forms of syndromic hearing loss demonstrate anomalies of one or more compartments of the ear (outer, middle and/or inner), suggesting an early developmental effect. One such autosomal dominant form, Branchio-Oto-Renal syndrome (BOR), has been described both clinically and genetically. A mutation in the human homologue of the *Drosophila* eyes absent (*EYA1*) was identified in affected individuals. We have recently described a mouse model of BOR syndrome arising from the insertion of a transposon in *Eya1* resulting in a hypomorph with inner ear and kidney anomalies. Utilizing this model we have begun to understand the developmental events underlying failed neurogenesis in this disorder. Further, we have utilized the genetic heterogeneity of mouse strains to begin to decipher the genetics of variable penetrance and expressivity in this form of syndromic hearing loss.

### **773 Evolution of the Mammalian Middle Ear**

**Gerald Fleischer**<sup>1</sup>

<sup>1</sup>Auditory Research - University of Giessen

Mammals are highly successful, living in all habitats of the world. Their body mass ranges from a few grams up to more than hundred metric tons. They adapted to flying, running, burrowing, to deep diving, and, of course, to the enormous variety of our technical environment. Frequency range of hearing extends from a few Hz up to more than 100 kHz. Although it may not be apparent, the middle ear evolved in various directions, starting with a humble collection of elements. In order to adapt to special requirements, great structural changes were needed. This evolutionary radiation tells a fascinating story of functional plasticity and adaptability.

Ears of 230 different mammalian species were anatomically examined. The samples included species of all sizes, from the tiniest shrews up to the huge baleen whales. All major biological types were covered, including man. Purpose of this survey was the collection of structural data for an understanding of the biomechanical aspects.

Starting from a primitive ancestral form, three major lines of structural and functional adaptations can be seen. One is towards a freely mobile ossicular chain, specialized

predominantly for low frequencies, as in man. Another is towards very small middle ears, specialized for high ultrasonic frequencies, as in bats. The third major line is towards the middle ear as found in dolphins and whales. Here, structural modifications of the skull were required, to achieve directionality of hearing. To adapt to the perception of high frequencies, dolphins gradually replaced the tympanic membrane by a thin ceramic-like bony plate and deeply modified the ossicular chain. In baleen whales, specialists for far-ranging low frequencies, the middle ear developed a mechanical low-frequency receiver that drives the ossicular chain. - These enormous structural developments across mammals were achieved by using and modifying the same basic components.

## **774 Non-Destructive Imaging for Middle Ear Research: Techniques and Application**

### **Examples**

**Willem F.S. Decraemer**<sup>1</sup>, Joris J.J. Dirckx<sup>1</sup>, W. Robert J. Funnell<sup>2</sup>

<sup>1</sup>*University of Antwerp*, <sup>2</sup>*McGill University*

The quantitative measurement of the three-dimensional (3-D) anatomy of the ear is of great importance in the making of teaching models and the design of mathematical models of parts of the ear, and also for the interpretation and presentation of experimental results. We will show how we used virtual sections from a commercial high-resolution x-ray computed tomography (CT) scanner to make realistic 3-D anatomical models for various applications in our middle-ear research. The important problem of registration of the 3-D model within the experimental reference frame is discussed. The commercial x-ray CT apparatus is also compared with x-ray CT using synchrotron radiation, with magnetic resonance microscopy, with fluorescence optical sectioning, and with physical (histological) serial sections. We will also show that Region-of-Interest scanning can be used to increase scanning resolution.

As an application example we will show how a 3-D model of the middle-ear ossicles can be used to transform experimental middle-ear ossicle vibration data into anatomically defined intrinsic reference systems. This is the same reference system used for mathematical middle-ear models, so that direct evaluation of computed results versus experimental data is possible. Animation of 3-D malleus motion, for example, also becomes more meaningful when presented in an appropriate intrinsic reference system. We will also show how the design of precise mathematical models can benefit from high-quality anatomical data nowadays provided by CT scanners. With the introduction of automation in the process of extracting 3-D models from an image stack of virtual sections it becomes possible to make dedicated mathematical models when different temporal bones are used in different experiments. An example of using templates for automatic segmentation will be shown.

Supported by Fund for Scientific Research (Flanders, Belgium), RAFO funding of the University of Antwerp and CIHR (Canada)

## **775 An Anatomical, Physiological and Mechanistic Analysis of Hearing Loss in Otosclerotic Middle Ears before and after Stapes Surgery**

**John Rosowski**<sup>1</sup>, Saumil Merchant<sup>2</sup>

<sup>1</sup>*Massachusetts Eye and Ear Infirmary*, <sup>2</sup>*Massachusetts Eye & Ear Infirmary*

Otosclerosis is a disease marked by the abnormal growth of bone around the stapedio-vestibular joint within the oval window. The new bone interferes with the sound-induced motion of the stapes producing conductive hearing losses of as large as 50-60 dB. The standard treatment for otosclerosis is surgical and entails the placement of an artificial stapes. The basic approach to 'stapedectomy' was developed nearly 50 years ago, but the procedure has been continuously refined since that time. We will review some recent work (performed by us and others) on the development of otosclerotic hearing loss as well as physiologic measurements and model analyses of middle-ear function in post-stapedectomy ears. The reviewed analysis of pathological anatomy and hearing in pre-surgery ears points out that the conductive hearing loss in otosclerosis is more closely related to changes in the ligamentous stapedial-vestibular joint (the annular ligament), and less related to bony fixation of the stapes. The model analysis suggests that the post-surgical results depend greatly on the diameters of the piston used as the replacement stapes and of the fenestra in which the piston sits; larger diameters are associated with improved hearing results. The analytic conclusions regarding the mechanism and degree of influence of the piston diameter on hearing results are supported by post-surgery hearing measurements as well as physiological results in live humans and mechanical measurements in cadaveric human temporal bones.

[Work Supported by the NIDCD]

## **776 The Influence from the Middle Ear Ossicles on Hearing by Bone Conduction**

**Stefan Stenfelt**<sup>1</sup>

<sup>1</sup>*Department of Signals and Systems, Chalmers University of Technology, Göteborg, Sweden*

Bone conduction (BC) stimulation involves several different physical and physiological phenomena and the literature have divided them and ascribed their importance differently. One common division used is to divide the BC components anatomically: (1) the outer ear, (2) the middle ear, and (3) the inner ear component. Here, the focus is on the middle ear component and the inertia of the ossicles that can influence hearing by BC. One way to investigate the effect of middle ear inertia on hearing by BC is by comparing the ossicles displacement at threshold stimulation by AC and BC. One may argue that, since the stapes footplate motion at AC stimulation can be seen as the input to the cochlea, similar stapes footplate displacement at hearing threshold with AC and BC stimulation indicates that the middle ear ossicles (or sound transmitted to the ear canal) do contribute to BC hearing. However, the motion at the stapes footplate can also be a

reflection of the fluid flow in the cochlea; the source for the footplate motion is the fluid flow in the cochlea and not the ossicles. A comparison of the stapes footplate displacement at human behavioral thresholds with AC and BC stimulation reveals that the relative footplate displacement with BC stimulation is 5 to 15 dB below that of AC stimulation for frequencies below 1 kHz. Between 1.1 and 1.8 kHz the displacements are similar, and for frequencies over 3 kHz, the BC footplate relative displacement is 10 to 25 dB greater than the AC footplate displacement at threshold stimulation. To better understand these results, a model for the ossicular inertia combined with a model of the inertial and compressional forces in the cochlea with BC stimulation was derived and fitted to measured data. The results from this model will be discussed in relation to the BC contribution from the middle ear ossicles. Moreover, the model explains some of the hearing effects found in middle ear pathologies.

### **777 Probing Human Middle-Ear Function using Otoacoustic-Emission and Reflectance Measurements**

**Douglas Keefe<sup>1</sup>**

<sup>1</sup>*Boys Town National Research Hospital*

The mechanics of the middle ear influence the forward propagation of acoustic energy from the ear canal to the region of otoacoustic emission (OAE) generation on the basilar membrane as well as the reverse propagation of the OAE from the cochlea back to the ear canal. Thus, an OAE measurement provides information on both cochlear and middle-ear function, but the problem remains of separating out their functional contributions. This presentation will review research related to this problem. Measurements of forward and reverse transmission through the middle ears of human-cadaver temporal bones and of animals quantify the middle-ear contribution, although such invasive measurements cannot be performed in human subjects. Using measurements of distortion-product and stimulus-frequency OAEs, methods based on the assumption of scaling invariance in the cochlea have been proposed to estimate non-invasively and indirectly the forward and reverse middle-ear transmission gains. Direct acoustical ear-canal measurements of middle-ear function that may be performed in human subjects include tympanometry and wideband acoustic transfer functions (ATF) such as reflectance and admittance. The wideband, input pressure spectrum to the middle ear at the tympanic membrane (TM) may be estimated using mid-canal pressure and reflectance measurements, and is similar to non-invasive spectral measurements on the TM using vibrometry. Just as OAEs predict the presence of a sensorineural hearing loss, so do ATFs predict the presence of a conductive hearing loss. This suggests that combined measurements may have clinical utility in hearing screening and diagnostic applications. One example is the ability of wideband ATFs to identify transient middle-ear pathology in a newborn hearing screening population, which may be useful in interpreting responses in normal-hearing infants in whom OAEs are absent. (Research supported by NIDCD grant DC003784)

### **778 The Middle Ear Does not Limit the Bandwidth of Hearing**

**Mario Ruggero<sup>1</sup>, Andrei Temchin<sup>1</sup>, Luis Robles<sup>2</sup>, Yun-Hui Fan<sup>1</sup>**

<sup>1</sup>*Northwestern University, <sup>2</sup>Universidad de Chile*

Ruggero and Temchin (PNAS 99: 13206-13210, 2002) reviewed the role of the middle ear of amniotic vertebrates after realizing that, in gerbil, 1) the bandwidth of stapes velocity is greater than that of behavioral thresholds; 2) neural thresholds and scala-vestibuli pressure near the stapes are comparably sensitive at ultrasonic and lower frequencies; 3) basilar-membrane vibrations near the stapes are as sensitive as those at more apical sites. The review showed that the bandwidth of stapes velocity is also greater than that of behavioral thresholds in turtle, pigeon, guinea pig, bat and chinchilla. At least in chinchilla, and probably also in guinea pig, the incudo-stapedial joint selectively boosts the magnitude of high-frequency vibrations (by 16 dB at 25 kHz, on average) [see abstract by Robles et al., this ARO MW meeting, 2005]. Phase-vs.-frequency curves of pressure in scala vestibuli in gerbil and of stapes vibration in gerbil, cat and chinchilla have roughly constant slopes (corresponding to pure delays) over wide frequency ranges. The foregoing evidence suggests that the middle ears of amniotic vertebrates act as nearly-ideal pressure transformers, with tympanic-membrane and incudo-stapedial joint responses combining to produce a wide-band input to the cochlea. In stark contrast, stapes vibrations in the temporal bones of human cadavers appear to be frequency-tuned at around 1 kHz. However, comparisons of the magnitudes of umbo or stapes vibrations in-vivo and post-mortem suggest that for frequencies > 1-2 kHz the former exceed the latter by amounts directly proportional to stimulus frequency (growing at a rate of 6 dB/octave). Furthermore, the bandwidth of umbo vibrations in living humans exceeds that of the audiogram. If post-mortem ossicular-vibration measurements sufficiently underestimate their in-vivo bandwidth, it may turn out that middle-ear transmission is as efficient and wide-band in humans as in other vertebrates.

### **779 An Approach Towards Understanding the Functional Consequences of Middle Ear Anatomy**

**Sunil Puria<sup>1,2</sup>, Jonathan Fay<sup>1</sup>, Charles Steele<sup>1</sup>**

<sup>1</sup>*Stanford University, Department of Mechanical Engineering, Mechanics and Computation Division,*

<sup>2</sup>*Department of Otolaryngology-Head and Neck Surgery, 300 Pasteur Drive, Stanford, CA 94305*

The functional significance of many gross anatomical features of the mammalian middle ear has yet to be understood. For example, why does the tympanic membrane (TM) have a conical shape? What is the advantage of its angular placement in the ear canal? Why do the TM sublayers have highly organized collagen fiber structure? Why does the malleus-incus interface have two saddle-shaped gaps as first described by Helmholtz? Moreover, what role do the suspensory ligaments play in the complicated 3D vibrations of the middle ear bones?

We address these issues in a biomechanical model of the cat and human middle ear. Asymptotic methods are used to calculate model responses (Fay, 2001 PhD Thesis, Stanford University), which differ from finite-element methods. The anatomical description for the cat middle ear is taken from the published literature whilst for the human middle ear we have developed methods to obtain morphometry from a microCT (Scanco, vivaCT 40) imaging system (Sim et al, ARO 2005). Anatomical data is combined with human cadaver temporal bone TM velocity, as a function of radial position, and 3D motions of the malleus-incus complex, in the computational model for individual ears. Results suggest that with a flat TM, sound transmission to the cochlea is reduced above a few kHz. An angular placement in the canal results in a larger area of the TM for the same canal diameter, which increases the middle ear pressure gain. The radial fibers on the inner portion of the TM results in effectively an orthotropic membrane while the outer circumferential fibers provide a low-impedance beam-like support for the higher impedance but orthotropic central portion allowing maximal sound transmission at both low and high frequencies. Our working hypothesis is that the suspensory ligaments are arranged with minimal pretension while maximizing motions along a rotational axis perpendicular to the stapes head. [Work supported in part by grant No. DC005960 from the NIDCD of NIH.]

### **780 Calcium Buffers in Mammalian Cochlear Hair Cells**

Shantini Mahendrasingam<sup>1</sup>, Robert Fettiplace<sup>2</sup>, Carole Hackney<sup>1</sup>

<sup>1</sup>Keele University, <sup>2</sup>University of Wisconsin-Madison

Endogenous calcium buffers ensure the spatial and temporal separation of calcium signaling pathways in hair cells. Here we used an immunoprecipitation technique to investigate their concentrations in hair cells before and after the onset of hearing (p12). Cochleas from young rats (p7 and 16) were fixed and embedded in LR-White resin. Ultrathin sections from apical and basal turns were incubated in polyclonal antibodies to calbindin and calretinin (Chemicon), parvalbumin- $\alpha$  (PV- $\alpha$ ) and parvalbumin- $\beta$  (PV- $\beta$ ) (SWant) or a monoclonal antibody to PV- $\beta$  (thanks to Dr MT Henzl) followed by gold-conjugated secondary antibodies. To determine their concentrations, measured amounts of each protein were dissolved in 10% bovine serum albumin in phosphate buffer, fixed to form gels and embedded in resin. Sections of each gel were labeled as for cochlear sections and concentrations calculated from comparative gold densities. PV- $\beta$  occurs at ~2 mM in outer hair cells (OHCs) and at <10  $\mu$ M in inner hair cells (IHCs) post-hearing. PV- $\beta$  is expressed at lower levels in pre-hearing OHCs (~0.25 mM) with more at the cochlear base than the apex. Calbindin-D28k is at higher levels pre-hearing in both IHCs and OHCs but levels fall to 0.2 mM or less post-hearing with the highest levels being found in the apical OHCs. PV- $\alpha$  and calretinin (which also occurs in supporting cells) occur at low levels (20-80  $\mu$ M) post-hearing in both types of hair cells with the level of PV- $\alpha$  falling in the IHCs between p7 and p16. Thus, IHCs appear to have lower levels of calcium buffering than

OHCs. This low level accords with estimates from physiological measurements (Moser and Beutner, 2000: Proc Natl Acad Sci 97:883-8) and with other biochemical findings (Yang et al. 2003: J. Neurobiol. 58: 479-92). The high concentration of calcium buffer in OHCs is comparable with skeletal muscle and implies an important role for calcium in their function. (Supported by the Steenbock endowment and NIH R01 DC01362).

### **781 Ca<sup>2+</sup> Current-Driven Nonlinear Amplification by the Mammalian Cochlea in Vitro**

Dylan Chan<sup>1</sup>, A.J. Hudspeth<sup>1</sup>

<sup>1</sup>The Rockefeller University

Two mechanisms have been proposed to underlie the mammalian cochlear amplifier: receptor-potential-based electromotility and Ca<sup>2+</sup>-driven active hair-bundle motility. To link the macroscopic phenomenology of the cochlear amplifier with these cellular mechanisms, we developed an *in vitro* preparation of the gerbilline cochlea that affords optical access to the sensory epithelium while mimicking its *in vivo* ionic and electrical environments. A two-compartment recording chamber permitted separation of endolymph and perilymph, and an applied transepithelial current reproduced the endocochlear potential. The preparation demonstrated intact forward and reverse mechanotransduction. Acoustic stimulation elicited microphonic potentials that were reversibly abolished by the transduction-channel blocker amiloride and by replacement of K<sup>+</sup> as the primary monovalent cation in the endolymph with the channel-impermeant NMDG. Transepithelial currents elicited electrically evoked hair-bundle movement. To assess the mechanical response of the cochlear partition, we measured the displacement of an inner-hair-cell hair bundle in response to acoustic frequency sweeps from 0.3-3.0 kHz, which spans the characteristic frequencies of the preparation. The response revealed a striking resonance and compressive nonlinearity diagnostic of the active process. Transduction-current blockade with amiloride abolished nonlinear amplification, whereas eliminating all but the Ca<sup>2+</sup> component of the transduction current by using NMDG-based endolymph did not. Turning the endocochlear potential on and off permitted fast and reversible observation of cochlear amplification; this manifestation of the active process also was sensitive to amiloride but persisted in the presence of NMDG-based endolymph. These results suggest that the Ca<sup>2+</sup> current is necessary and sufficient to drive the cochlear active process and support the hypothesis that active hair-bundle motility underlies cochlear amplification.

### **782 Fast Adaptation and Hair Bundle Mechanics in Rat Outer Hair Cells**

Robert Fettiplace<sup>1</sup>, Helen Kennedy<sup>2</sup>, Andrew Crawford<sup>3</sup>

<sup>1</sup>University of Wisconsin-Madison, <sup>2</sup>Bristol University, UK, <sup>3</sup>University of Cambridge, UK

The properties of the hair cell mechano-electrical transducer (MET) channels and how they influence hair bundle mechanics have been well documented in lower

vertebrates. In the turtle, transduction exhibits fast adaptation with a time constant varying inversely with hair cell characteristic frequency (CF). Fast adaptation reflects calcium-dependent re-closure of the MET channels, which can in turn elicit a mechanical reaction that moves the hair bundle. To extend these results to mammals, we have recorded MET currents in outer hair cells of acutely isolated cochleas of P6 to P12 rats. In response to step deflection of the hair bundle, MET currents activated with a time course indistinguishable from the stimulus, and then adapted with a time constant less than 0.1 ms. As in turtle, both the size and adaptation rate of the current depended on external calcium concentration. Comparison of two cochlear locations with CFs of 4 and 14 kHz showed that cells with the higher frequency location had larger MET currents and faster adaptation than those at the lower frequency location. We also examined the mechanical properties of outer hair cell bundles using stimulation with flexible fibers whose motion was determined by photodiode imaging. The force-displacement relationship of the hair bundle was very non-linear over the range where the MET channels were gated and in some cells showed evidence of a negative slope region similar to that previously observed in frog saccular hair cells. The non-linearity was sensitive to external calcium and developed with a time course similar to fast adaptation. We conclude that fast adaptation in outer hair cells operates on a time scale appropriate for cycle-by-cycle regulation at the hair cell CF. We suggest adaptation is linked to force generation by the hair bundle that may contribute to the cochlear amplifier.

Supported by NIH grant RO1-DC01362 to RF.

### **783 Fast Electromechanical Amplification in the Lateral Membrane of the Outer Hair Cell.**

**Joseph Santos-Sacchi<sup>1</sup>, Lei Song<sup>1</sup>, Enrique Navarrete<sup>1</sup>**

<sup>1</sup>*Otolaryngology and Neurobiology, Yale University*

Prestin shows a behavior somewhat akin to, but notably different from the stereociliar bundle adaptation process. That is, during a step voltage stimulus there is a time-dependent shift in the motors' Boltzmann distribution along the stimulus axis, but unlike bundle adaptation, the shift is of opposite polarity, resulting in mechanical amplification, not adaptation (Santos-Sacchi et al., 1998). While we have modeled this process as resulting from a relaxation in voltage dependent membrane tension, the recent discovery of chloride's role in prestin activity and a lateral membrane chloride conductance may prove significant. Here we report on the speed, and Cl and tension dependence of this amplificatory process.

One way to evaluate the speed of this phenomenon is to follow the exponential change in prestin-generated nonlinear capacitance (NLC) during a step change in voltage, as it arises from the shift in NLC voltage dependence. We have measured rates which are well fit with a stretched exponential function, indicating a multi-exponential process. Exponential components below 1 ms are found, and are likely limited by the speed of voltage clamp. In order to determine whether lateral membrane chloride flux and accumulation within the sub-plasma

membrane space contribute to the process, we made measures with different chemical driving forces for chloride across the OHC membrane under whole cell voltage clamp (Cl: 5 mM patch pipette; 1,5,140 mM extracellular). Regardless of extracellular chloride concentration, the amplificatory process and its time course remained intact. We then compared the time course of NLC shift due to a rapid change in tension of the OHC membrane before and after trypsin digestion of the cytoskeleton. In either case, the exponential components present during voltage steps were not apparent. These results may indicate that the amplificatory process is intrinsic to prestin and not governed by either membrane tension or chloride flux.

Supported by NIH NIDCD DC 00273.

### **784 Calcium-Calmodulin-Dependent Contraction in Auditory Hair Cells of the Frog Inner Ear.**

**Nasser Farahbakhsh<sup>1</sup>, Peter Narins<sup>1</sup>**

<sup>1</sup>*UCLA*

At the last ARO meeting (2004), we reported that in hair cells of the rostral segment of the amphibian papilla (AP), from the leopard frog, *Rana pipiens*, increases in the concentration of the intracellular free calcium, induce cell-length shortening. These shortenings are composed of two partially-overlapping phases: an initial rapid iso-volumetric contraction, and a slower length decrease accompanied with swelling, suggesting movement of salt and water across the cell membrane in the latter case. We now show that it is possible to unmask the iso-volumetric contraction by delaying the cell swelling with the help of K<sup>+</sup> or Cl<sup>-</sup> channel inhibitors, such as quinidine or furosemide. Furthermore, it appears that the longitudinal contraction in these cells is Ca<sup>2+</sup>-calmodulin-dependent. In the presence of W-7, a calmodulin inhibitor, only a slow, swelling-dependent phase could be observed. These findings suggest that in contrast to the mammalian auditory outer hair cells, the amphibian rostral AP hair cells possess a Ca<sup>2+</sup>-calmodulin-dependent contractile mechanism capable of mediating length change in response to extracellular stimuli. Such a mechanism might be utilized by the auditory efferent neurotransmitters for adaptive modulation of sensitivity and frequency selectivity in the amphibian papilla.

Supported by NIH grant no. DC-00222 to PMN.

### **785 Extracellular Potentials and the Cochlear Amplifier**

**Anders Fridberger<sup>1</sup>, Jacques Boutet de Monvel<sup>1</sup>, Jiefu Zheng<sup>2</sup>, Ning Hu<sup>2</sup>, Yuan Zou<sup>2</sup>, Tianying Ren<sup>2</sup>, Alfred Nuttall<sup>2,3</sup>**

<sup>1</sup>*Karolinska Institutet, Stockholm, Sweden*, <sup>2</sup>*Oregon Health & Science University, Portland, OR*, <sup>3</sup>*Kresge Hearing Research Institute, Univ. of Michigan, Ann Arbor, MI*

During sound stimulation, receptor potentials are generated within the sensory hair cells of the cochlea. Prevailing theory states that outer hair cells use the potential-sensitive motor protein prestin to convert receptor potentials into fast alterations of cellular length or stiffness

that boost hearing sensitivity almost 1000-fold. However, receptor potentials are attenuated by the filter formed by the capacitance and resistance of the cell's membrane. This attenuation would limit cellular motility at high stimulus frequencies, rendering the above scheme ineffective. Therefore, Dallos and Evans (Science 267:2006-9, 1995) proposed that extracellular potential changes within the organ of Corti could drive cellular motor proteins. These extracellular potentials are not filtered by the membrane. To test this theory, both electric potentials inside the guinea pig organ of Corti and basilar membrane vibration were measured in response to acoustic stimulation. Vibrations were measured at sites very close to those interrogated by the recording electrode, using laser interferometry. Close comparison of the measured electrical and mechanical tuning curves and time waveforms, and their phase relations revealed that those extracellular potentials indeed could drive outer hair cell motors. However, to achieve the sharp frequency tuning that characterizes the basilar membrane, additional mechanical processing must occur inside the organ of Corti.

Supported by the Swedish Research Council and NIH NIDCD DC 00141.

### **786 Basilar-Membrane Responses in the Cochleae of Adult Chinchillas and Gerbils, Either Post-Mortem Or In-Vivo, Do not Have the Minimum-Phase Property**

**Yun-Hui Fan<sup>1</sup>, Mario Ruggero<sup>1</sup>**

<sup>1</sup>Northwestern University

In minimum-phase systems, a given amplitude response has a unique phase response. We ask the question: do basilar-membrane (BM) vibration responses have the minimum phase property? We use two approaches to answer this question. The first is to ascertain whether the minimum phase of a given magnitude-vs.-frequency response is identical to the actual phase-vs.-frequency response. If the computed and actual phase responses are not identical, then it is concluded that the original responses do not have the minimum-phase property. The second approach is to ascertain whether the Nyquist plot of the responses encircles the origin in the clockwise direction. If so, then the response does not have the minimum-phase property. We tested BM responses, culled from the literature, from apical and basal sites of adult chinchilla cochleae, both post-mortem and in-vivo. BM responses from adult and neonatal gerbils (age: 14-20 days after birth) were also tested. BM responses in adult cochleae, either post-mortem or in-vivo, do not have the minimum-phase property. Furthermore, the BM responses in adult cochleae are still nonminimum-phase after removal of the signal-front delay. BM responses are closer to being minimum-phase at apical cochlear sites and for high-intensity stimuli. These results are consistent with the findings of Recio, Narayan and Ruggero (pp. 325-331 in Diversity in Auditory Mechanics, ed. by E. R. Lewis et al., World Scientific, 1997) but dispute the reports by Zweig (Cold Spring Harbor Symp. Quant. Biol., 619-633, 1976) and Koshigoe and Tubis (J.A.S.A. 71: 1194-1200). In

contrast with results for adult cochleae, BM responses at the extreme base of the cochlea of gerbil neonates do possess the minimum-phase property. Overstreet, Temchin and Ruggero (J. Physiol. 545.1: 279-288, 2002) questioned "whether the BMs of (neonate) gerbils actually sustain traveling waves". The present results suggest that true traveling waves must lack the minimum-phase property.

### **787 ATP- $\gamma$ -S Shifts the Operating Point of Outer Hair Cell Transduction Towards Scala Tympani.**

**Richard Bobbin<sup>1</sup>, Alec Salt<sup>2</sup>**

<sup>1</sup>Kresge Hearing Research Lab, Department of Otolaryngology, LSU School of Medicine, New Orleans, LA, <sup>2</sup>Department of Otolaryngology, Washington University School of Medicine, St. Louis, MO.

ATP- $\gamma$ -S, an ATP receptor agonist, suppresses the cubic distortion product otoacoustic emission (DPOAE) and enhances the quadratic DPOAE while PPADS, an ATP receptor antagonist, has opposite effects (Chen et al., Hear. Res. 118: 47, 1998; Kujawa et al., Hear. Res. 76: 87, 1994). According to a model proposed by Frank and Kosl (Hear. Res. 98: 104, 1996) these effects of the drugs are consistent with the hypothesis that ATP affects mechano-electrical transduction and the operating point of the outer hair cells (OHCs). This hypothesis was tested by monitoring the effect of ATP- $\gamma$ -S on the operating point of the OHCs. Guinea pigs anesthetized with urethane and with sectioned middle ear muscles were used. Cochlear microphonics (CM) was recorded differentially across the basal turn before and after perfusion (20 min) of the perilymph compartment with artificial perilymph (AP) and ATP- $\gamma$ -S (1- 333  $\mu$ M) dissolved in AP. The technique described previously (Sirjani et al. JASA 115: 1219, 2004) was used to calculate the operating point from CM recorded in response to an intense (106-118 dB SPL) low frequency (200 Hz) tone. Compared to the initial perfusion with AP, ATP- $\gamma$ -S (3 - 333  $\mu$ M) in a dose responsive manner enhanced peak clipping of the positive, scala tympani peak of the CM, and significantly shifted the operating point towards positive values (towards scala tympani). Following a single perfusion with 333  $\mu$ M ATP- $\gamma$ -S a significant degree of recovery of the operating point was observed after washing with AP. Multiple perfusions of AP had no significant effect on the operating point. These results are consistent with an ATP- $\gamma$ -S induced static movement of the organ of Corti towards scala tympani.

Supported by grants DC04994 (RB) and DC01368 (AS) from the National Institute of Deafness and Other Communication Disorders.

## **788** The Significance of Length Scale on Measurements of Tectorial Membrane Elasticity

**Brett Shoelson**<sup>1</sup>, Emiliios Dimitriadis<sup>2</sup>, Richard Chadwick<sup>1</sup>

<sup>1</sup>*Section on Auditory Mechanics, NIDCD, Bethesda, MD 20892*, <sup>2</sup>*DBEPS/OD, NIH, Bethesda, MD 20892*

In a previous publication [1], we used atomic force microscopy (AFM) to measure and map the elasticity of the tectorial membrane (TM). Using different probe tips, we indented the tissue first on the length scale of a single stereocilium and then on the scale of a stereocilia bundle. In general, the tissue was found to be approximately 70% softer on the larger length scale ( $2.00 \pm 1.24$  kPa vs.  $6.54 \pm 4.18$  kPa). We suggested that the apparent decrease in elasticity is consistent with the theory of strain-hardening introduced by the sharper tip, but ultimately concluded that "the exact nature of the difference in moduli obtained by probing at different scales remains unclear; the apparent increase in elasticity with a sharper tip likely also reflects structural differences in the TM at the different length scales of the AFM probes." In the current study, we further examine the nature of the length-scale dependency by probing a series of poly(vinyl alcohol) gels on macro-, micro-, and nano-scales. For macro- determinations, we measured the contact radius resulting from indentation with a 3-mm steel sphere. Micro- and nano-measurements were made with microsphere-affixed and unmodified Si<sub>3</sub>Ni<sub>4</sub> AFM probes, respectively. In a preliminary series of measurements of PVA gels, we found insufficient evidence to attribute the length-scale dependency entirely to strain-hardening, and we conclude that our TM measurements likely reflect structural length-scale differences.

Reference: 1. Shoelson, B., et al., Evidence and implications of inhomogeneity in tectorial membrane elasticity. *Biophys J.*, 2004; 87(4):2769-2777.

## **789** Noise-Induced Adaptation of Stimulus Frequency Otoacoustic Emission and Cochlear Microphonic Residuals in Gerbil

**Shawn Goodman**<sup>1</sup>, Douglas Keefe<sup>1</sup>, JoAnn McGee<sup>1</sup>, Edward Walsh<sup>1</sup>

<sup>1</sup>*Boys Town National Research Hospital*

Stimulus frequency otoacoustic emissions (SFOAEs) associated with low-level sinusoidal probes may be useful in studying the medial olivocochlear (MOC) reflex because elicitors suppressing the SFOAE may also evoke the MOC reflex, whereas SFOAE probes do not evoke the reflex (Guinan et al., 2003, JARO). Previous human measurements of noise-induced adaptation of SFOAEs showed weak or absent effects at low elicitor levels of a notched broadband noise (Goodman & Keefe, 2004, ARO abstr.). At higher elicitor levels, most test ears showed adaptation after the elicitor was gated off, some of which was not attributed to the middle-ear muscle (MEM) reflex. To determine whether these effects are due to the MOC reflex, SFOAEs and cochlear microphonics (CM) were measured in anesthetized Mongolian gerbils using a similar measurement paradigm to that used for humans.

Probe tones were presented at 2 and 10 kHz, and a broadband noise was used as the elicitor. In each measurement, the probe tone was gated on for 1350 ms followed by a 650 ms baseline recovery period. The elicitor was gated on 250 ms after the probe tone with a 500 ms duration. The SFOAE suppression of the probe produced by the elicitor was measured using a residual procedure. Baseline measurements were compared with measurements made after paralysis, after severing the olivocochlear bundle (OCB) at the level of the IVth ventricle, and post-mortem. Residual SFOAE responses in gerbil were qualitatively similar to responses in humans. At high elicitor levels, residuals in SFOAEs and some CM recordings were measurable for hundreds of ms after the elicitor was gated off. Post-elicitor residuals were present in paralyzed animals, after complete OCB section, and for several hours post-mortem. These data suggest that some or all of the residuals are due to adaptation processes intrinsic to the cochlea, rather than the influence of MOC or MEM efferent reflexes. (Supported by NIDCD grants DC007023, DC00013, DC04566, DC03784)

## **790** Addition of Spectrin to the Lateral Wall Modifies Outer Hair Cell Mechanical Properties

**Heather Jensen-Smith**<sup>1</sup>, Alex Bien<sup>2</sup>, Richard Hallworth<sup>1</sup>

<sup>1</sup>*Creighton University*, <sup>2</sup>*University of Nebraska Medical Center*

The mechanical properties of the outer hair cell (OHC) lateral wall are important in determining how effectively OHC motility is communicated to the organ of Corti. The OHC cortical cytoskeleton is thought to contribute to its mechanical properties. The cortical cytoskeleton has an unusual configuration, consisting of circumferential actin filaments linked by longitudinal spectrin filaments. We show that, in development, spectrin appears in the cortical cytoskeleton of gerbil OHCs after post-natal day 3 (P3). To test the hypothesis that the addition of spectrin to the cortical cytoskeleton contributes to OHC mechanical properties, we measured the ratio of the shear modulus ( $\mu$ ) to the area modulus (K), a key measure of membrane mechanical properties, in isolated OHCs using hypo-osmotic challenge. Length and diameter strains in response to exposure to 260 mOsm L-15 (from 300 mOsm) were measured using video microscopy. We obtained a  $\mu/K$  ratio of 0.046 for adult gerbil OHCs, a value close to the previously reported values for guinea-pig OHCs of 0.054 (Ratnanather et al., *J.A.S.A.*, 99: p. 1025, 1996) and 0.13 (Iwasa and Chadwick, *J.A.S.A.*, 92: p. 3169, 1992). The  $\mu/K$  ratio obtained from developmental OHCs (P0 to P12) did not differ significantly from adult OHCs ( $F(5,218)= 1.75$ ,  $p = 0.142$ ). Thus the  $\mu/K$  ratio of the OHC lateral wall is not significantly altered over the period in which the actin-spectrin cortical cytoskeleton is elaborated. However, robust changes in radial and axial strains were observed in developmental OHCs ( $F(6,217)= 22.01$ ,  $p < 0.0001$ ;  $F(6,217)= 30.19$ ,  $p < 0.0001$ , respectively). Radial strain evoked by osmotic challenge increased, while axial strain increased in magnitude, in the negative direction. These results strongly support the



hypothesis that the OHC cortical cytoskeleton influences OHC mechanical properties.

(Supported by NIH (DC02053) and the Clare Booth Luce Foundation)

## **791 Negative Damping by Hair Bundles Can Sharpen Tuning in the Alligator Lizard Cochlea**

**A.J. Aranyosi<sup>1</sup>**, Dennis Freeman<sup>1</sup>

<sup>1</sup>MIT

Hair cell bundles have been shown to generate force in several vertebrate species. However, it is not clear how such force generation can increase the sharpness of tuning in the cochlea. The alligator lizard cochlea provides a simple context in which to examine the contribution of active mechanisms to cochlear tuning. The free-standing region of this cochlea has no travelling wave and no tectorial membrane, so mechanical tuning results from the interaction of hair bundles with fluid. Nonetheless, this system has sharp tuning at low sound levels, and significant level-dependent tuning. Measurements of the mechanical tuning of hair bundles at 85-100 dB SPL are consistent with the tuning of hair cell receptor potentials at these levels. A hydrodynamic model shows that the sharpness of this tuning is limited by fluid viscosity, suggesting that some active mechanism is necessary to sharpen tuning at lower levels. We have extended the model by adding an active force at the level of the hair bundle, and compared the frequency response at various sound levels to that of hair cell receptor potentials. Three types of active mechanism were considered: a negative stiffness, a negative damping, and an added torque, each acting over a limited range of hair bundle deflections. The mechanism most consistent with measured tuning curves was a negative damping, which counteracted about 90% of the fluid-generated damping and operated over a range of deflections of about 10-20 nm. This negative damping generates a peak force equivalent to about 2 pN, roughly consistent with the force exerted by hair bundles in a frog sacculle preparation (Martin et al, 2000). In contrast, the negative stiffness reduced the sharpness of tuning at lower sound levels, and the added torque caused little change in tuning. Thus an active hair bundle that operates as a negative damping provides a plausible explanation for the level-dependent sharpening of tuning in this cochlea.

## **792 Role of the ROCK-LIM kinase-Cofilin Pathway in the Regulation of Outer Hair Cell Motility**

**Nozomu Matsumoto<sup>1</sup>**, Federico Kalinec<sup>1</sup>

<sup>1</sup>Gonda Dept. of Cell & Molecular Biology, House Ear Institute

Cochlear outer hair cells (OHCs) change their shape by two independent mechanisms, namely slow and fast motility. Slow motility involves cytoskeletal reorganization, while fast motility (or electromotility) results from voltage-driven conformational changes of a membrane-embedded protein. Both mechanisms are at the core of the active process of cochlear amplification. We have previously

published evidence that the Rho-ROCK signaling pathway, which is known to regulate the organization and dynamics of cytoskeletal structures, can induce changes both in slow and fast OHC motility (Kalinec et al., 2000, Zhang et al., 2003). This result strongly supports the idea that both mechanisms are regulated by the cytoskeleton. However, the precise mechanism of regulation and the molecular targets of the Rho-ROCK pathway are still unknown.

We investigated the role of two downstream targets of the Rho-ROCK signaling pathway: LIM kinase (LIMK) and cofilin. By using automatic analysis of video images during whole-cell patch recording, we investigated both OHC slow and fast motility and evaluated the effect of a natural RhoA activator (lysophosphatidic acid; LPA), a pharmacological inhibitor of ROCK (Y27632), and a peptide containing the phosphorylation site of cofilin (S3) as a competitive inhibitor of LIMK-cofilin coupling.

LPA decreased OHC length during stable membrane potential (-70 mV) but did not affect the amplitude of fast motility. Y27632, in contrast, elongated the cells and abolished the OHC fast motility either when applied alone or in combination with LPA. The effect of S3, either applied alone or in combination with Y27632, was similar to that elicited by Y27632.

Our results suggest that LIMK and cofilin play an important role in the regulation of both slow and fast OHC motility. These results further advance our understanding of the cell and molecular mechanisms responsible for the regulation of OHC motility and cochlear amplification.

## **793 Cloning and Characterization of CTL2 Isoforms**

**Pavan Kommareddi<sup>1</sup>**, Thankam Nair<sup>1</sup>, Kelley Kozma<sup>1</sup>, Takeharu Kanazawa<sup>2</sup>, Steven Telian<sup>1</sup>, Alexander Arts<sup>1</sup>, Thomas Carey<sup>1</sup>

<sup>1</sup>KHRI, <sup>2</sup>CCGC

Choline transporter-like protein 2 (CTL2) is a target of antibody mediated hearing loss. Antibodies bind to CTL2 in vivo and result in hair cell and hearing loss in animal models. We sequenced CTL2 from inner ear cDNA and found that exon 1 differed significantly from the reference sequence in the NCBI database. Further analysis revealed that CTL2 has at least four isoforms under the control of as many promoters. We named the isoforms P1-P4. The P1 and P2 isoforms are full length and differ only in exon 1. The P1 isoform of CTL2 has an alternate exon 1 (exon 1a) that is located 22.9kb upstream of the P2 exon 1 (exon 1b). P1 (exon 1a) is the predominant isoform found in the inner ear of humans and guinea pigs. Exon 1a encodes ten amino acids whereas exon 1b encodes 12 leading to a 2 amino acid difference in the size of the full length of the polypeptides specified by P1 and P2 of 704 and 706 amino acids respectively. To further characterize P1 and P2 CTL2 isoforms we determined the mRNA expression patterns in mouse tissues using RT-PCR. With the exception of the inner ear, the P2 isoform predominates in colon, heart, lung, kidney and stomach. P1 predominates in inner ear, brain, small intestine, and liver. To study the cellular localization and protein characteristics we cloned CTL2 P1 and P2 full length cDNAs and the open reading

frames into the pGEM-T cloning vector and subcloned the ORFs into various mammalian expression vectors in frame with a histidine tag and green fluorescent protein. CTL2 expression as measured by GFP fluorescence localized to the membrane and the endocytic vesicles consistent with its membrane location in supporting cells. Stably transfected mammalian cells should be useful for functional studies of the CTL2 isoforms.

Supported by the Townsend Fund, NIH R01 DC03686, TG DC00011, P30 AR048310 and P30 DC05188.

### **794 CTL2 Distribution in Animal Tissues**

**Loc Thang<sup>1</sup>**, Pavan Kommareddi<sup>1</sup>, Thankam Nair<sup>1</sup>, Thomas Carey<sup>1</sup>

<sup>1</sup>*University of Michigan*

Recently, we reported that the inner ear supporting cell antigen defined by the KHRI-3 monoclonal antibody is the guinea pig homologue of the human CTL2 protein, a member of the choline transporter-like family. Antibodies to CTL2 can bind to supporting cells in vivo and induce hearing loss in adult guinea pigs. CTL2 has multiple isoforms including the full length isoforms CTL2-P1 and CTL2-P2 which have promoters separated by 22.9 kb and use alternate first exons. CTL2 P1 appears to predominate in the inner ear. In addition, there are two short isoforms that share the C-terminal domain. We have studied predominantly the P1 and P2 isoforms. At the RNA level, both isoforms appear to be expressed in mouse colon, heart, and lung, although the P2 isoform predominates in all of the tissues examined except for brain and liver in which P1 dominates. To independently assess the expression of the CTL2 isoforms at the protein level, new polyclonal antibodies are raised against the CTL2-P1 and CTL2-P2 exon one specific peptides. In addition to the 4 isoforms, CTL2 also has alternate splice forms. To study the expression of the various isoforms and alternative splice forms, a CTL2 C-terminal antibody that will recognize all of the isoforms and the alternate splice forms has been raised. When KHRI-3 immunoprecipitates of guinea pig cochlear lysate were probed with the C-terminal antibody it recognized the same doublet (68-72kd) as the KHRI-3 antibody. Using these antibodies we can determine the distribution of CTL2 proteins in tissues. CTL2-P1 and CTL2-P2 isoforms will have relatively the same molecular weight. However, with the specific CTL2-P1 and CTL2-P2 antibody we can distinguish between the two isoforms. Alternate splice forms of CTL2 antigen have smaller molecular weight than CTL2-P1 and CTL2-P2 and will be recognized by the CTL2 C-terminal antibody.

Supported by the Townsend Fund, NIH R01 DC03686, TG DC00011, P30 AR048310 and P30 DC05188.

### **795 Transmembrane Topologic Organization of TMC1**

**Valentina Labay<sup>1</sup>**, Tomoko Makishima<sup>1</sup>, Andrew Griffith<sup>1</sup>

<sup>1</sup>*Section on Gene Structure and Function, NIDCD, NIH*

Dominant and recessive mutant alleles of *TMC1/Tmc1* (transmembrane channel-like gene 1) cause hearing loss in humans and mice (Kurima et al., *Nature Genetics*, 2002; Vreugde et al., *Nature Genetics*, 2002). *Tmc1* mRNA is

expressed in cochlear and vestibular hair cells, but its function is unknown. The mammalian *TMC* gene family has seven other members, all of which are strongly predicted to encode proteins containing 6 to 10 transmembrane domains (Kurima et al., *Genomics*, 2003). In order to provide a foundation for identifying the function and potential interacting protein partners of TMC1, we have begun to define the transmembrane topologic organization of TMC1 heterologously expressed in Cos7 cells. GFP-tagged TMC1 expressed in Cos7 cells results in a reticular expression pattern consistent with the location of endoplasmic reticulum. Specific rabbit antisera against the N-terminus and the C-terminus of mouse TMC1 were used in cytoimmunofluorescence and protease protection assays (Otto & Smith, *J. Biol. Chem.*, 1994; Lin et al., *Mol. Biol. Cell*, 2003) to show that both the N- and C- termini of TMC1 are cytoplasmically oriented. This topologic structure is shared with the superfamily of transmembrane channels that includes TRP channels. We are currently generating a series of constructs with a hemagglutinin epitope tag inserted in predicted hydrophilic loop regions to experimentally define the transmembrane domains and topologic orientation of internal loops of TMC1. These results will also be presented and form a basis for future studies of the structure and function of TMC1 in neurosensory hair cells.

### **796 Multi-Genomic Analysis of Prestin Gene Regulation.**

**Thomas Weber<sup>1</sup>**, Jian Zuo<sup>1</sup>

<sup>1</sup>*St. Jude Childrens Research Hospital*

Within the cochlea expression of prestin is restricted to the outer hair cells suggesting a very strict regulation of the gene. Our aim is to identify the genomic regions that form the prestin promoter and to learn how this precise expression pattern can be retained. We have recently shown data pointing to the presence of a minimal promoter located around the transcriptional start site (Weber et al., *Assoc Res Otolaryngol.* 27, abstract 1046). The transactivation capacity of the fragments used in these studies however was weak (6fold induction) when reporter gene assays were performed in 293-cells. Therefore, in this study we tested our fragments using the cochlear UB-OC1 hair-cell-line described in Rivolta et al. (2002) for transient transfections. We still observed a very weak transactivation capacity which declined even further when UB-OC1 cells were transfected after several days under differentiating conditions. This could be explained by the presence of transcriptional repressors or the lack of activators in this cell line or simply by the lack of important cis-acting elements in our constructs which are crucial for a strong prestin expression. In order to identify additional putative regulatory regions we performed a comprehensive multi-genomic in silico analysis of the prestin gene including mouse, rat, human and chimpanzee genomic sequences (<<http://genome.ucsc.edu/>>). We searched for areas with a high grade of conservation between species along the length of the gene. We found several clusters of highest conservation covering a region of 7,5 kb, which only partly overlaps with the promoter fragments described earlier. We will analyze this area for the presence of

conserved binding sites and present data underlining their relevance for the transcriptional regulation of prestin.

Supported by the American Lebanese Syrian Associated Charities (ALSAC), NIH Cancer Center Support CORE grant (CA21765), and NIH grants to J.Z. (DC05168, DC06471).

### **797 Further Molecular Characterization of The Cytocaud in Shaker 2 Mice**

Lisa Beyer<sup>1</sup>, Jill Karolyi<sup>2</sup>, Qing Fang<sup>2</sup>, Sally Camper<sup>2</sup>, David Kohrman<sup>1</sup>, **Yehoash Raphael<sup>1</sup>**

<sup>1</sup>Kresge Hearing Research Institute, Univ. of MI, <sup>2</sup>Dept. of Human Genetics, Univ. of MI

The shaker 2 (*sh2*) mouse has a mutation in the unconventional myosin *Myo15* gene that results in congenital deafness and circling behavior. Auditory and vestibular hair cells of *sh2* mutants are characterized by abnormally short stereocilia. In addition, vestibular and inner hair cells display a cytocaud: a long actin-rich tail-like extension projecting from the basal end of the cell. While pirouette (*pi*) mice have a similar cytocaud pathology, this structure is not common among congenitally deaf mice. We now report characterization of the cytocaud in terms of its molecular composition, temporal sequence of formation, and genetic requirements. Normal stereocilia are immunoreactive for the actin cross-linking proteins espin and fimbrin. We determined that cytocauds in both *pi* and *sh2* mutants contain fimbrin, but no detectable espin. The absence of espin demonstrates the molecular dissimilarity between stereocilia and cytocauds. Based on phalloidin staining, cytocauds can be detected in inner hair cells of *pi* mice as early as postnatal day 3 (P3), but in *sh2/sh2* cochleae they first appear much later, around P13. Thus, the development of cytocaud pathology is different in *pi/pi* and *sh2/sh2* mutants. Double mutants were generated to explore the genetic requirements for cytocaud pathology. *Myo7a*, *Myo15* double mutants formed cytocauds similar to those observed in *Myo15* single mutants. However, no cytocauds were detectable in mice lacking both *Myo6* and *Myo15* function, whereas *Myo6* deficiency did not block cytocaud formation in *pi/pi* mutants. These studies suggest that despite the similarities in cytocaud pathology of *pi* and *sh2* mutants, the ontogeny and genetic requirements are different. A greater understanding of the etiology of inner hair cell pathology in these mice is important for assessing the therapeutic potential for correction of this type of deafness. Supported by NIDCD grants R01-DC05401, R01 DC05053 and P30-DC05188.

### **798 Expression and Mutation Analysis of Grxcr1, the Gene Affected in the Mouse Deafness Mutant Pirouette**

Kristina Hunker<sup>1</sup>, Hana Odeh<sup>1</sup>, Lili Zheng<sup>2</sup>, Kate Barald<sup>1</sup>, Yehoash Raphael<sup>1</sup>, James Bartles<sup>2</sup>, **David Kohrman<sup>1</sup>**

<sup>1</sup>University of Michigan, <sup>2</sup>Northwestern University

The mouse mutant pirouette (*pi*) exhibits profound hearing loss and circling behavior inherited as autosomal recessive traits. Analysis of inner pathology in *pi/pi* homozygotes has

previously indicated abnormally thin stereocilia during sensory cell maturation, and the appearance of abnormal, actin filament bundles ('cytocauds') in all inner hair cells and a subset of vestibular hair cells. The defective gene in pirouette mice, *Grxcr1*, is expressed in neuroepithelial cells in the cochlea and encodes a 290 amino acid protein that contains a region of similarity to glutaredoxins, enzymes that reduce oxidized cysteines on cellular proteins during normal homeostasis and under oxidative stress conditions.

Transfection experiments with GRXCR1 fusion proteins have demonstrated a close association of GRXCR1 with actin filament-rich structures on the dorsal/apical surface of cultured cells. These structures contain parallel actin filament bundles that are qualitatively similar to the bundles found in the core of stereocilia. Along with the distinctive pathologies in pirouette mutants, this localization of GRXCR1 is consistent with a role for the protein in controlling actin cytoskeletal architecture in the apical region of hair cells. We have characterized a paralogous gene, *Grxcr2*, which exhibits an inner ear-specific expression pattern similar to that of *Grxcr1*. The GRXCR2 protein also localizes to actin filament-rich structures in transfected cells, suggesting it may play a similar role in regulating actin organization in the inner ear.

We have expanded our transfection studies to additional cultured cell types, including lines derived from the developing otocyst. GRXCR1 hybrid proteins exhibit similar localization to actin filament-rich projections in these cell types. We have also begun to analyze GRXCR1 mutant proteins in order to define sequences necessary for localization and other aspects of function.

### **799 Hearing Loss in Thyroid Hormone Deficient Mice is Alleviated by Thyroid-Rich Diet**

Jill Karolyi<sup>1</sup>, Lisa Beyer<sup>2</sup>, Gary Dootz<sup>2</sup>, Frank Probst<sup>1</sup>, Karin Halsey<sup>2</sup>, David Dolan<sup>2</sup>, **Yehoash Raphael<sup>2</sup>**, Sally Camper<sup>1</sup>

<sup>1</sup>Dept. of Human Genetics, Univ. of MI, <sup>2</sup>Kresge Hearing Research Institute, Univ. of MI

Thyroid hormone (TH) insufficiency causes variable hearing loss and mental deficiency in humans. Rodents lacking TH have hearing loss that has been attributed to lowered endocochlear potential (EP), tectorial membrane abnormalities, delayed development of the sensory epithelium, and impaired synaptogenesis. We examined three genetically defined strains of hypothyroid mice for development of hearing and response to oral TH replacement initiated during late gestation and continued through 6 weeks of age. These strains lack pituitary thyroid stimulating hormone (TSH) and have undetectable levels of serum TH. *Prop1<sup>df</sup>* and *Pit1<sup>dw</sup>* mutants fail to develop the cells that produce TSH, and *Cga<sup>tm1Sac</sup>* mutants are unable to make the alpha subunit critical for TSH bioactivity. ABR audiometry showed variable, but significant, hearing loss in mutants of each strain at 3 and 6 weeks of age relative to normal littermates. TH-enriched chow significantly alleviated hearing loss in 3-week old mutants of each strain. The *Cga<sup>tm1Sac</sup>* strain was selected for further characterization. Mutants appeared to have

normal hair cell cytoarchitecture in the organ of Corti. Although no obvious differences in the mutant and control tectorial membranes were observed by light microscopy, cochlear development was clearly delayed in *Cga* mutants. DPOAE was absent, and EP was 41mV. The spiral ligament had striking morphological abnormalities that could have contributed to the low EP and deafness in mutant animals. We conclude that the identified pathologies are delay in organ of Corti development, low EP, and spiral ligament abnormalities. Oral TH supplement administered during the critical period of hearing development in mice can prevent hearing loss associated with congenital hypothyroidism of heterogeneous genetic etiology.

Supported by NIDCD grants R01-DC05401 and R01 DC05053 and P30-DC05188.

## **800** Characterization of the Hurry-scurry Knockout Mouse and Reporter Gene Expression

**Chantal Longo-Guess**<sup>1</sup>, Leona Gagnon<sup>1</sup>, Sandra Gray<sup>1</sup>, Qing Yin Zheng<sup>1</sup>, Heping Yu<sup>1</sup>, Kenneth Johnson<sup>1</sup>

<sup>1</sup>The Jackson Laboratory

The hurry-scurry (*hscy*) mutation is a spontaneous mutation that exhibits a circling and head bobbing phenotype. Mutant mice are deaf as early as 26 days after birth. SEM and histological examination of mutant mice shows a loss of inner and outer hair cells in the organ of Corti. Using a positional cloning approach, we have identified the *hscy* mutation to be a missense mutation in a novel uncharacterized gene. This novel gene is approximately 7.9 kb in size and is composed of 4 exons. It encodes a 219 amino acid protein that is a member of the tetraspan family of small proteins consisting of four transmembrane helices. Here we report on our characterization of a targeted disruption of the hurry-scurry gene and our expression analysis of a  $\beta$ -galactosidase reporter gene.

We produced a hurry-scurry knockout by replacing exons 1 and 2 of the *hscy* gene with  $\beta$ -gal/neo. The resulting plasmid was linearized and transfected into a 129 ES cell line. Homologous recombination was identified by using PCR primers specific to the 5' arm of the construct and to the  $\beta$ -gal sequence. Correctly targeted ES clones were injected into C57BL/6J blastocysts. The resulting chimeras were bred to C57BL6/J, and pups were selected for germ line transmission.

Mice that are homozygous for the hurry-scurry targeted null allele exhibit a phenotype much the same as mice homozygous for the spontaneous mutation. At approximately three weeks of age, the mice exhibit a rapid circling and head bobbing behavior and they are also deaf.

The inclusion of  $\beta$ -galactosidase in the knockout construct allowed for gene expression studies in mice with the targeted allele. We see pronounced expression in cochlear hair cells as well as in hair cells of the saccule, utricle, and crista ampullaris. We do not see any expression in the adult inner ears, suggesting that the hurry-scurry gene may be important in the development of the hair cells. These results confirm earlier protein expression results

obtained through immunofluorescence with a peptide antibody specific to the hurry-scurry protein.

This work was supported by grant DC04301 from NIH.

## **801** Genetic Mapping of a Mouse Mutation Associated with Otitis Media

**Qing Yin Zheng**<sup>1</sup>, Belinda Harris<sup>1</sup>, Patricia Ward-Bailey<sup>1</sup>, Heping YU<sup>1</sup>, Roderick Bronson<sup>1</sup>, Leah Rae Donahue<sup>1</sup>, Kenneth Johnson<sup>1</sup>, Muriel Davisson<sup>1</sup>

<sup>1</sup>The Jackson Laboratory

Otitis media (OM) is one of the most common human diseases, accounting for 22 million visits annually to physicians in the United States. OM is affected by multiple factors including eustachian tube (ET) structure and function, immune status, innate mucosal defense, genetic susceptibility, and pathogens. Infectious disease can be viewed as a battle between hosts and pathogens, in which the commands are encoded in their genomes respectively and are then executed by gene products including antibodies of the host and drug-resistance mechanisms of bacteria. Several lines of evidence indicate that genetics plays an important role in human OM. The mouse has emerged as the premier animal model for human disease research, and genetic models of OM represent potentially powerful tools for identifying the biological and genetic factors underlying human OM. OM is relatively common in mice. Here we report a mutant mouse strain with head bobbing behavior named *Gom1* has a very high incidence of OM. Six out seven mutant mice were confirmed to have OM by histology. *Gom1* is a new dominant mutation that spontaneously arose in a colony of C3H/HeJ inbred mice at The Jackson Laboratory. The human homolog of the gene responsible for the *Gom1* phenotype in mice may play a role in the etiology and pathogenesis of some cases of human OM. A small panel of intercross mice was used to map the *Gom1* locus to the middle region of mouse chromosome (Chr) 10. The genetic map position of the mouse *Gom1* gene suggests that the homologous human gene may be located on Chr 10q22-23.

This work is supported by NIH grants DC005846

## **802** Gene Targeting and Homologous Recombination for USH1C Gene

**Xue Zhong Liu**<sup>1</sup>, Qing Yin Zheng<sup>2</sup>, Xiao Mei Ouyang<sup>1</sup>, Li Lin Du<sup>1</sup>, Kenneth R Johnson<sup>2</sup>, Denise Yan<sup>1</sup>

<sup>1</sup>University of Miami, <sup>2</sup>The Jackson Laboratory

Mutations in USH1C gene are the causes of Usher syndrome type 1C as well as certain forms of non-syndromic deafness. The gene is composed of 28 exons, including 20 that are constitutive and 8 that are alternatively spliced in the mouse. USH1C gene encoding a PDZ-containing protein, harmonin, is thought to play a central role in the USH1 genes pathway, mediating organization of the hair cell and its stereociliary bundle. To further understand the role of harmonin in the pathogenesis that leads to USH1, we have used the technique of gene targeting by homologous recombination to generate USH1C null mice. The mouse *Ush1c* clone was isolated from a 129 Sv6/Sv Ev Tac bacterial artificial

chromosome (BAC) library. The exons 1-4 of the gene were replaced with a beta-gal reporter gene downstream of the Ush1c promoter used to drive beta-gal expression. Two arms consisting of a 3.7 kb-5'homologous region and a 4 kb-3'homologous region were generated via polymerase chain reaction (PCR) using genomic DNA and subcloned into a vector containing beta-gal, neomycin resistant gene cassette (Neo) and the herpes simplex virus thymidine kinase gene cassette (TK). Linearized targeting construct was electroporated into R1 ES cells. By Southern blot analysis, two clones were found properly targeted on both the 5' and 3'ends, from a screening of 172 different ES colonies, yielding a homologous recombination rate of ~1.16%. Following transfer of 193 injected blastocysts into 17 foster mothers of one of the positive clones, we have obtained 30% newborn mice with 60% of them presented 75%-100% contribution in the coat color and had a 26:14 male to female ratio. We are presently establishing homozygous mouse lines. Generation and characterization of an usher 1c knockout mouse would provide a means to understand the bases for the sensory defects associated with Usher syndrome and other auditory disorders.

The work is supported by NIH DC 05575 and DC 005846)

### **803 In Situ Localization and Temporal Expression of Mouse *Vlgr1*, the Gene Mutated in Human Usher Syndrome type IIc (USH2C).**

**Michael D. Weston<sup>1</sup>**, Sonia M.S. Rocha-Sanches<sup>1</sup>, Ken A. Morris<sup>1</sup>, Kirk W. Beisel<sup>1</sup>

<sup>1</sup>*Creighton University*

Usher syndrome type II is a genetically heterogeneous autosomal recessive disease of congenital hearing loss and progressive retinitis pigmentosa. Three genetic subtypes (USH2A-C) and 2 genes have been implicated in the disease process. Both *USH2A* and *VLGR1* (USH2C) genes encode proteins that are very large (>500kD) putative membrane bound receptors. Human *VLGR1* mutations have also been associated with both febrile and afebrile seizures. Murine *Vlgr1* mutants manifest audiogenic seizures that are most likely a secondary effect of a primary *Vlgr1*- mediated hearing impairment. Published data have shown that most rodent strains can be rendered susceptible to audiogenic induced seizures by prior acoustic insults (genetic hearing impairment, aminoglycosides, and acoustic trauma) when this priming event occurs during a short critical period in postnatal development.

Mouse *Vlgr1* expression studies in brain have demonstrated alternative splice variants, but the diversity and temporal expression of *Vlgr1* in the postnatal (P) mouse inner ear and retina is unknown. We are currently performing whole mount in situ hybridization to localize *Vlgr1* mRNA in both rat and mouse P0, P8, P21 and P35 cochleae. Preliminary data are consistent with low level expression in the neuroepithelium of the cochlea including spiral ganglion (SG) cells, inner and outer hair cells (HCs) and Hensen cells. Expression is limited, with qualitatively more expression signal in HCs than SG at P21 and a

reciprocal pattern at P0, suggesting a radial gradient of *Vlgr1* expression through postnatal cochlear development. RT-PCR data indicate that novel tissue specific *Vlgr1* transcripts are expressed from mouse cochlea and retina. These data suggest that tissue-specific protein motif exclusion caused by alternative mRNA splicing produces a diversity of VLGR1 protein isoforms that may impact the types and strengths of protein-protein interactions with other, yet to be discovered, VLGR1 binding partners. Such knowledge will be necessary to determine the biologic function of VLGR1 and how its dysfunction leads to the manifestation of Usher syndrome and, perhaps, to seizure disorders as well.

### **804 Physical and Genetic Interaction Between Usher 1 Genes**

**Denise Yan<sup>1</sup>**, Qing Yin Zheng<sup>2</sup>, Fang Li<sup>1</sup>, Xiao Mei Ouyang<sup>1</sup>, Li Lin Du<sup>1</sup>, Kenneth R Johnson<sup>2</sup>, Xue Zhong Liu<sup>1</sup>  
<sup>1</sup>*University of Miami*, <sup>2</sup>*The Jackson Laboratory*

Usher syndrome is the most common form of combined deafness and blindness. Usher type I (USH1), the most severe form, is characterized by profound congenital deafness, constant vestibular dysfunction, and pre-pubertal onset retinitis pigmentosa. At least seven genetic loci have been linked to USH1, and five of the relevant genes have been cloned. They encode myosin VIIa (USH1B), harmonin (USH1C), cadherin 23 (USH1D), protocadherin 15 (USH1F) and SANS (USH1G). Harmonin, the protein encoded by USH1C, has been shown to bind, via its PDZ (postsynaptic density, disc large, zonula occludens)-domains with the products of other Usher syndrome genes. Homozygous mutant mice for Usher 1 genes are phenotypically indistinguishable. They all characterized by deafness, vestibular dysfunction and disorganized, splayed stereocilia. Given the important role that harmonin may play in the shaping of the hair bundle as a coherent unit and the similarity in histopathology among the Ush1 mouse models, we sought to determine functional interaction between harmonin and the other usher 1 proteins. By means of co-transfection experiments, we confirm that there is an in vitro interaction between the Usher 1 genes. Our data show that harmonin physically interacts with Myosin VIIa and PCDH15, as does CDH23 with PCDH15 protein. We have used the mutant alleles Ush1c (dfcr), Myo7a (sh1-8J), Cdh23 (v-2J) and Pcdh15 (av-3J) to generate ush1c/ush-b,-d,-f, and -g double heterozygous mice to test for genetic interaction in vivo. We found no evoked auditory brainstem response (ABR) threshold shifts in doubly heterozygous mice from all crosses at 22 days of age. Currently, we are investigating whether the mutant alleles of Ush1 genes can genetically interact to cause age-related hearing loss.

The work is supported by NIH DC 05575 and DC 005846)

## **805 Expression of Neural Fate Markers During Early Sensory Epithelial Development in Mouse**

Steven Raft<sup>1</sup>, Herson Quinones<sup>2</sup>, Jane Johnson<sup>2</sup>, Neil Segil<sup>1</sup>, Andrew Groves<sup>1</sup>

<sup>1</sup>House Ear Institute, <sup>2</sup>UT Southwestern Medical Center

During inner ear development, the basic Helix Loop Helix genes *Ngn1* and *Math1* are required for specification of neural and sensory hair cell fates, respectively. In the mouse otic epithelium, onset of *Ngn1* expression precedes that of *Math1* by roughly three days of development, paralleling the well-characterized temporal sequence of neural and sensory hair cell specification in mammals and birds. However, recent results suggest that commitment of otic epithelial cells to a neural fate continues through the time of sensory hair cell specification, although spatial relationships between regions of neural and sensory epithelial competence remain largely unexplored. Using transgenic reporter mice in conjunction with in situ hybridization, we have compared expression patterns of *Ngn1* and other markers of neural fate with those of *Math1* and various markers of nascent sensory epithelia between the stages of E11.5 and E14.5. Neural fate marker expression is absent from the developing cristae/ampullae at all stages analyzed. By contrast, the presumptive and definitive utricle and saccule express neural markers and produce delaminating cells at all stages tested. In the utricle, *Ngn1*- and *Math1*-positive domains are mutually exclusive by E13.5. The cochlea shows a restricted area of neural fate marker expression at its base at E12.5, but no neural markers tested are detected in the cochlea at later stages. These studies reveal that neurogenesis persists in specific regions of the developing vestibular system through a period of sensory hair cell specification.

## **806 Examination of the Atonal bHLH Family of Transcription Factors in the Developing Mouse Ear**

Ken A. Morris<sup>1</sup>, Ryan P. Basham<sup>1</sup>, S.M.S. Rocha-Sanchez<sup>1</sup>, Bernd Fritzsche<sup>1</sup>, Kirk W. Beisel<sup>1</sup>

<sup>1</sup>Department of Biomedical Sciences, Creighton University, Omaha, NE, USA

Recent data using basic-helix-loop-helix (bHLH) gene mutations have shown that *Neurog1* and *Atoh1* are essential for sensory neuron and hair cell formation, respectively. However, studying their interaction and combined effects suggest that some undifferentiated precursors of hair cells form even in the absence of both genes. Further, certain downstream genes of hair cells such as the neurotrophin *Bdnf* show an uneven dependency on *Atoh1*. This raises the possibility that more than the three currently known bHLH genes (*Atoh1*, *Neurog1*, and *Neurod1*) are expressed in the developing ear.

A panel of fifteen bHLH genes in the Atonal-related protein family was selected for study. Representative full- or partial-length cDNA clones were obtained and primer sets were designed for each of these genes. RT-PCR was performed using total RNA isolated from the otocysts of

developing mice at embryonic days (E) 10.5 and 11.5. All of the genes except *Atoh7* were detected at these developmental stages. The identities of the resulting amplicons were verified by restriction digestions and sequence analyses. Inner ear expression patterns are being examined using riboprobes in whole mount in situ hybridization studies of E10.5 and E11.5 otocysts. The expression patterns of these genes are being compared with those of *Atoh1* and *Neurog1* to investigate possible interactions or complementary roles. In addition, the transcript levels of these genes are being quantified using real-time TaqMan PCR. These studies will aid us in determining if other bHLH genes are involved in hair cell and afferent neuronal development. Our overarching goal is to establish the regulatory pathways associated with neuronal, neurosensory, and non-sensory tissues in the developing inner ear.

## **807 Math1 Regulates Development of the Cochlear Sensory Epithelium**

Chad Woods<sup>1</sup>, Mireille Montcouquiol<sup>1</sup>, Matthew Kelley<sup>1</sup>

<sup>1</sup>NIDCD

The bHLH transcription factor *Math1* has been shown to play a key role in the development of the inner ear. However, some controversy has persisted regarding its specific role. In particular, separate results have suggested that *Math1* could act to define the entire prosensory domain or alternatively, that its role is limited to differentiation of hair cells. In an effort to clarify the role of *Math1*, we generated an inducible version by fusing the *Math1* open reading frame to a tamoxifen-specific form of the estrogen receptor. The resulting fusion protein was inactive in the absence of tamoxifen (Tx), but could be activated to induce hair cell formation by continuous exposure to Tx. To recapitulate the normal pattern of *Math1* expression, clusters of cells within Kolliker's organ were transfected with *Math1*-ER in cochlear explants. *Math1*-ER was then transiently activated using Tx. Analysis of cell fates within transfected clusters indicated that transfected cells had developed as both hair cells and supporting cells. Moreover, the relative percentage of hair cells within each cluster could be increased by inhibiting the Notch pathway, indicating a role for Notch in sorting of individual cell fates. Finally, transfection with endogenous *Math1* also induced the formation of clusters of hair cells and supporting cells, but in these cases, all transfected cells developed as hair cells while supporting cells were recruited from surrounding, untransfected cells. These results demonstrate that while *Math1* is expressed in cells that will develop as supporting cells, the expression of *Math1* is not required for supporting cell development, indicating that *Math1* does not act to specify the prosensory domain. Instead, developing hair cells appear to generate two signals, an inhibitory signal mediated through Notch, that inhibits neighboring cells from developing as hair cells and a second, unidentified signal, that induces those same cells to develop as supporting cells.

## **808 Spatiotemporal Gradients of Innervation and Cell Proliferation in the Prenatal Cochlea**

**Stephen Echteler<sup>1</sup>, James Davis<sup>1</sup>**

<sup>1</sup>*The Children's Hospital of Philadelphia*

Precise topographic mapping between neurons of the spiral ganglion and hair cells of the organ of Corti is a hallmark of the mammalian cochlea. The mechanisms by which this topography is established are largely unknown (Rubel and Fritzsche 2002). Moreover, in mice, spiral ganglion neurons first innervate the cochlear sensory epithelium on embryonic (E) day 13, when cytologically distinct hair cells are not yet evident and the cochlea is less than one-quarter of its mature length (Sher, 1971). Therefore, neuronal topography must be established between specific segments of the spiral ganglion and organ of Corti while both of these structures are growing. At present, no studies have examined the spatiotemporal relationship between cochlear innervation and cellular proliferation within the developing spiral ganglion and organ of Corti. We addressed this issue by labeling proliferating cells in the prenatal cochlea on E13.5 through E 15.5 by cumulative injections of BrdU or by immunostaining for phosphohistone H3. Developing nerve fibers were subsequently visualized by immunostaining for neurofilament 150KD and newly differentiated hair cells were labeled by immunostaining for Myosin VI protein. We show that within each turn of the developing cochlea, the first auditory nerve fibers enter the organ of Corti when the spiral ganglion is adjacent to the cochlear duct and cellular proliferation is continuing within the spiral ganglion. As innervation proceeds within each turn of the cochlea, the formation of the spiral limbus displaces the spiral ganglion into the modiolus and away from its target tissue. This displacement is substantial, from E13.5 to E18.5 there is a seven-fold increase in the length of fibers between the spiral ganglion and the auditory sensory epithelium within each turn of the cochlea.

## **809 Developmental Expression of the Homeobox Transcription Factor Prox1 in the Murine Organ of Corti**

**Olivia Bermingham-McDonogh<sup>1</sup>, Jennifer Stone<sup>1</sup>, Clifford Hume<sup>1</sup>, Elizabeth Oesterle<sup>1</sup>**

<sup>1</sup>*Univ. of Washington*

The mammalian auditory epithelium is composed of a complex array of sensory hair cells and non-sensory supporting cells. The molecules that regulate specification, differentiation, and patterning among these cells are beginning to be characterized. Transcription factors are excellent candidate regulatory molecules for these processes, because they directly influence gene expression. The homeobox transcription factor, Prox1, regulates cell cycle exit and differentiation in specific neuronal subtypes in the mammalian retina. Prox1 has been localized to the developing inner ear of zebrafish and is highly expressed in sensorigenic and neurogenic regions of the avian otocyst. Here, we characterize Prox1 expression in developing and mature mammalian organ of Corti. Prox1 protein was detected in sections and whole-mount preparations of embryonic and postnatal organ of

Corti in Swiss Webster and CBA mouse strains using immunofluorescence. At E16, Prox1 protein is seen in the nuclei of developing hair cells and supporting cells throughout the organ of Corti. By E18, Prox1 immunoreactivity is restricted to some supporting cell nuclei, spanning from the inner pillar cells to the outermost Deiters' cells. Between P1 and 8 weeks of age, Prox1 immunoreactivity in supporting cell nuclei shows a progressive downregulation, starting in supporting cells located in the center of the organ and spreading outwards. The precise pattern of Prox1 immunoreactivity varied across the length of the organ, with the basal end showing a more advanced, downregulated pattern than the apical end. This pattern of Prox1 expression does not support a role for Prox1 in cell cycle exit but does suggest it may be important for cellular differentiation during organ of Corti development.

## **810 Expression Patterns of GATA3 in the Developing Chick Inner Ear**

**Andrew J. Drescher<sup>1</sup>, Mark E. Warchol<sup>1</sup>**

<sup>1</sup>*Department of Otolaryngology, Washington University School of Medicine*

Differentiation of the inner ear is a complex process that involves regional proliferation and apoptosis, and is orchestrated by differential gene expression. GATA3 is a zinc-finger transcription factor that is expressed in the embryonic ear and brain, and partial loss of GATA3 leads to syndromic hearing loss. During early development, GATA3 is expressed in neurons of rhombomere 4, and in the developing otic vesicle and associated mesenchyme. At later stages, it is expressed in the developing utricle, spiral ganglion, and cochlea. Notably, GATA3 expression in the mature utricle is limited to the striolar reversal zone. In order to further understand the role of GATA3 in otic development, we have characterized GATA3 expression in the developing chick ear between embryonic days 3-7. In the E3 otocyst, GATA3 expression is restricted to the lateral region and is complementary to the medial expression of PAX2. By E4, GATA3 is present in the dorsal otocyst (which will form the vestibular organs), and in a patch of cells on the ventral-medial otocyst (which has been described as a 'hot spot' of apoptosis- Lang et al., JCN, 2000). By E5, expression is observed in mesenchymal cells outside the ventral otocyst, and in a patch of cells in the dorsal-lateral otocyst that corresponds to the location of the developing utricle. Interestingly, cells in the mesenchyme adjacent to the utricular region also express GATA3. By E6, GATA3 is present in the cochlear duct and utricular region, but is absent from the most dorsal otocyst (where the semicircular canals will form). GATA3 expression at E7 shows partial overlap with the developing sensory epithelium of the utricle; this region may later form the striola. Further studies will attempt to modify GATA3 expression in these regions, in order to elucidate its role in structural determination.

(Supported by grants from the NIH and NASA)

### **811** Dynamic Pattern of Expression of NT3 in the Postnatal Inner Ear

Mitsuru Sugawara<sup>1,2</sup>, Konstantina Stankovic<sup>1,2</sup>, M. Charles Liberman<sup>2,3</sup>, Gabriel Corfas<sup>1,3</sup>

<sup>1</sup>Children's Hospital Boston, <sup>2</sup>Massachusetts Eye and Ear Infirmary, <sup>3</sup>Harvard Medical School

NT3 is essential for normal development of hair cell afferent innervation. In adult ears, the pattern of NT3 expression and its biological roles are not understood. Studies of transgenic mice in which erbB receptor signaling is blocked in cochlear supporting cells in adults suggest that neuregulin-induced NT3 expression is important for survival of spiral ganglion neurons. In these mice, which express a dominant-negative erbB receptor in inner ear supporting cells, the cochlea develops normally, but by P30, type I spiral ganglion neurons degenerate. Immediately preceding this degeneration, there is a specific and significant reduction in the levels of NT3 mRNA in the cochlea.

To understand the normal pattern of NT3 expression during postnatal development, we analyzed cochlear and vestibular organs from P0 to adult using real-time quantitative RT-PCR and a lacZ reporter mouse in which cells expressing NT3 also express  $\beta$ -gal, allowing for histochemical visualization.

The RT-PCR showed age-related decrease in NT3, with a 20- and 3-fold decrease from P0 to P25 in cochlear and vestibular portions, respectively. The lacZ staining patterns were consistent with the RT-PCR results. At P0, NT3 was strongly expressed in supporting cells and hair cells of all vestibular and cochlear sense organs, Reissner's membrane, saccular and utricular membranes and the dark cells adjacent to canal organs. With increasing age, staining decreased monotonically in all cell types. In the cochlea, by P15 there was a longitudinal gradient (apex > base) and radial gradient (IHC > OHC area). In vestibular maculae, staining gradients were: striolar > extrastriolar regions, supporting cells > hair cells and type-II > type-I hair cells. By P135, cochlear staining was restricted to IHCs and their supporting cells and was much stronger in the apex than the base. These data are consistent with NT3 being involved in the loss of type-I ganglion cells in DNerb4 mice.

R01 DC04820 (GC) and P30 005029 (MCL).

### **812** Estrogen Receptors in Rat in the Inner Ear During Different Stages of Pregnancy

Rusana Simonoska<sup>1</sup>, Annika Stenberg<sup>1</sup>, Britt Masseroni<sup>2</sup>, Lena Sahlin<sup>2</sup>, Malou Hultcrantz<sup>1</sup>

<sup>1</sup>Dept of Otorhinolaryngology, KNV, Karolinska Hospital and Intitute, <sup>2</sup>Dept of women and child health, Karolinska Intitute

Background: Older women in menopause, in normal population tend to develop more severe hearing loss compared to males. In Turner Syndrome (loss of one X chromosome), results in a short stature, failure to enter puberty spontaneously and infertility. Ear and hearing problems are common among these patients and affects outer, middle and inner ear. Middle-aged women frequently

complain of a rapid onset of social hearing problems, due to rapid aging of the ear (presbycusis). Can estrogen have an impact on hearing? Aim: 22 rats in 4 different groups in different time periods of pregnancy and 16 fetuses in 2 groups, have been investigated in order to study the effect of estrogen and estrogen receptors in the inner ear during inner ear development. Methods: All specimens were smeared and stained immunohistochemically for estrogen receptors and Peripherin. Results: Estrogen receptors are present in the inner ear of the rat and differ during pregnancy and fetal stadium. Conclusion: Estrogen receptors are present in the inner ear and are up- or down regulated depending on the stage of pregnancy and fetal period, proposing that estrogen may affect hearing.

### **813** Expression of Robo1 and Robo2 in the Developing Inner Ear

Jennifer Bayer<sup>1</sup>, Heather Aloor<sup>1</sup>, Takako Kondo<sup>1</sup>, Eri Hashino<sup>1</sup>

<sup>1</sup>Indiana University School of Medicine

Members of the Roundabout (Robo) family are transmembrane receptors and bind their ligands, Slit proteins. Four members, Robo1-4, have been thus far identified in the mouse. Slit-Robo signaling has been implicated in axon guidance of sensory neurons and development of lung, limb and kidney. Little, however, is known about a potential role for Robo proteins in inner ear development. To determine which Robo protein plays a major role in inner ear development and to elucidate its specific functions, we investigated spatio-temporal expression patterns of *Robo1* and *-2* in the mouse inner ear using quantitative RT-PCR and *in situ* hybridization. Our RT-PCR analysis with inner ear cDNA at E9, E10, E14, E18, P5 and P20 revealed that *Robo2* expression was 10-times higher than *Robo1* expression at all developmental stages examined. Both *Robo1* and *-2* mRNAs were detectable as early as E9, and up-regulated thereafter. The expression levels reached their peaks at E14, after which they declined and became undetectable by P5 (*Robo1*) or P20 (*Robo2*). Whole-mount *in situ* hybridization analysis with E9 embryos showed that strong *Robo2* expression was seen in the anterodorsal region of the otic epithelium. At E14, positive signals were confined to the sensory epithelia of the cochlea and vestibule. At P1, *Robo2* expression was detected in supporting cells of the organ of Corti. In contrast, sensory hair cells and the spiral ganglion were devoid of *Robo2*. A similar expression pattern was observed for *Robo1*. The significantly higher expression of *Robo2* compared to *Robo1* strongly suggests that Robo2 plays a primary role in inner ear development. In addition, the absence of Robo1 and *-2* in spiral ganglion neurons suggests that these proteins may not play a role in axon guidance in the cochlea.



## **814 Slit/robo Signaling in the Developing Cochlea**

**Audra Webber<sup>1</sup>**, Lynne Bianchi<sup>2</sup>, Yael Raz<sup>3</sup>

<sup>1</sup>University of Pittsburgh School of Medicine, Pittsburgh, PA, <sup>2</sup>Neuroscience Program, Oberlin College, Oberlin, Ohio, <sup>3</sup>Department of Otolaryngology, University of Pittsburgh, Pittsburgh, PA

The *slit* proteins and their *robo* receptors participate in guiding developing sensory neurons to their central and peripheral targets. While earlier studies revealed expression of these genes in the otic vesicle, little is known about the role of this signaling pathway in inner ear morphogenesis. This aim of this study was to determine the cell-specific expression of the various *slit* and *robo* genes in the developing inner ear. Whole-mount *in situ* hybridization was performed on developing mouse cochleae during the period of spiral ganglion neurite extension towards the organ of Corti. Results reveal that *slit3* and *robo1* are expressed in restricted bands along the cochlear spiral between embryonic day 13 (E13) and E 15.5. *Slit3* expression was restricted to the neural aspect of the sensory epithelium whereas *robo1* expression was limited to a complementary abneural band. The restricted and complementary expression of *slit3* and *robo1* during the period of neurite outgrowth suggests that this signaling pathway may play a role in shaping neural connectivity in the developing cochlea.

Supported by University of Pittsburgh Medical Student Summer Research Program to AW and Pennsylvania Lions, University of Pittsburgh CMRF, AHRF Wiley Harrison Memorial Research Grant and NIDCD K08 DC006676 to YR.

## **815 Espin Protein Expression during Early Ear Development and Stereociliogenesis**

**Gabriella Sekerkova<sup>1</sup>**, Lili Zheng<sup>1</sup>, Patricia Loomis<sup>1</sup>, Enrico Mugnaini<sup>1</sup>, **James Bartles<sup>1</sup>**

<sup>1</sup>Northwestern University Feinberg School of Medicine

Espins are multifunctional actin cytoskeletal proteins in the parallel actin bundle at the core of hair cell stereocilia and are the target of mutations that cause deafness and vestibular dysfunction in mice and humans. We have examined the distribution of espin proteins by immunohistochemistry during prenatal (E10-19) and postnatal (P1-35) development in rats. We detected two distinct patterns of espin protein expression during inner ear development. One, which was unexpected, encompassed early development and was characterized by strong and homogenous immunostaining of the otic pit (E10.5) and, at later stages, the otocyst and endolymphatic duct/sac. At E14, the entire cochlea and vestibular system showed this homogeneous staining. By E16.5-E17 espin immunostaining showed evidence of down-regulation in cells other than developing hair cells. The immunostaining associated with this early wave of espin expression was specific in that it was not observed with preimmune IgG. Importantly, it was observed in wild-type mice and heterozygous jerker mice, but not in homozygous jerker mice, which lack espin proteins. Moreover, it coincided with the appearance of known espin

isoforms on western blots. Consistent with a role in stereocilium elongation/maintenance, the second wave of espin expression surrounded stereociliogenesis. Espin-positive hair cells, which showed espin accumulation at their apical surface, first appeared in maculae at E14. Vestibular hair cells in maculae and cristae showed strong staining of stereocilia by E16 and E18, respectively. The number of espin-positive cochlear hair cells with labeled stereocilia increased from E16 onward, in a gradient from base to apex along the cochlea. During postnatal development, obvious gradients in espin levels arose, and these were positively correlated with stereocilium length. These results suggest that espins function during multiple epochs in the development of the inner ear. (NIH DC004314 to JRB)

## **816 Expression of Ribeye in Zebrafish**

**Yvonne Bradford<sup>1</sup>**, Nina Woodworth<sup>1</sup>, William Roberts<sup>1</sup>

<sup>1</sup>University of Oregon

Ribbon class synapses are found in the sensory receptors and neurons of the inner ear and retina. Characteristically these synapses have a presynaptic osmiophilic dense body, or ribbon, that is surrounded by tethered synaptic vesicles. Due to the ribbon's close proximity to the active zone and synaptic vesicle associations, it has been hypothesized to be involved in synaptic vesicle cycling at the synapse. Previously Schmitz *et al.* (2000) described a ribbon specific protein, RIBEYE, which localizes to the synaptic ribbon in antibody studies and appears to be a component of ribbons in human, cow, and rat.

In humans, RIBEYE is encoded by the *CTBP2* gene, which also encodes C-terminal binding protein 2 (CtBP2). CtBP2 acts as a transcriptional co-repressor that binds zinc finger proteins, and RIBEYE is a cytoplasmic protein that has been suggested to be a structural component of ribbon class synapses. To understand how novel developmental and physiological functions can evolve from a single gene, we have been investigating the genomic structure and embryological function of *CTBP2* in zebrafish and pufferfish. We have previously shown that the last common ancestor of fish and mammals had a single copy of the *CTBP2* gene, and that a later duplication in the fish lineage generated a second copy of this and several flanking genes in pufferfish and zebrafish. This duplication resulted in the production of Ribeye-a and Ribeye-b. *In situ* analysis of these transcripts in zebrafish suggest that Ribeye-a and Ribeye-b are differentially expressed in the sensory receptors and neurons of the inner ear and retina. To further understand the function of RIBEYE at ribbon synapses we are currently using morpholinos to block translation of Ribeye transcripts.

## **817** Developmental Analysis of Calretinin in the Rat Cochlea

Young Ho Kim<sup>1</sup>, Ji Yeong Park<sup>2</sup>, Byung Yoon Choi<sup>2</sup>, Min-Hyun Park<sup>2</sup>, Jun Ho Lee<sup>1</sup>, Chong-Sun Kim<sup>2</sup>, Sun O Chang<sup>2</sup>, Seung Ha Oh<sup>2</sup>

<sup>1</sup>Department of Otolaryngology, Seoul National University, College of Medicine, Seoul Municipal Borama, <sup>2</sup>Seoul National University, College of Medicine, Seoul, South Korea

**Background and Objectives :** Calcium-binding proteins are known to play an important role in the regulation of intracellular calcium concentrations. Calretinin(CR) is a neuron specific, high affinity cytosolic calcium-binding protein of the EF-hand family and expressed in the organ of Corti and most of neurons of mammals. In the mouse inner ear, inner hair cells and most of Corti's ganglion neurons show expression of calretinin from the embryonic stage through the adult stage, whereas outer hair cells are known to be expressed from P1(postnatal day 1), disappearing before P22. It is known that rats show the expression of calretinin in inner hair cells and most of spiral ganglion cells. This study was performed to observe the change of expression and amount of calretinin during the maturation period in the rat cochlea.

**Materials and Methods :** Sprague-Dawley rat cochlea collected from each stage (P5, P17, P35) were analyzed using 2D gel electrophoresis, proteomic analysis, Western blot analysis, and fluorescence immunocytochemistry.

**Results :** In P17 and P35, calretinin was identified as two spots at an isoelectric point (pI) of 4.9 and a molecular weight of 29 kDa in the analysis of the rat cochlea proteins using proteomic analysis, which is thought as a result of posttranslational modification, especially phosphorylation. P17 and P35 revealed remarkable existence of calretinin in 2D gel electrophoresis and Western blot, whereas P5 demonstrated its existence little. In fluorescence immunocytochemistry, P17 and P35 showed the calretinin immunoreactivity of similar intensity in inner hair cells and most ganglion neurons, but P5 displayed a very faint immunoreactivity.

**Conclusion :** Compared with early neonatal stage, an amount of calretinin remarkably increases during the critical period of the cochlear maturation and is maintained till young adult stage. In the rat inner ear, these results suggest that calretinin may have a specific role as a calcium-binding protein since the cochlear maturation.

## **818** Analysis of Fgf3 Reporter Expression in the Mouse Otic Vesicle

Androulla Economou<sup>1,2</sup>, Mark Maconochie<sup>2</sup>

<sup>1</sup>Developmental Neurobiology, National Institute for Medical Research, Mill Hill, London, UK, <sup>2</sup>School of Life Sciences, University of Sussex, Brighton, UK

Fgf3 is required for inner ear induction in mammals, avians and zebrafish, and performs this role through co-operation with other members of the FGF family. However, Fgf3 expression is also prominent in the developing inner ear after induction of the otic vesicle. Mouse mutants for Fgf3 alone display highly variable inner ear phenotypes, where presentation of phenotypes may be complicated by the

expression of other FGF ligands in the developing inner ear. Some of these additional ligands should be able to signal through the same receptors. In order to begin to accurately delineate which roles are carried out by Fgf3, the identity of cells expressing Fgf3 in inner ear development is an important first step. Further, in order to circumvent the difficulty of using non-radioactive *in situ* hybridisation for highly sensitive detection of Fgf3 expression, we have developed transgenic mice with an Fgf3 reporter which includes regulatory elements responsible for driving the inner ear domain of endogenous Fgf3 expression. Analysis of transgenic mouse embryos carrying the Fgf3 reporter reveals that expression is restricted to the lateral aspect of the antero-ventral compartment of the otic vesicle.

## **819** Notch1 Activation Demonstrated *In Situ*, During Mouse Inner Ear Development of the Late Embryonic and Post-Natal Stage

Junko Murata<sup>1</sup>, Akinori Tokunaga<sup>2</sup>, Hideyuki Okano<sup>2</sup>, Arata Horii<sup>1</sup>, Tamotsu Harada<sup>3</sup>, Katsumi Doi<sup>1</sup>, Manabu Tamura<sup>1</sup>, Takeshi Kubo<sup>1</sup>

<sup>1</sup>Osaka University Medical School, Department of Otolaryngology, <sup>2</sup>Keio University School of Medicine, Department of Physiology, <sup>3</sup>Kawasaki Medical School, Department of Otolaryngology

Notch signaling pathway has been thought to play an important role in the development of the alternating mosaic pattern of the hair cells and supporting cells in mammalian inner ear, mainly based on the result of function-loss experiment using *Jagged2* mutant mice. However, the precise spatio-temporal activation pattern of Notch1 in the cochlear development has remained unknown. We tried to map the active state of Notch1 *in situ* by immunohistochemistry using a specific antibody that recognizes the processed form of the intracellular domain of Notch1 (actN1) (Tokunaga A et al., 2004). The activated state of Notch1 has not been elucidated at developing cochlear duct of E14.5. We found a population of Notch1-activated cells around Math1-positive cells at E15.5. These Notch1-activated cells were all PCNA-positive at E15.5, and they existed just medial to a wide zone of PCNA-negative cells. Most of actN1-positive cells became PCNA-negative at E16.5. By E17.5, the organ of Corti is patterned into one row of inner and three rows of outer hair cells. ActN1 was detected in the cells surrounding these hair cells, which were thought to become supporting cells. At P0, the mouse organ of Corti is not matured yet, but the primitive supporting cells-like immature Deiters cells can be identified. Notch1 was activated in these primitive supporting cells, and faint immuno-reactive product of actN1 was observed in GER. Notch1 activation had almost disappeared at P3 stage.

This is the first report to demonstrate *in situ* that Notch1 was transiently activated in the supporting cell lineage during the development of mammalian cochlea, indicating a crucial role of Notch pathway in hair cell and supporting cell differentiation. In addition, we suggest that Notch pathway may have some other important functions in inner ear development, such as the determination of pro-

sensory cell population and the migration of ganglion neurons. In combination with mutant mice strategy, our morphological study add more insights into the better understanding of inner ear development and differentiation.

### **820 Large Scale Gene Expression Profiles of Mouse Early Inner Ear Development.**

**Samin Sajan<sup>1</sup>**, Mark Warchol<sup>1</sup>, Michael Lovett<sup>1</sup>

<sup>1</sup>Washington Univ Med School

Studies of inner ear development to-date have examined the influence of a relatively small number of genes. To further understand pathways in this important process and to obtain a measurement of normal gene expression, we micro-dissected inner ear structures from mouse embryos at stages E9 to E15 in half-day intervals (covering the earliest structures of the inner ear up until the appearance of differentiated hair cells). Gene expression profiles were derived using Affymetrix mouse gene chips. Two litters per developmental stage were obtained, the structures were dissected and duplicate gene-chips were hybridized. Genes were selected that were reproducibly differentially expressed by at least 1.5-fold between any two stages, and self-organizing maps created to identify genes with similar expression patterns. We found 528 genes to be differentially expressed across the time course, of which 10% had previously been shown to be expressed in the inner ear. Genes with relatively high expression at early stages (E9-E9.5) included *Dachshund 2*, *Choroidermia*, *Kinesin family member 1B*, and *NeuroD6*. At the stage E12.5 and beyond, we compared gene expression between the cochlea and the vestibular organs and found 384 differentially expressed genes. From this list, 111 genes exhibited heightened expression in the cochlea in all stages compared to the vestibular organs, and included genes such as *TGFB2*, *Forkhead Box G1*, *IRF6*, *SOX21* and *Frizzled-related 1*. The vestibular organs showed a heightened expression of 125 genes in all of these stages, some of which were *Zic3*, *Zic4*, *Cyclin dependent kinase 5 (p35)*, *BMP2*, and *Otoraplin*. Many of these observations have been validated by quantitative-PCR and/or in-situ hybridizations. This study provides new candidate pathways for further investigation in specifying the complex structural components of the inner ear and in the genetics of hearing loss and/or its restoration.

### **821 Profiling Gene Expression Associated with the Onset of Hearing**

**Ellen Reisinger<sup>1</sup>**, David Meintrup<sup>2</sup>, Dominik Oliver<sup>1</sup>, Bernd Fakler<sup>1</sup>

<sup>1</sup>Universitaet Freiburg, <sup>2</sup>Universitaet der Bundeswehr Muenchen

The developing rodent inner ear is an ideal object to study the molecular mechanisms underlying the unique performance of the mammalian cochlea, since major maturation processes and the onset of hearing take place postnatally. Morphological and physiological changes are inextricably coupled to the expression of a series of cochlea-specific proteins that are in part responsible for inherited hearing disorders. The aim of the present study

was identification of genes involved in the maturation of the organ of Corti.

Using the mRNA differential display technique on organs of Corti of P0 and P14 rats we identified 174 different transcripts that are upregulated during postnatal development. From these transcripts 103 are coding for proteins of known function, 63 transcripts either code for proteins of unknown function or hypothetical proteins or were assigned to expressed sequence tags (ESTs). Eight transcripts could not be assigned to any published mRNA sequence. The known proteins serve most different cellular functions including intracellular signaling pathways, control of growth and differentiation and regulation of protein biosynthesis and degradation. Furthermore, a number of synaptic or vesicular proteins as well as ion channels and cytoskeletal proteins were shown to be upregulated.

Together, our results give insight into the various molecular processes required for the onset of hearing. Furthermore, it seems suggestive that at least some of the uncharacterized proteins or mRNAs might be candidates for deafness genes.

### **822 Down Syndrom and Hearing Loss : Is There an Evidence of Morphological Changes in the Inner Ear ?**

**Annelies Schrott-Fischer<sup>1</sup>**, Xilong Yu<sup>1</sup>, Mario Bitsche<sup>1</sup>, Rudolf Glueckert<sup>1</sup>

<sup>1</sup>ENT Department

The stria vascularis is essential for the production and maintenance of high potassium concentration in the cochlear duct and endocochlear potential. Primary abnormalities of the stria vascularis can result in cochleosacular degeneration.

Atrophy of the stria vascularis has been identified as a possible cause of slowly progressive sensorineural hearing loss. Cases with strial atrophy as the only observable morphological changes are usually characterized by flat pure tone audiometric thresholds. Presbycusis is evident in Down syndrome after the first decade of life. The exact aetiology of this hearing loss remains unclear. The aim of our study was to determine whether any abnormalities associated with Down syndrome can be observed even at very early gestational ages compared to normal stria development.

The expression of intermediate filaments (cytokeratin, nestin and vimentin) and NaK/ATPase, is shown during gestational maturation of the foetus using immunohistological methods. Intermediate filament proteins were used to assess their cell type. Na-K/ATPase was stains marginal strial cells and is responsible for the generation of high potassium concentration in the cochlear duct and the positive endocochlear potential.

Epithelial cytokeratin was evident from gestational week 13 in the marginal cells. Gestational maturation leads to an increased intensity in staining for cytokeratin. In week 13 Vimentin staining is obvious in all stria layers. At a later stage of maturation Vimentin is only expressed in intermediate and basal cells. Nestin staining pattern was similar to that of Vimentin with the exception that it is

absent in basal cells. No change in the expression of these proteins could be observed. Likewise, Electron microscopy confirmed normal maturation, suggesting unimpaired development of the stria vascularis in temporal bones with Down syndrome.

The study was performed in accordance with the guidelines of the Declaration of Helsinki.

The work presented was supported by the FWF Project Nr. P15948 -BO5 and the Austrian Nationalbank (Jubiläumsfond) Nr 8745.

### **823 Localization of 5-HT in Developing Auditory Brainstem Neurons**

**Ann Thompson<sup>1</sup>, Jean Shih<sup>2</sup>, Jean Lauder<sup>3</sup>**

<sup>1</sup>Univ. of Oklahoma Hlth Sci Ctr, <sup>2</sup>Univ. of Southern California, <sup>3</sup>Univ. of North Carolina at Chapel Hill

A neurotransmitter in the adult, serotonin (5-HT) serves as an epigenetic signal and neurotrophic factor during development. Evidence in rodents suggests that 5-HT plays a developmental role in the auditory brainstem. Serotonin has been shown to alter synaptic currents in the lateral superior olive (LSO) in the postnatal gerbil [1]. The 5-HT transporter is expressed by auditory brainstem neurons during postnatal development in the wild type mouse [2]. The 5-HT transporter is believed responsible for the transient appearance of 5-HT in developing auditory brainstem neurons [3].

To further study 5-HT expression in the immature auditory brainstem, brain sections from 7 day old mice were immunohistochemically processed with an antibody against 5-HT. We used male mice with a deletion of the *Mao a* gene, the monoamine oxidase A knock out (MAO A KO), which have increased brain levels of 5-HT during perinatal development [4].

As initially reported [3], many 5-HT-immunoreactive (IR) cell bodies were observed in the LSO. In addition, we observed numerous labeled axons in the lateral lemniscus (LL). 5-HT-IR axon terminals were observed in the dorsal nucleus of the LL (DNLL) and the inferior colliculus (IC). In the DNLL and central nucleus of the IC (CNIC), the 5-HT-IR axon terminals were relatively large in size and were arranged pericellularly. This is unlike the typical fine, *en passant* type innervation in the external nucleus of the IC of the same mouse, and in the CNIC of the wild type adult mouse. This staining pattern indicates that the postnatal expression of 5-HT in the mouse occurs along a particular ascending pathway originating in the LSO, traveling through the LL, and terminating in the DNLL and CNIC. Further studies will investigate the presence of other elements of the 5-HT phenotype by neurons of the same ascending pathway from the LSO.

1. Fitzgerald, K., and Sanes, D. (1999) Serotonergic modulation of synapses in the developing gerbil lateral superior olive. *J Neurophysiol*, 81:2743-2752.

2. Thompson, A., and Lauder, J. (2004) Postnatal expression of the serotonin transporter in auditory brainstem neurons. *Dev Neurosci*, in press.

3. Cases, O. et al. (1998) Plasma membrane transporters of serotonin, dopamine and norepinephrine mediate serotonin accumulation in atypical locations in the developing brain of monoamine oxidase A knock-outs. *J Neurosci*, 18:6914-6927.

4. Cases, O. et al. (1995) Aggressive behavior and altered amounts of brain serotonin and norepinephrine in mice lacking MAOA. *Science*, 268:1763-1766.

### **824 SK2 in the Cochlea**

**Claudia Braig<sup>1</sup>, Harald Winter<sup>1</sup>, Martina Knirsch<sup>2</sup>, Ulrike Zimmermann<sup>1</sup>, Karin Rohbock<sup>1</sup>, Iris Köpschall<sup>1</sup>, Jutta Engel<sup>2</sup>, Marlies Knipper<sup>1</sup>**

<sup>1</sup>Tuebingen Hearing Research Center, Molecular Biology,

<sup>2</sup>Institute of Physiology Dept. II, University of Tuebingen

Hair cells are the targets of olivocochlear fibers that carry efferent inhibitory feedback from the brain. In particular, IHCs initially are contacted by olivocochlear efferent fibers that make contacts with IHCs before targeting OHCs (Simmons et al., 1996). In the adult system IHCs are innervated mainly by afferent fibers, having few if any remaining efferent contacts (Liberman et al., 1990). In contrast, adult OHCs are the principal targets of cholinergic olivocochlear efferents (Guinan, 1996). The efferent feedback to IHCs and OHCs is predominantly provided by the release of acetylcholine (ACh), that acts on AChR a 9/a 10 subunits. In OHCs and IHCs calcium influx through the receptor complex is presumed to activate nearby calcium-dependent SK2 channels, leading to inhibitory postsynaptic currents (Oliver et al., 2000; Elgoyhen et al., 1994, 2001; Glowatzki et al., 2000). Accordingly, we note the localization of SK2 channel protein during the early (IHC), respectively late (OHC) postnatal period.

Aiming to identify transcriptional regulators for SK2 we could identify thyroid hormone (TH) as one of the presumptive modulators. While under hypothyroid conditions the SK2 protein in OHCs is completely absent most interestingly SK2 expression persists in IHCs.

Using in situ hybridisation, immunohistochemistry, reporter gene study, RT-PCR and EMSA we start to elucidate the obvious differential regulatory role of TH on SK2 ion channels in IHCs and OHCs.

Supported by a grant from the Deutsche Forschungsgemeinschaft DFG KN316/4-1 and Interdisciplinary Center of Clinical Research (Tuebingen, Germany).

## **825** Understanding the Developmental Origins of the Mammalian Superior Olivary Complex

David M. Howell<sup>1,2</sup>, W. Jason Morgan<sup>1,2</sup>, Albert S. Berrebi<sup>1,3</sup>, George S. Spirou<sup>1,4</sup>, Peter H. Mathers<sup>1,2</sup>

<sup>1</sup>Sensory Neuroscience Research Center, Dept. of Otolaryngology, WVU School of Medicine, <sup>2</sup>Dept. of Biochemistry and Molecular Pharmacology, WVU School of Medicine, <sup>3</sup>Dept. of Neurobiology and Anatomy, WVU School of Medicine, <sup>4</sup>Dept. of Physiology and Pharmacology, WVU School of Medicine

Developing neurons utilize multiple guidance cues to reach their appropriate destination. Much is known about the anatomy and electrophysiology of cells in the adult auditory brainstem, but the molecular factors directing cell specification and migration of these nuclei remain relatively unknown. For example, neurons comprising the superior olivary complex (SOC) are known to originate in the rhombic lip around mid gestation; however, their birth location within the rhombic lip and migratory route are not known. The lack of understanding and the paucity of markers for these early cells have hindered efforts to identify mechanisms that establish auditory brainstem topography.

We find that SOC neurons express RNA for three cell surface receptors, *DCC*, *robo1* and *robo2*, during their migration into the ventral brainstem. These receptors direct growth cone guidance and cellular migration in various pathways throughout the central nervous system. Both *netrin1* and *slit1*, secreted ligands for *DCC* and *robo*, respectively, are expressed in the brainstem at locations consistent with a role in the guidance of SOC neurons. As early as E12.5, probes for *DCC*, *robo1* and *robo2* label cells in migratory streams that originate from the rostral-most extent of the brainstem and extend caudally on the ventral surface of the brainstem toward the adult SOC position. SOC neurons maintain *DCC*, *robo1* and *robo2* expression as they segregate into discrete SOC nuclei. The utilization of these factors in SOC cell migration is supported by the disruption of the SOC and the absence of the MNTB in P0 mice that are homozygous for a mutation in the *DCC* gene. Furthermore, analysis of the brainstem in P0 mice carrying no functional copies of the *netrin1* gene shows a similar disruption of the SOC with an ablation of the MNTB. Given these results, we suggest that a functional *netrin-DCC* and *slit-robo* signaling system is necessary for the migration of SOC neurons.

(Supported by NIH/NCRR grant P20 RR15574)

## **826** Identification of in Vivo Inner Ear Coup-TFI Targets

Celina Montemayor<sup>1</sup>, Feng Lin<sup>1</sup>, Scott D. Pletcher<sup>1</sup>, Fred A. Pereira<sup>1</sup>

<sup>1</sup>Baylor College of Medicine

Chicken Ovalbumin Upstream Promoter Transcription Factors (COUP-TFs) are orphan members of the nuclear receptor superfamily. Although their ligand and precise function are unknown, the presence of COUP-TF homologues across species—from metazoans to humans

—and their stunning interspecies similarity indicate that these nuclear receptors play an essential role that has been conserved across evolution. There are two members of this family in mice: COUP-TFI and COUP-TFII, and although they have overlapping expression patterns, knockout studies have revealed that each has a vital, specific developmental function. COUP-TFI is mainly expressed in the central and peripheral nervous system, and the COUP-TF<sup>-/-</sup> mice exhibit perinatal mortality, with malformations in the glossopharyngeal ganglion, loss of cortical layer IV, and defects in axonal arborization. Of particular interest to our lab, COUP-TFI<sup>-/-</sup> mice exhibit a deafness phenotype correlated with a gradual degeneration of the basal turn of the organ of Corti before functional hearing is established. To better understand the function of this orphan receptor, we seek to identify *in vivo* targets of COUP-TFI and its role in development of the mouse inner ear. We obtained microarray gene expression profiles of wild-type and COUP-TFI<sup>-/-</sup> inner ear tissue. Analysis of identical and experimental replicates revealed a list of 256 genes that are significantly different across genotypes. After verification by qRT-PCR of inner ear expression, promoter sequences from such genes will be scrutinized for evolutionary conservation and for matches to a COUP binding-site matrix based on existing literature. Candidate COUP-target genes will also be studied through promoter-reporter gene assays and chromatin immunoprecipitation to determine direct targets.

## **827** The Intracellular Localization of Biotinidase Correlates with Proliferation and Differentiation of Cell Types in the Auditory System During Development.

Craig Brumwell<sup>1</sup>, D. Kent Morest<sup>1</sup>, Barry Wolf<sup>2</sup>

<sup>1</sup>Neuroscience Dept., Univ. of Conn. Med. Ctr, Farmington,

<sup>2</sup>Research Dept., Conn. Children's Med. Ctr, Dept. of Pediatrics, Univ. of Conn. Med. School, Hartford

We are studying a genetic form of sensorineural hearing loss due to biotinidase deficiency. Biotin is an essential vitamin. Biotinidase is responsible for cleaving and recycling biotin from biocytin and from dietary protein-bound sources. This frees biotin for use in the cell body. Biotinidase can biotinylate histones in the nucleus. We hypothesize that biotinidase is present at key stages in the development of the auditory system. To examine the role of biotin and biotinidase in cellular development, cultures were used to study the intracellular expression in cell lines. FIRST, as an example of a non-neuronal cell, NIH 3T3 fibroblasts were studied. Biotinidase immunostaining revealed signal in the nucleus and cytoplasm, and, in many cells, it was associated with the nuclear envelope. Biotin localization by avidin labeling revealed a nuclear signal. In situ RT-PCR for RNA revealed a similar pattern. SECOND, as an example of a neuron, the B104 cell line was grown in defined media, with or without biotin. Biotinidase immunostaining showed nuclear localization with biotin (2.7µg/ml), but a reduced nuclear signal without biotin. Biotin was localized in the nucleus. THIRD, biotinidase localization was studied in a ventral otocyst cell line (VOT) (gift of M. Holley), which gives rise to ganglion

cells and other epithelial cells. The biotinidase immunostaining had a nuclear signal when VOT cells were proliferating. In contrast, when cells were differentiating, only some nuclei were immunopositive. Biotin was similarly localized in the differentiating cells. Tuj1 (neuronal tubulin) immunostaining was then done with VOT's to determine if localization and cell-fate were linked. The results showed that biotinidase localized in the nucleus in differentiating neuronal precursors, with Tuj1 in the cytoplasm. In summary, the findings show that biotinidase has a different intracellular distribution depending on cell fate.

(Supported by Safra Research Fund.)

## **828** Spatiotemporal Expression of *Fam3c* in the Developing Mouse Inner Ear

Valentina Pilipenko<sup>1</sup>

<sup>1</sup>CHMC

Spatiotemporal Expression of *Fam3c* in the Developing Mouse Inner Ear

Daniel Larson, Valentina V. Pilipenko, Daniel I. Choo, John H. Greinwald, Jr.

*Center for Hearing and Deafness Research, Division of Pediatric Otolaryngology, Cincinnati Children's Hospital Medical Center and the University of Cincinnati College of Medicine, Cincinnati, OH, United States*

Previously we have reported overlapping expression patterns of the *Fam3c* and *Nkx5.1* genes in proliferating epithelial cells in the developing semicircular canals at embryonic day (E) 15.5. Sequence analysis of the *Fam3c* promoter region suggested a role for *Nkx5.1* in *Fam3c* function. These findings suggest that *Fam3c* may be a downstream target gene for the *Nkx5.1* transcription factor in semicircular canal development. By studying the expression of *Fam3c* in the inner ear at the otocyst and post natal stages, further insight into the molecules involved in the pathways of inner ear development can be gained.

We performed *in situ* hybridization on the mouse E9-E12, E18.5 and postnatal day (P) 2 inner ear cryosections. At the otocyst stage *Fam3c* showed expression both in the otocyst epithelium and in the periotic mesenchyme surrounding the newly formed otocyst, where as *Nkx5.1* expression was detected only in the otocyst epithelium. At E18.5 and P2, *Fam3c* expression was not detected in the semicircular canals, but at P2 expression was present in the organ of Corti region of the cochlea. Interestingly, strong expression of *Fam3c* was also noted in the developing hair follicles in the dermis.

Thus, at the otocyst stage *Fam3c* and *Nkx5.1* showed overlapping but distinct expression patterns. Further studies are underway to delineate the role of *Fam3c* in inner ear development and the specific relationship with other related molecules, such as *Nkx5.1*

## **829** Expression Patterns of Tbx Genes in The Developing Mouse Inner Ear

Heather Aloor<sup>1</sup>, Takako Kondo<sup>1</sup>, Eri Hashino<sup>1</sup>

<sup>1</sup>Indiana University School of Medicine

The T-box (Tbx) genes encode a family of transcription factors that have a conserved DNA-binding domain called the T-box. Tbx genes play a role in developmental processes such as cell type specification, limb formation, and regulation of morphogenetic movements. Among more than 20 Tbx genes discovered thus far, Tbx1 has been shown to control sensory vs. neural specification in the developing inner ear. However, little is known about other members of the Tbx family in inner ear development. To identify other Tbx genes that play a role in inner ear development, we investigated spatio-temporal expression patterns of Tbx2, -3 and -5 in the mouse inner ear using quantitative RT-PCR and *in situ* hybridization, and compared them to the expression pattern of Tbx1. Our RT-PCR analysis with E10 otocyst cDNA revealed that Tbx1 expression was the highest, followed by Tbx2 (40% of Tbx1) and then Tbx3 (18% of Tbx1). The expression of all Tbx1, Tbx2 and Tbx3 was down-regulated at later embryonic stages and became barely detectable at P5. Expression of Tbx5 was not detectable in the inner ear at any developmental stages examined. Whole-mount *in situ* hybridization analysis with E9 embryos showed that strong Tbx3 expression was confined to the lateral side of the otic epithelium. At E10, Tbx3-positive regions remained in the lateral region, but particularly strong expression was seen in anterior and posterior ends of the otocyst. A similar, but more ubiquitous expression pattern was seen for Tbx2. No Tbx2 or -3 expression was detected in the mesenchyme of the second pharyngeal arch. At E14, strong Tbx3 expression was found in the organ of Corti and vestibular epithelia. The expression domain of Tbx2 or -3 only partially overlaps with that of Tbx1, which is confined to the posterior region of the otocyst and the periotic mesenchyme (Raft et al., 2004). These results suggest that Tbx2 and/or -3 might play a different role in inner ear development than Tbx1.

## **830** Changes in Expression of Musashi 1 in Guinea Pig Vestibular Endorgans Following Gentamicin-Induced Damage

Tatsuya Yamasoba<sup>1</sup>, Chie Miyajima<sup>1</sup>, Kenji Kondo<sup>1</sup>, Hideyuki Okano<sup>2</sup>

<sup>1</sup>University of Tokyo, <sup>2</sup>University of Keio

Musashi1 (Msi1) is expressed in neural stem/progenitor cells, astroglial progenitor cells and astrocytes in the central nervous system (CNS), which indicates that this protein is a neural stem cell marker. It has been demonstrated that Msi1 may be a Notch activator by translationally suppressing the synthesis of m-numb and that Notch lateral inhibition plays an important role in the development of the mammalian inner ear. In the current study, we investigated Msi1 expression in normal and damaged vestibular endorgans in mature guinea pigs.

Albino male guinea pigs (250-350 g) were used. Experimental animals received gentamicin (GM) topically to the left middle ear spaces and controls saline.

Experimental animals were euthanized 1, 3, 7, and 28 days following surgery and controls 7 days following it. The temporal bones were fixed, decalcified, dehydrated, and embedded in paraffin. Sections were incubated in 3 % H<sub>2</sub>O<sub>2</sub> in methanol, block solution, 1:2000 PBS dilution of rat anti-Msi1 monoclonal antibody, and a peroxidase-conjugated secondary antibody, and allowed to react with diaminobenzidine.

In controls, there was no immunoreactivity in the hair cells, while Msi1 immunoreactivity was observed in the nuclei of the supporting cells in both the macula and ampulla. Three days following GM application, the damage to the hair cells became evident but Msi1 expression was unchanged. Seven days following GM treatment, the hair cells were severely degenerated and Msi1 immunoreactivity was diffusely spread into the cytoplasm of the supporting cells. The Msi1 expression returned to be nuclear predominance pattern 28 days following GM application, and a few nuclei of the hair cells in the utricle were immunopositive to Msi1. It has been shown that Msi1 is localized predominantly in the cytoplasm of CNS progenitor cells and that in the mouse inner ear the subcellular localization of Msi1 changes from cytoplasmic predominance to nuclear predominance during the first 2 weeks after birth. Considering these findings, diffuse spread of Msi1 expression into the cytoplasm of the supporting cells soon after the completion of hair cell injury suggests that Msi1 plays some role, such as introduction of hair cell regeneration, during scar formation in the vestibular organs. A small amount of hair cells, which became immunopositive to Msi1 after scar was well formed, might be differentiated from the supporting cells.

### **831 The Generation of Cell Colonies Following Dissociation of Sensory Epithelial Sheets from the Newt Inner Ear**

**Ruth Taylor<sup>1</sup>, Andrew Forge<sup>1</sup>**

<sup>1</sup>*University College London*

Investigations into dedifferentiation of supporting cells prior to cell cycle re-entry and the mechanism of supporting cell division have directed our research to establish cultures that initially comprise only supporting cells and hair cells.

Cultures of small groups of cells explanted from the sensory epithelium of the adult newt sacculle can be maintained for over 6 weeks. Sheets of cells from the saccular macula and surrounding epithelium were detached from the underlying mesenchymal tissue of the sacculle using thermolysin. Cells were dissociated into clusters of up to 20 cells, but individual cells were also generated, by trituration and plated onto laminin coated Mattek dishes. After 7-10 days, these cells attached and lost their differentiated characteristics to become a monolayer of cells. Previous studies using newt sacculles cultured within the intact otic capsule to investigate regeneration have shown that proliferation of the supporting cells is absent or at an extremely low level in undamaged sensory epithelia but upregulated following hair cell ablation with gentamicin. In this study, the dissociated cells were taken from undamaged sensory epithelia and progressed to form cell colonies in which

dividing cells were readily observed. They survived several passages. Immunohistochemistry using ZO-1, an epithelial marker, showed that they retained epithelial cell characteristics. Maintenance of colonies for a further 14 days without change of culture medium resulted in cells adopting a neuronal-like morphology that were  $\alpha$ -tubulin III (TuJ1) and neurofilament 200 positive. Many cells sent out long, fine processes to connect with cells in close proximity. It would appear that dissociated cells from the sensory epithelia dedifferentiate, re-enter the cell cycle to proliferate and defined culturing conditions induce them to redifferentiate into a neuronal-like cell, suggesting plasticity in the saccular epithelial cells as found in other newt tissues.

### **832 Differential Expression of Prostaglandin E Receptors in Skin and Airway Wounds of Fetal, Weanling and Adult Rabbits**

**Ha-Sheng Li-Korotky<sup>1,2</sup>, Patricia Hebda<sup>1,2</sup>, Chia-Yee Lo<sup>2</sup>, Joseph E. Dohar<sup>1,2</sup>**

<sup>1</sup>*University of Pittsburgh School of Medicine,* <sup>2</sup>*Children's Hospital of Pittsburgh*

**Objective:** We previously demonstrated that fetal airway mucosal healing is regenerative and scarless and that a gene encoding prostaglandin E<sub>2</sub> (PGE<sub>2</sub>) receptor 4 (Ptger4) was induced in fetal skin wounds but suppressed in adult skin wounds 12h after wounding. The goal of this study is to define age-dependent, tissue-specific expression profiles of this gene family encoding Ptger1, Ptger2, Ptger3, and Ptger4 in both skin and airway wounds. **Design:** Skin and airway incisional wounds were made in fetal (gestation day 21-23), weanling (4-6 weeks) and adult (>6 months) rabbits. Non-wounded and wounded tissues were collected at 12h (all age groups), 24h (weanling skin and airway wounds) and 48h (weanling airway wounds) after injury. Expression levels of Ptger genes were assayed by real-time PCR. **Results:** By comparing the basal levels of Ptger gene family members, Ptger4 was relatively, abundantly expressed in both non-wounded skin and airway of all age groups. At 12h in skin wounds, expression levels of Ptger4 increased over 3 fold in fetus, no significant change in weanling rabbits, but decreased over 3 fold in adults compared with that in age-matched non-wounded tissues. The suppression of Ptger4 gene expression remained unchanged up to 24h in postnatal skin wounds. By contrast, at 12h in airway wounds, Ptger4 molecular activity decreased over 2 fold in fetuses, but increased about 5 fold in weanling animals and about 2 fold in adults. The augmented levels of Ptger4 expression were over 4-fold and sustained up to 48h after wounding in postnatal airway wounds. **Conclusions:** Differential expression profiles of the Ptger gene family in the context of the age-dependent and tissue-specific wound repair suggest that Ptger4 is prominently involved in the PGE<sub>2</sub>-mediated fetal scarless wound repair and adult wound scar formation.

### **833 Breed Differences in Mitotic Activity in Young Chickens Following Acute Sound Exposure**

**Christina Kaiser**<sup>1,2</sup>, Douglas Girod<sup>2</sup>, Dianne Durham<sup>1,2</sup>

<sup>1</sup>Anatomy and Cell Biology, University of Kansas Medical Center, Kansas City, KS, USA, <sup>2</sup>Otolaryngology/Head and Neck Surgery, University of Kansas Medical Center, Kansas City, KS, USA

Previous studies from our laboratory have shown that young egg layer chickens are more susceptible to acute sound exposure than young broiler chickens. Egg layer birds are more likely to display severe cochlear damage (Kaiser et al, Soc. for Neuroscience Abstracts; 2003) and more robust CNS metabolic changes (Kaiser et al., ARO Abstracts; 2004). In this study, we examine the capacity of egg layer and broiler birds to regenerate new cochlear hair cells following acute sound exposure. Young egg layer or broiler chickens (10-17 weeks) were placed into a sound attenuated chamber and exposed to a 1500 Hz pure tone at 120 dB SPL for 24 hours. Following either 24 or 72 hours of recovery, birds were given a single, subcutaneous injection of bromodeoxyuridine (BrdU) and sacrificed 6 hours later. Cochleae were dissected as whole mounts and processed for BrdU immunocytochemistry to reveal mitotically active cochlear cells. In both breeds, BrdU-labeled cells were seen only in the cochlear regions damaged during sound exposure. In egg layer birds, the majority of BrdU-labeled cells were seen 24 hours after sound exposure; fewer BrdU-labeled cells were seen after 72 hours of recovery. Preliminary results in broiler birds show robust labeling at both 24 and 72 hours, with labeling at 72 hours greater than that seen in egg layer birds. These results suggest that mitotic replacement of hair cells may occur over a more protracted period of time in broiler birds. It is not known whether breed differences exist in the total number of regenerating hair cells.

Supported by NIDCD R01 DC01589, R21 DC004982, and the KUMC Biomedical Research Training Program.

### **834 Analysis of Myosin VI and VIIa During Avian Sensory Hair Cell Regeneration**

**Luke Duncan**<sup>1,2</sup>, Juila Anderson<sup>1</sup>, Jonathan Matsui<sup>1,3</sup>, Dominic Mangiardi<sup>1,4</sup>, Douglas Cotanche<sup>1,5</sup>

<sup>1</sup>Otolaryngology, Children's Hospital, 300 Longwood Ave, Boston, MA, United States, <sup>2</sup>Chemistry, Holy Cross College, 1 College Street, Worcester, MA, United States, <sup>3</sup>Department of Molecular and Cellular Biology, Harvard University, Cambridge, MA, <sup>4</sup>Biomedical Engineering, Boston University, 44 Cummings Street, Boston, MA, <sup>5</sup>Otology & Laryngology, Harvard Medical School, 243 Charles Street, Boston, MA

A single 300 mg/kg subcutaneous injection of gentamicin induces apoptotic death within the proximal end of the chick basilar papilla. Avians have the capacity to regenerate lost hair cells from the surrounding supporting cells. When the apoptotic hair cells are ejected from the basilar papilla, it induces the supporting cells to re-enter the cell cycle, which we monitored via BromodeoxyUridine (BrdU) uptake in the inner ear. The motor proteins myosin VI and myosin VIIa are observed to change their

distributions within regenerating hair cells over time. Multiple injections of BrdU were used to indicate hair cells that have arisen from mitotic origins. The first signs of BrdU labeling are seen in the proximal end of the basilar papilla, 65 hours after gentamicin treatment. No myosin labeling is observed in the regenerating hair cells until myosin VI is first expressed, 96 hours after gentamicin treatment. Myosin VIIa is not expressed until 120 hours after injection. At the onset of labeling, both myosins uniformly labeled the cytoplasm of regenerating hair cells, but they were still excluded from the nucleus. Myosin VI was transiently expressed at the base of the stereocilia around 96 hours but is not expressed at 144 hours. Myosin VIIa labeled the growing stereociliary bundle. A temporal study of the progression of hair cell regeneration was performed by administering a single injection of BrdU, collecting samples 4 hours later. Control levels of mitotic activity were indicated by BrdU labeling at 60 hours after gentamicin treatment, indicating that mitotic activity had not begun. In the time between 65 and 72 hours, the number of BrdU labeled cells increase greatly in the proximal end of the cochlea. In the following 24 hours, the center of BrdU labeling shifts towards the distal end of the damaged region, indicating a temporal shift in mitotic activity similar to the progression of gentamicin damage. There is a rapid decrease of mitotic activity between 96 and 120 hours after injection, with only a few BrdU labeled nuclei in the distal end of the damage region. By 144 hours, BrdU levels subside to control levels.

Supported by NIH/NIDCD Grant #DC01689, the Children's Hospital Otolaryngology Foundation Research Fund and the Sarah Fuller Fund.

### **835 Binding Kinetics of Proteins Involved in Repair of Traumatized Hair Cells in the Sea Anemone (*Haliplanella Luciae*).**

**Michele Green**<sup>1</sup>, Glen Watson<sup>1</sup>

<sup>1</sup>University of Louisiana Lafayette

Hair bundle mechanoreceptors located on the tentacles of sea anemones detect swimming movements of their prey. The hair bundles are derived from a multicellular complex in which a sensory neuron is surrounded by 2-4 supporting cells. The hair bundles are severely damaged by 1 h exposure to calcium-depleted seawater but then spontaneously recover normal structure and function within 4 h of returning to seawater containing calcium. This recovery is based on the secretion of specific proteins that we named 'repair proteins.' A partial purification of repair proteins on Sepharose columns yields a fraction (fraction beta) that has biological activity comparable to the complete repair protein mixture. We here report on the binding kinetics of 2 fractions derived from fraction beta obtained from an ion exchange column. Fraction beta was injected into a DEAE-Trisacryl ion exchange column equilibrated to a low salt buffer. A salt gradient to 2 M was imposed to the column and fractions collected. The ion exchange fractions 10, 11, 36, 37, 38 and 39 were immunoreactive in a dot-blot assay using anti-beta. Fractions 10 and 11 were pooled as were fractions 36-39. The pooled fractions were biotinylated and then used to



label live tissue after a 1h trauma caused by exposure to calcium-depleted seawater. After specified incubations in the biotinylated beta fractions, the tissue was fixed and patterns of labeling were examined using a confocal microscope. At 10 minutes, fraction 10-11 binds the sensory neuron and supporting cells. By 20 minutes, labeling remains circular, but expands in the total area labeled. Labeling continues to expand to the maximum at 30 minutes. Fraction 36-39 shows similar patterns of labeling to fraction 10-11 through the first 20 minutes, after which time the area labeled drastically decreases. Thus, the components of these fractions label hair bundles dynamically but with differences in their labeling patterns. Supported by NIDCD DC05514.

### **836** Auditory Hair Cell Replacement and Hearing Improvement After Math1 Gene Therapy in Mature Deafened Guinea Pigs

*Masahiko Izumikawa<sup>1</sup>, Shelley Batts<sup>1</sup>, Karen Abrashkin<sup>1</sup>, Donald Swiderski<sup>1</sup>, David Dolan<sup>1</sup>, Yehoash Raphael<sup>1</sup>*  
<sup>1</sup>Kresge Hearing Research Institute, Univ. of MI

**Abstract.** Sensorineural deafness caused by hair cell (HC) loss is permanent because lost HCs are not replaced. The bHLH transcription factor Math1 < is an essential gene for HC differentiation during cochlear development. We recently demonstrated that adenovirus-mediated overexpression of Math1 < generates new HCs in the organ of Corti of mature deafened guinea pigs. To further characterize the outcome of Math1 gene transfer in the deafened cochlea, young adult guinea pigs were systemically deafened by kanamycin and ethacrynic acid, resulting in complete bilateral elimination of HCs in cochlear turns 1-3 and profound deafness, verified by ABR audiometry. Four days after the insult, an adenovirus vector was inoculated into the scala media of the left cochlea. Gene inserts were Math1 (Ad. Math1), Math1 and GFP (Ad. Math1-GFP) or controls (Ad.empty or Ad.GFP). SEM analysis five weeks post Math1 inoculation revealed immature HCs in the organ of Corti. At two months, the surface of the auditory epithelium contained numerous cells with mature stereocilia bundles. Cross sections of the auditory epithelium revealed normal appearing inner HCs, whereas in the outer HC area, new HCs were poorly differentiated. Epi-fluorescence examination of ears inoculated with Ad. Math1-GFP, revealed that many new HCs were GFP positive. No regenerated HCs or GFP-positive cells were found in any of the control animals or contralateral ears. Two months after Ad. Math1 inoculation, ABR thresholds in Math1 inoculated ears were significantly better than contralateral ears and control groups at all tested frequencies (4, 8, 16, and 24 kHz). These data further implicate transgenic Math1 expression as a signal for generating new HCs, and demonstrate the ability of this treatment to improve auditory thresholds in deafened animals.

Supported by GenVec, NIH/NIDCD Grants R01-DC01634, R01-DC05401, R01-DC05053, and P30-DC05188.

### **837** Induction of Supporting Cell Proliferation in the Cochlea using AdV5 Encoded shRNA Targeting p27kip1 mRNA in Vivo.

*Rende Gu<sup>1</sup>, Carol Pierce<sup>1</sup>, James LaGasse<sup>1</sup>, Huy Tran<sup>1</sup>, Jerry Glattfelder<sup>1</sup>, Eric Lynch<sup>1</sup>, Jonathan Kil<sup>1</sup>*  
<sup>1</sup>Sound Pharmaceuticals, Inc.

Our group has stimulated supporting cell proliferation in wild type mouse cochlear cultures using liposome mediated antisense oligonucleotides and adenovirus encoded shRNAs that target and inhibit p27kip1 mRNA (Kil et al., 2001, ARO; Kil et al., 2004, ARO). We have developed CMV promoter expression constructs to include co-expression of GFP in cells that are infected. These second generation CMV-GFP-IRES-p27 shRNA adenovirus were validated in cell and organ cultures for their ability to express GFP and to drive down p27 mRNA and protein levels. For in vivo analysis, we delivered 2 ul of 8e10 ifu/mL adenovirus in a single bolus injection through the lateral wall of the cochlea in six to eight week old Swiss Webster mice. As a control, adenovirus encoding random sense shRNA was encoded on the same GFP-IRES-encoding vector and delivered in the same manner. To identify proliferating cells, BrdU was delivered systemically during the recovery phase through a subcutaneous mini osmotic pump. Following recovery, mice were sacrificed and the cochlea collected for histologic analysis. Whole cochlea were immunoreacted for BrdU and GFP, and visualized under fluorescence microscopy. Using this approach, the tropism of the AdV for Deiter's cells in vivo is high. Mice treated with AdV encoding p27 shRNA had BrdU (+), GFP (+) cells within the organ of Corti. Mice treated with the control random sense shRNA-GFP vector had significant infection of Deiter's cells but no BrdU. These novel findings extend what we have reported previously for neonatal cochlear cultures. Quantitative analysis of the ratio of GFP (+) to BrdU (+) cells within the organ of Corti will be presented. Evaluation of physiologic recovery in the context of injury and longer recovery intervals is on going.

### **838** Differential Regulation of Chaperonin Subunits during Scarless Wound Healing

*Sandeep Kathju<sup>1</sup>, Adam Abdulally<sup>1</sup>, Duane Oswald<sup>1</sup>, Sandy Johnson<sup>1</sup>, Elaine Blyskun<sup>1</sup>, Fen Ze Hu<sup>1</sup>, J Christopher Post<sup>1</sup>, Garth D Ehrlich<sup>1</sup>*

<sup>1</sup>Allegheny Singer Research Institute

**Introduction:** Adult mammalian tissues heal injury with scar formation. Although useful in sealing an injured area, scar can itself be a source of significant morbidity, interfering with respiration, hearing, speech, restricting movement, etc. In contrast, mammalian fetal tissue can heal without scar. We have undertaken to identify gene products differentially expressed during scarless wound healing through several expressomic techniques; differential display has identified the eta subunit of chaperonin containing T-complex polypeptide (CCT-eta) as one such differentially regulated message.

Methods: Incisional wounds were made on New Zealand white fetal rabbits at gestational age 20 days; wounds were also placed on the dorsums of the mothers. Twelve hours post-injury the wounds were excised from both fetal and adult rabbits; unwounded control tissue was also harvested. Total RNA extracted from these tissues was used as a template in differential display reactions to generate tissue-specific gene expression fingerprints. Up- and down-regulated amplimers were characterized and their differential expression confirmed by limiting dilution RT-PCR.

Results: Several differentially expressed amplimers were noted to correspond to the eta subunit of chaperonin containing T-complex polypeptide. Limiting dilution RT-PCR confirmed that CCT-eta was indeed specifically down-regulated in healing fetal wounds. In other systems, all 8 subunits of CCT had been observed to display coordinated regulation. Therefore, primers were designed (using mouse and human sequences) to the remaining 7 subunits and tested on rabbit tissues in limiting dilution RT-PCR reactions. This revealed that CCT-eta is the only subunit specifically down-regulated in healing fetal wounds, whereas CCT-alpha is specifically down-regulated in healing adult wounds.

Conclusion: Using RACE (rapid amplification of cloned ends) we have isolated full-length clones of rabbit CCT-eta, CCT-alpha, and CCT-beta. These clones allow for the further exploration of post-transcriptional and transcriptional mechanisms important in scarless wound healing through the study of 3' untranslated and adjacent promoter regions.

### **839 Advances in Organ Culture Methods for the Study of Avian Auditory Hair Cell Regeneration**

Rachel Nehmer<sup>1</sup>, Jialin Shang<sup>1</sup>, Jennifer Stone<sup>1</sup>

<sup>1</sup>Univ. of Washington

The avian auditory epithelium (AE) normally generates no new hair cells after birth. However, when hair cells are killed experimentally in mature birds, mitotic activity among sensory progenitors cells (SPCs) is stimulated, and new functional hair cells are formed. In vitro methods provide an excellent means to explore mechanisms underlying this renewed sensory cell production. In this study, cochlear ducts (CDs) from P7 chickens were cultured between 1 and 7 days. Cultures were exposed to streptomycin (78 µM) for 2 hours or for the entire culture period. Culture conditions varied according to media (DMEM, EBSS/BME) and supplements (1-10% fetal bovine serum, with or without 1 mM pyruvate). Bromodeoxyuridine was added to cultures to assess SPC proliferation, and cultures were labeled with hair cell markers to assess patterns of hair cell damage and regeneration. We observed a significant effect of media and supplements on the spatial pattern and levels of mitotic activity in SPCs. In DMEM, SPCs in abneural and neural regions of the AE throughout its length showed marked proliferation between 2 and 4 days in vitro. Rates of proliferation were inversely proportionate to, but the spatial pattern was not dependent upon, serum concentration. In EBSS/BME (which in contrast to DMEM

contains no pyruvate), significantly less SPC division was seen, and most was in the proximal end. However, when pyruvate was added to EBSS/BME, levels of SPC division increased to become comparable with DMEM, with the majority of mitotic cells located along the abneural edge, in a manner independent of serum concentration. Preliminary qualitative analyses suggest that spatial patterns of cell division in each condition do not correlate with hair cell loss. Many new hair cells were detected immunologically by 6-7 days in vitro. Current investigations are underway to determine if levels and patterns of new hair cell differentiation are dependent upon culture media or supplements.

### **840 NF-kappaB is a Survival Factor for Immature Auditory Hair Cells**

Ivana Nagy<sup>1</sup>, Daniel Bodmer<sup>1</sup>

<sup>1</sup>University Hospital Zurich

Death of auditory hair cells (HC) in the inner ear as a consequence of aging, disease, acoustic trauma, or exposure to ototoxins results in irreversible hearing loss. Despite intense effort, little is known about the molecular mechanisms that underlie protection of these valuable cochlear elements. Here we examined the role of NF-kappaB, a ubiquitous transcription factor that plays a major role in the regulation of many apoptosis- and stress-related genes, in mediating HC survival. We analyzed organ of Corti (OC) explants of 5-day old rat pups, and found evidence of a constitutively active form of NF-kappaB that localizes predominantly to the outer and inner HCs. Selective inhibition of NF-kappaB through use of a cell-permeable inhibitory peptide caused transcriptional down-regulation of *gadd45beta*, an anti-apoptotic NF-kappaB target, activation of caspase-3 and cell death by apoptosis. In contrast to p5 animals, immunohistochemical analysis showed differential staining patterns for RelA (p65) in the cochleae of adult animals and no evidence of NF-kappaB in the OC. Taken together, our data suggest an important function for NF-kappaB in promoting survival of immature auditory hair cells.

### **841 Alexander's Law Revisited**

Benjamin Jeffcoat<sup>1</sup>, Alexander Shelukhin<sup>1</sup>, Alexander Fong<sup>1</sup>, William Mustain<sup>1</sup>, Wu Zhou<sup>1</sup>

<sup>1</sup>University of Mississippi Medical Center

It is well known that the slow phase velocity of a nystagmus changes as a function of the gaze direction. Alexander's Law states that the beat direction of the nystagmus is the determining factor for the amplitude of the slow phase velocity. Our hypothesis is that the modulation of the slow phase velocity is due to the activation levels of motoneuron pools associated with different eye positions. This hypothesis and Alexander's Law make the same prediction for peripheral vestibular lesions or equivalent cold water stimulation. However, they make opposite predictions under conditions of activation of peripheral vestibular end organs or equivalent warm water stimulation. To test this hypothesis, binocular eye positions were recorded (infrared video-based eye tracker) in normal human subjects (N=3) when they were given cold and

warm water caloric stimulation in total darkness. Once nystagmus reached steady-state, subjects were instructed to look 10 degrees to the left and right. Alexander's Law was examined by measuring the correlation coefficient between the slow phase eye velocity and the eye position for each eye. One of the three subjects exhibited significant Alexander's Law. During cold water stimulation, there was an increase of the slow phase velocity in the contralateral gaze direction, which is consistent with both our hypothesis and the Alexander's Law. During warm water stimulation, however, there was also an increase of the slow phase velocity in the contralateral gaze direction, which is not consistent with the Alexander's Law, but is consistent with our hypothesis. We also examined the conjugacy of the slow phase, which is a controversial issue in the literature. We found that the slow phase was conjugate in two subjects and disconjugate in one subject. As our subject population increases in this ongoing project, we will be able to either extend or restate Alexander's Law.

### **842 Transient Elimination of Bilateral Vestibular Functions Makes Postural Changes in Guinea Pig.**

**Hiroataka Hara<sup>1</sup>, Hiroaki Shimogori<sup>1</sup>, Kenji Takeno<sup>1</sup>, Takefumi Mikuriya<sup>1</sup>, Hiroshi Yamashita<sup>1</sup>**

<sup>1</sup>*Department of Otolaryngology, Yamaguchi University School of Medicine*

By the progress of space technology, humans will have the opportunity to live in space, and this has created a need to elucidate the effects of altered gravity on the peripheral vestibular organs. To investigate microgravity effects on vestibular organs, we have constructed a ground-based simulation model of microgravity.

Blocking vestibular inputs without injuring the peripheral vestibular organs would at least simulate an influence of vestibular input in a microgravity environment. In this paper, we show the animal model by means of continuous bilateral intracochlear administration of Tetrodotoxin (TTX) by osmotic pump and show the behaviors changes during TTX administration and after TTX discontinuation.

By eliminating the central gliosis and neurochemical changes that accompany mechanical destruction of the peripheral vestibular organs, this model permits unconfounded examination of peripheral changes that occur in the absence of vestibular inputs like in space, and enables examination of the central changes that occur when vestibular inputs are resumed.

### **843 A Guinea Pig Model for Blockage of Vestibular Input with Intact Vestibular Endorgan using TTX by Osmotic Pump**

**Kenji Takeno<sup>1</sup>, Hiroaki Shimogori<sup>1</sup>, Hiroataka Hara<sup>1</sup>, Kazuma Sugahara<sup>1</sup>, Tsuyoshi Takemoto<sup>1</sup>, Kuniyoshi Tanaka<sup>1</sup>, Takefumi Mikuriya<sup>1</sup>, Hiroshi Yamashita<sup>1</sup>**

<sup>1</sup>*Yamaguchi University*

[Background]

On the earth, we always feel gravitation. However, in a space life, we lose bilateral vestibular input, and so we can adapt ourselves to circumstances. To investigate the

mechanisms of vestibular compensation in the loss of bilateral vestibular function, we developed animal model for transient and reversible blockage of vestibular input using tetrodotoxin (TTX) by osmotic pump. Recently, we reported that no histological damage was found in the crista and macula in animal with TTX administration for 1 week by using osmotic pump.

└─mObjects└─n

We investigated the vestibular function changes in the guinea pig which received transient vestibular input blockage by TTX administration using osmotic pump.

└─mMaterials and Methods└─n

We used male Hartley guinea pigs. At first, animals were examined vestibulo-ocular reflex (VOR) and caloric test (0.5ml/10sec). Sequentially, intracochlear administration of TTX (10<sup>-6</sup>g/ml) was performed by osmotic pump bilaterally for 3 days. After 3 days infusion of TTX, VOR and caloric test were examined, sequentially catheters were clamped. After 7 days from clamping, VOR and caloric test were examined.

└─mResults└─n

After 3 days from operation, Caloric response and VOR gain were vanished. After 7 days from clamping, Caloric response was almost recovered as pre-operative value, but VOR gain showed insufficient recovery compared with pre-operative value.

└─mConclusion└─n

These data indicate that transient blockage with bilateral intracochlear administration of TTX may be useful for studying the central vestibular response to recurrent or episodic vestibular disruption in the intact vestibular system.

### **844 Rapid Administration of Edaravone Protects Vestibular Periphery from AMPA-Induced Vestibulotoxicity in the Guinea Pig**

**Hiroaki Shimogori<sup>1</sup>, Kazuma Sugahara<sup>1</sup>, Kuniyoshi Tanaka<sup>1</sup>, Tsuyoshi Takemoto<sup>1</sup>, Kenji Takeno<sup>1</sup>, Hiroshi Yamashita<sup>1</sup>**

<sup>1</sup>*Yamaguchi University School of Medicine*

Ischemic injury is one of the major causes of inner ear diseases. The ischemic injury induced elevation of glutamate concentration in the cochlear perilymph. Glutamate is the most likely neurotransmitter between hair cells and primary afferents in the inner ear. But excessive glutamate also has toxic effects on the inner ear. The aim of this study was to evaluate effects of edaravone, one of the free radical scavengers clinically used, on AMPA-induced peripheral vestibular disorder like ischemic injury.

Thirty-five Hartley guinea pigs with normal Preyer's reflexes and normal tympanic membranes were used in this study. Intracochlear administration of AMPA (10 mM) was performed at 0.6 ml/hr for 5 minutes by a syringe pump (n = 30). Edaravone (3 mg/ml)-soaked gelform was put on the round window membrane just after AMPA administration (group A, n = 7), 12 h after AMPA administration (group B, n = 7), 24 h after AMPA administration (group C, n = 9). In 7 animals out of 30, AMPA administration was performed without edaravone

(group D). As a control group, a same amount of artificial perilymph was administered intracochlearly (group E, n = 5).

One week after operation, in the group A, a mean value of caloric response time in the lesioned side/ caloric response time in the intact side (time ratio) was statistically higher than that in the group C or D. There was no statistical difference between the group A and group B, or the group A and group E with respect to the time ratio.

Our results indicate the possibility that topical application of edaravone may be one of the candidates for treatment of vertigo induced by ischemia, and that administration of edaravone within 12 h after lesions are made shows an sufficient effects.

#### **845 Discharge Properties of Otolith Afferents in the Normal C57BL/6 Mouse**

Hong Ju Park<sup>1,2</sup>, David M Lasker<sup>1</sup>, Lloyd B Minor<sup>1</sup>

<sup>1</sup>Department of Otolaryngology-Head and Neck Surgery, Johns Hopkins University, <sup>2</sup>Konkuk University

Extracellular recordings were made from 95 otolith afferents recorded in the left superior vestibular nerve in anesthetized 2-3 month old C57BL/6 mice maintained at a core body temperature of 36° C. Animals were rotated (nose out) about an earth-vertical axis that was offset 50 cm from the center of rotation in order to obtain tangential acceleration. Sinusoidal rotations were delivered at 0.5-12 Hz with peak tangential acceleration ranging from 0.04-0.47g. Maximum sensitivity vectors were determined for 46 otolith units by tilting the animal 20°, 0° and -20° in the inter-aural and naso-occipital planes. We used these findings to localize afferents into four regions relative to the striola: medial anterior (MA, n = 23), medial posterior (MP, n = 14), lateral posterior (LP, n = 4) and lateral anterior (LA, n = 3). Sensitivity vectors for the MP and LA units aligned closely with the earth-horizontal plane. MA units aligned best with the animal tilted approximately 43° left ear down. LP units aligned best with the animal tilted approximately 31° right ear down. By virtue of their location within the superior vestibular nerve and their polarization vectors, it is likely that these afferents innervated the utriculus.

Firing rates, measured with the head in the horizontal position, of regular ( $CV^* < 0.1$ , n = 66), intermediate ( $0.1 < CV^* < 0.2$ , n = 5) and irregular ( $CV^* > 0.2$ , n = 19) otolith afferents were  $45.5 \pm 16.5$ ,  $36.3 \pm 24.0$ , and  $34.0 \pm 14.9$  sp/s, respectively. For regular afferents, sensitivity and phase lead re acceleration were  $46.7 \pm 12.2$  (sp/s)/g and  $-0.4 \pm 8.5^\circ$  at 0.5 Hz and did not differ across frequencies ( $p > 0.1$ ). For irregular afferents, sensitivity measured  $237.7 \pm 128.8$  (sp/s)/g at 0.5 Hz. Sensitivity rose as a function of frequency with a 79% increase at 12 Hz. Phase lead re acceleration for these afferents was  $19.1 \pm 8.2^\circ$  at 0.5 Hz and  $32.0 \pm 16.9^\circ$  at 12 Hz and did not differ across frequencies ( $p > 0.3$ ).

Regular otolith afferents showed no change in sensitivity and a phase of approximately 0° across the range of frequencies used in this study and could be modeled with a simple gain term. Irregular afferents showed an increase in gain and a constant phase lead of approximately 25°

with increasing frequency. The sensitivity and phase of these irregular afferents were well fit with a gain and fractional derivative term ( $75 \cdot s^{0.27}$ ). Supported by NIH R01 DC02390.

#### **846 Intratympanic Gentamicin in Human Subjects: A Lesion Intermediate Between Canal Plugging and Surgical Destruction**

Matthew Stewart<sup>1</sup>, Charles C. Della Santina<sup>1</sup>, Americo Migliaccio<sup>1</sup>, Lloyd Minor<sup>1</sup>, John Carey<sup>1</sup>

<sup>1</sup>Otolaryngology, Head and Neck Surgery, Johns Hopkins School of Medicine

In human subjects, intratympanic (IT) gentamicin treatment for Ménière's disease decreases the angular vestibulo-ocular reflex (aVOR) gain in response to ipsilateral head thrusts. Studies in the chinchilla (abstracts 62, 813) show that this aVOR gain reduction is accompanied by severe reduction of afferent sensitivity to head acceleration and loss of type I hair cells and stereocilia on type II cells. However, the treatment does not silence the spontaneous firing of these afferents. This situation should be analogous to that created by canal plugging (CP). We used 3D magnetic search-coil recordings to compare the aVOR in response to canal-plane head thrusts between 3 groups of human subjects: an unusual group of subjects with single CP (N=4), unilateral IT gentamicin-treated subjects (N=17), and surgical unilateral vestibular destruction (SUVD) subjects (N=13). Ipsilateral excitatory aVOR gains for plugged canals and gentamicin-treated canals averaged  $0.45 \pm 0.12$  and  $0.35 \pm 0.13$ , respectively; ipsilateral gains in SUVD subjects averaged  $0.25 \pm 0.09$  (mean  $\pm$  s.d). These results suggest that the lesion created by IT gentamicin is intermediate between SUVD and CP. Preservation of ipsilateral vestibular afferent firing after IT gentamicin and CP may be responsible for the increased values of these gains over those after SUVD. The relatively greater response seen after CP may be due to contributions from (i) other ipsilateral canals, (ii) otolith organs, and/or (iii) greater afferent activity in the plugged canal.

Supported by NIH/NIDCD K08DC006216, R03DC005700, K23DC00196, R01DC02390, T32DC00027, P03DC05211

#### **847 Structural and Ultrastructural Changes in Chinchilla Semicircular Canal Cristae and Utricular Maculae After Intratympanic Gentamicin Treatment**

Lee Ching Anderson<sup>1</sup>, Timo Hirvonen<sup>2</sup>, Mohamed Lehar<sup>1</sup>, Casey Vogelheim<sup>3</sup>, John Carey<sup>1</sup>

<sup>1</sup>Johns Hopkins University School of Medicine, <sup>2</sup>Helsinki University Central Hospital, <sup>3</sup>Northern Michigan University

Intratympanic (IT) gentamicin treatment is used to treat vertigo in Ménière's disease. While known as "chemical labyrinthectomy," IT gentamicin does not stop spontaneous vestibular afferent firing, although sensitivity to stimuli is markedly reduced (Hirvonen et. al., 2002). We hypothesize that some vestibular hair cells (HC) and synaptic specializations are preserved to provide the synaptic input required for such firing. Adult chinchillas

received a single unilateral IT gentamicin injection (26.7mg/ml), with contralateral ears as controls. Animals were euthanized at 2 periods after treatment: early (14-28 d) or late (3 mo). Semicircular canal cristae were sectioned for light and electron microscopy. Treated cristae had a 40% reduction ( $p=0.02$ ) in vestibular HC nuclei number per transverse section, with loss of all type I HC but no change in type II HC number. Of the remaining type II hair cells, there was a 61% decrease in the proportion of hair cells with stereocilia ( $p<0.001$ ). Neuroepithelial height was reduced by 20% ( $p=0.02$ ). There was no net change in the total number of afferent boutons in contact with type II HC. However, more type II HC had afferent contacts after treatment (early: 42%, late: 88%,  $p=0.02$ ), but the number of afferent contacts per type II HC decreased (early: 25%,  $p=0.03$ ; late: 50%,  $p=0.0001$ ). The number of efferent bouton endings decreased with time after treatment ( $p=0.05$ ). The number of ribbon synapses per section was reduced by 50% ( $p=0.03$ ), with no change in the ribbon synapse-to-HC ratio. Utricular maculae were also sectioned for light microscopy. Treated utricular maculae had a 41% reduction ( $p=0.01$ ) in vestibular HC nuclei number per transverse section, with loss of all type I HC but no change in type II HC number. Hair cell loss was greater in the striolar region (90% reduction,  $p=0.005$ ) than in the extrastriolar region (33% reduction,  $p=0.02$ ). A single IT gentamicin treatment is not a complete labyrinthectomy. Remaining hair cells have synaptic specializations and afferent bouton contacts but lose their stereociliary bundles. These results help explain the findings of spontaneous vestibular afferent firing but reduced sensitivity to vestibular stimuli after IT gentamicin treatment. Preservation of spontaneous firing may decrease the adaptive burden for central vestibular nuclei compared to surgical labyrinthectomy.

### **848** 3D Vestibuloocular Reflex, Afferent Responses and Crista Histology in Chinchillas After Unilateral Intratympanic Gentamicin

Charles C. Della Santina<sup>1</sup>, Americo A. Migliaccio<sup>1</sup>, HongJu Park<sup>1,2</sup>, lee-Ching Wu Anderson<sup>1</sup>, Patpong Jiradejvong<sup>1</sup>, Lloyd B. Minor<sup>1</sup>, John P. Carey<sup>1</sup>

<sup>1</sup>Dept. of Otolaryngology-Head & Neck Surgery, Johns Hopkins School of Medicine, <sup>2</sup>Konkuk Univ., Korea

We sought to correlate changes in the vestibuloocular reflex (VOR) with vestibular nerve activity and histologic appearance of cristae in chinchillas treated with intratympanic gentamicin (ITG). We measured eye movements with 3D search coils during  $3000^\circ/s^2$  transient head rotations in 7 awake chinchillas 3 wks after unilateral middle ear injection of 26.7 mg/mL gentamicin. Single unit vestibular nerve activity and responses to head rotation were then examined under barbiturate anesthesia, and a subset of animals were perfused and sectioned for light microscopy.

Horizontal, LARP (left-anterior/right-posterior) and RALP VOR gains were  $0.35\pm 0.21$ ,  $0.52\pm 0.37$  and  $0.37\pm 0.27$ , respectively, for head rotation to the treated side and  $0.88\pm 0.26$ ,  $1.17\pm 0.34$  and  $1.09\pm 0.38$  to the intact side.

VOR latency was longer for ipsilesional ( $24.2\pm 5.7$ ,  $24.6\pm 8.6$ ,  $30.1\pm 6.6$  ms) than for contralesional ( $13.5\pm 3.7$ ,  $19.0\pm 6.3$ ,  $15.9\pm 4.6$  ms) rotations. VOR gains for an animal treated with ITG in the presence of middle ear inflammation showed intermediate VOR gain and latency.

Single-unit responses of 56 intact side afferents were consistent with published normative data. The 99 treated-side units recorded had below-normal spontaneous rates; 90 had no response to head rotation or tilt, and 9 (all in 2 animals with relatively preserved VOR gain) had detectable but below-normal responses to head rotation or tilt.

Histologic exam of 2 animals to date showed a marked loss of Type I hair cells in treated-side cristae ( $0.3\pm 0.6$  cells/transverse cross section vs  $21.0\pm 5.0$ ), no change in density of Type II hair cells ( $19.0\pm 4.6$  vs  $19.0\pm 2.6$ ) and preservation of afferent fibers in the crista.

The reduced VOR response after ITG corresponds to marked loss of afferent sensitivity, partly preserved spontaneous activity, and a marked reduction in the number of Type I hair cells.

Supported by NIH/NIDCD K08DC006216, R03DC005700, K23DC00196, R01DC02390, T32DC00027, P03DC05211

### **849** Comparative Features of Dynamic Response Characteristics Among Semicircular Canal Afferent Neurons

LF Hoffman<sup>1</sup>, DJ Hirsch-Shell<sup>1</sup>, MG Paulin<sup>2</sup>

<sup>1</sup>Geffen School of Medicine at UCLA, <sup>2</sup>University of Otago

Primary afferent neurons projecting from the central region of the semicircular canal cristae may exhibit either calyx-only (C) or dimorphic (D) dendritic morphology. It has been previously shown that this morphologic distinction has a physiologic correlate in that C afferents are characterized by lower measures of response gain than D afferents. However, the systems response transfer functions have yet to be examined in detail to elucidate the common features of response dynamics among afferents representing these morphologic subpopulations. In view of the distinction in dendritic morphology, such an analysis may provide insight into factors associated with these common physiologic features (i.e. locus of crista innervation).

Transfer functions were determined from the response discharges of chinchilla horizontal semicircular canal afferents to discrete sinusoidal and band-limited Gaussian stimuli. In the present study we focused upon afferents exhibiting spontaneous discharge coefficients of variation (CV)  $> 0.2$ . These afferents exhibited response sensitivities to 0.8 Hz stimuli ( $30^\circ/s$ ) ranging between 0.4 and 2.0 spikes-s<sup>-1</sup>/deg-s<sup>-1</sup>. All exhibited phase leads (re: velocity) that ranged between  $14^\circ$  and  $40^\circ$ . Preliminary analyses of these data indicate that afferents with high 0.8 Hz sensitivities (putative D afferents) exhibited increasing sensitivities and phases in response to high stimulus frequencies. Afferents with low 0.8 Hz sensitivities (putative C afferents) exhibited sensitivities and phases that were relatively constant at the high frequencies tested in the present study. These analyses suggest the factor(s) responsible for the high frequency lead term in putative D

afferents is not common to putative C afferents, and therefore likely not specifically associated with crista innervation locus. Supported by DC05059 (LFH), an NSF IGERT traineeship (DJHS), and the Royal Society of New Zealand (MGP).

### **850** Directional Sensitivities of the Otolith System

Timothy Hullar<sup>1</sup>, Elizabeth Lamont<sup>1</sup>, Robert Mallery<sup>1</sup>

<sup>1</sup>Washington University School of Medicine

The responses of single primary semicircular canal and otolith afferents to sinusoidal stimulation have been extensively documented. Less well understood is the degree to which combinations of these afferents may contribute to conveying information to the brain. In particular, groups of afferents may improve the temporal or spatial accuracy of the system. The three semicircular canals, for instance, have been shown in many species to lie at nearly 90 degrees to one another, allowing rotations in all three dimensions to be represented with the highest sensitivity possible.

We tested the hypothesis that linear accelerations are also collected and represented with equal sensitivity in all three dimensions. We used histologic methods to determine the topographic contours of the otolith organs of normal mice (C57/BL6, JAX). We used scanning electron microscopy to create maps of hair cell orientations on the saccular and utricular maculae of the same strain. Approximately 5000 randomly distributed hair cells were mapped per otolithic membrane. We then digitally combined these data sets to create a representation of the surfaces of the otolith organs and the vectors of the direction of activation of the hair cells in the otolith organs in three-dimensional space.

We found that the vectors of hair cell maximum sensitivity were not uniformly distributed in three dimensions. Otolith hair cells appeared to overrepresent the anterior-posterior direction compared to other directions. Unlike the semicircular canals, which are oriented orthogonally to represent rotations in any direction with great sensitivity, the otolith organs are therefore likely to be particularly effective at coding accelerations in this direction. This arrangement may have functional implications for the ability of the otolith organs to encode the direction and magnitude of linear accelerations and may be related to more commonly encountered directions of linear acceleration in the behaving animal.

### **851** Model and Experimental Data for the Utricular Medial and Lateral Partitions Based on the Unilateral Centrifugation Test

Floris Wuyts<sup>1,2</sup>, Benson Ogunjimi<sup>3</sup>

<sup>1</sup>Dept of Biomedical Physics, University of Antwerp, <sup>2</sup>Dept of ENT, University Hospital of Antwerp, Belgium,

<sup>3</sup>University of Antwerp

The utricle consists of a medial and a lateral part, with opposite polarization vectors. By using the recently refined technique of unilateral centrifugation (Wuyts et al, 2004) we have new data to investigate the sensitivity and relative functionality of the medial and lateral partitions of the

human utricle, based on an extension of the theoretical model by Kondrachuk (2003).

We investigated in 10 healthy subjects the ocular counter rolling (OCR), recorded with 3D video oculography. The subjects were rotated around a vertical axis on a rotary chair at a speed of 400 degrees per second. During the ongoing rotation the subjects were slowly laterally translated over a distance of 8 cm. During this procedure, the axis of rotation moves sideways and when the excursion is less than 4 cm, both utricles are stimulated in opposite directions. Once beyond 4 cm, both utricles are stimulated in the same direction, but with largely different centrifugal forces. The utricular sensitivity (US) is represented by the slope of the OCR as a function of the apparent tilt of the head center. Based on the slopes of the 10 subjects, we determined the prevalence of medial and lateral partitions of the utricle.

The test paradigm can be divided in two parts: a) when the axis of rotation is positioned between both utricles (i.e. < 4 cm):  $\langle US \rangle = -0.253 \pm 0.017$  (degree OCR/tilt head center); b) when the axis is positioned beyond the utricles (4cm<axis<8 cm) the  $\langle US \rangle = -0.196 \pm 0.020$ . Using a modified model of Kondrachuk, these data indicate that the medial partition of the utricle provides a response twice as prominent as the lateral part.

Our findings also corroborate that a great asymmetry exists between left and right utricles.

Kondrachuk A.V.(2003) Qualitative model of otolith-ocular asymmetry in vertical eccentric rotation experiments, *Hear.Res.* 178(1-2),59-69.

Wuyts F., Hoppenbrouwers M., Pauwels G., Van de Heyning P. (2003) *J of Vestib. Res.* 13(4-6):227-34.

### **852** Otolith Receptor Formation During Development.

J. David Dickman<sup>1</sup>, David Huss<sup>1</sup>

<sup>1</sup>Washington University

We are interested in understanding otolith system development in birds. In the present study, we examined the formation of otoconia, receptor cells, stereocilia organization, and afferent innervation during embryogenesis and early post-hatch development in Japanese quails. The utricular and saccular maculae were fixed by intralabyrinthine perfusion, then harvested on each embryonic day from E3 – E15 and every 7 days post-hatch from P0 - P42 (adult). Stereocilia polarization was quantified across the macular surfaces (SEM). At E6, stereocilia were diffusely arranged and chaotic, but from E8 – adult, reversal line architecture was established and stereocilia polarizations were topographically organized. Otoconia were observed to first develop at E5 in the saccule, followed by 8 – 12 hours (E6) in the utricle. Initially, the core of the otoconia consisted of a double fluted shape that quickly appeared to calcify into a barrel shape with trihedral faceted ends. Otoconial measurements established a mature average of 11µm in length, 5µm in width and a sustained 2.5:1 length/width ratio regardless of size. Developing afferents were examined using retrograde tracers (HRP or BDA), video microscopy, and 3D reconstruction. Only

bouton afferents innervated the macular epithelium, from E4 – E10. At E12, the first dimorph afferents were observed, with calyx afferents forming from E14 and continuing through post-hatch development.

Supported in part by funds from NIH DC003286 and NASA NNA04CC52G.

### **853 Efferent Innervation of the Chinchilla**

#### **Vestibular Endorgans**

**Yaser Maksoud<sup>1</sup>**, Anna Lysakowski<sup>1</sup>

<sup>1</sup>*Univ. of Illinois at Chicago*

The brainstem sends efferent fibers to the vestibular labyrinth. This study addresses the question of whether there is a differential distribution of this efferent innervation within the sensory epithelium. Purcell and Perachio studied the vestibular efferent projection in the gerbil (*J Neurophysiol* 78: 3234-48, 1997). They concluded that ipsilateral (I) group e (iE) projects to the central zone of the crista (CZ) and striola of the utricle (S), and contralateral (C) group e (cE) projects to the peripheral zone (PZ) and extrastriola (ES). A recent electrophysiological study in the chinchilla showed that contralateral stimulation leads to large responses in irregular units (Marlinski et al., *JARO* 5: 126-43, 2004). We decided to study this question in the chinchilla, an animal model for which there is much physiological data on the vestibular periphery. Eight animals were injected stereotaxically with 10% BDA in the left group e. After a 2 wk survival, endorgans were dissected, reacted, flat-mounted, and reconstructed with NeuroLucida. Data from 7 contralateral and 7 ipsilateral endorgans were analyzed. We found that contralateral efferents produce more extensive innervation than ipsilateral ones: tree length (C: 1044  $\mu\text{m}$  vs I: 476  $\mu\text{m}$ ;  $p < 0.01$ ), surface area (C: 2816  $\mu\text{m}^2$  vs I: 1275  $\mu\text{m}^2$ ;  $p < 0.01$ ), volume (C: 890  $\mu\text{m}^3$  vs I: 433  $\mu\text{m}^3$ ;  $p < 0.02$ ), and average bouton (B) count/tree (C: 108 vs I: 81;  $p < 0.01$ ). The cE:iE bouton number ratio is 1.4:1 and the cE:iE parent axon (PA) number ratio is 1.6:1. There were no significant differences between innervation patterns of PZ (ES) and CZ (S), as reflected by their bouton densities, 4.95 and 5.30 boutons/100  $\mu\text{m}^2$ , respectively ( $p > 0.3$ ). The ratio of total peripheral to central bouton numbers reflects the surface area difference between the peripheral and central sensory epithelium, roughly 2:1. We conclude that ipsilateral and contralateral brainstem efferent neurons each project to both zones of chinchilla vestibular endorgans.

Supported by NIDCD R01-02521.

### **854 4-Aminopyridine Modulates Adaptation and Uncovers Calcium Action Potentials in the Vestibular Afferent Neurons**

**Francisco Mercado<sup>1</sup>**, Agenor Limón<sup>2</sup>, Cristina Pérez<sup>1</sup>, Rosario Vega<sup>2</sup>, Enrique Soto<sup>2</sup>

<sup>1</sup>*Instituto de Fisiología Celular, UNAM*, <sup>2</sup>*Instituto de Fisiología, BUAP*

The aim of this work is to define the participation of ionic currents in the sensory coding of rat's vestibular system afferent neurons. The characteristics of ionic currents,

action potential and discharge pattern of cultured afferent neurons were studied with or without presence of channel blockers. The cells were registered using the whole cell patch clamp technique, in both, voltage and current clamp conditions. The recordings were done in normal saline or  $\text{Na}^+$  free saline solutions as indicated. Cultured afferent neurons (18-24 hrs) from neonatal rats (P5-P10) had a resting membrane potential of  $-58.4 \pm 6$  mV ( $n = 51$ ). When the neurons were stimulated with current pulses they typically fired one single action potential with an amplitude of  $66 \pm 15$  mV and  $1 \pm 0.3$  ms duration ( $n = 51$ ). The application of 10 mM 4-AP ( $n = 32$ ) significantly reduced the inactivating outward current and increased the action potential duration up to 500%, blocked the afterhyperpolarization in a 80% and unmasked a TTX resistant calcium-dependent plateau phase. In 47% of the cells 4-AP converted the firing properties to a current pulse injection (100 pA, 2s) from phasic to tonic; in 19% firing was converted to a slowly adapting type response (in about 500 ms); and in 34% of the cells the response remained a single action potential. In 27.3% of the cells, the application of 10 mM 4-AP induced a regular spontaneous discharge. These results indicate that vestibular afferent neurons in primary culture express a 4-AP sensitive currents which contribute to the action potential waveform, adaptation time course to electrical stimulation, and that constitute a counterweight to calcium current mediated excitability.

This work was partially financed by CONACyT grant 40672 to RV. FM and CP are recipients of CONACyT fellowships 185844 and 185855 respectively.

### **855 KCNQ Potassium Channels in Vestibular Afferent Neurons.**

**Cristina Pérez-Flores<sup>1</sup>**, Agenor Limón<sup>2</sup>, Rosario Vega<sup>2</sup>, Enrique Soto<sup>2</sup>

<sup>1</sup>*Instituto de Fisiología Celular, UNAM*, <sup>2</sup>*Instituto de Fisiología, BUAP*

There is evidence that the family of KCNQ potassium channels (KCNQ1- 4) is expressed in the inner ear (Kubisch et al., 1999). KCNQ4 channels are expressed in type I hair cells and in calyx ending afferent neurons in the vestibular system (Kharkovets et al., 2000). The aim of this work was to determine the effect of the KCNQ blocker XE-991 on the outward current in vestibular afferent neurons.

Recordings were performed in vestibular ganglia afferent neurons isolated from Wistar rats (postnatal days 7-10) held in primary culture (18-24 hrs). Neurons were recorded using whole cell patch clamp technique. External solution consisted of (in mM): NaCl 140, KCl 5.4,  $\text{MgCl}_2$  1.2,  $\text{CaCl}_2$  1.8, HEPES 10 and Glucose 10. Internal solution contained (in mM): NaCl 10, KCl 125,  $\text{CaCl}_2$  0.134, EGTA 10, HEPES 5, Mg ATP 2, Na GTP 1. The perfusion of XE-991 (0.03 to 10  $\mu\text{M}$ ) decreased the neuron outward current up to 45% ( $n = 25$ ). The dose response curve showed an  $\text{IC}_{50}$  of 1  $\mu\text{M}$ . In current clamp, 10  $\mu\text{M}$  XE-991 revealed an oscillatory postdepolarization without repetitive spike discharge in response to current pulse injection ( $n = 5$ ).

These results suggest that cultured vestibular afferent neurons express KCNQ type potassium currents which are

sensitive to XE-991. It has been proposed that KCNQ2/KCNQ3 and KCNQ3/KCNQ5 heteromers are the molecular constituent of the M current (Schroeder et al., 2000; Lerche et al., 2000); thus, in calyx ending neurons that are contacted by cholinergic efferent axons, the KCNQ channels could lead to an M like current.

Supported by a grant from Consejo Nacional de Ciencia y Tecnología de México (CONACyT) grant 40672 to RV. CP is a recipient of a CONACyT fellowship (185855).

## **856** Electrophysiology and Modeling of Vestibular Calyx Terminals

Katherine Rennie<sup>1</sup>, Michele Streeter<sup>1</sup>, Tim Benke<sup>1</sup>, Anna Taylor Moritz<sup>2</sup>

<sup>1</sup>University of Colorado Health Sciences Center,

<sup>2</sup>University of Washington

Calyx fibers are the primary vestibular afferent neurons postsynaptic to type I vestibular hair cells and are named for their unmyelinated cup shape terminals, which encase the basolateral surface of one or more type I hair cells. As a first step to understanding the initiation and propagation of action potentials in vestibular afferents contacting type I hair cells, we have used whole cell patch clamp to record ionic currents and action potentials from calyx terminals. Type I hair cells with attached calyx endings were dissociated from the semicircular canals and utricles of Mongolian gerbils.

As previously described, a voltage-dependent transient inward current and sustained outward potassium currents were present in calyx terminals (Rennie ARO abstract 1070, 2003). Potassium currents were blocked with cesium in the patch electrode solution or with extracellularly applied 20  $\mu$ M linopirdine and 1 mM 4-aminopyridine. Transient inward currents activated positive to -60 mV from holding potentials of -80 mV and more negative. Inward currents activated and inactivated rapidly, had a maximum peak amplitude of  $0.99 \pm 0.64$  nA ( $n = 18$ , mean  $\pm$  SD), a half-inactivation of approximately -81 mV and were blocked more than 80 % by 100 nM tetrodotoxin ( $n = 4$ ). These properties are consistent with a conventional neuronal Na<sup>+</sup> current.

The calyx afferent has been modeled in the NEURON simulation environment. The parameters governing the activation of the ion channels were optimized with a genetic algorithm to match kinetic data from our whole cell recordings. The model consists of a series of cylindrical compartments that represent the inner and outer calyx membrane (6 compartments each), the base of the calyx (4 compartments) and a short segment of the axon (5 compartments). We will use the model to investigate how the distribution of voltage-gated ion channels alters the discharge characteristics of the calyx afferent.

Supported by NIDCD DC03287 and the American Hearing Research Foundation.

## **857** Bundle Mechanics Depends on Bundle Structure in Turtle Utricle.

Corrie Spoon<sup>1</sup>, Ellengene Peterson<sup>2</sup>, Wally Grant<sup>1</sup>

<sup>1</sup>Virginia Tech, <sup>2</sup>Ohio University

It is generally supposed that hair bundle structure affects bundle mechanics. Computational models support this suggestion, but we lack direct experimental evidence relating bundle mechanics to specific structural features of hair bundles on vestibular hair cells. To address this, we are examining the static stiffness of turtle utricular bundles that differ in structure.

We deflected bundles with flexible glass whiskers of known stiffness applied to the tip of the kinocilium. The base of the whisker was attached to a piezoelectric linear actuator and oscillated at 0.5 Hz. Displacements of the whisker base were measured using an extrinsic Fabry-Perot interferometer. Displacement of the whisker tip (i.e., bundle deflection) was measured using a dual photodiode array. Bundle stiffness was calculated from the bundle deflection, whisker deflection, and whisker stiffness. We visualized bundles using DIC optics, and we measured the following features: array length (distance from tall to short end of the bundle), and heights of kinocilia, tallest stereocilia, and shortest stereocilia. From these we calculated a KS ratio (ratio of kinocilium height to height of the tallest stereocilia) and slope ((tallest - shortest stereocilia)/array length) because computational analyses suggest that these features are likely to affect bundle stiffness.

Our results to date are based on 11 bundles in striolar zones 2 (type II hair cells only) and 3 (type I and II hair cells) and the adjacent medial extrastriola (type II hair cells only); all bundles were medial to the line of polarity reversal. We find that bundle stiffness decreases systematically from the line of polarity reversal toward the medial extrastriola. Bundle stiffness is negatively correlated with KS ratio (Spearman  $R = -0.81$ ;  $p < .01$ ) and positively correlated with bundle slope (Spearman  $R = 0.72$ ;  $p < .05$ ). Thus, bundle stiffness depends significantly on bundle heights.

## **858** Differences Between Hair Bundles of Type I Hair Cells in Turtle Utricle.

Jingbing Xue<sup>1</sup>, William Moravec<sup>1</sup>, Ellengene Peterson<sup>1</sup>

<sup>1</sup>Ohio University

In amniote vestibular organs, type I hair cells contact pure calyx and dimorphic afferents; it is unclear whether differences between type I hair cells contribute to observed physiological differences between these two afferent types. In turtle utricle, type I hair cells are restricted to a subdivision of the striola, zone 3, which contains both type I and type II hair cells. Within zone 3 there is a spatial gradient in two features of type I bundles: stereocilia number and the ratio of kinocilium height to the height of the tallest stereocilia (KS ratio). Computational models (Silber et al., 2004, *Hear. Res.*, in press) and experiments on living hair cells (Rennie and Ricci, ARO 2004; Spoon, Peterson, Grant, ARO 2005) suggest that these features affect bundle mechanics and transduction currents.



Both stereocilia numbers and KS ratios increase significantly from lateral to medial within zone 3 (Moravec and Peterson, ARO 2004; Xue and Peterson, ARO 2004). To see how these features vary with afferent type, we used confocal microscopy of utricular wholemounts and slices stained with antibodies to calretinin and  $\beta$ -III tubulin to visualize calretinin-positive (Cal+) calyces (putative calyx afferents) and calretinin-negative (Cal-) calyces (putative dimorphic afferents), respectively. This material reveals that Cal+ calyces occupy most of zone 3; in contrast, Cal- calyces are restricted to a narrow band at the medial margin of zone 3. This spatial pattern suggests that type I hair cells supplying the two classes of calyx-bearing afferents may differ in stereocilia counts or bundle heights (KS ratio). In support of this hypothesis, simultaneous bundle staining with acetylated  $\alpha$ -tubulin and phalloidin to visualize kinocilia and stereocilia, respectively, indicates that type I hair cells supplied by Cal+ calyces have significantly lower KS ratios than those supplied by Cal- calyces (Mann-Whitney U = 11,  $p < 0.0005$ ). Type II hair cells have the highest KS ratios in zone 3; they are most common in medial zone 3, where they are opposed to the outer face of both Cal+ and Cal- calyces.

### **859** Information in Posterior Canal Afferents of the Turtle, *Trachemys (Pseudemys)* Scripta.

**Michael Rowe**<sup>1</sup>, Alexander Neiman<sup>1</sup>

<sup>1</sup>*Ohio University*

We have used an in vitro turtle preparation to characterize response properties of posterior canal afferents in terms of information theory. Afferents were stimulated by mechanical indentation of the posterior duct via a small hole in the bony canal. Glass micropipettes were used to record extracellular spikes from afferent axons in the posterior division of the VIIIth nerve. Stimulus waveforms were band-limited Gaussian white noise, with cutoff frequencies ranging from 10 to 50 Hz. For individual afferents, total entropy of its spike train was estimated from the response to a 10 minute long segment of noise. The variability of afferent responses to repeated presentations of the same 5-30 sec. noise segment was used to characterize "noise" entropy. Mutual information rate between afferent response and noise stimulus was then obtained by subtracting the noise entropy from the total entropy. Mutual information rates ranged from 13 -70 bits/sec. when all possible spike patterns were considered, but were considerably lower when only individual spikes were considered (7 - 34 bits/sec). These differences indicate the existence of significant correlations in afferent spike trains. Additional analyses further indicated that information was coded not only in spike rate, but also in the temporal pattern of inter-spike intervals. Information rates increased as the stimulus bandwidth increased, indicating that these afferents are able to encode stimulus frequencies as high as 50 Hz.

### **860** Development of Image Analysis Technique of Vestibulo-Collic Reflex in Laboratory Animal

**Makoto Hashimoto**<sup>1</sup>, Kenji Takeno<sup>1</sup>, Koichi Watanuki<sup>1</sup>, Hirotaka Hara<sup>1</sup>, Takuo Ikeda<sup>1</sup>, Hiroaki Shimogori<sup>1</sup>, Hiroshi Yamashita<sup>1</sup>

<sup>1</sup>*Department of Otolaryngology, Yamaguchi University School of Medicine*

There is no established method of evaluating the vestibulo-spinal reflex in laboratory animal. We tried to develop the measurement of vestibulo-collic reflex (VCR), one of the vestibulo-spinal reflex, in alert guinea pigs using a method for obtaining calibrated head tilt images. Hartley guinea pigs were immobilized to the cage, fixed to a turntable apparatus, with their neck movable freely. Two marks were made on animals, tip of nose and top of head, respectively. For sinusoidal rotation, different conditions were designed (peak angular velocity : 60deg/sec, period : 3sec ; peak angular velocity : 90deg/sec, period : 4.5sec). During sinusoidal rotation, movement of the head and neck was recorded on videotapes using an infrared charge-coupled device (CCD) camera. We stored the video images on a computer, and head tilt was analyzed. The analysis was performed using public domain NIH image program (developed by U.S. National Institute of Health). It was proved that head tilt, which synchronized sinusoidal rotation to the opposite direction, was caused by VCR. The more angular velocity we supplied, the larger VCR was produced. These data indicate that the VCR in guinea pigs could be quantitatively measured. It is expected that our method would be useful to evaluate vestibular function in animal models.

### **861** Regulation of Connexin-Mediated Cell-Cell Signaling: Development of Peptidomimetic Inhibitors

**W. Howard Evans**<sup>1</sup>

<sup>1</sup>*Cardiff University Medical School*

Cells are invariably in partnership with others and communicate directly and extensively. Connexins (Cx) are nonglycosylated proteins in vertebrates that function as oligomeric membrane channels facilitating cell-cell signaling. In gap junctions, docked Cx hexameric channels organised as linear arrays at cell contact points allow direct intercellular signaling exemplified by propagation of calcium waves and unidentified small ions and molecules across groups of cells. Calcium wave spread also occurs in a paracrine mode by release of ATP across nonjunctional plasma membrane Cx hemichannels. Specific pharmacological inhibition of Cx mediated signaling can be a powerful tool for its analysis. Short peptides corresponding in sequence to selected extracellular loop domains are 'clean' reversible reagents allowing manipulation of signaling in cells expressing various Cxs owing to the conserved sequences on the two exposed loop domains of these proteins. Patch clamp studies show that binding of Cx peptidomimetics blocks electrical conductance of Cx hemichannels. In metabolic stress, Cx peptidomimetics block the release of ATP and calcium signaling by cells occurring via the hemichannels.

The mechanism of action on cell signaling via Cx channels by this new class of inhibitors is now being elucidated.

### **862 Connexin 43 in the Avian Inner Ear: A Role in Asymmetric Coupling of Supporting Cells?**

Regina Nickel<sup>1</sup>, David Becker<sup>2</sup>, Andrew Forge<sup>1</sup>

<sup>1</sup>Centre for Auditory Research, University College London, <sup>2</sup>Department of Anatomy and Developmental Biology, University College London

Previous fluorescence recovery after photobleaching (FRAP) studies in the intact sensory epithelia of the inner ear of chick hatchlings revealed asymmetric transfer of calcein via gap junctions between the supporting cells of the basilar papilla, but not those of the utricular macula (Abstract #1120, ARO 2003).

This difference in the characteristics of the dye spread appears to coincide with the differential expression of connexin 43 (cx43) in the sensory epithelia. Cx43-immunoreactive sites, whose size and density gradually decrease from the proximal to the distal end, were detected between supporting cells of the basilar papilla. Double immunofluorescence and immunogold labelling of thin sections showed cx43 to co-localise with the inner ear-specific chicken connexin 31 (c-cx31) within gap junction plaques of the auditory supporting cells. No cx43-positive gap junction plaques, however, were detected in the sensory epithelium of the utricle.

To further corroborate the role of cx43 in the asymmetric coupling of supporting cells, cx43 was transiently knocked down in organotypic cultures of the basilar papilla using antisense oligodeoxynucleotides (ODNs) and its effect on dye transfer is currently examined utilizing FRAP.

These comparative functional and morphological studies suggest that c-cx31/cx43 junctions play a role in the asymmetric spread of calcein, which may underlie directional gap junction pathways in the avian inner ear.

Supported by Defeating Deafness

### **863 Effects of Active or Passive K<sup>+</sup>Transport Blockage on Connexin 26 Expression in Gerbil Type II Fibrocyte Cultures**

Fenghe Liang<sup>1</sup>

<sup>1</sup>Medical University of South Carolina

Fenghe Liang 1, Chunyan Qu 1, Zhijun Shen 1, Bradley A. Schulte 1, 2

Departments of Pathology and Laboratory Medicine; Otolaryngology, Head and Neck Surgery, Medical University of South Carolina, 165 Ashley Ave, Charleston, SC 29425

Recycling of K<sup>+</sup> in the cochlea is essential to the transduction by auditory hair cells and maintenance of the endocochlear potential. Current K<sup>+</sup> recycling models suggest that type II spiral ligament fibrocytes actively take up perilymphatic K<sup>+</sup> via Na-K-ATPase, and pass it to type I fibrocytes through gap junctions formed by connexin 26 and/or connexin 31 for eventual return to endolymph. Disruption of gap junctions in mutant mice models and

certain forms of human recessive hereditary hearing loss results in reduction of the endocochlear potential and deafness (Minowa 1999, 2002;Kelsell 1997, 2004). These mouse mutants generally exhibit pathologies in fibrocytes or their contacts with neighboring cells. Theoretically, interference with any one-step in the complex K<sup>+</sup> recycling procedure could produce positive or negative feedback effects on downstream and/or upstream elements of the pathway. To investigate this question, we evaluated the effects of selective blockade of active and passive ion transport processes on connexin 26 (Cx26) expression in cultured type II spiral ligament fibrocytes. Type II fibrocytes in culture extend multiple dendrites that form direct contacts between cells. Na-K-ATPase, the Na-K-2Cl cotransporter (NKCC1) and Cx26 were expressed at steady levels in cells passages up to 18 times as judged by immunocytochemistry and Western blots. Incubation with either the Na-K-ATPase inhibitor Oubain (1 mM) or the NKCC1 blocker Bumetanide (0.1 mM) for 36 hours significantly reduced the expression of Cx26, in contrast, incubation with the BK channel blocker IBTX (50 mM), the L-type Ca<sup>+</sup> channel blocker Nifedipine (0.1 mM) or the chloride channel blocker DIDS (0.2 mM) had little effect on Cx26 levels. Further work is needed to determine if the inhibition of active K<sup>+</sup> uptake can influence gap junction formation or integrity in cell types upstream and/or downstream to the site of inhibition.

### **864 Differential Effects of Connexin26 Mutations on Ionic and Biochemical Permeabilities of Gap Junctions Studied in Vitro**

Yanping Zhang<sup>1</sup>, Wenxue Tang<sup>1</sup>, Shoab Ahmad<sup>1</sup>, Yasmin Elhady<sup>1</sup>, Ping Chen<sup>1</sup>, Xi Lin<sup>1</sup>

<sup>1</sup>Emory University School of Medicine

Mutations in connexin26 (Cx26) and Cx30 genes are major causes of congenital nonsyndromic deafness in human. However, little is known about how these mutations cause hearing impairment. The aim of this project is to investigate whether some deafness-causing Cx26 mutations differentially affect ionic and biochemical permeabilities of gap junctions (GJs). To evaluate ionic permeability with high efficiency, we developed an imaging method to measure intercellular Ca<sup>++</sup> transfer through GJs. This new method enabled us to quickly survey the effect of a large numbers of Cx mutants on ionic permeability. The Cx mutants were also tested for their effects on the biochemical permeability using fluorescent dye diffusion assay. We have tested both Cx26 (R75W, W44C, delE42, R184Q, D179N, C202F, V84L, R143W, V27I and E114G) and Cx30 (T5M, G11R, A88V, V37E) mutants. GJs comprised of eGFP-fused Cx26 and Cx30, either homo- or hetero-merically assembled were studied. Most Cx mutants (except for Cx26D179N, Cx30G11R, Cx30A88V and Cx30V37E) formed GJs in the cell membrane and most mutants completely disrupted the Ca<sup>++</sup> permeation through GJs. However, GJs comprised of Cx26 mutants W44C and R143W showed residual Ca<sup>++</sup> permeation with altered diffusion kinetics. Cx26V84L, Cx30T5M showed nearly normal Ca<sup>++</sup> permeation through GJs. All Cx

mutants we tested disrupted the biochemical coupling of cells as measured by fluorescent dye (propidium iodide) diffusion across GJs. Our study suggested that most Cx mutations associated with hereditary sensorineural deafness resulted in a complete interruption of the Ca<sup>++</sup> permeation through either homo- or hetero-meric GJ channels comprised of Cx26 or/and Cx30. However, residual Ca<sup>++</sup> permeation shown by Cx mutants W44C, R143W, V84L and T5M suggested that Cx mutations specifically affect the biochemical permeability through GJ channels are sufficient to cause hearing impairment.

### **865 ATP Connexin Hemichannel Release in the Cochlea** **Hong-Bo Zhao<sup>1</sup>**

<sup>1</sup>*Dept. of Surgery – Otolaryngology, University of Kentucky Medical Center, Lexington, KY 40536*

Although it has been known for a long time that extracellular ATP in the cochlea can modify cochlear functions, it is still a puzzle about where intracochlear ATP comes from. In the cochlea, connexins express extensively in the cochlea supporting cells and the apical face of the sensory epithelium incubates in the low Ca<sup>++</sup> endolymph. Here, we reported that the connexin hemichannels in the cochlea could release ATP under a low Ca<sup>++</sup> condition. The guinea pig cochlea was exposed after removal of the stria vascularis and incubated in a low Ca<sup>++</sup> extracellular solution. The incubation solution was sampled and its ATP concentration was measured by a bioluminescent-based method, using an EDTA-containing luciferin-luciferase assay kit with a luminometer. Under the low extracellular Ca<sup>++</sup> condition, the ATP concentration increased 5~10-fold from the base line. The maximum of ATP release was 18.66 ± 4.05 nM (n=8), which is in the physiological range of ATP concentration in the cochlea. The ATP increase could be blocked by gap junction channel blockers, octonal and carbenoxolone, and high extracellular Ca<sup>++</sup>. Other hemichannel blockers, Gd<sup>3+</sup> and Mg<sup>++</sup>, also could block ATP release. P2 receptor blockers, however, could not block this ATP release. Inhibition of other ATP release pathways also did not significantly affect this ATP release. The data suggested that the connexin hemichannel can open to release ATP under physiological conditions in the cochlea and may play an important role in cochlear intercellular signaling and nutrition. Connexin mutation may abolish this ATP release disturbing nutrient supply to cause cell degeneration.

Supported by NIH/NIDCD DC04618 and DC05989

### **866 Gap Junctions Contribute to Intercellular Propagations of Ca<sup>++</sup> Waves in Supporting Cells in the Cultured Cochlea of Mice**

Wenxue Tang<sup>1</sup>, Yanping Zhang<sup>1</sup>, Shoab Ahmad<sup>1</sup>, Ping Chen<sup>1</sup>, **Xi Lin<sup>1</sup>**

<sup>1</sup>*Emory University School of Medicine*

Cells in the sensory epithelia and the lateral wall in the cochlea are coupled intercellularly by gap junction (GJ) channels. Dysfunctions of GJ channels account for about

half of hereditary non-syndromic childhood deafness cases. However, how GJs contribute to the cochlear functions is currently unclear. Utilizing the extensive GJ network preserved in supporting cells maintained in organotypic cultures of the cochlea of mice, we studied whether GJs mediated the intercellular Ca<sup>++</sup> signaling in the supporting cells.

Intercellular propagations of transient increases in intracellular Ca<sup>++</sup> concentrations (Ca<sup>++</sup> waves) were triggered by a slight mechanical deformation to the cell membrane of a single cell. Under the conditions that Ca<sup>++</sup> waves propagated through activations of purinergic receptors were blocked by using saturating concentrations of either ATP (20 μM) or purinergic antagonists (e.g., 200 μM suramin), Ca<sup>++</sup> waves persisted in the supporting cells. These Ca<sup>++</sup> waves in the supporting cells, however, were blocked by applications of GJ blockers (e.g., flufenamic acid (100 μM)). These results suggest that GJ-mediated intercellular diffusion of Ca<sup>++</sup> signaling molecules mediated the propagation of Ca<sup>++</sup> waves in the supporting cells. GJs in the cochlea are traditionally believed to participate in the intercellular ionic couplings (e.g., diffusion and recycling of K<sup>+</sup>). Our results provided first evidence supporting that GJs contribute to the intercellular biochemical couplings in the cochlea by facilitating propagations of intercellular Ca<sup>++</sup> waves.

### **867 Establishment of the Intrastrial Space Compartment by Claudin-11 Based Tight Junction Strands is Required for Generation of EP**

**Shin-ichiro Kitajiri<sup>1,2</sup>**, Tatsuo Miyamoto<sup>2</sup>, Akihito Mineharu<sup>3,4</sup>, Noriyuki Sonoda<sup>2</sup>, Kyoko Furuse<sup>5</sup>, Masaki Hata<sup>5</sup>, Hiroyuki Sasaki<sup>5,6</sup>, Yoshiaki Mori<sup>3</sup>, Takahiro Kubota<sup>3</sup>, Juichi Ito<sup>1</sup>, Hiroshi Takenaka<sup>4</sup>, Mikio Furuse<sup>2</sup>, Shoichiro Tsukita<sup>2</sup>

<sup>1</sup>*Dept. of Otolaryngology-Head and Neck Surgery, Kyoto University Graduate School of Medicine,* <sup>2</sup>*Dept. of Cell Biology, Kyoto University Graduate School of Medicine,* <sup>3</sup>*Dept. of physiology 2, Osaka Medical College,* <sup>4</sup>*Dept. of otolaryngology, Osaka Medical College,* <sup>5</sup>*KAN Research Institute,* <sup>6</sup>*Department of Molecular Cell Biology, The Jikei University School of Medicine*

Claudins are cell adhesion molecules working at tight junctions (TJs) that are directly involved in compartmentalization in multicellular organisms. The cochlea includes a rather peculiar compartment filled with endolymph. This compartment is characterized by high K<sup>+</sup> concentration (L`150 mM) and a positive endocochlear potential (EP) (L`90 mV), both indispensable conditions for cochlear hair cells to transduce acoustic stimuli to electrical signals. These conditions are thought to be generated by the stria vascularis, which is adjacent to the endolymph compartment. The stria vascularis itself constitutes an isolated compartment delineated by two epithelial barriers, marginal and basal cell layers. Since TJs of basal cells are primarily composed of claudin-11, claudin-11-deficient (Cld11<sup>-/-</sup>) mice were generated with an expectation that the compartmentalization in stria vascularis in these mice would be affected. Auditory

brainstem response measurements revealed that Cld11-/- mice suffered from deafness; though no obvious gross morphological malformations were detected in Cld11-/- cochlea, but freeze-fracture replica electron microscopy showed that TJs disappeared from basal cells of the stria vascularis. In good agreement with this, tracer experiments showed that the basal cell barrier was destroyed without affecting the marginal cell barrier. Importantly, in the endolymph compartment of Cld11-/- cochlea, the K<sup>+</sup> concentration was maintained around the normal level ( $\sim 150$  mM), whereas the EP was suppressed down to  $\sim 30$  mV. These findings indicated that the establishment of the stria vascularis compartment, especially the basal cell barrier, is indispensable for hearing ability through the generation/maintenance of EP, but not of a high K<sup>+</sup> concentration in the endolymph.

### **868 The Expression of Aquaporin-5 (AQP5) in Outer Sulcus Cells (OSC) is Related to Direct Contact to the Endolymphatic Space**

**Bernhard Hirt**<sup>1,2</sup>, Zhenya Penkova<sup>1</sup>, Karina Gultig<sup>1</sup>, Andrea Muller<sup>1</sup>, Marcus Muller<sup>1</sup>, Hubert Lowenheim<sup>1</sup>

<sup>1</sup>Tübingen Hearing Research Center, University of Tübingen, <sup>2</sup>Dept. of Anatomy, University of Tübingen

In order to maintain inner ear sensory function volume and ionic composition of the inner ear fluids must be tightly regulated. The lateral wall of the cochlear duct has been proposed to play a major role in endolymph secretion. On molecular level, transmembrane proteins called aquaporins act as selective water channels and play a fundamental role in fluid homeostasis. In the lateral wall aquaporin 5 (AQP5) is localized in the outer sulcus cells (OSC) and the epithelial cells of the spiral prominence with a base to apex gradient in adult rats (Mhatre et al., 1999).

This study examines the developmental expression pattern of aquaporin 5 in rat by immunolabeling of AQP5 at different postnatal stages. Analysis of cellular localisation and subcellular expression domains were performed with epifluorescence and confocal laser scanning microscopical techniques. Colocalisation with the tight junction marker occludin and analysis of semithin sections were performed to show cell contacts to the endolymphatic space.

We could detect AQP5 in OSC and epithelial cells of the spiral prominence along the entire length of the lateral wall in postnatal rat until p4. The expression started to diminish in the basal turn at p8 and was limited to 25% of the total length at p32 in the apical turn. This loss of expression coincides with the loss of direct contact of OSC with the endolymphatic space. During development of the cochlea the apical membrane of OSC becomes covered by claudius cells. Subcellularly the localisation of AQP5 showed no polarized expression pattern.

### **869 Aquaporins (Water Channel) Expression in the Human Inner Ear**

**Ivan Lopez**<sup>1,2</sup>, Gail Ishiyama<sup>3</sup>, Robert W Baloh<sup>4</sup>, Akira Ishiyama<sup>5</sup>

<sup>1</sup>UCLA School of Medicine, <sup>2</sup>Surgery Department, <sup>3</sup>Neurology department UCLA School of Medicine,

<sup>4</sup>Neurology Dept UCLA School of Medicine, <sup>5</sup>Surgery Dept UCLA School of Medicine

Aquaporins (AQPs) are water channel proteins that play central roles in the handling of water in mammalian tissues. The inner ear is equipped with mechanisms that ensure tight volume control in the face of osmotic stress imposed by activity dependent ion fluxes or extrinsic factors, and AQPs likely play an important role. Expression of AQPs 1, 2, 4, and 5 has been reported in the rat, mouse and guinea pig inner ear. AQP2 is expressed in the endolymphatic sac of guinea pig and human. AQP expression has not been determined in the human inner ear, cochlea and vestibule. Thus, in the present study, we determine the expression of AQPs 1-9 in the human cochlea and vestibular endorgans. Temporal bones were obtained from autopsy within 3-5 hours post mortem from individuals with no history of vestibular or auditory problems (age ranging from 85-95 years old; n=4). The cochlea and vestibule were microdissected from the temporal bones, and then immersed in 4% paraformaldehyde for 6 hours. Twenty-micron cryostat sections were made, and incubated with affinity-purified rabbit antiserum against the AQPs 1-9 (1:500 in PBS, Chemicon, Temecula CA). Positive controls included midmodiolar sections of rat and mouse cochlea. Negative controls included omission of the antibody and antigen absorption. Specimens were analyzed using light, fluorescent and laser confocal microscope. In the vestibular endorgans, AQP1 localized to the blood vessels located in the cristae and utricular stroma. AQP4 and AQP6 were confined to supporting cells of the cristae ampullaris and macula utricule. However, there was differential localization: AQP4 was detected mainly in the basal portion of supporting cells, and AQP6 was confined to the apical portion of supporting cells. In the cochlea, AQP1 was found in fibrocytes of the spiral ligament. AQP4 localized to the inner sulcus cells and Claudius cells. AQP6 immunoreactivity localized to the apical portion of interdental cells in the spiral limbus and in supporting cells of the organ of Corti. There was no differential regional expression of AQPs expression in the apical vs. basal cochlea. Inner ear cochlear and vestibular hair cells and nerve fibers were not AQP immunoreactive. The expression of AQPs in the human cochlea and vestibular periphery are indicative of a role of AQPs in the human inner ear.

### **870 Amiloride-Sensitive Potassium and Sodium Absorption by Semicircular Canal Duct Epithelium of the Rat**

**Tao Wu**<sup>1</sup>, Satyanarayana R. Pondugula<sup>1</sup>, Donald Harbidge<sup>1</sup>, Daniel C. Marcus<sup>1</sup>

<sup>1</sup>Kansas State University

We have shown that SCCD epithelia absorb Na under glucocorticoid (GC) control [Pondugula et al., *Am J Physiol*, 2004]. This absorptive process can be inhibited by amiloride (K<sub>i</sub>  $\sim 1$   $\mu$ M) and benzamil (K<sub>i</sub>  $\sim 0.1$   $\mu$ M), consistent with the pharmacologic fingerprint of the classical epithelial Na channel (ENaC) that has a very high selectivity for Na over K and consists of  $\alpha$ -,  $\beta$ - and  $\gamma$ -

subunits. Transcripts for all three subunits are present in SCCD [Pondugula et al. (2004) AJP]. Controversy remains about the Na over K selectivity of ENaC in different subunit stoichiometry, which is of special importance in the context of the high K concentration of endolymph. We sought 1) functional evidence by RNA interference for participation of  $\alpha$ -ENaC in the amiloride-sensitive short circuit current (*amil-I<sub>sc</sub>*) across SCCD; 2) to determine if SCCD could sustain an *amil-I<sub>sc</sub>* in the presence of luminal K and absence of luminal Na; 3) to demonstrate amiloride-sensitive Na & K currents at the whole cell level by patch clamp. Neonatal rat SCCD epithelial cells were cultured to confluence on permeable supports for measurement of *amil-I<sub>sc</sub>* and on glass coverslips for patch clamp recording. Transfection of cultures for 24 h with siRNA against  $\alpha$ -ENaC led to a decrease in *amil-I<sub>sc</sub>* of about 30-40% compared to transfection with nonsense siRNA, which had no effect on *amil-I<sub>sc</sub>*. The *amil-I<sub>sc</sub>* with apical K was about 16-20% of that with apical Na. Inward whole cell currents were found to be inhibited by replacement of Na with NMDG and by application of 10  $\mu$ M amiloride; inward current was also reduced by amiloride with K as the only conducting cation (gluconate or methanesulfonate as anions). These results support the notion that SCCD provides an additional parasensory pathway for K recirculation in the vestibule and that this occurs through an amiloride-sensitive conductive pathway in the apical membrane of SCCD epithelial cells. Supported by NIH NIDCD R01-DC00212.

### **871 Chloride Secretion by CFTR in Semicircular Canal Duct Epithelium is Regulated by cAMP Activation of Protein Kinase A**

**Suresh B. Kampalli<sup>1</sup>**, Satyanarayana R. Pondugula<sup>1</sup>, Joel D. Sanneman<sup>1</sup>, Nithya N. Raveendran<sup>1</sup>, Daniel C. Marcus<sup>1</sup>  
<sup>1</sup>*Kansas State University*

Semicircular canal duct (SCCD) epithelia contribute to the homeostasis of vestibular endolymphatic ion composition by Cl secretion under adrenergic control via cAMP. We sought to determine whether cAMP regulated secretion is via protein kinase A (PKA) & the Cl channel CFTR, as found in many Cl-secreting epithelia. The equivalent short circuit current (*I<sub>sc</sub>*) was measured on confluent primary cultures. Forskolin ( $EC_{50}$ : 0.8  $\mu$ M; an activator of adenylyl cyclase (AC)), 8-Br-cAMP ( $EC_{50}$ : 180  $\mu$ M) and 8-pCPT-cAMP (100  $\mu$ M) each stimulated *I<sub>sc</sub>*, as did the nonselective phosphodiesterase (PDE) inhibitor IBMX (250  $\mu$ M) and the selective cAMP-specific PDE-4 inhibitor R0-20-1724 (100  $\mu$ M), demonstrating constitutive activity of AC. Stimulation was greater after exposure to glucocorticoids. Expression of PDE-4 was shown by gene microarray. Both gene array and RT-PCR results demonstrated the presence of transcripts for CFTR; microarrays revealed expression of other Cl channels, although not activated by cAMP. The specific CFTR inhibitor CFTR<sub>inh-172</sub> (5  $\mu$ M) decreased AC-stimulated *I<sub>sc</sub>* and increased  $R_T$ ; *I<sub>sc</sub>* was also decreased by the less-specific inhibitor flufenamate (100  $\mu$ M). Preliminary results

showed that *I<sub>sc</sub>* was stimulated by direct activation of PKA [N6-BNZ-cAMP; 200-500  $\mu$ M] but not by guanine nucleotide exchange factor [GEF; 8-pCPT-2-O-Me-cAMP (100  $\mu$ M)], another cAMP dependent signal pathway. *I<sub>sc</sub>* was partially inhibited in the presence and absence of HCO<sub>3</sub> by basolateral bumetanide (50  $\mu$ M), a blocker of Na,K,2Cl-cotransport. Inhibitors of other anion transporters were ineffective. Neither DNDS (500  $\mu$ M) nor gadolinium (100  $\mu$ M) affected *I<sub>sc</sub>* from either side. These results show that cAMP-stimulated Cl secretion into endolymph by SCCD is at least partially mediated via PKA activation of CFTR and that basolateral uptake of Cl is partially mediated by a Na,K,2Cl-cotransporter, which was found to be present by microarray (NKCC1). Supported by NIH-NIDCD grant R01-DC00212, NCRR P20 RR17686 & P20 RR16475.

### **872 Model of Ion Transport in the Stria Vascularis**

**Imran Quraishi<sup>1</sup>**, Robert Raphael<sup>1</sup>  
<sup>1</sup>*Rice University*

Many cases of genetic deafness are due to mutations in ion channel and transporter genes. These membrane channels and transporters maintain the endocochlear potential and endolymphatic potassium concentration. The precise nature of their individual contributions is poorly understood. We are developing a computational model to evaluate these contributions, taking advantage of disparate electrophysiological data from the cochlea and other tissues. Results regarding ion regulation by the stria vascularis are presented. The tissue is divided into compartments along physical and functional boundaries, with intercompartmental fluxes defined in terms of individual ion currents. Steady state ion concentrations and electrical potentials within the compartments are solved numerically. Equations for ion currents are based upon data from the cochlea, where available, or similar currents in other systems. Steady state concentrations and potentials are calculated for isolated marginal, intermediate, and basal cells, as well as components of the intact stria vascularis. Predictions for the effects of specific transporter and ion channel activity levels on the intrastrial and endocochlear potential will be given.

### **873 Further Development of a Three-Dimensional Model of Substance Distribution in the Cochlea after Round Window Application**

**Stefan Plontke<sup>1</sup>**, Norbert Siedow<sup>2</sup>, Alec N. Salt<sup>3</sup>, Hans-Peter Zenner<sup>1</sup>, Raimund Wegener<sup>2</sup>

<sup>1</sup>*Dept. of Otorhinolaryngology, HNS, Tübingen Hearing Research Center (THRC), University of Tübingen,*

<sup>2</sup>*Fraunhofer Institute of Industrial Mathematics, Kaiserslautern, Germany,* <sup>3</sup>*Dept. of Otolaryngology, Washington University in St. Louis, USA*

The local delivery of drugs to the round window membrane for the treatment of inner ear disorders is a promising alternative to systemic therapy. Since direct measurements of drug concentration time courses in the

human inner ear (as required in phase I clinical studies) is not presently possible, computer simulations provide a valuable tool for estimating drug concentrations in the inner ear for phase II clinical studies.

Although our initial one-dimensional simulation model provides a good representation of the longitudinal distribution of drugs, its ability to accurately predict the radial distribution of drugs (across and between scalae) is limited. A three-dimensional model has therefore been developed which better represents the complex geometry of the inner ear and is better able to represent radial drug movements from scala tympani into the vestibule. In our current studies we are working to reconcile the results from the two modelling approaches. The calculated results for different application conditions were compared between the two models starting with a simple geometry, specifically straight, tapered tubes with application through a permeable membrane at the base. Differences between algorithms have been evaluated and, in some cases, errors have been corrected. For the straight tubes, the concentration profiles calculated by the two models are now comparable.

We are now evaluating the influence of curvature of the inner ear compartments on the diffusion process. In adding curvature into the 3D representation, cross-sectional areas, volumes and areas of inter-compartment interaction (such as through the spiral ligament) become distorted. Comparisons of the differences between 3D-structures, and results from the original 1D-model will establish how the more complex geometry influences calculated drug movements.

Supported by grants from the Federal Institut of Risk Assessment, ZEBET WK 1-1328-171 to SP and NIDCD DC01368 to ANS.

### **874 The Use of Microdialysis for Quantification of Dexamethasone and Flourescein Entry Into Scala Tympani During Round Window Application**

H. Hahn<sup>1</sup>, B. Kammerer<sup>2</sup>, A. DiMauro<sup>1</sup>, H.-P. Zenner<sup>1</sup>, A. N. Salt<sup>3</sup>, S. Plontke<sup>1</sup>

<sup>1</sup>Dept. of Otorhinolaryngology Head and Neck Surgery, Tuebingen Hearing Research Center (THRC), <sup>2</sup>Dept. of Clinical Pharmacology, University of Tuebingen, Germany, <sup>3</sup>Dept. of Otolaryngology, Washington University, St. Louis, USA

Before new drugs for treatment of inner ear disorders can be studied in controlled clinical trials it is of importance to characterise their pharmacokinetics in the inner ear fluids in animal experiments. Since volume samples of inner ear fluids cause considerable artifacts, microdialysis has been shown to be an advantageous sampling technique. The aim of this study was to quantitatively compare round window entry rates into scala tympani (ST) for two substances – a flourescent marker and a clinically used glucocorticoid.

Flourescein 10 mg/ml and dexamethasone 8 mg/ml were continuously applied to the round window membrane (RWM) in guinea pigs in vivo. Concentration in perilymph at the base of ST was measured using microdialysis.

The concentration reached in ST was higher for flourescein ( $225 \pm 341\text{mg/ml}$ ) than for dexamethasone ( $124 \pm 122\text{mg/ml}$ ). Considerable concentration differences were found between animals, by approximately a factor of 40 for flourescein and 10 for dexamethasone.

The wide range of measured concentrations was not caused by analysis of the substances because dexamethasone and flourescein were analysed by different methods and the concentration ratio between the two substances was nearly constant throughout the experiments ( $2 \pm 0.77$ , after correction for differences in concentrations applied). Since microdialysis is a continuous sampling technique, variations are also unlikely to be a problem of intersample variation. Instead, it is more likely that the variation in drug levels reached in ST correlates with differences in animals. Specifically, the RWM permeability properties appear to vary considerably between individuals. This variation has already been reported by other authors (Salt & Ma, Hear Res 2001;154:88-97 and Salt & Hale, Abstr. ARO 2004).

Microdialysis is an effective method of measuring drug concentration in the base of ST close to the RWM. The wide range of concentration could be of potential clinical interest since the middle ear environment might be changed during a surgical procedure for RWM drug delivery.

Supported by Univ. of Tuebingen fortune-project no: 1001-0-0 (SKRP)

### **875 Potassium Channel Expression in Rat Utriclar Epithelium.**

Karen Hurley<sup>1</sup>, Meng Zhong<sup>1</sup>, Ruth Anne Eatock<sup>1</sup>

<sup>1</sup>Baylor College of Medicine

Over 80% of type I hair cells in rat vestibular epithelia express a negatively activating K conductance,  $g_{K,L}$ . In the rat utricular macula,  $g_{K,L}$  first appeared at postnatal day (P) 7, later than in the mouse. From P7-P14, the voltage of half-maximal activation changed from  $-33 \pm 2.1$  mV (8 cells) to  $-76 \pm 2.1$  mV (37) and maximum conductance increased from  $36 \pm 9.6$  (7) to  $152 \pm 18.5$  (16) nS. It has been proposed that  $g_{K,L}$  comprises KCNQ4 K channel subunits. But after P7, KCNQ4-like immunoreactivity is principally in type I calyces and some type II hair cells (Lysakowski et al., this meeting). At P8, single-cell RT-PCR experiments on type I cells yielded PCR products for KCNQ3 and KCNQ5 in 6/9 cells each (5 cells expressed both). All 9 cells were negative for KCNQ4. These data argue against  $g_{K,L}$  being a KCNQ4 conductance but leave open the possibility that it includes other KCNQ subunits.

Several results suggest that some type I cells express ether-a-go-go related (erg) K channels. Type I cells in extrastricular/peripheral zones of vestibular epithelia label with an erg antibody that recognizes erg1, 2 and 3 (ibid). In rat utricular type I cells (>P13),  $g_{K,L}$  fell into three categories of sensitivity to erg blockers (10  $\mu\text{M}$  WAY-123,398 and E-4031): (1) strongly blocked (~90%; 14 cells); (2) somewhat blocked (40%; 6 cells); (3) not blocked (8 cells). Single-cell RT-PCR at P8 on 6 type I hair cells yielded products corresponding to erg subunits in all

cells. One cell expressed erg1, 2 and 3; 2 cells expressed erg2 and 3; and 3 cells expressed just erg3.

Thus, some type I cells express KCNQ3 and/or 5 subunits and some express erg subunits, especially erg3. For cells in which  $g_{K,L}$  was partly blocked by erg blockers,  $g_{K,L}$  may comprise both KCNQ and erg channels. Antibody staining (ibid) suggests that subunit expression varies with epithelial zone.

Supported by NIDCD grant DC00290.

### **876 Expression Pattern of Voltage-Dependent K<sup>+</sup> Channels During Development of Rat Vestibular Endorgans.**

**Anna Lysakowski<sup>1</sup>, Sophie Gaboyard<sup>1</sup>, Steven D. Price<sup>1</sup>**

<sup>1</sup>*Univ. of Illinois at Chicago*

In the inner ear, expression of different K channels plays a major role in differentiating hair cell types and epithelial zones. We investigated the expression of KCNQ3, KCNQ4, and erg alpha subunits, plus mink-related peptide 1 (MiRP-1), a partner of erg1, in developing vestibular endorgans. These subunits are candidates for K conductances in hair cells and afferent neurons (Hurley et al., this meeting). Immunocytochemistry was performed on postnatal day (P) 0, P4, P6, P8, P14, P21 and adult rat vestibular epithelia. We found KCNQ3 immunoreactivity in all hair cell types and epithelial regions from P0 to adult; labeling intensity increased with age. All hair cells were immunoreactive for KCNQ4 at P0, but staining in most hair cells disappeared by P8. KCNQ4 staining appeared in calyx afferents in the central/striolar zones as they began to form; between P4 and P21 staining became more intense and spread into the peripheral/extrastriolar region. KCNQ4 expression in adult maculae and cristae was confined to calyx inner faces, in the bottom 2/3 of central/striolar calyces and the bottom 1/3 of peripheral/extrastriolar calyces, and some type II hair cells. Immunoreactivity to erg1 was seen in afferent fibers from P0 to adult, beginning with central/striolar afferents and spreading to peripheral/extrastriolar afferents. In adult, all calyces expressed erg1, but staining was more intense in peripheral/extrastriolar dimorphic afferents than in central/striolar calyx afferents. A pan-erg antibody against all 3 erg subunits labeled calyces and hair cells beginning at P0. With development, staining became more intense in the periphery/extrastriola than in the central/striolar zones. MiRP-1 immunoreactivity was first observed at P0 in all hair cells and supporting cells. From P4 to adult, MiRP-1 immunoreactivity increased in hair cells, supporting cells (especially at their apices), and the bases of calyces.

Supported by NIDCD grant DC02290.

### **877 Identification of T-type Calcium Channel Currents in Sensory Cells in the Inner Ear**

**Liping Nie<sup>1</sup>, Dwayne D Simmons<sup>2</sup>, Michael Anna Gratton<sup>3</sup>, Ebenezer N Yamoah<sup>1</sup>**

<sup>1</sup>*University of California, Davis*, <sup>2</sup>*Washington University School of Medicine*, <sup>3</sup>*University of Pennsylvania*

Auditory and vestibular hair cells are endowed with voltage-gated Ca currents that produce multiple Ca-

dependent functions. L-type channels (Cav1.3) and currents have been identified in several hair cell preparations using both functional and molecular biological assays. Moreover, there are circumstantial reports suggesting that hair cells express non-L type currents as well. Yet, direct functional and molecular evidence for the existence of the non-L type channels is lacking. Careful analysis of the whole-cell and single-channel Ca current data from hair cells showed that: 1) In sharp contrast to the L-type current, the magnitude of non L-type currents in Ca/Sr were similar to the Ba currents. This is consistent with the permeation properties of a T-type current. 2) The  $i_{Ca}$  of the I-V relation of the whole-cell current was eliminated by low concentrations of Ni (20  $\mu$ M), mibefradil (100 nM), and kurtoxin (300 nM), known blockers of T-type currents. We characterized the localization of the T-type Ca channel, Cav3.1, expression in the cochlea using immunohistochemistry and immunoelectron microscopic techniques. Mid-modiolar sections (5  $\mu$ m) of cochlear tissue fixed with 4% paraformaldehyde were reacted (1:250) with a polyclonal antibody for Cav3.1. Following incubation in biotinylated secondary antibody, the sections were treated with avidin-biotin complex reagent. Reactive sites were visualized by development in a 3,3'-diammonibenzidine-H<sub>2</sub>O<sub>2</sub> substrate medium. Positive staining was observed in the basolateral membrane of neurosensory cells in the inner ears of mice. Immuno-gold electron labeling of Cav3.1 showed gold particles that were aligned with the plasmalemma in the basal portion and the cytoplasm of hair cells. Some label was also observed in supporting cells. Moreover, we also demonstrated that the Cav3.1 channels were differentially expressed during development. The role of T-type Ca currents in hair cells will be discussed.

This work was supported by grants to ENY NIH-DC03828, DC04523, and NIH-DC006442 to MAG.

### **878 Molecular Cloning of Inner Ear-Specific T-Type Ca<sup>2+</sup> Channels in the Mouse**

**Liping Nie<sup>1</sup>, Hoi Ting Tsang<sup>1</sup>, Judilee N Dinglasan<sup>1</sup>, Ebenezer N Yamoah<sup>1</sup>**

<sup>1</sup>*University of California, Davis*

T-type Ca<sup>2+</sup> channels have been implicated in a variety of physiological processes including neuronal firing, hormone secretion, smooth muscle contraction, cell proliferation and development. It has been demonstrated that there are three subtypes of T-type Ca<sup>2+</sup> channels: a1G, a1H, and a1I. Here, we report the expression and the cloning of T-type Ca<sup>2+</sup> channels in the mouse inner ear. RNA expression of T-type Ca<sup>2+</sup> channels was investigated by RT-PCR using subunit-specific primers. The results indicated that three types of T-type Ca<sup>2+</sup> channels, a1G, a1H, and a1I, are expressed in the mouse cochlea, while only a1G and a1I are expressed in the utricle. The relative abundance of different T-type channels expressed in the mouse inner ear was determined. Furthermore, the a1G Ca<sup>2+</sup> channel was cloned from a mouse cochlea cDNA library using a multiple-probe strategy. Four different probes were designed based on a known sequence of a1G Ca<sup>2+</sup> channel from the mouse brain and were used for the cDNA library screening. The full-length a1G Ca<sup>2+</sup>

channel was assembled from overlapped clones. The sequencing analysis indicates that the mouse inner ear-specific  $\alpha 1G$   $Ca^{2+}$  channel is similar but not identical to the  $\alpha 1G$   $Ca^{2+}$  channel from brain. A functional study of the cloned channel will be discussed.

This work was supported by grants to ENY NIH-DC03828, DC04523.

### **879 CSlo Interacting Proteins in the Inner Ear.**

**Pownima Joshi<sup>1</sup>**, Haresha Samaranayake<sup>1</sup>, Alberto Ortega<sup>1</sup>, Joseph Santos-Sacchi<sup>1</sup>, Dhasakumar Navaratnam<sup>1</sup>

<sup>1</sup>*Yale University*

BK channels in hair cells are critical for normal hearing. In some vertebrates, BK channels play a critical role in frequency selectivity of hair cells, being responsible for the changing frequency of membrane potential oscillation along the tonotopic axis (electrical resonance). In addition, these channels are clustered and co-localized with voltage gated Ca channels. In seeking to understand the molecular underpinnings of the changing kinetic properties of these channels and their physical clustering and co-localization, we undertook a yeast two hybrid assay using a C terminal fragment of the BK channel as bait to interrogate a chick cochlea cDNA library. We found several proteins to interact with the Slo protein under high stringency conditions. These proteins included Dickkhopf related protein 3 (Wnt pathway), neuronal microtubule/neurofilament associated protein kinase, TNRC protein 11, RACK 1, CLN 3 like protein and several other proteins of indeterminate function. These proteins were shown to interact with the Slo C terminal bait fragment by immunoprecipitation. Since these proteins have been shown to alter the kinetics and localization of other ion channels we hypothesize that these proteins serve a similar function in chick hair cells.

Supported by NIH DC 00273 (JSS) and DC05352 (DN).

### **880 Voltage-Gated Calcium Channel Alpha-1 and Beta Subunit Interactions in Saccular Hair Cells**

**Neeliyath A. Ramakrishnan<sup>1</sup>**, Matthew J. Dickson<sup>1</sup>, Khalid M. Khan<sup>2</sup>, Marian J. Drescher<sup>1</sup>, Dennis G. Drescher<sup>1,3</sup>

<sup>1</sup>*Department of Otolaryngology, Wayne State University School of Medicine, Detroit, MI,* <sup>2</sup>*Department of Biological Sciences, Aga Khan University, Karachi, Pakistan,*

<sup>3</sup>*Department of Biochemistry-Molecular Biology, Wayne State University School of Medicine, Detroit, MI*

Functional interactions between alpha-1 and beta subunits of voltage-gated calcium channels (VGCC) modulate calcium current properties in hair cells. The alpha-1 and beta subunits physically interact through an AID (alpha-interaction domain) in the I-II intracellular loop of the alpha-1 subunit and a BID (beta-interaction domain) in the beta subunit. We have cloned and sequenced splice variants of alpha-1D (Cav1.3), alpha-1B (Cav2.2), beta-1, and beta-2a subunits from a trout saccular hair cell layer. Using

affinity-purified antibodies, we immunohistochemically localized both alpha-1D and alpha-1B subunits to saccular hair cells. To study subunit interactions in vitro, we cloned and expressed regions of the VGCC subunits as fusion polypeptides, utilizing pRSET vector, Ni affinity columns, and western blot detection with anti-Xpress monoclonal antibody. Surface plasmon resonance binding studies were performed with purified beta-1 and beta-2a subunits as ligands (amine-coupled on a CM5 sensor chip) and purified alpha-1 subunit fusion polypeptides as analytes. For immunoprecipitation studies, fusion polypeptides were synthesized in a coupled transcription-translation system. The alpha-1 subunit I-II loop splice variants, cloned in pGBKT7 vector (containing a cMyc epitope at the N-terminal), and the beta subunits, cloned in the pRSET vector (containing a Xpress epitope), were translated in vitro. The fusion polypeptides containing alpha-1 and beta subunit polypeptides were allowed to interact and subsequently immunoprecipitated using anti-cMyc monoclonal antibody and protein A-agarose. Bound polypeptides were denatured and the beta subunit polypeptide was detected by western blot using anti-Xpress antibody. The results demonstrated interaction of the beta-1 subunit with a Cav1.3 hair-cell I-II loop splice variant containing exon 9a. These studies reveal the nature of VGCC subunit interactions in the hair cell.

### **881 Extrasynaptic Localization of Inactivating BK Channels in Mouse Inner Hair Cells**

**Sonja Pyott<sup>1</sup>**, Richard Aldrich<sup>1</sup>

<sup>1</sup>*Stanford University*

Auditory hair cells from non-mammalian vertebrates are electrically tuned to specific sound frequencies primarily by the interactions of voltage-gated calcium channels and BK potassium channels colocalized at synaptic active zones. Mammalian inner hair cells are not electrically tuned, and, yet, BK channels are also thought to reside at active zones. Using patch clamp recordings and immunofluorescence, we characterized BK channel expression in mouse inner hair cells. Both electrophysiology and immunoreactivity show that BK channel expression is developmentally regulated. Unexpectedly, these channels have inactivating currents and are clustered near the apex of the cell away from synaptic sites near the base. These results indicate a novel function of BK channels in mammalian inner hair cells and provide a framework for future research.

### **882 Kappa Opioid Receptor Activation Inhibits Calcium Current in Cochlear Hair Cells.**

**Enrique Soto<sup>1</sup>**, Rosario Vega<sup>1</sup>, Angelica Almanza<sup>1</sup>

<sup>1</sup>*Universidad Autónoma de Puebla*

There is increasing evidence that the opioid system has a role in hearing. To provide further evidence for such a role, the action of kappa opioid receptor (KOR) agonists on the outward currents and on the  $Ca^{2+}$  current were studied in outer and inner hair cells (OHC, IHC). Hair cells were



enzimatically dissociated from P14 to P17 Long Evans rats. Cells were voltage clamped and the action of KOR agonist U-50488 was studied in total outward currents from OHC ( $n = 6$ ) and IHC ( $n = 12$ ).  $1 \mu\text{M}$  U-50488 produced a 52% decrease in outward current magnitude in both cell types. To define if this action of U-50488 was due to  $\text{Ca}^{2+}$  activated  $\text{K}^+$  current lack of activation after  $\text{Ca}^{2+}$  current inhibition, as reported in vestibular hair cells (Vega and Soto, 2003), solutions to isolate the  $\text{Ca}^{2+}$  current were used. Extracellular solution consisted of (in mM) NaCl 55, CsCl 30, TEA 23,  $\text{BaCl}_2$  20,  $\text{CaCl}_2$  0.1, HEPES 10, glucose 10. Intracellular solution was (in mM) CsCl 75, TEA 23,  $\text{CaCl}_2$  0.1, EGTA 10, NMDG 80, GTPNa 0.5, ATPMg 2, HEPES 10. Calcium current from OHC ( $n = 6$ ) was of the high voltage activated type (around -40 mV) and with no significant inactivation during 2 s pulse. The application of  $1 \mu\text{M}$  U-50488 ( $n = 3$ ) produced a  $63 \pm 21\%$  partially reversible decrease of the  $\text{Ca}^{2+}$  current. These results indicate that KOR activation modulates  $\text{Ca}^{2+}$  current in hair cells influencing the cell excitability via the  $\text{Ca}^{2+}$  activated  $\text{K}^+$  current and the neurotransmitter release. Opioid modulation of auditory function may be significant in controlling auditory sensitivity and it may have a significant role in pathological process such as hyperacusis and tinnitus.

This material is based on work supported by a grant from the University of California Institute for México and the United States (UC-MEXUS) and the Consejo Nacional de Ciencia y Tecnología de México (CONACyT) grant 40672 to RV.

### **883 Fast Activation and Inactivation of BK Currents in Rat Inner Hair Cells (Ihc): The Implication of $\beta$ Auxiliary Subunits**

Emilie Hoang-Dinh<sup>1</sup>, Didier Dulon<sup>1</sup>

<sup>1</sup>EA 3665 Université de Bordeaux 2, France

Large-conductance calcium-activated  $\text{K}^+$  (BK) channels are known to be a key component of the fast repolarizing currents of inner hair cell (IHC). These channels allow IHC to function as fast mechano-electrical transducers and to phase-lock the receptor potential with sound up to the kHz (Kros et al. 1998; Skinner et al. 2003). Similar to voltage-gated  $\text{K}^+$  channels, BK channels contain a tetramer of pore-forming  $\alpha$  subunits encoded by the slo1 gene (KCNMA). In many tissues, this tetramer may also be associated with auxiliary  $\beta$  subunits that define several important functional properties of the channels (such as calcium, IbTX sensitivity and inactivation). Four members of the BK  $\beta$  subunit family issued from four different genes (KCNMB1, KCNMB2, KCNMB3, KCNMB4) have been identified. The participation and the role of such regulatory  $\beta$  subunits in the fast BK currents expressed in mammalian hair cells remain uncertain. The goal of our study was to investigate the participation of such regulatory subunits in the BK currents of inner hair cells.

Patch-clamp recordings in mature IHC isolated from rat cochleae (P18-P22) showed that the fast repolarizing  $\text{K}^+$  currents were sensitive to 10 mM intracellular BAPTA, confirming their calcium dependence. IbTX and paxilline, two potent inhibitors of BK channels, inhibited this fast

outward  $\text{K}^+$  currents of IHC. The sensitive currents to both toxins displayed a fast transient component (tau activation ranging between 0.5 to 1 ms and tau inactivation ranging between 2.4 to 3.0 ms) and a sustained non-inactivating component. A more effective inhibition was observed with paxilline ( $20 \mu\text{M}$ ) compared to IbTX ( $100 \text{ nM}$ : a concentration largely above  $\text{IC}_{50}$ ), indicating a lower sensitivity to IbTX. RT-PCR experiments from P19 rat organ of Corti showed the expression of  $\beta 1$ ,  $\beta 4$  in agreement with Langer et al. (2003) but also the presence of the more recently discovered  $\beta 3$  subunits (Xia et al. 2000). Interestingly,  $\beta 3$  subunits are known to confer in heterologous expression systems fast inactivation and IbTX resistance to BK currents, in agreement with our electrophysiological recordings in IHCs. The cellular expression of these different  $\beta$  regulatory subunits along the cochlear partition is currently under investigation.

### **884 Tissue-Specific Alternative Splicing of Full-Length KCNMA1 (Slo) Splice Variants**

Thomas Bell<sup>1</sup>, Jun Kong<sup>1</sup>, Locke Emily<sup>1</sup>, Carl Oberholtzer<sup>1</sup>

<sup>1</sup>University of Pennsylvania School of Medicine

Large conductance (BK) calcium-activated  $\text{K}^+$  channels are widely expressed in the nervous system and BK channels play a key role regulating several cellular functions such as neurotransmitter release, burst firing in Purkinje neurons, and the intrinsic frequency tuning of auditory hair cells (Wang et al., 2001; Swensen and Bean, 2003; Fettiplace & Fuchs 1999). The pore-forming alpha-subunit is encoded by single gene (KCNMA1 or Slo) and mice lacking the KCNMA1 gene display several dysfunctions such as progressive hearing loss, cerebellar ataxia and reduced burst firing in cerebellar Purkinje neurons (Sauabier et al., 2004; Ruttiger et al., 2004). In neurons the functional diversity among BK currents has yet to be fully resolved, but expression of multiple Slo splice variants is likely an important factor. Previous studies have demonstrated that the Slo gene is subjected to extensive tissue-specific (Tseng-Crank et al; 1994) and cell-specific alternative splicing (Navaratnam et al. 1997; Rosenblatt, et al. 1997). However, these studies focused on the expression patterns of alternatively spliced Slo exons in isolation and did not establish the linkage between splice sites. The goal of this study is to identify the populations of native full-length Slo transcripts in two functionally distinct tissues in which BK currents play key physiological roles: the chick basilar papilla and cerebellum. Single gene Slo cDNA libraries were constructed from basilar papilla and cerebellar RNA using long-range RT-PCR in order to determine the dominant full-length Slo transcripts. A genomic map of the Slo gene was also constructed by screening a chicken genomic library and the chicken genomic database to establish the exon borders and gene structure of the Slo gene. The minimal Slo variant contains 27 exons and full-length transcripts frequently contained at least one alternatively spliced- 66% in cerebellum and 40% in basilar papilla. The BK currents in auditory hair cells and Purkinje neurons are likely to be derived from the contribution of several different Slo splice isoforms, therefore identifying the number native splice isoforms that are expressed in these tissues will be useful

in determining the functional impact Slo splicing plays in the physiology of the inner ear and cerebellum. Supported by DC02755 to J.C.O.

### **885 Expression of Voltage-Gated Calcium Channels in the Rat Vestibular Periphery**

Betty Tsai<sup>1</sup>, Julian Woollorton<sup>1</sup>, Ruth Anne Eatock<sup>1</sup>

<sup>1</sup>*Baylor College of Medicine*

The L-type Ca<sup>2+</sup> channel alpha subunit, Ca<sub>v</sub>1.3, is the dominant pore-forming Ca<sup>2+</sup> channel subunit in cochlear hair cells (Kollmar et al. 1997), where it is responsible for the vesicular release of glutamate (Spassova et al. 2001). However, Ca<sub>v</sub>1.3-null mice lack vestibular deficits (Platzer et al. 2000) and about half of the voltage-gated Ca current persists in the vestibular hair cells of Ca<sub>v</sub>1.3-null mice (Dou et al. 2004). Candidate alpha subunits for this current include other L-type (Brandt et al. 2003), N-type (Lopez et al. 1999; Rodriguez-Contreras and Yamoah 2001) and R-type subunits (Martini et al. 2000). Primary vestibular neurons have multiple voltage-gated Ca<sup>2+</sup> channel currents (Desmadryl et al. 1997), which may participate in retrograde transmission onto hair cells (Demêmes et al. 2000) or activation of Ca<sup>2+</sup>-gated K<sup>+</sup> currents.

We investigated expression of Ca<sup>2+</sup> channel alpha subunits in the utricular maculae, semicircular canal cristae, and vestibular ganglia of neonatal rats. The maculae and cristae were isolated from underlying tissue after treatment with thermolysin. We performed reverse-transcription PCR with nested primers. For the initial round of amplification, we used a degenerate primer set (Takahashi et al. 2003) to amplify Ca<sub>v</sub>1.1-1.4 (L-type) and Ca<sub>v</sub>2.1-2.3 (P/Q, N, and R-types, respectively). The amplified product was then subdivided for further amplification with primer sets specific to each Ca<sup>2+</sup> channel subunit. PCR products were confirmed by sequencing. In all three tissues (maculae, cristae, and ganglia), we obtained PCR products corresponding to the L-type subunits Ca<sub>v</sub>1.2 and 1.3, the P/Q-type subunit Ca<sub>v</sub>2.1, the N-type subunit Ca<sub>v</sub>2.2, and the R-type subunit Ca<sub>v</sub>2.3. Supported by NIDCD grant DC02290.

### **886 Is TRPA1 the Transduction Channel?:**

#### **Localization in Vertebrate Hair Cells**

Melissa A. Vollrath<sup>1,2</sup>, Duan-Sun Zhang<sup>1,2</sup>, Paul A. Gray<sup>1,3</sup>, Shuh-Yow Lin<sup>1,4</sup>, Kelvin Y. Kwan<sup>1,2</sup>, Daniel Tamasauskas<sup>1,2</sup>, David P. Corey<sup>1,2</sup>

<sup>1</sup>*Dept. of Neurobiology, Harvard Medical School*, <sup>2</sup>*Howard Hughes Medical Institute*, <sup>3</sup>*Dana Farber Cancer Institute*, <sup>4</sup>*Dept. of Biology, Massachusetts Institute of Technology*

NOMPC, a member of the TRP-channel superfamily, participates in mechanotransduction in fruit fly bristles and zebrafish hair cells. Although no NOMPC homologues have been found in mammals, we hypothesized that the mammalian hair-cell transduction channel would be a TRP family member. To identify candidates, we performed in situ hybridizations for all 33 mouse TRP superfamily members. In situ hybridization on mouse sections, aged E17 to P0, showed TRPA1 message in the organ of Corti

and in the utricle. While label was faint, the pattern was more suggestive than for any other TRP, so we pursued TRPA1.

To determine the subcellular localization of TRPA1, we generated antibodies to the C-terminus of mouse TRPA1 and purified them against two different peptides. The antibodies recognized a single, appropriately-sized band in immunoblots from bullfrog and zebrafish eye. Additionally, on immunoblots prepared from HEK293 cells expressing a GFP::TRPA1 fusion, a single band co-labeled with our TRPA1 antibody and a GFP antibody.

In mouse cochlea, the antibody labeled hair-cell stereocilia, as well as the Golgi apparatus of Hensen's cells. In mouse vestibular system, stereocilia and kinocilia were labeled. Antibodies also cross-reacted with bullfrog saccular hair cells: they prominently labeled stereocilia tips but not their bases, and labeled kinocilia and the pericuticular zone. Both antibodies gave similar staining patterns that were eliminated by excess peptide. Finally, we treated bullfrog sacculles with BAPTA or La3+, treatments shown to cut tip links and to cause redistribution of the tip-link protein cadherin-23. TRPA1 immunoreactivity in stereocilia was greatly reduced following treatment. TRPA1 is appropriately located to be part of the transduction channel of vertebrate hair cells.

### **887 Is TRPA1 the Transduction Channel?**

#### **Suppression by Morpholino Oligonucleotides in Zebrafish**

Shuh-Yow Lin<sup>1,2</sup>, Melissa Vollrath<sup>1,3</sup>, Daniel Tamasauskas<sup>1,3</sup>, Jaime Garcia-Anoveros<sup>4</sup>, David Corey<sup>1,3</sup>  
<sup>1</sup>*Dept. of Neurobiology, Harvard Medical School*, <sup>2</sup>*Dept. of Biology, MIT*, <sup>3</sup>*Howard Hughes Medical Institute*, <sup>4</sup>*Northwestern University*

TRP channels have been implicated in transduction by various sensory receptors, including including those sensing mechanical stimuli. Antibody localization suggested a role for TRPA1 in mouse inner ear, so we asked whether a TRPA is essential for hair-cell function in zebrafish. We first found two homologs of TRPA in the zebrafish genome, termed drTRPA1 and drTRPA2. drTRPA1 was detected in zebrafish inner ear by RT-PCR. To understand the functions of drTRPA1 and drTRPA2, we used morpholino anti-sense oligonucleotides to inhibit protein expression in zebrafish embryos, and assessed function by electrophysiology and FM1-43 imaging at 60-70 hours post fertilization.

FM1-43 accumulation by lateral-line hair cells was inhibited by morpholinos targeting drTRPA1 but not drTRPA2, with fluorescence intensity of individual neuromasts reduced by ~50%. Similarly, FM1-43 injections into the otocyst labeled fewer hair cells in fish injected with drTRPA1 morpholinos than in fish with control morpholinos.

We tested the function of the inner hair cells by measuring the microphonic potentials from the otocyst, elicited by a stimulus probe placed nearby. Microphonic potentials were reduced by two thirds, for drTRPA1 morpholinos compared to controls. To rule out possible developmental effects, we counted phalloidin-labeled hair bundles and

found no substantial reduction in cell number that could account for the decrease in microphonic potentials or FM1-43 labeling.

To verify the effectiveness of the morpholinos, we used immunoblots to assess drTRPA1 protein levels in the morphants. Gene-specific morpholinos, but not the control, reduced protein expression. By sequencing RT-PCR products, we also found that a morpholino targeting a splice junction caused a frame shift and stop before drTRPA1's transmembrane domains.

This evidence is consistent with the idea that drTRPA1 mediates mechano-transduction in zebrafish hair cells, as has also been proposed for zebrafish NOMPC.

### **888** Is TRPA1 the Transduction Channel? Expression and Suppression in the Embryonic Mouse Utricle

Gwenaelle S.G. Geleoc<sup>1</sup>, Matthew P. Hoffman<sup>2</sup>, Jaime Garcia-Anoveros<sup>3</sup>, Andrea Amalfitano<sup>4</sup>, David P. Corey<sup>5,6</sup>, Jeffrey R. Holt<sup>1</sup>

<sup>1</sup>Depts. of Neuroscience and Otolaryngology, University of Virginia School of Medicine, <sup>2</sup>Matrix and Morphogenesis Unit, CDBRB, NIDCR, <sup>3</sup>Depts. of Anesthesiology and Physiology, Northwestern University Institute for Neurosciences, <sup>4</sup>Dept of Pediatrics, Duke University Medical Center, <sup>5</sup>Dept. of Neurobiology, Harvard Medical School, <sup>6</sup>Howard Hughes Medical Institute

The onset of mechanotransduction in hair cells of the mouse utricle occurs within 18 hours between embryonic day (E) 16 and E17 (Géléoc and Holt, Nat Neurosci, 2003). We reasoned that expression levels of mRNAs that encode transduction elements might peak around this time point. To identify candidate transduction channels, we did quantitative RT-PCR for TRP channels in mouse utricles between E14 and E19. TRPA1 expression peaked at E17 and was therefore selected for further examination.

To test TRPA1 function by suppressing expression, we generated multiply deleted adenoviral vectors (-E1, -pol, -pTP) that encoded siRNAs specific to either transmembrane domain five (Ad14) or six (Ad6) driven by the H1 promoter. Green fluorescent protein (GFP) driven by the constitutively active CMV promoter was included as a marker. A third adenovirus that contained just the CMV-driven GFP sequence was used as a control (AdGFP). Sensory epithelia of embryonic mouse utricles were excised at E15 and placed in organotypic culture for 2-4 days and exposed to Ad14, Ad6, or AdGFP at titers ranging from 10<sup>5</sup> to 10<sup>8</sup> infectious particles/ml.

We first examined the infected utricles for FM1-43 loading. FM1-43 fluorescence was reduced by 32±5% (n=41) in Ad14 infected cells and by 69±8% (n=20) in Ad6 infected cells, relative to uninfected controls, but was within 5±14% of controls (n=11) in Ad-GFP positive cells. Next we deflected hair bundles and recorded transduction currents. We found no significant difference between transduction current amplitude in uninfected control cells (130±16 pA, n=10) and those infected with AdGFP (103±28 pA, n=6). However, Ad14-infected cells had mean currents of 34±13 pA (n=4) while Ad6-infected cells had maximal currents of 20±12 pA (n=10).

The expression peak at E17 and suppression of FM1-43 uptake and transduction currents by specific siRNAs suggest that TRPA1 is an essential component of the mechanotransduction apparatus in mouse utricle hair cells.

### **889** Hair Cell-Transducer Properties of TRPA1, an Ancestral Channel for Pain and Hearing

Keiichi Nagata<sup>1</sup>, Anne Duggan<sup>1</sup>, Gagan Kumar<sup>1</sup>, Jaime Garcia-Anoveros<sup>1</sup>

<sup>1</sup>Northwestern University

The channels that underlie most forms of sensory mechanotransduction in mammals, including those in auditory hair cells and mechanonociceptors, are unknown. The mouse TRPA1 channel is expressed by most small neurons of dorsal root, trigeminal and nodose ganglia, localized to their sensory fibers, and activated by icilin, isothiocyanates, and other pain-producing chemicals. TRPA1 is not expressed in any other major organ except in the inner ear, where we find it in both supporting and hair cells of sensory epithelia (organ of Corti, utricle, sacculus and crista ampularis), and can be detected in hair cell stereocilia. Thus TRPA1 is a potential transducer for both nociceptors and hair cells. In support of this proposed role, heterologously expressed TRPA1 channels share many properties with the hair cell transducer: block by gadolinium, amiloride, gentamicin and ruthenium red, a 100 pS conductance that is reduced to 55 % by calcium, potentiation followed by closure by calcium entering the channel and reopening by depolarization, a feature also in keeping with a role in nociception. Nematodes, which lack hair cells but do have mechanosensory and nociceptive neurons, have an ortholog to TRPA1 that is expressed in some of them and mediates avoidance to the channel agonist icilin. We conclude that TRPA1 orthologs play a widespread and ancestral role in nociception and mechanotransduction, and suggest that vertebrate hair cells and nematode ciliated mechanosensory neurons derive from an ancestral, TRPA1-expressing sensory neuron.

### **890** Mutant Analysis Reveals Whirlin as a Dynamic Organiser in the Growing Stereocilium

Steve Brown<sup>1</sup>, Yoshi Kikkawa<sup>2</sup>, Philomena Mburu<sup>1</sup>, Sue Morse<sup>1</sup>, Stuart Townsend<sup>1</sup>

<sup>1</sup>Mammalian Genetics Unit Harwell, <sup>2</sup>Tokyo Metropolitan Institute of Medical Science

Stereocilia on the surface of hair cells are vital for the process of auditory transduction. Stereocilia develop in bundles with a regular staircase pattern, whose actin core is organised such that the barbed ends of actin filaments are located at the stereocilia tips where there is a continuous cycle of renewal of actin filaments by addition of actin monomers. What little we know of the molecular processes that control actin polymerisation and stereocilia growth come from studies of mouse mutants with defects in stereocilia development, including the shaker2 (myosin XVa) and whirler mutants. The PDZ protein whirlin is

known by virtue of the whirler mutation to be involved in the process of stereocilia organisation (Mburu et al, Nature Genetics 2003). We have investigated the expression of whirlin and myosin XVa in developing stereocilia in wild-type and whirler and shaker2 mutants. Whirlin localises to the actin-free zone at the tips of stereocilia. Expression of whirlin is dynamic during stereocilia growth demonstrating an ordered appearance and fade-out across the stereocilia rows and revealing a novel molecular gradation of process traversing the developing stereocilia bundle. Fade-out of whirlin in inner hair cells precedes that of outer hair cells consistent with the earlier maturation of inner hair cell stereocilia. In myosin XVa mutants in which stereocilia are shortened, whirlin is still expressed in the stereocilia tips but fade-out is accelerated. The data indicate that whirlin is a critical and dynamic organiser for proteins involved in stereocilia elongation and actin polymerisation.

### **891 TRPA1 Channel Expression in Sensory Epithelia of the Inner Ear and in Nociceptors of Sensory Ganglia**

**Gagan Kumar<sup>1</sup>, Anne Duggan<sup>1</sup>, Jaime García-Añoveros<sup>1</sup>**  
<sup>1</sup>Northwestern University

TRPA1 is a channel with 17 ankyrin repeats that has been proposed as a receptor for pain. We performed in situ hybridization (ISH) and immunohistochemistry (IHC) to determine its pattern of expression. We find TRPA1 mRNA in the three ganglia (dorsal root, trigeminal and nodose) that contain nociceptive neurons as well as in the sensory epithelia of the inner ear, but find no TRPA1 mRNA in any other major organ (brain, heart, liver, kidney, skeletal muscle, lung, spleen, bladder, testis, whisker pad skin, or superior cervical ganglion). Within sensory ganglia, TRPA1 is expressed by 56.5 % of all DRG neurons, 36.5 % of all trigeminal ganglia neurons, and 28.4 % of all nodose ganglia neurons. Size distribution plots show that, in all three types of ganglia, expression is restricted to the majority of the smaller neurons, the nociceptors. TRPA1 protein was also found in the nociceptors, both at their cell bodies and at their sensory processes in target organs such as the bladder, as expected if TRPA1 functions in the primary sensory transduction of nociceptors.

In inner ear, TRPA1 immunoreactivity was detected, both by western blot and by IHC, in all the sensory epithelia: organ of Corti, utricle, sacculus and crista ampularis. TRPA1 was present surrounding the apical side of utricular supporting cells and of inner and outer pillar and Deiter cells of the organ of Corti. However, low levels of TRPA1 protein were also detected in both vestibular and cochlear hair cells, where it localized to the sensory bundles. The expression pattern and localization of TRPA1 suggests it may be a component of the transduction channel complex of both hair cells and nociceptor neurons.

### **892 Opening Single MET-Channels in Mammalian Outer Hair Cells by AFM**

**Stefan Fink<sup>1</sup>, Assen Koitschev<sup>2</sup>, Hans-Peter Zenner<sup>3</sup>, Matthias G. Langer<sup>1</sup>**

<sup>1</sup>Dept. of Applied Physiology, University of Ulm,

<sup>2</sup>Tuebingen Hearing Research Center (THRC), <sup>3</sup>Dept. of Otorhinolaryngology, University of Tuebingen

Perception of sound relies on transformation of incoming sound waves (mechanical stimulation) into electrical signals, called mechano-electrical transduction (MET). It is still unknown how the transduction channel can respond to applied forces within microseconds and how the transduction machinery overcomes the limit of channel gating noise. Here, instead of using conventional stimulation methods addressing the entire hair bundle, an atomic force microscopy (AFM) sensor was used displacing single tallest stereocilia within intact hair bundles. Individual stereocilia were scanned by AFM while single-channel currents of mammalian outer hair cells (OHC) were simultaneously measured by patch clamp using the whole-cell, voltage-clamp configuration.

In contrast to single-channel recordings obtained by stimulation of entire hair bundles AFM stimulation of single stereocilia yielded intrinsic channel gating with continuous transitions between open and closed state rather than step-like responses. This observation suggests a gate flickering between open and closed state with rate constants far beyond the recording bandwidth of 3 kHz. Observed current responses likely reflect the average open probability of the transduction channel rather than transitions between open and closed state at full bandwidth. Assuming a gating noise equally distributed over very large bandwidth (exceeding the upper frequency limit of hearing) the current noise level would reduce improving the signal to noise ratio and the sensitivity of hearing.

### **893 Combined AFM and Patch clamp in Hearing Research: A powerful Tool for Probing Single Mechanosensitive Ion Channels in the Mammalian Inner Ear**

**Matthias G. Langer<sup>1</sup>, Assen Koitschev<sup>2</sup>, Hans-Peter Zenner<sup>3</sup>, Stefan Fink<sup>1</sup>**

<sup>1</sup>Dept. of Applied Physiology, University of Ulm,

<sup>2</sup>Tuebingen Hearing Research Center (THRC), <sup>3</sup>Dept. of Otorhinolaryngology, University of Tuebingen

Perception of sound relies on mechanosensitive ion channels located in the stereocilia of so-called hair cells. Usually the entire hair bundle is mechanically stimulated by an attached glass fiber or by fluid jet application rather than displacing individual stereocilia. Thus, single-channel recordings with common stimulation methods are limited to artificial hair bundles with only few intact transduction channels, which is either due to morphological damage or to application of low extracellular Ca<sup>2+</sup>. Here, we present a new experimental approach combining the nanomanipulation capability of Atomic Force Microscopy (AFM) with patch clamp. Single-channel currents in intact, untreated mammalian outer hair cells (OHC) were

measured by patch clamp in response to displacement of individual stereocilia using a sharp AFM tip. Detected single-channel transduction currents of 6.4 pA (single-channel conductance: 76 pS) reveal a kinetic that differs from current recordings that have previously been observed by other investigators with conventional stimulation methods.

### **894 The Structure of Tip Links and Kinocilia Links in Avian Sensory Hair Bundles**

Vladimir Tsuprun<sup>1</sup>, Patricia Schachern<sup>1</sup>, Michael Paparella<sup>1</sup>, Richard Goodyear<sup>2</sup>, Guy Richardson<sup>2</sup>

<sup>1</sup>University of Minnesota, <sup>2</sup>University of Sussex

Recent studies have indicated that the tip links and kinocilia links of sensory hair bundles in the inner ear have similar properties and share a common epitope (Goodyear and Richardson, 2003), and that cadherin 23 may also be a component of each link type (Siemens et al., 2004). Transmission electron microscopy was therefore used to study and compare the fine structure of the tip links and kinocilia links in avian sensory hair bundles. Tannic acid treatment revealed a thin strand, 150 - 200 nm long and 8-11 nm thick, present in both link types. Fourier analysis of link images showed that the strand of both link types is formed from two filaments coiled in a helix-like arrangement with an axial period of 20 - 25 nm, with each filament composed of globular structures that are about 4 nm in diameter. Differences in the radius and period of the helix-like structure may underlie the observed variation in the length of tip and kinocilia links. The similar helix-like structure of the tip links and kinocilia links is in accord with the presence of a common cell-surface antigen (TLA antigen) and similarities in the physical and chemical properties of the two link types (Goodyear and Richardson, 2003). The spacing of the globular structures comprising each filament of the two link types is similar to the 4.3 nm center-to-center spacing reported for the globular cadherin repeat (Boggon et al., 2002), and is consistent with the suggestion (Siemens et al., 2004, Corey and Sotomayor, 2004) that cadherin 23 is the tip link.

### **895 The Role of Myosin-1c's Calmodulin-Binding Domains in Binding to Hair-Bundle Receptors**

Kelli Phillips<sup>1,2</sup>, Anindita Biswas<sup>1,2</sup>, Janet Cyr<sup>1,3</sup>

<sup>1</sup>Sensory Neuroscience Research Center, West Virginia University School of Medicine, <sup>2</sup>Dept. of Biochemistry and Molecular Pharmacology, West Virginia University School of Medicine, <sup>3</sup>Dept. of Otolaryngology, West Virginia University School of Medicine

Myosin-1c (Myo1c) is essential to the mechanosensitive process of slow adaptation in vestibular hair cells. As the slow adaptation motor, Myo1c must interact with other components of the transduction channel complex. Indeed, Siemens *et al.* (Nature **428**:950-54, 2004) have demonstrated that Myo1c interacts with cadherin 23, a component of the tip link, when the two proteins are expressed in human embryonic kidney cells. However, it is unclear whether these two proteins interact directly and whether this interaction occurs within the hair bundle.

To examine the binding of Myo1c with components of the transduction apparatus, we employ an *in situ* binding assay that allows for the visualization of the interaction of Myo1c recombinant fragments to specific intracellular binding sites, located at the tips of stereocilia, which we term "receptors". This interaction is mediated by Myo1c's neck region, specifically at its second calmodulin-binding IQ domain. Myo1c:receptor interactions are influenced by surrounding Myo1c IQ domains and blocked by excess calmodulin (CaM). To further characterize Myo1c's interactions with stereociliary receptors, mutations within the IQ consensus sequence of each Myo1c IQ domain were made to block CaM interaction. The number of CaM molecules bound to the mutated Myo1c fragments was evaluated by densitometry analysis, and the recombinant proteins were used in our *in situ* binding assay to ascertain the role that CaM bound at each IQ domain plays in receptor binding. In addition, we are also investigating the identity of Myo1c receptors, specifically focusing on the potential interaction of Myo1c with cadherin 23.

(Supported by NIH RO1 DC006402)

### **896 Cholesterol Modulates Mechanotransduction and Lipid Diffusion in Hair Bundles**

Diane Ronan<sup>1</sup>, Peter Gillespie<sup>1,2</sup>

<sup>1</sup>Oregon Health and Science University, <sup>2</sup>Vollum Institute

Specialized lipid domains in the membranes of hair bundles regulate mechanotransduction (Hirono et al., Neuron, in press). Cholesterol may play a particularly important role as it has been previously shown to be a major component of hair cell stereocilia (Jacobs and Hudspeth, 1990; Forge, 1991) and, in other cell types, this sterol modulates ionic channel activity and mechanical properties of the plasma membrane. Here we show that sequestration of cholesterol with methyl- $\beta$ -cyclodextrin (MBC) reversibly slows adaptation and increases resting open probability without decreasing total transduction current in isolated bullfrog saccular hair cells. Motivated by this result, we examined whether the plasma membrane of the hair cell has regions that are differentially influenced by cholesterol modulation. A useful technique for defining the lipid-domain structure of the plasma membrane is to measure the lateral diffusion of fluorescently-labeled lipids after bleaching different defined areas (fluorescence recovery after photobleaching, or FRAP). We labeled isolated bullfrog saccular hair cells with the membrane probe di-8-ANEPPS, bleached rectangular regions of the hair bundle and apical plasma membrane, and monitored recovery of fluorescence over time. We find that when bleaching the tip of the hair bundle, the fluorescence recovers quite rapidly back towards control values. Bleaching either the whole bundle or the apical plasma membrane causes a much slower and partial recovery. After depletion of cholesterol with MBC, however, even in cells which did not recover well from the control bleach, the recovery is much more rapid and complete. The increased lipid mobility after cholesterol treatment is consistent with FRAP studies on other cell types, but the effect is much more pronounced in

hair cells. In addition, the MBC treatment caused a large increase in the steady-state fluorescence. Removal of cholesterol may increase the pool of diffusible lipid by altering a diffusion barrier, such as tight junctions. We will further examine this idea, and will measure whether smaller regions within the hair bundle itself have different lipid mobility and sensitivity to cholesterol modulation.

### **897 Longitudinal Distribution of Drugs in Perilymph Assessed by Cochlear Action Potentials.**

**Alec Salt<sup>1</sup>**, Shane Hale<sup>1</sup>

<sup>1</sup>*Department of Otolaryngology, Washington University Medical School, St. Louis, MO*

Although chemical marker studies indicate that the spread of substances in the fluids of the ear is dominated by passive diffusion, it has not been established whether this principle is generally applicable to all substances. In the present study, we have used the spread of suppression of cochlear responses to quantify the spread of drugs applied to perilymph. We injected one of three drugs: tetrodotoxin, sodium kainite or furosemide at 50 or 100 nl/min into scala tympani perilymph of the basal or third turn. Injection pipettes were sealed into the bony otic capsule to prevent artifacts from perilymph leakage. Cochlear action potential (AP) thresholds were monitored as a function of time for frequencies from 1 kHz to 23 kHz in half or quarter octave steps. Thresholds were established in an automated procedure using a 10  $\mu$ V response criterion. Sensitivity was determined for up to 10 test frequencies at 2 min intervals during the 90 min period following drug injection. For tetrodotoxin and kainite, the spread of response suppression as a function of frequency and time was in close agreement with simulations of the spread of drug along the scala. In contrast, for furosemide, the initial threshold changes close to the injection site were consistent with the drug's effects, but furosemide also induced threshold elevations at distant sites in a manner inconsistent with longitudinal diffusion of drug along the scala. The findings suggest that furosemide may be spreading by other mechanisms, such as via the vasculature, or that local effects of furosemide on one part of the endolymphatic system are influencing endolymph status, and function, at distant sites. The results with TTX and kainate validate the use of AP thresholds as a method to quantify the dispersal characteristics of an applied drug, but the anomalous findings with furosemide show that for some drugs, alternative mechanisms may need to be considered.

This study supported by NIH/NIDCD grant DC01368

### **898 Expression Patterns of Connexin29 in the Cochlea of Mice**

**Wenxue Tang<sup>1</sup>**, Yanping Zhang<sup>1</sup>, Shoab Ahmad<sup>1</sup>, Ping Chen<sup>1</sup>, Xi Lin<sup>1</sup>

<sup>1</sup>*Emory University School of Medicine*

Gap junctions (GJs) facilitate intercellular communications by providing conduits linking the cytoplasm of attached cells. Each GJ is an intercellular channel consisting of a

pair of connexons in apposed cell membranes that meet and align by multiple disulfide bonds within the intercellular space. Connexons are made of six protein subunits called connexins (Cx). Twenty different Cx genes have been found in the human genome so far, and 19 in that of the mouse. The importance of Cxs in normal cochlear functions has been demonstrated by a large number of genetic studies showing that about half of inherited childhood non-syndromic deafness cases are caused by mutations in the Cx gene. Our previous work showed that Cx26, Cx30, Cx29 and Cx43 are the four most abundantly expressed Cx subtypes in the cochlea of mice. Cx29 is a relatively new member of the Cx family, whose expression has not been characterized in the cochlea. Western blot results revealed that Cx29 expression levels were dramatically up-regulated after birth. Postnatal levels of Cx29 were at least 20 times higher than the prenatal level. Cx29 expression in the cochlea was further increased by about 50% at the adult stage. Immunolabeling identified high levels of Cx29 in the myelinating schwann cells along the processes of the auditory nerve, and a much lower level in a subset of fibrocytes bordering the stria vascularis. It is known that mutations in Cx32 cause a demyelinating peripheral neuropathy, X-linked Charcot-Marie-Tooth disease in humans (Bergoffen et al., 1993). However, previous work by others showed that mice lacking Cx32 only showed very mild peripheral phenotype. It is known that Cx29 interacts with Cx32 (Altevogt et al., 2002). Therefore, our findings offered the possibility that dysfunction of Cx29 could be involved in auditory neuropathy.

### **899 Cochlear Function in BETA2/NeuroD1 Transgenic Mice**

**Ann Marie Visosky<sup>1</sup>**, Jang Cho<sup>2</sup>, Ming-Jer Tsai<sup>2</sup>, Fred Pereira<sup>1,2</sup>, John Oghalai<sup>1</sup>

<sup>1</sup>*The Bobby R. Alford Department of Otolaryngology-Head and Neck Surgery, Baylor College of Medicine,*

<sup>2</sup>*Department of Molecular and Cellular Biology, Baylor College of Medicine*

BETA2/NeuroD1 is a beta helix-loop-helix transcription factor expressed in the mammalian endocrine pancreas, neuroendocrine cells of the gut and portions of the central and peripheral nervous systems. BETA2/NeuroD1 is essential for neuronal differentiation and null mice have a near complete absence of spiral ganglion neurons and a loss of central neuronal targets. Additionally, the cochlear duct is shortened and there are some inner hair cells found within the outer hair cell region of the organ of Corti. Heterozygotes, however, have normal cochlea and neuronal anatomy. We recorded auditory brainstem responses (ABRs) and distortion product otoacoustic emissions (DPOAEs) in 8 week old BETA2/NeuroD1 null mutants, heterozygotes and age-matched, wild type controls. ABRs were evoked with a 5 msec sine wave tone pip. The stimulus intensity range was 10-90 dB SPL over the frequency spectrum of 4-80 kHz. DPOAEs were elicited using F2=1.2\*F1 and L2=L1. The stimulus intensity range was 20-80 dB SPL over the frequency spectrum of F2=4-43 kHz. We found that BETA2/NeuroD1 null mice have no ABRs and no DPOAEs. Heterozygote

mice have ABR and DPOAE thresholds similar to age-matched, wild type controls. The absence of ABR responses in the BETA2/NeuroD1 null mice is not surprising given their lack of spiral ganglion cells. However, the absence of DPOAEs suggests that there are profound physiologic consequences of this mutation, beyond the lack of innervation. Further studies are underway to determine if this represents a problem with the endocochlear potential or anatomic changes within the organ of Corti.

Supported by NIDCD Grant K08 DC006671 (to JSO) and DC04585 (to FAP)

## **900 Central Auditory Nerve Degeneration in Knockout Mice Lacking the Taurine Transporter**

**Haiyan Jiang**<sup>1</sup>, Dalian Ding<sup>1</sup>, Marcus Müller<sup>2</sup>, Ulrich Warskulat<sup>3</sup>, Dieter Häussinger<sup>3</sup>, Richad Salvi<sup>1</sup>

<sup>1</sup>Center for Hearing and Deafness, SUNY at Buffalo,

<sup>2</sup>Universität Tübingen, <sup>3</sup>Heinrich-Heine University

Taurine, one of the most abundant free amino acids, plays an important role in calcium and cell volume regulation, and antioxidant defense. Taurine is transported into cells by the sodium-dependent taurine transporter (TAUT) encoded by the *taut* gene. TAUT is expressed in glia, vascular endothelium and some neurons. Taurine is expressed at high levels in the inner ear; therefore we hypothesize that taurine transporter KO mice (*taut*<sup>-/-</sup>) would show enhanced degeneration in the inner ear and auditory nerve, myelinated by glia and Schwann cells on central and peripheral processes respectively. To test this hypothesis, we measured the auditory brainstem response (ABR) and harvested the cochlear tissue from *taut*<sup>-/-</sup> mice and WT mice. ABR thresholds were ~12 dB and 20 dB higher in KO mice than WT mice at 4 and 6 mo of age respectively and ABR amplitude was greatly reduced. Inner ear and auditory nerve pathology was evaluated at 3, 6 and 18 mo old KO and WT mice. *Taut*<sup>-/-</sup> mice exhibited an accelerated loss of outer hair cells and inner hair cells (IHC) compared to WT mice consistent with elevated ABR thresholds and reduced amplitudes. Peripheral auditory nerve fibers were present in the habenula perforata except in regions of the cochlea associated with missing IHC and spiral ganglion neurons (SGN). Loss of SGN was greater in *taut*<sup>-/-</sup> mice than WT mice. Interestingly, the central region of auditory nerve fibers in the modiolus showed significantly more degeneration in *taut*<sup>-/-</sup> KO than WT mice. Significantly, most of the glial cells in the central portion of the auditory nerve were missing in *taut*<sup>-/-</sup> mice, but were present in WT mice. These results suggest that loss of the taurine transporter in glial cells may exacerbate degeneration of auditory nerve fibers in addition to accelerating age-related hair cell loss.

Supported by NIH grants P01 DC03600-01A1 & R01 DC06630-01 and DFG Sonderforschungsbereich 575 "Experimentelle Hepatologie"

## **901 The Inhibition of Nifedipine on an Inward Current Evoked by ATP in Isolated Hensen's Cells of Guinea-Pig Cochlea**

**Xingqi Li**<sup>1</sup>, Jianxiong Li<sup>2</sup>, Jun Liu<sup>1</sup>

<sup>1</sup>Institute of Otolaryngology, Chinese PLA General

Hospital, <sup>2</sup>Department of Oncology, Chinese PLA General Hospital

Previous studies suggested that Hensen's cells in cochlea contributed an important role in maintaining the chemical and electrical homeostasis of the organ of Corti. ATP played an important role as an extracellular chemical messenger in the cochlea to change the ionic and micromechanical environment of hair cells. Previous studies suggested that nifedipine could partly protect the noise induced hearing loss by changing the function of Hensen's cells. To study whether the effect of nifedipine on Hensen's cell is related with the modulation effect on ATP, we studied the nifedipine's effect on the ATP induced currents recorded from the Hensen's cell. Hensen's cells were isolated from the adult cochlea of guinea pigs. They are identified by their characteristic lipid inclusions and then settled on Poly-L-lysine coated cover slips. The whole cell patch-clamp was used to record ion currents in Hensen's cells. Drugs were delivered to the cell by a micromanifold system made by three 100 µm diameter microtubules. An inward current was induced by ATP (0.1 to 10 mM) from the Hensen's cell. The current was reversible blocked by suramin (100 µM), a purinergic antagonist. When ATP (1 mM) and nifedipine (10 µM) were applied together, the inward current induced by ATP was blocked. Our results suggest nifedipine can inhibit ATP induced inward current recorded from Hensen's cell and this effect may be related with the nifedipine's protection effect on noise exposure.

## **902 Analysis of Mouse Cochlear Afferents Having Voltage-Gated Sodium Channels (Nav)**

**J.L. Winslow**<sup>1</sup>, W.A. Hossain<sup>2</sup>, M.N. Rasband<sup>3</sup>, D.K. Mores<sup>2</sup>

<sup>1</sup>U Toronto, <sup>2</sup>U CT Health Ctr, <sup>3</sup>CT Health Ctr

Use of antibodies has demonstrated presence of sodium channels on Types I and II cochlear afferents respectively from inner hair cells (IHCs) and outer hair cells (OHCs). Previous simulation of these fibers as passive membrane dendrites with low  $R_m < 1 \text{Kohm} \cdot \text{cm}^2$  showed that single synaptic pulses can trigger APs at the foramen nervosa (FN) where myelin begins for Type I; but, not for Type II which are unmyelinated and have synaptic input from 10 OHCs (Winslow, 1990. Prog. Neurobiol.34:91-105). Using a contemporary value  $R_m = 50 \text{Kohm} \cdot \text{cm}^2$ , HC synaptic input to both fibers can trigger APs at FN.

Our current simulation assumes that Nav1.6 channels are on the unmyelinated regions of both types distal to the FN and at nodes of Ranvier of Type I. K<sup>+</sup> channels occur at juxtaparanodes. Type II fibers have pan-Nav labeled channels on their axons central to FN and on the soma, and we assume they are co-localized with K<sup>+</sup> channels.

Nav1.6 is present on the ganglionic initial axon segments of both types. We compartmentalize the different regions, use kinetic equations for these channels and solve for the AP voltages over time and location. This model is used to test hypotheses about efficacy of the Nav channels in supporting APs. (Supported by NIH grants and Computational Neuroscience Fund)

### **903 Recordings from Spiral Ganglion Cells obtained in the Gerbil Hemicochlea**

**Adrian Muenscher<sup>1</sup>**, Claus-Peter Richter<sup>1</sup>

<sup>1</sup>*Northwestern University, Chicago, IL*

Two types of spiral ganglion cells can be distinguished, type-I and type-II cells. Type-I cells form contacts with inner hair cells, while type-II cells contact outer hair cells. Classification of spiral ganglion cells is mostly based on the innervation pattern. However, differences in morphology and electrophysiology also exist. While extracellular and intracellular recordings, which were made with sharp pipettes, are numerous for type-I spiral ganglion cells, fewer results are available for patch recordings from type-II spiral ganglion cells. Patch recordings were commonly obtained from cultured cells that were harvested from young animals (<10 days).

In our study, we examine spiral ganglion cells in an acute adult spiral ganglion cell preparation, the hemicochlea.

The hemicochlea is an isolated gerbil cochlea cut in half along its mid-modiolar plane. The modiolus is removed carefully from the cochleae. Next, one of the half modioli is mounted in an experimental dish on the stage of an upright microscope for measurements. After identifying the SG cells by location and morphology under the microscope, a measuring pipette (tip aperture ~1.5µm, resistance <5mΩ) is approached towards the cell. After the pipette formed a seal with the cell's membrane, voltage-current relations (I/V-curves) were recorded at a holding potential of -80 mV. In addition to voltage clamp measurements, similar measurements were performed in current clamp. Differences between two morphologically distinguishable cell populations will be discussed.

Supported by the Georgia Birtman Endowment Fund

### **904 Roles for Glutamate Receptor Subtypes in Calcium Oscillations in Dissociated Chick Cochlear Neurons**

**Brian Manning<sup>1,2</sup>**, William Sewell<sup>1,2</sup>

<sup>1</sup>*Eaton-Peabody Laboratory, Massachusetts Eye and Ear Infirmary*, <sup>2</sup>*Dept. of Otolaryngology and Laryngology, Harvard Medical School*

Auditory neurons express both ionotropic and metabotropic glutamate receptors. While AMPA-selective, ionotropic glutamate receptors are considered to mediate moment-by-moment afferent auditory neurotransmission, the functional roles of NMDA and metabotropic receptors are enigmatic. We have explored the ability of ligands for these receptor subtypes to alter intracellular calcium concentrations in dissociated chick auditory ganglion cells using Fura-2 ratiometric analysis, and confirmed the expression of these receptor subtypes on these cells using

immunohistochemistry and confocal microscopy. Cochlear ganglion neurons frequently displayed spontaneous oscillations in intracellular calcium concentration. The occurrence of these oscillations could be decreased in experiments in which antagonists for AMPA- and NMDA-receptor subtypes were present during tissue dissection and ganglia dissociation. Oscillations could also be eliminated in the presence of caffeine, implicating calcium release from intracellular stores. Application of agonists for all three receptor types produced increases in intracellular calcium that lasted long after the agonist had been washed out, though responses to agonists for each subtype differed. Agonists examined included dihydroxyphenylglycine (DHPG), an agonist for group I metabotropic receptors, as well as NMDA and AMPA. Prominent responses included an increase in the magnitude of calcium oscillations (DHPG), a transient increase in calcium concentration (AMPA and DHPG), and a prolonged increase in calcium concentration (NMDA). These results imply a functional role for these receptor subtypes in cellular processes that exhibit time courses on the order of seconds to minutes, rather than milliseconds, such as might be required to regulate the fidelity and stability of auditory transmission.

### **905 Cochlear Excitation and Synchronized Across-Frequency Neural Response: Modeling the Neural Response to Schroeder-Phase Harmonic Complexes in Several Species**

**Otto Gleich<sup>1</sup>**, Marjorie Leek<sup>2</sup>, Robert Dooling<sup>3</sup>

<sup>1</sup>*ENT-Department, University of Regensburg, Germany*,

<sup>2</sup>*Walter Reed Army Medical Center, Washington, DC USA*,

<sup>3</sup>*University of Maryland, College Park, MD, USA*

Harmonic complexes whose component phases increase or decrease with increasing frequency can result in large masking and perceptual differences, even though their long-term spectra do not differ. It is thought that the traveling wave associated with frequency specific delays along the cochlear partition critically affects processing of these harmonic complexes. Here we analyse how the time dependent change of frequency within one period of a harmonic stimulus interacts with the frequency specific delays along the cochlear partition in several species. We compare these model calculations with the amplitude of the compound action potential (CAP) measured with electrodes placed at the round window or penetrating directly into scala tympani, reflecting the degree of neural synchronization. Modeling and CAP measures were carried out for guinea pig, gerbil, canary, zebra finch and budgerigar, for a range of harmonic Schroeder complexes. The relative timing of each frequency within a harmonic period of the stimulus was added to the frequency-specific cochlear delays appropriate to each species to obtain a frequency dependent temporal representation of a given harmonic complex at the level of the auditory nerve. The maximum range of frequencies activated within a sliding 0.5 ms time window was assessed throughout the period. Our analysis shows that the maximum frequency range (in octaves) that can be activated by a 0.5 ms time window



within a single period of a harmonic complex is a good predictor of the CAP amplitude across a range of harmonic complexes and species. All species show a maximum synchronization varying between 0.2 and 3.6 octaves that is significantly correlated with CAP amplitudes (range 19 – 83 mV). This indicates that the degree of synchronization, estimated by CAP amplitude, is proportional to the distance along the cochlear partition activated within a time window of 0.5 ms. [Work supported by NIH and the DFG Str275-4/3].

### **906 Cochlear Frequency Map of the CBA/J Mouse: An Anatomical and Physiological Study**

Alejandro Rivas<sup>1</sup>, Karen Montey<sup>1</sup>, Michael Muniak<sup>1</sup>, Bradford May<sup>1</sup>, David Ryugo<sup>1</sup>, Howard Francis<sup>1</sup>

<sup>1</sup>Johns Hopkins University

The relationship between structure and function is an invaluable context with which to explore biological mechanisms of normal and dysfunctional hearing. The systematic representation of frequency across auditory structures is a first principle of auditory organization, and commences in the cochlea. With the mouse emerging as an important animal model for auditory research, there is need for a cochlear frequency map that is derived directly from electrophysiological and anatomical measurements. Previous maps for the mouse relied on assumptions about critical bands (Ehret et al., 1975) or estimated structure-function assessments in noise-damaged cochleae (Ou et al., 2000). Mueller et al. (ARO Abst., 2004) presented a frequency map for the CBA/J mouse cochlea based on physiological tuning measurements in the cochlear nucleus, staining with horseradish peroxidase, and serial section reconstructions of cochleae. Concerns about the accuracy of anatomic data based on the reconstruction of sectioned material prompted our examination of the mouse cochlear map using whole mount surface-preparations.

We present a cochlear frequency map in the CBA/J mouse based on measurements of frequency tuning between 4-60 kHz followed by injections of fluorescent dextran amines in the cochlear nucleus. The brightest location of fluorescent signal in retrogradely labeled radial fibers was determined and normalized as the percent distance from the apex. A place-frequency map was generated that resembled the Mueller et al. (2004) map in the apex but differed in the base. Although we did not observe single-unit responses at frequencies below 4 kHz, our results reveal that frequencies between 4-60 kHz are logarithmically distributed along the cochlea. Thus as observed in other mammalian species, there is a linear-distance to log-frequency relationship for the mouse cochlea.

Supported by NIH/NIDCD grants DC05909, DC05211, DC00232, and DC00143.

### **907 Stereology for Morphometric Analysis of Cochlear Innervation**

Yu Saito<sup>1</sup>, Alejandro Rivas<sup>1</sup>, Mohamed Lehar<sup>1</sup>, Peter Mouton<sup>2</sup>, David Ryugo<sup>1</sup>, Howard Francis<sup>1</sup>

<sup>1</sup>Johns Hopkins University, <sup>2</sup>Stereology Resource Center

The morphometry of afferent terminals and their synapses has implications for how auditory signals get transferred to the brain. The study of innervation structure at inner hair cells (IHCs) is needed to understand the pre- and post-synaptic mechanisms that underlie normal and abnormal hearing. Due to the labor-intensive demands of serial section electron microscopy, a more time-efficient approach was sought. We applied an unbiased stereological protocol that assesses innervation density and terminal morphometry at IHCs in C57BL/6J mice.

A stereological protocol consisting of disector pairs separated by a single section (Rivas et al., ARO Abstr, 2004) was refined to estimate the number of nerve endings, synaptic membrane thickenings, and synaptic bodies per IHC. We used this protocol in 19 IHCs from the 16 kHz location in 5 animals, and compared results to an analysis of semi-serial sections of 11 IHCs from 3 animals. Using systematic-random sampling, disector pairs separated by a distance of 0.16-0.18  $\mu\text{m}$  were examined, and nerve endings ( $Q_{ne}$ ), synapses ( $Q_{syn}$ ) and synaptic bodies ( $Q_{sb}$ ) were counted when present in the reference section and absent in the lookup section. The estimated total number of terminals, synapses and synaptic bodies per IHC ( $N_{IHC}$ ) were determined by multiplying  $\Sigma Q_{ne}$ ,  $\Sigma Q_{syn}$  and  $\Sigma Q_{sb}$ , by the fixed section-sampling fraction ( $k$ ). Estimates of  $N_{IHC}$  for synaptic membrane thickening and synaptic bodies in 5 mice (mean $\pm$ SD: 16.1 $\pm$ 2.7 and 18.3 $\pm$ 2.0) were within 10% of that determined using a serial analysis of alternate sections in 3 mice (17.1 $\pm$ 2.3). An analysis of variance suggests no significant difference between disector pair and semi-serial section data, and biological variability accounted for most of the variance in the stereological data.

Supported by NIH/NIDCD grants DC05909, DC05211, DC00232, and DC00143, and an NOHR grant.

### **908 Noise Exposure Shifts the Frequency Representation in the Mouse Cochlea**

Marcus Mueller<sup>1</sup>, Jean W.T. Smolders<sup>1</sup>

<sup>1</sup>J.W.Goethe-University, Physiology II, Theodor-Stern-Kai 7, 60590 Frankfurt, Germany

We recently presented a physiological place-frequency map of the CBA/J mouse cochlea, based on physiologically characterized and subsequently labeled auditory nerve fibers (Müller et al., Hear. Res., in press). Relative to this map the anatomical map derived from noise exposed C57BL/CBA F1 hybrid mice (Ou et al., 2000, Hear. Res. 145) is shifted by about an octave towards lower frequencies. We suggest that noise trauma alters basilar membrane vibration, resulting in a shift of the most sensitive frequency of auditory nerve fibers towards lower frequencies. However, the frequency shift observed after noise exposure in other species (cat, guinea pig) is less than an octave. To quantify the frequency shift in the

mouse, we measured changes in characteristic frequency (CF) resulting from acute noise exposure.

Micropipettes filled with 3 M KCl were advanced into the cochlear nucleus of anesthetized mice. When an auditory unit was isolated, a frequency tuning curve was determined from which CF and CF-threshold were derived. Then mice were exposed to noise (2 octaves bandwidth, centered at CF, 110 dB SPL, 4 min.) and frequency tuning curves of the same unit were determined for up to 30 min post-exposure.

After noise exposure the CF shifted to lower frequencies by about 1 octave. The shift was frequency dependent, increasing from 0.8 octaves at a (pre-exposure) CF of 10 kHz to 1.2 octaves at 50 kHz. Post exposure CF-thresholds ranged from 61 to 79 dB SPL, the most sensitive units having the largest threshold shift.

The observed 1 octave shift of CF after noise exposure is large enough to explain the observed discrepancy between the physiological and anatomical place-frequency maps. The CF-shift in the mouse is about twice that reported in guinea pig and cat. Considering that the slope of the place-frequency map in mouse (1.25 mm/octave) is about half that in cat and guinea pig, the absolute shift in mm along the basilar membrane is similar in all three species.

Supported by the DFG, SFB 269, B1

## **909 A Frequency-Position Function for the Human Spiral Ganglion**

**Divya Sridhar**<sup>1</sup>, Olga Stakhovskaya<sup>2</sup>, Patricia A. Leake<sup>2</sup>  
<sup>1</sup>University of Miami, <sup>2</sup>University of California, San Francisco

Characteristic frequencies for cochlear implant (CI) electrode stimulation sites are currently estimated based on the Greenwood frequency-position equation for the organ of Corti (OC). However, contemporary perimodiolar CI designs target the spiral ganglion (SG), and there is evidence that represented frequency in the SG may be significantly offset from that on the OC.

The goal of this study was to derive a frequency-position function for the SG. Surface preparations of osmium-stained cadaveric cochleae (n=7) fixed <14 hours postmortem were examined; the OC and SG were measured, and radial fiber trajectories were traced to define a series of frequency-matched coordinates. Mean OC length was 32.71±2.38 mm; mean SG length was 13.96±0.82 mm; mean SG/OC ratio was 0.42±0.02. Frequency-matched points, expressed as percentage of total SG vs. OC length, demonstrated a consistent intersubject correlation that was best fit by a cubic function, which permits derivation of SG frequency by substitution into Greenwood's equation. Data also included the first estimates of SG critical band width and its variance as a function of position along the cochlea; unlike that of the OC, SG critical band width decreases from base to apex. Thus, if CI electrodes are spaced evenly, frequency resolution of stimulation decreases in lower frequencies.

The longitudinal position of CI electrodes in the cochlea can be correlated with pitch perception for each electrode

as well as with threshold, growth of loudness, and speech intelligibility. As subjects with greater residual hearing and better SG survival receive implants and advances in CI design permit more spatially precise stimulation, and accurate frequency map for the SG provides a basis for matching subjects' speech processor maps to the appropriate frequencies of CI stimulation sites, potentially increasing clinical benefits.

(Research supported by a Doris Duke Clinical Research Fellowship to D.S.

and NIDCD Contract #N01-DC-3-1006)

## **910 The Human Spiral Ganglion: Ultrastructure, Survival Rate and Implications for Cochlear Implants**

**Rudolf Glueckert**<sup>1</sup>, Kristian Pfaller<sup>2,3</sup>, Anders Kinnefors<sup>4</sup>, Helge Rask-Andersen<sup>4</sup>, Anneliese Schrott-Fischer<sup>5</sup>

<sup>1</sup>Medical University Innsbruck, Department of Otolaryngology, <sup>2</sup>Medical University Innsbruck, Department of Histology and Molecular Cell Biology, <sup>3</sup>Department of Histology and Molecular Cell Biology, Institute of Anato, <sup>4</sup>Department of Otolaryngology Uppsala University Hospital, Sweden, <sup>5</sup>Department of Otolaryngology Medical University of Innsbruck, Austria

Our knowledge about the ultrastructure of the human spiral ganglion is still limited. More information about its morphology, organization and spiral ganglion cell (SGC) survival in deaf people may give us a better understanding regarding mode and site of electrical stimulation of the neural elements in patients with cochlear implants and contribute to a model of electrostimulation that takes into account the characteristics of the human cochlea.

Scanning (SEM) and Transmission (TEM) Electron Microscopy of temporal bones from normal hearing and a long term deaf demonstrate the differences in organization of neuronal structures and gives indications about the SGC survival rate in humans.

Specimens were obtained at surgery for large life-threatening petro-clival meningioma. Excellently preserved human tissue could be obtained after decalcification and observation in a Field Emission Scanning Electron Microscope.

The delicateness of structures at the modiolar wall is shown in macerated and surgical specimen and represents possible sites for cochlear implant insertion traumata. Peculiarities of the human spiral ganglion like mostly absent myelinisation, close physical interaction and concentration of neurons in the apical region are shown the first time using SEM.

A thin fibrous network arranged-like layer covered with a thin mesothelial sheet is situated between the nerve fibre containing bony columns. Infrequently dispersed holes of varying diameter in that tissue enables direct fluid communication between the scala tympani and the modiolus. A cochlea from a man who was deaf for more than 50 years displays the retrograde degeneration pattern found in human. Loss of SGCs was highest in the base with significantly smaller neurons, peripheral processes degenerated and fibrosis in the scalae could be observed. Myelin distortions in the cochlear nerve points out impaired

function of SGCs. The benefit of perimodiolar and deep inserted electrodes is discussed.

The authors are supported by the European Community Project QLG3-CT-2002-01463 (BIOEAR), the Austrian Science Foundation FWF project P15948-B05 and the National Bank Foundation Österreichische Nationalbank 8745, the Swedish Scientific Council (VR proj no. 03908) Hörselskadades riksförbund (hrf) and Stiftelsen Tysta Skolan.

### **911 Three-Dimensional Cochlear Imaging and Informatics**

**Arne Voie<sup>1</sup>, Eugene Saxon<sup>1</sup>, Mailee Hess<sup>1</sup>**

<sup>1</sup>*Spencer Technologies*

This presentation describes the first-year results of a project to improve the imaging technique of Orthogonal-Plane Optical Sectioning (OPFOS) (Voie, Hear Res, 172: 120-129, 2002) and to generate high-resolution image stacks of the intact cochlea. The immediate goals of this project were to develop (1) automated image acquisition of optical sections, (2) efficient feature extraction algorithms, and (3) software for morphometric analysis and 3D visualization. Longer range goals are to introduce this cochlear imaging modality to the hearing research community, to provide a high-resolution 3D cochlear anatomical database for web-based access and analysis, and to develop advanced computational tools for the study of cochlear form and function. Hardware improvements to the OPFOS system include the use of a high-resolution digital camera and macro zoom lens, stepper motor motion control for translation and rotation stages, and removable specimen chambers that maintain their spatial register when interchanged. LabVIEW routines were written to control all motorized stages and perform image acquisition from a remote PC, eventually enabling the instrument to be operated from a remote site via the internet. In addition to megapixel imaging and high magnification, the OPFOS images were further enhanced using a higher quantum efficiency fluorescent dye and digital image manipulations to improve axial resolution beyond normal optical limits. A high resolution image stack of a guinea pig cochlea is presented to demonstrate the capabilities of the digital OPFOS system. The data volume was composed of 5 micron voxels and was re-sectioned in a spiral sequence in order to obtain true measurements of cross section areas of the scalae. Results of these measurements and 3D reconstruction of the cochlea are presented.

This work was supported by a grant from NIH/NIDCD: R43DC006310-01A1

### **912 Were Hearing Sensitivities of Freshwater Fishes Selected by the Ambient Noise in their Habitats?**

**Sonja Amoser<sup>1</sup>, Friedrich Ladich<sup>1</sup>**

<sup>1</sup>*University of Vienna, Institute of Zoology, 1090 Vienna, Austria*

Fishes have evolved an astonishing diversity in hearing abilities. Hearing generalists such as salmonids and

perches detect low frequency sounds (< 1 kHz) at relatively high sound intensities, whereas hearing specialists detect sounds over a broader frequency range (up to several kHz) at much lower sound intensities.

We hypothesize that the enhanced sensitivities of specialists, such as carps and catfishes evolved due to low ambient noise levels in certain freshwater habitats (stagnant and slowly flowing inland waters). At higher noise levels such as in running waters and in the sea, enhancing hearing sensitivity would be of no adaptive advantage due to masking effects of the habitat. To test this hypothesis, noise levels and spectra of four different freshwater habitats near Vienna were recorded and played back to native fish species while measuring their auditory thresholds using the AEP recording technique. Two of the four noise types represent quiet habitats (backwater of the Danube River and the Lake Neusiedl) and two rather noisy habitats (Triesting Stream and Danube River). We chose hearing specialists such as the common carp *Cyprinus carpio* and the gudgeon *Gobio gobio* (family Cyprinidae) and hearing generalists such as the European perch (*Perca fluviatilis*, Percidae). Preliminary data show that the carp's hearing is masked by the stream and river noise by up to 40 dB in its best hearing range (500-1000 Hz) but is not affected by the lowest natural noise level. In contrast, the perch's hearing thresholds were only slightly affected (approx. 10 dB) by the highest noise levels encountered in natural environments.

Our results indicate that hearing abilities of cyprinids are well adapted to the lowest noise levels encountered in freshwater habitats and that their hearing is masked in some parts of their distribution range. Hearing in perches, however, is only minimally masked because they evolved in noisy (marine) environments.

### **913 Patterns of Cochlear Pathology, Neural Activity in the Inferior Colliculus, and Psychophysical Evidence of Tinnitus in Chinchillas**

**Thomas Brozoski<sup>1,2</sup>, Carol Bauer<sup>1,2</sup>, Jeremy Turner<sup>1,3</sup>, Donald Caspary<sup>1,3</sup>**

<sup>1</sup>*Southern Illinois University School of Medicine*, <sup>2</sup>*Division of Otolaryngology*, <sup>3</sup>*Department of Pharmacology*

Tonndorf (1981) hypothesized that specific patterns of stereocilia damage in the cochlea led to aberrant neural activity perceived as tinnitus. Kaltenbach, et al. (2002) reported cochlear outer hair cell (OHC) damage produced by systemic cisplatin led to neuronal hyperactivity in the dorsal cochlear nucleus. The present experiment further examined the relationship between cochlear damage, neural activity, and tinnitus. Young adult chinchillas were trained and psychophysically tested for tinnitus using the method of Brozoski et al. (2002). After discrimination functions were determined for broadband noise (BBN), and 1, 2, 4, 6, 8, 12 kHz tones, performance-matched groups were exposed once unilaterally to the following: Acoustic trauma (n = 6, 4 kHz, 85 dB, 60 min), Cisp (n = 7, cisplatin, 1.32 µg, 15 min direct round window (RW) application), Carb (n = 7, carboplatin, 8 µg, 15 min direct RW application), and control (n = 5, no treatment).

Following exposure, the animals were evaluated for tinnitus. At the conclusion of the experiment, single neuron activity was recorded from tonotopic layers of the inferior colliculus (IC) using a linear electrode array, and cochleas were removed for quantitative morphometry. Distinct patterns of ipsilateral cochlear damage were obtained with each of the treatments; cochleas contralateral to the exposed ear (bilateral for controls) were unaffected. Despite the distinct patterns of cochlear pathology displayed by each experimental group, all experimental groups displayed psychophysical evidence of tonal tinnitus in the vicinity of 1 kHz: Their 1 kHz discrimination was significantly different than that of the controls ( $p = 0.044$ ), but not significantly different from one another ( $p = 0.688$ ). The results and their implication for understanding the pathophysiology of tinnitus was interpreted in the context IC neural activity.

### **914 Effects of Unilateral Removal of the Lateral Olivocochlear System in Mice**

**Keith Darrow**<sup>1,2</sup>, Stephane F. Maison<sup>1,2</sup>, M. Charles Liberman<sup>1,2</sup>

<sup>1</sup>*Eaton-Peabody Laboratory, Massachusetts Eye and Ear Infirmary*, <sup>2</sup>*Program in Speech and Hearing Bioscience and Technology, Harvard-MIT Division of HST*

The olivocochlear (OC) system in mammals has medial (MOC) and lateral (LOC) components. MOC cholinergic effects on OHCs have been well studied. The unmyelinated LOC system, which projects to the dendrites of auditory nerve fibers, is more poorly understood; however, LOC terminals contain several neurotransmitters and may exert both suppressive and excitatory effects.

In the present study, we probe LOC function in mice by selective unilateral removal of LOC innervation via stereotaxic injection of melittin, a neurotoxin, into the lateral superior olive (LSO), where LOC fibers originate. Cochlear effects are characterized by bilateral measurement of DPOAEs and ABRs. Lesion success is evaluated using brainstem sections stained for acetylcholinesterase and cochlear whole mounts immunostained for a cholinergic marker. MOC function is assessed by measuring cochlear suppression evoked by brainstem shocks to the OC bundle.

Results have been obtained from 19 mice with unilateral injection. In 8 "hit" cases, the LSO was partially destroyed; in 11 "miss" cases, the LSO remained intact. In all "miss" cases, ABR and DPOAE responses were similar on lesion vs. control side. In "hit" cases, DPOAEs were bilaterally symmetrical, however ABR response magnitudes were always asymmetrical. The degree, frequency region, and even the sign of the changes in neural response varied. This variation may correlate with the size or position of the LSO lesion. Four cases with selective loss of the medial limb showed a 30-50% increase in high frequency (>16kHz) ABR responses; two cases where both medial and lateral limb were hit, showed 25-50% decrease in response across all frequencies (5.6-45.25kHz).

The results suggest a complex interaction of excitatory and inhibitory effects of the LOC on auditory nerve activity, and the possibility that different LOC subgroups,

expressing different transmitters, are spatially segregated within the LSO.

Research supported by T32 DC00038, RO1 DC0188 and P30 DC05209.

### **915 Do All Normal-Hearing Humans Have a Medial-Olivocochlear Acoustic Reflex Response?**

**Bradford Backus**<sup>1</sup>, John Guinan<sup>2</sup>

<sup>1</sup>*Speech & Hearing Bioscience & Technology, Harvard-MIT Division of Health Science & Technology*, <sup>2</sup>*Mass. Eye & Ear Infirmary, Harvard Medical School*

Previous studies that measured the medial-olivocochlear reflex (MOCR) in humans did not focus on characterizing MOCR strength across the normal-hearing population. As a result, it is not known whether all normal-hearing people have an MOCR response and little is known about the range and variation of MOCR strengths. A grasp of both these issues would help to address questions regarding the role of the MOCR in hearing.

We measured MOCR strength in 21 normal-hearing adults using stimulus-frequency otoacoustic emissions (SFOAEs). We tested all normal-hearing subjects who were able to sit quietly enough to be measured, i.e. produce < -10 dB SPL noise floor (3 of 24 did not sit still enough). MOCR strength was quantified by calculating the percent change in total SFOAE amplitude (SFOAE amplitude was estimated using two-tone suppression) in response to 60 dB SPL contralateral broadband noise. Since SFOAE amplitude varies significantly across frequency in a given ear, MOCR strengths at two nearby frequencies (one at 1 kHz and one within 10% of 1 kHz) were averaged to produce the overall MOCR strength reported here.

We have been able to measure a statistically significant MOCR effect and quantify the MOCR strength in every case, indicating that all normal-hearing people have an MOCR response. Our measurements also show that MOCR strength varies appreciably across individuals (10%-56% of ISFOAEI in our 21 subjects, mean 30% +/- 13% sd).

Supported by NIDCD R01 DC005977, P30 DC005209

### **916 The Multi-Modal Middle Ear of the Cape Golden Mole (*Chrysochloris asiatica*)**

**Urban Willi**<sup>1</sup>, Gary Bronner<sup>2</sup>, Peter Narins<sup>1</sup>

<sup>1</sup>*UCLA*, <sup>2</sup>*University of Capetown*

The hypertrophied malleus in some genera of golden moles (*Chrysochloridae*) has been well-described, but never investigated experimentally in this family nor any other subterranean mammal. The enlarged malleus appears to represent an adaptation for detecting low-frequency (<300Hz) ground vibrations that propagate particularly well in the animal's natural habitat. When exposed to seismic disturbances, the inertia of the malleus head results in relative motion between the ossicular chain and the skull, resulting in an effective stimulus for the inner ear. In this study we focused on the functionality of the middle ear of *Chrysochloris asiatica*, the Cape golden

mole. The middle ear anatomy, the distribution of mass and its suspension in the middle ear cavity, suggest several distinct degrees of freedom. We used vertical and horizontal vibration (B&K, type 4809; 50Hz-1kHz) as well as airborne sound in closed field (periodic chirp; 0.5-10kHz) as stimuli and recorded the motion of the ossicular chain by means of Scanning Laser Doppler Vibrometry. The ossicular chain of *C. asiatica* responds to both vertical and horizontal vibrations, but also to airborne sound. Vertical and horizontal vibrations of the skull cause a pendulum-like motion of the ossicular chain in the corresponding direction due to the inertia of the malleus head (resonance  $\sim 125\text{Hz} \pm 40\text{Hz}$ ). In contrast, airborne sound causes the ossicular chain to rotate about an axis running through the short process of the incus and the center of mass of the malleus head (resonance  $\sim 115\text{Hz}$  and  $2\text{kHz}$ ). The three modes, initiated either by a vertical or horizontal vibration or airborne sound, can be described by three nearly orthogonal rotations. Thus, the middle ear of the Cape golden mole not only exhibits adaptations that favor airborne sound transmission to the inner ear, but also those that facilitate detection of low-frequency vibrations that propagate efficiently in soils. Supported by NIH grant DC-00222 to PMN.

### **917** Displacement and Deformation of the Middle Ear Ossicles under Static Pressure Load

**Steve A. Maas**<sup>1</sup>, Richard D. Rabbitt<sup>2</sup>, Jeffrey A. Weiss<sup>2</sup>, Willem F. Decraemer<sup>1</sup>, Joris J.J. Dirckx<sup>1</sup>

<sup>1</sup>Biomedical Physics, University of Antwerp, Antwerp, Belgium, <sup>2</sup>Dept. of Bioengineering, University of Utah, Salt Lake City, UT

Accurate measurement of middle-ear ossicle displacements at static ear canal pressures is challenging because of the difficult access to the middle ear and the smallness of the displacements, which are moreover three-dimensional (3D). We used a micro CT-scanner for the measurements and a relatively new computational method, termed hyperelastic warping (Rabbitt et al., 1995 SPIE 2573:252) to calculate the displacements, as well as the deformations, of the middle ear ossicles as a function of static pressure load. Sequences of micro CT-images were acquired from temporal bones of gerbils under static ear canal pressure loads ranging from -45 to +45 hPa. These image data were used to track the 3D motion and deformations of the ossicles using an image-deformation method termed hyperelastic warping. The great strength of this method is that the deformation follows the laws of continuum mechanics resulting in a physical admissible one-to-one mapping between template and target. For this, geometrically accurate finite element (FE) models were generated for each of the ossicles using template image data collected in the reference configuration (zero pressure case). The difference between template image data acquired in the reference configuration vs. the target image data acquired in the deformed configuration was used to drive the deformation of the FE model. The warping algorithm displaced and deformed the FE models of the ossicles in order to align the deformed template with

the target data. Results show a nonlinear pressure-displacement relationship.

Supported in part by NIDCD R55 DC05585 and NSF #BES-0134503. Additional funding provided by Prof. Dr. Dirk Van Dyck (VisionLab, UA). We acknowledge Stefan L.R. Gea for recording the CT-images.

### **918** The Effects of Complex Stapes Motion on the Response of the Cochlea in Guinea Pigs

**Damien Sequeira**<sup>1</sup>, Christian Breuninger<sup>2</sup>, Albrecht Eiber<sup>2</sup>, Alexander Huber<sup>1</sup>

<sup>1</sup>Department of Otorhinolaryngology, Head and Neck Surgery, University Hospital of Zurich, Switzerland,

<sup>2</sup>Institute B of Mechanics, University of Stuttgart, Germany

Recent studies into the vibration modes of the stapes in response to acoustic stimulation of the normal ear have revealed a complex movement pattern of its footplate. These complex vibrations can be expressed as one translational displacement and two rotational movements around the long and short axes of the stapes. At low frequencies the vibrations are predominantly piston-like (translational), but they become increasing rocking-like (rotational) at middle and high frequencies. Contrary to what occurs in the case of the translational component, the rotational components produce no net volume displacement of cochlear fluid at some distance from the footplate. Therefore, according to the classical theory, it is hypothesized that the rotational motion of the stapes is considered to be lost energy that is not transformed into a hearing sensation. It is the goal of an ongoing study to test this hypothesis. In a previous experiment, desired movement patterns of the stapes superstructure were elicited by varying the input parameters of a custom-built, three-axis piezoelectric actuator, which was monitored using a three-dimensional laser Doppler interferometer. Hence, having proven the feasibility of this test stand in vitro, it is presently the objective to test this specific measuring setup in vivo on anesthetized guinea pigs. This experimental phase combines the electrophysiological measurements of the cochlear potentials and this mechanical measurement setup. Both the cochlear microphonic and compound action potential are recorded with regards to piston-like, rocking-like and arbitrary movement patterns of the stapes superstructure. The results of these experiments will be presented at the meeting.

### **919** Boost of Transmission at the Incudo-Stapedial Joint of Chinchilla Middle Ear

Luis Robles<sup>1</sup>, Andrei Temchin<sup>2</sup>, Yun-Hui Fan<sup>2</sup>, Mario Ruggero<sup>2</sup>

<sup>1</sup>Universidad de Chile, <sup>2</sup>Northwestern University

As a follow-up of a review that disputed commonly held views of middle-ear vibration (Ruggero and Temchin, PNAS 99: 13206-13210, 2002), we are re-examining ossicular vibrations in the chinchilla middle ear, using better stimulus and recording methodologies than previously available (Ruggero et al., 1990, JASA 87: 1612-

1629). The initial results showed that the magnitudes of stapes vibration velocity have "a relatively flat frequency spectrum ... up to at least ... the high-frequency cut-off of hearing" (Temchin et al., ARO MWM Abstracts 25: 154, 2002). Here we extend those findings. The vibratory responses to tones of the stapes and the incus were measured near the incudo-stapedial joint using a laser velocimeter and a wide-band acoustic-stimulus system. The velocity magnitude of stapes vibrations was relatively constant (~0.1 mm/s/Pa) up to 32 kHz and decreased at a rate of ~20dB/oct at higher frequencies. Phase lag relative to pressure in the external ear canal increased approximately linearly, with a slope equivalent to a pure delay of 76  $\mu$ s. These results show that, consistent with the PNAS review (Ruggero and Temchin, op. cit.), the chinchilla middle ear behaves as a wide-band pressure transformer which transmits acoustic signals into the cochlea even at frequencies far exceeding the cut-off of hearing. Both the large bandwidth and the delay of the middle-ear responses appear to originate principally at the tympanic membrane, since they are present in incus vibrations. These features, however, are refined by a wide peak in the magnitude of the stapes-re-incus transfer function accompanied by a large phase lag. The magnitude peak boosts stapes vibrations by about 16 dB at 25 kHz, further flattening the magnitude middle-ear transfer function. The phase lag extends the range of constant delay to about 20 kHz. Both the peak and phase lag are considerably reduced after experimentally stiffening the incudo-stapedial joint.

## **920 Interspecies Variation in Cat Family: Ear Acoustics & Evoked Potentials**

**Howard Chan**<sup>1,2</sup>, William Peake<sup>1,2</sup>, John Rosowski<sup>2,3</sup>, Edward Walsh<sup>4</sup>, JoAnn McGee<sup>4</sup>

<sup>1</sup>M.I.T., <sup>2</sup>Mass Eye & Ear Infirmary, <sup>3</sup>Dept. Otolaryngology and Laryngology, Harvard Medical School, <sup>4</sup>Boys Town National Research Hospital

With the goal of relating interspecies variations to ethology and habitat we have focused on the 36 species of the cat family (Felidae). With data from 34 species we have shown that ear dimensions generally increase with skull size (Peake and Rosowski, 1997, "Diversity in Auditory Mechanics", E.R. Lewis et al., Eds. World Scientific, pp.3-10.) and (with measurements in 11 species) that acoustic input-admittance magnitude is also positively correlated with size (Huang et al., 2000, J. Comp. Physiol. A 186: 447-465). For the one felid species that lives exclusively in deserts (the sand cat, *Felis margarita*) measurements show that ear-canal and bullar dimensions are unusually large for the size of the skull and that the acoustics of the external and middle ear make the ear more effective in absorbing acoustic power than the ears of domestic cats (which are about the same size) (Huang et al., 2002, J. Comp. Physiol. A. 188: 663-681). We have suggested that this interspecies difference might represent an adaptive change to the desert habitat that provides more sensitive low-frequency hearing and longer "ear shot" to detect sounds over large distances in the open desert space. To test this hypothesis we have now made measurements in anesthetized animals of acoustic input-admittance of ears

along with hearing thresholds based on auditory brainstem responses (ABR). This combination of measurements has been made in specimens of four species. We have focused attention on the sand cat because of its demonstrated specializations in ear structure and acoustic function. We have been successful in measurements in 24 ears of sand cats, and from 4-6 ears in 3 other exotic species (Pallas' cat, serval, bobcat). ABR derived threshold vs frequency curves will be compared to admittance measurements to test the hypothesis that hearing sensitivity is influenced by the acoustic admittance at the tympanic membrane. (Supported by NIH. Carried out with the cooperation of The Living Desert, Palm Desert, CA and the School of Veterinary Medicine, North Carolina State U., Raleigh, NC).

## **921 Manubrium and Eardrum Vibrations in the Rat**

Fadi Akache<sup>1</sup>, Sam J. Daniel<sup>2</sup>, **W. Robert J. Funnell**<sup>3</sup>

<sup>1</sup>BioMedical Engineering, McGill University,

<sup>2</sup>Otolaryngology, McGill University, <sup>3</sup>BioMedical Engineering & Otolaryngology, McGill University

The rat is an attractive species for hearing research. It is relatively inexpensive and the middle-ear structures are easily approachable. With the recent addition of rats to the list of species whose genomes have been mapped, the rat could become even more valuable for hearing research. Few measurements of middle-ear mechanics have been made in the rat, however, and then only at the umbo. The goal of the present study is to begin to characterise the mechanical behaviour of the rat manubrium and eardrum. Vibration measurements were made using a Polytec laser Doppler vibrometer. The stimuli were sinusoidal sweeps to 10 kHz, with a closed sound system. Small (90 - 150  $\mu$ m diameter) glass beads were used as targets for the laser. Displacements were measured at multiple points on the manubrium and on the eardrum, and repeated measurements were made at each point. Measurements were generally fairly repeatable over a period of an hour or so, but there was considerable variability from animal to animal. Manubrial displacements generally showed a maximum in the range of 2.5 to 4 kHz, and a second maximum in the range of 7.5 to 9.5 kHz. The shape of the frequency response was usually similar at the three points on the manubrium. Displacements on the eardrum were larger than on the manubrium; in some animals the shape of the frequency response on the eardrum was similar to that on the manubrium, but in some animals the shapes were quite different. A 3-D model of the rat middle ear is being developed based on x-ray microscopic computed tomography using a SkyScan 1072 scanner, with the goal of developing a finite-element model for comparison with the experimental measurements.

## **922 Middle and Inner Ear Stiffness Measurements in the Bottlenose Dolphin, *Tursiops truncatus***

Brian Miller<sup>1</sup>, David Mountain<sup>1</sup>, Aleks Zosuls<sup>1</sup>, Seth Newburg<sup>1</sup>, Darlene Ketten<sup>2</sup>

<sup>1</sup>Boston University, <sup>2</sup>Woods Hole Oceanographic Institution

The frequency range of hearing varies greatly across different mammalian species. These differences between species are believed to be due to differences in the middle-ear transfer function and to differences in the cochlear mechanics. Both the cochlear frequency-place map and the middle-ear transfer function depend on the stiffness-place map of the basilar membrane. The middle-ear transfer function is also strongly influenced by the middle-ear stiffness. The purpose of this study was to measure these parameters for the bottlenose dolphin (*Tursiops truncatus*), a species specialized for very high-frequency hearing and echolocation.

Middle-ear stiffness was measured using a force probe that applied a known displacement to the stapes footplate from within the cochlea and measured the restoring force. The basilar membrane point stiffness was measured using a similar but more sensitive force probe. It was found that the bottlenose dolphin middle ear has a stiffness of  $1e17 \text{ Pa/m}^3$ , and the point stiffness of the basilar membrane has a gradient from 20 N/m near the base to 1.5 N/m near the apex.

These stiffness measurements will be used to develop a model of cochlear and middle-ear mechanics in order to predict the *Tursiops* audiogram. Once the model is validated it will be extended to predict the audiograms of other cetacean species for which it is not feasible to measure the audiograms behaviorally.

Funded by ONR

## **923 Somatosensory and Bone Conduction Pathways in Elephant Signal Detection: Implications for Reception of Acoustic and Seismic Signals**

Caitlin O'Connell-Rodwell<sup>1</sup>, Thomas Hildebrandt<sup>2</sup>, Sarah Partan<sup>3</sup>, Jason Wood<sup>1</sup>, Timothy Rodwell<sup>1</sup>, Rhonda Keefe<sup>3</sup>, Darlene Ketten<sup>4</sup>, Christina Alarcon<sup>1</sup>, Donna Bouley<sup>1</sup>, Byron Arnason<sup>5</sup>, Lynette Hart<sup>6</sup>, Sunil Puria<sup>1</sup>

<sup>1</sup>Stanford University, <sup>2</sup>IZW, Berlin, <sup>3</sup>University of South Florida, <sup>4</sup>Woods Hole Oceanographic Institution, <sup>5</sup>Tezar, Inc., <sup>6</sup>University of California, Davis

Elephants produce, detect and respond to vocalizations in the range of 20 to 200 Hz, having primitive derived ears, specialized for low-frequency audition. During these vocalizations, a seismic replicate is propagated in the ground. It has been suggested that the elephant ear may be capable of detecting these seismic signals via bone conduction or via vibrational mechanoreceptors in the feet, similar to those in the elephant's trunk. Here we describe both pathways, including an anatomical adaptation of a muscle surrounding the external meatus of the ear of both the African and Asian elephant and suggest a possible function for these adaptations related to signal detection.

The muscles surrounding the meatus contract upon tactile stimulation, occluding the opening. We suggest that this sphincter-like adaptation may function to dampen air-borne vibrations, possibly allowing the elephant to focus on seismic signals with reduced background noise from air-borne signals. Behavioral data suggest that a somatosensory pathway may facilitate seismic detection but that the orientation of elephants during playback experiments suggest that bone conduction may play a role in localization. Because the muscles of the two ears may contract independently, the adaptation may further assist in the localization of low frequency sounds and seismic signals.

## **924 Evaluation of a New Diagnostic Apparatus for Ossicular Fixation using Human Temporal Bones: Comparison with Vibration Measurements by a Laser-Doppler Velocimeter**

Takuji Koike<sup>1</sup>, Shinji Hamanishi<sup>2</sup>, Toshimitsu Kobayashi<sup>3</sup>, Hideko Nakajima<sup>4</sup>, Michael Ravicz<sup>4</sup>, Saumil Merchant<sup>4</sup>, John Rosowski<sup>4</sup>, Hiroshi Wada<sup>2</sup>

<sup>1</sup>The University of Electro-Communications, <sup>2</sup>Tohoku University, <sup>3</sup>Tohoku University Graduate School of Medicine, <sup>4</sup>Harvard Medical School, and Eaton-Peabody Laboratory

The evaluation of ossicular mobility is an important parameter in decisions regarding surgical repairs of diseased ears as well as for the post-surgical improvement in hearing level. To evaluate ossicular mobility in surgery, direct measurement of mobility has been investigated using a laser Doppler velocimeter (Huber et al. 2001) and by using a piezoelectric ceramic device that directly vibrates the stapes (Gyo et al., 2000). A hand-guided device for measuring stapes mobility (Hofmann et al., 1999; Zahnert et al., 2001) has also been developed. This device measures stapes impedance at high frequency, i.e., 2.4 kHz, where, stapes impedance includes the impedances of the stapes, annular ligament, and the cochlea. In the case of ossicular fixation, measuring the stiffness component of the impedance of the ligaments and tendons, which is greater than that in the normal ear, is important. However, the impedance measured at a high frequency of more than 1 kHz contains not only the stiffness component, but also the mass and damping components of the ossicles and the cochlea. A low frequency or static measurement is therefore advantageous for detecting a slight change in the stiffness component due to fixation of the ossicles.

We have developed an apparatus that quasi-statically measures the load and displacement of the ossicles, where the stiffness defined by the slope of the load-displacement curve has been used as an index of ossicular mobility. In a pilot study, this apparatus was used to measure the ossicular stiffness in human temporal bones at the stapes and the malleus body before and after the ossicles were artificially fixed. These results were compared with simultaneous estimates of ossicular mobility obtained with a laser Doppler velocimeter (LDV). Although the data set is small, an inverse correlation was

seen between the ossicular stiffness measured with our apparatus and the vibration amplitude of the ossicles. This result suggests that our apparatus has the ability to detect the difference in stiffness between fixed and normal ears, and gives support to the idea that our device could be a useful tool in the surgical estimate of ossicular disorders.

### **925 Soft Tissue Morphometry of the Malleus-Incus Complex**

**Jae Hoon Sim<sup>1</sup>**, Vicki Li Lung<sup>1</sup>, Sunil Puria<sup>1,2</sup>

<sup>1</sup>Stanford University, Mechanical Engineering - Mechanics and Computation Division, <sup>2</sup>Otolaryngology-Head and Neck Surgery, 300 Pasteur Drive, Stanford, CA 94305

In developing an accurate and comprehensive biomechanical model of the human middle ear, anatomical measurements are both necessary and important. Traditional histological methods for soft tissue morphometry of human cadaver temporal bone middle ears are destructive and can take several months before results are obtained. Physiological measurements of the middle ear are often made with different ossicular manipulations and these include ossicular disarticulation and removal of the eardrum. MicroCT imaging is a modality that provides non-destructive imaging at each stage of manipulation with as little as 10  $\mu$ m resolution. We show that microCT imaging, so far used for high-density tissue such as the ossicles and surrounding bone, can also be used to image such soft tissues of the middle ears as the tympanic membrane, the incudo-malleol joint (IMJ), and suspensory ligaments and tendon. These images are used for geometric characterization of soft tissues with 3D volume reconstruction. Results from two cadaver temporal bone ears indicate that the IMJ has a shape that is best described by two orthogonal saddles as first described by Helmholtz. The thickness of the joint varies from 0.07 to 0.275 mm with the maximum appearing in the anterior-posterior region. The tensor tympani tendon can be described by a 1.55 mm long tapered cylinder whose diameter varies from 0.4 to 1.0 mm, while the superior ligament attached to the malleus has a shape of a cylindrical bar of 0.26 mm diameter and 1.1 mm length. The tensor tympani tendon is tilted by about 30 degrees from the medial-lateral axis, and the superior ligament is tilted by about 73 degrees from superior-inferior axis of our experimental frame. The anterior and lateral ligaments of the malleus and the two posterior ligaments of the incus are best described by polyhedrons with the largest dimension being 0.97, 0.51, 0.67 and 0.57 mm, respectively. [Work supported in part by grant No. DC005960 from the NIDCD of NIH.]

### **926 The Effect of Methodological Differences in the Measurement of Stapes Motion of Live and Cadaver Ears**

**Wade Chien<sup>1,2</sup>**, Mike Ravicz<sup>1</sup>, Saumil Merchant<sup>1,2</sup>, John Rosowski<sup>1,2</sup>

<sup>1</sup>Eaton-Peabody Lab, Massachusetts Eye & Ear Infirmary, Boston MA, <sup>2</sup>Department of Otolaryngology and Laryngology, Harvard Medical School, Boston, MA

Fresh cadaveric temporal bones have been used extensively as a model for studying middle-ear mechanics. To support this use, measures of middle-ear input, e.g., umbo velocity and middle-ear input immittance, have been found by several groups to be similar between live and cadaveric ears [Rosowski et al., ARO 2004]. In the single extant study of middle-ear output in live human patients [Huber et al., 2001], stapes velocity magnitude was similar at high frequencies to that measured in cadaveric ears by several groups but was significantly lower at low frequencies. Possible sources of this difference include post-mortem changes in middle-ear properties and methodological differences between studies. In this study we explore the effect of differences in measurement technique on stapes velocity in temporal bones.

Stapes velocity was measured in fresh cadaveric temporal bones with a laser-Doppler vibrometer by two methods: (1) through a small opening in the facial recess, as in live ears during surgery; and (2) through an enlarged facial recess with the stapedius tendon cut, as in previous studies of stapes velocity in cadaveric bones. Enlargement of the facial recess allowed the measurement angle between the laser and the stapes footplate to be varied between 20-30 degrees (as in the surgical approach) to 70-80 degrees (as in previous cadaveric studies). Cutting the stapedius tendon, enlarging the facial recess, and increasing the laser measurement angle all produced small but significant increases in the measured stapes velocity at low frequencies. The combination of these effects can explain most, if not all, of the differences in stapes velocity measurements between temporal bones and live ears.

Funded by NIDCD.

### **927 Alignment of Manubrium Mallei: Relation to Arcus Zygomaticus, Frankfort Plane, Visual Plane, and Mastoid Pneumatization**

**N Todd<sup>1</sup>**

<sup>1</sup>Emory

Background: There is no consensus why the manubrium of the malleus, as viewed clinically through the external ear canal, generally points downward and posterior.

Objectives: To depict the alignment of the handle of the malleus, viewed clinically through the external auditory canal, relative to the zygomatic arch, the Frankfort plane and a visual plane proxy, and relative to the horizontal semicircular canal. Also, to assess bilateral symmetry, and manubrium alignment relative to mastoid pneumatization.

Study Design: Post-mortem anatomic dissection of 41 bequeathed adult crania without clinical otitis.



Methods: The line of the manubrium as viewed through the external ear canal was measured relative to the Frankfort plane, to a proxy of the visual plane, and to the zygomatic arch. Mastoid sizes were determined radiographically. In a subset of ten crania additionally studied by computed tomography, the manubrium position was checked relative to the horizontal semicircular canal.

Results: Relative to the zygomatic arch and Frankfort and visual planes, the range of manubrium angles was at least 45 degrees. Bilateral symmetry was found, each  $r > .42$  (95% confidence interval .13 to .65). Relative to the horizontal canals, the range of manubria angles was 30 degrees, with symmetry suggested. Alignment did not correlate with mastoid pneumatization.

Conclusions: Manubrium orientation as viewed through the external auditory canal is not obviously explicable. Though bilaterally symmetrical, manubrium orientation is unrelated to mastoid pneumatization.

### **928 Middle-Ear-Cavity and Ear Canal Pressure Driven Stapes Velocity Responses in Human Cadaveric Temporal Bones**

**Kevin O'Connor<sup>1,2</sup>, Sunil Puria<sup>1,2</sup>**

<sup>1</sup>*Stanford University, Department of Otolaryngology-Head and Neck Surgery, 300 Pasteur Drive, Stanford,*

<sup>2</sup>*Department of Mechanical Engineering, Mechanics and Computation Division, Durand Building, Stanford*

In 1970, Richard L. Goode proposed that a likely site for an implantable hearing aid is inside the middle ear cavity (MEC), as opposed to in the ear canal (EC) as in conventional hearing aids (Am. Acad. Ophth. Otol.). To test the efficacy of such a drive mechanism, measurements of drive pressure ( $P_d$ ) and stapes velocity ( $V_{st}$ ) were performed on cadaveric temporal bones with a sound source placed in the EC as well as in the closed MEC. For both drive conditions, transfer function (TF) measurements of  $P_d$  to  $V_{st}$  were performed both with an intact and cut ossicular chain (OC) in order to compare the proportions of sound transmission due to the OC versus due to pressure within the MEC airspace ( $P_{mec}$ ), between 100 Hz to 20 kHz. With an intact OC, the TF magnitudes and angles are very similar for the EC drive and MEC drive (open EC) cases below 5.5 kHz. Cutting the OC in the EC drive case causes a reduction of up to 46 dB in sound transmission below 10 kHz, implying that the OC rather than  $P_{mec}$  is responsible for most of  $V_{st}$  for EC drive below 10 kHz. Cutting the OC in the MEC drive case, however, shows that the TF is very similar to the intact case above 7 kHz, implying that for MEC drive,  $P_{mec}$  rather than the OC is primarily responsible for  $|V_{st}|$  above 7 kHz. A dip of around 24 dB in the MEC drive TF magnitudes that occurs between 8 and 12 kHz is therefore also likely to be caused by  $P_{mec}$ , as opposed to the OC. The presently measured EC drive TF magnitudes are very similar to a past measurement (Aibara et al., 2001 Hear. Res.) below 0.8 kHz, but with a shallower slope (-2.3 dB/oct vs. -6.7 dB/oct.) above 1.5 kHz, a difference we attribute to our use of the natural EC and tympanic membrane (TM) angle instead of a perpendicular EC and TM angle due to the artificial EC as is commonly used in cadaver temporal

bone measurements. [Work supported in part by the Dept. of Otolaryngology, a gift from Implanted Acoustics, Inc., and grant No. DC005960 from the NIDCD of NIH.]

### **929 Development of Middle-Ear Admittance in Humans**

**Beth Prieve<sup>1</sup>, Shamsuddin Chasmawala<sup>1</sup>, Michael Jackson<sup>1</sup>**

<sup>1</sup>*Syracuse University*

Description of the development of human middle-ear characteristics in humans is critical for understanding the development of central auditory processing. Many studies in human neonates and adults exist, but few data on developing infants and toddlers are available. Middle-ear analysis was done as part of a larger study of longitudinal changes of otoacoustic emissions in infants and toddlers. Twenty-two infants were studied regularly from four weeks to two years of age, when possible. Twenty-two adult subjects were tested using the same schedule as a control group. Tympanometry was performed using probe frequencies of 226, 400, 630, and 1000 Hz. Middle-ear admittance and phase were calculated from tympanograms with ear-canal phase higher than 65 degrees and were analyzed according to the Vanhuyse model. To maximize data for statistical power, tympanograms for 5 age groupings were studied: 8-15, 16-31, 32-59, 60-95 and 96-153 weeks. Repeated-measures ANOVAs using infant and adult ear-canal phase angle, middle-ear admittance and middle-ear phase were run at each frequency. For most measures at each frequency, age-by-group interactions were found, indicating changes with development and differences between infants and adults. Infant ear-canal phase angle was significantly lower than adult phase angle, suggesting that infant ears may not follow some assumptions underlying tympanometry. Although middle-ear admittance increased with age, it was lower for infants than for adults at all frequencies. Middle-ear phase angles in all ages were higher than those in adults for all frequencies. Mean data for all age groups except the youngest were well-fit by a simple RLC model. Compliance of the middle ear and corner frequency of the low-frequency roll-off calculated from the model indicated that compliance increased with age and corner frequency decreased with age. Results suggest that developmental changes in the human middle ear can be modeled using a simple RLC model that has been used by other researchers to describe the low-frequency filter function of the adult middle ear.

Research supported by NIDCD R29 02028

### **930 Wideband Measurements of the Acoustic Stapedius Reflex in Human Infants**

**Patrick Feeney<sup>1</sup>, Chris Sanford<sup>1</sup>, Jessica Day<sup>1</sup>, Bethany Kershner<sup>1</sup>**

<sup>1</sup>*University of Washington*

Wideband changes in energy reflectance induced by the contralateral acoustic stapedius reflex were examined in 5 six-week-old infants and in 1 young adult using wideband shifts in admittance and energy reflectance (YR). The probe signal consisted of 40-ms electrical chirps with a

bandwidth from 0.2 to 10 kHz. The overall level of the chirps was set at 65 dB SPL for adult testing and 55 dB SPL for infant testing as calibrated in a Zwislocki occluded ear simulator. The reflex activator presented to the contralateral ear was a band-pass noise from 0.25 to 11 kHz presented at a maximum overall level of 90 dB SPL measured in the ear canal. An experimental run consisted of the presentation of five baseline-activator pairs by varying the activator level from 90 to 70 dB SPL in 5 dB steps. Two such runs were completed for adults and infants unless the subject's state precluded additional measurements. Reflex-induced YR shifts were then obtained by subtracting measurements obtained during a quiet baseline from those obtained in the presence of a contralateral activator noise. Reflexes were detected by calculating a cross-correlation between one-twelfth-octave measurements of YR for the highest activator level and responses to lower levels. The reflex-induced shifts in YR for the infant ears were similar in pattern to adult responses, but were shifted higher in frequency by around .5 kHz. Infant reflexes were more successfully detected when the cross-correlation was calculated from 1 to 8 kHz, whereas adult reflexes were more successfully detected for a cross-correlation from .25 to 2 kHz. This wideband acoustic reflex method may be useful in capturing the most robust frequency region for acoustic reflex detection across postnatal middle-ear development. Work supported by a grant from the Royalty Research Fund, University of Washington.

### **931 Tympanic Membrane and Middle Ear System Vibration Modes Predicted by 3-Dimensional Finite Element Model**

Rong Gan<sup>1</sup>, Ben Feng<sup>1</sup>, Tao Cheng<sup>1</sup>

<sup>1</sup>University of Oklahoma

A 3-dimensional finite element (FE) model of the human ear which included the external ear canal, tympanic membrane, ossicular bones, middle ear suspensory ligaments/muscles, and middle ear cavity was created based on a complete set of histological section images of a left ear temporal bone (Gan et al, Ann Biomed. Eng., 32 (6): 847-859, 2004). This model was validated by comparing model-predicted displacements at the stapes footplate and tympanic membrane (TM) with published experimental measurements on human temporal bones, particularly, with the data measured simultaneously on the footplate and TM using double laser interferometers (Gan et al., Otol. & Neuro., 25: 423-435, 2004). Obviously, the work published was focused on middle ear transfer function for sound transmission from the ear canal to the stapes through ossicular chain. In this paper, we report the studies on TM and middle ear system vibration modes in response to sound stimulation in the ear canal. The acoustic-structural coupled "two-chamber", that is, "ear canal-TM & ossicles-middle ear cavity", FE analysis was conducted on the model. The results included: 1) the effect of sound source location in ear canal on pressure distributions in the canal and middle ear cavity; and 2) changes of the TM modal shape in response to mechanical properties of the TM. Finally, the model-predicted results were compared with experimental data

measured in human temporal bones. The results reported here further demonstrated the applications of our 3-D FE model in study of acoustic-mechanical transmission from the ear canal to middle ear. (Supported by Oklahoma Center for the Advancement of Science & Technology)

### **932 Development of the Human Tympanum and Mastoid as Assessed by Distribution of Osteoblasts and Osteoclasts**

Naofumi Kuwahata<sup>1</sup>, Koichi Omori<sup>1</sup>, Chiaki Suzuki<sup>2</sup>, Iwao Ohtani<sup>3</sup>, Teruhisa Suzuki<sup>1</sup>

<sup>1</sup>Fukushima Medical University, <sup>2</sup>Fujita General Hospital,

<sup>3</sup>Fukushima Rosai Hospital

(Objective) Development of the human tympanum and mastoid process displays different stages, and individual differences exist. Previous research has attempted to ascertain development of the human temporal bone and direction of development of the human tympanum and mastoid. However, no detailed histopathological studies have examined distribution of osteoblasts and osteoclasts in temporal bone. To ascertain the normal developmental processes of the tympanum and mastoid, the present study observed the distribution of osteoblasts and osteoclasts at different times and locations.

(Subjects) Of human temporal bone stored in the Department of Otolaryngology at Fukushima Medical University, 63 samples from subjects ranging from week 30 of gestation to 29-years-old were used.

(Methods) Samples were divided into three groups: fetal group (before birth); child group (<15-years-old); and adult group (≥15-years-old). Distribution of osteoblasts and osteoclasts was assessed on two sides of the temporal bone: the middle ear cavity side; and the bone marrow side.

(Results) (1) Compared to the adult group, numbers of osteoblasts and osteoclasts were significantly higher in fetal and child groups. (2) Numbers of osteoblasts and osteoclasts were significantly higher in the mastoid than in other areas. Number of osteoclasts was higher on the middle ear cavity side, while number of osteoblasts was higher on the bone marrow side.

(Conclusions) Almost no osteoblasts or osteoclasts were seen in adult bone, suggesting that the tympanum and mastoid are morphologically mature after 15-years-old. The results suggest that bone formation and resorption are particularly active in the mastoid, and that the middle ear cavity expands by a combination of repeated bone resorption on the middle ear cavity side and bone formation on the marrow side.

### **933** Quinine-Induced Changes in C-Fos and Arc Gene Expression in Rat Cochlear Nucleus

Guang Yang<sup>1</sup>, Wei Sun<sup>1</sup>, Ming Li<sup>2</sup>, Ping Wang<sup>1</sup>, Dalian Ding<sup>1</sup>, Ed Lobarinas<sup>1</sup>, Richard Salvi<sup>1</sup>

<sup>1</sup>Center for Hearing and Deafness, University at Buffalo,

<sup>2</sup>Department of Otolaryngology, YueYang Hospital, ShangHai University of Chinese Traditional Medicine

Subjective tinnitus is a phantom auditory sensation that can be induced in humans by high doses of quinine. Quinine-induced tinnitus has also been measured in rats using behavioral techniques; however, the neural mechanisms that give rise to quinine-induced tinnitus are poorly understood. Recent studies (Chen et al., ARO, 2004) indicate that high doses of quinine, as well as salicylate, increases the mean spontaneous firing rate of bursting neurons in brain slices from the dorsal cochlear nucleus (DCN). To gain insight into the biological mechanisms that might alter spontaneous activity patterns in the cochlear nucleus, we looked for changes in expression of several genes implicated in synaptic plasticity. The immediate early gene c-fos has frequently been used as a marker of neuronal activation because of its low expression under normal conditions and its rapid increase following stimulation. Arc, also referred to activity-regulated cytoskeleton-associated protein or Arg3.1, is induced via NMDA-receptor dependent mechanisms and plays an important role in memory related processes. Since both genes have been implicated in synaptic plasticity and tinnitus, we used quantitative RT-PCR to assess changes in their expression in the cochlear nucleus of rats treated with quinine (150 mg/kg). Treatment with 150 mg/kg of quinine had little effect on Arc and c-fos expression 1 h following treatment; however, significant increases in Arc and c-fos expression were observed at 3 h post-injection. Expression of Arc and c-fos declined toward control (saline) levels by 8 h. Changes in c-fos and Arc expression are also being examined in other brain regions and will be related to behavioral measures of quinine-induced tinnitus. These results suggest that activity and synaptic plasticity related genes such as c-fos and Arc may play a role in tinnitus induced by quinine.

Research supported by grants from the American Tinnitus Association and NIH R01 DC06630-01

### **934** A Computational Model of the Development of Tinnitus-Related Hyperactivity in the Early Auditory Pathway

Roland Schaeffe<sup>1</sup>, Richard Kempter<sup>1</sup>

<sup>1</sup>Institute for Theoretical Biology, Humboldt University Berlin

Tinnitus is the perception of a sound in the absence of acoustic stimulation. In many cases, tinnitus is associated with hearing loss in the high-frequency range. The pitch of the tinnitus sensation is correlated to the extent and range of the hearing impairment (Henry et al., ITS Proceedings 1999). The question of how hearing loss leads to the development of tinnitus, however, still remains unanswered.

In animals, hearing loss induced by acoustic trauma leads to signs of tinnitus (Heffner et al., Hear. Res. 2002). A manifestation of tinnitus-related changes in the auditory pathway is found in the dorsal part of the cochlear nucleus, which is the first neuronal processing stage in the auditory pathway. In the dorsal cochlear nucleus (DCN) of animals with behavioral evidence of tinnitus, the spontaneous neuronal activity is significantly increased (Kaltenbach et al., Neurosci. Lett. 2004). These experimental results present a paradox situation: hearing loss leads to an overall decrease of auditory nerve activity, but there is increased spontaneous activity, or 'hyperactivity' in the DCN.

We address the question of tinnitus development from a theoretical perspective, following the hypothesis that the auditory pathway can be modified by sensory experience. Plasticity mechanisms like activity-dependent changes in synaptic weight or neuronal excitability are to ensure proper information processing. Hearing loss, however, causes drastic changes in the input received by the auditory system, and this imbalance might lead to the development of pathological hyperactivity in the brain stem.

In order to explore this hypothesis, we set up a computational model of the auditory nerve (AN) and the DCN. The model captures how the population firing rate of AN fibers depends on the intensity of acoustic stimuli and the integrity of inner and outer hair cells of the cochlea. Changes in the activity of the auditory nerve are assumed to drive a homeostatic compensation mechanism in output neurons of the DCN. Therefore, synapses from the AN to DCN neurons obey rules of homeostatic plasticity to maintain a pre-set target value of mean activity of the postsynaptic neuron. After hearing loss, our model develops hyperactivity in those parts of the DCN that are innervated by the damaged parts of the cochlea. The amount of hyperactivity depends on the amount of cochlear hair cell damage. The observed hyperactivity patterns are similar to those seen in animals.

Supported by the DFG, Ke 788/1-2,3

### **935** Identification of Hyperactive Cells in the DCN of a Noise-induced Tinnitus Model, using Spike Classification and Juxtacellular Labeling

Paul Finlayson<sup>1</sup>, James Kaltenbach<sup>1</sup>

<sup>1</sup>Wayne State University

Prior exposure to intense sound leads to chronic spontaneous hyperactivity of DCN neurons. Thus far, little is known about the changes underlying this hyperactivity at the cellular level. In the present study, we examined the characteristics of spontaneously active (SA) cells in the DCN of the hamster. Normal animals had no prior manipulation (n=15). Control (n=5) and exposed (n=5) animals were anesthetized for 4 hours, and either exposed to quiet or 127 dB SPL, 10 kHz continuous tone using a headphone coupled to the left ear, respectively.

Spontaneous activity of single units (SU, n=130) with CFs between 8 and 15 kHz were recorded 28 days later in the ipsilateral DCN, using glass micropipettes (8-14 Mohm).

The shape of spike waveforms did not change when the proximity of the recording electrode was varied. Classification of spike waveforms yielded 2 distinct groups, based on principal component analysis and hierarchical clustering; A. Multiphasic spikes having a W-shaped waveforms, and B. Multiphasic spikes with an M-shaped waveform. The fine details of W- and M-shaped spikes varied considerably, but there was virtually no overlap between these two groups. The durations of W-shaped spikes were considerably longer than M-shaped spikes. Moreover, after exposure to intense sound, the proportion of SA DCN cells with W-shaped spikes declined from 65% to 38%, while the proportion of SA cells with M-shaped spikes increased from 35% to 62%.

Since these changes could reflect either a shift in the types of SA cells, or changes in the physiology of cells, juxtapositional labeling of cells is being employed in an effort to resolve this issue. After recording SU properties, neurobiotin was electroporated into cells with positive 3 to 5 nA current pulses. To visualize labeled cells, sections (60  $\mu\text{m}$ ) of fixed DCN tissue were processed, using an ABC kit and the DAB chromagen reaction. The soma, dendritic trees, and axonal processes of the major cell types of the DCN, including fusiform, giant, cartwheel and stellate cells, have been well labeled. Correlation of SA, spike waveform and morphologic identity of normal and hyperactive cells will demonstrate whether changes in the physiology or types of SA cells are affected after intense noise exposure.

(Support NIDCD grant R01 DC03258)

### **936 Physiological Baselines for Assessing Tinnitus in the Inferior Colliculus of CBA/J Mice**

**Hiroshi Hidaka<sup>1</sup>**, Wei-Li Ma<sup>1</sup>, Bradford May<sup>1</sup>

<sup>1</sup>*Center for Hearing and Balance and Dept. of Otolaryngology-HNS, Johns Hopkins University*

Previous physiological studies have implicated the polysensory projections of the dorsal cochlear nucleus (DCN) as a generator site for tinnitus. Hypothesized abnormal discharge rates ascend from the DCN to the central nucleus of the inferior colliculus (IC) where they commingle with potentially normal inputs from virtually all major auditory nuclei. In the cat, these separate influences may be isolated by identifying the subset of IC neurons that manifest the unique physiological properties of the DCN. Although rodent species have played a critical role in behavioral and physiological assessments of tinnitus, there is no similar system for linking abnormal activity in the DCN to the higher levels of auditory processing that give rise to tinnitus percepts.

As a first step toward defining a tinnitus pathway, this study examined the physiological properties of single units in the IC of CBA/J mice. Neural responses were analyzed in the context of existing systems of classification that are based on excitatory bandwidth. This tuning is dictated by inhibitory inputs that are mapped in the frequency domain by suppressing spontaneous rates (SRs) with pure tones. To minimize the confounding effects of anesthesia on SRs, our recordings were made in sedated mice using relatively

non-invasive surgical procedures. This preparation is ideal for verifying the increased SRs that are predicted by hyperactivity models of tinnitus. Here, we summarize the physiological baselines of response types in the IC of normal mice. A companion abstract describes how these properties are influenced by tinnitus induction.

This research was funded by a grant-in-aid from the Tinnitus Research Consortium and by NIH grant DC05211.

### **937 Unilateral Noise Exposure Causes Low-Frequency Enhancement of Spontaneous Activity in the Ipsilateral Cochlear Nucleus and the Contralateral Inferior Colliculus of Intact and Decorticate Rats**

**Thomas J. Imig<sup>1</sup>**, Dianne Durham<sup>1</sup>

<sup>1</sup>*University of Kansas Medical Center*

Tinnitus often results from noise exposure and is believed to reflect aberrant spontaneous activity (SA) in the auditory system. We used 2-deoxyglucose (2DG) to characterize changes in SA in brainstem nuclei following noise exposure. One week following unilateral exposure to 1 h of 114 dB SPL, 14 – 19 kHz band pass noise, cortically intact and decorticate unanesthetized rats were injected with 2DG and kept in a quiet sound chamber during 2DG uptake. Optical density measurements were obtained in low (LF), middle and high frequency (HF) areas of the dorsal (DCN) and anteroventral (AVCN) cochlear nuclei, and in the central nucleus of the inferior colliculus (ICc). Intact and decorticate rats showed enhanced 2DG labeling in LF areas of the ipsilateral DCN and AVCN and in the contralateral ICc, i.e. the LF area was more densely labeled than the HF area of each nucleus as compared to controls. In intact animals, LF enhancement was due to a decreased HF labeling density. In decorticate animals, it was due to a decreased HF density and increased LF density. Weaker changes in contralateral CN and ipsilateral IC include a significant HF enhancement in contralateral AVCN of intact animals and in contralateral DCN of decorticates. One interpretation of intact – decorticate differences is that descending systems provide negative feedback to the DCN, AVCN and ICc. Decortication removes negative feedback and causes an increase in activity. Changes in brainstem SA may reflect changes in auditory nerve SA where noise damage has been shown to cause a decrease in SA. Noise exposure would be expected to cause greatest damage to HF hair cells and it is in the HF region of brainstem nuclei where there is a decrease in SA. LF enhancement may be a neural correlate of tinnitus, as tinnitus pitch frequency has been reported to correspond with the low frequency edge of hearing loss in humans with unilateral sensorineural hearing loss. Supported by NIDCD DC01589.

### **938 Differential Gene Expression in Two Models of Tinnitus**

**Avril Gene Holt<sup>1</sup>**, Catherine Lomax<sup>1</sup>, Margaret Lomax<sup>1</sup>, Richard Altschuler<sup>1</sup>

<sup>1</sup>*University of Michigan*

Tinnitus can be a debilitating condition that decreases the quality of life for many people. Central tinnitus can occur in people with no hearing deficit as well as those that have hearing loss that ranges from mild to profound. In an investigation of the pathways involved in tinnitus, the changes in gene expression were studied in two different animal models of tinnitus. Animals were divided into three different experimental groups: (1) exposed to a 10 kHz 118 dB tone for four hours, (2) exposed to a 16 kHz 105 dB tone for one hour and (3) non noise-exposed. Exposure to the 10 kHz tone resulted in a permanent threshold shift (PTS) of 80 dB resulting in profound hearing loss. In contrast the 16 kHz tone resulted in a temporary threshold shift (TTS) with normal hearing completely restored by 5 days after the exposure. The expression of 40 neurotransmitter related genes were assessed in the cochlear nucleus (CN) and inferior colliculus (IC) in all three experimental groups 5 days following the exposure. Each experimental group consisted of 4 RNA pools for each brain region, each comprised of the CN or IC from 4 rats. Surprisingly, real time RT-PCR (qRT-PCR) for GABA receptor related genes (GABA A beta 1, GABA A beta 2, GABA A beta 3, GABA A gamma 1, GABA A gamma 2, GABA alpha 1, GABA alpha 3, GABA alpha 5, GAD 65), glycine receptor related genes (glycine alpha 1, glycine alpha 2, glycine alpha 3), and glutamate receptor related genes (GluR 1, GluR 2, GluR 3, GluR K2, NMDAR 1A, NMDAR 2A, NMDAR 2B, NMDAR 2C, NMDAR 2D), and other neurotransmitter related genes suggest that many of the genes are differentially expressed in a similar fashion for both the PTS and TTS models of tinnitus. By comparing various noise over-stimulation models that produce behavioral tinnitus, but result in different anatomical and physiological characteristics we will be able to identify changes in gene expression that are common to all tinnitus models and may be important in the identification of mechanisms that underlie this condition.

### **939 Noise-Induced Hyperactivity in the Dorsal Cochlear Nucleus: Dependence of Onset Time on Exposure Level.**

**James Kaltenbach<sup>1</sup>**, Jinsheng Zhang<sup>1</sup>

<sup>1</sup>*Dept. of Otolaryngology, Wayne State University, Detroit, MI 48201*

Intense sound exposure causes increased spontaneous activity in the dorsal cochlear nucleus (DCN) of laboratory animals. Several lines of evidence suggest that this hyperactivity may represent a neural correlate of tinnitus. For example, behavioral studies indicate that the same exposure conditions that cause hyperactivity in the DCN also cause animals to experience tinnitus. One weakness of DCN hyperactivity as a model of tinnitus is that its onset is delayed relative to the onset of noise induced-tinnitus in humans. For example, animals exposed to a tone at 125-130 dB SPL (4 hrs) do not develop hyperactivity in the

DCN until 5 days after exposure. In contrast, psychoacoustic studies indicate that humans exposed to a tone at 90-120 dB SPL (5 mins) develop tinnitus immediately after the exposure. One possible explanation for this discrepancy is that, unlike the more moderate, non-traumatizing sounds employed in experimental studies to induce tinnitus in humans, the higher sound levels used to induce hyperactivity cause severe cochlear damage. To address this possibility, we sought to determine whether earlier onsets of DCN hyperactivity might be observed following more moderate exposure conditions. One group of hamsters was exposed to a 10 kHz tone for 4 hours at levels between 80 and 115 dB SPL. A second group served as unexposed controls. Electrophysiological recordings of multiunit spontaneous activity were performed on the surface of the DCN one day following the exposure. Comparison of DCN activity profiles from the two groups revealed higher levels of spontaneous activity in exposed animals than in controls. In numerous exposed animals whose DCNs displayed hyperactivity, histological evaluations demonstrated no appreciable hair cell loss throughout the cochlea. These results indicate that moderate levels of exposure which do not cause hair cell loss cause hyperactivity in the DCN with onset times more comparable to those of human noise-induced tinnitus.

### **940 Altered Levels of S6-P and eEF2-P, Regulators of Protein Synthesis, in Guinea Pig Cochlear Nucleus After Unilateral Cochlear Ablation**

**Sanoj Suneja<sup>1</sup>**, Zhicheng Mo<sup>1</sup>, Steven Potashner<sup>1</sup>

<sup>1</sup>*Neuroscience, University Of Connecticut Health Center*

Unilateral cochlear ablation (UCA) in adult guinea pigs induced plasticities in brain auditory pathways, including synaptogenesis and synaptic reorganization in the ventral cochlear nucleus (vCN) and altered transmitter release and receptor activity. Certain changes were accompanied by altered signal transduction and transcription factor activation, which may alter gene transcription and protein synthesis. Protein synthesis can be regulated at initiation of mRNA translation and at protein elongation. To determine if protein synthesis is altered by UCA, we used Western blotting of whole tissue lysates of the CN subdivisions to quantify levels of phosphorylated (i.e., activated) S6 (S6-P), an initiation factor, and eEF2 (eEF2-P), an elongation factor. At 3 days, when cochlear nerve endings had degenerated, S6-P levels declined in the ipsilateral CN but were near normal contralaterally. Between 3 and 7 days, S6-P recovered in the ipsilateral vCN, coincident with a period of synaptogenesis and accumulation of synaptosomal proteins and synaptophysin, a synaptic vesicle protein (Benson et al. Synapse 25:243 1997). S6-P was also elevated in the contralateral vCN. By 60 days, S6-P levels declined in the vCN, except in the ipsilateral anteroventral (AVCN) CN, where the level was elevated. Levels were also elevated in the dorsal (DCN) CN. At 3 days, eEF2-P levels were elevated in the posteroventral (PVCN) CN but not in other subdivisions. Between 3 and 7 days, eEF2-P levels declined in all CN subdivisions and were elevated again by

60 days in the DCN bilaterally and in the ipsilateral vCN. At 60 days, contralaterally, levels were near normal in the AVCN but remained elevated in the PVCN. These changes are consistent with protein synthesis regulation during periods of signal transduction (Suneja & Potashner J. Neurosci. Res. 73:235 2003) and transcription factor activation (Mo et al. 2005, ARO Poster) that may have shaped plasticities after UCA. (Supported by DC00199)

#### **941 CREB-P Levels Change in Guinea Pig Brain Stem Auditory Nuclei After Unilateral Cochlear Ablation**

Zhicheng Mo<sup>1</sup>, Sanoj Suneja<sup>1</sup>, Steven Potashner<sup>1</sup>

<sup>1</sup>*Neuroscience, University Of Connecticut Health Center*

After unilateral cochlear ablation (UCA) in young adult guinea pigs, the appearance of various plasticities in auditory pathways suggested modified phenotypic behaviors of auditory neurons. Cochlear nerve loss presumably altered signal transduction, which, in turn, changed gene expression and protein synthesis. We have quantified the levels of phosphorylated CREB (CREB-P) as an index of this process. CREB-P is a transcription factor that binds to DNA and facilitates gene expression, which is presumably followed by translation of mRNA to make proteins (Bonnie & Ginty, Neuron 35:605 2002). In these studies, the left cochlea was removed and Western blotting was employed to quantify CREB-P and total CREB in whole tissue lysates of the anteroventral (AVCN), posteroventral (PVCN) and dorsal cochlear nucleus, the lateral and medial superior olive, the medial nucleus of the trapezoid body, and the central nucleus of the inferior colliculus (ICc) for up to 145 postlesion days. Levels of total CREB were relatively unchanged. During the first postlesion week, however, CREB-P levels were depressed in all the tissues, except in the ICc and PVCN, where they were elevated approximately 2-4 fold. At 60 days, CREB-P levels were elevated above the levels in unlesioned controls by 1.5-7.5 fold. By 145 days, CREB-P levels again declined in all the nuclei, except in the ICc and AVCN (ipsilateral), where levels were elevated 2-7.5 fold. The main elevation of CREB-P levels at 60 days preceded the UCA-induced upregulation of glutamatergic transmitter release that developed in many of the auditory brain stem nuclei between 60-145 postlesion days (Potashner et al. Exptl Neurol 148:222 1997). In the CN, the 60 day elevation of CREB-P also coincided with elevations of initiation and elongation factors that regulate protein synthesis (see Suneja et al, 2005, ARO poster). Thus, the findings suggest CREB contributed to the UCA-induced plasticities. (Supported by DC00199)

#### **942 Lithium Increases Bcl-2 Expression in the Chick Cochlear Nucleus and Protects Against Deafferentation-Induced Cell Death**

Angela Bush<sup>1</sup>, Richard Hyson<sup>1</sup>

<sup>1</sup>*Florida State University*

Approximately 20-30% of neurons in the avian cochlear nucleus, nucleus magnocellularis (NM), die following deafferentation (i.e. deafness produced by cochlea

removal). Cell death is generally accepted to be a highly regulated process involving a variety of pro-survival and pro-death molecules. Chronic administration of lithium has been shown to modify the expression of these molecules and to reduce neuronal death in other systems. We have recently reported that chronic administration of lithium decreases the amount of cell death seen after cochlea removal in the chick; saline-treated birds showed 22.4% cell death, but only 9.8% death was observed in birds that were treated with lithium. Lithium did not alter the total number of neurons on the intact side of the brain, but prevented death on the deafferented side of the brain. The present experiment examines a possible mechanism of lithium's neuroprotective effect. Previous studies suggest that the pro-survival molecule, Bcl-2, may play a role in regulating cell death following deafferentation. Perhaps lithium has its neuroprotective effect by upregulating Bcl-2 protein, thereby defending the NM neurons from the effects of deafferentation. To test this hypothesis, post hatch chicks were treated with LiCl or saline for 17 consecutive days. On the 17th day, birds were perfused with 4% paraformaldehyde and brain sections were processed using immunocytochemistry for Bcl-2. To control for variation in labeling intensity produced by processing variables, sections from both saline- and lithium-treated subjects were incubated and reacted together. Bcl-2 labeling in NM neurons was greater in birds treated with lithium than in birds given saline. These data support the hypothesis that lithium imparts its neuroprotective effect by altering the expression of genes that regulate cell death.

#### **943 Differential Gene Expression of Glutamate Receptor Subunits and related Transporters following Deafness**

Mikiya Asako<sup>1</sup>, Avril Gene Holt<sup>2</sup>, Margaret Lomax<sup>2</sup>, Richard Altschuler<sup>2</sup>

<sup>1</sup>*Kansai Medical University*, <sup>2</sup>*University of Michigan*

There is increasing evidence of changes in levels of inhibitory and excitatory amino acids and their related receptors induced by activity dependent plasticity in the auditory brainstem. We have previously used real time RT-PCR (qRT-PCR) to show changes in GABA and glycine receptor related gene expression in the rat cochlear nucleus (CN) 3 days, 3 weeks and 3 months following bilateral cochlear ablation. In the current study we use qRT-PCR to examine changes in expression of glutamate receptor subunits and associated transporters following deafening. Male Sprague-Dawley rats, 200-300g, with normal hearing, were divided into four groups each containing 12 rats: Group 1 - normal hearing control animals, age matched to Group 3; Group 2 - bilaterally deafened by cochlea ablation and assessed 3 days following deafening; Group 3 - bilaterally deafened by cochlear ablation and assessed 3 weeks following deafening; Group 4 - bilaterally deafened by cochlear ablation and assessed 3 months following deafening. To generate three different pools of CN mRNA for each condition, each group of 12 rats was randomly divided into three sub-groups of four rats each. Many receptor subunits (GluR1, GluR2, GluR3, GluR4, NMDAR2a-d,

NMDAR3) showed an initial decrease in expression at 3 days and 3 weeks and then increased expression over normal at 3 months. NMDAR1, on the other hand, showed a large initial increase 3 days after deafening followed by a decrease at 3 weeks and close to normal expression by 3 months. Expression of glutamate transporters had a similar pattern of change with VGLT1&2, GLAST, EAAC1 and GLT1 showing an initial decrease in expression at 3 days, a return to close to normal levels at 3 weeks with an increase over normal expression by 3 months.

**944 Complementary Changes in Synaptic Plasticity, Glial Processes, and NT-3 Localization in the Mouse Cochlear Nucleus (CN) Following a Single Episode of Acoustic Trauma.**

Jennifer Bendiske<sup>1</sup>, D. Kent Morest<sup>1</sup>

<sup>1</sup>Univ. of Connecticut Health Center, Dept. of Neuroscience

Previously, we reported in the anterior portion of the posteroventral CN (PVCN-A) a gradual loss in optical density measurements of synaptic vesicle protein SV-2 immunostaining in mice (C57Bl/6JxCBA/J) that survived for 1, 2, 4, or 8 weeks following a single exposure to 6hrs of white noise (4-16 kHz at 110dB SPL). The present study expands on these findings by examining SV-2 labeling in specific locations (perisomatic vs. neuropil). The data indicated that SV-2 loss occurs in two waves, with a transient recovery in between. SV-2 is lost from perisomatic and neuropil locations by week 1, after which there is a recovery to near control values in both locations by week 2. After the apparent recovery, there is a sustained loss of SV-2 through week 8. Complementing the change in SV-2 are alterations in labeling for GLT-1, a glial glutamate transporter. E.g., at the times when SV-2 labeling is diminished, detection of GLT-1 is elevated. In contrast to SV-2 and GLT-1, the expression of NT-3 is maintained throughout the time course. Our data also indicate that NT-3 is in synaptic endings and the surrounding glial processes, as suggested by co-localization of NT-3 with both SV-2 and GLT-1. This dual localization may explain the apparent maintenance of NT-3 in the weeks following noise exposure. NT-3 may up regulate in one cell type (e.g. glia) at one stage of the pathological sequence and down regulate in another (synaptic endings) at the same stage. The net effect would be the maintenance of overall protein levels. In sum, the waves of expression of molecules associated with glia and synaptic endings at neuropil and perisomatic sites may play a role in axo-glial interactions in the synaptic plasticity following acoustic trauma. Supported by NIH grants F32 DC006120 and RO1 DC00127.

**945 Degeneration in the Synaptic Nests of the Cochlear Nucleus Following Acoustic Overstimulation in a Model for Noise-induced Hearing Loss: An Electron Microscope and Immunogold Study**

Munirathinam Subramani<sup>1</sup>, Maya Yankova<sup>1</sup>, D Kent Morest<sup>1</sup>

<sup>1</sup>University of Connecticut Health Center

Synaptic nests are specialized clusters of synaptic endings that are not separated by glial processes which express high-affinity glutamate transporters (e.g., GLT1). Without the transporters, noise induced hyperactivity could increase extracellular glutamate in the nest. This may produce synaptic degeneration by an excitotoxic process. We hypothesize that glial processes expressing GLT1 infiltrate the nests as a compensatory response to noise. To test this hypothesis, we have examined the fine structure of synaptic nests in the dorsal subdivision of anterior part of the posteroventral cochlear nucleus (PVCNAd) and lateral lamella of the small cell shell in normal and noise-exposed mice. F1 hybrid (C57/BxCBA/J) adult mice were exposed to white noise (4-16 kHz) at 115 dB SPL for 6 hrs. After survival times of 3.5-120 days, exposed and age-matched unexposed control mice were prepared for electron microscopy. Serial-section reconstructions showed synaptic nests weaving through the neuropil for long distances. The nests were clearly distinguishable from the glomeruli. In the 3.5-30 day survivals, astrocytic processes invaded the synaptic nests and increased the extent of glial-synaptic contacts. Where glial processes contact degenerating endings, they hypertrophy and express glial fibrillary acidic protein. However, the glial processes contacting normal nest endings had a pale, watery appearance with few glial filaments. This appearance distinguishes them as supportive astrocytes, different from the phagocytic processes of microglial cells or reactive astrocytes. To confirm this distinction, we found that the supportive astrocytic processes entering the synaptic nests were labeled for GLT1 by post-embedding immunogold. Our data suggest that there is significant plasticity and ultrastructural reorganization in the synaptic nests of the cochlear nucleus in a model for noise-induced hearing loss.

Supported by NIH Grant DC00127.

**946 Fibroblast Growth Factor Receptor (FGFR1) in the FGF2 Overexpresser Mouse Appears at the Right Time and Place to Rescue Synaptic Endings in the Cochlear Nucleus after Noise Damage**

Chrystal D'Sa<sup>1</sup>, D. K Morest<sup>1</sup>

<sup>1</sup>Dept of Neuroscience, University of Connecticut Health Center, Farmington, CT

In adult mammals, a single noise exposure can damage cochlear hair cells and cause degeneration of axonal endings in the cochlear nucleus (CN). Possible mechanisms for the axonal and synaptic degeneration are loss of trophic support and/or excitotoxicity in the CN.

FGF2 may be involved in either mechanism. Previously we found that the high levels of FGF2 in the overexpresser reduce terminal degeneration in the CN, based on optical density measurements for synaptic vesicle protein (SV2). In the present study, we quantified the number of objects or clusters immunostained for SV2 in the anterior part of the posteroventral CN at 7 days after noise in the FGF2 overexpresser mouse. The results were compared to appropriate controls. This analysis presented two main types of clusters: peri-somatic clusters, which represent axo-somatic endings, and neuropil clusters, which represent axo-dendritic endings. The large axo-somatic clusters are dominated by cochlear nerve endings, while the small clusters include inhibitory endings. In the wild type, there is a decrease in the number of both neuropil and peri-somatic clusters. In the overexpresser, there is a decrease in the number of neuropil and small peri-somatic clusters, while the number of large peri-somatic clusters increases. At the same time, FGFR1 decreases in the axons and dendrites (neuropil) and increases in the peri-somatic regions. These changes were not seen in the wild type. The interaction of FGF2 with its high-affinity receptor FGFR1 may be part of the mechanism by which FGF2 protects the peri-somatic pre-synaptic endings from damage after noise.

(Supported by NIDCD)

#### **947 Short Term Synaptic Depression and Recovery in the AVCN Endbulb Synapse in Mice with Age-Related Hearing Loss**

**Yong Wang<sup>1</sup>**, Paul Manis<sup>1</sup>

<sup>1</sup>UNC-CH Department of Otolaryngology/Head and Neck Surgery 1115 Biometrics Building, CB#7070 University of North Carolina Chapel Hill, NC 27599-7070

Age related hearing loss is accompanied by changes in synaptic function at the endbulb of Held synapse in the anteroventral cochlear nucleus (AVCN). These changes include a reduction of spontaneous mEPSCs, a slowing of mEPSC decay time course, a decrease in vesicle release probability, and functionally, a reduction of bushy cells' ability to entrain to high frequency auditory nerve stimuli. These changes in synaptic function involve both presynaptic and postsynaptic mechanisms. Considering the importance of the endbulb synapse in coding temporal information of the auditory signal, it is critical to understand how these changes in synapse performance affect synapse function in cells affected by hearing loss. To that end, we used a mouse model of age-related hearing loss, DBA mice, and in a slice preparation, characterized synaptic depression and recovery for high frequency nerve shocks. In contrast to the substantial depression reported for young medial nucleus of the trapezoid body (MNTB) neurons, we found, at 33°C, in mice of 21 or 45 days of age, that the synaptic responses to 20 stimuli at 100 Hz were only depressed by about 10%, and responses to 200Hz and 300 Hz shocks were depressed by about 50% at the end of the train. Higher frequency shock trains resulted in a faster recovery of the synaptic release, consistent with the posited role of intracellular Ca accumulation in the recovery. We found that hearing loss

does not appear to have an effect on the synaptic depression as measured at 33 °C, despite having an effect on the initial vesicle release probability as measured at 22 °C. This may suggest a homeostasis of the synapse in adult animals, which maintain a delicate balance between the number of release sites and release probability at the endbulb synapse.

(Supported by NIH DC04551 to PBM).

#### **948 Responses of Dorsal Cochlear Nucleus Neurons to Trigeminal Stimulation are Altered Following Noise Damage.**

**Susan Shore<sup>1</sup>**, Jianzhong Lu<sup>1</sup>, Seth Koehler<sup>1</sup>

<sup>1</sup>University of Michigan

Trigeminal projections to the cochlear nucleus terminate in its granule cell domains (Shore et. al., J. Comp. Neurol. 2000; Zhou and Shore, J. Neurosci. Res. 2004). We have previously demonstrated that trigeminal stimulation produces excitatory, inhibitory and complex responses in DCN units. When paired with broadband noise (BBN), trigeminal stimulation can suppress or enhance the firing rate in response to BBN, reflecting multi-sensory integration (Shore and Lu, ARO, 2004). Based on evidence that multi-sensory neurons in other systems show enhanced plasticity after de-afferentation, we investigated the effects of noise damage on trigeminal – evoked DCN unit responses.

Guinea pigs were anesthetized and exposed to wideband noise (2-20 kHz) at 105, 114, or 120 dB SPL for 4 hours. Pre- and post exposure ABRs detailed the threshold shifts evident after one or two weeks, at which time unit responses to trigeminal and acoustic stimulation were measured. A bipolar stimulating electrode was placed stereotaxically into the ipsilateral trigeminal ganglion and unit responses from DCN units were obtained using a 16-channel silicon electrode. Electrical stimuli were applied as bipolar pulses, 200  $\mu$ sec per phase, at intervals of 200 ms, with amplitudes ranging from 10-100  $\mu$ A.

Noise exposed animals showed a greater proportion of inhibitory, and a very small number of excitatory responses compared to normal. In addition, noise-damaged animals showed lower thresholds and shorter latencies to trigeminal stimulation than normal animals.

These results suggest that projections from the trigeminal system to the CN are altered after hearing loss. The impact of these alterations is yet to be elucidated but could be involved in plastic changes which may lead to perceptions of phantom sounds (“tinnitus”) which can be modified by manipulations of somatic regions of the head and neck (“somatic tinnitus”).

Supported by NIH grant R01 DC004825 and Tinnitus Research Consortium.



## **949 Protein Synthesis in Central Auditory System Nuclei Following Conductive Hearing Loss**

**Ken Hutson<sup>1</sup>**, Dianne Durham<sup>2</sup>, Debara Tucci<sup>1</sup>

<sup>1</sup>Duke University Medical Center, <sup>2</sup>University of Kansas Medical Center

We have used malleus removal in the young gerbil as a model to study the effects of conductive hearing impairment on central auditory system (CAS) function. Previous studies have shown a decrease in CAS activity and metabolism following this manipulation (Tucci et al., 1999, 2001). In order to understand some of the cellular events associated with this change in activity, we initiated the current study to investigate protein synthesis in CAS nuclei immediately (6 hours) following conductive hearing loss (CHL), cochlear ablation (CA) or a sham procedure (SH; anesthesia only) in postnatal day 21 gerbils. Protein synthesis was assessed using tritiated leucine incorporation (Steward and Rubel, 1985). Brains were embedded in paraffin, and coronal sections through the auditory brainstem were mounted on slides and processed by standard autoradiographic techniques. CAS nuclei (AVCN, MTB, and LSO) were sampled under 63X oil magnification. NIH Image software was used to determine cell area and density of silver grains. Cellular incorporation was measured as fractional density (density of silver grains/cell area). For each animal, background level incorporation was estimated by measuring cells in the abducens nuclei. Background corrected CAS fractional density values were then analyzed across the experimental conditions. Preliminary results suggest that overall the auditory brainstem of CHL animals differ from both CA and SH animals. Relative to CA or SH animals, CHL animals demonstrate elevated mean levels of leucine incorporation. Although at present our sample size is small, (four animals per condition), the greatest differences in leucine incorporation appear in MTB and LSO. Future studies will address the possibility that the present results reflect only immediate (6 hour) alterations in protein synthesis, which may change or even reverse over longer time periods and in response to environmental acoustic demands.

## **950 Auditory Midbrain Implants in Acute and Chronic Experiments**

**Guenter Reuter<sup>1</sup>**, Mino Lenarz<sup>1</sup>, Uta Reich<sup>1</sup>, Nadine Marquardt<sup>1</sup>, Marc Klingberg<sup>1</sup>, Gerrit Paasche<sup>1</sup>, Jim Patrick<sup>2</sup>, Thomas Lenarz<sup>1</sup>

<sup>1</sup>Dept. of Otolaryngology, <sup>2</sup>Cochlear Ltd.

Auditory brainstem implants with electrodes positioned in the NC are used for the auditory habilitation of patients with neural deafness [1]. Alternative concepts for targeted tonotopic stimulation of the higher auditory areas, such as colliculus inferior (IC), are currently under investigation [2,3]. In collaboration with Cochlear Ltd. (Sydney), a 4 mm 20-channel rod electrode was developed, electrode contacts being arranged in a circle on a rod at 200 µm intervals. This electrode inserted in IC allowed measuring acoustically evoked potentials in acute experiments and also electrical stimulation of IC. In chronic experiments the

same type of electrode was inserted in the IC. Parallel to a non-stimulated control group daily stimulation with commonly used speech processor and impedance measurements are performed.

Electrode insertion in IC proved to be easy and reproducible. In acute experiments acoustically evoked potentials can be recorded with multi channel set up in the IC in a frequency dependent manner on the auditory cortex or in cortical layers of AI. Stimulating the IC via the IC electrode electrically, comparable potentials were measured parallel on 16 channel in the auditory cortex. A clear input-output characteristic was seen as a clear dependency of pulse length and threshold.

Long-term studies carried out in order to investigate the safety and feasibility of this approach. Animals implanted with these electrode in IC showed no noticeable neurological and motoric diseases in time range up to few months. First experiments with electrical stimulation in IC during speech processor evoked no avoidance reaction. In behaviour tests animals with deafness (neonatal or adult) react on short loud sounds with attention and visual searching. There is no visible pain reaction. In the first 30 days weeks after implantation there is no increase the impedance of electrode contacts.

More long-term animal studies with and without stimulation are running. Histological comparison of IC after 3 month stimulation and control experiments help to analyse insertion trauma and tissue growth during stimulation. The goal is auditory rehabilitation in patients suffering from neural deafness more efficiently than surface electrodes places on the cochlear nucleus.

## **951 Neural Correlates of Temporal Processing in the Inferior Colliculus of Mice Lacking the Kv3.1 Voltage-Gated Potassium Channel**

**Anita Jeyakumar<sup>1</sup>**, Nicholas Schmuck<sup>1</sup>, Paul Allen<sup>1</sup>, Rolf Joho<sup>1</sup>, Joseph Walton<sup>1</sup>

<sup>1</sup>University of Rochester

Delayed rectifier potassium current regulation and diversity are essential for signal processing and integration in neuronal circuits. This is especially evident in the auditory brainstem where many different types of voltage-gated potassium channels (VGPCs) are found. The Shaw family of VGPCs play an important role in the neurons which discharge at high frequencies in a sustained manner or fire repetitively to stimuli. These experiments were performed in order to investigate the functional consequences of a loss of the Kv3.1 channel on in vivo coding of static and dynamic sound envelopes. Specifically, we examined 3 stimulus conditions: 1) thresholds and amplitude by intensity functions to tone and noise bursts, 2) encoding silent gaps embedded in noise and 3) encoding of 100% sinusoidal amplitude modulated (SAM) noise in 3 genotypes, +/+, +/- and -/-. Kv3.1 mice were developed on a mixed background of 3 strains, 129/Sv:C57BL/6:ICR (at about 25:25:50). Recordings were obtained from monopolar electrodes (25-40 µm tips) lowered to 500µm and 1500 µm into the central nucleus of the IC. Gap stimuli consisted of two 50 ms noise bursts (NB1 & NB2)

separated by quiet gaps varying from 0.25 to 96 ms, including a no gap control. SAM noise bursts were 200 msec in duration with modulation frequencies ranging from 10 to 1500 Hz. Each set of stimuli were presented at 60 and 80 dB SPL. We calculated RMS amplitudes (GAPS) and power spectrums (SAM) in 3 time windows in order to compute the respective gap functions and modulation transfer functions. Preliminary data analysis indicates that minimal gap thresholds (MGTs) and the recovery of NB2 amplitude are not affected in KO mice. The SAM upper cutoff frequency ranged from 80 to 300 Hz, and was only slightly lower in KO mice. Results will be discussed in terms of the role of the Kv3.1 in reducing the width of action potentials and as a specialization for enabling neurons to transmit high-frequency temporal information.

## **952 A Behavioral Study of Adult Barn Owls: The Precision and Long-Term Stability of Head-Orienting Responses to Auditory and Visual Stimuli**

**Duck Kim**<sup>1</sup>, David Schneider<sup>2</sup>, Yi Zheng<sup>1</sup>, Andrew Moiseff<sup>2</sup>  
<sup>1</sup>University of Connecticut Health Center, <sup>2</sup>University of Connecticut

The barn owl has been an effective animal model for studies of auditory localization and its adaptive plasticity. We undertook a behavioral study of the system as behavioral assessments provide information that cannot be obtained from physiological assessments alone and behavioral data are less available than physiological data. In preparation for a study of the progression of the adaptive plasticity in adults, we examined the stability of localization behavior measured repeatedly over a long period. We measured head-orienting responses of three adult barn owls (> 7 mo old) using a search coil system. To determine the relationship between the auditory and visual systems, we measured, in each testing session, the owl's responses to free-field sounds and lights, ranging in azimuth from +/- 38 deg in steps of 6.3 deg at 0 deg elevation. Duration of stimuli were 0.7~3.3 s.

To quantify the precision and variability of the auditory and visual responses, we computed: (1) linear regressions of the responses versus the targets yielding slope and intercept (Poganiatz et al., 2001); and (2) the standard deviations of the errors of the responses relative to the target (variability<sub>1</sub>) and relative to the regression line (variability<sub>2</sub>). We observed that, for both sound and light, the regression line typically had a slope of 0.80 ~ 0.99 and a negligible intercept. The variability<sub>1</sub> of the auditory responses ranged typically from 1.2 to 7.0 deg. The variability<sub>2</sub> of the auditory responses was smaller than variability<sub>1</sub>. The two variability measures of the visual responses tended to be smaller than the auditory counterparts. The auditory and visual responses tended to be concordant although exceptions were encountered. The results also indicate that the slope and variabilities of both auditory and visual responses may vary over time. Such potential variation of the responses over time must be taken into account in future studies of adaptive plasticity of the system.

## **953 Object Discrimination in the Flying Bat, *Eptesicus fuscus***

**Ben Falk**<sup>1,2</sup>, Tameeka Williams<sup>1,3</sup>, Murat Aytakin<sup>1,4</sup>, Kaushik Ghose<sup>1,4</sup>, Cynthia Moss<sup>1,4</sup>

<sup>1</sup>University of Maryland, College Park, <sup>2</sup>Dept. of Psychology, <sup>3</sup>Dept. of Biology, <sup>4</sup>Dept. of Psychology, Institute for Systems Research, Neuroscience and Cognitive Science Program

Echolocating bats emit high frequency sounds and listen to the returning echoes to develop an auditory representation of their environment. Bats use the intensity, interaural difference cues and the delay of sonar echoes to determine the size, location, and distance of targets. Bats may also use echolocation to determine the shape and texture of sonar targets, but the acoustic cues associated with these features have not yet been established. This study was designed to measure target discrimination by echolocation in the FM bat, *Eptesicus fuscus*, and to determine the acoustic features used to perform such a task.

In this experiment we adopted a new procedure for testing object discrimination in free-flying bats by training animals to hit a tethered target (S+) in the presence of alternative tethered targets (S-). If the bat hit S+, it received a food reward on a landing platform. S+ was always a smooth bead, and S- was one of several textured beads. Bats successfully learned this discrimination, but their performance depended on the characteristics of any given S-. Echoes from the beads were measured by broadcasting computer generated FM sonar pulses and recording the returns. Spectrum and intensity parameters were characterized for each target, and only beads that returned mean echo levels within 3 dB of each other were used in the discrimination task. The bat's 3-D flight path was reconstructed using stereo images taken from high speed video recordings. The bat's sonar cries were recorded for each trial and analyzed off-line. In selected trials, the bat's sonar vocalizations were also recorded using a microphone array that permitted reconstruction of the beam pattern, allowing us to study the bat's head-directing behavior in this task. The results of this study demonstrate that *E. fuscus* can discriminate fine differences between objects and quantifies the auditory cues it uses for this task. Supported by NSF, Howard Hughes, UM Senior Summer Scholars.

## **954 Directional Hearing in the Gerbil (*Meriones Unguiculatus*)**

**Julia Maier**<sup>1</sup>, Georg Klump<sup>1</sup>

<sup>1</sup>Oldenburg University

The Mongolian gerbil's low-frequency sensitivity is similar to that of humans (Ryan, 1976, JASA 59: 1222-1226). Therefore it has become a model organism for studying the physiological mechanisms of sound source localization in azimuth (e.g., Brand et al. 2002, Nature 417: 543-574). So far, localization thresholds had only been determined for broad-band noise (Heffner & Heffner 1988, Behav Neurosci 102: 422-428). Here we report localization thresholds for tones and narrow-band noise stimuli (bandwidth 300 Hz) with center frequencies of 0.5, 1, 1.5,

2, 4 and 8 kHz in addition to thresholds for broad-band noise. All stimuli had a duration of 125 ms including 25-ms Hanning ramps and had a mean overall level of 60 dB SPL that was randomly varied by  $\pm 6$  dB.

We tested the accuracy of azimuth sound localization of 7 gerbils in a 2AFC paradigm with food rewards. Their task was to report if stimuli were presented from the left or the right side by choosing the appropriate direction in a y-maze (threshold 75% correct response). The angle between pairs of speakers left and right of the midline was 10°, 30° or 60° as seen from the position of the gerbil at a distance of 85 cm. Sounds were either presented from the front (N = 4) or from the back (N = 3). Gerbils stimulated from the front had localization thresholds that ranged from 20.4° to 30.3° for tones and from 19.5° to 36.9° for narrow-band noise. The best thresholds were found between 1 and 2 kHz. However, there was no significant difference in the performance for stimuli of different frequencies. The threshold for broad-band noise was 23.4° and 22.3° for varying and fixed levels, respectively. For most signals, gerbils stimulated from the back had significantly higher thresholds than gerbils stimulated from the front. The results are discussed with reference to the duplex theory of sound localization.

Supported by the DFG within the international graduate school "Neurosensory Science, Systems and Applications" and FOR 306

### **955** Localization of Stimuli that Produce the Franssen Effect in Mammals

**Micheal Dent**<sup>1</sup>, Joel Weinstein<sup>2</sup>, Luis Populin<sup>2</sup>

<sup>1</sup>University at Buffalo, SUNY, <sup>2</sup>University of Wisconsin

When measuring the auditory illusory Franssen Effect (FE), subjects are presented with two sounds from two different locations in space; one a transient tone with an abrupt onset and immediate ramped offset and the other a sustained tone of the same frequency with a ramped onset which remains on for several hundred ms. When listeners report hearing only one sound at the location of the transient signal, even though that sound has ended and the sustained one is still present at another location, the FE is said to be operating. The FE has been explored using discrimination procedures in humans and results show that it occurs with pure tones of ~1-1.5 kHz (Yost et al., JASA, 1997), conditions where sound localization is difficult in humans. The FE has also recently been found to occur in domestic cats at higher frequencies using sound localization instead of discrimination procedures, and results showed that the listeners actually perceive the illusory fused object at the location of the transient sound source (Dent et al., JASA, 2004).

Previous studies in humans have employed discrimination procedures, making it difficult to link the FE to sound localization mechanisms. Here, we measure the FE using, for the first time in humans and non-human primates, localization procedures. Humans and non-human primates were outfitted with eye coils to measure gaze movements using the magnetic search coil technique. Paired FE and single source stimuli were presented from various locations in azimuth and the listeners were

required to orient towards the perceived location of the auditory object. Results show that all three species of mammals localize FE illusory stimuli near the location of the transient sound source in a similar manner. These results demonstrate that the FE is a robust auditory illusion capable of causing large errors in localizing sounds under certain conditions.

Funded by NIH DC03693, NSF IBN-9904770, and The Deafness Research Foundation to LCP

### **956** Echo Suppression in Echolocating Bats: Influence of Semantic Meaning?

**Maïke Schuchmann**<sup>1</sup>, Lutz Wiegrebe<sup>1</sup>

<sup>1</sup>Ludwig-Maximilians-Universitaet

Echoes are an essential part of the natural environment. They include misleading spatial information of a sound source and produce acoustic mirror images of objects.

Accurate sound localization is enabled by the perceptual suppression of the misleading spatial information of echoes. Only the directional information of the sound which reaches the ear first dominates the perceived position of a sound source (localization dominance).

A previous study showed that echolocating bats show no localization dominance when either echolocation calls or impulses were used as stimuli (Schuchmann et al.; ARO 2004).

The present study investigated whether there is localization dominance when a stimulus with a semantic meaning is used. This stimulus was a recording of a *Megaderma lyra* contact call. This call contains a frequency-modulated, multiharmonic complex (duration about 15-20 ms; the 15 kHz fundamental is the strongest harmonic). This complex is followed by a series of multiharmonic echolocation calls (duration 0.5-1.5 ms;  $f_0 = 22$  kHz; strongest harmonics are 3, 4, or 5). Note that these echolocation calls do not cause any localization dominance by themselves.

These contact calls were played back in a lead-lag paradigm via two ultrasonic loudspeakers with a lead-lag delay of 0 to 12.8 ms.

All tested individuals of *M. lyra* preferred the first of two contact calls when there was a lead-lag delay of 0.2 to 0.8 ms.

The occurrence of localization dominance with *M. lyra* contact calls could result from either the semantic meaning of the stimulus or the spectro-temporal structure. Control data testing these alternatives will be presented.

### **957** The Role of the External Ear Tragus in Obstacle Avoidance by Echolocation in the FM-bat, *Eptesicus fuscus*

**Chen Chiu**<sup>1</sup>, Cynthia Moss<sup>1</sup>

<sup>1</sup>Neuroscience and Cognitive Science Program, University of Maryland, College Park

The role of the external ear tragus in obstacle avoidance by echolocation in the FM-bat, *Eptesicus fuscus*

The external ears collect and filter the sound used by echolocating bats to localize sonar targets. There are two major components of bats' external ears, the pinna and the

tragus. The size and shape of the tragus vary with bat species, especially for Microchiropteran bats. Previous studies suggest that the tragus contributes to elevation-dependent characteristics of the bat's head-related transfer function (Wotton et al., *J. Acoust. Soc. Am.*, 1996), as well as vertical localization performance in bats echolocating from a platform (Wotton and Simmons, *J. Acoust. Soc. Am.*, 2000). The purpose of this experiment is to examine the role of the tragus in spatially-guided flight of the FM bat, *Eptesicus fuscus*.

The experimental setup consisted of a 1.2mx1.2m frame hanging from the ceiling of a large flight room, containing an array of 0.05 mm diameter wires arranged in a grid. Horizontally stretched wires were parallel and separated by a distance of 3.25cm, except for a 30 cm opening whose position within the grid changed across trials. Vertical wire avoidance was also tested for comparison. The bat's task was to find the opening in the grid and fly through it without touching the wires. Two high-speed video cameras recorded the bat's flight path, and a microphone array was used to measure the horizontal and vertical directional aim of the sonar beam pattern as it performed the obstacle task. Bats were tested under two conditions, with tragus and without tragus. Preliminary results show that tragus deflection initially reduced the bat's success rate flying through the lower openings in the horizontal grid but not the upper ones. The drop in success rate following tragus deflection could last few days but performance would recover. These data suggest that the tragus contributes to vertical localization below the bat's eye-nostril plane, but the bat can compensate for tragus manipulations by changing its flight path. *Supported by NSF.*

### **958 The Effects of Stimulus Duration, Level, and Spectral Content on Sound Localization in Cats**

Janet L. Ruhland<sup>1</sup>, Daniel J. Tollin<sup>1</sup>, Tom C.T. Yin<sup>1</sup>

<sup>1</sup>*Department of Physiology, University of Wisconsin, Madison, WI USA*

Sound azimuth is based on two binaural cues, interaural differences in the time of arrival and level of the sounds at the ears. Sound elevation is based on patterns of the broadband power spectra at each ear that result from the direction-dependent acoustic filtering properties of the head and pinnae. We hypothesized that stimulus manipulations that alter the presumed peripheral representation of sound spectra at the ears would result in greater detriment of localization accuracy for sources varying in elevation than azimuth. To test that hypothesis, we examined the influence of stimulus duration, level, and spectral content on sound localization in the cat. Cats were trained using operant conditioning to indicate the apparent locations of sounds via gaze shift (combined eye and head movements). Stimulus manipulations formed a 5 X 5 matrix of sound level (10, 25, 40, 55, and 70 dB attenuation from maximum) and duration (5, 10, 25, 40, and 164 ms). For each combination of stimulus level and duration, localization performance was summarized by the slope (or gain) of the linear regression relating the

localization responses of the cats to the target positions. In general, localization accuracy in azimuth improved with increasing stimulus level and duration. Localization accuracy in elevation also improved with increased stimulus duration. However, unlike for sources in azimuth, localization of sources in elevation for all durations tended to deteriorate at both high and low sound levels, the shortest durations more sharply than the long. The poor localization of source elevation for these conditions is consistent with the hypothesis that broadband spectral shape is critical for sound localization in elevation since the representation of source spectrum at the auditory periphery would likely be compromised at very low and very high stimulus levels. Supported by grants NIDCD DC00116 and DC02840

### **959 A Sensori-Motor Model of Sound Localization in the Echolocating Bat, *Eptesicus fuscus***

Murat Aytakin<sup>1</sup>, Cynthia F. Moss<sup>1,2</sup>

<sup>1</sup>*Neuroscience and Cognitive Science Program, University of Maryland, College Park,* <sup>2</sup>*Institute of System Research, University of Maryland, College Park*

Echolocating bats produce ultrasonic vocalizations and use echoes reflected from objects in the path of the sound beam to localize obstacles and track insect prey on the wing. Their success in spatial orientation depends on both auditory information processing and adaptive motor control. In this study we developed a computational model for sound localization that monitors the auditory consequences of changing head position and captures the relations between head movement and localization cues.

Auditory input is dependent on the acoustic characteristics of the sound source and its location with reference to the head. This model learns to predict auditory consequences of small head movements by monitoring their effect on the acoustic information received at the ears. Since the received acoustic information contains directional information about the sound source and depends on the spectral characteristics of the signal, our model's behavior is influenced by both. We will show that the model learns different directional features as cues for sets of sounds with different statistical characteristics.

Unlike sound localization models that are based on a priori localization cues, such as interaural time and level differences (ITD and ILD), this model learns to use directional cues (derived from both spatial and sound source characteristics) to localize sound sources. We believe that this modeling approach will provide insight to the computation of sound source location by the auditory system. We report the results of our study using an echolocating bat, *Eptesicus fuscus*, as a model system, but the approach can apply more generally to all mammals.

## **960 Spatial Unmasking at a Spectrally Sparse Cocktail Party**

**Antje Ihlefeld<sup>1</sup>, Eric Larson<sup>1</sup>, Barbara Shinn-Cunningham<sup>1</sup>**  
<sup>1</sup>*Boston University*

Spatially separating a target from a simultaneous masker improves speech intelligibility during selective listening. Here, two experiments investigated such "spatial unmasking" when competing signals were processed to reduce peripheral masking.

Speech signals were band-pass filtered into 16 non-overlapping third-octave bands. On each trial, the envelopes of eight randomly selected bands were used to modulate sine-wave carriers at the corresponding center frequencies, which were then summed to produce a spectrally sparse speech-like signal. The eight remaining bands were processed similarly to form a competing signal with negligible spectral overlap for that trial. Signals were presented over headphones with spatial cues derived from manikin head-related transfer functions.

The first experiment tested whether the amount of spatial unmasking in selective listening varies with the fidelity of the spatial cues used to control perceived source location. After accounting for energy effects, the amount of spatial unmasking was similar when spatial cues are (1) all present, (2) present only in the modulation envelopes, and (3) present only in the sinusoidal carriers.

The second experiment examined spatial unmasking in selective listening (subjects reported the content of the target, which contained a predetermined call sign) and divided listening (subjects reported the content of both simultaneous signals). A priori knowledge about the signals' locations was also manipulated. In selective listening, spatial unmasking was significant but a priori knowledge about the source locations had no effect. In divided listening, no spatial unmasking was found.

Results suggest that regardless of spatial cue fidelity, perceived spatial separation improves the ability to selectively attend a quiet signal in the presence of a more intense competing source, and that prior knowledge about where to listen may not be critical for spatial unmasking.

[supported by ONR N00014-04-1-0131]

## **961 Directionality of Echolocation Calls recorded in the Field from Bats hunting over water, *Myotis daubentonii*, *Noctilio leporinus*, *N. albiventris***

**Annemarie Surlykke<sup>1</sup>, Lasse Jakobsen<sup>1</sup>, Elisabeth Kalko<sup>2</sup>**  
<sup>1</sup>*University of Southern Denmark*, <sup>2</sup>*University of Ulm*

In the field bats emit sonar signals that differ significantly from what they emit in the lab. Thus, field recordings are indispensable in order to understand the adaptations and constraints of echolocation. However, making field recordings under controlled conditions is a challenge, because bats fly in darkness at uncontrollable distance emitting highly directional signals. Flying bats turn unpredictably in all directions. In order to minimize the variation, we recorded from bats that hunt over water i.e. moving mainly in 2 dimensions: Daubenton's bat, *Myotis daubentonii*, in Denmark, and bulldog bats, *Noctilio*

*leporinus* and *N. albiventris* in Panama. We used 3 microphones in a 2 m linear array placed ca. 0.5 m above the water.

*M. daubentonii* emits short broad-band FM signals around 100 to 40 kHz. By cross-correlating, TOAD's (Time Of Arrival Differences) between the microphones were found and used to find the bat's positions for each signal and consequently the bat's flight path. Assuming the bat aimed its sonar beam in the flight direction, the angles to the microphones were calculated for each cry. A major problem in the analysis was the signal reflected from the water surface, which created strong interference patterns and deep notches in the spectrum. A method was developed to subtract the reflected signals from the recordings. The results show that the beam-width is decreasing as frequency increases. The attenuation at 30° off-axis is around -5 dB at 45 kHz and -15 dB at 65 kHz. Results of similar experiments with the Bulldog bats are presented. Here, the analysis was more difficult, because of the characteristics of their echolocation signals, which are longer starting with an almost constant frequency and ending in a short downward sweep that may occasionally be omitted. Also, they fly at high speed, creating Doppler shifts of the recorded signals that may differ considerably between the microphones.

## **962 Identifying a Bird in a Chorus: How Target and Masker Statistics Influence Spatial Unmasking**

**Erol Ozmeral<sup>1</sup>, Virginia Best<sup>1</sup>, Frederick Gallun<sup>1</sup>, Kamal Sen<sup>1</sup>, Barbara Shinn-Cunningham<sup>1</sup>**  
<sup>1</sup>*Boston University*

Spatial separation of competing sound sources improves the ability to understand a signal, an effect known as spatial unmasking. Speech signals (which contain modulation, common across-frequency onsets and offsets, harmonic elements, and other spectro-temporal features that affect source segregation) show large effects of spatial unmasking. This study attempts to uncouple the importance of spectro-temporal features in speech from the influence of linguistic and semantic content.

In the current study, listeners identified zebra finch calls, which share many properties with speech but that lack semantic and linguistic content, in the presence of various masking sources. Listeners were trained to identify five individual zebra finches from their calls presented in quiet. Three maskers with the same long-term spectro-temporal content but with different short term statistics were derived from six other, unfamiliar birdsongs: (1) a chorus (random combinations of three unfamiliar songs); (2) song-shaped noise (broadband noise whose spectral magnitude equaled the average spectral magnitude of the unfamiliar song ensemble); and (3) modulated chorus noise (song-shaped noise multiplied by the envelope from a random chorus masker). Listeners identified familiar songs presented with one of the three maskers to test how the amount of masking and the amount of spatial unmasking depended on the short-term masker statistics. Using generic HRTF filtering, the target was simulated from straight ahead; the masker was either simulated from

straight ahead or to the right. Monaural performance was measured to determine what portion of any effects could be attributed to energetic changes at the better ear.

Similar to results from previous speech studies, spatial unmasking was found for birdsong identification. Furthermore, both the amount of masking and the influence of spatial separation depended on the statistical structure of the competing signal.

[supported by AFOSR FA9550-04-1-0260]

### **963** Dynamic Influence of Eccentric Gaze on Sound Localization

**Babak Razavi**<sup>1</sup>, Ashley R. Glade<sup>2</sup>, William E. O'Neill<sup>1</sup>, Gary D. Paige<sup>1</sup>

<sup>1</sup>University of Rochester, <sup>2</sup>Iowa State University

Eccentric gaze is reported to bias visually-guided sound localization. This may reflect an error in how eye position signals are utilized to internally realign visual and auditory space during changes in gaze. Alternatively, an eye movement might provoke a gradual shift in our sense of 'straight-ahead' toward the new eye position. This might induce a comparable shift in our registration of multi-modal space. We quantified the influence of eccentric gaze on sound localization in human subjects while fixating eccentric targets for varying durations.

Subjects were tested in a dark echo-attenuated room, heads fixed, while facing a cylindrical screen at 2m, behind which a non-visible speaker on a robotic arm presented auditory targets (0.1-20 kHz noise; 150-ms bursts at 5 Hz) in a random sequence across the frontal field ( $\pm 50^\circ$  Az  $\times$   $\pm 25^\circ$  El). Targets were localized using a joystick-mounted laser pointer. Eye position was monitored using EOG. During sustained gaze (minutes), subjects fixated 1 of 5 visual fixation spots (Center, L20°, R20°, D20°, or U20°) continuously while localizing sound using their peripheral visual field. In a transient gaze task, gaze and pointer were centered at the onset of each trial, until 1 of the 5 fixation spots appeared (randomly intermixed). Subjects then shifted and held their eyes on the spot while localizing the auditory target over the subsequent few seconds.

Results demonstrate that eccentric fixation shifts sound localization toward gaze angle. In azimuth, the shift approached half the angle of sustained gaze—less so in elevation and with more variance. The shift was far less pronounced for transient gaze. No systematic changes in spatial gain appeared, only general (DC) shifts. Another experiment (extended-transient task) tracked the effect following eye movements over time and showed that the shift develops exponentially, with an average time constant of roughly half a minute. For comparison, sound localization was assessed during combined gaze-laser pointing. A ~10% overshoot in spatial gain appeared but without a DC shift. This effect was absent in other tasks. Results are consistent with a time- and gaze-dependent adaptation of auditory space based upon a slowly shifting internal signal related to eye position.

NIH grants R01-AG16319, P30-DC05409, T32-GM07356 & T32-EY07125.

### **964** Measuring Precedence Effect Buildup using Subjective Scaling Methods

**Pavel Zahorik**<sup>1</sup>

<sup>1</sup>University of Louisville

Past research has demonstrated that listeners' abilities to detect or discriminate changes in a single echo are diminished after repeated presentations of both source and echo. This buildup of echo suppression (precedence effect buildup) along with the release from suppression when dramatic changes are made to the spatial relationship of source and echo are taken as evidence of a complex neural process that adapts and suppresses the acoustical contributions of the listening environment. These effects have seldom been evaluated in more complex and realistic listening environments with multiple echoes or reverberation. One reason for this is the difficulty in modifying echo detection/discrimination paradigms for use with multiple echoes and/or reverberation. Here a method of subjective scaling is described that may easily be applied to the study of suppression effects in such complex environments. The method tracks listeners' estimates of perceived echo/reverberation strength throughout the course of a stimulus presentation sequence and was found to produce results that are both reliable and consistent with previously published echo detection data in which precedence effect buildup was studied using a source and single echo on the frontal horizontal plane. Additional stimulus conditions in which the delay between source and echo was varied within the presentation sequence were also found to produce predictable results.

### **965** Click versus Click-Click: Influence of a Preceding Stimulus on Sound Localization

**Norbert Kopco**<sup>1,2</sup>, Virginia Best<sup>1</sup>, Barbara Shinn-Cunningham<sup>1</sup>

<sup>1</sup>Boston University, <sup>2</sup>Technicka Univerzita, Kosice, Slovakia

Previous studies of sound localization have observed spatial interactions between sound objects presented simultaneously or with very small inter-stimulus delays. For stimuli presented in rooms, we have observed such interactions at much longer delays (up to 300 ms). The aim of the current study was to better characterize how preceding stimuli influence sound localization over these time scales.

We examined the localization of two-ms-long target clicks presented with or without an identical preceding click. The clicks were presented from loudspeakers located in the frontal horizontal plane in a moderately reverberant room. Preceding and target clicks had angular separations of up to 90° and temporal separations of up to 500 ms. The preceding click had two main effects: (1) it increased the variance in target localization responses and (2) it shifted the mean response, especially for large angular separations (greater than 50°) where the mean was shifted towards the location of the preceding click. Both effects decreased with increased temporal separation.

Analysis of interaural cues for the click-pair stimuli suggest that acoustic interactions between the reverberant tail from

the preceding click and the direct sound of the target click cannot explain the observed effects. We hypothesize that neural dynamics in spatial processing, operating over longer time scales than many other known spatial-processing mechanisms (such as the precedence effect), contribute to the observed phenomenon.

[work supported by NIH R01 DC05778-02, AFOSR FA9550-04-1-0260 and NAS/NSF INT-0002341]

### **966 The Use of Interaural Time Difference in Spectral and Temporal Grouping.**

**Ade Deane-Pratt<sup>1</sup>, David McAlpine<sup>1</sup>**

<sup>1</sup>*Department of Physiology and UCL Ear Institute, University College London*

Interaural time difference (ITD) is the primary cue to sound-source localisation in the horizontal plane but its importance in auditory scene analysis is uncertain. In the presence of a single sound-source ITD can be used for temporal grouping, but spectral grouping by common ITD is weak. Modern place-code models of ITD representation suggest that straightness of activation across frequency in the  $\tau$ -f plane encodes perceived lateral location. However, recent data suggest that a rate-code model of neurons tuned for interaural phase difference exclusively within  $\pm 1/2$  cycle may be a more apt. A new model that relies on a rate-code is presented to account for sequential and spectral grouping by ITD and auditory stream segregation.

### **967 Redesign of the Simulated Open Field Environment and its Application in Audiological Research**

**Bernhard Seeber<sup>1</sup>, Ingrid Zellner<sup>1</sup>, Ervin Hafter<sup>1</sup>**

<sup>1</sup>*University of California, Berkeley*

The Simulated Open Field Environment (SOFE) uses independently controlled loudspeakers in an anechoic chamber to simulate realistic auditory scenes with sources and echos. As such, directional characteristics of the simulated stimuli are maintained throughout head movements. Unlike virtual environments based on Head Related Transfer Functions (HRTFs), these stimuli are heard without the incumbrance of earphones, allowing easy comparisons between subjects with normal hearing, hearing aids (HA's) and cochlear implants (CI's) Matlab based software allows control of 48 auditory channels through speakers whose amplitude responses in the range 0.310 kHz are equalized to  $\pm 0.7$  dB and a few  $\mu$ sec of delay. Echoes are computed for virtual rooms using the mirror-image method which allows for accurate representation of the reverberant environment. A synchronized, high resolution video projector, controlled by a separate computer, produces virtual 3-dimensional displays subtending a visual arc of nearly 90°. With these, a subject can use a track ball to place simulated visual objects in a way that describes the perceived azimuth, elevation and distance of the sounds. A first study in the new facility has considered the use of near-speaker panning to achieve still higher spatial resolution. Measures of a listener's ability to tell stimuli panned with the traditional sin/cosine law from sounds coming from a

single speaker at the panned location. There we have found reasonably high performance, even with separations as small as 7.5°. Those detections are based primarily on differences of loudness and timbre created by interference patterns near the listeners head. Use of an HRTF-based model to produce filters that reduce the level and timbral cues produce a reductions in discrimination of the panned and real sounds without erasing their common localization. Continued work examines the importance of lesser cues such as apparent source-width. A working affiliation with the Douglas Grant Cochlear Implant Center at U. C. San Francisco will soon allow for patients with bilateral CI's to be brought into the SOFE for studies of spatial hearing as well as the possible use of a simpler variant of this facility for training those skills. A similar relation with the Starkey Hearing Institute will bring in patients with various HA.s.

### **968 Effects of an Additional SAM Tone on the Responses of Inferior Colliculus Neurons to a SAM Tone with Varied Modulation Depth**

**Hongzhe Li<sup>1</sup>, Jennifer Henderson Sabes<sup>2</sup>, Donal G Sinex<sup>3</sup>**

<sup>1</sup>*University of Washington,* <sup>2</sup>*University of California, San Francisco,* <sup>3</sup>*Utah State University*

Responses to sinusoidally amplitude modulated (SAM) tones with varied modulation depth (m) were recorded from neurons located in the central nucleus of the inferior colliculus of chinchillas. Discharge rate monotonically varied with m (rate-m function). Phase locking to the modulator frequency (fm), measured by vector strength, increased monotonically with m (synchrony-m function). The response synchronized to fm usually locked to the modulation peaks. Responses to one SAM tone (the target) were re-measured with an additional SAM tone (the interferer), in-phase with the same fm and with m=1, but whose carrier frequency was located 0.2 to 2 octaves away from that of the target. Such dual SAM-tone configuration mimicked the stimulus used to investigate psychophysical modulation detection interference. Introducing the interferer could produce responses that phase-locked to fm even when the target m=0. The response phase locked to either the peaks or valleys of the stimulus modulation, suggesting that the effect of the interferer SAM tone could be either excitatory or inhibitory. Notable changes were observed: inhibitory interferers typically shifted down the rate-m functions, while excitatory interferers often slightly shifted up synchrony-m functions. Overall, inhibitory interferers caused greater modification in rate-m and synchrony-m functions than excitatory interferers did; greater modification in these functions was observed when the separation in target-interferer carrier frequency was small (e.g. 0.2 oct) than when it was large (e.g. 2 oct).

In some neurons, effects of interferer out-of-phase with the target were also examined. In the in-phase condition, with an inhibitory interferer, response phase usually locked to the modulation valleys. Similarly, if an excitatory interferer was presented out-of-phase with the target, response phase could also lock to the modulation valleys with comparable synchrony. The similarity was also observed between the in-phase condition with excitatory interferers

and out-of-phase condition with inhibitory interferers. This suggests that reversing interferer phase plays little role on modifying response phase across neurons, and possibly the amount of average response synchrony. (Supported by NIDCD DC00341)

### **969 Inferior Colliculus Neurons Extract Temporal Features of Signals Presented in Background Noise**

**Kathy Barsz<sup>1</sup>, Joseph Walton<sup>1</sup>**

<sup>1</sup>*University of Rochester Medical Center*

Extracting features in noisy backgrounds is a remarkable capability of the auditory system. Previous research has shown the importance of temporal cues in this process; speech sounds can be distinguished based on temporal features alone. We studied the neural basis for this by measuring minimum gap thresholds (MGTs) and modulation transfer functions (MTFs) of the same single IC units recorded from normal hearing C57 and CBA mice. Stimuli were presented at optimum levels in quiet and in continuous background noise (CBN: 6 dB SNR). MGT was defined statistically as the shortest gap that elicited a reduced response in the gap or increased response after the gap; if MGT was minimally changed in CBN the unit was classified as specialized for gap encoding. MTFs were analyzed for both rate encoding (rMTF) and phase-locking (sMTF). The rMTF included any modulation frequency which elicited a markedly stronger response than the other frequencies tested. The sMTF included those units in which a clear phase-locked response occurred to the AM envelope. If either measure was minimally changed in CBN relative to quiet, the unit was classified as specialized for AM encoding. When CBN masked the temporal encoding, the unit was classified as non-specialized. Our preliminary analysis indicated that 47 of 100 units were specialized for encoding both gaps and AM in 6 dB SNR, 17 units were specialized for gaps only, 17 units were specialized for AM only, and 19 units were non-specialized, i.e. they encoded neither gaps nor AM in 6 dB SNR. The proportions were strikingly similar in C57 and CBA samples. Thus, in young, normal hearing mice, 80% of IC units were specialized for temporal encoding in CBN, and over half of those encoded both gaps and AM in CBN. These results indicate that a large proportion of IC neurons can encode both static (various gap durations) and dynamic (various AM rates) temporal features in high levels of background noise. Supported by USPS PO1 AG09524

### **970 Responses of Inferior Colliculus Neurons to Simultaneous Complex Tones with Different Fundamental Frequencies**

**Donal Sinex<sup>1</sup>, Hongzhe Li<sup>1</sup>**

<sup>1</sup>*Utah State University*

The auditory system can segregate sounds that overlap in time and frequency, if the sounds differ in acoustic properties such as fundamental frequency (f<sub>0</sub>). However, the neural mechanisms that underlie this ability are poorly understood. Responses of neurons in the inferior

colliculus (IC) of the chinchilla to simultaneous complex tones with different f<sub>0</sub> were measured, to determine how the representation of competing sounds differs from the representation of single complex tones. As reported previously, IC responses to single harmonic complex tones usually have no stimulus-related temporal pattern, or they may exhibit a simple envelope modulated at f<sub>0</sub>. When a second harmonic tone was added, complex slowly-modulated discharge patterns were observed. The response envelope varied with the difference in f<sub>0</sub> and with overall level. The envelope also varied with the relative levels of the two tones; complex temporal patterns were observed when levels were equal, but as the level difference increased, the discharge pattern reverted to that associated with single harmonic tones. A computational model of spectral integration developed in a previous study of mistuned tones was able to reproduce the temporal patterns elicited from IC neurons by competing complex tones. This suggests that the processes incorporated in the model, notably narrowband envelope extraction and integration across relatively large frequency ranges, contribute to the representation of simultaneous complex tones.

### **971 Mapping of Neurons Selective for Sinusoidal Frequency Modulations in the Inferior Colliculus of the Big Brown Bat, *Eptesicus Fuscus*.**

**Qi Yue<sup>1</sup>, Ellen Covey<sup>1</sup>, John H. Casseday<sup>1</sup>**

<sup>1</sup>*University of Washington*

Most communication and echolocation sounds, including those used by big brown bat, contain frequency-modulated components, including sinusoidal frequency modulation (SFM). Previous studies have shown that some neurons in the inferior colliculus (IC) of the big brown bat are specialized for responding to SFM signals. In this study, we examined the responses and locations of SFM-selective neurons in the IC, using extracellular recordings. When an SFM-selective neuron was encountered, we first characterized its response to different SFM parameters and then marked the site with a small iontophoretic injection of biotin dextran amine (BDA). We classified cells as SFM-selective if they responded exclusively or best to SFM, and did not respond to pure tones. All of the SFM-selective cells that we obtained showed high sensitivity to at least one of the four main parameters that we varied, SFM center frequency, modulation rate, modulation depth and amplitude. Most of the SFM-selective cells had extremely low thresholds, usually below 15 dB SPL. Most also had closed response areas, i.e., had an upper threshold as well as a lower one. These findings indicate that most SFM-selective cells only respond to a narrow range of amplitude. For SFM-selective cells with spontaneous activity, the spontaneous activity was eliminated throughout the stimulus when the sound amplitude was above their upper threshold, with spontaneous discharge resuming after the stimulus was over. This finding indicates that the amplitude tuning of these neurons was likely created by inhibitory inputs. The histological data revealed that all SFM-selective cells were



located in the rostro-dorsal part of the IC. No SFM-selective cells were found below 1000 microns depth in the IC. The anatomical data also indicates that SFM-selective cells are found in clusters within the rostral and dorsal part of the IC.

Supported by NIH grants DC-00287 and DC-00607.

### **972 The Neural Basis of Temporal Coding in the South African Clawed Frog**

Taffeta Elliott<sup>1</sup>, Jakob Christensen-Dalsgaard<sup>2</sup>, Darcy Kelley<sup>1</sup>

<sup>1</sup>Columbia University, <sup>2</sup>Southern Denmark University

The calls of the South African clawed frog, *Xenopus laevis*, consist of trains of clicks. The two female calls differ primarily in click rate and elicit distinct behavioral responses in males. To understand how the auditory system processes click rate, we investigate the representation of calls in the auditory nerve, the dorsal medullary nucleus (DMN), and the laminar nucleus of the torus semicircularis. We record *in vivo* in frogs stimulated with both pure tones and recorded calls. Auditory nerve fibers and DMN cells show no preference for click rate but synchronize to click envelopes. Preliminary recordings in the TS indicate that some cells may be selective for lower click rates characteristic of female call types. Rate-sensitive cells found in a preliminary experiment discharged phasically with single spikes or bursts when presented with pure tones.

### **973 Neural Responses Selective to Duration in the Inferior Colliculus of Guinea Pigs**

Jian Wang<sup>1</sup>

<sup>1</sup>Dalhousie University

Duration information of acoustic signals is clearly encoded as duration turning in neural responses in auditory neurons of echolocating animals. It has been suggested that, neural tuning to the duration of sound would provide an additional filter beside those for frequency and intensity in those animals. Such duration turning has also been reported in non-specific mammals in a few studies of recent years, but has not been extensively studied. In this study, duration turning of single neurons in the inferior colliculus (IC) of guinea pigs were evaluated in response to narrowband as well as broadband signals of different duration at different presenting levels. Weak duration turning was evident in more than 50% of IC neurons. Those who showed duration turning to narrowband signal may not show similar turning in response to broadband signals. In some neurons, antagonists to inhibitory neurotransmitters were applied through microiontophoresis to evaluate the role of local inhibition on duration turning.

### **974 Responses to Amplitude Modulation in Inferior Colliculus and Thalamus**

Lucy Anderson<sup>1</sup>, Trevor Shackleton<sup>1</sup>, Alan Palmer<sup>1</sup>

<sup>1</sup>MRC Institute of Hearing Research, Nottingham, NG7 2RD, UK

We compare the responses of neurones in the inferior colliculus (IC) and medial geniculate nucleus (MGN) of the

anaesthetised guinea pig to sinusoidally amplitude modulated signals. In the IC, we recorded single unit activity to 100% amplitude-modulated best-frequency tones, while in the MGN we used 100% amplitude modulated noise, because responses were recorded using an eight channel multi-electrode array which simultaneously spanned different best frequencies. Both rate (rMTFs) and synchronised rate modulation transfer functions (tMTFs) were measured. MTF types found in the IC were consistent with previous IC reports, and were also observed in the MGN. In both IC and MGN, rMTFs showed a variety of shapes while tMTFs tended to be either low pass or band pass. MTF's of IC neurones showed a greater response modulation, higher best modulation frequencies, and upper-frequency limits for significant synchronisation compared to MGN neurones. Band pass tMTFs were more commonly observed in the IC (51%) than in the MGN (30%). We also tested the hypothesis that the medial division of the MGN might signal amplitude variations to higher frequencies than the ventral division. However, while 16% of medial MGN neurones were capable of following modulation frequencies  $\geq 200$  Hz, the ventral MGN also contained 4% of neurones which could follow these higher rates. The present results are consistent with the hypothesis that sensitivity to temporal variations in the stimulus envelope becomes progressively restricted to lower frequencies ascending the auditory pathway.

### **975 Predicting Responses of Neurons in Bat Inferior Colliculus to Social Communication Calls**

Sari Andoni<sup>1</sup>, Na Li<sup>1</sup>, George Pollak<sup>1</sup>

<sup>1</sup>University of Texas at Austin

In order to better understand how neurons in the inferior colliculus (IC) process complex social communication calls, a spectral-temporal receptive field (STRF) was derived using dynamic moving ripple stimuli. We recorded the extracellular response to a set of upward and downward moving ripple stimuli, which make the Fourier basis components of the spectral-temporal domain. Reverse correlation technique was then utilized to derive a linear representation of excitation and inhibition that drive or suppress the response of the cell for a given spectral and temporal range. For the vast majority of cells, the best frequency (BF) obtained from the STRF was in strong agreement with the BF obtained from the classical tuning curve. To further verify the validity of the STRF model, a large set of species-specific social communication calls were convolved with the STRF and a predicted response of the cell was obtained for each call. The predicted response was then correlated with the actual response of the cell to these specific calls and a correlation coefficient was calculated. In many cells the predicted response was highly correlated with the actual response of the cell, which showed that the STRF had captured most of the response properties of these cells. Given a large set of bat social communication calls that are different in their spectral and temporal properties, we were able to extract the properties that inhibit or excite cells in the IC as well as accurately

predict the total response of each cell to these specific calls. Supported by NIH Grant NS 00268.

### **976 Intracellular Responses of Inferior Colliculus Neurons to a Train of Sound Pulses in Awake Little Brown Bats**

**Sergiy Voytenko<sup>1</sup>, Alexander Galazyuk<sup>1</sup>**

<sup>1</sup>*NEOUCOM, Rootstown, OH*

Sounds in the real world seldom occur in isolation. In spite of this, most studies for the auditory system have employed low repetition-rate stimuli. It is unclear whether these basic neural response properties are applicable to real-world situations where sounds usually occur in rapid succession. Recently we showed that the majority of inferior colliculus (IC) neurons respond to isolated sound pulses with long-lasting suppression of their spontaneous but not driven activity. This long-lasting suppression averaged 200 ms and was particularly evident at high intensities. Results of this study suggest that such suppression is presynaptic. In order to get further insight into this phenomenon we investigated intracellular driven responses in IC neurons during this selective response suppression. Postsynaptic potentials were recorded in awake little brown bats in response to short (4 ms) frequency modulated pairs of sound pulses (downward sweep from 80 to 20 kHz) with varied inter-pulse intervals varying from 1 to 300 ms. Sound level of the first pulse (pulse) was fixed at 80 dB SPL, whereas the second pulse (probe) level was either the same or 20 dB weaker than the first. Our data show that in more than half of IC neurons, postsynaptic responses to pulse and probe stimuli were similar and independent of inter-pulse interval. However, some neurons showed response facilitation to the probe during a limited time after the unit's response to the pulse. During this time, the unit's spontaneous activity was deeply suppressed. Since, driven responses of nearly every IC neuron contain both excitatory and inhibitory components, the response facilitation to the probe involved a change in balance between excitation and inhibition. An increase of inhibition could also create facilitation via an enhanced postinhibitory rebound. Research is supported by grant from the National Institute for Deafness and Other Communicative Disorders (NIH R01 DC005377).

### **977 Comparison of Online and Offline Spike-Sorting to Classify Multi-Channel Receptive Field Recordings from Mouse Inferior Colliculus Neurons**

**Joseph Walton<sup>1</sup>, Paul Allen<sup>1</sup>, Kathy Barsz<sup>1</sup>**

<sup>1</sup>*University of Rochester*

Simultaneous multi-electrode recordings place demands on analysis techniques not usually encountered in single-unit electrophysiology. Here we compare online spike sorting with 2 different offline spike sorting and clustering techniques applied to multi-unit activity (MUA) and single units (SU) recorded from the mouse IC using a 16 channel multi-electrode (courtesy of CNCT, Univ. Michigan) and OpenEx (TDT) front end. The OpenEx platform allowed for real-time display of neural events that exceed a voltage

threshold. Events were sampled at 24 kHz, stored with 30 data points per event, and coded as MUA or SU (S/N >2:1). To verify the quality of the real time sort, we performed offline spike sorting manually, based on the first two principle components (PC) of the events. Comparison of the PCA based sort with online sorting illustrated that the online sort leads to substantial overlap of the classes in PC space. We then passed the PCs that accounted for >90% of the variance to AutoClass (AC), an unsupervised Bayesian analysis package. This method also resulted in over classification because the PC decomposition is weighted by the most numerous waveforms in the data; hence it tends to overfit to MUA and miss SU classes. Finally, we used the complete event waveform, comprised of 30 data points (1.25 msec), as input to AC. The results indicate that this method is more sensitive to voltage excursions from the mean at a given time point, which is characteristic of SU rather than MUA, and appears to yield more appropriate classifications. In each method the measurement error (intrinsic variability in the voltage/time waveform) was computed, and this influences the sort by establishing the voltage difference samples need to have to be considered potential members of different classes. We use these data to address the question of what constitutes the optimal sorting of combined MUA and SU events.

Supported by USPHS grant PO1 AG09524 and Glenn/AFAR (PA).

### **978 Adaptive Temporal Processing and the Precise Encoding of Vocalizations in the Songbird Auditory Midbrain**

**Sarah M. N. Woolley<sup>1</sup>, Frederic E. Theunissen<sup>1</sup>**

<sup>1</sup>*University of California, Berkeley*

Temporal processing is important for discriminating among and identifying vocalizations. In humans and songbirds, accurate vocal perception is possible when the auditory input is largely temporal. And impairments in speech perception are correlated with temporal processing disorders. Mechanisms whereby populations of auditory neurons encode the acoustic features that characterize vocalizations are not understood. Songbirds are skilled in auditory discrimination; they learn to distinguish among and recognize the songs of other birds. We used Spectro-temporal Receptive Fields (STRFs) to study the neural coding of a control, synthetic sound called modulation-limited (ml) noise versus the coding of conspecific song in the zebra finch auditory midbrain region, the mesencephalicus lateralis, pars dorsalis (MLd). We found that the time/frequency tuning of most single neurons (80%) differs when birds hear ml-noise and when birds hear song. During the processing of ml-noise, time/frequency tuning is variable across cells. During the processing of song, auditory tuning becomes more similar across cells, particularly in the temporal domain. Tuning adaptations during the processing of song reduce frequency selectivity, increase the rate of temporal modulation tuning and increase spiking precision across cells. The result is a population response that can precisely encode the temporal patterns of rapidly changing

sounds. Models of population responses to song, constructed using STRFs, suggest that the adaptations in temporal processing when birds hear song facilitate the accurate neural representation of a song's temporal information. This coding accuracy for the temporal information which characterizes a song is suggested as a neural mechanism for the behavioral discrimination of individual songs. Supported by: NIH grants DC05087 and MH59189

### **979 Neural Correlates of Across Channel Gap Detection in the Mouse Inferior Colliculus**

**Nicholas Schmuck<sup>1</sup>**, Paul Allen<sup>1</sup>, Joseph Walton<sup>1</sup>

<sup>1</sup>*University of Rochester*

Psychoacoustic measures of temporal acuity, using the classical gap detection paradigm, are thought to involve only one perceptual channel. Phillips and colleagues used a spatial gap paradigm to explore across-channel gap detection in the free-field by moving the second marker along the azimuthal plane. As the second marker moved into the contralateral spatial hemisphere gap thresholds increase systematically. In this study we searched for a neural correlate of cross-channel gap detection in the IC of 10 young CBA mice. Bipolar metal electrodes having tip diameters of 25-50  $\mu\text{m}$  and tip-to-tip spacing of 50-100  $\mu\text{m}$  were lowered into the dorsal ( $\sim 500 \mu\text{m}$ ) and ventral ( $>1300 \mu\text{m}$ ) IC under stereotaxic control. The standard gap series consists of two broadband noise bursts (NB1 and NB2), each 50 ms in duration separated by a silent gap having durations of 0.25 to 196 ms (log spacing), and single control NB1 fixed at  $-60^\circ$ . The NB2 speaker was fixed on a robotic arm and moved to  $-50^\circ$ ,  $0^\circ$ ,  $+60^\circ$  and  $+90^\circ$  azimuth. To control for binaural level differences the NB2 intensity was increased in 10 dB steps. Automated analysis of the RMS response of the near-field evoked potentials (NFAEPs) to NB1 and NB2 was done using a custom LabView program. Stimulus intensity affects gap recovery, with decreasing intensity yielding increased MGTs and impaired recovery rates and times. These effects increase as the second marker moves into the contralateral spatial hemisphere. Increasing the NB2 intensity at  $+60^\circ$  served to compensate for the binaural level difference effect on MGT, however the function never completely recovered, only to a level comparable to that at  $+0^\circ$ . Recording depth also affected gap encoding, with the effects of spatial separation of noise bursts producing greater impairment of gap recovery in the ventral IC. Finally, increasing the NB2 intensity by 20 dB at  $+60^\circ$  facilitates more complete recovery in ventral recordings as compared to recovery in the dorsal IC.

Supported by USPHS grant PO1 AG09524.

### **980 Spectro-Temporal Receptive Fields for Multiple-Single Unit Clusters and for Correlated Activity Between Unit Clusters in Cat Primary Auditory Cortex.**

**Jos Eggermont<sup>1</sup>**, Masahiko Tomita<sup>2</sup>

<sup>1</sup>*University of Calgary*, <sup>2</sup>*Niigata University*

Recordings were made from the right primary auditory cortex in 17 adult cats using two eight-electrode arrays. We recorded the neural activity under spontaneous firing conditions and during random, multi-frequency stimulation, at 65 dB SPL, from the same units. 281 multiple single-unit (MSU) recordings were stationary, through 900 s of silence and during 900 s of stimulation. The cross-correlograms of 545 MSU pairs with peak lag times within 10 ms from zero lag time were analyzed. Stimulation reduced the correlation in background activity and as a result the signal-to-noise ratio of correlated activity in response to the stimulus was enhanced. The cross-correlation for spikes contributing to the STRF depended much stronger on the STRF overlap than the cross-correlation during either silence or for spikes that did not contribute to the STRF (OUT-STRF). Compared to that for firings during silence the cross-correlation for the OUT-STRF spikes was much reduced despite the unchanged firing rate. This suggests that stimulation breaks up the large neural assembly that exists during long periods of silence into a stimulus related one and maybe several others. As a result, the OUT-STRF spikes of the unit pairs, now likely distributed across several assemblies, are less correlated than during long periods of silence. Reconstructed spectro-temporal receptive fields (STRFs) for coincident spikes showed larger STRF overlaps, and showed that coincident neural activity serves to sharpen the resolution in the spectro-temporal domain. Overlaps between all pairwise coincident spikes for all electrodes in the arrays were constructed and compared to those for coincidences between triplet recordings. As expected, the correlated-firing triplet-STRFs were sharpened compared to the pair-correlation ones. Comparisons were made between the correlated-firing STRFs and the uncorrelated-firing STRFs with respect to the amount of information they conveyed about the stimulus.

### **981 Response Modulation to Ongoing Broadband Sounds in Primary Auditory Cortex**

**Barak Shechter<sup>1</sup>**, Sridhar Kalluri<sup>1</sup>, Peter Marvit<sup>1</sup>, Heather D. Dobbins<sup>1</sup>, Yadong Ji<sup>1</sup>, Didier A. Depireux<sup>1</sup>

<sup>1</sup>*University of Maryland, Baltimore*

It is well-known that background noise does not interfere with one's ability to attend to a specific auditory stream. Driven by previous reports of adaptation to persistent stimuli in other brain regions, we investigated short term (1-2 sec) adaptive effects in the primary auditory cortex of an awake ferret (*Mustela putorius*). Electrophysiological data was obtained in response to the presentation of structured narrowband and broadband sounds. We demonstrate cortical response modulation to changes in

the structure of the spectrotemporal envelope of the stimulus.

### **982 The Neuronal Representation of Pitch in the Auditory Cortex of Awake Primates**

Daniel Bendor<sup>1</sup>, Xiaoqin Wang<sup>1</sup>

<sup>1</sup>Johns Hopkins University

Although the auditory system is cochleotopically organized, sounds are perceptually ordered according to their pitch rather than frequency. Complex sounds composed of multiple harmonically related frequency components produce a pitch, which is determined by the fundamental frequency (f<sub>0</sub>) of their periodicity and is unchanged when the harmonic at f<sub>0</sub> is removed ("missing fundamental" harmonic complex). Information related to a sound's pitch is embedded in the interspike intervals of the auditory nerve and further processed at higher auditory centers including the inferior colliculus. Lesion studies have indicated that auditory cortex is necessary for pitch perception. Because the average upper limit of stimulus synchronized firing in auditory cortex falls close to the lower limit of pitch (~30 Hz), the cortical representation of pitch is likely based on a rate/place code. Here we report the existence of neurons along the anterior lateral border of primary auditory cortex (AI) in awake marmoset monkeys that responded to both low frequency pure tones and missing fundamental harmonic complexes with the same pitch. These neurons did not respond significantly to the individual components of the missing fundamental harmonic complex. In addition, the response to a missing fundamental complex was unaffected by the addition of a 1-2 octave noise masker matched in sound level and centered at the sound's f<sub>0</sub>. These findings show that low frequency pitch (< ~500 Hz) is encoded by neurons in a region near the lateral portion of the low frequency border between primary auditory cortex (AI) and the rostral field (R).

Support Contributed By: NIH grants DC 03180 (X.W.), F31 DC 006528 (D.B.), DC 05211 (P30 Research Core)

### **983 Responses of Neurons in Primary Auditory Cortex of Marmoset Monkeys (Callithrix jacchus) Trained to Discriminate the Direction of Frequency Modulated Sweeps**

Ralph E. Beitel<sup>1</sup>, Maike Vollmer<sup>1</sup>, Steven W. Cheung<sup>1</sup>, Ben H. Bonham<sup>1</sup>, Benedicte Philibert<sup>1</sup>, Michael M. Merzenich<sup>1</sup>, Christoph E. Schreiner<sup>1</sup>

<sup>1</sup>W.M. Keck Center for Integrative Neuroscience, Otolaryngology-HNS, UCSF, San Francisco, CA

Animal vocalizations and human speech include frequency-modulated (FM) components that provide important spectral and temporal information in auditory perception. In this study we compared neuronal responses in primary auditory cortex (AI) evoked by FM sweeps in naïve and trained marmoset monkeys. The AI tonotopic map in this species spans from about 1 to 16 kHz, with isofrequency contours organized in an open fan-like fashion on the lateral surface of the temporal gyrus.

Discrimination of FM sweep direction was used in training. The signals (six sequential upward or downward sweeps; 125 ms ISI; 2-18 kHz; 33.2 octave/s) were presented randomly from a speaker. Monkeys initiated trials and were rewarded with a drop of juice for correct detection of FM sweep direction (downward or upward). Perceptual learning was documented to asymptotic levels of performance (~90 % correct detection).

Nine hemispheres in five anesthetized monkeys (three trained, two naïve) have been densely mapped using metal microelectrodes. Based on evoked spike counts, preliminary results show that: 1) direction selectivity varies with neuronal characteristic frequency (CF), changing in preference from upward to downward sweeps as CF increases; 2) for downward sweeps the latency of response increases as CF decreases; and 3) for upward sweeps the latency increases as CF increases. Our presentation will emphasize the effects of behavioral training on neuronal responses to upward and downward FM sweeps.

Supported by NS 34835, NS 10414, DC 02260, Veterans Affairs Medical Research

### **984 Neural Representations of Temporally Modulated Signals in the Medial Geniculate Body of Awake Marmoset Monkeys**

Edward Bartlett<sup>1</sup>, Xiaoqin Wang<sup>1</sup>

<sup>1</sup>Johns Hopkins University

In subcortical auditory nuclei, neurons represent temporal modulations primarily with spikes that are synchronized with the stimulus waveform or envelope. In the auditory cortex of awake primates, rapid temporal modulations are transformed into firing-rate based representations, while slow temporal modulations are represented by stimulus-synchronized discharges. While numerous studies have examined temporal coding in the inferior colliculus (IC) and auditory cortex, there have been relatively few studies of the medial geniculate body (MGB) of the thalamus, particularly in unanesthetized conditions. We tested the temporal processing capabilities of MGB neurons in awake marmoset monkeys using sinusoidally amplitude-modulated stimuli and repetitive click stimuli. We found that discharges of most MGB neurons were synchronized to a range of modulation frequencies intermediate between those of IC and auditory cortex. Unlike responses in the anesthetized MGB, a sizeable proportion of MGB neurons also displayed nonsynchronized discharges at high modulation frequencies. The nonsynchronized MGB responses appeared at higher modulation frequencies than those observed in auditory cortex and were complementary to the difference in the limits of synchronized responses in these two neural structures. Some MGB neurons exhibited both synchronized and nonsynchronized discharge patterns at low and high modulation frequencies, respectively, which was rarely observed in the auditory cortex. These observations suggest that synchronized and nonsynchronized discharges present in single MGB neurons may be processed differentially by separate populations of cortical neurons. Alternatively, the synchronized MGB responses

may represent feedforward inputs from IC, whereas the nonsynchronized responses may arise from corticothalamic feedback.

Supported by a grant from the Deafness Research Foundation (ELB) and NIH grants DC006357 (ELB), DC01380 (XW), DC05211 (P30 research core).

### **985 On the Spectro-Temporal Representation of Feature Onsets in AI**

Heather Dobbins<sup>1</sup>, Peter Marvit<sup>1</sup>, Barak Shechter<sup>1</sup>, Sridhar Kalluri<sup>1</sup>, Yadong Ji<sup>1</sup>, Didier Depireux<sup>1</sup>

<sup>1</sup>UMD, Baltimore

We are investigating how feature onsets of broadband stimuli such as speech are represented in the firing patterns of cortical neurons. However, a feature onset can be confounded by a stimulus onset, since there is a considerable change in level from silence to the level of the stimulus played. A level change of this magnitude tends to drive cortical neurons to respond no matter to which features they respond best. To circumvent this issue, a stimulus was used which contains transitions in features without a change in the mean level. This allows an examination of the encoding of feature onsets and offsets, or transients within a stimulus, by themselves - disentangled from the stimulus onset and offset responses (i.e. the abrupt and large change in level). In our experiments, we present these special broadband sounds to an awake ferret and use a multi-electrode array to record neuronal responses from the primary auditory cortex. We have found that there are different features in the stimuli transitions which are represented in the firing patterns of cortical neurons.

### **986 Differential Effects of Iontophoretic Application of the GABAA-Antagonists Bicuculline and Gabazine in Primary Auditory Cortex**

Simone Kurt<sup>1</sup>, John M. Crook<sup>2</sup>, Henning Scheich<sup>1</sup>, Holger Schulze<sup>1</sup>

<sup>1</sup>Leibniz Institute for Neurobiology, Magdeburg, Germany,

<sup>2</sup>Univ. of Newcastle, UK

The temporal structure of the envelope of speech sounds plays an important role in speech segmentation. Neurons in the primary auditory cortex (AI) have been shown to code for such slow amplitude modulations by phase-locking their responses to the envelope of sound. Here we investigate the role of intracortical inhibition in this type of temporal stimulus processing.

Single and multi-unit responses to pure tones and sinusoidally amplitude modulated (AM) tones were recorded from the left AI in anaesthetized and unanaesthetized Mongolian Gerbils before, during and after microiontophoretic application of one of the GABA<sub>A</sub>-receptor antagonists bicuculline (BIC) and Gabazine (SR) (15-80 nA; 10±2 min).

Before the application of one of the GABA<sub>A</sub>-receptor antagonists, responses of most units to AM tones showed phase-locking to the AM envelope at periodicities below 30 Hz. When GABA<sub>A</sub>-mediated inhibition was blocked by

application of either antagonist, we observed an increase of spontaneous and sound evoked activity. Interestingly, whereas a broadening of the spectral receptive fields was observed during the BIC condition, such broadening was not observed under the SR condition, but the effects of BIC and SR were similar when BIC was applied in very low doses. Furthermore, any phase-locked discharges that were seen in the AM responses before drug application were eliminated during application of BIC in high doses, but not during application of BIC in low doses or SR.

We conclude from these results that the broadening of frequency receptive fields and the disappearance of the phase-locked response components observed under high doses of BIC can not be explained by the BIC-induced blocking of GABA<sub>A</sub>-mediated inhibition, but rather seems to result from secondary BIC effects, e.g. the known influence of BIC onto Ca-dependent K-channels (cf. Heyer et al., 1981, *Neurology* 31:1381-1390). In contrast to what is reported in the literature the sharpness of tuning in AI therefore does not seem to be influenced by GABA<sub>A</sub>-mediated inhibition.

**Supported by DFG (German Science Foundation, grants SCHU 1272/1-2,3)**

### **987 Representation of Temporally Structured Acoustic Stimuli in Gerbil Auditory Cortical Neurons: Influences of Repetition Rate and Sound Intensity**

Dagmar Isheim<sup>1</sup>, Bernhard Gaese<sup>1</sup>, Manfred Koessl<sup>1</sup>

<sup>1</sup>J.W. Goethe University

We investigated the neuronal firing in cortical neurons synchronized to temporal features of acoustic stimuli. As temporally structured stimuli we used sinusoidally amplitude-modulated signals (SAM), repetitive tone pips, and click stimuli. Extracellular recordings in the gerbil primary auditory cortex were performed under ketamin/xylazine-anaesthesia, and acoustic stimuli were presented under free-field conditions.

In general, slow repetition rates up to 30 Hz are well represented in the temporal firing pattern of primary auditory cortical neurons, whereas neuronal responses at higher repetition rates were restricted to stimulus onset. Primary auditory cortical neurons reacted almost entirely in a low-pass manner. Only few neurons exhibited a band-pass characteristic. No strong differences were found between the different stimulus types.

Synchronization of neuronal activity was strongly influenced by varying sound intensity in a range well inside the tuning curve. Neurons either showed a monotonic increase in synchronization of neuronal firing with increasing sound intensities, or their synchronization was only strong in a restricted intensity range. Neuronal behavior in these cases depended on the stimulus type used, and three main classes of neurons could be distinguished: Firing patterns were either equal for all 3 stimulus types, or differed between SAM and the other stimuli used. About half of the neurons displayed monotonic increase of neuronal firing with higher sound intensity regardless of stimulus type. About 40% of the neurons showed monotonic increase to tone pips but

responded to SAM only in a a restricted range. The remaining neurons showed restricted firing independent of stimulus type.

Pharmacological manipulation with the GABAa-antagonist Bicucullin revealed changes in overall firing rate but had only little effect on the degree of temporal synchronization to the stimuli.

### **988 Macroscopic Spectro-Temporal Characterization of Primary Auditory Cortex Activity.**

**Nikolaos Kanlis<sup>1</sup>**, Shihab Shamma<sup>2,3</sup>, Jonathan Simon<sup>2,4</sup>, Didier Depireux<sup>5</sup>

<sup>1</sup>Raycap Corp, <sup>2</sup>University of Maryland, College Park, <sup>3</sup>Institute for System Research, <sup>4</sup>Institute for Systems Research, <sup>5</sup>University of Maryland, Baltimore

Using a single tungsten electrode, extracellular field potential recordings (EPs) were obtained along neuronal columns of the Primary Auditory Cortex of barbiturate-anaesthetized Ferrets (*Mustela Putorius*), in response to a complete set of broadband-dynamic acoustic stimuli (moving ripples). Starting from the pial surface at 0microns the electrode tip was advanced with depth-step increments of 100microns down to 1000microns - 1500microns, in a linear fashion perpendicular to the known laminar organization.

The EPs recorded along the different columnar depths displayed time-locked behaviour in response to dynamic ripples, similar to that reported in the literature for their Action potential (AP)counterparts (Shamma et.al 1998, Klein et.al 2000, Depireux et.al 2001), and with range of ripple-velocity-locking, covering most of the modulation-rate range mammalian brain is known to follow ( $\pm 30\text{Hz}$ ). With EPs in essence capturing the aggregate synaptic neural population activity, the construction of STRFs using those EPs (assuming quadrant separability), allowed us to quantitatively characterize the Spectro-Temporal properties of populations as a whole. Further, the parameters of those STRFs allowed us to make direct comparisons with the single-cell recording cases, and thus shed light on the transformations taking place as our view shifts from single-cell behaviour to macroscopic population activity. As expected from the nature of the EPs, there is definately an "averaging quality" governing the calculated STRFs, but this averaging taking place in the Transfer-Function (TF) domain. Specifically, there is strong evidence that only the common spots in the TFs of the contributing to the AEP neural elements eventually survive the AEP summation. Thus, the resulting aggregate TF functions appear with a single very distinct peak around a specific value of moving ripple velocity, a fact that is evident in the inseparability indices of the STRFs. This sharpening of the TF function manifests itself as ripple-like features and a "disperse" quality on the STRF side, e.g. without a central/focal frequency-time point.

### **989 Temporal Pattern Codes for Animal Vocalisations in Ferret Auditory Cortex**

**Jan Schnupp<sup>1</sup>**, Thomas Hall<sup>1</sup>, Bashir Ahmed<sup>1</sup>

<sup>1</sup>Oxford University

In 2001, Wang and Kadia compared responses from cat and marmoset (A1) to natural and time-reversed marmoset "twitter" calls. They reported that marmoset A1 neurons often "prefer" the natural to the time reversed call, while cat cortex did not exhibit any such specificity. Their data suggest that, within primate cortex, vocalisations may be represented through the activity of highly call specific neurons. However, while carnivores like cats lack call-specific neurons for vocalisations of other species, they still have to be able to detect and distinguish the vocalisations of many different species of animals. It seems highly likely that the "general purpose" auditory cortex of these animals represents such stimuli in the dynamic discharge pattern of cortical neurons, but so far little is known about the nature of this putative temporal code, its temporal resolution, or its information capacity.

We recorded responses to the same set of twitter calls used by Wang and Kadia from 236 auditory cortex units of 5 domitor/ketamine anaesthetised ferrets. As expected, spike rates carried only minimal amounts of information about call identity. We then devised a temporal pattern classifier algorithm to estimate the information contained in the temporal discharge patterns. Our algorithm used principal component analysis to reduce the dimensionality of the temporal patterns, and then assigned individual responses to the individual stimulus classes according to the "distance" of the response to other responses evoked by each stimulus. The proportion of correct classifications enables us to estimate the mutual information between stimuli and responses. For some units, the amounts of information contained in the temporal discharge pattern reached very respectable levels (up to 1.9 bits, compared to an entropy in the stimulus space of 2.6 bits). Over half of the units studied carried significant amounts of information about stimulus identity in their temporal response pattern, and of these ca 90% perform above chance in natural vs. time-reversed twitter discriminations. By repeating this analysis with coarser or finer binning of the temporal response patterns we were able to estimate the temporal resolution at which this temporal pattern information is represented. For most units, this decoding process worked optimally at temporal resolutions between 10 and 50 ms.

#### References

Wang X, Kadia SC (2001) Differential representation of species-specific primate vocalizations in the auditory cortices of marmoset and cat. *J Neurophysiol* 86:2616-2620.

## **990 Entropy-Based Analysis of Neuronal Spike Train Synchrony to Auditory Cyclic Stimulation.**

Yoshinao Kajikawa<sup>1</sup>, Troy Hackett<sup>2</sup>

<sup>1</sup>Vanderbilt University, Department of Psychology,

<sup>2</sup>Vanderbilt University School of Medicine, Department of Hearing & Speech Sciences

Synchronization of neuronal response to cyclic sound is often quantified by vector strength, assuming the temporal pattern is unimodal within a cycle. Its significance can be examined by the Rayleigh test. We analyzed synchronization of cortical neurons to repetitive trains (1 to 24 Hz) of upward sweeping frequency modulated tones (from 2 to 8 or 6 to 12 kHz, 30 msec duration) recorded in the auditory cortex of the ketamine-anesthetized marmoset monkey. Responses of some neurons were well entrained up to 20 Hz repetition rate. Other neurons showed good phase-locking, but also had multi-peaked phase histograms. Vector-based analyses were not applicable to those. Accordingly, we devised a new analysis method of synchronization based on entropy that can account for complex synchronization patterns, along with a statistical test of this analysis. Since the temporal structure of any spike train is determined by the serial order of inter-spike intervals, spike trains of degraded temporal patterns can be obtained by shuffling their serial sequence. From these shuffled spike trains entropic measures can be obtained and compared with the value of the original spike train. If it has a significant temporal pattern, then it will depart from the range of shuffled spike trains. Application of this analysis to data from the marmoset produced consistent results with visually apparent, but complex synchronization.

## **991 Effect of Stimulus Ensemble on Cortical Receptive Fields: A Comparison Between Rippled Noise and Natural Stimuli**

Nima Mesgarani<sup>1</sup>, Serin Atiani<sup>1</sup>, Mounya Elhilali<sup>1</sup>, Shihab Shamma<sup>1</sup>, Jonathan Fritz<sup>1</sup>

<sup>1</sup>Center for Acoustic and Auditory Research, Institute for Systems Research, University of Maryland

How do cortical neurons represent the acoustic environment? In previous work, we have described the linear filter properties of A1 cortical neurons by studying responses to static or dynamic rippled noise stimuli, and computing the neuronal spectrotemporal receptive field (STRF). In the present study, we probed neuronal responses in primary auditory cortex of awake ferrets with a variety of other complex acoustic stimulus ensembles. The stimulus set included two classes of natural sounds: (1) ferret vocalizations (FV) recorded from infants and adults, (2) human speech (HS) sounds (male and female voices) consisting of various sentences in English from the TIMIT database. In addition, we explored the linearity of cortical processing by predicting responses to a third stimulus set of rippled noise representations of speech sounds.

We recorded A1 neuronal responses in the awake ferret to these classes of complex natural stimuli to estimate

STRFs, using standard reverse correlation techniques. We compared FV-STRFs and HS-STRFs to the STRFs derived from responses to TORCs (temporally orthogonal ripple combinations) presented to the same individual neurons. Previous studies have suggested that the responses of cortical neurons to ripple stimuli and to English vowels can be well predicted by the linear STRF. Here, we also asked how well the TORC-STRF could predict responses to natural sounds and compared these predictions with those derived from the FV-STRFs and HS-STRFs. Based on these results, we discuss the influence of the stimulus basis set on the derived receptive field, and investigate the value of the *linear* receptive field model as a descriptor of sound processing in A1.

## **992 A Role for the Non-Primary Auditory Pathway in the Encoding of Slow Temporal Information: Implications for Speech Envelope Encoding**

Daniel Abrams<sup>1</sup>, Trent Nicol<sup>1</sup>, Nina Kraus<sup>1</sup>

<sup>1</sup>Northwestern University

A question that has gone largely unanswered in the neuroscience literature is that of the role of the non-primary auditory pathway. Here we provide evidence that this pathway may be essential to the encoding of slow temporal information in acoustic signals, which, in the case of speech, is critical for perception. In the somatosensory system, it has been shown that primary and non-primary nuclei in thalamus and cortex encode increases in stimulus rate between 2-8 Hz in fundamentally different ways: primary neurons show decreases in spike count, but constant response latencies; non-primary neurons show increases in response latencies. It has been hypothesized that a "phase-locked loop" characterizes this non-primary thalamocortical circuit, and could serve as an essential mechanism for encoding low-frequency temporal information in the somatosensory system (Ahissar et al., Nature, 406, 302-306). The implication for the auditory system is that a similar loop, with comparable connections and response latency characteristics, could provide an essential mechanism for encoding low-frequency temporal features (e.g., the speech envelope) of sound. To address this issue, temporal response properties of primary and non-primary auditory nuclei of the thalamus and cortex in anesthetized guinea pig were measured following presentation of click trains between 2-17 Hz. Preliminary results indicate that, with increasing click rate, response latencies increase only in the non-primary pathway while primary response latencies remain stable, suggesting that auditory and somatosensory systems share a similar mechanism for encoding low-frequency temporal information. These data suggest an important role for the elusive non-primary auditory pathway in the encoding of complex acoustic signals.

Supported by NIH R01 DC01510-10.

**993 Primary Auditory Cortex Forward Spectral Masking Dynamics in Squirrel Monkeys with Mild Unilateral Hearing Loss**

**Benedicte Philibert<sup>1</sup>**, Haruka Nakahara<sup>1</sup>, Christoph E. Schreiner<sup>1</sup>, Steven W. Cheung<sup>1</sup>

<sup>1</sup>*University of California San Francisco*

Mild unilateral low frequency hearing loss was induced in two adult squirrel monkeys by exposing them to a 1 kHz tone at 136 dB SPL for 3 hours under general anesthesia. The left ear was protected with acoustic foam. Six months later, frequency specific auditory brainstem responses confirmed the hearing loss configuration. Microelectrode recordings were performed in the primary auditory cortex (AI) that was contralateral to the impaired ear. A two-tone paradigm was used to measure forward spectral masking behavior.

Suppression was estimated by evaluating the reduction of activity imparted by one tone on the following tone. Each tone was 50msec in duration. The second tone, fixed in frequency to the CF of the neuron and 10-20 dB above response threshold, was presented 50 msec after the end of the first tone. The first tone varied in frequency, from -2 to +2.25 octaves centered about CF (20 conditions total). Suppression of the second tone response was quantified by normalization to the unmasked tone response. Suppression was strongest when the first and second tones were close in frequency. A comparison of average suppression index (2 normal animals (n = 106 CF > 1.4 kHz, n = 65 CF < 1.4 kHz); 2 hearing loss animals (n = 68 CF > 1.4 kHz, n = 75 CF < 1.4 kHz) ) for masker frequencies within an octave of CF, 0.5 to 1.5 octaves above CF and 0.5 to 1.5 octaves below CF showed the following: 1) For CFs above 1.4 kHz, there was no difference in the amount of suppression in all three frequency regions. 2) For CFs below 1.4 kHz (within the potential area of damage), suppression was substantially reduced at CF but not above or below CF in the hearing loss group. These data show different inhibitory strengths for separate neuronal populations (CFs < 1.4 kHz versus CFs > 1.4 kHz) following mild SNHL.

This work was supported by grants DC-02260, NS-34835, and VA Medical Research.

**994 Subdividing Cat Primary and Non-Primary Auditory Areas in the Cerebrum with Neurofilament Proteins Expressing SMI-32**

**Jeffrey G. Mellott<sup>1</sup>**, Estelle Van der Gucht<sup>2</sup>, Charles C. Lee<sup>3</sup>, David T. Larue<sup>3</sup>, Jeffery A. Winer<sup>3</sup>, Stephen G. Lomber<sup>1</sup>

<sup>1</sup>*The University of Texas at Dallas*, <sup>2</sup>*Katholieke Universiteit Leuven*, <sup>3</sup>*University of California at Berkeley*

Neurofilament protein revealed by the monoclonal antibody SMI-32 reliably identifies 13 areas in cat visual cortex. Here, we employed SMI-32 labeling to immunocytochemically characterize and delineate all areas of the cat auditory cortex. Cortical labeling was concentrated among 1) pyramidal cells within layers III, V, and VI and 2) dendritic features in all layers except I. Both criteria differentially labeled more than 10 behaviorally,

physiologically, and anatomically recognized auditory cortical areas of the cat. These 10 areas displayed individually unique patterns of affinity for the SMI-32 antibody: primary auditory cortex (AI), secondary auditory cortex (AII), dorsal zone (DZ), posterior auditory field (PAF), ventral posterior auditory field (VPAF), ventral auditory field (VAF), temporal cortex (T), insular cortex (In), anterior auditory field (AAF), and the auditory region of the anterior ectosylvian sulcus (fAES). Cortical borders fit into one of three categories: 1) sharp, 2) transitional, and 3) indefinite. Most borders were considered transitional, since transitions between areas were gradual. Cortical borders, PAF-VPAF and AII-VAF were sharp. For example, in PAF the somata are stained in layers III and V, while in VPAF only layer V contains immunopositive somata. The only cortical border considered indefinite was fAES/ectosylvian visual area (EVA) which was not unexpected given the multisensory functionality of AES. Physical variations in AES made it more difficult to discern these local boundaries. The distinct neurofilament protein revealed for each of the 10 cortical regions was replicated and observed in each case regardless of which of the three laboratories processed the immunocytochemistry. The ability to distinguish auditory areas with SMI-32 is a valuable correlative technique for experimental identification of cerebral areas in electrophysiological, anatomical, and/or behavioral investigations. *Supported By: NSF IBN0424582 & NIDCD R01DC02319.*

**995 Spatial and Non-Spatial Processing of Auditory Stimuli in the Ventrolateral Prefrontal Cortex**

**Yale Cohen<sup>1</sup>**, Brian Russ<sup>1</sup>, Gordon Gifford<sup>1</sup>, Ruwan Kiringoda<sup>1</sup>, Katherine MacLean<sup>1</sup>

<sup>1</sup>*Dartmouth College*

In primates, it is hypothesized that a “dorsal” cortical pathway processes the spatial attributes of a stimulus, and a “ventral” pathway processes the non-spatial attributes. We tested the spatial and non-spatial response properties of neurons in an area of the ventral pathway, the ventrolateral prefrontal cortex (vPFC). In the first set of experiments, we tested 48 vPFC neurons using procedures mirroring those used to test the spatial and non-spatial properties of neurons in the auditory cortex (Tian et al., 2001). During a visual-fixation task, single-unit recordings were obtained while 1 of 7 different vocalization exemplars were presented from 1 of 7 speakers that spanned a range from 60° left to 60° right. vPFC neurons were significantly modulated by the non-spatial and spatial attributes of an auditory stimulus. The sensitivity of vPFC neurons was intermediate between that seen in areas in the auditory cortex hypothesized to be functionally specialized for processing the spatial attributes (caudomedial belt) and non-spatial attributes (anterolateral belt). In a second set of experiments, we tested 71 vPFC neurons using experimental procedures mirroring those we used to test the spatial and non-spatial properties of neurons in the lateral intraparietal area (area LIP). During a visual-fixation task, single-unit recordings were obtained while vocalizations or band-pass noise were presented from the location of a neuron’s response-field peak or a



location 180° contralateral; these two locations were separated by 24°. Once again, vPFC neurons were modulated by both the spatial and non-spatial attributes of an auditory stimulus. On average, the selectivity of vPFC neurons for the spatial and non-spatial attributes of an auditory stimulus was comparable to that in area LIP. Together, these data suggest that substantial spatial and non-spatial processing occurs in both the dorsal and ventral pathways.

### **996 Spatial Sensitivity of Neurons in the Anterior Field (AAF) of Cat Auditory Cortex**

Ian A. Harrington<sup>1</sup>, G. Christopher Stecker<sup>2</sup>, Ewan A. Macpherson<sup>1</sup>, John C. Middlebrooks<sup>1</sup>

<sup>1</sup>University of Michigan, <sup>2</sup>VA Research Service, Martinez CA

We evaluated the spatial tuning properties of neurons in the anterior auditory field (AAF) and compared them with those previously observed in the primary (A1) and posterior auditory fields (PAF). Together, AAF and A1 constitute the cat's auditory core, whereas PAF is one of several higher-order fields of the auditory belt. We recorded extracellular responses from the right hemispheres of  $\alpha$ -chloralose-anesthetized cats. Stimuli were 80-ms noise bursts presented from loudspeakers spaced 20 degrees apart in azimuth or elevation. Consistent with its inclusion in the auditory core, response latencies in AAF were short, indeed, slightly shorter than in A1, and rate-level functions were highly monotonic. In contrast to PAF, response latencies in AAF and A1 were not strongly modulated by changes in stimulus location. Several measures of spatial tuning were derived from rate-azimuth functions (RAFs). Azimuth centroids—defined as the spike-count weighted center of mass of the RAF peak—were undefined for the majority of AAF units because their spike counts were so weakly modulated, particularly at higher stimulus levels. When centroids could be defined, they were located near the lateral pole of the contralateral hemifield (−90°) or near the acoustic axis of the contralateral pinna (−45°). The transmission of spatial information was estimated using a pattern recognition algorithm that classified the temporal pattern of each neural response according to the sound source location likely to have elicited it. Perhaps not unexpectedly, neurons in AAF and A1 transmitted less spatial information than neurons in PAF. These results indicate that AAF shows no specialization for spatial hearing and, thus, suggest that it participates in auditory functions that generalize across space.

Supported by: NIDCD, NSF-DBI, UM CNCT (NIH NCRR)

### **997 Proximity Trumps Stimulus Level in Cortical Masking**

Leonard Kitzes<sup>1</sup>, Kyle Nakamoto<sup>1</sup>, Jiping Zhang<sup>1</sup>

<sup>1</sup>University of California, Irvine

Responses of single units in the primary auditory cortex (A1) to a matrix of CF tones varying in inter-aural level (ILD,  $\pm 20$  dB) and average binaural level (ABL, 0 - 70) typically exhibit a focus of maximal responses that systematically decline as stimuli progressively depart from

the optimal stimuli. The level response area (LRA) can occupy a small or large portion of the binaural matrix. The preferred binaural combinations (PBC, i.e., the set of contiguous stimuli that evokes  $\geq 80\%$  of the maximal response) is often a small portion of the LRA. The centers of the PBCs vary over the entire ILD and ABL range. Those of monotonic and nonmonotonic units occupy the upper and lower ranges of ABL, respectively.

We assessed the influence of stimulus history on cortical LRAs. Recording the responses of single units in AI of pentobarbital anesthetized cats to a forward masking paradigm (ISI  $\geq 50$  ms), we have determined that (1) the closer the masker is to the PBC, the greater the contraction and reduction of the LRA. A high level masker has minimal or no effect on a low ABL-range LRA and, similarly, a low level masker has minimal or no effect on a high ABL-range LRA. (2) A contracted LRA remains organized in that stimuli within the control PBC evoke the strongest responses. (3) There is directionality to the masking in that the portion of the LRA closest to the masker contracts most. This directionality suggests the selective inhibition of inputs to the LRA. (4) At the level of the individual trial, the suppression does not depend on the size of the response to the preceding masker. The LRA contraction is stimulus dependent, not response dependent.

Therefore, the LRA of AI neurons is not a hard-wired response parameter. The size, shape and response-magnitude of the LRA are conditioned by the stimulus history. Broad LRAs in the quiet may be useful for stimulus detection; LRAs contracted by preceding stimuli may be useful for stimulus discrimination.

### **998 Thalamocortical Connections of the Medial Belt Auditory Cortex of Marmoset Monkeys**

Lisa de la Mothe<sup>1</sup>, Suzanne Blumell<sup>2</sup>, Yoshinao Kajikawa<sup>1</sup>, Troy A. Hackett<sup>1,2</sup>

<sup>1</sup>Vanderbilt University, Department of Psychology,

<sup>2</sup>Vanderbilt University, Department of Hearing and Speech Sciences

The current working model of primate auditory cortex groups areas into three levels of processing. A primary level, the core, is surrounded by a secondary level, the belt, medial and lateral to the core. A third level of processing, the parabelt, is located lateral to the belt. The medial belt areas lie adjacent to the fundus of the lateral sulcus on its ventral bank, which poses difficulties for direct access and study. Accordingly, little is known about the connections of these areas. In the present study, the thalamocortical connections of the rostral (RM) and caudal (CM) medial belt areas were determined by placing tracer injections into medial belt and surrounding auditory areas of the marmoset monkey (*Callithrix jacchus jacchus*). Both areas received projections from the medial and dorsal divisions of the medial geniculate complex (MGC). Labeled cells in the anterodorsal (MGad) division were present with CM injections, but absent after RM injections. In the posterodorsal division (MGpd), labeled cells were found ventrally after RM injections and dorsally after CM

injections. CM also received strong inputs from the supragenulate, limitans, medial pulvinar, posterior, and intralaminar nuclei. Thalamic inputs to RM appeared to come mainly from the MGC. The patterns of connections are consistent with the presence of multisensory convergence in the caudal belt, and support the hypothesis that CM and RM represent functionally distinct areas of the medial belt cortex.

### **999** Suppression of Hearing Following Electrical Stimulation of Human Auditory Cortex

**Albert Fenoy**<sup>1</sup>, Meryl Severson<sup>1</sup>, Igor Volkov<sup>1</sup>, John Brugge<sup>1,2</sup>, Matthew Howard<sup>1</sup>

<sup>1</sup>University of Iowa, <sup>2</sup>University of Wisconsin

During electrical stimulation mapping (ESM) neurosurgical patients report percepts while electrical pulse trains (50-100 Hz) are delivered to localized cortical regions. Here we describe in two patients with chronically implanted intracranial electrode arrays suppression of their hearing when ESM stimuli were applied to localized regions of the superior temporal gyrus (STG). One patient also experienced tinnitus suppression. These findings are related to auditory evoked potential maps obtained using a variety of acoustic stimuli and, in one patient, to results of electrical stimulation tract tracing. MRI and intra-operative photographic images aided in anatomically localizing recording and stimulating sites. Suppression of hearing airborne sound and of tinnitus was induced by electrical stimulation of circumscribed regions of STG auditory cortex. Moving the stimulating electrode as little as 5 mm could eliminate the effect. Both patients experienced suppression effects with electrical stimulation of acoustically mapped sites within Heschl's gyrus. One patient experienced similar effects when the stimulus was applied to auditory area PLST on the posterior lateral STG (Howard et al. 2000). In both cases suppression effects persisted for seconds following electrical stimulation. These findings confirm Penfield's original observations and are consistent with two recent reports. By combining electrical stimulation mapping with electrophysiological recording we are gaining new insights into the functional organization of human auditory cortex. (Supported by DC04290, Hoover Fund)

De Ridder D et al. *J. Neurosurg* 100: 560-564, 2004.

Howard MA et al. *J. CompNeurol* 416: 76-92, 2000.

Penfield W and Perot P. *Brain* 86: 595-696, 1963.

Sinha SR et al. *Neurology* (in press), 2004.

### **1000** Identification of Brainstem Auditory Pathways Targeted by Cortical Axons

**Diana Coomes**<sup>1</sup>, Brett Schofield<sup>1</sup>

<sup>1</sup>University of Louisville

Multilabeling techniques were applied in guinea pigs to identify brainstem circuits that are targeted by auditory cortical projections. In each experiment, we injected an anterograde tracer into auditory cortex (AC) to label corticofugal axons. We also injected one or more retrograde tracers into different subcortical structures -

cochlear nucleus (CN), superior olivary complex (SOC), inferior colliculus (IC), or medial geniculate nucleus (MG) - to label specific brainstem pathways. We then examined retrogradely labeled cells for evidence of contacts by anterogradely-labeled cortical axons.

In the CN, we observed contacts between cortical axons and cells that project to the ipsilateral or contralateral IC. Contacts were present on the same side as the injected cortex as well as on the opposite side, and were present in both the dorsal and ventral CN.

In the SOC, we observed contacts on cells that project to the IC or the CN. Contacts were more common on the side ipsilateral to the injected AC, and were observed in almost all SOC nuclei. On both sides of the brain, contacts occurred on cells that project to the ipsilateral or contralateral IC as well as on cells that project to the ipsilateral or contralateral CN.

In the IC, we observed contacts on cells that project to the MG, the SOC or the CN. Contacts were present in the dorsal cortex and external cortex of the IC ipsilateral to the cortical injection.

In summary, corticofugal projections contact both ascending and descending pathways that originate at many brainstem levels. One result is a network of pathways that provide multiple routes for descending corticofugal influence. For example, cortex could affect the CN via direct projections as well as indirect (i.e., disynaptic) pathways through the IC and SOC. The cortical projections also establish a series of loops by which cortex could affect activity at many points within the ascending pathways. The results suggest that multiple routes could underlie corticofugal effects at each level of the brainstem auditory pathways.

### **1001** A Cortical Analysis of the Laterality of the Planum Temporale in Hearing, Hearing-Impaired and Central Auditory Processing Disorder Subjects

**J. Tilak Ratnanather**<sup>1,2</sup>, Clare Poynton<sup>1</sup>, Elvan Ceyhan<sup>1</sup>, Anne Osdoit<sup>2,3</sup>, Dana Boatman<sup>3</sup>

<sup>1</sup>Center for Imaging Science, Johns Hopkins University, Baltimore, MD 21218, <sup>2</sup>Dept of Biomedical Engineering, Johns Hopkins University, Baltimore, MD 21218, <sup>3</sup>Depts of Neurology and Otolaryngology, Johns Hopkins Univ. Sch. of Medicine, Baltimore, MD 21218

The highly lateralized planum temporale (PT) is the substrate of speech and language processing in the human auditory cortex. Recent imaging studies (Emmorey et al., *PNAS*, 100, 10049, 2003; Penhune et al., *NeuroImage*, 20, 1215, 2003) have shown structural differences in auditory cortex of hearing (H) and hearing-impaired (HI) subjects. Other studies have shown differences in functional responses in the PT in HI and central auditory processing disorders (CAPD) subjects. But little is known about the morphometric properties of the PT in these groups, particularly non-signing HI subjects using hearing-aids.

Semi-automated methods (Ratnanather et al., *NeuroImage*, 20, 359, 2003) were used to analyze MRI scans of 20 subjects (H: n=9; CAPD: n=8; HI: n=3).

Regions enclosing the superior temporal gyrus were masked, segmented into gray (GM) and white (WM) matter tissues that were used to generate the GM/WM surface. Distances of GM voxels closest to the delineated PT surface were collected to give the PT GM cortical mantle. A labeled cortical mantle depth map associating a distance with each GM voxel (Miller et al., PNAS, 100, 15172, 2003) was also generated.

The volume and surface area in the left PT were significantly larger than in the right for the H subjects (resp.  $p = .0075$ ,  $p = .0027$ ). The left PT surface area was smaller in CAPD than in H subjects ( $p = .0478$ ). The left PT was thinner than the right in each group ( $p \approx .0000$ ). Stochastic ordering for PT thickness between groups showed  $LHI < LH$ ,  $LCAPD < LH$ ,  $RHI > RH$  and  $RHI > RCAPD$  ( $p \approx .0000$ ) where L and R respectively denote left and right. The results are discussed in light of the suggestion that the left PT is thinner due to its cortical columns being farther apart than in the right PT accounting for processing differences (Harasty et al., Lateral, 8,247,2003).

Supported by R01-DC005645, P41-RR15241 and NOHR.

### **1002 Primary Auditory Corticocortical Connections in the Normal Mouse**

Noah Meltzer<sup>1</sup>, David Ryugo<sup>1</sup>

<sup>1</sup>Johns Hopkins University

Cochlear implantation yields variable performance outcomes. Prelingually deafened individuals exhibit poorer outcomes compared to postlingually deafened individuals. Functional imaging studies of such individuals seem to correlate area of auditory-evoked cortical activation to implant benefit. Collectively, the studies suggest that auditory stimulation activates widespread cortical regions in normal hearing individuals but activates only primary auditory cortex in long-term, congenitally deaf individuals. One possible explanation for these observations is that auditory corticocortical connections develop abnormally in the absence of sound stimulation.

A first step in understanding the impact of deafness on auditory corticocortical organization is to determine the connection pattern in a strategic animal model. We used a combination of electrophysiological response properties, frequency mapping, cytochrome oxidase histochemistry, and neuronal tracers to describe a pattern of corticocortical projections in normal hearing mice. Following dye injections into primary auditory cortex and a 7-14 day survival, cortical tissue was flattened and sectioned. Distribution plots of retrogradely labeled cell bodies revealed a reproducible corticocortical connection pattern ( $n=5$ ). The location of these cells was inferred to be in cortical areas 1, 2, 18a, 36, 36a, 22, 40, 41, and entorhinal cortex (Caviness 1975; Woolsey 1975; Wallace 1984).

These data represent a description of the primary auditory corticocortical connections in the mouse. The results suggest that we can utilize the mouse as a model for testing ideas about the effects of deafness on corticocortical connections. It is our working hypothesis that some variable outcomes in cochlear implant users

may be understood by investigating the effects of deafness on cerebrocortical organization in the mouse.

Supported by NIH/NIDCD grant DC00232 and DC00027.

### **1003 Investigating Auditory-Visual Interactions in Ferret Auditory Cortex**

Jennifer Bizley<sup>1</sup>, Fernando Nodal<sup>1</sup>, Israel Nelken<sup>2</sup>, Andrew King<sup>1</sup>

<sup>1</sup>University of Oxford, <sup>2</sup>Hebrew University, Jerusalem

Recent imaging, electrophysiological and anatomical studies in a range of species suggest that the incidence of multisensory convergence in the cortex is much greater than previously thought. We used multi-electrode recording techniques to investigate the response properties of large numbers of neurons located in different areas of ferret auditory cortex. Stimuli were broadband noise bursts delivered to the contralateral ear or light flashes that filled much of the visual field of the contralateral eye, presented either simultaneously or separately. Based on measurements of mutual information between the spike discharges and the stimulus eliciting them, we found that the auditory responses of around 35% of neurons recorded throughout much of the auditory cortex were significantly modulated by the presence of simultaneous visual stimulation. In non-tonotopic auditory cortex and tonotopically-organised secondary areas, and on the fringes of the primary areas, we observed a range of multisensory interactions, including both response enhancement and response suppression. Neurons exhibiting a robust response to visual stimulation by itself were most often, but not exclusively, found on the anterior ectosylvian gyrus, which has previously been reported to receive auditory, visual and tactile inputs. These visual responses had onset latencies ranging from 50-200 ms. Multi-channel linear array recordings revealed that multisensory interactions were present in all cortical layers. These data suggest that there are widespread multisensory interactions occurring in what are traditionally defined as modality-specific areas. The presence of such interactions lends weight to the argument that few cortical areas are, in fact, truly unisensory. Rather, areas of sensory cortex appear to be dominated by one modality, while receiving other inputs that can modulate neuronal responses to the dominant modality.

### **1004 Thalamocortical Columns in the Guinea Pig Primary Auditory Cortex**

Mark Wallace<sup>1</sup>, Lucy Anderson<sup>1</sup>, Trevor Shackleton<sup>1</sup>, Alan Palmer<sup>1</sup>

<sup>1</sup>MRC Institute of Hearing Research, Nottingham, NG7 2RD, UK

In the visual system thalamic afferents carry sensory information which is then processed within a vertically arranged column in the primary visual cortex. A similar process may occur in auditory cortex and we tested to see if there was columnar processing in the primary auditory area (AI) of the guinea pig. A conspecific vocalization (chutter) was used along with pure tones to measure response latency and best threshold. The chutter has a rich source of acoustic transitions which can produce a

complex series of changes in the firing probability of auditory neurones in the forebrain. The stimuli were presented to anaesthetised guinea pigs via a closed sound system. Cortical units in AI responded to 63 different combinations of the 17 transitions within the chatter that affect firing probability. Units in the medial geniculate body gave the same types of specific, combination response patterns as occurred in the cortex and it seems likely that each structure contains the same range of response combinations. When cortical units were recorded in orthogonal tracks the best thresholds and latencies to pure tones, in layers II to IV, were usually very similar. By contrast when tangential tracks were used the thresholds and latencies often showed sudden large changes. In orthogonal tracks the correlations between the responses to chatter, from units in layers II and III, were usually very high ( $R^2 > 0.8$ ) whereas in tangential tracks there were sudden changes in the type of response to chatter. Thus all three parameters studied provided evidence of functional modules in the outer layers of AI where units have very similar response properties.

### **1005 Effects of Sleep on Processing Complex Sounds in Auditory Cortex**

**Elias Issa<sup>1</sup>, Xiaoqin Wang<sup>1</sup>**

<sup>1</sup>*Johns Hopkins University*

The behavioral state of an animal influences how sounds are processed in the auditory system. One important behavioral state relevant to survival is sleep. During sleep the auditory system still receives external inputs, but few sounds reach conscious perception. How the brain is processing these sounds differently remains largely unclear. Previous studies using limited stimulus ensembles have suggested that the change in cortical responses between asleep and awake states is a nonspecific change in response gain. Here, we have studied the neural responses of single units in the auditory cortex of the common marmoset while the animal naturally slept. We determined the animal's state of vigilance based on the spectral content of the EEG. We used a variety of simple and complex sounds to more completely characterize the change in neural responses between awake and asleep states. These stimuli included tones, noise, amplitude or frequency modulated tones, random spectral stimuli, click trains, and marmoset vocalizations. We hypothesized that slow-wave sleep (SWS) alters stimulus specificity in addition to attenuating overall firing rate. Consistent with this hypothesis, we found that, although ~65% of units changed their response for at least one stimulus set between wakefulness and SWS, a number of units showed a decrease in response for one stimulus set while increasing response for another stimulus set. Interestingly, the changes in firing rate appear to depend on the spectral content of stimuli. For broadband stimuli, the firing rate was often higher in the awake state. For tonal stimuli, the firing rate was often higher when the animal was in SWS. This difference suggests that the response gain for spectrally rich sounds is higher when the animal is awake and has implications for the degradation of spectral integration in auditory cortex during sleep.

Supported by a Whitaker Fellowship (EI) and NIH grants DC01380 (XW) and DC05211 (P30 Research Core).

### **1006 Histiotypic Methylphenidate-Induced Reduction of Spontaneous Activity in Cultured Auditory Cortical Networks.**

**Kamakshi Gopal<sup>1,2</sup>, Guenter W. Gross<sup>1,2</sup>**

<sup>1</sup>*University of North Texas*, <sup>2</sup>*Center for Network Neuroscience*

Dopamine plays an important role in motivation, attention (including auditory attention), reward and cognition. Methylphenidate (MPH or Ritalin) is a widely used drug in the treatment of attention deficit and hyperactivity disorder. Auditory processing disorders are commonly associated with attention disorders; hence, MPH is often prescribed to those with auditory processing disorders. MPH increases the availability of dopamine in the synaptic cleft by blocking the dopamine transporters. This increase in dopamine is thought to decrease the background firing rates and increase signal-to-noise ratios among the target neurons. It is postulated that this would enhance task specific signals and enhance the saliency of the incoming stimuli. The study characterized the effects of acute application of MPH on spontaneously active auditory cortical networks (ACN) growing in culture on multielectrode arrays. Auditory cortical neurons dissociated from auditory cortices of 15-16 day old mouse embryos were grown on photoetched multielectrode arrays, which contained 64 transparent indium-tin oxide electrodes. Mature ACNs (at least 21 days in vitro) that were spontaneously active were coupled to the recording chambers for continuous extracellular recording of multisite action potentials before and after ACNs were exposed to various concentrations of MPH. Results from 10 ACNs (total number of neurons = 281) indicated that serial additions of 1-300  $\mu$ M MPH produced repeatable and quantifiable inhibition of the spike rate and burst rate activity. The IC<sub>50</sub> mean  $\pm$  S.E. for spike rates was  $170 \pm 13.9 \mu$ M. The inhibitory effects induced by MPH were reversible with a complete medium change. These results are comparable to published animal experiments, and demonstrate that nerve cells in culture retain pharmacological characteristics of the parent tissue.

### **1007 Tonotopic Representation of Stop Consonant Place of Articulation in Primary Auditory Cortex (A1) of the Awake Monkey.**

**Mitchell Steinschneider<sup>1</sup>, Yonatan Fishman<sup>1</sup>**

<sup>1</sup>*Albert Einstein College of Medicine*

In order to clarify neural mechanisms involved in the representation of stop consonant place of articulation (POA), we physiologically tested the hypothesis that onset spectral features are important for phonetic discrimination. This hypothesis proposes that /b/ and /d/ contain diffuse spectra maximal at lower and higher frequencies, respectively, while /g/ has a more compact spectrum maximal at intermediate frequencies (Blumstein & Stevens, JASA 1980: 67, 648-662). Multiunit activity evoked by the synthetic syllables /ba/, /ga/ and /da/ was

recorded in A1. The syllables differed in their spectral location of frication at stimulus onset, and direction and duration of formant transitions. Relative amplitudes of the speech-evoked responses were compared to predicted ranks defined by the responses to tones centered at the points of frication. Despite marked overlap in formant frequencies, responses reflecting POA were partly determined by the onset spectral characteristics of the syllables and the tonotopic sensitivity of the recording sites. Longer intervals of analysis led to a decrement in response specificity. Response specificity was enhanced for the longest duration formant transition stimuli (80ms). We conclude that A1 responses support the hypothesis that onset spectral features of stop consonants are important for POA discrimination. Relevance to normal perception and that occurring in some people with developmental language disorders will be discussed. Supported by DC00657.

### **1008** Development of Selectivity for the Direction and Rate of Frequency Modulated Sweeps in the Pallid Bat Auditory Cortex

**Khaleel Razak<sup>1</sup>, Zolan Fuzessery<sup>1</sup>**

<sup>1</sup>*University of Wyoming*

While neural selectivity for the rate and direction of frequency modulated (FM) sweeps is present in the auditory cortex of several species, the time course of development of selectivity and the developmental changes in mechanisms that shape selectivity are unknown. The pallid bat is well suited to address these issues for several reasons. It uses a stereotyped downward FM sweep (60-30 kHz, 3-5msec duration) to echolocate. Nearly 75% of neurons in its auditory cortex (best frequency >30 kHz) are selective for the direction and rate of its echolocation call. The mechanisms underlying selectivity in the adult cortex are known. Direction selectivity arises due to low-frequency (LF) inhibition arriving earlier than excitation. Upward sweeps will evoke inhibition first and cause a reduced response than a downward sweep. FM rate selectivity arises due to delayed high-frequency (HF) inhibition. A slow downward FM sweep will allow inhibition to catch up with excitation. A fast FM sweep, however, will allow excitation to occur before inhibition arrives. In this study, we determined how selectivity and the underlying mechanisms change during development of pups maintained in cages with their mothers. An adult level of selectivity for downward FM rate is present in even 2-3 weeks old pups. The relative delay in arrival time, strength and bandwidth of HF inhibition are indistinguishable from adults. Direction selectivity, however, is found only in 25% of the neurons even up to 5-7 weeks of age. In contrast to adults, the relative arrival time of LF inhibition is delayed. Bandwidth and strength of inhibition are smaller in pups up to 5-7 weeks of age. At 12 weeks, arrival time, bandwidth and strength of LF inhibition and direction selectivity are adult-like. Thus, low and high-frequency inhibition to FM-selective neurons follow different time courses of maturation and these differences cause a delayed development of selectivity for FM direction, but not rate.

### **1009** Topographical Laminar Distribution of Receptive Field Parameters in the Primary Auditory Cortex of the Cat

**Craig A. Atencio<sup>1</sup>, Christoph E. Schreiner<sup>1</sup>**

<sup>1</sup>*Bioengineering Graduate Group, Coleman Memorial Laboratory, Department of Otolaryngology, UCSF*

While the topographical organization of response parameters in the primary auditory cortex of the cat has been systematically addressed relatively few studies have analyzed how these parameter distributions change along the depth of the cortex. Basic features, such as the organization of characteristic frequency, have been elucidated though parameters such as sharpness of tuning and monotonicity have not been described in complete detail. Using the anesthetized cat we made orthogonal electrode penetrations and recorded the responses of single neurons at multiple depths along iso-frequency contours in the primary auditory cortex to tone bursts of varying frequency and level. From these recordings we reconstructed the depth profiles of characteristic frequency, latency, threshold, sharpness of tuning, and monotonicity. While CF, threshold, and monotonicity were relatively constant across depth, latency and sharpness of tuning varied systematically. Latency was shortest at depths of 0-200 microns, 750-1000 microns, and 1600-2000 microns, roughly corresponding to layer 1, lower layer 3 and layer 4, and layer 6, respectively. Sharpness of tuning also varied with depth, generally showing broader receptive fields at deeper depths. Topographically the sharpness of tuning profiles changed as well. In the central narrowly tuned region tuning remained relatively constant. In the dorsal narrowly tuned region tuning was sharpest in the input layers and become broadly tuned in the output layers of the cortex. Thus latency and sharpness of tuning are different in the input layers than the output layers. We conclude that response characteristics of single neurons in the output layers are not simple reflections of input layer neuron characteristics and may reflect differences in how auditory stimuli are processed in different layers in the auditory cortex.

### **1010** Context-Dependent Receptive Fields in AI

**Arnaud Norena<sup>1</sup>, Naotaka Aizawa<sup>2</sup>, Jos Eggermont<sup>2</sup>**

<sup>1</sup>*CNRS - LYON*, <sup>2</sup>*University of Calgary*

Tuning properties of auditory neurons are usually assessed with pure tones presented at a low rate (single-frequency method). The corresponding tuning curve is often "v-shaped" - the frequency selectivity of the neurons decreases as the intensity increases. A critic of this method is that pure tones do not exist in the real world (vocalizations for instance are complex in the time and the frequency domains). This method does not seem adequate to reveal functional properties of neurons. In this context, other methods have been designed to derive tuning properties of auditory neurons from complex stimuli (multi-frequency methods). In these methods, the tuning properties of neurons are represented as a function of time: the responses obtained then form the "spectro-temporal receptive field" (STRF) of the neurons.

Here we compared the tuning properties of neurons in AI derived from both methods. Frequency was varied over 5 octaves. In the single-frequency method, pure tone were presented at a rate of 4/s. In the multi-frequency method, an independent Poisson train of pure tones was created for each frequency (same mean rate over frequencies). The mean rate of each frequency was adjusted in such a way that the overall presentation rate was 20, 120 or 240 stim/sec.

The results showed that frequency selectivity of AI neurons was greater with multi-frequency method than with the single-frequency method. In addition, some neurons that were single-peaked (one maxima in the firing rate) with the single-frequency method were observed to be multi-peaked (2 or more maximas in the firing rate) with the multi-frequency method. Interestingly, the peaks were not randomly distributed over frequency: instead, there was an octave relationship between the peaks. These results suggest that the tuning properties of neurons is dynamic and strongly dependent on the context. Finally, the octave distance between distinct maximas in the STRF of AI neurons may have important functional implications.

### **1011 Refined Electrode Design for Impedance Measurements using the Four-Electrode Reflection Coefficient Technique**

**Alan Micco<sup>1</sup>, Claus-Peter Richter<sup>1</sup>**

<sup>1</sup>*Northwestern University Feinberg School of Medicine*

Cochlear implants electrically stimulate residual spiral ganglion cells to restore hearing sensation in severely to profound hearing impaired individuals. The patterns of cochlear current flow can be determined by measuring the impedances of cochlear structures. In previous studies, we have measured the resistivities for selected structures using the four-electrode reflection coefficient technique. The purpose of this study was to refine the electrode design by using glass electrode pipette to allow us to measure smaller structures in the cochlea. The larger wire electrodes were too large to get into the turns of the cochlea to measure key target structures such as the basilar membrane and the modiolar areas in the gerbil hemicochlea. The new refined electrode was created using tetra-glass which was pulled to have a very small tip. Silver wire was placed into the chambers along with normal saline. Hemicochlea preparations were made from normal hearing adult gerbils. Resistivity measurements were taken along the basilar membrane of the gerbil hemicochlea preparation. Results showed that within 2 diameters of the electrode width from the target structure, 95 % of the voltage changes are seen. The advantages of the refined electrode include the ability to create almost any size electrode. A small tip area can be created obviating the concern about the effect of surface contour on the measurements. Finally the ability to alter the direction of the tip allows for measurements of target structures on the cochlea that were inaccessible with our standard wire electrodes. These refinements will allow us to make more precise resistivity measurements, as well as create a more complete electroanatomic map of the cochlea.

Supported by the Silverstein Grant in Neurology

### **1012 Optically-Evoked Acoustic Nerve Activity**

**Claus-Peter Richter<sup>1</sup>, Agnella Izzo<sup>1</sup>, Joseph T. Walsh<sup>1</sup>, E. Duco Jansen<sup>2</sup>**

<sup>1</sup>*Northwestern University, <sup>2</sup>Vanderbilt University*

In contemporary cochlear implants, the injected electric current is spread widely along the scala tympani and across turns of the cochlea. Consequently, stimulation of spatially discrete spiral ganglion cell populations is difficult. One goal of implant device development is to design cochlear implants that can stimulate smaller populations of spiral ganglion cells. We introduce a completely novel concept, optical stimulation of spiral ganglion cells, to accomplish extremely discrete stimulation. Using an infrared optical source with an in vivo animal preparation, we can evoke compound actions potentials (CAPs) in the auditory nerve that are qualitatively the same as acoustically-evoked CAPs. Control experiments were made, in which animals were deafened acutely using a cocktail of kanamycin given intraperitoneally, followed by ethacrynic acid injected intravenously. Acoustically evoked CAP amplitudes decreased rapidly, while the optically evoked CAP amplitudes remained unchanged. The results from the latter experiments indicate that optical stimulation is not a result of an artifact from the optical source, a mechanical stress wave in the cochlear fluids, or a photochemical reaction. The long-term impact of these experiments is to design and build safe "optical cochlear implants" with significantly improved spatial selectivity for spiral ganglion cell stimulation. As a consequence, it is expected that these cochlear implants will provide significantly more independent frequency bands to the implant user. The result would be better speech recognition, especially in noisy environments.

### **1013 Safe Ranges for Optical Cochlear Neuron Stimulation**

**Agnella D. Izzo<sup>1</sup>, Claus-Peter Richter<sup>1</sup>, Joseph T. Walsh, Jr.<sup>1</sup>, E. Duco Jansen<sup>2</sup>**

<sup>1</sup>*Northwestern University, <sup>2</sup>Vanderbilt University*

Cochlear implants are intended to be used over many years by the patient and, therefore, the device cannot be harmful to the auditory neurons. However, the use of a laser to stimulate auditory neurons has the potential to damage the cells if laser parameters are not selected properly. To date only our limited pilot data are available providing safe laser parameters, such as energy, spot size, length of continual stimulation, and placement of the fiber, while stimulating the auditory system. The present experiments are designed to rigorously establish the parameters that allow the safe use of the optical energy without damaging spiral ganglion cells. It could be shown that laser energy can be increased by at least 30 dB between compound action potential threshold and damage to the nerve, (2) that continuous stimulation of time periods up to at least three hours do not deteriorate the CAP amplitude significantly, (3) spot sizes of 100  $\mu\text{m}$  provides a sufficiently large stimulation signal to elicit auditory

response, and (4) the best results for stimulation is achieved if the fiber is placed directly opposite and in close proximity to the spiral ganglion cells. Furthermore, we expect that the deafening protocol deteriorates cochlear function. The experiments did not indicate that the nerve fiber is damaged from long-term stimulation.

### **1014 Effect of Electrical Stimulation on Spiral Ganglion Survival in Animals with Early-Acquired Hearing Loss.**

**Olga A. Stakhovskaya<sup>1</sup>, Gary T. Hradek<sup>1</sup>, Patricia A. Leake<sup>1</sup>**

<sup>1</sup>*University of California San Francisco*

Previously, we reported that electrical stimulation from a cochlear implant (CI) has significant trophic effects on spiral ganglion cell (SGC) survival in neonatally deafened cats. In this study we explored developmental critical period(s) by examining a different deaf animal model. Kittens were deafened at 30 days of age by ototoxic drug administration identical to that used in neonates. Profound hearing losses occurred by 48-56 days of age. Unilateral electrical stimulation with bipolar electrodes and temporally challenging signals (325pps) was initiated immediately after deafening and continued over periods of 35-37 weeks to match stimulation in neonatally deafened animals. Two subjects deafened at 30 days and half of the neonatally deafened group also received GM1 ganglioside, but due to the absence of any significant effect of GM1, the data were combined for animals with and without GM1 treatment.

Animals deafened at 30 days of age (n=3) demonstrated a highly significant increase (more than 20%) in SGC survival in the stimulated ears as compared to the deafened control side, suggesting that electrical stimulation significantly enhanced SGC survival in this group. At the same time, these preliminary data did not show a significant difference in SGC survival between the 30-day deafened and neonatally deafened groups. Although auditory pathways are still immature at 30 days of age, deafening in this older group was initiated after the development of adult-like spontaneous activity in the auditory nerve and adult-like auditory brainstem responses, in contrast to the neonatally deafened group. Thus, these interesting results did not provide evidence for a developmental critical period at least during the first postnatal month. Delaying the onset of deafness by more than 30 days and initiating stimulation immediately thereafter did not provide additional benefit for SGC survival over the long term.

*Supported by NIDCD Grant #RO1 DC000160 and Contract #N01-DC-3-1006.*

### **1015 Long-Term Sensorineural Hearing Loss Induces Functional Changes in the Rat Auditory Nerve**

**Robert Shepherd<sup>1,2</sup>, Lloyd Roberts<sup>2</sup>, Antonio Paolini<sup>1,2</sup>**

<sup>1</sup>*The Bionic Ear Institute*, <sup>2</sup>*The Department of Otolaryngology, University of Melbourne*

Loss of cochlear hair cells in the rat initiates degenerative change within the primary auditory neurons (ANs) of the

cochlea. These degenerative changes include loss of peripheral processes, demyelination, and ultimately cell death. This pathology will affect the biophysical processes involved in action potential generation and propagation to an electrical stimulus via a cochlear implant. We measured the response properties of ANs - with particular reference to their refractory behaviour - in normal, short- (9 weeks) and long-term (>52 weeks) deafened rats. AN loss was moderate in the short-term and severe in the long-term deafened animals. AN activity was elicited using a brief electrical stimulus delivered via a bipolar electrode array implanted into the cochlea. The general response properties of ANs recorded from deafened cochleae were similar to those observed in normal cochleae; i.e. a monotonic increase in the probability of firing and a decrease in response latency and temporal jitter with increasing stimulus intensity. However, the absolute refractory period was significantly prolonged in animals deafened > 12 months (P=0.0026). Deafened animals also exhibited a highly significant increase in threshold compared with normal controls (P<0.001). These functional changes have implications for recipients of cochlear implants and potential therapies directed toward halting or reversing AN pathology.

### **1016 Degradation in Topographic Specificity (Frequency Resolution) of Spiral Ganglion Projections to the Cochlear Nucleus After Neonatal Deafening is not Reversed by Chronic Electrical Stimulation**

**Patricia Leake<sup>1</sup>, Russell Snyder<sup>1,2</sup>, Gary Hradek<sup>1</sup>, Leila Chair<sup>1</sup>, Ben Bonham<sup>1</sup>**

<sup>1</sup>*University of California San Francisco*, <sup>2</sup>*Utah State University*

Previously, we studied the development of spiral ganglion (SG) projections to the cochlear nucleus (CN), using the neuronal tracer Neurobiotin™ to label small sectors of the SG representing a narrow frequency range. SG projections in normal pre-term kittens showed clear tonotopic organization at 60 days gestation, several days before auditory nerve spontaneous activity emerges and long before hearing onset. But when normalized for CN size, projections in AVCN, PVCN and DCN were 53, 36 and 32% broader, respectively, in neonates than in adult cats. Thus, significant refinement of these pathways occurs in early postnatal life.

This study examined SG projections in 5 adult cats that were deafened neonatally by ototoxic drug administration. At 6-8 weeks of age, animals received a unilateral cochlear implant that delivered electrical stimuli on 2 bipolar channels for 14-34 weeks. Preliminary data show that the basic tonotopic order of SG projections was intact in these deaf animals, but when normalized for the smaller size of the CN, projections were significantly broader than in controls. Laminae in AVCN, PVCN and DCN were all 30-45% broader than normal. Further, there was no significant difference between projections in the stimulated vs. unstimulated CN in the deaf cats. However, it must be noted that selectivity of stimulation, assessed by threshold

vs. depth functions in the inferior colliculus, varied widely among subjects.

Our findings suggest that normal auditory experience may be essential for precise refinement of the SG to CN projections. In early-deafened animals the tonotopic order is established and preserved into adulthood, but topographic specificity (inferred frequency resolution) of the primary afferent input to the central auditory system is significantly degraded. Moreover, electrical stimulation from an implant was not sufficient to induce normal refinement of this pathway.

*Supported by NIDCD Grant RO1DC000160 and Contract N01-DC-3-1006*

### **1017 The Effect of Post-Implant Cochlear Fibrosis on Residual Hearing**

**Chul-Hee Choi**<sup>1</sup>, Ross E Tonini<sup>2</sup>, Patricia A Leake<sup>3</sup>, Daniel C Chelius<sup>1</sup>, John S Oghalai<sup>1</sup>

<sup>1</sup>*Baylor College of Medicine,* <sup>2</sup>*Texas Children Hospital,*

<sup>3</sup>*University of California San Francisco*

Intracochlear scarring is one of well-described sequelae of cochlear implantation. We developed a mathematical model of passive cochlear mechanics to predict the impact that this might have upon residual acoustical hearing after implantation. The cochlea was modeled using lumped impedance terms for scala vestibuli (SV), scala tympani (ST), and the cochlear partition (CP). The damping of ST and CP was increased in the basal one half of the cochlea to simulate the effect of scar tissue. We found that increasing the damping of the ST predominantly reduced basilar membrane vibrations in the apex of the cochlea, while increasing the damping of the CP predominantly reduced basilar membrane vibrations in the base of the cochlea. We also measured changes in residual hearing after cochlear implantation by comparing the pre-operative to post-operative auditory steady-state evoked responses in 12 children. The average loss after implantation ranged from 3-10 dB across the frequency range. According to our model, ST damping must not have increased more than 100 times normal and CP damping must not have increased more than 10 times normal. As long as intracochlear scarring continues to occur with cochlear implantation, there will be limitations on the hearing preservation.

Supported by NIH grants: NIDCD DC05131 and National Organization for Hearing Research Foundation

### **1018 Simulating Time-Varying Electrical Stimulation of the Auditory Nerve using a New Integrate-And-Fire Model.**

**Mark Robert\***

A widely-used cochlear implant stimulation strategy for restoring normal hearing uses the time envelope of the input signal to modulate the amplitudes of fixed-rate pulse trains that are directed to tonotopically appropriate electrodes. A consequence of this steady electrical stimulation rate is the entraining of the neural response to the pulse rate of these carrier signals. As a result of this so-called phase locking, fibers in the stimulated region of

the auditory nerve are thought to be collectively in the same refractory state and hence are essentially unresponsive to any irregularly or weakly time-varying components of the signal. Strategies to conserve the presence of these components in the signal envelope include the addition of an optimal amount of noise to the signal (Chatterjee & Robert, 2001, *JARO* 2:159-171) and driving the system into a less synchronous state with a high frequency "conditioner" signal (Rubinstein et al., 1999, *Hearing Research* 127(1-2):108-118). The work presented here is from the validation of a new model developed to simulate these strategies as part of a broader effort looking at how the electrically-stimulated auditory system processes time-varying stimuli. An integrate-and-fire model extended to respond to extracellular current, this model improves the mapping of electric potential to neural response. Results agree qualitatively with animal data described by Dynes & Delgutte (1992, *Hearing Research* 58(1):79-90) for sinusoidal electrical stimuli, showing that synchronization falls with higher frequencies (> 1 kHz) and discharge rate increases with level. The model confirms the important role a cell's refractory period plays in phase-locking. Results from ongoing validation and additional simulation work investigating the sources of large variability in synchronization at high frequencies described by Dynes & Delgutte will be presented.

### **1019 Inferior Colliculus Responses to Two-channel Cochlear Implant Stimulation**

**Steven Bierer**<sup>1</sup>, Ben Bonham<sup>1</sup>, Russell Snyder<sup>1</sup>

<sup>1</sup>*University of California, Epstein Laboratory*

For normal hearing listeners, the perception of one tone can be suppressed by the presence of another. With cochlear implant listeners, a similar phenomenon occurs, albeit one that does not involve the suppressive mechanisms of the auditory periphery. We explored the nature of central mechanisms of suppression by stimulating with intracochlear electrodes and recording neural activity across the central nucleus of the inferior colliculus (ICC). Single and multi-unit activity from the ICC of the anesthetized guinea pig was recorded with a 16-channel electrode spanning the cochleotopic representation. First, single- and two-tone acoustic responses were obtained. With the recording electrode fixed in place, the guinea pig was then deafened and an 8-electrode cochlear implant was inserted into the scala tympani. Pulse trains were presented as bipolar pairs between neighboring electrodes (BP+0) or between alternating electrodes (BP+1). Two-channel stimulation was achieved by interleaving pulse trains from different bipolar pairs, with one channel varying in cochleotopic location and intensity and the other fixed. With the 1-channel stimulation, the extent of activation across the ICC was fairly restricted and reflected its cochleotopic organization. Each recording site, therefore, could be characterized by its best stimulus channel. For some recording sites, activity evoked by the best channel could be suppressed by stimulation on a second channel. The suppression was often greatest when the stimulation channels were adjacent (BP+0) or overlapping (BP+1). This finding is consistent with acoustic studies



demonstrating lateral suppressive sidebands. At low rates of stimulation (50 pps), when responses to the two stimulation channels were well separated in time, the occurrence of pulses from the fixed channel could suppress responses to the other channel, even when the fixed channel itself produced only a modest response.

### **1020 Effects of Combined Acoustic and Electric Stimuli: Single Auditory Nerve Fiber Responses**

Charles Miller<sup>1</sup>, Heil Noh<sup>2</sup>, Paul Abbas<sup>1</sup>, Barbara Robinson<sup>1</sup>, Kirill Nourski<sup>1</sup>, Fuh-Cherng Jeng<sup>1</sup>

<sup>1</sup>University of Iowa, <sup>2</sup>The Catholic University of Korea

As some cochlear-implant users have residual hearing and implantation criteria may continue to relax, we are investigating how combined acoustic and electric stimuli affect the response of auditory nerve fibers. Our work (cf. Nourski et al. abstract) and that of Killian et al. (1994) have shown that the electrically evoked compound action potential (ECAP) is influenced by the simultaneous presentation of acoustic noise. Also, complex post-stimulatory effects are observed after noise offset. Single-fiber studies were performed to elucidate the physiology underlying these and other effects.

Anesthetized cats were used in acute sessions. A minimally invasive intracochlear electrode was used to preserve acoustic sensitivity. The electric stimuli was a 250 pps electric pulse train presented for a duration of 200-550 ms. An acoustic noise burst was presented 50 ms after train onset and turned off prior to train offset.

In general, the synchronized response to the electric pulse train was decreased during the presentation of the acoustic noise. After noise offset, there was generally a period of reduced responsiveness that recovered over a 100 ms period. These trends are consistent with previous ECAP results.

Unexpected results were also obtained. First, rates of adaptation to acoustic and electric stimuli could differ markedly. In some cases, adaptation was faster for electric stimuli than for acoustic stimuli. We attribute this to distinct excitation mechanisms for the two modalities. Furthermore, while the acoustic stimulus often partially masked the electric response, at least one fiber showed a unique response in which the acoustic noise facilitated the electric response. Finally, we attribute the complex pattern of ECAP recovery (observed after offset of the noise) to refractory and temporal properties of the auditory nerve fibers. These patterns may need to be considered for the optimal design of speech processors when applied to specific users.

### **1021 Forward Masking in Cat Inferior Colliculus using Combined Electric and Acoustic Stimulation of the Cochlea**

Maike Vollmer<sup>1</sup>, Jochen Tillein<sup>2</sup>, Ben Bonham<sup>1</sup>

<sup>1</sup>University of California, San Francisco, <sup>2</sup>University of Frankfurt

Combined electric and acoustic stimulation (EAS) has been applied successfully to cochlear implant users with

residual low frequency hearing. Using a forward masking paradigm, we examined the spectro-spatial interactions of EAS on inferior colliculus (IC) neurons. Anesthetized normal hearing cats were implanted with a scala tympani electrode array. An earphone was sealed to the auditory meatus for acoustic stimulation. Neural activity was recorded simultaneously at 16 sites along the tonotopic gradient of the central nucleus of the IC. A 20-ms electric probe was preceded by a 50-ms acoustic masker. Probe and masker were systematically varied in intensity and frequency.

At low intensities, electric probe frequencies >1 kHz evoked activity at primary IC locations that corresponded to the probe frequency. This activity was masked when the electric probe was preceded by acoustic stimuli at the same frequency.

At higher intensities, the electric probe evoked additional activity at a secondary IC location corresponding to the cochlear site of the stimulating electrode. This activity was masked by acoustic frequencies that corresponded to the same cochlear site. Strength of masking was generally increased by increasing masker intensity.

Similar masking effects occurred when the electric probe was replaced by an acoustic probe (two-tone masking) at either the frequency of the electric probe or a frequency corresponding to the cochlear site of electrical stimulation.

The results indicate that EAS produces complex spatial interactions in the central auditory system. The extent of these interactions is dependent on the intensities and spectral characteristics of both electric and acoustic stimulus components. The results also suggest that electric stimulation evokes low-threshold acoustic-like electrophonic responses as well as high-threshold direct activation of the auditory nerve.

(Supported by NOHR, NIH N01 DC-2-1006, NIH N01 DC-3-1006 and MedEI)

### **1022 Prevention of Synaptic Abnormalities by Cochlear Implantation in Cats**

Erika Kretzmer<sup>1</sup>, Tan Pongstaporn<sup>1</sup>, Charles-André Haenggeli<sup>2</sup>, Charles Limb<sup>1</sup>, John Niparko<sup>1</sup>, David Ryugo<sup>1</sup>

<sup>1</sup>Johns Hopkins University, <sup>2</sup>Hôpitaux Universitaires de Genève

Congenital deafness causes changes throughout the central auditory system, including abnormalities in protein synthesis, initiation of cell death, and altered axonal projections. We studied the specific synaptic changes found in the endbulb of Held, a prominent terminal of auditory nerve fibers. We have demonstrated deafness-induced hypertrophy of endbulb synapses that accompanies a delay in the late peaks of EABR responses. In the present study, we show that electrical stimulation of the auditory system via a cochlear implant prevents the formation of abnormal synapses.

Kittens exhibiting bilateral, congenital deafness were surgically fitted at 3 months of age with 6-channel cochlear implants designed by Advanced Bionics. Stimulation was begun at 4 months and continued for 2 to 6 months, 5 days a week, 7 hours a day. At least 2 channels were activated in each experimental cat. Electrically-evoked

cochlear potentials (ECAPs and EABRs) and behaviorally-appropriate responses to sound imply that the central auditory system was activated by the implant. At the end of the stimulation period, we harvested brain and cochlear tissue for light and electron microscopy.

We reconstructed and measured endbulbs in hearing, deaf, and implanted cats using serial section electron micrographs. As previously reported, endbulb synapses from deaf animals were hypertrophied ( $0.39 \pm 0.45 \mu\text{m}^2$ ) as compared to those from normal hearing animals ( $0.11 \pm 0.06 \mu\text{m}^2$ ). In contrast, endbulb synapses from implanted cats were similar in size ( $0.14 \pm 0.13 \mu\text{m}^2$ ) to those from the normal hearing cats of the same age. Surprisingly, endbulb synapses contralateral to the implant also exhibited a near normal appearance ( $0.21 \pm 0.21 \mu\text{m}^2$ ), implying a widespread effect of unilateral stimulation. These data could influence intervention strategies for deaf patients.

*Supported by NIH grants RO1 DC00232, DC005864, DC05211, the Emma Liepmand Fund, and a gift from Advanced Bionics Corp.*

### **1023 Gross Synaptic Currents in A1 Demonstrate Delayed and Altered Synaptogenesis in Deafness**

**Andrej Kral<sup>1,2</sup>, Jochen Tillein<sup>2</sup>, Silvia Heid<sup>2</sup>, Rainer Hartmann<sup>2</sup>, Rainer Klinke<sup>2</sup>**

<sup>1</sup>Laboratories of Integrative Neuroscience, <sup>2</sup>Institute of Sensory Physiology and Neurophysiology

The field A1 was investigated during development in cochlear implanted electrically-stimulated congenitally deaf and hearing cats. Lowest cortical thresholds in A1 were assessed using surface Ag/AgCl electrodes (d=1mm) with pulsatile stimulation. At 10 dB above threshold the field A1 was mapped with glass microelectrodes. At the place of largest activity local field potentials were recorded in all cortical layers and gross extracellular layer-specific synaptic currents were determined using the current-source-density method.

In hearing controls, young cats (up to 2 months) had large CSD signals which decreased in amplitude after the 2nd month of life. At the age of 4 weeks, the synaptic activity was concentrated mainly in the superficial (supragranular) cortical layers II and III. At 2-3 months activity increased also in deeper cortical layers (V and VI) and reached mature patterns (Kral et al., 2000, Cereb Cortex 10:714) after the 4th month p.n.

Very young deaf animals (4-6 weeks p.n.) had less synaptic activity in the auditory cortex than age-matched controls (mean sink amplitude  $317.4 \mu\text{V}/\text{mm}^2$  in deaf vs.  $2313.3 \mu\text{V}/\text{mm}^2$  in hearing controls, Wilcoxon-Mann-Whitney two-tailed test,  $p < 0.001$ ). At 2 months, CSD peak amplitudes did not differ between deaf and hearing group ( $1318 \mu\text{V}/\text{mm}^2$  in deaf vs.  $2459.9 \mu\text{V}/\text{mm}^2$  in controls). At 3 months p.n. the sink amplitudes reached their maximum in deaf cats and became significantly larger than in hearing controls ( $2804.8 \mu\text{V}/\text{mm}^2$  in deaf vs.  $1486.6 \mu\text{V}/\text{mm}^2$  in controls, Wilcoxon-Mann-Whitney two-tailed test,  $p = 0.02$ ). The amplitudes at this age in deaf better corresponded to those in 1 month old hearing control (non-

significant difference). However, infragranular activity was more comparable to age-matched controls. At 4 months, the deaf animals showed CSD profiles corresponding to adult deaf cats characterized by reduced activity in infragranular layers and smaller overall mean CSD amplitudes (Kral et al., 2000, Cereb Cortex 10:714). The present study reveals that congenital deafness delays the functional "synaptic overshoot" by 2 months in field A1. Subsequently it leads to a more pronounced developmental reduction of mean synaptic activity and by that to a sensitive period (comp. Kral et al., 2002, Cereb Cortex 12:797).

Supported by Deutsche Forschungsgemeinschaft (SFB 269 C1).

### **1024 Effects of Hair Cells on Cochlear Implant Psychophysical Detection Thresholds**

**Bryan E. Pfingst<sup>1</sup>, Gina L. Su<sup>1</sup>, Deborah J. Colesa<sup>1</sup>, Richard A. Altschuler<sup>1</sup>**

<sup>1</sup>University of Michigan

Studies examining the relationship between psychophysical detection thresholds and spiral ganglion cell survival patterns have produced mixed results, with some studies showing negative correlations and others not. A potential complicating factor in these studies is the presence of hair cells. Since many implanted patients have some residual hearing prior to implantation and since the implantation procedure does not necessarily destroy hair cells, it is reasonable to expect that some individuals with cochlear implants have some functioning inner hair cells. The presence of hair cells presumably would be a benefit for the survival of spiral ganglion cells and thus potentially increase sensitivity of the auditory system to electrical stimulation. On the other hand, recent studies have shown that hair cells can reduce the electrically-evoked compound action potential of the auditory nerve (Hu et al., Hearing Research, 2003, 185, 77-89). In this study we examined effects of the presence of hair cells on psychophysical detection thresholds for electrical stimulation of cochlear implants in guinea pigs. Guinea pigs were either deafened with cochlear perfusion of neomycin and implanted with a multichannel cochlear implant (n = 2), or they were simply implanted without chemical deafening (n = 6). In this group of 8 animals, hair cell survival ranged from near normal to completely absent. Psychophysical detection thresholds for animals with moderate to good hair cell survival were an average of 7 dB higher than those for animals with severe hair cell loss, even though spiral ganglion cell survival was much higher in the animals with surviving hair cells. These data are consistent with the hypothesis that hair cells produce spontaneous activity in the auditory nerve, thus reducing the sensitivity of the system to electrical stimulation. This work was supported by NIH/NIDCD R01 DC03389 and P30 DC05188.

## **1025 Physiological Measures of Auditory Nerve Activation by Current Steering**

**Ben Bonham**<sup>1</sup>, Russell Snyder<sup>1</sup>, Scott Corbett<sup>2</sup>, Tim Johnson<sup>2</sup>, Steve Rebscher<sup>1</sup>

<sup>1</sup>*Epstein Laboratory, Dept of Otolaryngology-HNS, Univ of Calif, San Francisco, CA,* <sup>2</sup>*Advanced Cochlear Systems, Snoqualmie, WA*

Current cochlear implants (CIs) employ a modest number (16-22) of electrodes to stimulate a small number (4-8) of discrete regions of the auditory nerve (AN) array. In CI patients, stimulation of individual electrodes (as monopoles) or adjacent/nearby electrode pairs (as bipoles) restricts the number of independently addressable regions of the AN array to at most the number of individual electrodes. Thus, CI stimulation using either of these paradigms results in stimulation of a small number of independent channels. In contrast, the normal ear can arguably be considered to have as many independent (though overlapping) acoustic channels as there are inner hair cells (~3500). There is currently no commercially implemented solution that increases the number of CI channels by increasing the number of physical electrodes (and consequently decreasing the spacing between electrodes). An alternative method that can be used to increase the number of independent CI channels is to change the way current is directed into the spiral ganglion by dividing, or steering, current among a local group of electrodes. This method can be employed with two effects. First, by sharing stimulus current between nearby (adjacent) electrodes, "virtual" electrodes can be created that lie between physical electrodes. Second, spread of activation of the AN can be decreased by shaping the field potential using countercurrent applied to adjacent electrodes. By measuring spread of activation along the tonotopic axis of the inferior colliculus, we have demonstrated that suitable division of stimulating current among a local group of electrodes can, but does not always, stimulate multiple independent, though overlapping, regions of the AN array. We have also demonstrated that injection of countercurrent into adjacent electrodes (i.e., partly tripolar stimulation) can, but does not always, reduce the spread of AN activation by a single implant electrode.

(Sponsored by NIDCD #N01-DC-02-1006)

## **1026 Estimates of Auditory Filter Shapes at Low Frequencies using Forward and Simultaneous Masking**

**Xuedong Zhang**<sup>1</sup>, Andrew J. Oxenham<sup>1</sup>

<sup>1</sup>*Research Laboratory of Electronics, Massachusetts Institute of Technology, Cambridge, MA 02139, USA*

A well-established method of estimating human auditory filter shape is to measure the masked threshold of a sinusoidal signal in a spectrally notched noise as a function of notch position and width.

Auditory filter shapes are affected by the cochlear nonlinearities. In particular, estimates using simultaneous maskers, where nonlinear suppression can play a role, have been found to lead to wider estimated filters than

forward (nonsimultaneous) masking. It is generally thought that forward masking provides an estimate of human cochlear tuning that is more suitable for comparison to data from physiological studies. However, such estimates apparently only exist for signal frequencies of 1 kHz and above.

The current study derived the auditory filter shapes in normal-hearing listeners using a variant of the notched-noise method for brief signals in forward and simultaneous masking. Signal frequencies of 250, 500, and 1000 Hz were tested. The signal level was fixed at 10 dB above absolute threshold in forward masking, and the masker threshold level was measured as a function of the width and position of the notch. The signal in simultaneous masking was determined such that noise levels used in forward and simultaneous masking were similar to each other in the absence of a notch. The results provide insights into human cochlear mechanics at low frequencies, and should assist in the development of nonlinear cochlear models.

[Supported by the ASA Hunt Fellowship and NIH DC03909.]

## **1027 ZEST as a Tool for Rapid Assessment of Frequency Discrimination**

**Michael Stahl**<sup>1</sup>, Soren Buus<sup>1</sup>, Mary Florentine<sup>1</sup>

<sup>1</sup>*Northeastern University*

The purpose of this study is to evaluate the ZEST psychophysical procedure (King-Smith et al., 1994) as a tool for rapidly and reliably measuring auditory discrimination thresholds. Thresholds for frequency discrimination were obtained by ZEST in 30 trials with a 2AFC paradigm. Subsequent analysis allowed calculation of thresholds for any number of trials up to 30. The stimuli were 600-ms tones at seven frequencies from 250 to 7000 Hz. Data for six normal listeners obtained with three different initial slopes (beta) of the assumed psychometric function indicate that reliable thresholds can be obtained in 10 to 15 trials. Likewise, simulations indicate that threshold estimates have only a slight percent error, which declines to less than 15% after only nine trials. The simulations also show that this bias can be reduced with only a small increase in the variability if the assumed psychometric function used by ZEST is made steeper than the listener's actual psychometric function, (i.e., if beta is increased from 1.23 to 6). Altogether these results suggest that ZEST combined with a 2AFC paradigm is a promising candidate for rapid and reliable assessment of discrimination thresholds.

## **1028 Rapid and Reliable Assessments of Psychoacoustic Thresholds**

**Sygal Amitay**<sup>1</sup>, David Hawkey<sup>1</sup>, Amy Nelson<sup>1</sup>, David Moore<sup>1</sup>

<sup>1</sup>*MRC Institute of Hearing Research*

In psychoacoustic studies there is often a need to establish performance indices very quickly (e.g. child hearing, training). The aim of this study was to establish the quickest and most reliable method for assessing

thresholds in backward masking and frequency discrimination tasks. Computer simulations based on signal detection theory suggested that for attentive observers a maximum-likelihood (ML) algorithm targeting the "sweet-point" on the psychometric function was both the quickest and the most reliable when coupled with a 3-alternative forced-choice (3-AFC) paradigm. However, the ML procedure targeting the sweet-point is highly susceptible to lapses in attention, a problem solved by targeting a lower point on the psychometric function. Staircase procedures are more stable for inattentive observers, but take longer to converge on a threshold. We compared these simulations with results from 20 adult listeners for two adaptive algorithms (staircase and ML targeting the 79% correct point on the psychometric function) and two response paradigms (3-interval 2-AFC AXB and 3-interval 3-AFC oddball) in a 2x2 design. Analysis was carried out both within and across listeners. No significant differences were found between methods in the backward masking detection task, which showed considerable variability. Consistent with the computer simulations, the 3-AFC oddball coupled with an ML algorithm was the "best method" in the frequency discrimination task, producing stable psychometric functions in as few as 20 trials. Test-retest reliability was also measured one week and three weeks following initial testing. Reliability was high. Training was observed in the frequency discrimination task, with significant performance gains between the first and second (160 trial) sessions and maintained learning in the third session. Further experiments comparing training with the same methods are currently underway.

### **1029 Test of the Linearity Assumption Underlying COSS Estimates of Listener Decision Weights**

**Robert Lutfi<sup>1</sup>, Walt Jesteadt<sup>2</sup>**

<sup>1</sup>*Univ. of Wisconsin, Madison, WI*, <sup>2</sup>*Boys Town Natl. Research Hosp., Omaha, NE*

In recent years COSS (conditioned-on-a-single-stimulus) analysis, and related correlational methods, have become increasing popular as a means of determining the relative reliance or weight listeners place on different components of a multicomponent stimulus in detection and discrimination tasks [Berg, *J. Acoust. Soc. Am.* 86, 1743-1746 (1989)]. A strong assumption of these methods is that listener decisions are based on a linear combination of the component predictor variables. Several conditions must be met to satisfy this requirement, but one in particular is that the slopes of COSS functions for single-tone stimuli not change significantly with tone level. We present contrary data in which COSS slopes for single tones increase with increasing level over most of the dynamic range of hearing (from 20-80 dB SPL). The results are discussed in terms of their implications for the interpretation of weights obtained in past studies, particularly those for which stimulus components are of unequal level. [Work supported by NIDCD].

### **1030 Auditory Brainstem Response Correlate of the Psychophysical Temporal Effect of Masking**

**Lata Krishnan<sup>1</sup>, Elizabeth Strickland<sup>1</sup>, John Durrant<sup>2</sup>**

<sup>1</sup>*Purdue University*, <sup>2</sup>*University of Pittsburgh*

#### **ABSTRACT**

A short duration signal in the presence of a longer duration masker is more difficult to detect when it is close to the onset of the masker than when the signal is delayed from the onset of the masker. This has been called overshoot or the temporal effect and the mechanisms underlying this phenomenon are still unclear. It has been hypothesized that the gain of the cochlear amplifier is decreased during acoustic stimulation with the masker thus decreasing the effectiveness of the masker in the long-delay condition.

This has been supported by the finding that listeners with cochlear hearing impairment show a reduced temporal effect. A physiological correlate of the temporal effect has been reported as well in terms of lower thresholds of stimulus frequency otoacoustic emissions in the long-delay condition.

The aim of this study was to evaluate a possible electrophysiological correlate to the psychophysical temporal effect. The temporal effect was measured in normal hearing listeners using a 10-ms 4000-Hz signal presented 2 ms after the onset of a 200 ms broad band noise (short-delay) or 202 ms after the onset of a 400 ms noise (long-delay). Auditory brainstem responses (ABR) were then obtained from the same listeners, using the same stimulus paradigm. The signal duration was shortened to 5 ms in order to produce a clearer ABR response. Recordings were obtained in the short-delay and long-delay conditions for a signal of 95 dB SPL with no masker and with the masker at 45, 55, 65 and 75 dB SPL. Latency and amplitude changes of Wave I and Wave V components as well as I-V interpeak intervals of the ABR were compared between the two main conditions as a function of masker level. The findings reveal differences in the ABR between the short- and long-delay conditions consistent with the psychophysical temporal effect. Detailed effects on individual ABR measures will be presented and interpreted to support the current theory underlying this effect.

### **1031 Infants' and Adults' Perception of Tone Chroma in Melodic and Scrambled-Note Conditions**

**Daniella Kim<sup>1</sup>, Lynne Werner<sup>1</sup>**

<sup>1</sup>*University of Washington*

In music, pitches are defined by height and chroma. Demany and Armand (1984) suggested that infants, like adults, perceive 2 notes an octave apart as having the same chroma. This is called octave equivalence. In previous reports we have shown that infants' perception of tone chroma is not yet adult-like (Kim and Werner, 2003). We found that infants learned to treat other melodic transpositions of a background melody as equivalent more quickly than octave transpositions of a novel 6-note melody. Our study and that of Demany and Armand

differed in method, but also in the melody used. The aim of the current study is to test infants' and adults' perceptions of 7th and 9th (chroma) transpositions of Demany and Armand's original 3-note sequence. All subjects were tested using an observer-based psychoacoustic procedure. Each subject was tested in two conditions. In the MELODY condition, subjects heard the standard 3-note melody randomly played in 1 of 4 octaves (Demany and Armand's condition). In the NOTE condition, subjects heard the standard background melody, each individual note could be played in 1 of 4 octaves. Target stimuli were transposed by a 7th or 9th. In both conditions, subjects were trained to respond to chroma transpositions and not octave transpositions. The number of trials it took to learn to respond to only chroma change was recorded. There was generally no difference in performance between conditions for either infants or adults. 66% of infants and 90% of adults reached an 80% correct criterion in 24.19 and 23.56 trials, respectively. Adults did better in the NOTE condition if they heard the MELODY condition first, but infants performed equally well in the two conditions, regardless of testing order. We conclude that both infants and adults can readily identify chroma changes and recognize octave equivalence, at least with a 3-note melody. Work supported by NIDCD DC00396 and DC04661.

### **1032** Discrimination of Rapid Frequency Modulated Sweeps as a Function of Direction, Frequency Span and Center Frequency

**Bernhard Gaese**<sup>1</sup>, Susan Wehner<sup>1</sup>

<sup>1</sup>Zoologisches Institut, J.W. Goethe Universität, Frankfurt a.M., Germany

There is strong evidence that human speech and animal communication calls share common acoustic characteristics and general principles of processing and that, both in humans and animals, temporally changing acoustic cues are of critical importance. Especially frequency modulation (FM) is a critical parameter of acoustic communication signals. In speech, rapid frequency transitions carry important information about plosive consonants.

Several studies in humans investigated the detection and discrimination of "slow" frequency modulated (FM) sweeps and found a strong dependence on the frequency span. Such "slow" upward FM sweeps were easier to detect and discriminate than downward FM sweeps in several studies in the literature. FM transitions in speech, however, are rapid and of larger frequency span. An advantage in detection of upward modulated sweeps for such rapid FM sweeps was so far only described in untrained subjects in a recent study (Gordon and Poeppel, *Acoust. Res. Lett. Online* **3**: 29; 2002). We followed this line of research in psychoacoustic experiments using trained subjects and, in addition, investigated possible differences in detection and discrimination between rapid upward and downward FM sweeps in greater detail.

No differences were obvious in the thresholds for detection of FM stimuli (2-100 octaves/s) in background noise

between upward and downward FM for trained subjects. Psychometric functions for upward FM, however, were steeper. Upward and downward FM sweeps were tested independently in 2IFC-discrimination experiments comparing sweeps of different modulation rate but constant direction. Small but consistent advantages in discrimination were again found for upward modulations in different frequency ranges (0.5-3 kHz). These results hint towards a direction-dependent mechanism for the processing of FM sweeps in general.

### **1033** Music Perception with Bone-Conducted Ultrasound

**Takefumi Sakaguchi**<sup>1</sup>, Tadashi Nishimura<sup>1</sup>, Hiroshi Hosoi<sup>1</sup>, Yoshiaki Watanabe<sup>2</sup>

<sup>1</sup>Nara Medical University, <sup>2</sup>Doshisha University

Previous studies reported that not only normal-hearing subjects but also profoundly deaf subjects could perceive speech sounds when the ultrasound were modulated by the speech sounds and presented via bone-conduction. Recently, one of the profoundly deaf subjects, who tried our bone-conducted ultrasound hearing aid (USHA) device, were able to understand speech sounds with USHA, and moreover, listen to music and even discriminate the differences of the music.

In this study, we have designed experiments to evaluate the ability of music perception, especially the ability of tempo discrimination, of the bone-conducted ultrasound listeners.

Four different drum sounds, of which tempo were 60, 80, 100, and 120 beats per minute (bpm), were made so as to be used as standard stimuli. Faster, slower, and same tempo drum sounds were also made as test stimuli. Standard and test stimuli were paired randomly with 1 s interval, and were presented to the normal-hearing and profoundly deaf subjects. Subjects were asked to answer whether the tempo of the test stimuli were "faster" or "slower" or "same" compared to the formerly presented standard stimuli.

Although correctly answered percentage of tempo discrimination experiment of bone-conducted ultrasound listeners were slightly poorer than the air-conducted audible sound listeners, it was better than the results of the cochlear implant listeners.

### **1034** Variable Effects of Spectral Resolution and Spectral Asynchrony on the Identification of Environmental Sounds

**Valeriy Shafiro**<sup>1</sup>, Yana Gilichinskaya<sup>2</sup>

<sup>1</sup>Rush University Medical Center, <sup>2</sup>City University of New York, Graduate Center

Previous research demonstrates that spectral resolution affects listeners' ability to identify familiar environmental sounds. Using a noise-excited vocoder simulation of a cochlear implant, Shafiro (2004, unpublished dissertation) showed that identification of environmental sounds tended to improve as the number of frequency channels increased. However, following the initial increase in identification performance, identification accuracy of a

large number of individual sounds decreased with further increases in the number of channels. It was hypothesized that this decrease resulted from the effects of spectral asynchrony introduced by unequal filter group delays across frequency channels. This hypothesis was not confirmed, however, by a follow-up experiment that attempted to equalize the amount of cross-channel asynchrony by using either long logarithmically spaced FIR filters, or linearly distributed 6th order Butterworth filters. One possible reason for the lack of an effect of spectral asynchrony could be the introduction of novel processing artifacts (e.g., ringing) that might have additionally distorted the stimuli and obscured effects of asynchrony. This interpretation is supported by the result that a larger number of sounds declined in accuracy at a lower number of frequency channels. To further examine possible effects of spectral asynchrony another experiment was conducted. The amount of spectral asynchrony was manipulated by limiting the number of times filtering is performed on each channel by the vocoder algorithm. Results indicate that multiple acoustic parameters including spectral resolution and spectral asynchrony play a role in the perception of environmental sounds. Implications of these results for the accuracy of acoustic models of cochlear implants are discussed.

### **1035 F0 Discrimination and Pitch-Strength Matching for Filtered Iterated Rippled Noise: The Correlation Between Different Measures of Pitch Strength**

**Lutz Wiegrebe<sup>1</sup>**, Alexandra Stein<sup>1</sup>

<sup>1</sup>*University of Munich*

It is generally assumed that listeners' capability to detect small changes in the fundamental frequency ( $f_0$ ) of a perceived complex sound ( $f_0$  difference limens,  $f_0$ DLs) is a good indicator of pitch strength. The use of iterated rippled noise (IRN) allows adjusting the pitch strength by manipulating the gain in the delay-and-add network used to generate IRN. Three experiments are presented which investigate the effect of gain changes on IRN  $f_0$ DLs.

In the first experiment,  $f_0$ DLs were measured for IRNs with reference  $f_0$ s of 90 and 250 Hz in three band-pass conditions ('low', 125-625 Hz; 'mid', 1375-1875 Hz; and 'high', 3900-5400 Hz). For a 90-Hz  $f_0$ , harmonics are spectrally resolved in the 'low' condition and unresolved in the 'mid' and 'high' condition. Correspondingly, for a 250-Hz  $f_0$ , harmonics are resolved in the 'low' and 'mid' condition and unresolved in the 'high' condition.

In the second experiment, the listeners reduced the IRN pitch strength in a spectrally resolved condition ('low' condition with  $f_0 = 90$  Hz or 'mid' condition with  $f_0 = 250$  Hz) to match the pitch strength in the corresponding unresolved condition ('mid' condition with  $f_0 = 90$  Hz or 'high' condition with  $f_0 = 250$  Hz).

In the third experiment,  $f_0$ DLs were remeasured for the pitch-strength reduced conditions ('low' condition with  $f_0 = 90$  Hz or 'mid' condition with  $f_0 = 250$  Hz).

The results show that although the listeners provided reliable pitch-strength matching in Experiment II, the  $f_0$ DLs in Experiment III were still much better for the pitch-

strength reduced spectrally resolved stimuli than for the spectrally unresolved stimuli. Thus, listeners showed different  $f_0$ DLs for stimuli which had the same pitch and were individually adjusted to have the same pitch strength. These results question the value of  $f_0$ DLs to assess pitch strength.

### **1036 Hearing Out Concurrent Harmonic Complex Tones**

**Christophe Micheyl<sup>1</sup>**, Andrew J. Oxenham<sup>1</sup>

<sup>1</sup>*MIT Research Laboratory of Electronics, Cambridge, MA*

Harmonic complex tones (HCTs) are an ecologically important class of sounds for both animals (vocalizations) and humans (speech and music). In natural settings, target HCTs often have to be heard out in a background of other sounds, including other HCTs (e.g., multi-talker conversation or orchestra). Numerous earlier studies have been devoted to concurrent vowel identification. However, little is still known regarding more basic detection and discrimination abilities of concurrent harmonic complexes other than vowels. This study measured threshold target-to-masker ratios (TMRs) for a) detection and b)  $F_0$ -discrimination HCT targets in the presence of another HCT as a function of 1) the nominal  $F_0$  of the target (100, 200, or 400 Hz), and 2) the average separation between the target and masker  $F_0$ s (-7, 0, or +7 semitones).  $F_0$ s and levels were varied to limit loudness or mean-rate cues. Other factors such as component-phase relationships and target-masker onset asynchronies, as well as conditions involving inharmonic-complex-tone or noise maskers, were also tested. The stimuli were bandpass-filtered between 1200 and 3600 Hz and lowpass-filtered noise was added to mask distortion products. In the detection task, threshold TMRs improved as the target  $F_0$  increased and as the masker  $F_0$  increased relative to that of the target. Inharmonic maskers and noise produced higher TMRs than HCT maskers. In the  $F_0$ -discrimination task,  $F_0$  differences between target and masker tones produced lower TMRs at the highest target  $F_0$  tested (400 Hz) but not at the lowest (100 Hz). Temporal asynchronies between the target and masker had a similar effect. The results suggest that peripheral frequency resolution limits the ability to benefit from sound-source segregation cues such as  $F_0$  differences or onset asynchronies when trying to detect, or track the  $F_0$  of, concurrent HCTs. [Supported by NIDCD R01DC05216]

### **1037 The Effect of a Flashing Visual Stimulus on the Auditory Continuity Illusion**

**Maori Kobayashi<sup>1</sup>**, Yoshihisa Osada<sup>2</sup>, Makio Kashino<sup>3</sup>

<sup>1</sup>*Rikkyo University*, <sup>2</sup>*NTT Communication Science Labs.*, *NTT Corporation*, <sup>3</sup>*Rikkyo University*, <sup>3</sup>*NTT Communication Science Labs.*, *NTT Corporation*

The effect of a visual stimulus on the auditory continuity illusion was examined. The auditory stimulus consisted of a 0.4-s, 500-Hz tone and a 0.2-s, 1/3-octave band-pass noise centered at 500 Hz, that were presented in an alternating fashion. The total duration was 4.45 s. The level of the noise was fixed at 60 dB SPL, and that of the tone was varied between 42 and 69 dB SPL at each trial.

The auditory stimulus was presented diotically through headphones. The visual stimulus was a series of white rings 5° in diameter, which flashed on a black background on a CRT monitor. In Exp. 1, 11 participants judged whether the tones were perceived as continuous in a 2AFC paradigm with and without the visual stimulus. The continuity limits (CL; a tone level at which the participant's judgment changed from continuous to discontinuous) were measured using the method of limits. In the flash condition, the white ring was synchronized with every onset of the noises. In the no-flash condition, only a fixation point was presented. The mean CL in the flash condition was approximately 2.2 dB higher than that in the no-flash condition ( $p < .05$ ), indicating that the visual stimulus enhanced the auditory continuity illusion. In Exp. 2, the effect of timing between the white ring and noise onset on the continuity illusion was examined. Eleven participants judged the apparent continuity of the tones using the same procedure as Exp. 1, under seven timing conditions (-200, -100, 0, 100, 200 ms of SOA, random timing at every noise onset, and no flash). The effect of the timing conditions on CL was significant ( $p < .01$ ). The CL in the 0-ms SOA condition was the highest among the five SOA values. No significant difference was found between the random condition and the no-flash condition, indicating that the difference was not due to distraction caused by the presence of the visual stimulus. Implications for the mechanisms of the continuity illusion and audiovisual interaction will be discussed.

### **1038** Limitations in Auditory Attentional Processing: The Auditory Attentional Blink vs. Backward Masking

Heidi Peeters<sup>1</sup>, David Gooler<sup>1</sup>

<sup>1</sup>University of Illinois at Urbana-Champaign

It is known that auditory processing is naturally associated with sequences of acoustic information. However, it is unclear how the processing of sequential auditory events is influenced by attentional capacity. It has been shown in the visual modality that when a target is identified in a stream of visual information, the recognition of a second target is compromised when appearing within a half second of the first target (Shapiro, Arnell, & Raymond, 1997). The period in which the second target is undetectable is referred to as the attentional blink. Exploration of this phenomenon in the auditory modality is not as well understood as it is in the visual modality. Mixed results have been obtained in which a distinct auditory attentional blink is not always present. An auditory attentional blink paradigm was adapted from procedures similar to previous attentional blink investigations. A stream of letters formed the distracters within which two targets (digits) were embedded. The time between targets and the number of distracters that followed the second target were varied. The results demonstrated that detection of the initial target was reduced when it was followed sequentially in time by a second target and only two distracting stimuli. When the number of distracters following the second target was increased to eight, detection of the second target was degraded beyond that of the first target. Detection of a

single target in a stream of distracters was always superior to performance in the two target paradigm. This may provide evidence that processing of auditory information triggering the attentional blink and backward masking phenomena follow similar processing in the auditory system.

### **1039** Distributed Brain Activation Involved in the Changes of Auditory Perceptual Organization: An Fmri Study on the Verbal Transformation Illusion

Hirohito Kondo<sup>1</sup>, Makio Kashino<sup>1</sup>

<sup>1</sup>NTT Communication Science Laboratories, NTT Corporation

Prolonged listening to a clearly spoken word repeated without pause produces a series of illusory changes for the physically unchanging word, which are known as the verbal transformations (VTs). A word "banana", for example, may be transformed into a variety of forms, including "nanba", "nanpa", "nappa", "nando", or "hana". We investigated human brain activity involved in the changes of perceptual organization in VTs using functional magnetic resonance imaging (fMRI). In experimental sessions, the word "banana", spoken by a female native speaker of Japanese, was presented repeatedly for 90 s diotically through headphones. Fourteen participants conducted two types of tasks in alternate sessions. One task was to respond to every transition in perceived verbal form, and the other to respond to clearly audible tone pips superimposed on the repeated word at random time intervals, both by pressing a button. The number of tone pips was matched individually with those of perceptual transitions. The behavioral results showed that the mean of median duration for one perceptual form was approximately 8.0 s (11.8 transitions for each session) and the number of different perceptual forms ranged from two to five across participants. We used an event-related procedure to identify brain activity at the time of perceptual transitions and tone detection. A group analysis indicated that the left insula, right temporal lobe, bilateral parietal lobe, and thalamus were activated both in perceptual transitions and tone detection. On the other hand, the bilateral prefrontal cortex, anterior cingulate cortex, and left inferior frontal cortex (Broca's area) were activated only in perceptual transitions. The primary auditory area was activated in tone detection but not in perceptual transitions. The results suggest that the changes of auditory perceptual organization in VTs involve activation in distributed brain regions outside the primary auditory area, especially in the frontal lobe.

### **1040** The Dynamics of Auditory Streaming

Minae Okada<sup>1</sup>, Shin Mizutani<sup>2</sup>, Makio Kashino<sup>2</sup>

<sup>1</sup>AI Incorporated, <sup>2</sup>NTT Communication Science Labs., NTT Corporation

Perceptual organization of tone sequence, or auditory streaming, is inherently a dynamic phenomenon, but its dynamics are not fully understood. In this study, we presented participants with a repeating pattern of tones for as long as 6 min, and analyzed the time series of reported

perceptual transitions. The test sequences were 900 repetitions of a triplet pattern composed of low-frequency tone (L) and high-frequency tone (H). The frequency difference ( $\Delta f$ ) between L and H was either approximately 1/12, 1/6, 1/3, 1/2, and 1 octave centered at 1kHz. The duration of each tone was 40 ms including raising and falling cosine ramps of 10 ms. The stimulus onset asynchrony (SOA) of adjacent L and H tones within a triplet was 100 ms. The SOA of neighboring triplets was 200 ms. Ten participants were instructed to listen to the test sequence without any particular listening attitude, and to report whether they perceived one stream (LHL-LHL-...) or two streams (L-L-... and H---H---...) by touching the corresponding keys of a response box whenever the percept changed. The test sequences were presented to the left ear through a headphone at 60 dB SPL. Each participant ran 10 sessions for each  $\Delta f$  condition. The results showed that (1) the percept switched frequently and randomly during the stimulus presentation in all  $\Delta f$  conditions after the initial build-up of streaming, (2) the time required for the build-up of streaming decreased as  $\Delta f$  increased, (3) the time-interval histogram for each of the two percepts conformed to the gamma distribution or the lognormal distribution, and (4) the mean number of streams and mean total duration of the "two streams" response increased as  $\Delta f$  increased. These results cannot be fully explained by previously proposed theories of auditory streaming, such as the peripheral channel theory, the pitch-jump detector theory, and the accumulation-of-evidence theory. We propose a theory of streaming incorporating neural dynamics.

### **1041 Visualizing Hair Bundles in Three Dimensions at Molecular Resolution: Extracellular Links, the Adaptation Machinery, and Lipid Rafts**

**Manfred Auer**<sup>1</sup>, A. J. Hudspeth<sup>1,2</sup>

<sup>1</sup>The Rockefeller University, New York, NY, <sup>2</sup>Howard Hughes Medical Institute

Employing electron-microscopic tomography, we examined the three-dimensional structure of hair cells from the bullfrog's sacculus. We observed the distinct structures of three types of extracellular link: tip links connecting adjacent stereocilia, basal links joining stereocilia just above their tapers, and kinociliary links that ligate stereocilia to the kinocilium. Tip links are straight, 140 nm long, 16 nm wide, and 8 nm thick. Basal links are arched or S-shaped and 200 nm long, whereas kinociliary links are pleated and range in length between 85-100 nm in length. Tip link and basal links, but not kinociliary links, exhibit a lower density at their midpoints. Assuming filamentous protein strands 8 nm diameter, these properties suggest that tip links are tetramers, consisting of two dimers joined at their ends. Basal links likewise appear to consist of two halves joined at their termini. Both basal and kinociliary links, but not tip links, form complexes containing multiple links. We also observed an auxiliary strand that extends from the top portion of a tip link and terminates about 100 nm above the link's upper

insertion. Our data obtained by electron tomography can be compared with models of cadherin 23 and fibronectin.

We visualized the insertional plaque that connects each tip link to the actin cytoskeleton and delineated electron densities that are consistent in size and shape with myosin molecules. We are currently analyzing these data in order to estimate the number of putative myosin molecules in each motor.

Using appropriate controlled detergent extraction protocols, we found in stereocilia a dense array of membrane patches, each 20-40 nm in diameter, that resist extraction with cold Triton X-100 but are sensitive to cholesterol-depleting reagents. We infer that stereociliary membranes contain a high density of lipid rafts, which are known to be involved in cellular signaling. As long as these lipid rafts remain intact, detergent extraction does not disrupt tip or basal links, presumably owing to their anchorage to the cytoskeleton.

This work was supported by grant DC00241 from the National Institutes of Health.

### **1042 Localization of Lipids to Distinct Domains in Hair Bundles**

**Peter Gillespie**<sup>1</sup>, Moritoshi Hirono<sup>1</sup>, Diane Ronan<sup>1</sup>, Guy Richardson<sup>2</sup>

<sup>1</sup>Oregon Health & Science University, <sup>2</sup>University of Sussex

Phosphatidylinositol 4-5-bisphosphate (PIP<sub>2</sub>) regulates slow adaptation, mediated by myosin-1c, and fast adaptation, thought to be controlled by Ca<sup>2+</sup> binding to the transduction channel (Hirono et al., Neuron, in press). Moreover, as PIP<sub>2</sub> is depleted from hair cells, mechanotransduction disappears. Motivated by these observations, we localized PIP<sub>2</sub> and other lipids in hair bundles. PIP<sub>2</sub> is excluded from the basal region of hair bundles and apical surfaces of frog saccular hair cells; in addition, detergent treatment shows that PIP<sub>2</sub> at stereocilia tips and in a band above the ankle-link region resists extraction, suggesting that it is immobilized by PIP<sub>2</sub>-binding proteins or by other means in these regions. Localization of a phosphatidylinositol lipid phosphatase, Ptpqr, to these PIP<sub>2</sub>-free domains suggests that Ptpqr maintains low PIP<sub>2</sub> levels there. In most cells, phosphatidylserine (PS), detected by fluorescent annexin V, is localized uniformly throughout stereocilia. In some cells, however, PS is concentrated in a band at the ankle links, in a region where PIP<sub>2</sub> is absent. Finally, as detected with fluorescent cholera toxin B subunit, the glycosphingolipid GM1 ganglioside is found in hair cells at stereocilia tips, in the ankle-link region, and at apical surfaces. Conversion of sialic acid-modified gangliosides to GM1 gangliosides with neuraminidase greatly enhances CTX reactivity in the taper and ankle-link region, suggesting that multiply-glycosylated gangliosides are concentrated there. Taken together, these results show that different lipid species are maintained in distinct domains in hair bundles



### **1043 Is TRPA1 the Transduction Channel?: Mechanics of the Ankyrin-Repeat Domain**

Marcos Sotomayor<sup>1</sup>, Eunice Cheung<sup>2</sup>, Klaus Schulten<sup>1</sup>, David P. Corey<sup>2,3</sup>

<sup>1</sup>University of Illinois at Urbana-Champaign, <sup>2</sup>Harvard Medical School, <sup>3</sup>Howard Hughes Medical Institute

NOMPC and TRPA1 are strong candidates for components of the transduction channel of vertebrate hair cells. They are unique among TRP channels in possessing a large number of ankyrin repeats preceding the transmembrane domains (29 or 17, respectively). While ankyrin repeats are often protein-binding sites, we wondered if the large number indicates another, perhaps mechanical function.

We explored the elastic properties of ankyrin repeats using extensive molecular dynamics simulations of existing crystallographic structures of 4 and 12 ankyrin repeats, and derived models of 17 and 24 ankyrin repeats. We have found a two stage elongation-unfolding mechanism by which ankyrin repeats respond to external forces. First, these large structures-- with intrinsic curvature formed by ankyrin repeats-- become straight when stretched using relatively small forces (~25 pN), and relax back in nanoseconds. Then, unfolding of individual repeats along with fragmentation of the structure occurs at larger forces (>100 pN). Calculated spring constants were similar to that measured for the gating spring in optical-trap experiments on frog hair cells.

We compared the calculated ankyrin elastic properties with the behavior of the EC2 domain of cadherin C, a protein similar to the tip-link protein cadherin23. The EC2 cadherin domain responds to external forces distinctly differently from ankyrin repeats. In addition, we found that Ca<sup>2+</sup> ions affect the pathway and forces required for unfolding.

Our results show that extension and spring constants found for large ankyrin-repeat structures are in agreement with the values predicted by the gating spring model of hair-cell mechanotransduction, suggesting that ankyrin repeats provide a flexible link between membrane channels and the cytoskeleton.

### **1044 Mechanoelectrical Transduction in Adult Inner Hair Cells**

Shuping Jia<sup>1</sup>, Peter Dallos<sup>2</sup>, David He<sup>1</sup>

<sup>1</sup>Creighton University, <sup>2</sup>Northwestern University

The inner hair cell (IHC) is one of two types of sensory receptor cells in the cochlea, the one that provides auditory information to the brain. IHCs respond to basilar membrane vibration by producing a receptor potential. The first steps towards the generation of the receptor potential are the deflection of the hair bundle, and the subsequent flow of transducer current through the mechanosensitive transducer channels at the tips of the stereocilia. Although IHC receptor potentials have been recorded from adult animals *in vivo*, using sharp electrodes, and in culture preparations of neonatal mice, the mechanotransducer current has not been recorded from adult animals. We simultaneously recorded IHC transducer currents and basilar membrane motion in a

gerbil hemicochlea to examine relations between transducer currents and basilar membrane (BM) displacements, and their variation along the cochlear length. Hemicochleae were prepared from 25- to 35-day-old gerbils. Transducer currents were recorded from IHCs in the apex and base of the hemicochlea during basilar membrane vibration evoked by a glass fiber positioned below the BM. The magnitude of the BM motion was measured by a photodiode-based system. Results show that transducer currents can be best fit with 2<sup>nd</sup> order Boltzmann functions. Maximum currents are of the order of 1.0~1.5 nA in both apical and basal cells. The operating range of the cells, however, is quite different. In line with our previous work with outer hair cells [He et al., *Nature*, 429: 2004], smaller BM displacement produces the same current in basal cells. Finally, there is a phase lead of IHC receptor currents re BM displacement (Supported by NIH grants to DH and PD).

### **1045 Prestin's Interaction with CFTR Enhances its Function**

Jing Zheng<sup>1</sup>, Sal Aguiñaga<sup>1</sup>, Charles T. Anderson<sup>1</sup>, Katharine Miller<sup>1</sup>, Peter Dallos<sup>1</sup>

<sup>1</sup>Northwestern University

Prestin is the motor protein of outer hair cells (OHCs) and plays an important role in the frequency selectivity and sensitivity of mammalian hearing. Prestin belongs to the solute carrier family 26 (SLC26A), but is unique for its voltage-driven motility and lack of anion transport. CFTR (cystic fibrosis transmembrane conductance regulator) is a cAMP-activated chloride channel, critical for the regulation of Cl<sup>-</sup> transport and fluid secretion in various tissues. Recently, it was discovered that CFTR modifies the function of some SLC26A proteins. Because prestin's function relies on Cl<sup>-</sup> anions, and CFTR is known to regulate Cl<sup>-</sup>, it is of great interest to explore the potential interaction between prestin and CFTR. By using RT-PCR and *in situ* hybridization, we discovered that CFTR mRNA is present in OHCs. The study of prestin/CFTR interaction was further investigated by measuring nonlinear capacitance (NLC), a signature of OHC motility. When CFTR cDNA alone was transfected into a human kidney cell line, no NLC was observed. When prestin and CFTR cDNAs were co-transfected into the cell line, however, cAMP-activated CFTR significantly increased voltage-dependent charge displacement in prestin/CFTR-expressing cells. Our data suggest that CFTR may be important for the regulation of OHC function. [Supported by Grant DC00089].

## **1046** Prestin's Partners: Molecular Interactions a Go-Go!

Jun-Ping Bai<sup>1</sup>, Haresha Samarnanayake<sup>2</sup>, Pownima Joshi<sup>2</sup>, Joseph Santos-Sacchi<sup>1</sup>, Dhasakumar Navaratnam<sup>2</sup>

<sup>1</sup>Otolaryngology and Neurobiology, Yale University, 333 Cedar Street, New Haven, CT, United States, <sup>2</sup>Neurology and Neurobiology, Yale University, 333 Cedar Street, New Haven, CT, United States

Prestin is a newly identified member of the anion transporter family that has been implicated in electromotility of outer hair cells. Though cells transfected with prestin display the many biophysical traits of the OHC motor, some differences have led us to speculate on multimeric interactions (Santos-Sacchi et al., J. Physiology, 2001). In trying to determine prestin's structure-function relationships we have previously demonstrated by serial truncations of its N and C termini that these intracellular termini are critical for electromotility. We hypothesized that these ends formed protein-protein interactions, and demonstrate here that prestin forms multimers using protein cross linking. In attempting to further define these interactions we used the C terminus of prestin (amino acids 495-744) as bait in a yeast two hybrid assay using a chick cochlea cDNA library, and identified several proteins that interacted under conditions of high stringency (-Ade; -His; -Leu; -Trp). These proteins included the beta-1 subunit of Na/K ATPase, and several proteins of as yet indeterminate function. We speculate that these proteins serve several functions including anchoring it to the underlying cytoskeleton. In further investigating prestin's interactions we used YFP and CFP tagged prestin to demonstrate via FRET that prestin molecules interact with other prestin molecules to form (homo)multimers. These data together suggest a complex molecular architecture underlying electromotility.

Supported by NIH DC 00273 (JSS) and DC05352 (DN).

## **1047** Proteomic and Biochemical Analysis of Prestin, the Outer Hair Cell Motor

Lisan Parker<sup>1</sup>, Michael Podgorski<sup>1</sup>, Xudong Wu<sup>1</sup>, Jian Zuo<sup>1</sup>

<sup>1</sup>St. Jude Children's Research Hospital

Electromotility of outer hair cells (OHCs) and cochlear amplification require prestin, the motor protein in the lateral wall plasma membrane of OHCs. The dynamic changes in OHC length in response to stimulation suggest that a tightly regulated motor complex composed of prestin:prestins interactions and/or prestin direct association with other membrane or cytosolic proteins contribute to OHC electromotility. To identify prestin interacting proteins, the last 100 or 246 residues of the mouse prestin C-terminus were expressed and purified as glutathione S-transferase (GST) tagged prestin carboxyl terminal fusion proteins. Lysates from various tissues including cochlea, brain and testes were used in pull-down assays with GST-prestin fusion proteins. In a complementary approach, prestin specific antibodies were cross-linked to agarose matrix or protein G beads. Tissue lysate was then incubated with the prestin antibody matrix to isolate prestin

protein complexes. Subsequently, the compositions of these complexes were determined by the use of multiple proteomic approaches, including 2D gel electrophoresis and mass spectrometry. Co-immunoprecipitation with prestin, Western blot analysis, and immunolocalization in the cochlea will be used to verify all proteins identified. Furthermore, the purified prestin C-terminal fusion proteins were used to investigate the biochemical and structural properties of prestin. Anion binding, phosphorylation and homomeric interactions of the prestin C-terminal fusion proteins were examined based on conserved features of the SLC26 superfamily. These studies will provide insights into the functions of prestin and makeup of the motor complex.

We thank J. Zheng, P. Dallos, and L. D. Madison for providing the prestin cDNA clone. This work is supported by the American Lebanese Syrian Associated Charities (ALSAC), NIH Cancer Center Support CORE grant (CA21765), and NIH grants to J.Z. (DC06471 and DC06471S1).

## **1048** Electro-Mechanical Transduction in the Absence of Prestin

Feng Qian<sup>1</sup>, William Brownell<sup>2</sup>, Bahman Anvari<sup>1</sup>

<sup>1</sup>Rice University, <sup>2</sup>Baylor College of Medicine

Cochlear outer hair cells (OHCs) are specialized sensory cells with a well-developed membrane motor capability in which the membrane protein prestin plays a central role. Combining optical tweezers with patch clamp techniques, we have studied the electro-mechanical transduction in membrane tethers formed from OHCs and human embryonic kidney (HEK) cells. After forming a membrane tether by optical tweezers, transmembrane voltage was changed, and the resulting membrane tether mechanical response was monitored continuously by an optically-trapped microsphere, which served as a micro-displacement or force sensor (Qian, et al, Rev. Sci. Instrum., 2004). Experimental results show that OHC and native HEK cell membrane tethers can respond mechanically to frequencies greater than 6kHz and 3kHz, respectively, though the patch clamp amplifier and pipette typically act as a low pass filter with a corner frequency below 1 kHz. The electrically evoked force from OHC tethers is nearly 20 times greater than that evoked from HEK tethers at high frequencies. Moreover, Both the OHC and the HEK cell membranes present different electro-mechanical transduction abilities as the membrane potential is changed. The transduction is greater with hyperpolarizing than with depolarizing potentials. The results confirm the ability of membranes to generate mechanical force in response to changes in the transmembrane potential even in the absence of prestin.

This research is supported by grant DC02775 from NIDCD

**1049 Theoretical Analysis of Electromechanical Effects on Tether Formation from Outer Hair Cells**

Emily Glassinger<sup>1</sup>, Robert Raphael<sup>1</sup>

<sup>1</sup>Rice University

Outer hair cells (OHCs) are necessary for the remarkable frequency discrimination and sensitivity of mammalian hearing. The integral membrane protein, prestin, is responsible for the outer hair voltage-dependent force generation and signature non-linear capacitance of outer hair cell. How prestin transduces electrical impulses into mechanical energy is not fully understood. Current theories suggest that prestin operates as either an area motor or as a nanoscale bending motor. Another hypothesis suggests that prestin amplifies the native voltage-dependent changes in membrane tension. To determine how prestin confers electromotility to the OHC membrane, an experiment which distinguishes in-plane area changes from nanoscale curvature changes must be conducted. One method to apply a large curvature deformation to a cellular membrane is to form a long, thin bilayer tube (tether) from the membrane surface. Recent tether experiments on voltage-clamped outer hair cells have measured force gains in OHCs and prestin-transfected HEK (human embryonic kidney) cells. Here we develop a theoretical framework to analyze how prestin's proposed modes of electromechanical coupling will affect tether conformation. The thermodynamic model of tether formation accounts for both active area and curvature changes as well as changes in interfacial tension.

**1050 Diversity of a1G Ca<sup>2+</sup> Channels and Their Functional Roles in the Mouse Inner Ear**

Liping Nie<sup>1</sup>, Judilee N Dinglasan<sup>1</sup>, Jerel Garcia<sup>1</sup>, Ebenezer N Yamoah<sup>1</sup>

<sup>1</sup>University of California, Davis

Alternative splicing is one of the major mechanisms for the functional diversity of the mammalian genomes. Here, we report the alternative splicing profile of a1G Ca<sup>2+</sup> channel in the mouse cochlea. A systematic RT-PCR method has been used to investigate alternative splicing of a1G Ca<sup>2+</sup> channels in the cochlea of adult CBA mice. The results showed that there are at least fourteen alternative splicings in the mouse cochlea, six of which are novel. Interestingly, all of the newly identified alternative splice forms occur at exon8 and exon9, and lead to the changes in the I-II linker of a1G Ca<sup>2+</sup> channel protein. Four of these splice variants have a shorter I-II linker (from 134 amino acid (aa) to 2aa), resulting from the exclusion of different regions in exon8 or exon9. Additionally, one splice variant has a longer linker (4aa). Moreover, in the case of the exclusion of exon9, the alternative spliced channel protein was truncated at the I-II linker. As a result, only the first transmembrane domain (domain-I) remained and was followed by a novel I-II linker with 51 distinct amino acids. It is well known that I-II linker of voltage-gated Ca<sup>2+</sup> channels is responsible for G-protein regulation of the channels as well as the interaction with

the auxiliary subunits. We predicted that these alternative splice variants probably result in the distinct channel properties and contribute to the inner ear specific-phenotype of a1G Ca<sup>2+</sup> channel. The experiments aimed at identifying the current properties of a1G Ca<sup>2+</sup> channel with different I-II linkers and their functional roles in the mouse inner ear are currently under investigation.

This work was supported by grants to ENY NIH-DC03828, DC04523

**1051 The Effect of the Beta Subunits on the Kinetic Properties of the BK Channel from Chick Hair Cells**

Alberto Ortega<sup>1</sup>, Haresha Samaranyake<sup>1</sup>, Joseph Santos-Sacchi<sup>1</sup>, Dhasakumar Navaratnam<sup>1</sup>

<sup>1</sup>Yale University

Electrical tuning is a mechanism used by certain vertebrate hair cells, including the chick and turtle, to discriminate between different frequencies of sound. The changing intrinsic oscillation frequency in hair cells along the tonotopic axis is brought about principally by the changing kinetic properties of the BK channel. Since native hair cell BK channels have kinetic properties that are different than those of heterologously expressed channels, we speculate that association with other proteins brings about the unique kinetic properties of the BK channels in hair cells. Beta subunits of the BK channels have been shown to affect the kinetic properties of the BK channel in hair cells and other systems. We have cloned three beta subunits from the chick basilar papilla the beta 1,2 and 4 subunits. Previously we showed the differential distribution of these channels in the chick basilar papilla. Here, using excised patch recordings, we show that the co-expression of the different beta subunits in Oocytes affect the kinetic parameters of the chick BK alpha subunit. While the beta subunits 1 and 4 prolong deactivation kinetics, the effect of the beta 1 subunit was several fold greater than that of the beta 4 subunit. Similarly, while the beta 1 subunit increased both Ca and voltage sensitivity, the beta 4 subunits effects on voltage sensitivity were dependent on the concentration of Ca. Thus, in keeping with the properties of the mammalian beta 4 subunit, the chick beta 4 subunit caused a rightward shift in conductance-voltage relations at 1micromolar Ca and a leftward shift at 50 micromolar Ca. The role of these subunits will be discussed in the context of electrical tuning.

**1052 Effects of Targeted Deletion of BK Channels on Inner Hair Cell Electrophysiology in vitro and Auditory Nerve Fiber Response in vivo**

Dominik Oliver<sup>1</sup>, Annette M. Taberner<sup>2,3</sup>, Matthias Sausbier<sup>4</sup>, Peter Ruth<sup>4</sup>, Bernd Fakler<sup>1</sup>, M. Charles Liberman<sup>2,3</sup>

<sup>1</sup>Dept. of Physiology II, University of Freiburg, Germany, <sup>2</sup>Eaton-Peabody Laboratory, Massachusetts Eye and Ear Infirmary, Boston MA 02114, <sup>3</sup>Program in Speech and Hearing Bioscience and Technology, Harvard-MIT,

Cambridge MA, <sup>4</sup>Dept. of Pharmacology and Toxicology, University of Tuebingen, Germany

In mammalian inner hair cells, two major outward-rectifying K<sup>+</sup>-currents are activated by depolarization: one fast (I<sub>k,f</sub>), the other slower (I<sub>k,s</sub>). The large conductance and fast kinetics of I<sub>k,f</sub> imply a role in shaping the voltage response of the IHC, even at relatively high frequencies. The pharmacological profile suggests that I<sub>k,f</sub> is carried by large-conductance, voltage- and Ca<sup>2+</sup>-gated K<sup>+</sup> channels (BK). We used BK deficient mice (BK<sup>-/-</sup>) to analyze the role of BK in mammalian cochlear processing.

Patch clamp recordings from IHCs revealed complete absence of the fast outward current in BK<sup>-/-</sup> mice, confirming the identity of I<sub>k,f</sub> as a BK current. There was no compensatory upregulation of other K<sup>+</sup> currents. To examine the role of BK in voltage signal processing, we injected sinusoidal currents at 2 kHz, shaped according to the mechano-electrical transducer characteristics. In wt cells, this resulted in saturating receptor potential (RP)-like voltage responses similar to RPs in vivo. In BK<sup>-/-</sup> mice, the current-evoked DC component was increased by ~66% and showed a slow relaxation, while the AC component was reduced by ~25%.

Auditory nerve responses in BK<sup>-/-</sup> mice were similar to wt in many respects, including threshold, sharpness of tuning, synchrony-level functions and dynamic range of rate-level functions. Abnormalities included a 15% increase in mean spontaneous rates and a 40% decrease in maximum rate (both onset and steady state).

These neural changes could arise from IHC depolarization due to loss of BK channels: sustained depolarization may directly affect the efficacy of the afferent synapse or - by reducing stereociliary Ca<sup>2+</sup> entry - shift the transducer set point rightward along the I<sub>x</sub>-curve, thus reducing sound-driven DC potentials and maximum neural rates.

Whatever underlies the rate anomalies, BK channels in mouse do not appear to play a major role in shaping the temporal aspects of auditory nerve response and are not required for normal frequency tuning.

### **1053 Voltage-dependent Sodium Channels in Rat Utricular Hair Cells**

**Julian Wooltorton**<sup>1</sup>, Karen Hurley<sup>1</sup>, Jasmine Garcia<sup>1</sup>, Ruth Anne Eatock<sup>1</sup>

<sup>1</sup>Baylor College of Medicine

The sodium (Na) currents in hair cells fall into three categories: TTX-sensitive and negatively inactivating, TTX-sensitive and less negatively inactivating, and TTX-insensitive and negatively inactivating. In hair cells of immature rat utricular maculae, we have identified two Na channel populations with different voltage ranges of inactivation, TTX sensitivity and localization within the macula. One current was TTX insensitive (53±4.8 [SEM] % reduction by 500 nM TTX; n=5 cells), had a negative half-maximal voltage of inactivation ( $V_{1/2(\text{inact})} = -93 \pm 0.5$  mV; n=66) and was found in 87% (48/55) of striolar hair cells. This current was also found in 32% (18/56) of hair cells from the surrounding extrastriola. The other current was TTX sensitive (76±8.1% block by 50 nM; n=3), had a less negative  $V_{1/2(\text{inact})}$  (-75±0.6 mV; n=45) and was found in

68% (38/56) of extrastriolar cells and only 13% (7/55) striolar cells. This current is not found in mature (postnatal day [P] 21) hair cells (Chabbert et al. 2003).

We screened thermolysin-treated P1 and P21/22 utricular maculae for all Na channel alpha subunits with the RT-PCR method. PCR products were detected for all TTX-sensitive subunits: Na<sub>v</sub>1.1, 1.2, 1.3 and 1.6 at both ages; 1.4 and 1.7 at P1 only. Of the 3 TTX-insensitive candidates, we found Na<sub>v</sub>1.5 at both ages. Hair cells were labeled for Na<sub>v</sub>1.2-, Na<sub>v</sub>1.6- and Na<sub>v</sub>1.5-like immunoreactivity (Gaboyard et al., this meeting). Together these results show that the TTX-insensitive current is likely to be through Na<sub>v</sub>1.5 channels. Our results also resolve the discrepancy between studies that describe the more negatively inactivating current in the mouse utricle (Rusch and Eatock 1997) and the less negatively inactivating current in the rat utricle (Chabbert et al. 2003): it is likely that the investigators sampled hair cells from the striola and extrastriola, respectively.

Support: NIDCD DC02290

### **1054 Expression Pattern of Voltage-Gated Na<sup>+</sup> Channels During Development of Rat Vestibular Endorgans.**

**Sophie Gaboyard**<sup>1</sup>, Steven Price<sup>1</sup>, Anna Lysakowski<sup>1</sup>

<sup>1</sup>University of Illinois at Chicago

Hair cells in the utricular macula of immature rats express two sodium (Na) currents with different voltage dependence. The less negatively inactivating current goes away with maturation and might correspond to NaV1.2 and/or NaV1.6 alpha subunits, which are expressed by these hair cells (Chabbert et al. 2003). The more negatively inactivating conductance has properties consistent with NaV1.5 alpha subunits (Wooltorton et al., this meeting). We have investigated the expression of these candidate subunits in the developing utricular maculae and cristae of postnatal day 1 (P1), P6, P12, and P21 rats by immunocytochemistry. NaV1.2 immunoreactivity was present in hair cells from P1 until P21, when staining intensity in the central/striolar region decreased. NaV1.6 immunoreactivity was present in hair cells at P1 and more intensely at P6; subsequently, intensity in hair cells faded, first in central/striolar regions and later in peripheral/extrastriolar regions. Over the same period, NaV1.6 immunoreactivity appeared in supporting cells, beginning in the central/striolar zone and spreading through the whole epithelium. By P21, NaV1.6 was present along supporting cell membranes, especially at the apex of the crista, whereas its expression in hair cells, especially type I, was weak. NaV1.5 immunoreactivity was evident in hair cells from P1 to adult. Our results support the suggestion that NaV1.5 subunits carry the negatively activating current of vestibular hair cells, and further suggest that this current persists in mature epithelia. Moreover, calyx afferents began to express the NaV1.5 subunit as soon as they formed, starting in the central/striolar zones and spreading throughout the epithelium. Supported by NIDCD grant DC02290.

### **1055** Synaptic Specializations in Turtle Auditory Hair Cells Support Role in Vesicle Trafficking for Synaptic Ribbons

Michael Schnee<sup>1</sup>, Max Lawton<sup>2</sup>, David Furness<sup>2</sup>, Timothy Benke<sup>3</sup>, Anthony Ricci<sup>1</sup>

<sup>1</sup>LSU Health Sciences Center, <sup>2</sup>Keele University,

<sup>3</sup>University of Colorado

Turtle auditory hair cells respond over a narrow frequency range, a consequence of an electrical tuning mechanism. This sharp tuning is transferred synaptically to the primary afferent neuron with high fidelity. Present work investigates presynaptic specializations responsible for accurate information transfer. Serial electron microscopic reconstruction of hair cells and synaptic ribbons from two frequency locations (~120 Hz and ~320 Hz) of the auditory papilla revealed a difference in number of release sites and density of vesicles near the ribbons. Calcium-dependent membrane capacitance changes that track vesicular release, found differences in rates and number of released vesicles that could in part be accounted for by scaling for the above morphological differences. A model of release derived from equilibration of vesicles between pools reproduced the three kinetic phases of release and demonstrated that increasing the number of release sites extends the frequency range over which synchronous synaptic activity can occur.

### **1056** Asynchrony and the Grouping of Vowel Components: Captor Tones Revisited

Brian Roberts<sup>1,2</sup>, Stephen D. Holmes<sup>1,2</sup>

<sup>1</sup>School of Psychology, University of Birmingham, Edgbaston, Birmingham, United Kingdom, <sup>2</sup>Neurosciences Research Institute, Aston University, Aston Triangle, Birmingham, United Kingdom

Asynchrony is an important grouping cue for separating sound mixtures. An incremented component makes a reduced contribution to vowel timbre when it begins before the other components. The basis of this effect was explored by adding a captor tone one octave above the incremented harmonic and synchronous with its leading portion (Darwin & Sutherland 1984, QJEP 36A: 193-208). The captor was too remote to evoke adaptation in peripheral channels tuned to the incremented harmonic, but nonetheless the contribution of that harmonic to vowel quality was partly restored. Hence, this restoration effect was thought to arise from the grouping of the leading portion of the incremented component with the captor, leaving the remainder to group with the vowel. This account has been tested using captors that begin asynchronously with the leading harmonic, or which are not harmonically related to it. If grouping by common onset and harmonicity is the underlying mechanism, asynchronous or inharmonic captors should be less effective in restoring the contribution of an asynchronous harmonic. The main findings are: (1) The captor is as effective when it begins before or after the onset of the leading component as when it begins in synchrony. (2) Captor efficacy is dependent on frequency proximity with the leading component, not on harmonic relations. (3) A noise-band captor is at least as effective as a tonal captor

of similar power and center frequency. (4) The effect of the captor is equivalent to attenuating the leading portion of the incremented harmonic by 6 dB. Together, these results indicate that high-level auditory grouping factors do not govern the captor effect. Instead, it is proposed that the efficacy of a captor in restoring the perceptual contribution of an asynchronous component to vowel timbre can be understood in terms of broadband inhibition within the cochlear nucleus (Pressnitzer et al 2001, J Neurosci. 21: 6377-6386). [Supported by BBSRC (UK) grant 6/S17805].

### **1057** Human Perception of Simultaneous Dichotic Speech Streams

Frederick J. Gallun<sup>1</sup>, Christine R. Mason<sup>1</sup>, Gerald Kidd, Jr.<sup>1</sup>

<sup>1</sup>Boston University

This study investigated the ability of listeners to process two simultaneously presented speech streams. One stream was presented to each ear and the task and stream was either specified in advance (single-task) or specified after the streams had been presented (dual-task). The tasks were either to recognize keywords in both simultaneously presented sentences (Exp. 1) or to recognize the keywords in one sentence and simply detect the presence of the other sentence (Exp.2). Sentences were presented in noise set at a level that reduced performance to roughly 90% correct when each task was performed alone with only one stream present. In Exp. 1, requiring identification of key words from either ear, listeners behaved as if they could process only one stream, while in Exp. 2, requiring key word identification in one ear and only detection of speech in the other, listeners successfully processed both. The results are discussed in the context of attentional resource theory and the ability of listeners to rapidly switch attention between streams.

### **1058** The Role of Suppression in Measures of Auditory Filter Bandwidths by Profile Analysis

Jennifer Lentz<sup>1</sup>, Melissa Ferrello<sup>1</sup>

<sup>1</sup>Indiana University

Profile-analysis thresholds were measured as a function of the number of stimulus components in the presence and in the absence of background noise for normal-hearing and hearing-impaired listeners. If suppression affects the measurement of auditory filters, wider bandwidths should be measured in the presence of noise. Hearing-impaired listeners, who do not have active cochleae, also should have wider auditory filter bandwidths in profile-analysis tasks. In this task, the number of components (N) at which masking begins to occur (the minimum in the function relating thresholds to N) reflects the frequency selectivity of the auditory system. A system with wider auditory filters should have a minimum profile-analysis threshold at a smaller N than a system with narrower auditory filters. Stimuli were the sum of 2 – 30 tones, ranging in frequency between 200 and 4000 Hz. The standard stimulus had equal-amplitude tones presented at 80 dB SPL per component, and the signal stimulus was created by alternately decreasing and increasing the levels of every

other component. In the noise-present condition, a 5000-Hz low-pass noise with a spectrum level of 50 dB/Hz was added to all signal and standard stimuli. For all listeners, thresholds fell with increasing N when N was small, and increased with increasing N when N was large. Minima in the functions relating thresholds to N were at about 4 components for the hearing-impaired listeners and at about 10 for the normal-hearing listeners, regardless of the presence or absence of background noise. As expected, data from hearing-impaired listeners were consistent with poorer frequency selectivity. For the normal-hearing listeners, the noise masker did not lead to wider auditory filter bandwidths because the minima were not altered by the presence of noise. This would suggest that the different auditory filter bandwidths obtained in notched-noise and profile-analysis tasks is not due to suppression. [Work supported by NIH.]

### **1059 Spectral Enhancement Revealed by Sinusoidal Spectral Modulation Masking Period Patterns.**

**Aniket Saoji<sup>1</sup>**, David A. Eddins<sup>1</sup>

<sup>1</sup>*Psychoacoustics Lab, Center for Hearing and Deafness, State University of New York at Buffalo*

An important component in the development of an overall framework for understanding auditory perception is knowledge of the internal representation of various spectral features. Previous studies have used the simultaneous and forward masking paradigms to determine masking patterns thought to reflect the internal representation of the chosen masker's complex spectral envelope. In the present study a more general approach was adopted based on the same masking technique. The internal representation of spectral envelope was estimated for noise carriers with sinusoidal spectral modulation producing spectral envelopes differing in spectral modulation frequency (0.25, 0.5, 1.0, 2.0, and 4.0 cycles/octave), phase (0,  $\pi/2$ ,  $\pi$ ,  $3\pi/2$ ), and depth (5, 15, and 25 dB SL). Simultaneous masking patterns indicate a reduction in spectral contrast for higher spectral modulation frequencies ( $\geq 2$  cycles/octave), consistent with the limits imposed by the frequency selectivity of the auditory system. Interestingly, forward masking patterns revealed considerable spectral enhancement as compared to the simultaneous masking patterns for the modulation frequencies of 1.0 and 2.0 cycles/octave. By mapping the internal representation of spectral envelope as a function of modulation frequency, depth, and phase, one can derive a space which, in theory, may be used to predict the internal representation of any arbitrary spectral envelope. (Work supported by NIH NIDCD DC04403).

### **1060 The Missing Target: Evidence of a Tone's Inability to Contribute to the Auditory Foreground.**

**Adrian KC Lee<sup>1</sup>**, Barbara Shinn-Cunningham<sup>1,2</sup>, Andrew Oxenham<sup>1,3</sup>

<sup>1</sup>*Harvard-MIT Division of Health Sciences and Technology, Speech and Hearing Bioscience and Technology,* <sup>2</sup>*Hearing*

*Research Center, Department of Cognitive and Neural Systems, Boston University,* <sup>3</sup>*Research Laboratory of Electronics, Massachusetts Institute of Technology*

A number of cues have been identified as contributing to formation of perceptual objects or streams across frequency and time. Here we investigate the specific influence of ITDs and frequency proximity on the grouping of an ambiguous target tone with competing temporal and spectral grouping cues.

The stimuli were repetitions of a three-tone sequence, consisting of a pair of pure tones followed by a harmonic complex. The harmonic complex was spectrally shaped by a synthetic vowel formant, producing the percept of a repeating vowel that occurred at a rate one-third that of a separate, ongoing stream of pure tones. The vowel was generated such that its perceived identity depended on whether or not one particular harmonic (the "target") was perceived in the complex (shifting the vowel from /eh/ when the target was perceived in the complex to /ih/ when the target was not perceived in the complex). Similarly, the perceived rhythm of the ongoing tone stream was heard as "regular" when the target was heard in the stream and "galloping" when the target was not in the stream. The ITDs and frequencies of the tones making up the stimuli were manipulated to explore how spatial and frequency cues influence across-time and across-frequency grouping.

Results show that the degree to which the target influences the vowel identity does not predict the degree to which it influences the tone stream rhythm. In some conditions, the tone is heard prominently in the tone stream and not in the vowel. However, in other conditions the target tone is not heard strongly in either the vowel or the tone stream. This phenomenon provides an interesting counterpart to the well-known duplex percept, in which a spectral component can contribute to two percepts simultaneously; in the present case, the "orphaned" tone contributes to neither percept. [Supported by ONR N00014-04-1-0131 and NIH DC05216.]

### **1061 Factors Affecting Perceptual Weighting of Acoustic Cues in a Categorization Task**

**Lori L. Holt<sup>1</sup>**, Andrew J. Lotto<sup>2</sup>

<sup>1</sup>*Carnegie Mellon University,* <sup>2</sup>*Boystown National Research Hospital*

The perception of complex sounds, such as speech, often requires the integration of information across multiple dimensions. The present experiments investigate the perceptual effectiveness or "weighting" of acoustic dimensions in a categorization task. Human listeners categorized sounds drawn from two input distributions lying within a two-dimensional acoustic space defining the center frequency (CF) and modulation frequency (MF) of frequency-modulated sinewaves. The 2-d acoustic space was scaled such that each dimension was psychophysically matched to be equally discriminable and, in the first experiment, equally informative for accurate categorization. Despite this normalization, listeners' category responses reflected a bias for use of CF. The CF bias was moderated when training distribution overlap was

increased along the CF dimension, thereby decreasing the informativeness of CF for the task. A reversal of weighting (MF over CF) was obtained when distribution variance was increased along the CF dimension. These results demonstrate that even when equally informative and equally discriminable, acoustic cues are not necessarily equivalently weighted in perception; listeners exhibit biases when integrating multiple acoustic dimensions. Drastic changes in cue weighting strategies can be effected by changes in input distribution parameters. Moreover, a final experiment demonstrates that listeners can be encouraged to re-weight acoustic dimensions by mere exposure to acoustic tokens varying along the less-preferred acoustic dimension. These methods provide potential insights into acquisition of speech sound categories, particularly second language categories for which cue weighting is a critical issue.

### **1062** Frequency Discrimination of Complex Tones as a Function of Harmonic Number and Component Phase; Teasing Out the Role of Component Resolvability and Temporal Fine Structure

**Brian Moore<sup>1</sup>**, Brian Glasberg<sup>1</sup>, Helen Flanagan<sup>1</sup>

<sup>1</sup>*University of Cambridge*

Thresholds for discriminating the fundamental frequency (F0) of a complex tone, F0DLs, are small when the tone contains low harmonics, but increase when the rank of the lowest harmonic is increased above about eight. It is usually assumed that performance is good for low harmonics because these harmonics are resolved in the peripheral auditory system, and that performance is poor for very high harmonics because only information about the temporal envelope of the stimulus is available. It remains unclear what mechanisms are involved for complex tones whose lowest harmonic has a rank in the range 8 – 13, for which performance is still reasonably good. It is possible that harmonics in this range are resolved to some extent, and that performance is based on resolved harmonics. Alternatively, pitch may be extracted from the time intervals between peaks in the temporal fine structure of the waveform close to adjacent envelope maxima. To assess these possibilities, F0DLs were measured for complex tones with three successive harmonics, as a function of the number of the lowest harmonic. The nominal frequency of the centre component of each complex tone was 2000 Hz, and the harmonic number was varied by changing the mean F0. A background noise was used to mask combination tones. The value of F0 was roved across trials to force subjects to make within-trial comparisons. Within each forced-choice trial, the number of the lowest harmonic was roved by  $\pm 1$  for each of the two intervals, to prevent subjects from using excitation pattern cues. The components were added with two different phase relationships. One (cosine phase) was designed to give a “peaky” waveform on the basilar membrane, while the other (alternating phase) was designed to give a much “flatter” waveform. If performance is based on resolved harmonics, component phase should not influence the results. If performance is

based on temporal fine structure (or envelope cues), the peaky waveform should lead to lower F0DLs. F0DLs were not influenced by component phase for low harmonic numbers, but were smaller for cosine than for alternating phase once the number of the lowest harmonic exceeded 8-10, suggesting that temporal fine structure plays a role in this range.

### **1063** Modulation Masking of Synchrony Detection

**Stanley Sheft<sup>1</sup>**, William A. Yost<sup>1</sup>

<sup>1</sup>*Parmly Hearing Institute, Loyola University Chicago*

Modulation filterbank models discard phase information above very low rates of amplitude modulation (AM). In contrast to this lowpass modeling assumption, results from synchrony-detection studies demonstrate ability to utilize envelope-phase information at moderate to high AM rates. One concern in applying these results to modeling is the extent to which they represent sensitivity to modulation phase versus processing a consequence of the envelope-phase manipulation. In the case of synchrony detection, spectral processing of the temporal modulation of the excitation pattern could cue the task. The present work evaluated modulation masking of synchrony detection in an attempt to estimate task dependence on modulation processing. In all conditions, the task was to detect incoherent modulation of two concurrent pure-tone carriers at 2.0 and 3.6 kHz. Modulation maskers were added as either a second component of the functions modulating the pure-tone carriers, or were introduced at intermediate spectral locations with either a noise band or pure tone as the modulation-masker carrier. Additional maskers were added to restrict within-channel listening or cuing by distortion products. Probe AM rate was 10, 20, or 40 Hz with modulation depth either 0.5 or 1.0. Masker AM rates ranged from 5 to 160 Hz. Modulation masking of synchrony detection was obtained primarily at the shallower probe AM depth. The masking functions, however, did not show tuning in the modulation domain. Manipulation of masker coherence or probe gating characteristics indicated a role of auditory grouping factors. As with streaming, when the probe carriers segregate, judgments of synchrony (temporal order) become difficult. The absence of significant modulation masking with a probe AM depth of 1.0 suggests the task does not rely on modulation processing per se, but rather reflects detection of cross-spectral synchrony with the envelopes acting as gating functions. [Supported by NIH DC005423.]

### **1064** The Role of Persistence in Forward Masking

**Magdalena Wojtczak<sup>1</sup>**, Neal F. Viemeister<sup>1</sup>

<sup>1</sup>*University of Minnesota*

Persistence of excitation extending beyond the offset of a stimulating sound has been proposed as a mechanism underlying forward masking. The persistence hypothesis was tested by comparing interaural level differences that led to a centered binaural image, between two partial-masking conditions, forward and simultaneous masking. It

was assumed that persistent excitation produced by a forward masker is equivalent to the excitation produced by an equally effective simultaneous masker. In the forward-masking condition, a 10-ms (5-ms rise/decay) 4-kHz signal was presented binaurally with a 5-ms delay after the offset of a monaural 150-ms 4-kHz masker. In the simultaneous-masking condition, the signal was added in 90-deg phase during the final 10 ms of the steady-state portion of the same masker. The levels of the maskers were adjusted to produce the same masked threshold. The level of the signal in the masked ear was set to 10, 20, and 30 dB above the masked threshold. Listeners adjusted the level of the 10-ms signal in the unmasked ear until it produced a centered image. Under simultaneous masking, the centered image was obtained when the levels of the 10-ms tone were approximately equal in both ears. Under forward masking, the result depended on the level of the signal in the masked ear. For the signal presented 10 dB above the masked threshold, the level of the tone in the unmasked ear needed for a centered image was about 20 dB lower than that in the masked ear, suggesting strong attenuation of the response to the signal by the forward masker. The difference between the levels of the 10-ms tones in both ears decreased as the level of the partially masked signal increased. The observed differences between forward and simultaneous masking suggest that the two types of masking cannot be accounted for by the same mechanism and that forward masking is better described as attenuation rather than persistence. [Work supported by Grant No. DC00683 from NIDCD].

**1065 Nonlinear Time-Frequency Analysis: A Dynamical Systems Approach**  
**Edward Large<sup>1</sup>**

*<sup>1</sup>Florida Atlantic University; Center for Complex Systems and Brain Sciences and Department of Psychology*

This talk will introduce a general model for nonlinear time-frequency analysis. I begin with a network of nonlinear oscillators, each tuned to a distinct eigenfrequency, driven by an external acoustic stimulus. Conceptually, this arrangement is similar to a bank of bandpass filters. Mathematical analysis of the network reveals general properties of nonlinear time-frequency analysis including amplitude compression, frequency detuning and nonlinear distortion. These properties are shown to be common to a family of physiological models that includes active cochlear models and oscillatory neural networks. I relate the properties of nonlinear time-frequency analysis to auditory percepts, including loudness and pitch. Finally, I propose a canonical time-frequency transform for acoustic stimuli, the Andronov-Hopf transform.

**Acknowledgments**

This research was supported by NSF grant BCS-0094229, awarded to the author



# Author Index

(Indexed by abstract number)

- Aalto, Heikki, 195  
Aarnisalo, A. A., 300  
Abbas, Paul, 75,1020  
Abdala, Carolina, 137  
Abdulally, Adam, 838  
Abe, Kousuke, 119  
Abrams, Daniel, 992  
Abrams, Harvey B., 164  
Abrashkin, Karen, 357,836  
Abu-Hamdan, Maher D., 643  
Ackley, Robert, 199  
Acuna, Dora, 538,586  
Adams, George, 400  
Adams, Joe C., 294,575,650  
Adato, Avital, 9  
Adelman, John P., 394  
Agapiou, John, 687  
Agrawal, Smita, 475,477  
Aguirre, Luis A., 289  
Ahmad, Shoab,  
290,864,866,898  
Ahmar, Nayef, 468  
Ahmed, Azad I., 145,146,149  
Ahmed, Bashir, 989  
Ahn, Joong Ho, 366,367  
Ahuja, Tarun K., 130  
Aizawa, Naotaka, 1010  
Akache, Fadi, 921  
Akil, Omar, 539  
Alagramam, Kumar N.,  
9,26,302,303  
Alam, Shaheen, 42,68  
Alarcon, Christina, 923  
Albert, Sebastien, 291  
Albinger, Andrea, 377  
Aldrich, Richard, 881  
Aletsee, Christoph, 637  
Alexander, Joshua, 485  
Alger, Heather, 618,629,649  
Allan, Chris, 168  
Allen, J. B., 337  
Allen, Jont, 757,758  
Allen, Paul,  
430,432,433,437,951,977,  
979  
Allen, Prudence, 168  
Allen, Susan, 274  
Almanza, Angelica, 882  
Alonso, Ophelia, 40  
Aloor, Heather, 813,829  
Altschuler, Richard A.,  
22,131,358,938,943,1024  
Alvarado, David, 280  
Alvarez, Araceli, 289  
Amalfitano, Andrea, 888  
Amarjargal, Nyamaa, 64  
Amitay, Sygal, 1028  
Amoser, Sonja, 912  
Anderson, Charles T.,  
616,1045  
Anderson, David J.,  
439,524,526  
Anderson, lee-Ching Wu,  
847,848  
Anderson, Ilona, 230  
Anderson, Julia K., 594,834  
Anderson, Lucy, 974,1004  
Anderson, Michael, 442  
Andoni, Sari, 129,975  
Andreeva, Nadejda, 64  
Angelaki, Dora, 174,177  
Angeli, Simon I., 59  
Antalis, Patricia, 145,147  
Anvari, Bahman, 334,1048  
Aouad, Rony, 665  
Arai, Maki, 401  
Aranyosi, Alexander J.,  
345,791  
Arenberg Bierer, Julie, 225  
Armstrong, W., 209  
Arnason, Byron, 923  
Arning, Erland, 363  
Arnold, Wolfgang,  
214,408,579  
Art, Jon, 530  
Arts, Alexander, 293,793  
Asadollahi, Ali, 691  
Asako, Mikiya, 361,943  
Ashida, Go, 119  
Atencio, Craig A., 1009  
Atiani, Serin, 716,991  
Atkin, Graham, 634  
Auer, Manfred, 1041  
Avissar, Michael, 69  
Aytekin, Murat, 953,959  
Bach-y-rita, Paul, 202  
Backes, Walter H., 456  
Backus, Bradford, 915  
Bae, Woo-Yong, 496  
Bagger-Sjöbäck, Dan, 491  
Bai, Donglin, 260  
Bai, Jun-Ping, 1046  
Bailey, Kelly, 215  
Baker, Kim, 51  
Bal, Ramazan, 444  
Balaban, Carey,  
29,172,178,532  
Balkany, Thomas J.,  
40,43,59,76  
Ball, Gregory F., 710  
Baloh, Robert W., 869  
Bamiou, Doris-Eva, 700  
Banai, Karen, 452  
Bandyopadhyay, Sharba, 670  
Banks, Juliane, 148,155  
Banks, Matthew I., 517  
Bao, Jianxin, 412,414  
Barald, Kate, 274,798  
Barbadora, Karen, 149  
Barco, Amy, 230,472  
Barrett, Kate, 296  
Barry, Peter, 544  
Barsz, Kathy, 969,977  
Bartles, James, 798,815  
Bartlett, Edward, 984  
Bartnik, Grazyna, 142  
Baschnagel, Andrew, 593  
Basham, Ryan P., 806  
Bashiardes, Stavros, 280  
Baskent, Deniz, 224,746,761  
Basta, Dietmar, 203  
Bastian, Amy, 198  
Bateman, Kristen, 296  
Battay, Jim, 243  
Batts, Shelley, 282,836  
Baucom, Jessica, 631  
Bauer, Carol, 431,913  
Bauer, Jay, 749  
Bauer, Karl, 545  
Baumann, Uwe, 160  
Baumgartner, Wolf-Dieter,  
37,474,478  
Bayer, Jennifer, 813  
Beal, Fabrice, 37  
Beaudoin, Kelly, 193  
Becker, David, 862  
Bee, Mark, 721  
Behne, Nicole, 453  
Beisel, Kirk W.,  
27,423,633,803,806  
Beitel, Ralph E., 983  
Bell, Steven, 163  
Bell, Thomas, 884  
Beltramello, Martina, 306  
Bendiske, Jennifer, 944  
Bendor, Daniel, 982  
Benke, Timothy, 856,1055  
Benson, Jennifer M., 525  
Bergeson, Tonya, 238  
Berk, Richard, 158  
Bermingham-McDonogh,  
Olivia, 809  
Berrebi, Albert S., 681,825  
Bertolotto, Cristina, 538  
Best, Virginia, 962,965  
Beurg, Maryline, 56  
Beyer, Lisa, 31,797,799  
Bhagat, Shaum, 196,200  
Bhargava, Ashish, 759  
Bhattacharya, Gautam,  
299,642  
Bhonagiri, Veena, 280  
Bian, Lin, 317,338  
Bianchi, Lynne, 274,814  
Bielefeld, Eric, 365,582  
Bien, Alex, 790  
Bierer, Steven, 1019  
Billig, Isabelle, 532  
Billings, Peter, 576  
Birnbauer, Marie, 222  
Biswas, Anindita, 895  
Bitoun, Pierre, 291  
Bitsche, Mario, 822  
Bizley, Jennifer, 1003  
Black, F. Owen, 202,534  
Blaser, Susan, 210  
Blasiolo, Brian, 275  
Bledsoe, Sanford C., 525  
Bleleck, Stefan, 671,673  
Blons, Helene, 291  
Bloomberg, Jacob, 534  
Blumell, Suzanne, 998  
Blumenthal, Kenneth, 592  
Blyskun, Elaine, 838  
Boatman, Dana, 1001  
Bobbin, Richard P., 563,787  
Boche, Jo Ellen, 297  
Bodmer, Amy, 230,472  
Bodmer, Morana, 377  
Bögel, Lars, 38  
Bohne, Barbara A., 574  
Bohorquez, Jorge,  
499,500,624  
Bok, Jinwoong, 548  
Bolz, Steffen-Sebastian, 408  
Bond, Chris T., 394  
Bonham, Ben H.,  
250,983,1016,1019,1021,  
1025  
Bonny, Christophe, 43,369  
Borenstein, Jeffrey T., 45,46  
Bossis, Ioannis, 628  
Bottiglieri, Teodoro, 363  
Bouley, Donna, 923  
Boulter, Jim, 395  
Bourdette, Dennis, 752  
Boutet de Monvel, Jacques,  
785  
Bowman, Glen A., 171  
Boyle, Richard, 530  
Brabet, Philippe, 604  
Bradford, Yvonne, 816  
Braig, Claudia, 545,824  
Brandon, Carlene, 609  
Bratt, Gene W., 143  
Braun, Allen, 747  
Brechmann, Andre, 453  
Bredberg, Göran, 41  
Breier, Joshua, 753  
Breneman, Katherine, 530  
Bresnahan, Glenn, 439  
Breuninger, Christian, 918  
Brewer, Carmen, 199  
Brey, Robert H., 536  
Briede, Thorsten, 352,579  
Brimjoin, Wm. Owen, 698  
Brittan-Powell, Elizabeth, 446  
Brodie, Hilary A., 63  
Broide, David, 151  
Bronner, Gary, 916  
Bronson, Roderick, 801  
Brooks, Andrew, 422,424,425  
Brors, Dominik, 637  
Brosch, Michael, 509  
Brough, Douglas, 52  
Brown, John, 450  
Brown, M. Christian, 91  
Brown, Steve, 890  
Brownell, William E.,  
382,610,611,612,615,617,  
618,619,1048  
Brozoski, Thomas, 431,913  
Bruce, Ian, 79  
Brugge, John, 999  
Brumwell, Craig, 827  
Brungart, Douglas, 242  
Brunso-Bechtold, Judy K.,  
695  
Brzezinski, Joseph, 22  
Buchinsky, Farrel J., 144,284  
Buckley, Kristi, 255  
Bukauskas, Feliksas, 306  
Burger, R. Michael, 434,435  
Burrows, Amy C., 154,156  
Bush, Angela, 942  
Buss, Emily, 472  
Butts, Sydney, 543  
Buus, Soren, 1027  
Buzanska, Leonora, 549  
Cai, Hongxue, 323  
Calais, Catherine, 291  
Cameron, Peter, 32  
Caminos, Elena, 90  
Camp, Jon, 536  
Campbell, Rob, 111  
Camper, Sally, 797,799  
Campero, Andrea, 271  
Cantor, Robert, 4  
Cao, Keli, 759  
Cao, Xiaojie, 20  
Carey, John P.,  
175,176,846,847,848  
Carey, Thomas, 293,793,794  
Carlyon, Robert P., 473,511  
Carney, Laurel H., 441,445  
Carrasco, Rafael, 708  
Carroll, Jeff, 734  
Caspary, Donald, 431,913  
Casseday, John H., 133,971  
Catalano, Peter, 193  
Catros, Helene, 291  
Cederroth, Christopher, 564  
Cedolin, Leonardo, 73,74  
Cenciarini, Massimo, 187  
Cerka, Amanda, 659,660,661  
Cerny, Ronald, 30  
Ceyhan, Elvan, 1001  
Chadwick, Richard, 323,788  
Chae, Sung-Won, 159,489  
Chair, Leila, 1016  
Chait, Maria, 455  
Chakrapani, S., 6  
Chalupper, Josef, 160  
Chan, Dylan, 781  
Chan, Gary, 343  
Chan, Howard, 920  
Chandrasekaran,  
Chandramouli, 331  
Chang, Sun O.,  
399,457,602,817  
Chase, Steven, 108  
Chasmawala, Shamsuddin,  
929  
Chatterjee, Monita, 227,228  
Chatterjee, Papri, 44,218  
Chavez, Eduardo, 151  
Cheatham, Mary Ann, 651  
Chelius, Daniel C., 382,1017  
Chen, Guang-Di, 373,580  
Chen, Hongbin, 522  
Chen, Jun, 24  
Chen, Lin, 89  
Chen, Ping, 541,864,866,898  
Chen, Zheng-Yi, 25,278  
Chen, Zhiqiang, 66,47  
Cheng, Alan, 400  
Cheng, Anbon, 656  
Cheng, Tao, 931  
Cherian, Neil, 205  
Chertoff, Mark, 78,317  
Cheung, Eunice, 1043  
Cheung, Steven W., 983,993  
Chien, Wade, 926  
Chinchilla, Sherol, 735  
Chiorini, John, 628  
Chiu, Chen, 957  
Chiu, Tzai-Wen, 126,134  
Cho, Jae-Gu, 159,489  
Cho, Jang, 899  
Cho, Yang-Sun, 309,503  
Choi, Byung Yoon,  
457,602,817  
Choi, Chul-Hee,  
334,621,1017  
Choi, Sukgui, 284  
Chole, Richard A., 488,490  
Christensen-Dalsgaard,  
Jakob, 110,972  
Chung, Jong Woo, 366,367  
Chung, Won-Ho, 153,309,597  
Church, Michael, 502  
Cioffi, Joseph, 23,33,34,35,36  
Clément, Gilles, 188  
Clendaniel, Richard,  
175,176,198  
Clifford, Sarah, 617,620  
Coale, Kathleen, 193  
Coburn, Michael, 132  
Coffey, Charles, 105  
Coffin, Allison B., 639  
Cohen, Helen, 184,190  
Cohen, Mazal, 167  
Cohen, Micah, 295  
Cohen, Nancy, 193  
Cohen, Yale, 995  
Cohen-Salmon, Martine, 261  
Cohn, Joseph, 172  
Colburn, H. Steven,  
441,443,476,728  
Coleman, John, 362  
Colesa, Deborah J., 525,1024  
Coling, Donald, 269,592  
Collazo, Andres, 541  
Collet, Lionel, 163  
Colletti, Vittorio, 523  
Collins, Leslie,  
521,741,742,743  
Cone-Wesson, Barbara, 449  
Conley, Stephen F., 284  
Coomes, Diana, 1000  
Cooper, Huw, 473  
Cooper, Nigel, 340  
Corbacelli, Elisa, 607  
Corbett, Scott, 1025  
Corey, David P.,  
25,278,886,887,888,1043  
Corfas, Gabriel, 811  
Corliss, Deborah, 563  
Corrales, C. Eduardo,  
559,560  
Cosgrove, Dominic, 299,642  
Costello, Michael, 48

Cotanche, Douglas A., 384,542,563,594,640,834  
Coticchia, James, 158  
Cotton, John, 529  
Couderc, Remy, 291  
Covey, Ellen, 133,678,971  
Cowan, Justin, 169  
Crawford, Andrew, 782  
Creedon, Thomas A., 164  
Cristobal, Ricardo, 33  
Crook, John M., 986  
Crosby, Patrick, 743  
Crumley, R., 209  
Crumling, Mark, 282  
Cuajungco, Math, 560  
Cuautle-Heck, Bessy, 709  
Cunniff, Chris, 286  
Cunningham, Lisa L., 608,609  
Cyr, Janet, 895  
D.M. Cortes, 6  
Dailey, Michael, 711  
Daleke, David, 3  
Dallos, Peter, 616,651,1044,1045  
D'Andrea, Susan, 173  
D'Angelo, William, 112  
Daniel, Sam J., 921  
Danilov, Yuri, 202  
Darrow, Keith, 914  
Daruwalla, Zeeba, 274  
Das, Gishnu, 10  
Dasika, Vasant K., 441  
David, Albert, 291  
Davidian, Danielle, 521  
Davidson, Amy L., 618  
Davis, Brianne, 501  
Davis, James, 808  
Davis, Kevin, 675  
Davis, Rick, 26  
Davis, Robin L., 66,67  
Davisson, Muriel, 801  
Day, Jessica, 930  
Dazert, Stefan, 637  
de Boer, Egbert, 320,325  
de La Garza, Amy, 141  
de la Mothe, Lisa, 998  
de Smit, Femke, 764  
de Zeeuw, Chris I., 308  
Dean, Isabel, 696  
Deane-Pratt, Ade, 966  
Decraemer, Willem F.S., 492,774,917  
Dejonckere, Philippe, 751  
del Castillo, Francisco J., 261,289  
del Castillo, Ignacio, 289  
Delgado, Rafael, 499,500,624  
Delgutte, Bertrand, 71,73,74,251  
Deliano, Matthias, 464,712  
Deligeorges, Socrates, 439  
Della Santina, Charles C., 175,846,848  
Delobel, Bruno, 291  
Demke, Joshua C., 107  
Deng, Youping, 24  
Denise, Pierre, 188  
Denoyelle, Françoise, 291  
Dent, Micheal, 955  
Deo, Niranjana, 333  
Depew, Aron, 157,498  
Depireux, Didier A., 697,981,985,988  
Derkey, Craig S., 284  
Desai, Anuradha, 65  
DeVenecia, Ronald, 91  
Dever, Dennis, 133  
Devore, Casey L., 407  
Devous, Michael, 255  
DeYoe, Edgar A., 465  
D'Haese, Patrick, 230,472  
Di Pasquale, Giovanni, 628

Diaz, Carmen, 90  
Dice, Bethany, 145,147,149  
Dickman, J. David, 174,177,275,852  
Dickson, Matthew J., 880  
Dietrich, Dalton, 40  
DiMauro, A., 874  
Dimitriadis, Emillos, 788  
Dinces, Elizabeth, 469  
Dinculescu, A., 300  
Ding, Dalian, 53,99,378,387,413,592,593,607,900,933  
Dinglasan, Judilee N., 878,1050  
Dirckx, Joris J.J., 492,774,917  
Divenyi, Pierre, 760  
Djiane, Alex, 10  
Dobbins, Heather D., 697,981,985  
Dobie, Robert, 161  
Doetzlhofer, Angelika, 281  
Dohar, Joseph E., 832  
Doi, Katsumi, 462,819  
Dolan, David F., 21,22,358,447,667,799,836  
Dollfus, Helene, 291  
Domanska-Janik, Krystyna, 549  
Donahue, Amy, 243  
Donahue, Leah Rae, 801  
Donepudi, Sreekrishna, 606  
Donfack, Joseph, 284  
Dong, Wei, 326  
Doolling, Robert, 77,313,446,905  
Dootz, Gary, 21,358,799  
Dopico, Richard, 145,146,149  
Dorman, Michael, 458  
Dormer, Kenneth, 48  
Doucet, John, 16  
Dowling, John, 542  
Downing, Mark, 236  
Downs, Daniel, 473  
Doyle, William, 148  
Drennan, Ward R., 220  
Drescher, Andrew J., 810  
Drescher, Dennis G., 643,880  
Drescher, Marian J., 643,880  
Dreyer, Anna, 71  
Driscoll, Colin, 536  
Dromard, Cecile, 564  
Drouin-Garraud, Valerie, 291  
D'Sa, Chrystal, 946  
D'Souza, Mary, 422,424,425  
Du, Bo, 99  
Du, Guo-Guang, 616  
Du, Li Lin, 59,802,804  
Du, Xiaoping, 55,606  
Du, Yafei, 412,414  
Duan, Maoli, 654  
Duane, Delimont, 299  
Dubno, Judy R., 480  
Duggan, Anne, 889,891  
Duggan, David, 286  
Duifhuis, Hendrikus, 764  
Dulon, Didier, 56,883  
Duncan, Luke, 834  
Duncan, R. Keith, 634  
Durham, Dianne, 833,937,949  
Duriez, Françoise, 291  
Durrant, John, 1030  
Dutia, Mayank, 515  
Duzhyy, Dmytro, 632  
Eatock, Ruth Anne, 875,885,1053  
Ebert, Charles S., Jr., 105  
Ebert, Jr., Charles S., 107  
Ebihara, Yasuhiro, 550  
Ebmeyer, Joerg, 151,153  
Ebmeyer, Umay, 151  
Echteler, Stephen, 808

Economou, Androulla, 818  
Eddington, Donald K., 476  
Eddins, David A., 86,732,1059  
Edge, Albert, 559,560  
Edmond, John, 586  
Edpao, Webster, 546,547  
Edwards, Jason, 233  
Egnisse, Rebecca, 23  
Egana, Ana, 542  
Eggermont, Jos J., 454,980,1010  
Eggers, Scott, 536  
Ehret, Guenter, 18  
Ehrlich, Garth D., 144,145,146,147,149,284,838  
Ehrlich, Nathan, 147,149  
Eiber, Albrecht, 918  
Eisen, Marc, 232  
Eisner, Frank, 461  
El-Amraoui, Aziz, 9  
Elgoyhen, A. Belen, 394,395  
Elhady, Yasmin, 864  
Elhilali, Mounya, 715,716,991  
Eliot, Marie-Madeleine, 291  
Elliott, Taffeta, 972  
Ellison, John C., 658  
Emadi, Gulam, 221  
Emily, Locke, 884  
Enas, Lija M., 569  
Ender, Frank, 691  
Endo, Tsuyoshi, 555,585  
Engel, Jutta, 824  
Engelhorn, Achim, 464,712  
Ensberg, Daniel, 464,712  
Epstein, Michael, 135  
Erbe, Christy, 33,34,35,36  
Erdos, Geza, 145,147  
Ernst, Arne, 203  
Esau, Katie, 78  
Escabi, Monty A., 714,717  
Eshraghi, Adrien A., 40,43,76  
Ettelman, Craig, 76  
Evans, Brad, 627  
Evans, Chris, 404  
Evans, W. Howard, 256,861  
Fabijanska, Anna, 142  
Fahey, Paul, 319  
Fairfield, Damon, 44  
Faix, Dennis, 194  
Fakler, Bernd, 821,1052  
Falk, Ben, 953  
Falk, Nicole J., 594  
Fan, Yun-Hui, 778,786,919  
Fang, Jie, 623  
Fang, Qing, 797  
Farahbakhsh, Nasser, 784  
Farkas, Daniel, 538  
Farkas, Dina, 691  
Farrell, Brenda, 612  
Faulkner, Andrew, 223,737  
Fauser, Claudius, 166,352,579  
Fausti, Stephen A., 143,752  
Fay, Jonathan, 779  
Fay, Richard R., 70  
Fechter, Laurence, 567  
Feeney, Patrick, 930  
Feinberg, Steven, 50  
Fekete, Donna M., 271  
Feldbauer, Noelle, 297,298  
Feldmann, Delphine, 291  
Felix, Richard, 680  
Fen, Weighong, 398  
Feng, Albert, 679  
Feng, Ben, 931  
Feng, Feng, 273  
Fenoy, Albert, 999  
Ferguson, Melanie, 169  
Ferrello, Melissa, 1058  
Fetoni, Anna Rita, 364

Fettiplace, Robert, 780,782  
Fielden, Claire, 473  
Fiering, Jason O., 45,46  
Fink, Stefan, 892,893  
Finlayson, Paul, 935  
Firszt, Jill B., 222,234,236,465  
Firzloff, Uwe, 719  
Fischel-Ghodsian, Nathan, 58  
Fishman, Yonatan, 510,1007  
Fitzakerley, Janet, 92  
Fitzgerald, Matthew B., 733  
Fitzgibbons, Peter, 84  
Fitzpatrick, Denis F., 658  
Fitzpatrick, Douglas C., 105,107  
Flanagan, Helen, 1062  
Fleischer, Gerald, 773  
Fletcher, Jack, 753  
Flore, Andrew, 157,498  
Florentine, Mary, 135,479,482,1027  
Flores-Otero, Jacqueline, 66  
Folkard, Tim, 169  
Fong, Alexander, 841  
Forbes, Michael L., 144  
Forge, Andrew, 7,258,630,831,862  
Formby, Craig, 142,237  
Forsythe, Thomas, 656  
Fourcin, Adrian, 206  
Fowler, Ben, 580  
Fowler, Karen, 246  
Foxton, Jessica M., 265  
Francannet, Christine, 291  
Francis, Howard, 906,907  
Franck, Kevin, 232  
Frangulov, Anna, 285,288  
Franklin, Samuel, 695  
Fransson, Anette, 41  
Free, Samantha, 700  
Freeman, Dennis, 341,342,343,344,345,791  
Frenz, Dorothy, 543,596  
Freyman, Richard L., 739  
Friberg, Ulla, 213  
Fridberger, Anders, 785  
Friedland, David, 23  
Friedman, Rick A., 772  
Friedman, Sarah, 84  
Friedrich, Victor L., Jr., 528  
Friesen, Lendra, 746  
Frisina, Robert D., 81,82,85,86,416,417,418,419,421,422,424,425,428  
Frisina, Susan T., 81,82,85  
Fritz, Jonathan, 715,716,991  
Fritzsch, Bernd, 273,423,633,806  
Fu, Qian-Jie, 226,735,736  
Fuchs, Manfred, 454  
Fuchs, Paul A., 353,396,397  
Fujiki, Nobuya, 704  
Fujinami, Yoshiaki, 591  
Fujioka, Masato, 577  
Fullarton, Lynne, 358  
Funabiki, Kazuo, 116,119  
Funnell, W. Robert J., 774,921  
Furman, Adam C., 69  
Furman, Joseph, 179,185,186,189  
Furness, David, 636,1055  
Furukawa, Masayuki, 151,153  
Furukawa, Shigeto, 103,117  
Furuse, Kyoko, 867  
Furuse, Mikio, 867  
Furze, Alexis D., 76  
Fuzessery, Zoltan, 132,1008  
Gaboyard, Sophie, 876,1054  
Gabriele, Mark, 690  
Gaese, Bernhard, 987,1032  
Gafur, Amir, 618

Gaggi, Wolfgang, 234,465  
Gagnon, Leona, 800  
Gagnon, Patricia M., 568  
Gai, Yan, 445  
Gail, Ishiyama, 404  
Galazyuk, Alexander, 976  
Gale, Jonathan, 360  
Gallun, Frederick J., 962,1057  
Galvin, John J., 226,736  
Gan, Rong, 931  
Gandour, Jack, 438  
Gans, Donald, 123,699  
Gans, Richard, 192  
Gantumur, Tsana, 214  
Gao, Wei-Qiang, 387  
Garabedian, Erea-Noel, 291  
Garadat, Soha, 754  
Garcia, Jasmine, 1053  
Garcia, Jerel, 359,398,1050  
Garcia, Meredith, 96,97  
García-Añoveros, Jaime, 887,888,889,891  
Garell, P. Charles, 459  
Garner, Cassie, 315,662  
Ge, Xianxi, 362,363  
Gea, Stefan L.R., 492  
Gearhart, Caroline, 567  
Geisler, Hyun-Soon, 545  
Geleoc, Gwenaëlle S.G., 888  
Gentner, Timothy Q., 710  
Gerke, Melissa, 215  
Ghaffari, Roozbeh, 341  
Ghose, Kaushik, 953  
Giampaola, Matthew M., 641  
Gibbons, Joanna, 708  
Gibson, Don, 48  
Gifford, Gordon, 995  
Gilihinskaya, Yana, 1034  
Gill, Ruth, 321  
Gillespie, Peter G., 346,376,380,626,638,896,1042  
Gillespie, Susan K.H., 638  
Gilley, Phillip, 458  
Girod, Douglas, 833  
Gittens, Joanne, 260  
Glade, Ashley R., 963  
Gladitz, John, 145,149  
Glasberg, Brian, 1062  
Glaser, Thomas, 21,22  
Glassinger, Emily, 1049  
Glatfelder, Jerry, 368,837  
Gleich, Otto, 905  
Glickman, Stephen E., 310  
Glickstein, Jonathan, 55  
Glowatzki, Elisabeth, 388,397,539  
Glueckert, Rudolf, 822,910  
Godar, Shelly, 475  
Goddard, Julie-Anne, 619  
Goebel, Joel, 197,535  
Goldberg, Jay M., 32,389,390  
Golding, Nace L., 94,682  
Gollapudi, Anantha S. B., 648  
Gomi, Takashi, 614  
Gong, Qin, 318  
Gong, Tzy-Wen, 358  
Gong, Xiangun, 260  
Goodman, Shawn, 789  
Goodyear, Richard, 9,894  
Gooler, David, 756,1038  
Gopal, Kamakshi, 1006  
Gordon, Jane S., 143  
Gordon, Karen, 210  
Gordon-Salant, Sandra, 84,313  
Gorga, Michael, 136,315,662  
Gottshall, Kim, 172,184,194  
Gould, Herbert, 606  
Gould, Robert, 32  
Goutman, Juan, 397  
Grandori, Ferdinando, 138

- Grant, John, 529  
Grant, L., 21  
Grant, Wally, 857  
Gratton, Michael Anne, 295,296,299,359,877  
Gray, Brianna, 563  
Gray, Lincoln, 718,753  
Gray, Paul A., 886  
Gray, Sandra, 800  
Green, Glenn, 286  
Green, Michele, 835  
Green, Steven, 42,44,68,218,711  
Green, Tim, 223  
Greenberg, David P., 149  
Greene, Nathaniel, 694  
Greeson, Jennifer N., 622  
Grégoire, Lucie, 283  
Greinwald, John, 287  
Griffin, Sarah, 106  
Griffith, Andrew, 625,795  
Griffiths, Tim, 265  
Grobman, Ariel, 76  
Groh, Jennifer, 694  
Grosh, Karl, 333  
Gross, Guenter W., 1006  
Gross, Johann, 64  
Grosveld, Frank, 308  
Groves, Andrew, 281,805  
Gstoettner, Wolfgang, 39  
Gu, Jianwen, 345  
Gu, Rende, 368,837  
Guan, Bing-Cai, 410,411  
Guan, Min-Xin, 58,60  
Guan, Yajun, 572,595  
Guimaraes, Patricia, 81,416  
Guinan, John J., 91,182,340,915  
Gultig, Karina, 868  
Gummer, Anthony W., 328,331,391  
Guo, S., 209  
Guo, Yu, 25  
Gurrola, Jose, II, 272  
Gutschalk, Alexander, 466,511  
Guyot, Jean-Philippe, 204  
Hackett, Troy A., 112,990,998  
Hackney, Carole, 780  
Hadjab, Saida, 713  
Haenggeli, Charles-André, 1022  
Hafidi, Aziz, 56  
Hafter, Ervin, 967  
Hahn, Caldwell, 446  
Hahn, H., 874  
Hain, Timothy, 749  
Haisfield, Christine, 715  
Hale, Shane, 897  
Hall, Ameer J., 118  
Hall, Thomas, 989  
Hall-Stoodley, Luanne, 147,149  
Hallworth, Richard, 790  
Halsey, Karin, 21,667,799  
Halvorsen, Michele B., 583  
Hamaker, Sara, 307  
Hamanishi, Shinji, 924  
Hamre, Kristin, 606  
Han, Dong-yi, 292  
Han, Mingbo, 412,414  
Han, Weiju, 347  
Hansen, Marlan, 44,218  
Hansen, Stefan, 637  
Haque, Asim, 174  
Hara, Akira, 570  
Hara, Hirotaka, 842,843,860  
Harada, Narinobu, 49  
Harada, Tamotsu, 819  
Harasztsi, Csaba, 391  
Harbidge, Donald G., 645,870  
Harding, Gary W., 574  
Hardy-Bruce, Karen, 745  
Hari, Riitta, 704  
Harkrider, Ashley, 87  
Harlan, Richard, 96,97  
Harper, Elizabeth, 362,363  
Harper, Nicol, 696,715  
Harrington, Ian A., 118,996  
Harris, Belinda, 801  
Harris, Jeffrey, 215  
Harris, Glenn, 286  
Harris, Thomas, 255  
Harrison, Robert, 701  
Harrison, Wilbur, 649  
Hart, Lynette, 923  
Hartmann, Rainer, 252,1023  
Harvey, Margaret, 632  
Hashimoto, Makoto, 860  
Hashimoto, Yasuyuki, 229,379,401  
Hashino, Eri, 551,552,813,829  
Hata, Masaki, 867  
Hatazawa, Jun, 462  
Hatfield, James S., 643  
Hatsusaka, Natsuko, 463  
Haupt, Michael, 158  
Haupt, Heidemarie, 64  
Häussinger, Dieter, 900  
Hauswirth, W.W., 300  
Hawkey, David, 1028  
Hawkins, R. David, 280  
Hawley, Monica, 142  
Hayes, Jay, 144,145,147,149  
Hay-McCutcheon, Marcia, 235  
He, David, 1044  
He, Jiao, 40,43  
He, Ning-ji, 480  
He, Wenxuan, 339  
Healy, Eric W., 744  
Hebda, Patricia, 155,832  
Hebert, Sylvie, 88  
Hedrick, Mark, 87  
Hedrick, Michelle, 562  
Hefeneider, Steven, 61,150,217  
Hegyi, Ivan, 377  
Heid, Silvia, 252,1023  
Heil, Peter, 484  
Heil, Tom, 665  
Heinks-Maldonado, Theda, 750,765  
Heinrich, Marco, 102  
Heinz, Michael, 72  
Helfer, Karen S., 739  
Heller, Stefan, 559,560  
Hemmert, Werner, 345  
Henderson Sabes, Jennifer, 968  
Henderson, Donald, 364,365,581,582  
Henkel, Craig K., 695  
Henry, Belinda, 477  
Henry, James A., 164  
Henson, Hillary, 322  
Henson, O'Dell, 536  
Heo, Jeong Hwa, 399  
Hernández, Olga, 676  
Herrmann, Barbara S., 182  
Herron, Timothy J., 171,467  
Hess, Mailee, 911  
Heydrick, Christopher, 708  
Hicks, Candace, 501  
Hidaka, Hiroshi, 121,936  
Hiel, Hakim, 396,539  
Higashi, Toru, 554,555,556,557  
Higgins, Nathan C., 714,717  
Highstein, Stephen, 530  
Higuchi, Masanori, 463  
Hildebrandt, Thomas, 923  
Hill, Jennifer K., 626  
Himeno, Chiemi, 49  
Hind, Sally, 169  
Hirono, Moritoshi, 1042  
Hirota, Sean, 586  
Hirsch, June C., 513,531  
Hirsch-Shell, D.J., 849  
Hirt, Bernhard, 868  
Hirvonen, Timo, 195,847  
Hoang-Dinh, Emilie, 883  
Hodges, Annelie, 231  
Hodges, Larry, 186  
Hoffer, Michael, 172,184,194  
Hoffman, Larry, 276,849  
Hoffman, Matthew P., 888  
Hogg, Justin, 149  
Holden, Laura, 234  
Holme, Ralph, 771  
Holmes, Stephen D., 1056  
Holstein, Gay R., 528,530  
Holt, Avril Genene, 131,938,943  
Holt, Jeffrey R., 638,888  
Holt, Joseph C., 32,389,390  
Holt, Lori L., 762,1061  
Holt, Rachael, 240  
Homaniacs, Gregg E., 652  
Hong, Sung Hwa, 309,503  
Honrubia, Dynio, 538  
Hooper, Rebecca, 354  
Hopkins, Michelle, 28  
Hordichok, Andrew, 588  
Horgan, Janet, 285  
Horii, Arata, 819  
Horn, David, 239  
Horowitz, Jay, 173  
Hosoi, Hiroshi, 1033  
Hossain, Waheeda A., 80,902  
Houde, John, 750,765  
Houston, Derek, 239  
Howard, MacKenzie, 434  
Howard, Matthew, 999  
Howell, David M., 825  
Hradek, Gary T., 1014,1016  
Hsu, Chi, 52  
Hsueh, Ju-Yin, 663  
Hu, Bo Hua, 364,365,581,582  
Hu, Fen Ze, 144,145,146,147,149,838  
Hu, Ning, 320,785  
Huang, Chenghang, 395  
Huang, Jie, 42  
Huang, MingQian, 25,278  
Huang, Ting-Ting, 605  
Hubbard, Allyn, 332,439  
Huber, Alexander, 918  
Hudspeth, A.J., 631,781,1041  
Hughes, Inna, 275  
Hughes, Larry, 431  
Hugnot, Philippe, 564  
Hullar, Timothy, 850  
Hultcrantz, Malou, 812  
Hume, Clifford, 809  
Hunker, Kristina, 798  
Hurle, Belen, 275  
Hurley, Karen, 875,1053  
Huss, David, 275,852  
Hutsell, Gayla, 245  
Hutsun, Ken, 949  
Hutter, Michele, 752  
Huynh, Kristin, 651  
Hwang, Chan Ho, 496  
Hwang, Soon-Jae, 159,489  
Hynes, Sarah, 365  
Hyson, Richard, 101,942  
Ide, Charles, 450  
Ignatova, Elena, 275  
Iguchi, Fukuichiro, 555,585  
Ihlefeld, Antje, 960  
Iida, Koji, 613  
Iizuka, Takashi, 305  
Ikeda, Katsuhisa, 305,316,613  
Ikeda, Takuo, 860  
Imig, Thomas J., 937  
Ingham, Neil, 671,673  
Inman, Jared, 157,498  
Isheim, Dagmar, 987  
Ishiyama, Akira, 869  
Ishiyama, Gail, 869  
Ison, James, 430,432,433,437  
Isosomppi, J., 300  
Issa, Elias, 1005  
Ito, Juichi, 554,555,556,557,558,585,867  
Ito, Ken, 420  
Itza, Erin M., 647  
Ivan, Lopez, 586  
Iwai, Koji, 555,557,558  
Iwaki, Takako, 462  
Iwasa, Kuni, 623  
Iwasaki, Satoshi, 229,379,401  
Iwasaki, Shinichi, 420  
Izumikawa, Masahiko, 31,282,357,836  
Izzo, Agnella D., 1012,1013  
Jabba, Sairam V., 646,647,648,653  
Jackson, Andrew, 737  
Jackson, Michael, 929  
Jackson, Ronald, 48,209,362,363  
Jacques, Steven L., 336  
Jagger, Daniel, 258,630  
Jain, Mahdvi, 716  
Jain, Roshini, 708  
Jakobsen, Lasse, 961  
Jansen, E. Duco, 1012,1013  
Janto, Benjamin, 145,149  
Jaquish, Dawn, 65  
Järlebarck, Leif, 301  
Jaynes, C. David, 690  
Jeffcoat, Benjamin, 841  
Jen, Philip, 19  
Jeng, Fuh-Cherng, 1020  
Jennings, J. Richard, 179  
Jenny, Andreas, 10  
Jensen-Smith, Heather, 790  
Jero, J., 300  
Jesteadt, Walt, 136,658,1029  
Jeyakumar, Anita, 951  
Ji, Ni, 374  
Ji, Yadong, 697,981,985  
Jia, Shuping, 1044  
Jiang, Haiyan, 99,378,413,593,607,900  
Jiang, Hong-Yan, 356,595  
Jiang, Zhi-Gen, 409,410,411  
Jin, Zhe, 301  
Jiradejvong, Patpong, 848  
Joannard, Alain, 291  
Jocz, Jennifer, 149  
Joensuu, J., 300  
Johansson, Marianne, 213  
John, Earnest, 157,498  
Johnson, Craig, 354  
Johnson, Don H., 504  
Johnson, Jane, 805  
Johnson, Jason, 286  
Johnson, Kaalan, 157,498  
Johnson, Katherine, 588,589  
Johnson, Kenneth R., 800,801,802,804  
Johnson, Sandra, 145  
Johnson, Sandy, 838  
Johnson, Scott, 551  
Johnson, Stuart, 635  
Johnson, Tiffany, 315,662  
Johnson, Tim, 1025  
Johnstone, Patti, 475  
Joho, Rolf, 951  
Jolly, Claude, 37  
Jones, Gary, 477,727  
Jones, Gavin, 362,363  
Jones, Sherri, 276  
Jones, Timothy, 276  
Jordan, Craig, 243  
Joris, Philip, 349,668  
Joshi, Pownrma, 879,1046  
Journal, Hubert, 291  
Juhn, Steven, 400  
Juiz, Jose M., 90  
Jung, Jae, 488,490  
Jung, Kak-Hyun, 159  
Jung, Timothy, 157,498  
Kabara, Lisa, 21,667  
Kachar, Bechara, 423,628,633  
Kadner, Alexander, 681  
Kahelin, Michael, 173  
Kaiser, Christina, 833  
Kajikawa, Yoshinao, 990,998  
Kalinec, Federico, 603,792  
Kalko, Elisabeth, 961  
Kallman, Jeremy, 584  
Kalluri, Sridhar, 981,985  
Kaltenbach, James, 683,935,939  
Kammerer, B., 874  
Kampalli, Suresh B., 645,871  
Kanazawa, Takeharu, 793  
Kane, Andrew S., 583  
Kaneko, Ken-ichi, 704  
Kaneko, Toshihiko, 361,391  
Kang, Eunjoo, 748  
Kang, Hun Hee, 366,367  
Kang, Hyejin, 748  
Kang, Myung-Koo, 496  
Kang, Xiaojuan, 467  
Kang, Young-Jin, 527  
Kanlis, Nikolaos, 988  
Kanneworff, Morten, 110  
Kanzaki, Sho, 577,591  
Karolat, Joerg, 632  
Karolyi, Jill, 797,799  
Kashino, Makio, 1037,1039,1040  
Kashio, Akinori, 54  
Kashtan, Clifford, 406  
Kasturi, Kalyan, 519  
Katbanna, Bharti, 450  
Kathju, Sandeep, 146,838  
Katz, Eleonora, 395  
Kaufman, Galen, 180,533  
Kawamoto, Kohei, 49,361  
Keefe, Douglas H., 136,658,777,789  
Keefe, Randy, 145,149  
Keefe, Rhonda, 923  
Keithley, Elizabeth M., 249,427,576  
Keller, Clifford, 113,114  
Kelley, Darcy, 972  
Kelley, Matthew W., 12,639,807  
Kelly, Jack B., 122,674  
Kemp, David, 663  
Kempter, Richard, 934  
Kempston, J. Beth, 61,98,217  
Kenna, Margaret, 247,285,288  
Kennedy, Helen, 782  
Kermany, Mohammad, 55  
Kerschner, Joseph E., 149,154,156  
Kershner, Bethany, 930  
Ketels, Kathleen, 546  
Ketten, Darlene, 922,923  
Khan, Khalid M., 643,880  
Khanikar, Prakash, 459  
Khimich, Darina, 392  
Kho, Soochuen, 404  
Kidd, Gerald, Jr., 1057  
Kidder, Gerald, 260  
Kiefer, Jan, 39  
Kiehl, Jessica, 170  
Kikkawa, Yayoi S., 303,890  
Kil, Jonathan, 368,837

- Kilgard, Michael, 708  
 Kilian, Susanne, 713  
 Kim, Bo Hyung, 400  
 Kim, Chong-Sun, 399,457,602,748,817  
 Kim, Daniella, 1031  
 Kim, Duck, 952  
 Kim, Eunsook, 351  
 Kim, HyungJin, 351,587,603  
 Kim, In-Young, 309,503  
 Kim, Ji Soo, 191  
 Kim, Jin Su, 457  
 Kim, Myung Soon, 503  
 Kim, SeJin, 587  
 Kim, Soo-Kyoung, 241  
 Kim, SungHee, 81,85  
 Kim, Tae-Soo, 554,555,556,557,585  
 Kim, Young Ho, 399,817  
 Kim, Young-Jin, 366  
 Kim, YunHa, 351  
 Kimball, Kay T., 190  
 King, Andrew, 111,1003  
 King, John, 231  
 King, Michael, 181  
 Kingfield, Jennifer, 230  
 Kinnefors, Anders, 910  
 Kiringoda, Ruwan, 995  
 Kirk, Karen I., 235  
 Kistler, Doris, 242  
 Kita, Tomoko, 554,555,556,557,558,585  
 Kitahara, Tadashi, 29  
 Kitajiri, Shin-ichiro, 867  
 Kitano, Hiroya, 703  
 Kitzes, Leonard, 50,997  
 Klapczynski, Marcin, 32  
 Klein, Thomas, 10  
 Klingberg, Marc, 950  
 Klink, Karin, 726  
 Klinke, Rainer, 39,252,1023  
 Klump, Georg, 721,722,726,954  
 Klump, Micah Bradshaw, 200  
 Knight, V. Bleu, 28  
 Knipper, Marlies, 304,545,713,824  
 Knirsch, Martina, 824  
 Knox, Glenn, 493  
 Knutsson, Johan, 491  
 Kobayashi, Maori, 1037  
 Kobayashi, Toshimitsu, 613,924  
 Koch, Dawn Burton, 236  
 Koehler, Seth, 948  
 Koehn, Fred, 65  
 Koessl, Manfred, 987  
 Kohno, Satoru, 462  
 Kohrman, David, 358,797,798  
 Koike, Takuji, 924  
 Koitschev, Assen, 892,893  
 Kojima, Ken, 554,555,556,558  
 Kollmar, Richard, 527  
 Komeda, Mototane, 361  
 Kommareddi, Pavan, 293,793,794  
 Kondo, Hirohito, 1039  
 Kondo, Kenji, 386,830  
 Kondo, Takako, 551,552,813,829  
 Kong, Jee-Hyun, 397,539  
 Kong, Jun, 884  
 Kong, Ying-Yee, 759  
 Konishi, Masakazu, 116,119  
 Konrad-Martin, Dawn, 143  
 Koo, Ja-Won, 191  
 Koo, Kevin, 542  
 Kopco, Norbert, 965  
 Kopke, Richard, 48,362,363  
 Kopschall, Iris, 824  
 Korsak, Rose, 586  
 Kos, Izabel, 204  
 Kotak, Vibhakar, 115  
 Kouzaki, Hideaki, 165,703  
 Kozma, Kelley, 793  
 Kral, Andrej, 252,1023  
 Kralick, Deanna, 76  
 Kraus, Nina, 452,992  
 Kretzmer, Erika, 1022  
 Krishnan, Ananthanarayan, 438  
 Krishnan, Lata, 1030  
 Kristiansen, Arthur G., 650  
 Kropp, Laura, 149  
 Kros, Corne, 635,771  
 Kubo, Takeshi, 462,819  
 Kubota, Takahiro, 867  
 Kucinski, Thomas, 497  
 Kucukoglu, Selin, 521  
 Kudo, Motoi, 95  
 Kujawa, Gerard J., 45  
 Kujawa, Sharon G., 45,46,47,182,429,569,584, 650  
 Kumagai, Izumi, 613  
 Kumar, Gagan, 547,889,891  
 Kuo, Sharon, 294  
 Kurima, Kiyoto, 625  
 Kuriyama, Hiromichi, 49,361  
 Kurokawa, Kiyoshi, 95  
 Kurt, Simone, 986  
 Kurtz, Isaac, 219,506  
 Kurtz, Stephen, 150  
 Kuwabara, Nobuyuki, 692  
 Kuwahata, Naofumi, 83,932  
 Kwan, Kelvin Y., 886  
 Kwon, John, 540  
 Kwon, See Youn, 503  
 L.G. Cuello, 6  
 Laback, Bernhard, 474,478  
 Labay, Valentina, 795  
 Lacombe, Didier, 291  
 Ladher, Raj, 270,537  
 Ladich, Friedrich, 912  
 Ladrech, Sabine, 604  
 Lafen, J. Brandon, 518,745  
 LaGasse, James, 368,837  
 Lahne, Manuela, 360  
 Laird, Dale, 260  
 Lake, Jennifer, 475  
 Lalwani, Anil K., 605  
 Lamont, Elizabeth, 850  
 Lancaster, Wayne, 283  
 Landsness, Eric, 534  
 Lane, Courtney C., 504  
 Lane, John (Jack), 536  
 Laneau, Johan, 520  
 Lang, Hainan, 381,550,562  
 Langemann, Ulrike, 721,722  
 Langer, Matthias G., 892,893  
 Langers, Dave R. M., 456  
 Langius-Eklöf, Ann, 208  
 Langner, Gerald, 266,709  
 Lanzoni, Irene, 607  
 Lapainis, Theodore E., 566  
 Large, Edward, 1065  
 Larsen, Erik, 73  
 Larson, Charles, 749  
 Larson, Eric, 960  
 Larue, David T., 689,994  
 Lasker, David M., 845  
 Lauder, Jean, 823  
 Lauer, Amanda, 483  
 Laurell, Göran, 208  
 Lauter, Judith, 460  
 Lautermann, Jürgen, 590  
 Lawton, Max, 1055  
 Laz, Amanda, 690  
 Lazimy, Yaniv, 444  
 Le, Tima, 427  
 Leahy, Kevin, 353  
 Leake, Patricia A., 250,909,1014,1016,1017  
 Leal, Suzanne M., 284  
 Lee, Adrian K.C., 1060  
 Lee, Charles C., 994  
 Lee, Choong Won, 157,498  
 Lee, Daniel, 91  
 Lee, Dong Soo, 457,748  
 Lee, Hyo-Jeong, 457,748  
 Lee, Jae Sung, 457  
 Lee, Jaechun, 55  
 Lee, JaeHyung, 587  
 Lee, Jun Ho, 399,817  
 Lee, Jungchan, 603  
 Lee, Sang Min, 309,503  
 Lee, Te-Chung, 53,705  
 Lee, Yuan Shain, 281  
 Lee, YuneSang, 748  
 Lee, Yun-Shain, 277  
 Leek, Marjorie, 483,905  
 Lefevre, Gaele, 9  
 Lehar, Mohamed, 847,907  
 Lei, Debin, 412,414  
 Leinung, Martin, 38  
 Leman, Jacques, 291  
 Lenarz, Minoo, 524,950  
 Lenarz, Thomas, 38,355,524,950  
 Lentz, Jennifer, 1058  
 Leuwer, Rudolf, 139,495,497  
 Levenson, Joshua, 147,149  
 Levenson, Robert, 275  
 Levine, Robert, 216  
 Lewin, A.S., 300  
 Lewis, M. Samantha, 752  
 Li, Chaoying, 268  
 Li, Cheng, 25  
 Li, Fang, 804  
 Li, Geming, 543,596  
 Li, Hongzhe, 968,970  
 Li, Jianxiang, 901  
 Li, Ming, 933  
 Li, Na, 129,975  
 Li, Xiaoming, 58  
 Li, Xingqi, 901  
 Li, Yan, 553,655  
 Li, Yao, 716  
 Li, Yi, 634  
 Liang, Fenghe, 405,601,863  
 Liang, Jianning, 486,487  
 Liao, Isaac H., 467  
 Liao, Zhijie, 610,611  
 Libby, Richard, 771  
 Liberman, M. Charles, 211,394,395,429,559,563, 569,584,652,770,811,914, 1052  
 Lichtenhan, Jeffery, 78  
 Liedert, Bernd, 590  
 Li-Korotky, Ha-Sheng, 29,148,832  
 Lilly, David, 752  
 Lim, David J., 587  
 Lim, Hubert H., 524,525,526  
 Limb, Charles, 747,1022  
 Limón, Agenor, 854,855  
 Lin, Feng, 540,615,618,619,629,826  
 Lin, Shuh-Yow, 886,887  
 Lin, Xi, 290,541,864,866,898  
 Lindberg, Belinda, 197,535  
 Lippincott-Schwartz, Jennifer, 2  
 Lis, Maciej, 592  
 Litovsky, Ruth, 475,477,727,754  
 Little, Nicole, 725  
 Litvak, Leonid, 221,236  
 Liu, Feng, 277  
 Liu, Haiying, 540,618,619  
 Liu, Jianzhong, 48,362,363  
 Liu, Jun, 901  
 Liu, Liangfa, 693  
 Liu, Qing, 67  
 Liu, Robert C., 706  
 Liu, Sheng, 740  
 Liu, Wei, 543  
 Liu, Xue Zhong, 59,802,804  
 Lo, Chia-Yee, 148,832  
 Lobarinas, Edward, 723,933  
 Lobdell, Bryce, 757,758  
 Lodde, Jill, 311  
 Loebach, Jeremy, 755  
 Lohr, Bernard, 446  
 Loizou, Philip, 519  
 Lomakin, Oleg, 675  
 Lomax, Catherine, 358,938  
 Lomax, Margaret, 358,938,943  
 Lomber, Stephen G., 118,994  
 Lonardo, Fulvio, 283  
 Long, Christopher, 473  
 Long, George, 505  
 Long, Glenis, 312  
 Longo-Guess, Chantal, 800  
 Lonsbury-Martin, Brenda, 140,141  
 Loomis, Patricia, 815  
 Lopez, Ivan, 404,869  
 Lotto, Andrew J., 1061  
 Louage, Dries, 668  
 Loughlin, Patrick J., 187  
 Louie, Raymond, 337  
 Lovett, Michael, 280,820  
 Lowenheim, Hubert, 868  
 Lu, Chun-ye, 292  
 Lu, Jianzhong, 948  
 Lu, Shan, 332  
 Lu, Weining, 294  
 Luan, Hongge, 183  
 Luján, Rafael, 90  
 Lundberg, Cecilia, 654  
 Lundberg, Yunxia (Yesha), 30  
 Lung, Vicki Li, 925  
 Luo, Huan, 470  
 Lustig, Lawrence, 353,539  
 Lutfi, Robert, 485,1029  
 Lutman, Mark E., 163,731  
 Luxon, Linda, 700  
 Lynch, Eric, 368,837  
 Lynch-Erhardt, Martha, 422,424,425,428  
 Lysakowski, Anna, 32,389,853,876,1054  
 Ma, Wei-Li, 121,936  
 Ma, Xiaofeng, 707  
 Maas, Steve A., 917  
 MacArthur, Carol, 150,217  
 MacLean, Katherine, 995  
 Macnamara, Rachel, 625  
 Maconochie, Mark, 818  
 Macpherson, Ewan A., 118,730,996  
 Madnani, Dilip, 596  
 Maganti, Rajanikanth J., 646,648,653  
 Mahendrasingam, Shantini, 780  
 Mahlke, Claudia, 709  
 Mahmood, U., 209  
 Maier, Hannes, 139,495,497  
 Maier, Julia, 580,954  
 Maison, Stéphane F., 394,395,652,770,914  
 Majdak, Piotr, 474,478  
 Maki, Katuhiro, 103,117  
 Makishima, Tomoko, 625,795  
 Maksud, Yaser, 853  
 Malhotra, Shveta, 118  
 Mallery, Robert, 850  
 Malmierca, Manuel S., 676,678  
 Mamedova, Natasha, 48  
 Mammano, Fabio, 306  
 Mandell, David, 155  
 Mangiardi, Dominic A., 594,640,834  
 Manis, Paul B., 93,516,947  
 Manning, Brian, 904  
 Mannström, Paula, 301  
 Manoussaki, Daphne, 323  
 Mansour, Suzanne, 268,537  
 Manuelito, Shannon J., 28  
 Mapes, Frances, 81,82  
 Mapes, Fray M., 85  
 Marcotti, Walter, 635,771  
 Marcus, Daniel C., 24,644,645,870,871  
 Marcus, Dawn, 185  
 Marietta, Chandler, 86  
 Mark, Sharayne, 541  
 Marlin, Sandrine, 291  
 Marquardt, Nadine, 950  
 Marquardt, Torsten, 729  
 Marshall, Allen, 105  
 Martens, Jan, 751  
 Martin, Gail, 269  
 Martin, Glen, 140,141,319  
 Martin, Kathryn, 458  
 Martin, Sophie, 564  
 Martinelli, Giorgio P., 528  
 Martinez Galán, Juan Ramon, 90  
 Martinez-Monedero, Rodrigo, 560  
 Marvit, Peter, 697,981,985  
 Masaki, Kinuko, 342,343,344  
 Mason, Christine R., 1057  
 Masseroni, Britt, 812  
 Mathers, Peter H., 825  
 Mathews, Paul J., 682  
 Matsui, Jonathan I., 542,594,834  
 Matsui, Minoru, 420  
 Matsumoto, Masahiro, 554,555,556,557  
 Matsumoto, Nozomu, 792  
 Matsunaga, Tatsuo, 370  
 Matthew W., Kelley, 272  
 Matthews, Scott, 336  
 May, Bradford J., 121,124,725,906,936  
 Mazhar, Amaan, 334  
 Mazurek, Birgit, 64  
 Mburu, Philomena, 890  
 McAlister, Erin, 313  
 McAlpine, David, 106,120,687,696,729,966  
 McCandless, Cyrus, 178  
 McCoy, Sharon, 150  
 McCrea, Robert, 183  
 McCullough, Brendan, 415  
 McDermott, Brian, 631  
 McFadden, Dennis, 310  
 McFadden, Sandra, 413  
 McGee, JoAnn, 297,298,299,789,920  
 McGinley, Matthew J., 444,684  
 McGuire, John, 50  
 McKay, Shawn, 283  
 McKenna, Michael J., 45,46,47,650  
 McLachlan, Elizabeth, 260  
 McMenamy, Alyssa, 708  
 McMillan, D. Randy, 297  
 Meehan, Daniel, 299  
 Meenderink, Sebastiaan W. F., 314  
 Meikle, Mary B., 164  
 Meintrup, David, 821  
 Melcher, Jennifer R., 466,511  
 Mellott, Jeffrey G., 994  
 Meltzer, Noah, 16,1002  
 Mercado, Eduardo, III, 705  
 Mercado, Francisco, 854  
 Merchant, Saumil, 211,768,775,924,926  
 Merriam, Elliott B., 517  
 Merzenich, Michael M., 702,983

Mescher, Mark J., 45,46  
Mesgarani, Nima, 991  
Metzger, Dennis, 152  
Metzger, Ryan, 694  
Meyer, Michaela, 70  
Meyer, Ted, 231  
Meyer, Thomas, 369  
Meyer-Rienecker, Hans, 201  
Meyers, Tanya, 154  
Meyer-zum-Gottesberge, Angela, 402  
Mhatre, Anand N., 605  
Micco, Alan, 1011  
Michaels, Leslie, 486,487  
Michel, Vincent, 9  
Micheyl, Christophe, 466,511,1036  
Middlebrooks, John C., 118,253,730,996  
Migliaccio, Americo A., 175,176,198,846,848  
Mikulec, Anthony, 47  
Mikuriya, Takefumi, 371,372,842,843  
Milenkovic, Ivan, 102  
Miller, Brian, 922  
Miller, Charles, 75,1020  
Miller, Diane L., 583  
Miller, Emilie, 346  
Miller, Josef, 41,370,571  
Miller, Joseph M., 37,355  
Miller, Katharine, 1045  
Mills, John H., 480  
Minami, Shujiro, 370,571,591  
Mineharu, Akihito, 867  
Minichiello, Liliانا, 633  
Minor, Lloyd B., 175,176,845,846,848  
Minowada, George, 269  
Mire, Patricia, 279  
Mireille, Montcouquiol, 272  
Mitalipov, Shoukhrat M., 451  
Mitchell, Tim, 56  
Mitchem, Kristina, 358  
Miyajima, Chie, 386,830  
Miyamoto, Richard, 239  
Miyamoto, Tatsuo, 867  
Miyazawa, Toru, 471  
Mizuta, Kunihiro, 229,379,401  
Mizutani, Shin, 1040  
Mlodzik, Marek, 10  
Mlynski, Robert, 637  
Mo, Zhicheng, 940,941  
Moghimi, Arash, 538  
Mohassel, Payam, 398  
Mohney, Kathryn, 646  
Moiseff, Andrew, 952  
Molavi, Diana, 16  
Molis, Michelle, 483  
Molloy, Anne, 747  
Montaudo, Renee, 192  
Montcouquiol, Mireille, 807  
Montemayor, Celina, 826  
Montey, Karen, 906  
Montgomery, Allen A., 744  
Moody-Antonio, Stephanie, 237  
Moon, Il Joon, 191  
Moon, So Young, 191  
Moonen, Marc, 520  
Moore, Anthony, 700  
Moore, Brian, 1062  
Moore, David, 169,1028  
Moore, Jason, 430,432,433,437  
Moore, Robert, 184  
Moravec, William, 858  
Morawski, Krzysztof, 624  
Moreno, Felipe, 289  
Moreno-Pelayo, Miguel A., 289  
Morest, D. Kent, 80,827,902,944,945,946

Morgan, Kaulani, 237  
Morgan, W. Jason, 825  
Mori, Yoshiaki, 867  
Morris, Ken A., 27,423,633,803,806  
Morrison, Richard, 600  
Morse, Sue, 890  
Morton, Cynthia, 294,307  
Moser, Tobias, 392  
Moss, Cynthia F., 953,957,959  
Motts, Susan D., 688  
Mou, Caihong, 43  
Moucha, Raluca, 708  
Moulin, Annie, 163  
Mountain, David C., 332,439,640,922  
Mouton, Peter, 907  
Mueller, Anne, 139  
Mueller, Marcus, 304,908  
Muenscher, Adrian, 903  
Mugnaini, Enrico, 815  
Mukherjee, Debashree, 350  
Muller, Andrea, 868  
Müller, Marcus, 868,900  
Müller, Martijn, 179  
Muniak, Michael, 906  
Murakoshi, Michio, 614  
Murata, Junko, 819  
Musicant, Alan, 112  
Musiek, Frank E., 700  
Mustain, William, 841  
Nagarajan, Srikantan, 765  
Nagashima, Reiko, 591  
Nagata, Keiichi, 889  
Nagura, Mitsuyoshi, 229,379  
Nagy, Ivana, 377,840  
Nair, Thankam, 293,793,794  
Nakae, Kaori, 49  
Nakagawa, Takayuki, 83,554,555,556,557,558,585  
Nakahara, Haruka, 993  
Nakai, Akira, 385  
Nakajima, Hideko, 924  
Nakamori, Akiko, 570  
Nakamoto, Kyle, 997  
Nakamura, Takaaki, 95  
Nakashima, Tsutomu, 62  
Nam, Jung-Hoon, 529  
Narins, Peter, 784,916  
Narui, Yuya, 316  
Nason, Robert, 488  
Nataraj, Kiran, 127  
Nathanson, Neil M., 652  
Navaratnam, Dhasakumar, 879,1046,1051  
Navarrete, Enrique, 783  
Neelon, Michael, 459  
Neely, Stephen, 315,662  
Nehmer, Rachel, 839  
Neiman, Alexander, 859  
Nelken, Israel, 508,691,1003  
Nelson, Amy, 1028  
Nemanov, Lyubov, 140  
Neubauer, Heinrich, 484  
Neubert, Wolfgang, 214  
Neuburger, Heidi, 518,738,745  
Newburg, Seth, 922  
Newlands, Shawn, 177  
Newman, Craig W., 164,205  
Newman, Dina, 422  
Ng, Philip, 615,627  
Ng, Thomas, 518  
Nicholas, Alexander, 101  
Nicholson, Bruce, 262  
Nickel, Regina, 258,862  
Nicol, Trent, 992  
Nicolae, Robert, 528  
Nicole, Trent G., 452  
Nicotera, Thomas, 364

Nie, Kaibao, 759  
Nie, Liping, 398,877,878,1050  
Niedermeyer, Hans, 214,352,579  
Niparko, John, 1022  
Nishimura, Hiroshi, 462  
Nishimura, Tadashi, 1033  
Nistico, Laura, 147,149  
Moser, Andrea, 160  
Nodal, Fernando, 1003  
Nogaki, Geraldine, 735,736  
Noh, Heil, 75,1020  
Nomoto, Yukio, 83  
Norena, Arnaud, 1010  
Northrop, Clarinda, 211  
Nourski, Kirill, 75,1020  
Nowotny, Manuela, 328  
Nuttall, Alfred L., 320,325,327,330,336,339,347,348,376,380,409,578,785  
Oas, John G., 173,193,205  
Oba, Sandra, 228  
Oberholtzer, Carl, 884  
Obstoy, Marie-Françoise, 291  
O'Connell-Rodwell, Caitlin, 923  
O'Connor, Kevin, 928  
O'Connor, Philip, 173  
Odeh, Hana, 798  
Oelke, Alisha, 648  
Oertel, Donata, 20,444,684  
Oesterle, Elizabeth, 809  
Oestreicher, Elmar, 352,408,579,713  
Offutt, George, 383  
Ogawa, Hiroshi, 83  
Ogawa, Kaoru, 370,571,577,591  
Ogawa, Makio, 550  
Oghalai, John S., 334,615,621,627,899,1017  
Ogita, Kiyokazu, 591  
Ogunjimi, Benson, 851  
Oh, Seung-Ha, 241,399,457,602,748,817  
Ohi, Frank W., 464,712  
Ohlemiller, Kevin K., 414,568  
Ohtani, Iwao, 932  
Okada, Minae, 1040  
Okano, Hideyuki, 386,577,819,830  
Okano, Hirotsuka James, 577  
Okano, Takayuki, 555,585  
Oku, Naohiko, 462  
Olarie, Margaritha, 289  
Oliver, Dominik, 821,1052  
Olivius, Petri, 451  
Olney, Daniel R., 417,418  
Olson, Elizabeth, 326  
Omelchenko, Irina, 578  
Omori, Koichi, 83,932  
O'Neill, William E., 433,437,698,963  
Onoda, Norihiko, 471  
Orem, Alex, 616  
Organ, Louise E., 622  
Oriel, Brad S., 182  
Ornitz, David M., 275  
Ortega, Alberto, 879,1051  
Ortiz, Jeanette A., 733  
Osada, Yoshihisa, 1037  
Osaka, Yasuhiro, 462  
Osdoit, Anne, 1001  
Osumi, Yasunori, 361  
Oswald, Duane, 838  
Ouyang, Xiao Mei, 59,802,804  
Overbeek, Paul A., 649  
Overson, Gary, 255  
Owens, K.N., 599

Oxenham, Andrew J., 71,466,511,1026,1036,1060  
Ozdamar, Ozcan, 499,500,624  
Ozmeral, Erol, 962  
Paasche, Gerrit, 38,950  
Paige, Gary D., 963  
Pak, Kwang, 151,153,553,597,655  
Palmer, Alan, 693,974,1004  
Palmer, Donna J., 627  
Paludetti, Gaetano, 364  
Pan, Luying, 559  
Pandya, Arti, 294  
Pandya, Pritesh, 708  
Paolini, Antonio, 1015  
Paparella, Michael, 894  
Papsin, Blake, 210  
Parameshwaran, Suchitra, 539  
Parazzini, Marta, 138,163  
Pardo, Patricia, 540  
Park, Byung-Gun, 496  
Park, Channy, 351,587  
Park, Hanho, 279  
Park, Hong Ju, 845,848  
Park, Ji Yeong, 602,817  
Park, Min-Hyun, 457,817  
Park, Raekil, 351,587  
Park, Seong Kook, 157  
Park, Sungyeol, 603  
Parker, Lisan, 1047  
Parker, Mark A., 384,563  
Parkinson, Aaron, 475  
Parrish, Jennifer, 431  
Parrish, Sarah, 61,217  
Parsons, Thomas D., 69,641  
Partan, Sarah, 923  
Pasanen, Edward G., 310  
Paschall, Dwayne, 501  
Patel, Andrew K., 605  
Patel, Aniruddh, 264  
Patel, Mihir R., 105,107  
Patel, Tejas, 359  
Paterson, Miles, 120  
Patrick, Jim, 524,950  
Patterson, Michael, 295  
Paulin, M.G., 849  
Pawlaczyk-Luszczynska, Malgorzata, 162  
Pawlowski, Karen S., 302,303  
Payne, Stacy, 231  
Peake, William, 920  
Peeters, Heidi, 1038  
Penkova, Zhenya, 868  
Pereira, Fred A., 540,615,618,619,627,629,649,826,899  
Pérez, Cristina, 854  
Pérez-Flores, Cristina, 855  
Perez-Gonzalez, David, 678  
Perozo, Eduardo, 6  
Persaud, Ricardo, 486,487  
Peters, B. Robert, 475  
Peters, Brian, 534  
Peterson, Ellengene, 857,858  
Petit, Christine, 9,261,291  
Petralia, Ron, 77  
Peusner, Kenna D., 513,531  
Pfaller, Kristian, 910  
Pfungst, Bryan E., 220,525,1024  
Pfister, Markus, 304  
Phatak, Sandeep, 757,758  
Philibert, Benedicte, 983,993  
Phillips, David S., 143  
Phillips, Gabriel, 606  
Phillips, Kelli, 895  
Piazza, Valeria, 306  
Pienkowski, Martin, 701  
Pierce, Carol, 368,837  
Pietola, L., 300

Pikkula, Brian, 334  
Piliipenko, Valentina, 828  
Pillai, Jagan, 565  
Pillers, De-Ann, 98  
Pintar, John E., 652  
Pirih, Primoz, 392  
Pirooz, Ali, 538  
Pisoni, David B., 235  
Place, Ned J., 310  
Pletcher, Scott D., 826  
Plinkert, Peter, 51  
Plontke, Stefan, 873,874  
Plyer, Patrick, 87  
Podgorski, Michael, 1047  
Poeppel, David, 468,470  
Pogal-Sussman, Tracy, 728  
Pohl, Ulrich, 408  
Poissant, Sarah F., 739  
Polak, Marek, 40,43,231  
Pollak, George, 128,129,975  
Polley, Daniel, 702  
Pondugula, Satyanarayana R., 24,644,645,870,871  
Pongstaporn, Tan, 685,1022  
Ponton, Curtis W., 454  
Poon, Becky B., 476  
Poon, Paul Wai-Fung, 126,134  
Popel, Aleksander, 610,611  
Popelka, Gerald, 436  
Popper, Arthur N., 70,583,639  
Popper, Paul, 23,33,34,35,36  
Populin, Luis, 955  
Portfors, Christine, 680  
Post, J. Christopher, 144,145,146,147,149,284,838  
Potashner, Steven, 940,941  
Pouyatos, Benoit, 567  
Poynton, Clare, 1001  
Praetorius, Mark, 51,52  
Prasad, Abhishek, 158  
Preston, Robert A., 145,146,149  
Previati, Maurizio, 607  
Price, Katharine, 416  
Price, Steven D., 876,1054  
Prieto, Jorge J., 689  
Prieve, Beth, 666,929  
Probst, Frank, 799  
Propst, Evan, 210  
Prosen, Cynthia, 124  
Prost, Robert W., 465  
Przynosch, David, 365  
Ptok, Martin, 206  
Puckett, Amanda, 708  
Puel, Jean-Luc, 369,564  
puel, Jean-Luc, 604  
Pujol, Jean-Louis, 604  
Puria, Sunil, 779,923,925,928  
Pyott, Sonja, 881  
Qian, Feng, 1048  
Qian, Jinyu, 732  
Qu, Chunyan, 405  
Quale, Mark, 92  
Quesnel, Alicia, 335  
Quinones, Herson, 805  
Quirk, W., 21  
Quraishi, Imran, 872  
Rabbitt, Richard D., 530,617,620,917  
Raft, Steven, 805  
Raible, David W., 598,599  
Raj-Koziak, Danuta, 142  
Ramakrishnan, Neelilyath A., 880  
Ramamoorthy, Sripriya, 333  
Ramkumar, Vickram, 350  
Raper, Jessica, 310  
Raphael, Robert M., 622,872,1049

- Raphael, Yehoash, 31,282,357,797,798,799,836
- Rapson, Ian, 656
- Rasband, Matthew N., 80,902
- Rask-Andersen, Helge, 213,403,910
- Rath, Nigam P., 275
- Ratnanather, J. Tilak, 1001
- Rauch, Steven D., 182
- Rauschecker, Josef P., 511
- Ravazzani, Paolo, 138,163
- Raveendran, Nithyanandhini N., 24,644,645,871
- Ravicz, Michael, 924,926
- Rawool, Vishakha, 170
- Raz, Yael, 814
- Razak, Khaleel, 1008
- Razavi, Babak, 963
- Razdan, Payal, 588
- Read, Heather L., 714,717
- Reavis, Kelly M., 143
- Rebscher, Steve, 250,1025
- Recio, Alberto, 672
- Recio-Spinoso, Alberto, 661
- Redfern, Mark S., 179,186,187,189
- Redfield, Rosemary J., 146
- Reetz, Guido, 37
- Regehr, Keil J., 407
- Regehr, Wade, 677
- Rehm, Heidi, 285,288
- Reich, Uta, 950
- Reidy, Patrick, 283
- Reinert, Thomas, 102
- Reisinger, Ellen, 821
- Reiss, Lina, 669
- Remus, Jeremiah, 742
- Ren, Tianying, 324,339,348,785
- Renken, Remco, 764
- Rennie, Katherine, 856
- Renvall, Hanna, 704
- Rerko, Michael, 738
- Reschke, Millard, 188
- Reuter, Guenter, 950
- Reynolds-Kenneally, Jessica, 10
- Ricci, Anthony, 1055
- Richard, Gabriele, 257
- Richards, Ayo-Lynn, 274
- Richardson, Dustin, 132
- Richardson, Guy, 9,344,894,1042
- Richter, Claus-Peter, 335,546,547,903,1011,1012,1013
- Ridgway, James, 209
- Rieger, Heike, 355
- Riley, Alison, 169
- Ringe, Wendy, 255
- Rinne, Teemu, 467
- Rinzel, John, 115
- Riquimaroux, Hiroshi, 720
- Rivas, Alejandro, 906,907
- Rivoli, Peter, 430,433,437
- Robb, Richard, 536
- Robenolt, Jaime, 690
- Robert, Mark, 1018
- Roberts, Brian, 1056
- Roberts, Lloyd, 1015
- Roberts, Patricia, 286
- Roberts, Richard, 192
- Roberts, William, 393,816
- Robertson, Nahid, 307
- Robinson, Barbara, 75,1020
- Robinson, Linda, 584
- Robinson, Shannon, 215
- Robles, Luis, 778,919
- Rocha-Sanchez, Sonia M.S., 423,633,803,806
- Roche, Joseph, 33,34,36
- Rodrigues, Aldo R., 684
- Rodriguez-Ballesteros, Montserrat, 289
- Rodwell, Timothy, 923
- Rogers, Cheryl F., 744
- Rogowski, Marek, 142
- Rohbock, Karin, 824
- Rohila, Neeru, 746
- Rohrseitz, Kristin, 160
- Roland, Peter, 255
- Ronan, Diane, 896,1042
- Rosahl, Thomas W., 652
- Rosen, Stuart, 167,223,737,763
- Rosenthal, Todd M., 528
- Rosowski, John, 212,775,920,924,926
- Rossoll, Wilfried, 637
- Roup, Christina M., 171
- Rowan, Daniel, 731
- Rowe, Michael, 859
- Rubel, Edwin W., 100,434,435,598,599,600,608,766
- Ruben, Robert, 57
- Rübsamen, Rudolf, 102,435,676
- Ruckenstein, Michael, 295
- Ruehlow, Lisa, 459
- Ruel, Jérôme, 369
- Ruggero, Mario, 318,661,778,786,919
- Ruhland, Janet L., 958
- Runge-Samuels, Christina L., 222,234,236,465
- Russ, Brian, 995
- Ruth, Peter, 304,1052
- Rutherford, Mark, 393
- Rüttiger, Lukas, 713
- Ryals, Brenda, 77
- Ryan, Allen F., 151,153,553,597,637,655
- Rybak, Leonard, 350
- Ryugo, David K., 16,685,906,907,1002,1022
- Rzadzinska, Agnieszka, 628
- Sabin, Andrew T., 730
- Sabine, Ladrech, 369
- Sabirov, Albert, 152
- Sabo, Diane, 248
- Sage, Cyrille, 25,278
- Sahlin, Lena, 812
- Saito, Yu, 907
- Sajan, Samin, 820
- Sakaguchi, Takefumi, 1033
- Sakamoto, Tatsunori, 554,555,556,557
- Salgado, Moses D., 63
- Salt, Alec N., 321,322,787,873,874,897
- Salvi, Richard J., 53,99,378,387,549,592,593,607,705,723,900,933
- Samaranayake, Haresha, 879,1046,1051
- Samuel, Erica A., 156
- Sanchez, Jason, 123
- Sandridge, Sharon A., 164,205
- Sanes, Dan, 115
- Sanford, Chris, 930
- Sangasilp, Nilubon, 197,535
- Sankila, E.-M., 300
- Sanneman, Joel D., 645,871
- Sanovich, Elena, 77
- Sans, Nathalie, 8
- Santi, Peter, 406,656
- Santos, Felipe, 598
- Santos-Sacchi, Joseph, 329,330,783,879,1046,1051
- Saoji, Aniket, 1059
- Sarampalis, Anastasios, 227
- Sasaki, Hiroyuki, 867
- Sasaki, Yasunari, 720
- Sato, Kunihiro, 576
- Saunders, James C., 69
- Sausbier, Matthias, 304,1052
- Sauter, Disa, 461
- Sauvaget, Elisabeth, 553,655
- Sawtell, Nathaniel, 680
- Sawyer, Drew, 627
- Saxon, Eugene, 911
- Sayed, Sameera, 145
- Scarborough, John D., 638
- Schachern, Patricia, 400,894
- Schacht, Jochen, 356,370,426,572,573,585,595
- Schacht, Keturah, 21,22
- Schachtele, Scott, 711
- Schaette, Roland, 934
- Schairer, Kim S., 658
- Scharf, Bertram, 482
- Scheeline, Alexander, 566
- Scheich, Henning, 453,464,712,986
- Scherer, Elias Q., 408
- Scherer, Hans, 64
- Scherer, Marc P., 331
- Schick, Bernhard, 51
- Schlaug, Gottfried, 267
- Schleifman, Erica, 146
- Schmerber, Sebastien, 291
- Schmid, Stephan, 377
- Schmidt, Marcus, 230
- Schmiedt, Richard A., 381,550,562
- Schmuck, Nicholas, 951,979
- Schnee, Michael, 1055
- Schneider, David, 952
- Schneider, Dieter, 201
- Schneider, Mark, 628
- Schnupp, Jan, 989
- Schoenwolf, Gary, 537
- Schoesser, Hansoerg, 233
- Schofield, Brett R., 15,688,1000
- Scholtz, Lars-Uwe, 201
- Schörnich, Sven, 719
- Schrader, Angela, 354
- Schreiner, Christoph E., 706,983,993,1009
- Schrott-Fischer, Anneliese, 822,910
- Schubert, Michael, 175,176,198
- Schuchmann, Maike, 956
- Schulte, Bradley A., 381,405,550,562,601
- Schulten, Klaus, 1043
- Schulz, Andreas, 111
- Schulz, Sara M., 21,22
- Schulze, Holger, 464,986
- Schweisguth, Francois, 11
- Sciarretta, Carla, 633
- Scott, Luisa, 94
- Scott, Sophie, 254,461,763
- Seeber, Bernhard, 967
- Seedorf, Hartwig, 497
- Segil, Neil, 277,281,541,805
- Sekerikova, Gabriella, 815
- Sekiya, Tetsuji, 554,555
- Sen, D., 337
- Sen, Kamal, 962
- Sendtner, Michael, 637
- Sequeira, Damien, 918
- Serrano, Elba E., 28
- Severson, Meryl, 999
- Sewell, William F., 45,46,47,904
- Sha, Su-Hua, 356,426,572,573,585,595
- Shackleton, Trevor, 693,974,1004
- Shafiro, Valeriy, 1034
- Shaikh, Aasef, 177
- Shamma, Shihab, 512,715,716,988,991
- Shan, Xiaojun, 705
- Shang, Jialin, 839
- Shannon, Robert, 224,523,746
- Shao, Mei, 513,531
- Shao, Qing, 260
- Sharma, Anu, 458
- Shaughnessy, Kathryn, 242
- Shechter, Barak, 981,985
- Shecter, Barak, 697
- Sheft, Stanley, 1063
- Shelukhin, Alexander, 841
- Shen, Kai, 145,146,149
- Shen, Yan, 292
- Shen, Zhijun, 405,601
- Shepherd, Robert, 1015
- Shera, Christopher A., 657
- Sheykholeslami, Kianoush, 699
- Shi, "Baker", 207
- Shi, Xiao-Rui, 347,376,380
- Shibuya, Terry, 50,209
- Shiga, Atsushi, 585
- Shih, Jean, 823
- Shim, Hee-Yeon, 309
- Shim, Katherine, 269
- Shim, Woo Sub, 191
- Shimizu, Takeshi, 165,703
- Shimogori, Hiroaki, 371,372,842,843,844,860
- Shin, Jeong Eun, 367
- Shin, Min-Sup, 241
- Shinder, Michael, 180,533
- Shinn-Cunningham, Barbara, 960,962,965,1060
- Shoelton, Brett, 788
- Shofner, William P., 724
- Shope, Cynthia, 382,612,615
- Shore, Susan, 22,686,948
- Shou, Jianyong, 387
- Shub, Daniel, 728
- Siebeneich, Wolfgang, 35
- Siedow, Norbert, 873
- Siegel, Jonathan H., 318,565,566,659,660,661
- Silverstein, Robert, 584
- Sim, Jae Hoon, 925
- Simmons, Charles, 538
- Simmons, Dwayne D., 354,877
- Simon, Jonathan Z., 455,468,470,988
- Simonoska, Rusana, 812
- Sinex, Donal G., 968,970
- Singh, Mandal, 146
- Singh, Ruchira K., 648,653
- Sininger, Yvonne, 449
- Sipp, James, 290
- Sisodiya, Sanjay, 700
- Sivakumaran, Theru, 307
- Skaggs, Jonathan, 105
- Skinner, Margaret, 234
- Skjõnsberg, Åsa, 667
- Slabu, Lavinia, 764
- Slightam-Wearne, Jonathan, 663
- Sliwinka-Kowalska, Mariola, 162
- Smalling, Jeremy, 679
- Smith, David W., 665
- Smith, Edward, 313
- Smith, Joseph, 666
- Smith, Michael E., 583
- Smith, Pauline, 169
- Smith, Richard, 343,767
- Smith, Roger W., 566
- Smith, Zachary M., 251
- Smolders, Jean W.T., 908
- Smythe, Nancy, 550
- Snow, Devon, 554
- Snyder, Evan Y., 563
- Snyder, Russell, 250,1016,1019,1025
- Snyder, William, 296
- So, Hongseob, 351,603
- Sokoman, Keith W., 710
- Sokolov, Yuri, 505,506
- Sokolowski, Bernd, 632
- Somma, Giuseppina, 649
- Sone, Michihiko, 62
- Song, Guiju, 336
- Song, Jae-Jun, 159,489
- Song, Jiakun, 583
- Song, Lei, 329,783
- Songer, Jocelyn, 212
- Sonoda, Noriyuki, 867
- Soose, Ryan, 155
- Sorce, Christopher T., 566
- Soriano, Joaquin, 90
- Soto, Enrique, 854,855,882
- Sotomayor, Marcos, 1043
- Soucek, Sava, 486,487
- Soukup, Garrett, 27
- Spahr, Anthony J., 221
- Sparto, Patrick J., 186,187,189
- Speck, Judy, 280
- Spector, Alexander A., 610,611,621
- Spencer, Nathan, 588
- Spicer, Samuel S., 381,405,550
- Spirou, George S., 825
- Spisak, Kristen, 238
- Spitzer, Philipp, 233
- Spoon, Corrie, 857
- Sridhar, Divya, 909
- Stachowiak, Michal K., 549
- Staecker, Hinrich, 51,52
- Stagner, Barden, 319
- Stagner, Bart, 140,141
- Stahl, Michael, 1027
- Stakhovskaya, Olga A., 909,1014
- Stallings, Valerie, 202
- Stankiewicz, Pawel, 649
- Stankovic, Konstantina, 811
- Stauffer, Eric A., 638
- Stecker, G. Christopher, 118,171,467,996
- Steel, Karen P., 771
- Steele, Charles R., 331,779
- Stein, Alexandra, 1035
- Stein, Murray, 215
- Steinberg, Elizabeth, 702
- Steinman, Aaron, 219
- Steinschneider, Mitchell, 510,1007
- Stemplinger, Ingeborg, 160
- Stenberg, Annika, 812
- Stenfelt, Stefan, 776
- Sterbing, Susanne, 112
- Sterbing-D'Angelo, Susanne, 109
- Sterns, Anita, 666
- Stevenson, Amy, 527
- Stewart, C. Matthew, 176
- Stewart, Christopher C., 733
- Stewart, Lauren, 265
- Stewart, Matthew, 846
- Steyger, Peter, 588,589
- Stickney, Ginger, 759
- Stjernschantz, Johan, 213,403
- Stocks, Rose Mary, 606
- Stone, Jennifer, 809,839
- Stoodley, Paul, 147,149
- Stöver, Timo, 38,355
- Strack, Daniela, 206
- Street, Sarah E., 93
- Street, Valerie, 584
- Streeter, Michele, 856
- Strehler, Emanuel, 626
- Strickland, Elizabeth, 1030

- Stripling, Roy, 172  
 Su, Gina L., 525,1024  
 Su, J., 209  
 Subramani, Munirathinam, 945  
 Suga, Nobuo, 13,707  
 Sugahara, Kazuma, 372,385,608,843,844  
 Sugai, Tokio, 471  
 Sugawara, Mitsuru, 811  
 Sukharev, Sergei, 5  
 Sultemeier, David R., 28  
 Sumner, Christian, 125  
 Sun, Hongyu, 122  
 Sun, Wei, 99,549,705,723,933  
 Sun, Xiao-Ming, 664  
 Suneja, Sanoj, 940,941  
 Sung, Young Ju, 309  
 Surlykke, Annemarie, 961  
 Susa, Ryan, 424  
 Sussman, Elyse, 469  
 Suzuka, Yuko, 463  
 Suzuki, Chiaki, 932  
 Suzuki, Mikio, 165,703  
 Suzuki, Mitsuya, 54  
 Suzuki, Teruhisa, 83,932  
 Svirskis, Gytis, 115  
 Svirsky, Mario, 240,518,738,745  
 Swiderski, Donald, 31,357,836  
 Syka, Josef, 17  
 Taberner, Annette M., 1052  
 Tabuchi, Keiji, 570  
 Tadros, Sherif, 82  
 Takahashi, Terry, 113,114  
 Takasawa, Masashi, 462  
 Takebayashi, Shinji, 557,558  
 Takemoto, Tsuyoshi, 371,372,385,843,844  
 Takemura, Keiji, 181  
 Takenaka, Hiroshi, 867  
 Takeno, Kenji, 371,372,842,843,844,860  
 Taki, Kousuke, 95  
 Talaska, Andra, 356,426,595  
 Talavage, Thomas, 518,745  
 Talmadge, Carrick L., 312,312,657  
 Tamaki, Chizuko, 199  
 Tamasauskas, Daniel, 886,887  
 Tamura, Manabu, 819  
 Tamura, Sunaho, 558  
 Tamura, Tetsuya, 555  
 Tan, Justin, 713  
 Tan, Wen-Hann, 384  
 Tanaka, Kuniyoshi, 371,372,385,843,844  
 Tang, Kang, 30  
 Tang, Louisa, 629  
 Tang, Qing, 740  
 Tang, Wenxue, 864,866,898  
 Taranda, Julian, 394,395  
 Tarantal, Alice, 544  
 Tarnawska, Grazyna, 162  
 Taslimi, Amir, 422  
 Tavartkiladze, George, 163  
 Taylor Moritz, Anna, 856  
 Taylor, N. Ellen, 518,745  
 Taylor, Ruth, 831  
 Telian, Steven, 293,793  
 Telischi, Fred, 624  
 Temchin, Andrei, 318,661,778,919  
 Tempel, Bruce L., 415,569,584  
 Thalmann, Ruediger, 275  
 Thang, Loc, 794  
 Theunissen, Frederic E., 978  
 Thiruvilangam, Prathapan, 149  
 Thomale, Jürgen, 590  
 Thomas, Jan Peter, 590  
 Thomas, Nathan A., 163  
 Thomas, Tamsin, 260  
 Thompson, Ann, 823  
 Thompson, Scott K., 417,418  
 Thonabulsombat, Charoensri, 451  
 Throckmorton, Chandra, 741,743  
 Thuroczy, Gyorgy, 163  
 Tian, Biao, 511  
 Tiblom-Ehrsson, Ylva, 208  
 Tillein, Jochen, 39,252,1021,1023  
 Tinling, Steven P., 63,544  
 Tobey, Emily, 255  
 Todd, N., 927  
 Todt, Ingo, 203  
 Tognola, Gabriella, 138,163  
 Tokunaga, Akinori, 819  
 Tollin, Daniel J., 104,958  
 Tolnai, Sandra, 676  
 Tomaskovic, Sonja, 764  
 Tomita, Masahiko, 980  
 Tomoda, Koichi, 463,471  
 Tong, Busheng, 654  
 Tong, Dan, 260  
 Tong, Ling, 131  
 Tonini, Ross E., 1017  
 Townsend, Stuart, 890  
 Tran Ba Huy, Patrice, 291,655  
 Tran, Huy, 368,837  
 Trejo, Lisa, 37,230,237  
 Tremblay, Kelly, 746  
 Trune, Dennis, 61,98,150,217  
 Russell, Larry, 448,514  
 Tsai, Betty, 885  
 Tsai, Ming-Jer, 899  
 Tsalighopoulos, Miltos, 163  
 Tsang, Hoi Ting, 878  
 Tso, May, 546  
 Tsukita, Shoichiro, 867  
 Tsumoto, Kouhei, 613  
 Tsuprun, Vladimir, 894  
 Tubis, Arnold, 657  
 Tucci, Debara, 949  
 Turecek, Rostislav, 102  
 Turick, Abby, 231  
 Turner, Jeremy, 431,913  
 Tuttle, David, 419  
 Tyler, Mitchell, 202  
 Tzounopoulos, Thanos, 448,680  
 Ubal, Valeria, 538  
 Uchida, Hikaru, 471  
 Ugrinov, Rosen, 382,612,615  
 Ukomadu, Chinweike, 294  
 Ulfendahl, Mats, 41,301,654,667  
 Ulmer, John L., 465  
 Uloza, Virgilijus, 163  
 Uloziene, Ingrida, 163  
 Underhill, Abigail, 694  
 Vajda, Viktor, 439  
 van De Water, Thomas R., 40,43,76,564  
 van der Giessen, Ruben, 308  
 van der Gucht, Estelle, 994  
 van der Heijden, Marcel, 349,668  
 van der Wees, Jacqueline, 308  
 van Dijk, Pim, 314,456,661  
 van Doorninck, J. Hikke, 308  
 van Heyningen, Veronica, 700  
 van Hoesel, Richard, 477  
 van Looij, Marjolein, 308  
 van Remmen, Holly, 605  
 VanBeek, Corinne, 155  
 Vanniasegaram, Iyngaran, 167  
 Vasama, Juha-Pekka, 704  
 Vasilyeva, Olga N., 416,428  
 Vazquez, Ana, 359,398  
 Veekmans, Kim, 233  
 Vega, Rosario, 854,855,882  
 Veile, Rose, 280  
 Veitch, Greg, 260  
 Verbny, Yakov I., 517  
 Verhey, Jesko, 671  
 Vernel, Huib, 751  
 Vestergaard, Martin, 481  
 Vetter, Douglas E., 278,394,395  
 Vicente-Torres, Maria Angeles, 426,572  
 Viemeister, Neal F., 1064  
 Viirre, Erik, 215  
 Villamar, Manuela, 289  
 Visosky, Ann Marie, 899  
 Visser-Dumont, Leslie, 137  
 Vogelheim, Casey, 847  
 Voie, Arne, 656,911  
 Voigt, Herbert, 440  
 Volkov, Igor, 999  
 Vollmer, Maïke, 983,1021  
 Vollrath, Melissa A., 278,886,887  
 von Unge, Magnus, 491  
 Vongphoe, Michael, 759  
 Voytenko, Sergiy, 976  
 Wachsmann-Hogiu, Sebastian, 538  
 Wackym, P. Ashley, 33,34,35,36,222,234,465  
 Wada, Hiroshi, 613,614,924  
 Wade, Travis, 762  
 Wadowsky, Robert W., 145  
 Wagner, Eva, 479,482  
 Wagner, Hermann, 691  
 Wagner, Todd, 194  
 Waldmann, Bernd, 494,495  
 Tsang, Conrad, 204  
 Wall, G. Michael, 157  
 Wallace, Mark, 1004  
 Wallen, Kim, 310  
 Wallhäuser-Franke, Elisabeth, 709  
 Walsh, Edward J., 297,298,299,789,920  
 Walsh, Joseph T., Jr., 1012,1013  
 Walton, Joseph, 951,969,977,979  
 Wang, Chih-Hung, 31  
 Wang, Eric, 488  
 Wang, Haobing, 211  
 Wang, Hong-Ning, 431  
 Wang, Jian, 973  
 Wang, Jianbo, 541  
 Wang, Jing, 369,604  
 Wang, Ping, 53,99,607,705,933  
 Wang, Qiong, 42  
 Wang, Qiu-ju, 292  
 Wang, Wen, 26  
 Wang, Xiaoqin, 507,982,984,1005  
 Wang, Yadong, 468,470  
 Wang, Yong, 947  
 Wangemann, Philine, 407,646,647,648,653  
 Warchol, Mark E., 275,280,810,820  
 Ward-Bailey, Patricia, 801  
 Wareham, Rachelle, 157,498  
 Warren, Jane, 461  
 Warren, Jason D., 265  
 Warskulat, Ulrich, 900  
 Wasserman, Stephen, 151  
 Watanabe, Yoshiaki, 1033  
 Watanuki, Koichi, 860  
 Waterman, Marjorie S., 419  
 Watson, Bracie, 244  
 Watson, Glen, 279,835  
 Webber, Audra, 814  
 Webber, Douglas, 586  
 Weber, Thomas, 545,796  
 Weber, Ursula, 10  
 Webster, Nicholas, 153  
 Wecker, Hermann, 166  
 Wefstaedt, Patrick, 355  
 Wegener, Raimund, 873  
 Wehner, Susan, 1032  
 Wei, Chaogang, 759  
 Wei, Dongguang, 654  
 Wei, Ling, 562  
 Weil, Dominique, 9  
 Weinstein, Joel, 955  
 Weiss, Jeffrey A., 917  
 Weiss, Thomas, 342  
 Weidele, Mary L., 310  
 Wenstrup, Jeffrey, 123,127,699  
 Wenthold, Robert, 8  
 Wentzel, Parri, 403  
 Wenzel, Gentiana I., 334,615,627  
 Wenzel, Sören, 497  
 Werner, Lynne, 1031  
 Werner-Reiss, Uri, 694  
 Wess, Jurgen, 652  
 Wester, Derin, 194  
 Weston, Michael D., 27,803  
 Whilby, Shani, 479  
 White, Ian, 274  
 White, John A., 441  
 White, Judith, 193  
 White, Patricia, 281  
 White, Perrin C., 297  
 Whitley, Elliott, 40  
 Whitlon, Donna S., 546  
 Whitmal, Nathaniel A., 739  
 Whitmer, William M., 724  
 Whitney, Susan, 186  
 Whitworth, Craig, 350  
 Wickesberg, Robert, 755  
 Wiegrebe, Lutz, 719,956,1035  
 Wiersinga-Post, Esther, 764  
 Wightman, Frederic, 242  
 Wiland, Jade, 461  
 Wiler, James A., 525  
 Willecke, Klaus, 259,261  
 Willi, Urban, 916  
 Williams, David, 771  
 Williams, Justin, 459  
 Williams, Tameeka, 953  
 Willott, James, 413  
 Wilson, E. Courtenay, 466,511  
 Wilson, Patricia, 561  
 Wilson, Richard, 752  
 Winer, Jeffery A., 14,689,994  
 Winslow, J. L., 902  
 Winter, Harald, 545,824  
 Winter, Ian, 671,673  
 Wisden, William, 652  
 Wise, Richard, 763  
 Wissel, Kirsten, 355  
 Withnell, Robert, 311  
 Witte, Mirko, 102  
 Witte, Robert, 536  
 Wojtczak, Magdalena, 1064  
 Wolf, Barry, 827  
 Wolf, Don P., 451  
 Wolf, Fred, 392  
 Wolford, Robert, 472  
 Wong, W., 25  
 Woo, Jihwan, 309  
 Wood, Jason, 923  
 Wood, Melissa, 212  
 Wood, Scott, 180,188,202  
 Woods, Chad, 272,807  
 Woods, Charles, 666  
 Woods, David L., 171,467  
 Woodworth, Nina, 816  
 Woolf, Nigel, 65  
 Woolley, Sarah M. N., 978  
 Woolley, Steven, 280  
 Woollorton, Julian, 885,1053  
 Wotring, Helena, 354  
 Wouters, Jan, 520  
 Wright, Anthony, 486,487  
 Wright, Beverly A., 733  
 Wright, Charles G., 26,302,303  
 Wright, Richard, 746  
 Wright, Tracy, 537  
 Wu, Doris, 548  
 Wu, Jiunn-Liang, 126  
 Wu, Jun, 10  
 Wu, Shu Hui, 122,130  
 Wu, Tao, 870  
 Wu, Xudong, 1047  
 Wuyts, Floris, 851  
 Wynshaw-Boris, Anthony, 541  
 Xia, Anping, 615,627  
 Xiang, Juanjuan, 468  
 Xie, Ruili, 128  
 Xu, Han, 89  
 Xu, Tian-Le, 89  
 Xu, Yisheng, 438  
 Xue, Jingbing, 858  
 Xu-Friedman, Matthew, 677  
 Yagi, Masao, 361  
 Yamada, Kanako, 463  
 Yamamoto, Hiroshi, 62  
 Yamashita, Daisuke, 370,571  
 Yamashita, Hiroshi, 371,372,385,842,843,844, 860  
 Yamashita, Toshio, 49,361  
 Yamasoba, Tatsuya, 54,386,830  
 Yamauchi, Daisuke, 645  
 Yamoah, Ebenezer N., 398,877,878,1050  
 Yan, Denise, 59,802,804  
 Yan, Jun, 18  
 Yan, Qingfeng, 58  
 Yang, Guang, 723,933  
 Yang, Hua, 30  
 Yang, Wei-yan, 292  
 Yang, Yu-Qin, 409,410,411  
 Yankova, Maya, 945  
 Yatsenko, Svetlana A., 649  
 Yau, Peter, 527  
 Yavuz, Erdem, 500,624  
 Ye, Qing, 39  
 Yeo, Nam-Kyung, 366  
 Yi, Eunyoung, 388  
 Yin, Pingbo, 715  
 Yin, Tom C.T., 958  
 Yip, Helena, 359  
 Yoder, Mervin, 551  
 Yoo, Donald, 619  
 Yoo, Ji-Yeon, 191  
 Yoo, Tai June, 55  
 Yoon, Yang-Soo, 756  
 Yoshino, Takahiko, 62  
 Yost, William A., 1063  
 Yotnda, Patricia, 540  
 Young, Eric, 108,442,669,670  
 Young, Rebecca, 592  
 Young, Wie-Yen, 60  
 Yu, Heping, 800,801  
 Yu, Ning, 375  
 Yu, Sam-Mi, 503  
 Yu, Shujun, 145  
 Yu, Susan, 149  
 Yu, Xilong, 822  
 Yue, Qi, 971  
 Yun, MyungJa, 603  
 Yun, Romy, 158  
 Yund, E. William, 171,467  
 Zahorik, Pavel, 964  
 Zalewski, Christopher, 199

Zamyslowska-Szmytke, Ewa,  
162  
Zatorre, Robert, 263  
Zecker, Steven, 452  
Zehnder, Andreas, 650  
Zellner, Ingrid, 967  
Zeng, Fan-Gang,  
522,734,740,759  
Zenner, Hans-Peter,  
873,874,892,893  
Zerbi, Marian, 472  
Zettel, Martha L., 421,425  
Zhan, Chan-De, 398  
Zhan, Xiping, 685  
Zhang, Duan-Sun, 886  
Zhang, Huiming, 674  
Zhang, Jinsheng, 683,939  
Zhang, Jiping, 997  
Zhang, Kechen, 442  
Zhang, Ming, 501  
Zhang, Roger, 505  
Zhang, Wei, 447  
Zhang, Xiaohui, 541  
Zhang, Xuedong, 1026  
Zhang, Yanping, 864,866,898  
Zhao, Hong-Bo,  
374,375,561,580,865  
Zhao, Hui, 60  
Zhou, Shan-Shan, 544  
Zheng, Jiefu,  
320,325,327,330,348,785  
Zheng, Jing, 616,651,1045  
Zheng, Lili, 798,815  
Zheng, Qing Yin,  
800,801,802,804  
Zheng, Xiaohan, 440  
Zheng, Yanping, 290  
Zheng, Yi, 952  
Zhong, Meng, 875  
Zhong, S., 25  
Zhou, Bin, 55  
Zhou, Guangwei, 182  
Zhou, Jianxun, 686  
Zhou, Wu, 841  
Zhou, Xiaoming, 19  
Zhou, Yi, 443  
Zhu, Xiaoxia,  
416,417,418,419,422,424,  
425,428  
Zhuang, HongXing, 270  
Zhuang, Lei, 490  
Zilany, Muhammad, 79  
Zimmermann, Ulrike, 545,824  
Zine, Azel, 43,564  
Zokoll, Melanie, 722  
Zoller, Jonathan, 96,97  
Zosuls, Aleks, 922  
Zou, YiHui, 270  
Zou, Yuan,  
320,325,327,348,785  
Zuo, Jian, 769,796,1047  
Zuo, Jiang, 545  
Zupancic, Steven, 501



**Association for Research in Otolaryngology**

Executive Offices  
19 Mantua Road  
Mt. Royal, NJ 08061

Phone: (856) 423-0041  
E-mail: [headquarters@aro.org](mailto:headquarters@aro.org)

Fax: (856) 423-3420  
Website: [www.aro.org](http://www.aro.org)